NREL
NATIONAL RENEWABLE ENERGY LABORATORY



Technical Report
NREL/TP-5200-60170
November 2013

Photovoltaic Module Reliability Workshop 2011

February 16–17, 2011

Technical Monitor: Sarah Kurtz

This report is available at no cost from the National Renewable Energy Laboratory (NREL) at www.nrel.gov/publications.

NREL is a national laboratory of the U.S. Department of Energy, Office of Energy Efficiency & Renewable Energy, operated by the Alliance for Sustainable Energy, LLC.
Contract No. DE-AC36-08GO28308

NOTICE

This report was prepared as an account of work sponsored by an agency of the United States government. Neither the United States government nor any agency thereof, nor any of their employees, makes any warranty, express or implied, or assumes any legal liability or responsibility for the accuracy, completeness, or usefulness of any information, apparatus, product, or process disclosed, or represents that its use would not infringe privately owned rights. Reference herein to any specific commercial product, process, or service by trade name, trademark, manufacturer, or otherwise does not necessarily constitute or imply its endorsement, recommendation, or favoring by the United States government or any agency thereof. The views and opinions of authors expressed herein do not necessarily state or reflect those of the United States government or any agency thereof.

Available electronically at http://www.osti.gov/bridge
Available for a processing fee to U.S. Department of Energy
and its contractors, in paper, from:
U.S. Department of Energy
Office of Scientific and Technical Information
P.O. Box 62
Oak Ridge, TN 37831-0062
phone: 865.576.8401
fax: 865.576.5728
email: mailto:reports@adonis.osti.gov

Available for sale to the public, in paper, from:
U.S. Department of Commerce
National Technical Information Service
5285 Port Royal Road
Springfield, VA 22161
phone: 800.553.6847
fax: 703.605.6900
email: orders@ntis.fedworld.gov
online ordering: http://www.ntis.gov/help/ordermethods.aspx

Cover Photos: (left to right) PIX 16416, PIX 17423, PIX 16560, PIX 17613, PIX 17436, PIX 17721

Printed on paper containing at least 50% wastepaper, including 10% post consumer waste.

NREL
NATIONAL RENEWABLE ENERGY LABORATORY

NREL's PHOTOVOLTAIC (PV) MODULE RELIABILITY WORKSHOP (PVMRW) brings together PV reliability experts to share information, leading to the improvement of PV module reliability. Such improvement reduces the cost of solar electricity and promotes investor confidence in the technology—both critical goals for moving PV technologies deeper into the electricity marketplace.

NREL's PVMRW is unique in its requirement that all participating companies share at least one presentation (either oral or poster). In most cases, participation from each company is limited to two people. These requirements greatly increase information sharing: If everyone shares a little information, everyone takes home a lot of information.

In 2011, the PVMRW themes included how to ensure long-term PV module performance by testing and monitoring and choosing the best materials, constructions, and testing methods for evolving module paradigms. Module durability topics were also addressed in the crystalline silicon, thin-film, and concentrator PV parallel sessions.

In addition to the oral sessions, the participants presented approximately 75 posters on PV reliability topics. Most of the participants shared their presentations for public posting; this document is a compilation of these. The success of the workshop is a direct result of the participants' willingness to share their results. We gratefully recognize the excellent contributions the community has made and thank all of the participants for the time and information they have shared.

The workshop was chaired by Peter Hacke with support from:

Ian Aeby
David DeGraaff
Neelkanth Dhere
Dan Doble
Ryan Gaston
Jennifer Granata
Peter Hacke
Peter Hebert
Michael Quintana
Ingrid Repins
Kurt Scott
Shirish Shah
Jim Sites
Govindasamy Tamizhmani
Kaitlyn VanSant
John Wohlgemuth

NREL
NATIONAL RENEWABLE ENERGY LABORATORY

TABLE OF CONTENTS

PLENARY SESSION A: DIAGNOSTICS OF FAILED AND DEGRADED MODULES

Degradation Mechanisms in Si Module Technologies Observed in the Field; Their Analysis and Statistics 1

Building for 25-year Durability in Amonix Solar Power Plants 26

Thin Film Module Reliability – Enabling Solar Electricity Generation 69

PLENARY SESSION B: METHODOLOGIES FOR PERFORMANCE, RELIABILITY, AND DURABILITY DETERMINATION— BABY STEPS TOWARD DETERMINATION OF A 25-YEAR WARRANTY

How to Set Up a Reliability Program for Photovoltaic Modules 111

From Climate Data to Accelerated Test Conditions 131

Monitoring System Performance 163

Methods for Analysis of Outdoor Performance Data 187

PLENARY SESSION C: UPSTREAM MATERIALS, MODULE COMPONENTS, AND STANDARDS

IGMA 25-Year Field Correlation Study 224

Physical Properties of Glass and the Requirements for Photovoltaic Modules 265

Reliability and Durability Evaluation of PV Connectors 283

Durability Testing for Module-attached Micro Inverters 308

How Standards Control Module Design for Better or Worse 317

PLENARY SESSION D: CUSTOMER EXPERIENCES WITH MODULES AND BALANCE OF SYSTEMS

PV Reliability and Performance: A Project Developer's Experience 331

CONCENTRATING PV SESSION

What Not to Do 352

Modeling Thermal Fatigue in CPV Cell Assemblies 373

Low Concentration Photovoltaics: Reliability and Durability Issues 385

Reliability Testing Of High-Concentration PV Modules and Soiling Issues 406
CPV Solar Cell Qualification Standard 427
Minimizing Variation in Outdoor CPV Power Ratings 441
International Quality Assurance Standards 456
Acrylic Materials in PV Applications: Making an Informed Choice 469

SILICON SESSION

Origin and Consequences of (Micro)-Cracks in Crystalline Silicon Solar Modules 506
Potential Induced Degradation 528
High Voltage Bias Testing of Specially Designed c-Si PV Modules 565
Failure Modes and Degradation Rates from Field-Aged Crystalline Silicon Modules 611
Analysis of Hot Spots in Crystalline Silicon Modules and their Impact on Roof Structures 642
PV Module Arc Fault Modeling and Analysis 664

THIN-FILM SESSION

Life Prediction for CIGS Solar Modules 680
Systems Approach to High Performance CIGS Material Set Including Flex Ultra-Moisture Barrier and Hi-Temp MLI Substrate 704
Durability of Ultra Barrier Solar Films for Flexible PV Applications 730
Calcium Based Test Method for Evaluation of Photovoltaic Edge-Seal Materials 749
Reliability and Application Challenges for Flexible Thin-Film (BIPV) Modules 768
Intrinsic Chemical Instability and Metastability in Photovoltaic Devices 787
Analysis of Alternate Methods to Obtain Stabilized Power Performance of CdTe and CIGS PV Modules 811

POSTER SESSION

GENERAL

Quantify Degradation Rates and Mechanisms of PV Modules and Systems Installed in Florida Through Comprehensive Experimental and Theoretical Analysis 829
Estimating the Degradation Rate of Photovoltaic Arrays Using a Two Component Nonlinear Model 830
Requirements for a Standard Test to Rate the Durability of PV Modules at System Voltage 831
Plextronics OPV Outdoor Testing 841
Photovoltaic DC Arc-Fault Circuit Protection and UL Subject 1699B 858

Photovoltaic Modules EDF EN Quality Control . . . 876
Statistical Modeling of Photovoltaic Reliability Using Accelerated Degradation Techniques . . . 877

CONCENTRATING PHOTOVOLTAICS

The Durability of Polymeric Encapsulation Materials for Concentrating Photovoltaic Systems . . . 878
Linking Accelerated Laboratory and Outdoor Exposure Results for PV Polymeric Materials . . . 879
Reliability of SOG for CPV Primary Optics . . . 880
PV Arc Fault Detector Challenges Due to Module Frequency Response Variability . . . 881
CPV Module Acceptance Angle Characterization . . . 882
Performance of a Low-cost, Low-concentration Photovoltaic System . . . 883
ACRYLITE® Acrylics for Reliable Long-Term Performance . . . 884
On the Development of Accelerated Aging Tests Based on Thermal Stress Impact to Assess the Reliability of 1000 Suns CPV Modules . . . 885
Correlations in Characteristic Data of Concentrator Photovoltaics . . . 886

CRYSTALLINE SILICON

NICE Modules Certification According to IEC-61215 and 61730 . . . 887
Mechanical Issues on Solar Modules and Encapsulated Components . . . 888
Outdoor Weathering of c-Si PV Modules in Various Climates - Measurement and Transfer of Module Data of PV-Modules via GPRS . . . 889
Progress on e-Modules Research and Production . . . 890
Development of a New Standard for Transport Simulation on Complete PV-Module Shipping Units in Combination with Thermo-Mechanical Stress . . . 913
Volume Resistivity of EVA Encapsulant Sheet . . . 914
Reliability Factors for Salvage Value of Photovoltaics . . . 921
Material Considerations for Crystalline Silicon PV Module Backsheets . . . 922
Automated Extraction of Cell Parameters in a Fully Packaged Solar Module . . . 923
Durability Test of Poly-Ethylen-Terephthalate (PET) Film for Backsheet . . . 924
Junction Box Qualification at REC Solar . . . 932
Comparison Between Outdoor Performances and Manufacturers' Flash Test Results of Crystalline Si PV Modules . . . 933
Study on Anti-reflection Coated Glass for Photovoltaic Modules . . . 934
Qualification and Lifetime Testing Protocols for Gen II Back Contact Solar Cells/Modules . . . 937

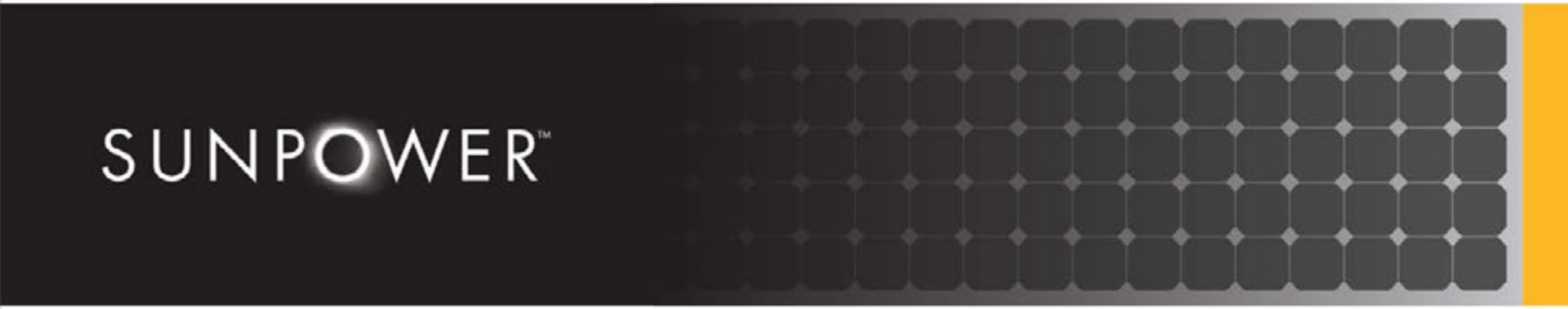
Characterization and Aging Study of Encapsulant (EVA) and Backsheet for PV Modules 949
Demonstration of the Benefits of Silicone Encapsulation of PV Modules in a Large Scale Outdoor Array 971
Evaluation and Analysis of 15 Years Exposure PV Module 972
PV-Integrated Microinverters in High-Reliability Rooftop Applications 978
Damp Heat Testing Longer than IEC Standards 988
Improvement of Reliability Using Four Bus Bar Cell 989
Developments in Weatherable Polyester Films for Photovoltaic Applications 990
Effect of Temperature on the Response of PV Modules to Mechanical Stress 991
Silicone Yellowing Due to Material Interaction in a CPV Application 992
Multi-Crystalline Silicon Solar Cell Modules: Crack Formation and Development due to Climate Chamber Thermal Cycle Testing 1002
New Acceleration Test for PV Modules Such as Burns or Interconnector Failures 1003
Solar Module Logistics Current Packaging Methodologies & Considerations 1004
Prediction of Critical Module Hot Spots Caused by Shunts in Silicon Solar Cells Using In-Line Thermography 1005
Advanced Fluoropolymer-Free, High-Grade PET-Based Backsheet Reaching Over 3,000 Hours DHT* 1006
Accelerated Test and Statistics Model Analysis of Degradation Performance for PV Module Lifetime Prediction 1007
Sensitivity of PV System Degradation Rates to Data Filtration 1008
Fast and Reproducible Test Method to Investigate Hot-Spot Sensitivity of c-Si Solar Cells 1009
LightSwitch™ ETFE Frontsheet 1010
c-Si PV Thresher Test 1011

THIN-FILM PHOTOVOLTAICS

Accelerated Weathering Testing Principles to Estimate the Service Life of OPV Modules 1012
From Rigid to Flexible: The Real Challenge of CIGS Module R&D 1013
A Decade of Combined Cycle Accelerated Testing 1014
Five Stages of a Solar Cell 1015
High Moisture Barrier Flexible Front Sheet for CIGS 1016
Product Reliability Challenges due to Packaging in A-Si Thin Films Modules 1017
Light Soaking Effects on PV Modules: Overview and Literature Review 1029

An Edge Sealing "Getter" Tape for Ultra-long Lifetime (up to 3000 hours) of Thin Film CIGS PV Modules 1054
Electroluminescence to Track Cell and Module Changes from Small-Area Cells to Large-Area Modules 1055
Highly Accelerated Weathering of CIGS Photovoltaics 1056
Stress Testing and Failure Analysis Methods for Determining the Reliability of Metal Buss Tapes 1057
Performance and Reliability Characterization of Conductive Inks for Solar Cell Front Grids and Busbars 1058
Temperature Study on a-Si:H Solar Cell Degradation with Different Loading Conditions 1059
Accelerated Ageing and Reliability of CIGS Thin Film Solar Cells 1060
Energy Production Comparison of Four Representative Solar Cell Technologies: mc-Si, a-Si, CIGS and OPV 1061
Keeping the Water Out for 25 Years 1062
Solar Attachment Adhesives for Building Applied Photovoltaic (BAPV) with Superior Bond Strength 1063
Effect of Long-Term Light Soaking on Shunts and Pmax in CIGS Solar Cells and Modules 1064
Strategies for Developing Barrier Films For Photovoltaics 1065
Understanding Degradation Pathways in Organic Photovoltaics 1066

NREL 2011 Photovoltaic Module Reliability Workshop
Golden, Colorado



Degradation Mechanisms in Si Module Technologies Observed in the Field; Their Analysis and Statistics

David DeGraaff, Ryan Lacerda, Zach Campeau, SunPower Corp

16 February 2011

Copyright © 2011 SunPower Corporation. All rights reserved.

Safe Harbor Statement

This presentation contains forward-looking statements within the meaning of the Private Securities Litigation Reform Act of 1995. Forward-looking statements are statements that do not represent historical facts and may be based on underlying assumptions. SunPower uses words and phrases such as "expects," “believes,” “plans,” “anticipates,” "continue," "growing," "will," to identify forward-looking statements in this presentation, including forward-looking statements regarding: (a) plans and expectations regarding the company’s cost reduction roadmap, (b) cell manufacturing ramp plan, (c) financial forecasts, (d) future government award funding, (e) future solar and traditional electricity rates, and (f) trends and growth in the solar industry. Such forward-looking statements are based on information available to the company as of the date of this release and involve a number of risks and uncertainties, some beyond the company's control, that could cause actual results to differ materially from those anticipated by these forward-looking statements, including risks and uncertainties such as: (i) the company's ability to obtain and maintain an adequate supply of raw materials and components, as well as the price it pays for such; (ii) general business and economic conditions, including seasonality of the industry; (iii) growth trends in the solar power industry; (iv) the continuation of governmental and related economic incentives promoting the use of solar power; (v) the improved availability of third-party financing arrangements for the company's customers; (vi) construction difficulties or potential delays, including permitting and transmission access and upgrades; (vii) the company's ability to ramp new production lines and realize expected manufacturing efficiencies; (viii) manufacturing difficulties that could arise; (ix) the success of the company's ongoing research and development efforts to compete with other companies and competing technologies; and (x) other risks described in the company's Annual Report on Form 10-K for the year ended January 3, 2010, and other filings with the Securities and Exchange Commission. These forward-looking statements should not be relied upon as representing the company's views as of any subsequent date, and the company is under no obligation to, and expressly disclaims any responsibility to, update or alter its forward-looking statements, whether as a result of new information, future events or otherwise.

© 2011 SunPower Corp.

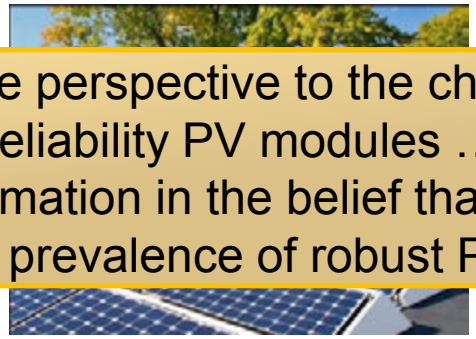
SunPower 2011: 25th Anniversary

- World-leading solar conversion efficiency
- >1.5 GW solar PV deployed
- Diversified portfolio: roofs to power plants
- 5 GW power plant pipeline
- Publicly listed on NASDAQ
- 2010: Revenue Guided >$2 billion
- 5,500+ Employees
- 550 MW+ 2010 production

SunPower brings a unique perspective to the challenge of deploying high-reliability PV modules …
… we are sharing this information in the belief that the entire industry benefits from a high prevalence of robust PV modules.



Residential: #1 US



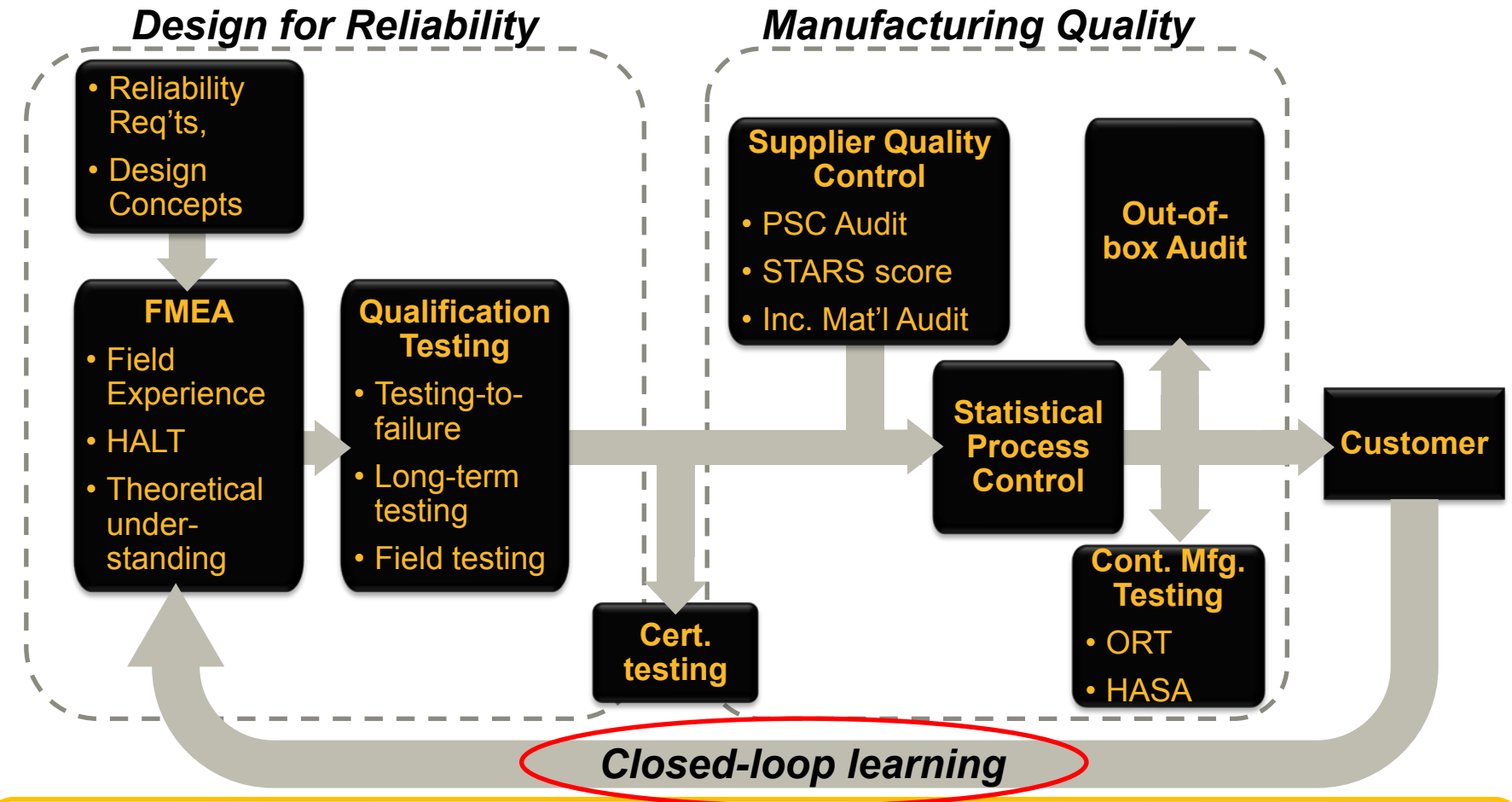
Commercial: #1 US



Power Plant Pioneer



Deploying high-reliability PV Modules: Overall Process



The overall process was articulated in D. DeGraaff, et. al., "*Qualification, Manufacturing, and Reliability Testing Methodologies for Deploying High-Reliability Solar Modules*," EUPVSEC Valencia Spain, Sept. 2010

The focus of today is Closed-loop learning from module field failures.

© 2011 SunPower Corp.

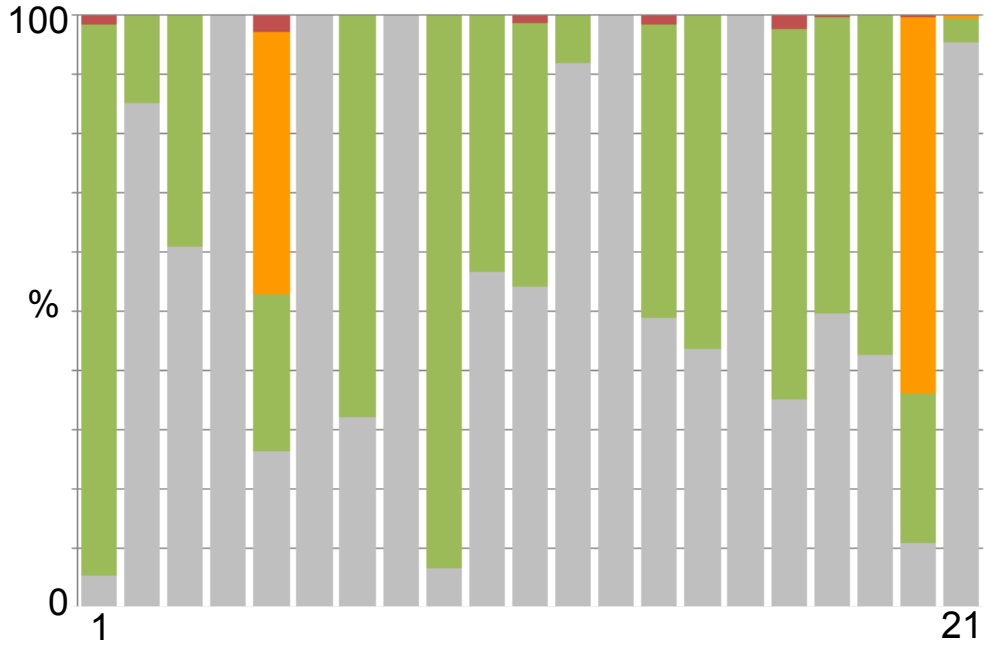
Closed-loop learning from field data

- While some data is significant, some does not have enough samples and is only qualitative.
- Every effort has been made to convey as much information as possible without indicating the names of any specific manufacturers.

ASTROPOWER	ISOFOTON	SANYO	SOLAR SEMICON.
ATERSA	KYOCERA	SHARP	SUNPOWER
BP SOLAR	PHOTOWATT	SHELL	SUNTECH
EVERGREEN	POWERLIGHT	SIEMENS	UNISOLAR
FIRST SOLAR	RWE SCHOTT	SOLARFUN	YINGLI
FLUITECNIK			

© 2011 SunPower Corp.

Field data sampling rates by manufacturer

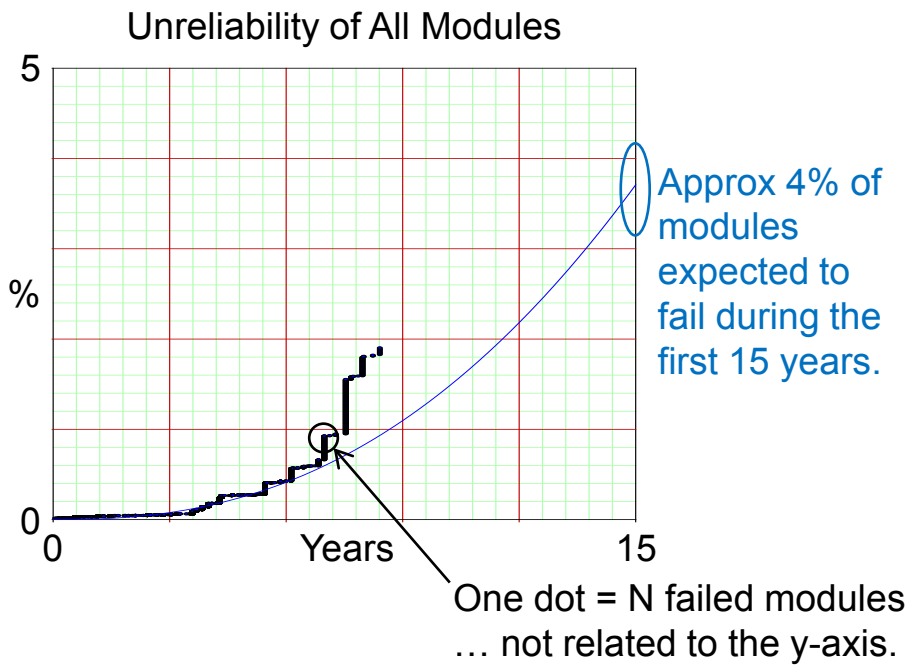


- Records from all sites with a power production warranty (includes string-level IV-curve tracing each year)
- Operations & Maintenance work orders
- Support incidents
- Corrective and Preventive Action records

- Fail – performance does not meet warranty
- Predicted to Fail – well-understood design problem shows these modules will not meet the warranty, but have not failed yet
- Pass – performance meets warranty
- Not Inspected

© 2011 SunPower Corp.

Field statistics: all modules



Notes:

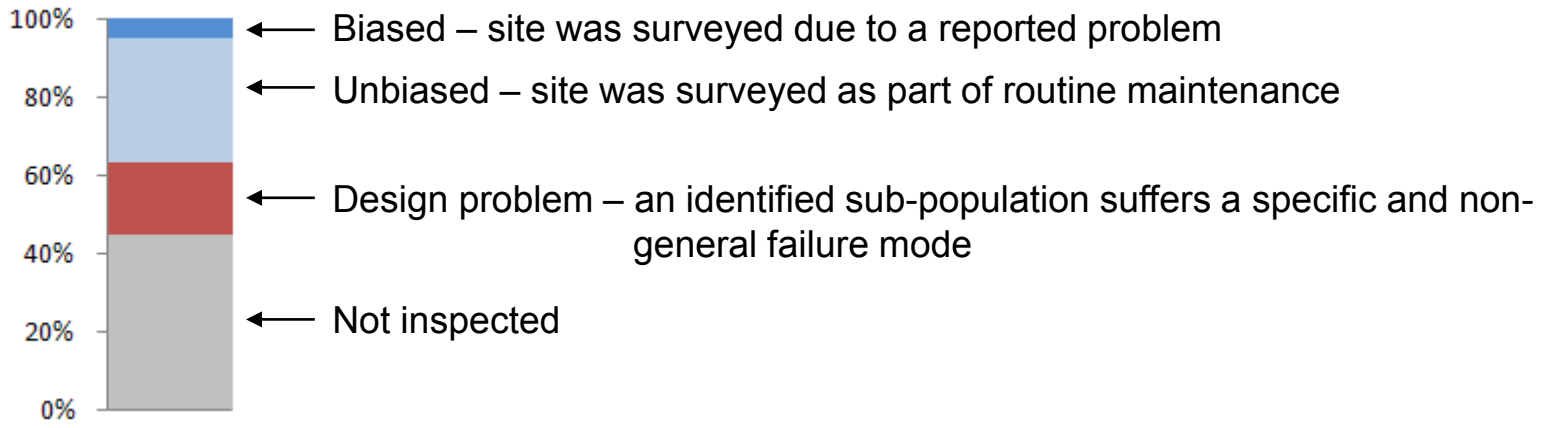
- *Line is a Maximum Likelihood Estimation Weibull fit with a changing number of good modules considered "suspensions."*
  - *Line up every single site with N_{pass} and M_{fail} data at the age of each inspection.*
  - *Find the most likely PDF that will result in that data (fit both the "passes" and the "fails").*
- *Extrapolation error is significant so failure rates should be considered qualitative.*

- A look at the entire fleet of modules suggests the expected reliability will not be met, but this is misleading:
  - Sampling is biased toward sites where customers have reported problems.
  - A high rate of failure for a few module designs is skewing the statistics of the entire fleet (although plot only shows actual failures and not predicted failures).

© 2011 SunPower Corp.

Field statistics: predicting reliability for a good design

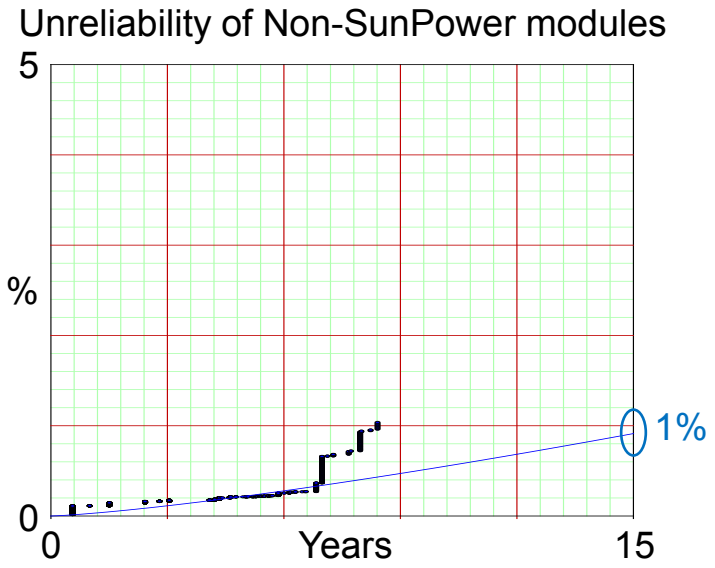
Entire fleet

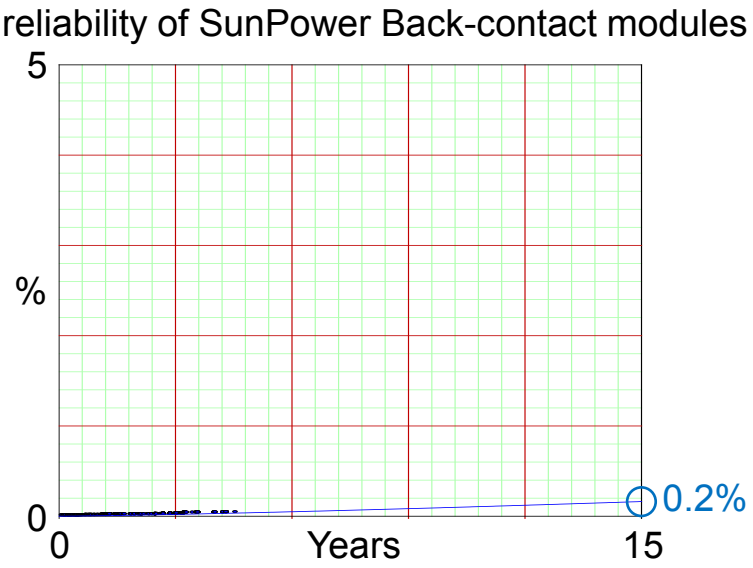


Apply the “unbiased” failure rates to the “not inspected” modules, and remove the “design problem” modules, to arrive at a **baseline fleet reliability** estimate …

© 2011 SunPower Corp.

Field statistics: predicting reliability for a good design



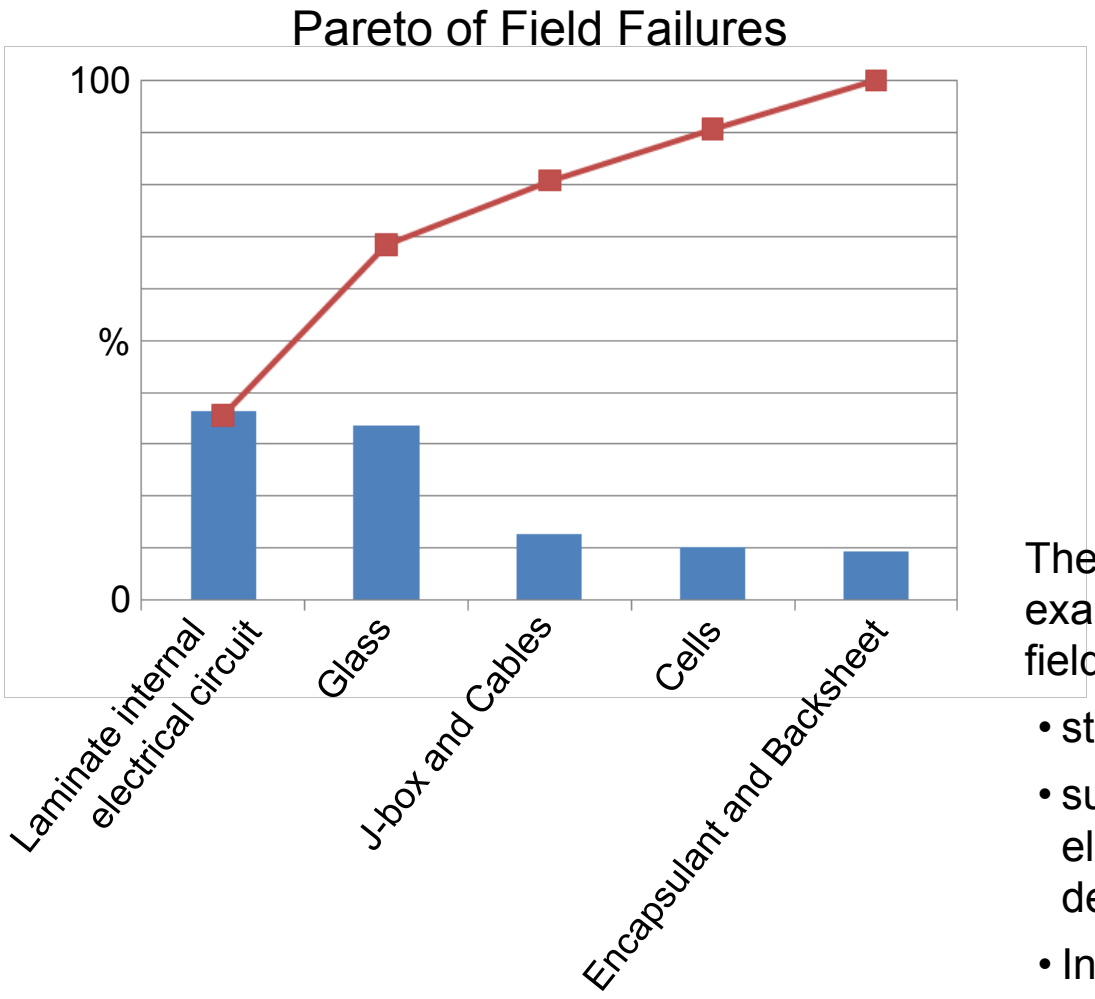


- A look at the fleet of modules *without identified design problems* gives a rough idea of the reliability of the fleet.
- This is only qualitative since the time period is not long enough, and bucketing a bunch of different failure modes into a single predictive Weibull fit is dubious.

The statistics suggests that:
- **Module reliability has a significant impact on Levelized-Cost-Of-Energy**
- **Flawed module designs wear-out quickly**

© 2011 SunPower Corp.

Specific field failures: their analysis and statistics



The next slides go through examples of these 5 groupings of field failures

- statistics when available
- suggestions for tests which could eliminate the failures in the design phase
- Includes the “design problems”

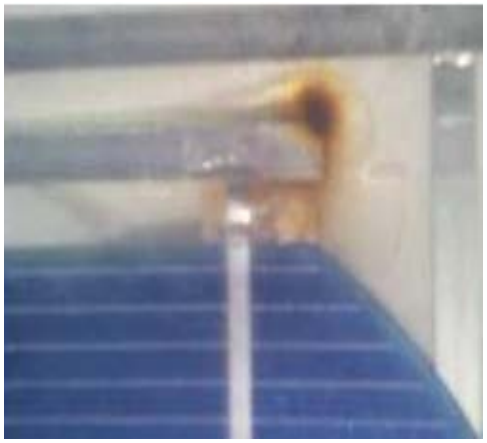
Manufacturers are not identified.

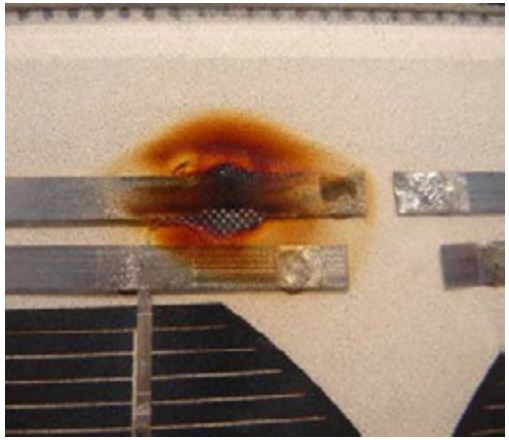
© 2011 SunPower Corp.

Laminate internal electrical circuit

- Failure mode: Hot solder joints causing EVA browning and backsheet damage
- Possible cause: weak solder joints

Mfg A: 0.3% failure rate





Mfg B: 1.5% failure rate

Mfg C: 2.9% failure rate



Front ←

Back →



© 2011 SunPower Corp.

Laminate internal electrical circuit

Mfg E: 0.1% failure rate



Front

Back



Brown EVA over the cell

Hot cell causes brown backsheet and cracking

- Tests that may cover these types of failures (after enough cycles):
  - DH with bias
    - Accelerates front metal corrosion.
  - TC with current
    - Reveals bad solder joints faster than TC alone because the current heats up the bad solder joints causing bubbled and burned backsheets.

© 2011 SunPower Corp.

Glass

- Failure mode: anti-reflective coating delamination
- Cause: tempering processes caused high stress and weakened adhesion.

SunPower: 0.03% failure rate (limited launch)

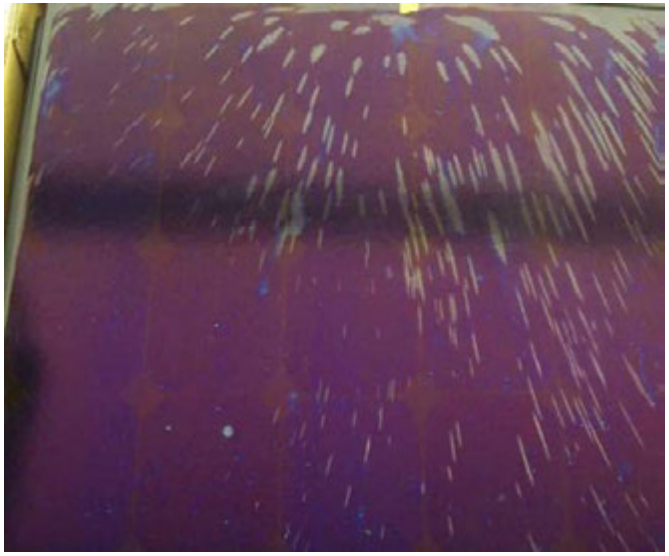
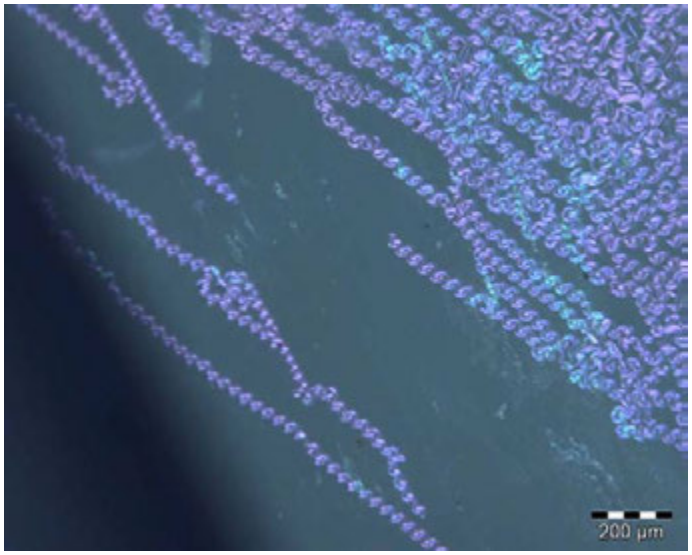


Photo of module with delaminating AR coating



Microscope image of delamination

© 2011 SunPower Corp.

Glass

- Failure mode: silicone residue from manufacturing caused increased soiling.
- Cause: greasy, hard-to-remove residue on modules due to cloth on laminate racks changing from teflon to silicone oil based coating.





Did not impact performance, but brought them all back for cleaning.

- Tests that may cover these types of failures after enough cycles:
  - Damp heat, Thermal cycling or humidity-freeze cycling
  - Water spray and outdoor exposure

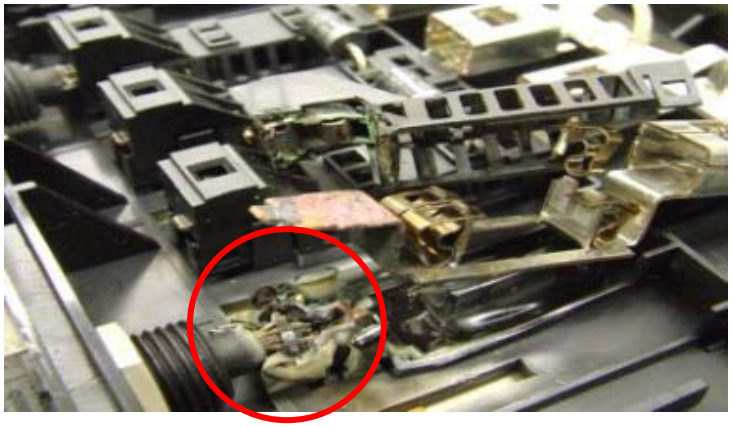
© 2011 SunPower Corp.

J-box and cables

- Failure mode: connectors disconnecting causing arcing
- Possible causes: connector designs susceptible to soiling, incorrect torquing or sizing of wire and grommet, embrittlement or creep of plastic over time, crimping problem

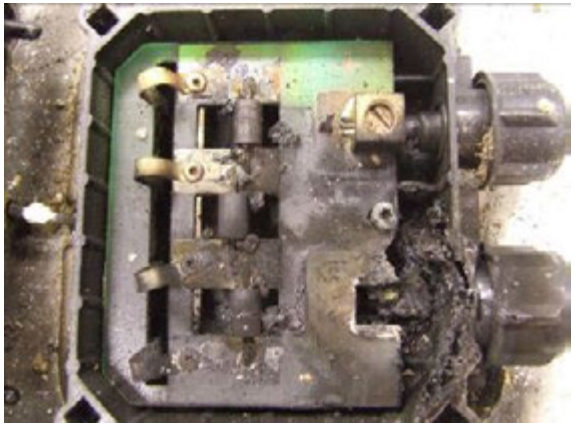
Mfg E: 0.4% failure rate

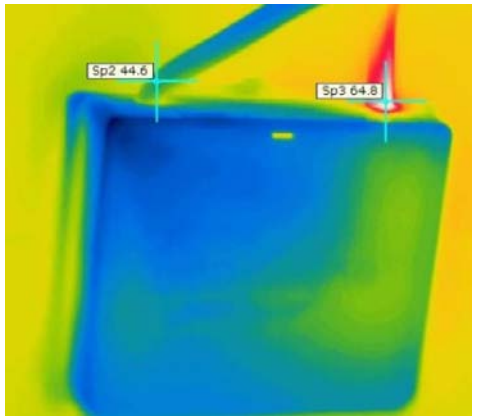




Mfg F

Mfg G



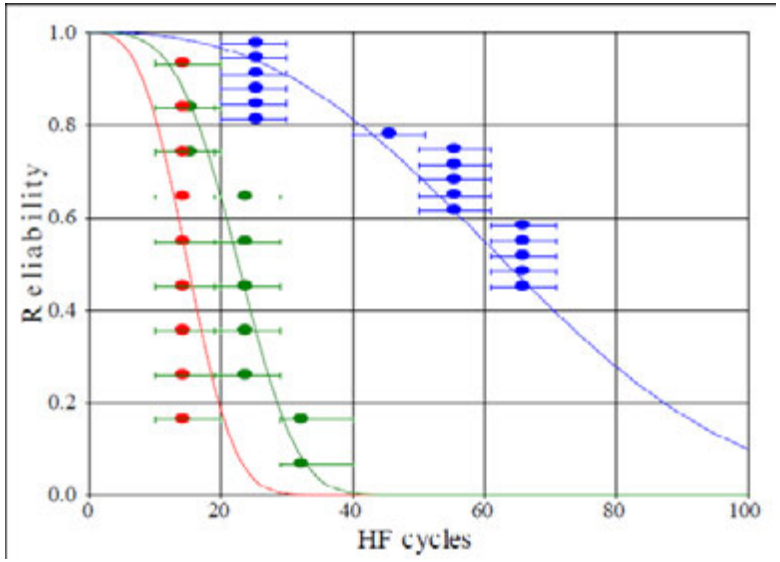


Mfg H: 50% j-boxes show defect (20C hotter)

© 2011 SunPower Corp.

J-box and cables

- Tests that may cover these types of failures:
  - HF50 on connector assemblies followed by dipping connectors in water bath to look for leakage.
    - Proved very good at comparing connector designs.



HF then leakage current testing on 3 cable/connector pairs

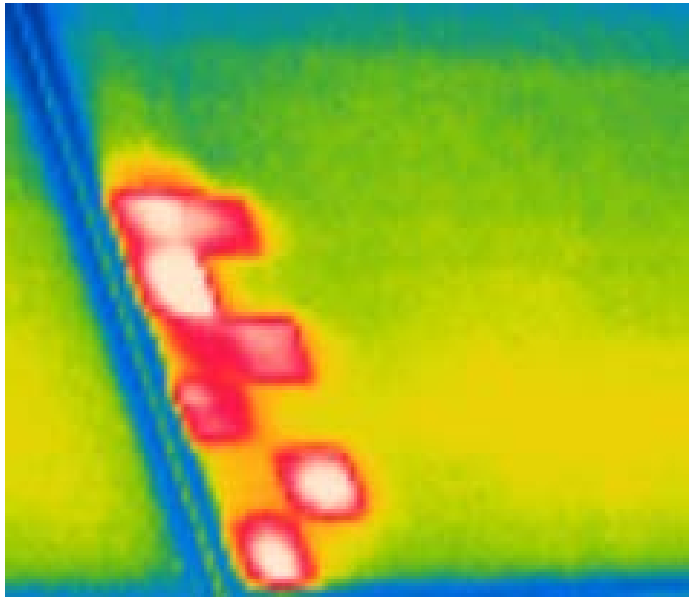
  - Temperature and Vibration
    - Reveals marginal connections, threads that will come loose and J-box adhesion

© 2011 SunPower Corp.

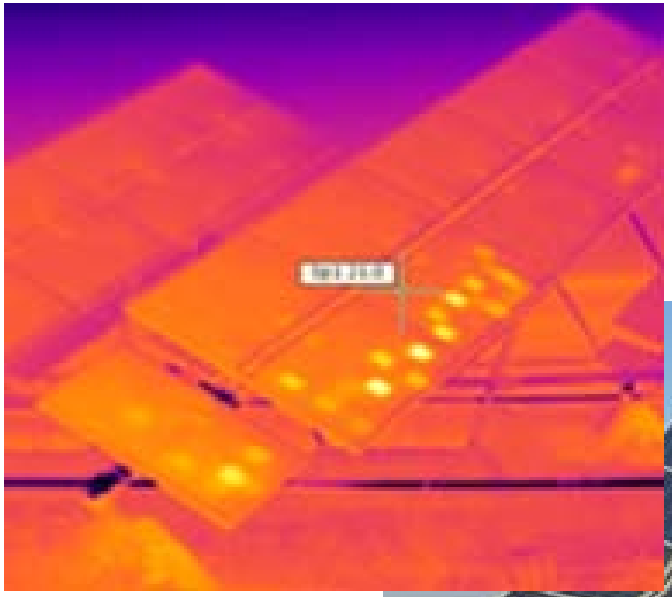
Cells

- Failure mode: Hot cells causing burned backsheets, delamination and sometimes cracked glass
- Possible cause: Unknown cell defect(s)

Mfg J: 1.2% failure rate



Mfg K





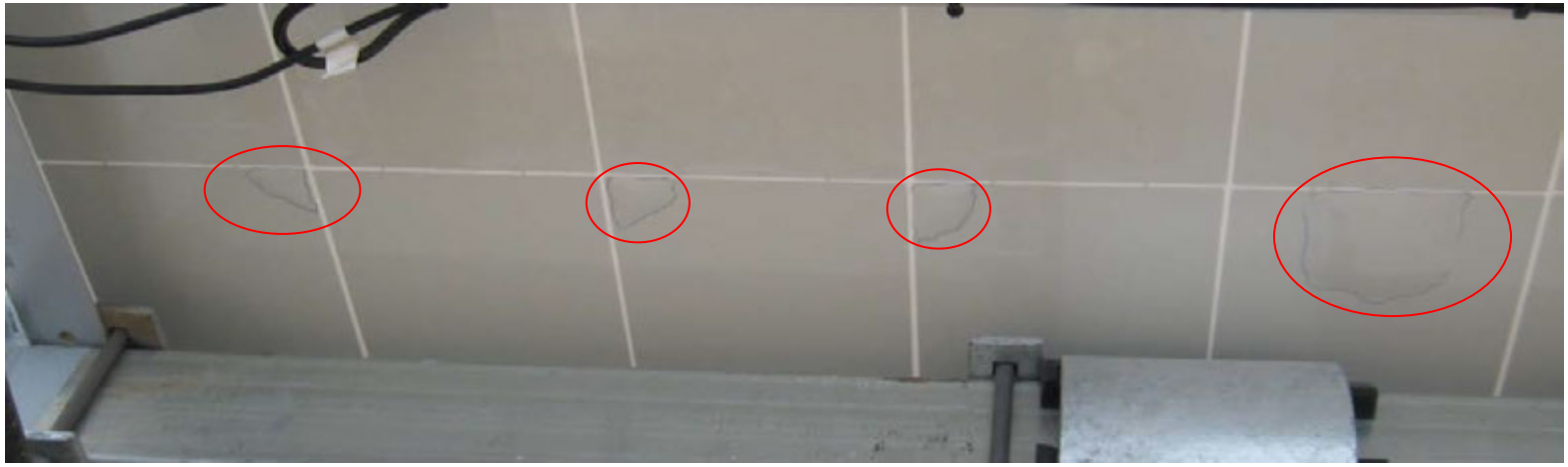
- Tests that may cover these types of failures:
  - Full screening for shunted cells at manufacturing
  - Dynamic load testing (1000 cycles at 2400 Pa) to quantify cell breakage

© 2011 SunPower Corp.

Encapsulant and backsheet

- Failure mode: Backsheet delamination
- Possible cause: unknown

Mfg J: 100% affected for this model



© 2011 SunPower Corp.

Encapsulant and backsheet

- Failure mode: EVA browning/yellowing
- Possible cause: EVA material variation

Mfg K: 50% affected

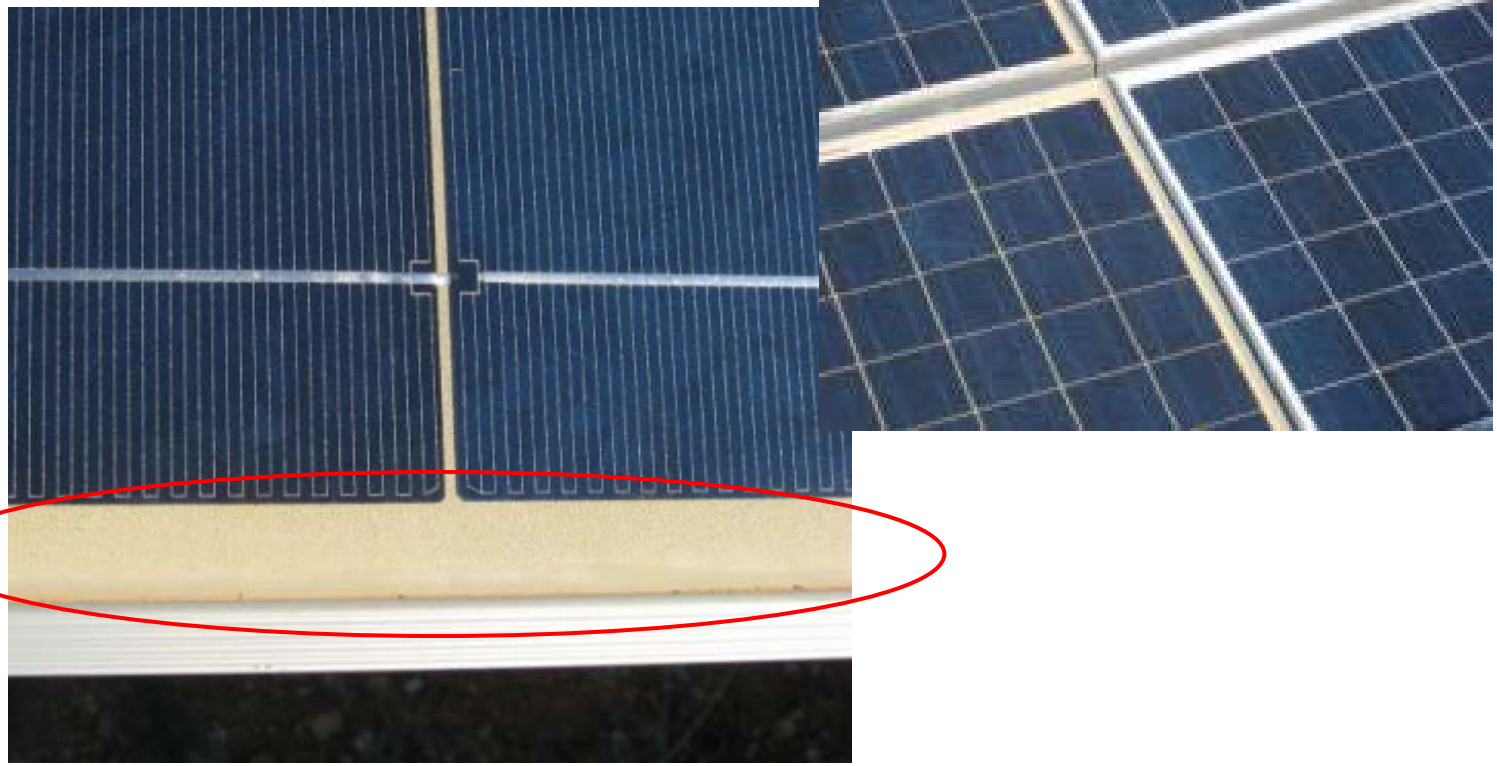


Image of browned EVA after one year in the field

© 2011 SunPower Corp.

Encapsulant and backsheet

- Failure mode: backsheet peeling off exposing backside of cell
- Possible cause: Unknown

Mfg M: 0.1% failure rate

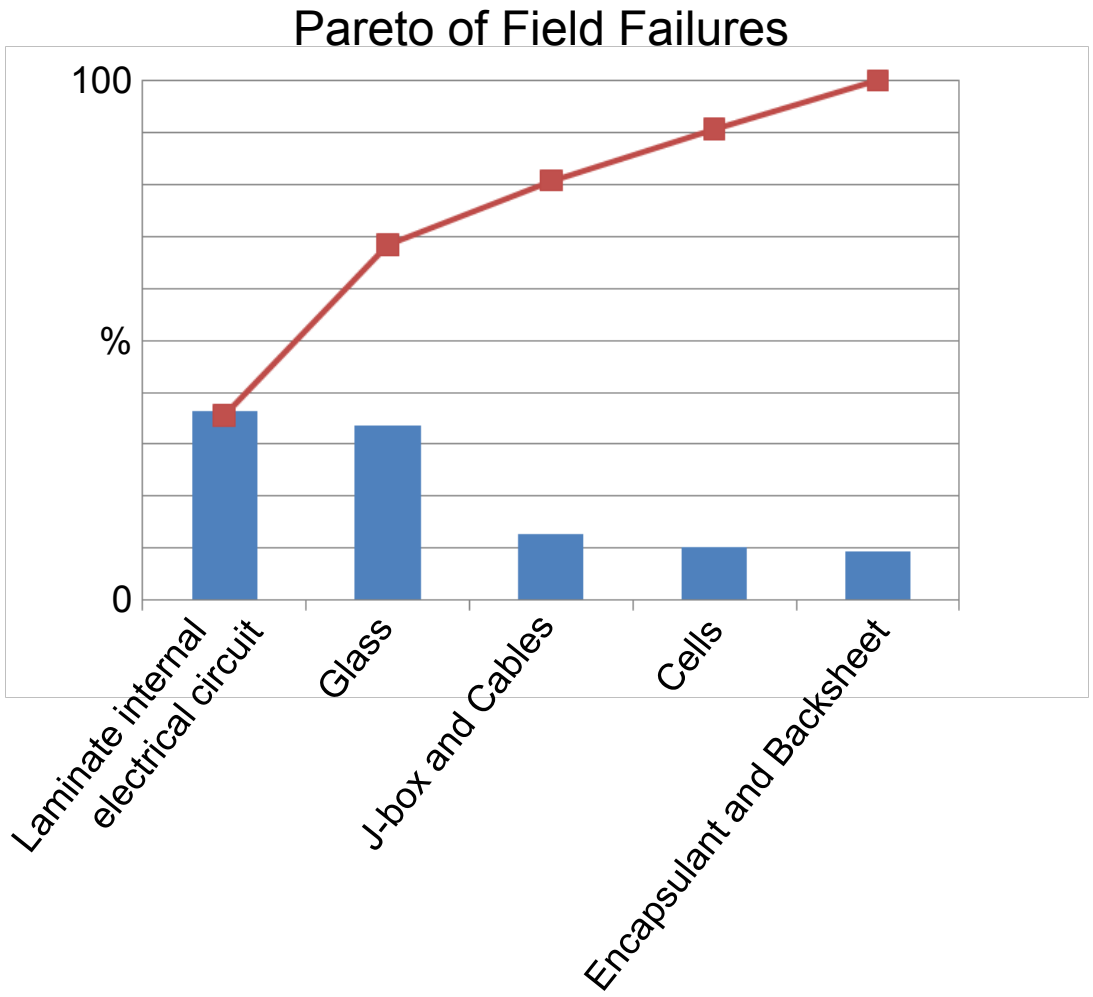


Image of a severely peeled backsheet from the field

- Tests that may cover these types of failures:
  - DH followed by wet leakage test
    - DH degrades the backsheet and the wet leakage test determines if the insulation integrity has been compromised. Partial Discharge testing is the most sensitive.
    - Also reveals both browning and backsheet peeling (requires more than 2000 cycles)
  - Accelerated UV testing (3x UV at 60C ambient for 5 days)
    - Browns EVA because it combines UV and temperature stress.
  - High temperature soak
    - Very effective in inducing bubbled backsheets.

© 2011 SunPower Corp.

Specific field failures: their analysis and statistics



© 2011 SunPower Corp.

Critters, Guns, and the Wrath of God



- Ants attracted to combiner boxes (warmth? electricity? safety?)
- Dead ants' bodies are acidic and corrosive

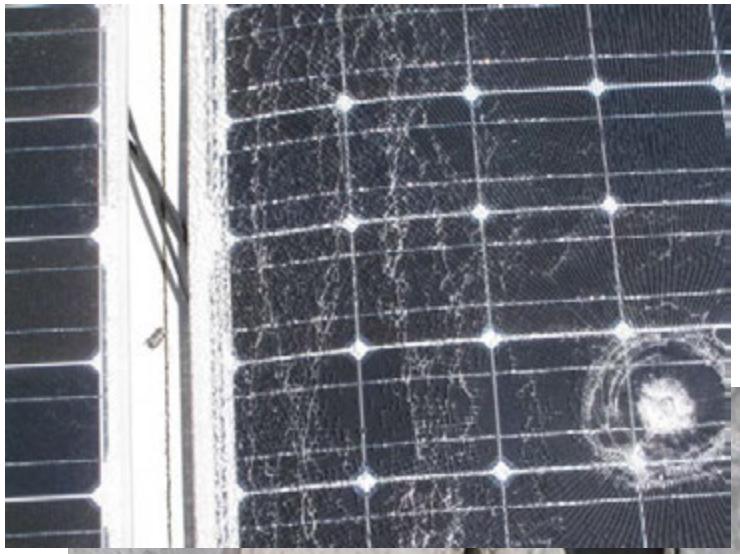


- Rats!



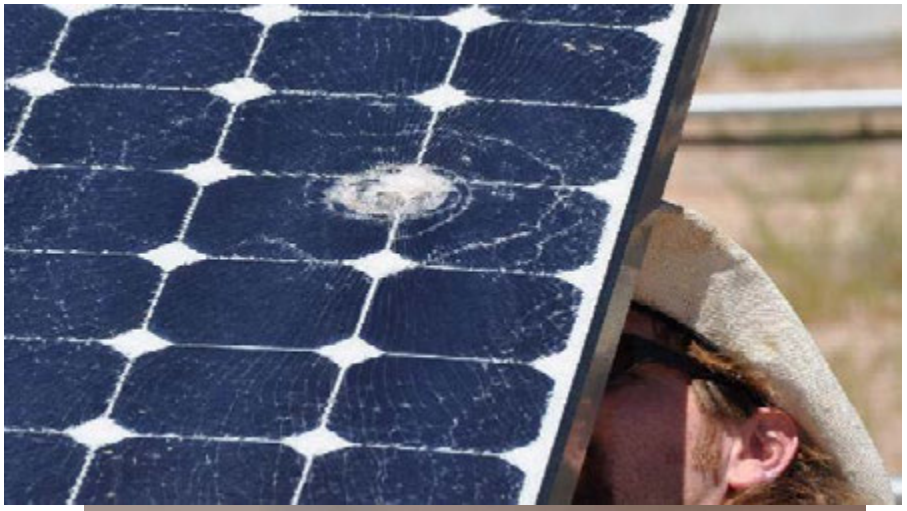
© 2011 SunPower Corp.

Critters, Guns, and the Wrath of God





- Bullet holes!

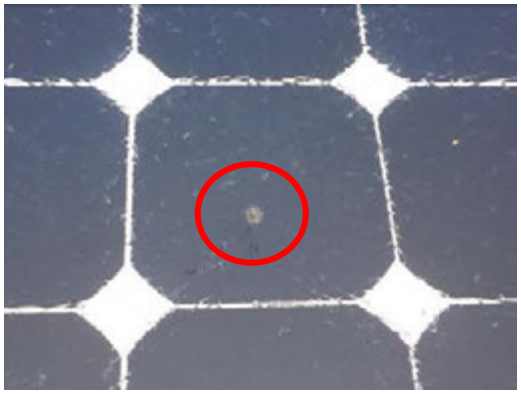




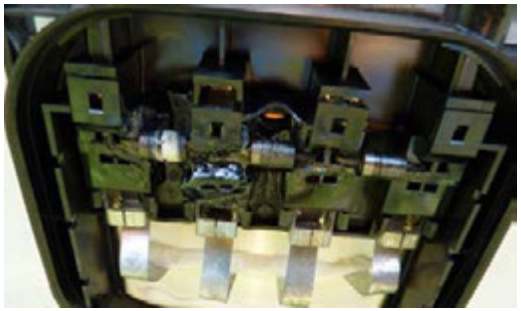
© 2011 SunPower Corp.

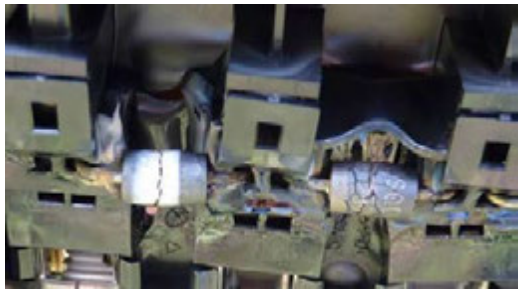
Critters, Guns, and the Wrath of God

- Direct-hit lightening strike: module works fine (!), but diodes were badly damaged



Point of contact on the glass





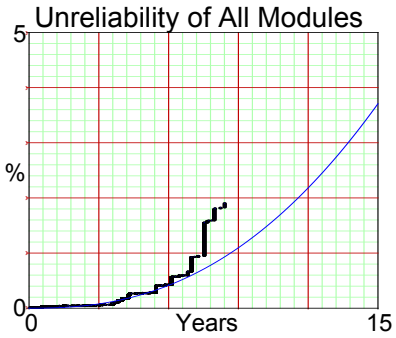


Backsheet damage

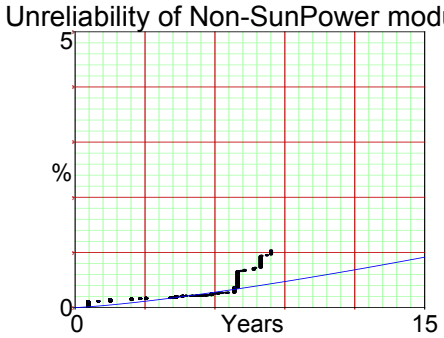


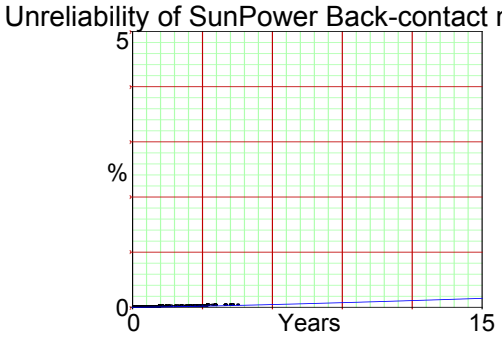
© 2011 SunPower Corp.

Conclusions



- Statistics on the entire fleet qualitatively suggest a reliability problem for a 25 year warranty, but are skewed:
  - Sample bias.
  - A few module types with a specific and non-general design problem.

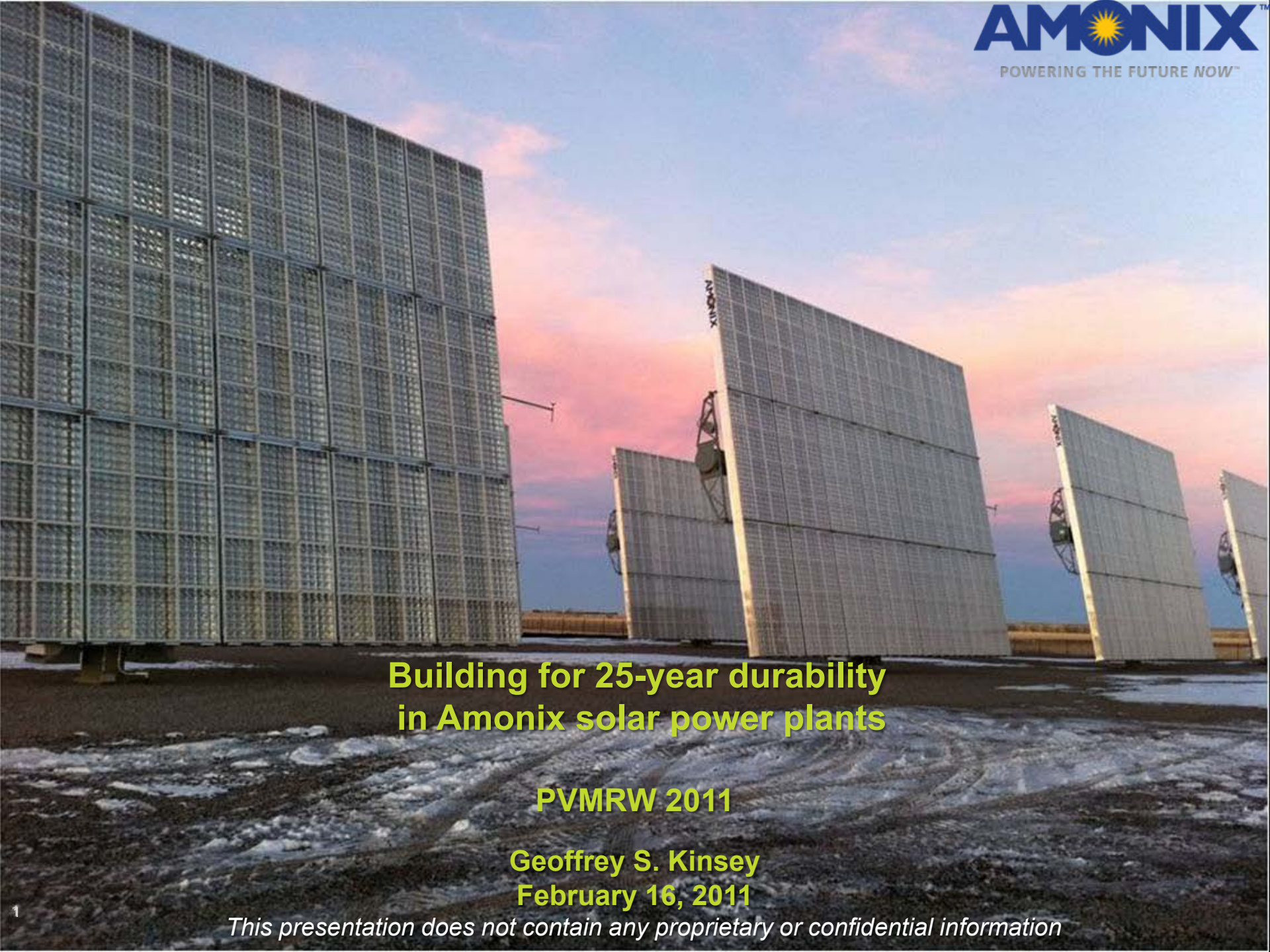




- If the bias is corrected, and key design problems tested out, the statistics qualitatively suggest:
  - High reliability is not a given, but is attainable.
  - Reliability and Quality play an important role in LCOE.

High reliability can be attained with careful testing that targets possible design problems, based on the physics of the failure modes, HALT testing, and field data.

© 2011 SunPower Corp.



Building for 25-year durability in Amonix solar power plants

PVMRW 2011

Geoffrey S. Kinsey

February 16, 2011

This presentation does not contain any proprietary or confidential information

The solar landscape



SUNPOWER
Q.CELLS
SUNTECH
SHARP
SOLON
Don't leave the planet to the stupid



nanosolar
HelioVolt
First Solar.
PrimeStar Solar
Making It Happen

Silicon PV

Thin-Film PV

SOLAR

DIFFUSE

CONCENTRATED



Concentrating Solar Power

ABENGOA SOLAR
acciona Energía
ausra
BrightSourceEnergy



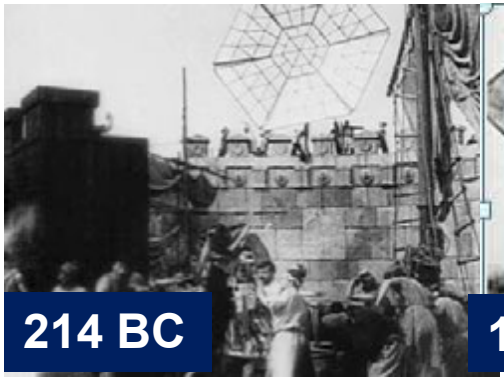
Concentrating PV (CPV)

Arima eco energy
sol3g
isofotón
SolFocus
Innovation Inspired by Nature
Concentrix solar

AMONIX
POWERING THE FUTURE NOW

History of CPV

CPV Progression











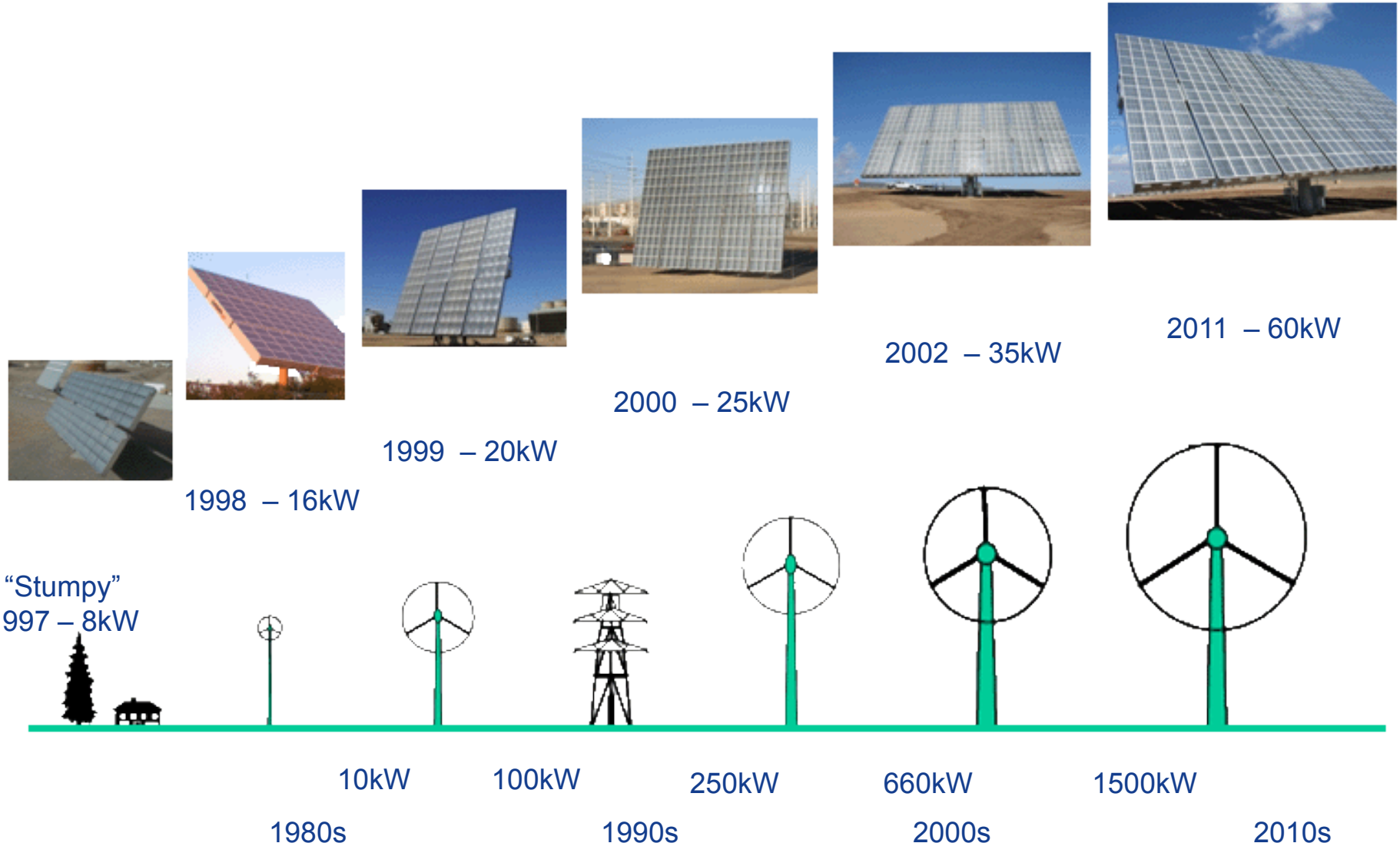






AMONIX
POWERING THE FUTURE NOW

Size supports durability



AMONIX
POWERING THE FUTURE NOW

Multijunction Solar Cell Transition

Same footprint almost doubles energy output



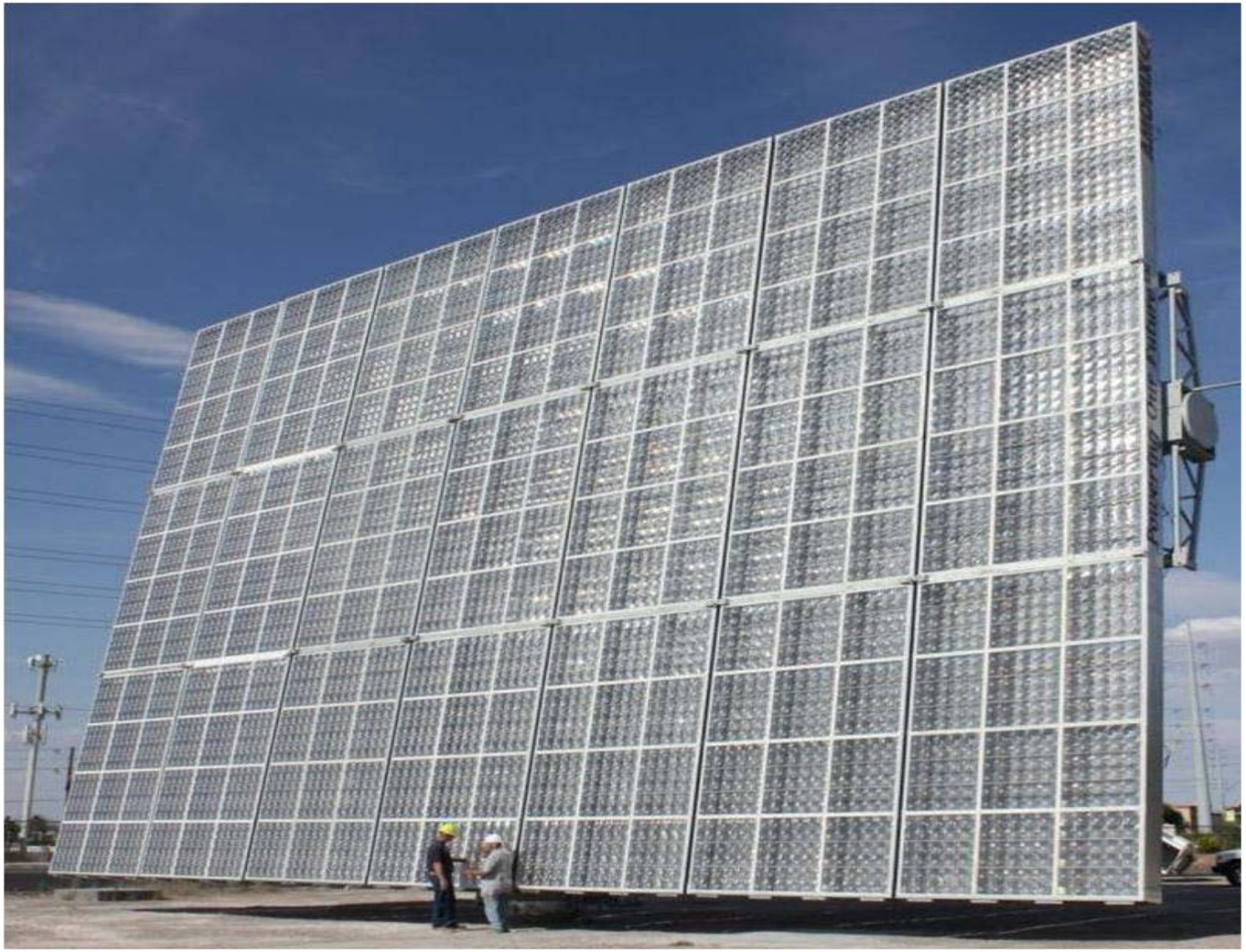
35kW Silicon Cell
(16% AC Efficiency)

60kW Multijunction Solar Cell
(27% AC Efficiency)



AMONIX
POWERING THE FUTURE NOW

Competitive today with established PV technologies



Amonix 7700 Solar Power Generator: 60 kW, 27% AC_{PVUSA}

AMONIX
POWERING THE FUTURE NOW

CPV community

DAIDO STEEL

Concentrix solar
Division of Soitec

SolFocus
Innovation Inspired by Nature

emcore
empower with light™





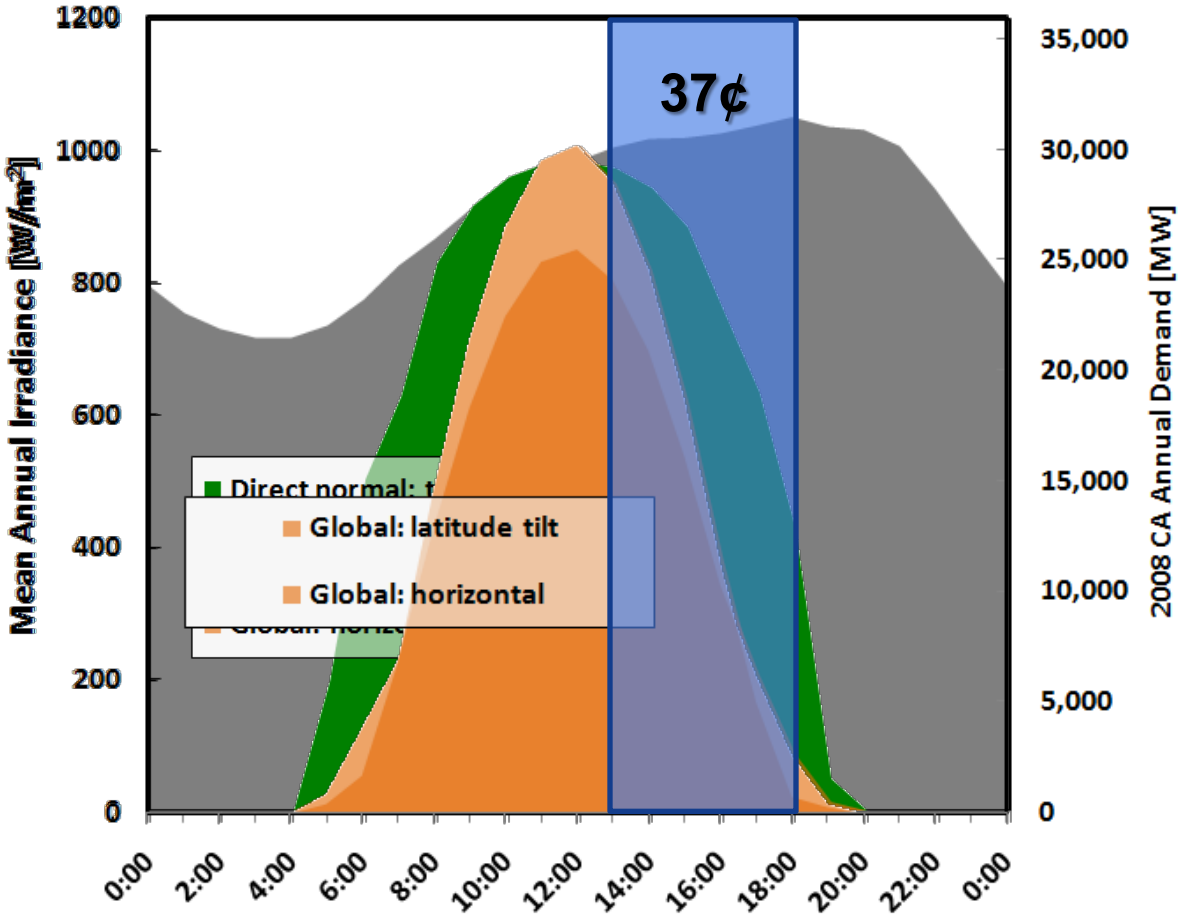


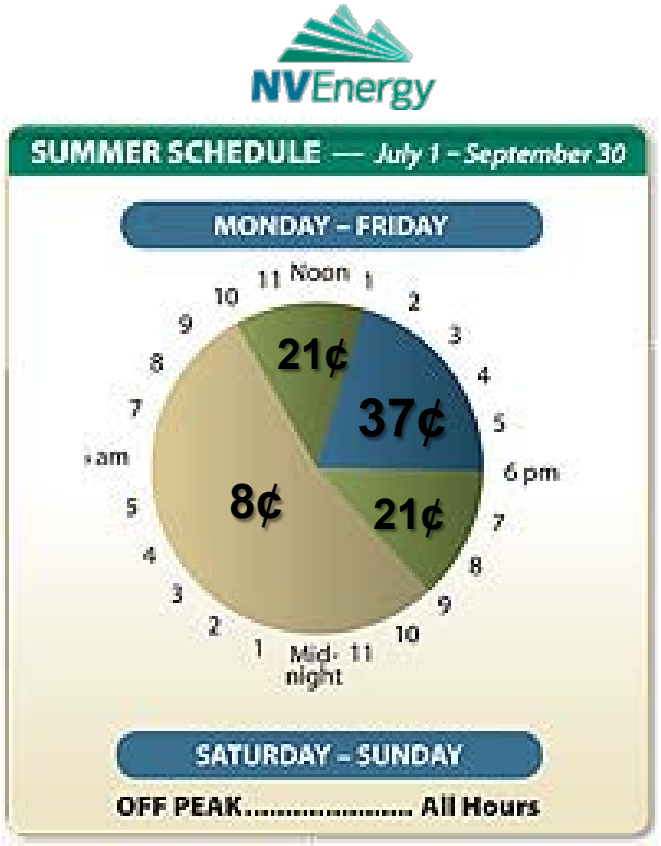


3-15 kW systems

AMONIX
POWERING THE FUTURE NOW

From power to *energy*





Rates per kW-hr

- Utility demand: flat output & high capacity factor.
- Two-axis tracking delivers a “flatter” output.
- CPV justifies the cost of dual-axis tracking

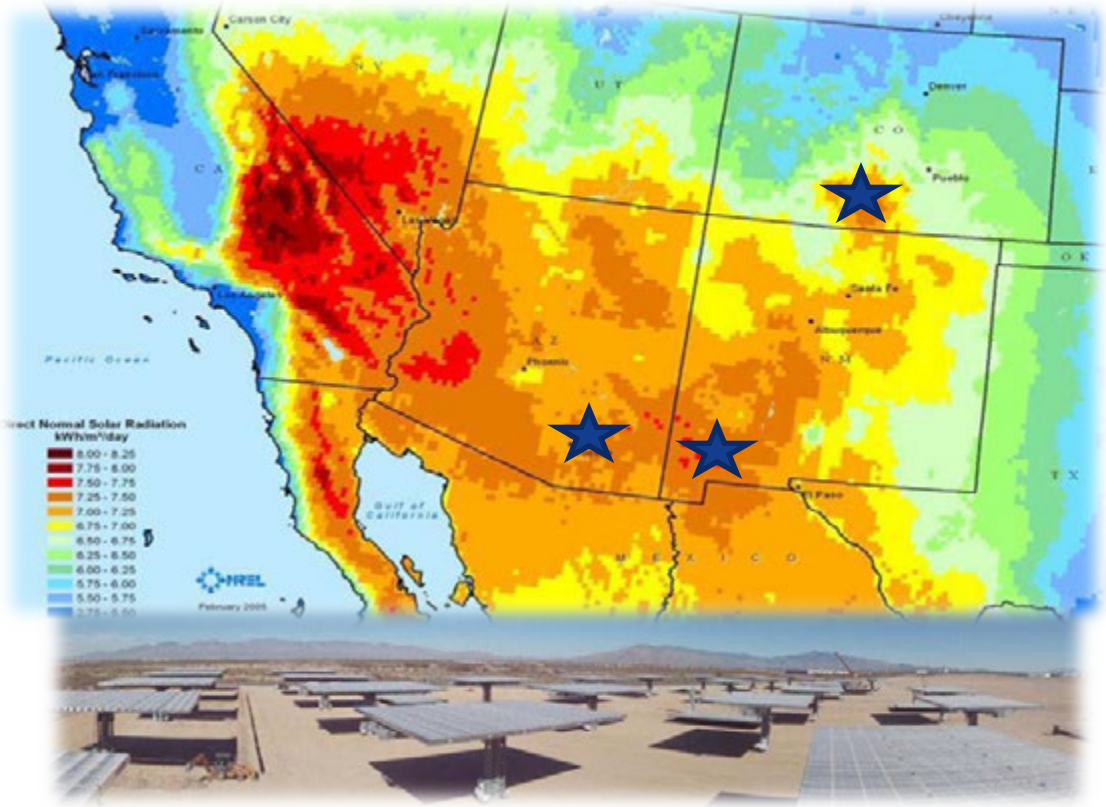
AMONIX
POWERING THE FUTURE NOW

Amonix CPV Projects

Robust Pipeline



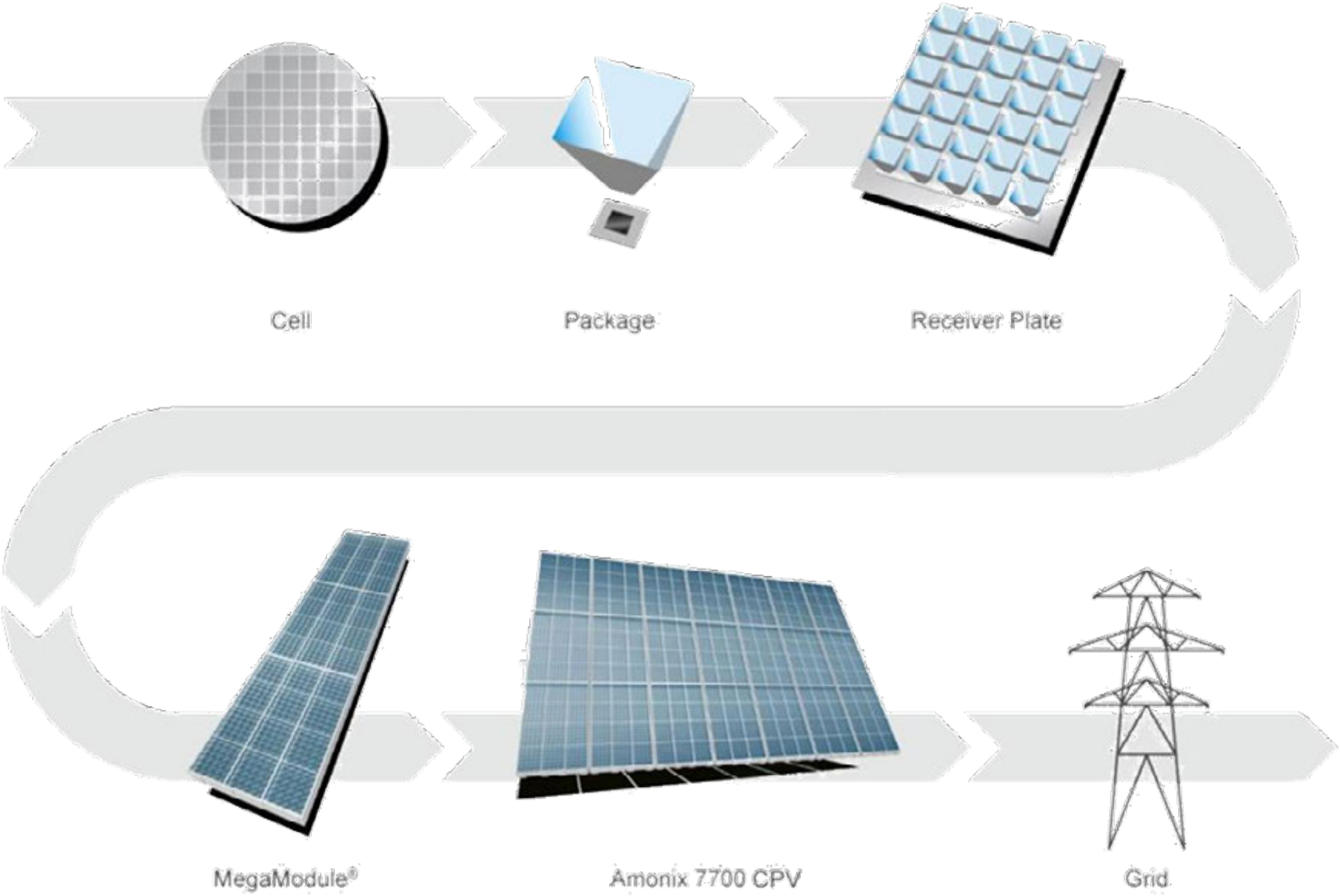




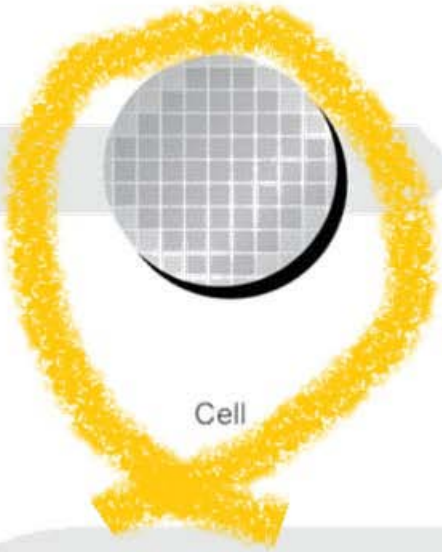
3MW Installed Last Quarter	50MW Under Construction

AMONIX
POWERING THE FUTURE NOW

Component levels



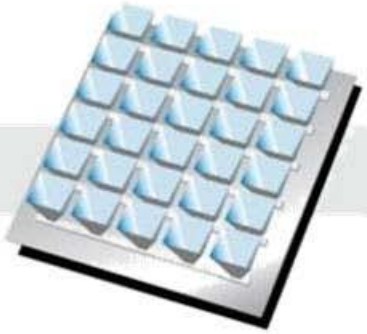
AMONIX
POWERING THE FUTURE NOW



Cell



Package



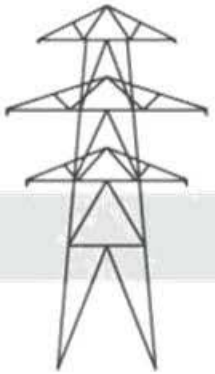
Receiver Plate



MegaModule®



Amonix 7700 CPV

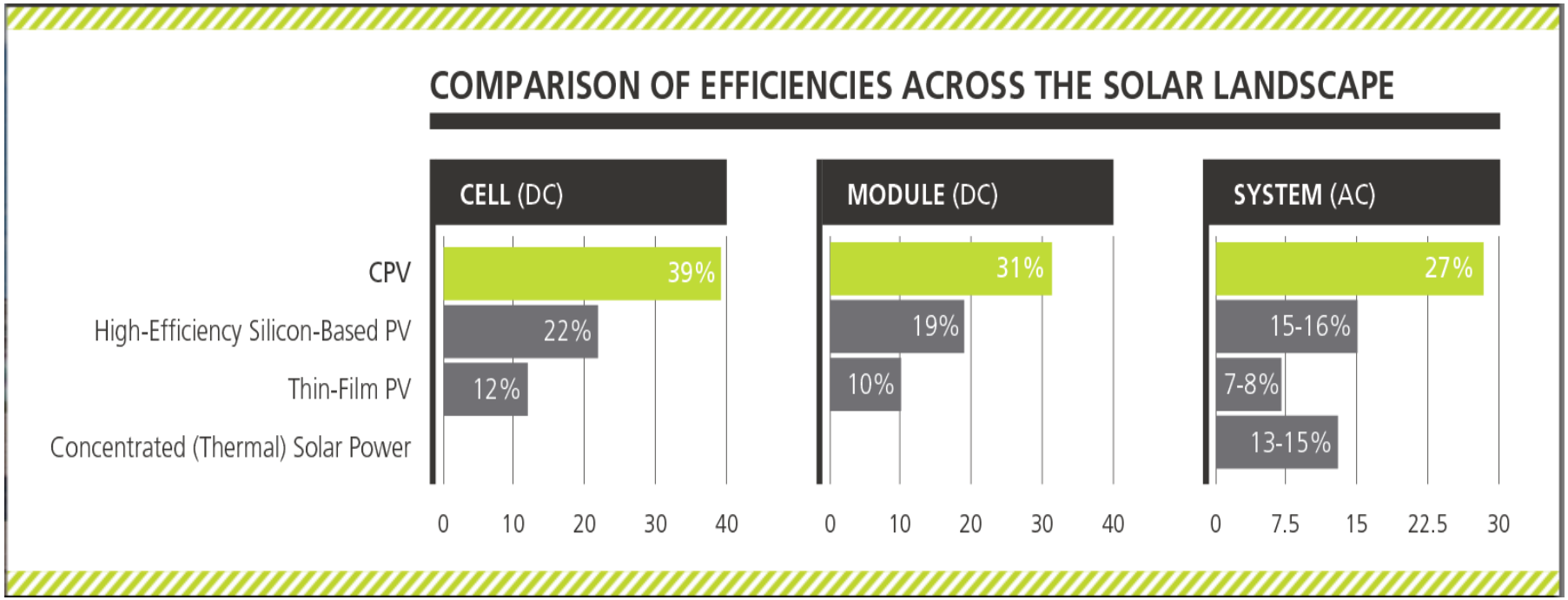


Grid

AMONIX
POWERING THE FUTURE NOW

III-V multijunctions deliver the highest efficiency

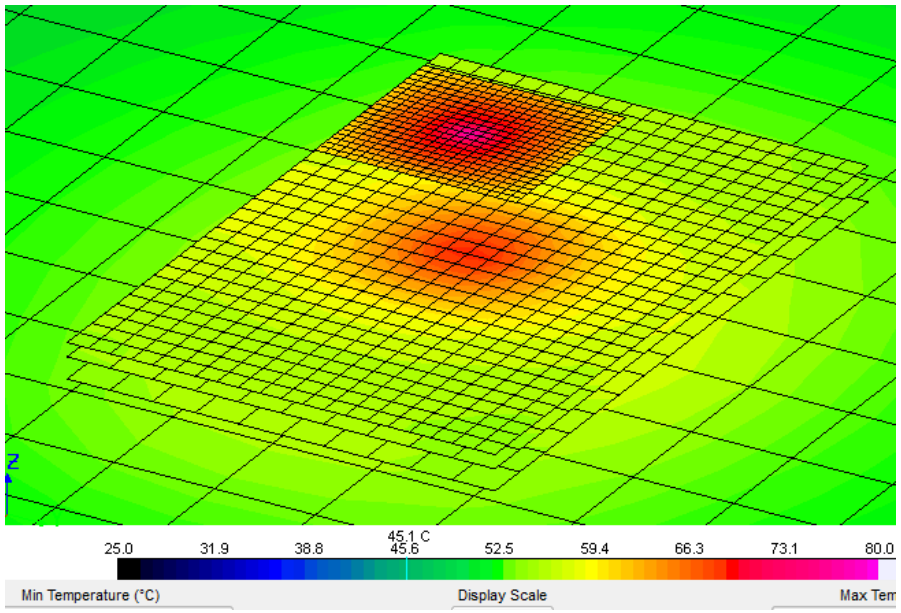
- 27% System, 31% Module, 39% Cell Efficiencies

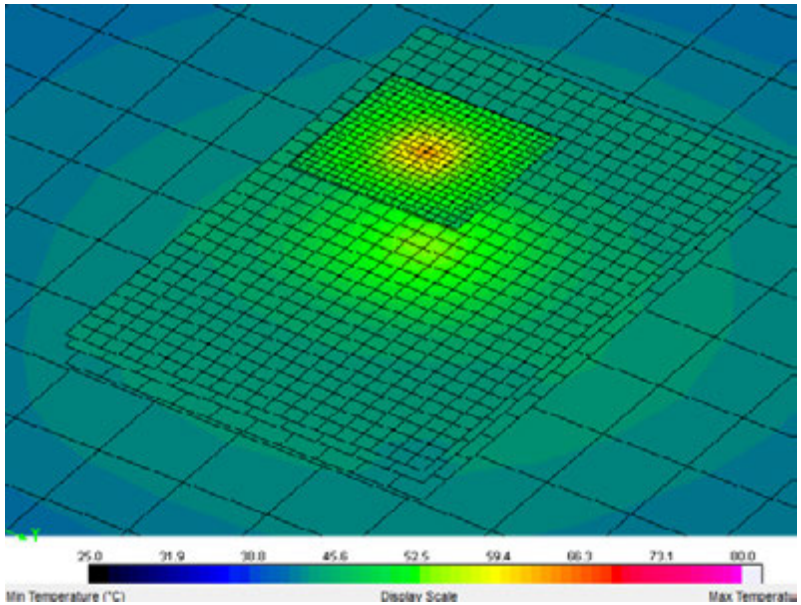


Higher efficiencies support reliability

AMONIX
POWERING THE FUTURE NOW

Thermal management





aggressive thermal management

high efficiency

durability

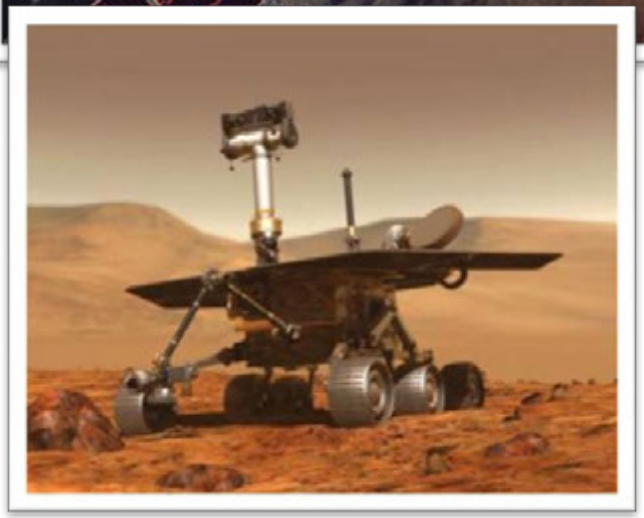
AMONIX
POWERING THE FUTURE NOW

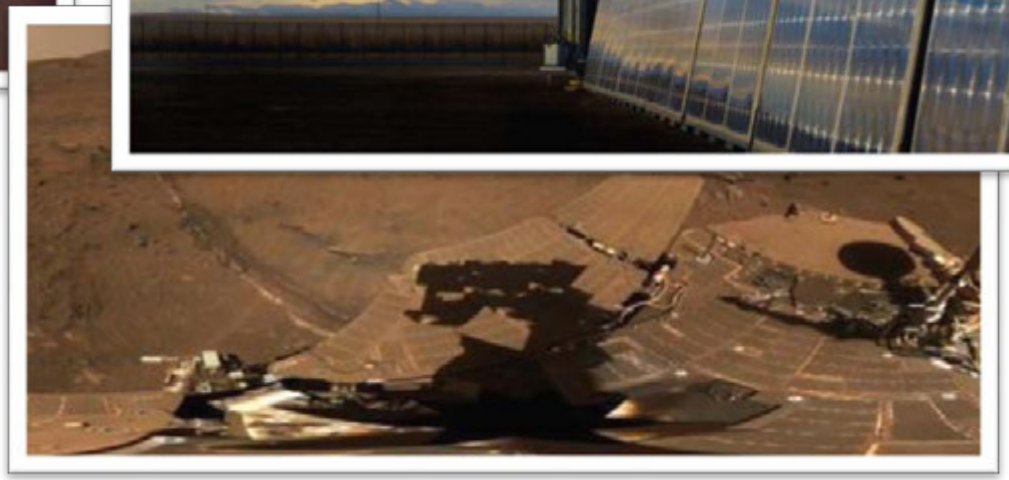
III-V multijunction solar cell: space heritage

Proven reliable in off- and on-planet operation



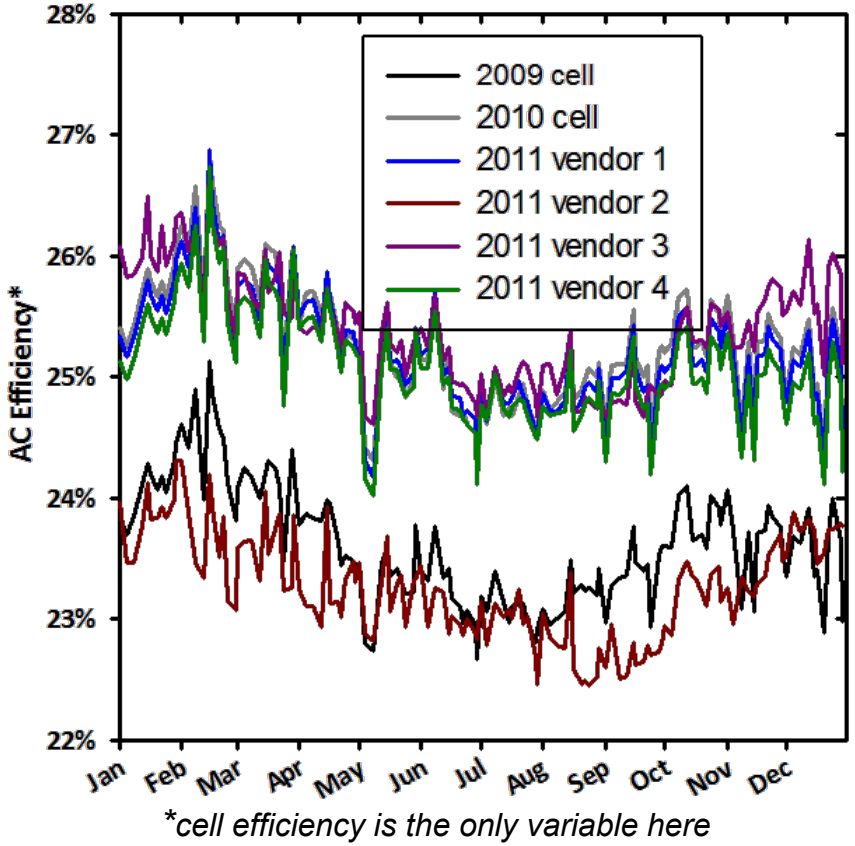




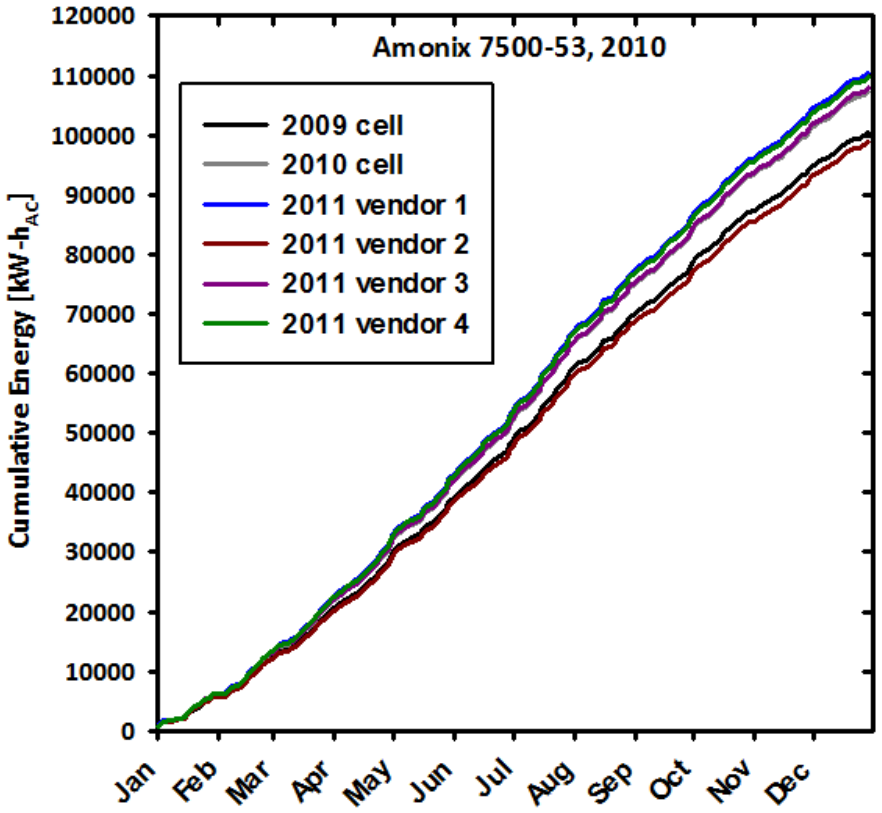


Multiple III-V multijunction cell vendors

Model of 7700-53 performance in Las Vegas

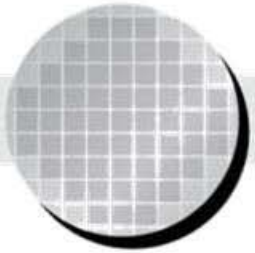


*cell efficiency is the only variable here



- field of vendors provides new insights in process improvements, design for reliability, & testing

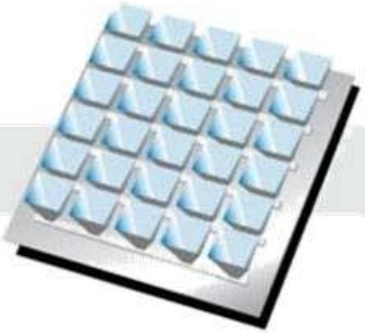
AMONIX
POWERING THE FUTURE NOW



Cell



Package



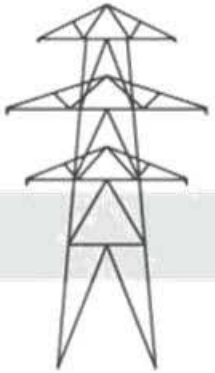
Receiver Plate



MegaModule®



Amonix 7700 CPV

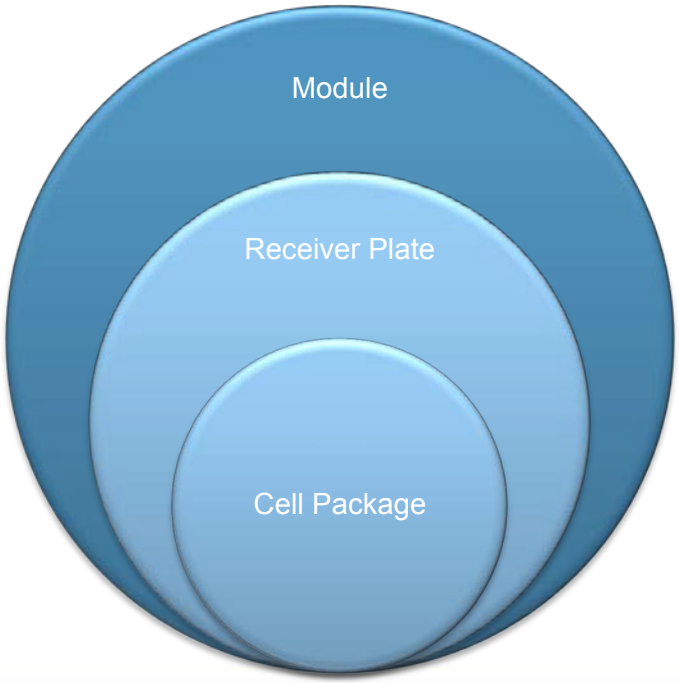


Grid

AMONIX
POWERING THE FUTURE NOW

On Going Reliability

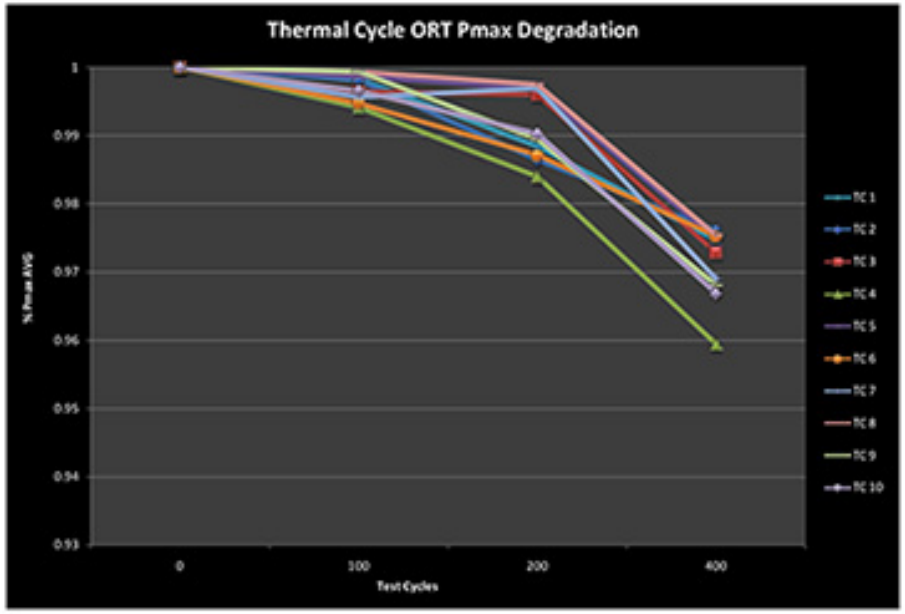
- Ongoing Reliability Testing is performed to monitor product reliability throughout manufacturing
- A comprehensive ORT will provide ongoing life data for the product, along with advance warning of dangerous shifts in manufacturing quality

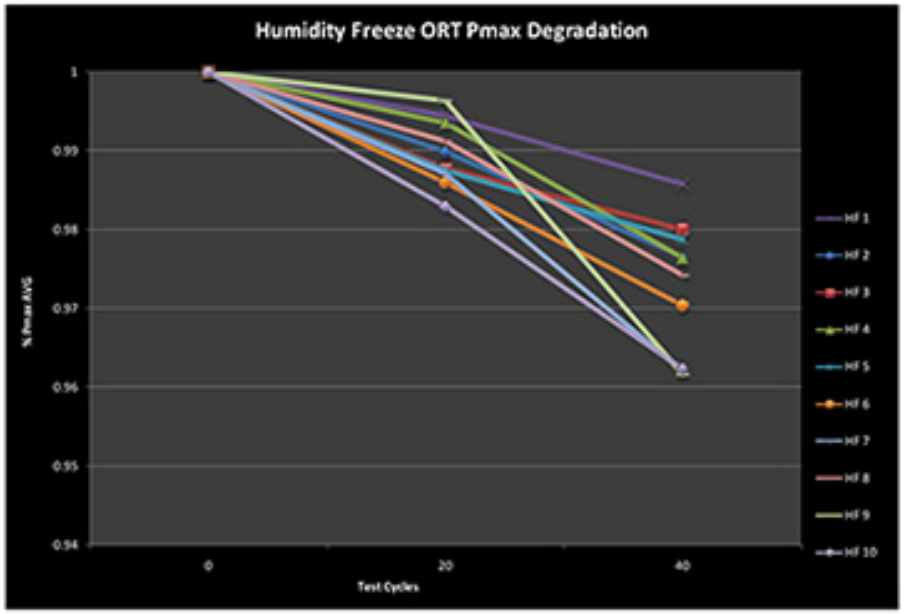


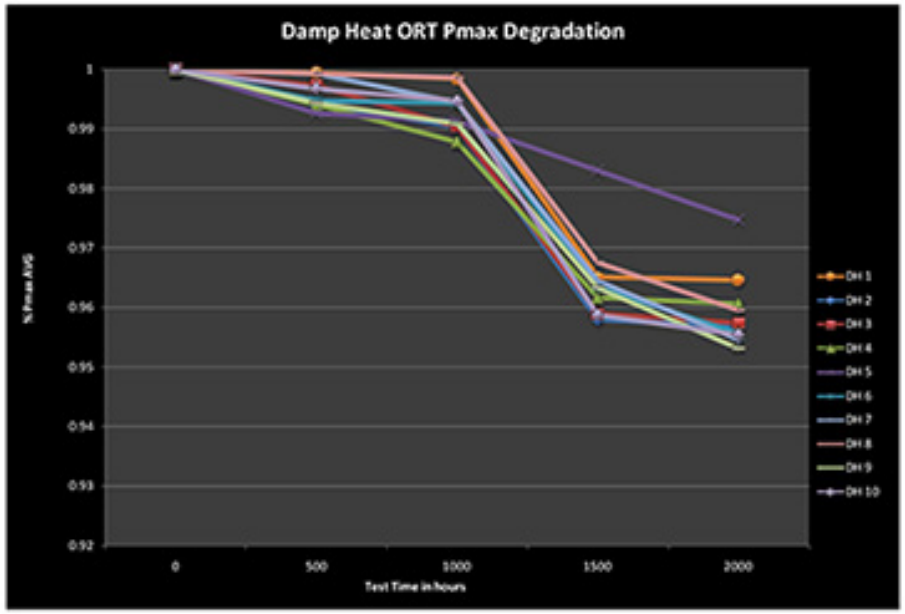
Confidential ©2010 Amonix, Inc.

Cell Package ORT

Test	Test Specification	Pass Criteria
Visual Inspection	IEC 62108 10.1	0 failures
Thermal Cycle (200 cycles)	IEC 62108 10.6	0 failures
Humidity Freeze (40 cycles)	IEC 62108 10.8	0 failures
Damp Heat (1000 hours)	IEC 62108 10.7	0 failures



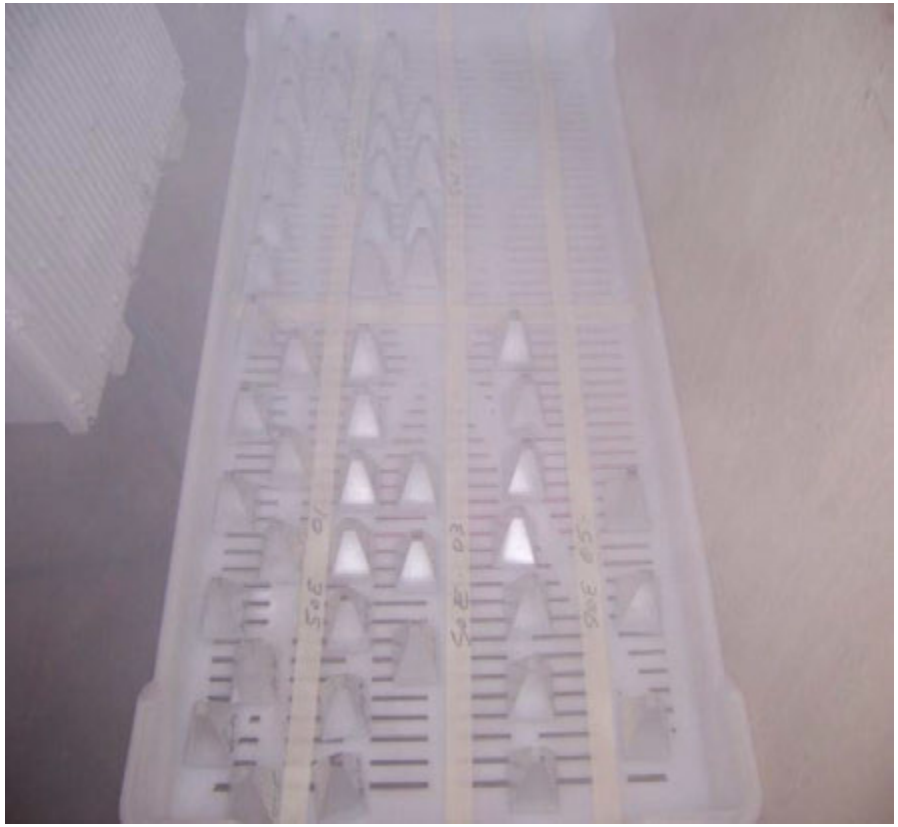
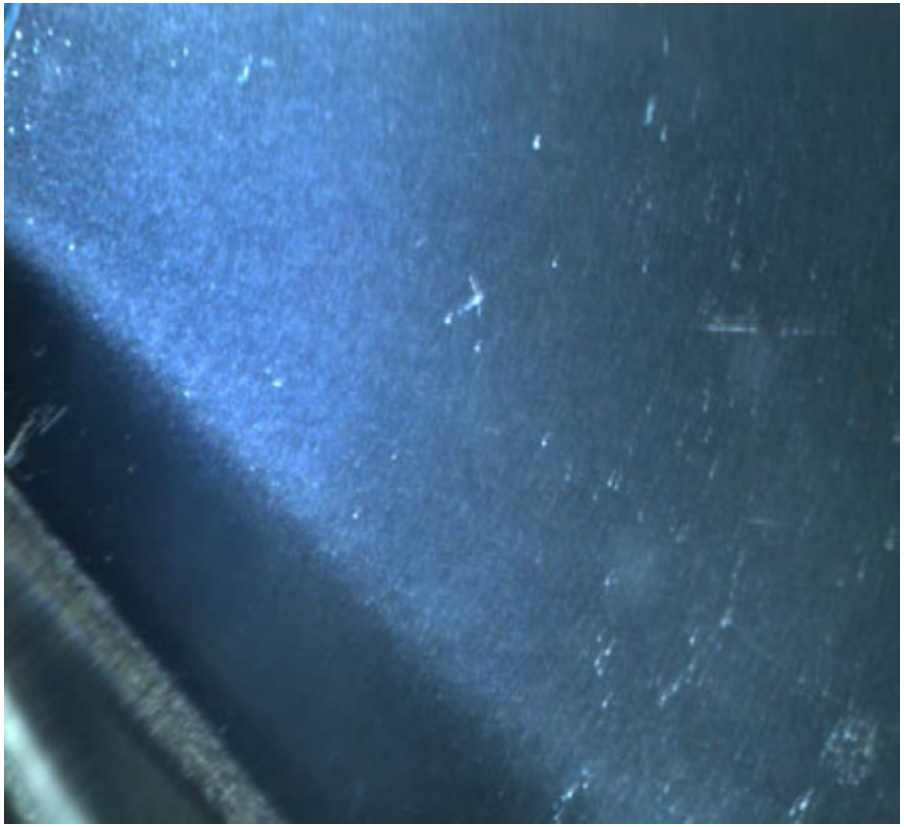




Confidential ©2010 Amonix, Inc.

Secondary Optics

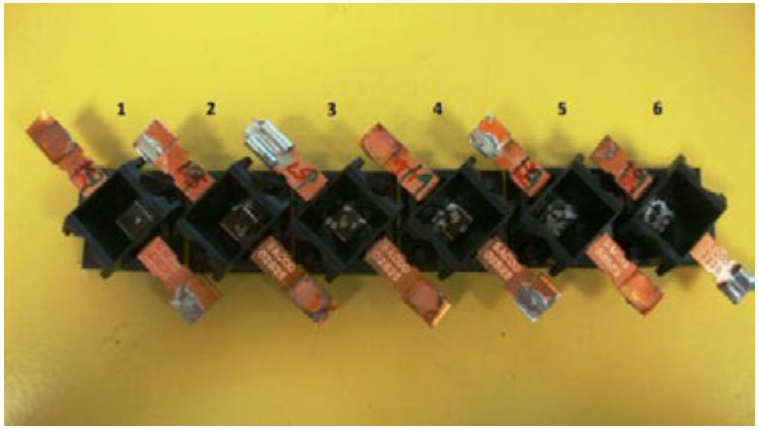
Extreme Salt Fog Conditions

Stress to 2X Mil-Std Requirements	Post Stress Analysis- No Tarnishing
	

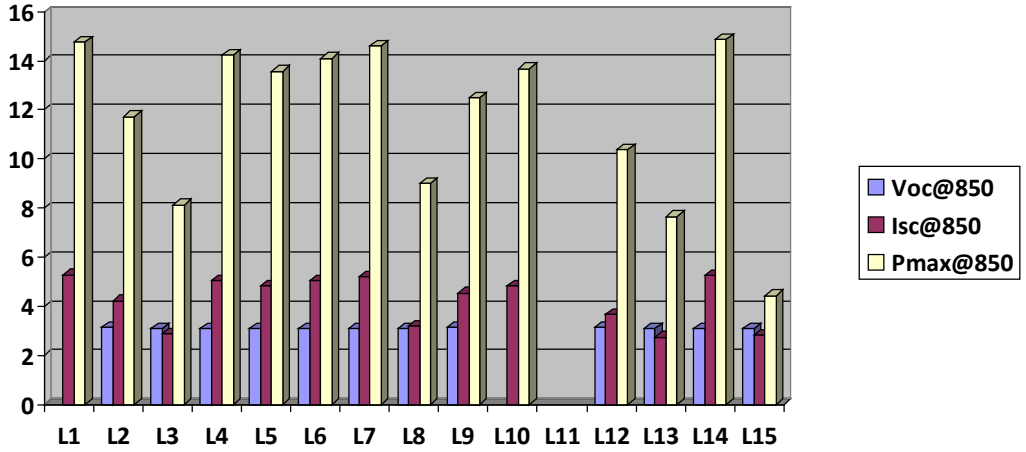
Confidential ©2010 Amonix, Inc.

Receiver Plate Debris Study

- Determine the amount of debris that causes a failure

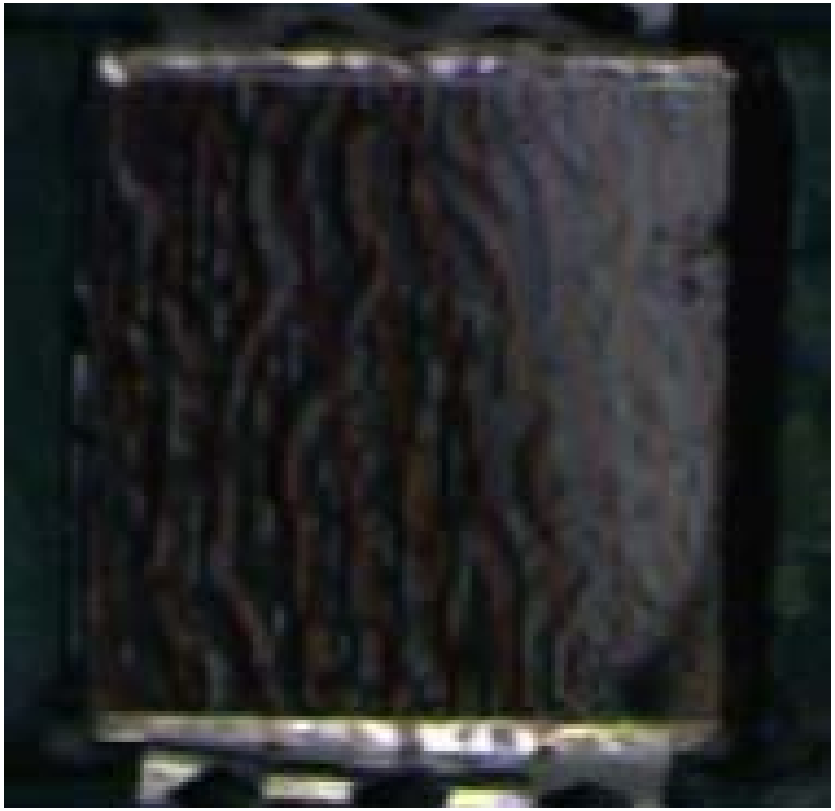






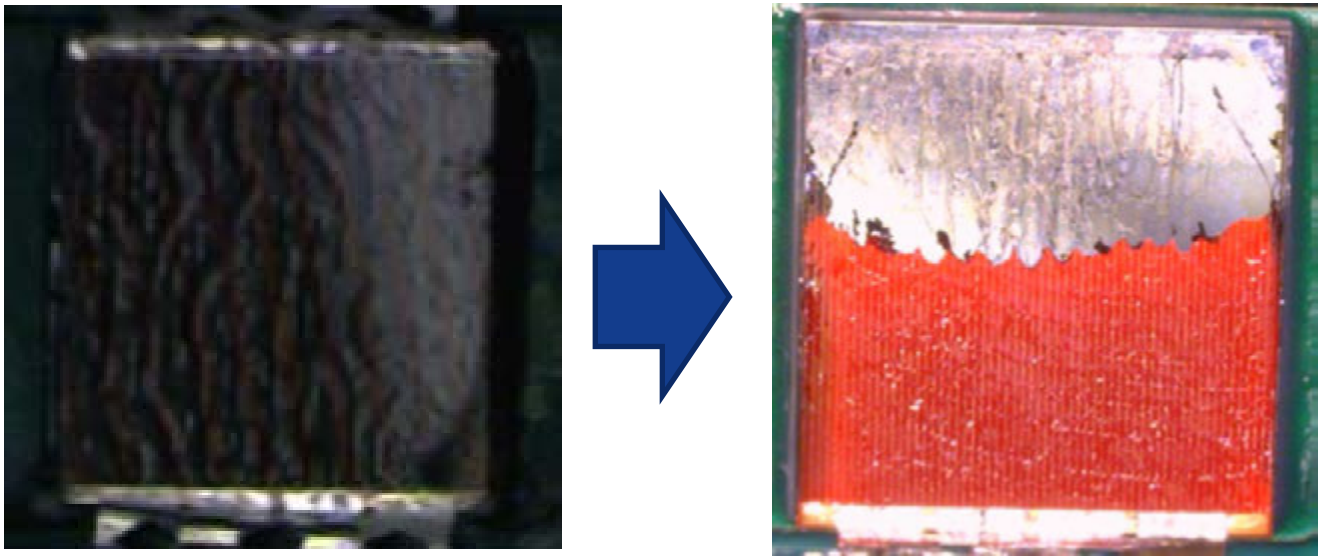
Confidential ©2010 Amonix, Inc.

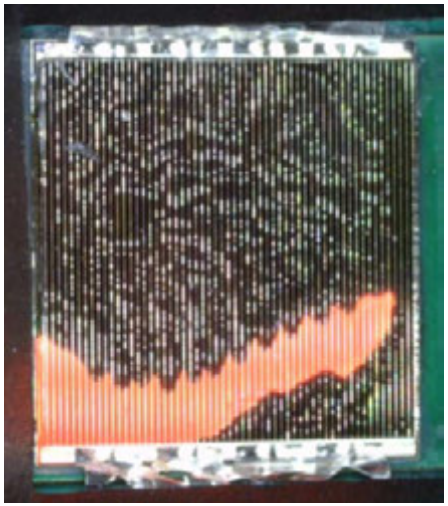
?

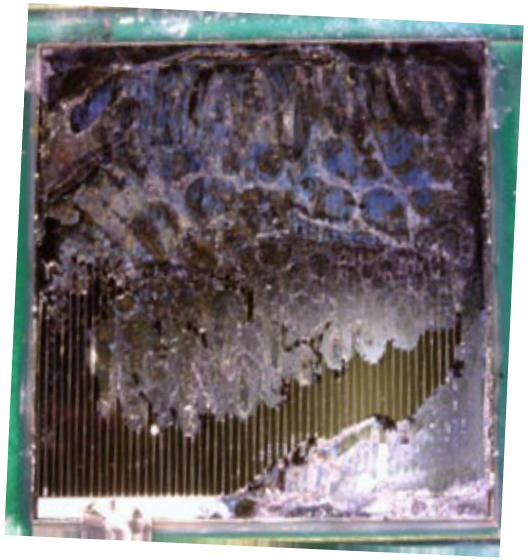


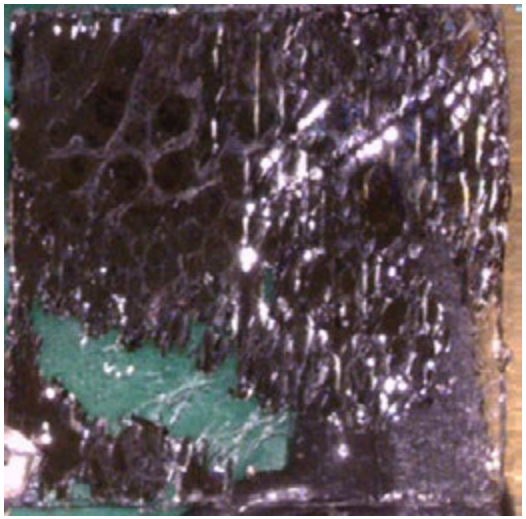
AMONIX
POWERING THE FUTURE NOW

Epitaxial exfoliation

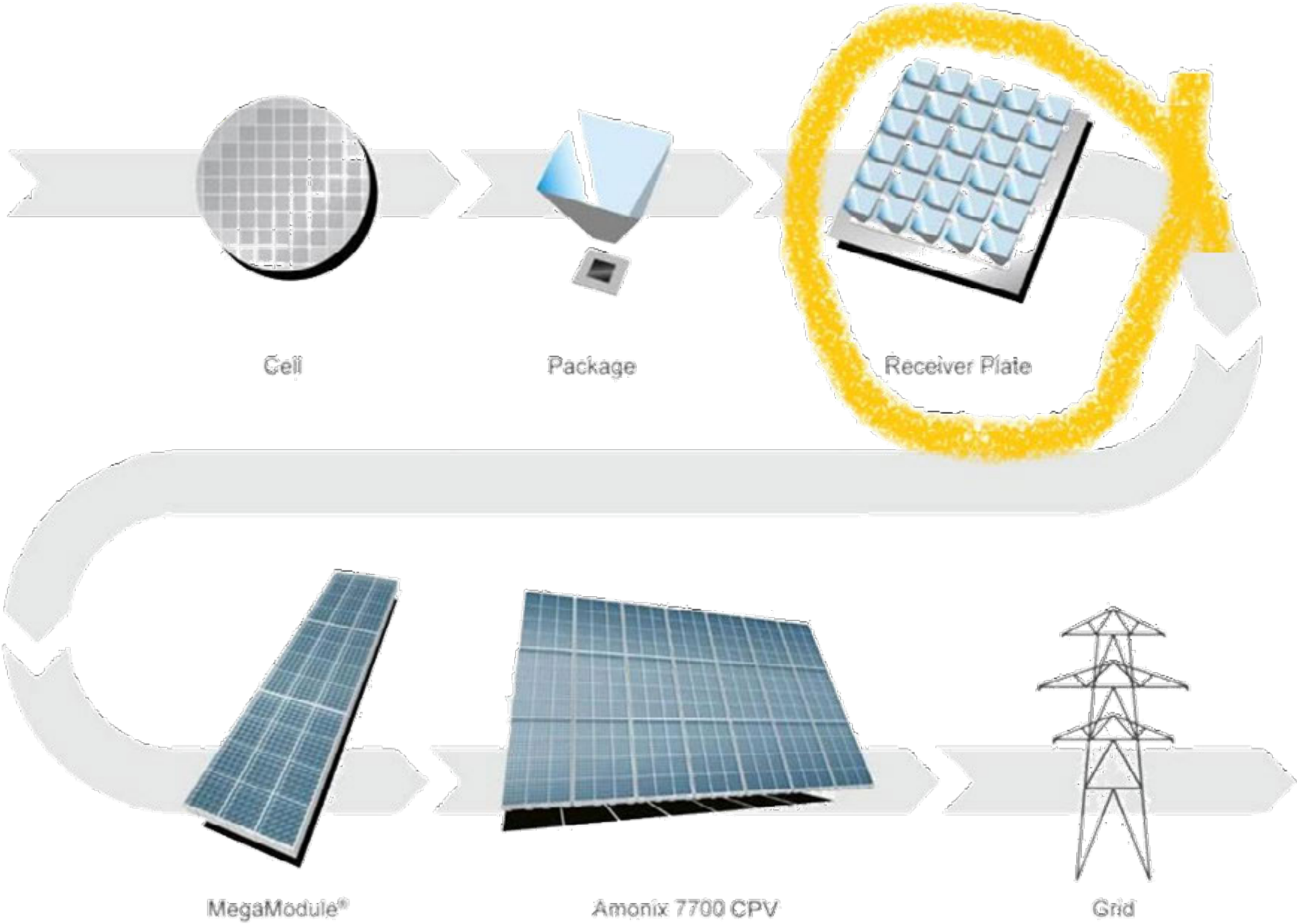








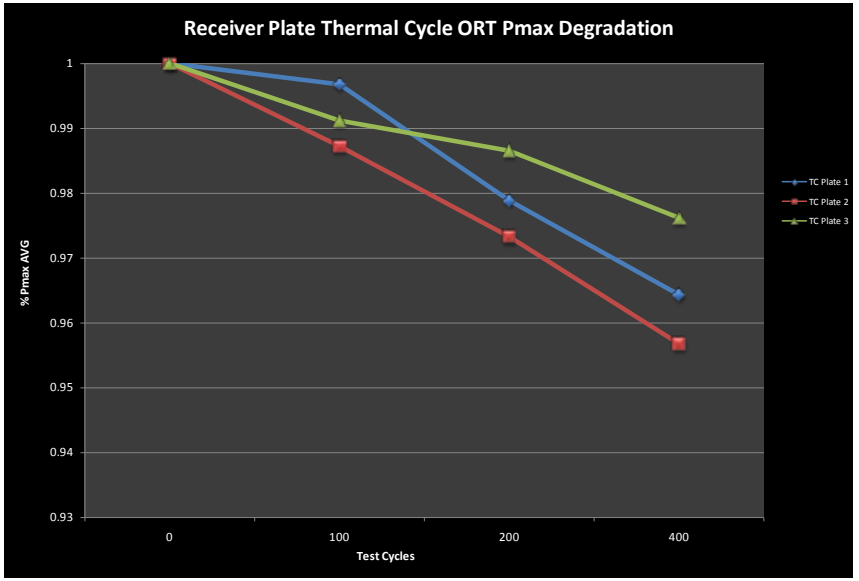
AMONIX
POWERING THE FUTURE NOW

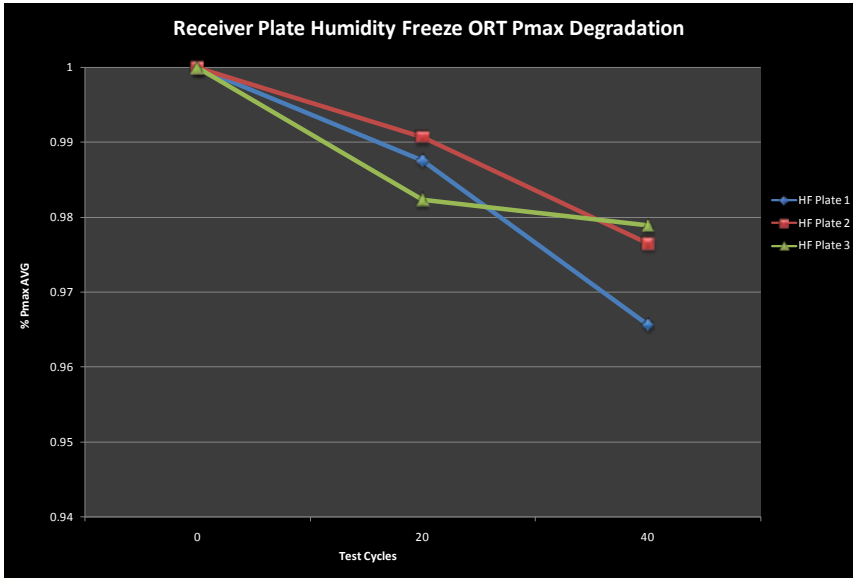


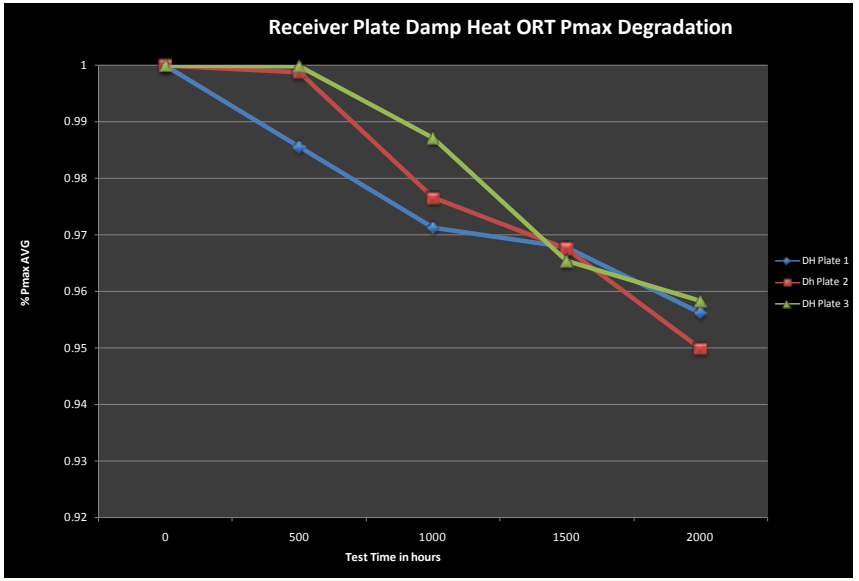
AMONIX
POWERING THE FUTURE NOW

Mini Module ORT

Test	Test Specification	Pass Criteria
Visual Inspection	IEC 62108 10.1	0 failures
Thermal Cycle (200 cycles)	IEC 62108 10.6	0 failures
Humidity Freeze (40 cycles)	IEC 62108 10.8	0 failures
Damp Heat (1000 hours)	IEC 62108 10.7	0 failures







Confidential ©2010 Amonix, Inc.

Material background: PMMA

- Amonix uses a Fresnel lens composed of PMMA acrylic

- Acrylic originally developed for aircraft canopies:
  - high broadband transmittance (~92%), superior to glass
  - good UV durability
  - one of the hardest plastics: resistant to soiling

- Different formulations of PMMA are now available:
  - recent use of UV inhibitors in PMMA extends the lifetime relative to pure PMMA material

Description

Poly(methyl methacrylate) (PMMA) is a clear, colorless polymer used extensively for optical applications. It is available commercially in both pellet and sheet form. Outstanding properties include weatherability and scratch resistance. The most serious deficiencies are low impact strength and poor chemical resistance

Properties

Glass transition temperature: 114°C.

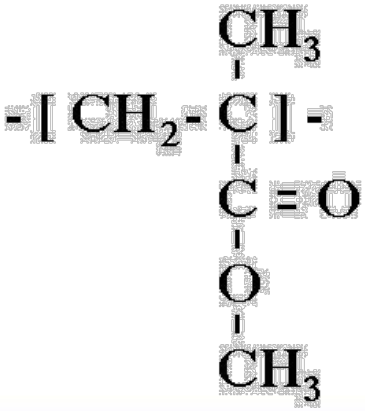
Amorphous density at 25°C: 1.17 g/cm^3.

Molecular weight of repeat unit: 100.12 g/mol.

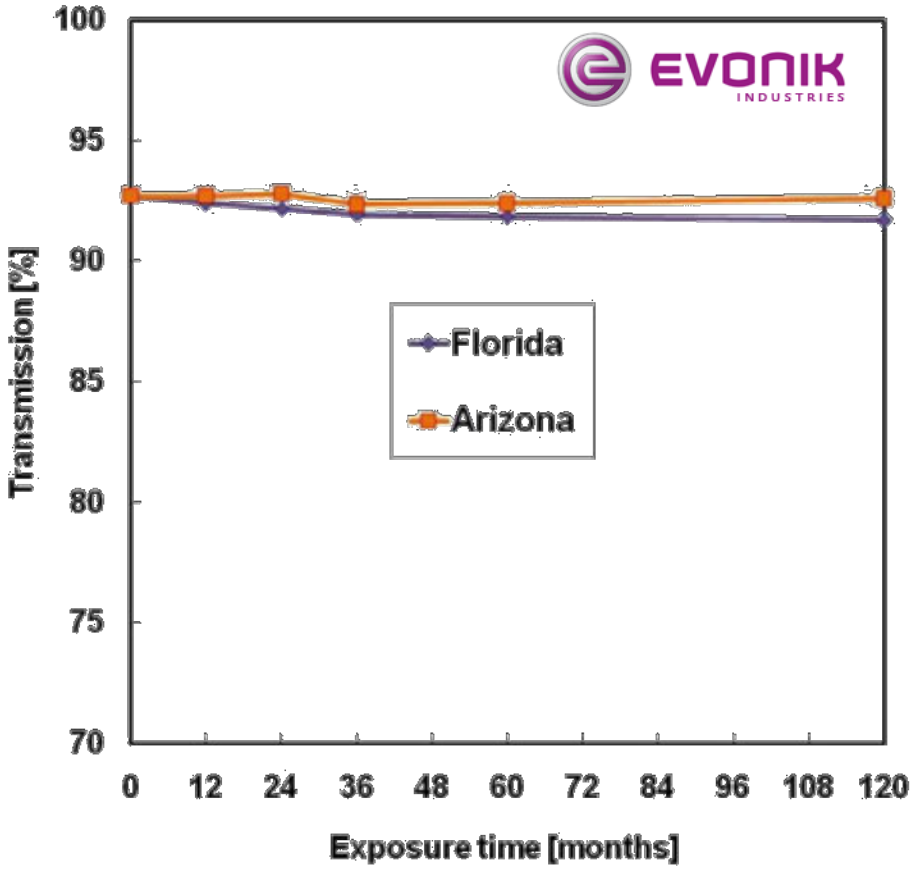
Typical physical properties

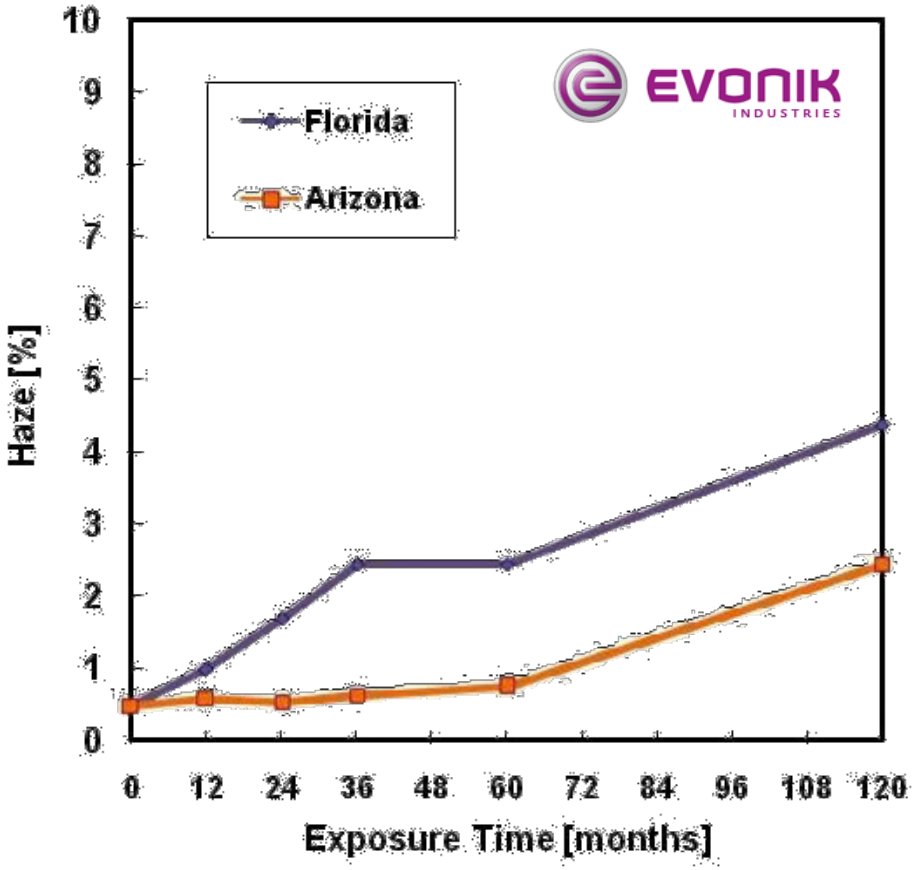
Repeat Unit

$C_5H_8O_2$



PMMA in outdoor exposure





- arid climate reduces rate of degradation

NREL study of PMMA for CPV

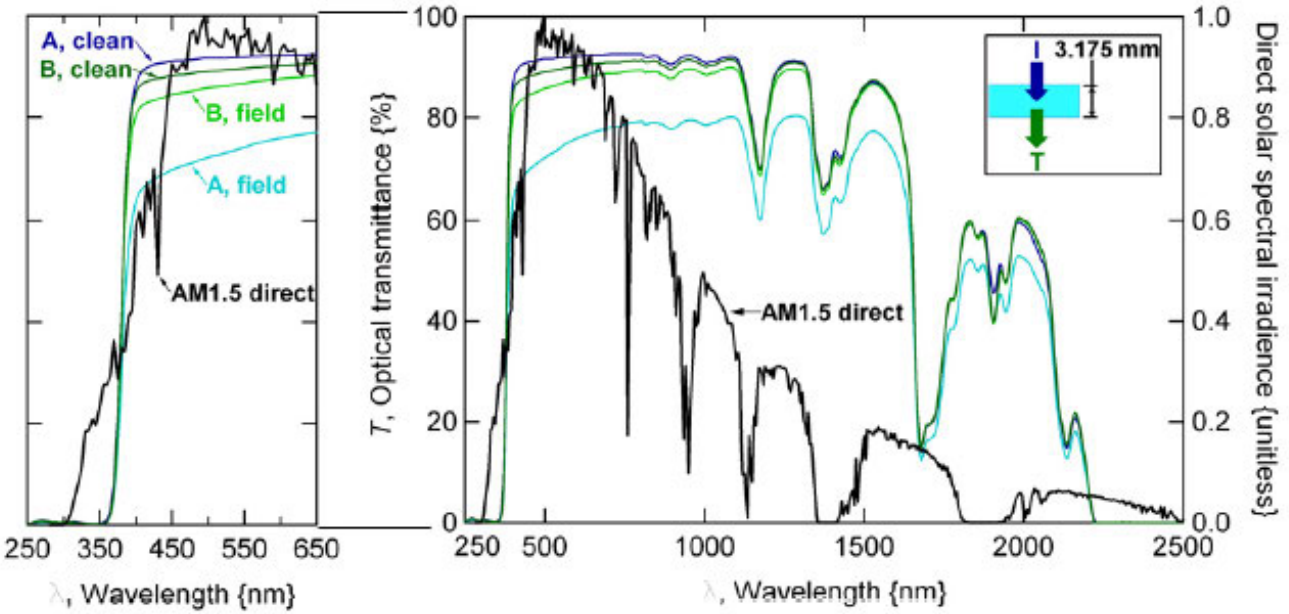


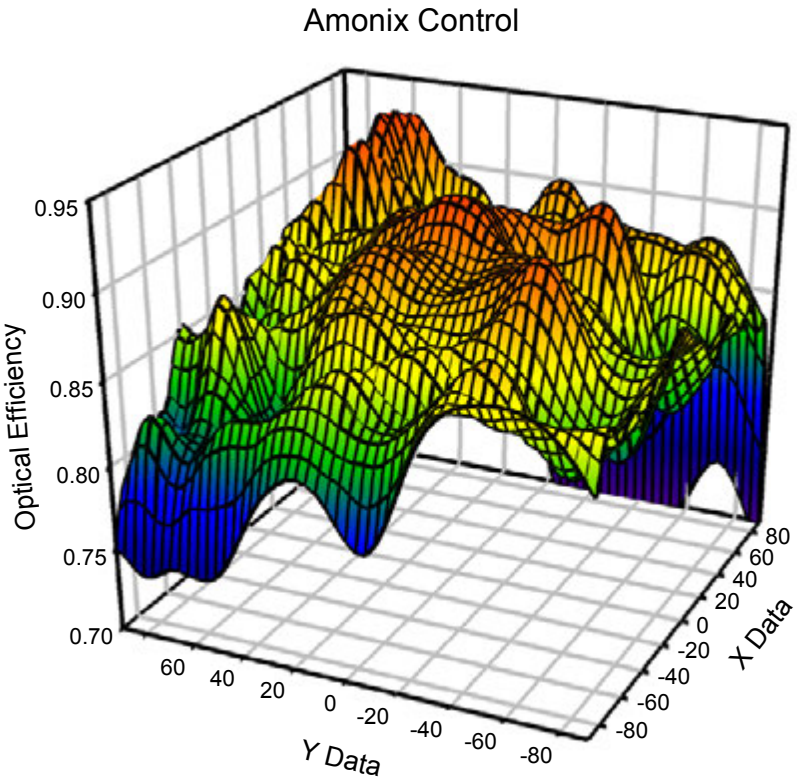
Figure 2: Measured optical transmittance (in air, compensated to h = 3.175 mm) for the most-soiled (fielded 22 years outdoors, "A") and next-most-soiled (fielded 8 years, "B") veteran lenses, relative to the normalized standard direct solar spectral irradiance [5]. Measurements were first made in the as-received condition and then after cleaning.

Strong attenuation of the blue region is not apparent for either of the cleaned sets in Figure 2. Use on a tracker tends to reduce exposure to airborne contamination, particularly if the module is maintained ≥2 meters above the ground [11].

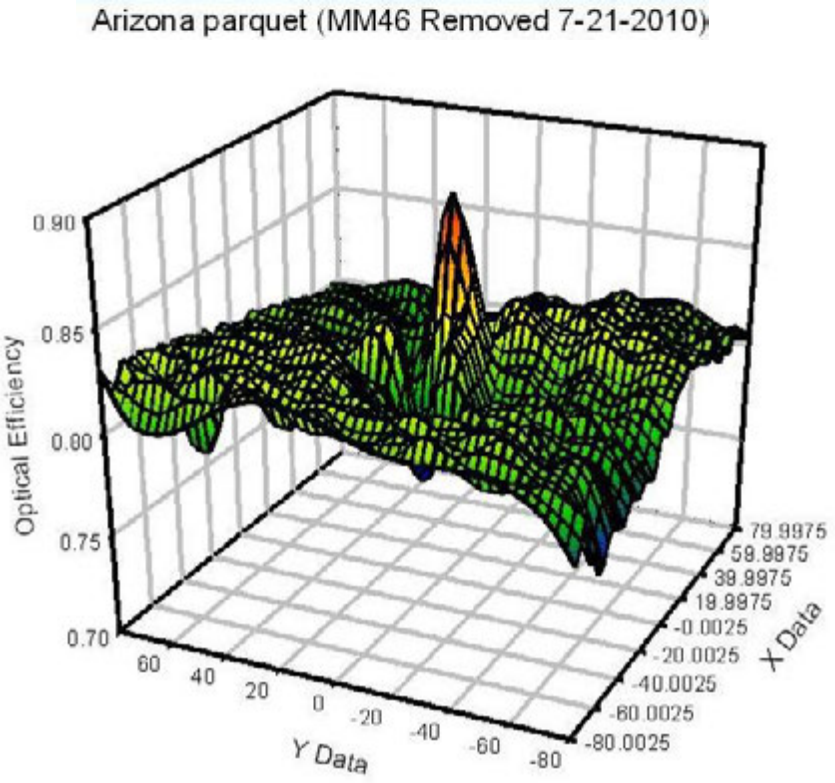
David C. Miller, Lynn M. Gedvilas, Bobby To , Cheryl E. Kennedy, and Sarah R. Kurtz, "Durability of Poly(Methyl Methacrylate) Lenses Used in Concentrating Photovoltaics", Proc. SPIE, 2010, 7773-02.

- **after cleaning, degradation in transmission is modest, <0.3%/year**

Amonix lenses fielded in Arizona



new lens: mean optical efficiency=85%



fielded lens: mean optical efficiency=81%

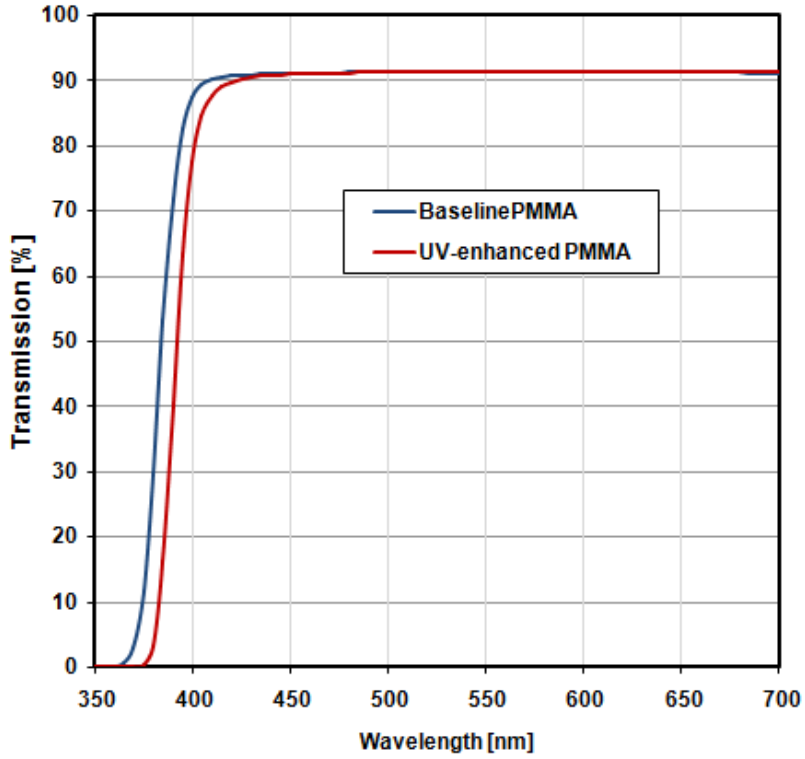
- laser map of lens surface quantifies mean optical efficiency
- lens from MM46 was installed c. 2001: decrease in optical efficiency of <0.4%/year

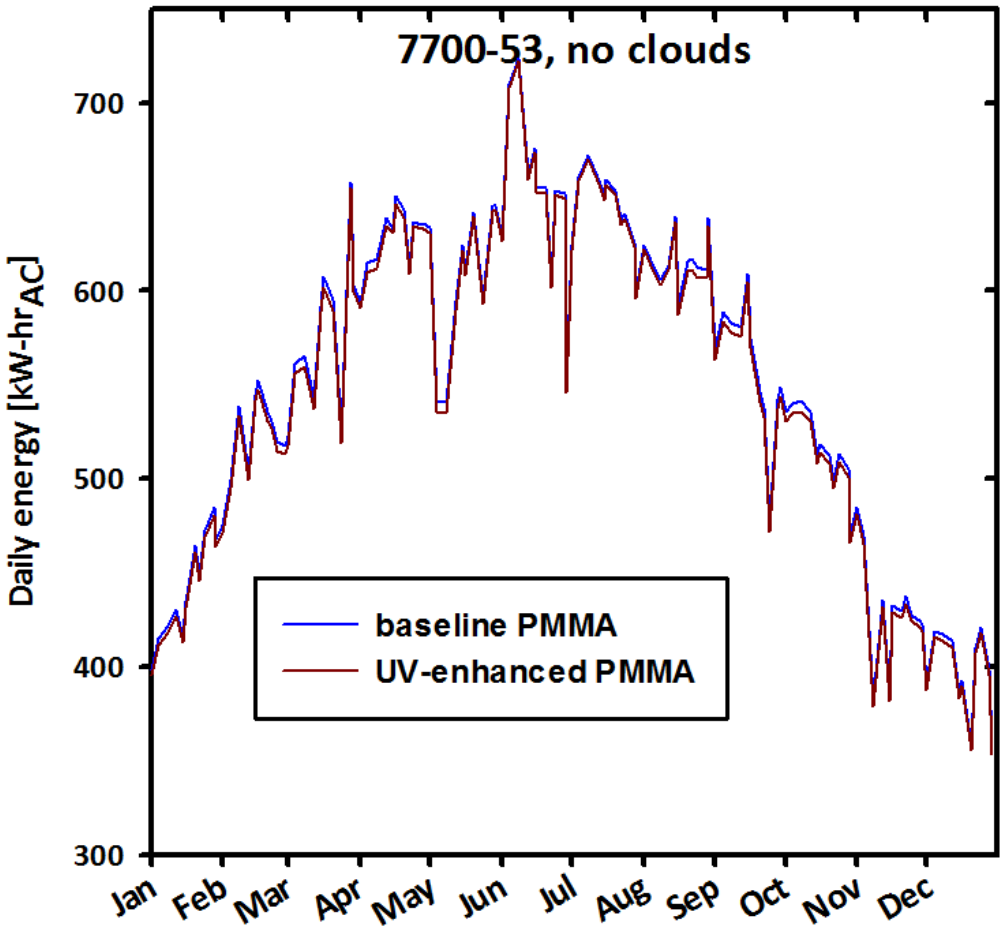
Lens Qualification

Test	Conditions	Configuration	Threshold
Performance	0°, 20°, 40° tilt	module	P_{mp}, characterization only
Damp heat	60° C, 60% relative humidity for 1000 hours	single lens element	$D_{optical\ efficiency}$<1%
		module	NP_{MP}>0.98
Temperature cycle	-40° to 110° C, 500 cycles	mounted to frame	$D_{optical\ efficiency}$<1%
Humidity freeze	after temperature cycle test: -40° to 60° C, 85% relative humidity, 20 cycles	mounted to frame	$D_{optical\ efficiency}$<1%
Abrasion resistance		single lens element	$D_{optical\ efficiency}$<1%
Impact test	per IEC 62108	mounted to frame	$D_{optical\ efficiency}$<1%
			no cracks (1x inspection)
UV test	Weather-Ometer, 1000 hours	bare lens sheet	$D_{optical\ efficiency}$<1%
		single lens element	NP_{MP}>0.98
	Outdoor concentrated test, 1000 hours	unpatterned sample	$DT_{350\text{-}1800nm}$<1%

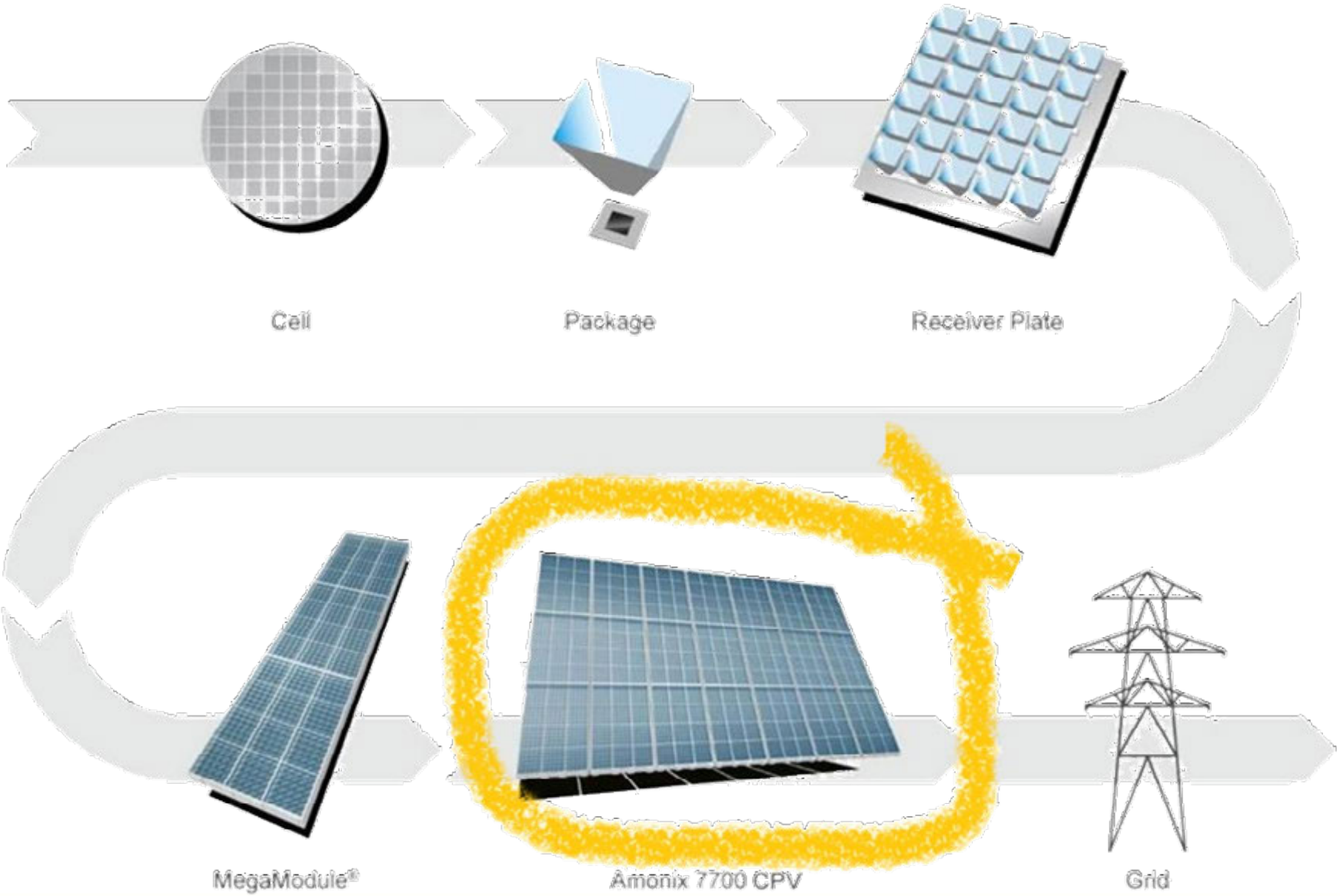
Confidential ©2010 Amonix, Inc.

Enhanced UV durability





- small decrement in energy generation provides substantial extension of lifetime



AMONIX
POWERING THE FUTURE NOW

Mega Module Transportation Qualification

- During shipment, the Mega Module can experience shock, vibration and compression which impact reliability

Test Condition	Test Description	Test Standard
Atmospheric Conditioning	Controller Temperature and Humidity	Mil-Std 810
Compression	Machine Apply and Release	Mil-Std 810
	Machine Apply and Hold	
	Weight and Load Spreader	
Vibration	Fixed Displacement	Mil-Std 810
	Random	
Shock	Drop	Mil-Std 810
	Incline Impact	
	Horizontal Impact	

Confidential ©2010 Amonix, Inc.

Competitive Advantages

Highest Efficiency, Low LCOE	Proven & Practical	Rapid & Flexible Deployment	Highest Energy Density
			
40% Cell, 31% Module	~20MW Deployed WW	"Drop and Connect" Deployment	Water-Free Power Production 5 acres per MW

AMONIX
POWERING THE FUTURE NOW

Low Factory Capital Investment

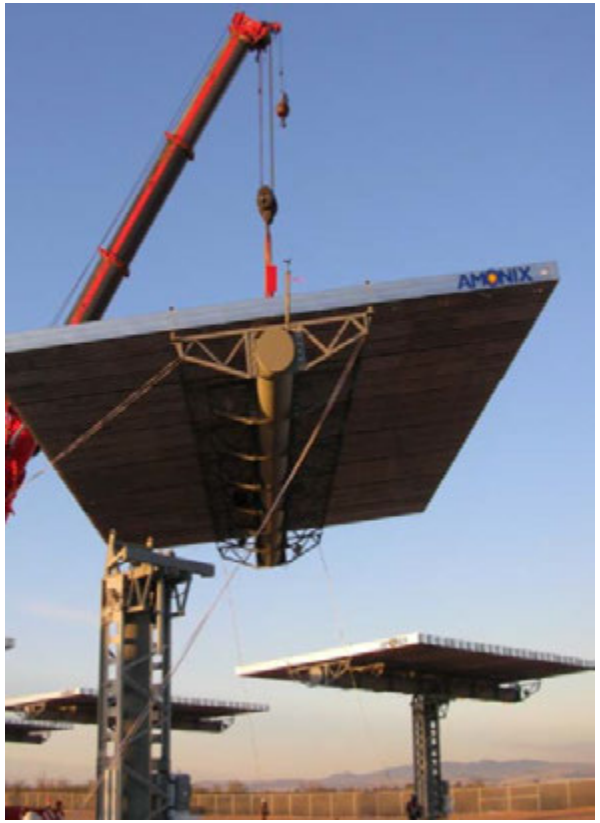
Leverages Existing Commodity and Fabrication Infrastructure



Distributed manufacturing



MegaModule® fabrication



Truck bed to field

Height provides wear & soiling resistance



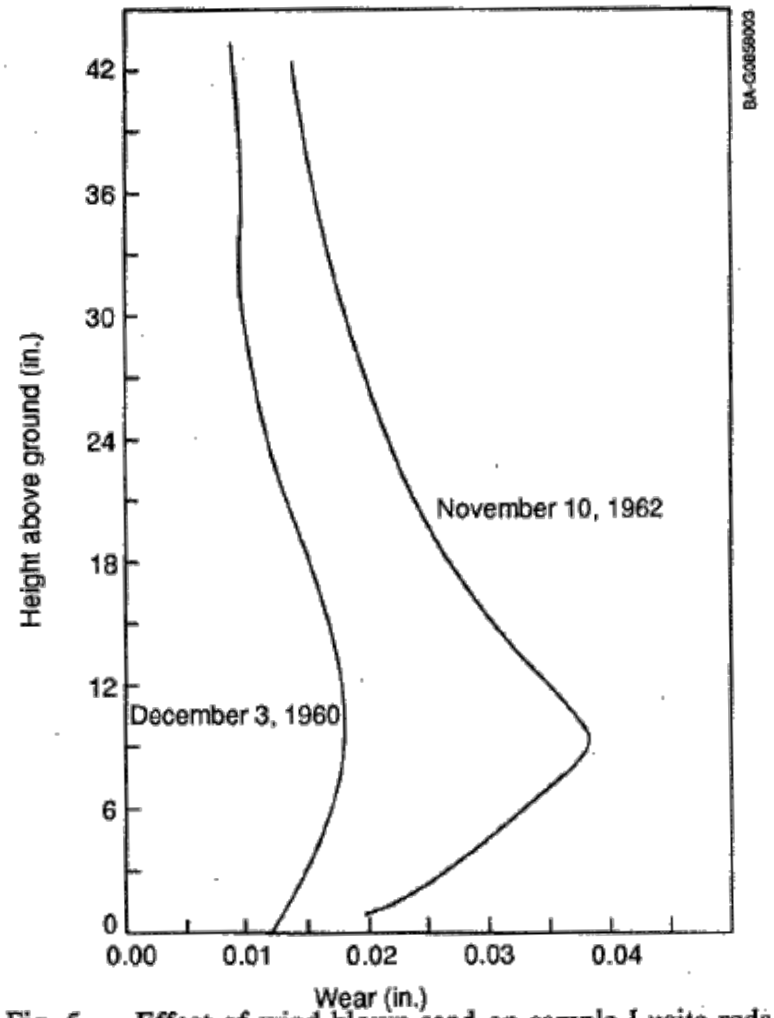


Fig. 5. Effect of wind-blown sand on sample Lucite rods

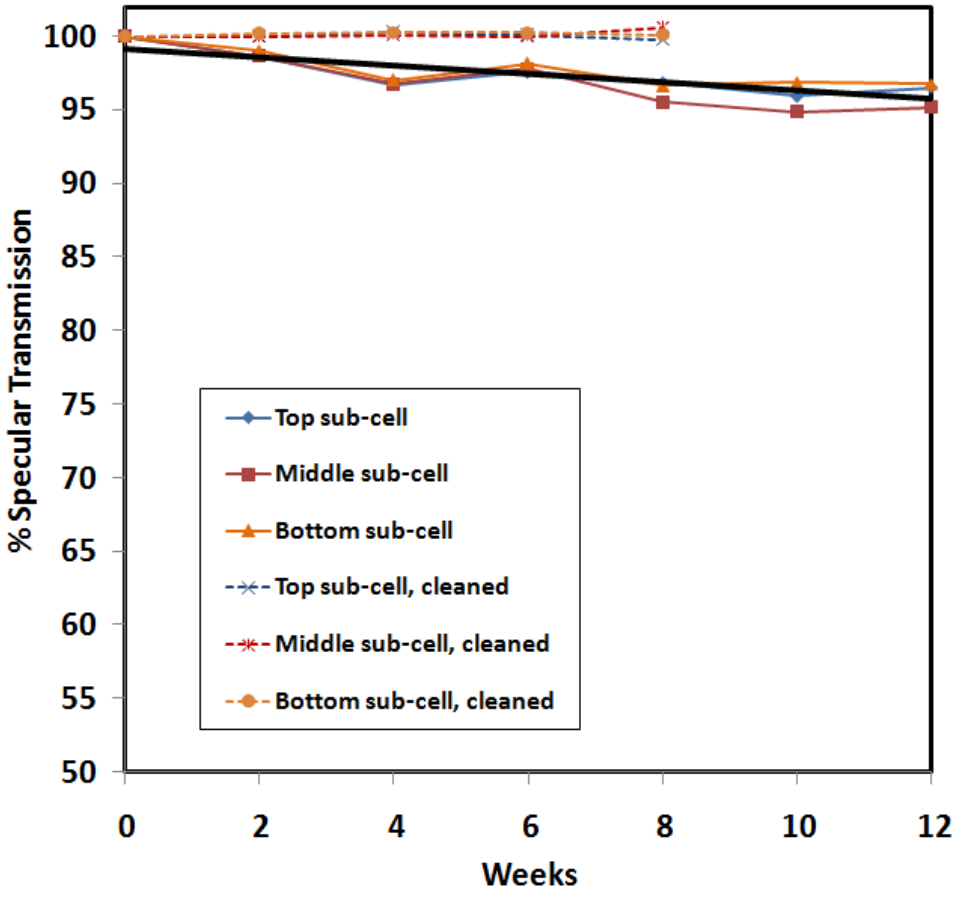
THE EFFECT OF SANDSTORMS ON PV ARRAYS AND COMPONENTS

John P. Thornton, P.E.
National Renewable Energy Laboratory, Golden, Colorado, U.S.A.

AMONIX
POWERING THE FUTURE NOW

Soiling in Las Vegas

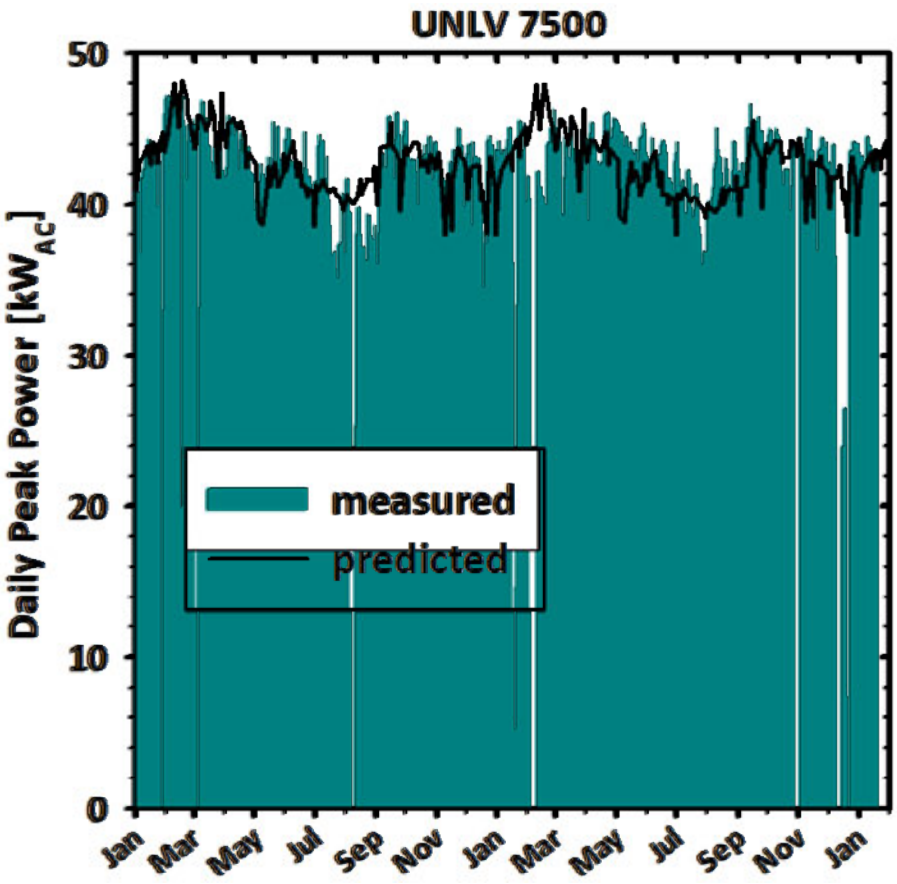


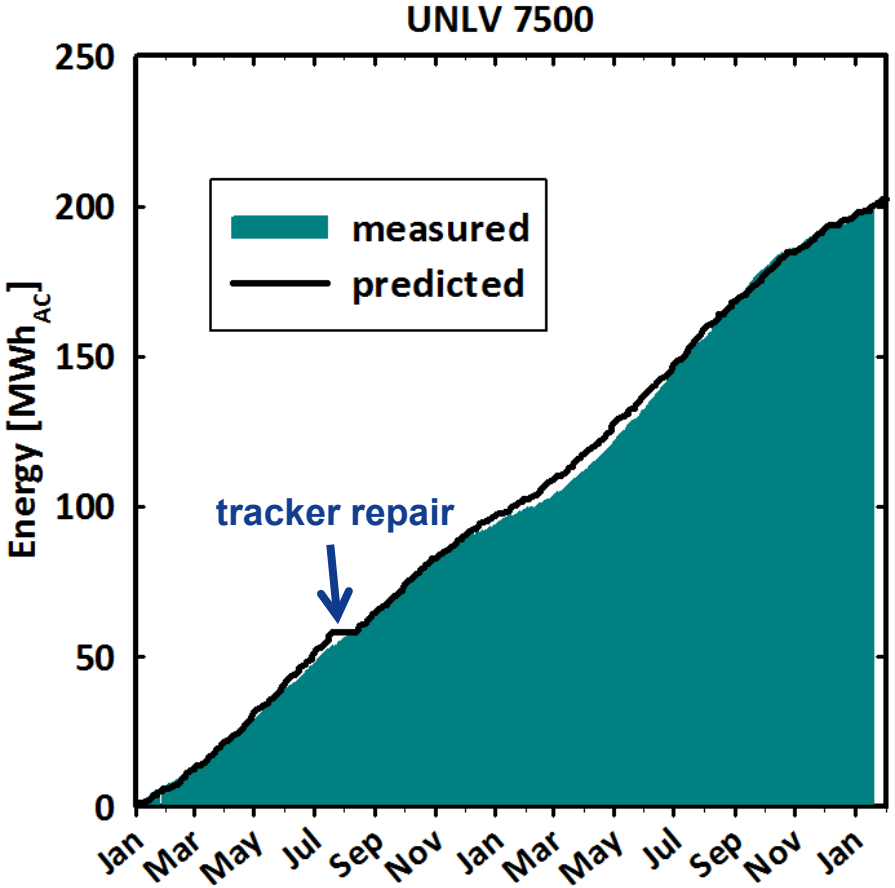


- mean soiling is around 2% near the Las Vegas strip

AMONIX
POWERING THE FUTURE NOW

Performance prediction: 2009-2011





- Generation is variable, but *predictable*
- <1% deviation from energy prediction after 2 years

AMONIX
POWERING THE FUTURE NOW

Rapid Installation and Deployment

- **CPV is utility grade**

From truck bed to tracking in days





- New, efficient installation process

AMONIX
POWERING THE FUTURE NOW

Problems remain:



AMONIX
POWERING THE FUTURE NOW

Solution: “RCMs”





AMONIX
POWERING THE FUTURE NOW

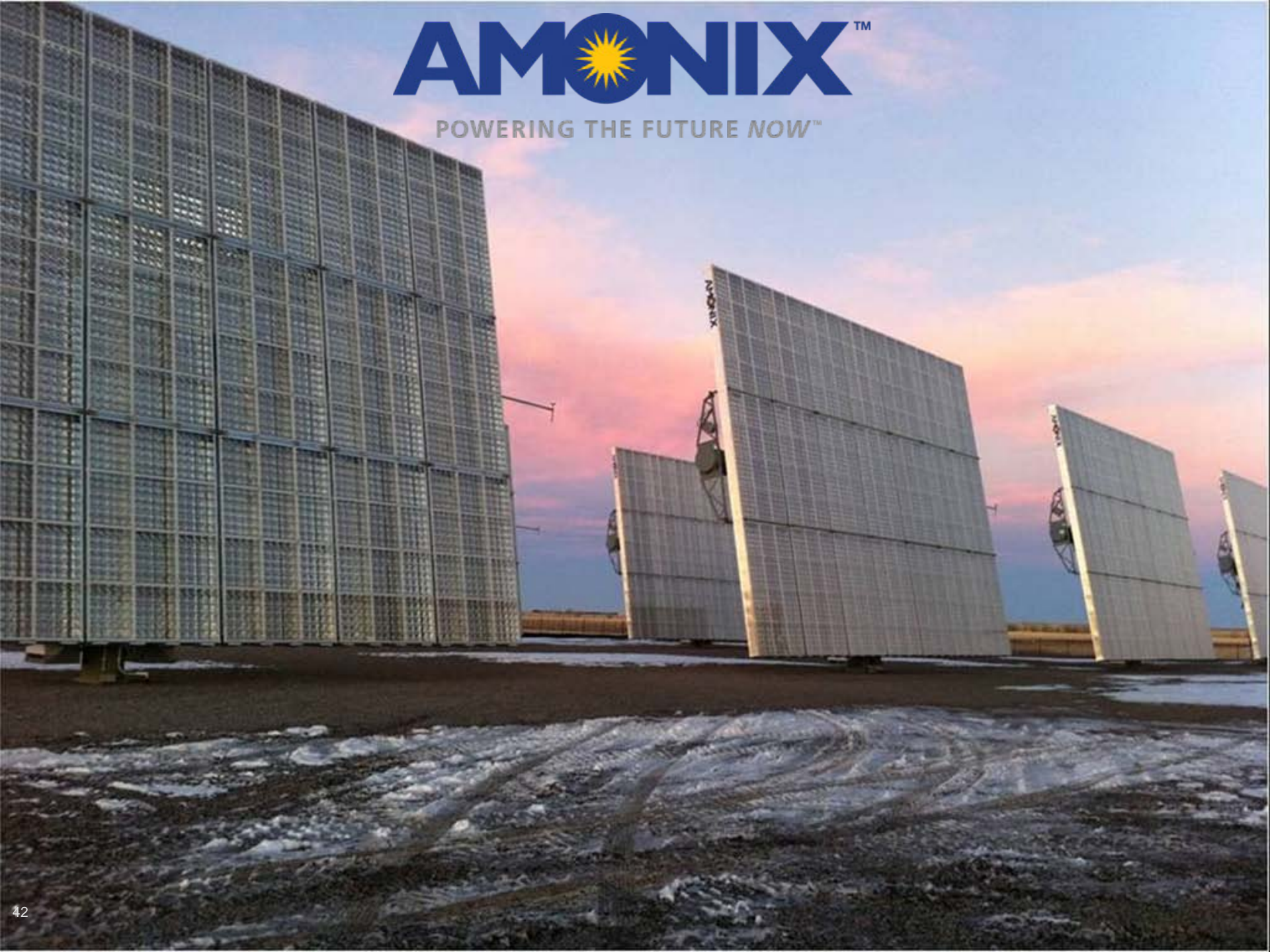
RCMs: Rodent Counter Measures





One more reason to install in the desert!

AMONIX
POWERING THE FUTURE NOW


AMONIX™
POWERING THE FUTURE NOW™


AMONIX™
POWERING THE FUTURE NOW™





Thin Film Module Reliability - Enabling Solar Electricity Generation

Markus Beck, Pedro Gonzalez, Richard Gruber, Jim Tyler





First Solar

Our Mission

To create enduring value by enabling a world powered by clean, affordable solar electricity.



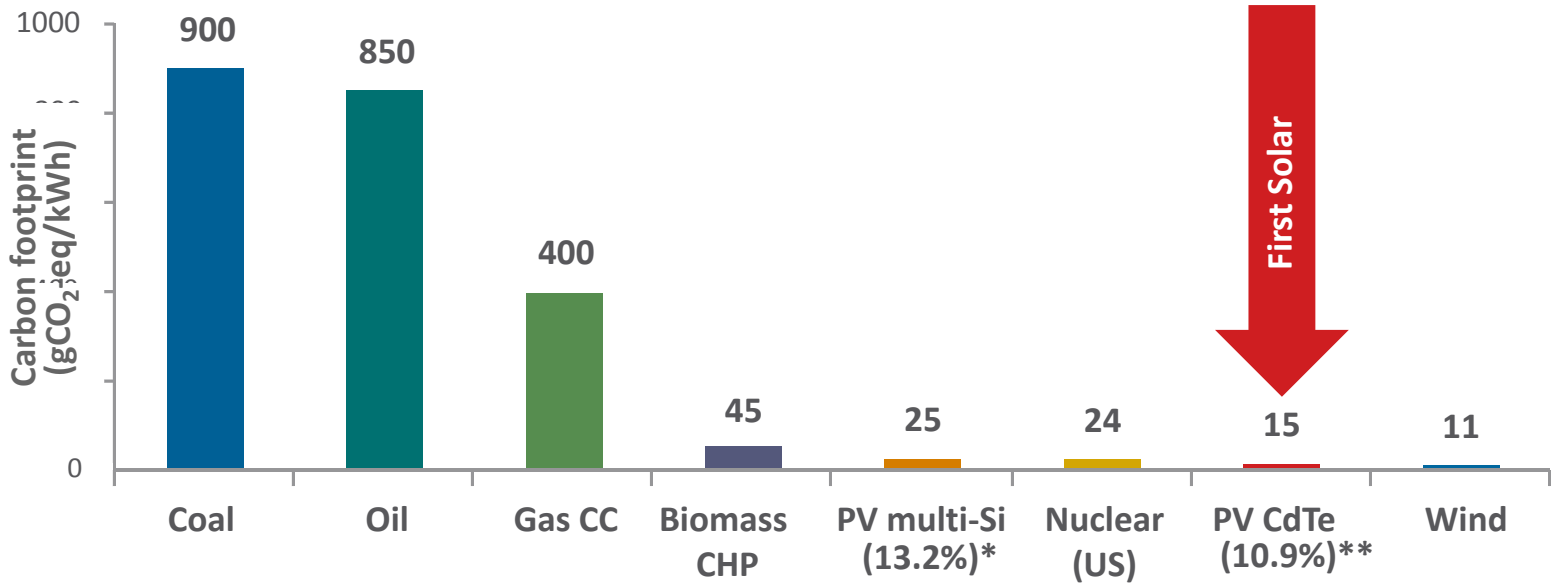




© 2009 First Solar, Inc.

Sustainable Environmental Profile

Carbon Footprint is a Fraction of Conventional Sources



Sources: *de Wild-Scholten, M., presented at CrystalClear Final Event in Munich on May 26, 2009. **de Wild-Scholten, M., 'Solar as an environmental product: Thin-film modules – production processes and their environmental assessment,' presented at the Thin Film Industry Forum, Berlin, April, 2009. Both PV technologies use insolation of 1700 kWh/m^2. All other data from ExternE project, 2003; Kim and Dale, 2005; Fthenakis and Kim, 2006: Fthenakis and Alsema, 2006; Fthenakis and Kim, in press.

© 2009 First Solar, Inc.

First Solar's Energy Payback Time (EPBT) < 1 year

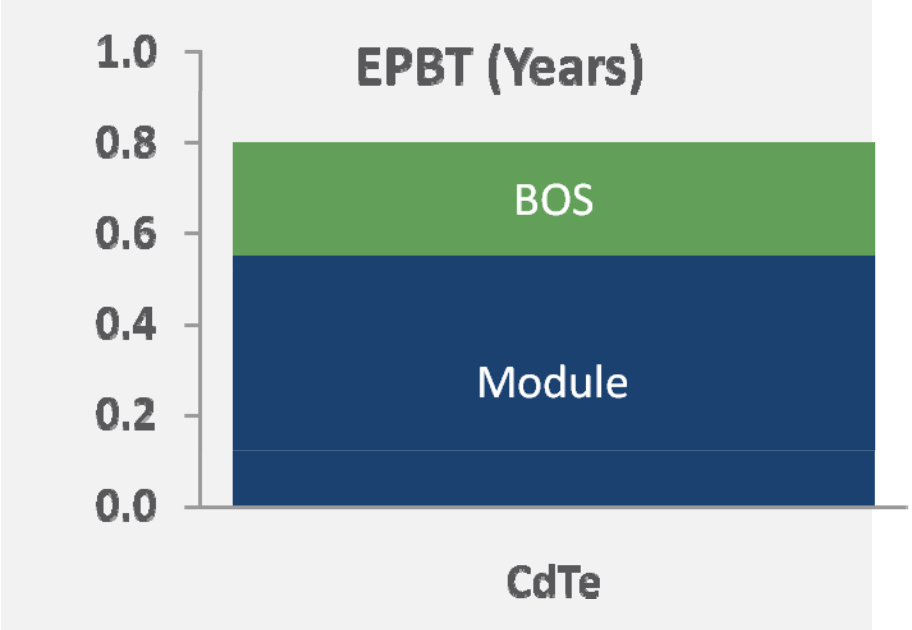
EPBT:

The amount of time
a system must operate to recover the energy that was required to fabricate the system

- EPBT = $E_{input}/(E_{output}/yr)$

Objective: Minimize EPBT

- Supports rapid scalability
- <1 year ensures industry growth does not create near term energy deficit



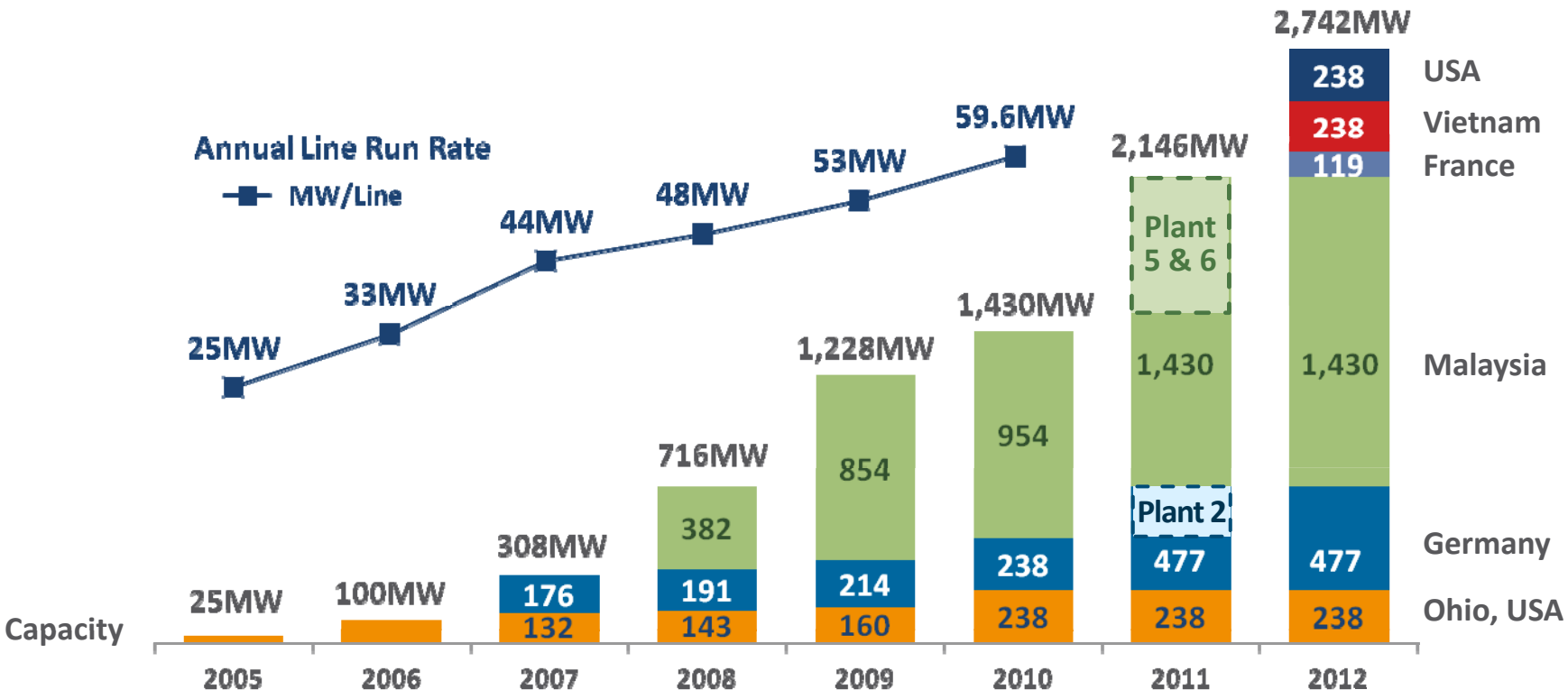
Note: Southern Europe 1700 kWh/m^2/year irradiance.

Source: de Wild-Scholten, M., 'Solar as an environmental product: Thin-film modules – production processes and their environmental assessment,' presented at the Thin Film Industry Forum, Berlin, April, 2009

© 2009 First Solar, Inc.

Production Capacity Growth (year-end capacity)

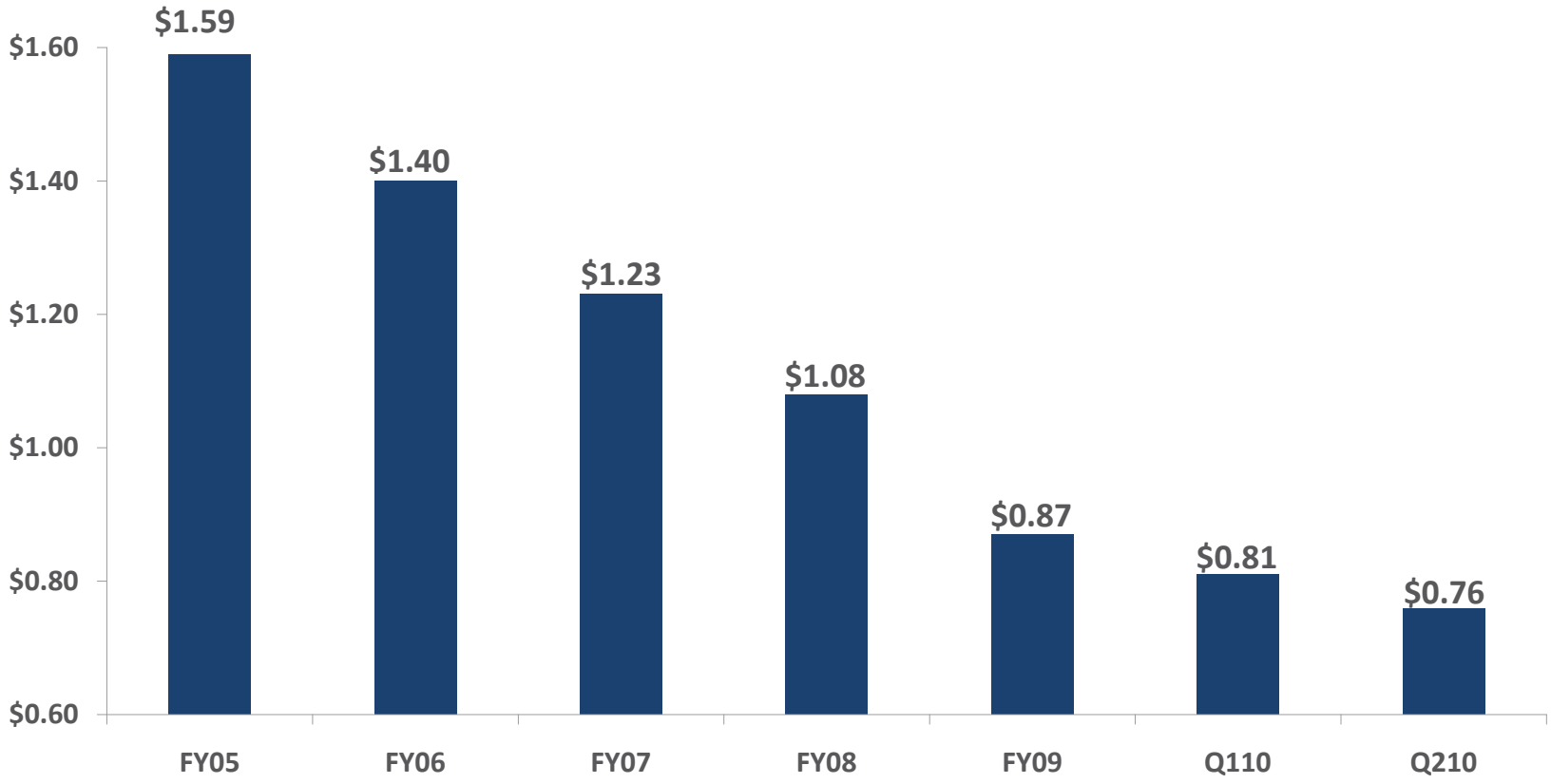
Current and announced capacity grows by 1.3GW (92%) to 2.7GW



Representation of year-end capacity. 2005 & 2006 based on Q4 06 run rate; 2007 based on Q4 07 run rate; 2008 based on Q4 08 run rate; 2009 based on Q4 09 run rate, 2010-2012 based on Q3 10 run-rate.

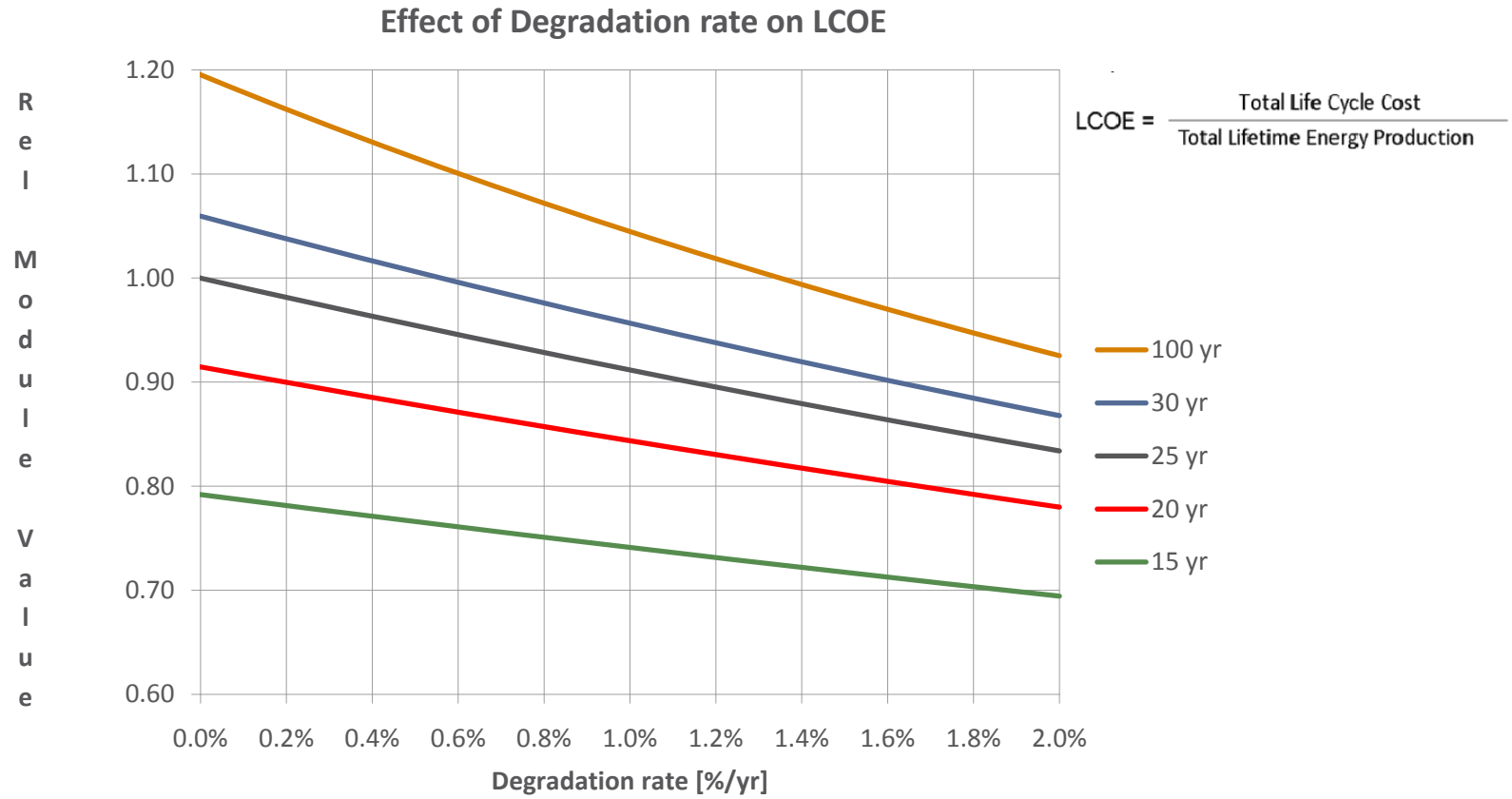
© Copyright 2010, First Solar, Inc.

Manufacturing Cost per Watt Trend



© 2009 First Solar, Inc.

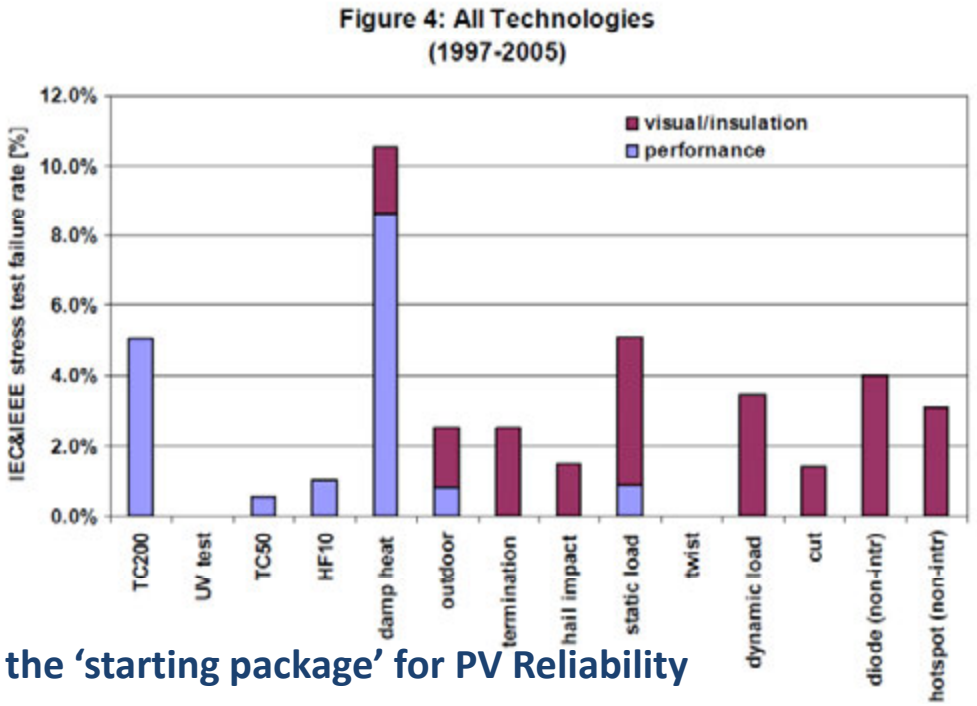
Reliability Impact on Module Value



$$LCOE = \frac{\text{Total Life Cycle Cost}}{\text{Total Lifetime Energy Production}}$$

© 2009 First Solar, Inc.

Module Failures from Qualification Testing



- **Qualification testing is the 'starting package' for PV Reliability**
- **Just a screening test for key design flaws/infant mortality**
- **No correlation to MTBF, long term OD performance, degradation**

TamizhMani, et al, "IEC And IEEE Design Qualifications: An Analysis Of Test Results Acquired Over Nine Years", 2008

© Copyright 2010, First Solar, Inc.

TF Module Failure Modes

Issue	Description	Tests	References	R&D need
Increase in series resistance after exposure to moisture	Moisture ingress is known to increase the series resistance of ZnO and some other materials commonly used in thin-film modules; this is a special issue for flexible products.	Damp heat	[27, 51] [41]	Development of thin-film products that are not sensitive to moisture or development of a barrier that keeps moisture out of sensitive layers.
Instability of thin-film layers caused by delamination and/or diffusion	Thin-film products usually require many layers; if any of these has poor adhesion, delamination may occur, often breaking the electrical connection between active layers. Also, Cu and other elements are known to diffuse, causing changes in how the cells perform.	Damp heat; temperature cycling	[18, 23, 52-57]	Develop understanding of the diffusion/delamination mechanisms, what affects them, and how to test for instabilities.
Nonuniformities in manufacturing, including scribe-line issues	Nonuniformities can lead to "weak diodes" that may then run hotter than the rest of the module, providing a weak point for degradation. Similarly, many other manufacturing nonuniformities (especially at scribe lines) can lead to reliability problems.	Damp heat; temperature cycling	[23, 58]	Much work is needed to understand what parameters must be carefully controlled during manufacturing and what nonuniformities can be tolerated.

Sarah Kurtz, et al, "Photovoltaic-Reliability R&D toward a Solar-Powered World", Proc. of SPIE 2009

© Copyright 2010, First Solar, Inc.

TF Module Failure Modes cont.

	Known and Anticipated Failure Modes & Degradation Mechanisms	Priority/Prob. of Success / Role for Labs (High-Medium-Low)	Diagnostic Technique / Qual Test (e.g., chamber tests, HVTB)	Comment
General	Corrosion leading to loss of grounding	H/H/H		
	Quick connector reliability	H/H/L		
	Improper installation leading to loss of grounding	H/H/L		
	Delamination	H/M/M		This is especially a problem for flexible packages
	Glass breakage	M/H/L		For products using glass
	Bypass diode failure	M/H/L		
	Inverter reliability	M/H/M		
Film Si	See items listed in "General" section			
	Electrochemical corrosion of SnO_2:F	M/M/L	Light soaking; Voltage biased damp heat[7]	
	Initial light degradation (a-Si)	L/L/L	Light soaking	
CdTe	Cell layer integrity – backcontact stability	H/H/H		
	Cell layer integrity – interlayer adhesion and delamination; Electrochemical corrosion of SnO_2:F	L/L/M	Voltage biased damp heat[7]	
	Fill-factor loss (increased series resistance and/or recombination)	H/M/H	Cell + Module Light soaking; Damp Heat	Screen at cell initially; then module
	Busbar failure - mechanical (adhesion) and electrical	H/H/M	IR Camera; Hot/humid vs. damp heat	Thermal stress[9]
	Shunt hot spots at scribe lines before and after stress	H/M/M	IR Camera; Hot/humid vs. damp heat	
	Weak diodes, hot spots, nonuniformities before and after stress	H/M/H	IR Camera; Hot/humid vs. damp heat	
CIS	Cell layer integrity – contact stability	H/H/H		Mo backcontact (all), the front contact is only a problem when the module is assembled from discrete cells
	Cell layer integrity – interlayer adhesion	M/H/M		
	Fill-factor loss (increased series resistance and/or recombination)	H/M/H	Cell + Module Light soaking; Damp Heat	Screen at cell initially; then module
	Busbar failure – mechanical (adhesion) and electrical	M/H/M	IR Camera; Hot/humid vs. damp heat	
	Notable sensitivity of TCO to moisture	H/M/H	Damp heat exposure	
	Moisture ingress failure of package	H/M/H	Hot/humid vs. damp heat	Flexible roofing products
	Cell–to-cell interconnect (discrete cells)	H/M/H	IR Camera; Hot/humid vs. damp heat	Flexible roofing products; this is a problem when discrete devices are interconnected into modules
	Notable sensitivity of TCO to moisture; need to pass damp heat test (non-shingle specific)	H/M/M	Damp heat exposure	
	Shunt hot spots at scribe lines before and after stress	H/M/M	IR Camera; Hot/humid vs. damp heat	
	Weak diodes, hot spots, nonuniformities before and after stress	H/M/H	IR Camera; Hot/humid vs. damp heat	
	Edge shunting	M/H/M		Discrete Cell – Flexible roofing products

Nick Bosco, "Reliability Concerns Associated with PV Technologies", NREL

© Copyright 2010, First Solar, Inc.

TF Module Failure Modes cont.

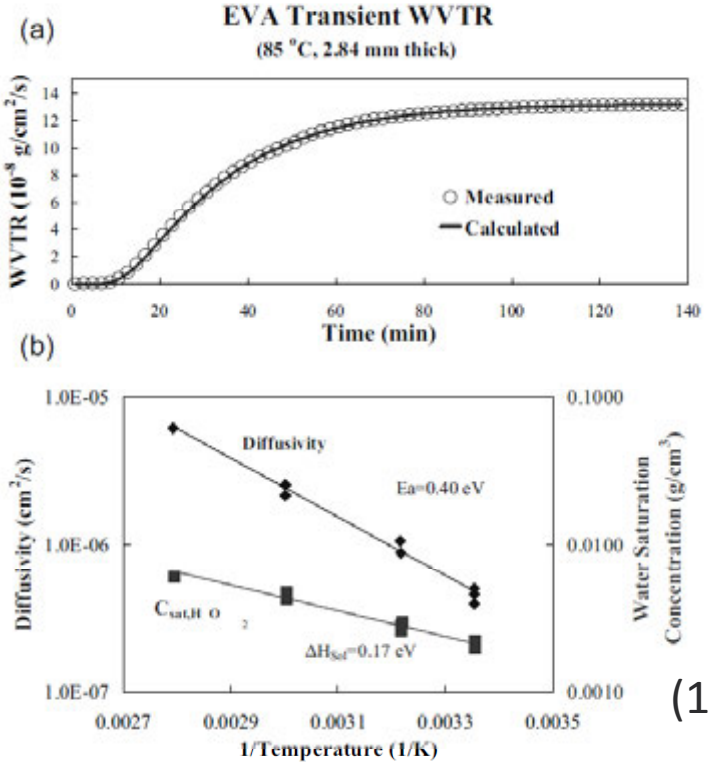
Table I. Thin-film failure modes and failure mechanisms

Failure modes	Effect on I–V curve	Possible failure mechanisms
1. Cell degradation		
a. Main junction: increased recombination[24]	Loss in fill factor, I_{sc}, and V_{oc}	Diffusion of dopants, impurities, etc. Electromigration
b. Back barrier; loss of ohmic contact (CdTe)[7,24,25]	Roll-over, cross-over of dark and light I–V, higher R_{ser}	Diffusion of dopants, impurities, etc. Corrosion, oxidation Electromigration
c. Shunting[26–28]	R_{shunt} decreases	Diffusion of metals, impurities, etc.
d. Series: ZnO,[23] Al[29]	R_{ser} increases	Corrosion, diffusion
e. De-adhesion SnO_2 from soda-lime glass[57,59]	I_{sc} decreases and R_{ser} increases	Na ion migration to SnO_2/glass interface
f. De-adhesion of back metal contact	I_{sc} decreases	Lamination stresses
2. Module degradation		
Interconnect degradation		
a. Interconnect resistance; ZnO:Al/Mo or Mo[23], Al interconnect[49]	R_{ser} increases	Corrosion, electromigration
b. Shunting; Mo across isolation scribe[23]	R_{shunt} decreases	Corrosion, electromigration
Busbar degradation	R_{ser} increases or open curcuit	Corrosion, electromigration
Solder joint	R_{ser} increases or open circuit	Fatigue, coarsening (alloy segragation)
Encapsulation failure		
a. Delamination[36–38]	Loss in fill-factor, I_{sc}, and possible open circuit	Surface contamination, UV degradation, hydrolysis of silane/glass bond, warped glass, 'dinged' glass edges, thermal expansion mismatch
b. Loss of hermetic seal		
c. Glass breakage		
d. Loss of high-potential isolation[50,56,57]		

T Mac Mahonm, "Accelerated Testing and Failure of Thin-film PV Modules" , Progress in PV 2004

© Copyright 2010, First Solar, Inc.

Humidity is an important stress factor



(1)

$$k = A_o \, e^{-\frac{E_a}{RT}}$$

Diffusivity of water follows an Arrhenius model

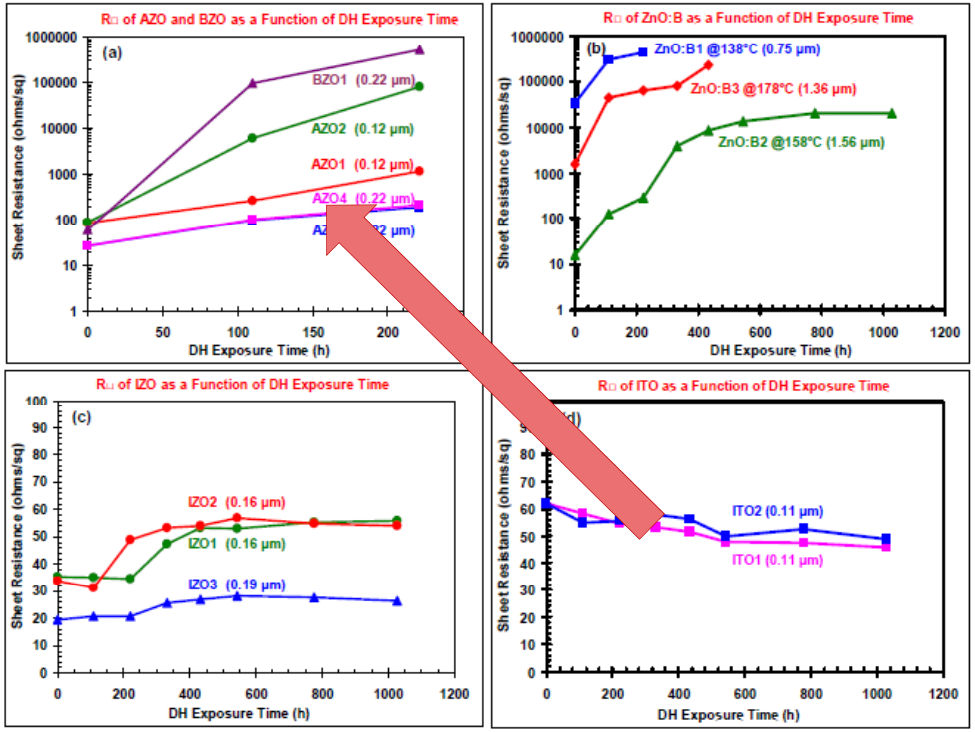
Choose materials that limit water ingress!

(1) M. Kempe, "Control of Moisture Ingress into Photovoltaic Modules" IEEE PVSC, 2005

(2) D. J. Coyle, H. A. Blaydes, J. E. Pickett et al., "Degradation kinetics of CIGS solar cells," Proceedings of the 2009 34th IEEE Photovoltaic Specialists Conference (PVSC 2009), pp. 001943-7, 2009.

© Copyright 2010, First Solar, Inc.

Humidity affects TCO's in different ways



x 10^4 worse

(1)

- **Choose materials that are less sensitive to water**

(1) F.J. Pern, R. Sundaramoorthy, C. DeHart, et al. " Stability of TCO Window Layers for Thin-Film Solar cells", Proc. of SPIE Vol. 7412 74120J-1

(2) Sundaramoorthy, R., et al., "Comparison of Amorphous InZnO and Polycrystalline ZnO:Al Conductive Layers for CIGS Solar Cells," 34th IEEE PVSC, (2009).

© Copyright 2010, First Solar, Inc.

Temperature is an important stress factor

- **Corrosion of conductive components**
- **Thermal degradation of polymers**
  - **Delamination of interfaces**
  - **Failure of adhesive/pottants**
- **Diffusivity of water**

$$k = A_o \, e^{-\frac{E_a}{RT}}$$

- **To find Activation Energy (Ea) we need to go beyond Damp Heat and test at different temperatures**

© Copyright 2010, First Solar, Inc.

Temperature is an important stress factor

Module Type	Mount	a	b	ΔT (°C)
Glass/cell/glass	Open rack	-3.47	-.0594	3
Glass/cell/glass	Close roof mount	-2.98	-.0471	1
Glass/cell/polymer sheet	Open rack	-3.56	-.0750	3
Glass/cell/polymer sheet	Insulated back	-2.81	-.0455	0
Polymer/thin-film/steel	Open rack	-3.58	-.113	3
22X Linear Concentrator	Tracker	-3.23	-.130	13

$$T_m = E \cdot \left\{ e^{a+b \cdot WS} \right\} + T_a$$

from ambient to module temperature

$$T_c = T_m + \frac{E}{E_o} \cdot \Delta T$$

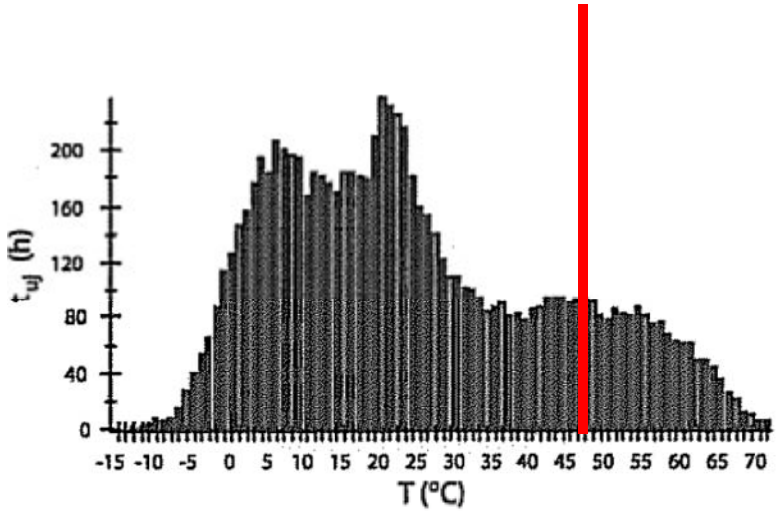
from module to cell (semiconductor) temperature

(1) King et al, "Photovoltaic Array performance model" Sandia SAND2004-3535, 2004

© Copyright 2010, First Solar, Inc.

Activation Energy & $T_{equivalent}$

- **$T_{equivalent}$ is the activation energy (Ea)-weighted average temperature for a system**
- **$T_{equivalent}$ is a function of the Activation energy**



$$\Delta P = Ae^{\frac{-E_a}{RT}}\Delta t$$

$$P = \sum_i Ae^{\frac{-E_a}{RT_i}}\Delta t_i = Ae^{\frac{-E_a}{RT_{Equivalent}}}\sum_i \Delta t_i$$

(1) McMahon, "Accelerated Testing and Failure of Thin-Film PV Modules" , Prog in PV, 2004

© Copyright 2010, First Solar, Inc.

Equivalent Temperature for Different Climatic Zones

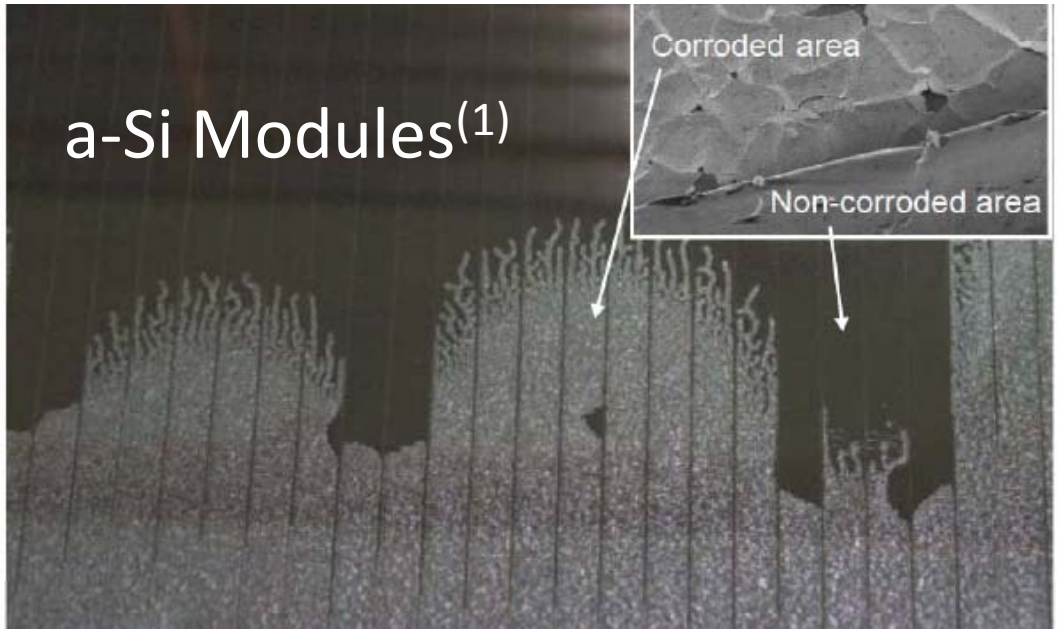
Mount:	Open rack glass-cell-glass		Close roof glass-cell-glass		Open rack glass-cell-polymer		Insulated back		Open rack polymer-cell-steel	
Ea→ Location↓	1.1 eV	2 eV	1.1 eV	2 eV	1.1 eV	2 eV	1.1 eV	2 eV	1.1 eV	2 eV
Riyadh	48.4	55.1	61.0	69.5	45.9	52.3	67.1	76.3	44.0	50.3
Kuwait	46.0	53.0	56.0	66.3	43.8	50.3	60.9	73.1	41.7	47.9
Bangkok	41.7	46.5	51.5	58.6	39.8	44.1	56.4	64.4	38.3	42.3
New Delhi	44.8	51.2	56.8	65.2	42.7	48.6	62.7	72.0	41.2	46.9
Seville	39.5	47.1	51.3	60.4	37.4	44.6	57.0	66.7	35.8	43.1
Munich	26.7	35.4	37.2	48.2	24.8	33.0	42.3	54.2	23.3	31.4
Phoenix	47.1	53.9	59.9	68.2	44.6	51.0	66.0	75.0	42.6	48.8
Yuma	43.8	50.2	54.9	63.0	41.6	47.7	60.3	69.2	39.9	45.8
Daytona	37.2	42.9	47.7	55.2	35.0	40.3	52.7	61	33.0	37.9
Miami	37.1	41.9	46.7	53.7	35.0	39.3	51.5	59.3	33.1	36.9

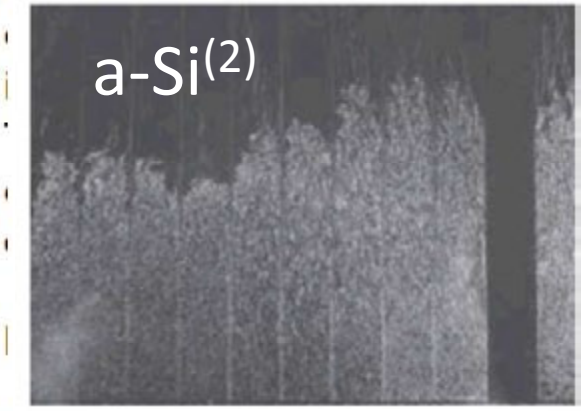
- **We can now answer the question "how long will my module last" for some degradation mechanisms**
- **What comes next? Correlate your lab model with real outdoor data**

Kent Whitfield, "Evaluation Of High-temperature Exposure Of Rack-mounted Photovoltaic Modules", PVSC IEEE 34th

© Copyright 2010, First Solar, Inc.

Voltage is an important stress factor





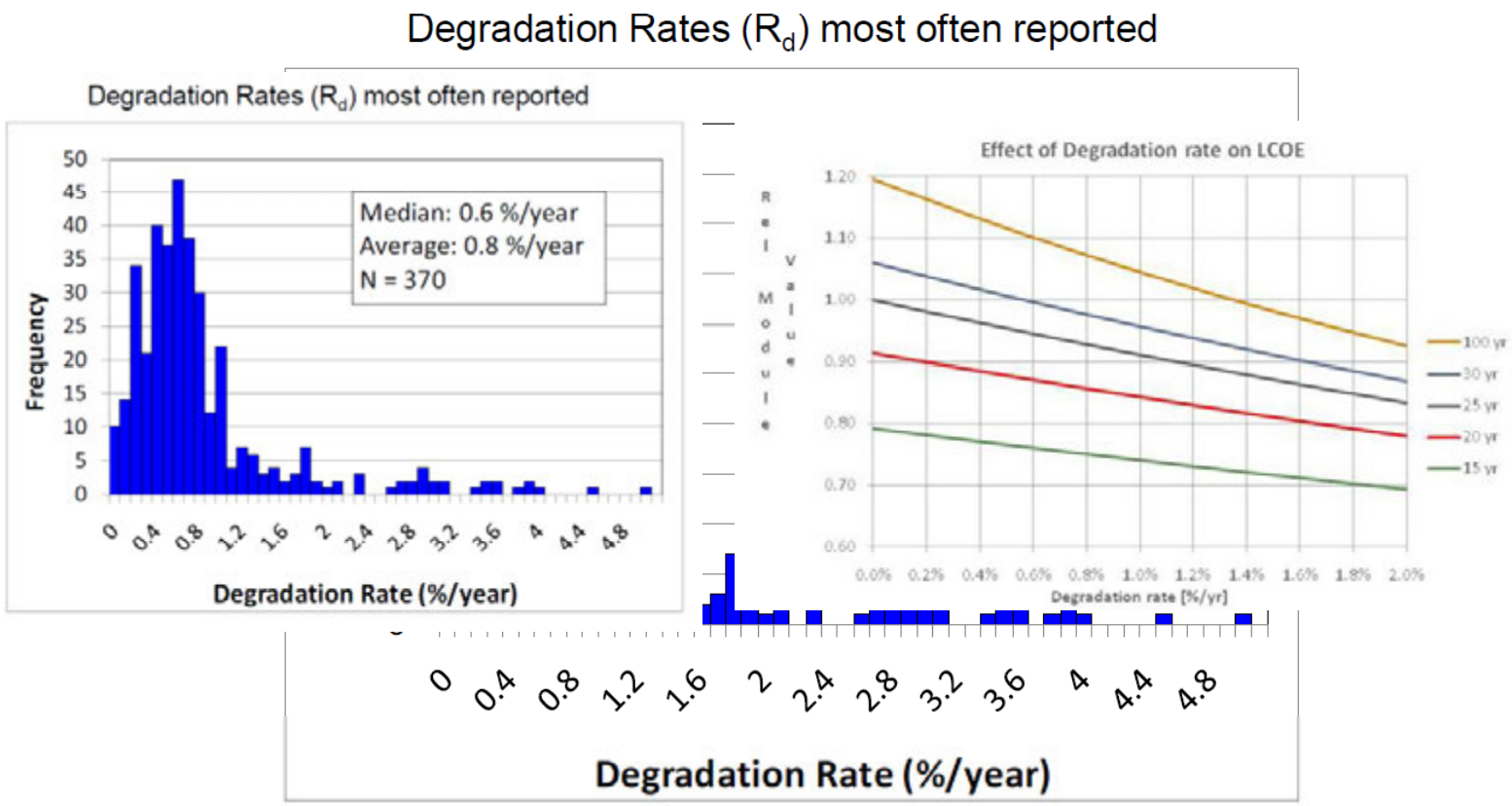
'Bar-graph' delamination

- **There are other stress factors, some of them not in the 'starter package'**

(1) Peter Hackle "Characterization of Multicrystalline Silicon Modules with System Bias Voltage Applied in Damp Heat ", 25th European Photovoltaic Solar Energy Conference and Exhibition. September, 2010
(2) T McMahon, "Accelerated Testing and Failure of Thin-film PV Modules" , Progress in PV 2004
(3) JPL- Mon, Ross (1984): "Predicting electrochemical breakdown in terrestrial photovoltaic modules"

© Copyright 2010, First Solar, Inc.

PV System Degradation rates



Dirk Jordan (NREL), "Degradation Rates", Feb-2010

© Copyright 2010, First Solar, Inc.

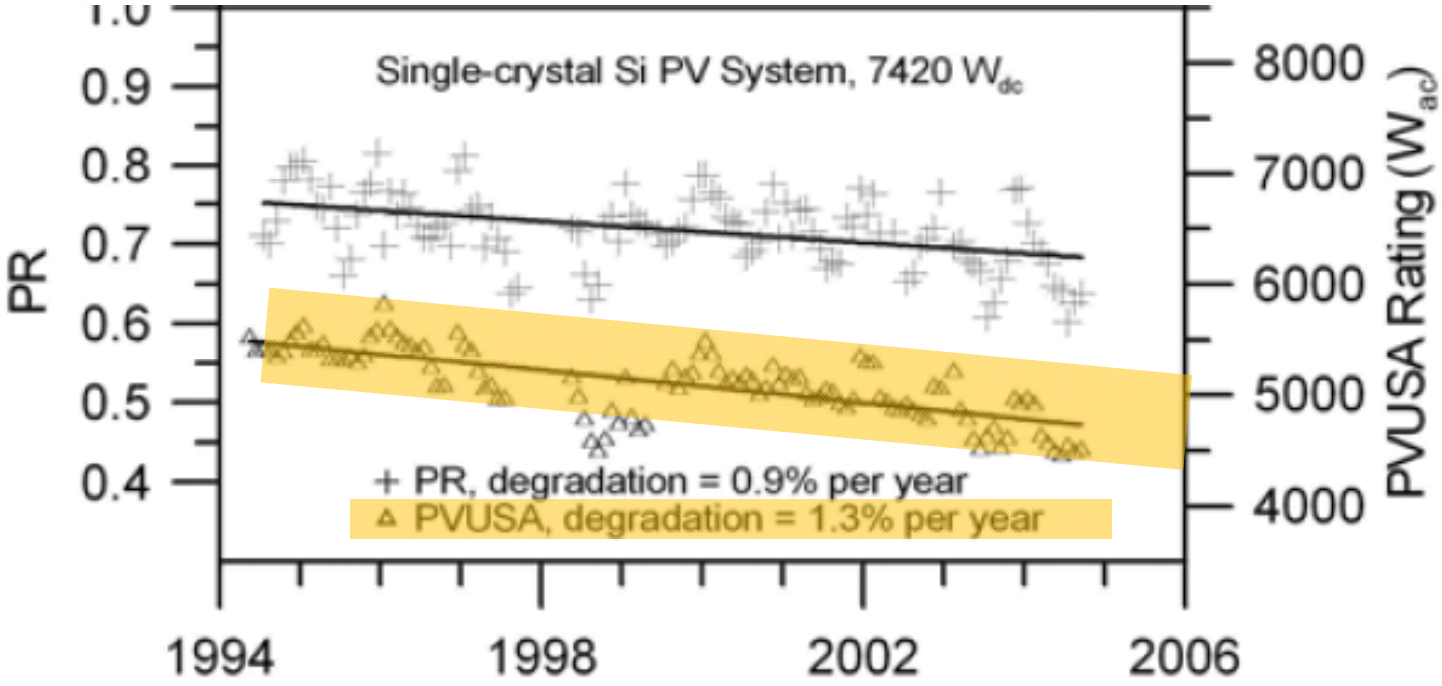
Outdoors Performance Monitoring

- **energy output** E **[amount of energy kW-AC]**
- **final PV system yield** $Y_f = E/P_0$ **[takes into account system size]**
- **performance ratio** $PR = Y_f/Y_r$ **[size + solar radiation]**
- **PTC ratio** PTC **[size + solar radiation + temperature/wind]**

IEC 61724 "Photovoltaic system performance monitoring-guidelines for measurement, data exchange, and analysis"

© Copyright 2010, First Solar, Inc.

Calculation of PV System Degradation rates

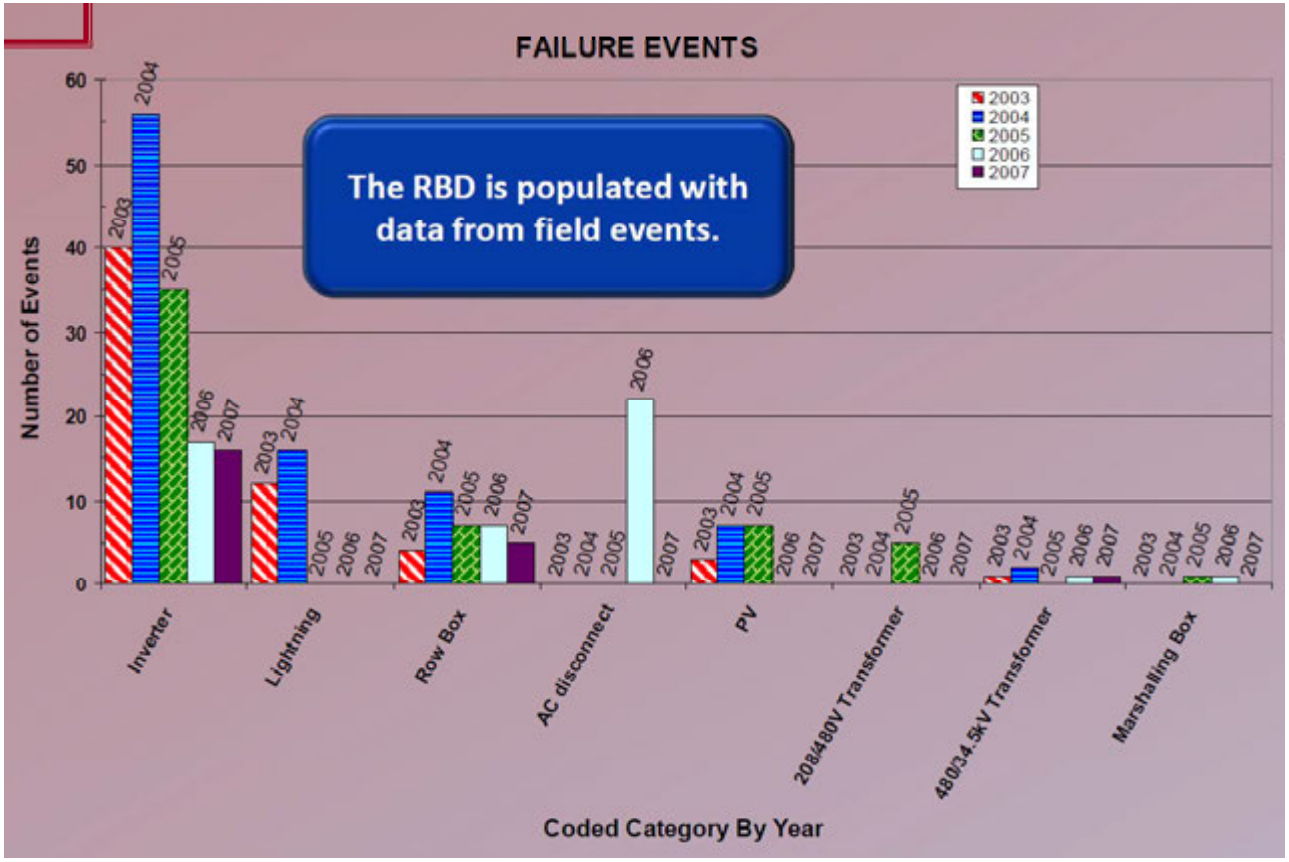


- **The variability on PTC(PVUSA) is lower than PR because it compensates for temperature**
- **+3 years of data is recommended to calculate degradation rates**

B. Marion, et al, "Performance Parameters for Grid-Connected PV Systems", 30th IEEE PVSC, 2005

© Copyright 2010, First Solar, Inc.

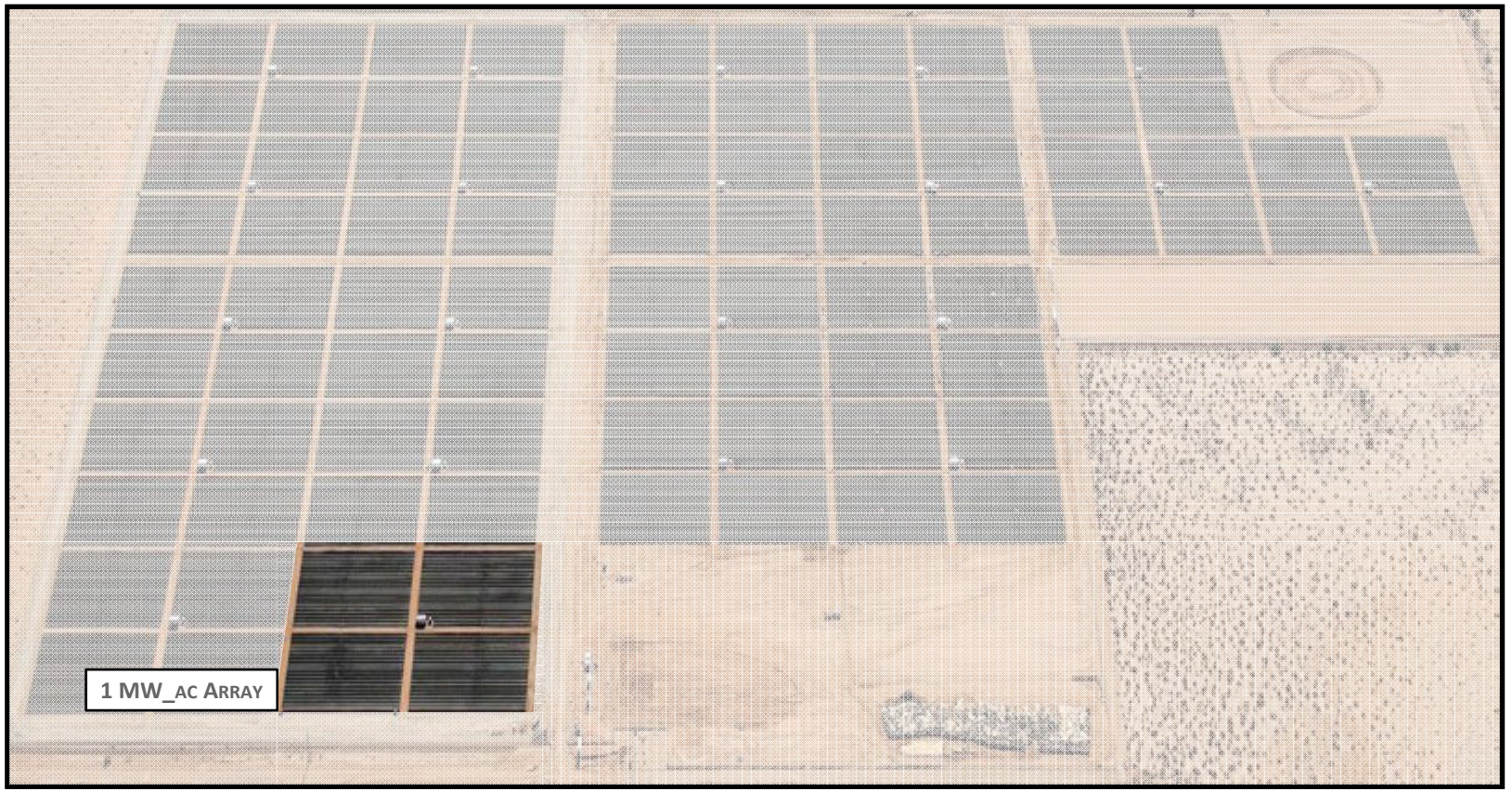
PV System Failure Events



M Quintana, J. Granata, et al. "Sandia'sPV Reliability Program", NREL PV Reliability Conference 2010. Sandia Poster

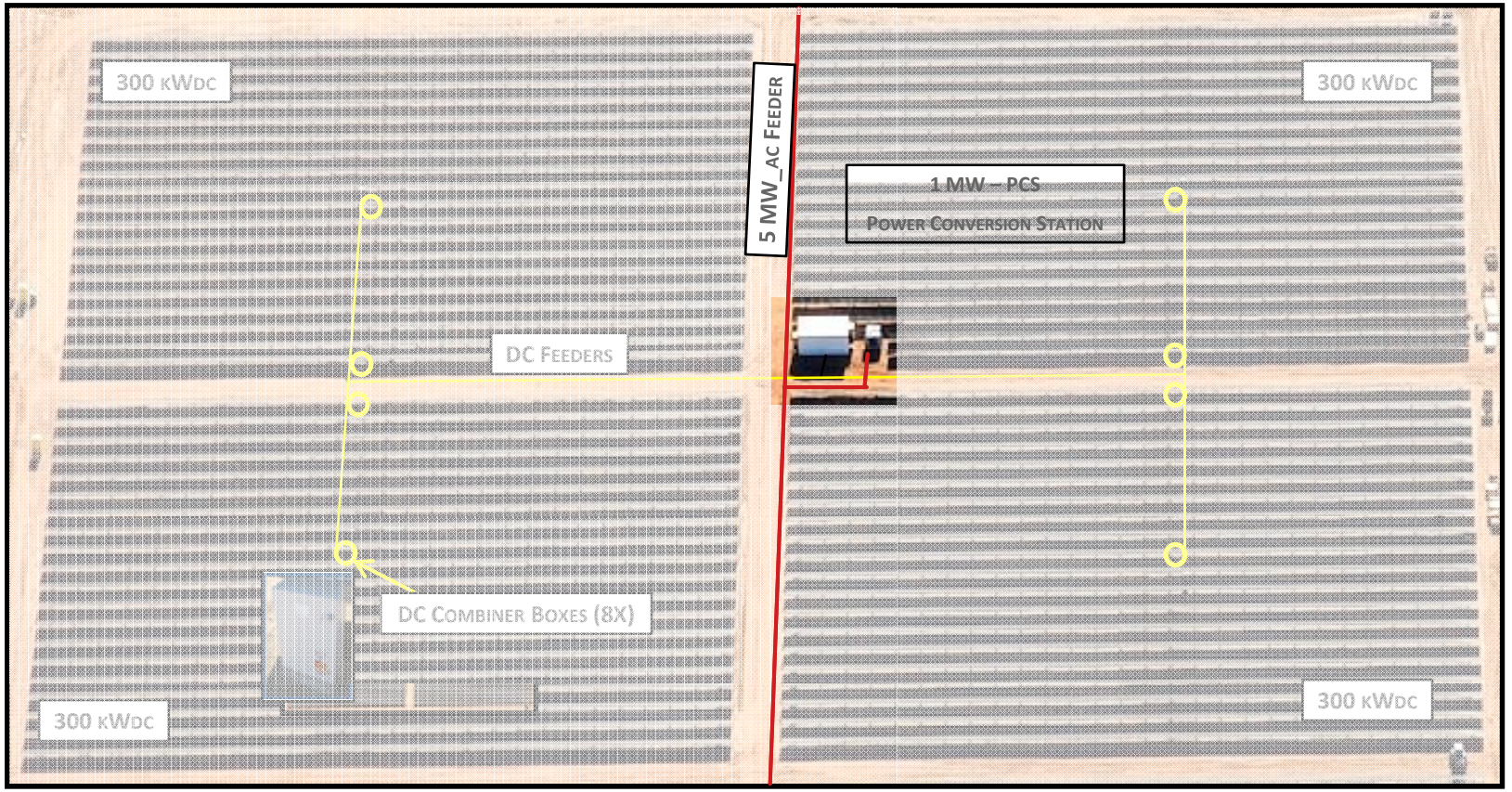
© Copyright 2010, First Solar, Inc.

21 MW Photovoltaic Power Plant: 21 x 1 MW Arrays



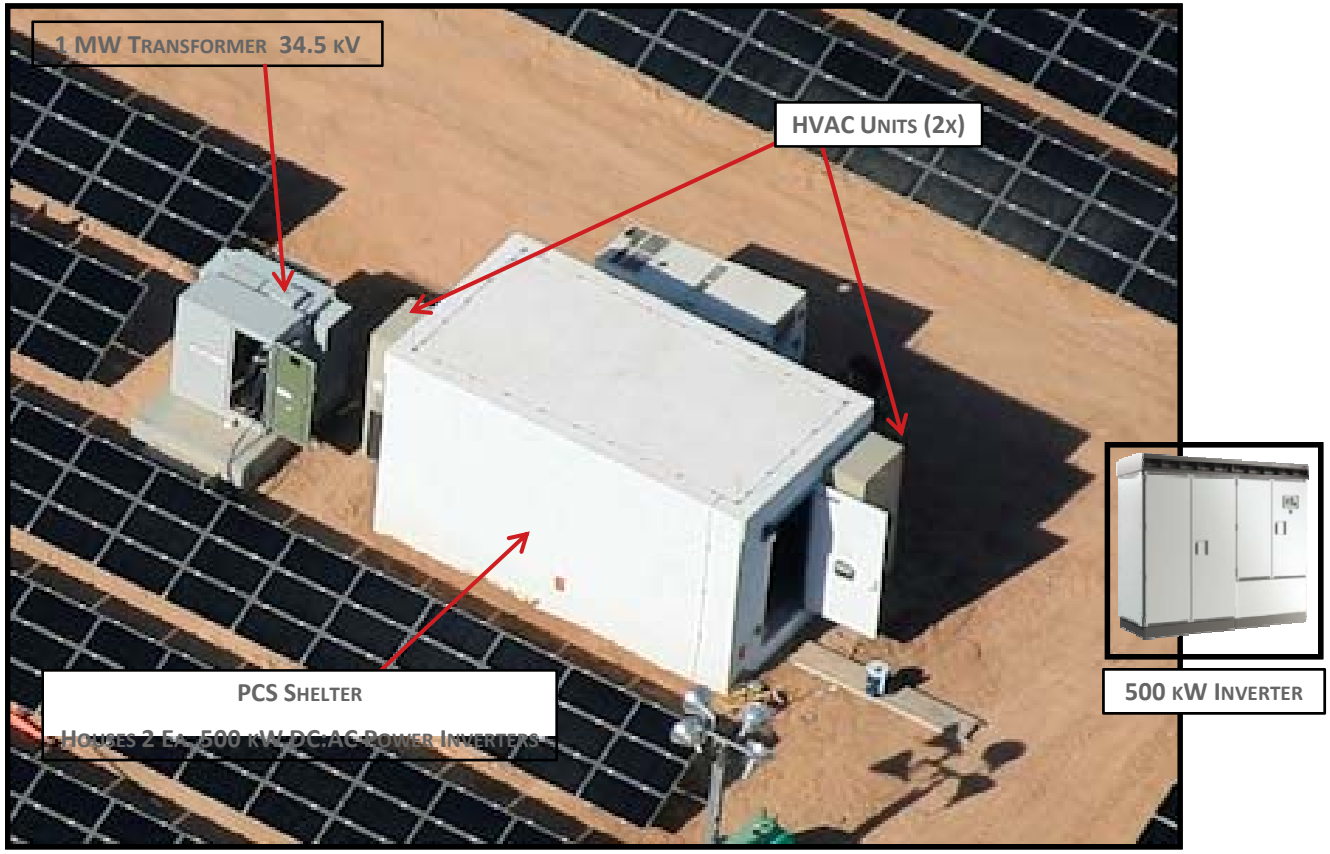
© 2009 First Solar, Inc.

1 MWAC ARRAY (1.2 MWDC)



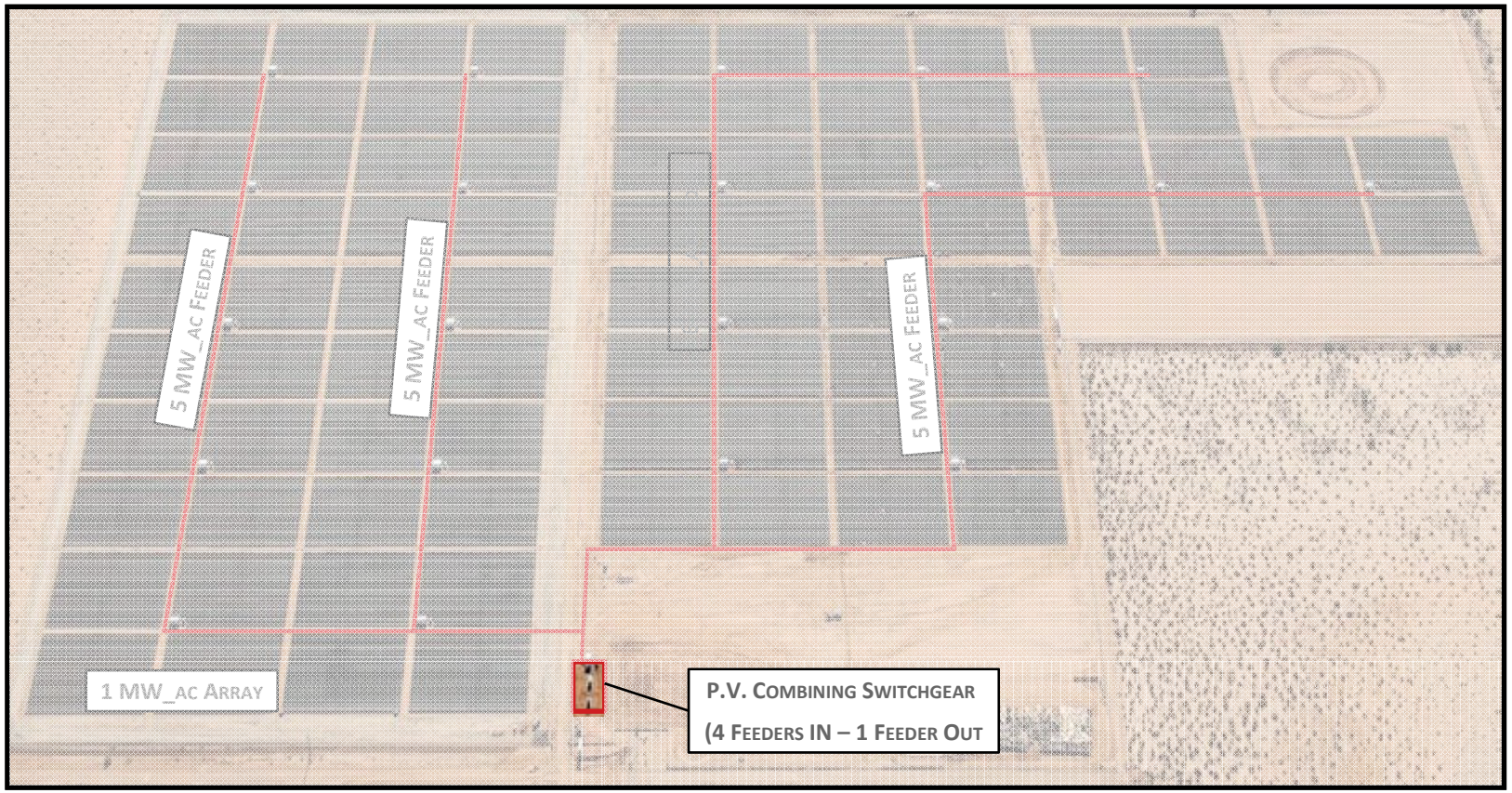
© 2009 First Solar, Inc.

1 MW PCS (Power Conversion Station)



© 2009 First Solar, Inc.

21 MW Photovoltaic Power Plant: 21 x 1 MW Arrays



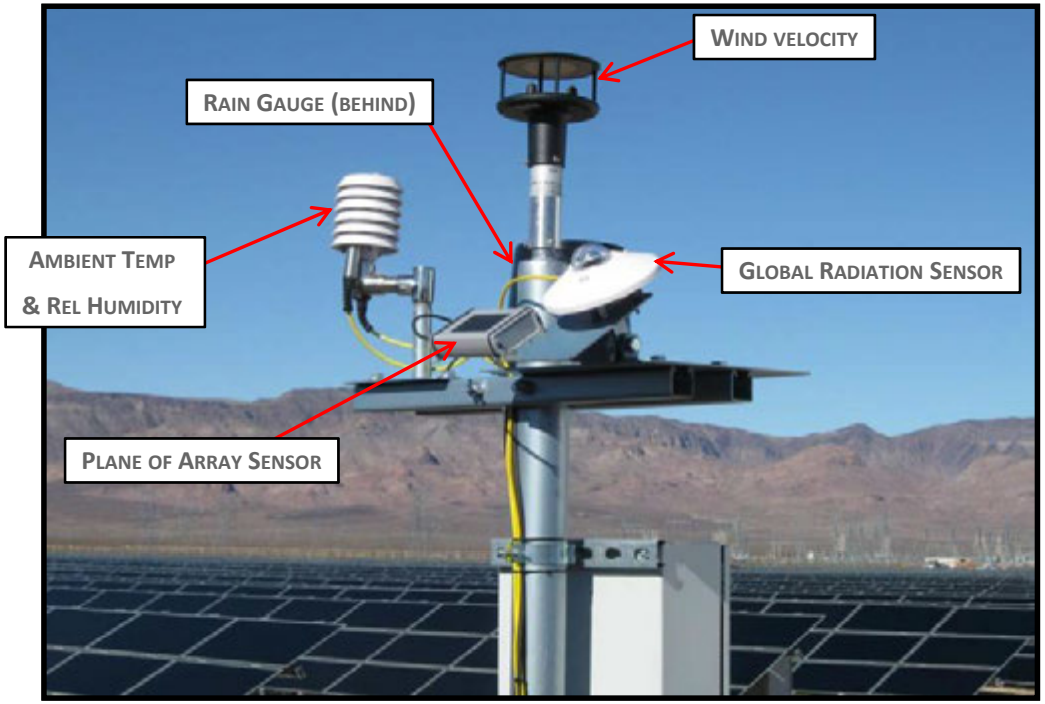
© 2009 First Solar, Inc.

21 MW PVCS (PHOTO VOLTAIC COMBINING SWITCHGEAR)



© 2009 First Solar, Inc.

METEOROLOGICAL STATION (2 EA.)



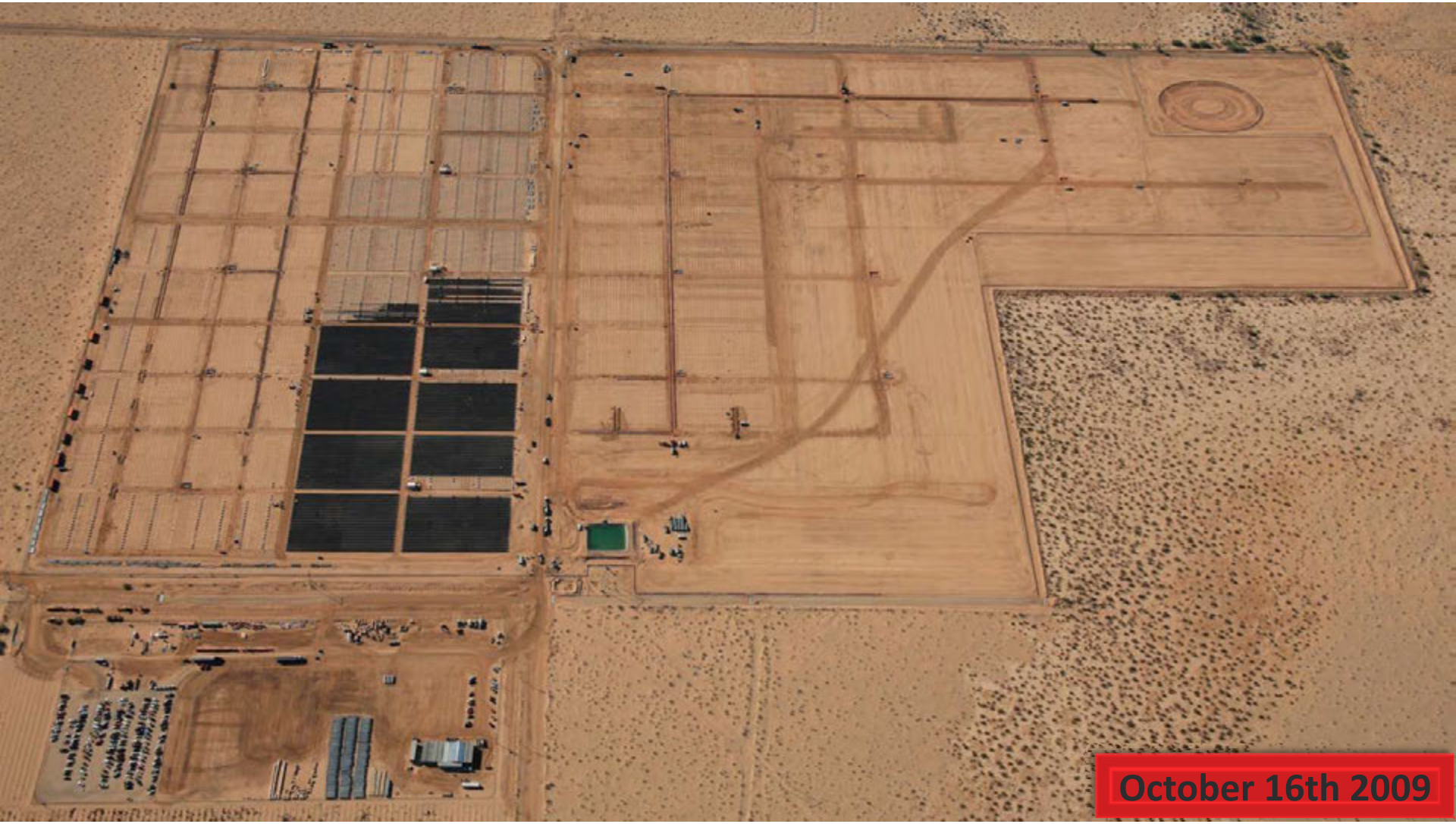
- **Irradiance, Temperature & WindSpeed needed to calculate PR's & PTC's**
- **Correlate your lab model with real outdoor data**

© 2009 First Solar, Inc.


September 25th 2009


October 2nd 2009


October 9th 2009


October 16th 2009


October 23rd 2009


November 3rd 2009


November 13th 2009


November 20th 2009

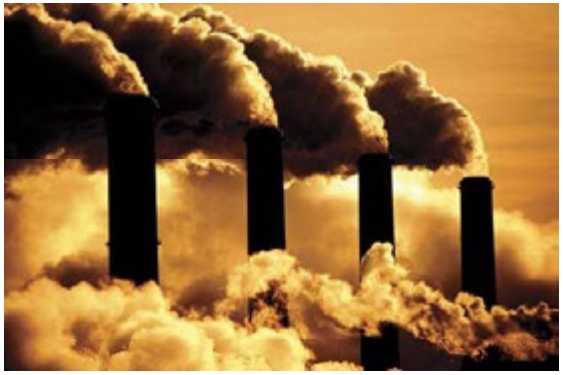

November 27th 2009

Environmental and Local Benefits

The project will power over 6,000 local homes









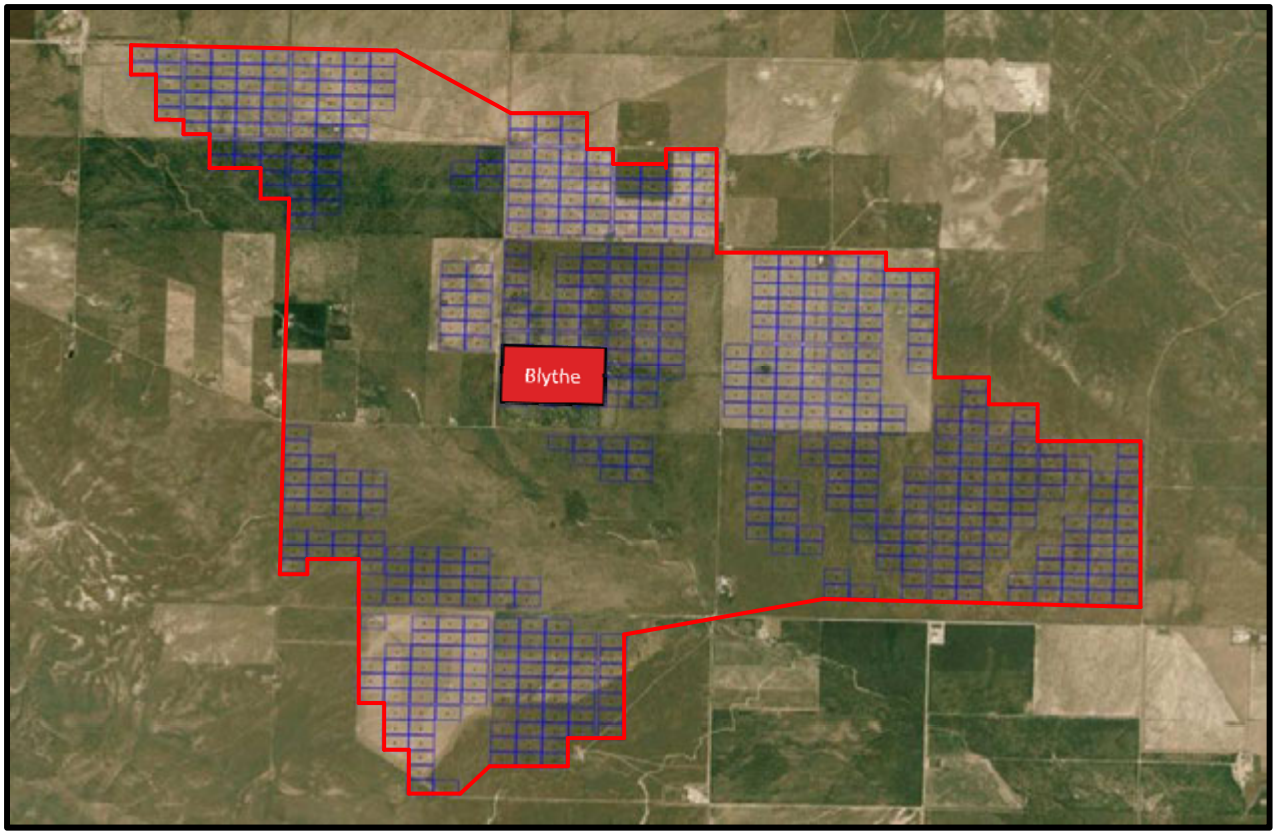
The project will avoid emissions of 12,000 metric tons of CO_2 – the equivalent of taking over 2,200 cars off the road.

© 2009 First Solar, Inc.

Utility-Scale Projects in Southwestern U.S. – 2.0 GW AC



From Blythe To Topaz



© 2009 First Solar, Inc.



Summary

- Module reliability is a driver for cost
- Module reliability does not dominate system reliability
- Module reliability enables affordable PV electricity
- Key module stress factors
  i. Humidity
  ii. Temperature
- What's needed
  - fundamental understanding of degradation mechanisms
  - correlation to real outdoor performance data
- First Solar enabling statistics at utility scale

© 2009 First Solar, Inc.



First Solar

thank you

Our Mission

To create enduring value by enabling a world powered by clean, affordable solar electricity.







© 2009 First Solar, Inc.

How to Set Up a Reliability Program for Photovoltaic Modules

Harry Guo ReliaSoft Corporation
Ryan Gaston Dow Chemical
Athanasios Gerokostopoulos ReliaSoft Corporation

ReliaSoft®

POWERHOUSE DOW SOLAR

Contents

- Reliability Challenges
- Scope of a Reliability Program Plan
- Reliability Management Concepts and Tools
- Statistic Methods and Tools Used in a Reliability Program
- Reliability Program Survey
- Reliability Program for PV Modules

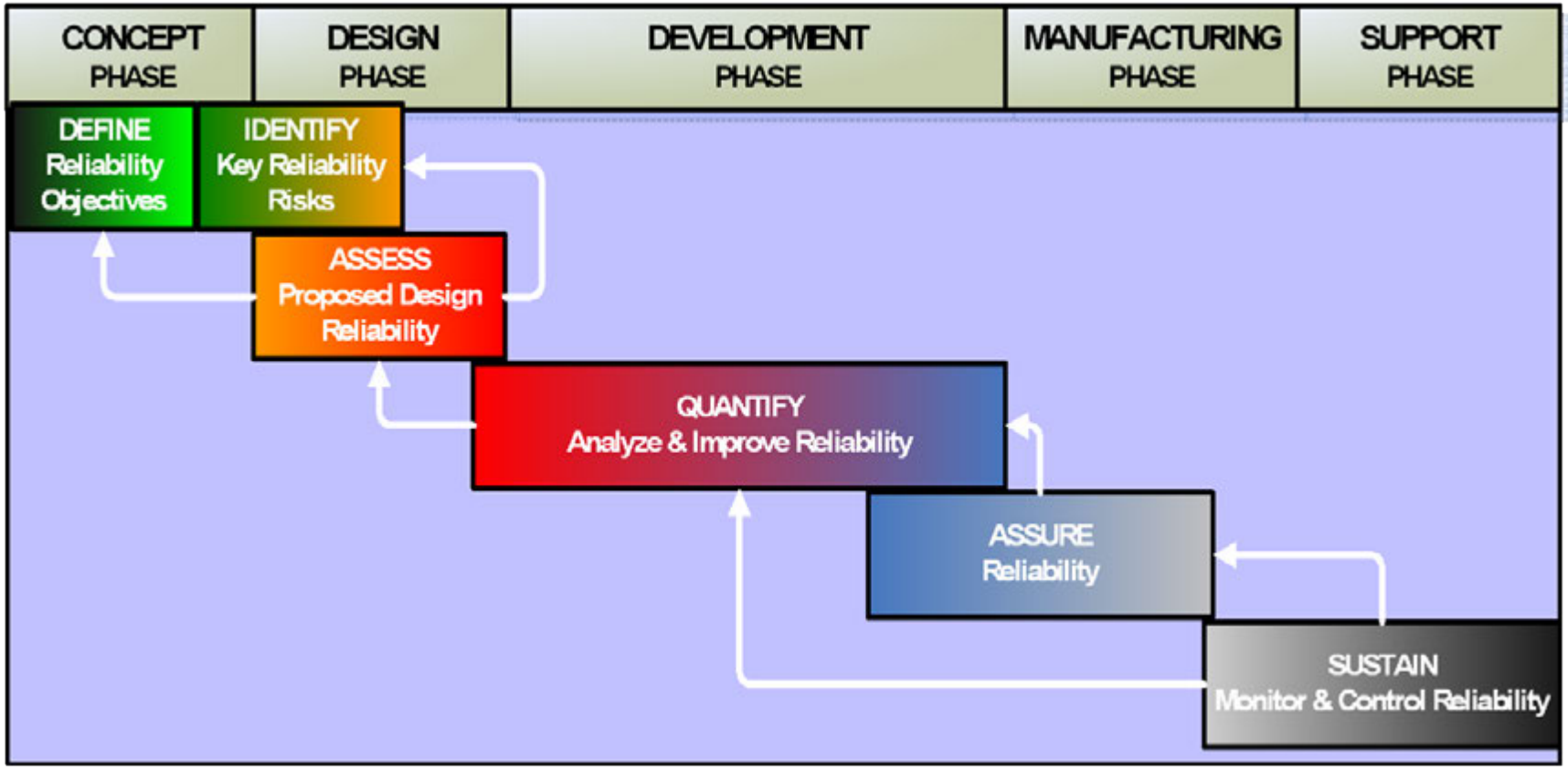
The Reliability Challenge

Most companies realize they have to balance three imperatives in order to develop highly reliable products and processes:

- Ensure that their products meet or exceed reliability requirements
- Meet project budget objectives
- Meet project timing objectives

Scope of a Reliability Program Plan

A Reliability Program Plan is a document that outlines the entire plan and set of action steps to achieve the reliability objectives for a project.



General Guidelines for Setting Up a Reliability Program

- **Set reliability objectives.**
- **Develop the specific action steps that will achieve the reliability objectives.**
- **Some resources for a reliability program:**
  - SAE JA1000/1: *Reliability Program Standard Implementation Guide*
  - ReliaSoft: *Blueprint for Implementing a Comprehensive Reliability Program*
  - Reliability Analysis Center: *Reliability Toolkit: Commercial Practices Edition*

Reliability Management Concepts and Tools

- **There are many standards on reliability management; for example, some of the military standards are:**
  - MIL-STD-2155 Failure Reporting, Analysis and Corrective Action System (FRACAS)
  - MlL-STD-785B Reliability Program for Systems and Equipment, Development and Production
  - MIL-HDBK-189 Reliability Growth Management

- **A FRACAS (failure reporting, analysis and corrective action system) is one of the most important management tools in a reliability program.**

Why FRACAS? Survey

- ***ReliaSoft* Survey shows FRACAS was ranked as the #3 important reliability task.**
- **In a survey published by the *IEEE Transactions on Reliability*, FRACAS was ranked #2 among reliability tasks with greatest effectiveness.**
- **In a similar survey published by the Reliability Analysis Center, FRACAS was ranked as the #1 important reliability task.**
- **To have a successful Reliability Program, you need to have an efficient FRACAS system!**
  - The characteristics of a closed-loop system provide the monitoring & control necessary to make FRACAS effective.
  - It causes the different groups/entities in the organization to effectively communicate and implement the corrective action and review its effectiveness.

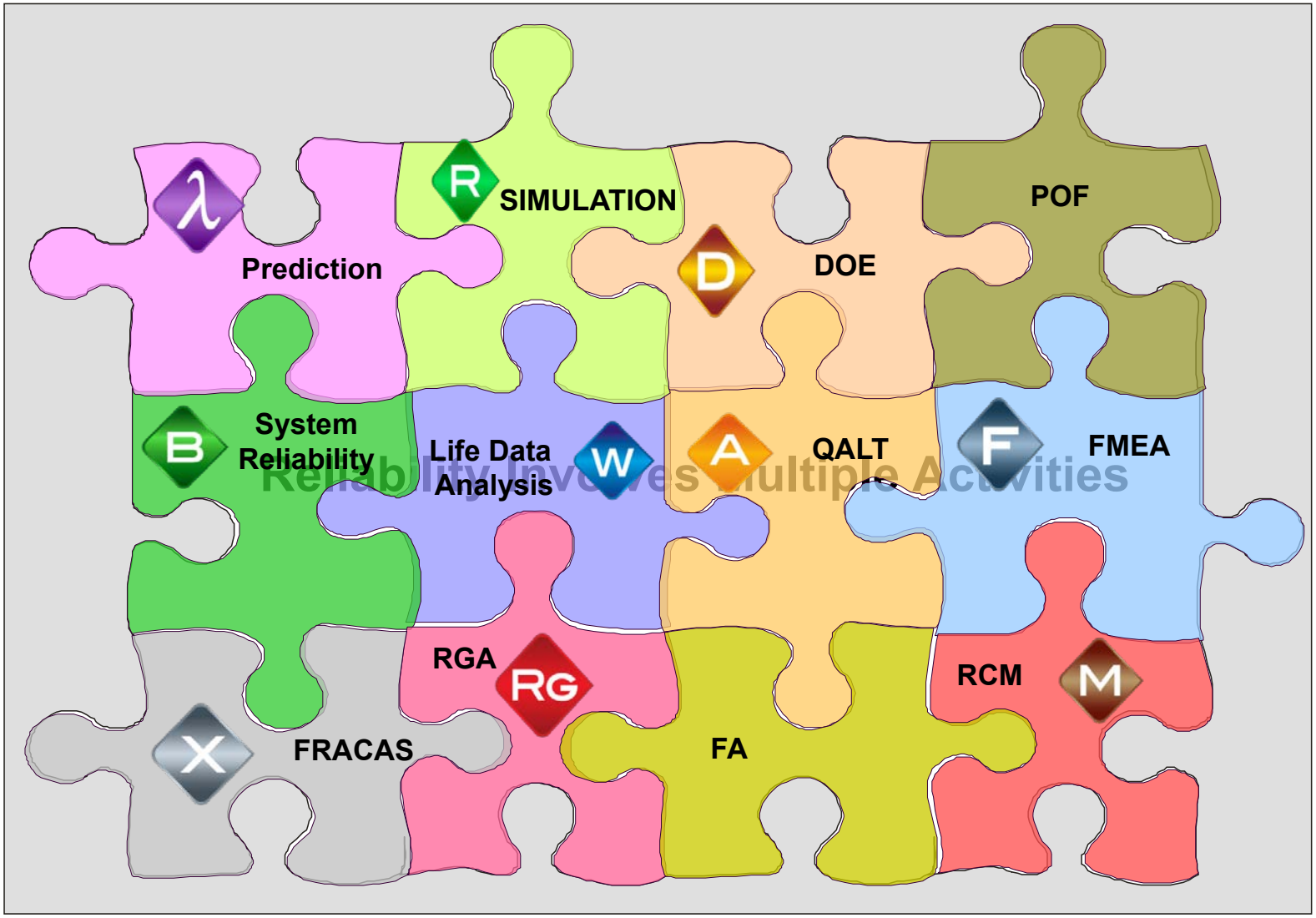
Why FRACAS? Benefits

- FRACAS promotes reliability improvement throughout the life cycle of a product. It can be used and applied during:
  - Initial product design/re-design to identify and eliminate known issues.
  - In-house development testing to improve the product, process or service.
  - Field testing.
  - Production and operations to increase efficiencies.
  - Capital equipment installation – reduce costs & time.
  - Supporting products in the field (end-user/customer).

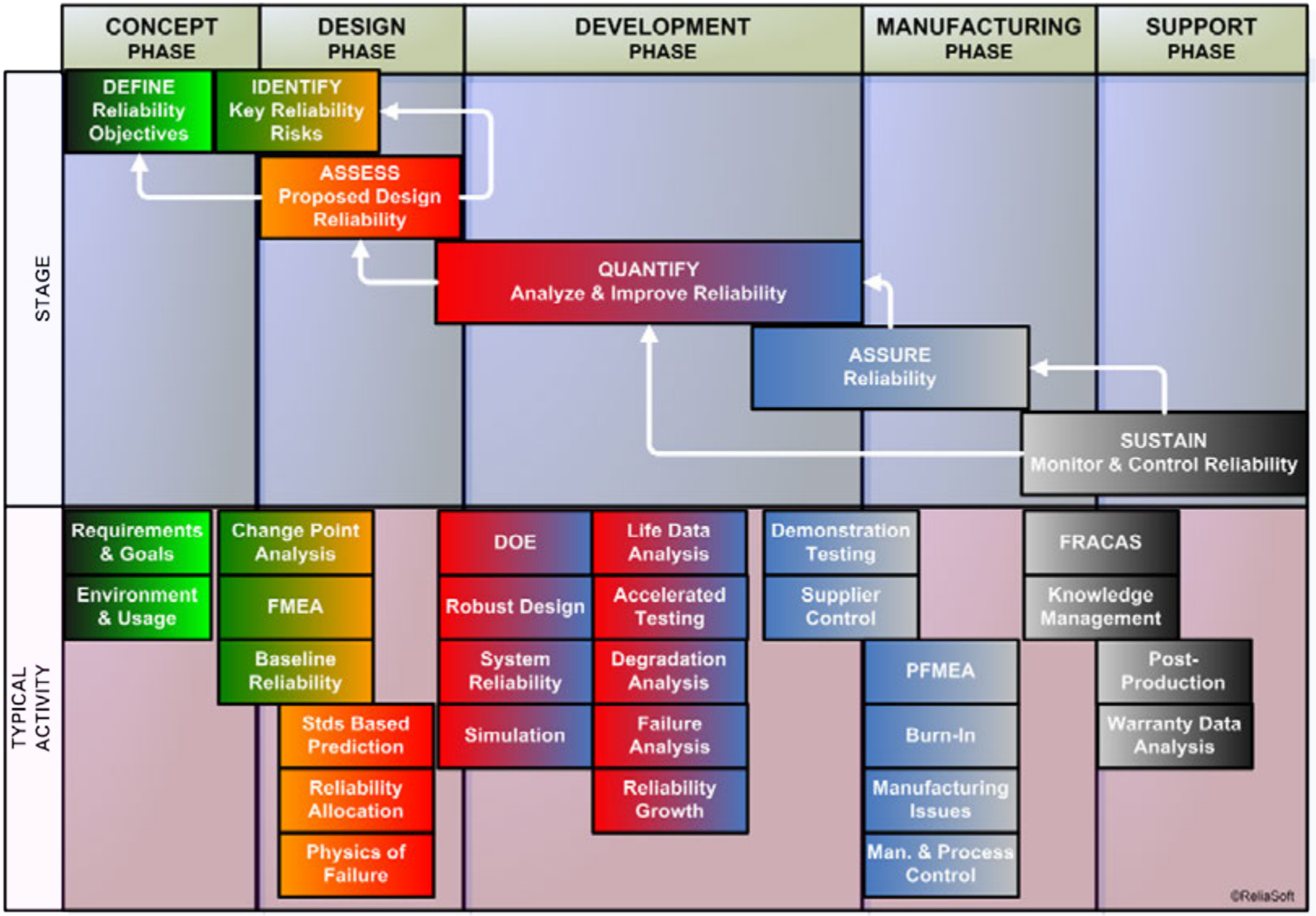
Why FRACAS? Benefits (*cont'd)*

- FRACAS promotes the reliability of a product or process by establishing a formal process followed by the entire organization:
  - Provides engineering data for corrective action and preventive action.
  - Identifies developing patterns of deficiencies.
  - Provides failure data for reliability analysis.
  - Helps avoid recurrence of failures in future designs.
  - Comprises a centralized lessons learned location that can help reduce time and effort for resolving both individual incidents as well as problems.
  - Essential for Quality/ISO certifications and audits.

Multiple Activities and Tools in Reliability Program



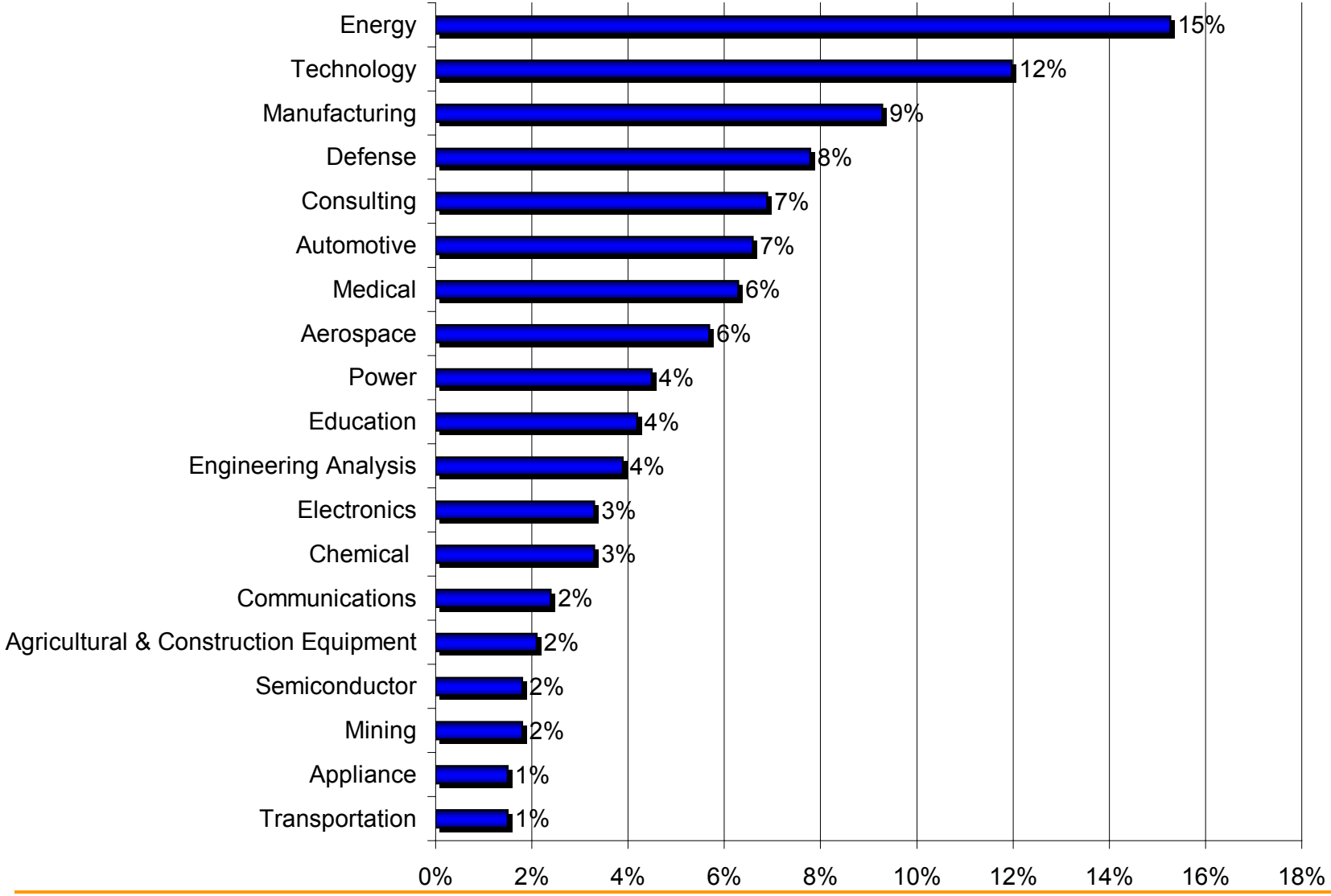
Micro Reliability: Statistic Tools Used in Reliability Program



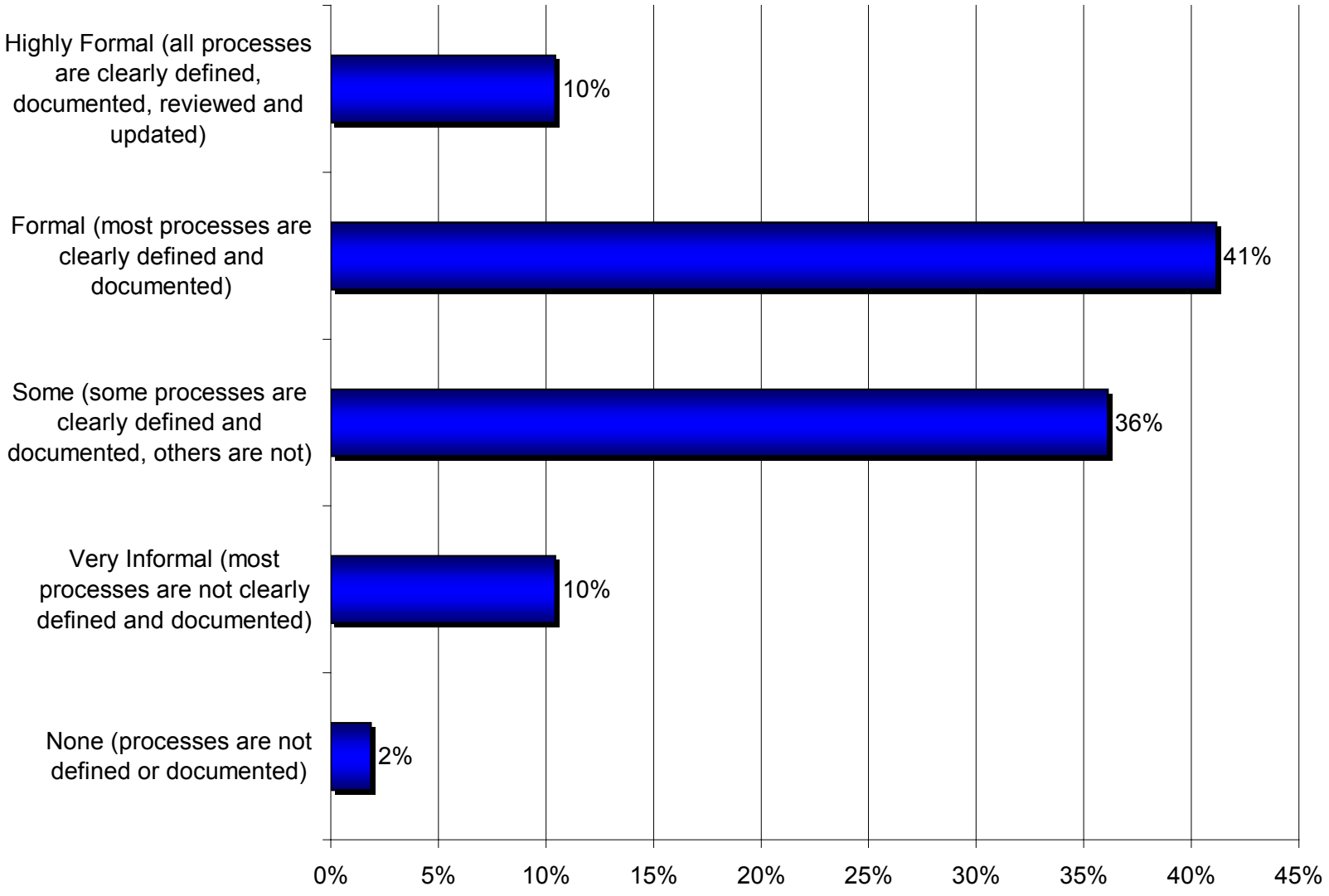
Reliability Program in Various Industries

- **In 2009, *ReliaSoft* conducted a survey on Reliability Programs from hundreds of companies.**
- **The survey tells us:**
  - How many of the companies have reliability programs and at what extent.
  - What are the commonly used tools in a reliability program.
  - And more….

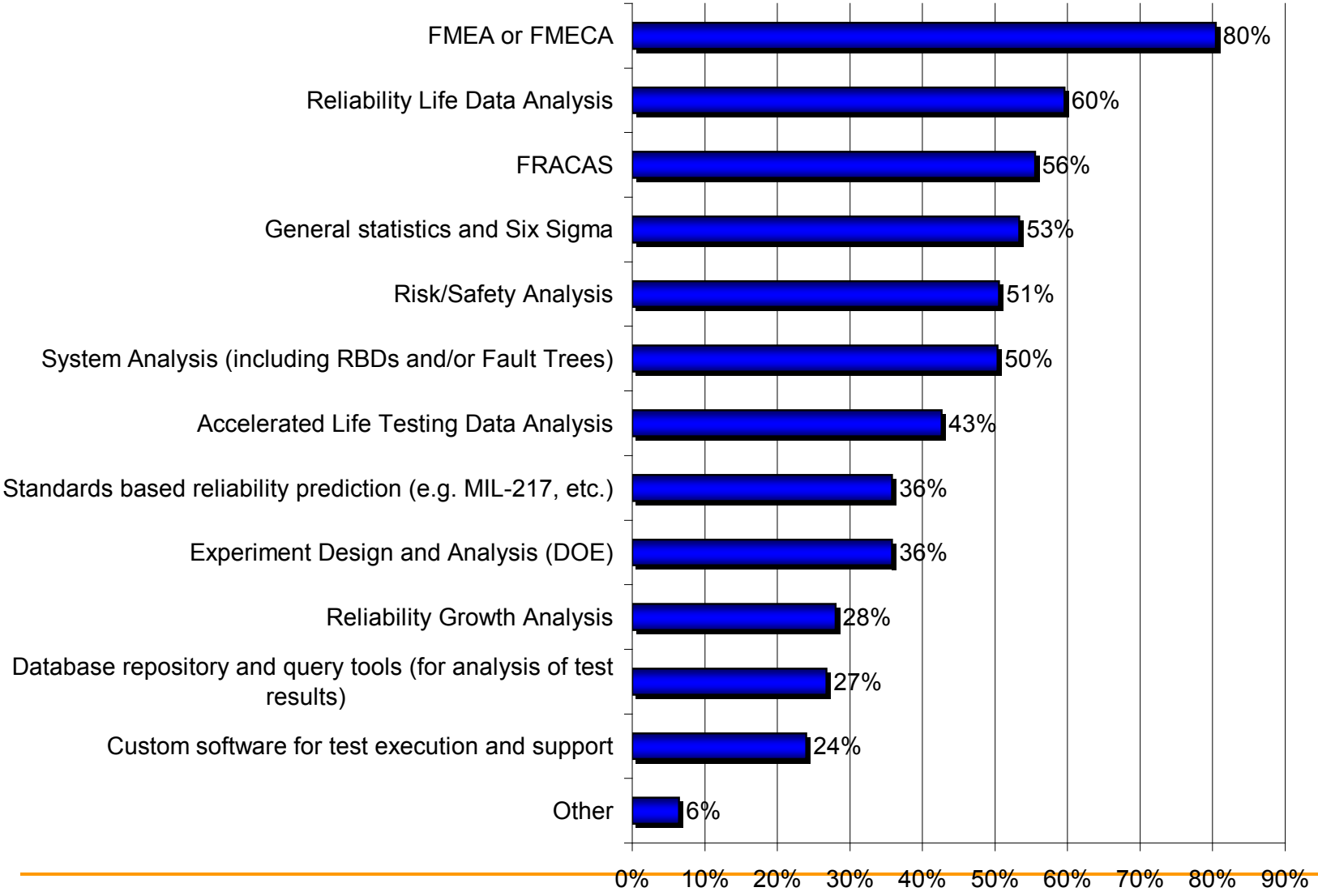
Industry Sectors Represents in the Survey



Status of Reliability Program at Various Companies



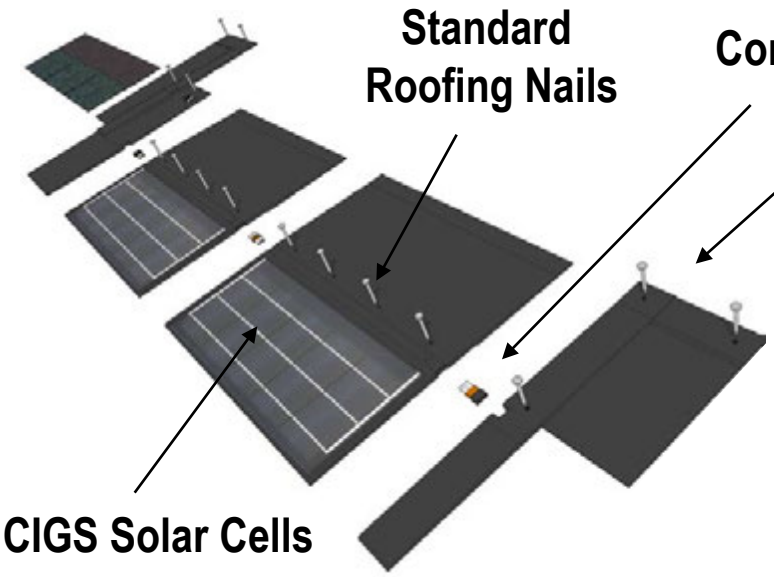
Management and Statistic Tools Used in a Reliability Program



Reliability Program for New PV Module Companies

- **How should a new PV module company set up a reliability program:**
  - Follow the reliability program guideline and tailor it for your company.
  - Use FRACAS to collect data and document all the mistakes and successes, and come up with acceptable plans for each reliability task.
  - Integrate reliability tasks with the concept, design, manufacturing and field use stages. Find out which reliability tasks can best benefit the company and start from them.
  - Start from small projects and show the benefit to managers. For example, use FMEA to identify failure modes and set up test plans; use HALT to identity the design flaws and thus improve the design.

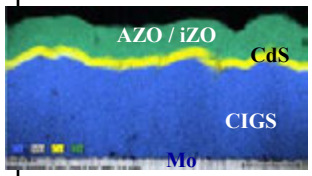
The Design… DOW™ POWERHOUSE™



Designed With A Roofer In Mind

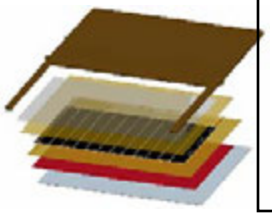
Need to overcome Design, Process, Installation Challenges to make a 20+ yr product

PV Knowledge
Thin Film Expertise
Process Knowledge
Efficiency Road Map





Reliability
20+yr Roofing product
20+yr PV product



Product Design
10 materials
Organic /inorganic matl
10X CTE; 100X Modulus diff

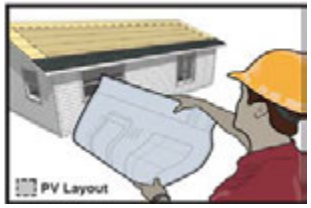
Roofing Product
PV product
One system

Power Conversion
Shading mitigation
Every home is different
DC to AC conversion



Process Steps
1000 x viscosity diff
Residual stresses



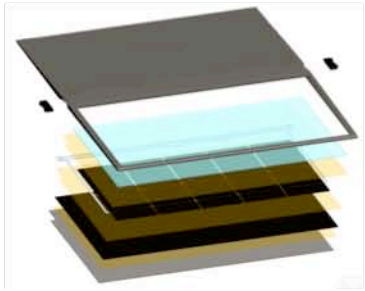


Channel
New Home/Reroofing
Design Capabilities

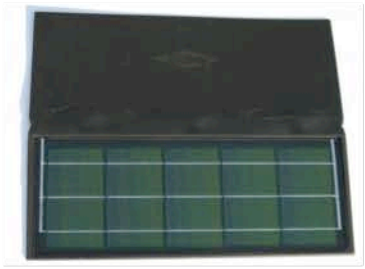
Reliability….



PV Cells



DOW™ POWERHOUSE™
Electrical Components & Materials



DOW™ POWERHOUSE™
Shingle



DOW™ POWERHOUSE™
Shingle Array

Test Protocols

- More than 10,000 parts tested/undergoing test
- Stress factors → temp, UV, hail, fire, rain, wind, ice, snow, humidity, electrical and force loads
- Reliability engineering tests "to failure" with focus on component, sub-system, and system level tests
- Application of modeling and physics of failure approach to derive transfer function between accelerated tests and life in field

Component



Sub-System



System



Lessons from Dow's Reliability Program

- It is never too early to start testing parts and prototypes – especially in regard to outdoor testing.
- Understand how qualification tests (IEC61646) and empirically derived standards based reliability approaches (ex. MIL-HDBK-217, Telcordia SR-332) apply.
- Virtual modeling and testing is critical.
  - Reduced costs and time for product development.
  - Link between accelerated testing and field life expectations.
- Multiple stress level testing is often required to derive appropriate acceleration factors.
- Both top down (system) and bottom up (component) approaches are useful.
- For a reliability program to be successful buy-in is necessary at all levels of the company and supply chain:
  - R&D, Manufacturing, Commercial, Supply Chain
  - Suppliers and Installers
  - Failure Reporting and Corrective Actions
- Suppliers may need assistance in understanding reliability requirements and setting up reliability programs.

From Climate Data to Accelerated Test Conditions

Michael Köhl

Fraunhofer Institute for Solar Energy Systems

Freiburg, Germany

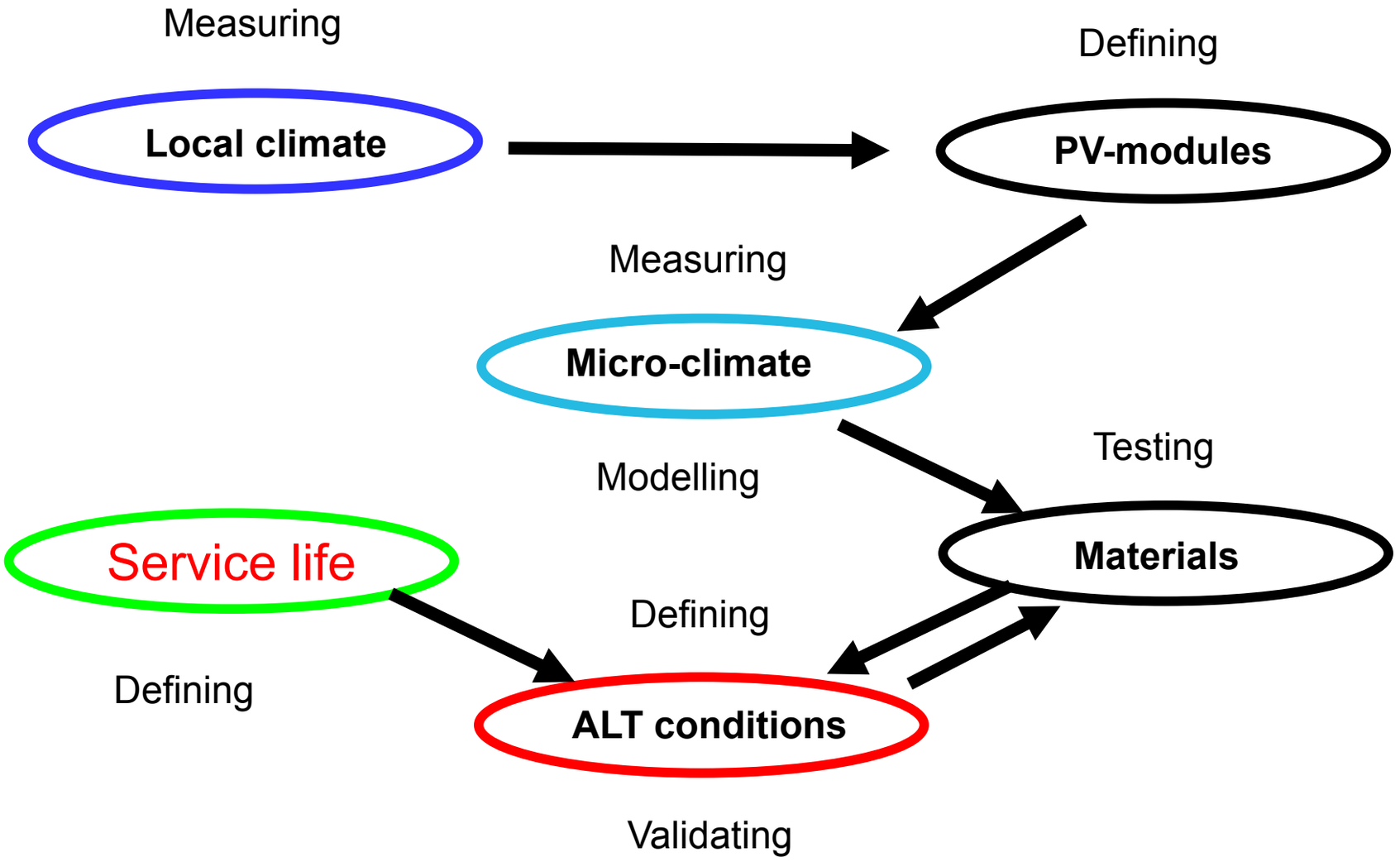
Presented at the PVMRW, Golden, February 2011

© Fraunhofer ISE

Fraunhofer ISE

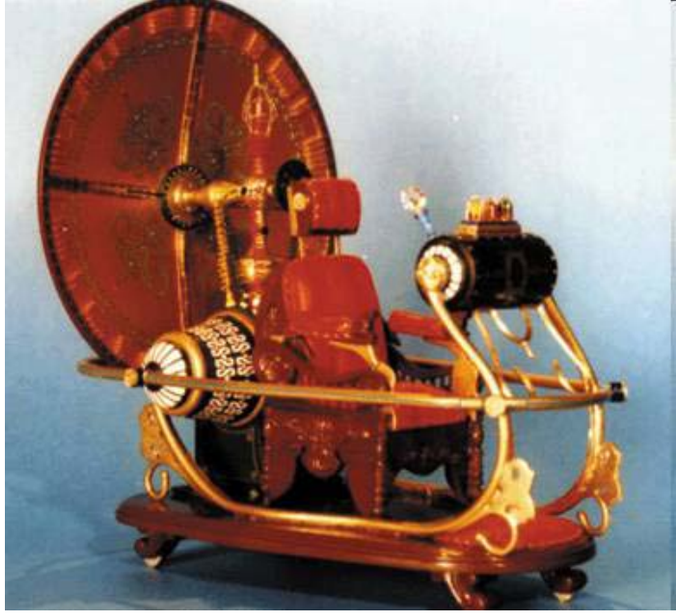
General methodology

Modeling the ALT conditions based on realistic loads



© Fraunhofer ISE

Simple deterministic model for aging processes: Time-transformation functions



Changes of property P after the testing time Δt_i

$$\Delta P = \Sigma^{m}_{j=1} \{$$

Temperature	$+ A\ \Delta t_i\ \exp[-E_A / RT_i]$
Moisture	$+ B\ \Delta t_i\ f(rh)_i\ \exp[-E_B / RT_i]$
UV-Radiation	$+ C\ \Delta t_i\ I^n_i\ \exp[-E_C / RT_i]$
T cycles	$+ D\ \Delta t_i\ f(\Delta T)_i\ \exp[-E_D / RT_i]$
Potential I D	$+ E\ \Delta t_i\ f(P)_i\ f_p(rh)_i\ \exp[-E_E / RT_i]$
Salt	$+ F\ \Delta t_i\ f(S)_i\ f_p(rh)_i\ \exp[-E_F / RT_i]$
……	$+ \ldots\ldots X\ \Delta t_i\ I^n_i\ f(X)_i\ \exp[-E_X / RT_i]\ \ldots\ldots\}$

Sample dependent degradation process parameters

Module temperature T

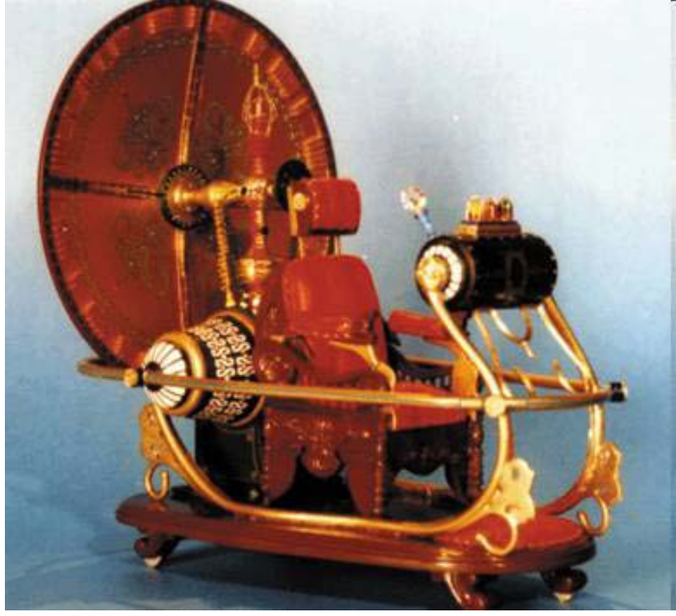
Micro-climatic stress factor

Time-interval Δt_i

Other degradation factors or synergistic effects

© Fraunhofer ISE

Simple deterministic model for aging processes: Time-transformation functions



Changes of property P after the testing time Δt_i

Degradation factor $\Delta P = \Sigma^{m}_{j=1} \{$

Temperature $+ A\ \Delta t_i\ \exp[-E_A / RT_i]$

Moisture $+ B\ \Delta t_i\ \mathbf{f(rh)_i}\ \exp[-E_B / RT_i]$

UV-Radiation $+ C\ \Delta t_i\ I^n_i\ \exp[-E_C / RT_i]$

Sample dependent degradation process parameters

T cycles $+ D\ \Delta t_i\ f(\Delta T)_i\ \exp[-E_D / RT_i]$

Potential I D $+ E\ \Delta t_i\ f(P)_i\ \mathbf{f_p(rh)_i}\ \exp[-E_E / RT_i]$

Salt $+ F\ \Delta t_i\ f(S)_i\ \mathbf{f_p\ (rh)_i}\ \exp[-E_F / RT_i]$

…… $+ \ldots\ldots X\ \Delta t_i\ I^n_i\ f(X)_i\ \exp[-E_X / RT_i]\ \ldots..\}$

© Fraunhofer ISE

Starting point: Outdoor exposure testing

Sites with extreme stresses

City or reference:

Freiburg Germany





Desert

Sede Boqer

Israel

Alpes

Zugspitze

Germany





Tropical

Serpang

Indonesia



Maritimes

Pozo Izquierdo

Gran Canaria

Monitoring degradation factors for modelling degradation

Measurement of module performance over time for validation of ALT

© Fraunhofer ISE

TÜVRheinland®
Genau. Richtig.

Fraunhofer ISE

End point: Outdoor exposure anywhere

Sites with climatic conditions known for one year at least

Examples (irradiation, wind, temperature, humidity data from 2007):

	Average temperature	Irradiation	UV dose
Goodwin Creek (warm and humid)	**16,6 °C**	**1631 kWh/m²a**	**83,20 kWh/m² a**
Desert Rock (Hot and dry)	**19,0 °C**	**2095 kWh/m²a**	**106,87 kWh/m² a**

© Fraunhofer ISE

Temperature

Difficulties:

1. Micro – climate (module temperature depends on module and climate)

2. Transient behaviour (changing temperature continuously, but delayed)

3. Accelerator for all degradation processes

Pay attention to thresholds changing degradation processes:

„ You never got a chicken by boiling an egg“

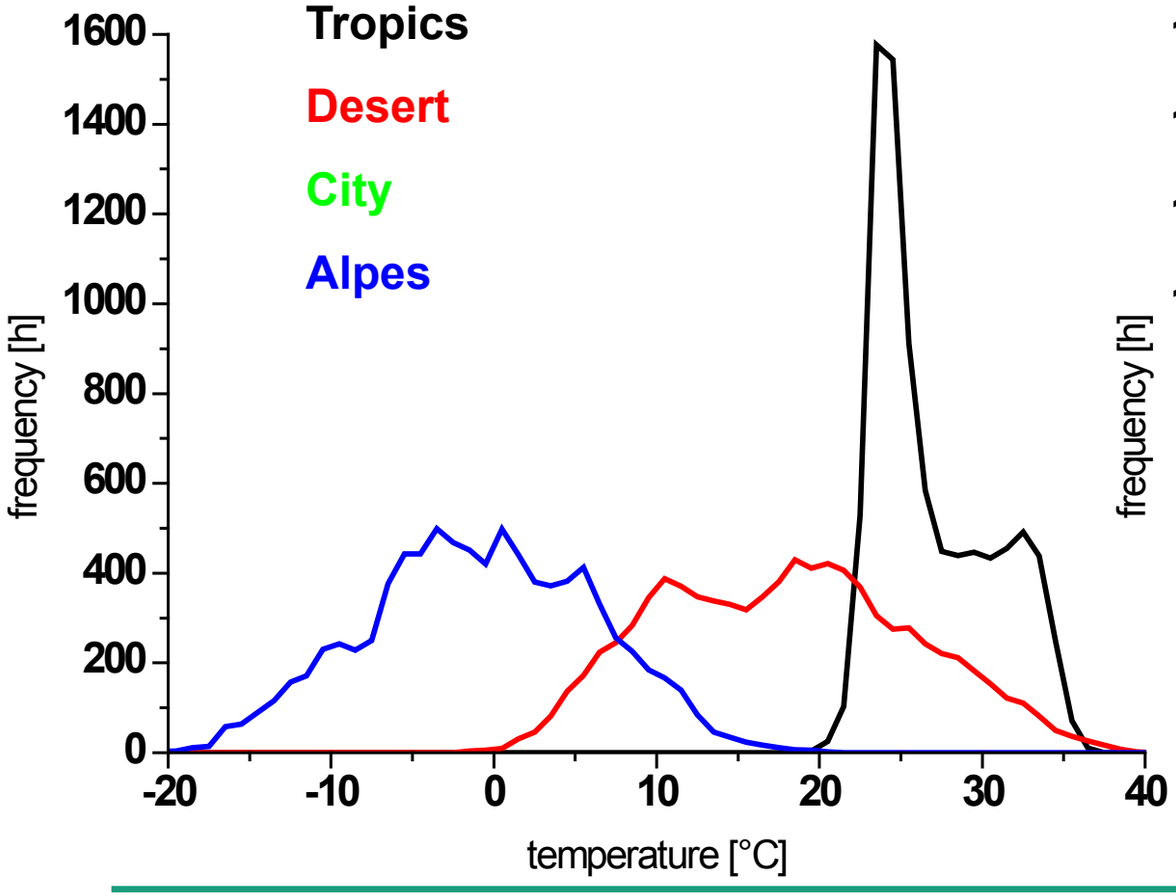
© Fraunhofer ISE

Outdoor testing

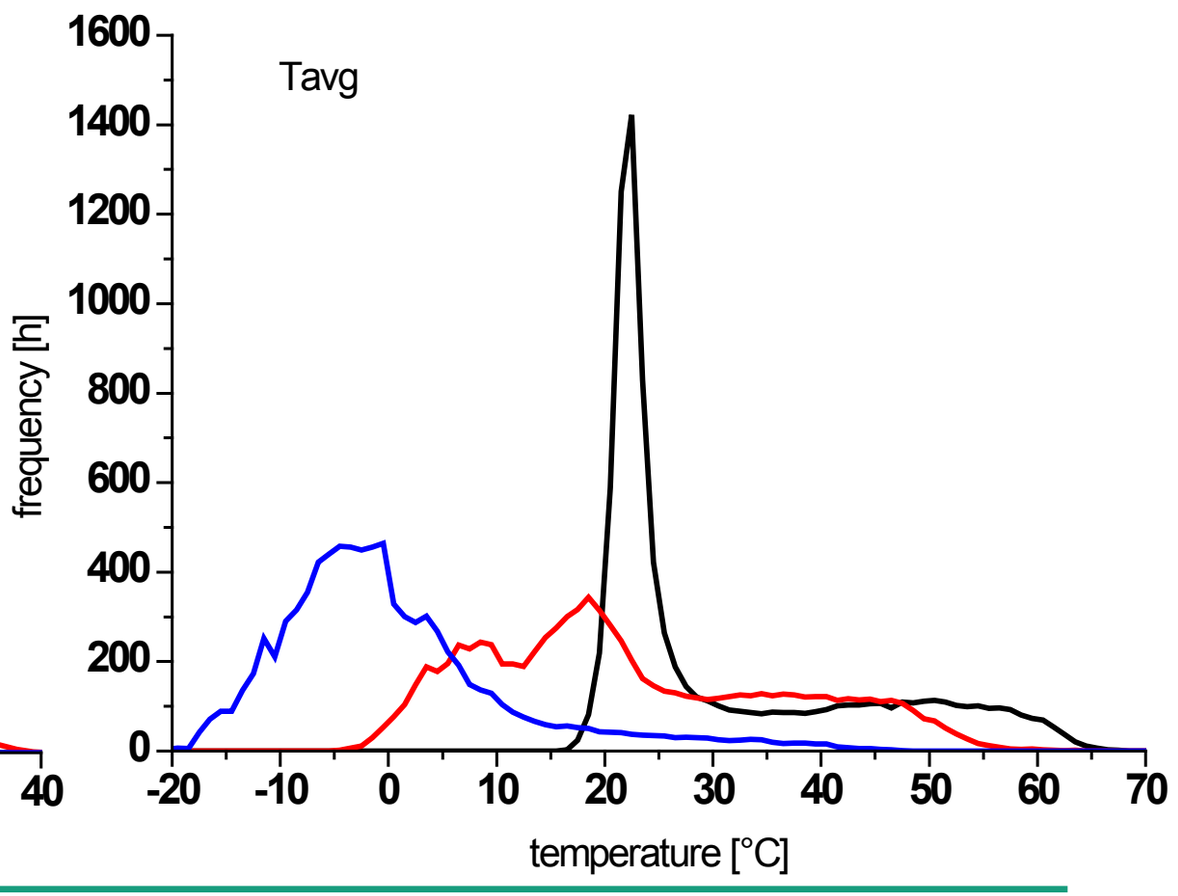
Temperature monitoring

Macro – climate => Micro – climate

Ambient temperature



Average module temperature (c-Si)



© Fraunhofer ISE

Fraunhofer ISE

Temperature evaluation for c-Si

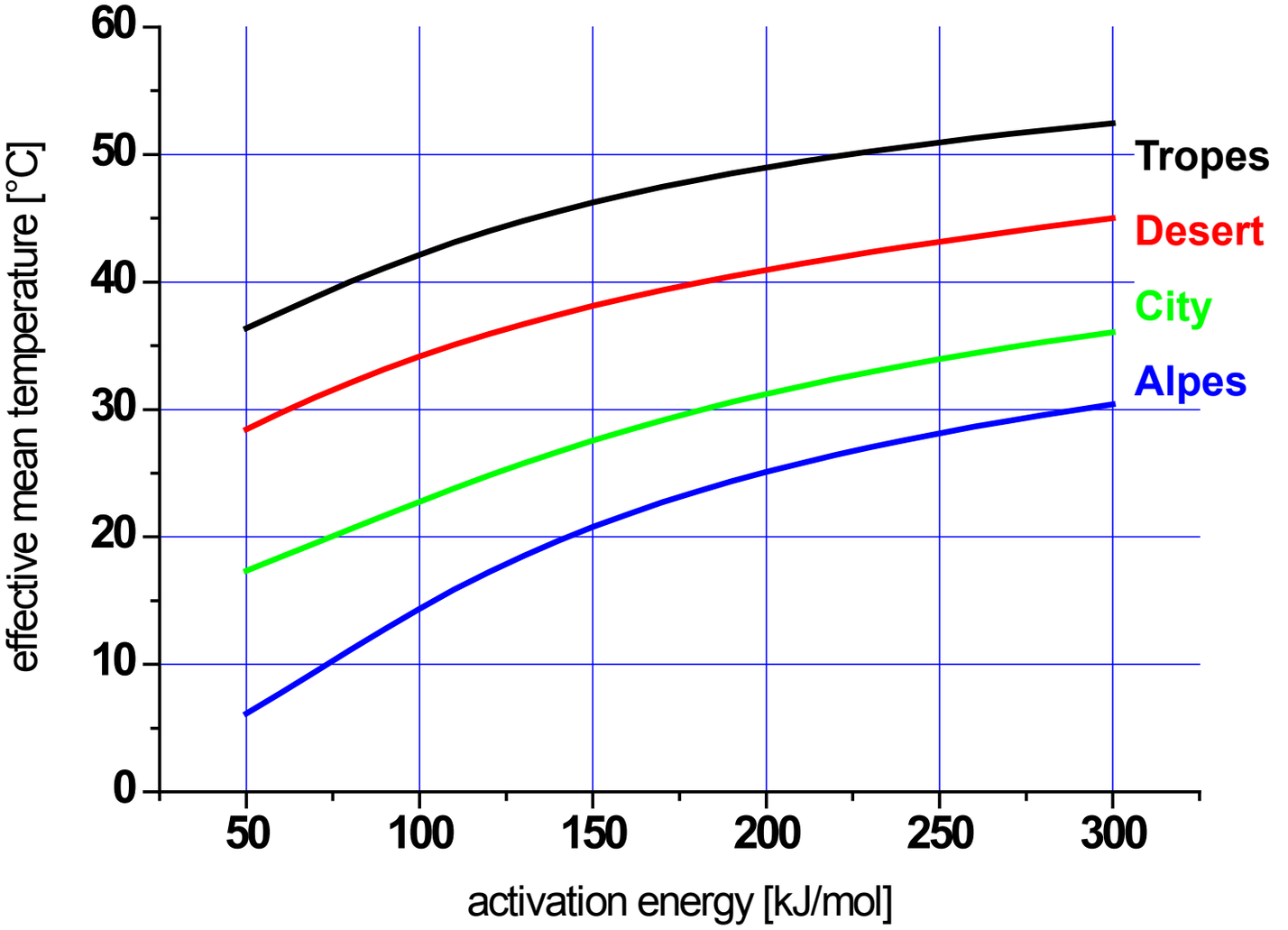
$$\exp[-E_p/RT_{eff}] = 1/(t_{max}-t_{min}) \sum^{tmax}_{tmin} \exp[-E_p/RT(t)]\Delta t$$

Effective Mean Temperature,

Constant test temperature that

Corresponds to the natural load in the same period

Depends on the activation energy of the degradation process



© Fraunhofer ISE

Life testing for degradation factor temperature

If their would be a degradation process without any external reaction partners

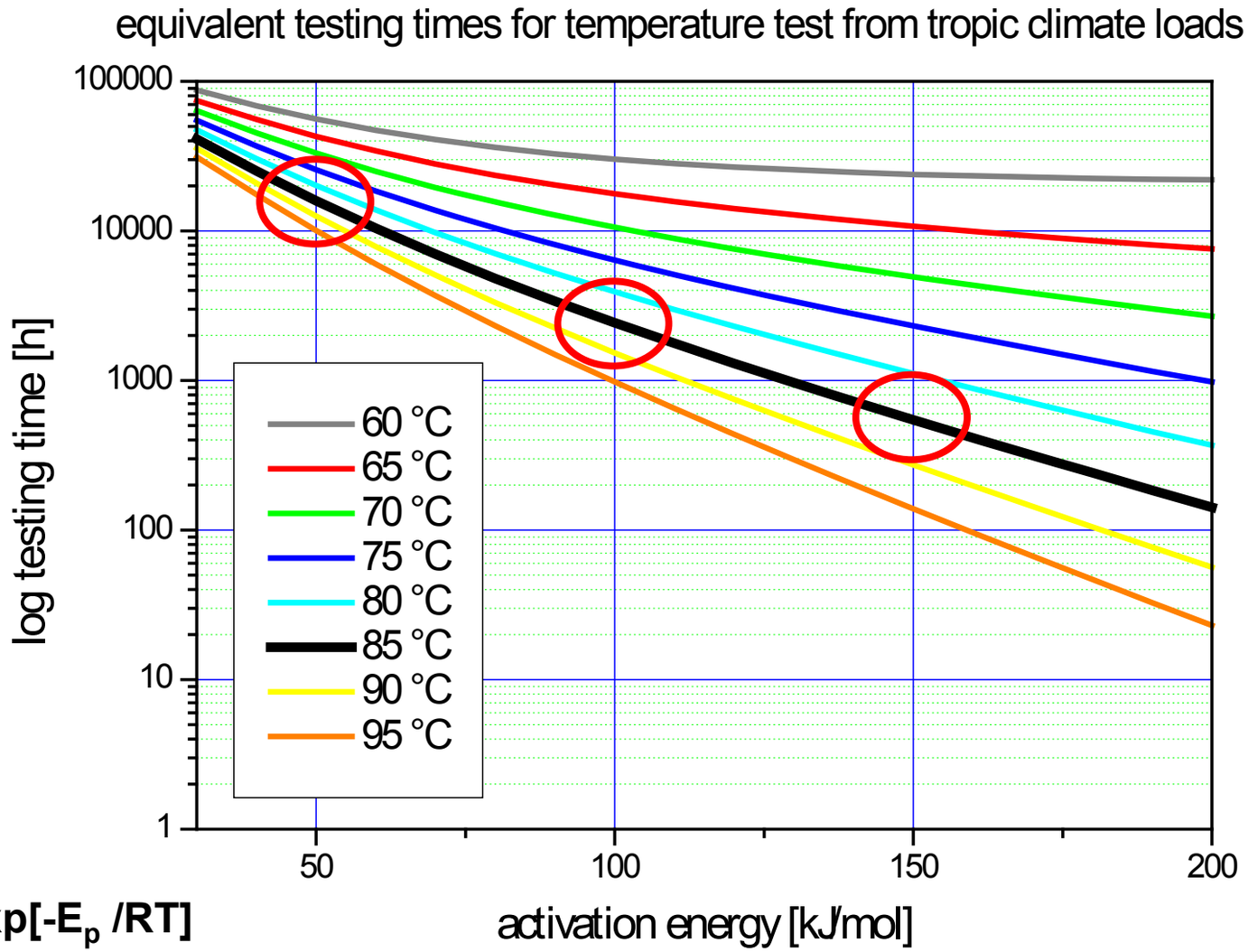
Might be tested simultaneously with the damp-heat test:

Some 100 to 10000 h

Equivalent Temperature Testing Times

for c-Si

for 25 a in tropical climates

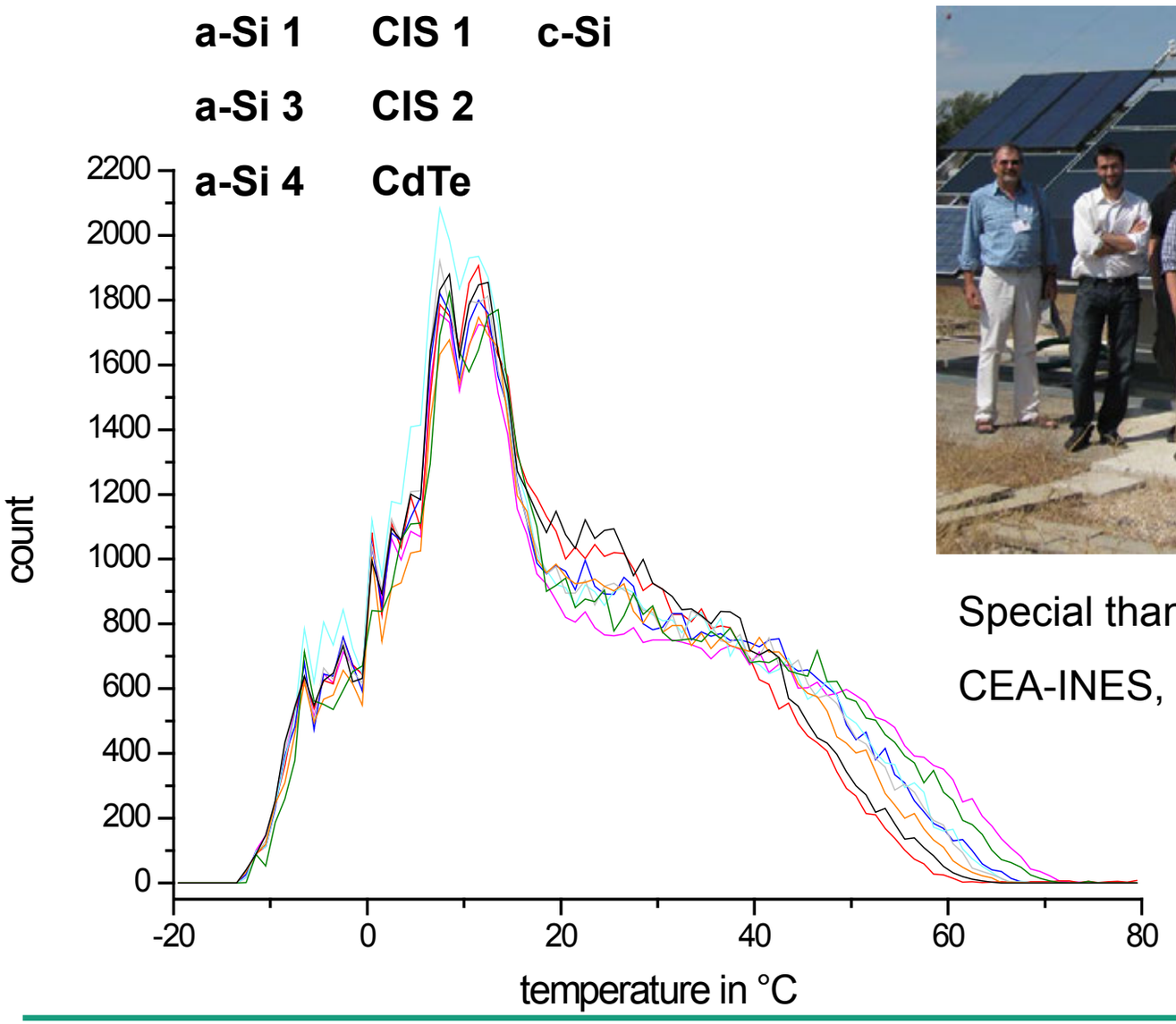


$t_{test} = 25*8760 \exp[-E_p /RT_{eff}] / \exp[-E_p /RT]$

© Fraunhofer ISE

Histogram of measured module temperatures in Cadarache, F

What about Thin Film Modules?





Special thanks to Antoine Guerin de Montgareuil, CEA-INES, Cadarache, France

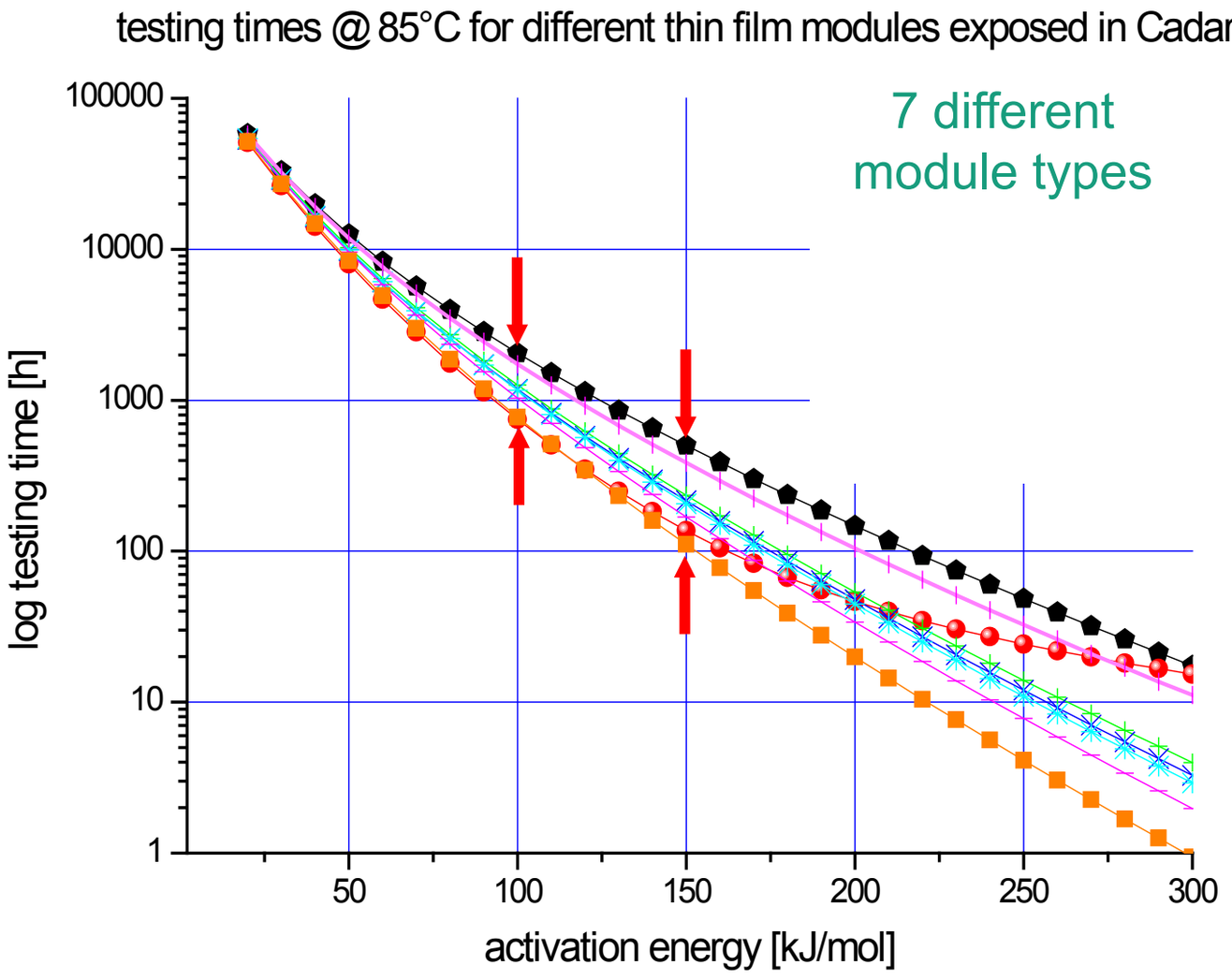
Module temperature for one year

© Fraunhofer ISE

Fraunhofer ISE

Corresponding temperature testing times at 85°C for 25 a exposure in Cadarache, France

based on monitored module temperatures



Different cell-types:

Factor 2 – 4 in testing time (depending on the degradation processes)

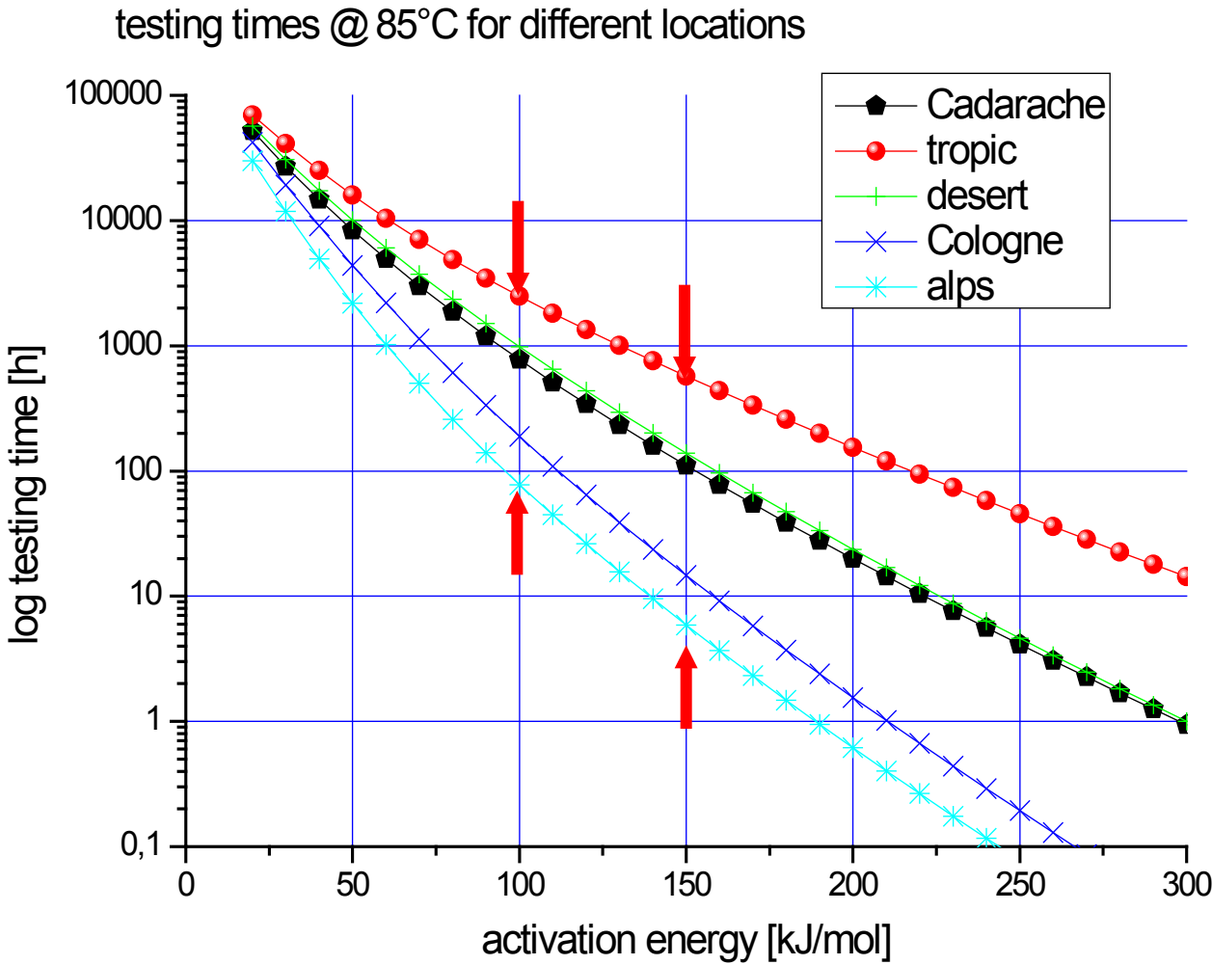
In the range of damp/heat

© Fraunhofer ISE

Fraunhofer ISE

Corresponding temperature testing times at 85°C for 25 a exposure of c Si modules in different climates

based on monitored module temperatures



Worst case tropics



Different climate-types:

Factor 20 – 100 in testing time (depending on the degradation processes)

© Fraunhofer ISE

Physical modeling of module temperature for each of the different module types using David Faiman's approach (could be King, Fuentes……as well)

Macro – climate => Micro – climate

Irradiation, wind, ambient temperature => T_{mod}

$$T_{\mathrm{mod}} = T_{amb} + \frac{H}{U_0 + U_1 \cdot \mathrm{v}}$$

T_{mod} module temperature

T_{amb} ambient temperature

v wind velocity

H solar radiation

	U1	U0
a-Si 1	10,7	25,7
a-Si 3	5,8	25,8
a-Si 4	4,3	26,1
CIS 1	3,1	23,0
CIS 2	4,1	25,0
CdTe	5,4	23,4
c-Si	6,2	30,0

U_0 , U_1 = module dependent parameters

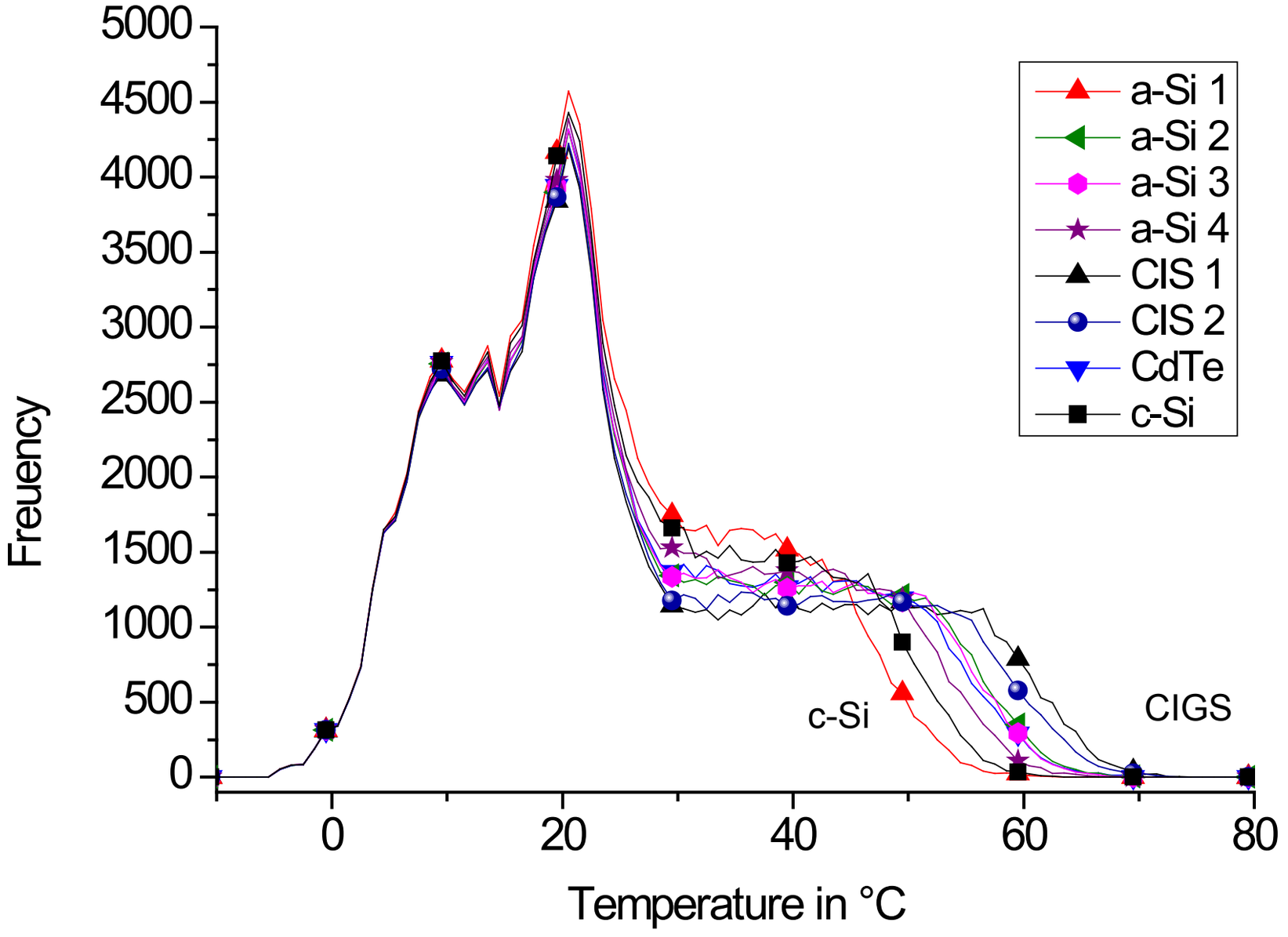
Neglected: IR-radiation exchange and natural convection

The parameters U are module-specific but location independent

M.Koehl et.al.: Modelling of the nominal operating cell temperature based on outdoor weathering, Sol. Energy Mat. Sol. Cells (2011)

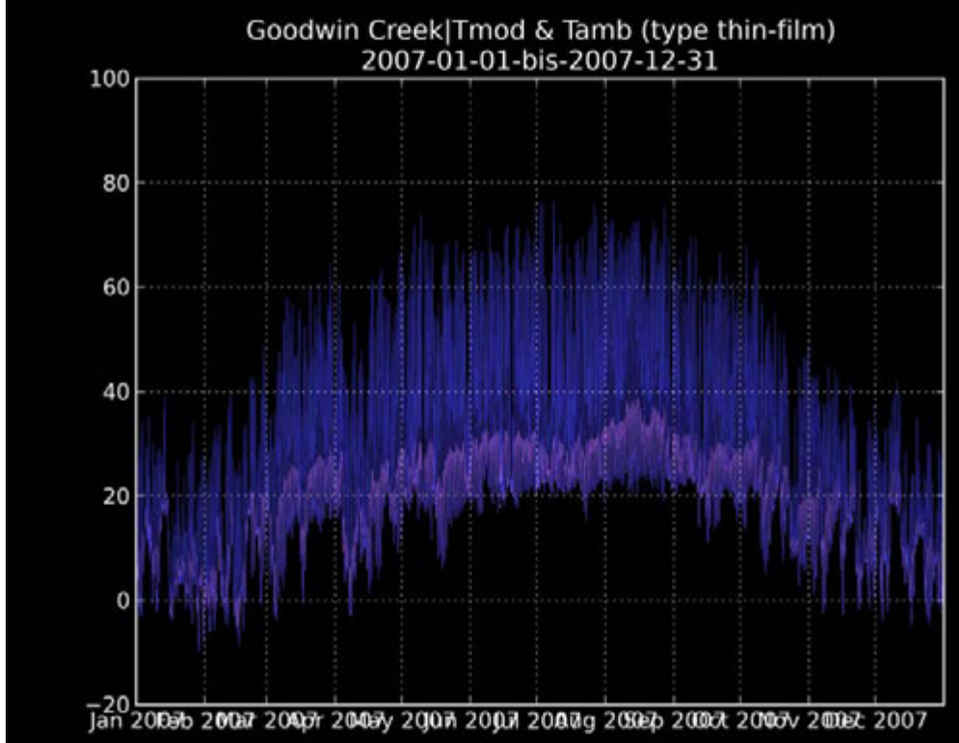
© Fraunhofer ISE

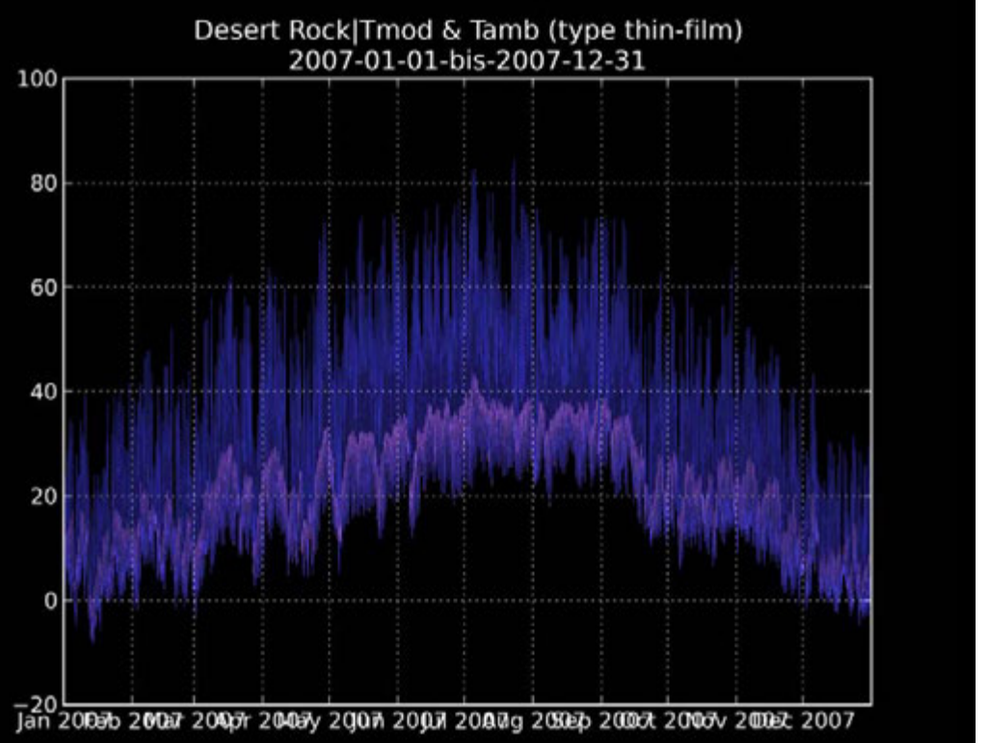
Histogram of simulated module temperatures in the Negev

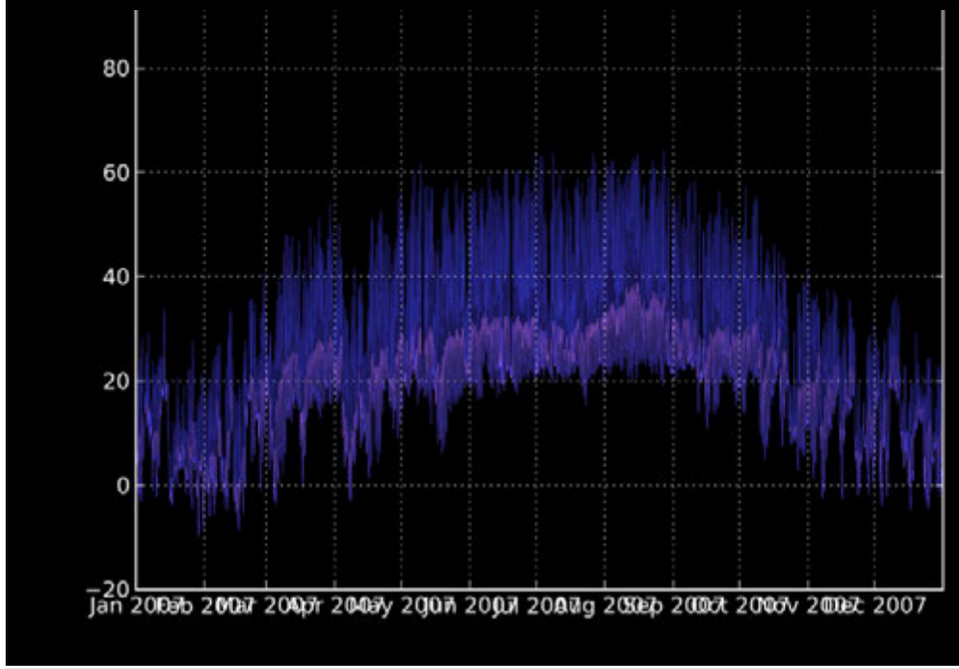


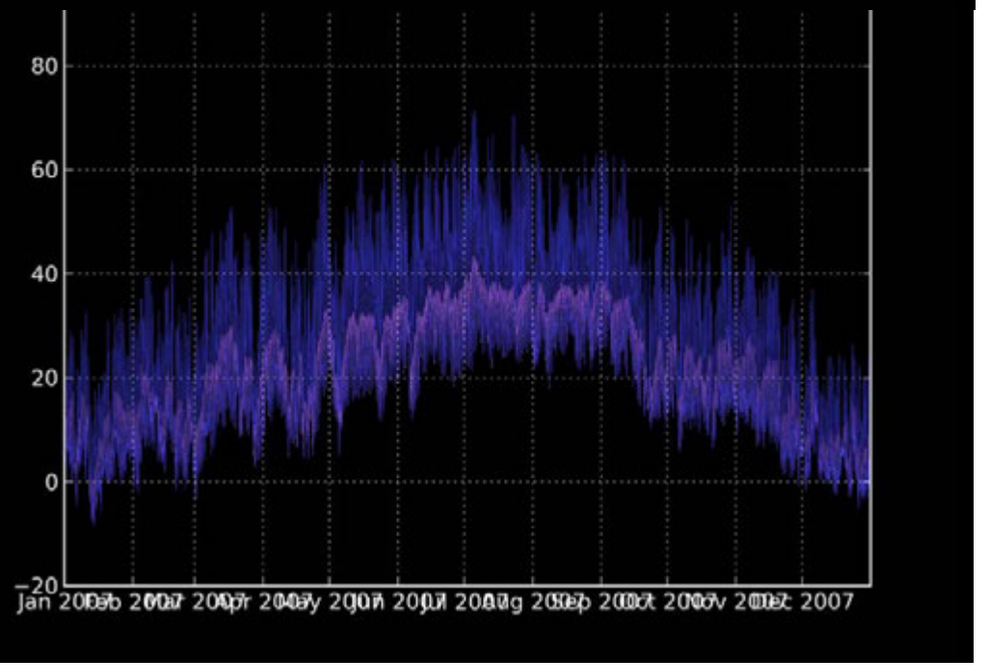
© Fraunhofer ISE

Fraunhofer ISE









© Fraunhofer ISE

Temperature load

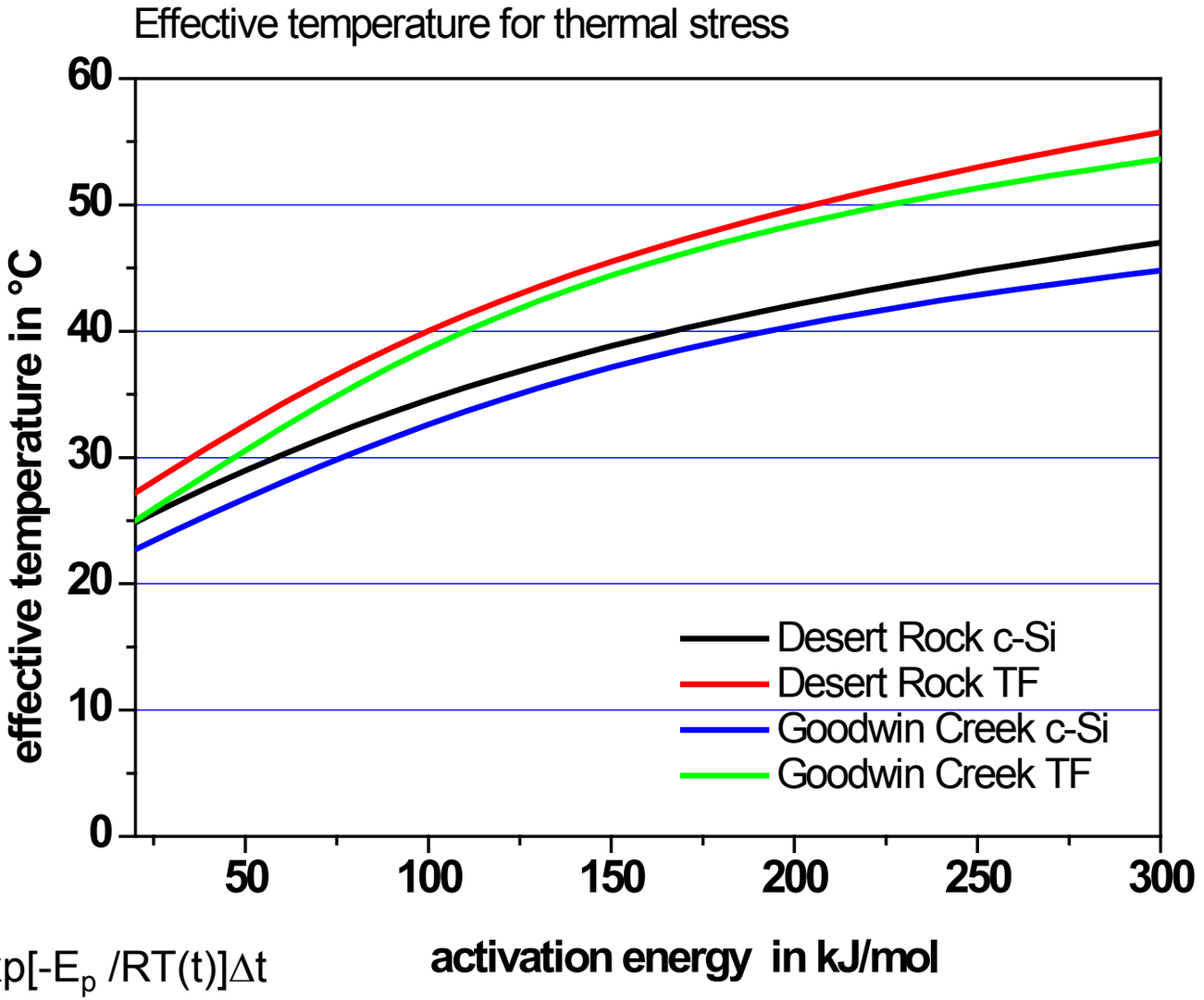
Accelerator for all degradation processes

Effective temperature:

The constant temperature needed for obtaining the same degradation as for outdoor exposure

Characteristic for location and module type

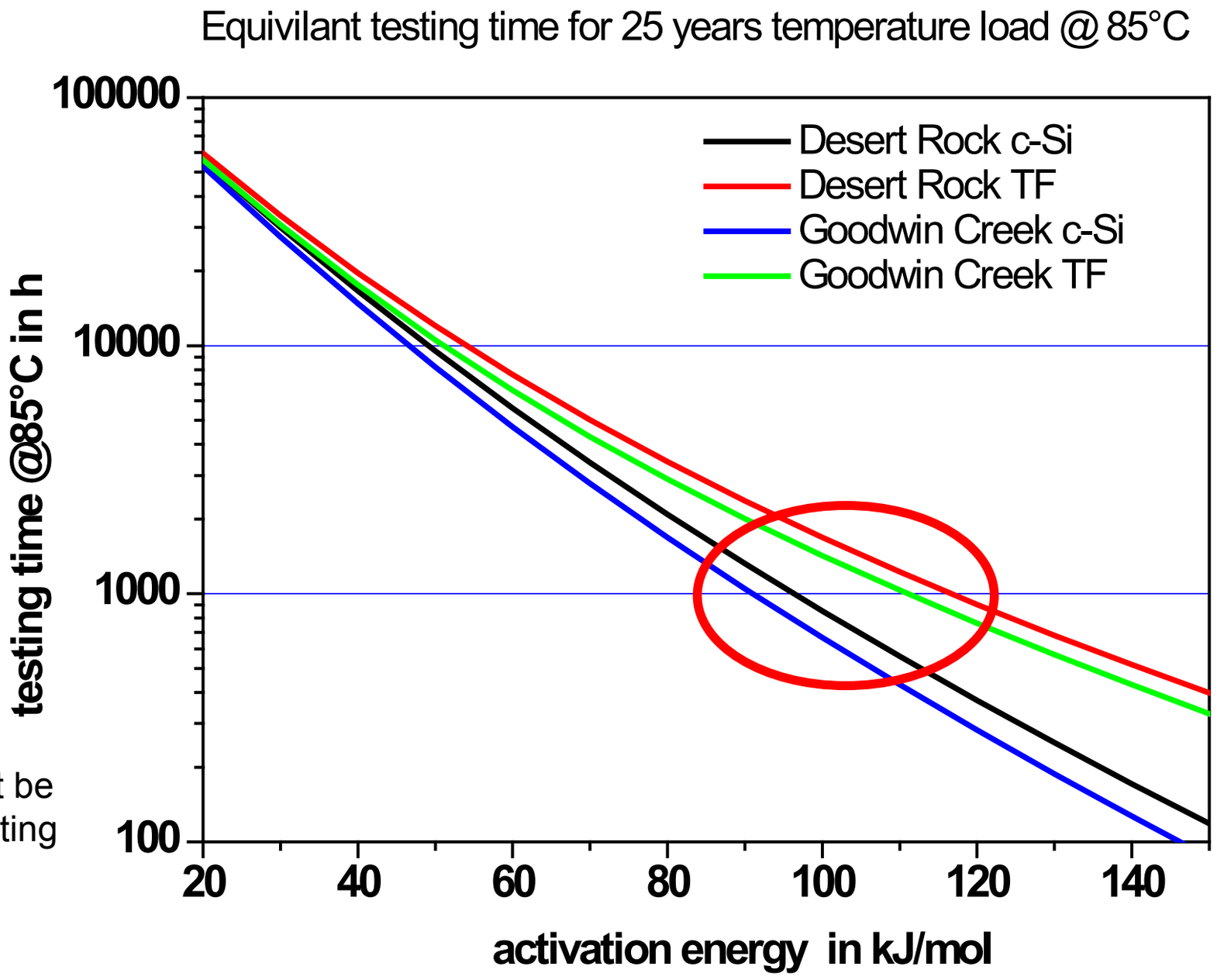
Type is more relevant here



$$\exp[-E_p/RT_{eff}] = 1/(t_{max}-t_{min}) \sum^{tmax}_{tmin} \exp[-E_p/RT(t)]\Delta t$$

© Fraunhofer ISE

Temperature testing



Temperature testing might be included in damp-heat testing without distinguishing the degradation processes

© Fraunhofer ISE

UV-radiation

Problems:

1. Measurement of UV-radiation

2. Reciprocity (Dose is I*t, or t = Dose/I)

3. Spectral sensitivity of the samples is not known

4. Differences of the UV-sources of the test facilities *

5. Temperature impact

**IEC TC82 WG2 – Round Robin for measurements of UV testing devices*

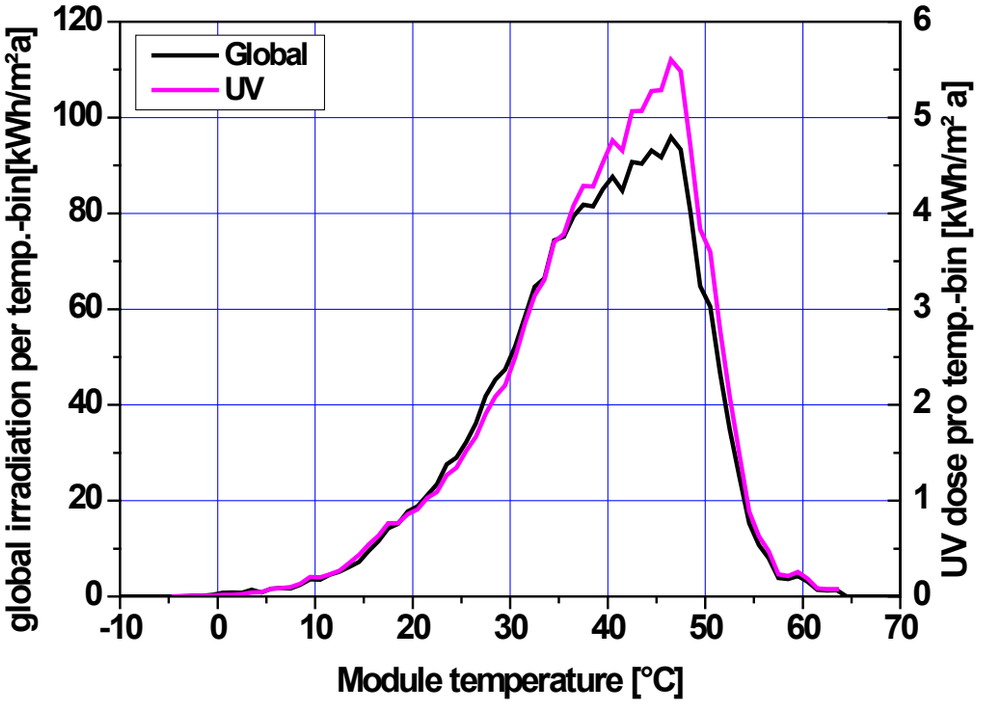
© Fraunhofer ISE

Outdoor testing

Radiation monitoring

Accumulated dose of UV- and solar radiation for one year in the desert:

120 kWh/m² (about 8 x IEC)

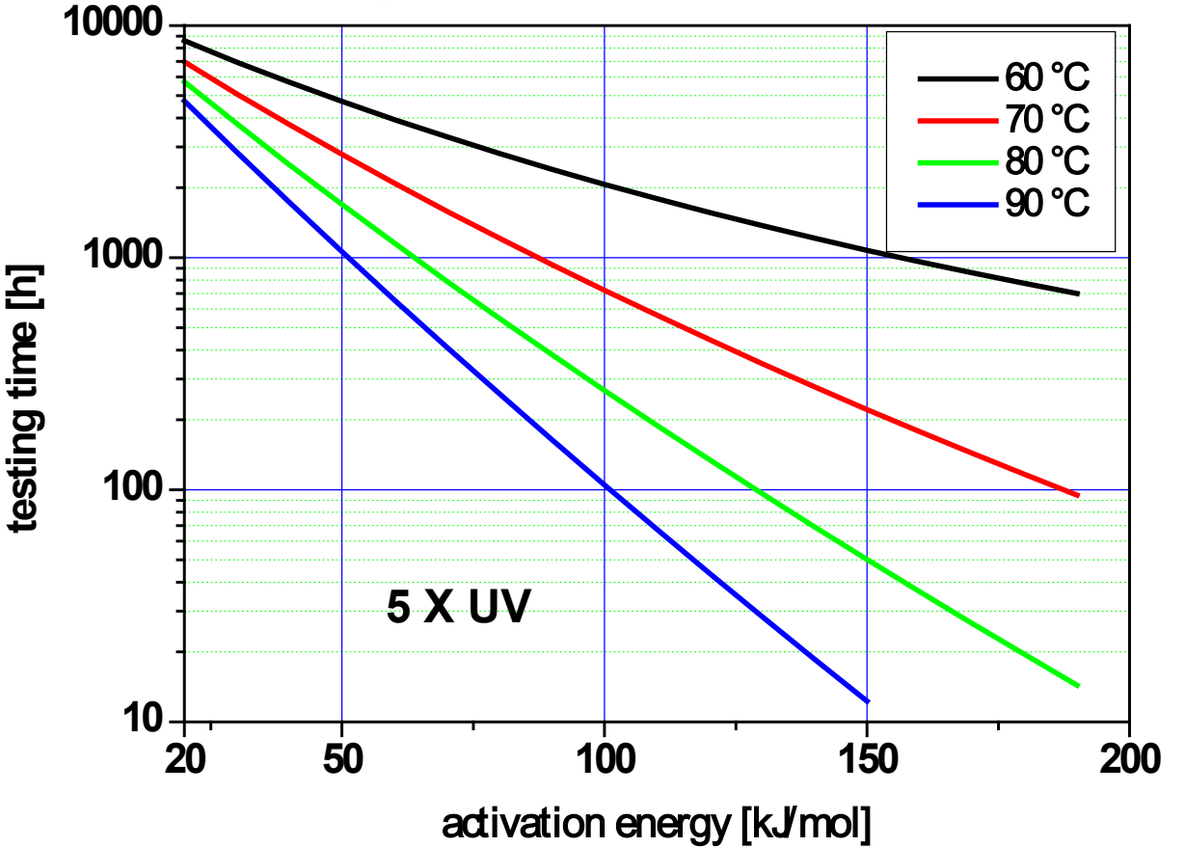


UV = 5.X % of solar radiation

Reciprocity: p = 1

$$t_{test} = (I_i / I_{test})^p \, \Delta t_i \cdot \exp\left[-(E_a / R)\cdot(1/T_{test} - 1/T_i)\right]$$

equivalent testing times for five suns UV test for desert climate loads



© Fraunhofer ISE

Fraunhofer ISE

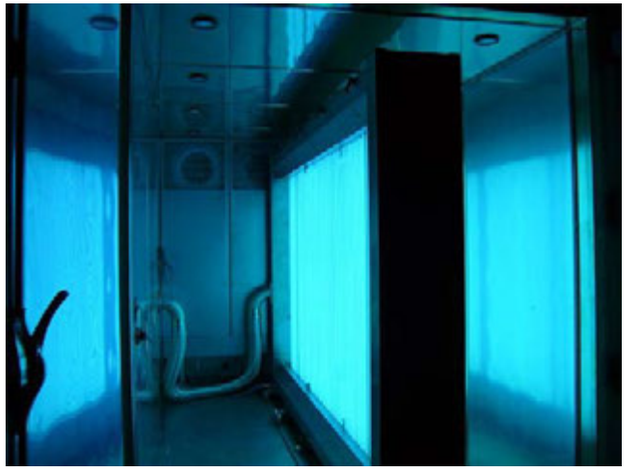
UV - radiation modelling

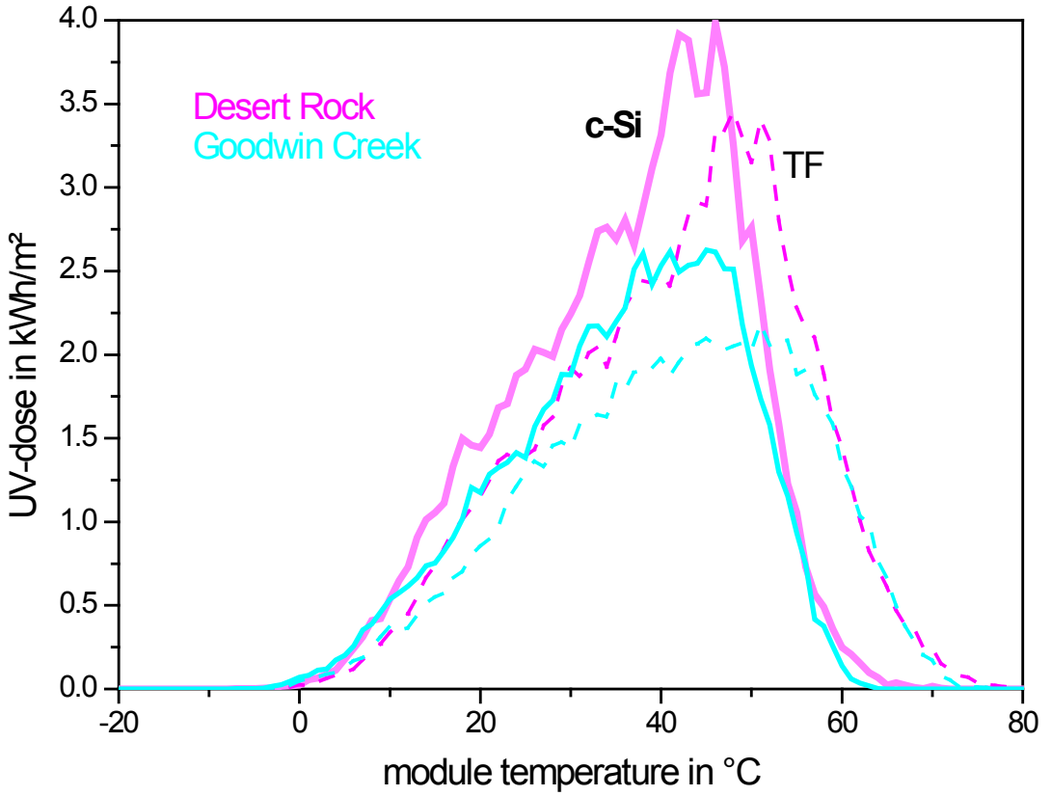
Desert Rock: **106 kWh/a m²**

Goodwin Creek: **83 kWh/a m²**

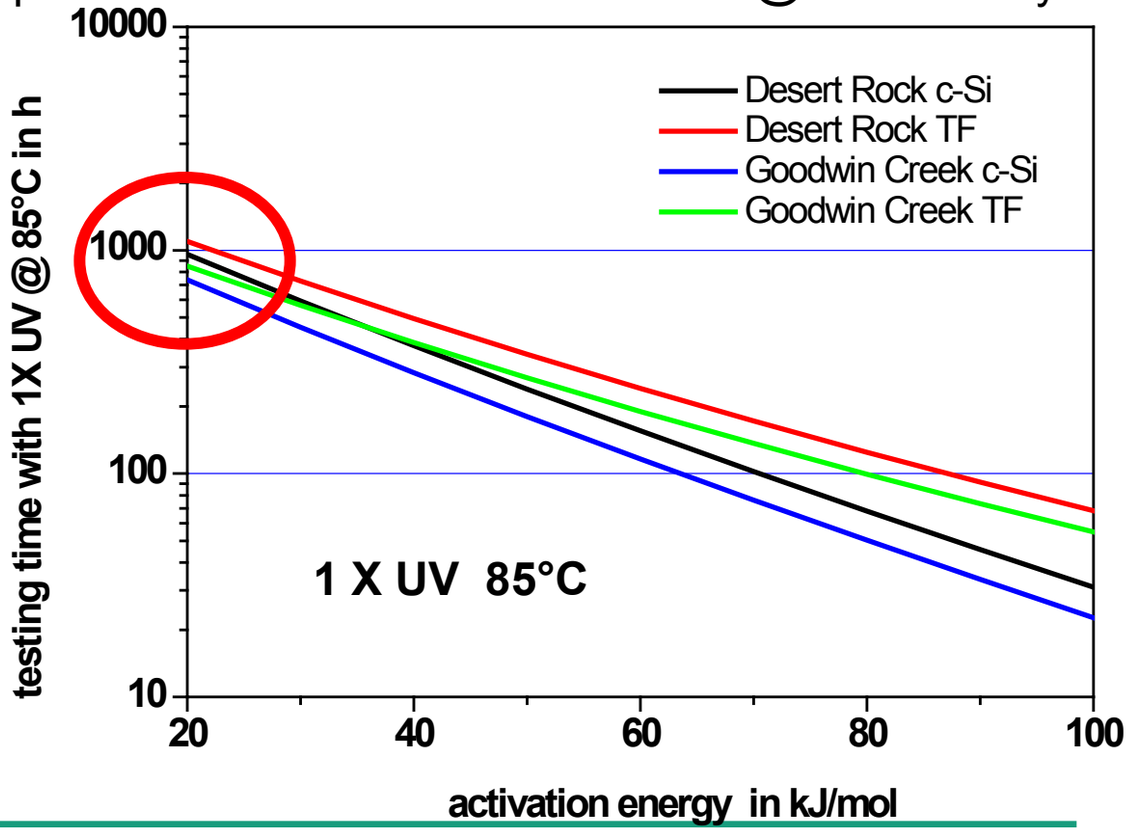
4-5 suns

Elevated temperature





Equivalent constant load for 1 sun UV @ 85°C for 1 year



© Fraunhofer ISE

Fraunhofer ISE

Humidity

Problems:

1. Assessing micro – climate

2. Transient behaviour (changing partial pressure gradients)

3. Slow diffusion in encapsulants or edge sealants (hard to accelerate)

=> non-uniform polymer degradation above cells after 4000h damp-heat*

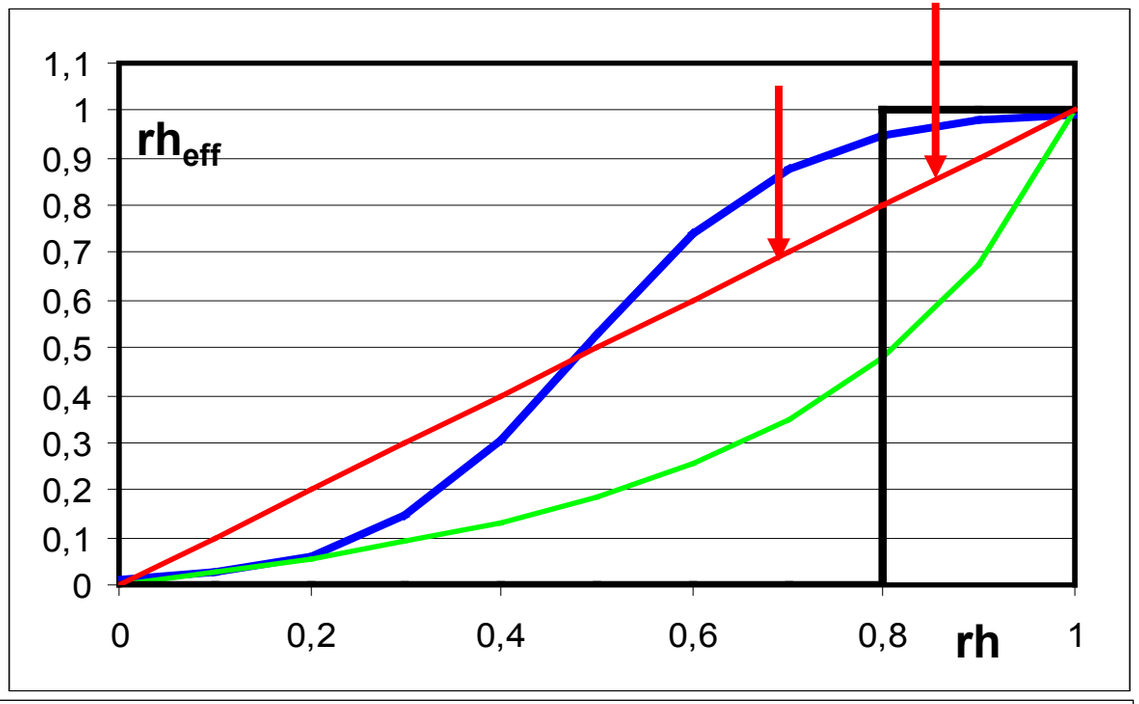
**C. Peike et.al.: Non-destructive degradation analysis of encapsulants in PV modules by Raman Spectroscopy, Sol. En. Mat. Sol. Cells (2011)*

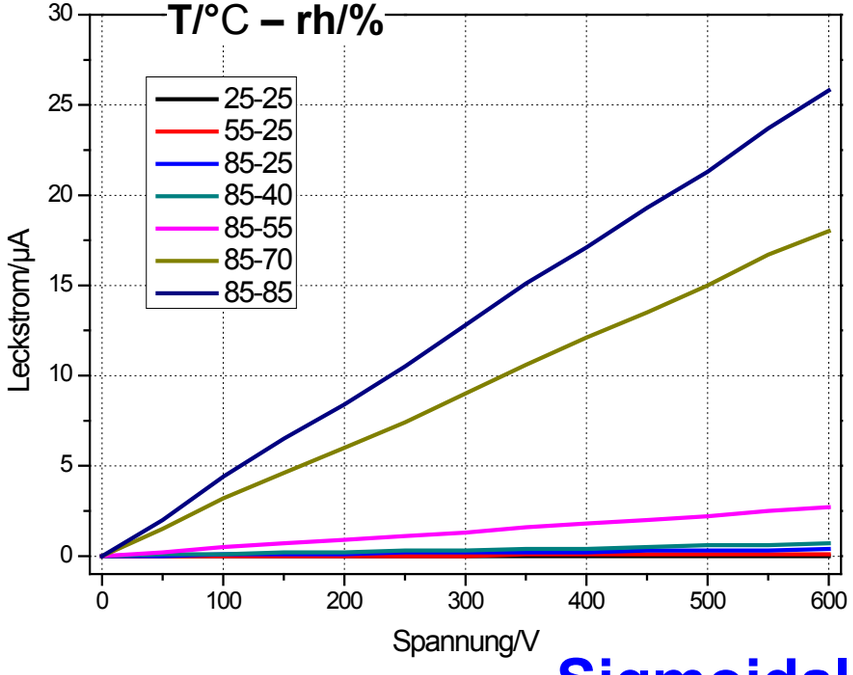
© Fraunhofer ISE

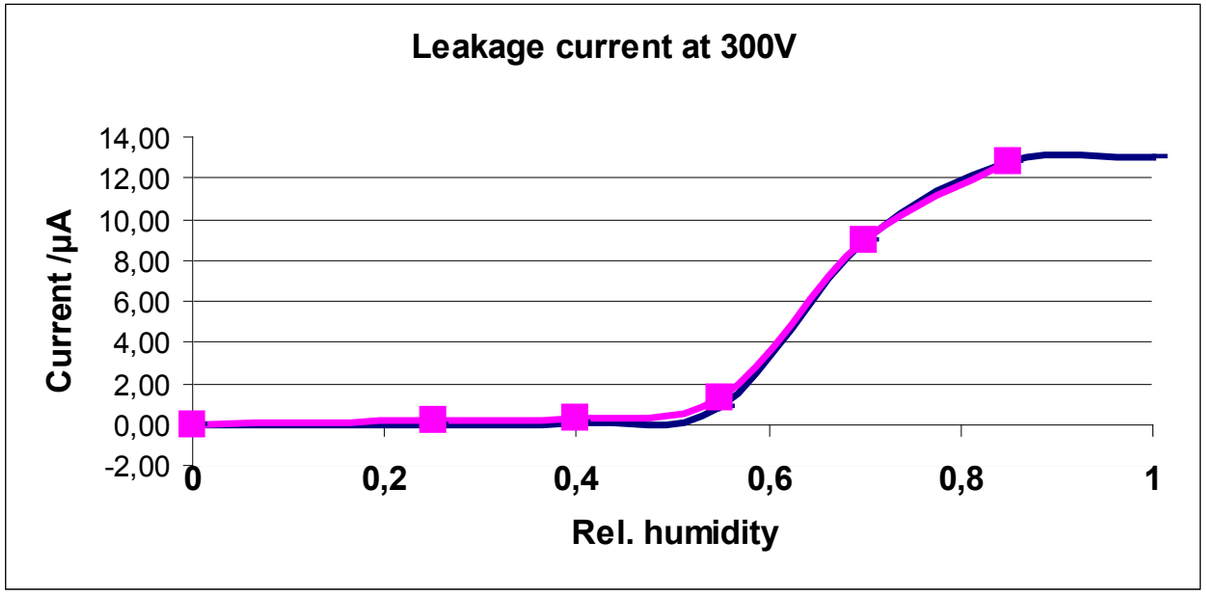
Effective humidity

Modelling humidity impact onto modules
based on surface humidity

- Climatic cabinet
- Leakage current







Sigmoidal Model: $I_{leak} = G/(G+ \exp(-rh*k) *(G/f(0)-1))$

© Fraunhofer ISE

Fraunhofer ISE

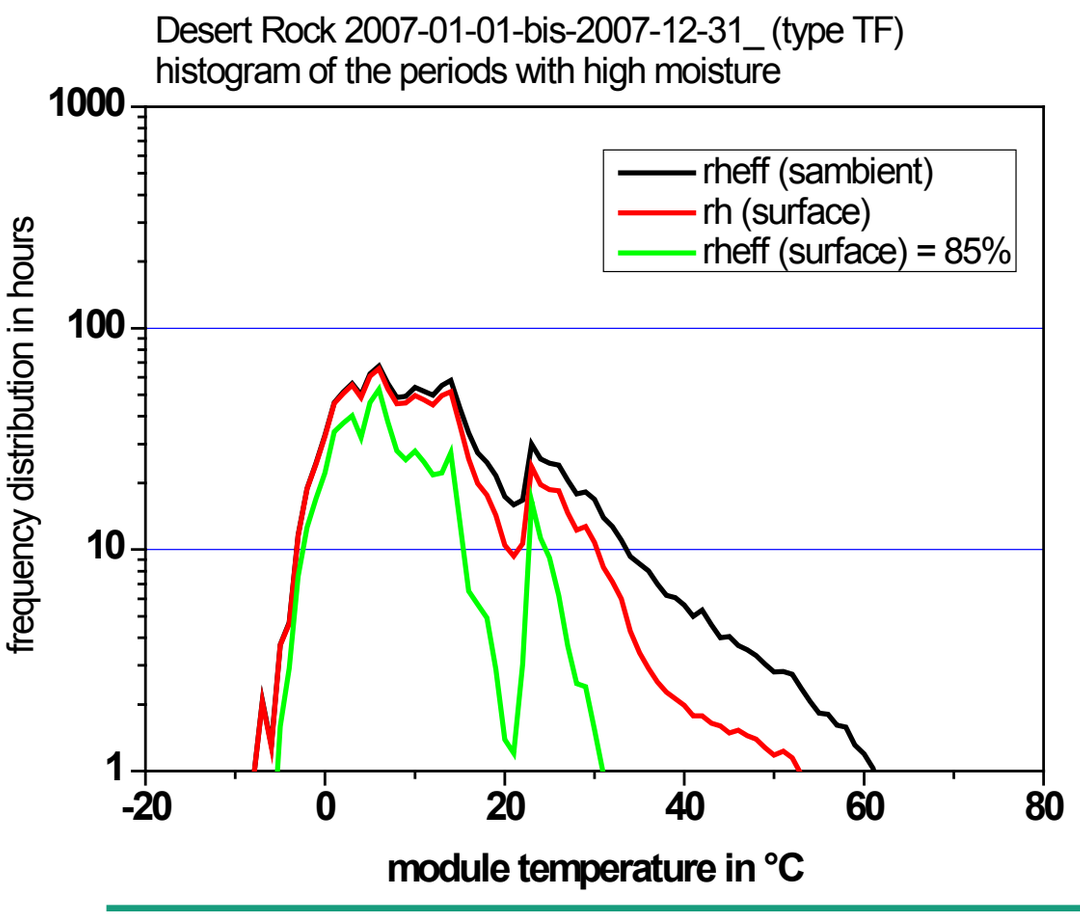
Simulated histograms of the relative humidity

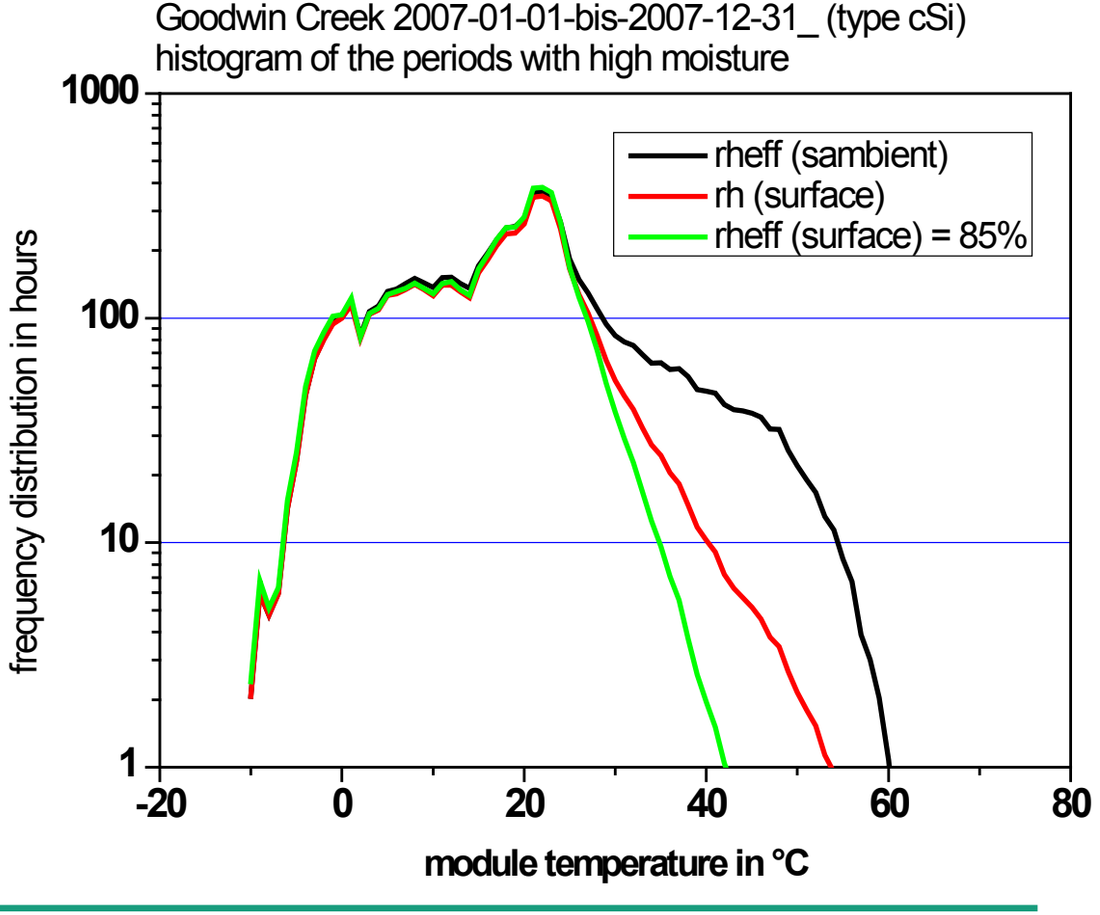
Ambient humidity = partial pressure / saturation pressure (T_{amb})

Surface humidity = partial pressure / saturation pressure (T_{modul})

Eff. Humidity: $rh_{eff} = 1/(1+ \exp(-rh*k) *(1/f(0)-1))$

Humidity dose: $\Delta t_{eff} = \Delta t * rh_{eff} / 0.85$





© Fraunhofer ISE

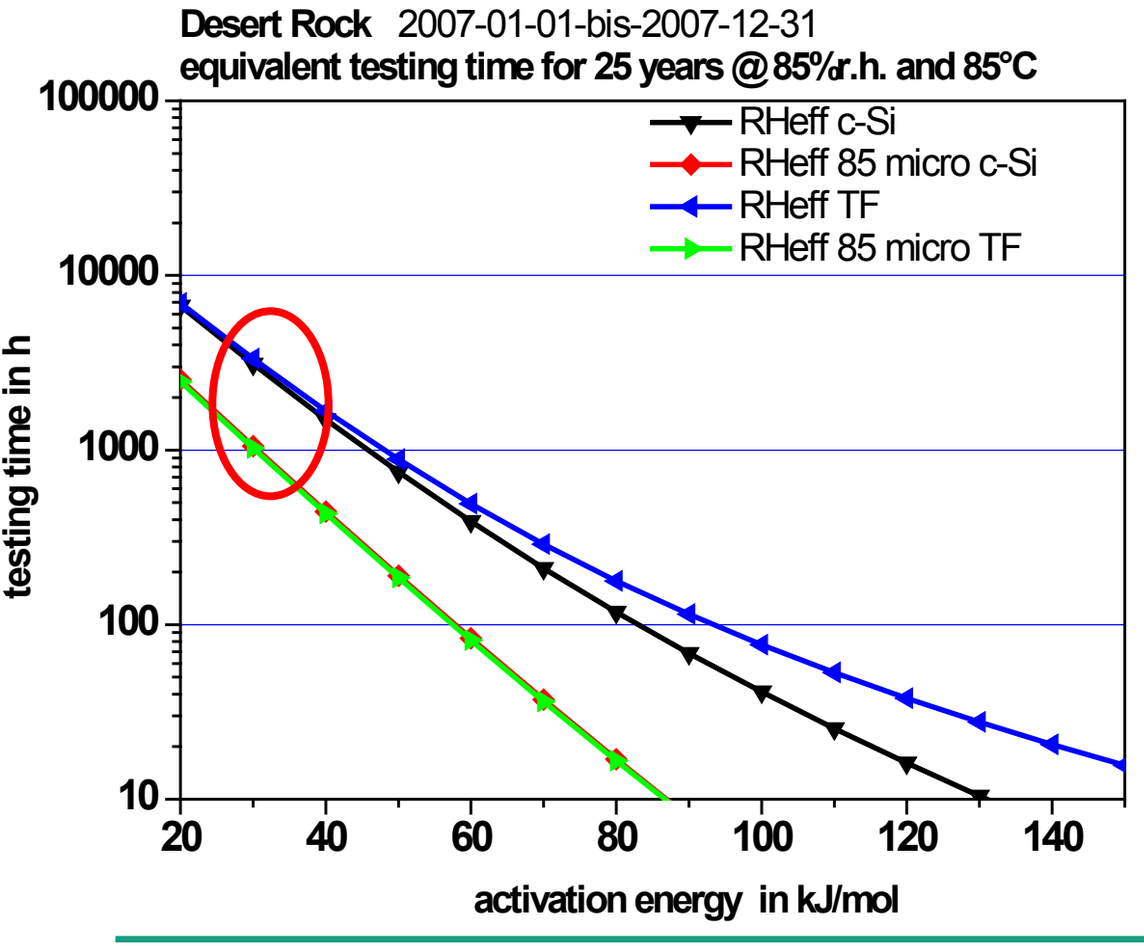
Fraunhofer ISE

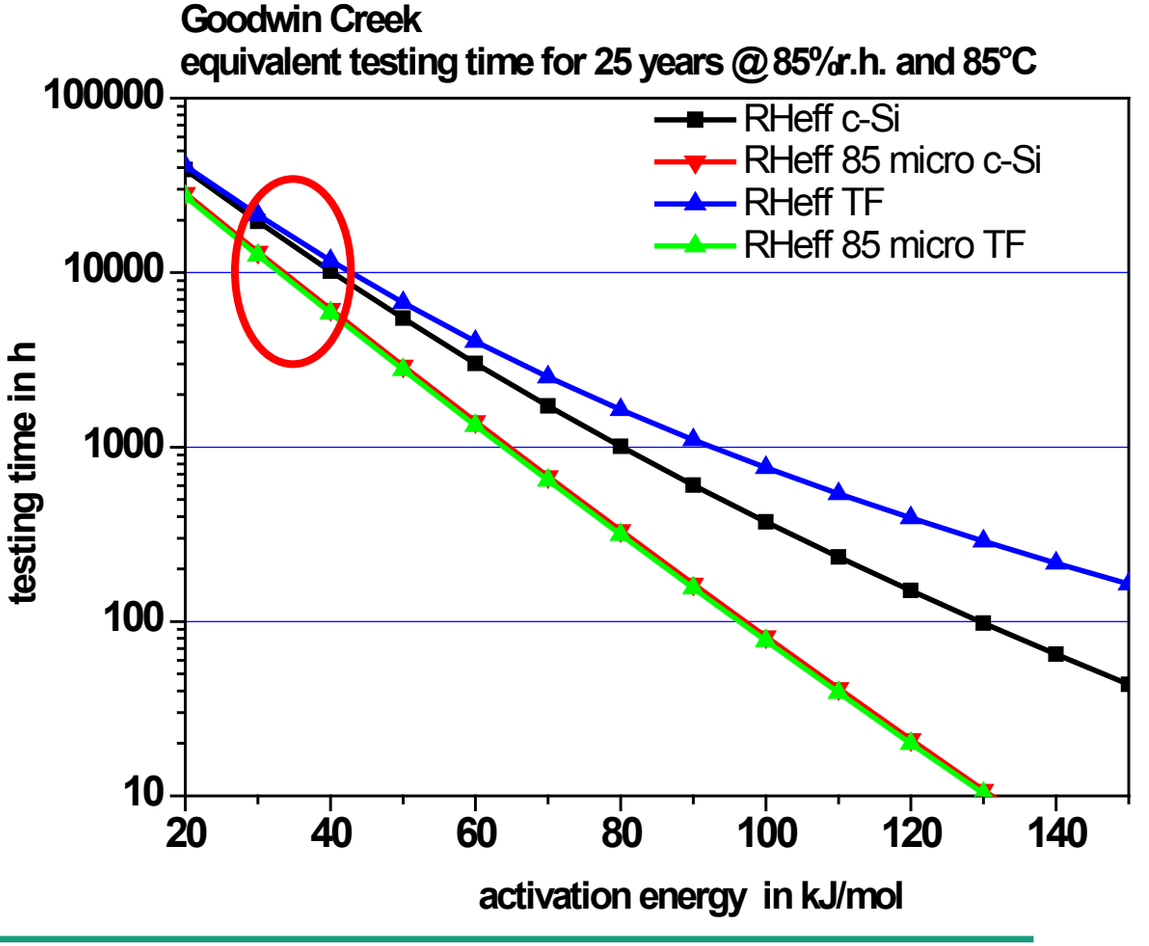
Damp-heat test conditions at 85°C and 85% rh

Considering the surface humidity instead of the ambient humidity reduces the testing time by a factor of 2 for humid and 3 for desert climates

Ten times longer testing time needed for the more humid site

The 1000h test suits for desert rock (could be 500 h)





© Fraunhofer ISE

Fraunhofer ISE

Testing times needed for service life testing (25 years)

Unfortunately strongly depending on the degradation processes in the materials

Test designs are needed which allow assessment of the material-dependent parameters in the time transformation functions

Service life testing times /h								
		E = 50 kJ/mol				**E = 100 kJ/mol**		
	Goodwin Creek		**Desert Rock**		**Goodwin Creek**		**Desert Rock**	
	c-Si	**TF**	**c-Si**	**TF**	**c-Si**	**TF**	**c-Si**	**TF**
Temperature (85°C)	8200	10500	9500	12000	666	1425	853	1680
Humidity (85/85)	2916	2780	191	185	82	77	4	4
UV (1sun @ 85°C)	4500	6700	6000	8500	575	1375	775	1700
UV (1sun no T-activation)	38000		48000					

© Fraunhofer ISE

Summary

Modelling the micro-climatic stress conditions

Time-series of climatic data

ambient temperature and humidity, solar irradiation, wind speed

Modeling the module temperatures

ambient temperature, solar irradiation, wind speed, module-specific coefficients (mounting situation might be considered)

Modeling the UV-radiation

5.5% of the solar radiation, module temperature

Modeling the effective surface humidity

ambient temperature and humidity, module temperature

© Fraunhofer ISE

Modelling the ALT conditions

Use a simple time-transformation function (Arrhenius based, eg)

Time, module temperature and other degradation factors, but separately first

Modeling the module temperature stress

as function of the material-specific activation energy,

(could be eventually included in damp-heat testing)

Modeling the UV-radiation impact

as function of the material-specific activation energy (which is low, UV-dose more important)

Modeling the moisture test

Higher test temperatures needed, as function of the material-specific activation energy,

© Fraunhofer ISE

What else is needed?

Validation of the time-transformation function

Or introduction of alternatices

Try to determine material dependencies like

activation energies for finding dose-response functions

Materials

Consider the other degradation factors,

Temperature cycling, frost-thaw, high pot, salt, ammonia……..

Micro-climate

Local climate

Define or adopt climate-classes and the respective stresses

Mapping, standardised ALT for each class or individual qualification

Or assess dose response-function and model for given location

ALT conditions

Define service-lifetime requirements

Design life-time, performance limit

Service life

© Fraunhofer ISE

Thanks for your attention

NREL for the invitation





To my colleagues

Daniel Philipp

Franz Brucker

Philipp Huelsmann

Markus Heck

Stefan Brachmann

Karl-Anders Weiss

Stefan Wiesmeier

To our partners

TÜV Rheinland

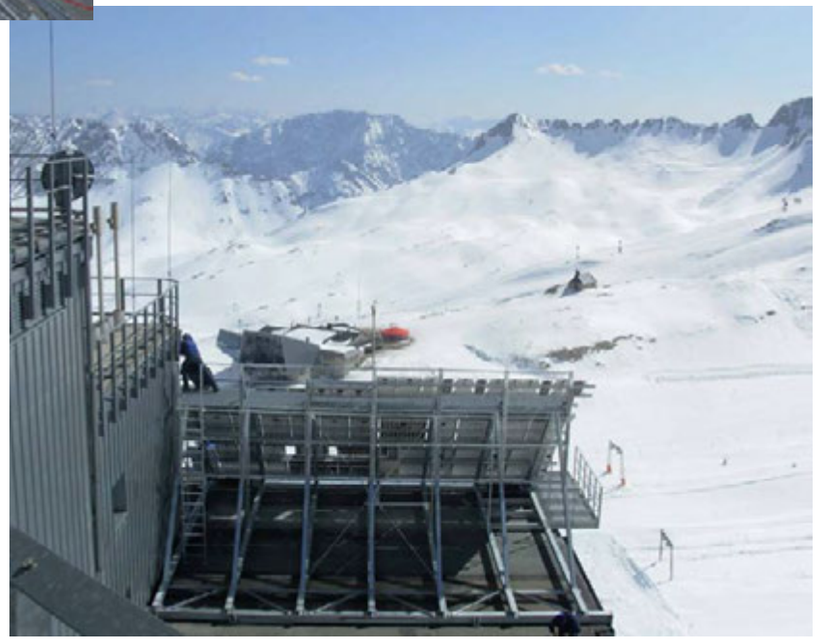
Schott Solar

Solarfabrik

Solarwatt

Solarworld

Solon



solar | glass Scheuten SCHOTT solar solar fabrik SOLARWATT SolarWorld SOLON AG für Solartechnik Fraunhofer ISE

Workshop on Reliability of PV-Modules

Testing

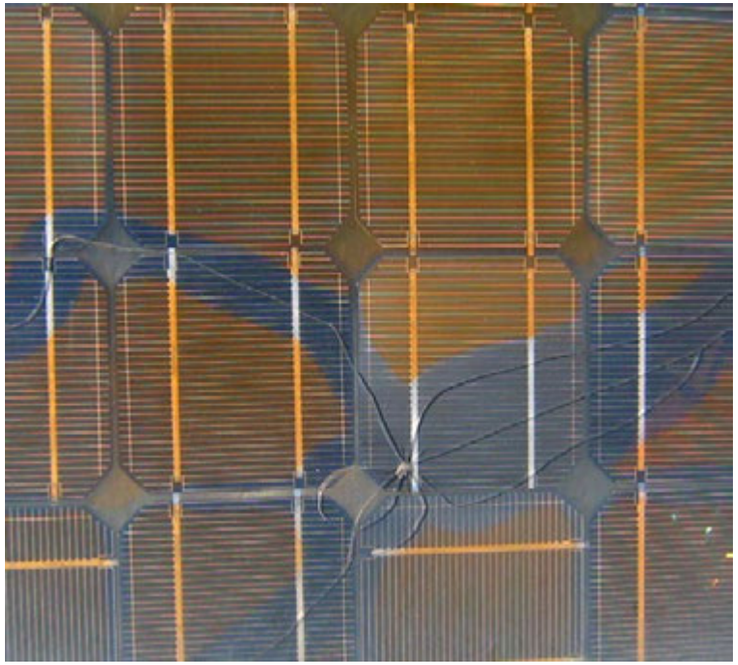
Analysing

Simulating module - reliabilty

Organised by Fraunhofer ISE and Humboldt-Univ. Berlin

Supported by JRC, PCCL, TÜV Rheinland, VDE - Institute

http://www-pbp.physik.hu-berlin.de/pvr/



Berlin - Adlershof

Germany

April 5 – 6 2011

Meeting of the IEC TC82 WG2

Sub-group on Back-Sheets

After the Workshop



© Fraunhofer ISE

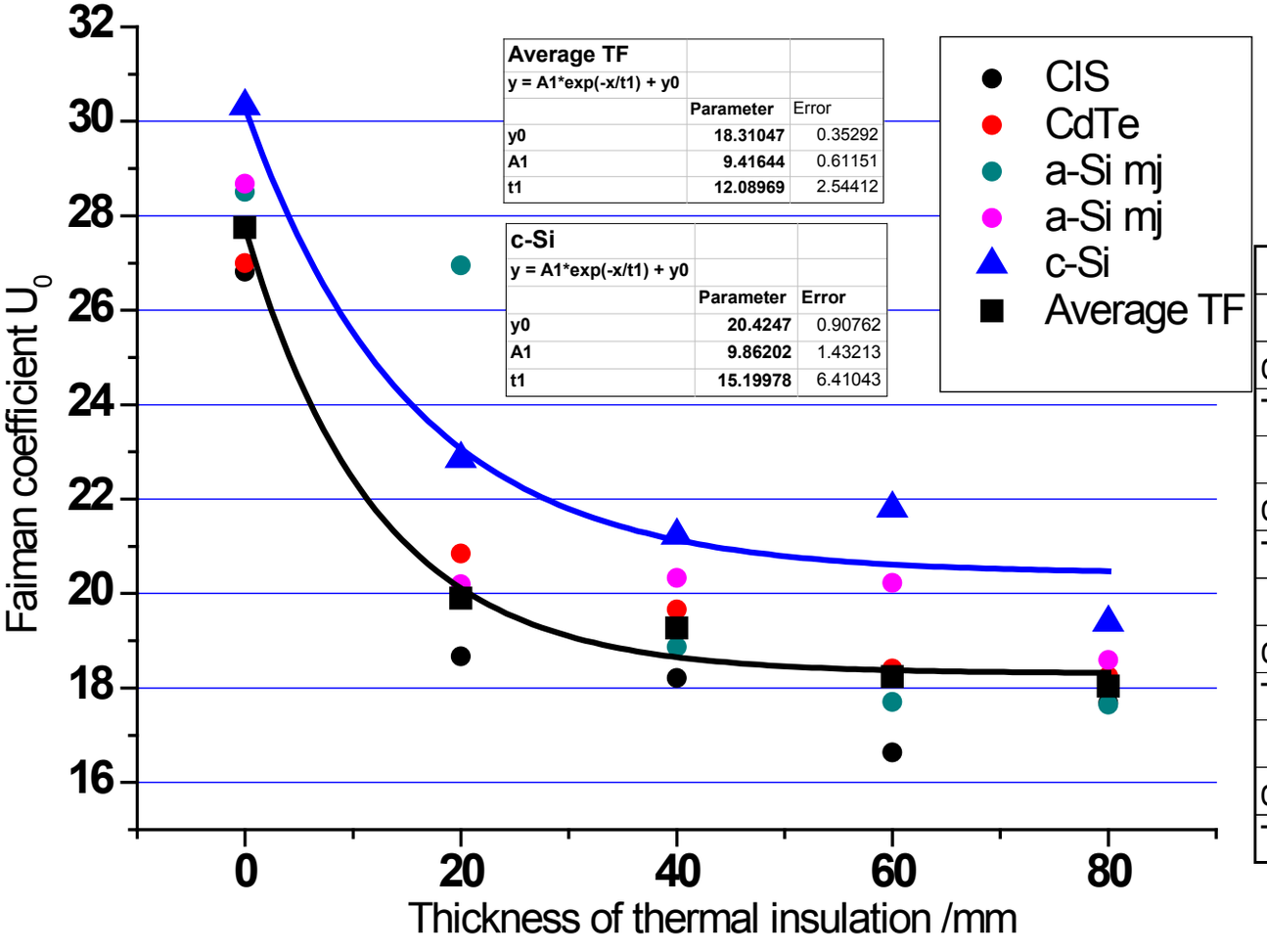
Fraunhofer ISE

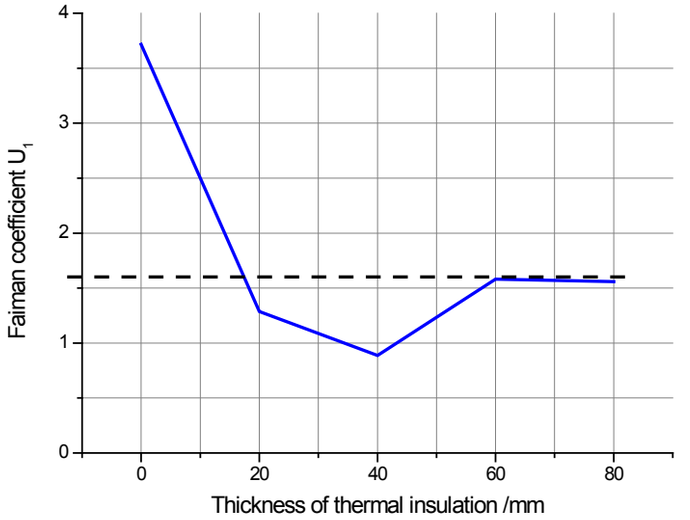
Temperature simulation towards BIPV

Increasing thermal insulation on the back-side

Short monitoring periods

Inclination 45°





Wind impact reduction by 50%

	Free		BIPV		45°	Incl.
	U0	U1	U0	U1		
c-Si	30	6	20	3		
TF	27,7	4	18,3	2		
c-Si	42,2		54,8		**NOCT**	800W
TF	43,7		59,4		Wind: 1 m/s	20°C
c-Si	40,2		51,3		**STC**	1000W
TF	44,3		58,0		Wind: 6 m/s	25°C
c-Si	68,3		85,0		**Maximum**	1000W
TF	71,1		89,6		Wind: 0 m/s	35°C

Module temperature up to 18 K higher

© Fraunhofer ISE

Fraunhofer ISE

NREL
NATIONAL RENEWABLE ENERGY LABORATORY

Monitoring System Performance



Venue: PV Module Reliability Workshop

Presenter: Keith Emery and Ryan Smith

Date: February 16, 2011

NREL/PR-5200-50643

NREL is a national laboratory of the U.S. Department of Energy, Office of Energy Efficiency and Renewable Energy, operated by the Alliance for Sustainable Energy, LLC.

Outline

Standards

- **National Electric Code**
- IEC 60904-1 **"Photovoltaic devices – Part 1: Measurement of photovoltaic current-voltage characteristics"**
- IEC 61724 "**Photovoltaic System Performance Monitoring – Guidelines for Measurement, Data Exchange and Analysis"**
- IEC 61829 "**Crystalline Silicon Photovoltaic array – On-site Measurement of I-V Characteristics**"
- ASTM E1036 "**Standard Test Methods for Electrical Performance of Nonconcentrator Terrestrial Photovoltaic Modules and Arrays Using Reference Cells"**
- ASTM E2527 "**Standard Test Method for Electrical Performance of Concentrator Terrestrial Photovoltaic Modules and Systems Under Natural Sunlight"**
- ASTM WK22009 "**Reporting Photovoltaic Non-Concentrator System Performance** "

Sources of Uncertainty

NREL's Approach to Local and Remote System Monitoring

Summary

IEC 60904-1 "Photovoltaic devices – Part 1: Measurement of Photovoltaic Current-Voltage Characteristics

- Voltage and Current measured with ±0.2 % Uncertainty in V_{oc} and I_{sc}
- Test and Reference device coplanar within ±2° and normal to the sun within ±5°.
- Reference cell and test device temperature measured with ±1 °C uncertainty.
- Optionally test device temperature determined via equivalent cell temperature method (IEC 60904-5)
- Spectral mismatch error correction if matched reference cell not used (IEC 60904-7).
- If reference cell >2 °C from calibration temperature corrections applied.
- Use IEC 60891 to translate for temperature and irradiance

ASTM E1036 **"Standard Test Methods for Electrical for Electrical Performance of Nonconcentrating Photovoltaic Modules and Arrays Using Reference cells"**

- Voltage and Current measured with ±0.1 % Uncertainty and 0.05% Resolution for V_{oc} and I_{sc}.
- Test and Reference device coplanar within ±2° and normal to the sun within ±10° or report incidence angle.
- Reference cell and test device temperature measured with ±1 ° C uncertainty, 0.1 ° C resolution.
- Spectral mismatch error correction applied (ASTM E973).
- Temperature and irradiance corrections applied if temperature more than 2° C from reference temperature or irradiance > 5% from reference irradiance correct using bilinear method. Otherwise current corrected to constant irradiance.
- Average Wind speed for 5 min prior to test.

IEC 61724 "**Photovoltaic System Performance Monitoring – Guidelines for measurement data exchange and analysis**"

Meteorology
- Total irradiance, in the plane of the array
- Ambient air temperature
- Wind speed

Photovoltaic array
- Output voltage
- Output current
- Output power
- Module temperature
- Mounting / tracker characteristics

Load
- Load voltage
- Load current
- Load power

Energy storage
- Operating voltage
- Current to/from storage
- Power to/from storage

Utility grid
- Utility voltage
- Each phase - Current to/from utility grid
- Power to/from utility grid

Back-up sources
- Output voltage
- Output current
- Output power


Meteorology
PV array
DC Disconnect
DC Monitoring
(V, I)
Utility-Interactive Inverter
AC Monitoring
(V, I, P, PF)
AC Disconnect
Meteorology
• Module Temp
• Ambient Temp
• Irradiance
Network
Utility Grid
Load
Data Acquisition System



Total Irradiance –

- Measured in plane of array
- Uncertainty including including Instrumentation < 5%
- Pyranometer
- Reference cell or cell in Module Package or Module (IEC 60904-2)

Ambient Temperature –

- Representative of Array Location
- Uncertainty including Instrumentation < 1° C

Wind Speed

- Measured at Height and Location Representative of Array
- Uncertainty including Instrumentation < 0.5 m/s for Speeds < 5 m/s, and <10 % of the reading for Speeds > 5 m/s

IEC 61724 "**Photovoltaic System Performance Monitoring – Guidelines for measurement data exchange and analysis**"

Module Temperature –

- Measured on back of 1 or more modules in representative of location
- Uncertainty including Instrumentation < 1° C
- location on module given in IEC 61829 method A (center of back surface of module in center of array field)
- Based upon V_{oc} and equivalent Cell temperature (IEC 60904-5)

Voltage and Current –

- ac and or dc
- Uncertainty including Instrumentation < 1% of reading

Power

- DC Calculated based upon instantaneous and not averaged readings or directly measured with wattmeter
- AC power accounts for power factor and harmonic distortion
- Uncertainty including Instrumentation < 2%

IEC 61724 "**Photovoltaic System Performance Monitoring – Guidelines for measurement data exchange and analysis**"

Appendix A - Data Acquisition - Irradiance, Temperature, Voltage, Current, Power

Sampling

- Parameters which vary directly with irradiance shall be sampled with 1 min or less interval. Parameters with larger time constants, an arbitrary interval may be specified between 1 min and 10 min. Special consideration for increasing the sampling frequency shall be given to any parameters which may change quickly as a function of system load.

Linearity

- The difference between measured and applied signal < ±1 % of full scale value at of 0, 20, 40, 60, 80, and 100 % of full scale.

Stability

- 100 % full scale dc signal applied for 6 h. Should the fluctuation of the input signal exceed ±0.2 %, the results shall be compensated by using a voltmeter with an accuracy better than ±0.2 %.

Integration

- Apply expected maximum sensor signal for > 6 h. Signal times interval within 1% of expected value. With shorted input integral less than 1% of maximum signal applied times interval.

dc or ac Power Rating to 20 ° C ambient temperature, 850 W/m² total irradiance, 4 m/s wind speed

Air temperature

- Resolution 0.1 ° C, Uncertainty < 1 ° C
- 1 to 2 m upwind , > 2m above ground
- See ASTM D6176 "Standard Practice for Measuring Surface Atmospheric Temperature with Electrical Resistance Temperature Sensors"

Wind speed

- Uncertainty less than 0.5 m/s
- 1 to 2 m upwind , > 2m above ground

Total direct beam irradiance

- ASTM E816, "**Standard Test Method for Calibration of Pyrheliometers by Comparison to Reference Pyrheliometers"**
- **Typical uncertainty < 1.5%**

ASTM WK22009 "**Standard Test Method for Reporting Photovoltaic Non-Concentrator System Performance**"

dc or ac Power Rating to agreed upon Reporting Conditions defined by an Ambient Temperature, Total Irradiance, and Wind Speed

Air temperature

- Resolution 0.1 ° C, Uncertainty < 1 ° C (ASTM D6176)

Wind speed

- Uncertainty less than 0.5 m/s
- ultrasonic preferred since no dead band for <0.5 m/s

Plane of Array irradiance

- Pyranometer
  - ASTM E824 Test Method for Transfer of Calibration From Reference to Field Radiometers "
  - ASTM G167 Test Method for Calibration of a Pyranometer Using a Pyrheliometer
- Matched Reference cell suitable for outdoor use (ASTM E1040)
  - secondary calibration according to ASTM E1362

ac power measured with less than 1.5% uncertainty

PV Irradiance detector

Reference Cells in metal package

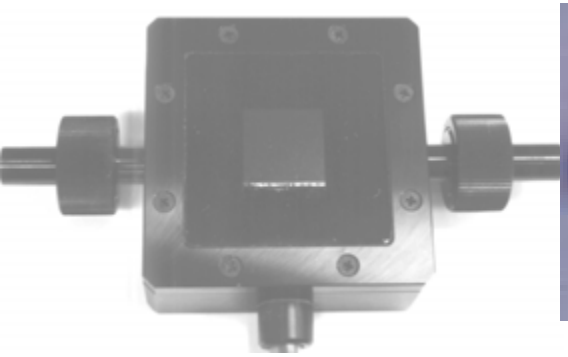
- Uncertainty in measuring the total irradiance of ± 1.5% provided that I_{sc} is temperature corrected and size is less than 2 by 2 cm
- Corrects for spectral effects to the reference spectrum. Exact correction if relative quantum efficiencies of reference and PV system identical
- Multiple intercomparisons among ISO 17025 accredited calibration labs suggest uncertainty less than ±2% for Si reference cells at 25 ° C
- Short-circuit temperature coefficient of Si is 500 to 850 ppm/° C depending on spectra measured under. In systems the temperature range may exceed 60 ° or a 3% error in irradiance if temperature not corrected for.
- Regression analysis of field data has a lower mean square error (less noisy)
- Time constant comparable to PV
- Temperature can be controlled potentially giving lower error in calibration

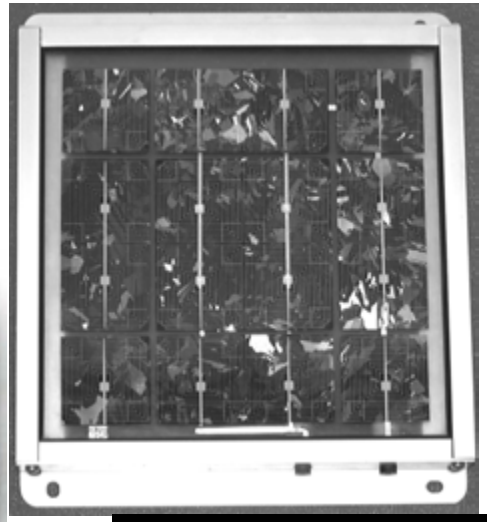
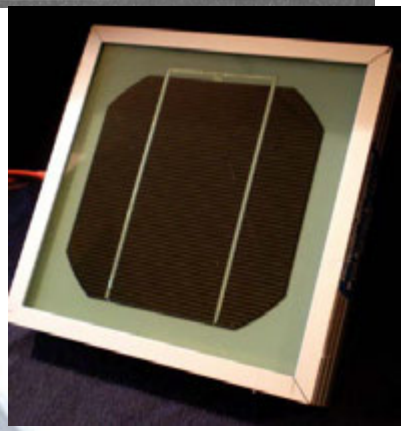
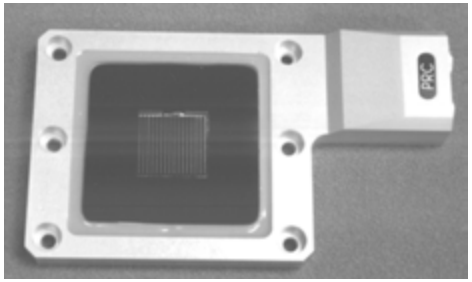
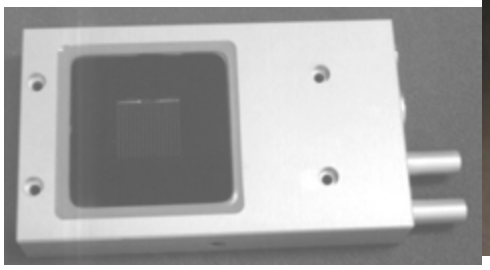
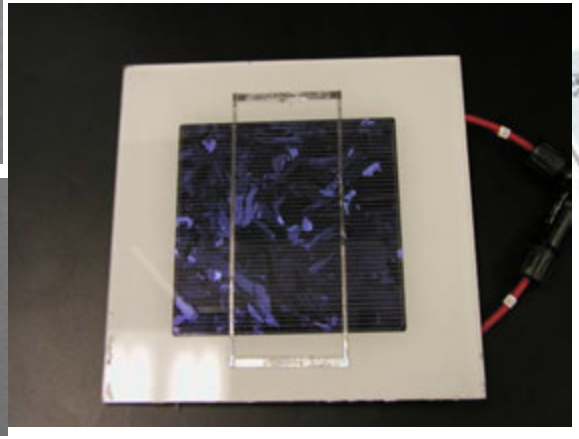
Cell in Module package

- Angular response similar to PV in system
- Quantum efficiency closer to module because packaging similar
- Thermal characteristics similar to PV system
- Slightly higher uncertainty than small area cells.

Reference Cell Packages

- Encapsulated
- Temperature sensor attached or other means to correct for temperature
- Packaged cell or cell in module package



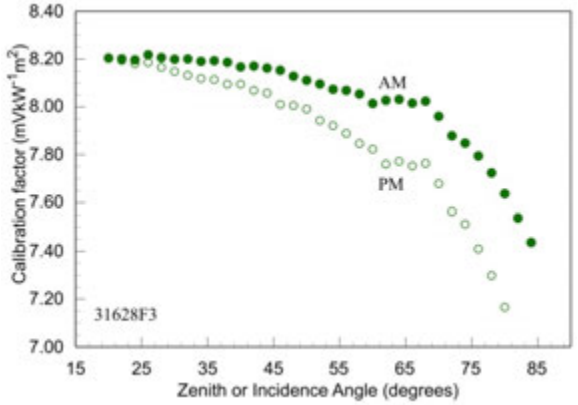







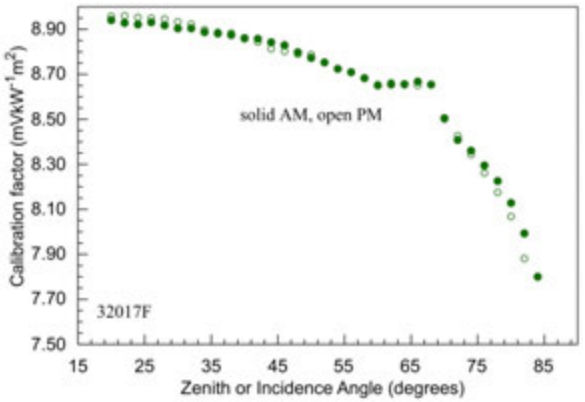

Pyranometer

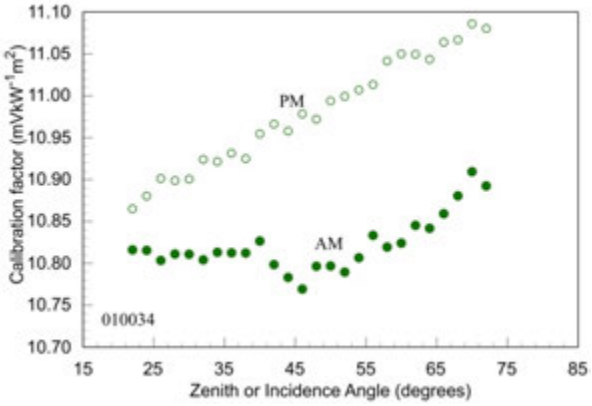
- Wide range of uncertainties depending on how calibrated (indoors using a sphere vs. outdoors, how mounted, and if corrections for temperature and angular response applied
- 1.5 % to >5% for WMO first class, potentially >20% for other units.
- "**WMO GUIDE TO METEOROLOGICAL INSTRUMENTS AND METHODS OF OBSERVATION"** http://www.WMO.int/pages/prog/www/IMOP/publications/CIMO-Guide/CIMO_Guide-7th_Edition-2008.html
- U_{95} for pyranometer calibration at NREL on a horizontal surface ±3 to 4% depending on multiple factors. Often different from indoor based calibrations by over 5%.
- Calibrated outdoors with respect to incident spectrum so calibration is **not** with respect to a reference spectrum Error for Si pyranometer not as large an error for thermopile based units.
- Usually calibrated on a horizontal surface. Calibration varies with tilt angle.
- Calibration dependent on cable orientation. Cable should face to north away from sun in northern hemisphere.
- Manufacturers often calibrate indoors with integrating sphere against a reference pyranometer.

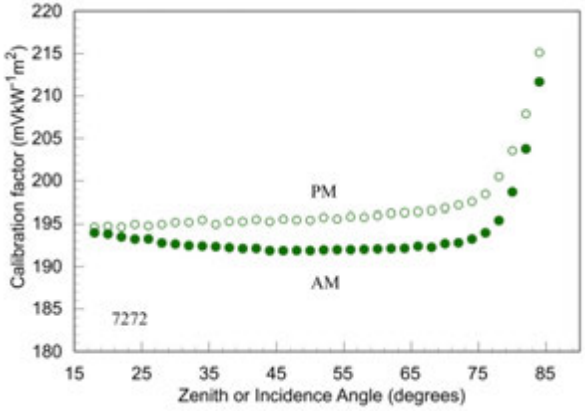
NREL single day Pyranometer calibrations, 2 degree bins

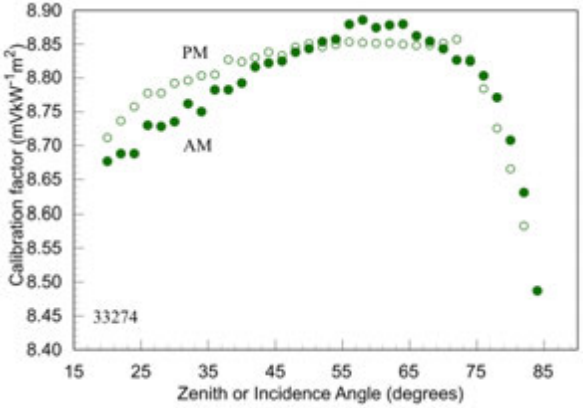
http://www.nrel.gov/aim/

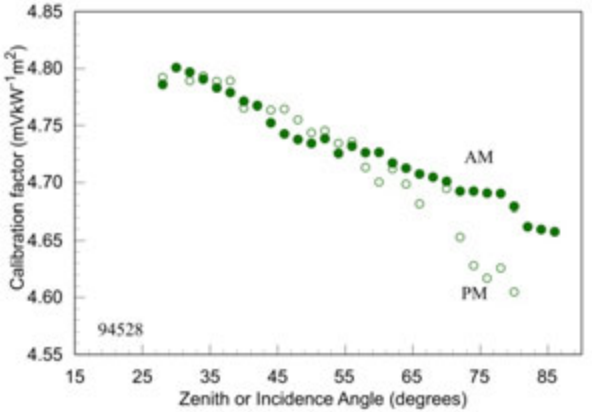


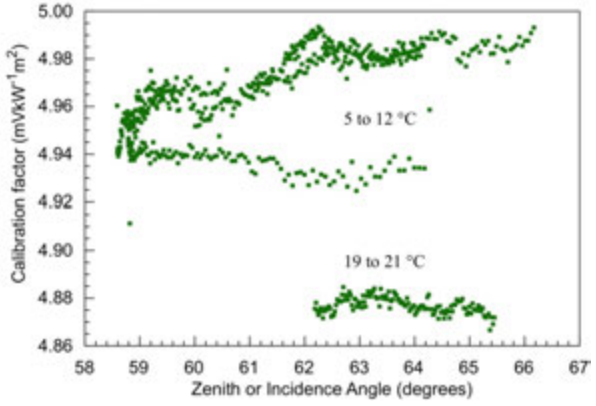


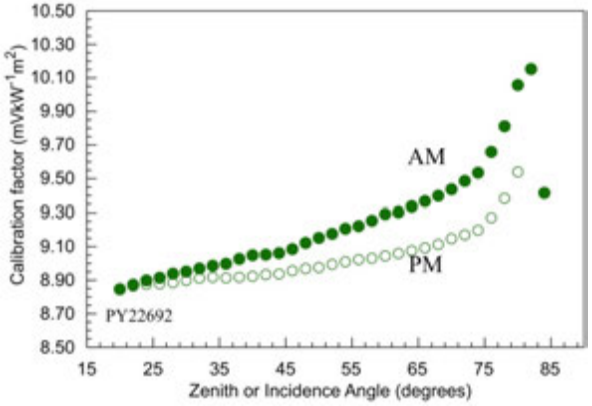


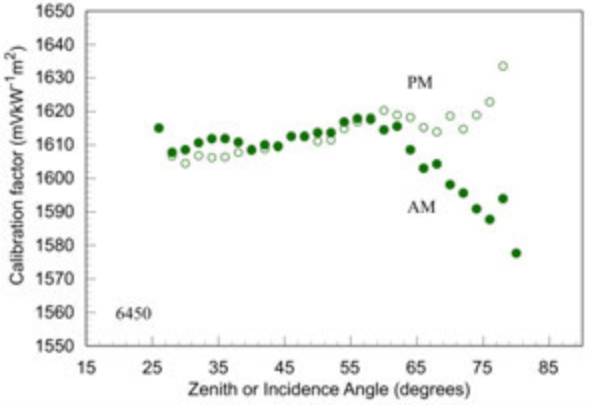






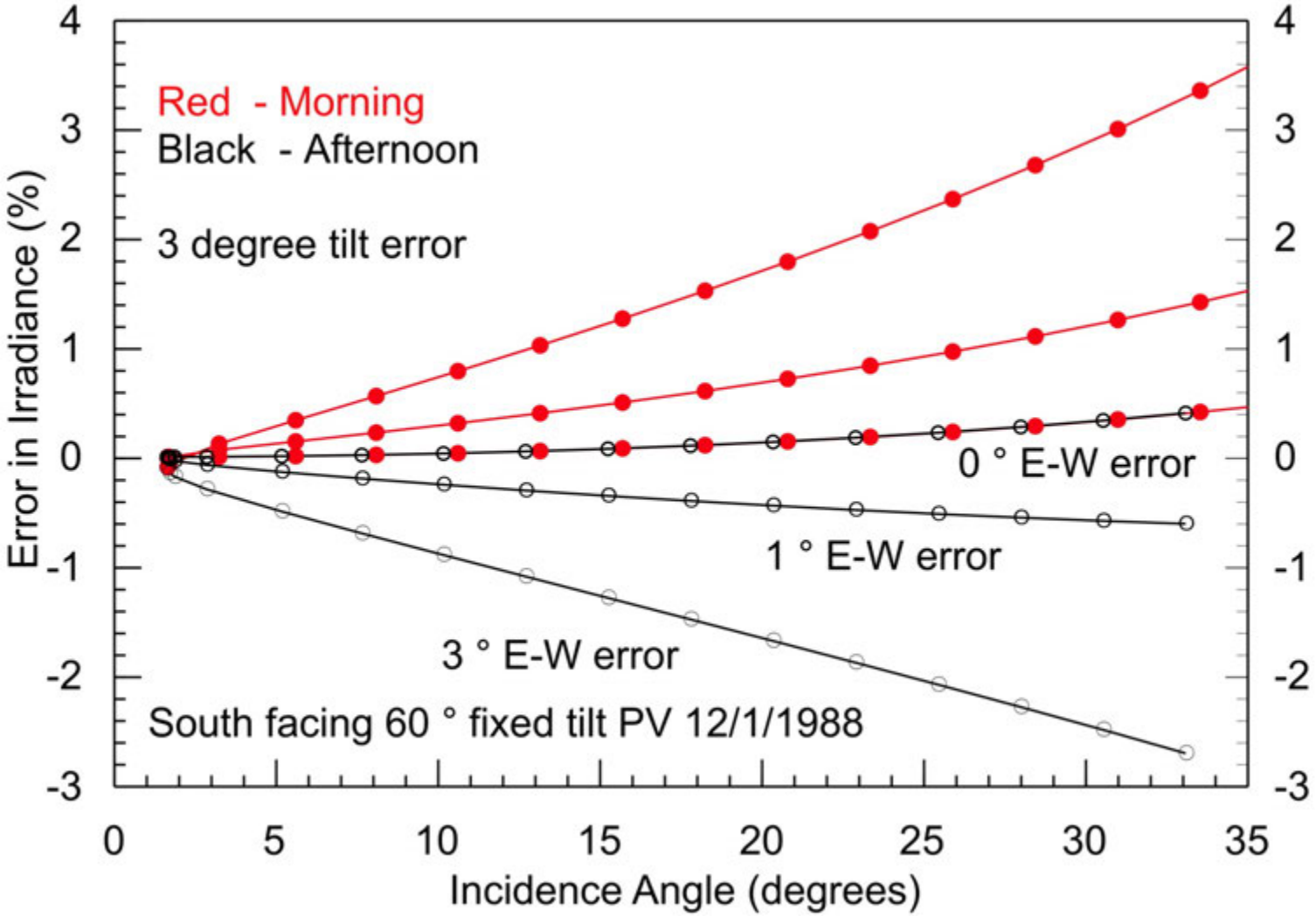






Leveling Error

How closely must irradiance sensor be aligned to PV array?
What is impact of PV modules in system misaligned with respect to each other?

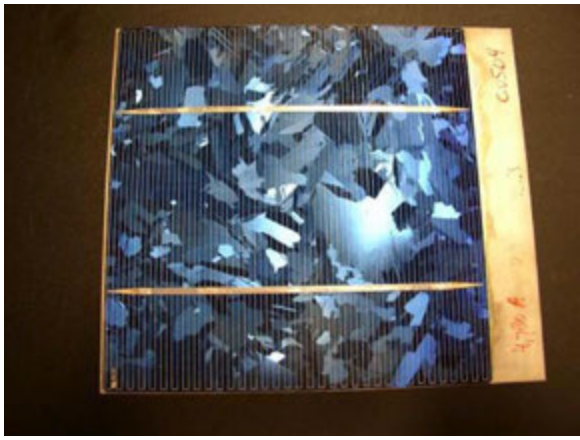


K.A. Emery, et al, "SERI Results from the PEP 1987 Summit Round Robin and a Comparison of Photovoltaic Calibration Methods," SERI tech. rep. TR-213-3472, March 1989.

Si secondary calibrations

Formal and informal secondary reference cell intercomparisons among ISO 17025 accredited or equivalent calibration labs suggest that the uncertainty is ±2% or less.

Cell	Calibrated	Isc (A)	Isc,ECN	ΔI (%)
100-A	ESTI 2002	3.020 ± 1.9%	3.032	+0.4
100-B	ESTI 2002	3.006 ± 1.9%	3.019	+0.4
100-B	NREL 2003	3.023 ± 2.0%	3.019	-0.1
125-A	ESTI 2002	4.780 ± 1.9%	4.816	+0.8
125-B	ESTI 2002	4.731 ± 2.0%	4.716	-0.3
125-C	NREL 2004	5.311 ± 2.0%	5.311	---
125-D	NREL 2004	5.380 ± 2.0%	5.393	+0.2
125-E	PTB 2004	4.752 ± 2.9%	4.724	-0.6
150-A	ESTI 2002	6.858 ± 1.9%	6.808	-0.7
150-B	PTB 2004	7.247 ± 2.8%	7.122	-2.2



Arvid van der Heide, Stefan Winter, Keith Emery, and Wim Zaaiman, "Comparison Between Large Reference Cells Calibrated by ESTI-JRC, NREL and PTB, Performed at ECN", Proc. 20th EU PVSEC, June, 2005.

NREL's Approach to Local and Remote System Monitoring

Successful monitoring requires understanding the entire data acquisition system.

Budget constraints may dictate to what extent monitoring is possible.

Local and remote monitoring applications can require different approaches.

Primary concepts for either monitoring application include:

- Select highly reliable hardware suitable for the end-use environment
- Decrease the susceptibility to external noise
- Choose sensors with low uncertainties and low drift
- In general, a simple system design is better
- Calibrate! Calibrate! Calibrate! - Calibration drift adversely impacts data quality and interpretation (next talk).

Typical NREL Installation







Choices

Reliable hardware is worth the cost!

- If the data is to be used for modeling or analysis than it needs to be as accurate and complete as possible. Unreliable hardware can impact results because of missing, inaccurate, or noisy measurements.
- Limit external noise by using good quality signal wires.
  - Foil shielded with drain wire or dense braided shield; one side only!
  - Transition between different thermal environments may require PTFE jacket
- Protect DAS hardware by using reliable fuses (especially on DC side of system)
- Use equipment rated for the worst-case temperature (usually 90° C).
- Monitoring equipment rated for range of ambient temperatures where deployed.
- A hardware suite of preference comes with experience (and from failures)
- A trustworthy communications interface and large internal storage is essential.

"Simple is better" - In our experience this is a true statement.

- Unnecessary signal conditioning increases uncertainty and creates more failure points.
- Passive devices with low thermal coefficients work very well.

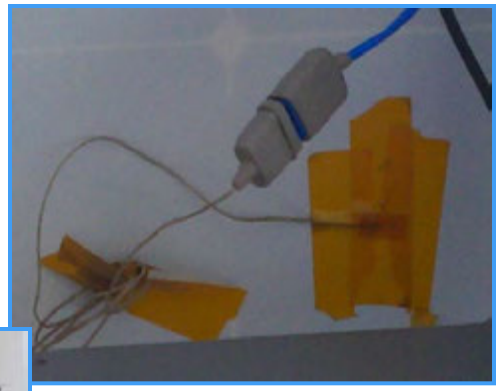
Calibrate

- Failure to do so impacts system rating uncertainty and degradation rates
- Don't blindly trust data sheets.
  - Often, the manufacturer calibration is valid for only one year.
- A complete end-to-end calibration, when possible, limits systematic errors.
- Periodic pyranometer calibrations (such as NREL's BORCAL) are essential!
  - 24 month schedule is normal, periodic inspection / cleaning of sensors

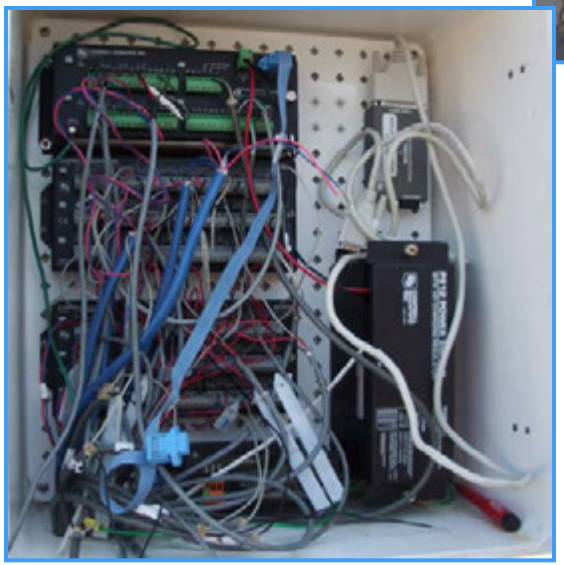
Keep it Clean

- Use devices designed and rated for the end-use environment
- Limit access to weather and vermin
- Use good wire management practices; label signal lines
- Make sure all measurement equipment is grounded





Degraded polyimide tape; potential for poor thermal contact



Poor wire management; lack of labeling.

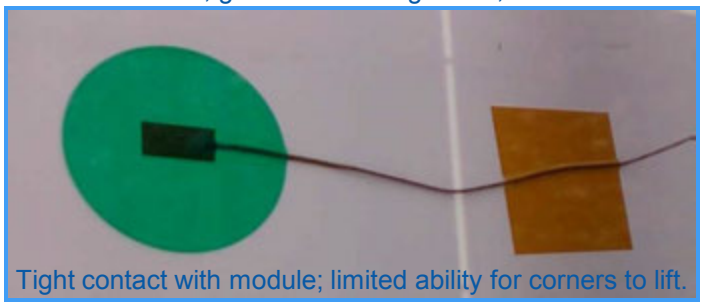


Corroded signal connections

vs.



Clean installation; good wire management; rated devices.



Tight contact with module; limited ability for corners to lift.

Recommendations

Topic	Recommendation	Reason
Measurement Interval	5-sec scans into 1-min averages	15-minute data (standard) cannot capture many system issues; 1-minute data provides the resolution needed for capturing transient system events such as inverter shutdown. 1-minute data also supports analysis which require more data points (degradation rate calculations, for instance). With the cost of hardware and storage decreasing there is no reason to avoid 1-minute (or sub-minute) data collection.
Analog Signal Lines	High quality PTFE Jacket; Shielded w/ drain wire	Experience has shown that PTFE jacketed signal lines are less susceptible to noise when going between different temperature environments. Also, PTFE has superior resistance against weather (UV, moisture, temperature) when used outdoors.
Outdoor Connectors	Rated for the environment; Use of protective boots.	Use all means to limit connector corrosion. Sunlight resistant boots must be used; unrated boots can crack and actually trap moisture within the connector housing.
Equipment Temperature Ratings	-55° C to 85° C	Equipment enclosures can see dramatic temperatures, especially if exposed to direct sunlight. Equipment must handle these extremes.
Enclosure Locations	In the shade	Direct exposure to sunlight can raise the interior temperature of an enclosure dramatically.
Thermocouple Attachment	Clean location and hands; Silicone adhesive; Round shape	Silicone adhesive has withstood outdoor testing very well. Limit contamination of the adhesive by cleaning the attachment location (w/ IPA) and your hands. Avoid touching the adhesive by using tape with a split carrier film. Square corners are prone to lifting; round dots limits lifting.
Inspection Interval	Visual checks quarterly	Check for: 1)Thermocouple detachment or tape embrittlement 2)Damage to exterior sensors (pyranometers, ambient temp sensors) 3)Evidence of moisture or vermin in enclosures 4)Loose connections at DAS / sensors
Calibration Interval	End-to-End Calibration Annually -Ambient temp above 15° C -Wind speeds below 3 m/s	Bench calibrations are done in an atypical environment (indoor is not equivalent to outdoor conditions). Calibration equipment can be affected by the surrounding environment. Limit temperature extremes and high winds which may cause offsets in the calibration hardware. End-to-end calibrations are necessary to limit uncertainties and systematic errors.

Monitoring Budget

As budgets for monitoring increase, the measurement data sources can be expanded.

- Allows for additional analysis options and backups

Component or Measurement	Data Source	Small → Budget → Large				
		Limited → Analysis Options[2] → Significant				
AC Energy Generation[1]	ANSI C12.20 Revenue Grade Meter			●	●	●
	Collected from Inverter	●	●	●	●	●
DC Energy Generation[1]	External Current and Voltage Transducers					●
	Collected from Inverter	●	●	●	●	●
Inverter Status and Errors	Collected from Inverter	●	●	●	●	●
Global Horizontal Irradiance	Thermopile Pyranometer					●
	Silicon Photodiode Pyranometer			●	●	
Plane-of-Array Irradiance	Thermopile Pyranometer					●
	Same-Technology Reference Cell / Module			●	●	●
	Silicon Photodiode Pyranometer	●	●	●	●	
Ambient Temperature	Thermocouple, RTD, Thermistor	●	●	●	●	●
Module Backsheet Temperature(s)	Thermocouple, RTD, Thermistor		●	●	●	●
Wind Speed	Ultrasonic Anemometer				●	●
	Cup Anemometer		●	●		

[1] The collection of both inverter and external energy generation data in the large budget scenario allows for comparisons between these two device types.

[2] Systems which collect higher quality data off of a greater variety of sensors allows for more significant analysis and have a greater benefit to PV performance and reliability research.

Summary

- The dominant error source in determining the system power is determining the plane-of-array irradiance
- Performance monitoring is significantly affected by the quality of the measurement hardware and the professionalism of the installation.
- Results of performance modeling have greater meaning if the measurement hardware is calibrated regularly.
- Calibration drift can invalidate all data since the previous calibration.
- No standards for system Energy rating, minimal standards for system power rating

NREL
NATIONAL RENEWABLE ENERGY LABORATORY

Methods for Analysis of Outdoor Performance Data



NREL

Dirk Jordan

2011 Photovoltaic Module Reliability Workshop

February 16, 2011

Golden, Colorado

NREL/PR-5200-51120

NREL is a national laboratory of the U.S. Department of Energy, Office of Energy Efficiency and Renewable Energy, operated by the Alliance for Sustainable Energy, LLC.

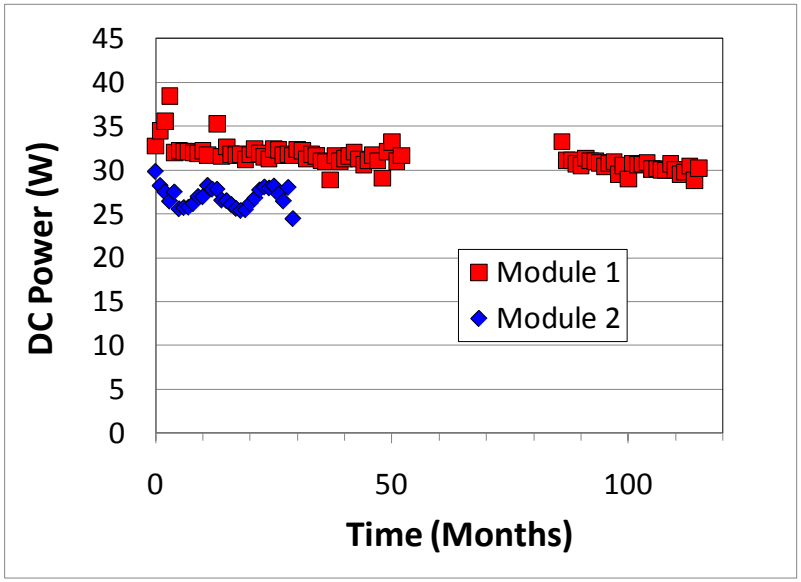
Outline

- Motivation: Impact of uncertainty in degradation rates (R_d)
- Methodologies
  1. IV data taken in discrete intervals
  2. Continuous data, PVUSA & Performance Ratio
  3. Additional methodologies for continuous data - Classical Decomposition, ARIMA
- Historical R_d and what we can learn from it.
  1. Methodologies
  2. Number of measurements
  3. Climate

Motivation

For solar industry to keep growing we need to accurately understand & predict how different technologies behave/change with weather, climate and time.

Change of power output with time is degradation rate (R_d)….uncertainty is very important too.



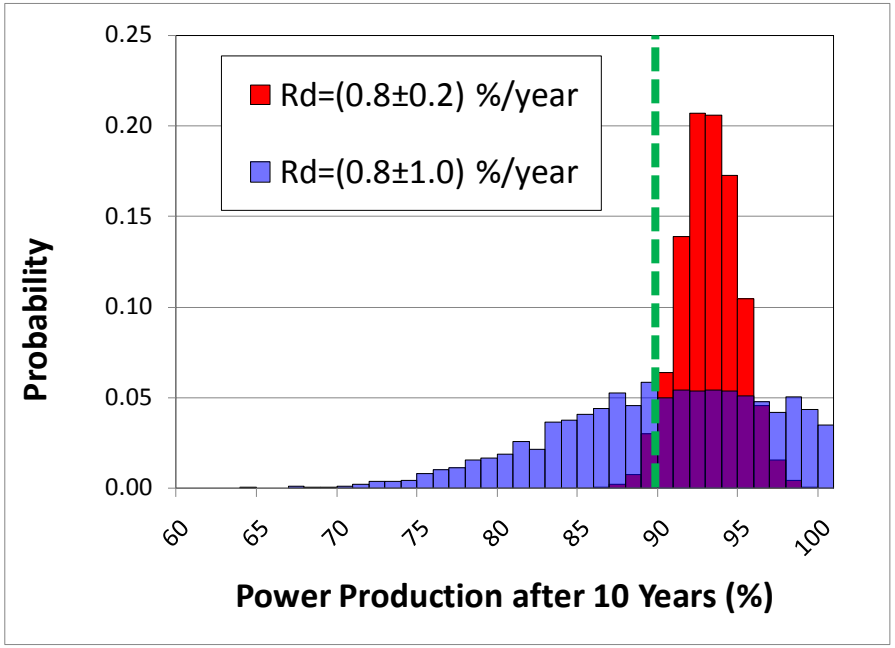
2 examples from NREL:
Different observation lengths, seasonality etc. → Leads to different uncertainties

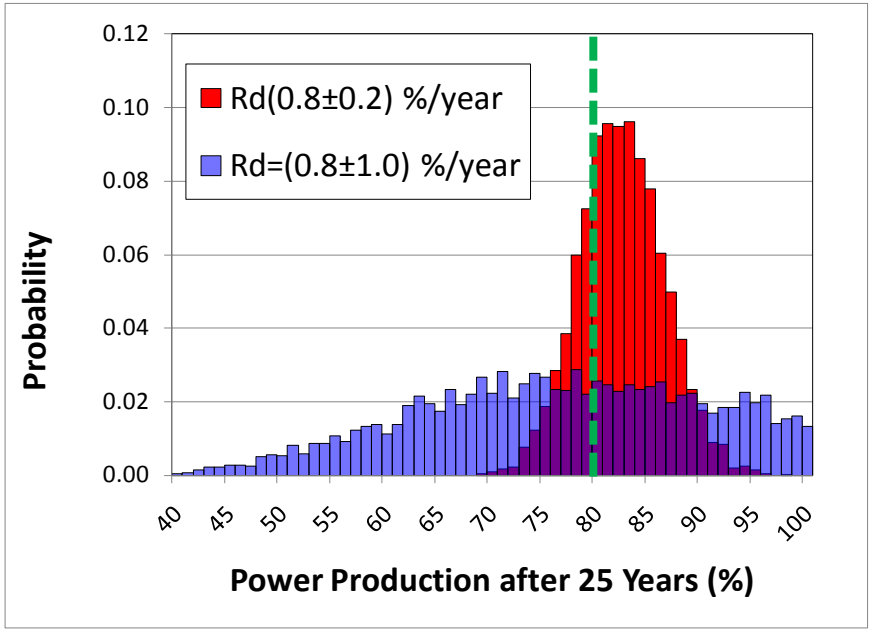
R_d (Module 1) = (0.8 ±0.2) %/year
R_d (Module 2) = (0.8 ±1.0) %/year

Same R_d but very different uncertainty

R_d Uncertainty Impact on Warranty

Manufacturer Warranty often twofold: 90% after 10 years, 80% after 25 years





Probability to default warranty:

1.0 %/year uncertainty = 46%
0.2 %/year uncertainty = 4%

$$Energy(Year_N) = \sum_{n=1}^{N} \frac{Energy(Year_1) \cdot (1 - R_d)^n}{(1 + r)^n}$$

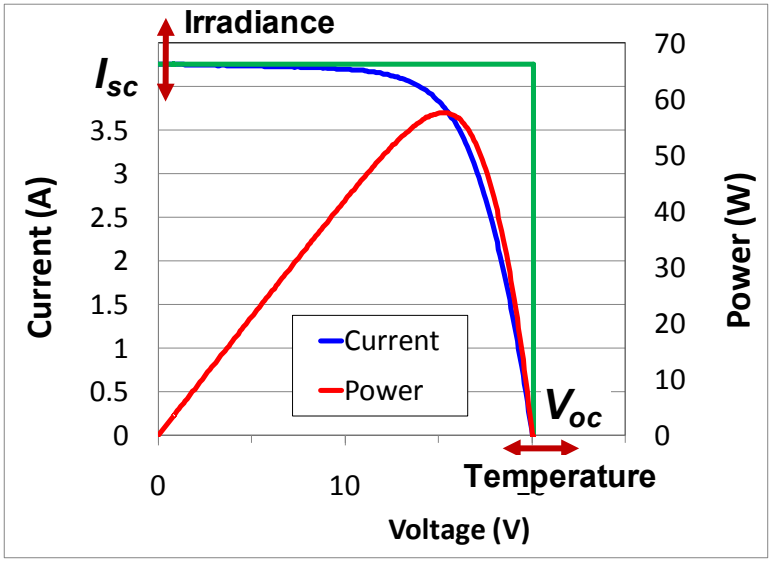
Probability to invoke warranty:

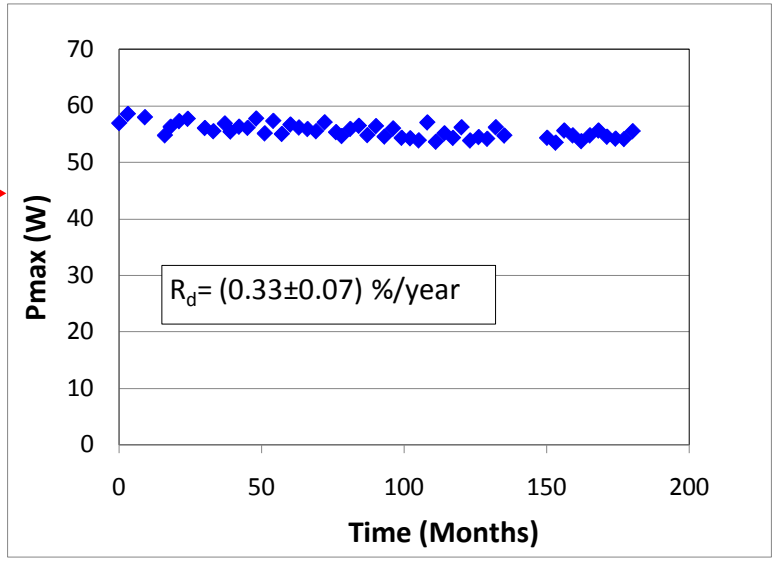
1.0 %/year uncertainty = 57%
0.2 %/year uncertainty = 24%

Higher R_d uncertainty significantly increases warranty risk

Degradation Rate (R_d)- Discrete Points

1. Translation to reference conditions (IEC60891)
2. Time series to determine degradation rate



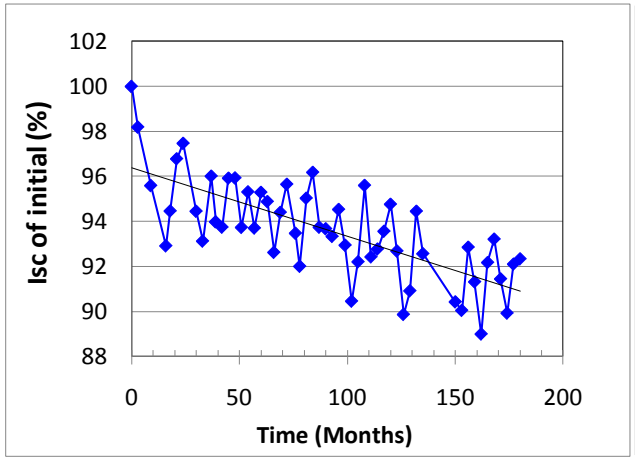


$$FF = \frac{P_{\max}}{I_{sc} \cdot V_{oc}} = \frac{I_{\max} \cdot V_{\max}}{I_{sc} \cdot V_{oc}}$$

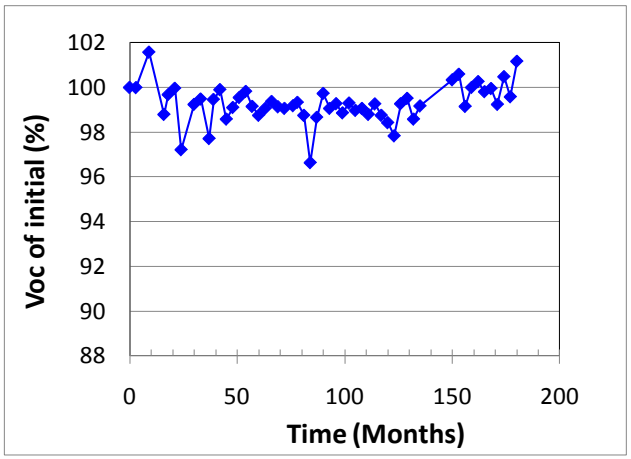
Quarterly taken I-V curves for degradation

Degradation Rate - Discrete Points

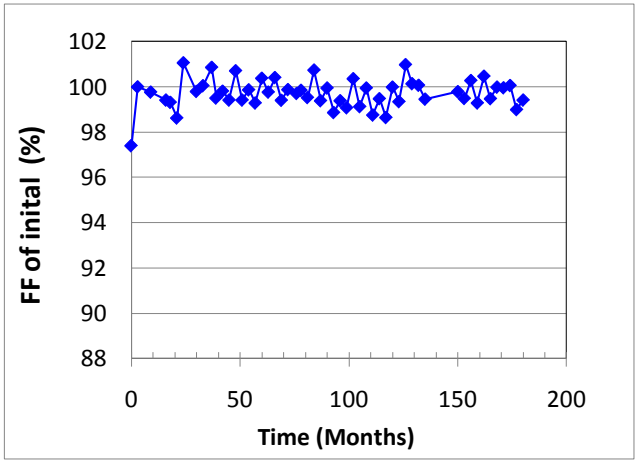
Short-circuit Current



Open-circuit Voltage



Fill Factor



Monocrystalline-Si

Degradation is due to decline in I_{sc}, (V_{oc} & FF are stable) → clues to degradation mechanism

Problem: 1. Labor-intensive, has to be clear sky
2. Large arrays → portable I-V tracer may not be available
3. Typically historical data not available

I-V curves provide clues to underlying failure mechanism

PV for Utility Scale Application (PVUSA)

The plant was originally constructed by the Atlantic Richfield oil company (ARCO) in 1983.

Provided electricity, data & experience in the 1980s and 1990s. Plant was dismantled in the late 1990s.

PVUSA Rating Methodology

Improved PVUSA models include Sandia & BEW model**

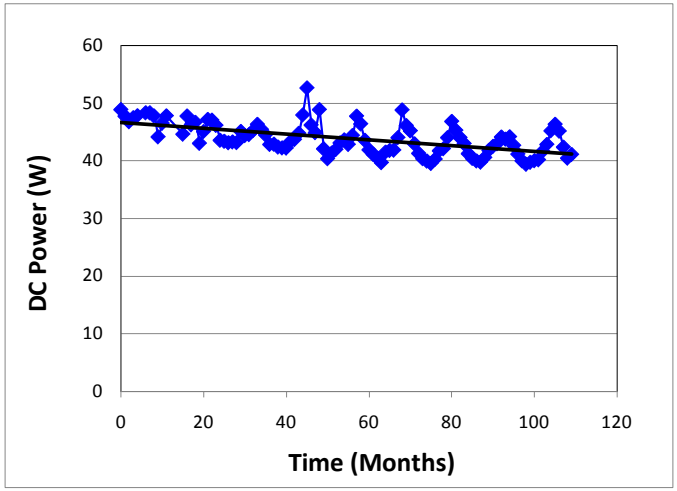
1. Step: Translation to reference conditions (use a multiple regression approach)

$$P = H \cdot (a_1 + a_2 \cdot H + a_3 \cdot T_{ambient} + a_4 \cdot ws)$$

H= Plane-of-array irradiance
$T_{ambient}$=ambient temperature
ws= wind speed
a_1, a_2, a_3, a_4= regression coefficients

Reference conditions:
PVUSA Test Conditions (PTC): E=1000 W/m^2, $T_{ambient}$=20ºC, wind speed=1 m/s

2. Step: Time series to determine degradation rate



Need basic weather station to collect $T_{ambient}$ and wind speed on top of irradiance

Seasonality leads to required observation times of 3-5 years* → long time in today's market

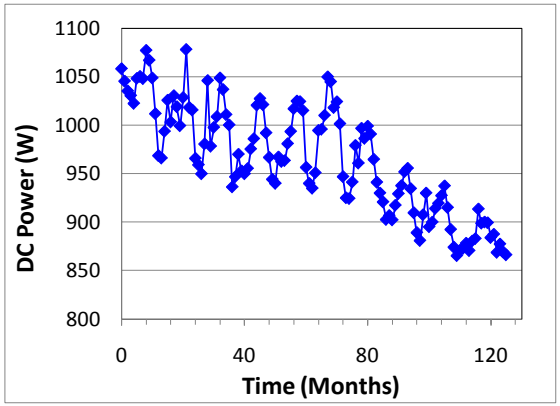
Long time required for accurate R_d

*Osterwald CR et al., Proc. of the 4th IEEE World Conference on Photovoltaic Energy Conversion, Hawaii, 2006.
**Kimber A. et al., Improved Test Method to Verify the Power Rating of a PV Project. Proceedings of the 34th PVSC, Philadelphia, 2009.

Classical Decomposition

Signal = Trend + Seasonality + Irregular

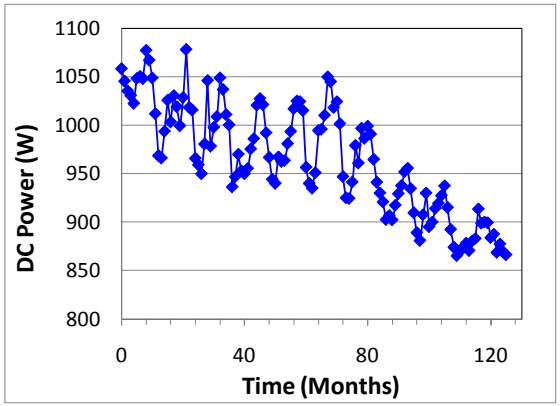
Original Data

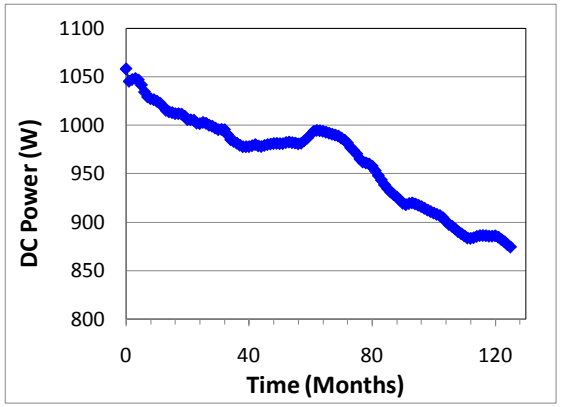


Classical Decomposition

Signal = Trend + Seasonality + Irregular

Original Data





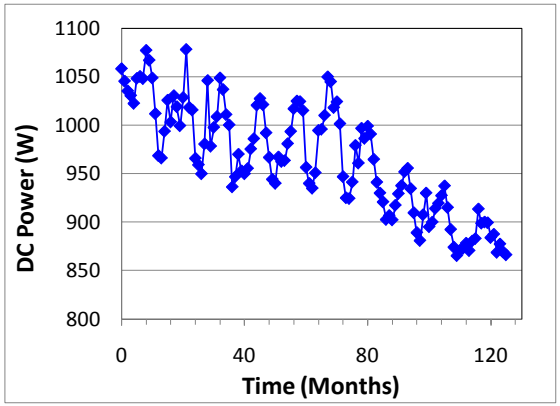
Trend

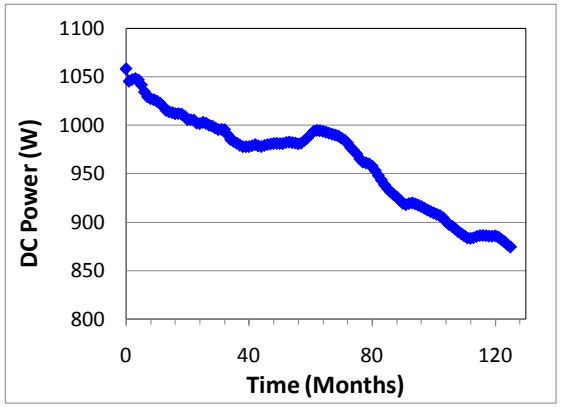
12-month centered-Moving Average

Classical Decomposition

Signal = Trend + Seasonality + Irregular

Original Data



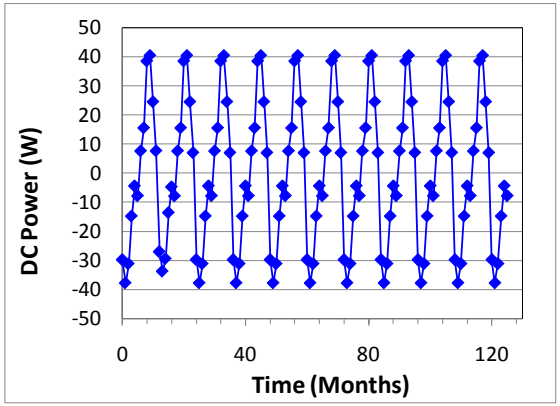


Trend

12-month centered-Moving Average

Seasonality

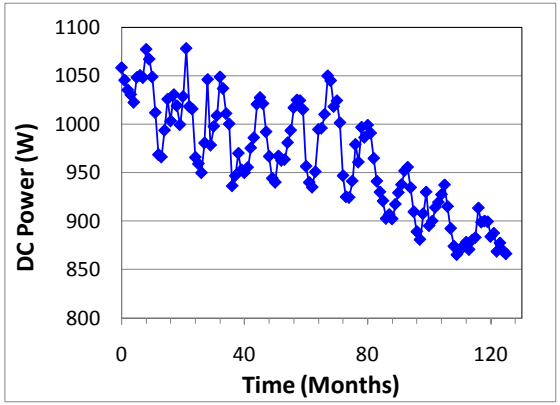
Average of each month for all years of observation

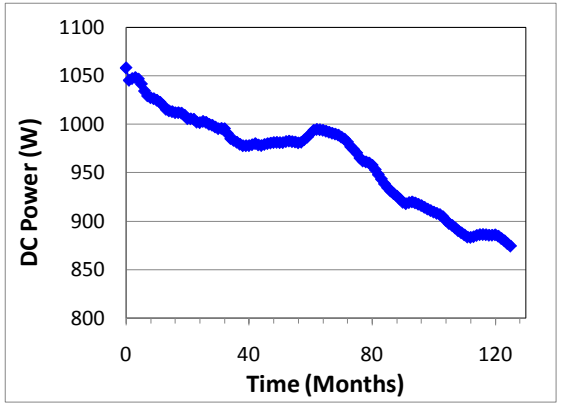


Classical Decomposition

Signal = Trend + Seasonality + Irregular

Original Data



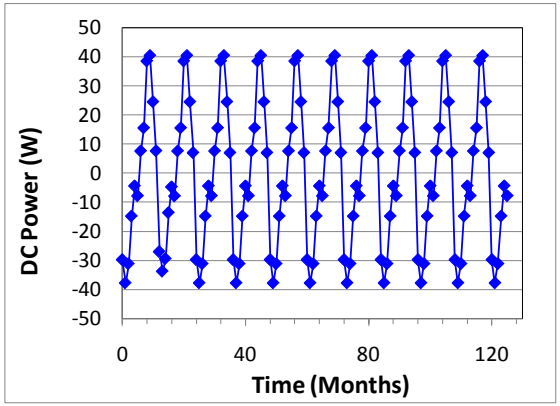


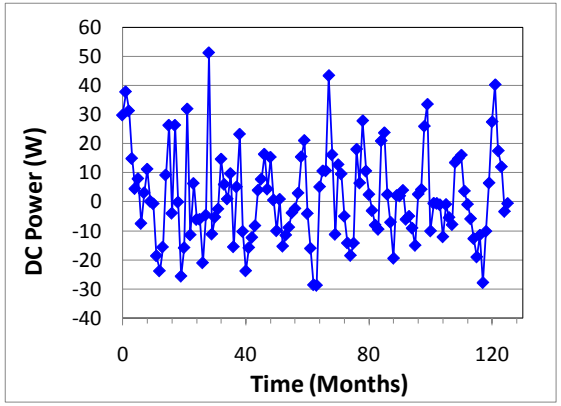
Trend

12-month centered-Moving Average

Seasonality

Average of each month for all years of observation





Irregular

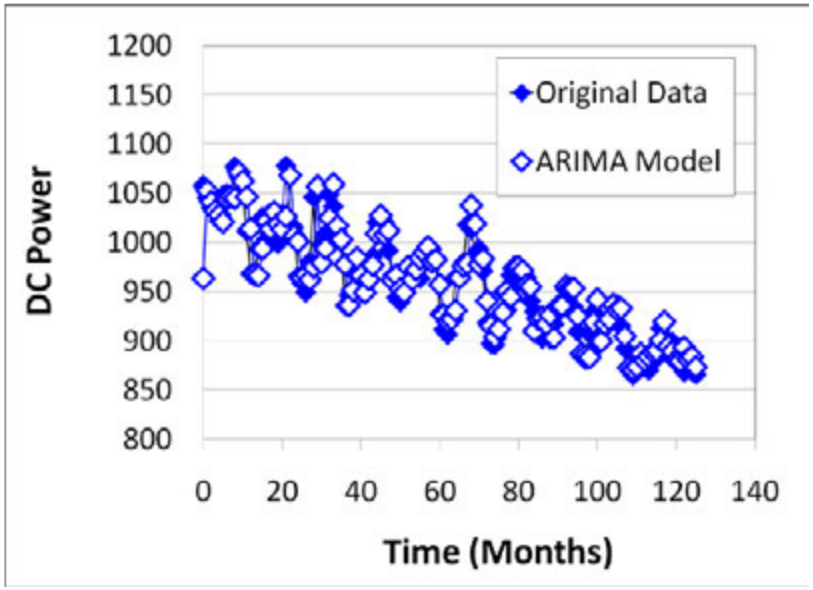
Determine R_d from Trend graph for higher accuracy

S.G. Makridakis et al., "Forecasting", New York, John Wiley & Sons 1997.

ARIMA

Auto**R**egressive **I**ntegrated **M**oving **A**verage (ARIMA)

Model trend & seasonality component w/ Linear Combination of weighted differences & averages



$$P_t - P_{t-12} - \phi \cdot P_{t-1} + \phi \cdot P_{t-13} = \delta + \varepsilon_t - \theta \cdot \varepsilon_{t-12}$$

ARIMA(100)(011)

P=Power
c, δ, ϕ, θ =constant
ε=noise

1. Built several Models → minimize noise component
2. Chose parsimonious model w/ aid of several selection criteria

2 free software packages, US Census Bureau, Bank of Spain: plug & play, sensitive to outliers!

Many statistical software packages include time series analysis (JMP, Minitab, R etc)
Developed script to make model selection less sensitive to outliers.

Use ARIMA to model data, then decompose

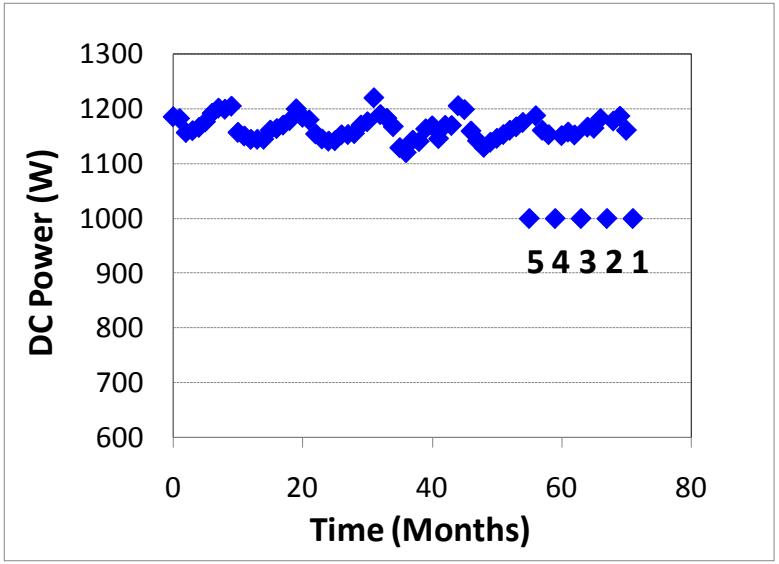
Box, GPP and Jenkins, G: Time series analysis: Forecasting and Control, San Francisco: Holden-Day, 1970.

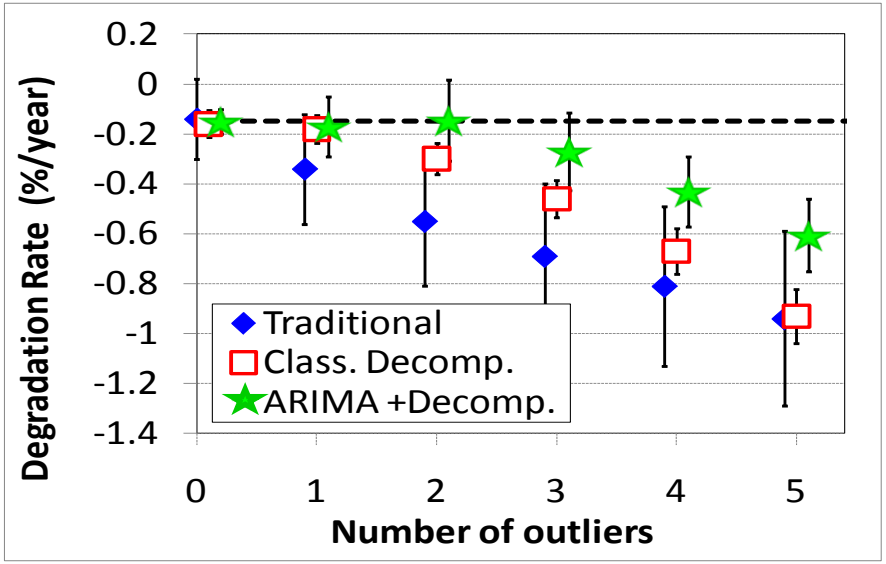
Outliers

Compare sensitivity of 3 methods to outliers

Procedure:

1. Dataset from NREL
2. Introduce outliers sequentially
3. Calculate R_d & study effect on all 3 methodologies





ARIMA most robust against outliers

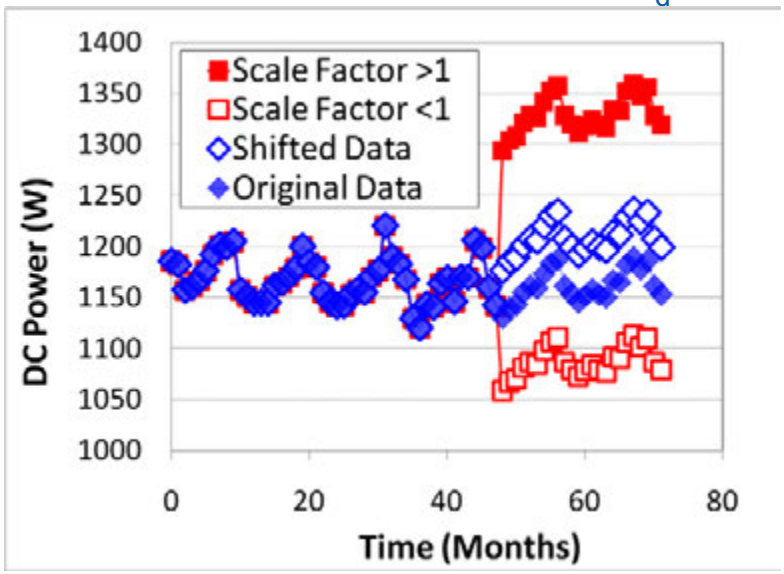
Data Shifts

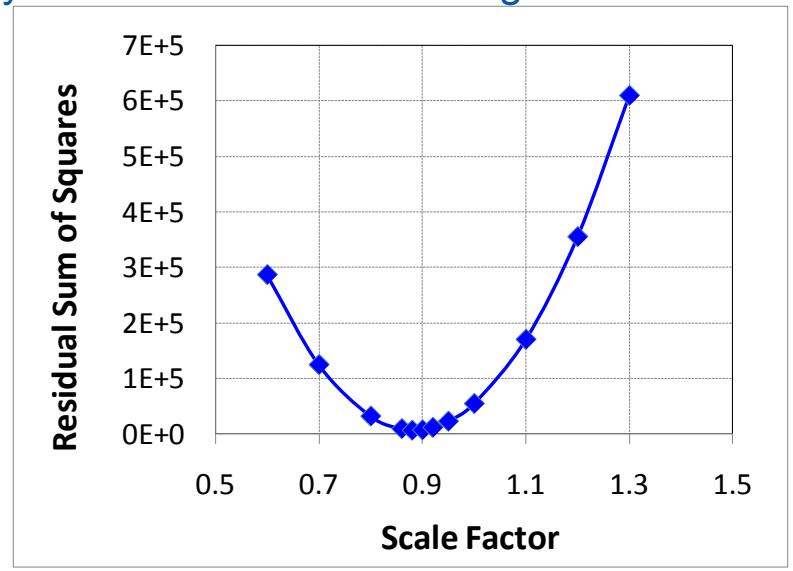
Compare sensitivity of 3 methods to data shifts

Example: inverter change

Procedure:

1. Dataset from NREL
2. Introduce a data shift deliberately
3. Multiply shifted section with a scaling factor
4. Calculate R_d & study effect on all 3 methodologies

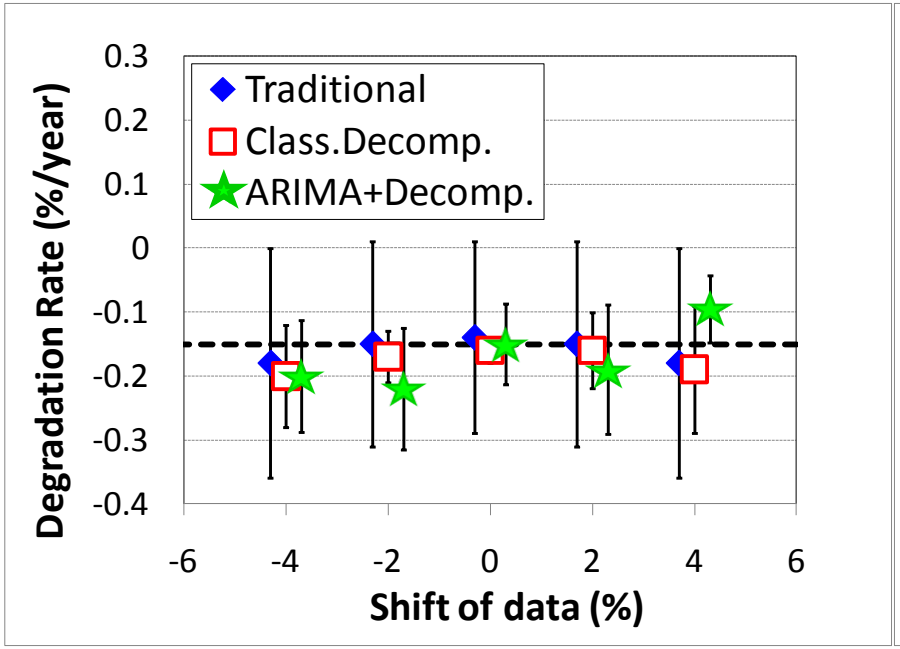




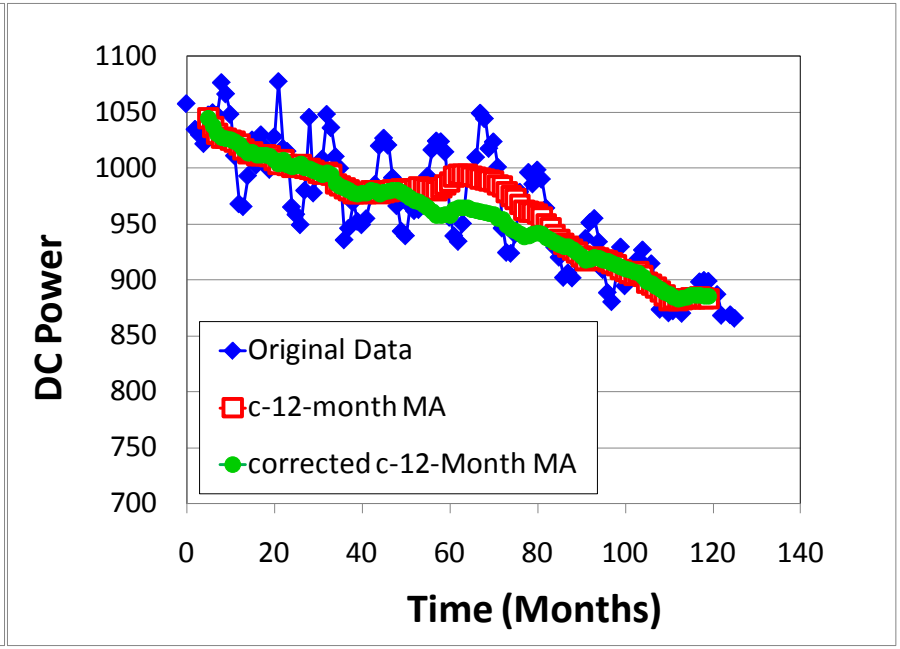
Correct data shifts by minimizing residual sum of squares

Data Shift Results

Results from induced shift



Real Shift – Blind test



Data shift correction procedure is successful for all 3 approaches.

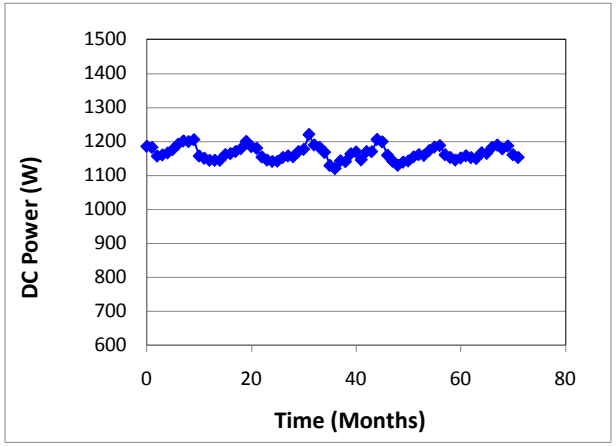
Data shift cause: Erratic ambient Temp sensor.
Misleading degradation rate if R_d calculated after shift.

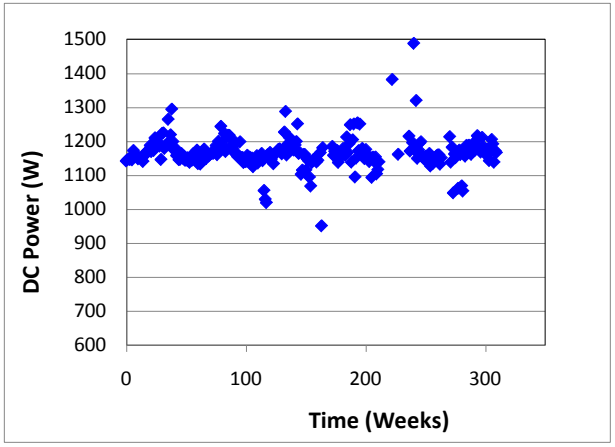
Residual minimization technique works on real shifts

PVUSA – Weekly Intervals

Multi-crystalline module

Monthly Intervals



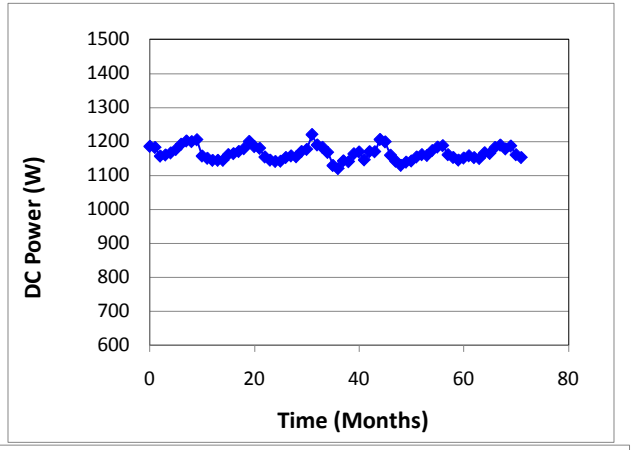


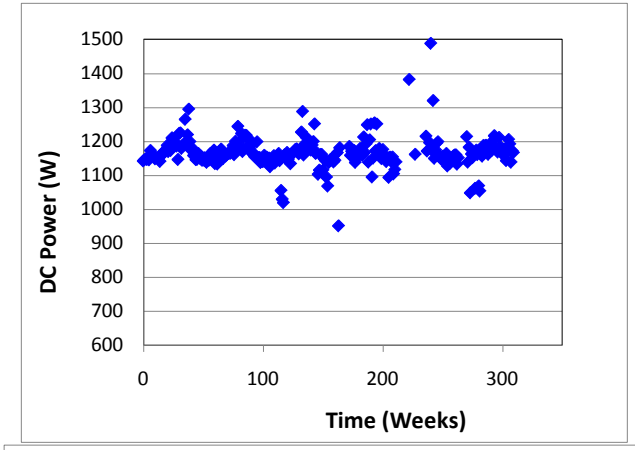
Weekly Intervals

PVUSA – Weekly Intervals

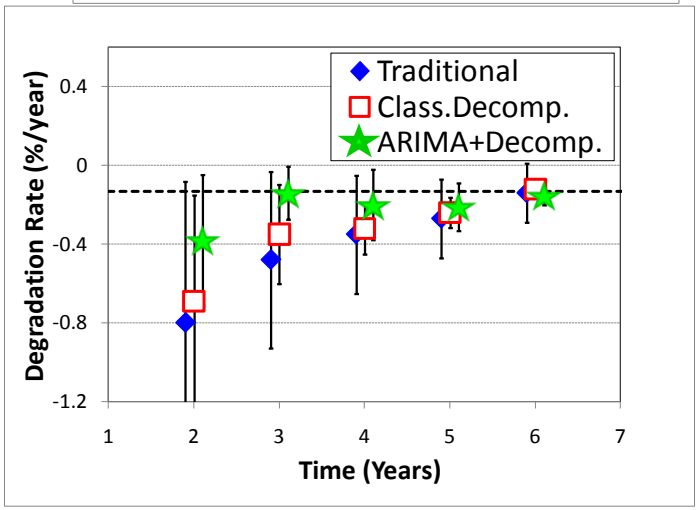
Multi-crystalline module

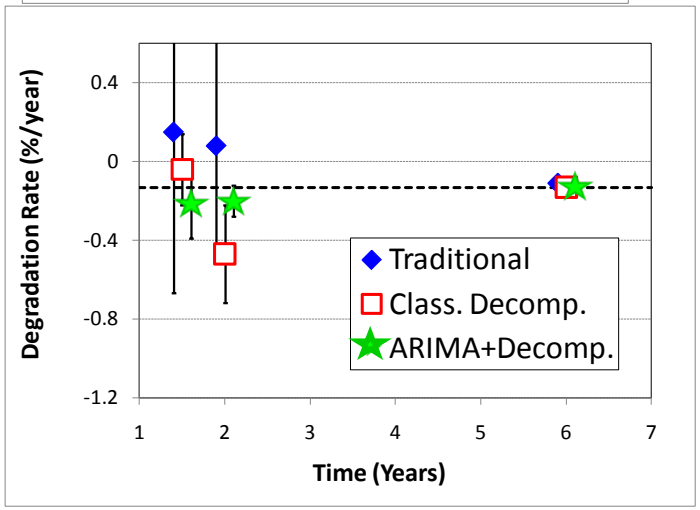
Monthly Intervals





Weekly Intervals

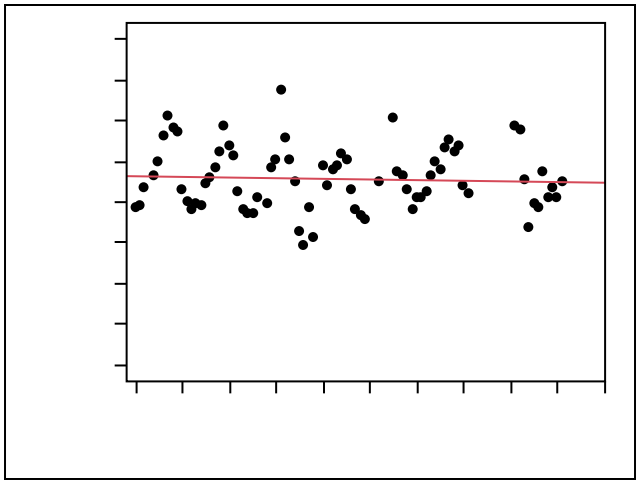




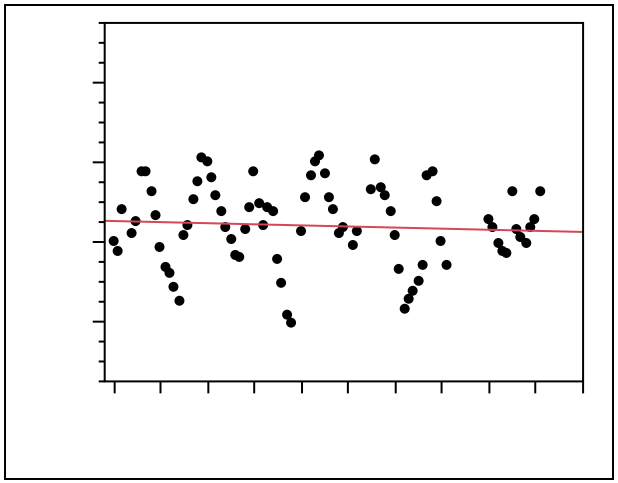
Weekly intervals → converges in less time

Performance Ratio

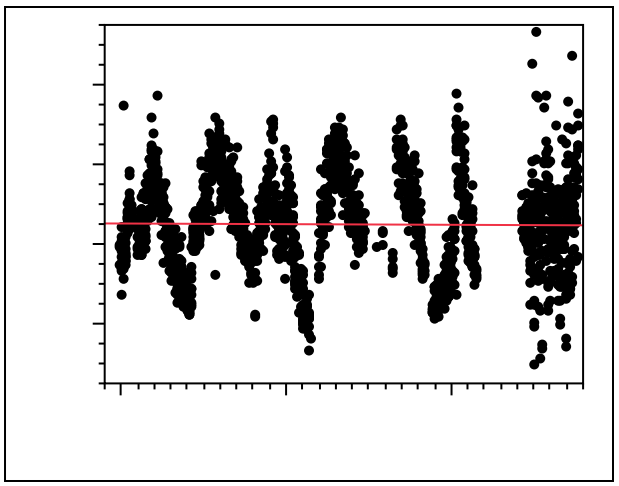
PVUSA



Monthly PR



Daily PR



Multi-crystalline Si system

$$Y_f = \frac{E}{P_0}$$

Y_f=Final Yield
E=Net Energy output
P_0=Nameplate DC rating

$$Y_r = \frac{H}{G}$$

Y_r=ReferenceYield
H=In-plane Irradiance
G=Reference Irradiation

$$PR = \frac{Y_f^*}{Y_r}$$

Can apply same modeling approaches to minimize seasonality

*B.Marion et al., "Performance Parameters for Grid-Connected PV Systems", Proc. 31st PVSC, Orlando, FL 2005.

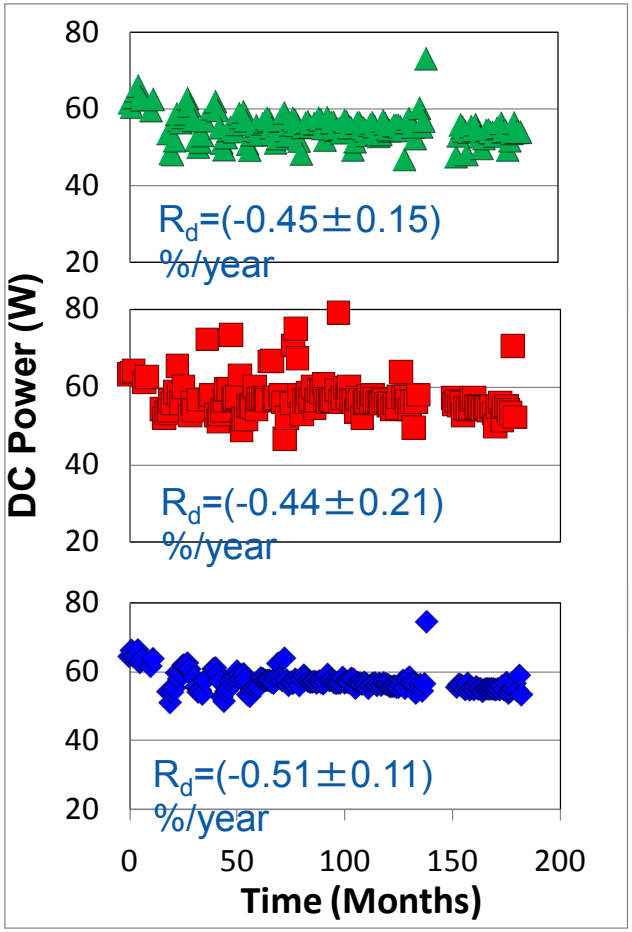
Data Filtering

Irradiance filtering interval

Too broad

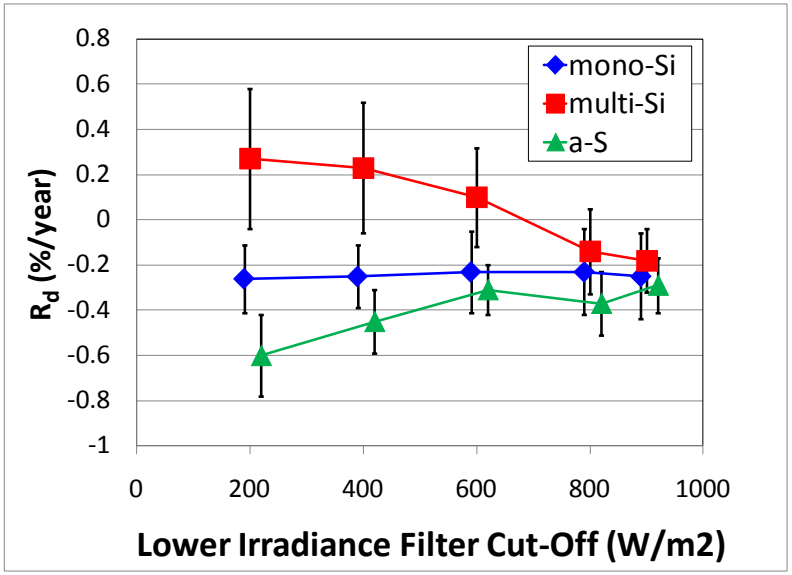
Too tight

best



mono-Si

PVUSA on 3 different modules



Example on how variable R_d may be depending irradiance filtering (may not be representative)

Filtering interval too tight or broad → R_d may be substantially different and uncertainty goes up

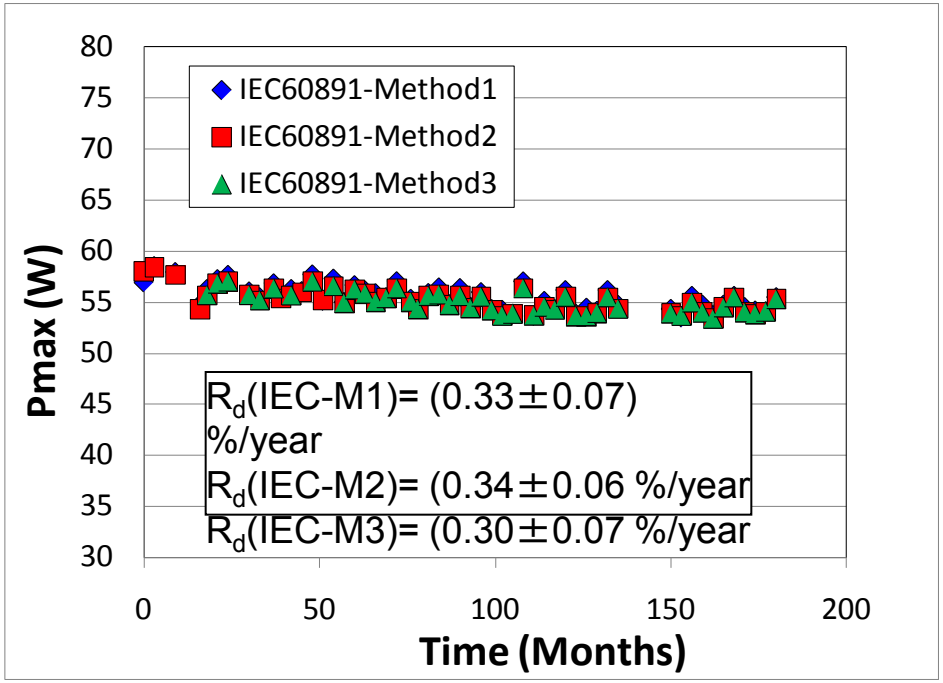
A. Kimber paper showed uncertainty may be reduced by using only sunny days

Data filtering has important impact on determined R_d

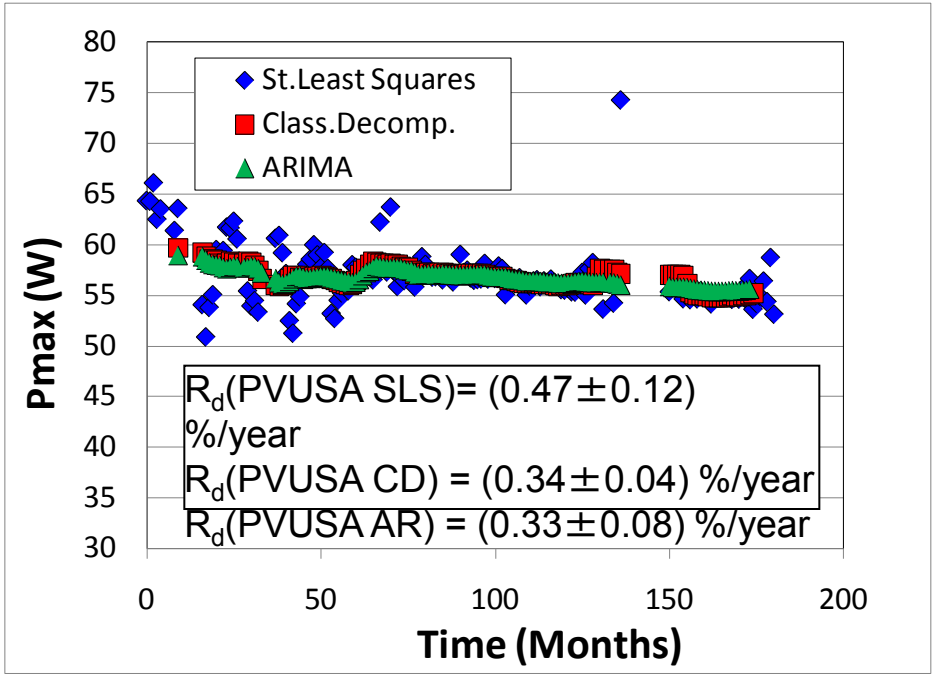
Kimber A. et al., Improved Test Method to Verify the Power Rating of a PV Project. Proceedings of the 34th IEEE PV Specialist Conference, Philadelphia, 2009.

Discrete vs. Continuous Data

IEC 60891



PVUSA



Quarterly taken IV + IEC translation less uncertainty than PVUSA

PVUSA + Modeling uncertainty is comparable to IEC method

Methodologies - Summary

	Time series	Data Type /# Data Pts.	Data Aqc.	Reference condition	Uncer-tainty	Outliers/ Dt.shifts sensitivity	Impleme ntation	Comments
PVUSA	**SLS**	continuous	DC, H, T, ws	PTC	ok?	high	easy	
	CD	"	"	"	good	medium	easy	
	ARIMA	"	"	"	best	low	difficult	Software & training required
PR	**SLS**	continuous	AC, H	----	ok?	high	easy	
	CD	"	"	"	good	medium	easy	
	ARIMA	"	"	"	best	low	difficult	Software & training required
IV-2	**SLS**	discrete, 2	I,V, H, T	STC, IEC60891	ok?	high	easy	difficult for larger arrays
IV-3+	**SLS**	Discrete, >2	"	"	best	low	easy	"

SLS: Standard Least Squares, CD: Classical Decomposition
H: in-plane irradiance, T: temperature, ws: wind speed

Contin. Data: Class.Decomp. may be good compromise

Discrete: Better take more than 2 measurements

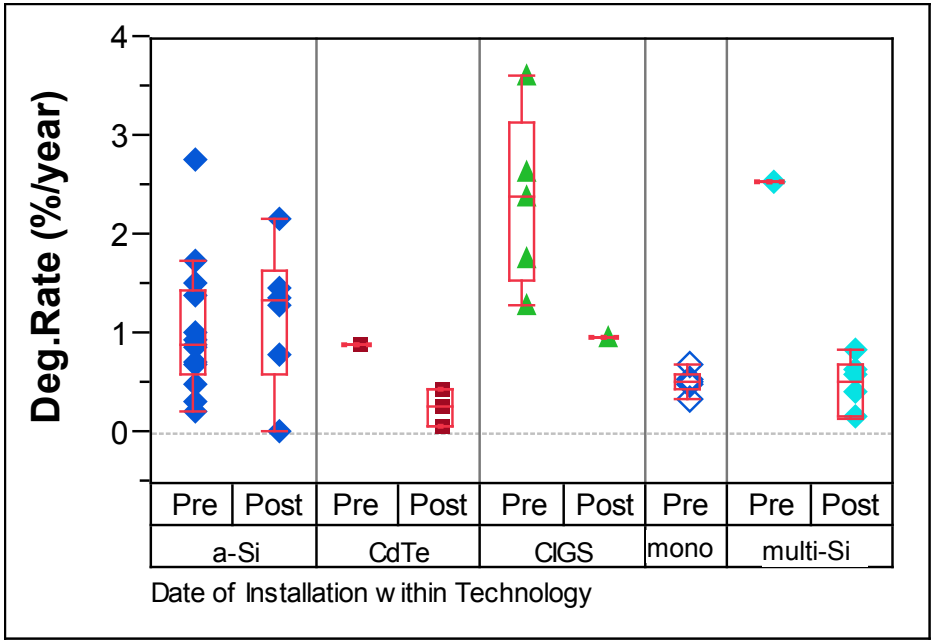
PERT – Degradation Rates

Performance Energy Rating Testbed = PERT



Photo credit: Warren Gretz, NREL PIX 03877.

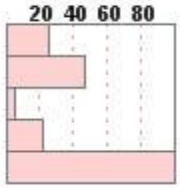
More than 40 Modules,
> 10 manufacturers,
Monitoring time: 2 yrs-16 yrs



Pre: Installed before year 2000
Post: Installed after year 2000

Variance Components

Component	Var Component	% of Total
Technology	0.3714	26
Date of Installation[Technology]	0.6886	47
Manufacturer[Technology,Date of Installation]	0.0782	5
Within	0.3151	22
Total	1.4533	100

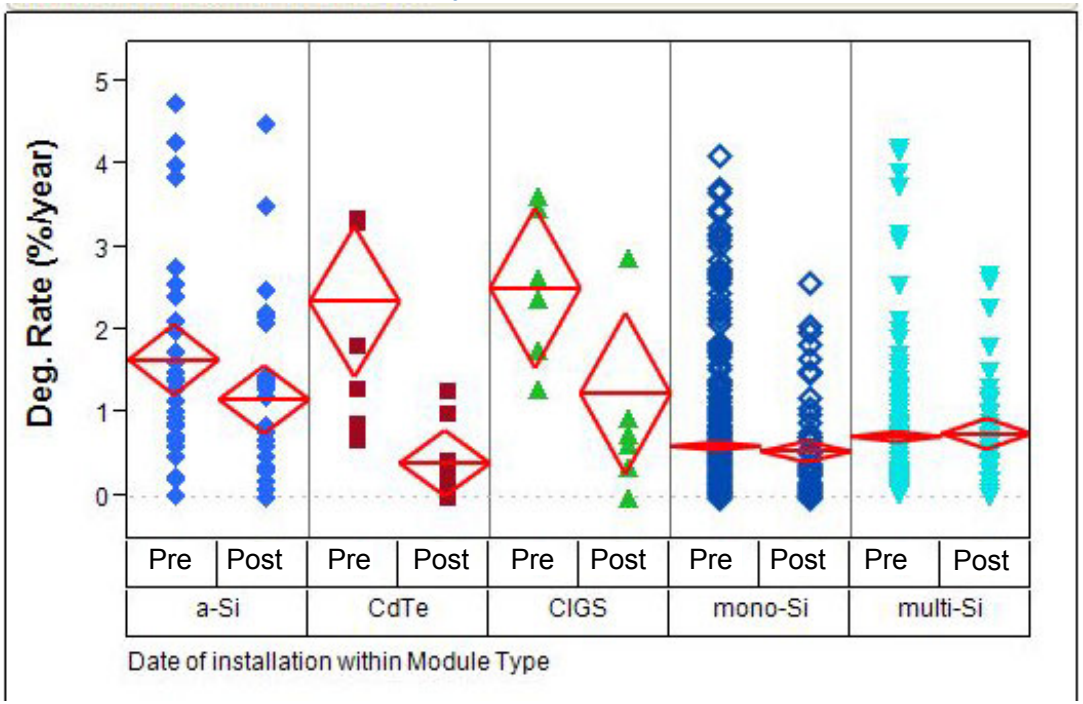


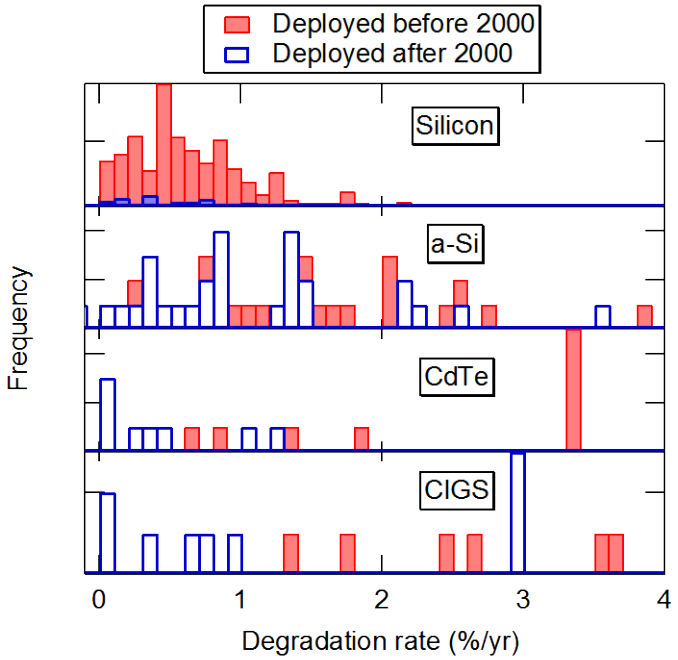
Appears that CdTe, CIGS & multi-Si improved

D.C. Jordan et al., Outdoor PV degradation comparison, Proc. IEEE PVSC, 2010, 2694.

Degradation Rates – Literature Survey

Number of R_d from literature: 1364 ca. 100 publications (see end)





Partitioned by date of installation: Pre- & Post-2000
Red diamonds: mean & 95% confidence interval

Crystalline Si technologies appear to be the same

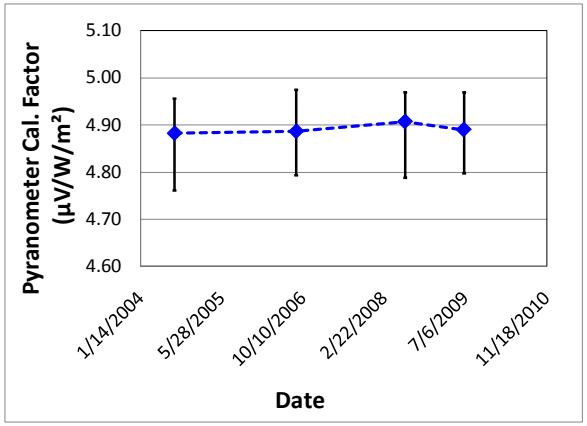
Thin-film technologies saw significant drop in R_d in last 10 years

NREL CIGS System



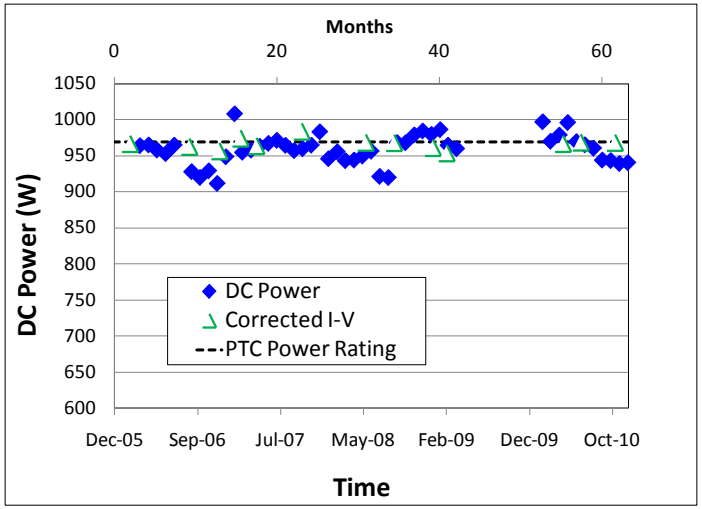
Shell Solar E80-C modules deployed at NREL. Photo credit: Harin Ullal, NREL PIX 14725

Pyranometer calibration



R_d	Statistical Uncertainty	Method	Interval
0.14	0.22	PVUSA Linear Fit	Monthly
0.57	0.21	PVUSA Cl.Decomp	Monthly
0.28	0.23	PVUSA ARIMA	Monthly
0.12	0.35	Performance Ratio Linear Fit	Monthly
0.61	0.10	PR Cl.Decomp	Monthly
0.47	0.13	PR ARIMA	Monthly
0.14	0.10	Performance Ratio Linear Fit	Daily
0.28	**0.22**	**Median ± pooled Standard deviation**	

PVUSA + Field I-V data

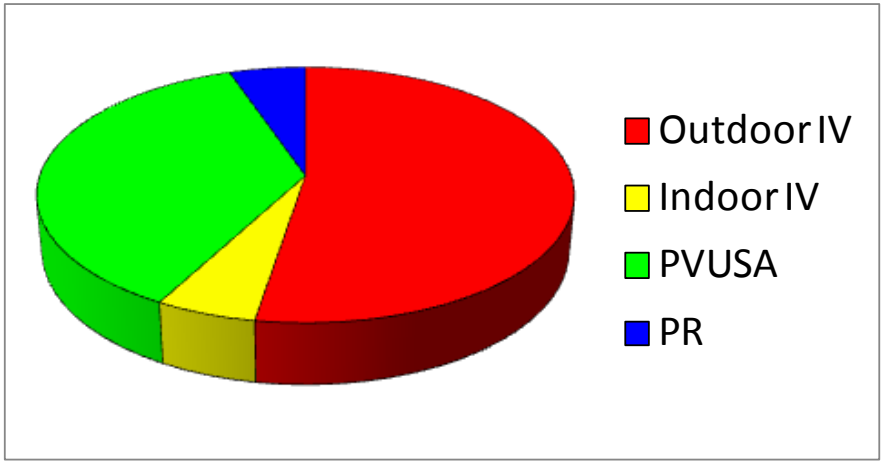


Deployed in Golden ,CO
Jan-06

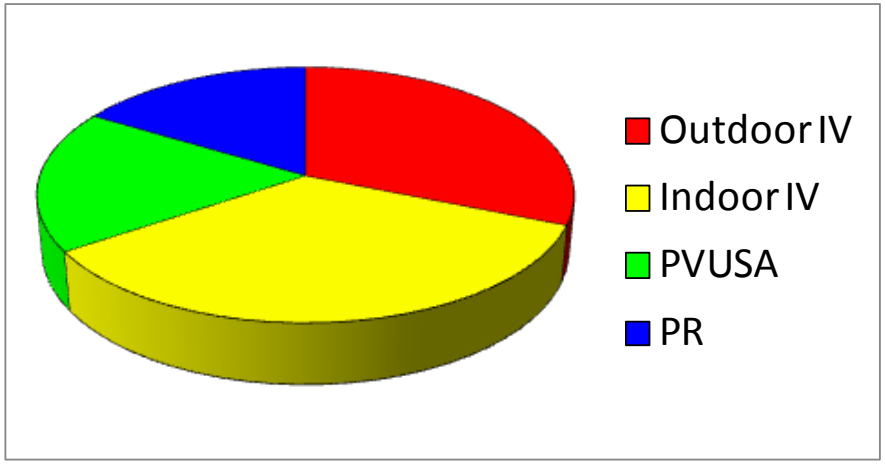
Results from this array appears to support findings from literature

Development of Methodologies

Pre 2000



Post 2000



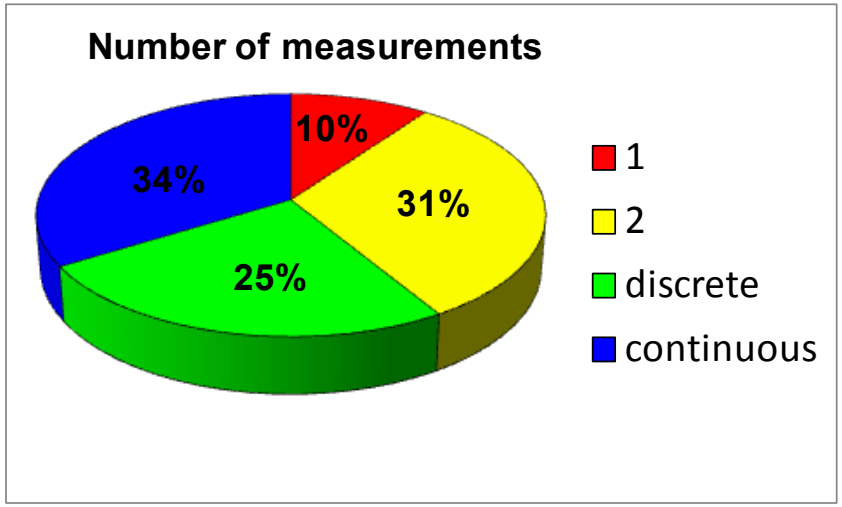
Percentage of Indoor IV has increased manifold → better tools

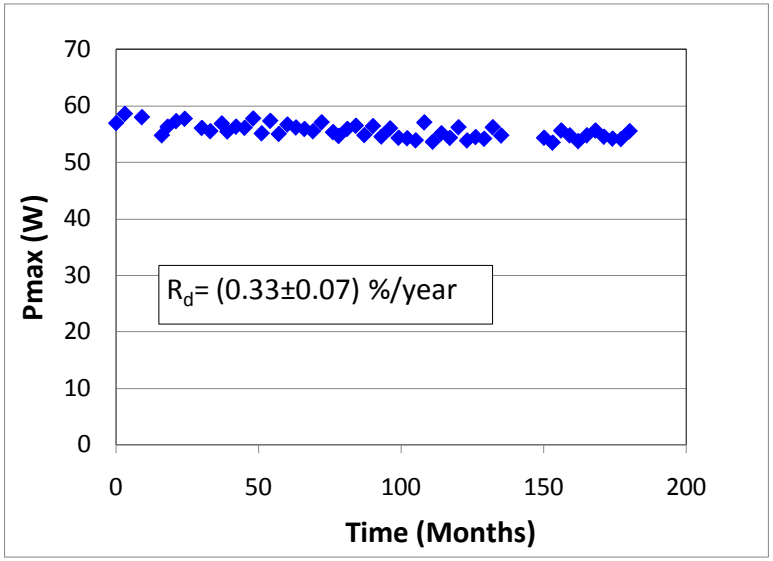
Percentage PR has increased → more installations, easy to collect AC data, don't necessarily need an entire weather station

Percentage PVUSA decreased significantly → pronounced seasonality & sensitivity to outliers

PVUSA methodology use has significantly declined

R_d literature – Number of measurements





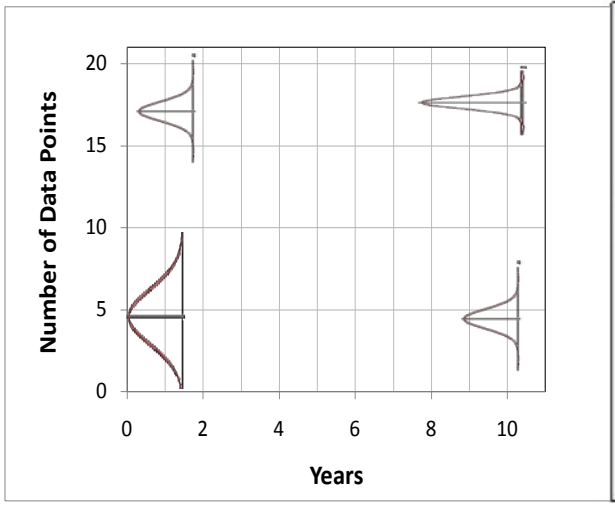
40% take only 1 or 2 measurements

1 Measurement: baseline no longer available or were never taken → have to compare to nameplate rating

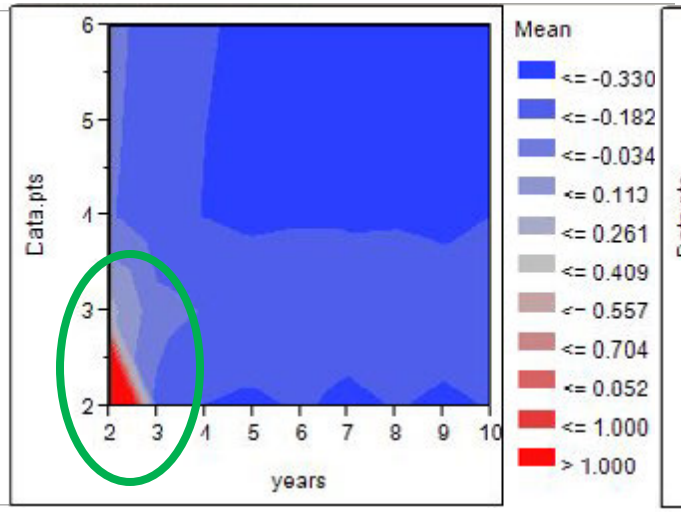
Procedure:
1.Take quarterly I-V data set
2.Randomly pick 2 data points & calculate Rd → repeat many times
3. Randomly pick 3 data points & calculate Rd → repeat many times
4.Rd will depend on # of data points & time span → can create 2D map

More than 40% of all R_d literature take only 1 or 2 measurements

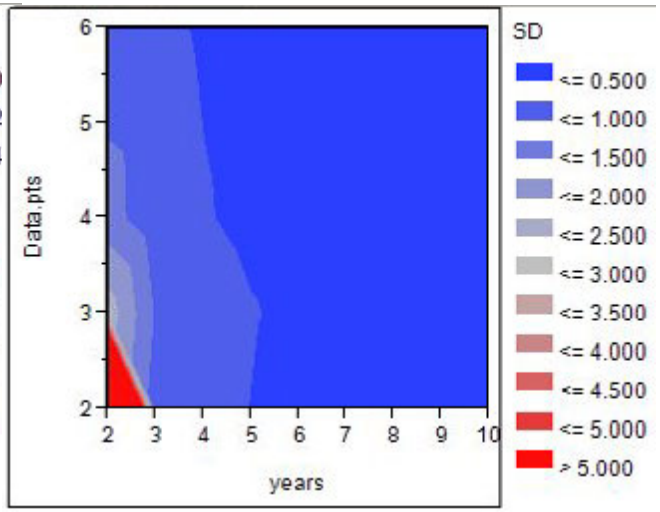
Effect of number of data points and years on R_d



Mean R_d



Standard Deviation



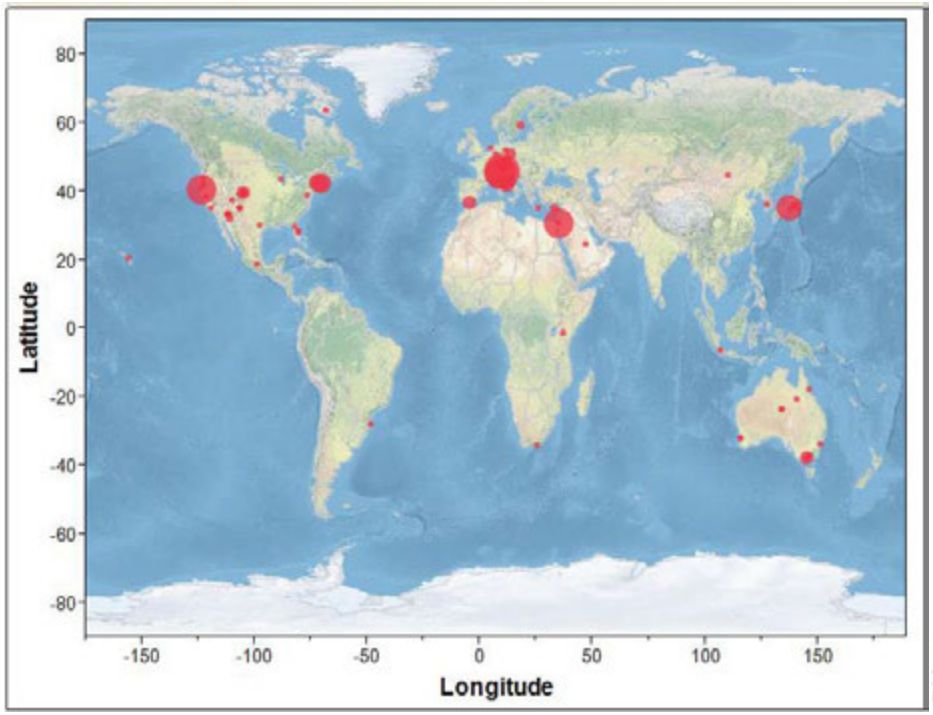
"True Rd"=-0.33 %/year (dark blue)

The curve is very steep for small data points and short time span

Even between 2-3 years can come close to "true Rd" simply by taken a few more data points

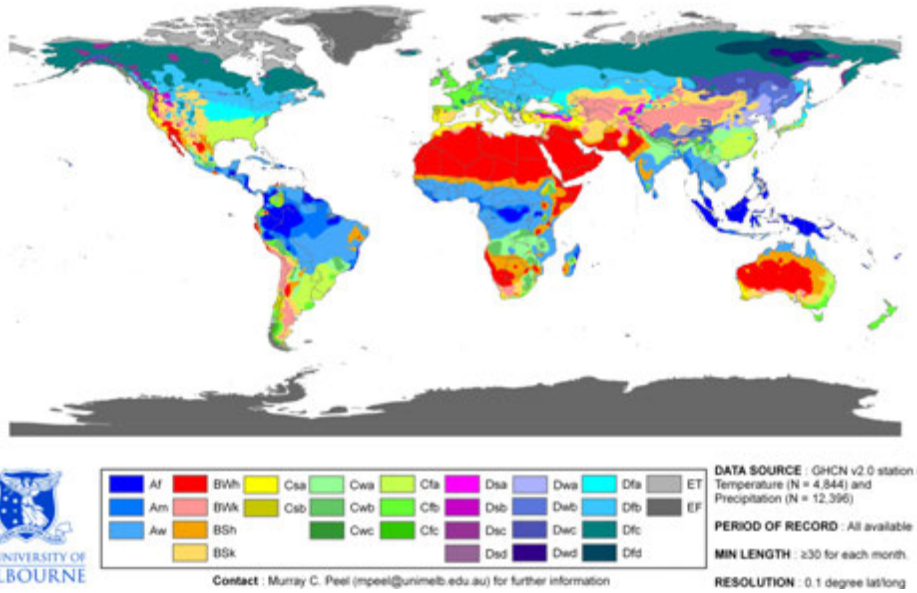
Would like to see more data points taken

Degradation Rates around the World



Size of circle: number of modules/systems tested

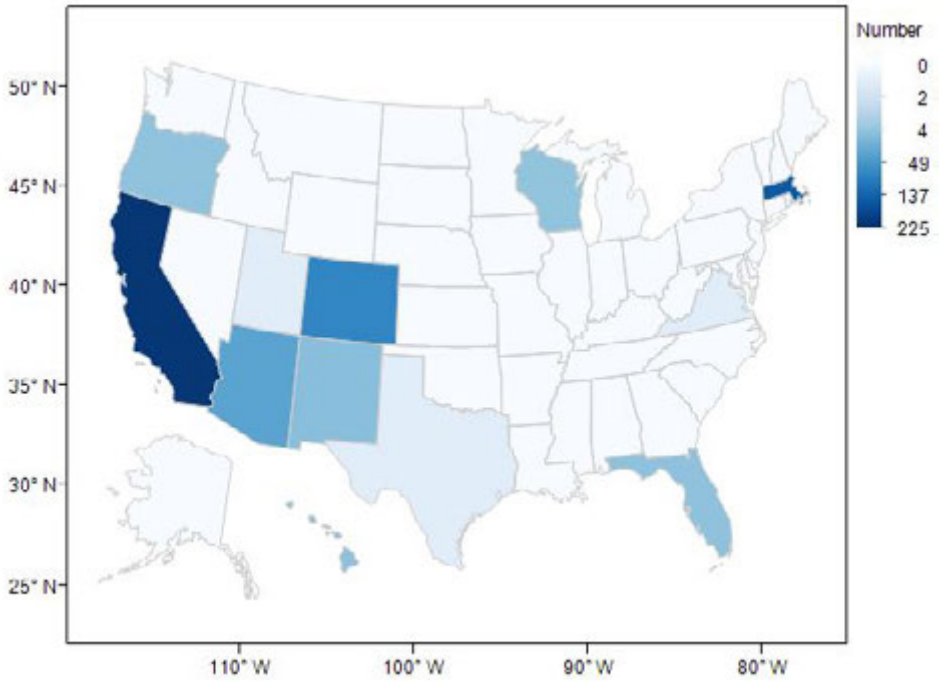
Köppen-Geiger climate map of the world (2007)



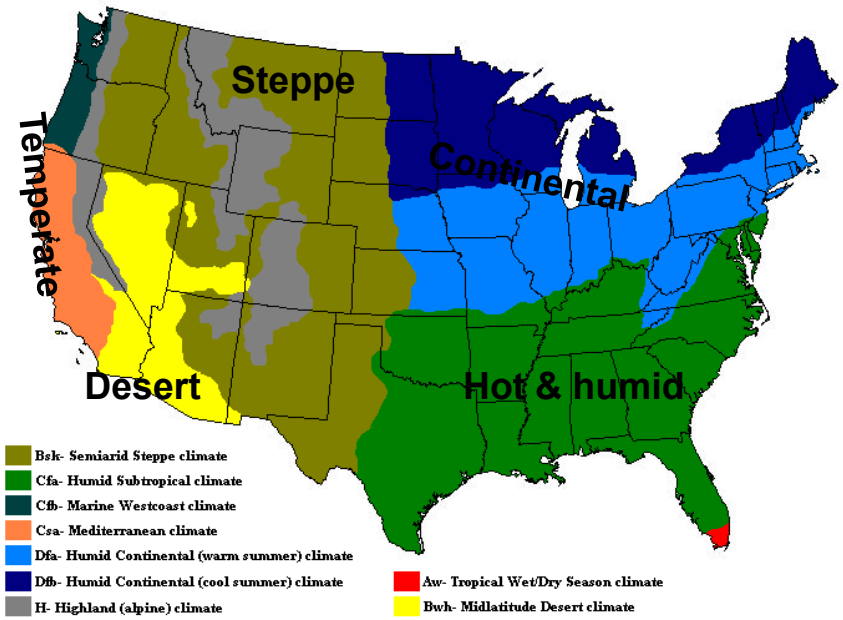
Main climates	Precipitation	Temperature	
A: equatorial	W: desert	h: hot arid	F: polar frost
B: arid	S: steppe	k: cold arid	T: polar tundra
C: warm temperate	f: fully humid	a: hot summer	
D: snow	s: summer dry	b: warm summer	
E: polar	w: winter dry	c: cool summer	
	m: monsoonal	d: extremely continental	

No reported degradation rates in many climate zones

Degradation Rates around the USA



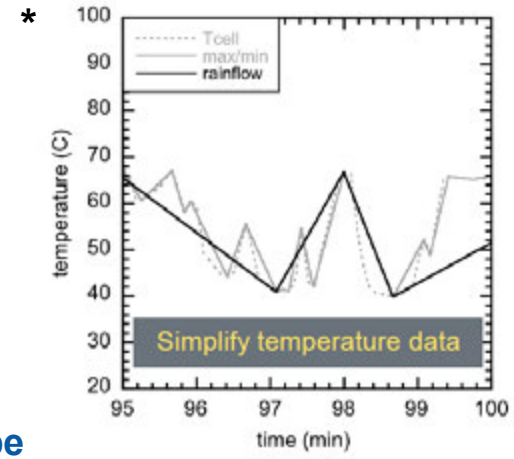
Climate Zones of the USA



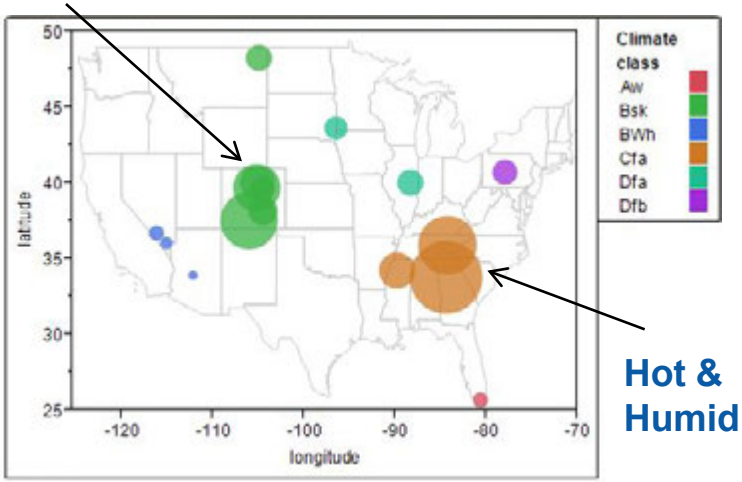
Similar picture as from around the world → some climate zones have not been investigated

No reported degradation rates in some climate zones

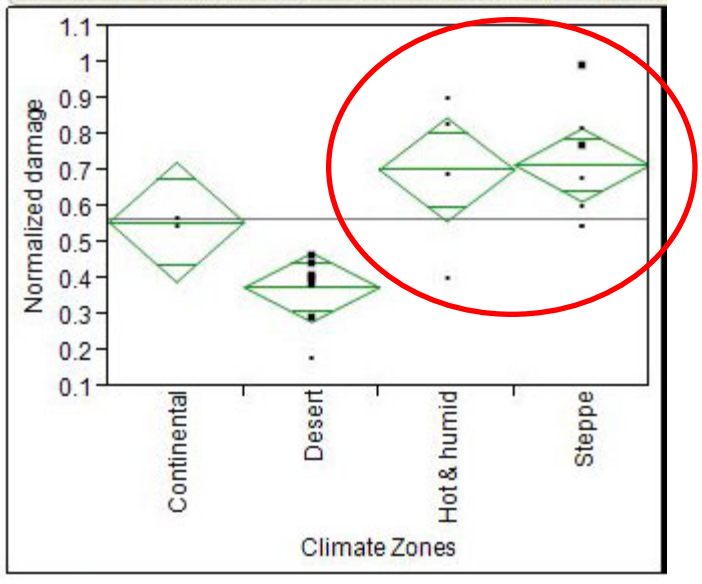
Rainflow Calculations



Steppe



Hot & Humid



Analysis of Variance

Source	DF	Sum of Squares	Mean Square	F Ratio	Prob > F
Clim.code2	3	0.57996071	0.193320	10.1472	0.0003*
Error	20	0.38103308	0.019052		
C. Total	23	0.96099379			

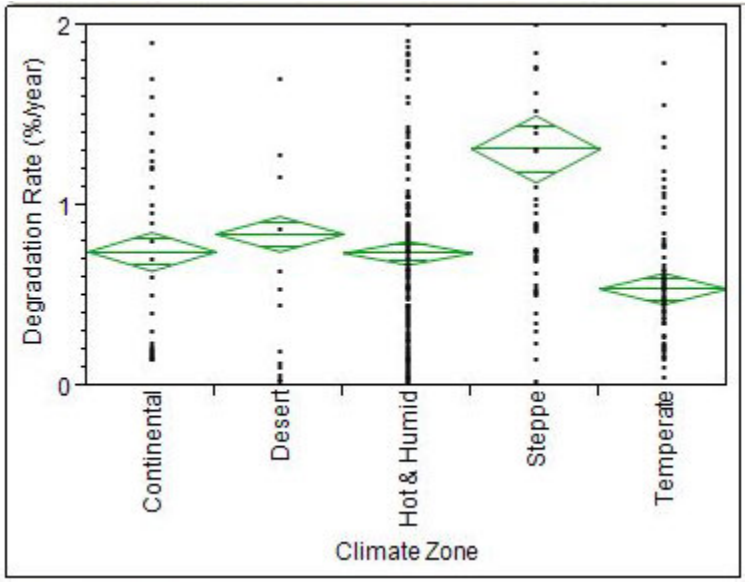
Steppe, Hot & humid show significantly higher damage than Desert & Continental climate.

Steppe Climate has high damage due to thermal cycling

*Quantifying the Thermal Fatigue of CPV Modules_Bosco__NREL_International Conference on Concentrating Photovoltaics_2010

Analysis of all R_d by climate

Pre 2000



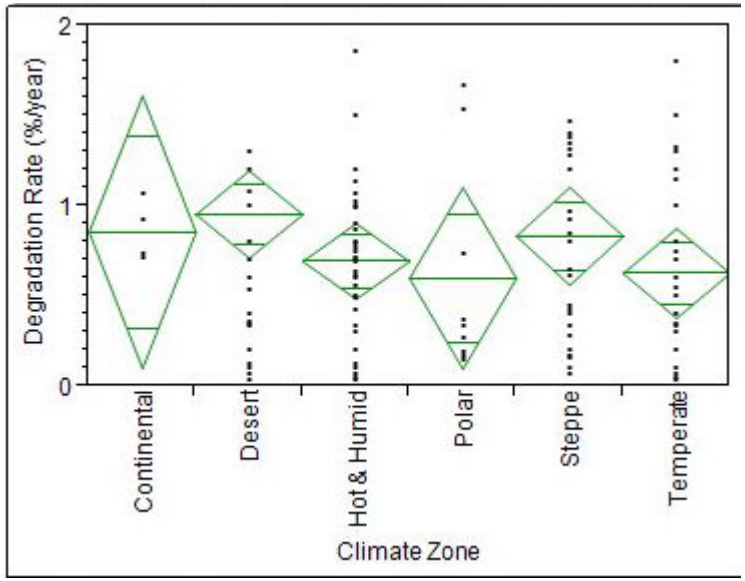
Analysis of Variance

Source	DF	Sum of Squares	Mean Square	F Ratio	Prob > F
Climate Code3	4	32.32	8.08	15.50	<.0001*
Error	1186	618.26	0.52		
C. Total	1190	650.58			

Steppe climate significantly higher.

All Technologies

Post 2000



Analysis of Variance

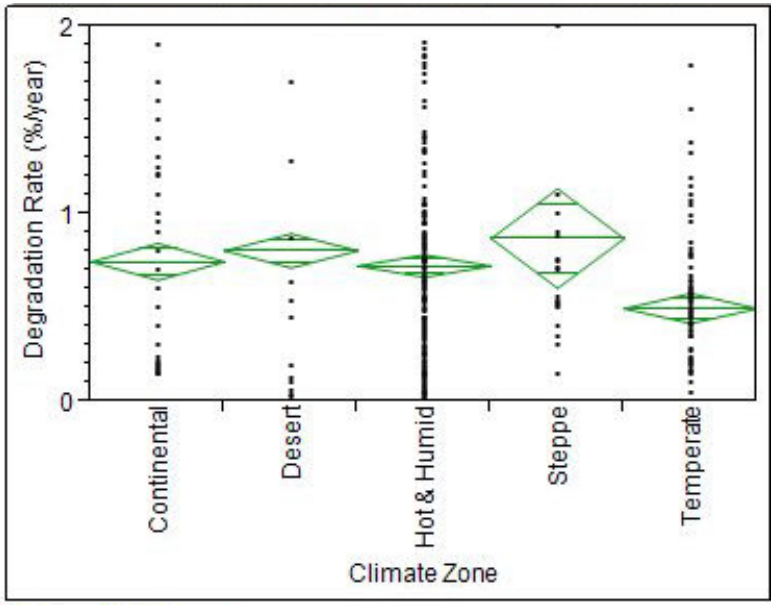
Source	DF	Sum of Squares	Mean Square	F Ratio	Prob > F
Climate Code3	5	2.78	0.56	0.95	0.4514
Error	166	97.25	0.59		
C. Total	171	100.03			

No significant difference.

Steppe Climate shows significantly higher R_d before 2000

Analysis of R_d by climate – c-Si

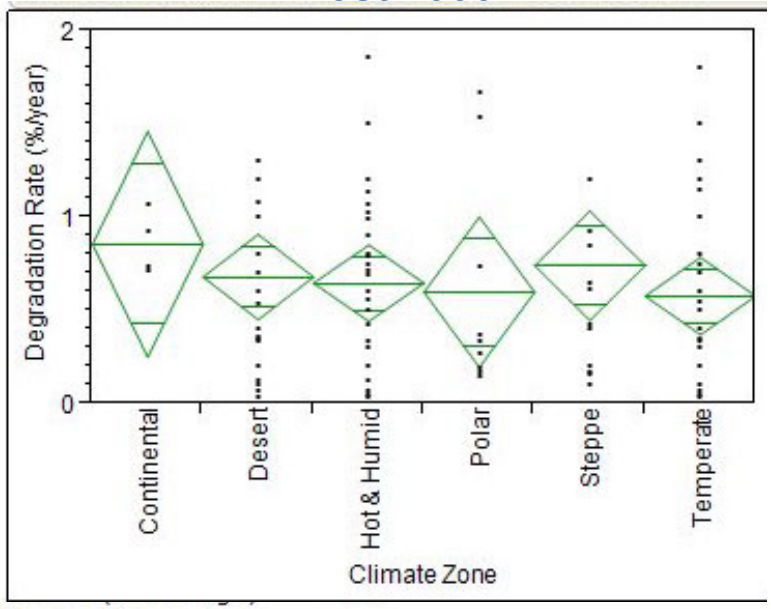
Pre 2000



Analysis of Variance

Source	DF	Sum of Squares	Mean Square	F Ratio	Prob > F
Climate Code3	4	14.53	3.63	8.28	<.0001*
Error	1138	499.39	0.44		
C. Total	1142	513.92			

Post 2000



Analysis of Variance

Source	DF	Sum of Squares	Mean Square	F Ratio	Prob > F
Climate Code3	5	0.53	0.11	0.29	0.9197
Error	121	45.15	0.37		
C. Total	126	45.69			

Similar but not as distinct trend for c-Si

Use of automated equipment, low stress ribbon effect visible…?

Steppe Climate shows significantly higher R_d before 2000

PVDAQ Project

PV Data Acquisition



Use data from government-funded and other projects

Performance data accessible on web page

Eliminate blank spots on the map

Conclusion

- Uncertainty can result in significant warranty risk
- Time series Modeling with continuous data (PVUSA, PR ..) can significantly reduce uncertainty
- Cont. Data: Class. Decomp. May be a good compromise between quality of results & ease of implementation.
- Discrete data: better practice to take more than 2 measurements.
- Analysis from literature and our own systems indicate that degradation rates have improved for installations after 2000.
- Have no data from many of the world's climate zones

Conclusion

- Uncertainty can result in significant warranty risk
- Time series Modeling with continuous data (PVUSA, PR ..) can significantly reduce uncertainty
- Cont. Data: Class. Decomp. May be a good compromise between quality of results & ease of implementation.
- Discrete data: better practice to take more than 2 measurements.
- Analysis from literature and our own systems indicate that degradation rates have improved for installations after 2000.
- Have no data from many of the world's climate zones

Need more data!

Acknowledgments

Thank you for your attention!

dirk.jordan@nrel.gov

Thank you to :
Sarah Kurtz
Ryan Smith
John Wohlgemuth
Nick Bosco
Peter Hacke
Bill Marion
Bill Sekulic
Kent Terwilliger
Rest of the NREL reliability team
Eric Maass

References

PVUSA progress report_Townsend_Endecon_1995.pdf
11 year field exposure_Reis_Humbold State CA_PVSC_2002.pdf
10 year PV review_Rosenthal_NM_PVSC_1993.pdf
Field test of 2400 PV modules_Hishikawa_Japan_PVSC_2002.pdf
Rd analysis c-Si_Osterwald_NREL_PVSC_2002.pdf
c-Si after 20 years_Quintana_Sandia_PVSC_2000.pdf
Rd c-Si_Machida_Japan_SEM&SC_1997.pdf
PV durability_King_Sandia_PiPV_2000.pdf
27+ years PV_Tang_ASU_2006.pdf
PV performance arctic college_Poissant_Canada_2006.pdf
20 year PV_Alawaji_Saudia Arabia_Renewable Energy Reviews_2001.pdf
Outdoor PV degradation_Vignola_UofOregon_ASES_2009.pdf
Perfromance analysis a-Si_Gregg_United Solar_PVSC_2005.pdf
Long-term performance of 8 PV arrays_Granata_Sandia_2008.pdf
Eff degradation c-Si_DeLia_Italy_2003.pdf
Long-term stability of the SERF_Marion_NREL_2003.pdf
double junction a-Si BIPV_Ruther_Brazil_2003.pdf
Performance losses_Mani_IPVR_2009.pdf
a-Si in different climates_Gottschalg_England_2001.pdf
a-Si in Sacramento_Osborn_Spectrum Energy_2003.pdf
Performance of a-Si in diff climates_Rüther_Brazil_2006.pdf
PV round robin_IEA Task2_Austria_2006.pdf
TISO-20 Jahre ARCO-PP.pdf
Anual report_LEEE-TISO_Switzerland.pdf
Field test in Mexico_Foster_New Mexico State_2005.pdf
c-Si of 22 years_Dunlop_EU_2006.pdf
Common degradation mechanism_Quintana_Sandia_IEEE_2003.pdf
Field test of c-Si in 1990_Sakamoto_Japan_PVenergyconv_2003.pdf
PV degradation_King_Sandia_2003.pdf
Outdoor PV in Sahara 3months_Saok_Algeria_2008.pdf
PV Greece_Kalykakis_Greece_2009.pdf
PV Korea_So_Korea_2006.pdf
Outdoor PV on Cyprus_Makrides_Cyprus_2009.pdf
DegRate for c-Si_Osterwald_NREL_2002.pdf
Outdoor testing at ASU_Mani_ASU_2006.pdf
PV Power production after 10 years_Cereghetti_Switzerland_2003.pdf
Degradation of a-Si_van Dyk_South Africa_SEM&SC_2010.pdf
20 year lifetime_Dunlop_EU_2005.pdf
Predicted long-term PV performance_Muirhead_Australia_PVScienceConf_1996.pdf
Long-term field age_Skoczek_Italy_2009.pdf
Degradationenergy payback_Davis_FSEC_2009.pdf
PV Performance analysis_Mau_Austria_2005.pdf
PV performance after field expsoure_King_Sandia_.pdf
Performance of 100 sites_Wolgemuth_BP_PVSC_2005.pdf
PV performance in different climates_Carr_Australia_SolarEnergy_2003.pdf
Outdoor monitoring_Dhere_FSEC_2005.doc
Energy rating for CPV_Verlinden_Australia_2009.ppt
Sytem performance_Wohlgemuth_IEEE_2002.pdf
performance of First Solar_Marion_NREL_2001.pdf
Degradation rates from PERT_Osterwald_NREL_2005.pdf
TEP study_Moore_Sandia_PIPV_2008.pdf
Improved Power ratingsd_Kimber_PVSC_2009.pdf
Degradation x-Si_Skoczek_Italy_PPV_2009.pdf
Field PV reliability_Vazquez_Spain_2008.pdf
PV degradation_Moore_Tucson Electric_2007.pdf
Relaibility 1kW a-Si_NREL_Adelstein_2005p.pdf
PV performance parameters_Marion_NREL_PVSC_2005.pdf
6 years 100 sites summary_Ransome_BP_PVSC_2005.pdf
Performance of a-Si in diff climates_Rüther_Brazil_2006.pdf
A-Si in Kenya_Jacobsen_Berkley_ASES_2000
Outdoor testing at ASU_Mani_ASU_2006.pdf
Field PV reliability_Vazquez_Spain_2008.pdf
PV durability_King_Sandia_PiPV_2000.pdf
PV in Saxony_Decker_Germany_1997.pdf
25 yearold PV modules_Hedstroem_Sweden_2006
Sunpower reliability_Bunea_Sunpower_PVSEC_2010.pdf
C-Si degradation_Morita_Japan_PVenergyconv_2003
Rd c-Si_Machida_Japan_SEM&SC_1997.pdf
c-Si after 20 years_Quintana_Sandia_PVSC_2000.pdf
Rd analysis c-Si_Osterwald_NREL_PVSC_2002.pdf
10 year PV review_Rosenthal_NM_PVSC_1993.pdf
11 year field exposure_Reis_Humbold State CA_PVSC_2002.pdf
PVUSA progress report_Townsend_Endecon_1995.pdf
Long-term PV FL_Hickman_FSEC_NRELworkshop_2010.ppt
Degradationenergy payback_Davis_FSEC_2009.pdf
PV degradation in moderate climate_Tetsuyuki_Japan_PiPV_2010
Outdoor PV Degradation comparison_Jordan_NREL_PVSC_2010.pdf
PV module characterization_Eikelboom_Netherlands_2000.pdf
Mean time before failure_Realini_ Switzerland_2003.pdf
PV EVA browing Negev Desert_Berman_Israel_SEM&SC_1995.pdf
PV modules Gobi desert_Adiyabat_Mongolia_PVSC_2010.pdf
Degradation rates from PERT_Osterwald_NREL_2005.pdf
PV performance parameters_Marion_NREL_PVSC_2005.pdf
Long-term reliability_Wohlgemuth_BP-2008.pdf
Outdoor Rd wo Irr_Pulver_UofA_PVSC_2010
20+ years PV_Bing_Massachusetts_PVMR2010_2010.pdf
Rd c-Si in Spain_Sanchez_Spain_PiPV_2011.pdf
Degradation Analysis PV plants_Kiefer_Fraunhofer_PVSEC_2010.pdf
Degradationsmessungen_Becker_Munich_2005.pdf
Long-term PV tsting_Hawkins_Australia_PVsec_1996.pdf
PV power at Telstra_Muirhead_Telstra_Au&NZSolar_95.pdf
Field performance a-Si_Osborn_CA_2008.pdf
Power drop rate_Kang_Korea_PVSEC_2010.pdf
PV reliability in 4 climates_Bogdanski_Germany_PVSEC_2010.pdf
Long-term CIS_Musikowski_Germany_PVSEC_2010.pdf
735 c-Si modules after 1 year_Coello_Spain_PVSEC_2010.pdf
PV performance arctic college_Poissant_Canada_2006.pdf

Notation: Title_Author_Institute/Country_Journal/Conference_Year

IGMA 25-Year Field Correlation Study

2011 Photovoltaic Module Reliability Workshop

Golden, Colorado

February 16 – 17, 2011



Presented by: A. William Lingnell, P. E.
Lingnell Consulting Services / IGMA Technical Consultant

Session Overview

- Insulating Glass Manufacturers Alliance (IGMA)
  - Introduction
  - Industry Standards
  - Certification cycle: administration, manufacture, auditing / inspection, testing
- IGMA Field Correlation Study
  - Phase 1: 1980 to 2005
  - Phase 2: 1990 to 2005

IGMA

Industry Standards and Programs

- Test Specification for Seal Durability
  - ASTM E 2188, E 2189 and E 2190 standards for insulating glass -current
  - ASTM E 773/E774 CBA standards for insulating glass – replaced with above

IGMA

Manufacture

Testing

Inspection







Inspector Label

SAMPLE IDENTIFICATION

Ser. No. _____

Date _____

Signature

Certification Cycle

IGMA

Test Specimens

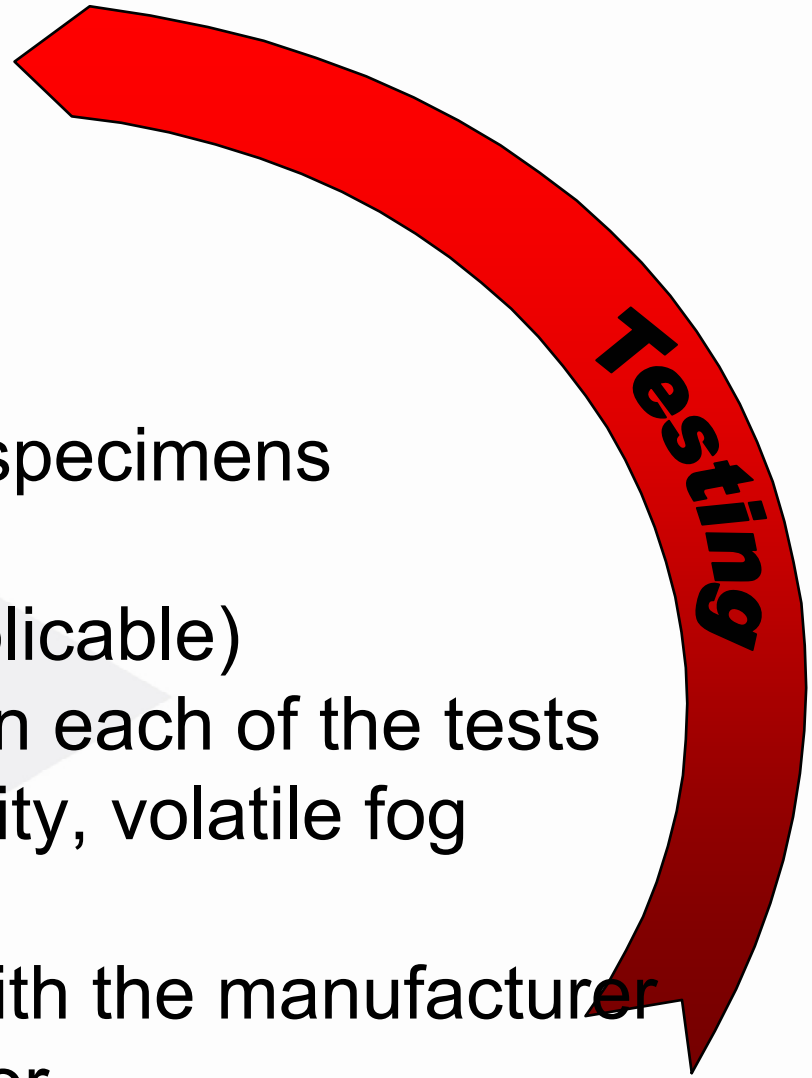
- Representative of manufacturers production
- 12 samples required for double glazed
- 14 samples required for triple glazed
- 14” X 20” samples
- Prescribed glass thickness to airspace width….why?
  - To establish set edge seal pressure

IGMA

IG Construction vs. Edge Seal Pressure

INPUT DATA					
Outboard Lite Thickness, mm	4.7	4.7	5.7	5.7	4.0
Inboard Lite Thickness, mm	4.7	4.7	5.7	5.7	4.0
IG Air Space, mm	6.5	12.7	6.5	12.7	12.0
IG Width, in.	14.00	14.00	14.00	14.00	14.00
IG Height, in.	20.00	20.00	20.00	20.00	20.00
Design Pressure Change, psi	-2.0	-2.0	-2.0	-2.0	-2.0
Comments	3/16" glass 1/4" airspace	3/16" glass 1/2" airspace	1/4" glass 1/4" airspace	1/4" glass 1/2" airspace	CAN & Euro Spec Unit
OUTPUT DATA					
Exterior Lite M.P. Stress, psi	1617	2330	1437	1903	2434
Exterior Lite Deflection, in.	0.028	0.041	0.021	0.027	0.051
Interior Lite, M.P. Stress, psi	1617	2330	1437	1903	2434
Interior Lite Deflection, in.	0.028	0.041	0.021	0.027	0.051
Final Air Space Pressure, psi	13.462	13.761	13.779	14.061	13.491
Air Space Pressure Differential, psi	0.76	1.06	1.08	1.38	0.79
Maximum Edge Seal Load, psi	5.34	7.42	7.55	9.53	5.54
Note: 2 psi pressure change is equivalent to a 0.70F airspace temperature change					

IGMA



- Receives test specimens
- Records and identifies test specimens
- Records initial dew points
- Records initial gas fill (if applicable)
- Records success or failure in each of the tests (weather cycling, high humidity, volatile fog
- Issues final report
- Maintains communication with the manufacturer and the program administrator

IGMA

Test Facility:

•Acknowledges receipt of test samples

•Records dew points at appropriate intervals

•Issues final test report indicating pass or failure of test samples



IGMA

Testing



- Initial Acknowledgement
- Dewpoints
- Initial gas content (if applicable)
- Weathercycling
- High Humidity Chamber
- Volatile Fogging Test
- Final gas content (if applicable)
- Final Test Report

IGMA

Weather Cycling
High Humidity
Volatile Fog





Accel. Weather Cycle test		**Fog Test**	
high temp	60+/- 3 C	type	full immersion box
low temp	-29+/-3 C	glass temp at corner	50 +/-3 C
UV source	F72T12BL/HO	glass temp other locations	50 +/-3 C
UV output	10 W/m^2	cooling plate temp	21 +/-3 C
moisture	30 min. spray	cooling plate area	0.018m^2 (150mm dia)
time per cycle	6 hr.	UV lamp	Osram Ultra Vitalux 300w
# of cycles	252	lamp output	400 μW/cm^2 @ 355 nm
total time	63 days		
High Humidity Test		**Evaluation criteria**	
Max temp.	60+/- 3 C	Frost point test	E546 w/ dry ice or CGSB 12.8 method
Min. temp.	(constant temperature)	max. frost point	-40 C
%RH	95% +/-5%	visible fog	no fog at arms' length
total time	42 days (14 days + 28 days)*		

IGMA

IGMA Field Correlation Study Results

The information contained in this presentation is the exclusive property of the Insulating Glass Manufacturers Alliance. Reproduction of any part of this presentation is strictly prohibited.

The IGMA field correlation study was continued at the mark to obtain information and data relating to the insulating glass performance over a of time from 1980 to 2005. The information obtained has been useful to help upgrade testing standards, determine performance criteria of insulating glass units, set glazing guidelines for the industry, as well as have a better understanding of the expected life of insulating glass.

IGMA

IGMA Field Correlation Study

- Introduction
- Purpose of Study
- Results
  - **10 years**
  - **15 years**
  - **25 years**
- Summary Comments on Study
- Conclusions

IGMA

The Three Analytical Methods

- **Experience:**
  - **OK if there are a relatively small number of failures**
- **Laboratory Analysis / Investigations:**
  - **Analysis – e.g. is the glass clean enough?**
  - **Investigation – e.g.: would something occur under these conditions?**
  - **OK when variables are few and can be accurately modeled**
- **Data Analysis:**
  - **Extremely good method if the underlying data is good**

IGMA

IGMA Field Correlation Study Introduction

1980 -2005 (Phase 1)

***Original study commissioned by SIGMA and HUD**
***Comparison of C, CB and CBA units**

- **The original 1980 study has certified units to class C, class CB and class CBA tested to the ASTM E 774 standard**
- **Frost points taken on the first seven years and visual inspections taken at 10, 15 and 25 years**
- **Some buildings not accessible, some replaced, security issues prevented inspection**
- **Approximately 75% of the original population was captured in the final inspection**

1990 – 2005 (Phase 2)

***Additional profiles added**
***Only CBA units were tracked**

IGMA

IGMA Field Correlation Study
Purpose of the Study

- **To determine the correlation of actual in-service insulating glass unit failures to the ASTM E 773 test method and ASTM E 774 specification for classifications C, CB, and CBA**
- **Summary of Accelerated Weathering Test Specification**

Class	High Humidity (days)	Accel. Weathering (cycles)	Frost Point
C	14	140	-34ºC(-30ºF)
B	+14	+56	-29ºC(-20ºF)
A	+14	+56	-29ºC(-20ºF)

IGMA

IGMA Field Correlation Study

In the 1980 original study sample size of 2,400 units in 140 buildings in the following 14 areas were included:

Boston *	**Atlanta ***	**Tampa ***
Cleveland *	**Minneapolis ***	**Dallas ***
Montana	**Denver**	**Phoenix ***
Sacramento	**Lake Tahoe**	**Seattle**
Portland	**San Francisco**	

- **40 manufacturing plants were represented**

*** Cites examined in 2005**

IGMA

IGMA Field Correlation Study
Seal Systems In 1980 – 2005 Study

- Single seal
  - Polysulfide
  - Permapol
  - Hot melt butyl

- Dual seal
  - Polyisobutylene/polysulfide
  - Polyisobutylene/silicone
  - Polyisobutylene/hot melt butyl
  - Hot melt butyl/silicone

IGMA

IGMA Field Correlation Study
Glazing System Types In Study

- **Residential 40% of study (in plant glazed)**
  - **Aluminum – marine gasket**
  - **Aluminum – dry interior and wet interior**
  - **Aluminum – both wet seals**
  - **Wood – marine gasket**
  - **Wood - both wet seals**

- **Commercial 60% of study (field glazed)**
  - **Aluminum – lockstrip**
  - **Aluminum – dry exterior and wet interior**
  - **Aluminum – tape exterior and dry interior**
  - **Wood – both wet seals**

IGMA

What is an IG Failure?

- The standard for visual failure was defined as “moisture, fog or dirt collection on the glass lite surfaces located within the air space,” exhibiting “permanent material obstruction of vision through the unit due to accumulation of dust, moisture or film on the internal surface of the glass.”

IGMA

Example of an IG Seal Failure



IGMA

Example of an IG Seal Failure



IGMA

Example of an IG Seal Failure

- 

IGMA

Example of an IG Seal Failure



IGMA

Example of an IG Seal Failure



IGMA

Large Commercial Building with Insulating Glass



IGMA

Frost Point Testing on Insulating Glass



IGMA

Results from the IGMA Field Correlation Study

Phase 1 – 1980 to 1990
(10 Year Mark)

IGMA

City	Class C	Class CB	Class CBA
Atlanta	1 of 99	0 of 21	O of 16
Boston	1 of 106	3 of 52	1 of 48
Cleveland	3 of 124	0 of 50	0 of 41
Dallas	36 of 144	1 of 12	1 of 163
Denver	2 of 68	--------	--------
Minneapolis	3 of 33	--------	3 of 216
Phoenix	8 of 49	1 of 20	0 of 60
Seattle	7 of 40	--------	0 of 130
Tampa	0 of 12	1 of 34	1 of 105
Portland, OR	5 of 95	--------	--------
Sacramento	--------	--------	2 of 74
San Fran. Santa Rosa, CA	--------	--------	18 of 113
Lake Tahoe	3 of 39	--------	0 of 12
Montana	--------	2 of 53	0 of 4
TOTAL FOGGED UNITS	**69 of 809**	**8 of 242**	**26 of 1049**
% FOGGED	**8.5%**	**3.3%**	**2.5%**

Total Failure Rate = 103 of 2100 = 4.9%

Results from the IGMA Field Correlation Study

Phase 1 – 1980 to 1995
(15 Year Mark)

IGMA

City	Class C	Class CB	Class CBA
Atlanta	7 of 101	0 of 21	1 of 16
Boston	1 of 106	3 of 72	2 of 28
Cleveland	9 of 123	--------	1 of 103
Dallas	24 of 129	--------	3 of 164
Denver	1 of 82\3	--------	0 of 47
Minneapolis	7 of 44	--------	5 of 217
Phoenix	2 of 43	3 of 21	0 of 66
Seattle	5 of 27	--------	0 of 133
Tampa	0 of 12	17 of 38	0 of 61
Portland, OR	18 of 92	--------	--------
Sacramento	--------	--------	3 of 56
San Fran. Santa Rosa, CA	--------	--------	27 of 114
Lake Tahoe	3 of 47	--------	0 of 9
Montana	--------	11 of 66	0 of 4
TOTAL FOGGED UNITS	**77 of 807**	**35 of 218**	**42 of 1,018**
% FOGGED	**9.5%**	**12.1%**	**4.1%**

Total Failure Rate = 153 of 2.043 = 7.5%

Phase 2 – 1990 to 2005

- New study started examining only “CBA” units incorporating new technology profiles to initial study:
  - Polyurethane and Swiggle ® sealants
  - Warm edge technology spacer designs
  - Bent corners
  - Low E glass
  - Internal grid systems
  - Argon-gas content

IGMA

Generalizations

- Little variation due to climatic conditions
- No failures in 80% of buildings
- 60% of failures were accelerated by glazing systems that held water at or near the edge sealant
- The findings of this study were one of the key determinants in eliminating the CBA system levels in the new ASTM standard E 2188, E 2189, E 2190

IGMA

Results from the IGMA Field Correlation Study

Phase 1 – 1980 to 2005
(25 Year Mark)

Phase 2 – 1990 to 2005
(15 Year Mark)

IGMA

IGMA Field Correlation Study - Phase 1
Field Study At 10, 15, 25 Years

# of Units	Class C	Class CB	Class CBA	Total Failure Rate (all units)	Adjusted Failure Rate CBA
2,100	69 of 809 (8.5%)	8 of 242 (3.3%)	26 of 1049 (2.5%)	103 of 2,100 (4.9%)	1.2%
2,043	77 of 807 (9.5%)	35 of 218 * (12.1%)	42 of 1,018 (4.1%)	153 of 2,043 (7.5%)	2.9%**
1,714	**85 of 791 (10.7%)**	**43 of 126 * (34.1%)**	**29 of 797 (3.6%)**	**157 of 1,714 (9.2%)**	**3.6%**

- *Due to small sample size and large number of units concentrated at one job site.
- **Re-stated percentage due to removal the two jobs with failures due to poor glazing.

IGMA

IGMA Field Correlation Study - Phase 1 & 2

Summary Survey Failure Rates

	Phase 1 1980 - 2005				Phase 2* 1990 – 2005
Years	25 Years		15 Years		15 Years
	C+CB	CBA	C+CB	CBA	CBA
Failure rate	**14.0%**	**3.6%**	**5.9%**	**2.9%**	**1.0%**
# of Units	917	797	1,025	1,018	10,944

* 10 years results of the same population show a failure rate of 0.12%

IGMA

IGMA Field Correlation Study Summary Comments

- **Glazing of insulating glass units is critical to long-term performance.**

  - Wet seal exterior had 10% the number of failures as dry seal on the exterior 1990 survey of original study

  - Two projects included in the study one with aluminum framing having marine gaskets and on site glazed units with lock strip gaskets demonstrated much higher failure rates, due to trapping water against the unit edge seal at the sill

- **Based on the data it is estimated that failure rate of the C + CB units is in excess of 20% due to the number of buildings re-glazed and known systems that were not properly performing to keep water away from the insulating glass edge**

- **The C + CB units (14%) in the 1980 study had 3 to 4 times the failures than the CBA units (3.6%)**

IGMA

IGMA Field Correlation Study Conclusions

- **Certification to class CBA of ASTM E 774 demonstrated much higher level of field performance than class C and CB.**
- **The Phase 1 and Phase 2 studies had failure rates of 2.9% and 1.0% respectively at 15 years for units certified to class CBA systems that were properly weeped for the 1980 and 1990 studies.**
- **Certification to class CBA in comparison to C and CB was in part justification for one level of testing as developed for ASTM E 2190.**

IGMA

Based on 25 Years of Performance!

- Best practices, proper glazing:

  TM-4000-02, IG Manufacturing Quality Procedures

  TM-4100-02, Preventing IG Failures

  TM-3000-04, North American Guidelines For Sealed Insulating Glass Units

  TB-1201-05, Minimum Dimensions for Sealant

- Insulating glass shall be certified to ASTM E 2190 (replacing ASTM E 774) for assurances of long term durability against fogging (seal failure) and glazed in accordance to IGMA standards

IGMA

IGMA Field Correlation Study
A New Study!

- Include new seal technologies since 1990 or those not included previously
- Gas filled units
- US and Canada for North American study (Energy Star™ zones)
- Use units certified to ASTM E 2190 and include some recent ASTM E 774 and CGSB 12.8 for comparison…..Main emphasis on ASTM E 2190

IGMA

Bridge Retrofitted with Insulating Glass



IGMA

Questions, Comments, etc.

IGMA INSULATING GLASS MANUFACTURERS ALLIANCE

- Bill Lingnell – Lingnell Consulting Services / IGMA Technical Consultant
  - Direct: (972) 771-1600 / Fax: (972) 771-0354
    - E-mail: lingnell@swbell.net

CORNING

Photovoltaic Glass Technologies

Physical Properties of Glass and the Requirements for Photovoltaic Modules

Dr. James E. Webb
Dr. James P. Hamilton

NREL Photovoltaic Module Reliability Workshop
February 16, 2011

Corning has a long history of life-changing innovations

1879 Glass envelope for Thomas Edison's light bulb



1915 Heat-resistant Pyrex® glass



1934 Dow Corning silicones



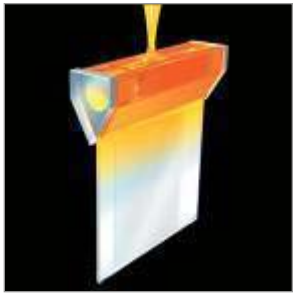
1947 Processes for mass producing the television bulb



1952 Glass ceramics



1960 Fusion draw process



1970 Specialty glass for NASA space missions



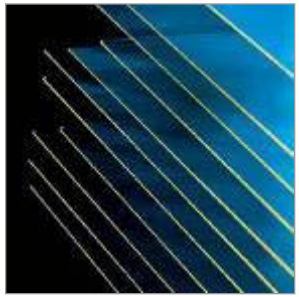
1972 First low-loss optical fiber



1984 Ceramic substrates for automotive catalytic converters



2006 AMLCD glass for TVs, notebook computers & monitors



© 2011 Corning Incorporated

Why is glass attractive for PV?

- Transparent
- Hermetic
- Durable
- Acceptable Strength
- Low Cost

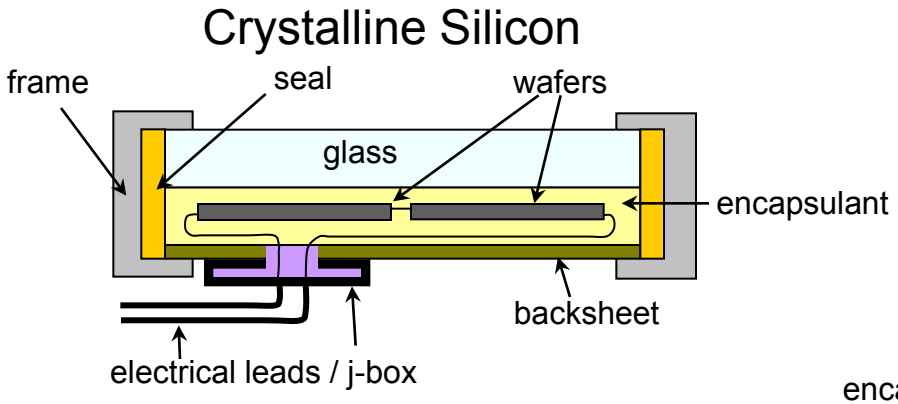
© 2011 Corning Incorporated

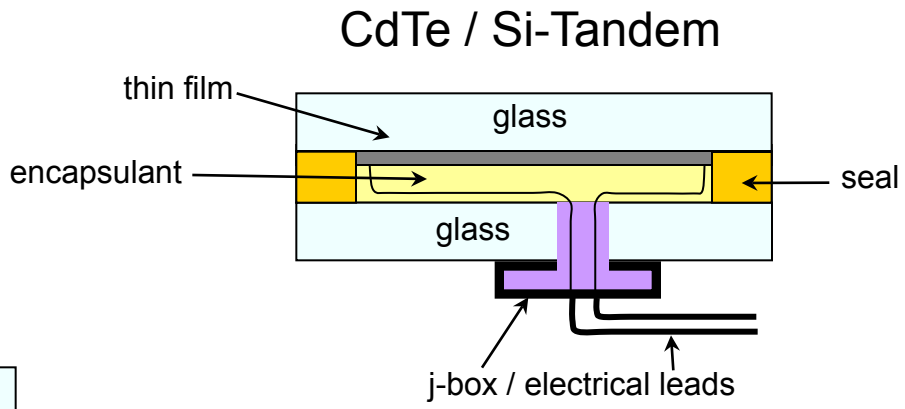
PV Module Requirements – where does glass fit in?

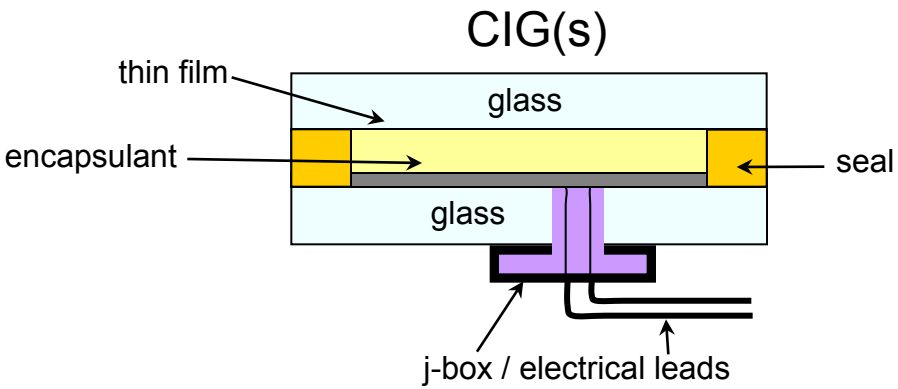
	Efficiency	Reliability	Weight
c-Si	✓	✓	✓
CdTe	✓	✓	✓
Si-Tandem	✓	✓	✓
CIGS	✓	✓	✓

© 2011 Corning Incorporated

Glass configurations for PV modules



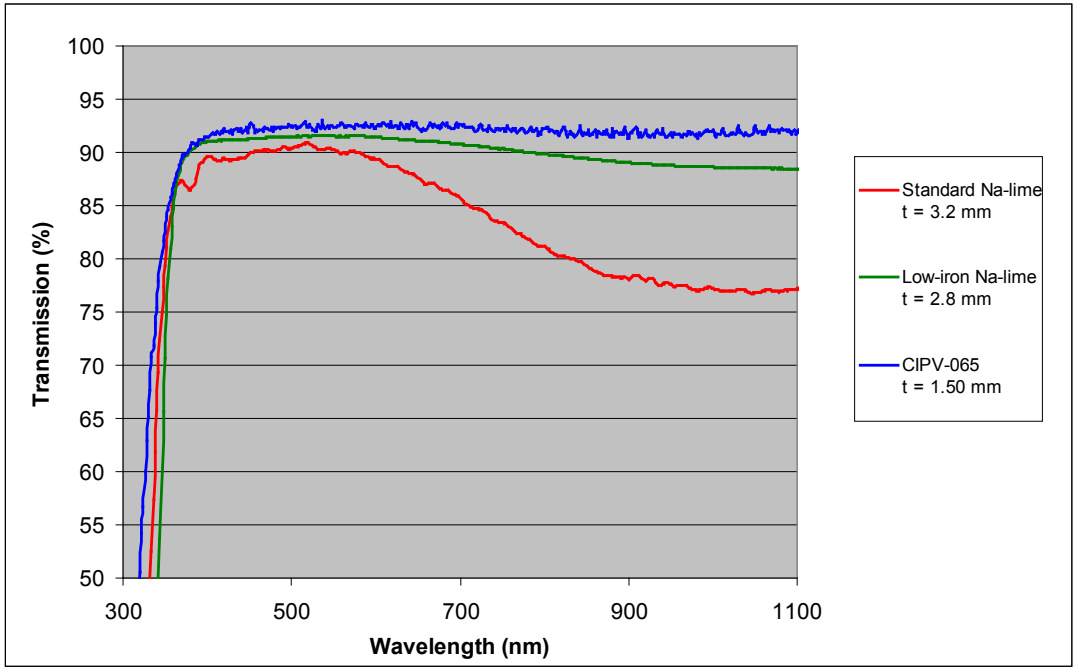




© 2011 Corning Incorporated

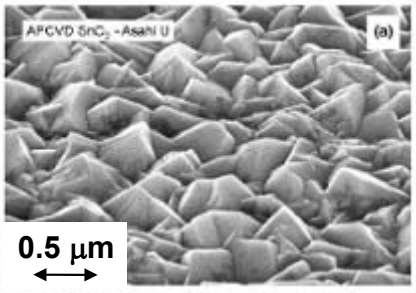
Glass can increase conversion efficiency

- Higher transmission
  - c-Si and thin film technologies
  - low-Fe and specialty glasses
- Enhanced light trapping
  - c-Si and thin film technologies
  - particularly Si-tandem

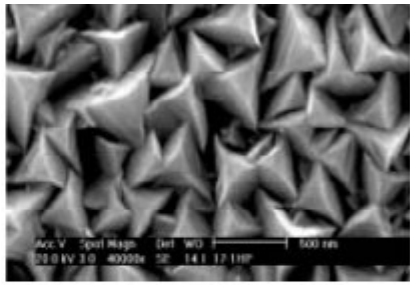


Light trapping demonstrated with TCO's for Si-Tandem

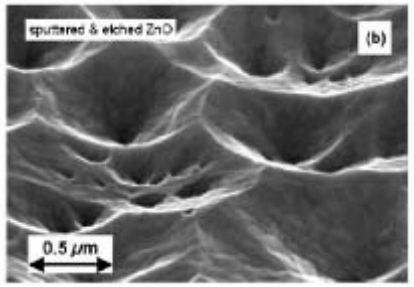
Similar opportunities for glass



SnO_2:F
Asahi, NSG, Guardian



ZnO:B
Oerlikon



ZnO:Al
Applied Materials

© 2011 Corning Incorporated

The highest efficiency CdTe cells have been produced on Corning's specialty glass

Organization & *Author*	Glass	Cell Efficiency	Author's Hypothesis
NREL *X. Wu*	Corning 7059	16.7%	• High temp • Cd stannate TCO
University of South Florida *C. Ferekides*	Corning 7059	15.8%	• High temp • Thin Cd Sulfide
University of Toledo *A. Compaan*	Corning 1737	14.0%	• Lack of impurities

© 2011 Corning Incorporated

Mechanical reliability assessment is composed of modeling, characterization, and testing

Modeling

Module size and support configurations

Stress analysis

Characterization

Surface and edge strength

Fatigue

Testing

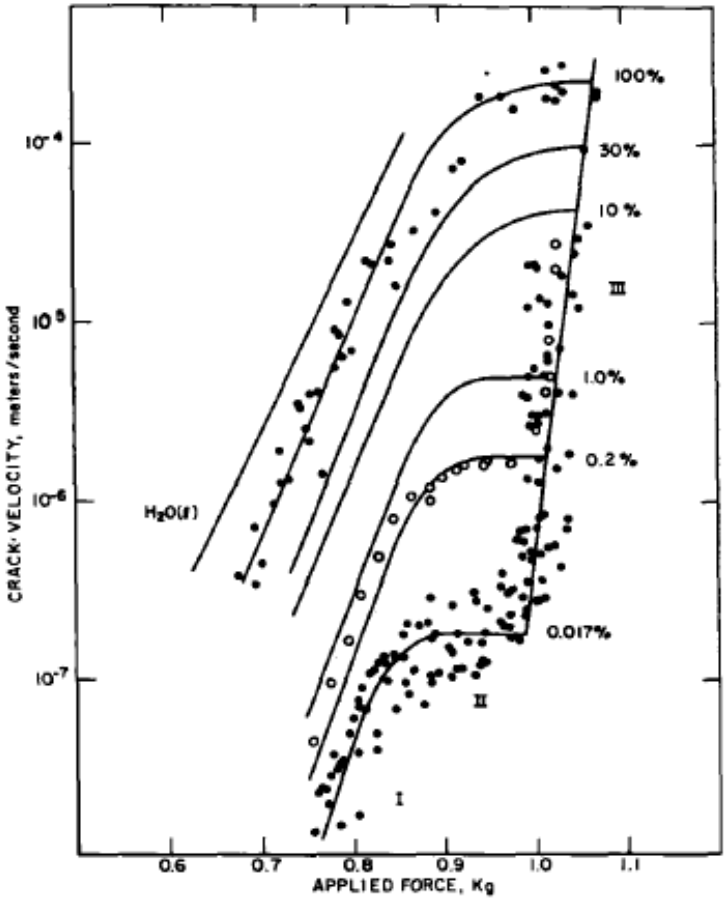
Snow load / hail testing

Wind load testing

Reliability assessment
- Reliability requirement
- Calculated reliability

© 2011 Corning Incorporated

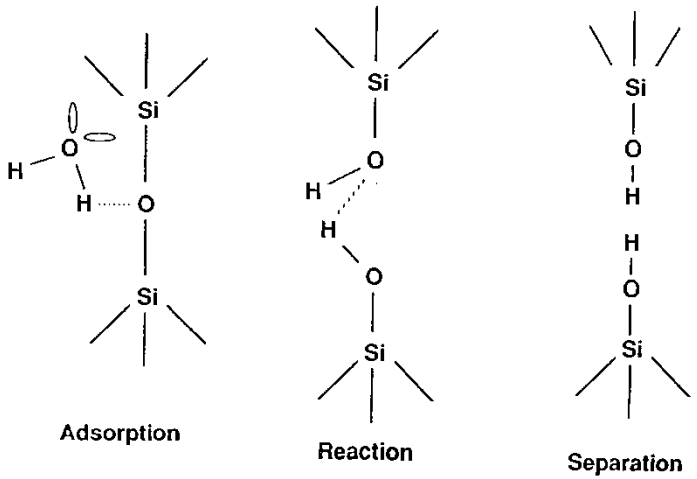
Glass fatigue – moisture effect on crack growth



S.M. Weiderhorn
"Influence of Water Vapor on Crack Propagation in Soda-Lime Glass"
J. Am.Ceram.Soc., Vol 50, No. 8, 407-414, 1967

$$SiO_2 + H_2O + \text{Stress} \Rightarrow Si(OH)_4$$

Molecular Flaw Growth Model
(Michalske and Freiman, 1983)



$$v = aK_I^n$$

n = fatigue exponent

© 2011 Corning Incorporated

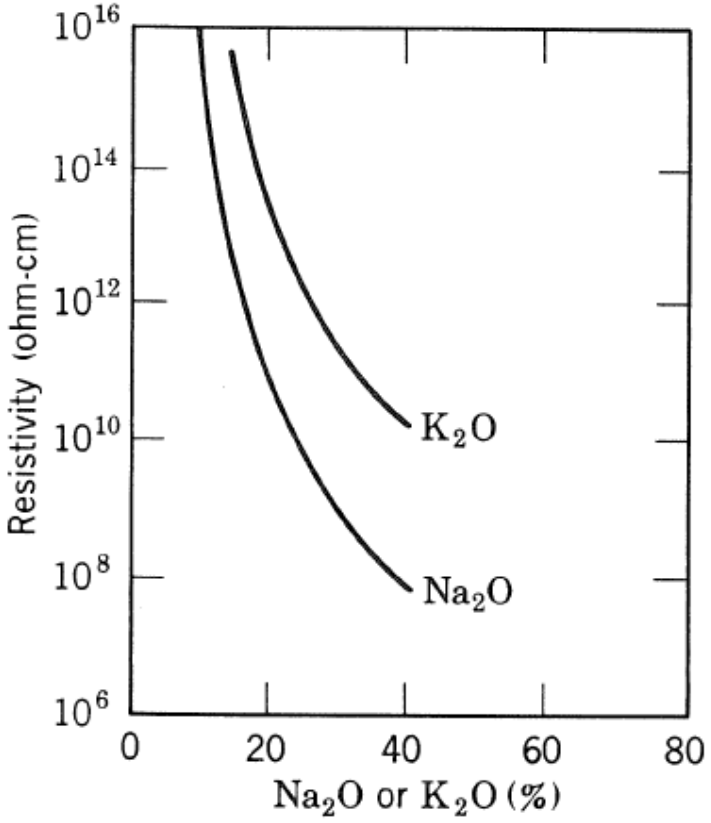
Increased fatigue exponent increases strength

Glass	Fatigue Exponent	Relative Strength (30 Year Life)
Soda-lime	~15	1.0
Corning PV glass	~20-23	1.4 – 1.6
Fused Silica (space shuttle windows)	~33	2.0

Specialty glass is ~50% stronger than soda lime

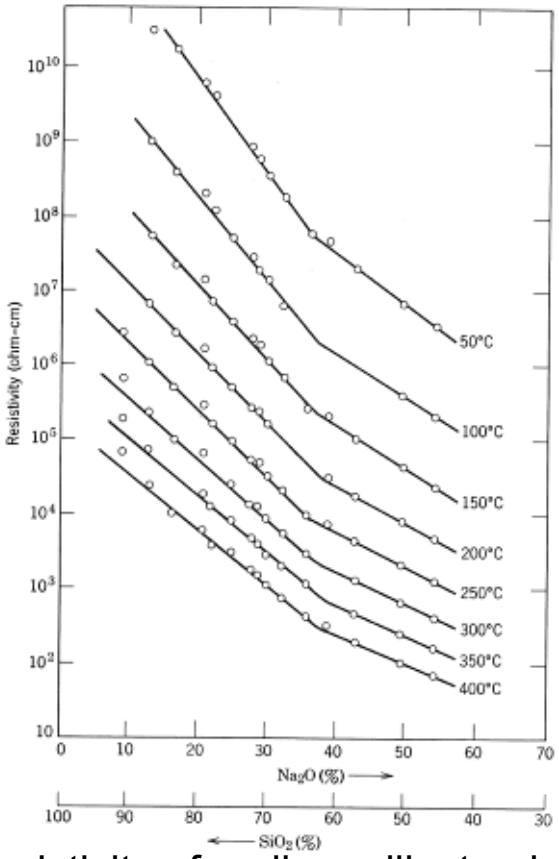
© 2011 Corning Incorporated

Glass resistivity decreases as alkali content increases



Resistivity of sodium and potassium-silicate glasses

Fulda M. (1927). *Sprechsaal*, **60**, 810.



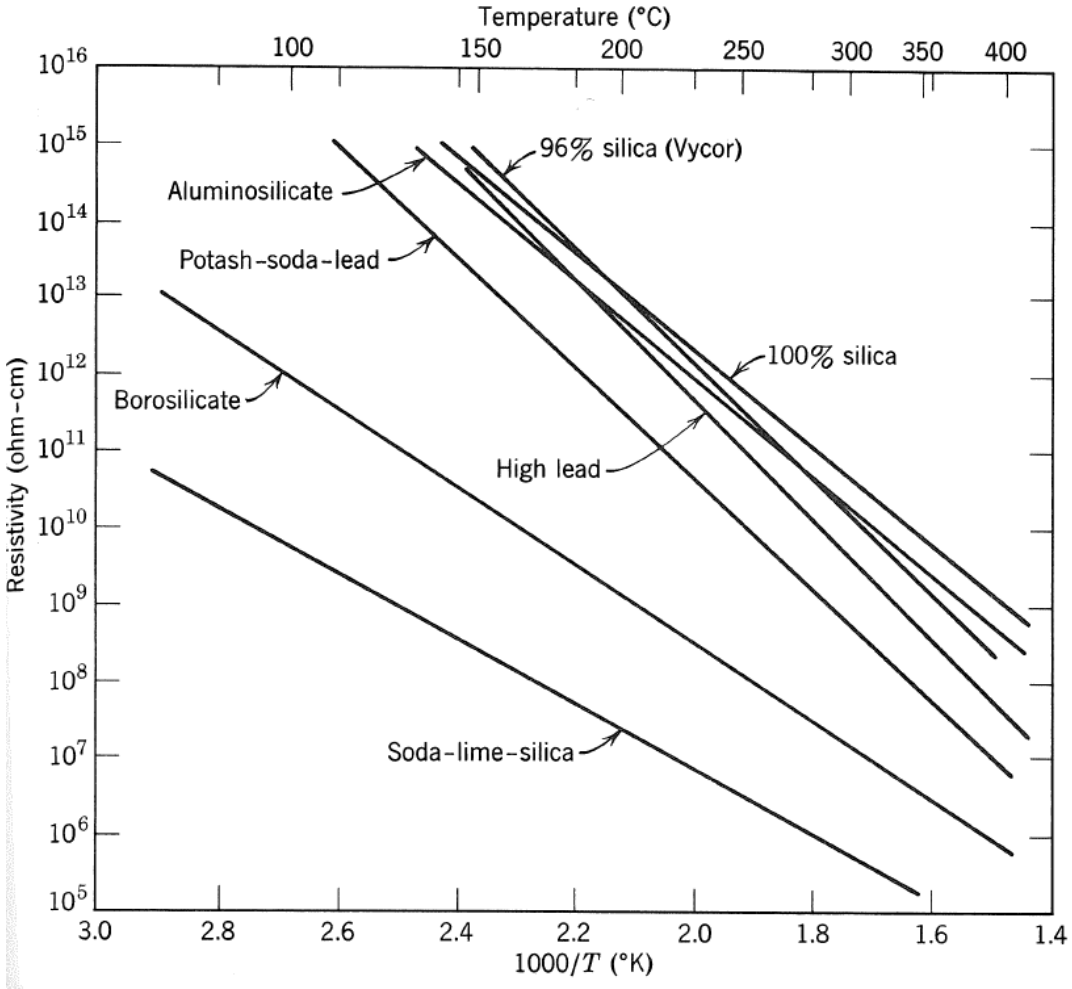
Resistivity of sodium-silicate glasses

Seddon E., Tippett E. J., Turner W. E. S. (1932). The Electrical Conductivity of Sodium Meta-silicate-Silica Glasses. *J. Soc. Glass Technol.*, **16**, 450.

Higher resistivity can improve electrical isolation performance

© 2011 Corning Incorporated

Specialty glasses can have resistivities up to 8 orders of magnitude higher than soda lime silica glasses

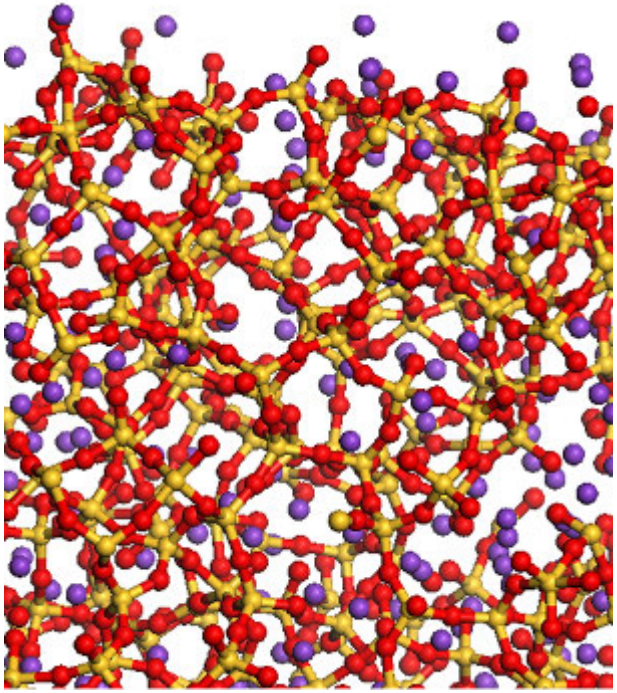


DC volume resistivity of commercial glasses

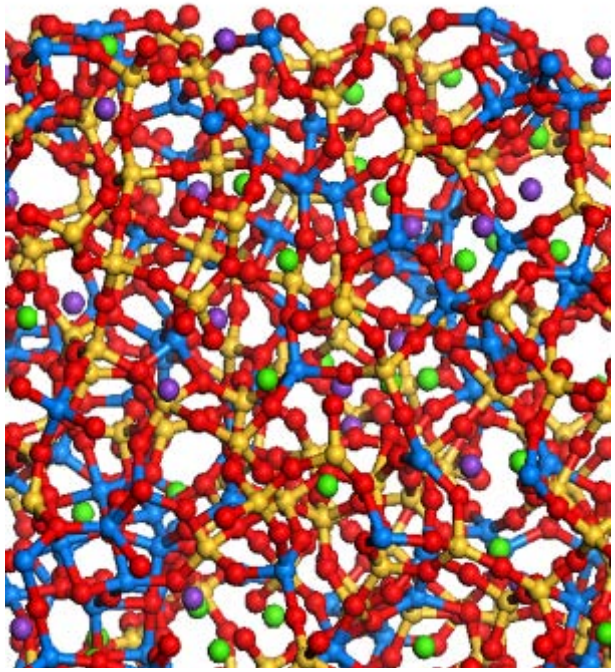
Kingery, Bowen, Uhlman (1976) *Introduction to Ceramics (2nd Ed.)*, p. 885, John Wiley & Sons

© 2011 Corning Incorporated

Glass structure modifications can improve durability



Multi-component silicate glass with non-bridging oxygens



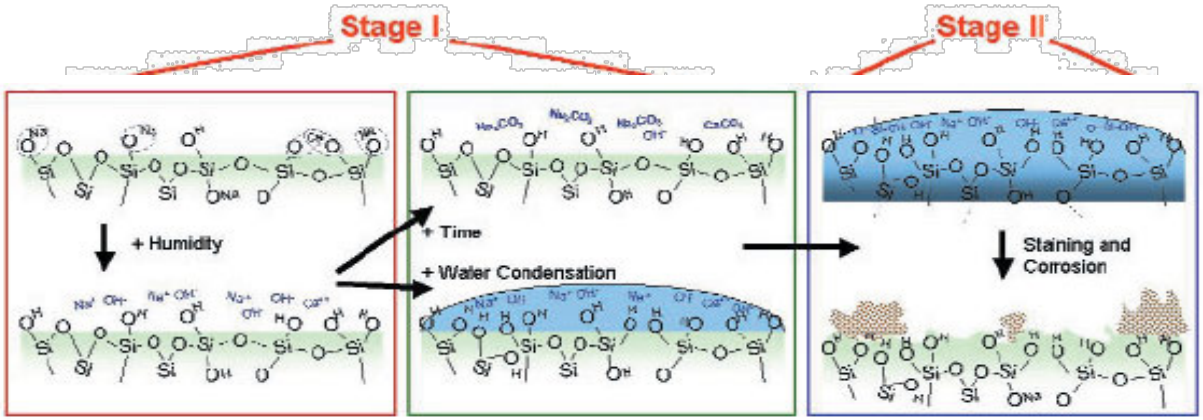
Fully polymerized multi-component silicate glass without non-bridging oxygens

Leed, E. A. and Pantano C.G. (2003). Computer Modeling of Water Adsorption on Silica and Silicate Glass Fracture Surfaces, *J. Non-Cryst. Sol.*, **48**, 325.

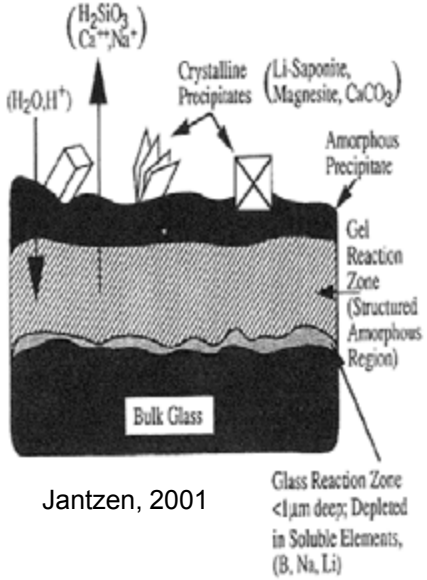
Elimination of non-bridging oxygens closes glass structure, significantly slows alkali and alkaline-earth migration, and improves chemical durability

© 2011 Corning Incorporated

Mechanisms of glass corrosion



R. A. Schaut, Pantano C.G., The Glass Researcher (2005)



Jantzen, 2001

- Weathering of float glass can be categorized into two stages:
  - "Stage I": Ion-exchange (leaching) of mobile alkali and alkaline-earth cations with H^+/H_3O^+, formation of silica-rich surface layer, pH rise in liquid film, and formation of soluble precipitates

$$\equiv SiO^- R^+ + H_2O \rightarrow \equiv SiOH + R^+OH^-$$

  - "Stage II": Dissolution of silica-rich glass network at pH >9 with degradation of surface and formation of insoluble precipitates (permanent staining)

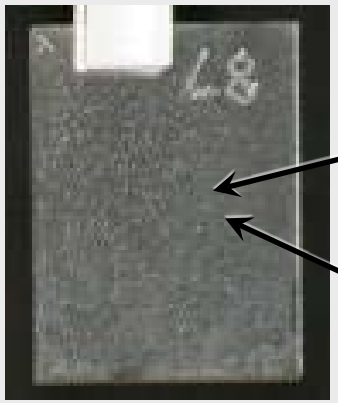
$$\equiv M\text{-}O\text{-}M\equiv + H_2O \leftrightarrow \equiv M\text{-}OH + HO\text{-}M\equiv$$

© 2011 Corning Incorporated

Weathering of glass – 30 days at 85°C / 85% r.h.



Soda-Lime-Silica



hazing
crystalline
precipitates

non-uniform
surface chemistry



Specialty Glass



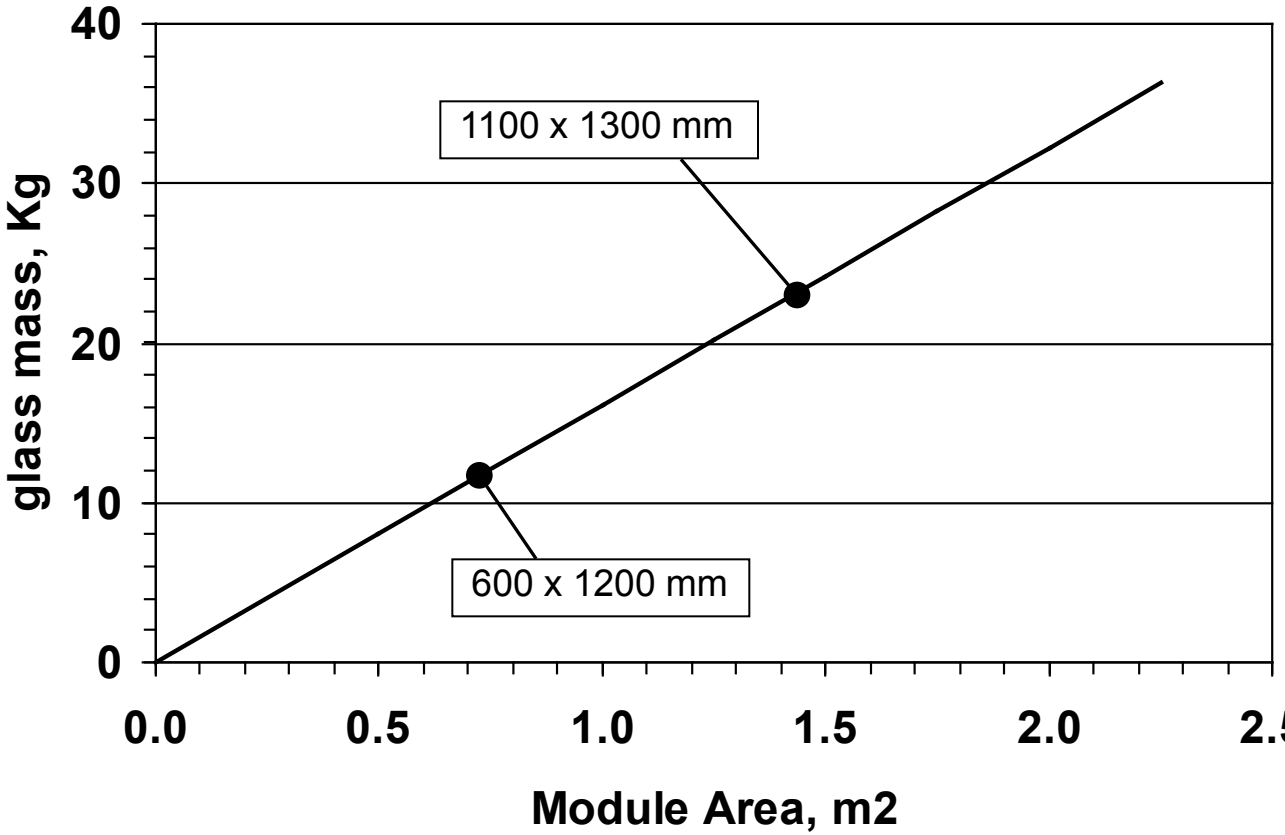
clear glass
with little or
no hazing

uniform
surface chemistry

Specialty glasses corrode much less than soda-lime-silica
Corrosion may negatively impact long-term module performance in field

© 2011 Corning Incorporated

Module weight driven by module size glass mass



Assumes thin film module with 2 sheets of 3.2 mm soda lime glass

Density = 2.5 g/cc

Typical Glass Densities

2.2 g/cc – Fused Silica
2.5 g/cc – SLG
3.1 g/cc – Lead Crystal

Thin glass and glass density can decrease module weight

© 2011 Corning Incorporated

In summary, glass has an important role in module performance and reliability

- Glass can:
  - increase module efficiency
  - improve mechanical reliability
  - improve electrical isolation performance
  - improve module durability
  - decrease module weight

© 2011 Corning Incorporated

CORNING

RELIABILITY AND DURABILITY EVALUATION OF PV CONNECTORS

Mani G. TamizhMani

Arizona State University
TUV Rheinland PTL

Acknowledgement:

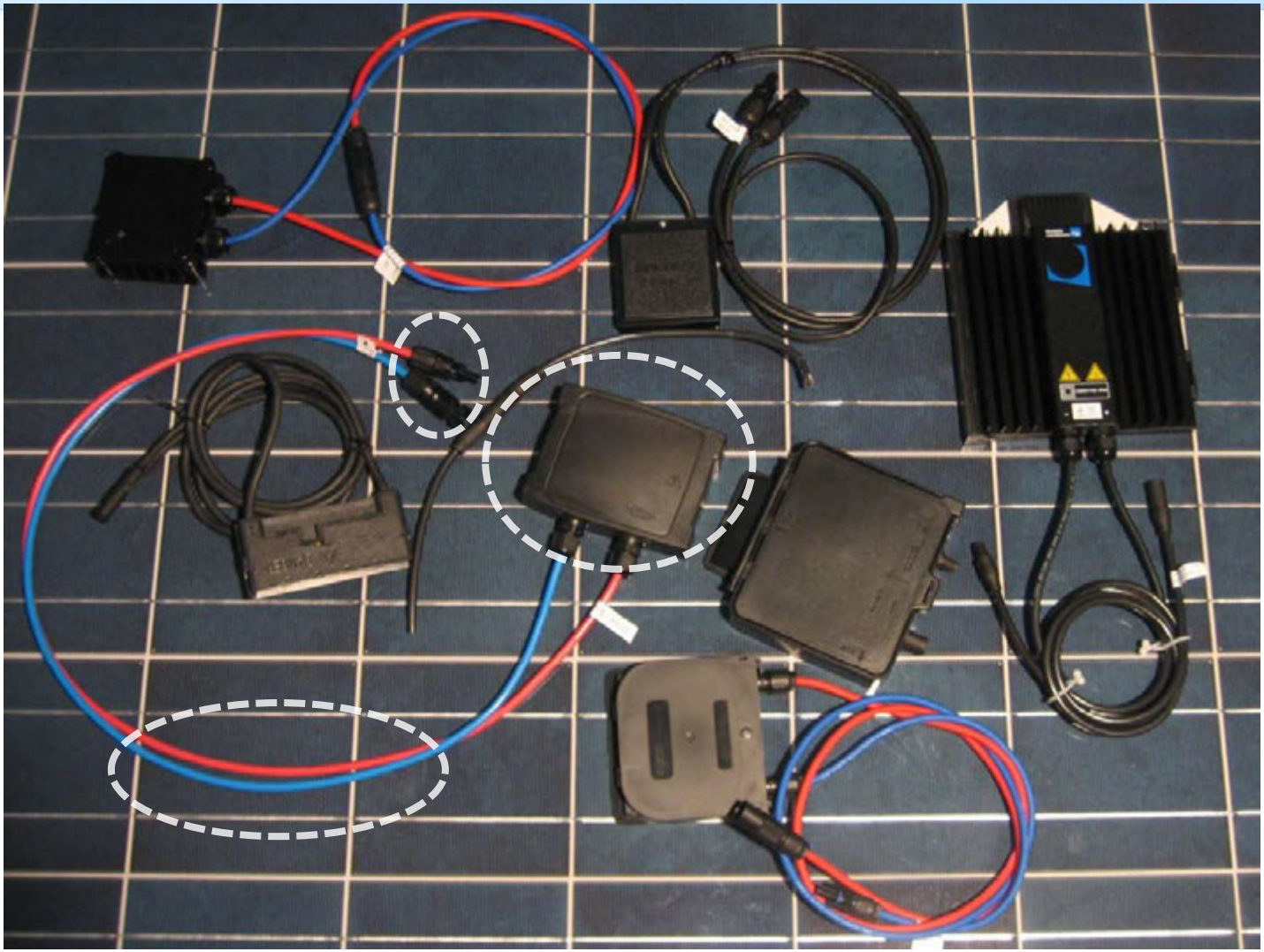
Funding support of BP Solar is gratefully acknowledged

Thanks to Mr. Guido Volberg of TUV Rheinland for sharing his experience in connector testing

ASU ARIZONA STATE UNIVERSITY

TÜVRheinland® Precisely Right.

PV module supply chain: Polymeric components



ASU Arizona State University
TÜVRheinland® Precisely Right.

Outline

PV Connectors

- Outdoor tests and results obtained @ ASU
  - Contact and cable resistance
- Indoor tests and results obtained @ TUV Rheinland
  - Contact resistance
- EN 50521 standard
  - A quick overview

ASU Arizona State University
TÜVRheinland® Precisely Right.

Why understanding PV connectors important

- Electrical safety
  - Arcing
  - High voltage (worse in flat roof puddles!)
- Contact resistance
  - Energy loss (kWh/kW)
  - Lifetime reduction (higher operating temperature)
  - Worse in hot-sunny location rooftops

ASU Arizona State University
TÜVRheinland® Precisely Right.

Connector types: Plug-in & Lockable



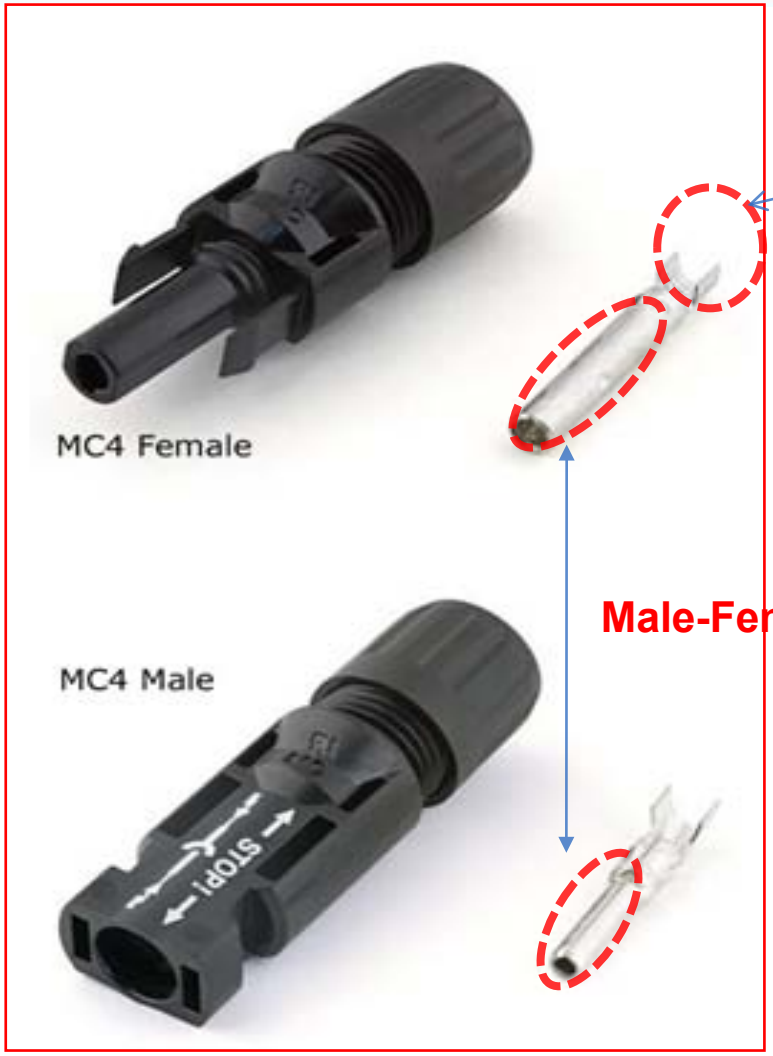




Source: www.civicsolar.com

ASU Arizona State University
TÜVRheinland® Precisely Right.

Contact resistance



Cable coupling

Male-Female contact

Source: www.civicsolar.com

ASU Arizona State University
TÜVRheinland® Precisely Right.

Field issues











ASU Arizona State University
TÜVRheinland® Precisely Right.

Field issues



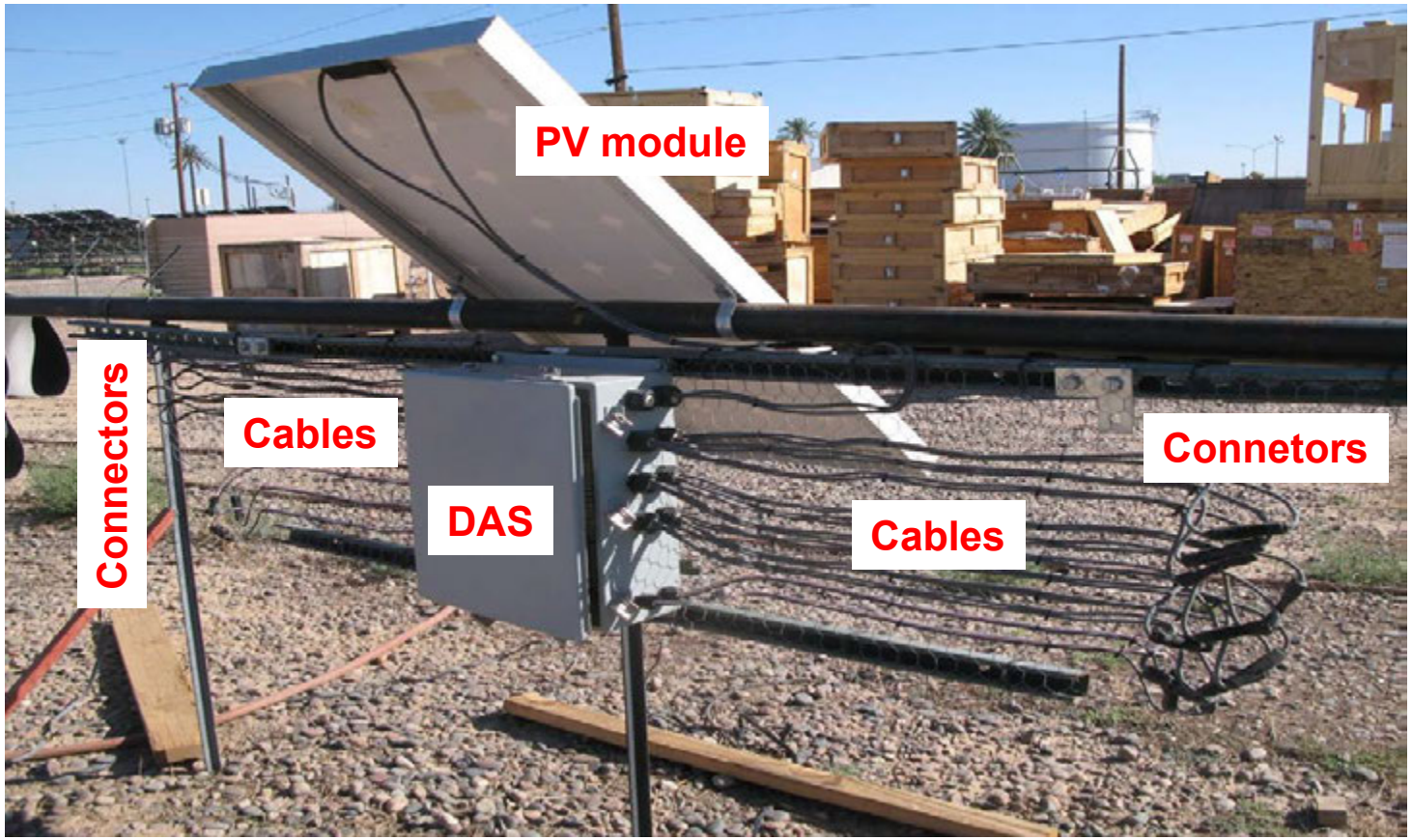
ASU Arizona State University
TÜVRheinland® Precisely Right.

Outdoor connector test @ ASU

- 19 connectors tested
- 2 meter long cables used
  - 12 AWG (for 14 connectors)
  - 14 AWG (for 5 connectors)
- 3 manufacturers
- 4 connector types
  - 1 plug-in
  - 3 lockable
- 1 PV module
- Outdoor exposure started in Nov. 2005 and the initial resistance measured
- Outdoor exposure continued and the second time resistance measured in Jun. 2006
- Outdoor exposure continued and every 6 min resistance monitoring started in Dec. 2008

ASU Arizona State University
TÜVRheinland® Precisely Right.

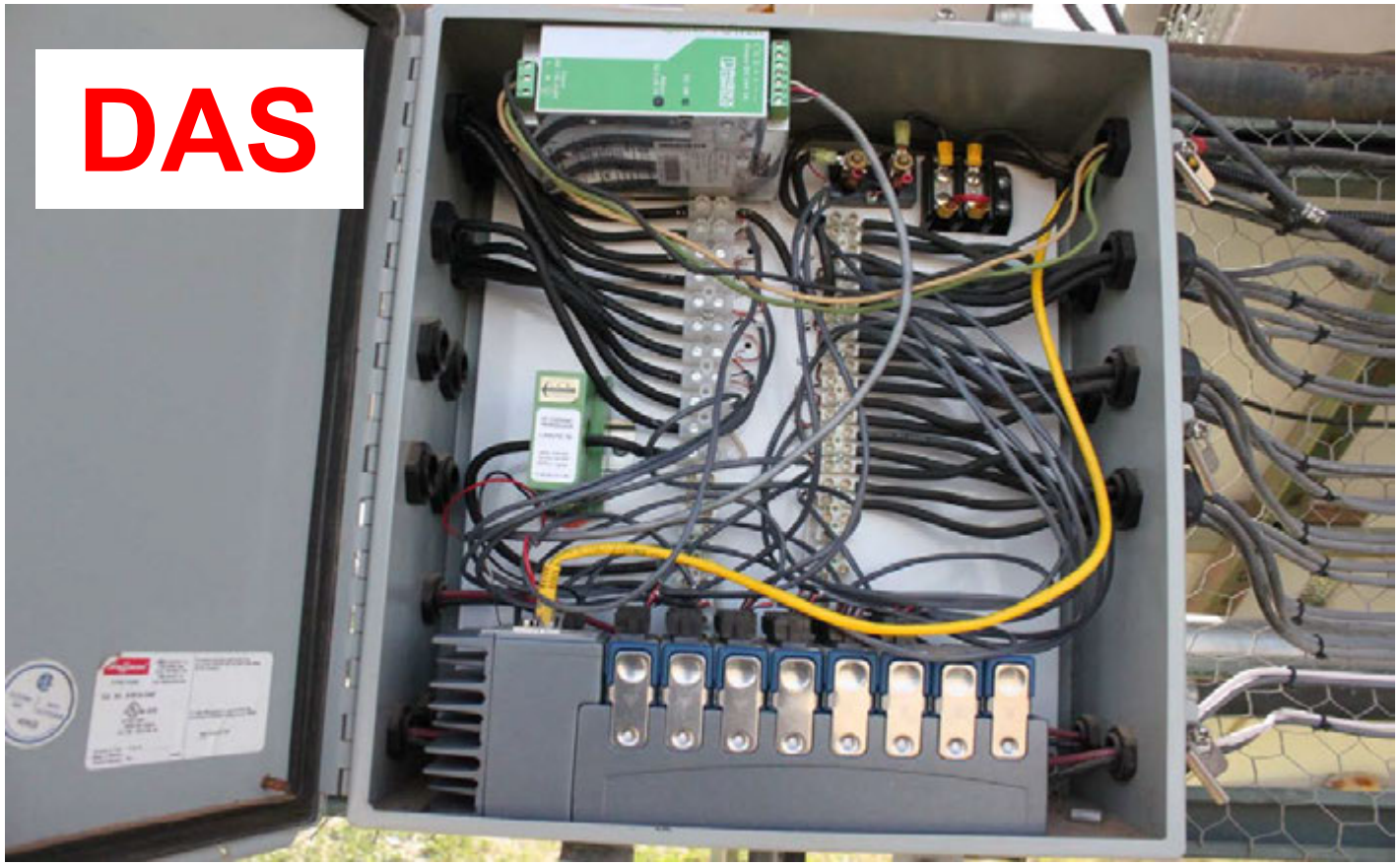
Outdoor connector test setup @ ASU



ASU Arizona State University

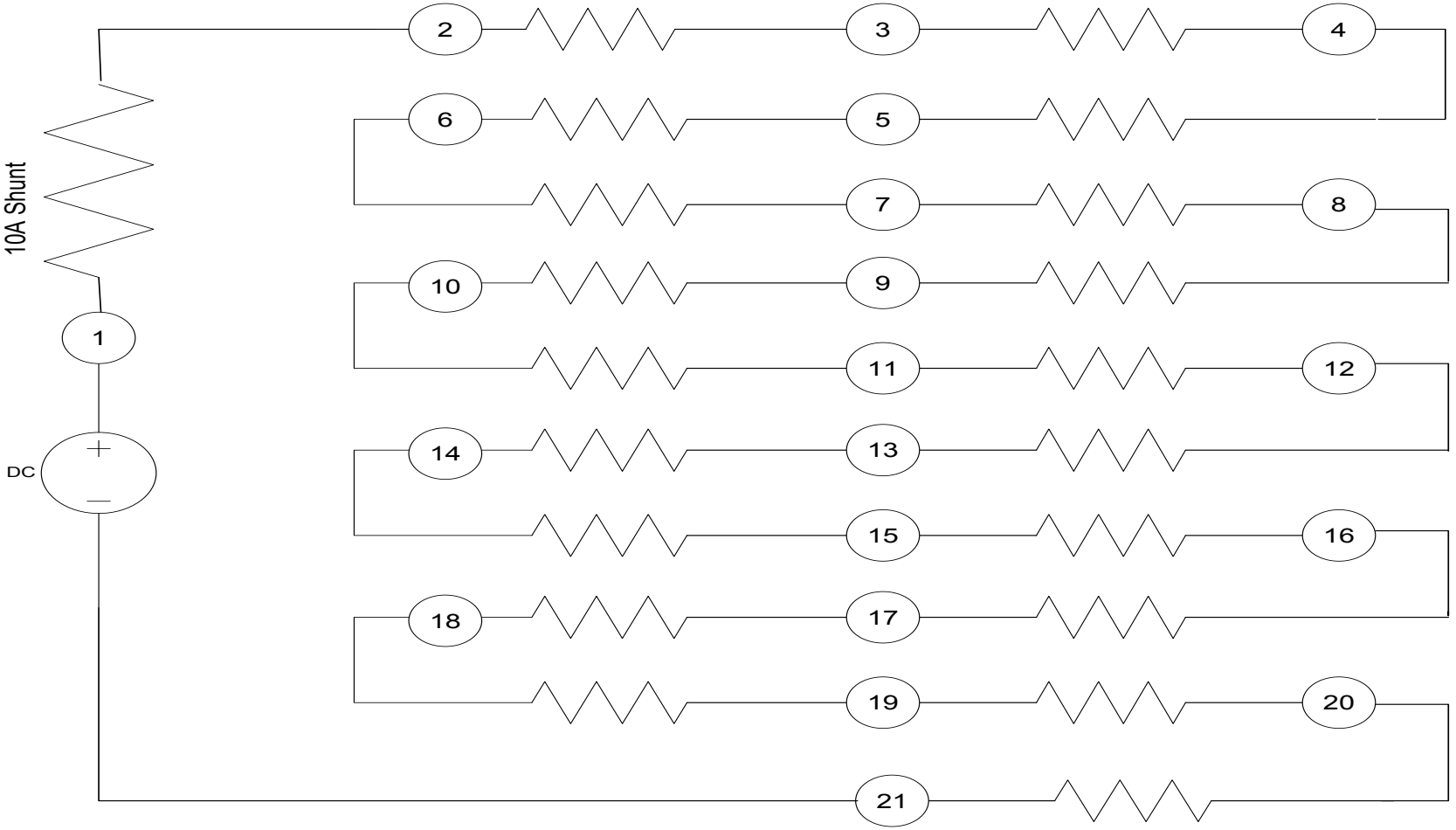
TÜVRheinland® Precisely Right.

Outdoor connector test setup @ ASU



ASU
ARIZONA STATE UNIVERSITY
TÜVRheinland®
Precisely Right.

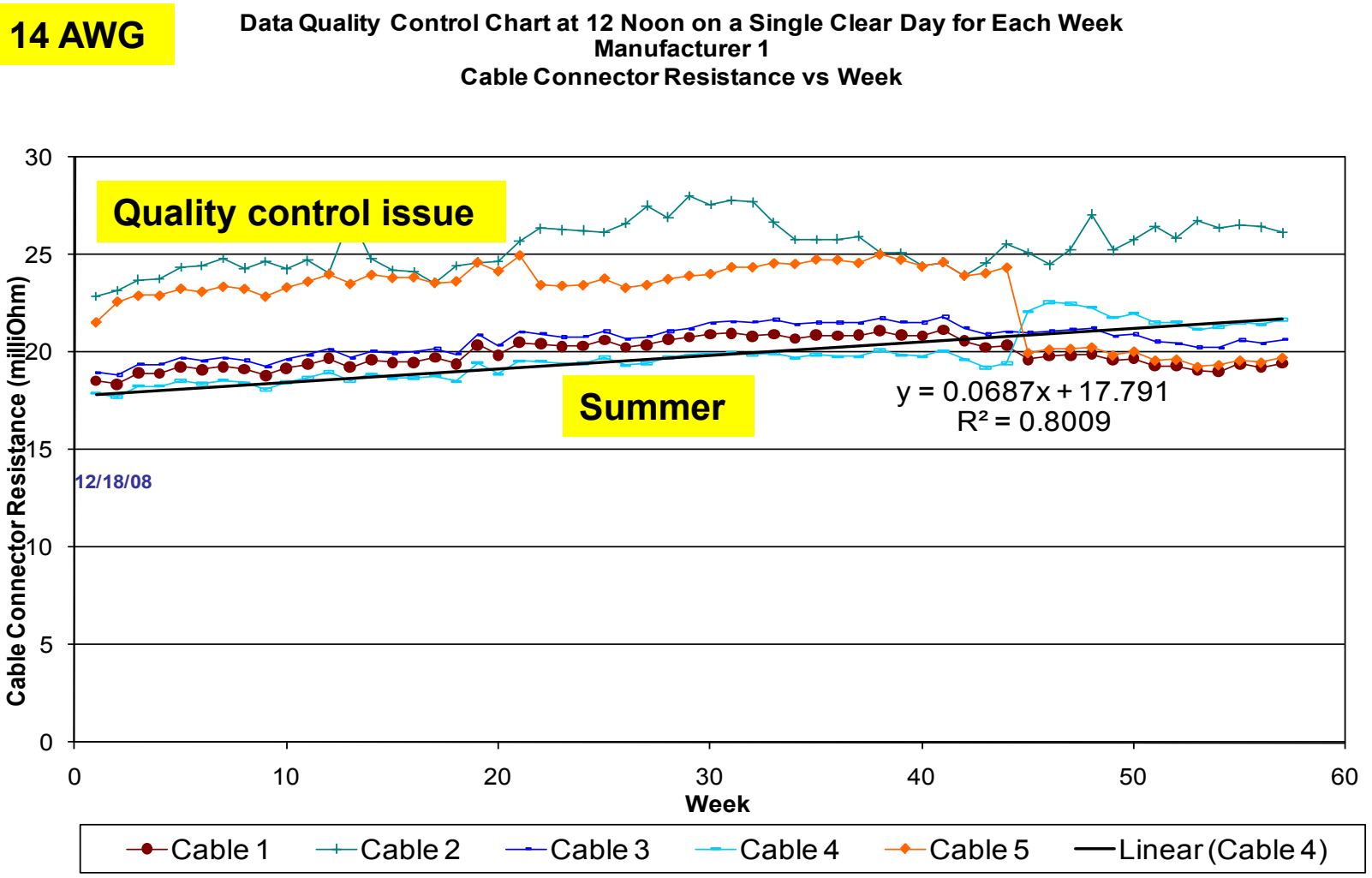
Outdoor connector test setup @ ASU



ASU Arizona State University
TÜVRheinland® Precisely Right.

Outdoor connector test results @ ASU

14 AWG

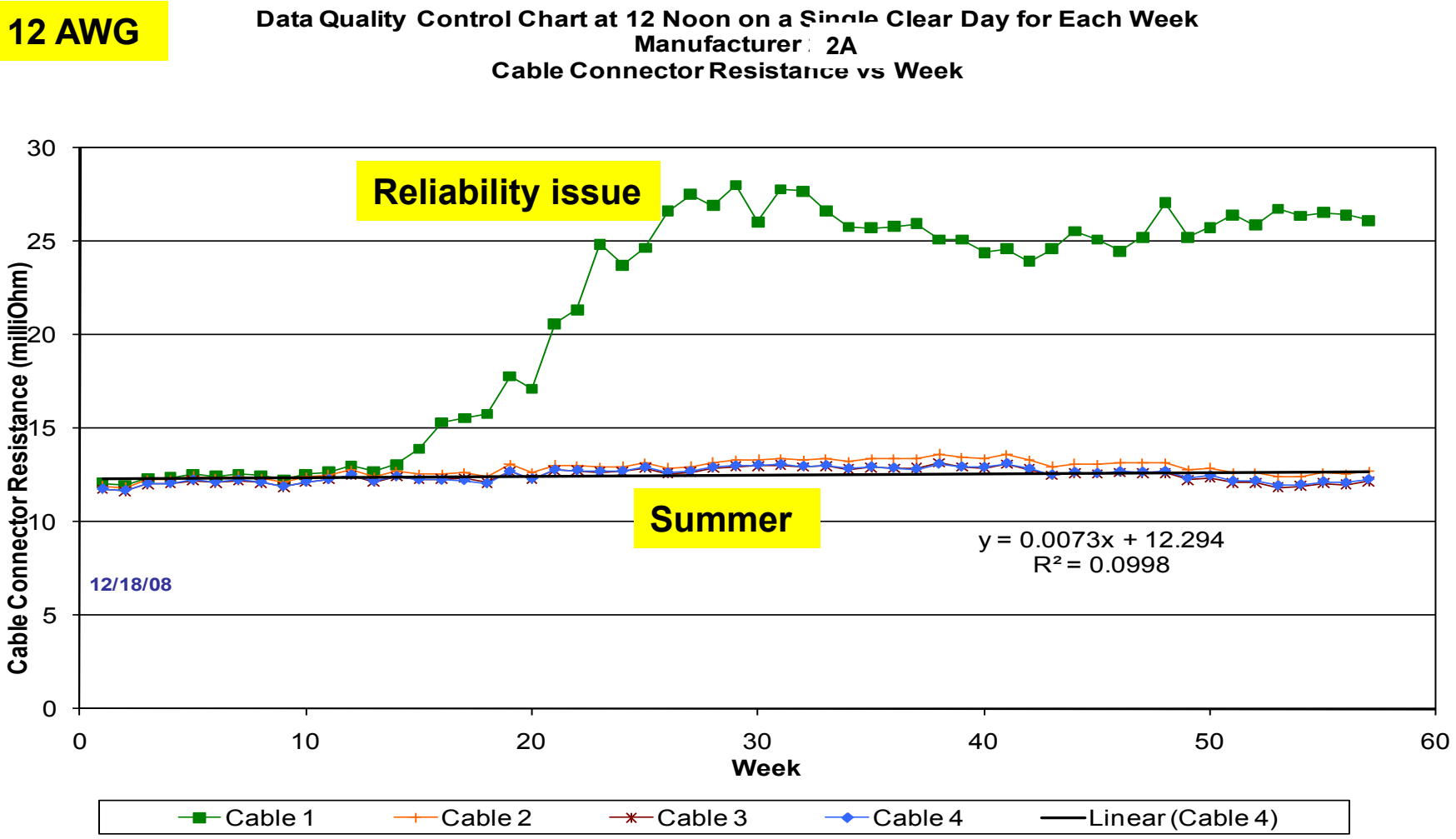


ASU Arizona State University

TÜVRheinland® Precisely Right.

Outdoor connector test results @ ASU

12 AWG

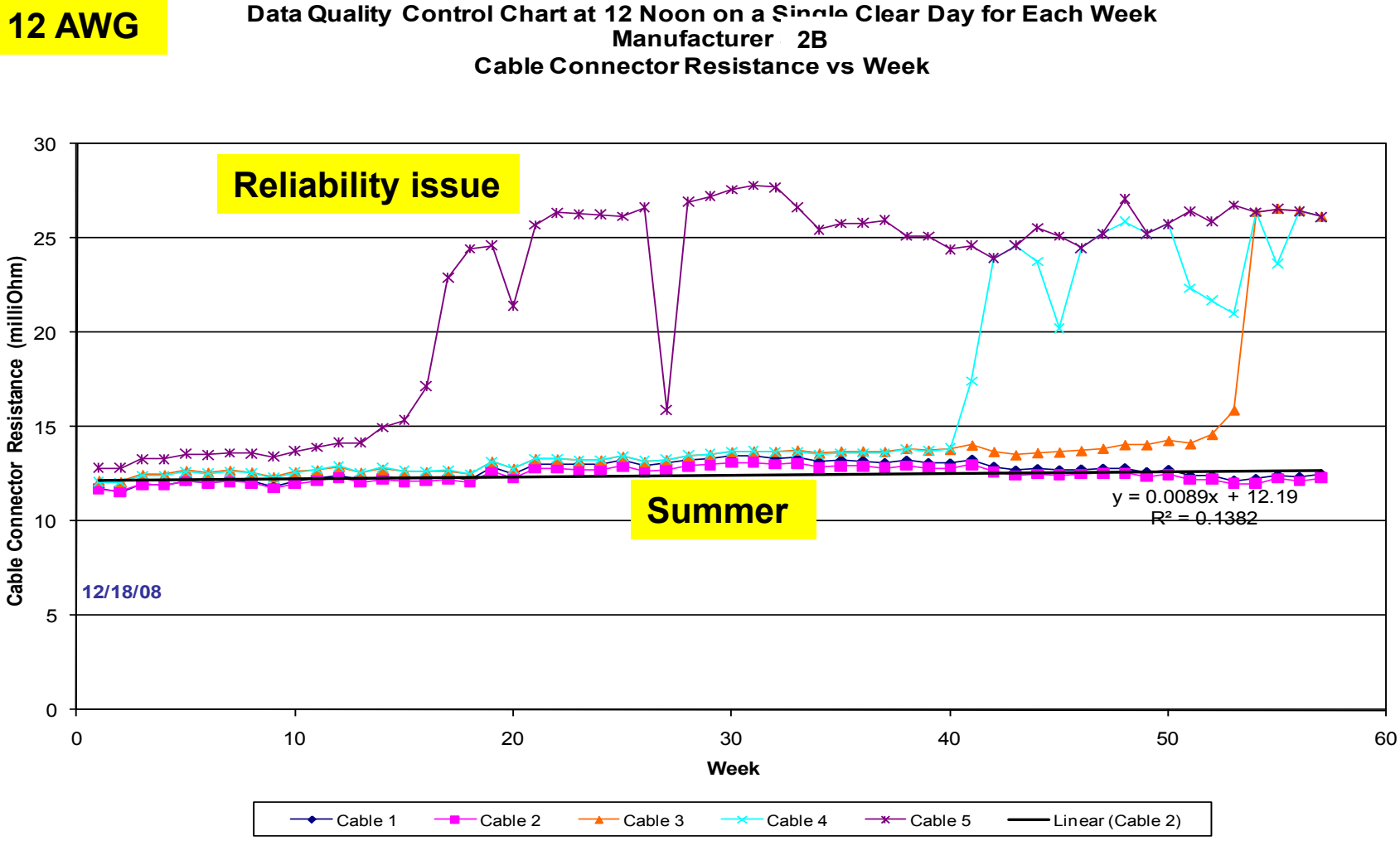


ASU Arizona State University

TÜVRheinland® Precisely Right.

Outdoor connector test results @ ASU

12 AWG

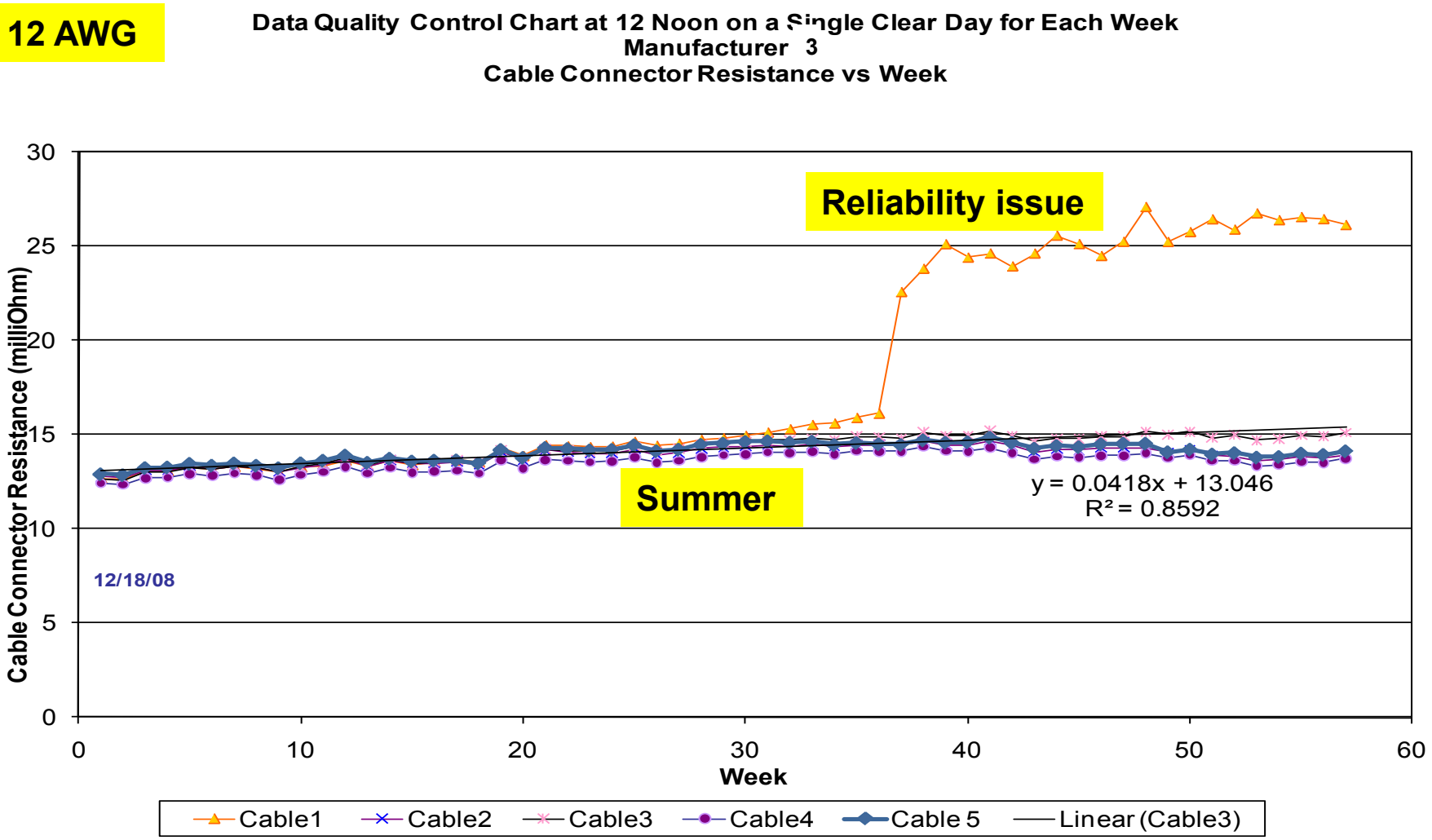


ARIZONA STATE UNIVERSITY

TÜVRheinland®
Precisely Right.

Outdoor connector test results @ ASU

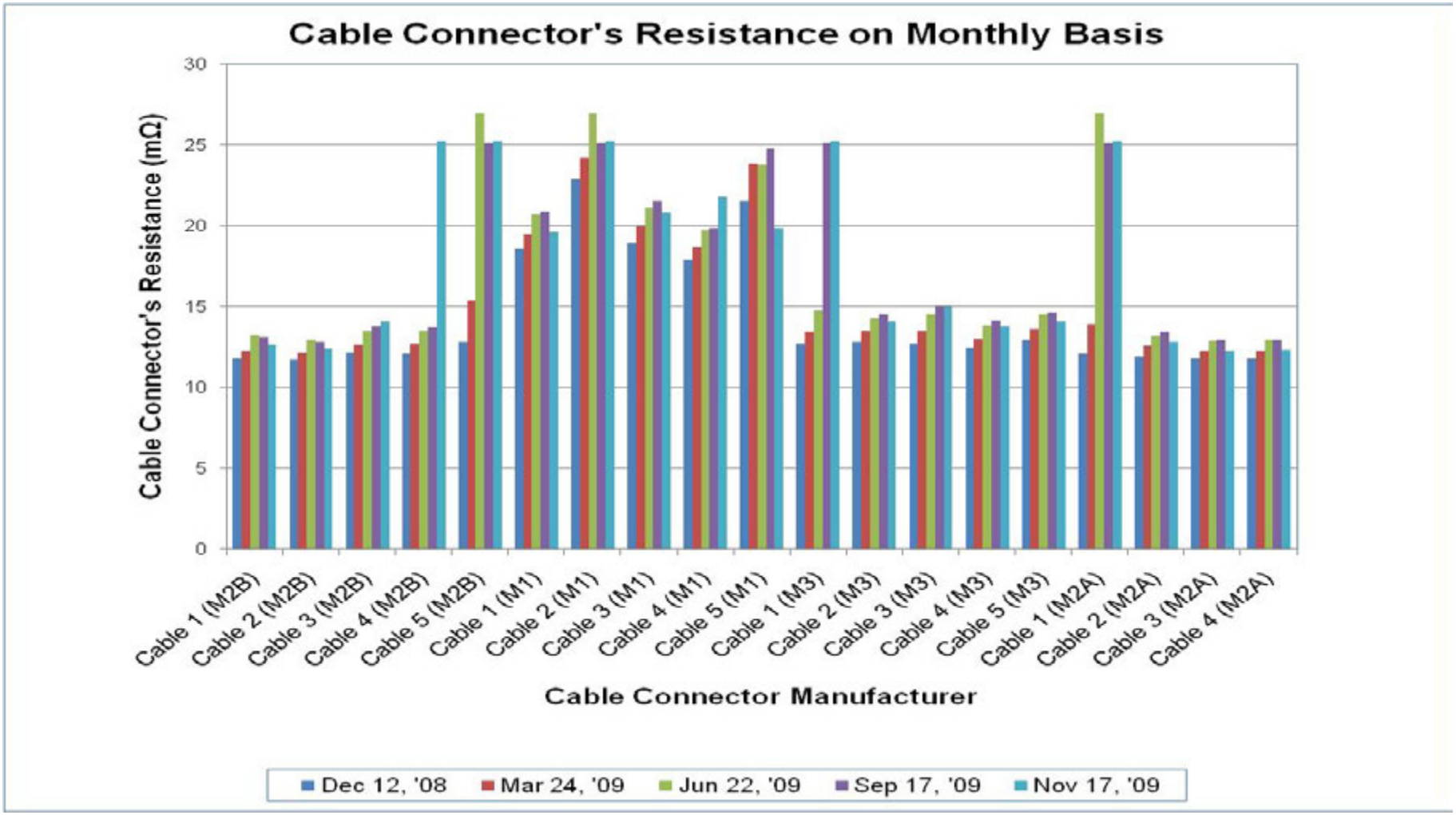
12 AWG



ARIZONA STATE UNIVERSITY

TÜVRheinland®
Precisely Right.

Outdoor connector test results @ ASU

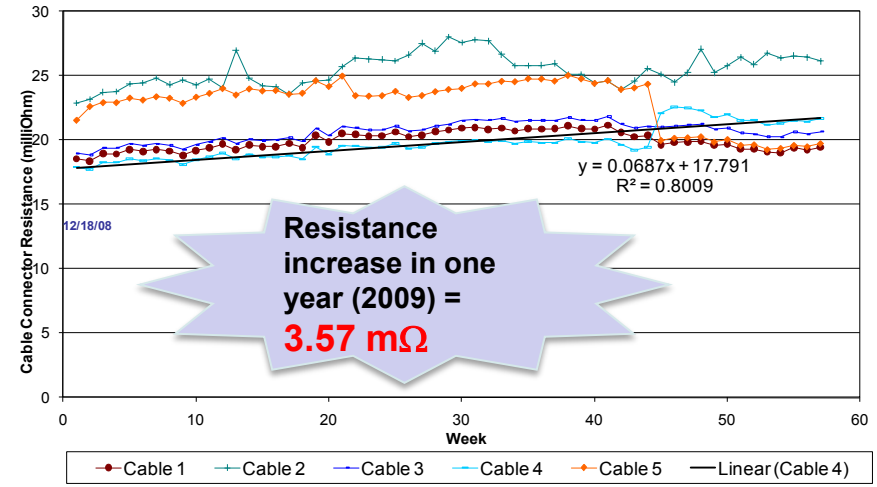


ASU Arizona State University

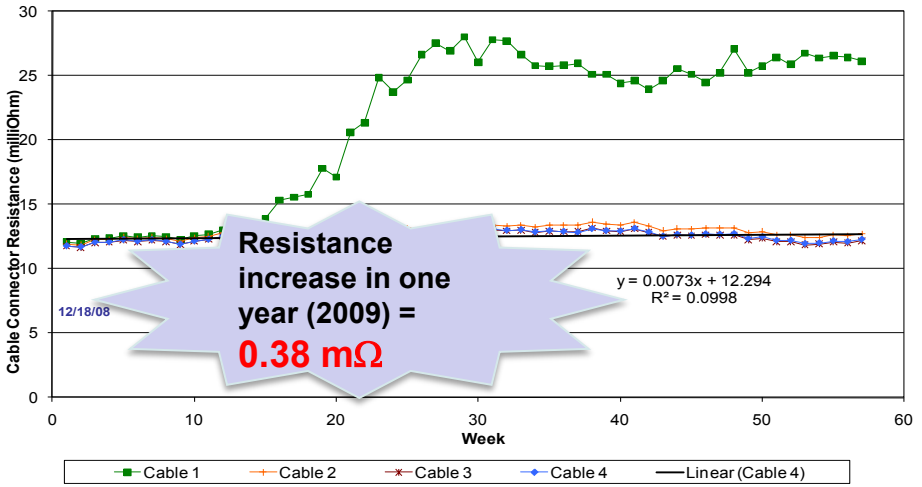
TÜVRheinland® Precisely Right.

Outdoor connector test results @ ASU

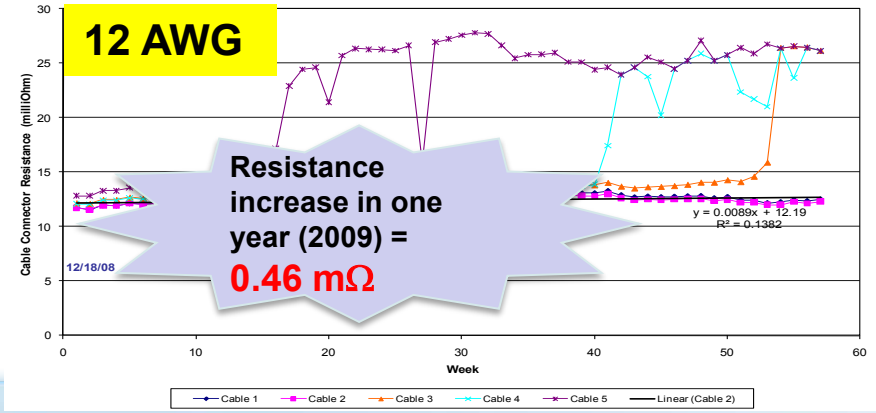
14 AWG



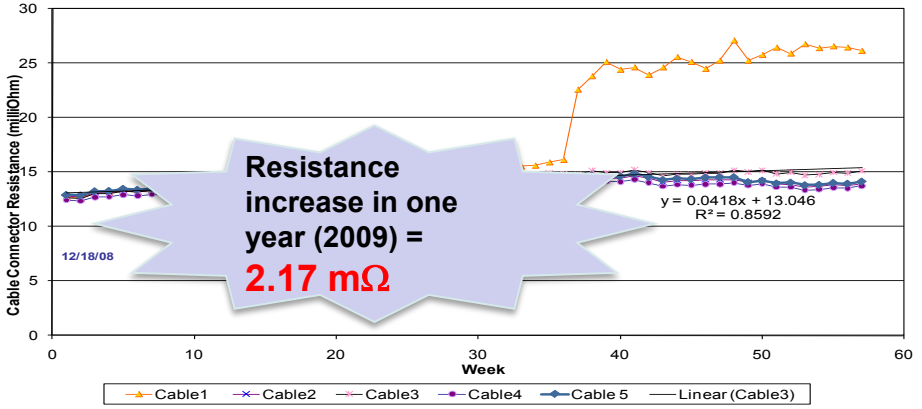
12 AWG



12 AWG



12 AWG



ARIZONA STATE UNIVERSITY

TÜVRheinland®
Precisely Right.

Outdoor connector test results @ ASU

All the connectors passed the wet megger test at 500 V_{dc} in Nov. 2010!

ASU Arizona State University
TÜVRheinland® Precisely Right.

Indoor connector test results @ TUV Rheinland
EN 50521: Contact resistance increase after stress test

STRESS TEST	PRJECT 1	PRJECT 2
BEFORE: 50 mechanical operating cycles test	2.5mm²: 2.60 mΩ	2.5mm² = 0.82 mΩ 6.0mm² = 0.49 mΩ
AFTER: 50 mechanical operating cycles test	2.5mm²: 2.62 mΩ	2.5mm² = 0.99 mΩ 6.0mm² = 0.51 mΩ
AVERAGE INCREASE (Group B): 6.6%	0.8%	12.4%
BEFORE: Temperature rise and dry heat tests	2.5mm²: 2.00 mΩ 6.0mm²: 1.36 mΩ	2.5mm² = 0.82 mΩ 6.0mm² = 0.46 mΩ
AFTER: Temperature rise and dry heat tests	2.5mm²: 2.01 mΩ 6.0mm²: 1.40 mΩ	2.5mm² = 0.91 mΩ 6.0mm² = 1.10 mΩ
AVERAGE INCREASE (Group C): 38.4%	1.7%	75.1%
BEFORE: Thermal cycling, damp heat and corrosion tests	6.0 mm²: 1.32 mΩ	2.5mm² = 0.75 mΩ 6.0mm² = 0.50 mΩ
AFTER: Thermal cycling, damp heat and corrosion tests	6.0 mm²: 1.45 mΩ	2.5mm² = 1.07 mΩ 6.0mm² = 1.82 mΩ
AVERAGE INCREASE (Group D): 81.6%	9.8%	153.3%

ASU Arizona State University
TÜVRheinland® Precisely Right.

EN 50521 Tests

DESCRIPTION
Initial sample/specimen activity
Select Samples for testing
Perform Incoming Inspection
Perform pre-conditioning of all test specimens
Mechanical test (Group A)
Visual and dimensional check
Marking durability test
Polarisation test
Termination test
Contact retention test
Cable anchorage test
Mechanical strength impact test
Low temperature mechanical strength test
Insertion and withdrawal force test
Coupling device effectiveness test

ASU Arizona State University
TÜVRheinland® Precisely Right.

EN 50521 Tests

Service life test (Group B)
Initial contact resistance measurement
Mechanical operation
Final contact resistance measurement
Contact earth measurement
Bending test
Thermal test (Group C)
Initial contact resistance measurement
Temperature rise test
Dry heat test
Visual and dimensional check
Final contact resistance measurement

ASU Arizona State University
TÜVRheinland® Precisely Right.

EN 50521 Tests

Climatic test (Group D)
Initial contact resistance measurement
Thermal cycle test
Damp heat test ***(& Humidity freeze test??)***
Dielectric strength tests
Corrosion test
Final contact resistance measurement
Degree of protection test (Group E)
Test finger access test
Manufacturer IP Code test (ingress)
Dielectric test

ASU Arizona State University
TÜVRheinland® Precisely Right.

EN 50521 Tests

Insulation material test (Group F)
Weather resistance test
Dielectric strength test
Outer housing insulation flammability test
Glow-wire test #1 (650°C)
Active parts insulation flammability test
Glow-wire test #2 (750°C)

ASU Arizona State University
TÜVRheinland® Precisely Right.

Planned future work

- Outdoor: Continuous monitoring of connector contact resistance
- Outdoor: Continuous monitoring of connector temperature using thermocouples
- Indoor: Measure connector contact resistance before and after TC500, DH2000, HF30 and dry heat tests for the same type of connectors as that of outdoor's
- Compare the outdoor connector results with indoor connector results
- Potentially determine the acceleration factor based on the indoor and outdoor test results

Thanks for your attention!

ASU Arizona State University
TÜVRheinland® Precisely Right.

Productive. Reliable. Smart. Safe.

Durability Testing for Module-attached Micro inverters

France Antelme
Senior Director, Product Verification

©2008 2010 Enphase Energy

Durability Strategy Considerations

- **Attached inverter subsystem durability should aim at that of the PV-Module host subsystem (15-25 year life)**
- **Inverter/Module Thermal and Mechanical closely coupled**
- **Durability testing of inverter must include all elements of the system. System test is unwieldy**
- **Subsystems could be tested alone – implies standardized test conditions that simulate the interaction of the PV module/Inverter subsystems**
- **Combined mix of Mechanical and Electrical/Electronic failure mechanisms for both subsystems is complex**

©2008-2010 Enphase Energy

PV-attached inverter failure mechanisms

- **Module/Inverter Interconnect System failures**
  - Corrosion
  - Moisture ingress
  - Mounting mechanical failure

- **Inverter Electromechanical/Mechanical failures**
  - PCB/Solder system mech. Integrity- Mechanical fatigue
  - Enclosure integrity – moisture ingress
  - Enclosure/Cabling – UV integrity

- **Inverter Electronic Device failure Mechanisms**
  - Passive components (Caps,Xfmers etc): Dielect/Ins bkdwn
  - Power devices(FETS etc): Various
  - Control (uP,IC,Memory): HCI, TDDB etc

©2008-2010 Enphase Energy

PV Module Failure mechanisms

Field Failure	Failure mechanism	Accelerated test
Interconnect Breakage	Thermal expansion & Contract	Thermal Cycling
De-lamination of Cell Metallization	Moisture penetration	Humidity Freeze
Corrosion of Cell Metallization	Moisture penetration	Damp Heat

Wohlgemuth, John, "Long Term Photo-Voltaic module reliability", NCPV and SPRM, 2003

- **PV Module failure modes and associated Accelerated lifecycle elements for comparison**
- **IEC 61215 is a module qualification test**
- **Variations/extensions of IEC-61215 have also been used by PV Module vendors to verify durability of PV modules**

©2008-2010 Enphase Energy

Attached inverter failure mechanisms

System Element	Failure mechanism	Accelerated test
Enclosure/Interconnect	Mechanical deformation, Moisture ingress, Corrosion, Dielectric breakdown	TC/HF/Damp heat UV precondition
PCB/Solder system	TCE mismatch, electromigration	HF/TC
Passive components	Dielectric, Insulation breakdown	HF/TC/Elevated Heat
Active devices	Many	TC/Damp Heat (Elevated temp)
Integrated circuit devices	HCI, TDDB etc	TC/HF/Damp heat

- **Attached inverter failure mechanisms are addressed by HF,TC and Damp Heat (Extended High temp operation)**
- **It is feasible to apply HF,TC and Damp heat as accelerated lifecycle tests for durability. Duration/mix?**

©2008-2010 Enphase Energy

Attached inverter Durability Test Elements

- **Durability testing –** Inverter subsystem failure mechanisms can be addressed with the same three elements applicable to the modules subsystem i.e. TC,HF, Damp heat
- **HF,TC, Damp Heat parameters/mix –** Need optimization for inverters
- **Lightning related issues–** i.e. lightning effects can be addressed by a derivative of standard inverter acceptance surge.
- **Independent Inverter Performance testing -** can be addressed with a standardized thermal profile

©2008-2010 Enphase Energy

Research needed

- **Thermal/thermoelectric effects** of the inverter attachment to the PV module backsheet
- **Standardized thermal profiles** against which we can execute performance tests on the individual inverters

©2008-2010 Enphase Energy

Standard updates ?

- **IEC-61215- standard update to take account of the Inverter attachment to the PV backsheet**
  - Module UUT orientations etc
- **Standardized test profiles/methodology to allow independent testing of Inverter and Module subsystems?**

©2008-2010 Enphase Energy

Conclusion

- **Majority of the failure mechanisms in PV attached inverter subsystems can be addressed with a variation of the mix of elements in IEC 61215 as accelerated lifecycle tests**
- **Optimization of HF,TC, Damp Heat parameters required for inverter: Excite all failure modes**
- **Require some optimization to Module qualification/durability testing to account for presence of Module/Inverter interconnect**

©2008-2010 Enphase Energy

NREL
NATIONAL RENEWABLE ENERGY LABORATORY

How Standards Control Module Design for Better or Worse



2011 PV Module Reliability Workshop

John Wohlgemuth,

February 16, 2011

NREL/PR-5200-51007

NREL is a national laboratory of the U.S. Department of Energy, Office of Energy Efficiency and Renewable Energy, operated by the Alliance for Sustainable Energy, LLC.

Introduction

- PV Modules should be designed and constructed to perform in a safe manner outdoor for at least 20 or 25 years.
- However, it appears that many modules are designed and their components are selected primarily to meet the requirements of the Performance Standards (IEC 61215 and IEC 61646) and Safety Standards (IEC 61730 and UL 1703).
- This presentation will explore the issues related to designing and building modules to meet standards rather than to survive in the field.

Why I believe Modules are Designed for Standards

- Too many cases where modules pass one of the tests from the qualification sequence but fail when the test is extended even a small amount.
- One case where new manufacturer's cells in standard package passed 1000 hours of damp heat with little power loss, but just extending to 1250 hours resulted in significant power loss > 20%.
- While at BP Solar we tested 10 crystalline silicon module types from 9 different manufacturers from all over the world, all qualified to IEC 61215.
  - Only 3 passed BP Solar's extended test protocol.
  - Most failed damp heat at 1250 hours.

Extending Test Duration for Cr-Si Modules Qualified to IEC 61215

Manufacturer	DMLC/TC/HF	1250 Hr DH	500 TC
A	Pass	Fail	Fail
B	Pass	Fail	Pass
C	Pass	Fail	Fail
D	Pass	Fail	Pass
E	Pass	Fail	Pass
F	Pass	Pass	Pass
G	Pass	Fail	Pass
H	Pass	Pass	Pass
J	Pass	Fail	Pass
K	Pass	Pass	Pass

What are the ramifications

- Qualification test is not a 25 year lifetime test.
- Qualification test does an excellent job of identifying design, material and process flaws that lead to premature failures (Infant mortality).
- Qualification test does not address wear-out mechanisms that limit lifetime.
- We do not have an accelerated test sequence that can assure 25 year lifetime in all terrestrial environment.
- Relying solely on the Qualification test sequence can mean no assessment or evaluation of how the module will actually perform long term in the field.

Over Design

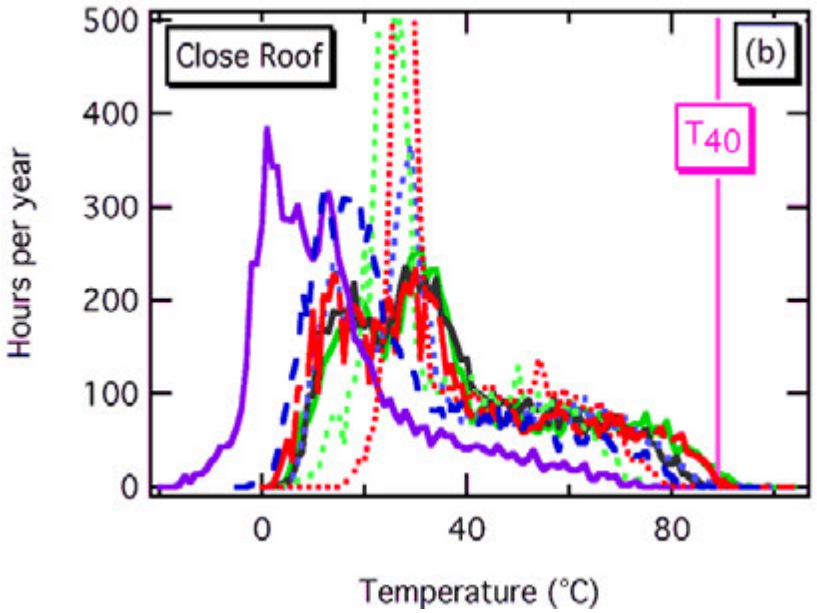
- The safety standards put requirements on the materials within the module.
- These requirements typically come from other fields.
- They may or may not be appropriate for PV applications.
- They often add unnecessary cost to the PV module.
  - Extra testing cost
  - Use of more expensive materials/components just to meet the requirements of the standard not to increase safety.
- Going to discuss 2 examples

RTI

- The UL RTI test has been included in both UL 1703 and IEC 61730.
- Both standards require any polymeric materials within the module to have an RTI rating equal to the temperature measured during the "Temperature Test - T_{40} " plus 20 °C.
- RTI is an exceeding long test (more than 1 year). So slows down and impedes the use of new materials.
- There is little scientific basis for the RTI test. It determines when a property has fallen to 50% of initial value no matter whether that loss of property has anything to do with its performance in the application.

RTI

- RTI usually used where the operating temperature is well known and fairly constant when an appliance is operating. **This is not the case for PV.**
- Modules rarely operate at even the temperature measured in the temperature test.
- Typical Module T_{40} = 90 °C
- See figure for a roof mount module in 6 locations including Saudi Arabia, one of the hottest places in the world.
- A module only spends a few hours a year above the T_{40} temperature and never reaches T_{40} + 20.



"EVALUATION OF HIGH-TEMPERATURE EXPOSURE OF PHOTOVOLTAIC MODULES" By Kurtz etal, TBP in **Progress in PV**

Partial Discharge Test

- IEC 61730 requires the back sheet material to have a partial discharge rating for the highest system voltage the module will be rated for (Typically 600 volts in the US and 1000 volts in Europe).
- The partial discharge test comes from the insulation industry and was typically used to evaluate the insulation on windings in transformers.
- Partial discharge is suppose to help predict wear out of the insulation material after long term exposure to electric fields.
- The test uses
  - 2 conductive planes with the backsheet sandwiched in between.
  - AC to excite the field and cause the discharges

Issues with Partial Discharge Test

- First issue is that there very few cases where the geometry in PV module resembles the test (backsheet sandwiched between 2 conductive planes).

In most cases there are no conductive materials touching the backsheet except maybe at the edges where the internal circuitry (cells and bus bars) must meet the clearance distance for the proposed voltage.

- Second issue is the use of ac rather than the dc that PV modules see.

Very little information is available to indicate that the AC test does anything to predict DC performance.

Why is Partial Discharge Test Important?

- Partial discharge test drives the construction requirements of the backsheet.
- Because of partial discharge test backsheets are much thicker (and therefore more expensive) than would be required to meet all other requirements in IEC 61730 or IEC 61215/61646.
- One module manufacturer estimated that this requirement adds $5 to $6 to the cost of every ~200 watt module.

Termination Requirements

- **Both UL 1703 and IEC 61730 have a similar requirement for module termination.**

"Strain relief shall be provided so that stress on a lead intended for field connection, or otherwise likely to be handled in the field, including a flexible cord, is not transmitted to the connection inside the module or panel." from UL1703

- **Good idea but implemented incorrectly.**
- **NRTL's have allowed this criteria to be met using a potting compound (such as silicone or epoxy).**
- **If the solder bond on the lead fails the pottant holds the lead in place allowing an arc to develop and possibly continue for an extended time period.**
- **This has been one of biggest PV safety issues.**

Solutions

- **For Design to Qualification Test:**

Develop a set of accelerated stress tests that predict module performance over 25 years in various terrestrial climates.

QA workshop In Tokyo in May, 2011

- **For RTI**

Replace RTI with requirements for materials that are developed specifically for the environments in which PV modules operate.

Underway in WG2 - Participate in this effort

- **For Partial Discharge**

Only require partial discharge test when module is designed to have conductive material in contact with the back of the backsheet. (Part of mounting system or metal foil for humdiity barrier)

Support this change in your national committee when voting on IEC 61730 edition 2

Solutions (Continued)

- **Termination Issue**

Latest draft of 61730 edition 2 changes wording on termination to require redundant electrical connections.

Support this change in your national committee when voting on IEC 61730 edition 2.

- **Redundancy Issue**

Replace UL 1703 with IEC 61730 so US industry isn't hampered by having to carry double safety certifications nor have to correct the problems in 2 standards.

Let UL, Solar ABCs and DOE know that this is a priority for US PV industry.

BORREGO SOLAR

PV RELIABILITY & PERFORMANCE

A PROJECT DEVELOPERS EXPERIENCE

Bradley Hibberd

Borrego Solar Systems

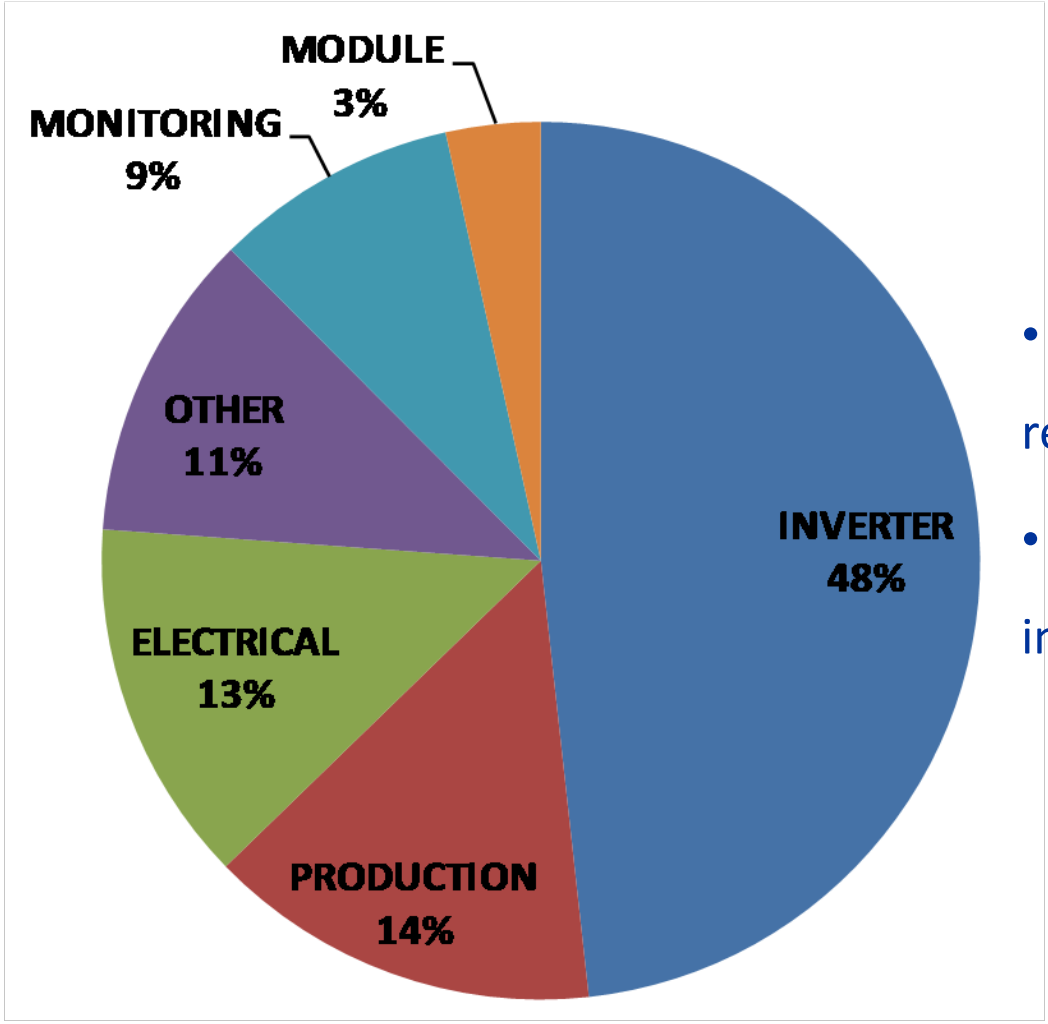
ABOUT US

- BORREGO SOLAR SYSTEMS
  - Established 1980
  - Offices in San Diego, Berkeley & Lowell, MA
  - Active in CA, NV, AZ, MA, NJ, PA, NY, CT, TX, OH
  - 70 Employees
  - Installed over 25MW of PV (1000+ Systems)
  - Project Developer & Integrator
  - Originally Residential, Now Commercial/Industrial/Utility Focussed`

OUTLINE

- SYSTEM RELIABILITY
  - Analysis of 5 Years of Service Data
- MODULE RELIABILITY
  - Summary of Experience
  - Photographs of Failed and Damaged Modules
- OUR RELIABILITY CONCERNS
  - Transportation
  - Installation Practices
  - Structural, Voltage, Shading, Moisture, Testing & New Products

SYSTEM RELIABILITY



- Analysis of 750 service cases reported through end 2010
- Residential and commercial installations.

SYSTEM RELIABILITY - BREAKDOWN

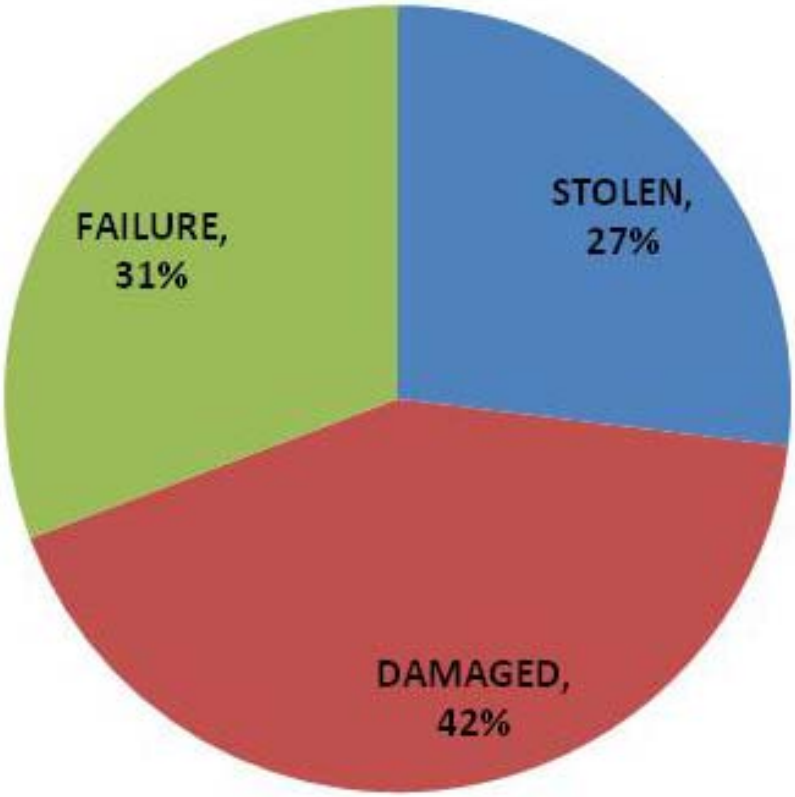
- INVERTER (48%)
  - Failure and Replacement (Complete/Partial) – Approx. 50%
  - Related Issues – Breakers/Fuses, AC Voltage, Turned Off
- PRODUCTION (14%)
  - Low Production Reported, Electricity Bill High
- ELECTRICAL (13%)
  - Installation Issues, Wiring Issues, Ground Faults, Tripping Breakers
- OTHER (11%)
  - Roof Leaks/Water in Conduit/Boxes, Damaged Tiles, Dirty Array, Rattling Modules, Bird/Rodent Issues, Other Damage
- MONITORING (9%)
  - Web Based Monitoring Not Working, Inverter/Local Monitoring Display Blank, Network Issues

MODULE RELIABILITY

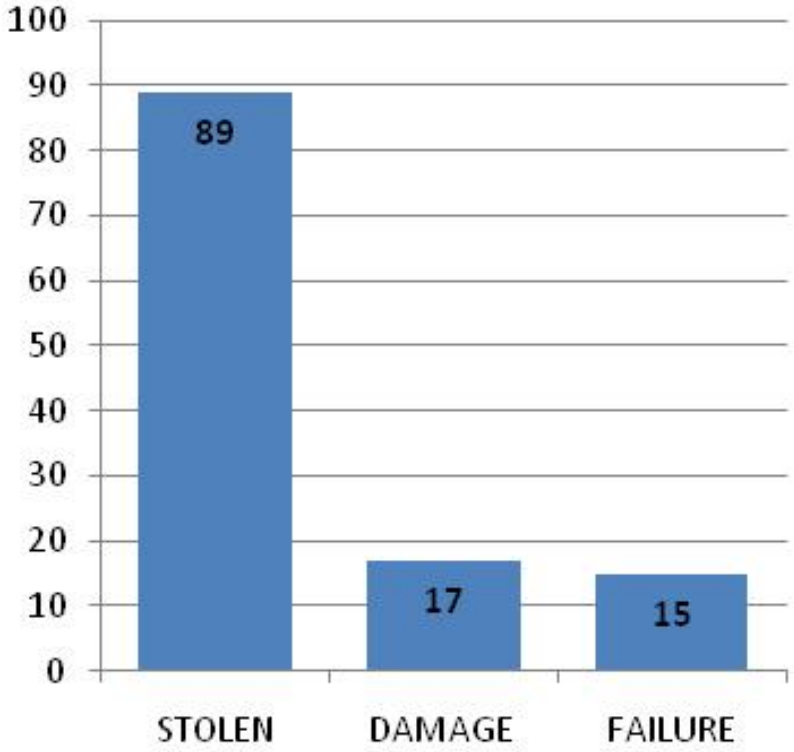
- INSTALLATION STATISTICS
  - 25MW / 125,000 Modules Installed
  - Modules from Sharp, Yingli, BP, Shell/Siemens/SolarWorld, Evergreen, First Solar, Kyocera, Uni-Solar, Sanyo, Kaneka
  - Residential & Commercial Installations
- DAMAGED DURING TRANSPORT/INSTALLATION
  - Quantity Unknown – Data Showing 60+ Modules ~0.05% of Installed
- DOA MODULES
  - DOA Modules - Appear OK, Non Functional
  - 2 Instances, 1 Module & 6 Modules – ~0.005% of Installed
  - Identified During Commissioning (V_{OC} testing)
- INSTALLED MODULE ISSUES
  - 3% Of Service Cases

MODULE RELIABILITY

% OF CASES (OF 3% MODULE CASES)



OF MODULES EFFECTED



MODULE RELIABILITY

- FAILURES
  - 7 Separate Incidents, 6 Different Brands, 15 Modules (0.01%)
  - Solder Bond, Seal, Structural, Corrosion & Hot Spot/ Failures
  - Replaced Under Warranty (Except One – Mounting Problem)
  - CAVEAT – These are Catastrophic Failures, We Expect There Are Unknown Non-Catastrophic Failures Reducing Performance
- DAMAGED
  - Majority from Customer Who Has Neighbor With 9 Hole Golf Course!
- STOLEN
  - Was a Growing Problem, Seems to Have Tapered Off, Better Security, Reduced Value, Focus on Commercial Systems

MODULE RELIABILITY - FAILURE



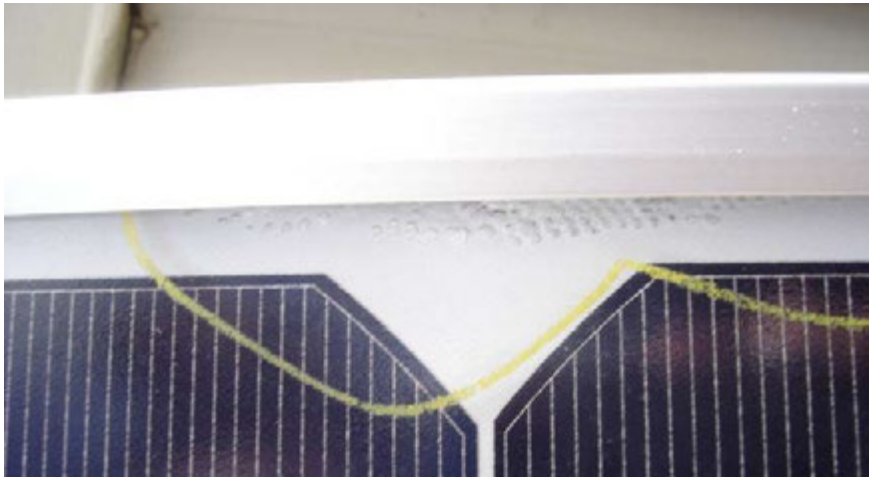


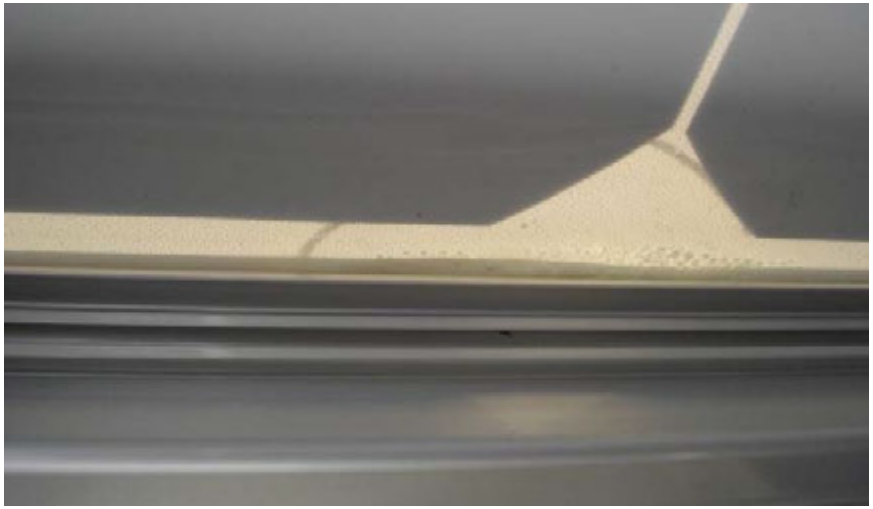




MODULE RELIABILITY - FAILURE



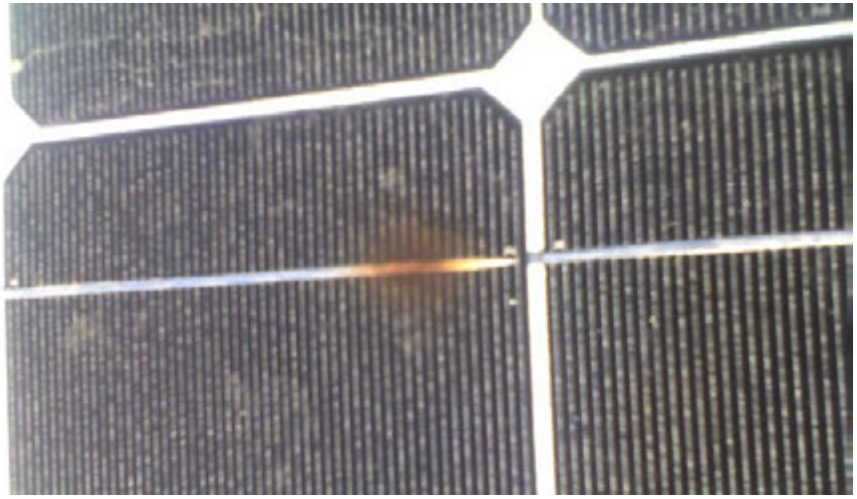


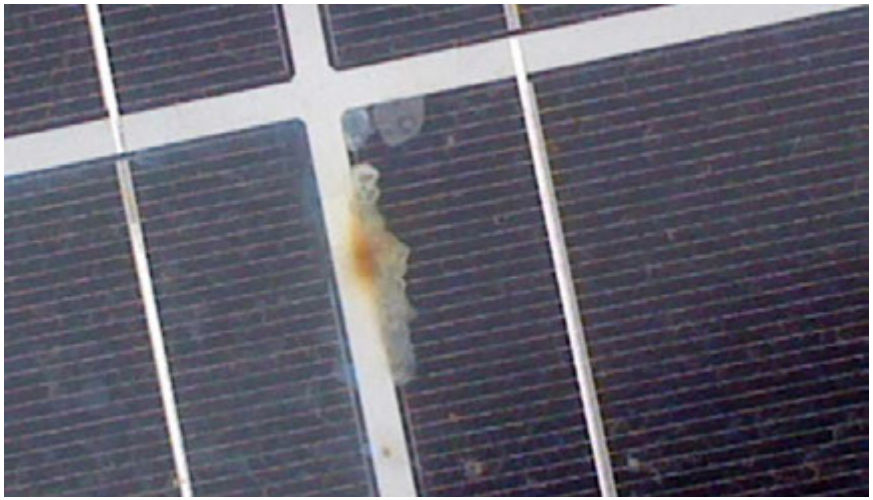




MODULE RELIABILITY - FAILURE



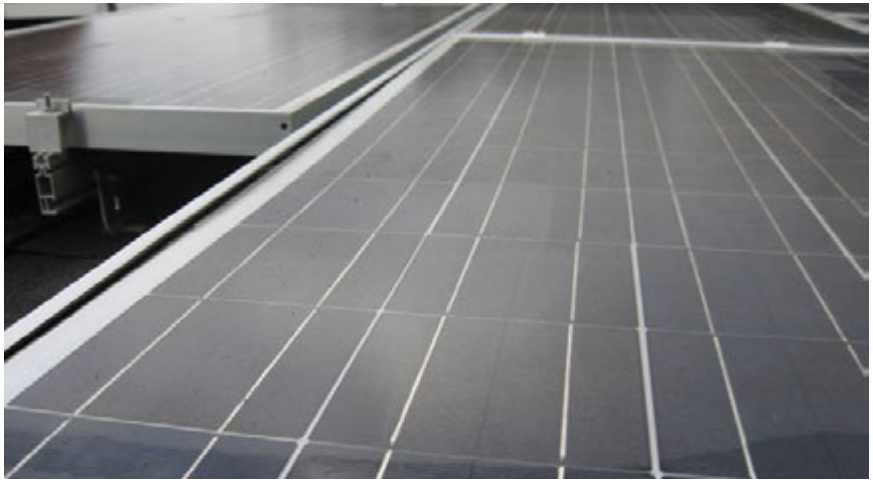




- CORROSION OR SOLDER BOND ISSUE?
  - LEFT – Same Module Type
  - ABOVE – Diff Module Type

MODULE RELIABILITY - FAILURES





- EDGE SEAL COMPROMISED
  - Ground Fault in Inverter
  - Inverters Replaced
  - Numerous Visits to Identify
- FRAME SEPARATION
  - Improper Module Support
  - Only 1 Module Impacted
  - Issue Corrected

MODULE RELIABILITY - DAMAGE









MODULE RELIABILITY – DAMAGE








OUR RELIABILITY CONCERNS

- TRANSPORTATION
  - What Issues in 5 or 10 Years From Transporting Modules?
  - What if Modules Were Unpackaged & Then Transported?
- INSTALLATION PRACTICES (PRE-FABRICATION)
  - Assemble Modules to Racking Off-Site (Warehouse)
  - Changes Some Construction to Manufacturing
  - Reduces Onsite Assembly, Craning Cost/Time,
  - Improved Quality
  - What Is Impact on Modules?
  - Planning on Testing Modules That Have Been Through Process

OUR RELIABILITY CONCERNS



TRANSPORT TO SITE





STORAGE/READY TO SHIP

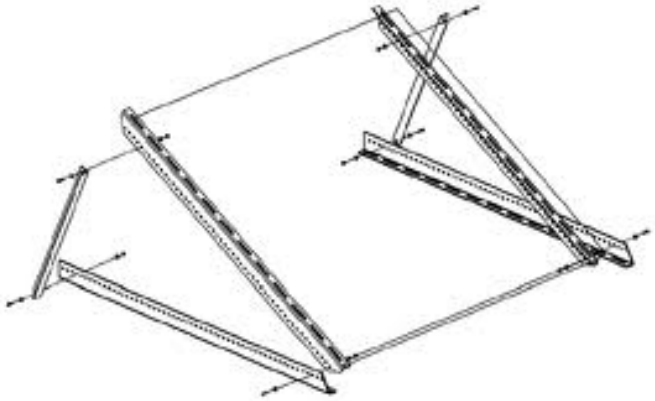
OUR RELIABILITY CONCERNS

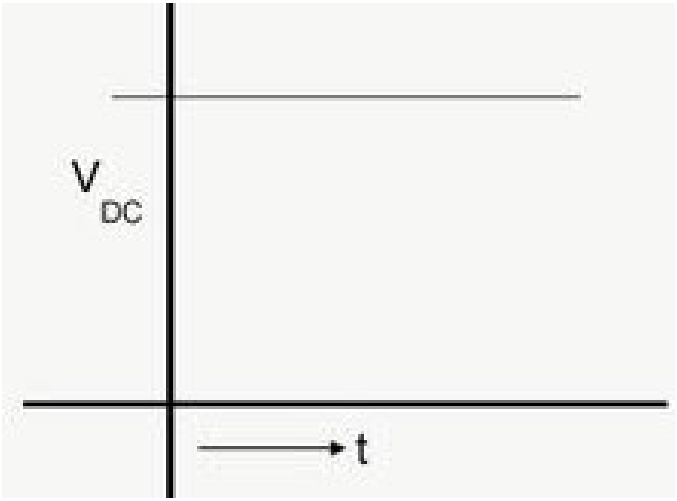

TRANSPORT TO SITE


ASSEMBLY ON SITE


CRANING TO ROOF

OUR RELIABILITY CONCERNS - OTHER





- STRUCTURAL SUPPORT
  - Can Racking Structures Reduce Cell Fracture (Or Conversely Promote It)?
  - How Significant is this Issue?
- VOLTAGE DEGRADATION
  - Does Module Voltage Change Over Time?
  - Industry Assumption is 50% V, 50% I
  - Limits System Design Flexibility OR Potentially Poorly Performing Systems

OUR RELIABILITY CONCERNS - OTHER

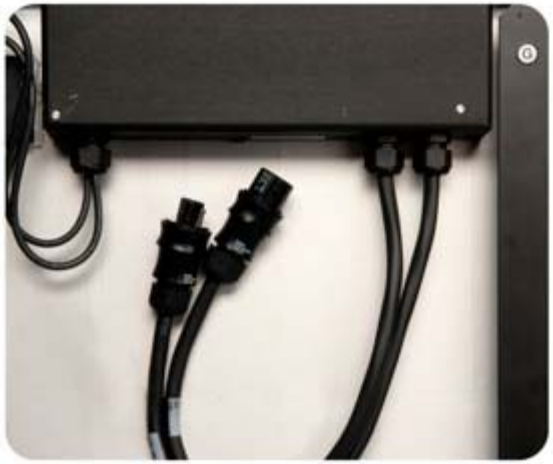




- SHADING
  - Is Consistent Shading on Portions of Modules a Long Term Issue?
- MOISTURE
  - Shallow Tilt/Water Pooling?
  - Consistent Snow Coverage?

OUR RELIABILITY CONCERNS - OTHER





- CIRCUIT TESTING – HIGH BIAS (MEGGER)
  - Can We Safely Megger Circuits Including Modules?
  - Large # of Circuits Not Currently Tested
  - Can Reduce Fire Danger if we Test
  - Need Best Practice Guide
- NEW PRODUCT RELIABILITY EVALUATION
  - Integrated Inverters/DC Converters/Intelligence
  - Need Standard Reliability Test

THANK YOU

SPECTROLAB

A BOEING COMPANY

BOEING

What Not to Do

Presented at NREL PV Reliability Workshop
Feb 17, 2011

Peter Hebert, John Frost, Rob Cravens and
Robyn Woo, Spectrolab, Sylmar, CA 91342

Source: Spectrolab, Inc.

Introduction

- This talk shares some experiences with failure analysis in CPV cells and assemblies

- In some cases, root cause and corrective actions are discussed.
  - These are examples of solutions.
  - They are not intended to claim that these are the best solutions, or that products with other design features will not work as well or better.

- This presentation does not contain any proprietary or confidential information

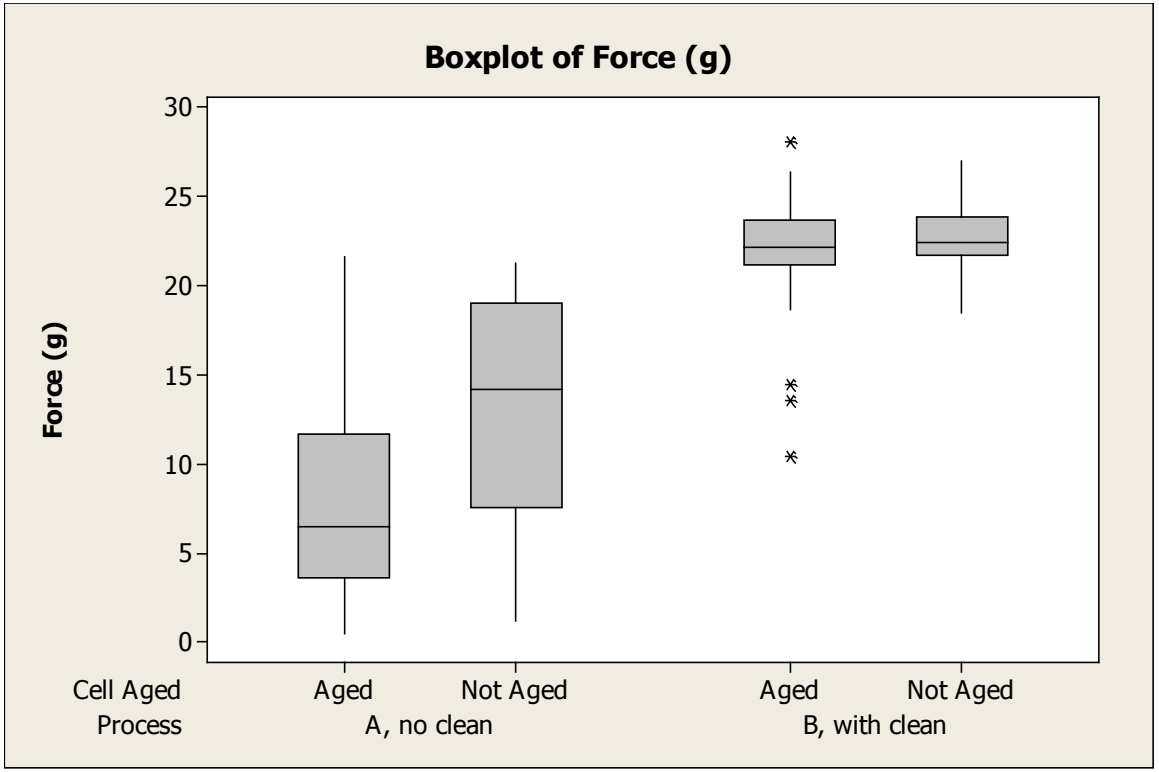
Agenda

- **Wire Bonding**
- Thermal Cycling
- Contamination in Cell Assembly I
- Contamination in Cell Assembly II
- Contamination in Enclosure I
- Contamination in Enclosure II

Cleaning Provides Higher Quality Bonds

- A split lot formed with several different groups of parts. Half parts were baked for 1 hr to simulate aging, half were not.
- Parts were wire bonded with two different processes.

Plasma Clean Improves Wire Bonding Robustness to Variation



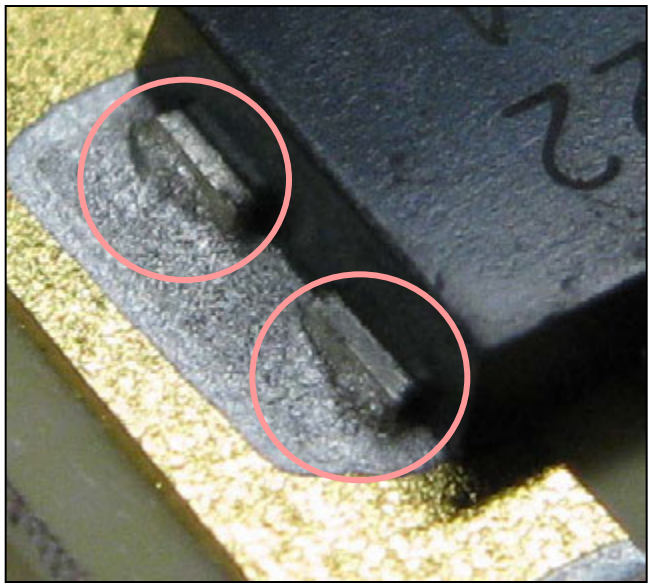
Agenda

- Wire Bonding
- **Thermal Cycling**
- Contamination in Cell Assembly I
- Contamination in Cell Assembly II
- Contamination in Enclosure I
- Contamination in Enclosure II

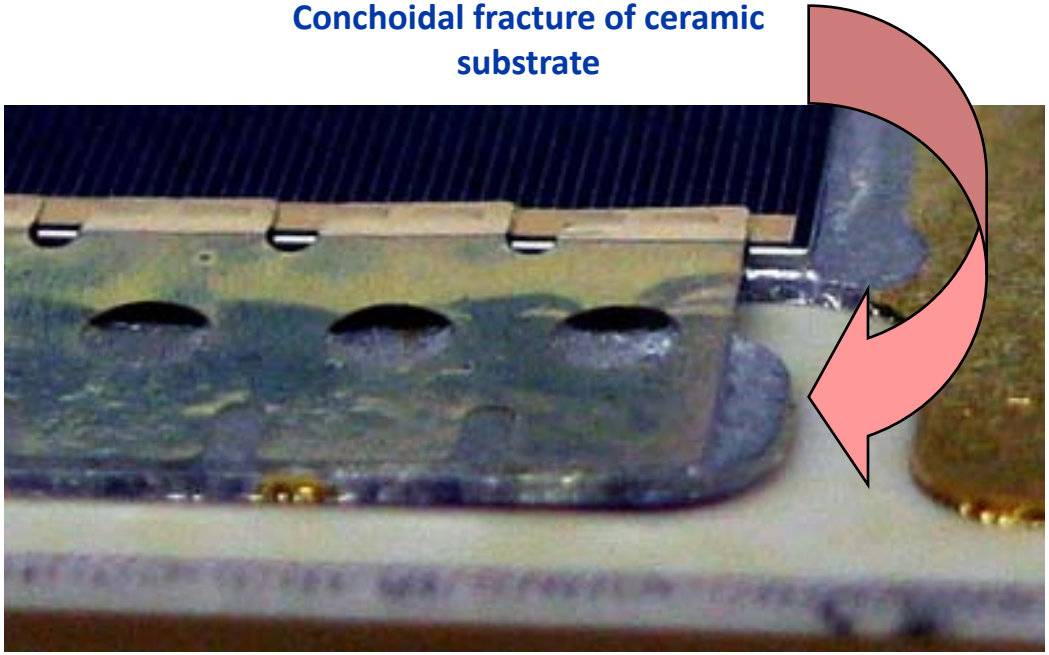
Assembly Design Failures

- Many CPV assemblies look similar, with cell bonded to DBC substrate. But reliable performance is in the details
- The following failures were observed after 500 IEC standard thermal cycles from -40C to +110C

Solder joint failure on surface mount diode



Conchoidal fracture of ceramic substrate

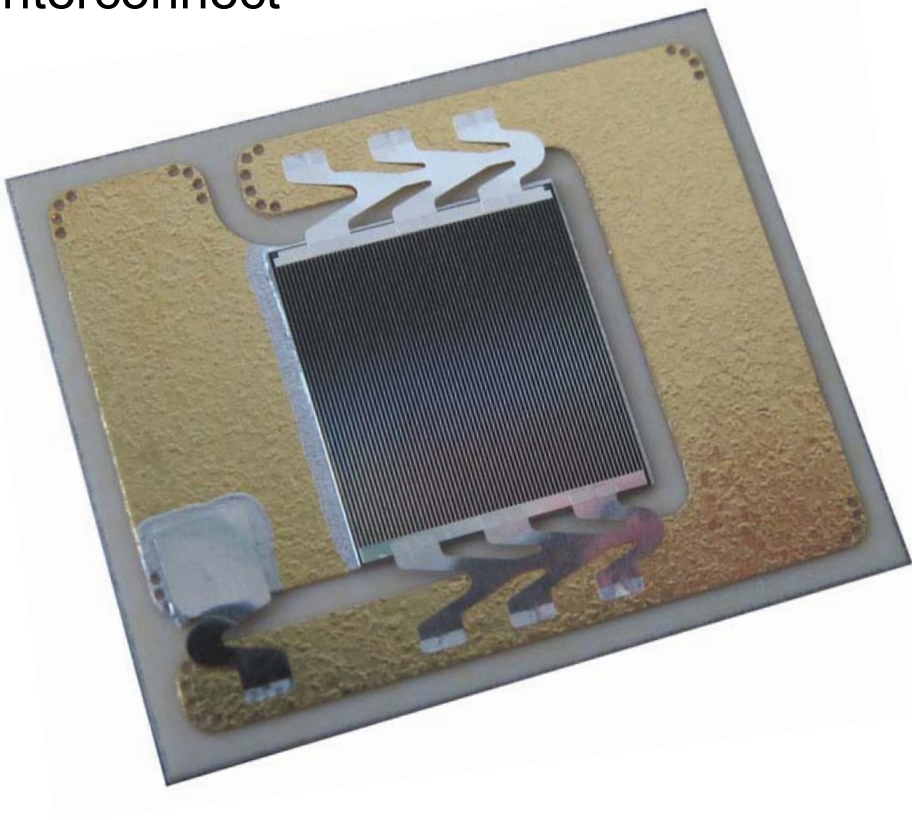


Corrective Actions

- Engineering to avoid most thermal cycle failures is well understood, it just requires requisite attention to detail
- Potential solutions to these failures include
  - Diode solder joint cracks
    - Stress relief in diode package
    - Less rigid attachment to substrate
  - Conchoidal fracture
    - Reduce thickness of Cu trace
    - Add dimples or other stress relief in Cu sheet
  - Solder disbond
    - Cleanliness and part preparation
    - Modeling and experiment with TIM material and process conditions

Improved Cell Assemblies

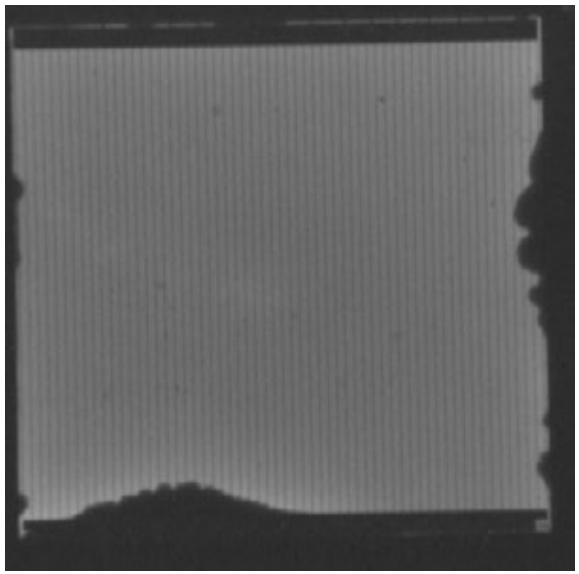
- New design
  - Improved stress relief in interconnect
  - Bare diode with stress relief in interconnect
  - 5 mil Cu thickness (from 8 mil)
  - Strategically placed dimples

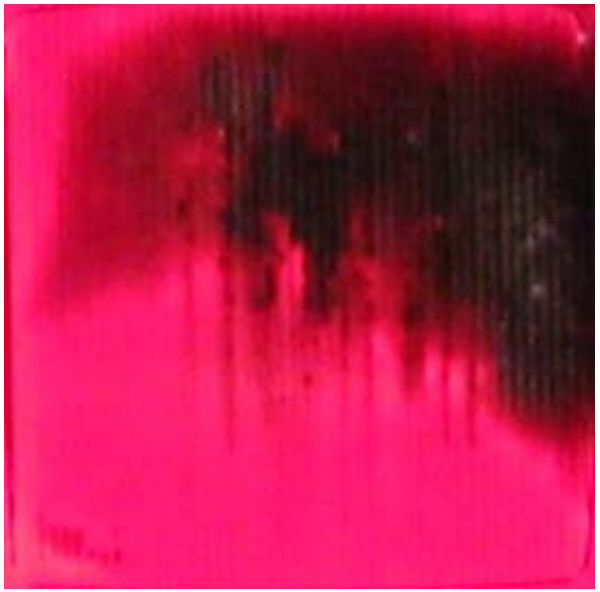


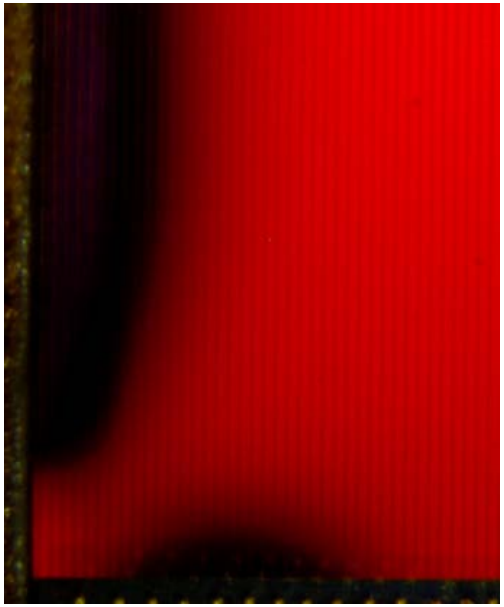
- Improved design shows no issues after new baseline of 1,500 thermal cycles from -40C to +110C

Cell Failures

- The electroluminescence images of cell failures look similar, but they have very different causes







Agenda

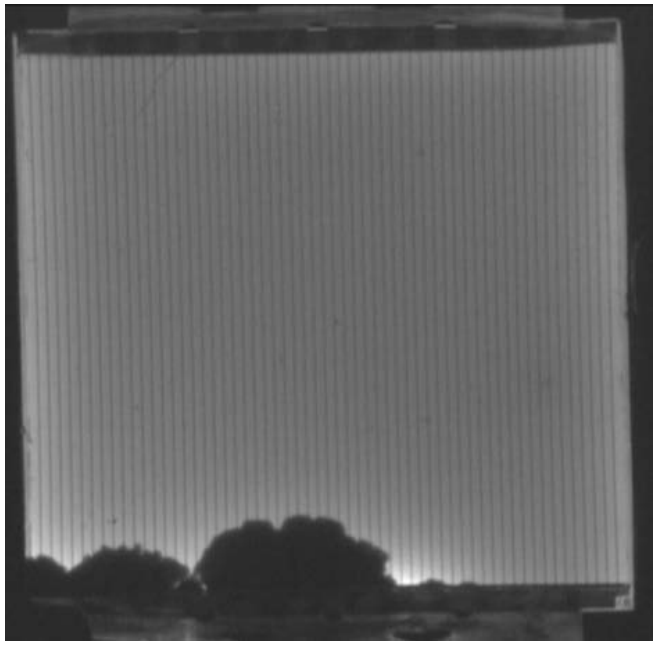
- Wire Bonding
- Thermal Cycling
- **Contamination in Cell Assembly I**
- Contamination in Cell Assembly II
- Contamination in Enclosure I
- Contamination in Enclosure II

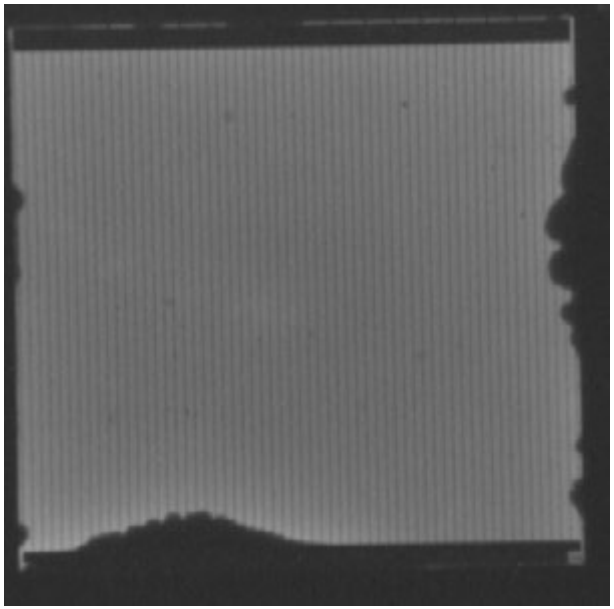
Contamination in Cell Assembly I

- Some assembly processes include liquid immersion, typically for flux removal or cleaning
- The solutions, even DI water, can become conductive from contamination or from material removed from the assembly
- If the solution becomes conductive, electrochemical reactions can occur
  - Driven by galvanic cell created between dissimilar materials (for example, Au-SnPb solder creates 0.65 V)
  - Driven by solar cell response to ambient indoor room lighting

Examples of Cell Damage

- Electrochemical reactions can perform many surprising feats
  - Plating of solder and substrate material on to cell surface
  - Wholesale or selective removal of cell layers





Recommendations to Avoid Electrochemical Reactions

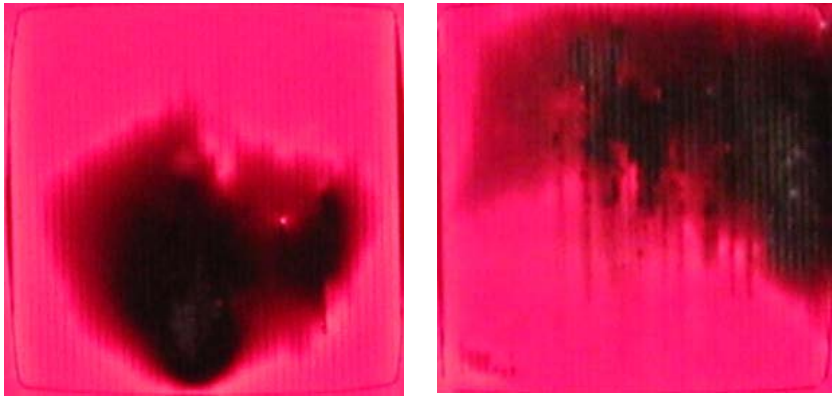
- If possible, minimize or eliminate aqueous processing
- Regularly test conductivity of the bath, not just water supply
- When possible, minimize lighting over baths
- Consider electrochemical potentials of materials in assembly design
- Protect metal and semiconductor surfaces with encapsulants and/or dielectric materials

Agenda

- Wire Bonding
- Thermal Cycling
- Contamination in Cell Assembly I
- **Contamination in Cell Assembly II**
- Contamination in Enclosure I
- Contamination in Enclosure II

Contamination in Cell Assembly II

- Cells began to degrade after several months on sun.



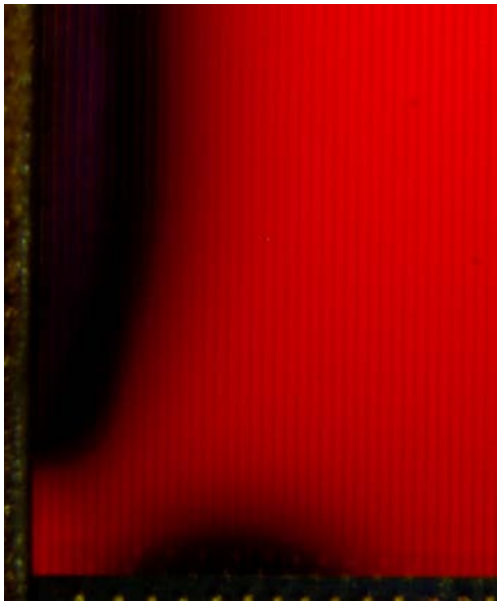
- Assembly process used solder flux and flux cleaner containing bromine
- EDX & ESCA scans did not detect bromine on cell surface after assembly.
- After being placed on sun, bromine attacked front metal and was found all over cell surface
- Recommendation – use halogen free flux and flux cleaner

Agenda

- Wire Bonding
- Thermal Cycling
- Contamination in Cell Assembly I
- Contamination in Cell Assembly II
- **Contamination in Enclosure I**
- Contamination in Enclosure II

Contamination in Enclosure I

- Cell degradation observed during module / system accelerated life tests



- Failure analysis showed cells shunted around the perimeter

- Further investigation found a contaminant within the module enclosure which was corrected before product release.

Agenda

- Wire Bonding
- Thermal Cycling
- Contamination in Cell Assembly I
- Contamination in Cell Assembly II
- Contamination in Enclosure I
- **Contamination in Enclosure II**

Contamination in Enclosure II

- In another case, chlorine off gassing from edge sealant caused corrosion within the module enclosure and created significant power loss within months of installation.
  - Did not directly attack cell
- Investigation showed the CM substituted a different edge seal from the one specified.
- Recommendation
  - Avoid halides at all phases.
  - Consider environment within the module

Conclusion

- This paper has described failure analysis of CPV components and modules at various levels of assembly and some potential solutions
- Some recommendations for reliability
  - Dimples and stress relief improve thermal cycle lifetime, but require larger substrate
  - Always maintain high resistivity in aqueous solutions and avoid voltage generators such as galvanic couples and light
  - Avoid halides in processing and as constituents of components inside modules
  - Protect cells with encapsulation, and design system to avoid damaging materials that can penetrate encapsulants

Acknowledgements

- The authors would like to acknowledge contributions and support from the entire Spectrolab team. Peichen Pien, Omar Al Taher, Randy Brandt, Jim Ermer, Russ Jones, Xiaobo Zhang, William Hong, Daniel Law and Mark Takahashi
- The authors would also like to thank various unnamed suppliers, customers and partners for useful data, discussions and support
- Some of this material is based upon work supported by the Department of Energy Solar America Initiative under contract DE-FC36-07G017052

NREL
NATIONAL RENEWABLE ENERGY LABORATORY

Modeling Thermal Fatigue in CPV Cell Assemblies



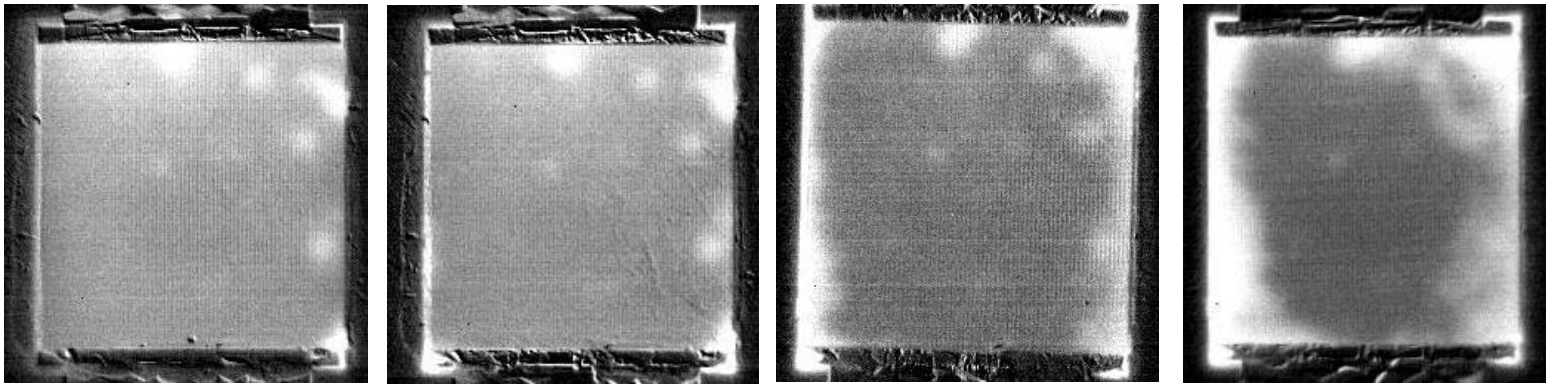
NREL PV Module Reliability Workshop

Nick Bosco
and Sarah Kurtz

February 16 2011

NREL is a national laboratory of the U.S. Department of Energy, Office of Energy Efficiency and Renewable Energy, operated by the Alliance for Sustainable Energy, LLC.

quantifying thermal fatigue



initial | 500 cycles | 1000 cycles | 1500 cycles

- Thermal fatigue will cause die-attach failure.
- How can we model this failure?
- Will this model result in a lifetime prediction?

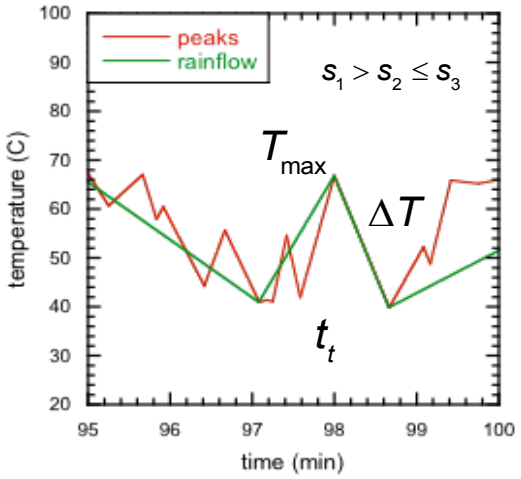
review: rainflow counting

1: CPV cell temperature modeling

$$T_{\text{mod}} = T_{amb} + E\exp(a + bW)$$

$$T_{cell} = \overline{T}_{\text{mod}} + \frac{E}{E_o}\Delta T$$

2: rainflow cycle counting



3: damage calculation

$$N_f = \frac{1}{2}\left(\frac{\Delta\gamma_p}{2\varepsilon_f}\right)^{\frac{1}{c}}$$

$$c = -0.422 - 6\cdot10^{-4}T_{mean} + 1.74\cdot10^{-2}\ln\left(1+\frac{360}{t_d}\right)$$

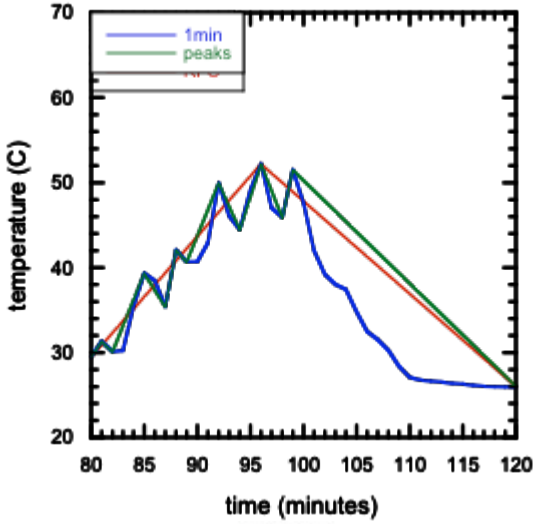
$$\Delta\gamma_p = \frac{\sqrt{2}FL}{2h}\Delta\alpha\Delta T$$

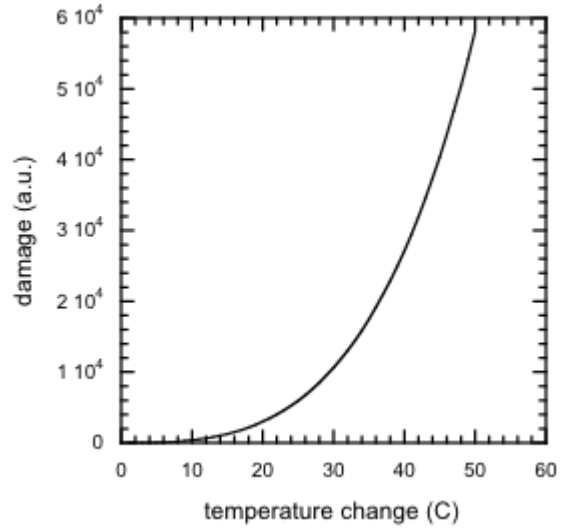
$$D = \sum_i \frac{n_i}{N_i}$$

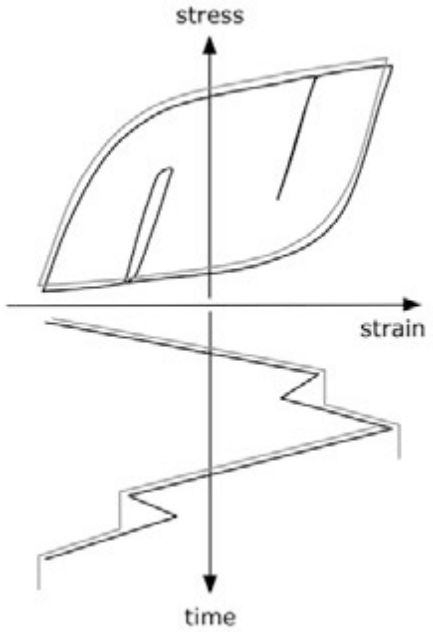
$$D = \sum_i \Delta T_i^{-\frac{1}{c_i}}$$

- Method can quickly analyze long time histories
- Several sources of error exist
- Not capable of differentiating between materials and designs*

review: rainflow counting



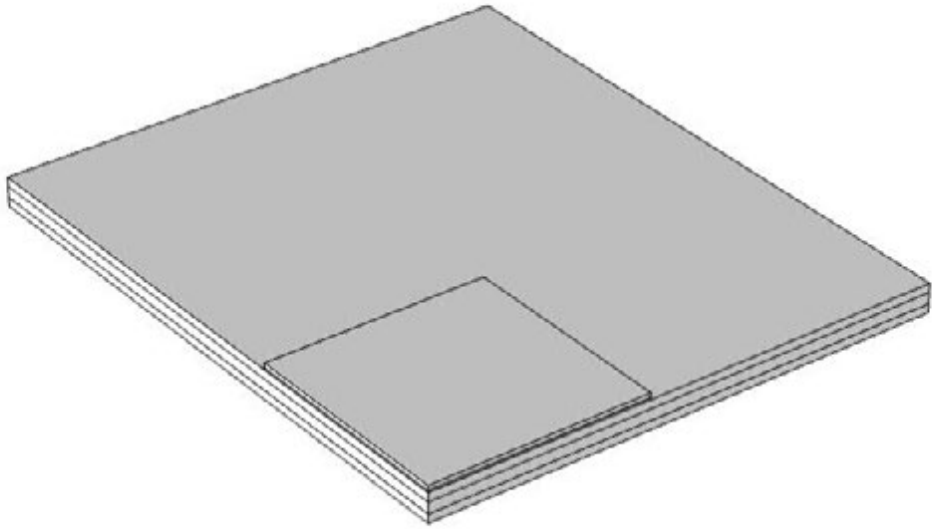




- Algorithm distills time history of temperature into discrete segments.
- Attempts to count only the “significant” segments.
- Damage is exponential with temperature change.

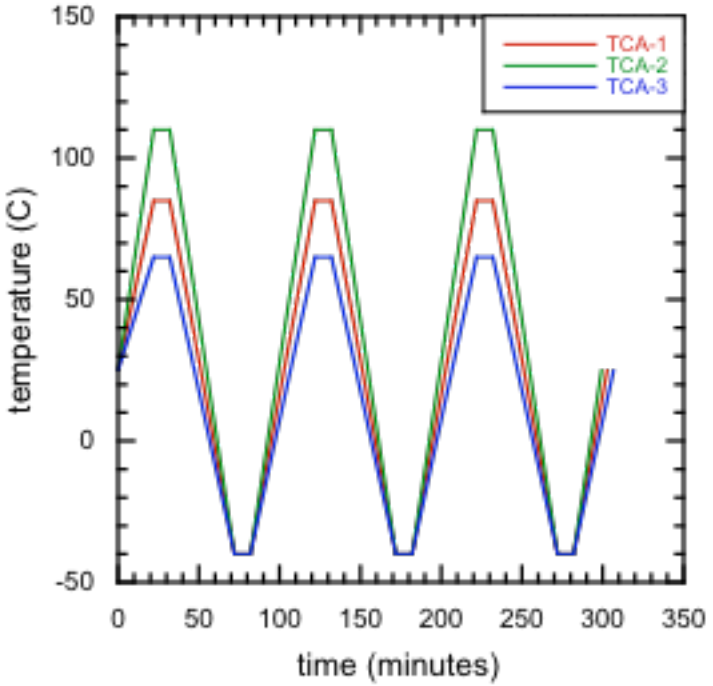
finite element modeling

FEM: CPV Cell Assembly



¼ model
1 cm^2 x 100 µm Ge die
50 µm eutectic Pb-Sn solder
650 µm DBC

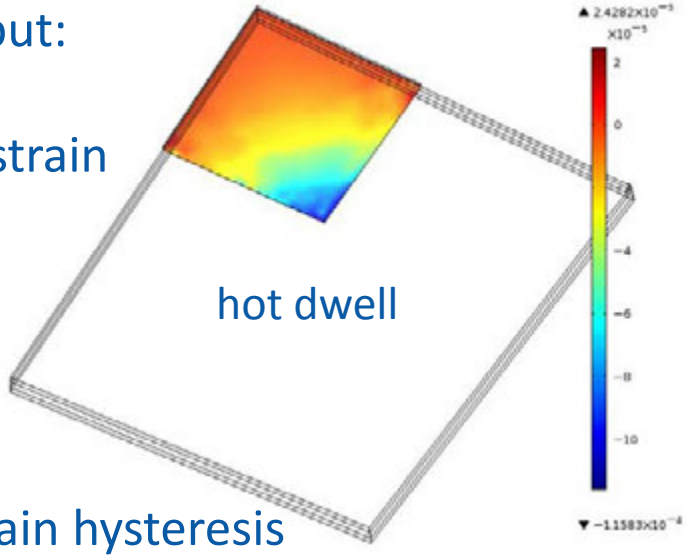
simulation: IEC 62108 thermal cycles

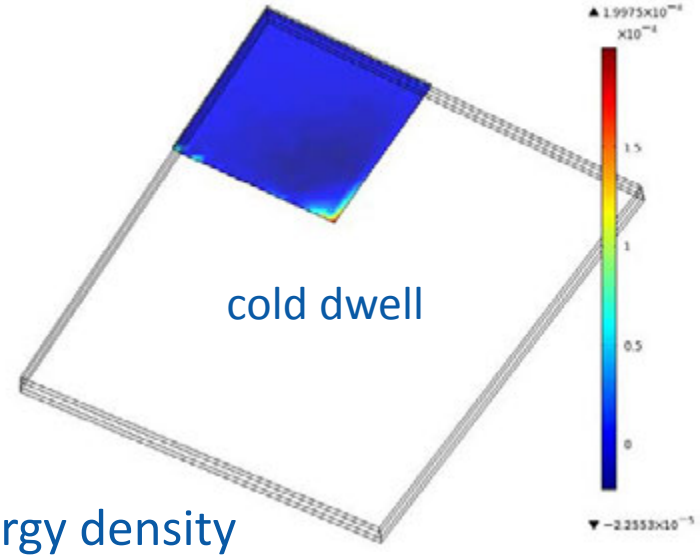


finite element modeling

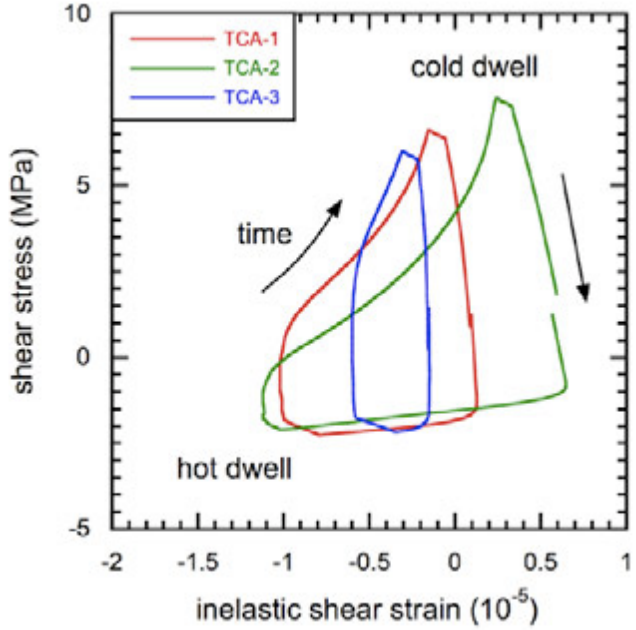
FEM output:

inelastic strain

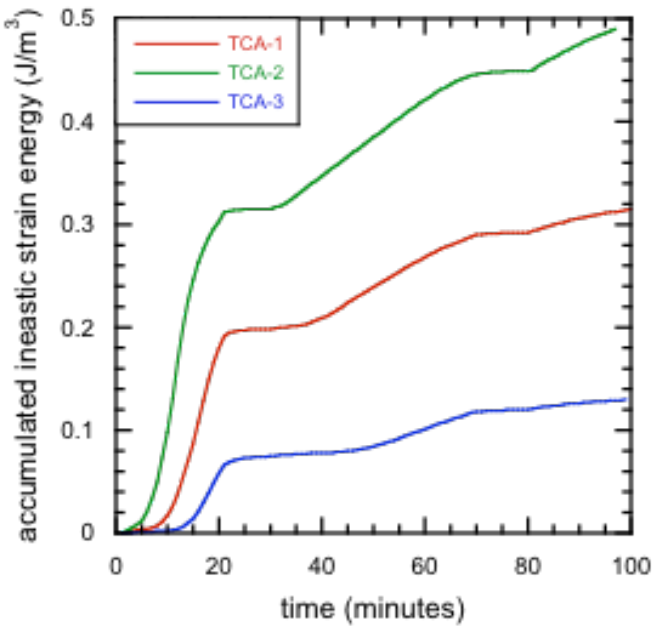




stress-strain hysteresis

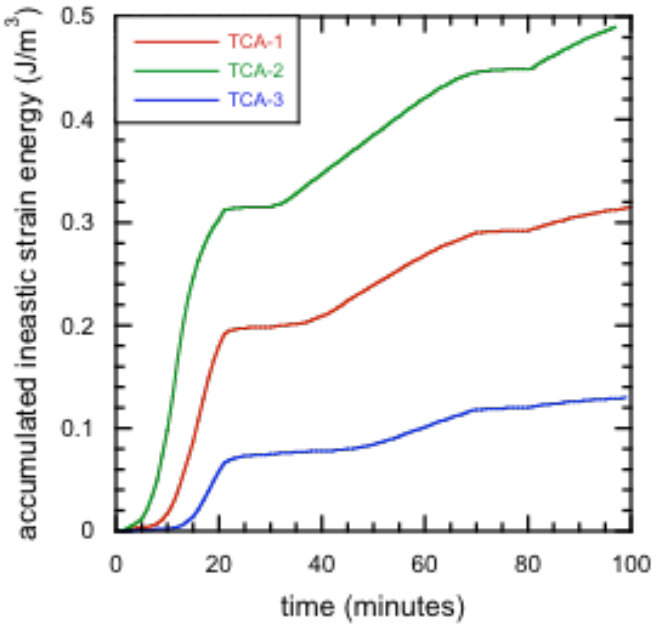


energy density



finite element modeling

damage calculation



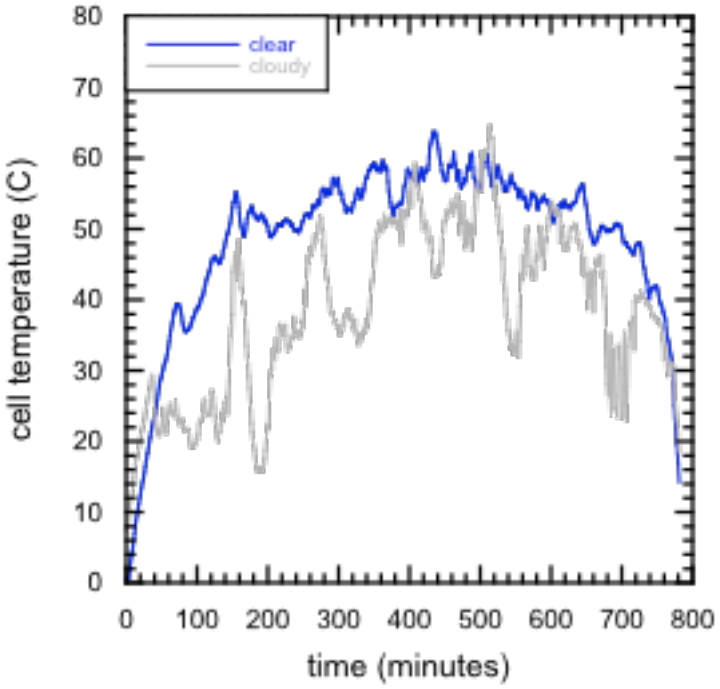
crack initiation: $N_o = K_1 \Delta W_{ave}^{\alpha}$

crack growth: $\frac{da}{dN} = K_2 \Delta W_{ave}^{\beta}$

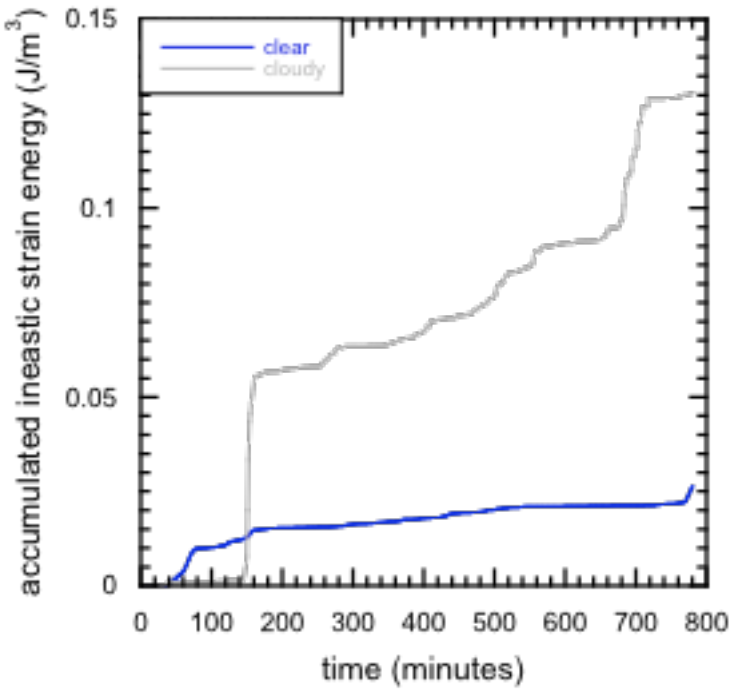
$$D = \frac{\Delta W_{acc}}{\Delta W_f}$$

finite element modeling

simulation: clear and partly cloudy days



FEM output: energy density

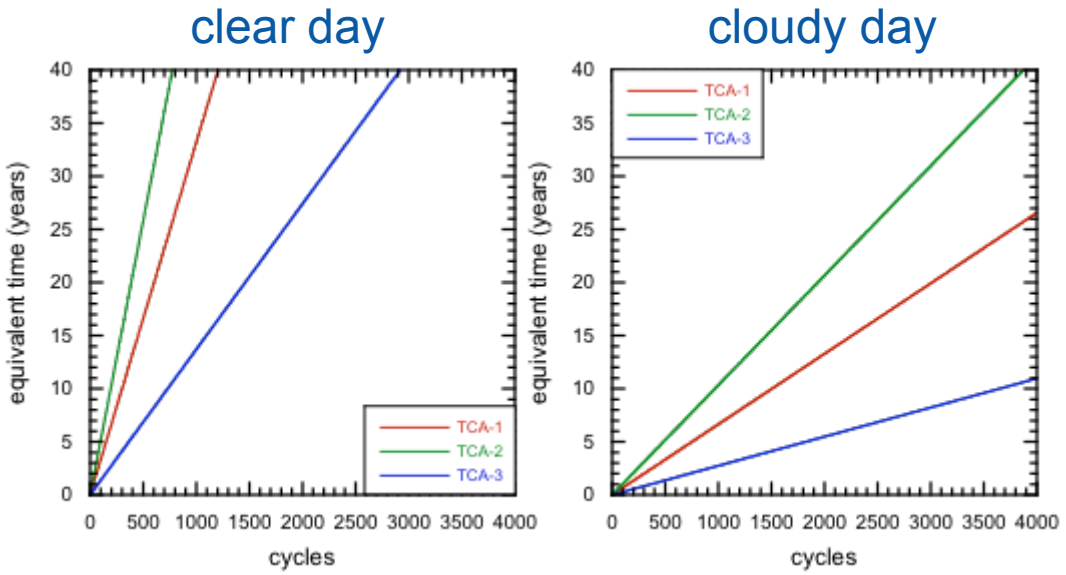


finite element modeling

Analysis:

Comparison of energy accumulated through thermal cycling and out door exposure provides for the calculation of equivalent times (acceleration factors)

$$t_{eq} = \frac{nD_{TCA}}{365D_{day}}$$



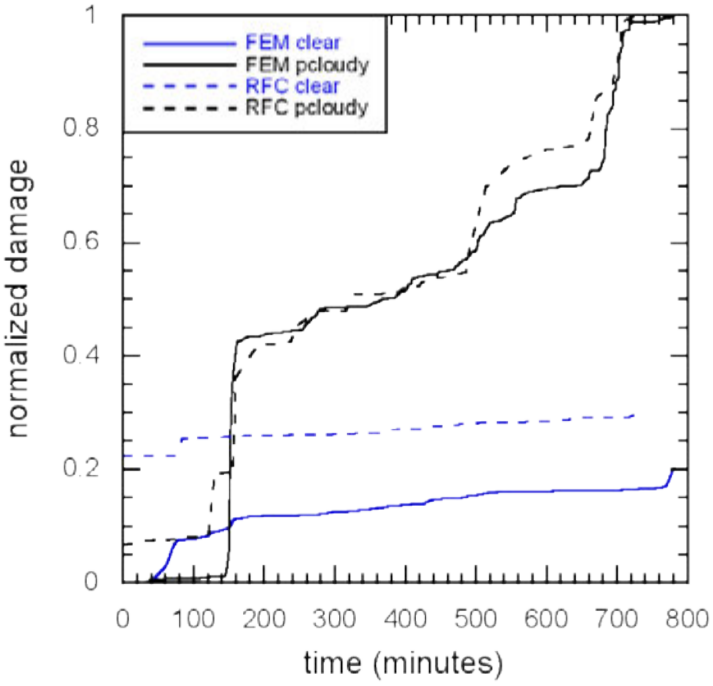
FEM

Standard	Option	n	t_{eq} clear	t_{eq} cloudy	N_{25} clear	N_{25} cloudy
IEC 62108	TCA-1	1000	33	6.5	750	3800
	TCA-2	500	26	5	480	2400
	TCA-3	2000	27	5.5	1800	9000

RFC

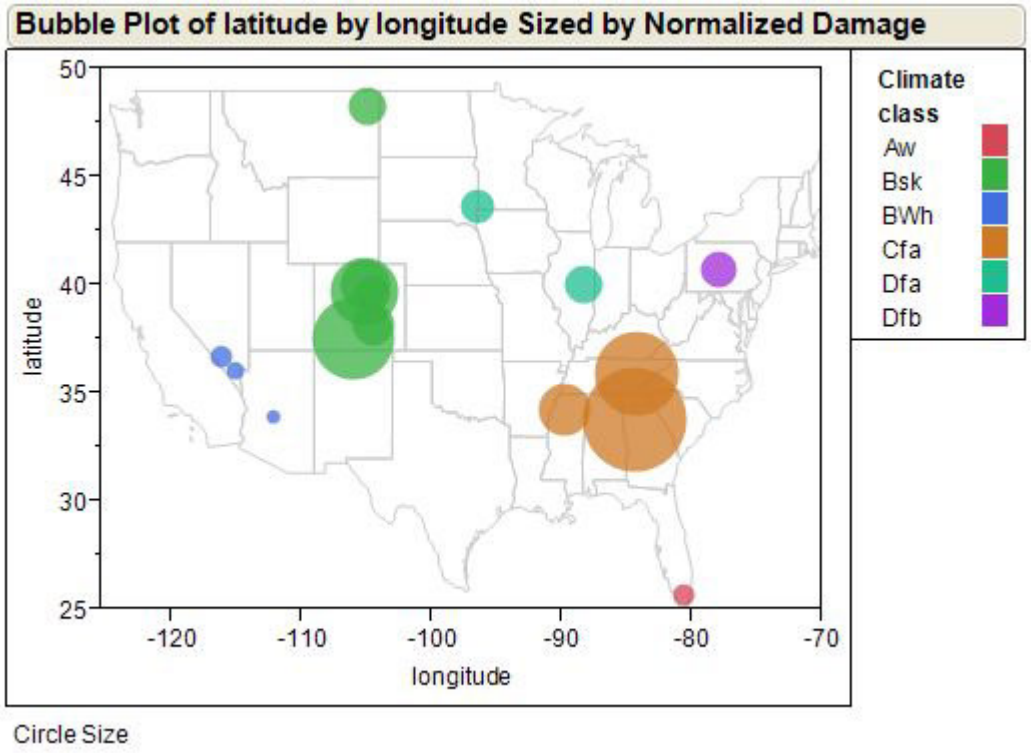
t_{eq} Golden years	t_{eq} Phoenix years	t_{eq} Miami Years
13.2	48	24
8.3	30	15
20.3	74	37

FEM vs. RFC



- All damage normalized with respect to the most damaging day.
- Only a 10% difference exists in the relative measurement.

RFC



- Bubble size: relative damage
- Bubble color: climate zone

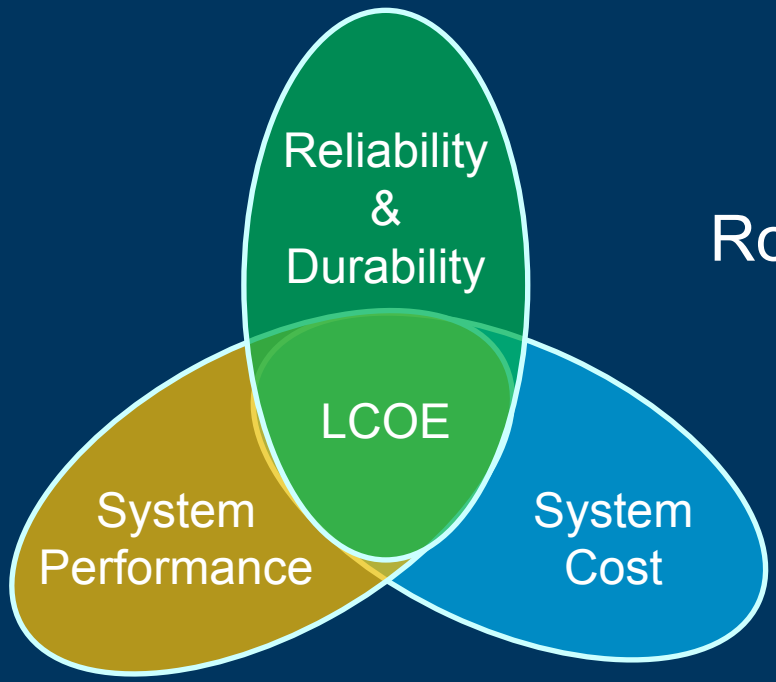
thoughts and future work

- RFC method shows promise for comparative studies between locations.
- Algorithm is convenient to quickly handle long time histories.

- FEM is capable of accurately quantifying the damage that causes failure.
- Accuracy should not be dependent on stress level.
- Models can differentiate between materials and geometries.
- Simulations are slow and expensive.

- Use FEM as a tool to refine algorithm and damage analysis
- Understand sources and magnitudes of error
- Goal: a more accurate RFC method with life prediction capabilities.

Low Concentration Photovoltaics: Reliability and Durability Issues



Roger H. French
Materials Science
Case School of Engineering
Case Western Reserve University
Cleveland OH 44106

roger.french@case.edu
http://dmseg5.case.edu/people/faculty.php?id=rxf131

This presentation does not contain any proprietary or confidential information.

Introduction

Require cost effective materials, components & design

- Design simplicity
- Typically conventional silicon cells

Can utilize conventional materials & construction

- High concentration challenges not essential
- Reliability and durability derive from conventional approaches
- e. g. c-Si cells, encapsulation

Challenge is cost-competitive, reliable LCPV technology

Calls for integrated optimization for reliability & lifetime

- Yielding lower cost and LCOE

Many LCPV efforts

Reflective efforts

Abengoa Solar NT
1.5 and 2.2X tracked
JX Crystals
3X
Megawatt Solar
20X
Replex
MAPV, fixed or tracked
LC2PV, tracked
Skyline High Gain Solar
~10X tracked
SunPower
7X tracked
tenKsolar
!2X, fixed, UV/IR shielding
Zytech Solar,

Refractive efforts

Solaria
~2X tracked

Need: Lifetime & Degradation Science for PV Modules

Qualification testing of systems not sufficient for reliability & lifetime

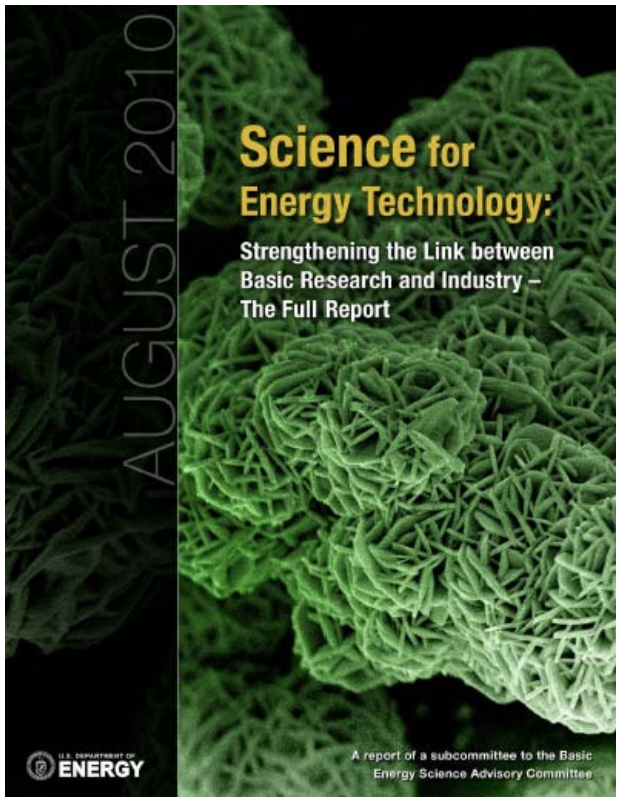
- To avoid excessively high degradation rates
- Dramatically reduced service lifetimes

Must determine degradation mechanisms and rates

- Scientific underpinning of reliability and qualification standards

Quantitative degradation rate modeling

- Connects materials, components, system
- To overall degradation rate, linearity, reciprocity
- And system lifetime performance



Science For Energy Technology Workshop

- Convened by U. S. DOE, Basic Energy Sciences

Science challenges across 9 areas of energy

PV prioritized research directions

- ***Photovoltaic module lifetime and degradation science***
- *Fundamental properties of photovoltaic interfaces*
- *Advanced photovoltaic analysis and computational modeling for scale-up*

http://www.er.doe.gov/bes/reports/files/SETF_rpt.pdf

Outline

2 characteristic LCPV systems:

- Replex's MAPV & LC2PV
  => LC2PV Poster

LCPV elements, stressors and design characteristics

- Primary optics, secondary optics, cell encapsulation, heat sinking

LCPV solar and environmental durability

- Materials examples: acrylics, outdoors, 4 Suns and 50 Suns
- Elements examples: Al/Ag mirrors, back & front surface mirrors, UV blocking mirrors

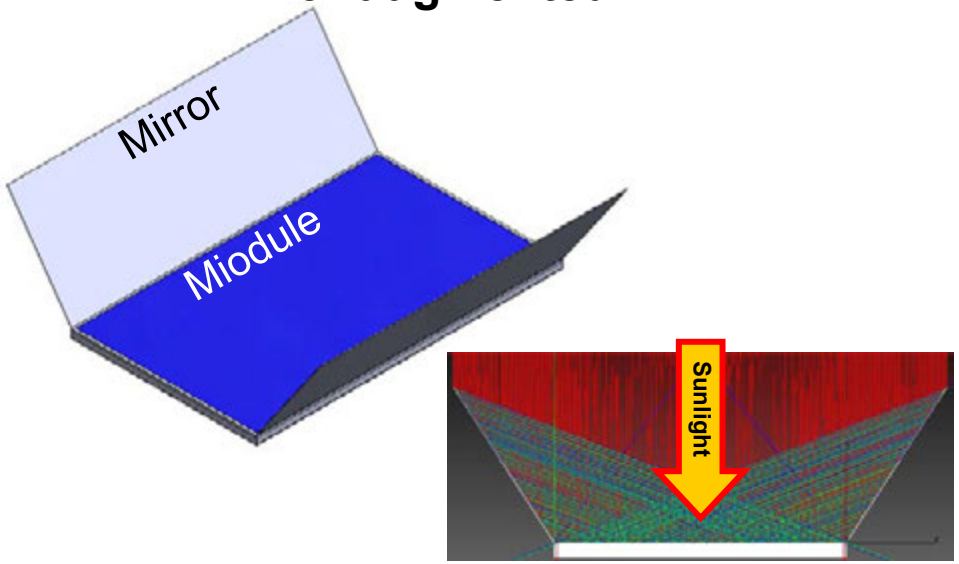
Cell encapsulation and thermal management

LCPV challenges

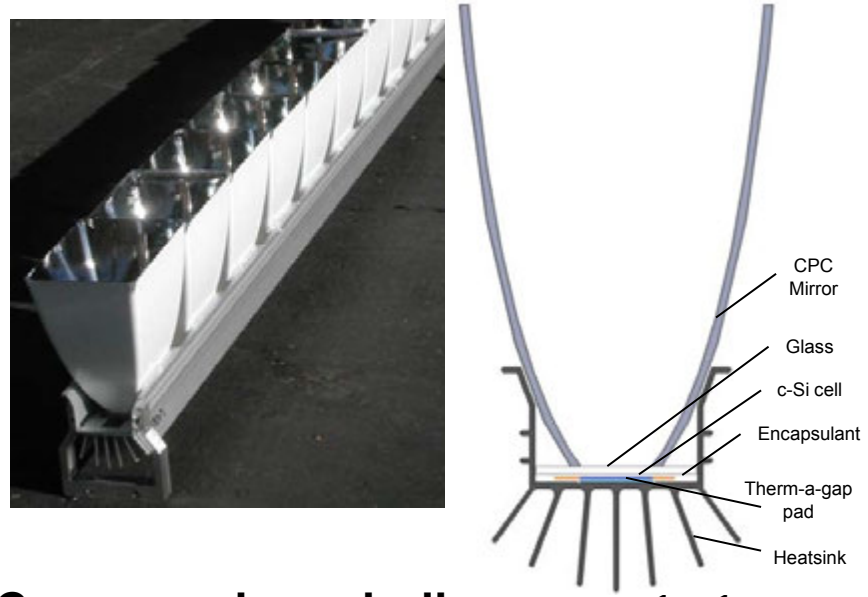
Conclusions

Two Replex LCPV Systems

MAPV: Mirror augmented PV



LC2PV: Low cost, low conc. PV



Flat mirrors & c-Si modules

- 1.15X (fixed)
- 1.5 to 2.2X (tracked)

Compound parabolic concentrator

10X geometrical concentration

Validation of LCPV degradation rates and lifetime needed

- Carrizo Plains / Arco Solar: R_d = 10%/yr degradation

Requires a materials/components/systems optimization approach

- Based on lifetime and degradation science
- Not just qualification testing results

LCPV Elements, Stressors and Design Characteristics,

LCPV elements

- 1 Sun optics
- Multi-sun optics
- Cell level encapsulation
- Silicon cells
- Dielectric isolation / thermal conduction
- Thermal management

Stressors

- Irradiance
- Temperature
  - Thermal degradation
  - Thermal expansion mismatches
- Humidity
  - Florida
  - Arizona
- Cycling
- Electrical
  - Current, voltage
  - Corrosion

Geometrical concentration

- MAPV - 1.5 to 2 Suns
- LC2PV - 5 to 10 Suns

Solar Mirror based optics

- Acrylic substrate
- Silver or aluminum mirrors
- First or second surface acrylic

Silicon cells

- Encapsulation
- Stringing and tabbing
- Heat sinking

LCPV cost constraints

- Performance & LCOE
- Manufacturability
- Durability
- Reliability
- Lifetime

LCPV Solar and Environmental Durability Issues

Acrylic solar durability

- PMMA: Arizona & Florida weathering
- PMMA: A new solar radiation durability metric: Induced absorbance to dose

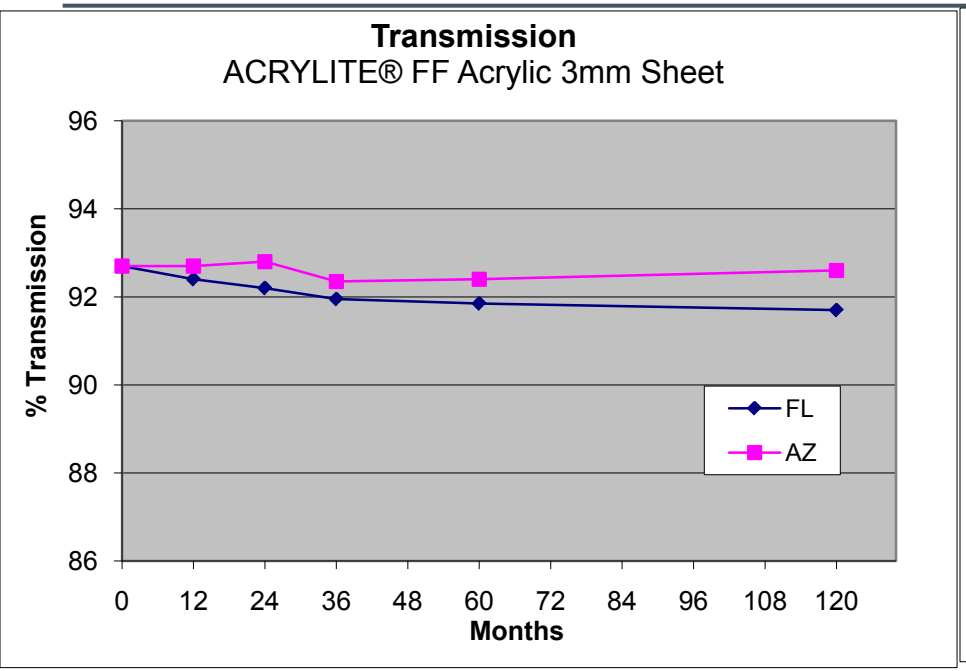
Solar mirror durability

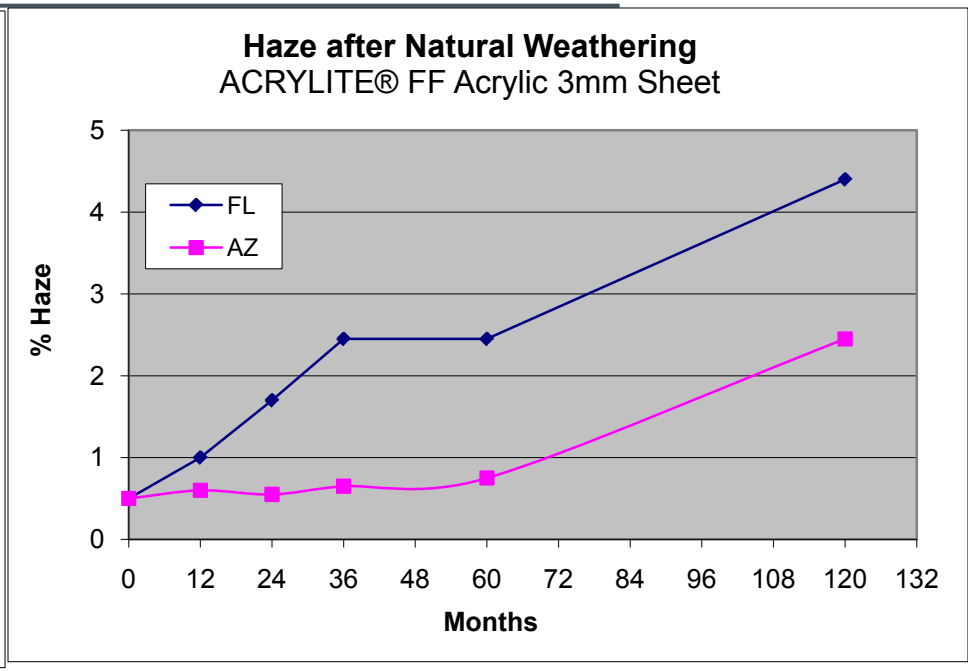
- Aluminum & silver mirrors: Arizona & Florida weathering
- Accelerated QUV testing of Al & Ag mirrors

Solar durability of back surface Al mirrors in a CPC

Cell encapsulation and thermal management

Natural Weathering of Acrylic Sheet: Arizona & Florida





Not much change in transmission

- Over 10 years exposure

Humidity in Florida increases

- Transmission drop
- Compared to AZ (dry)

Haze also affected by humidity

- Rate of change higher in FL

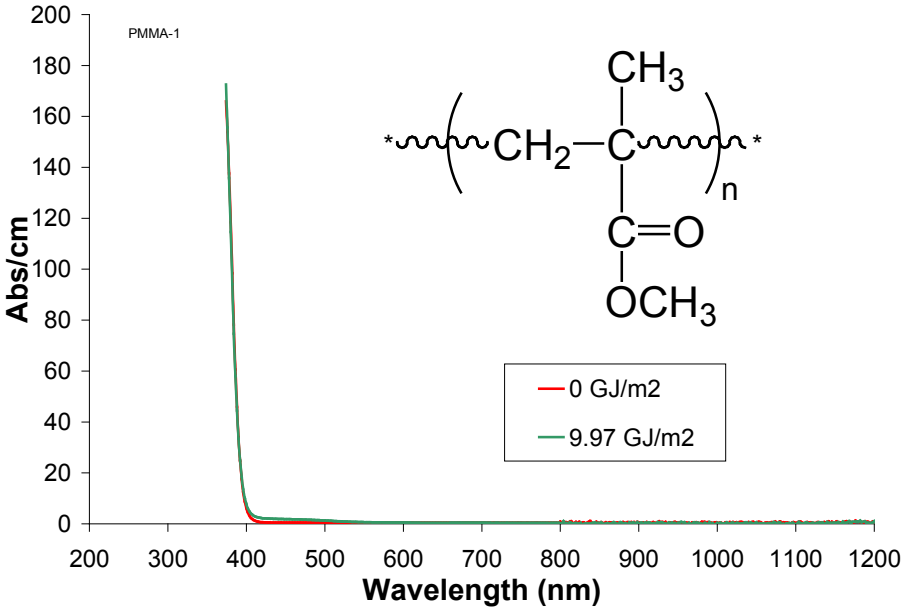
What are quantitative requirements?

- On material for this LCPV application?

Varies with system/element design

- Yes/No answer not germane

Induced Absorbance to Dose: PMMA-1 @ 3.8 kW/m2 Irradiance



75 mm film with UV stabilizers

- Shows strong absorption edge at 400 nm

Annual 1Sun Dose = 9.3 GJ/m2

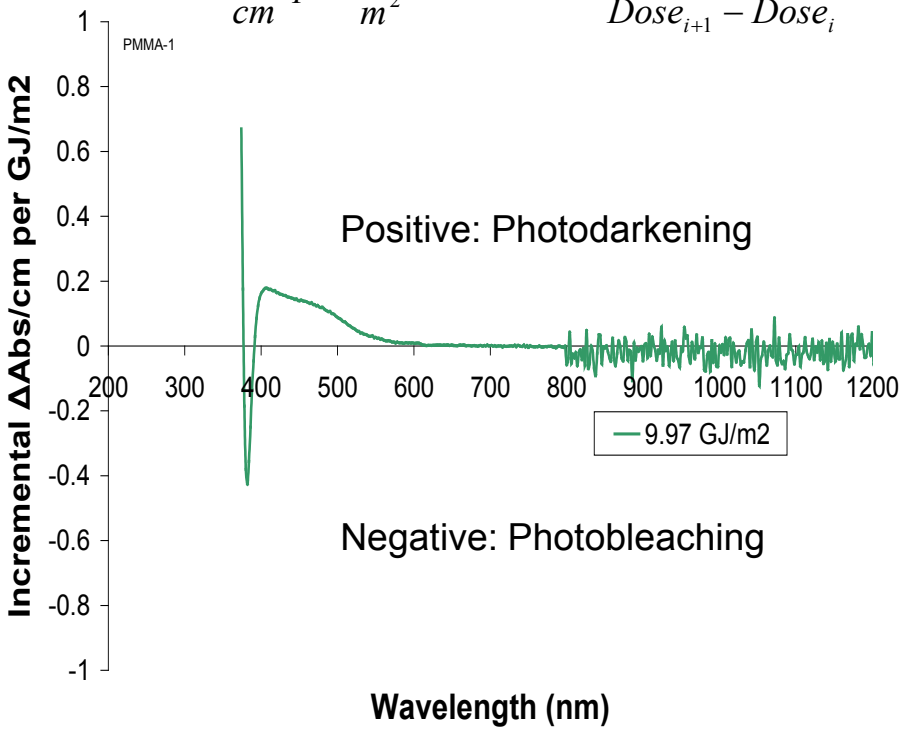
Photodarkening at 400-600 nm

Some photobleaching below 400 nm

Quantitative degradation rates R_d

Induced Absorbance To Dose

$$Incremental\ \frac{Abs}{cm}\ per\ \frac{GJ}{m^2}\ Dose \equiv \frac{Abs_{i+1}(\lambda)/cm - Abs_i(\lambda)/cm}{Dose_{i+1} - Dose_i}$$



Not all acrylics are alike

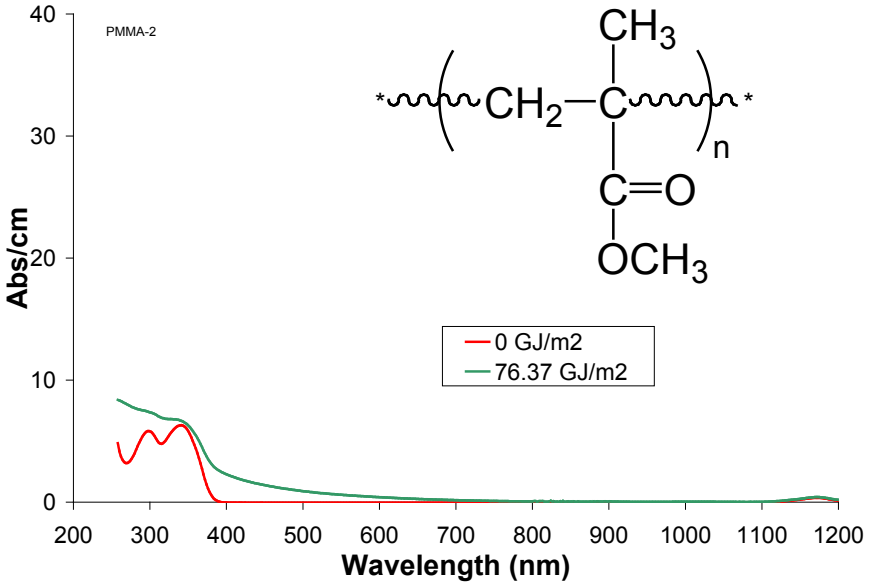
Need sufficient durability

- Without excessive cost of ownership

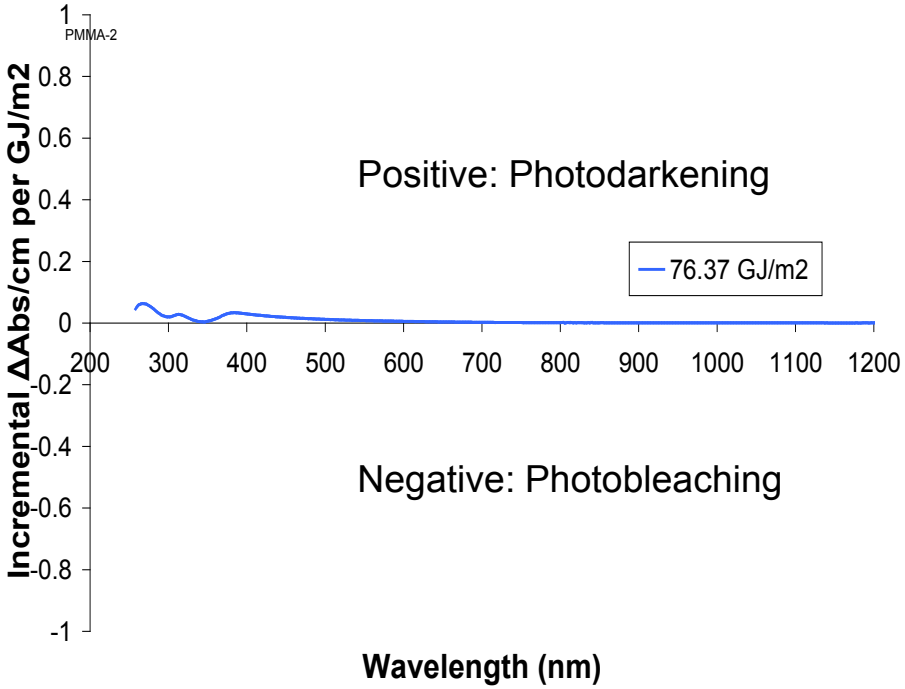
Optimize material to application

Induced Absorbance to Dose: PMMA-2 @ 48 kW/m2 Irradiance

Optical Absorbance/cm



Induced Absorbance To Dose



1.6 mm thick sheet with UV stabilizers

- Shows strong absorption edge at 400 nm

After ~76 GJ/m2 exposure

- Photodarkening at 250-600 nm
- No photobleaching observed

Much lower degradation rates

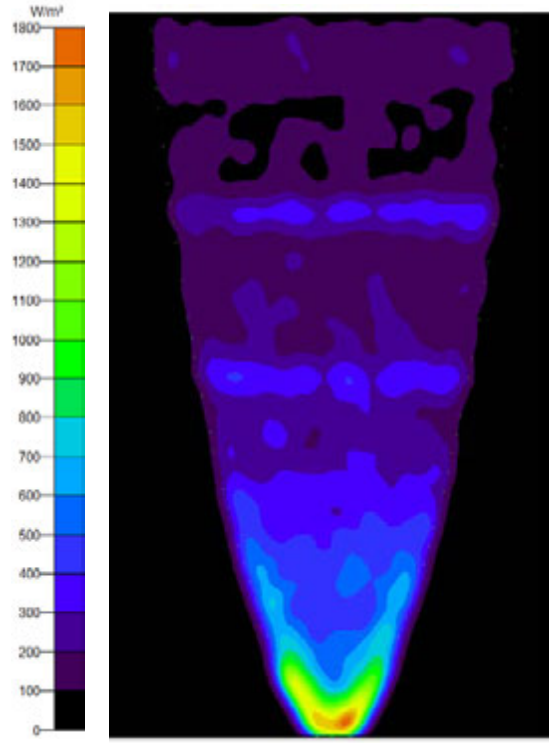
- Than highly stabilized PMMA-1

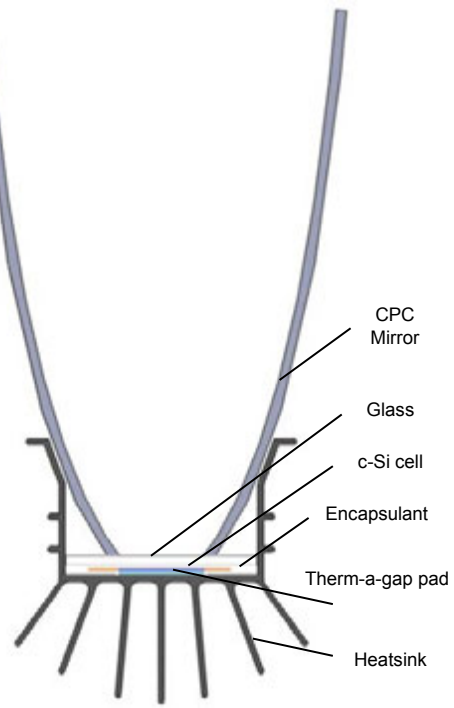
Check linearity & reciprocity

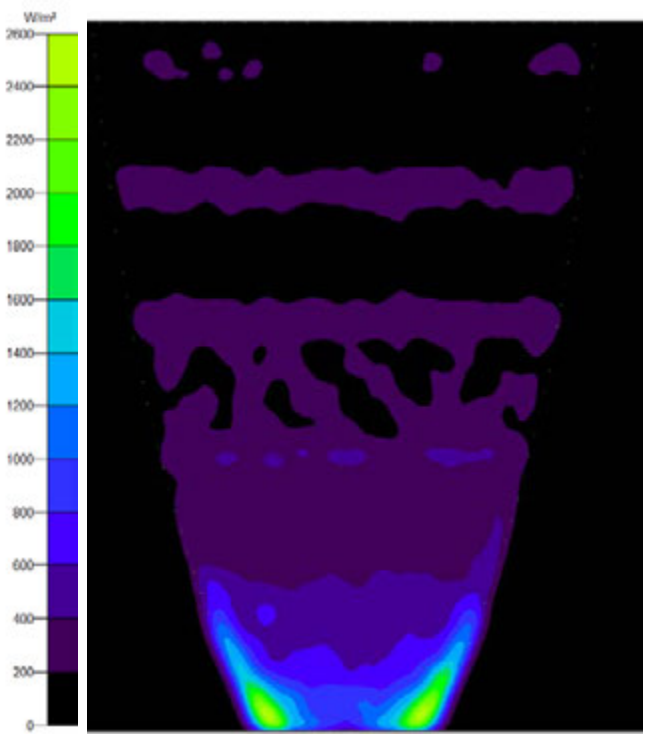
Then Use for accelerated testing

- Or real time 50 Sun testing

Expected Irradiance on LC2PV CPC Reflector







Non-tracking N/S direction

Max irradiance = 1.8 kW/m²

Tracking E/W direction

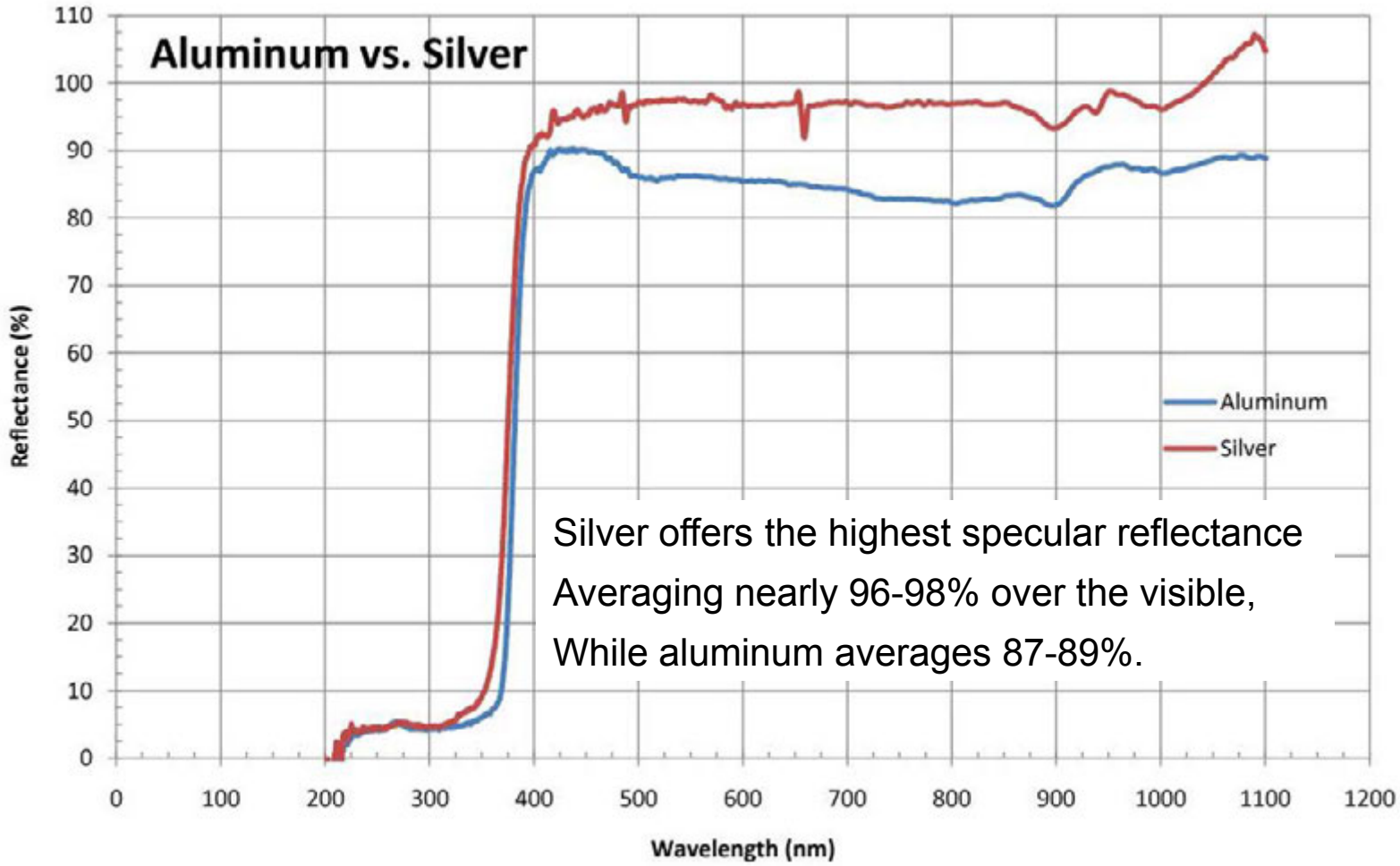
Max irradiance = 2.8 kW/m²

What are critical material requirements? Not just qual. testing requirements

- MAPV PO: 1 Sun Irradiance. LC2PV: 2.8 Sun Irradiance in some areas

Must optimize materials, componets and system for durability & lifetime

Optical Efficiency: Al vs. Ag Back Surface (BS) Mirrors

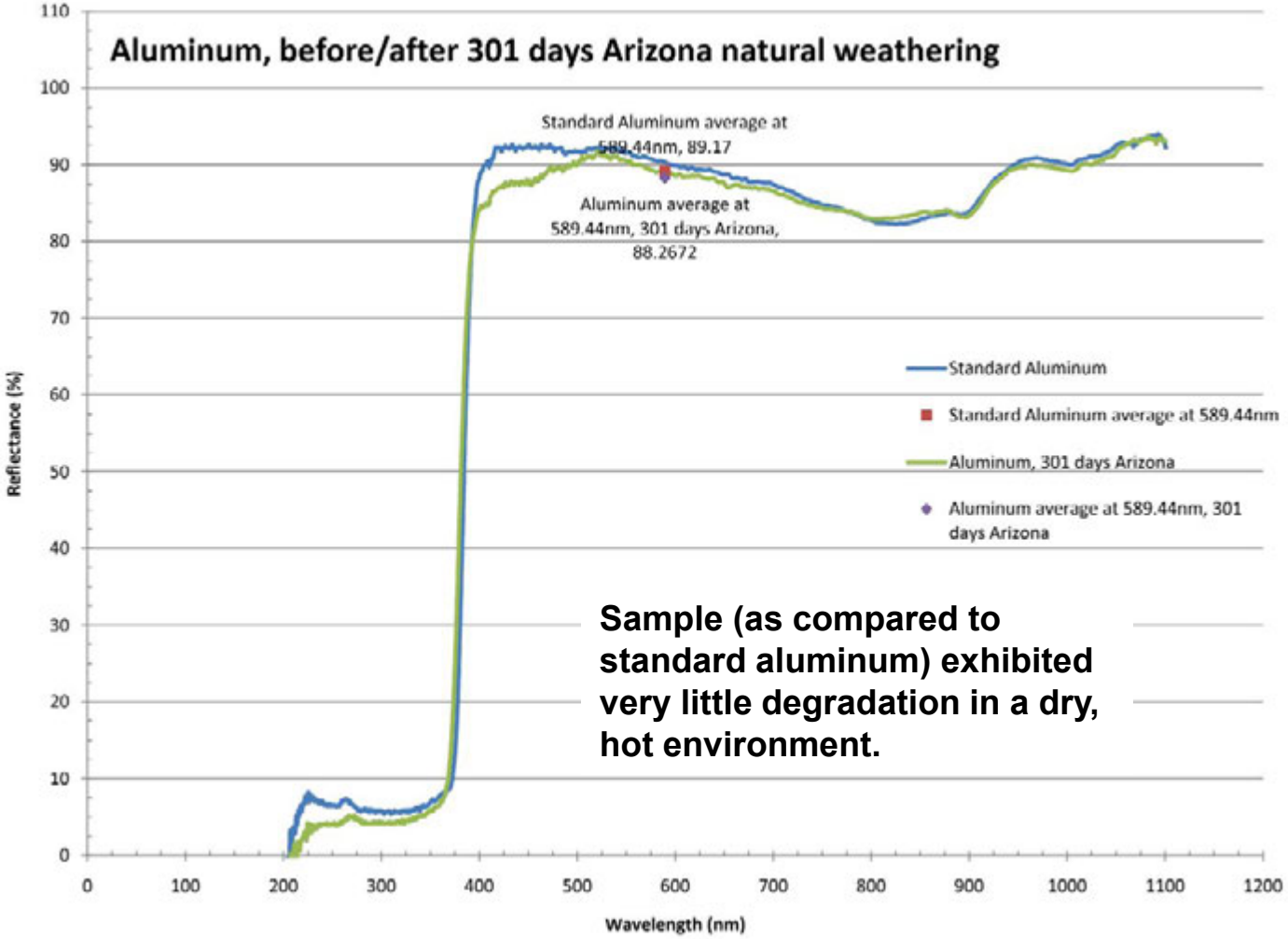


High reflectivity of silver, improves optical efficiency and performance

- But increases costs, and reduces durability and lifetime

Must carefully avoid increasing cost of ownership

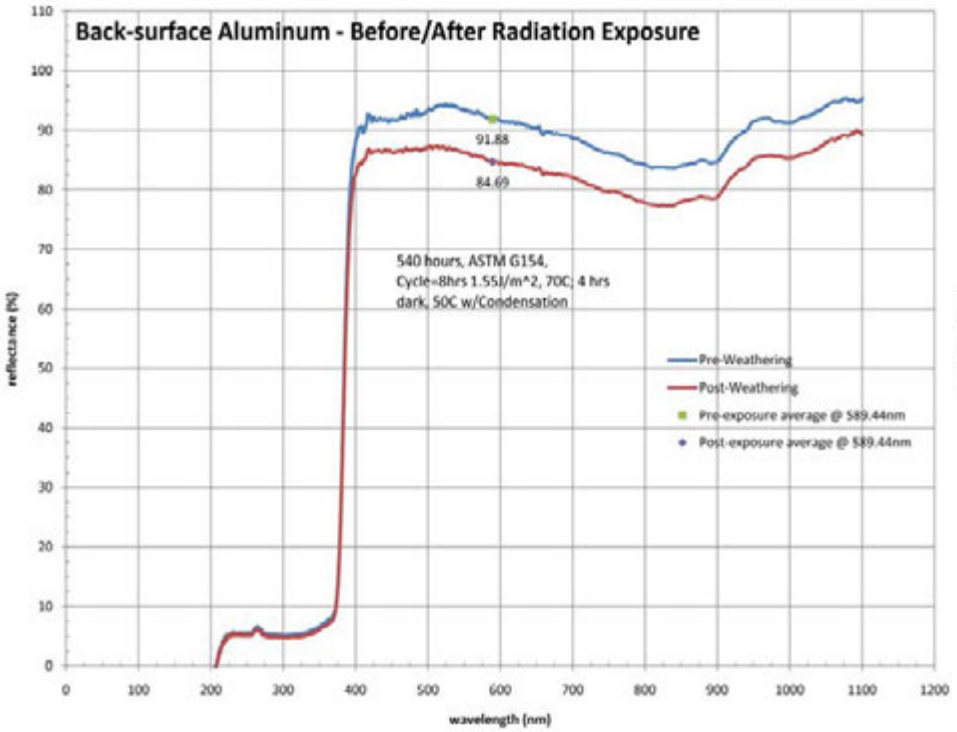
Al/Back Surface Mirror Durability: Arizona Outdoors

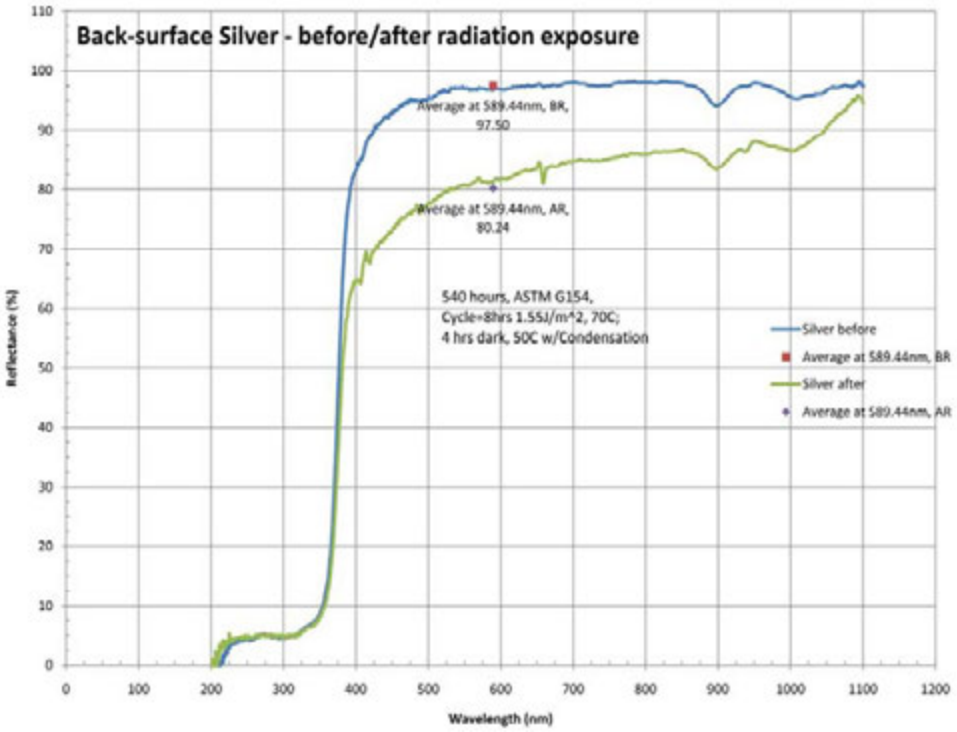


Sample (as compared to standard aluminum) exhibited very little degradation in a dry, hot environment.

Aluminum back surface mirrors show good durability

Al/Back Surface Mirror Durability: Accelerated Testing





QUV exposures with condensing humidity and heat during dark periods

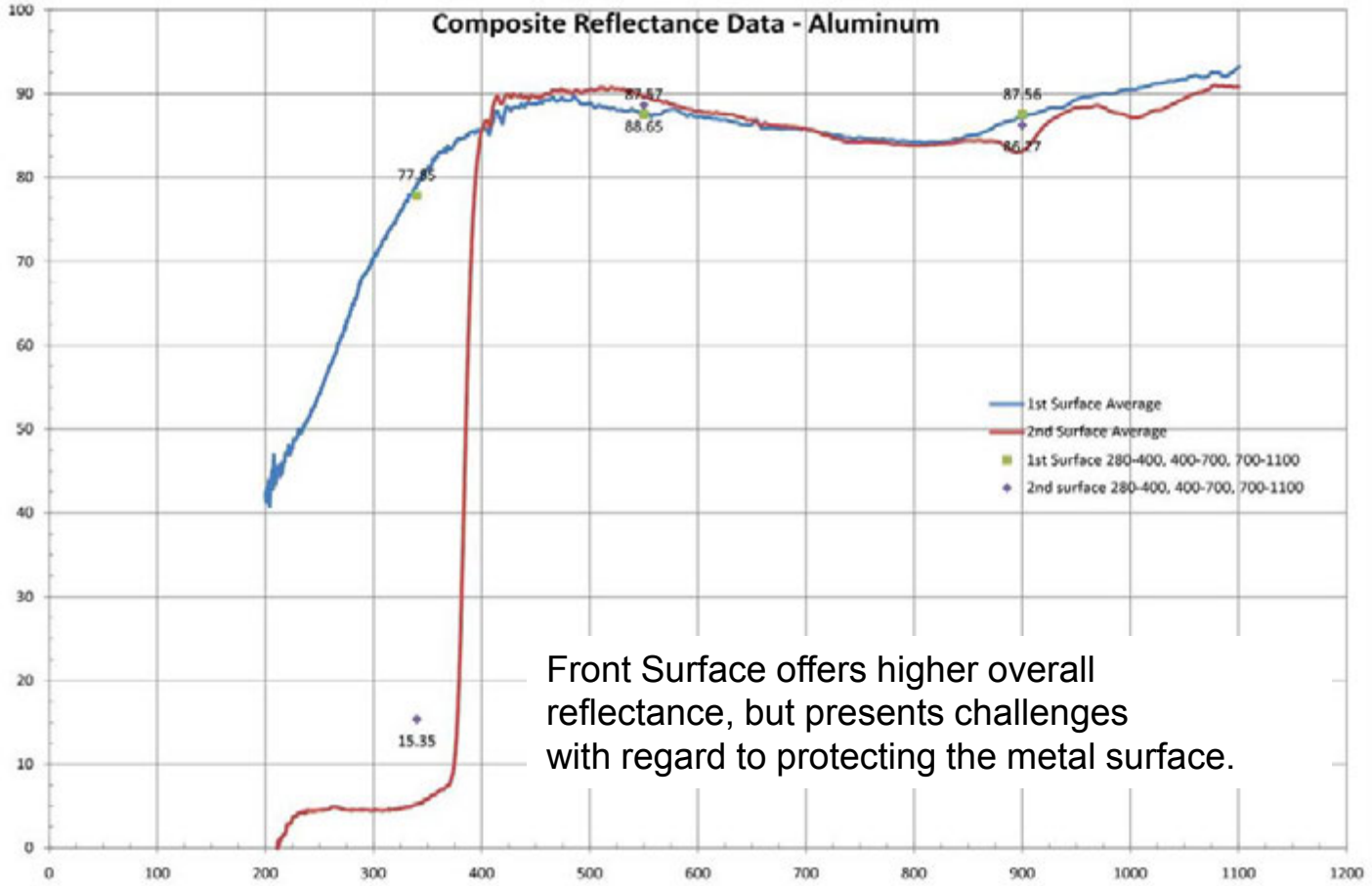
- Compare to Florida natural weathering

Aluminum/BS mirror: average 7% reduction in specular reflectance

Silver/BS mirror: average 17% reduction in specular reflectance

Aluminum/BS mirrors more durable in humid conditions

Al Back vs. Front Surface Mirrors: Optical Efficiency

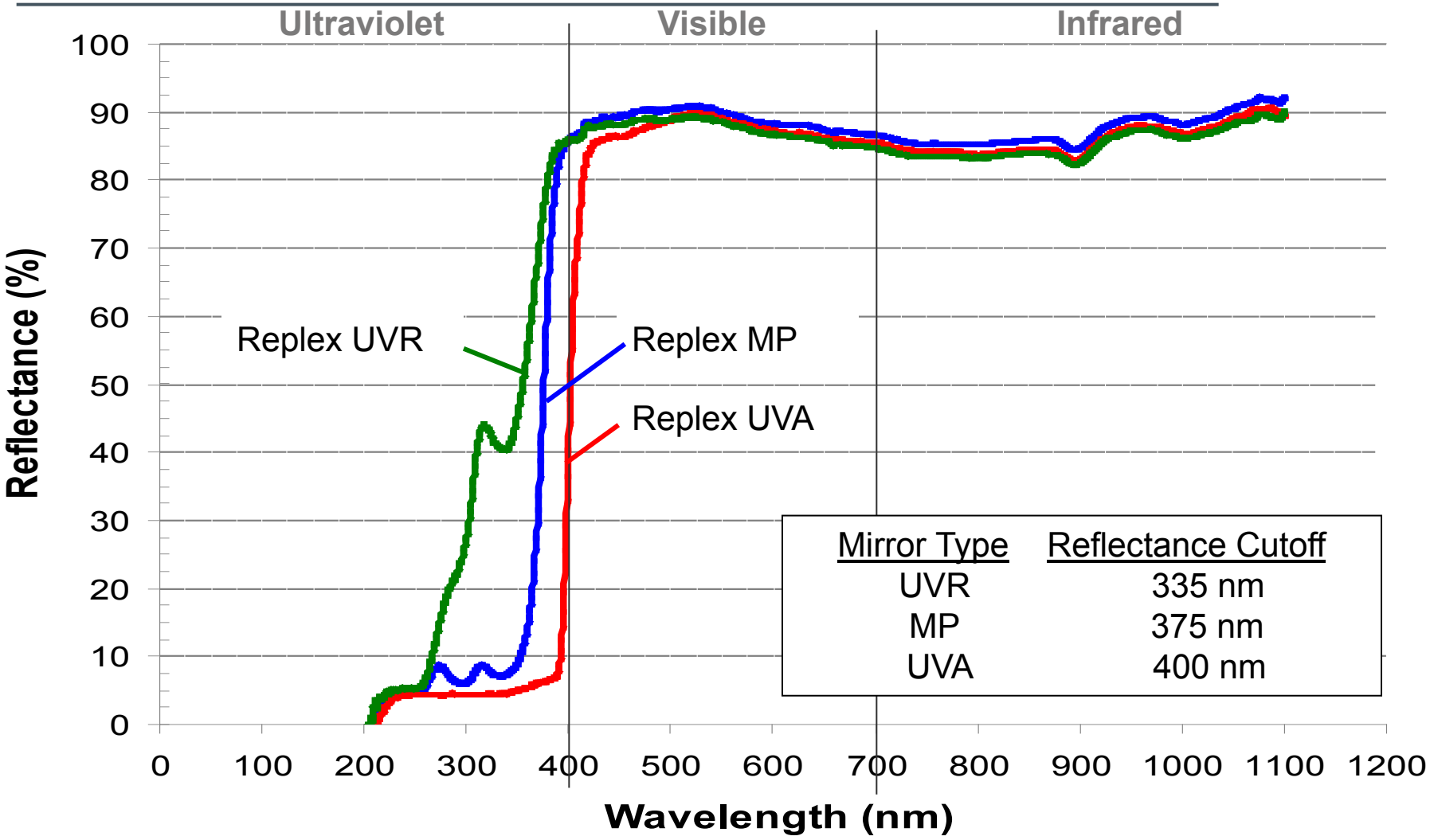


Front surface mirrors reflect UV and have similar visible reflectance

Back surface mirrors don't reflect UV, reduce UV exposure of cell encapsulation

- With similar optical efficiency when used with c-Si cells

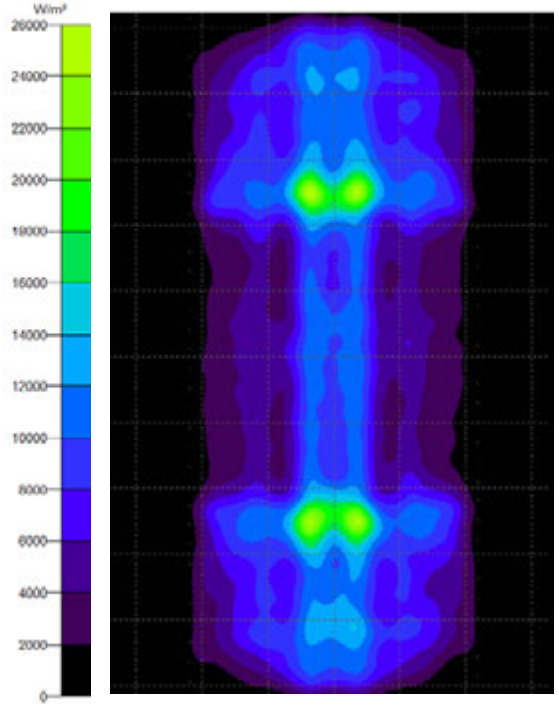
Replex UV Selective Al/Back Surface Mirrors

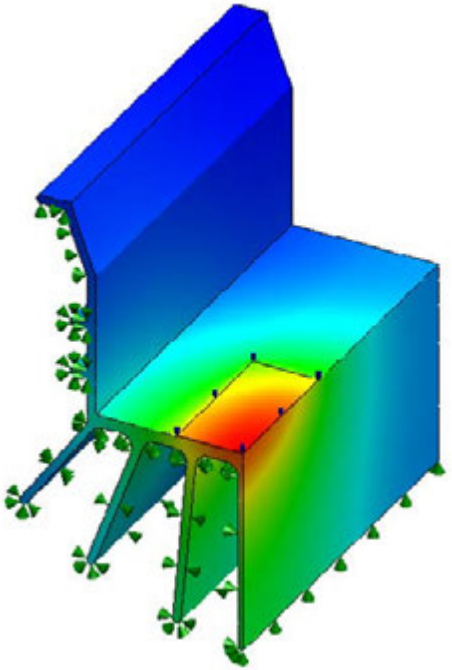


And back surface mirrors allow tuning of UV absorption edge

- Creating wavelength selective mirrors

Cell Level Irradiance and Thermal Management





10X CPC geometrical concentration

- Average cell irradiance = 6.9 kW/m^2

Hot spot, max conc. on cell = 26X

Encapsulation durability concern

Some decrease in performance

- But doesn't justify cost of secondary optic

Thermal management of cell

- Using aluminum heat sink,

7X area ratio: cell to heat sink

- Also aligns optics

Heat sinking a cost challenge

- not a technical challenge

LCPV Challenges

Using standard materials and components

- Under “accelerated” conditions

Maximizing optical efficiency

Sufficient, but cost effective, materials & component durability

- Acrylic
- Mirrors

Resistive losses due to more current out of standard cells

Cost of Manufacture

- Complexity
- Manufacturing throughput
- Cost model for design decisions

Conclusions

Interactive optimization essential

- Of materials, components (mirror, cell etc.) and system
- Not just materials and vendor choices by qual. testing and price

LCPV allows conventional materials and components

- And requires close attention to cost-effective technology choices

PV performance focus, can obscure important durability and lifetime choices

- High initial performance with high degradation rate

Essential efforts for reliable, durable, long-lived systems

- Quantitative degradation mechanisms and rates
- Detailed knowledge of system characteristics
- Detailed knowledge of environmental conditions and variability

i.e. a clear understanding of materials, components, and system



CASE SCHOOL
OF ENGINEERING

CASE WESTERN RESERVE
UNIVERSITY

System Designs:

- MAPV - 1.5 to 2 Suns
- LC2PV - 5 to 10 Suns

Solar Mirror based

- Acrylic Substrate
- First or Second Surface Acrylic
- Silver or Aluminum Reflectors

Silicon Cells

- Encapsulation
- Stringing and Tabbing
- Heat Sinking

LCPV Cost Constraints

- Manufacturability
- Durability
- Reliability
- Lifetime

emcore

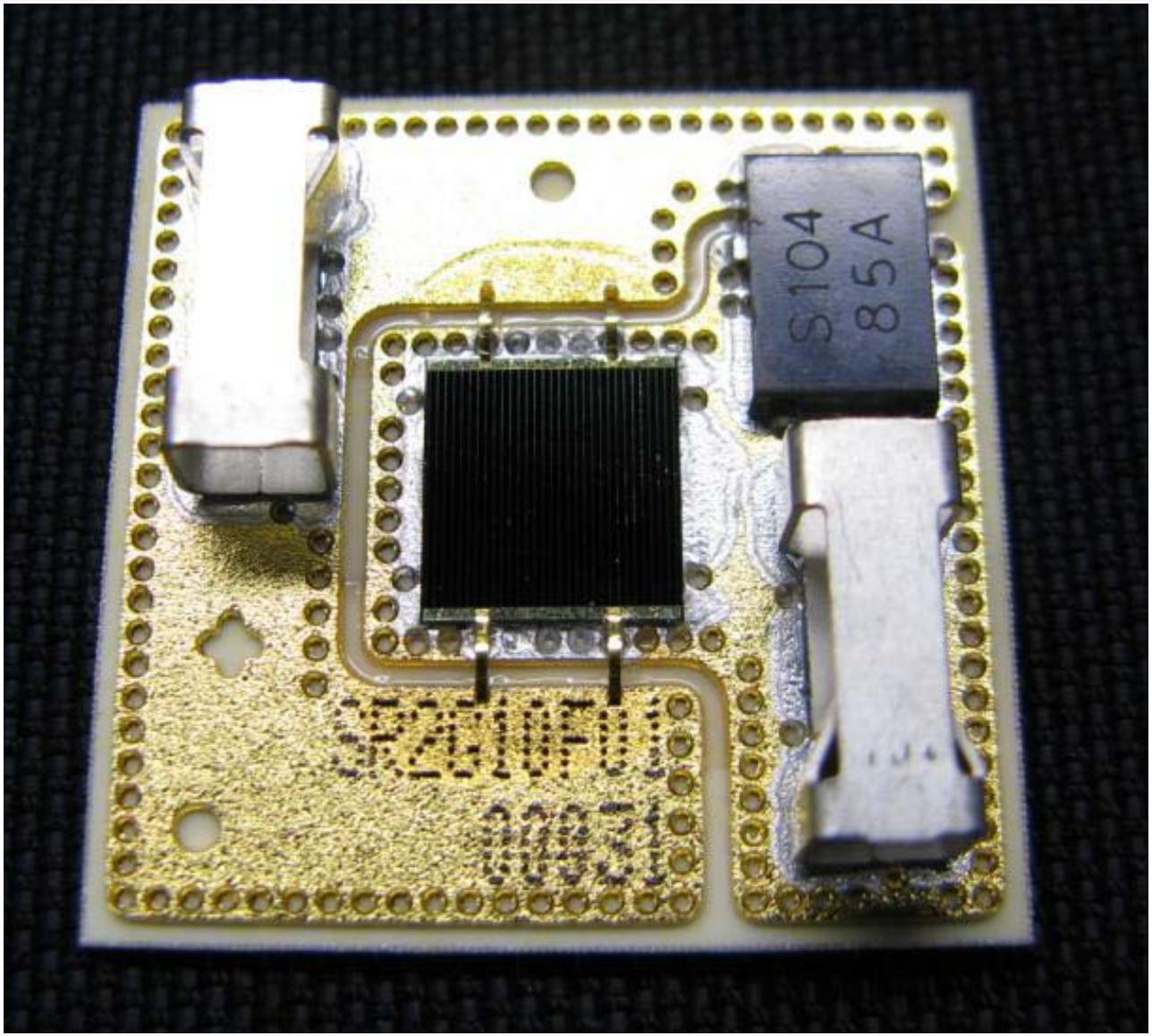
empower with light™

Reliability Testing Of High-Concentration PV Modules And Soiling Issues

Michael Winter
Greg Flynn
Jim Foresi
Phil Blumenfeld
Rick Hoffman
Ian Aeby
Theo Romero

This presentation does not contain any proprietary or confidential information

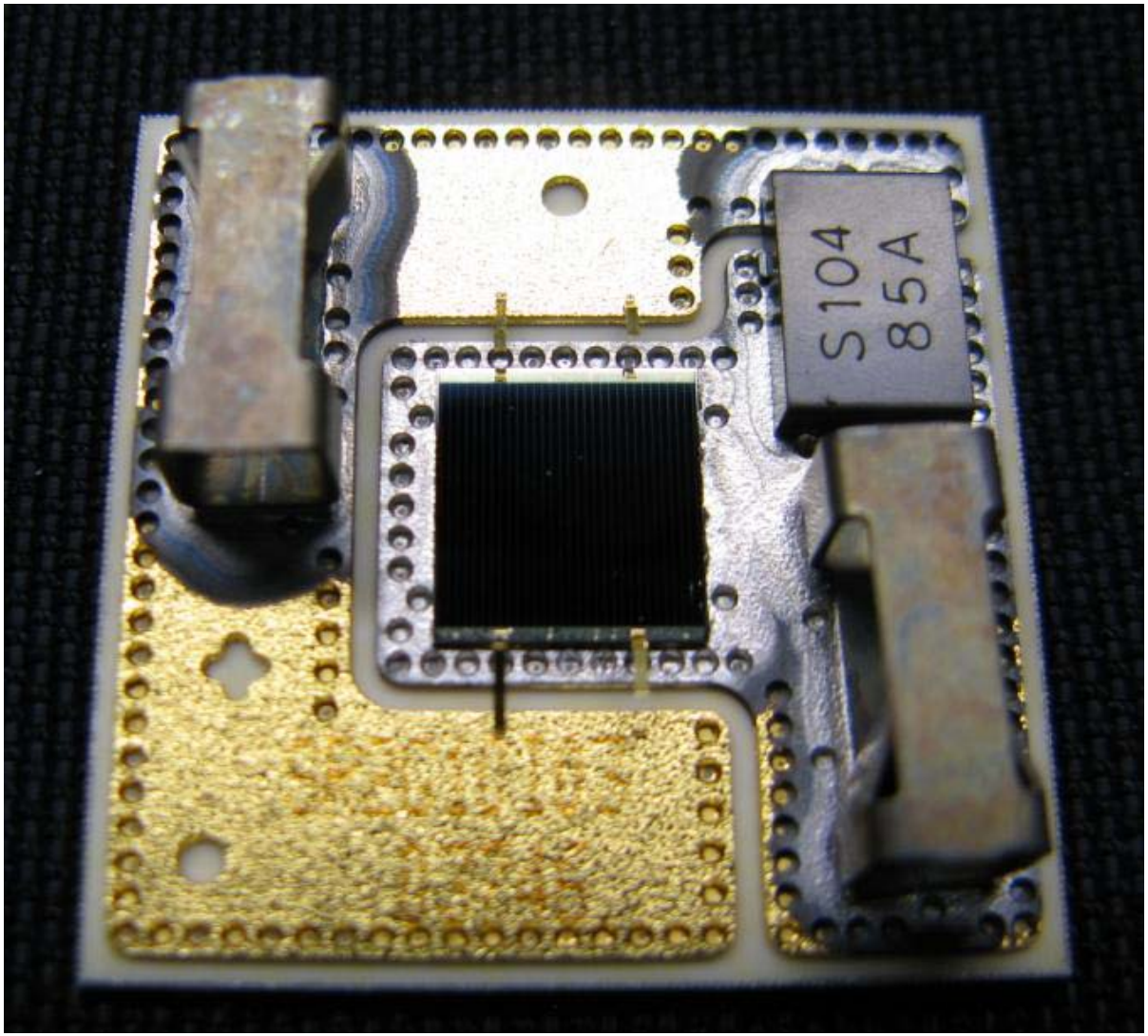
5.5 mm x 5.5 mm III-V cell on diffusion bonded copper substrate



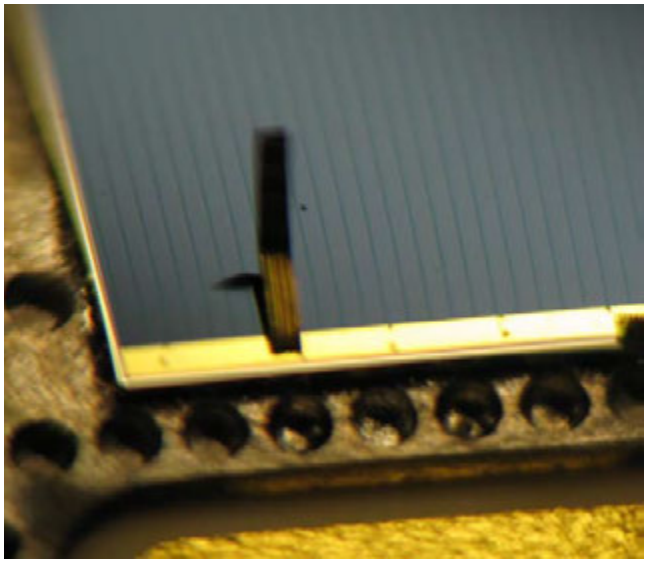
Qualification plan draws from IEC 62108 and various military standards

1	Thermal Aging for Intermetallics	300ºC	Pass
2	Powered Thermal Cycling	-40 to 110ºC	TBD
	Stud Pull		TBD
3	Humidity Freeze	-40 to 110ºC pre-condition -40ºC to 85ºC test	Pass
	Stud Pull		TBD
4	Damp Heat	85ºC	Pass
5	Mechanical Shock	30" drop	Pass
	Vibration	random vibration	Pass
	Liquid-Liquid Thermal Shock	-55 to 125ºC	Pass
6	ESD Damage Threshold	8kV	TBD

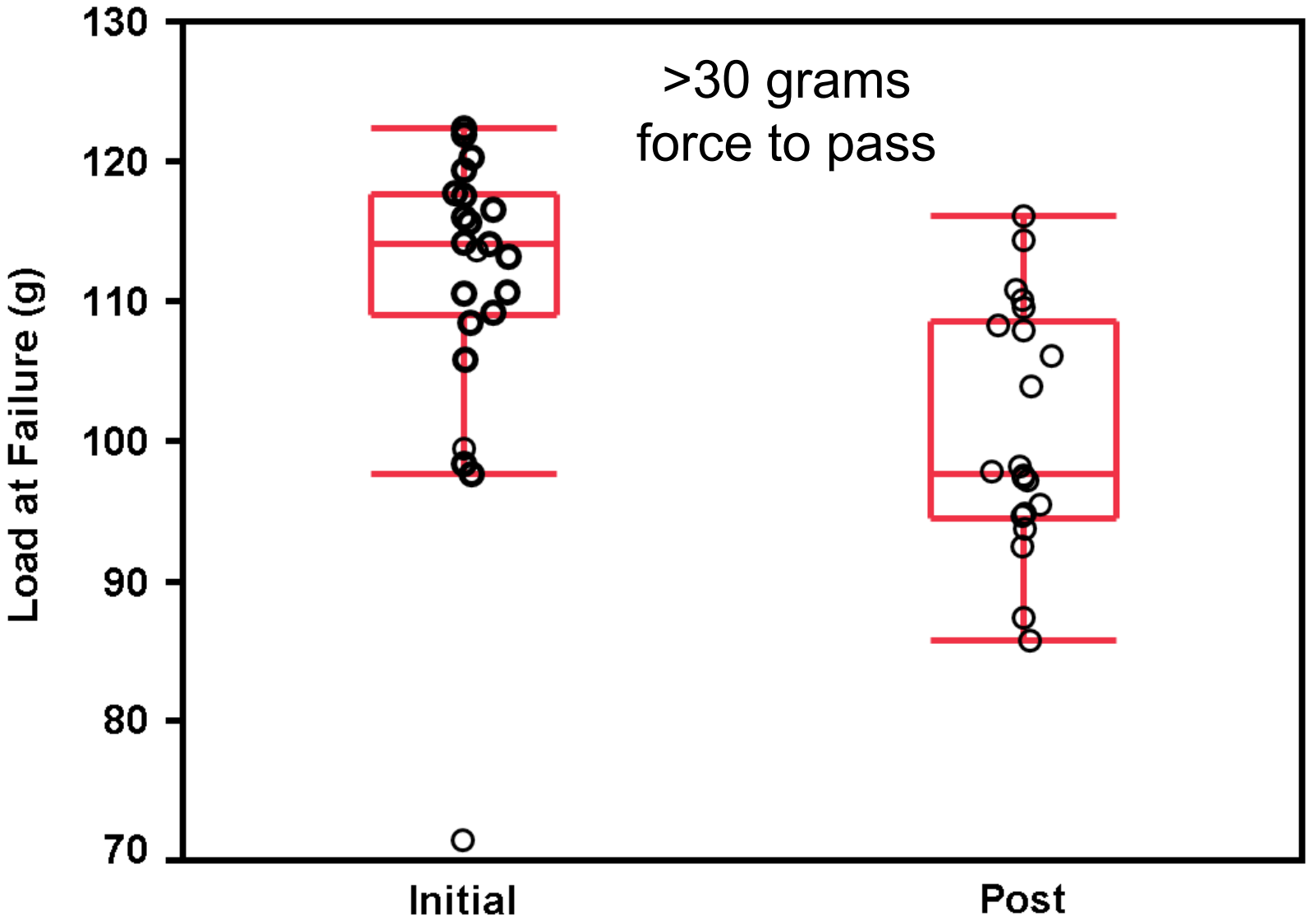
Thermal aging does not result in intermetallic phases and ribbons fail first



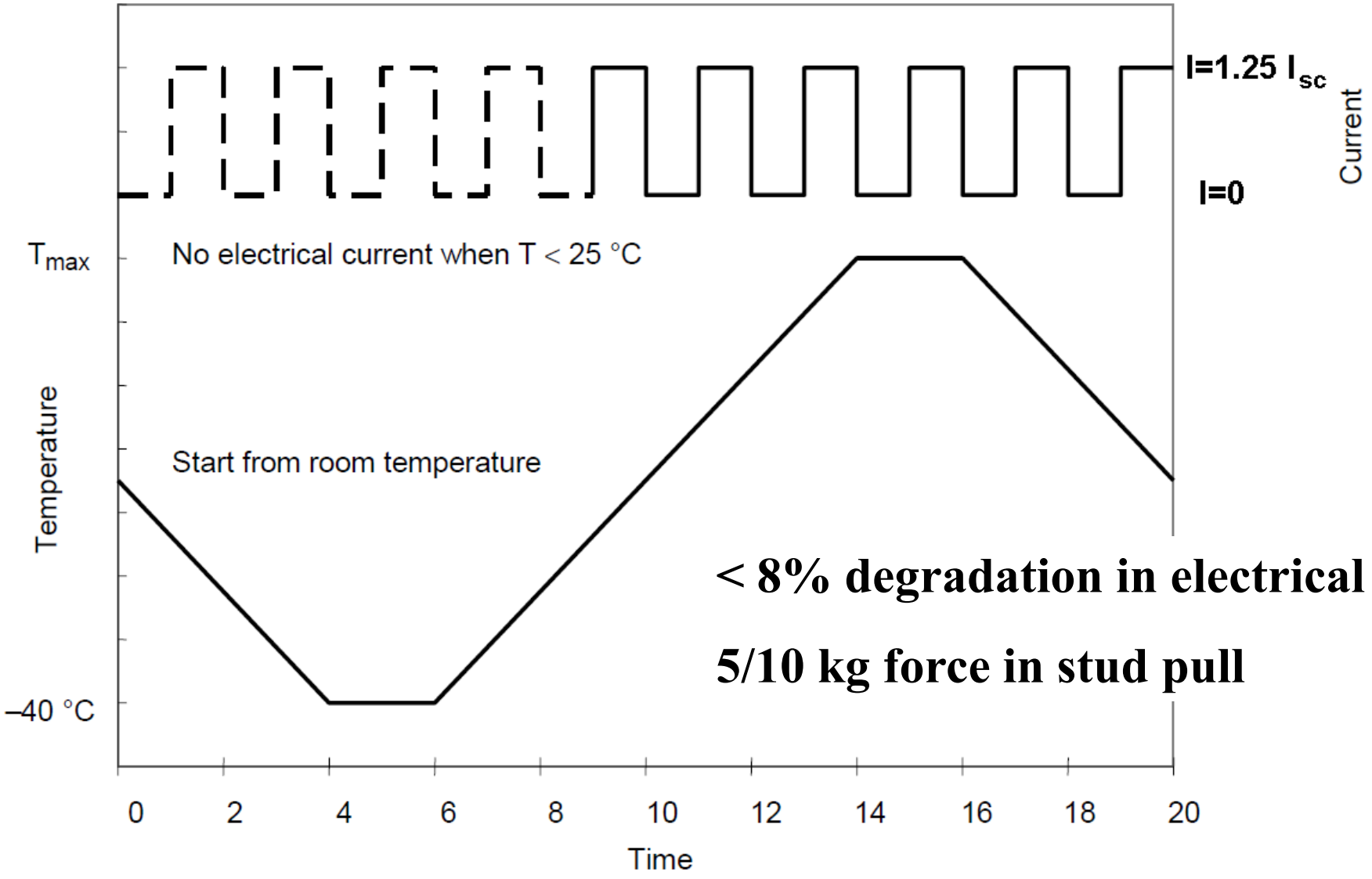
300ºC for 1h



Thermal aging of ribbon bonds does not significantly reduce pull strength



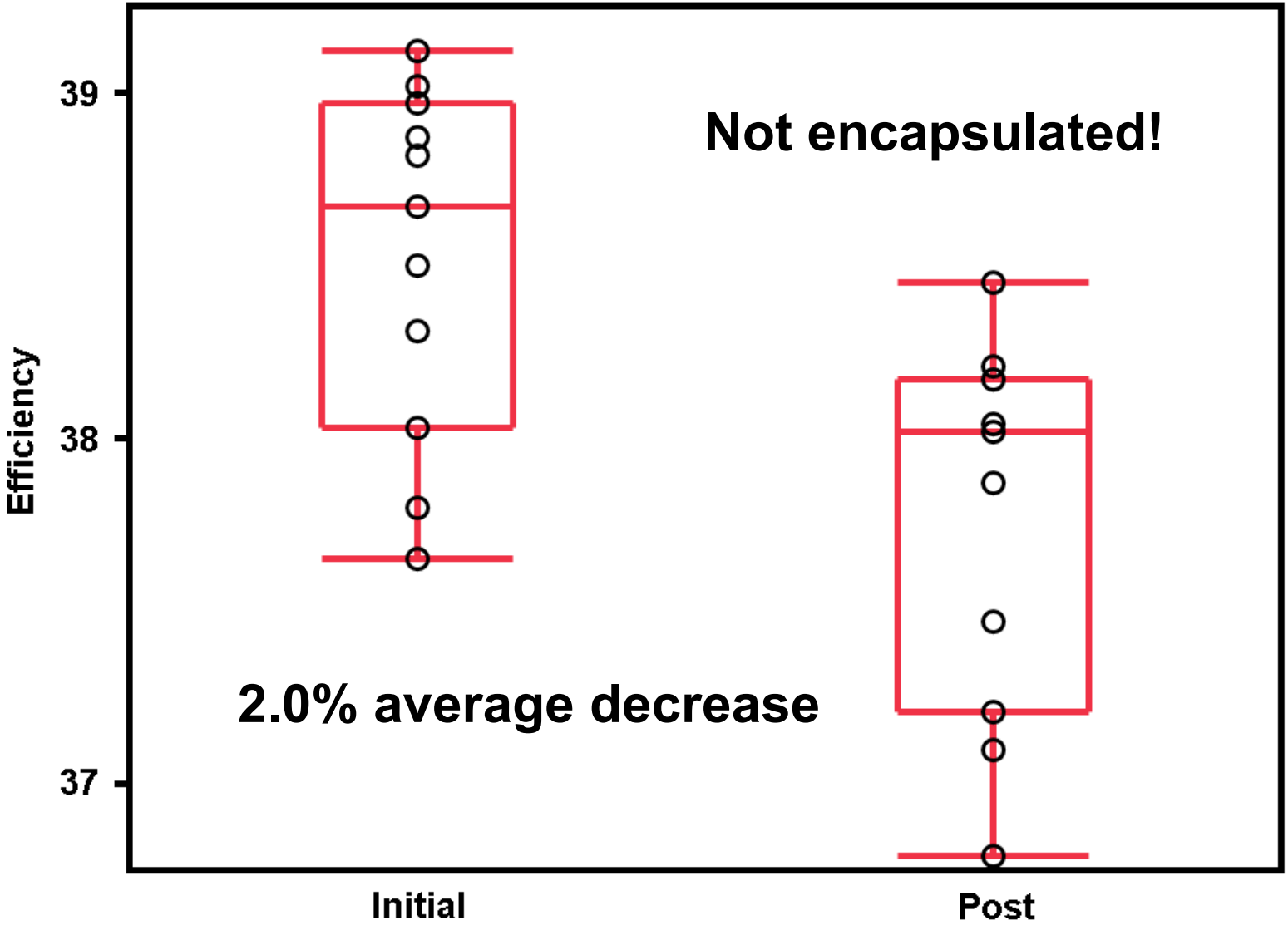
Powered thermal cycling for electrical properties and stud pull for solder adhesion



< 8% degradation in electrical

5/10 kg force in stud pull

Damp freeze impacts efficiency, but the decrease is less than 8%



Damp heat impacts efficiency, but the decrease is less than 8%



Efficiency

39

38

37

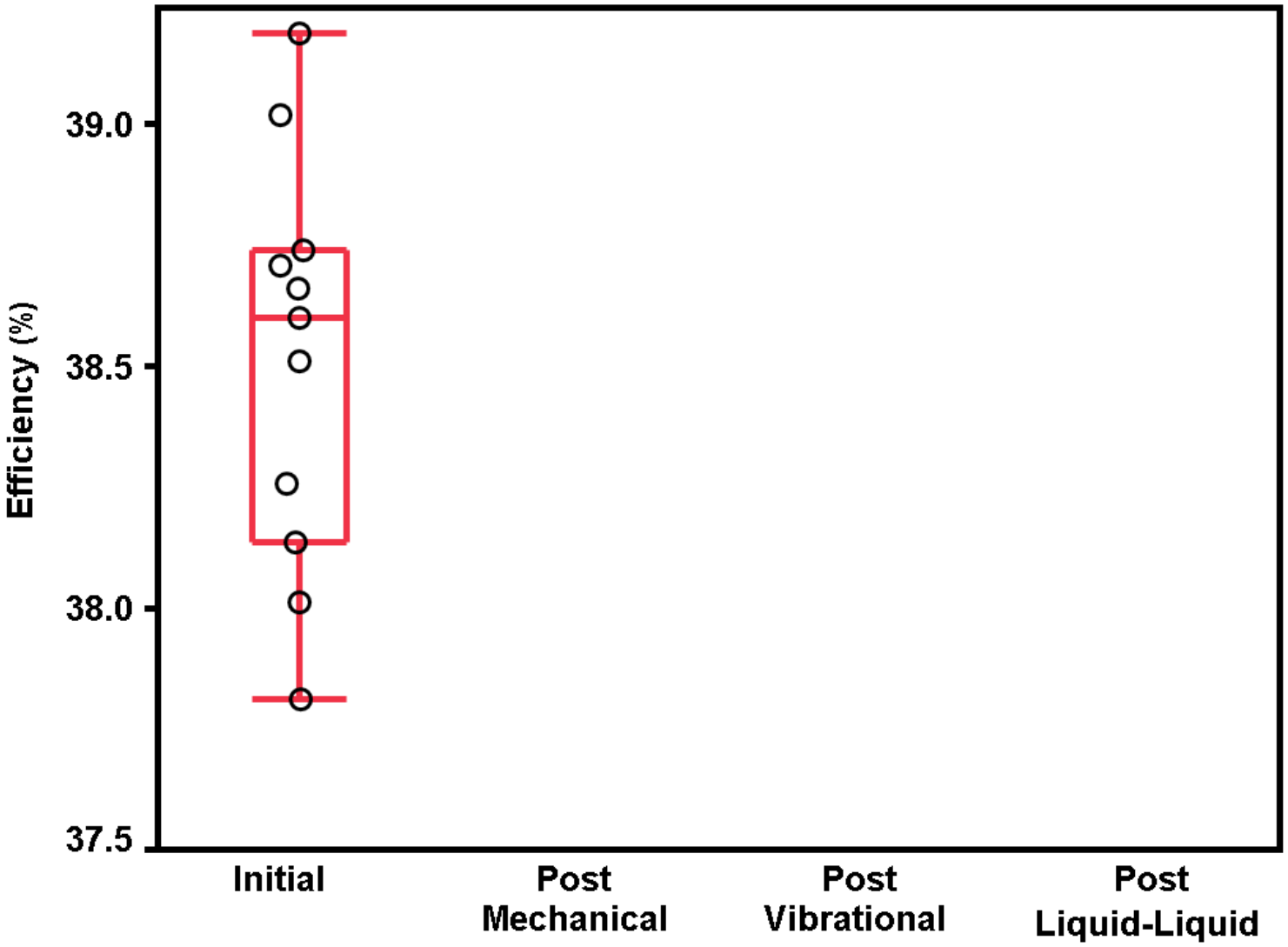
36

2.4% average decrease

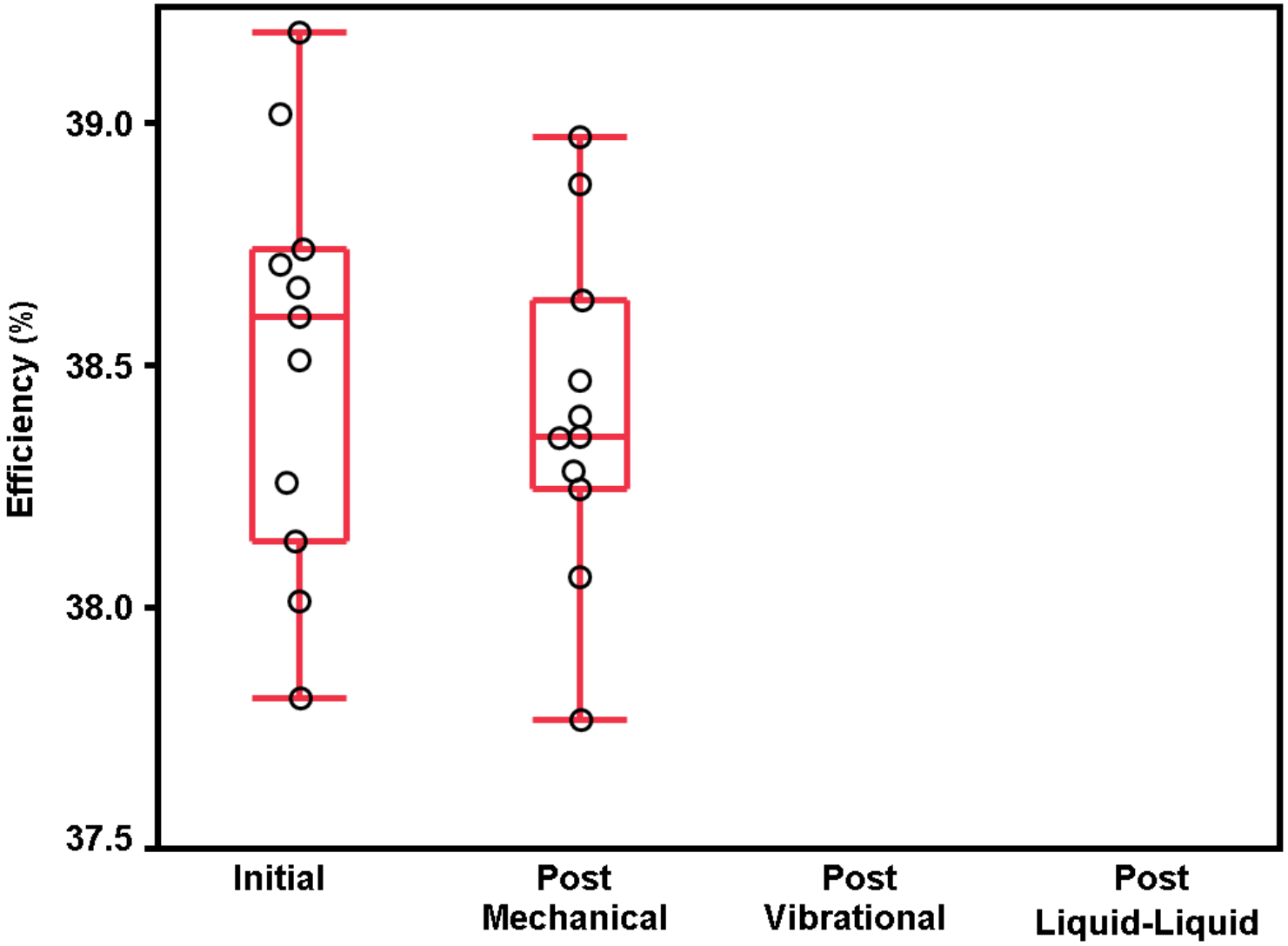
Initial

Post

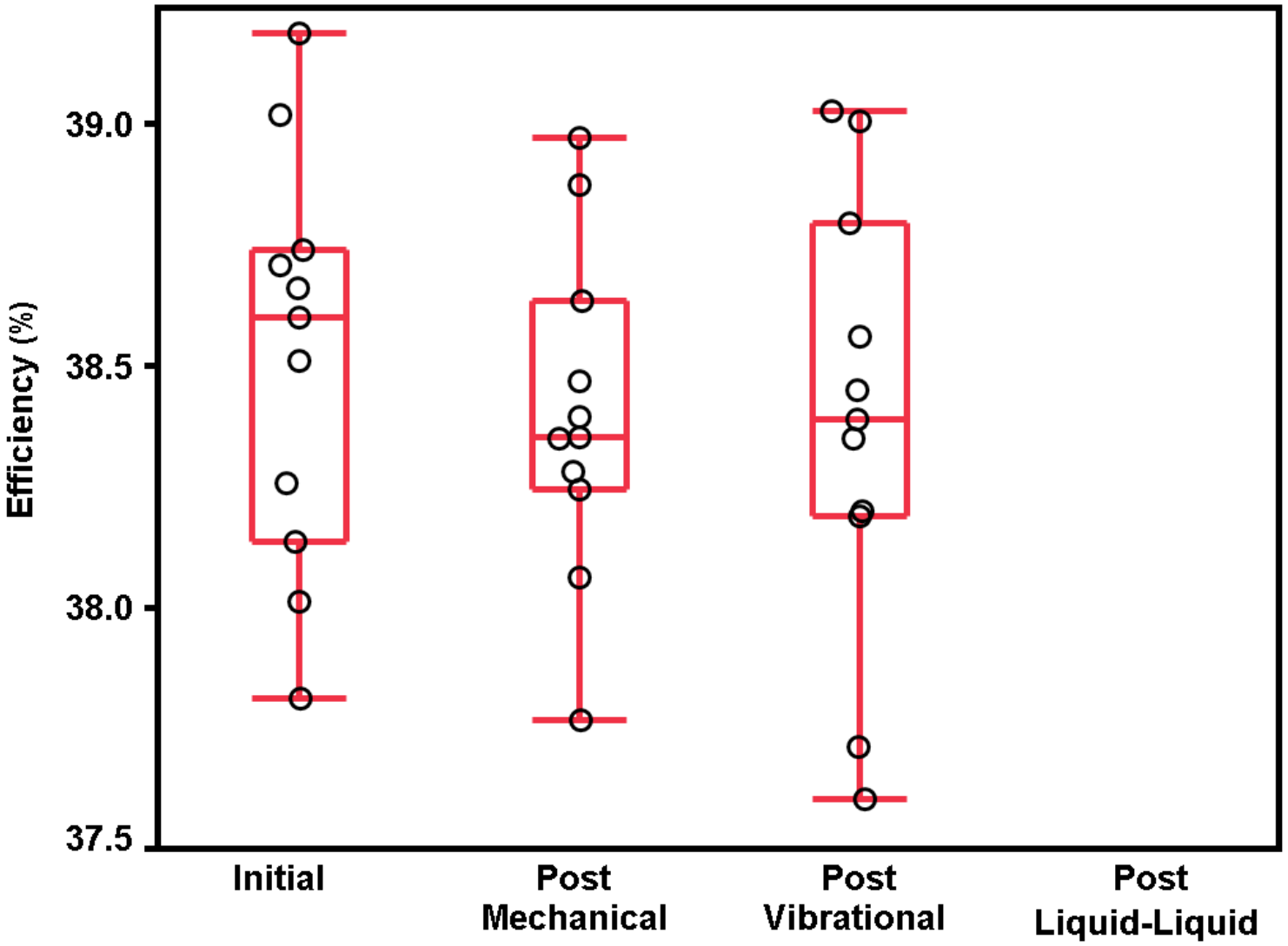
Initial efficiency whisker plot showing an average efficiency between 38% and 39%



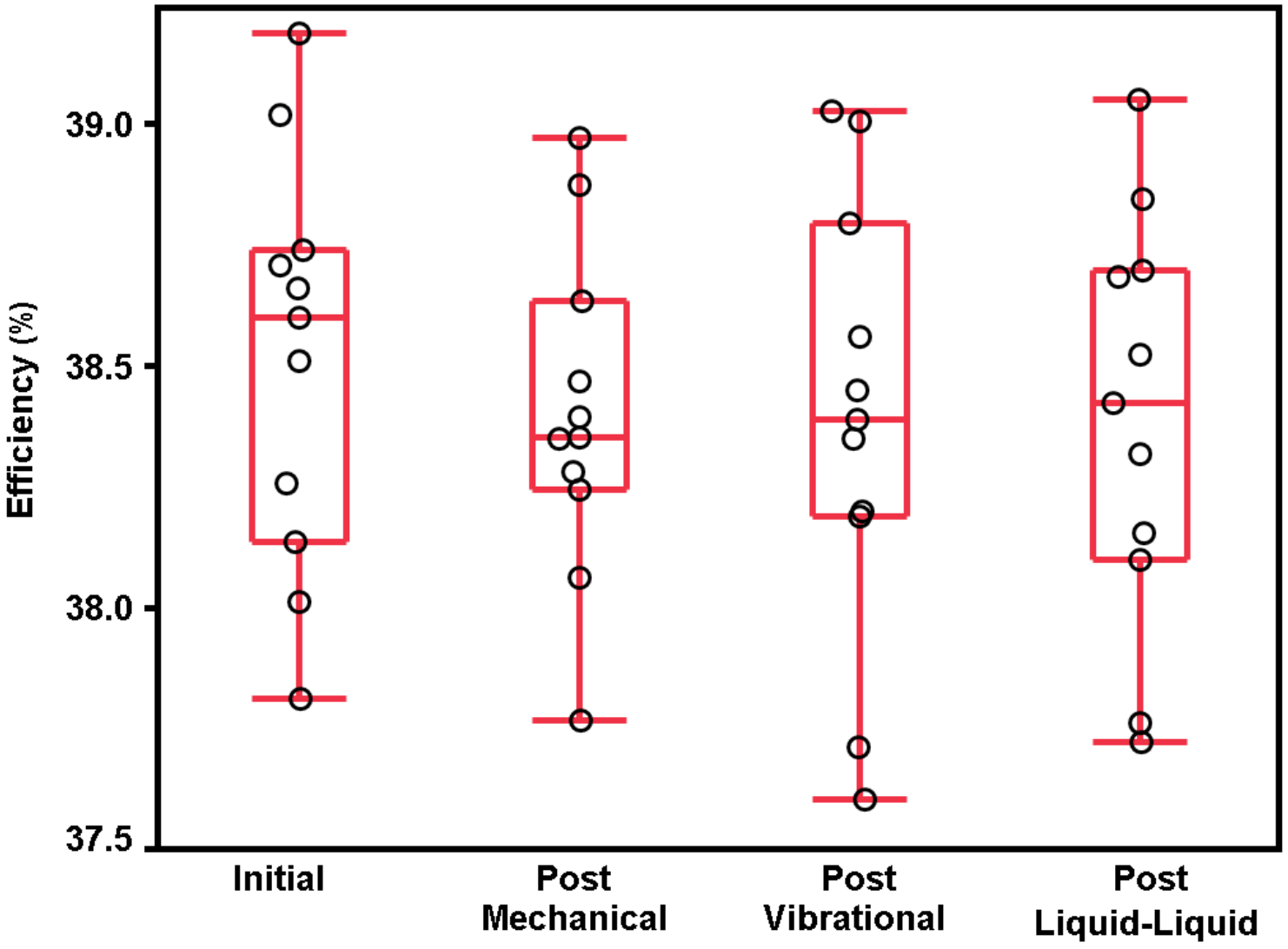
Efficiency whisker plot after mechanical stress showing no difference after the test



Efficiency whisker plot after vibrational stress showing no difference after the test



Efficiency whisker plot after liquid-liquid shock showing no difference after the test



Electrostatic discharge damage threshold



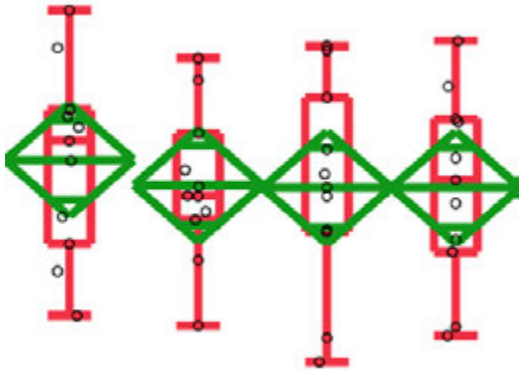
I-V measurements

ESD followed by I-V in increments

leakage current < 8 mA at 2.2 V

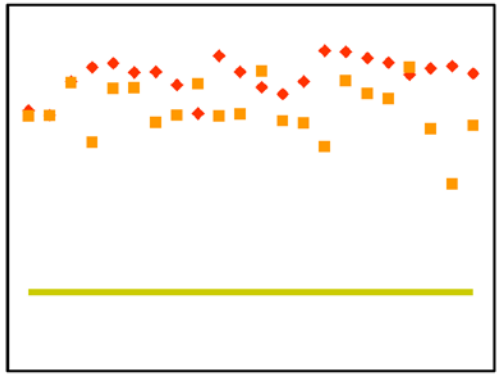
similar parts to 4kV have shown
<1 mA at 2.2 V

The 5.5 x 5.5 mm sub-assembly is a robust product against strife testing



Thermal and mechanical shock have no effect on efficiency

Thermal aging does not compromise ribbon bond strength





Humidity with temperature impacts performance, but within acceptable limits

Effect of soiling on PV performance

Air Force test location in Maui (leeward side)



Panels near the ground were untouched elevated panels cleaned weekly





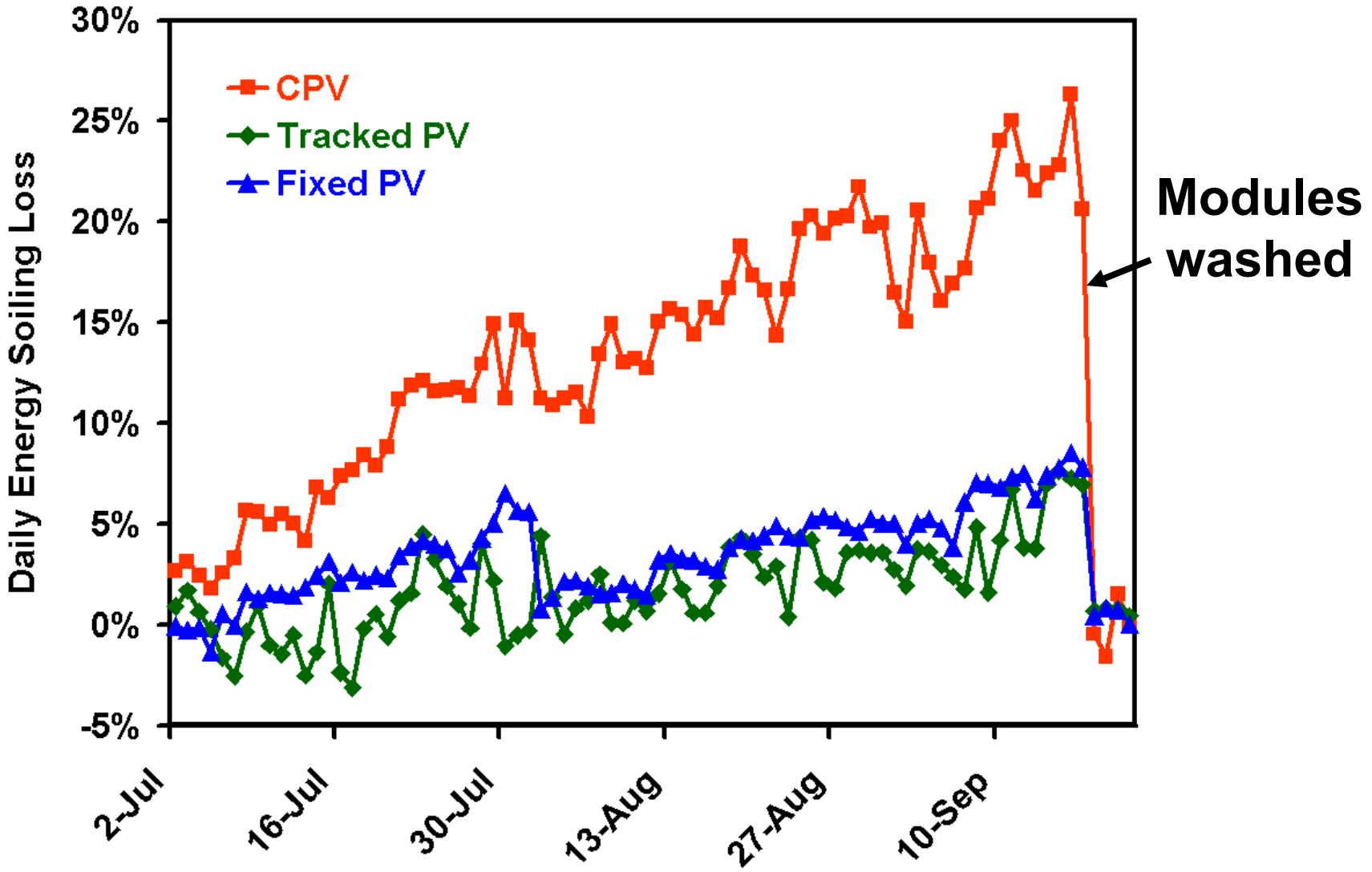
CPV soiling performance evaluation criteria

Soiling loss calculated using the following

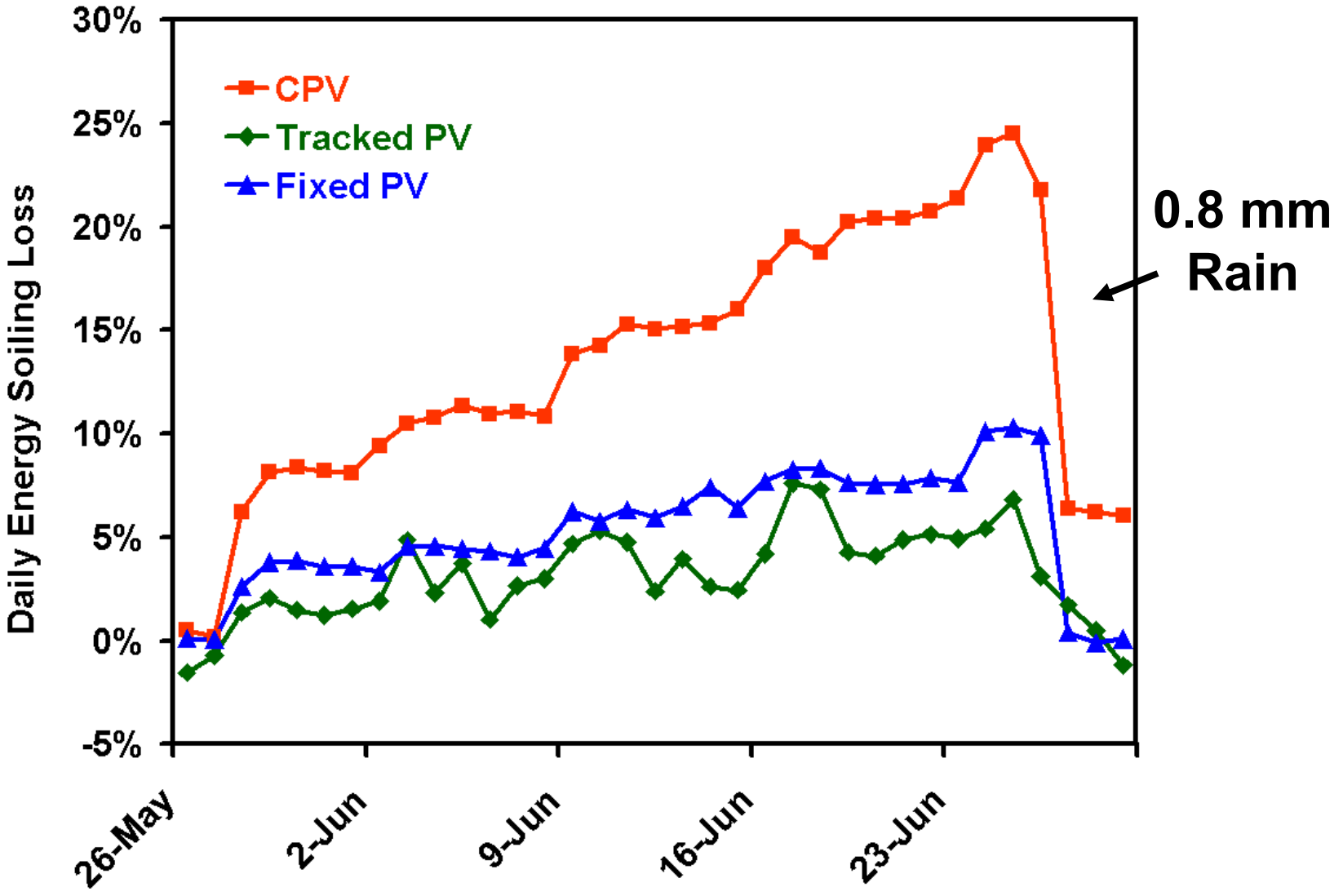
$$SL = \frac{E_{clean} - E_{dirty}}{E_{clean}}$$

Dirt accumulates at high rates in this environment

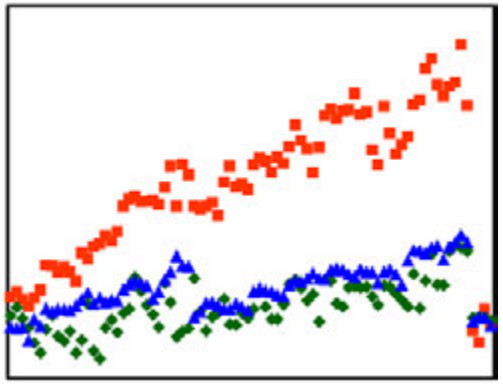
Dirt accumulation on CPV has a strong impact on electrical performance



Dirt accumulation may be easily removed by small (0.8 mm) rain events



Clean lenses are crucial for efficient CPV power generation



The data show what we knew:
Dirt accumulation affects efficiency



Washing and rain events restore performance to as-installed



Soiling effects and mitigation measures will be site and season dependent



CPV Solar Cell Qualification Standard

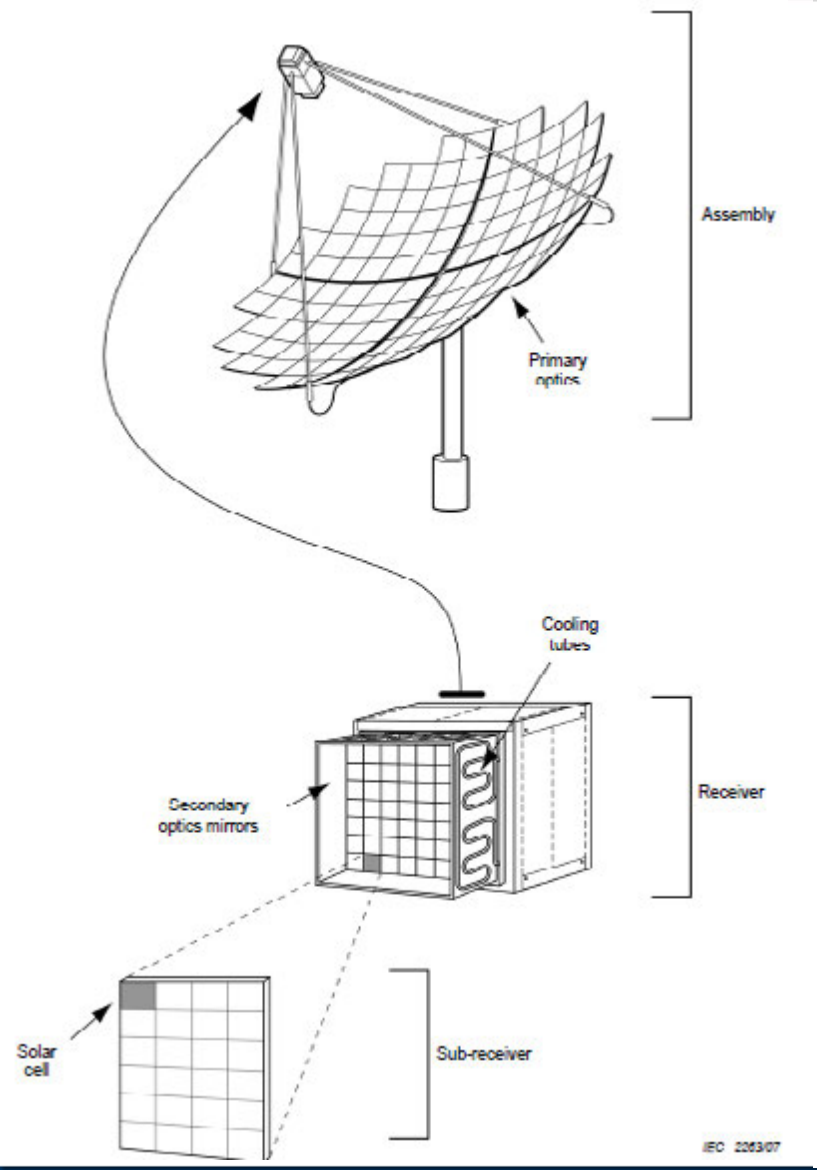
NREL PVMW 17-Feb-2011

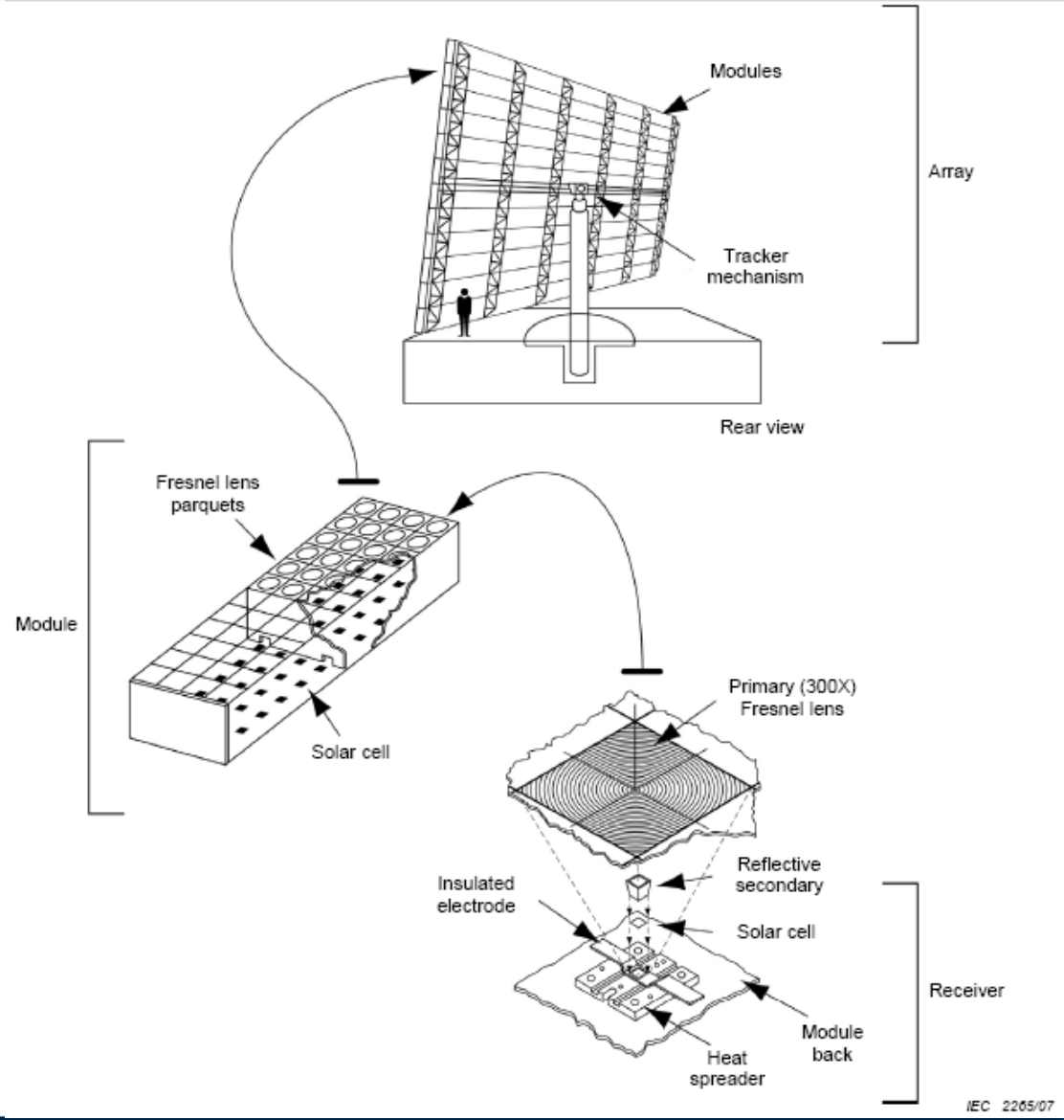
IEC TAG-82 WG-7

Outline

- Intro
- Review of PV Qualification Standards
  - National
  - International
  - Relationship with Other IEC Standards and Drafts
  - PV Cell Standards
- Proposed CPV Solar Cell and Receiver Package Qualification Standard
- IEC WG-7 Survey Results
- Open Discussion

CPV Systems and Subcomponents





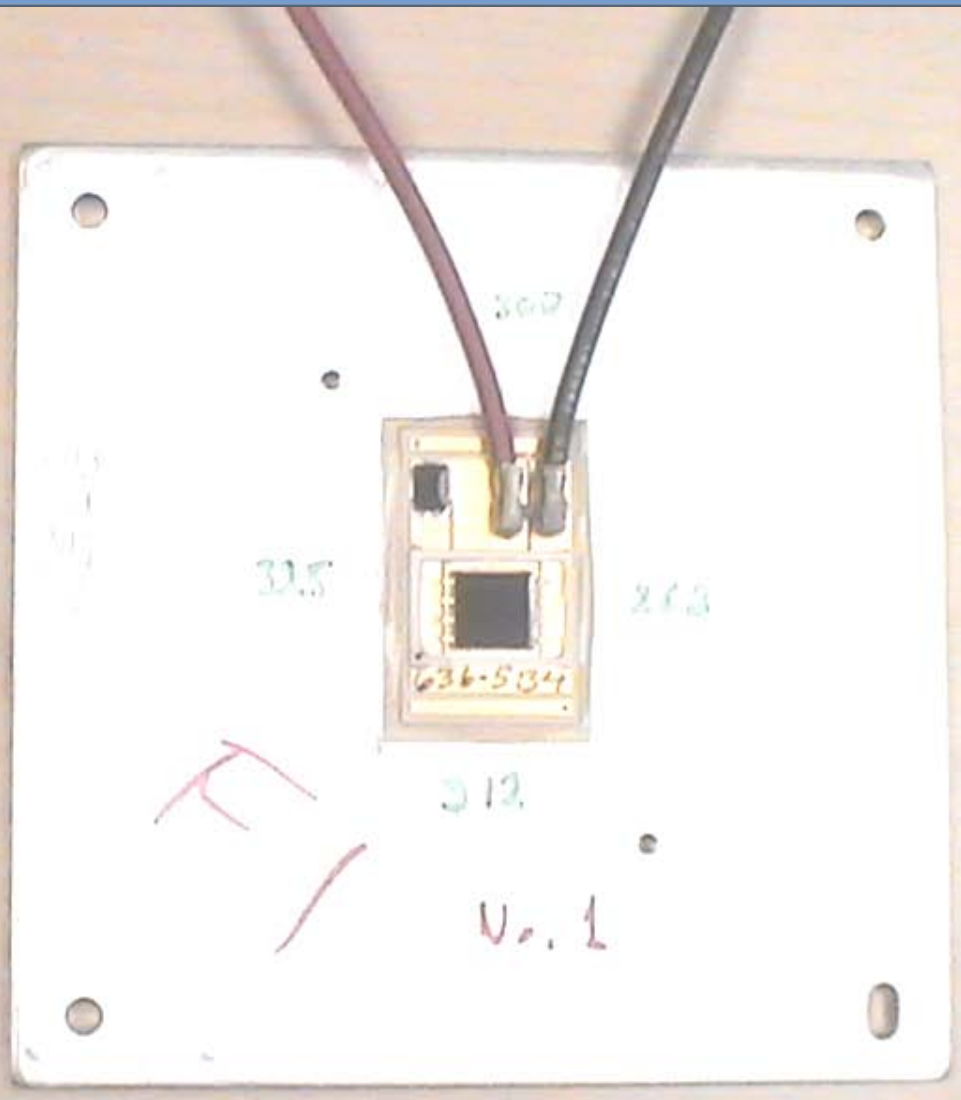
Definitions



Bare Cell
or
Device



Receiver
(Rx)



Receiver Assembly

Standards Overview

- **Electronic and Optoelectronics Component Qualification Standards**
  - Telcordia e.g. GR-468-CORE Issue 2, September 2004,
    - Reliability Assurance Requirements for Optoelectronic Devices Used in Telecommunications E
  - IEC e.g. 61751 ed1.0,
    - Laser modules used for telecommunication - Reliability assessment.
- **PV for Space Power Applications**
  - AIAA S-111-2005
    - Qualification and Quality Requirements for Space Solar Cells
  - ECSS-E-ST-20-08C
    - Photovoltaic assemblies and components
- **PV Cells**
  - Solar America Initiative (SAI) Procurement Specification Proposal
- **PV and CPV Modules and System Level**
  - IEC 61215 and IEC 62108
    - PV and CPV modules and assemblies – Design qualification and type approval.
  - IEEE Std 1513-2001
    - Recommended Practice for Qualification of CPV Receiver Sections and Modules

Relationships with other IEC CPV Standards

- IEC 62688 CPV Safety Standard
- Tracker Technical Specification
- IEC 62670 (CPV Module and Assembly Performance Testing and Energy Rating)
- CPV Performance based on 61853-2
- Acceptance test
- Energy Performance Ratio
- IEC 62108 revision
- Cell Qualification Standard
- Specification of Concentrator Cell Description
- Other standards and comments

- In addition, wherever possible, CPV standards mimic other IEC PV standards
  - (e.g. 62108/61215 and the c-Si cell procurement guidelines.)

Solar America Board for Codes and Standards (Solar ABCs)

emcore
empower with light™

Solar America Board for Codes and Standards Report

CRYSTALLINE SILICON TERRESTRIAL PHOTOVOLTAIC CELLS –

Supply Chain Procurement Specification Guideline

Prepared by

Govindasamy TamizhMani
Arizona State University
Photovoltaic Reliability Laboratory

March 2009

c-Si PV Cell Procurement Guideline

PERFORMANCE PARAMETER	SYMBOL (UNIT)	
Short circuit current @ STC	I_{sc} (A)	
Open circuit voltage @ STC	V_{oc} (V)	
Current at maximum power @ STC	I_{mp} (A)	
Voltage at maximum power @ STC	V_{mp} (V)	
Maximum power @ STC	P_{mp} (W)	
Fill factor @ STC	FF (%)	
Cell efficiency @ STC	(%)	
Cell efficiency tolerance @ STC	(%)	
Production Tolerance @ STC	I_{sc} (%)	
	V_{oc} (%)	
	I_{mp} (%)	
	V_{mp} (%)	
	P_{mp} (%)	

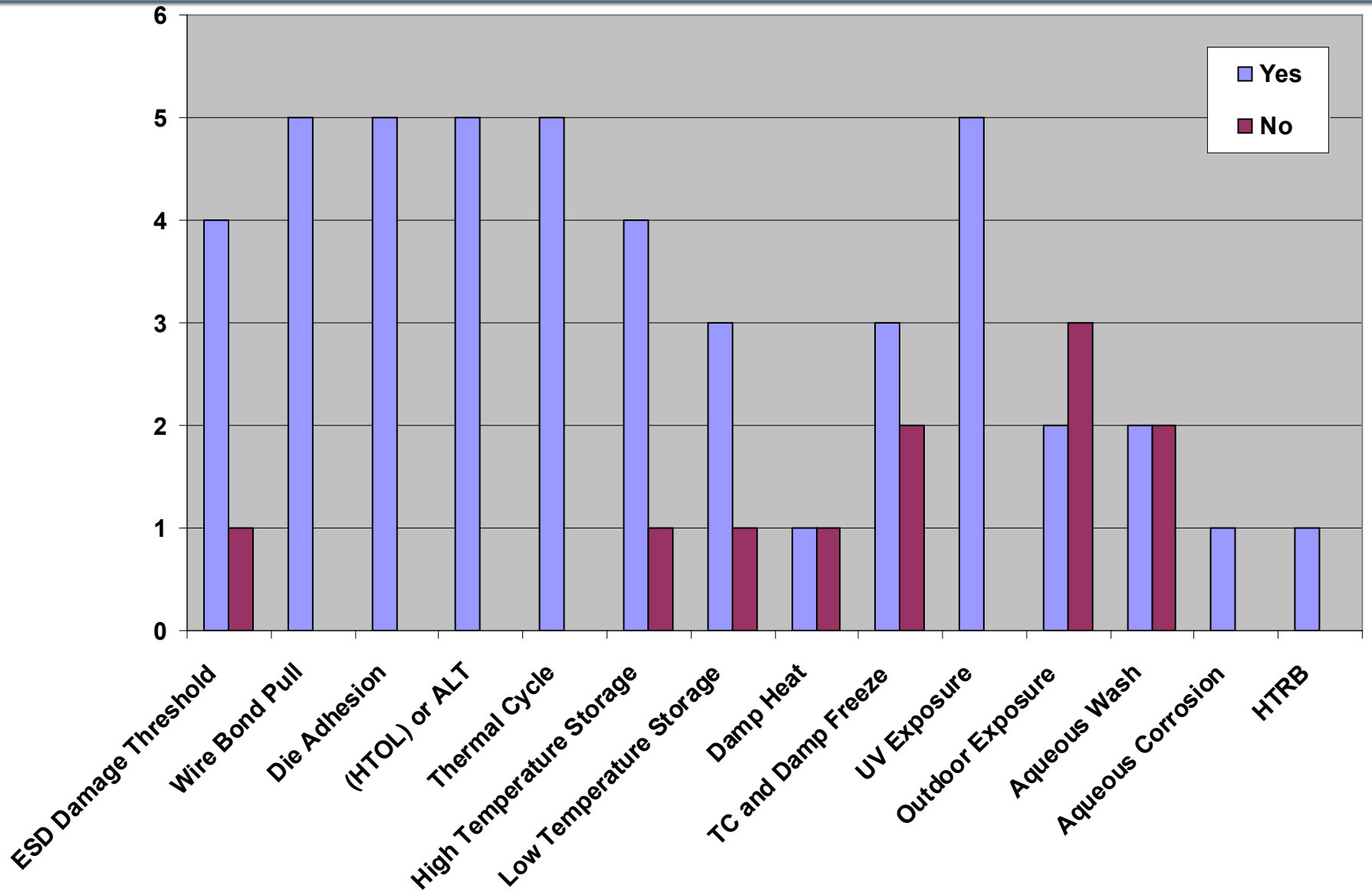
Proposed CPV Cell Qualification Tests

Stress Test Name	Cell Test Conditions
ESD Damage Threshold	Incremental Voltage tests for HBM and CDM to establish damage threshold. Dark IV.
Wire bond pull	Wire or ribbon bond, pull until failure, record mode and yield force.
Die Adhesion	Solder or adhesive die attach, pull to failure, record mode and yield force.
(HTOL) or ALT	T = T_{OP} (max), I = max tolerable, 5k hours. DIV (info only) and Flash test pre stress and at periodic pull points.
Thermal Cycle	T = -40 C to Tmax. 1k cycles for T max = 85 C, 500 cycles for T max = 110 C, 2k cycles for Tmax = 65 C, periodic light bias or no bias, dwell >10 min within ±3°C of extremes. 10 to 18 cycles per day. DIV (info only) and Flash test pre stress and at end.
High Temperature Storage	Ts (max) or 85C for 2000 hours.
Low Temperature Storage	Ts (min) or -40C 72 hours.
Damp Heat	1k hours at 85 C, 85% RH or 2k hours 65 C, 85% RH, DIV (info only) and Flash test pre stress and at periodic pull points.
TC and Damp Freeze	Precondition per 10.06 for 200 cycles, Tmax = 85 C, 100 Cycles Tmax = 110 C, 400 cycles Tmax = 65 C, Tmax and 85% RH for 20 hours, ramp down to -40 C for 4 hours, 20 cycles for Tmax = 85 C, 40 cycles for Tmax = 65 C. DIV(info only) and Flash test pre stress, after precondition, and at end.
UV exposure	Expose to a total dose of 2.5 kWhrs/cm^2, Lambda < 400 nm. DIV (info only) and Flash test pre stress and at periodic pull points. (Concurrent with HTOL.)
Outdoor Exposure	Expose to a total dose of 5 kWhrs/cm^2, DNI > 30 W/cm^2. DIV (info only) and Flash test pre stress and at periodic pull points. (Concurrent with HTOL.)
Aqueous Wash	Dice saw or typical semiconductor conditions (160 F, 2 psi.)

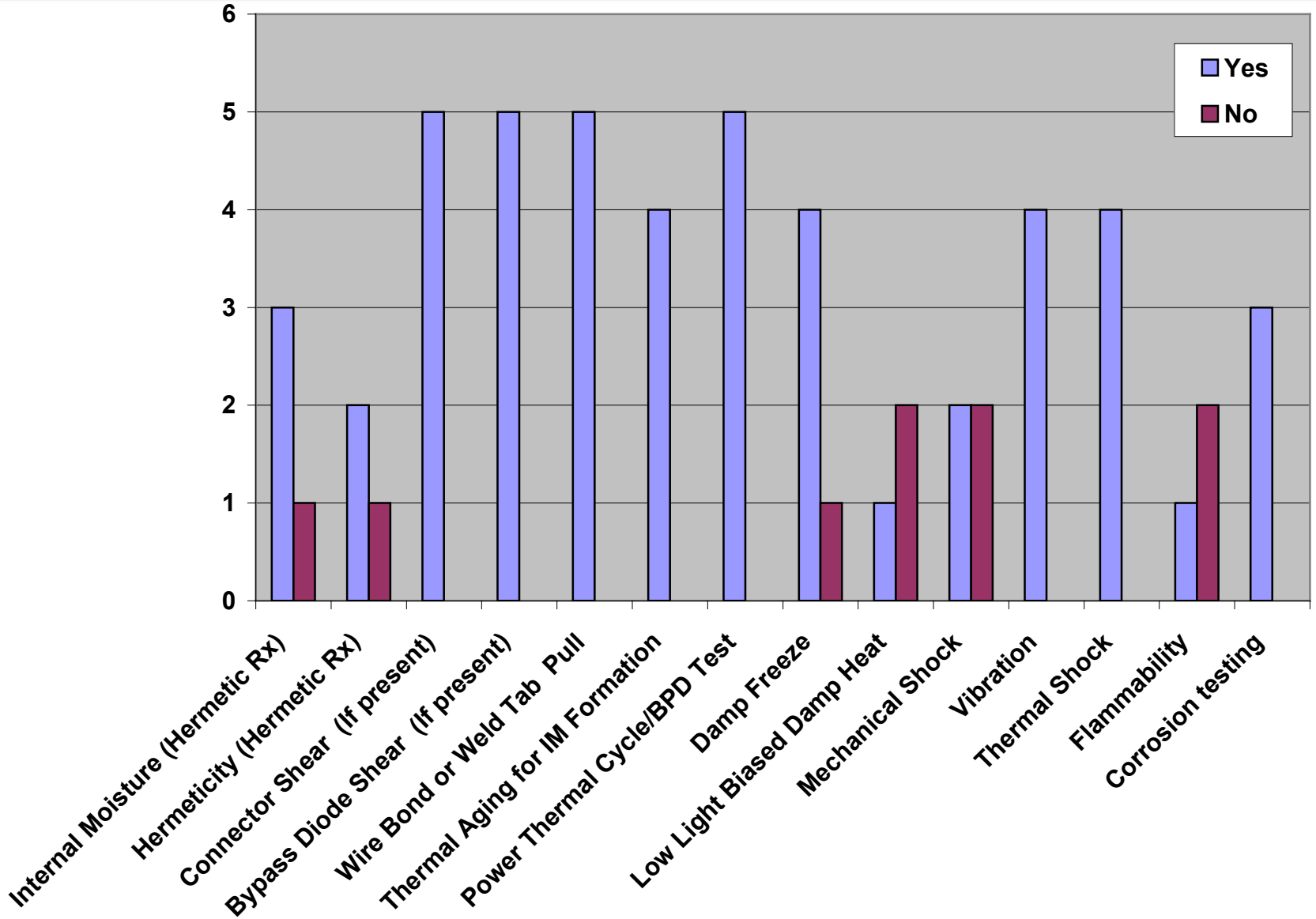
Proposed Receiver Package Qualification Tests

Parameter	Conditions
Internal Moisture (Hermetic Rx)	Bake at >100°C for 16 to 24 hours, RGA
Hermeticity (Hermetic Rx)	He bomb, leak detector
Connector shear (If present)	Shear tool
Bypass Diode shear strength (If present)	Shear tool
Wire bond or weld tab pull strength	Pull tool
Thermal aging for intermetallic formation	300C for 1 hour aging
Power thermal cycle/bypass diode thermal test	-40C to 110C for 500 cycles, IR or joule heating subcycles
Damp Freeze	Same sample as power temp cycle (for required TC preconditioning), 85C/85% RH for 20 hours, ramp down to -40 C for 4 hours, 20 cycles.
Low Level Light Biased Damp heat	Light Biased to ≥ 0.9 Voc, 85C/85% RH for 1000 hours
Mechanical Shock	Terminal peak sawtooth of amplitude 30gs and duration of 15 mSec (See figure 516.5-10 and Tables 516.5-III and IV.)
Vibration	Random vibration exposure.
Thermal Shock	Storage temperature extremes, > 60°C/min rate, 1 min dwells
Flammability	For packages with flammable components only.

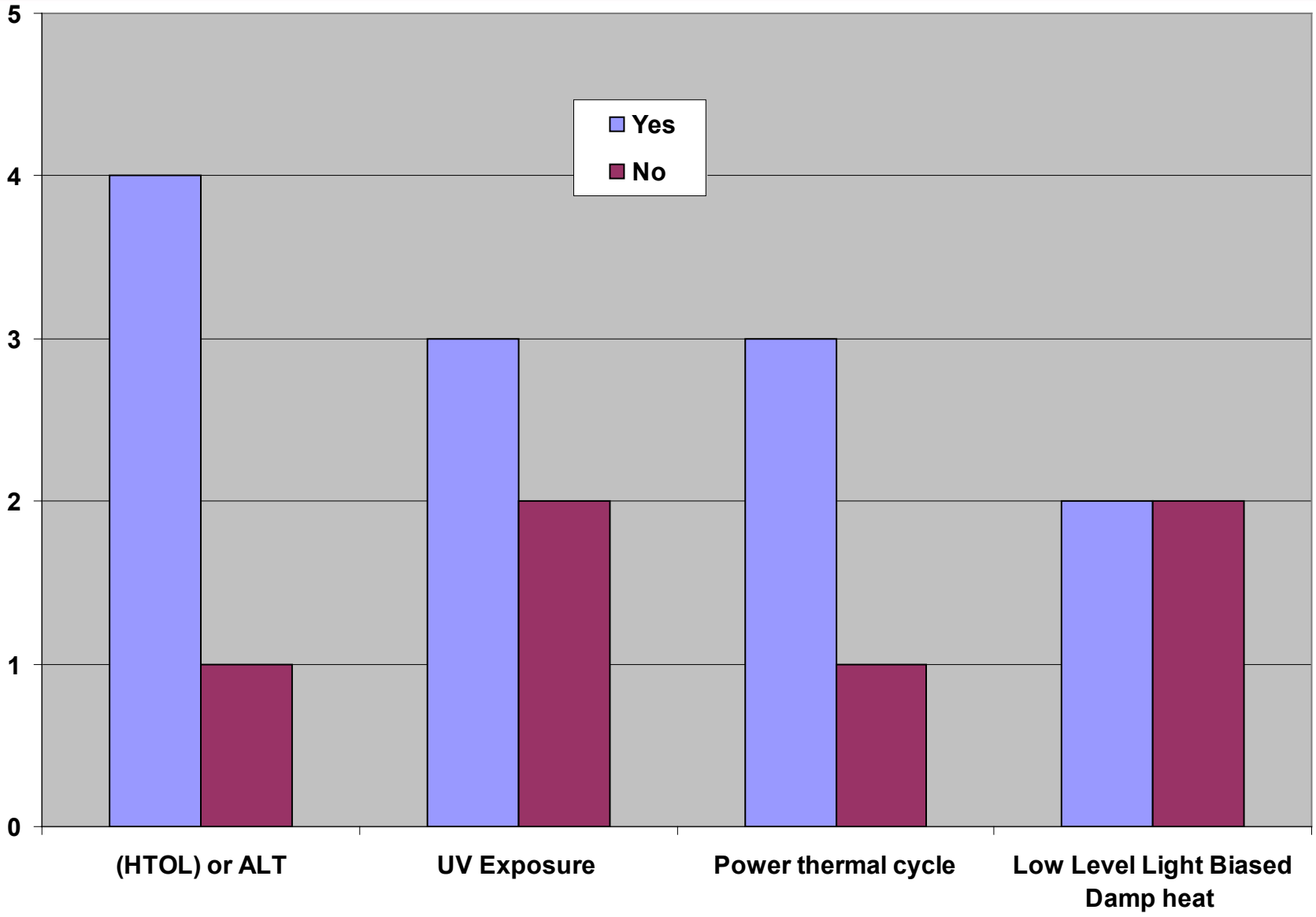
Cell Qualification Poll Results



Receiver Package Qualification Poll Results



Rx Package Qualification ALT Poll Results



emcore
empower with light™

Will the proposed standard(s) meet your needs?

NREL
NATIONAL RENEWABLE ENERGY LABORATORY

Minimizing Variation in Outdoor CPV Power Ratings



2011 Reliability Workshop, Golden CO

Matthew Muller

2/16/2010

NREL/PR-5200-51122

NREL is a national laboratory of the U.S. Department of Energy, Office of Energy Efficiency and Renewable Energy, operated by the Alliance for Sustainable Energy, LLC.

Outline

- NREL CPV testbed and its use in examining outdoor CPV power ratings
- IEC 62670 ,outdoor CPV power ratings, motivations and challenges
- ASTM E2527, a method for rating CPV module power outdoors
- Month to month variation in power ratings using ASTM method
- Attempts to improve the ASTM regression or develop an alternative
- Results to modifications to regression filtering and additional approaches
- Conclusions/Recommendations

NREL CPV Testbed & Outdoor Power Ratings

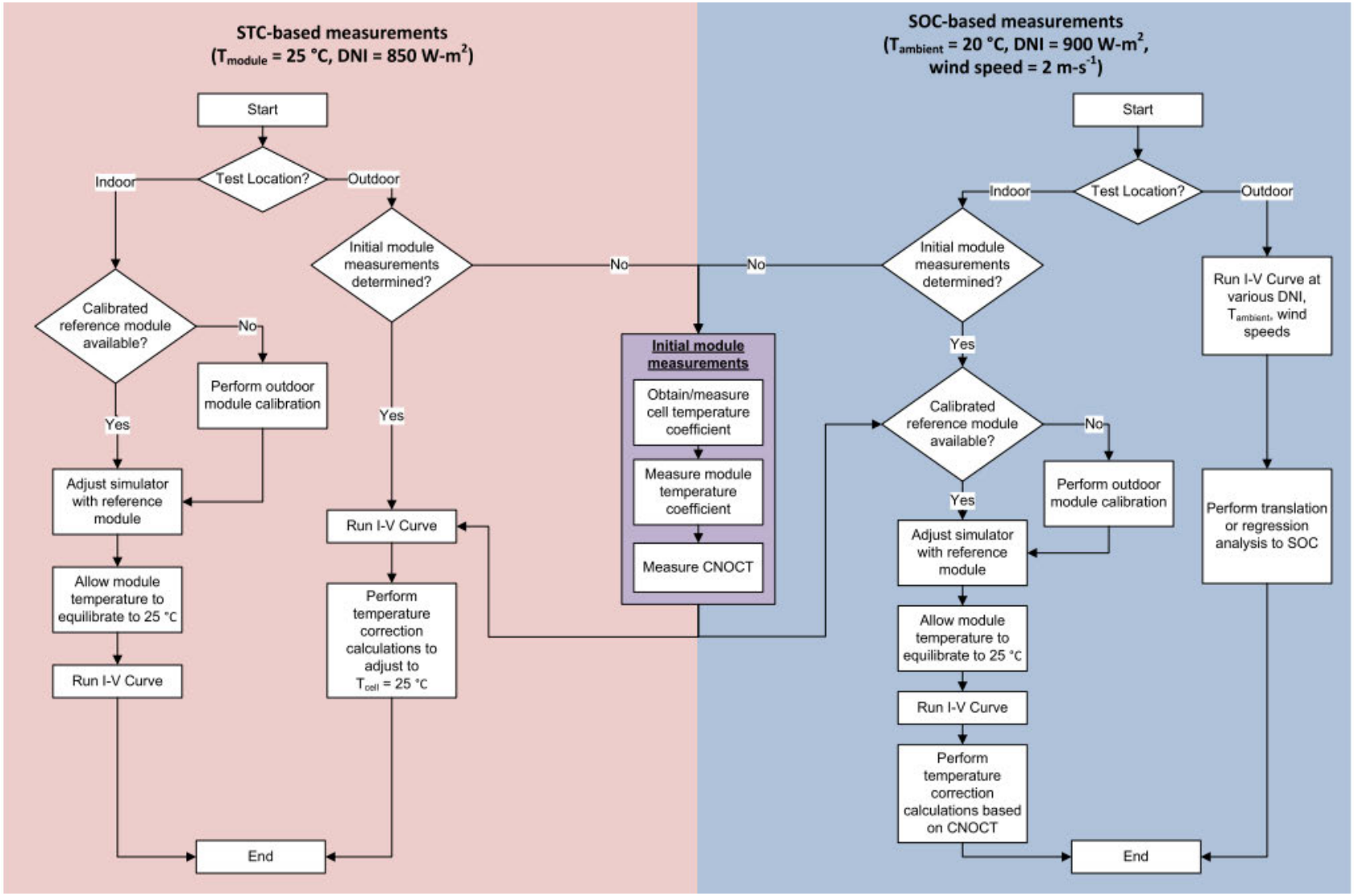
- 2-axis tracker (+/-0.15 degree sun pointing error)
- Data acquisition provides module peak power tracking
- IV sweeps, 5 minute intervals
- DNI, GNI, wind speed, Tambient, Tmodule, and tracking error are measured
- Spectral data (SRRL)



- A unique data set of various CPV lens and module architectures
- Understanding CPV performance variation and supporting standards development

IEC 62670 and Outdoor CPV Power Ratings

Concentrator Standard Operating Condition (CSOC)
Tambient (20C), DNI (900W/m2), Wind speed (2m/s) G173/AM 1.5 Spectrum



Outdoor Power Ratings, WHY? HOW?

- A need to characterize module thermal performance
  - Flat plate, ~25C above ambient at 1sun
  - CPV , ?? Degrees C above ambient
    - 300-1300X concentration varies the heat dissipation needed
    - Not all heat sinks are created equal
  - Outdoor temperatures → module/lens expansion/contraction
    - Does this impact performance?
- A need to characterize module spectral performance
  - It is well know that performance of triple junction cells is dependent on spectrum but how does this play out in a module and can it be quantified without specialized data
- If the above is the WHY? What about HOW?
  - IEC62670 describes CSOC but has not established a clear method
  - Method must provide consistent results from lab to lab (<5% variation)
  - Method must work for various CPV architectures without specialized information from the manufacturer

ASTM E2527, An Existing Method
CPV Module Power Rating Outdoors

- Measure module maximum power and meteorological parameters
- Apply the following regression to the data set, reject if standard error too high

$$P_{max}=DNI(a_1+a_2DNI+a_3T_{ambient}+a_4Wind)$$

Report Pmax @(T_{amb}=20C,W=4m/s,DNI=850W/m^2)

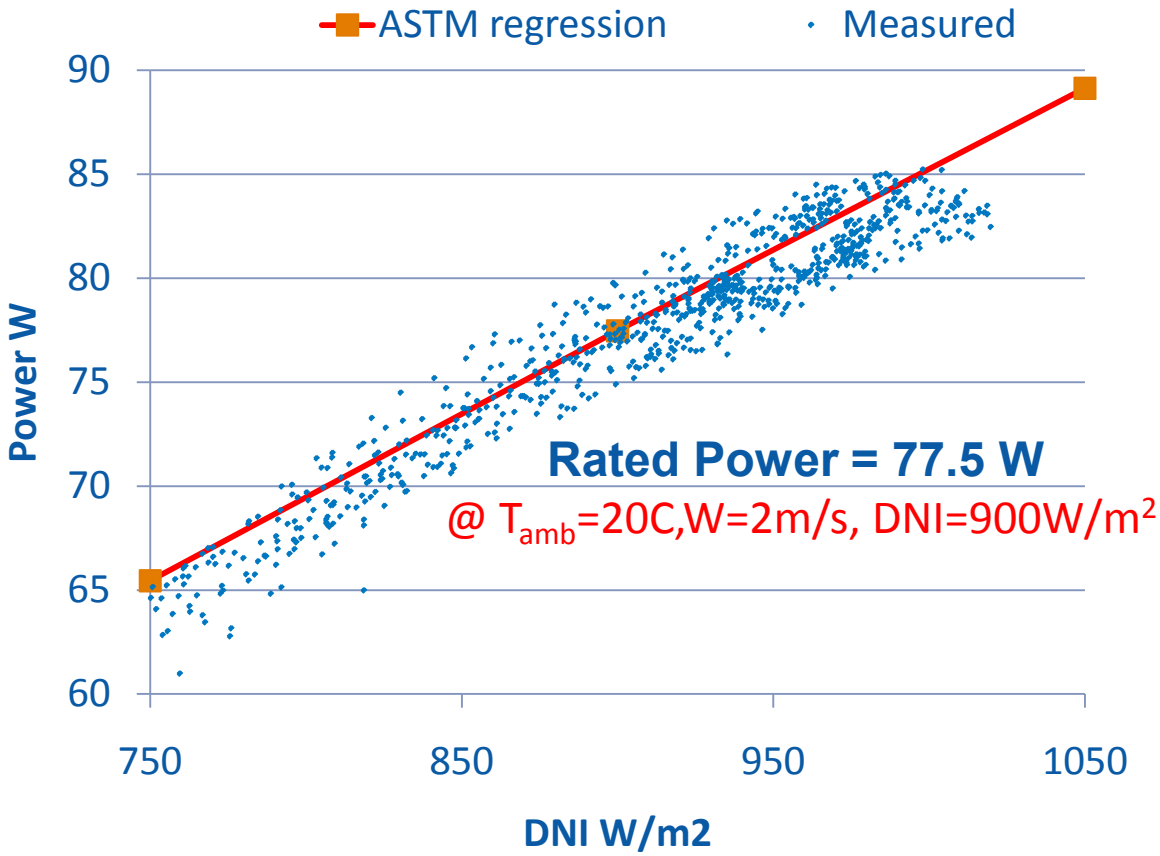
- In this presentation CSOC or (T_{amb}=20C,W=2m/s,DNI=900W/m^2) is used

- ASTM calls for the following restrictions on data for the regression
  - 10C <= T_{amb} <= 30C
  - DNI >= 750W/m^2
  - The average wind speed for the 5 minutes prior to a measurement is <= 5m/s
  - Reject if visible clouds are within 10 degrees of sun

- Cloud restriction is approximated by rejecting a 10 minute DNI deviation >2%

- Other restrictions applied above and beyond ASTM criteria
  - Reject if Diffuse radiation is > 140W/m^2
  - Reject if Tracking error is > 0.15 degrees

ASTM 2527 Applied to Sept 2010 data

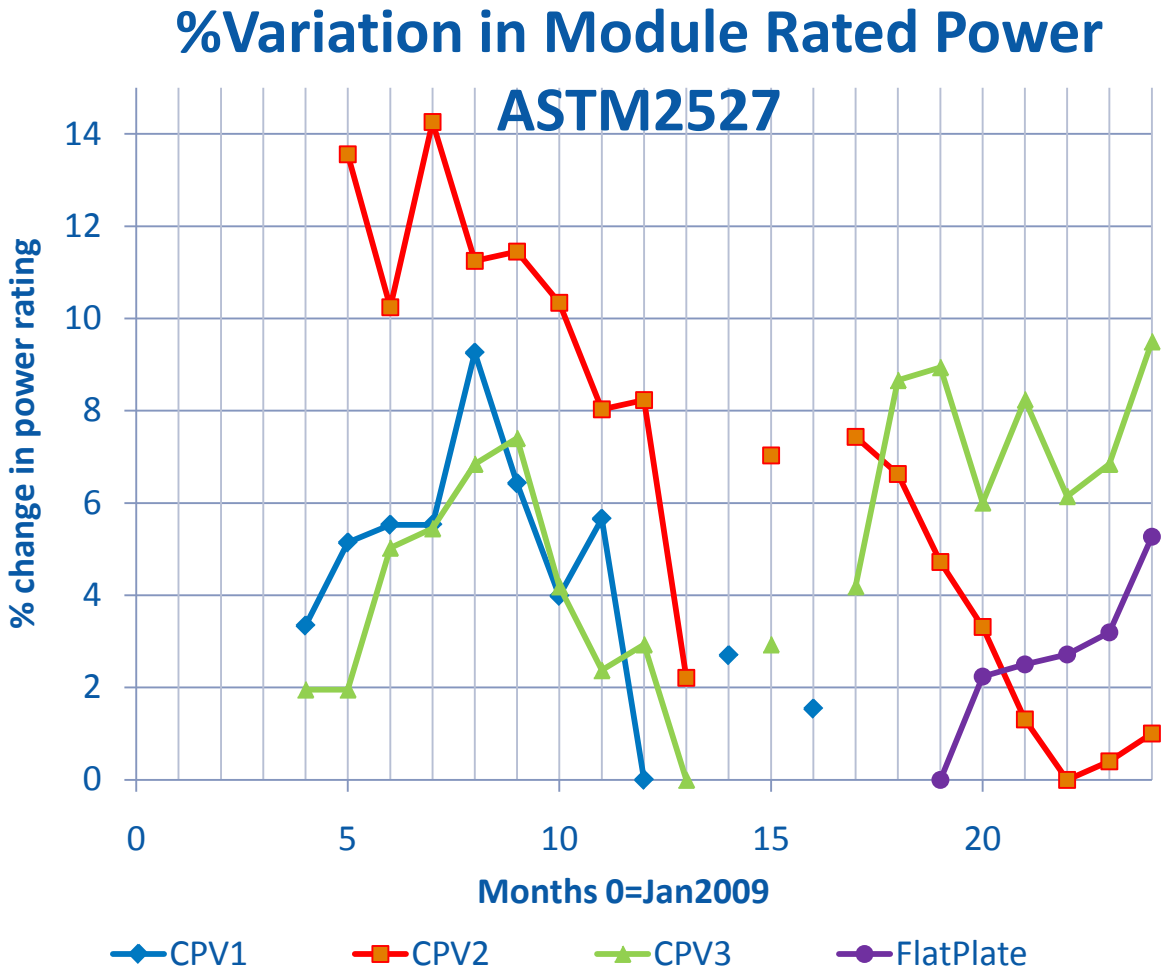


- How much will the Rated Power for a CPV module if this procedure is applied over multiple months??
- The answer not only depends on outdoor conditions but also on the module technology!

- The graph shows the % variation in a modules monthly power rating as compared to lowest monthly rating over the 2 years

- For example, CPV1 had its lowest rating in month 12, while the rating in month 11 was almost 6% greater

- Note that CPV2 appears to be degrading in the 2nd year.

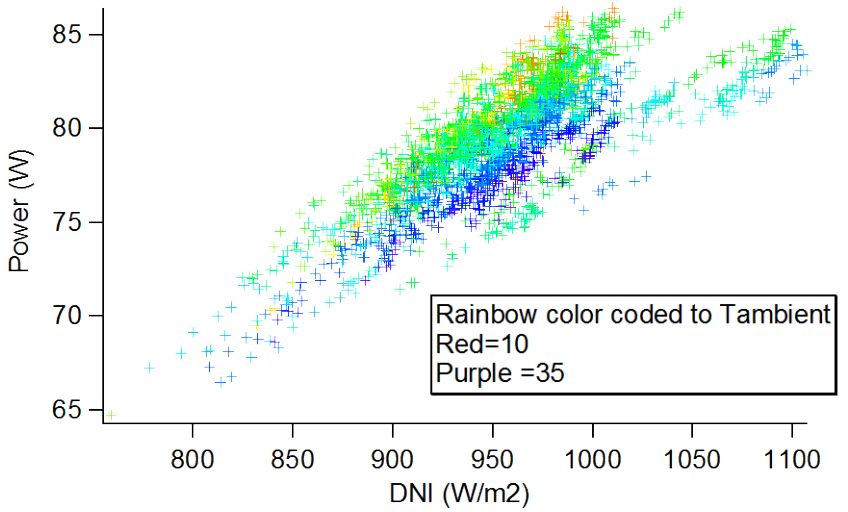


- WHY so much variation with the regression results?
  - AM neglected?
  - Lens performance neglected?
  - Moisture in modules, soiling, alignment varies?
  - Regression gives too much weight to outliers?

Can other variables improve the regression?

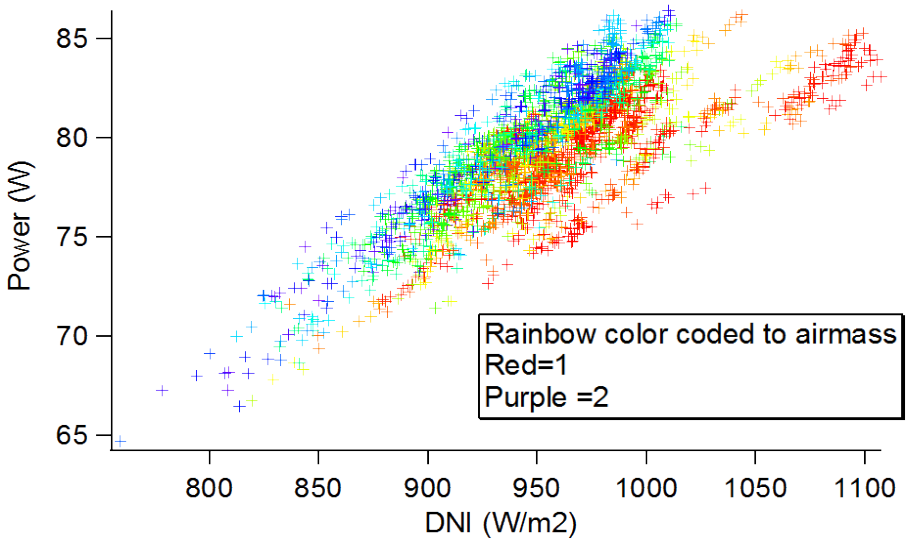
Efficiency correlates with the following

- Tambient
- Tmodule
- DNI and GNI
- AM



Efficiency (after temp correction) correlates with

- DNI and GNI
- AM
- Precipitable water vapor (moderate to weak)
- Turbidity (weak)
- In some cases there is positive correlation with Tambient, consistent with lenses that go out of alignment at low temperatures



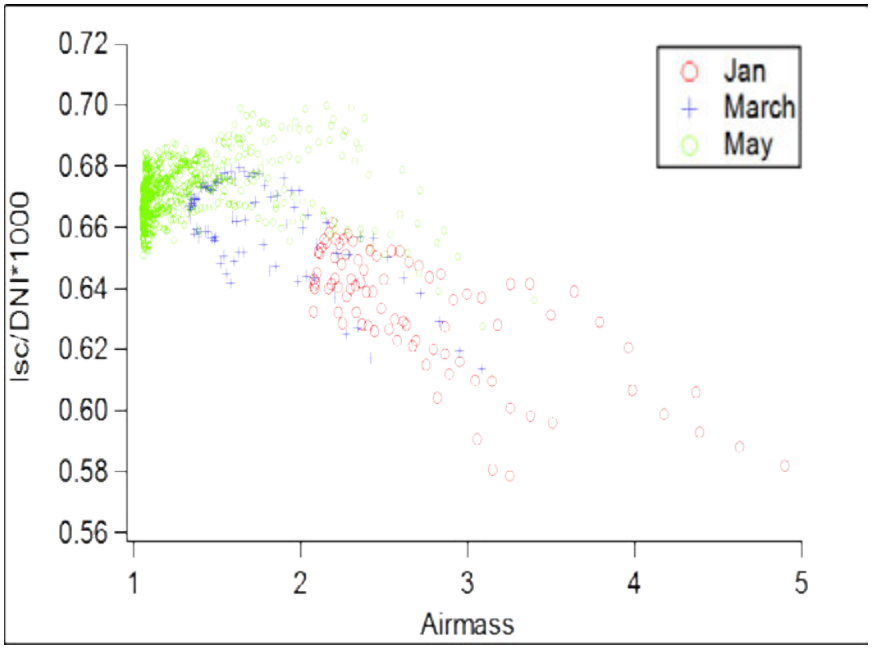
Regressions examined

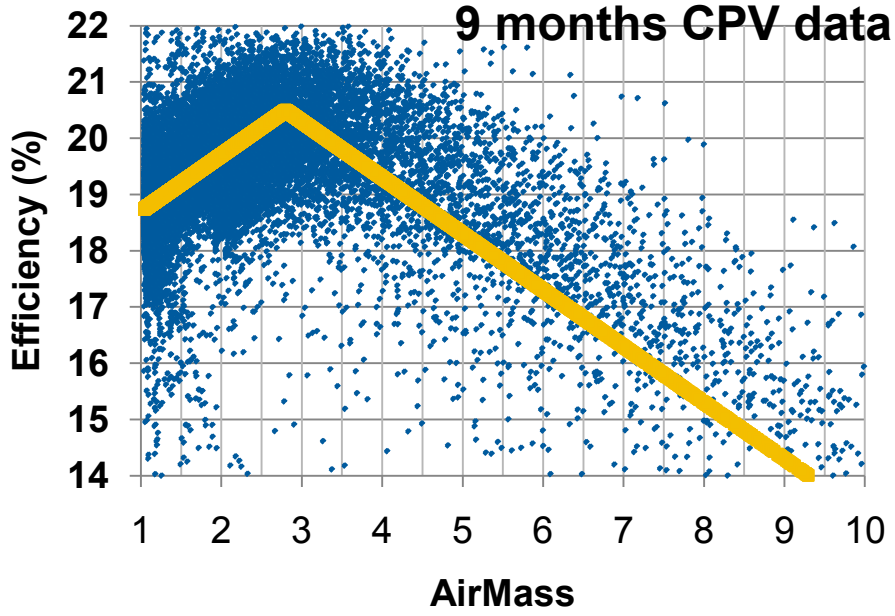
•New regressions were tested on yearly data sets using linear and nonlinear combinations of the variables on the previous slide

•The "best fit" for yearly data, judged by lowest standard error and the Tstat on the included variables, was $Power_{temp\ corrected} = a_1 DNI + a_2 DNI^2 + a_3 AM + a_4 WaterVapor$

• The existing ASTM regression with AM included also performed well.

•When the "best fit" and the modified ASTM regression were tested on monthly data the monthly variation in power became worse. (Graphs show one reason why)





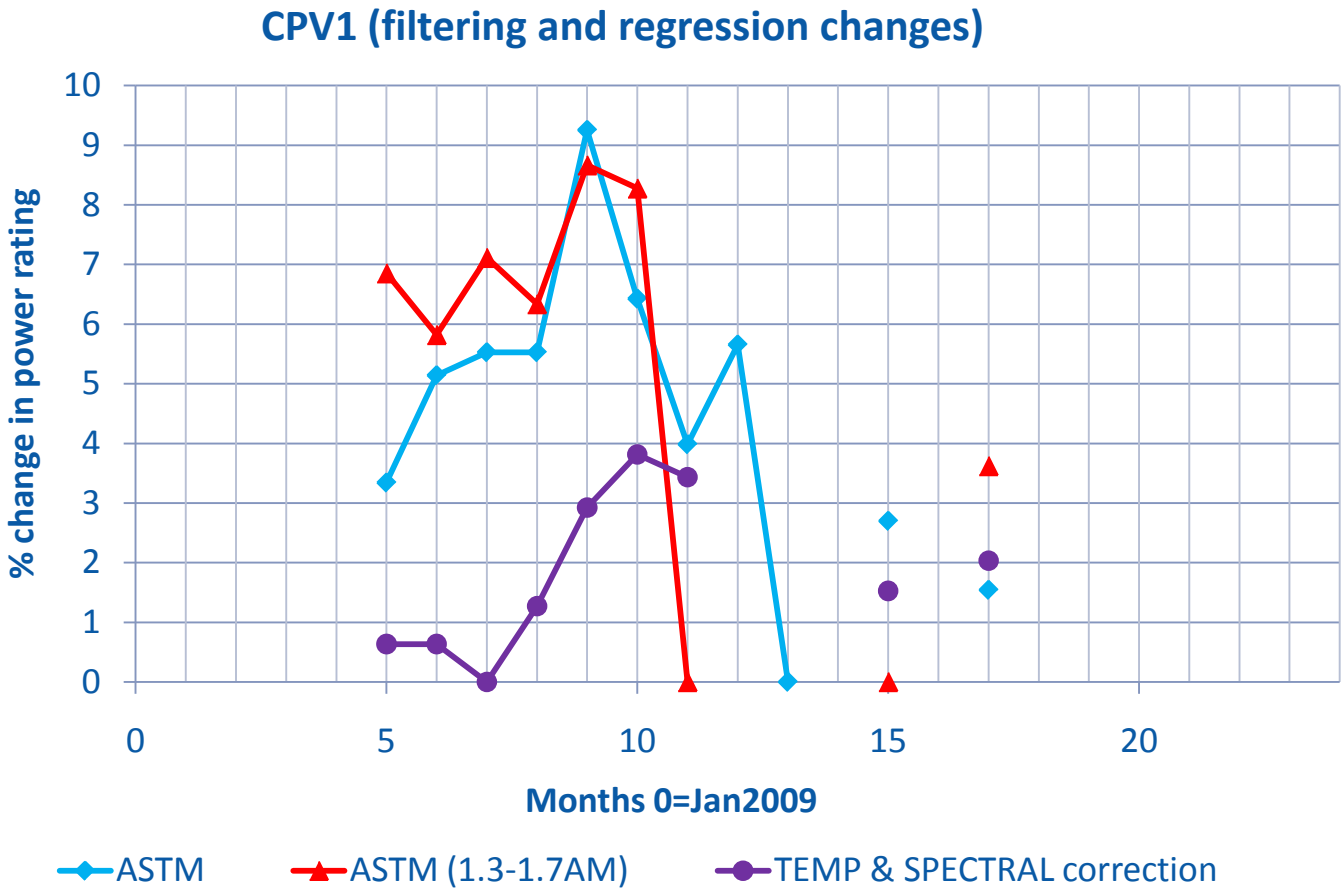
- The graphs on the previous slide show how monthly regressions can fail to accurately model spectral performance variations

- As an alternative, can spectral filtering (specifically limitting airmass from 1.3 to 1.7) reduce variation in the ASTM power rating?

- As another alternative, would variation be reduced if monthly data is corrected for temperature, airmass, and precipitable water vapor before running a simple regression using DNI and DNI^2?
  - Only accept airmass values less than 2
  - Assume efficiency increases 1% absolute per unit of AM
  - Assume efficiency increases 0.6% per cm of PWV
  - Exclude any data points that have a PWV below 0.4cm
  - Exclude ambient temperatures below 15C

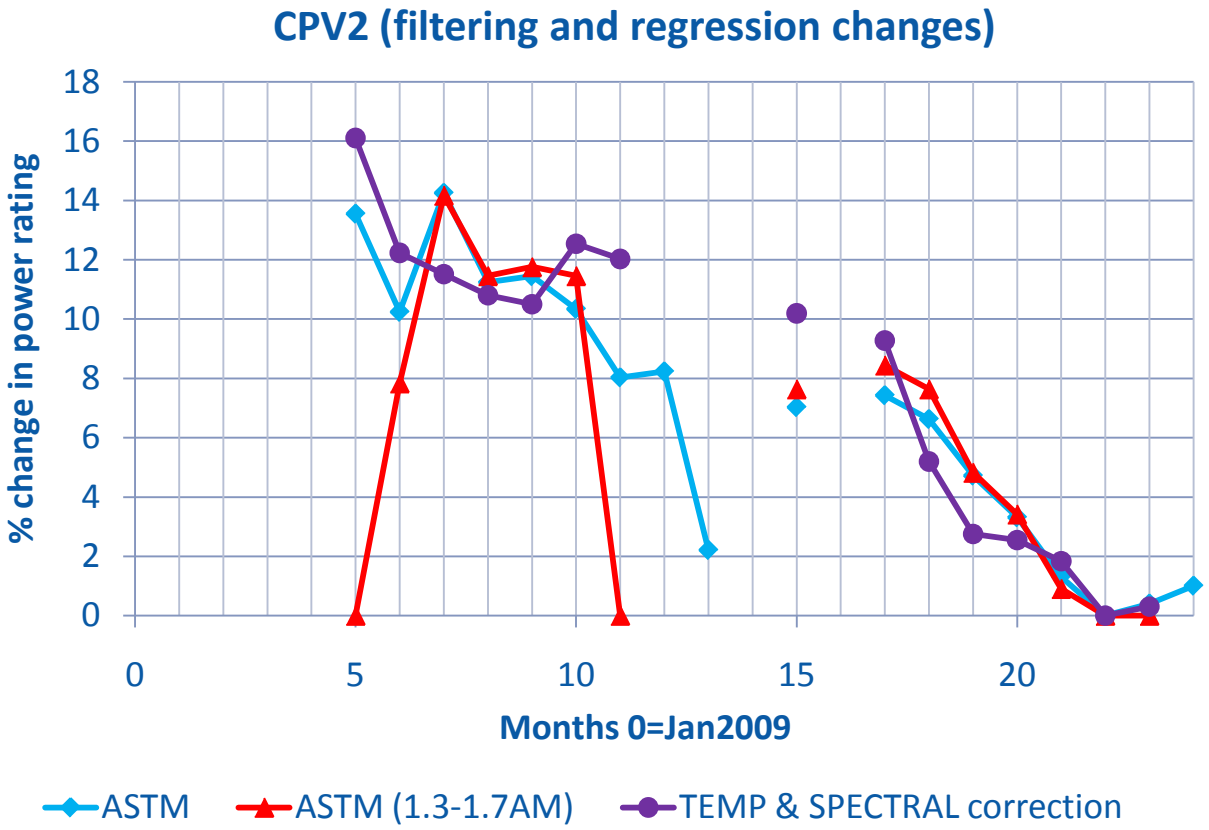
Regression modification results CPV1

- The tight filter on airmass eliminates Dec ,Jan but there is still ~9% variation
- The simple regression with corrected data reduces variation to ~4%



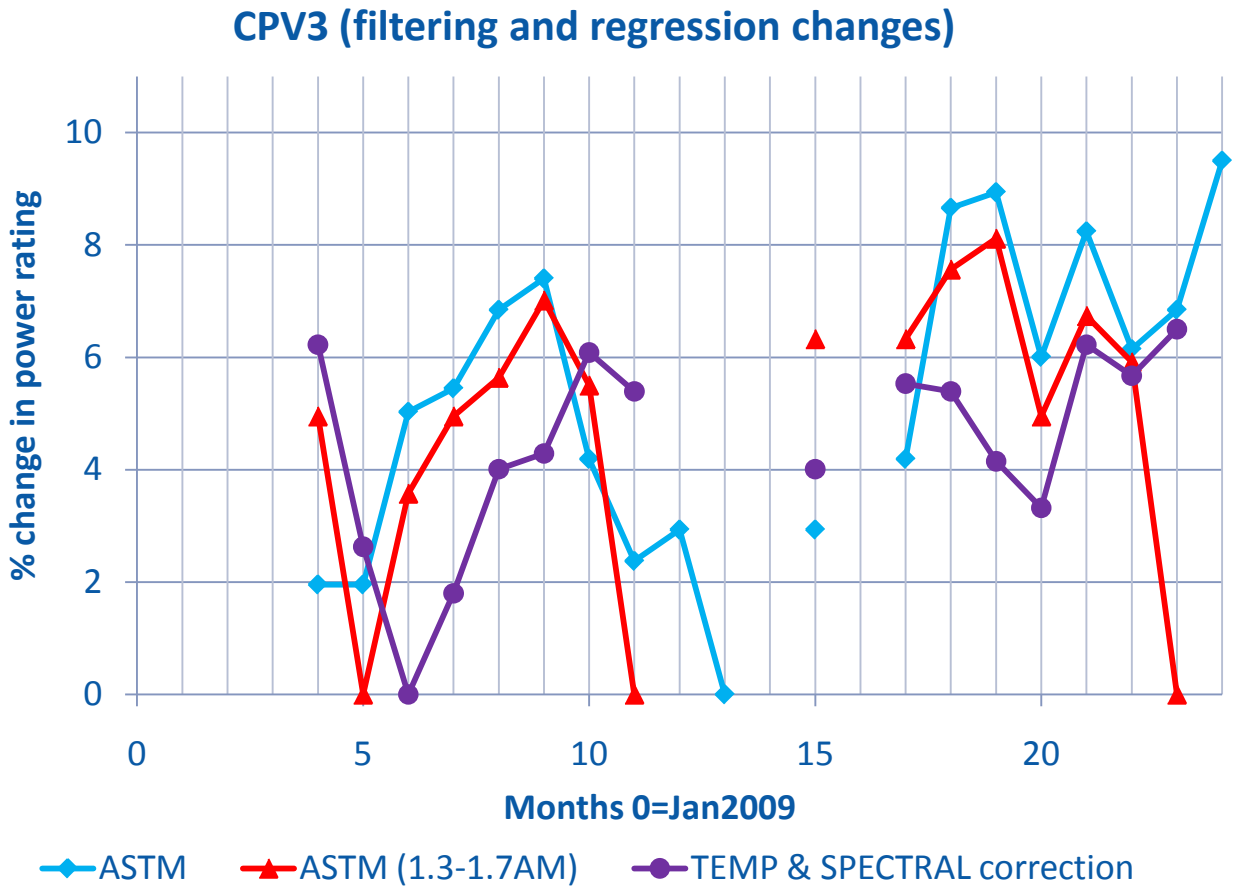
Regression modification results CPV2

- Airmass filtering again removes Dec,Jan but variation is still high
- Ignoring 2010 degradation, corrected data has a variation of ~6%



Regression modification results CPV3

- Again airmass filtering removes Dec, Jan with only a slight reduction in variation
- Corrected data still has a variation of 6.5%, June 2009 looks questionable



Conclusions and Recommendations

- Data sets for outdoor CPV power ratings should not include data points with a geometric airmass greater than 2
  - Performance begins to decline at airmasses greater than 2 or 3
  - This does little to help predict performance at AM1.5
- Ambient temperatures below 15 C have the potential to skew power ratings due to lens misalignment at low temperatures (true for some modules)
- Monthly regressions as a method for calculating CPV outdoor power ratings show too much variation (At least for data collected in Golden Colorado)
- Correcting outdoor data for temperature and spectral variation shows some potential to reduce month-to-month variation in outdoor CPV power ratings.

NREL
NATIONAL RENEWABLE ENERGY LABORATORY

International Quality Assurance Standards



PV Module Reliability Workshop

Golden, CO

Sarah Kurtz, Peter Hacke, John Wohlgemuth, Michael Kempe, Masaaki Yamamichi, Participation of others is solicited

February, 2011

This presentation has no confidential information

NREL/PR-5200-51123

NREL is a national laboratory of the U.S. Department of Energy, Office of Energy Efficiency and Renewable Energy, operated by the Alliance for Sustainable Energy, LLC.

Background

Many are asking for tests to make more quantitative predictions about PV modules:

- Companies: want to test to validate warranty
- Customers: easily compare quality of products
- Investors: establish acceptable risk
- Insurance companies: calculate risk

Many groups have begun developing tests that "go beyond IEC 61215"

Quality Assurance
(two parts)

1. Quality of design to withstand stresses in local environment (defined by climate and application)
2. Consistent quality from manufacturing line

We propose:

To work together internationally to create quality assurance standards – we will discuss this at a workshop in Japan in May, 2011

Benefits of Semi-quantitative QA Standards

- Customers can more easily assess quality/durability of products and choose the product that best meets their needs
- PV companies can better align product design with desired applications, potentially enabling lower costs
- Established companies can differentiate their (more durable) products
- New companies can better demonstrate durability of their new products
- Investors can better assess risk for investments anywhere in the world
- Insurance companies can begin to relate field performance to QA history

Example of Possible Rating System – Presented to Stimulate Discussion

Stress	Rating system	Accelerated test	Environmental definition
Voltage	Numeric value for maximum system voltage	As per IEC 61215, or revised to be applied during damp heat	System voltage
Temperature	Classes Hottest, Hot, Warm, Cool	Damp heat, possibly with voltage bias applied	Estimate assuming Arrhenius type behavior and create maps for rack and roof mounting
Thermal cycling	Class A, B	Thermal cycling as per IEC 61215, but two levels of 400 or 1000 cycles	Make map; partly cloudy locations have fastest degradation
Humidity	Class Humid, Dry	Damp heat, possibly with voltage applied	Average humidity; make map
Snow	Numeric rating for kg of static load	IEC 61215 static load test	Snow load from local building code
Marine environment	Numeric severity rating	Existing IEC test	Distance from ocean
Hail	Numeric rating for size of hail ball	Current default is 25 mm; method is already defined in 61215	Generally, people know the size of hail to plan for, but maps are not easily available
UV	Class A, B	Class A designed for high-altitude site	
Wind	Numeric rating for maximum wind gust	Combination of dynamic load test, vibration, and?	Maximum wind speed seen during gusts; available through weather data
Transportation	Rough/Smooth	Vibration	Type of transport: truck on paved and unpaved roads, train, etc.
Farmland	Pass/Fail	Use ammonia test being drafted by WG2	Agricultural area

Steps to Creating Quantitative Test

1. Define most important failure mechanisms to quantify
2. Collect suggestions for useful tests from engineers around the world (leveraging years of testing experience)
3. Select tests that have the potential to be useful (cost effective way to obtain valuable information)
4. Apply new tests to modules with known field experience
5. Create new IEC standard to define semi-quantitative tests that were useful
6. Through modeling, provide community with maps to show how the test results relate to field performance in different climates/applications

Failure Mechanisms
Which are most important to quantify?

Type of failure/degradation	Related stresses
Broken interconnects, solder bond failures	Thermal cycling, mechanical
Broken cells	Thermal cycling, vibration, mechanical
Corrosion, including electrochemical corrosion; corrosion leading to loss of grounding	Humidity, heat, bias V, dry/wet high pot
Delamination and/or loss of elastomeric properties of encapsulant	Humidity, heat, humidity-freeze, UV, dry/wet high pot
Encapsulant discoloration	UV, heat
Broken glass; structural failures	Mechanical
Hot spots	Hot spot
Junction box and module connection failures	Thermal cycling, humidity, heat, humidity-freeze
Bypass diode failure	Heat (applied to diodes)
Open circuiting leading to arcing	Thermal cycling
Ground fault from backsheet degradation	UV
Ground faults	Dry/wet high pot

Many of the tests are easy to make quantitative

- Thermal cycling test can easily be extended to more cycles
- Mechanical load is already defined to allow testing for different loads and some companies already use glass of different strength for high snow-load applications
- Hail test already allows testing for different size hail balls
- Salt spray test is already defined for multiple environments

QA of Manufacturing Process

- Currently each company has its own QA program (some are better than others)
- Currently there is no consensus guideline for factory inspection or periodic retest
- If a company gets a 61215 certification from a test lab that does not do factory inspections, the certificate may remain valid indefinitely even if the company maintains no QA program – how does a customer know?
- Is IECEE the right organization to implement the needed guidelines, using standards defined by other standards organizations?

Primary Challenge

Combined effects of temperature, humidity, voltage bias and light are very difficult to quantify

- These stresses appear in the environment in highly varying ways
- Simultaneous application of these stresses is expensive
- How can we define a “damp heat test with bias voltage” that can be quantitatively correlated with field performance?

Possible approaches

- UV may be applied to mini module with similar structure
- Voltage bias may be applied during damp heat
- To define four levels of thermal endurance, we could use two different temperatures and two different times

History of Si module qual. test: JPL (Jet Propulsion Lab) Block buys

Test	I	II	III	IV	V
Year	1975	1976	1977	1978	1981
Thermal Cycle (° C)	100 cycles -40 to +90	50 cycles -40 to +90	50 cycles -40 to +90	50 cycles -40 to +90	200 cycles -40 to +90
Humidity	70 C, 90%RH, 68 hr	5 cycles 40 C, 90%RH to 23 C	5 cycles 40 C, 90%RH to 23 C	5 cycles 54 C, 90%RH to 23 C	10 cycles 85 C, 85%RH to -40 C
Hot spots	-	-	-	-	3 cells, 100 hrs
Mechanical load	-	100 cycles ± 2400 Pa	100 cycles ± 2400 Pa	10000 cyc. ± 2400 P	10000 cyc. ± 2400 Pa
Hail	-	-	-	9 impacts 3/4” - 45 mph	10 impacts 1” - 52 mph
NOCT	-	-	-	Yes	Yes
High pot	-	< 15 µA 1500 V	< 50 µA 1500 V	< 50 µA 1500 V	< 50 µA 2*Vs+1000

JPL Block buys led to dramatic improvements – can we learn from this?

- One study claimed (Whipple, 1993):
  - Pre-Block V: 45% module failure rate
  - Post-Block V: <0.1% module failure rate

- Primary differences for Block V included:
  - 200 instead of 50 thermal cycles
  - Humidity freeze
  - Hot spot test

- If we pool the community's data, can we identify the most useful tests?

Do you have suggestions?

Write your suggestions here:

Or, contact Sarah.Kurtz@nrel.gov or any of the other authors

Acrylic Materials in PV Applications:

Making an Informed Choice

Evonik Cyro LLC
Acrylic Polymers
Peter Colburn

NREL PV Reliability Workshop Feb 17, 2011



EVONIK
INDUSTRIES

Topics

1. Outdoor Acrylic Applications
2. What is Acrylic?
3. UV Absorption Characteristics
4. Degradation Mechanisms
5. Protection Systems
6. Weathering Performance

Acrylic Use History









1930 1950 1970 1990 2010







Reliability: Proven Weatherability of Acrylic

Automotive

- Lighting
- Pillar covers
- Mirror housings











Reliability: Proven Weatherability of Acrylic

EVONIK INDUSTRIES

Architectural Glazing

















Limited (10 Year) Warranty

Acrylite® ACRYLIC SHEET

Reliability: Proven Weatherability of Acrylic

Aircraft Glazing

- Helicopter glazing
- General aircraft glazing
- Commercial aircraft cabin windows
- Fighter canopies and windshields
- Glider canopies







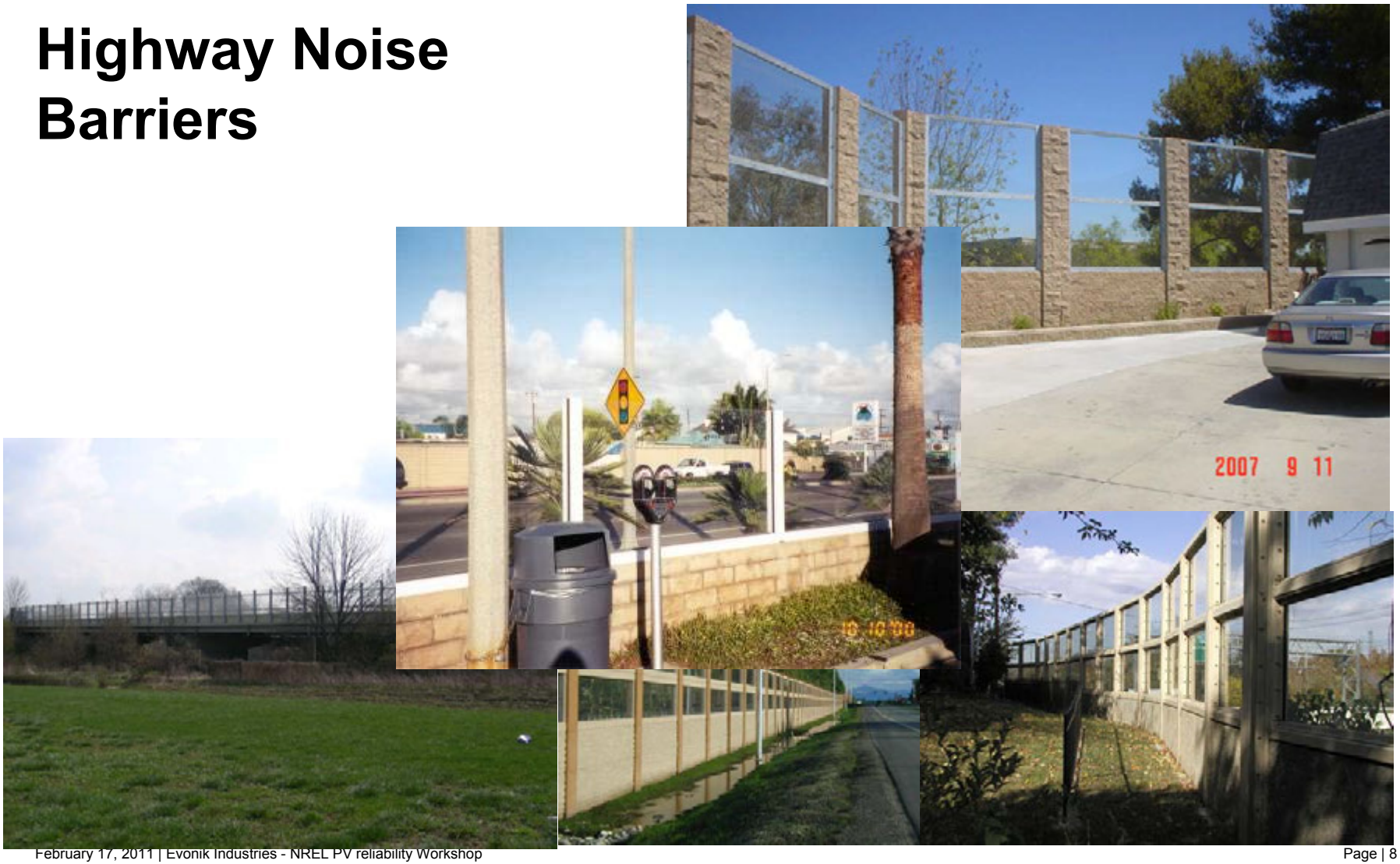
Reliability: Proven Weatherability of Acrylic

Signage



Reliability: Proven Weatherability of Acrylic

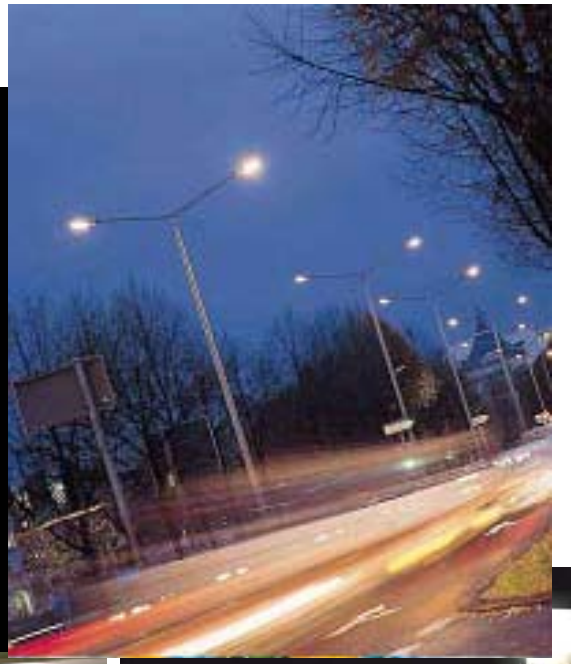
Highway Noise Barriers



Reliability: Proven Weatherability of Acrylic

HID & Outdoor Lighting Applications







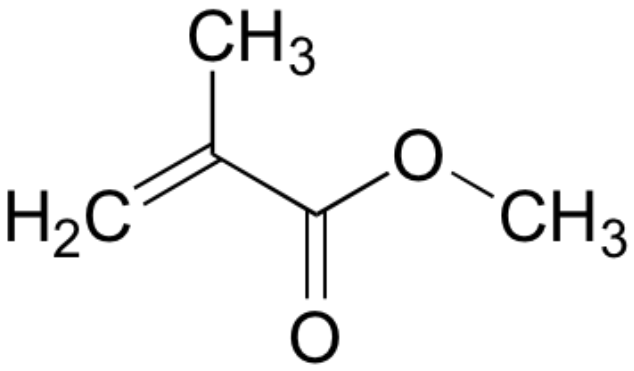




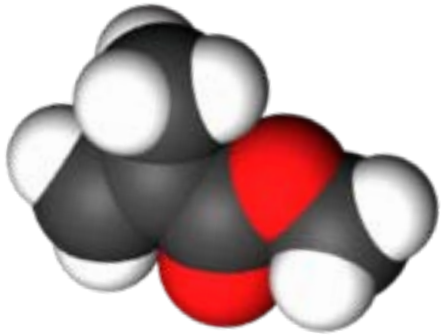
Topics

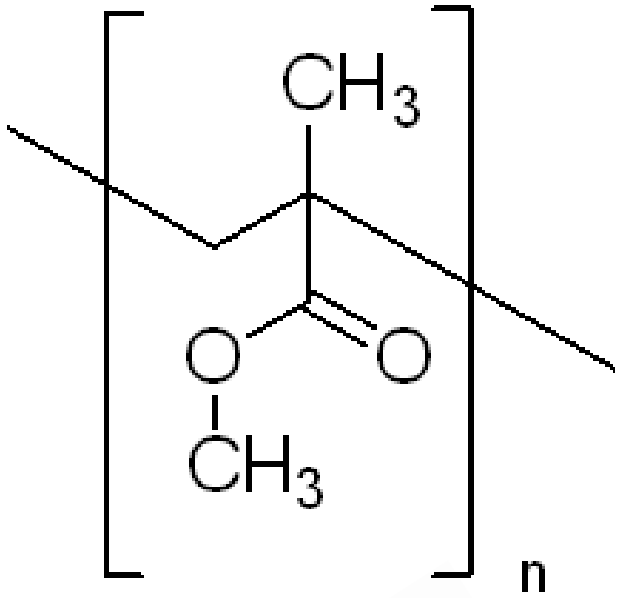
1. Outdoor Acrylic Applications
2. What is Acrylic?
3. UV Absorption Characteristics
4. Degradation Mechanisms
5. Protection Systems
6. Weathering Performance

What is Acrylic?

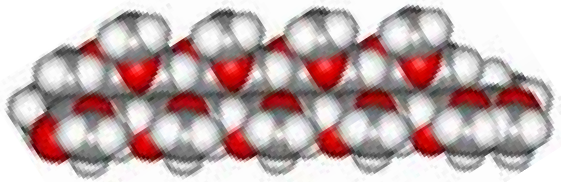


methyl methacrylate



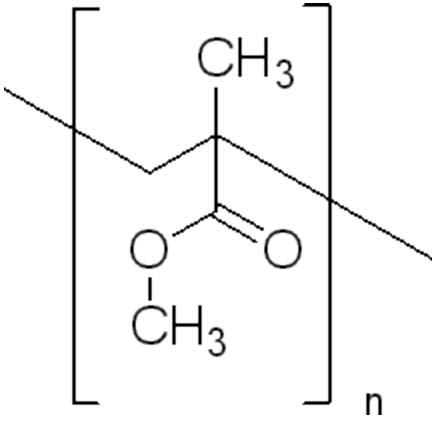


Polymethyl methacrylate



What is “acrylic”?

- Polymethylmethacrylate: -(MMA)$_n$-
  - PMMA is an ester
- Monomer – Methyl methacrylate
- Comonomer (methyl or ethyl –acrylate)
- Additives
  - Lubricants
  - Stabilizers
  - Colorants



Key Performance Characteristics

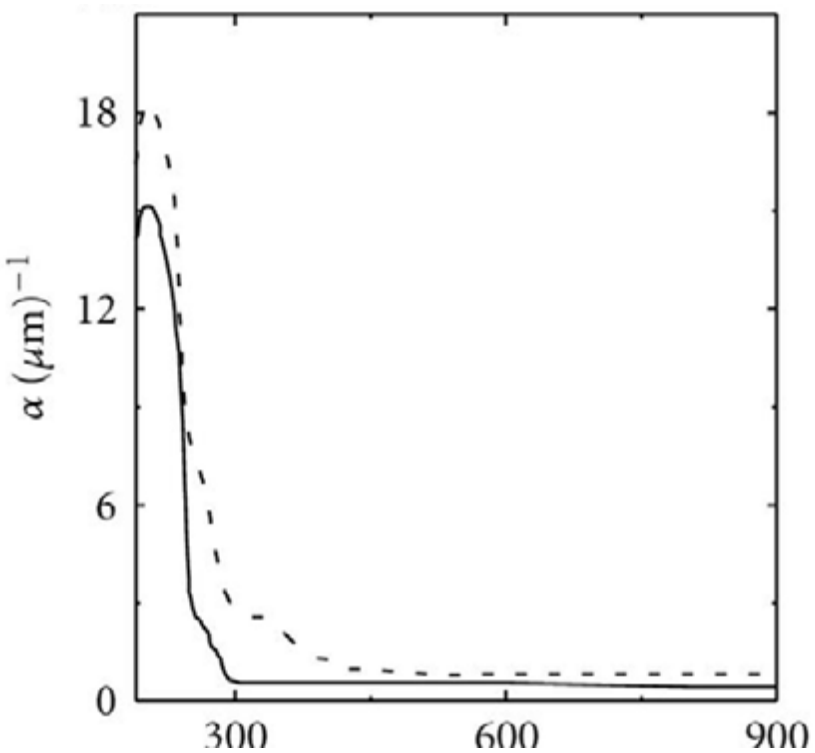
- Long Term Stability in Outdoor Environments
- Additional Protection Systems
- Excellent Surface Hardness
- Light Weight
- Outstanding Transmittance & Optical Clarity
- Optical Design Flexibility and Control

Topics

1. Outdoor Acrylic Applications
2. What is Acrylic?
3. **UV Absorption Characteristics**
4. Degradation Mechanisms
5. Protection Systems
6. Weathering Performance

UV Stability

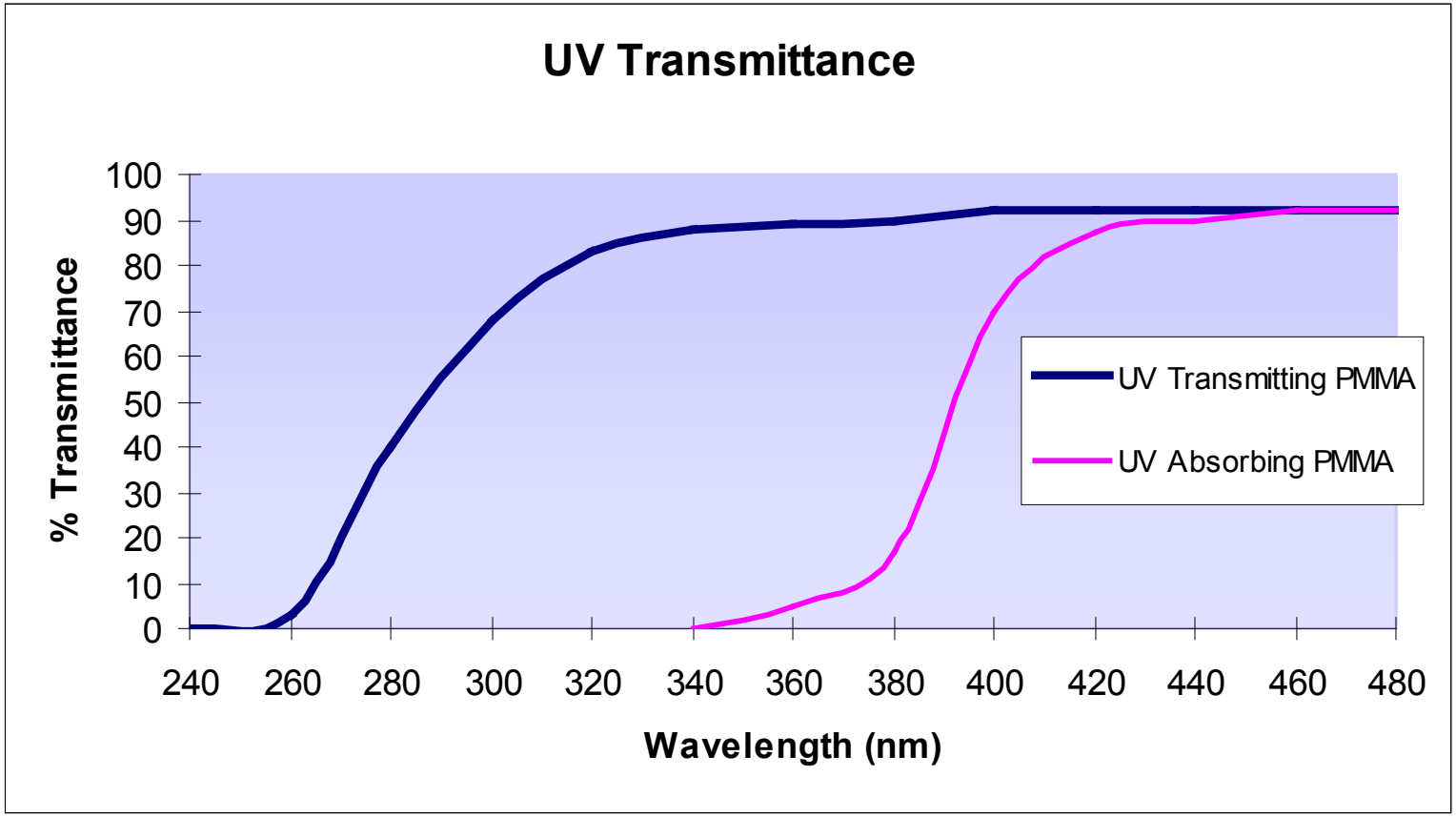
The outstanding stability of PMMA to sunlight results primarily from weak absorption of acrylic in the UV-region.



R.M. Ahmed, International Journal of Photoenergy, Volume 2009 (2009), Article ID 150389, "**Research ArticleOptical Study on Poly(methyl methacrylate)/Poly(vinyl acetate) Blends**

UV Stability

Acrylic is naturally UV transmitting, and can be modified with UV protection systems.



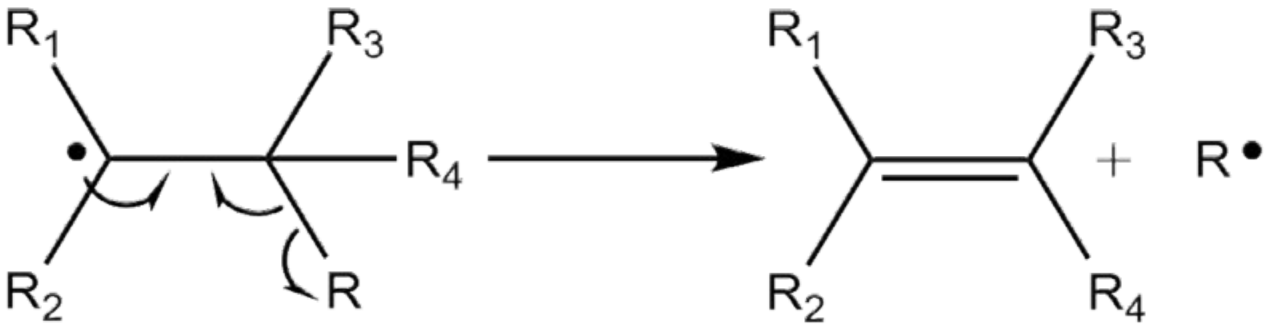
Topics

1. Outdoor Acrylic Applications
2. What is Acrylic?
3. UV Absorption Characteristics
4. **Degradation Mechanisms**
5. Protection Systems
6. Weathering Performance

Degradation Mechanisms

Chain scission by exposure to extreme temperature or radiation conditions produces alkyl radicals that can react with oxygen to form peroxy radicals, chain termination can lead to creation of aldehydes, ketones or alcohols. Activation energy is ~260 kcal/mole at 130,000 mw. **Thermal degradation of polymeric materials**, Krzysztof Pielichowski, James Njuguna, 2005, pg 101

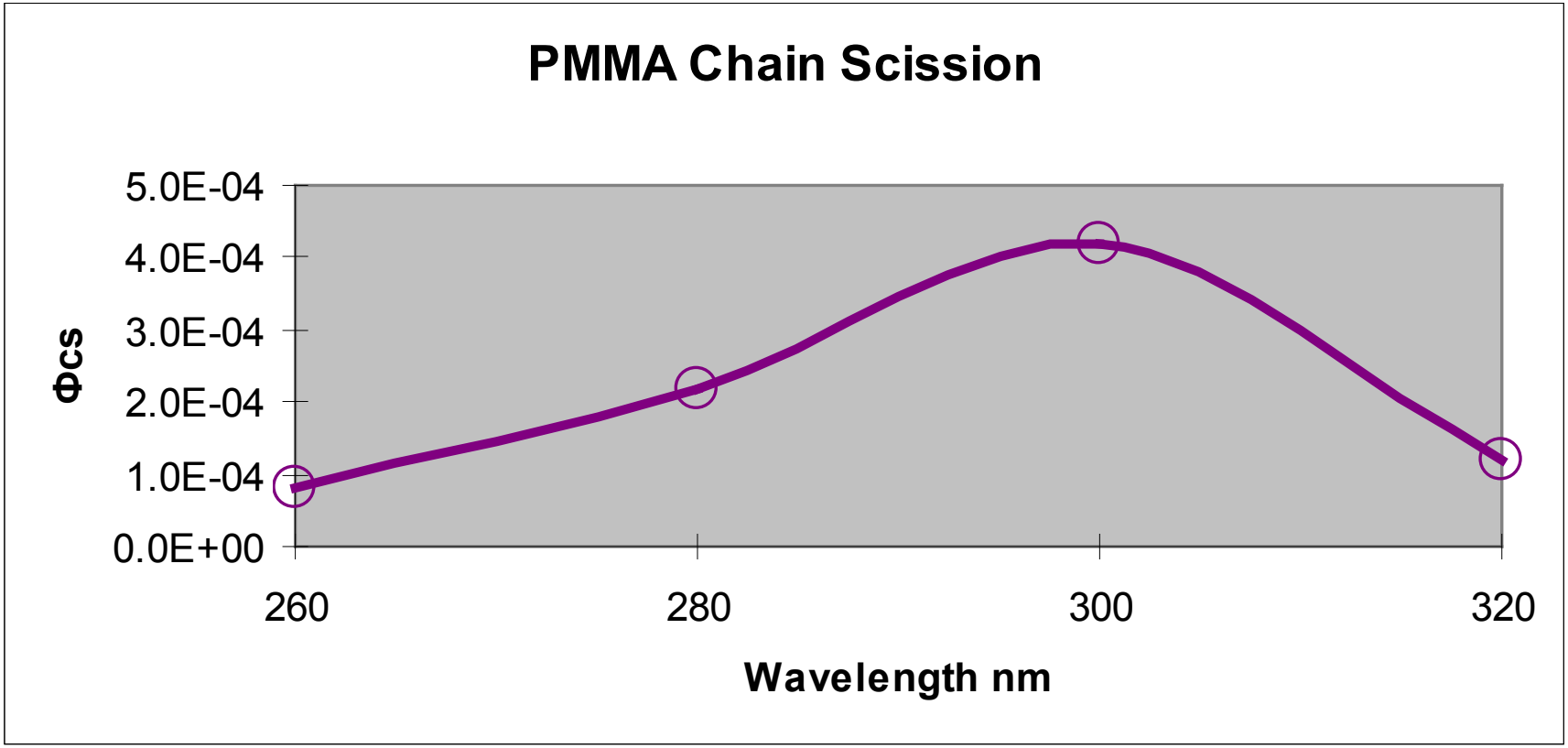
Alkoxy radicals may abstract H or undergo beta-scission. (unlikely).



Beta scission mechanism

Degradation Mechanisms
Main Chain Scission - PMMA

The quantum yield for main-chain scission of polymethylmethacrylate shows a maximum at 300 nm.



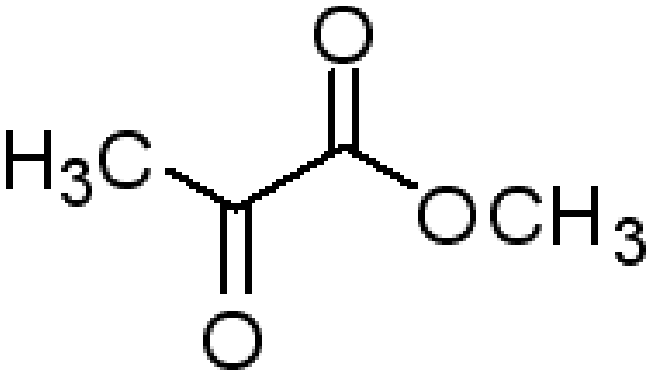
Mitsuoka, T.; Torikai, A.; Fueke, K. *J. Appl. Pol. Sci* **1993**, *47*, 1027

Photo-oxidation

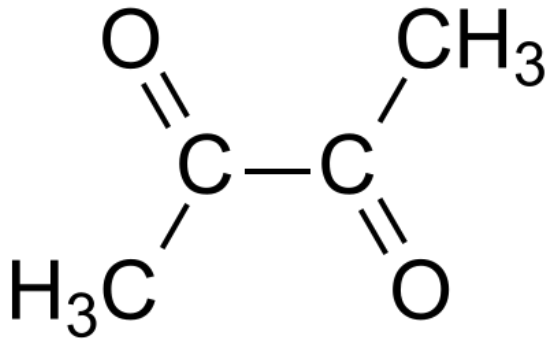
- Initiation of PMMA photo-oxidation is attributed to the decomposition of the ester groups by radiation in the range of 300-330 nm.
- In the presence of oxygen, radical-initiated oxidation occurs with the onset of photolysis.
- Another initiation scenario is the sensitizer effect of MMA-monomer: A photo-excited residual monomer transfers its energy to oxygen yielding singlet O_2 which reacts with monomer to form a hydroperoxide.

Oxidation of Residual MMA

In pyrolysis, polymethylmethacrylate can degrade via oxidation of by-products into methyl pyruvate or diacetyl.[1] Oxidation of residual MMA can produce these products as well. These materials are chromophores that can cause yellowing.



Methyl pyruvate

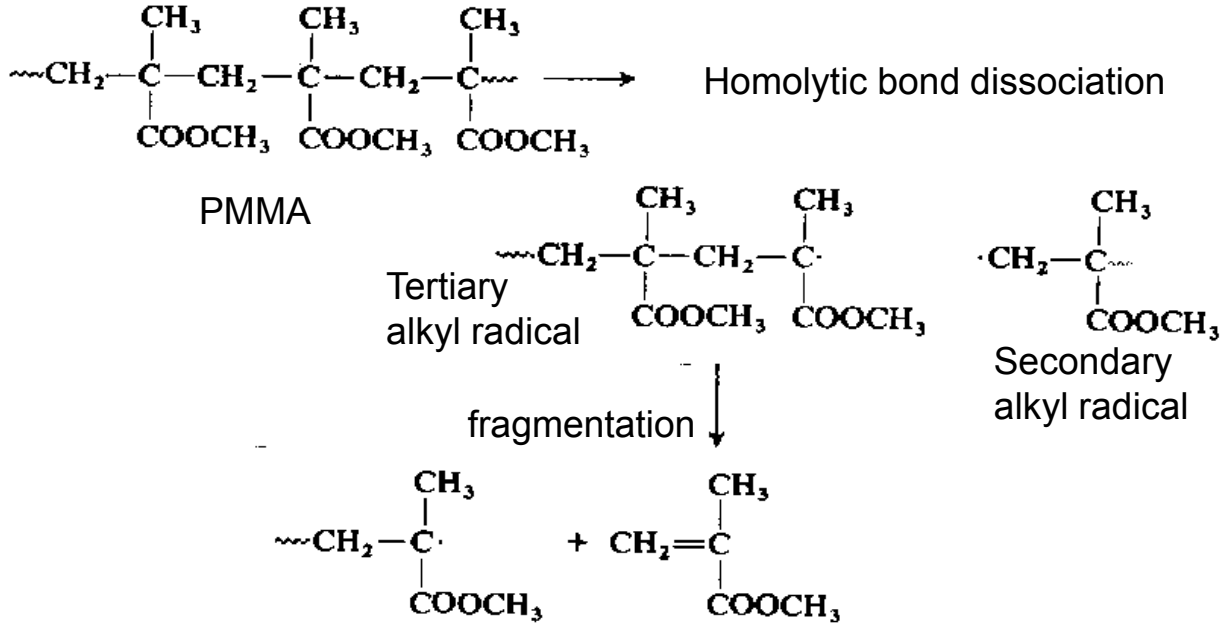


Diacetyl (2,3-butanedione)

1. Mukundan, Thekkekara and Kishore, Kaushal (1987) *Structure and pyrolysis of poly(methyl methacrylate peroxide): a thermochemical approach.* In: Macromolecules, 20 (10). pp. 2382-2385.

Thermal Effects

- Degradation occurs in processing above 300°C.
- Oxidation and chain scission can be accelerated at temperatures above 90°C in the presence of intense UV radiation in the range of 300-330nm.



Topics

1. Outdoor Acrylic Applications
2. What is Acrylic?
3. UV Absorption Characteristics
4. Degradation Mechanisms
5. **Protection Systems**
6. Weathering Performance

Protection Systems

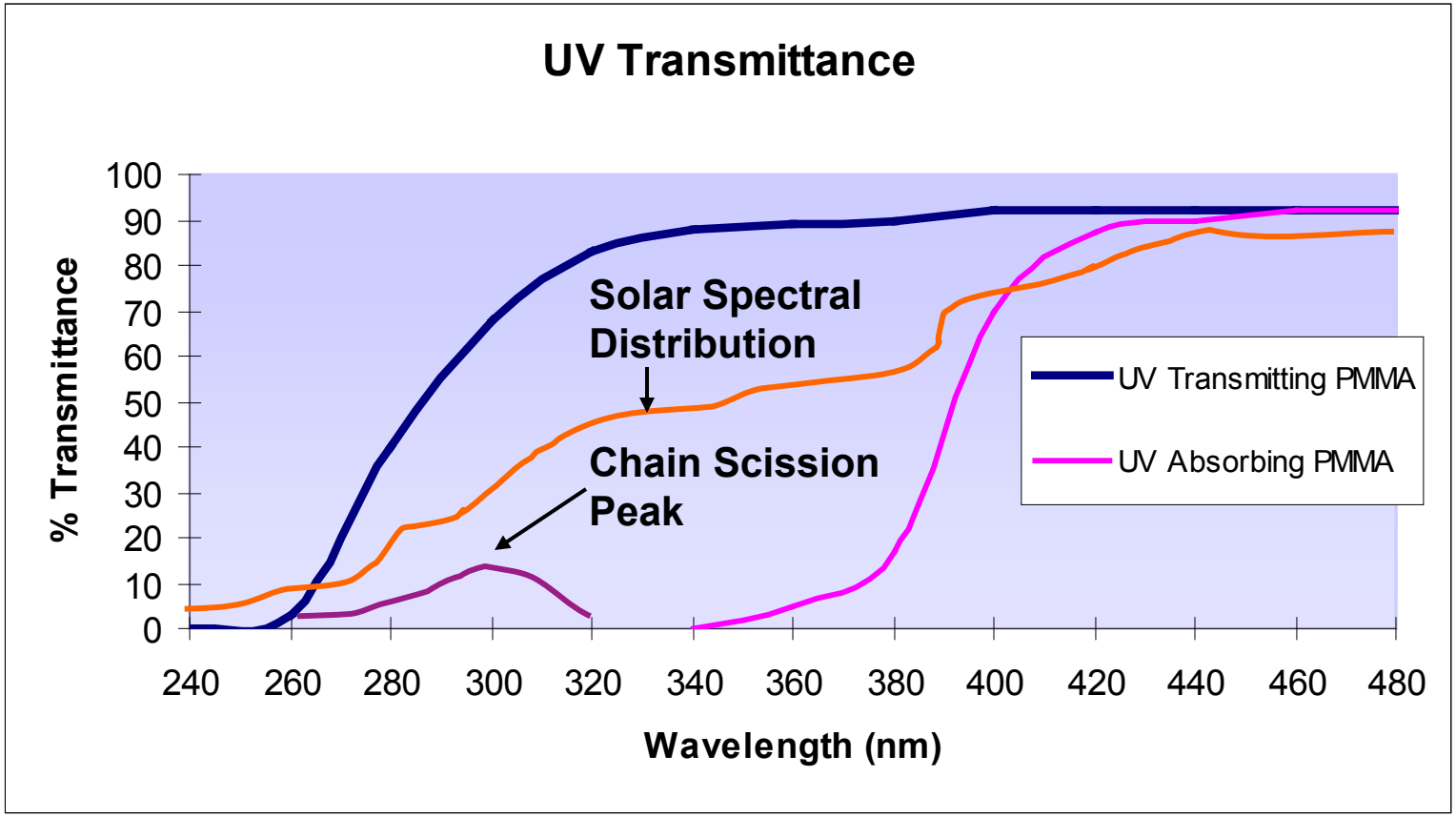
UV Absorbers

STABILIZERS

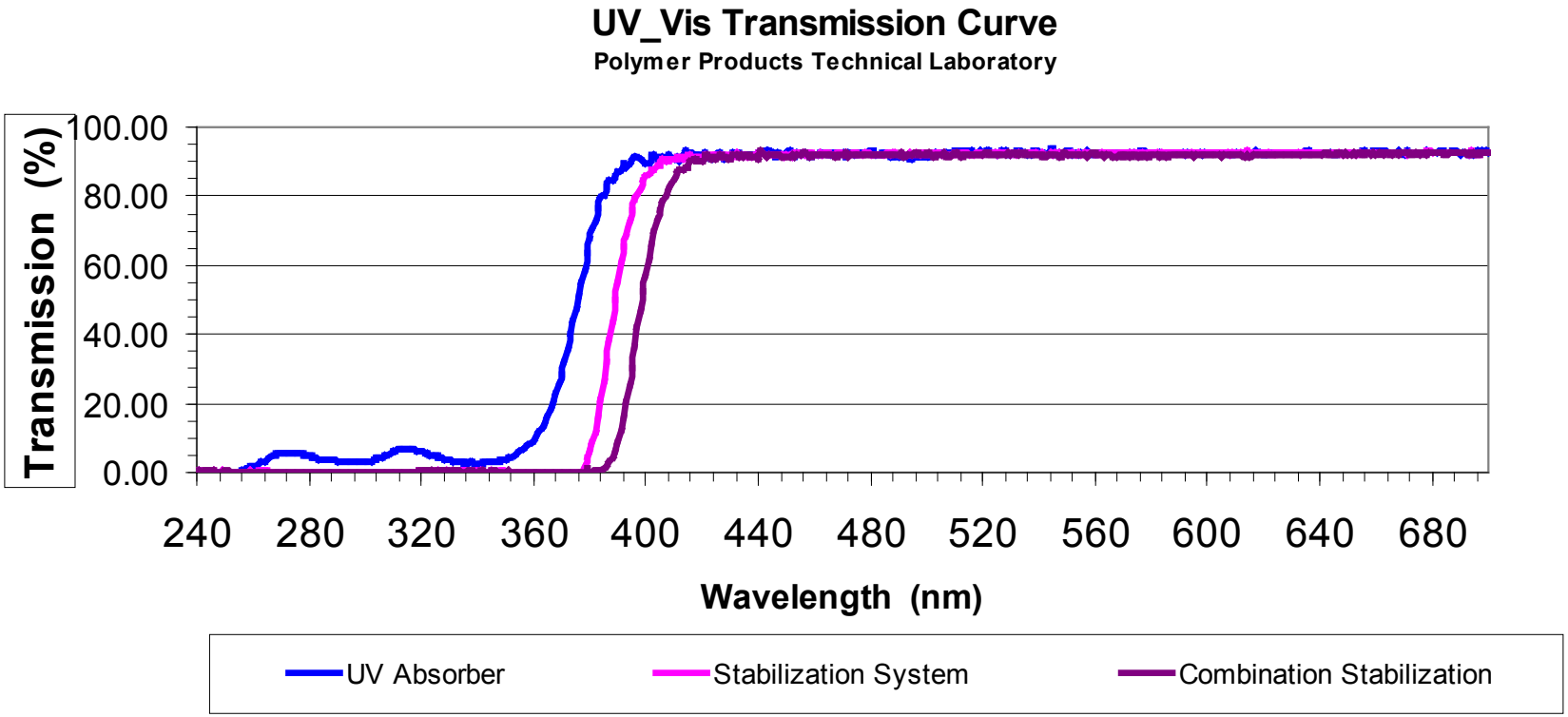
Combination Systems

Protection Systems

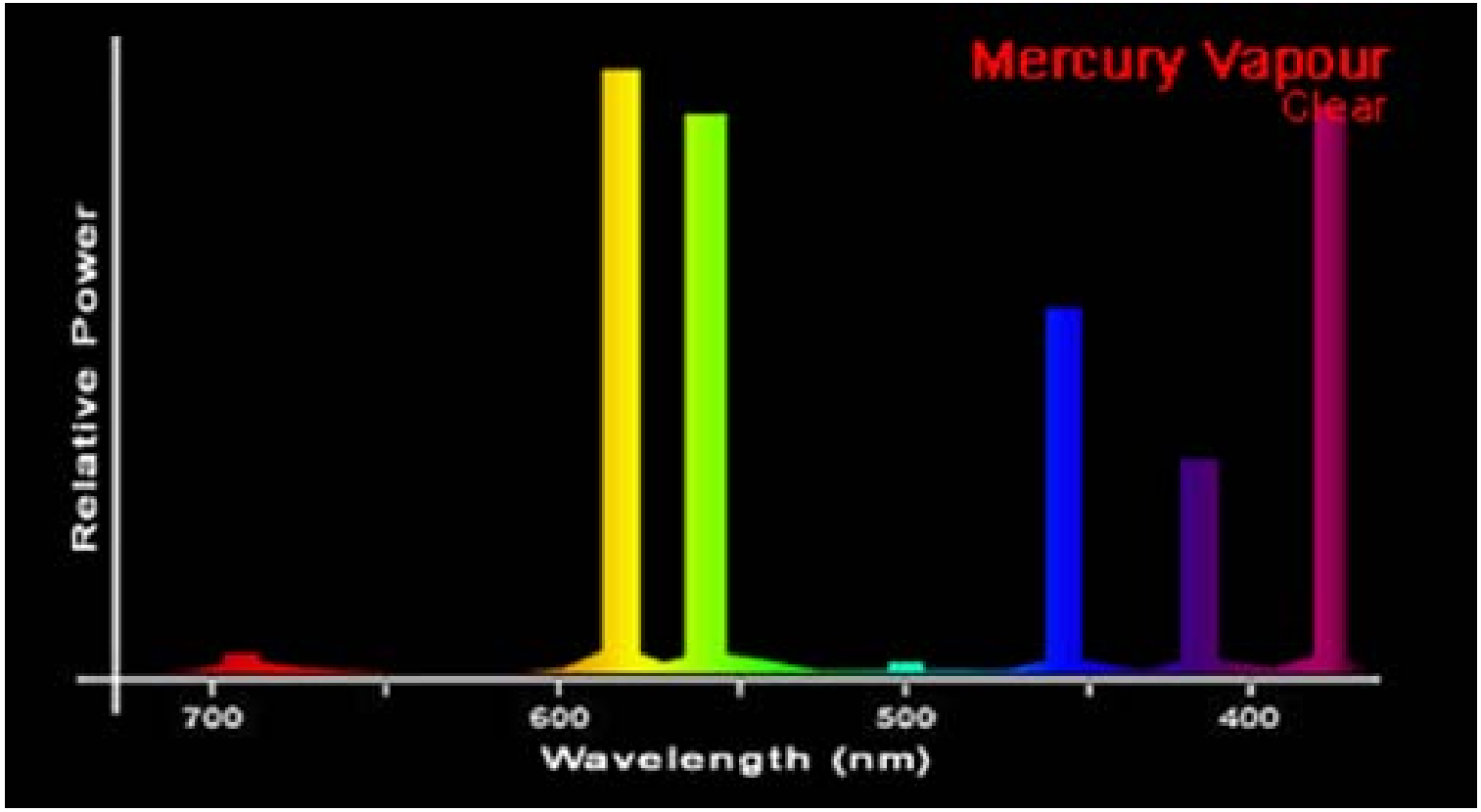
UV Absorbing PMMA blocks UV light in the region at which chain scission peaks.



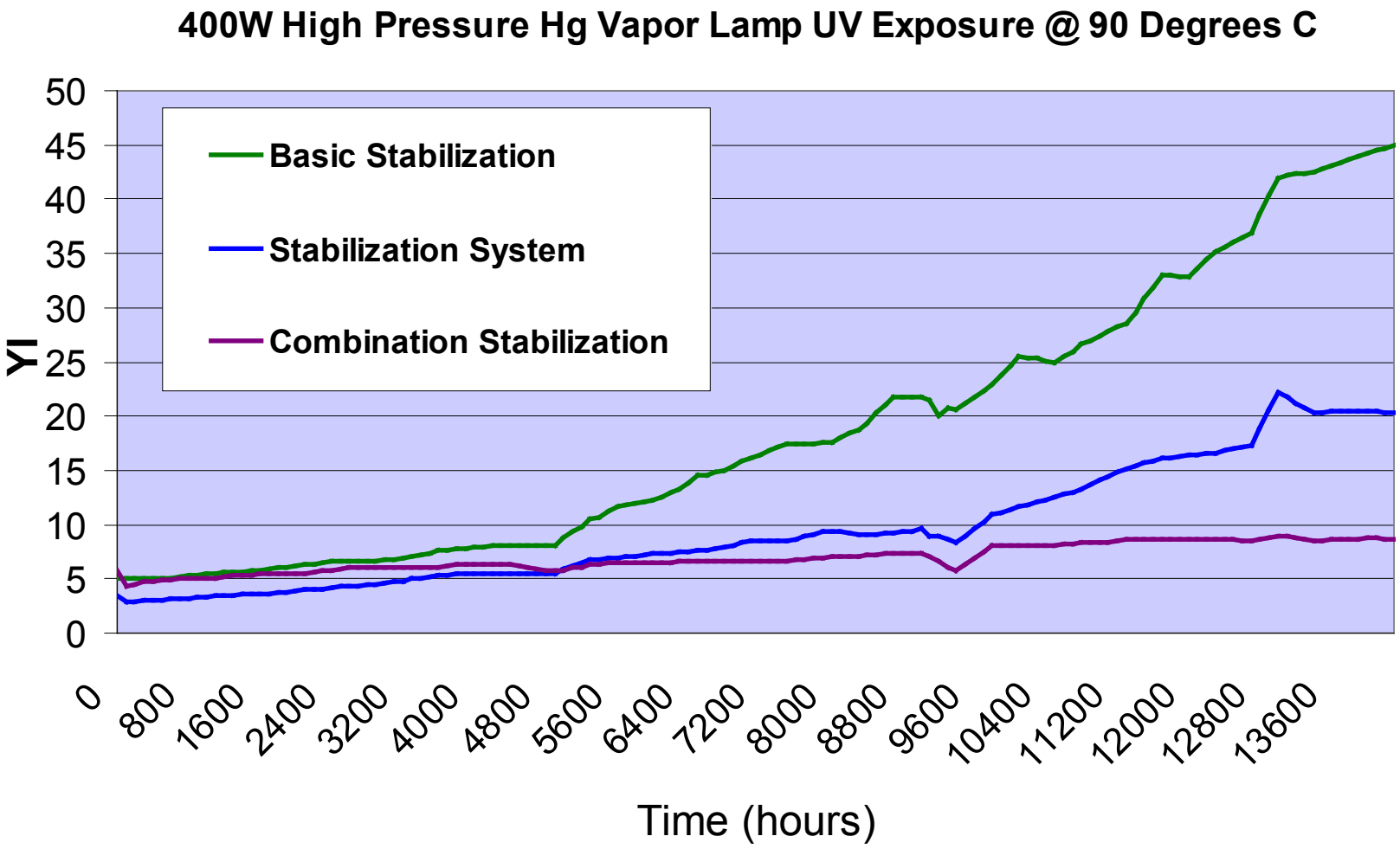
Protection Systems



High Pressure Hg Vapor Lamp



High Intensity UV and Heat Exposure



Topics

1. Outdoor Acrylic Applications
2. What is Acrylic?
3. UV Absorption Characteristics
4. Degradation Mechanisms
5. Protection Schemes
6. **Weathering Performance**

Weathering Variables

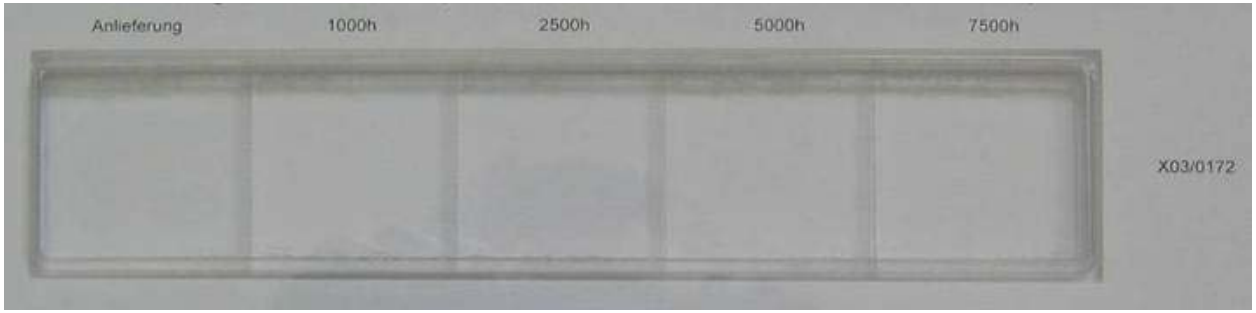
sun radiation (UV + vis + IR)
+ water (moisture)
+ mechanical stress (from diffusion, temperature, …)
+ temperature changes
+ microorganisms (algae, fungi, …)
+ time (1a, 2a, 3a, 5a, 10a and more)



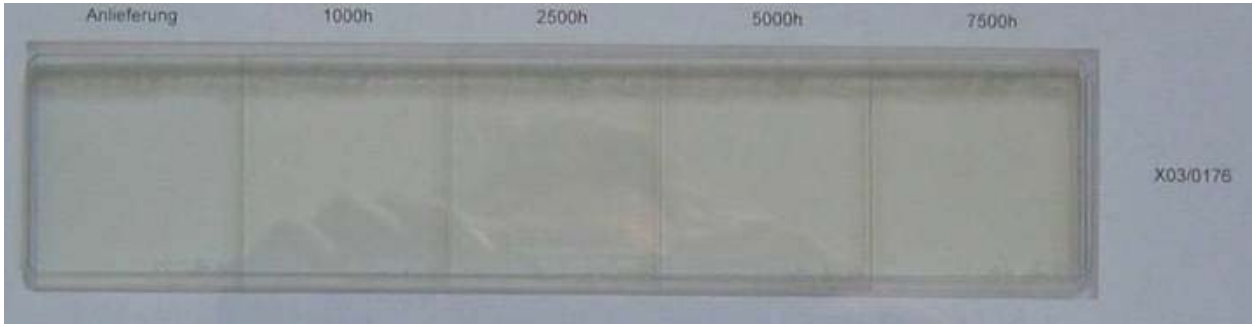


7500 hrs Xenon Arc Weathering

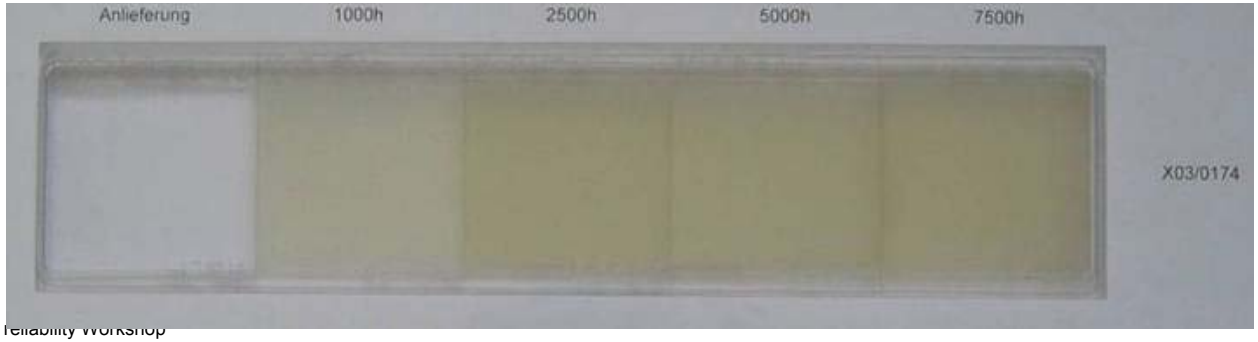
ACRYLITE®



PC UV-protected

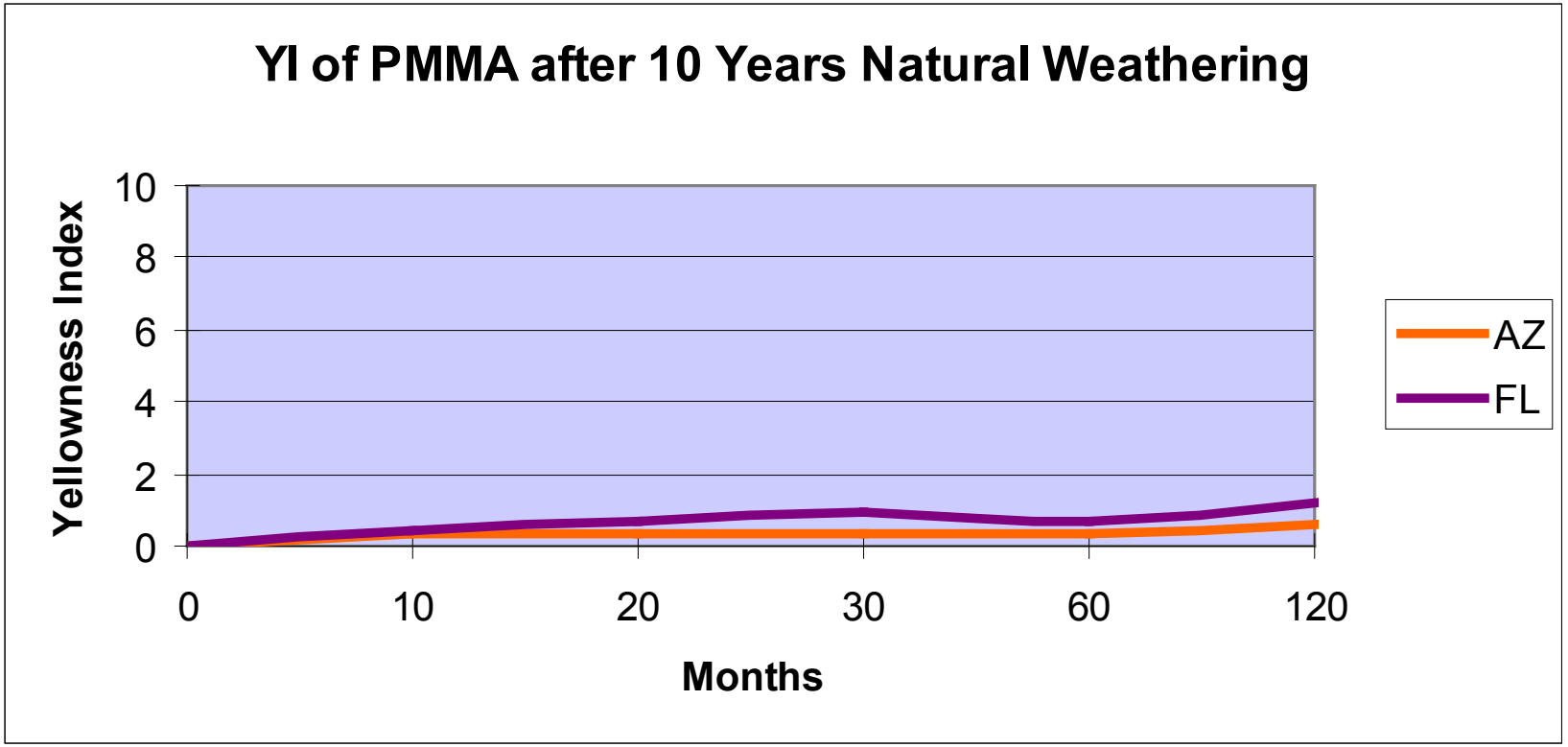


PC



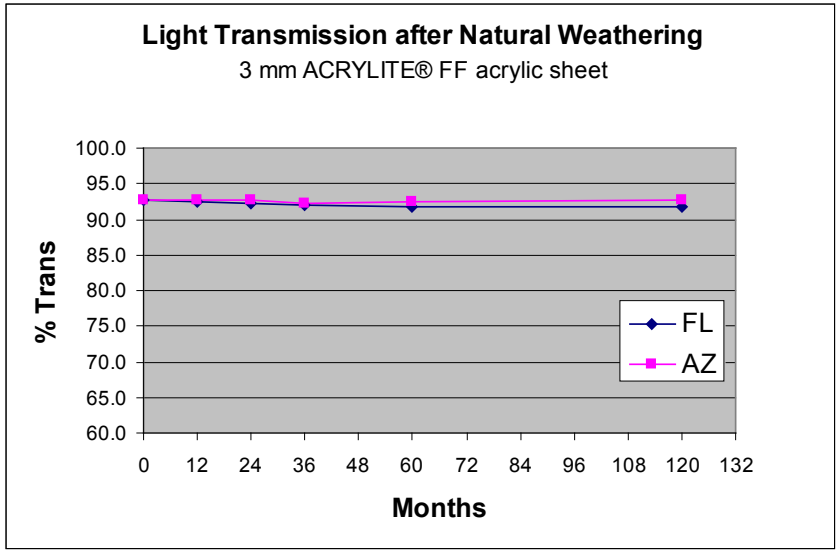
PMMA
10-Year On-Sun Weathering Results

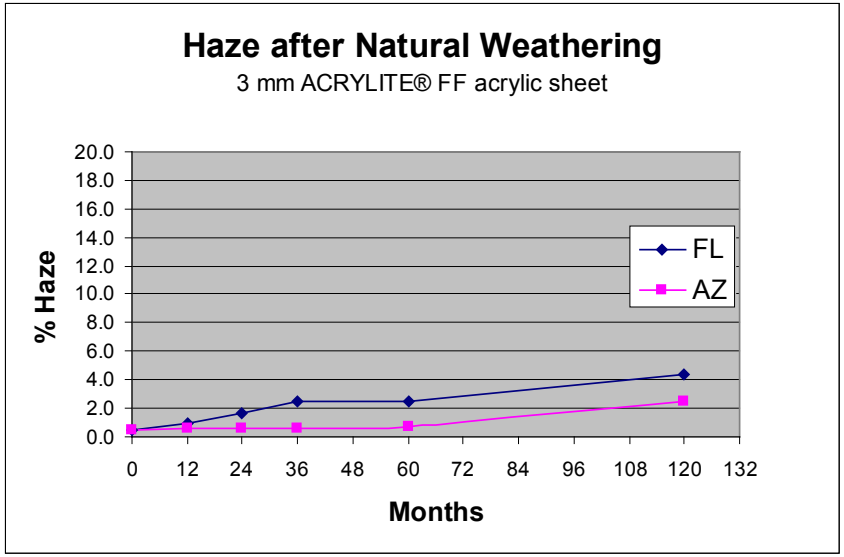
- Virtually no yellowing of acrylic in 10-year outdoor weathering in AZ and FL
- YI = 1.0 is nearly imperceptible to the eye when viewed through the material



10-Year On-Sun Weathering Results

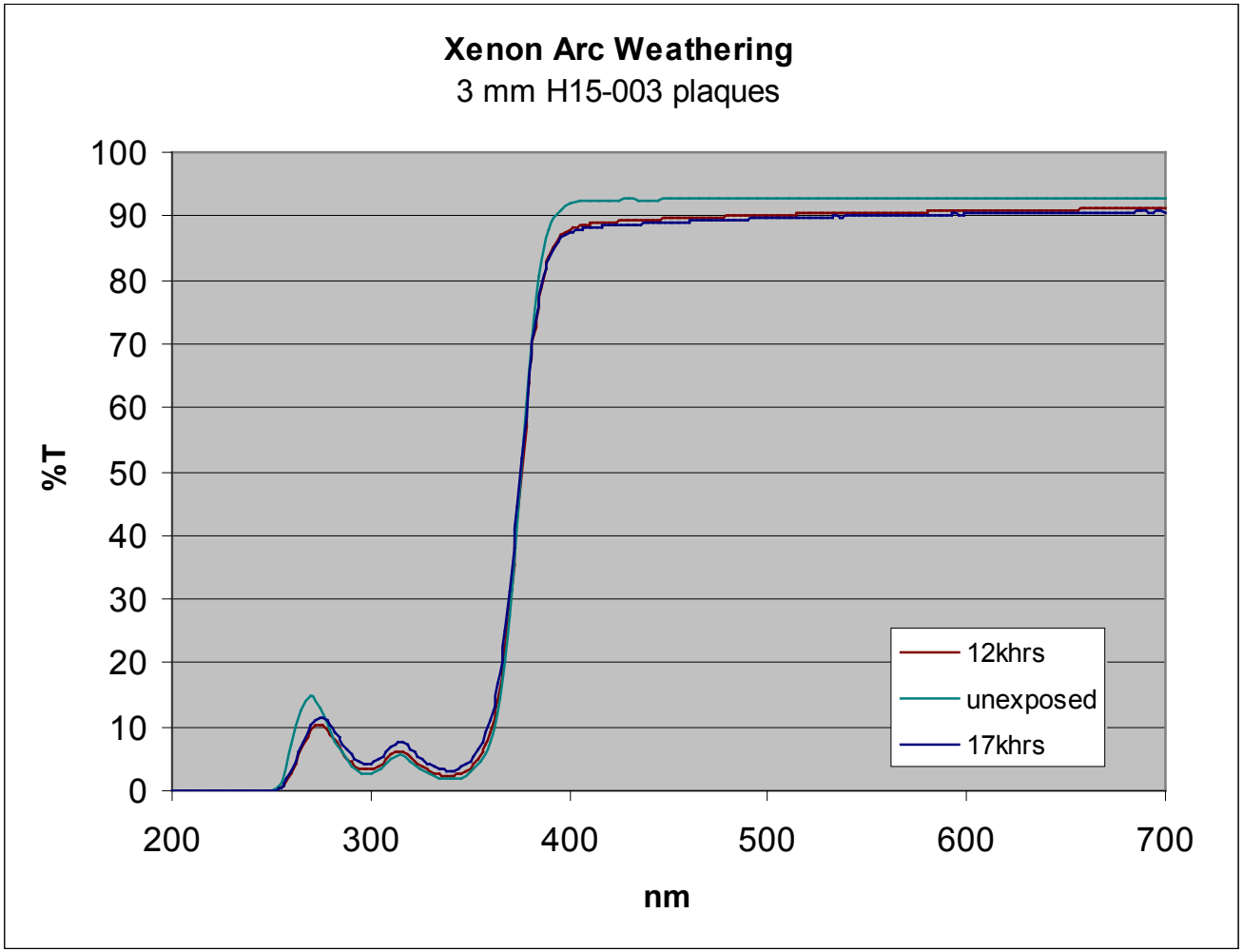
- Overall light transmission remains high and haze remains low after 10 years in outdoor weathering environments
- Florida environment has much more moisture and tends to increase haze somewhat





Xenon Arc Weathering Results

Long term stability



1khr = 1 year; “17-year” Xenon Arc Weathering %T = 88.1% @ 410 nm

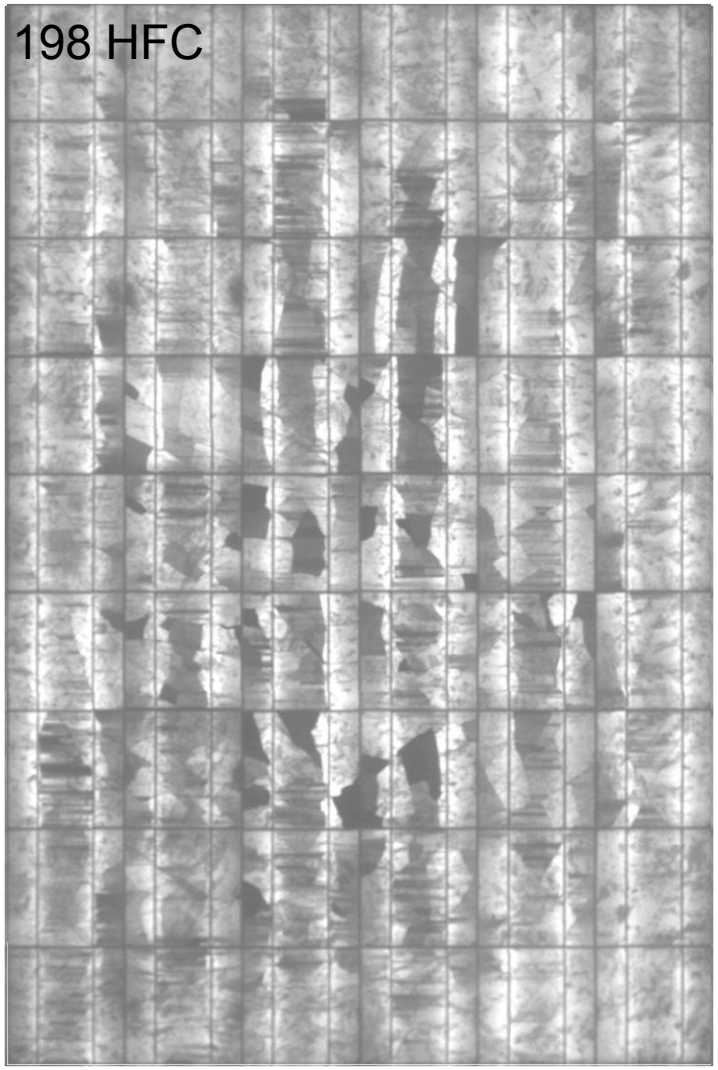
Probability of Failure

Failure Mode	Mechanism	Probability
Yellowing from UV Exposure	Oxidation of residual Monomer	High if monomer is present in sufficient quantities
Weakness from UV Exposure	Chain Scission	Low – Insufficient UV Exposure at Earth's Surface
Yellowing from processing	Chain Scission and oxidation of low molecular weight fractions from processing at temperatures above 300°C	Low – Depends on process conditions
Yellowing from UV exposure at High temperatures	Chain Scission and oxidation of low Mw fractions with intense UV radiation and heat	Depends on material, design and ambient temperature conditions
Mechanical (cracks)	High stress level and stress concentration point	Depends on application design and material preparation.

What Does This All Mean?

- Application design relative to material properties is important.
- High Residual MMA can cause yellowness through oxidation that creates chromaphores.
- Chain scission occurs at very low levels, if at all, creating minor low molecular weight fractions.
- Protective formulation systems can be used to minimize oxidative, thermal, and UV influences on molecular structure.
- All polymethyl methacrylate materials are not created equal.


EVONIK
INDUSTRIES



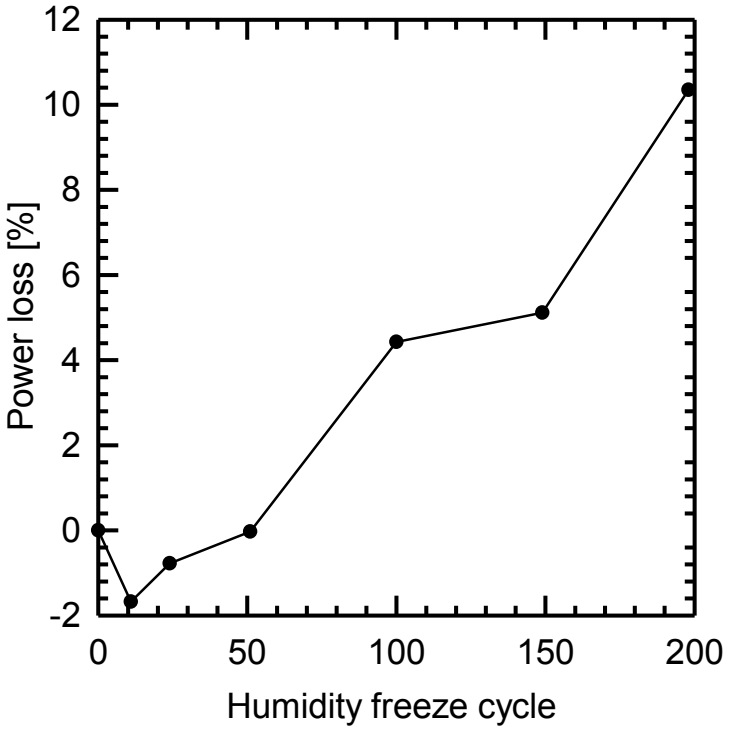
Origin and Consequences of (Micro)-Cracks in Crystalline Silicon Solar modules

M. Köntges[1], I. Kunze[1],
S. Kajari-Schröder[1],
X. Breitenmoser[2] and B. Bjørneklett[2]

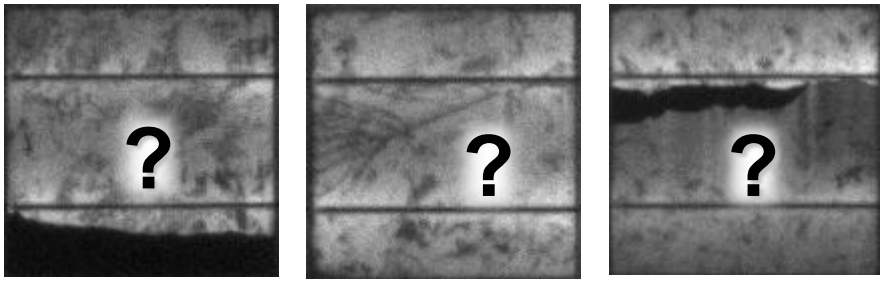
[1]Institute for Solar Energy Research Hamelin
[2]REC Solar AS

Motivation / Outline

Initially all cells show micro cracks



- Crack detection methods
- Influence on power generation
- How much cracking is acceptable ?
- Origin of statistical distribution of cracks

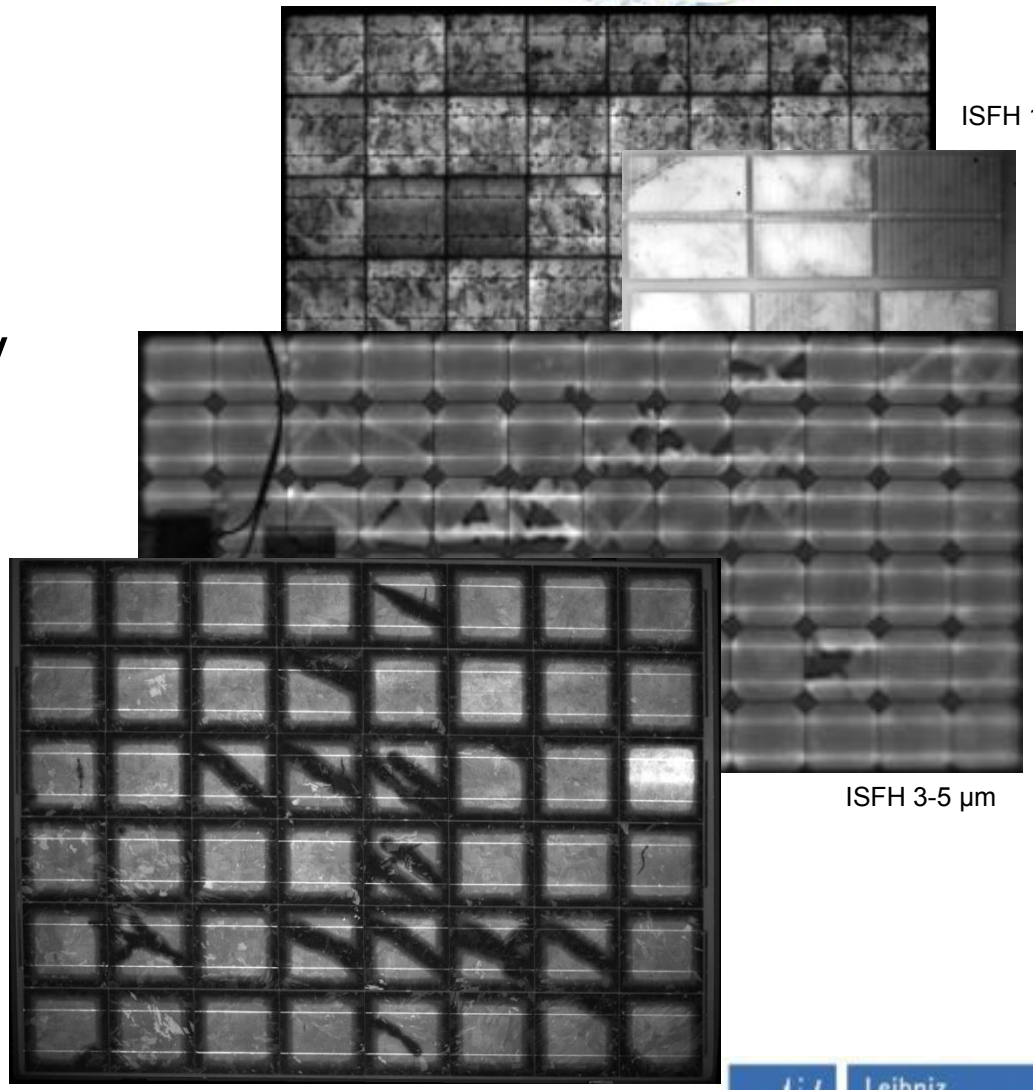


M. Köntges, et al., Sol. Energy Mater. Sol. Cells (2011),doi:10.1016/j.solmat.2010.10.034
M. Köntges, et al., 25th EUPVSEC (Valencia, Spain, 2010,WIP) , 4BO.9.4

Leibniz Universität Hannover

Crack detection in the PV module

- Electroluminescence[1]
- Si photoluminescence
- Dark lock-in thermography



ISFH 1150 nm

ISFH 3-5 µm

ISFH 534 nm

After aging, indirect

- EVA fluorescence[2] oxidation/vanishing of fluorescing molecules through cracks

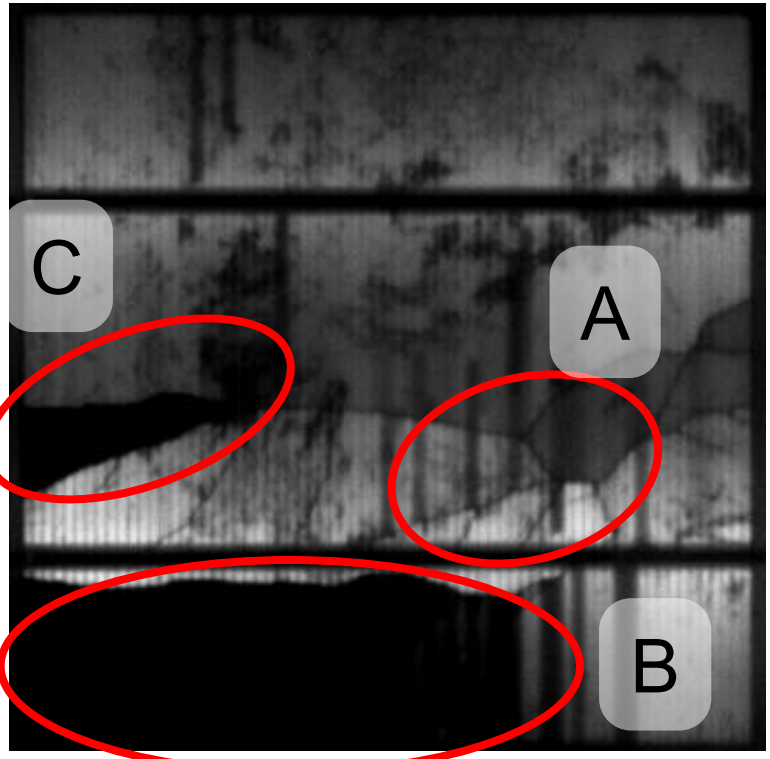
[1]T. Fuyuki, et al., *Applied Physics Letters* **86** (2005) 262108
[2]J. Schlothauer, et al., Photovoltaik International 10 (2010), 149-154

Leibniz Universität Hannover

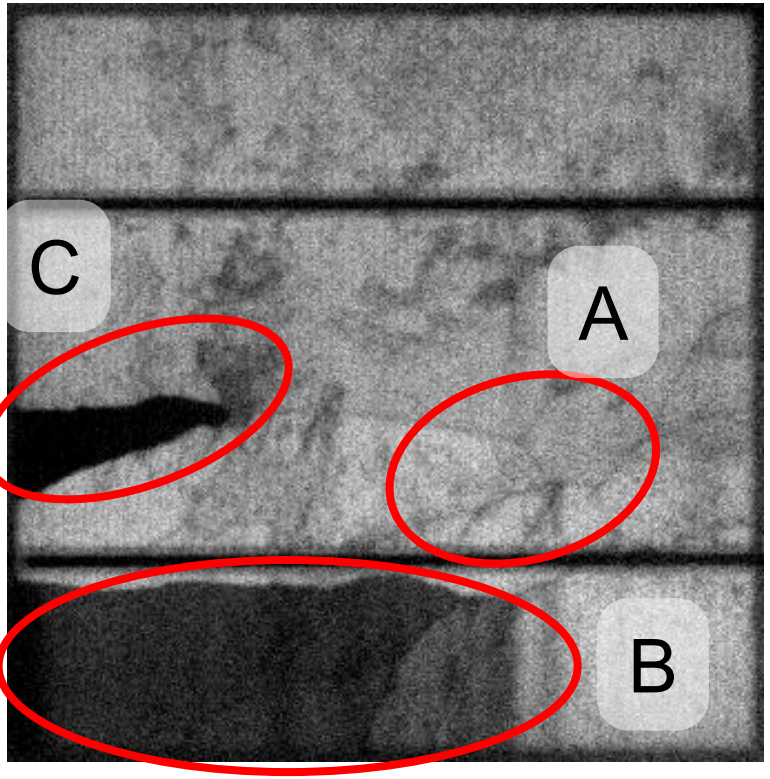
Infuence on power generation ?

Crack mode definition

EL image @ I_{sc}



EL image @ 1/10 I_{sc}



Crack mode:

A ➔ no increased resistivity

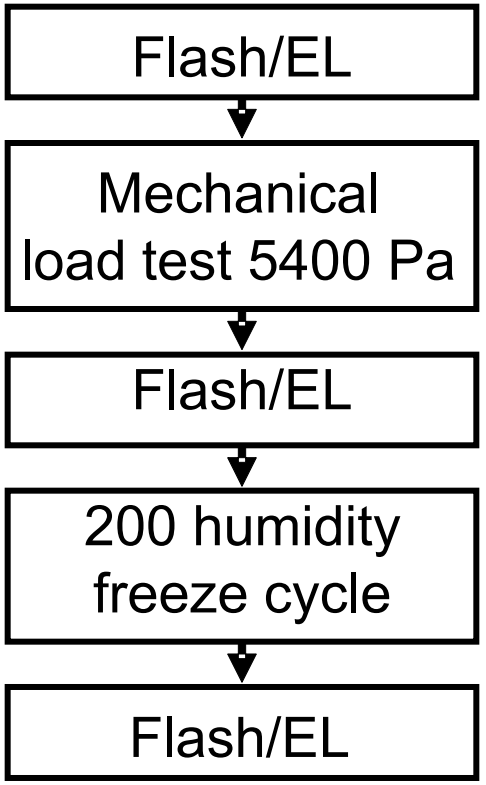
B ➔ still connected but increased resistivity

C ➔ disconnected, inactive cell area

Leibniz Universität Hannover

Experimental

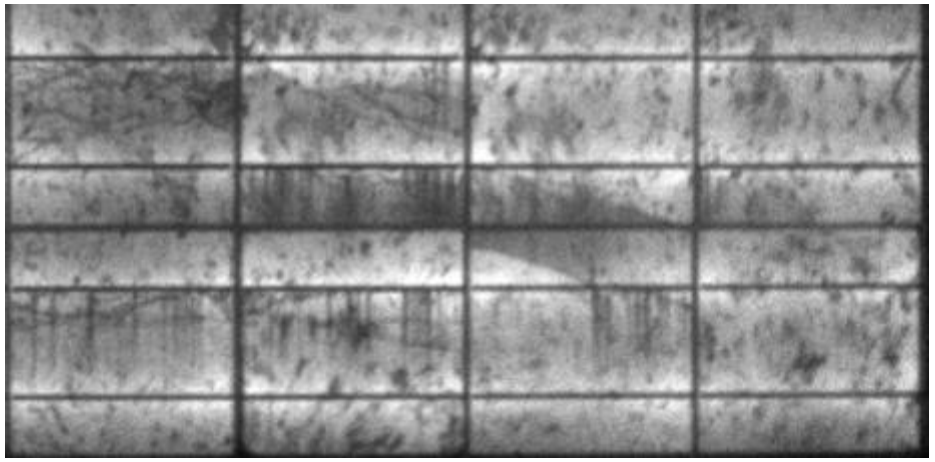
- 230 W modules with 60 15.6 cm² cells
- Inflict cracks to cells in PV module by mechanical load test (IEC 61215)
- Stress cracked cells by 200 HFC (similar to IEC 61215)
- Determine power loss due to mechanical load
- Determine power loss after 200 HFC aging



Find influence of cracks to PV module power

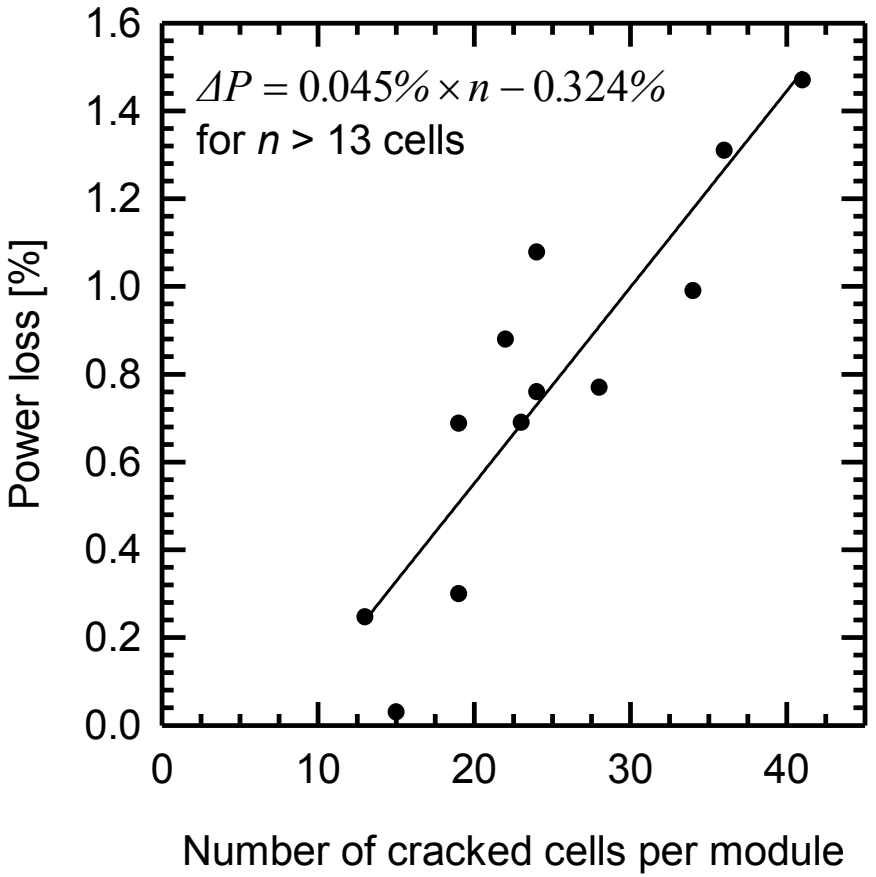
Transportsimulation + TC: S. Pingel et al., 24th EUPVSEC (2009, Hamburg, Germany, WIP) 4AV3.49
Simular test: Wohlgemuth et al., 23rd EUPVSEC (2008, Valencia, Spain, WIP) 4EP1.2

Mode A cracks

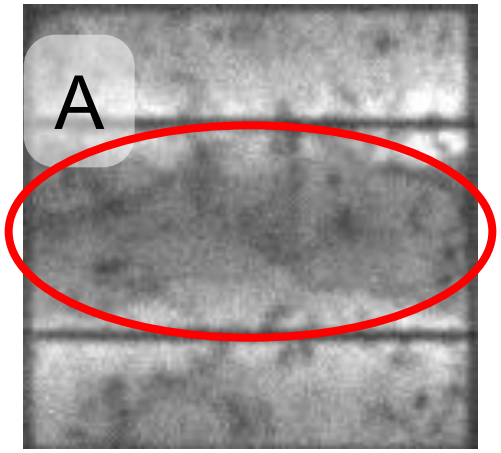


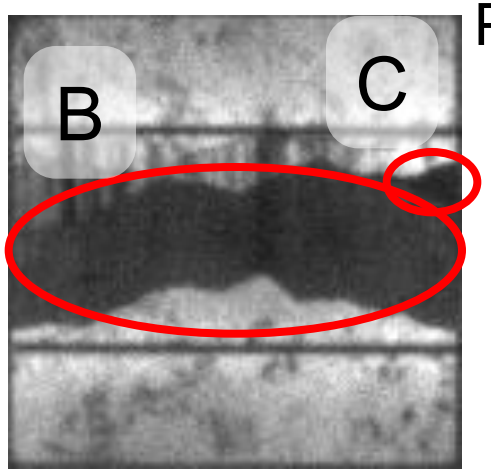
- Some solar cells with cracks
  ➔ power loss not measurable
- Half of cells show cracks
  ➔ only approx. 1% power loss
- All cells show micro cracks
  ➔ < 2.5% power loss

PV modules of 60 x 15.6 cm cells



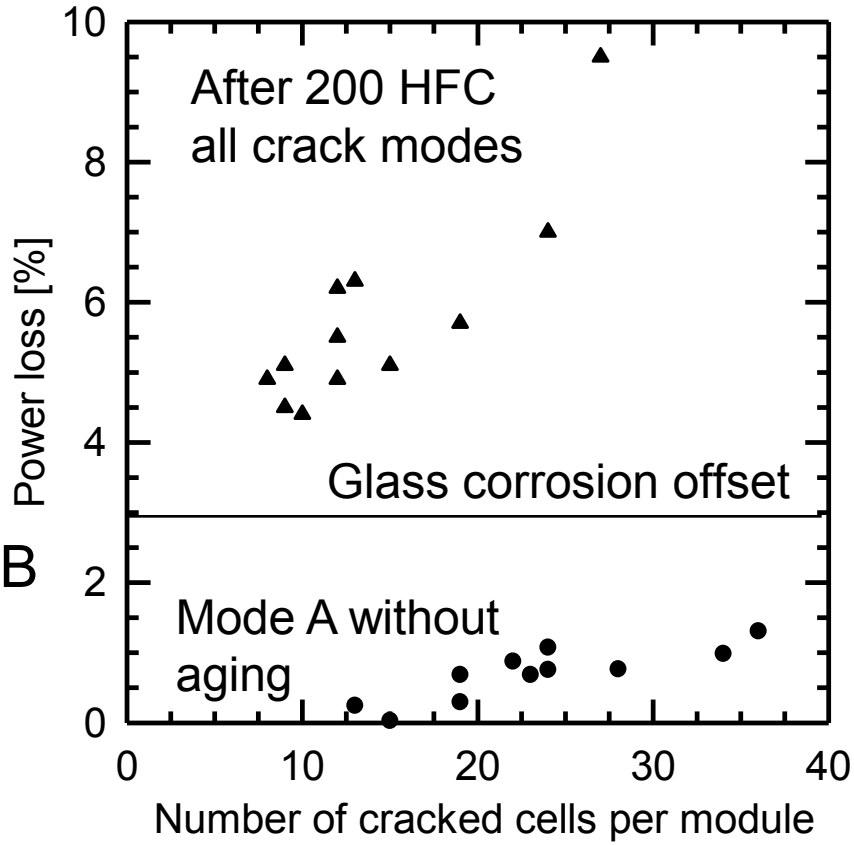
After 200 humidity freeze cycle





PV modules of 60 x 15.6 cm cells

- 3% degradation offset due to glass corrosion (I_{sc} loss)
- Predominant change from mode A to B
- Few cases A to C
- Power loss increases with no. of cracked cells



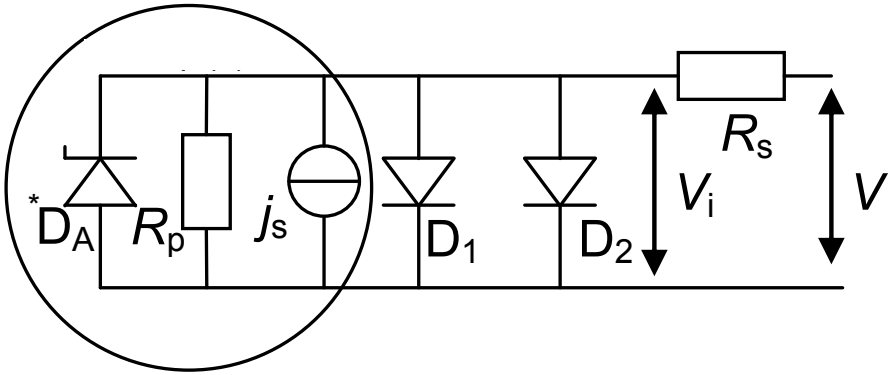
How much cracking is acceptable ?

PV module simulation

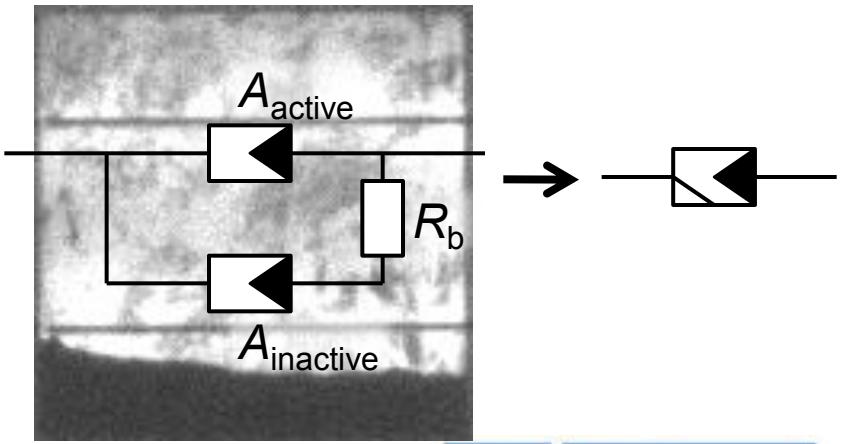
Aim: Power loss simulation due to mode C cracks

- LT Spice for electrical simulation
- Two diode model for each cell
- Power loss due to defective cell is influenced by breakdown voltage
- Breakdown model of Alonso-Garcia*
- Break resistance R_b connect broken cell area $A_{inactive}$

Cell equivalent network

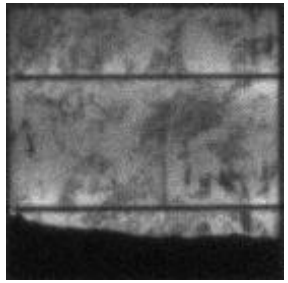


New symbol for broken cell

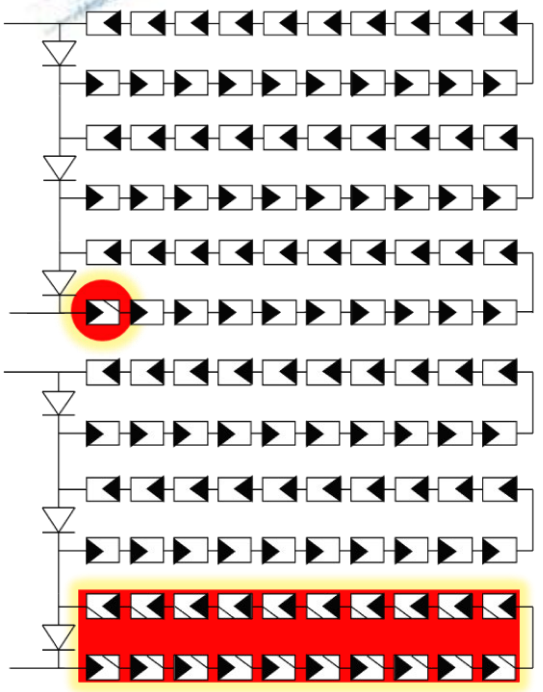


*M.C. Alonso-Garcia et al., *Solar Energy Materials & Solar Cells* **90** (2006) 1105–1120

Worst case scenarios



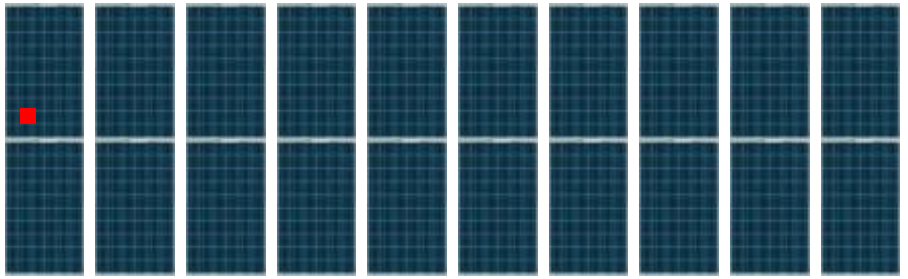
Power loss due to crack mode C



I Single defective cell in a PV module

II Multiple defective cells in a double string

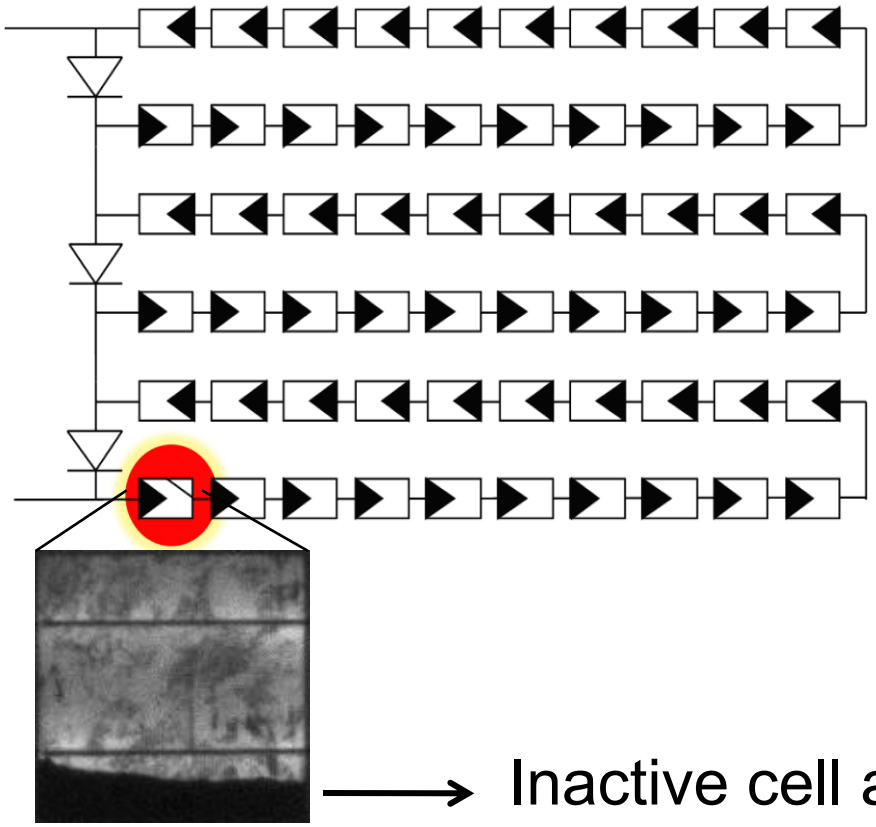
III One PV module with single defective cell in a PV array



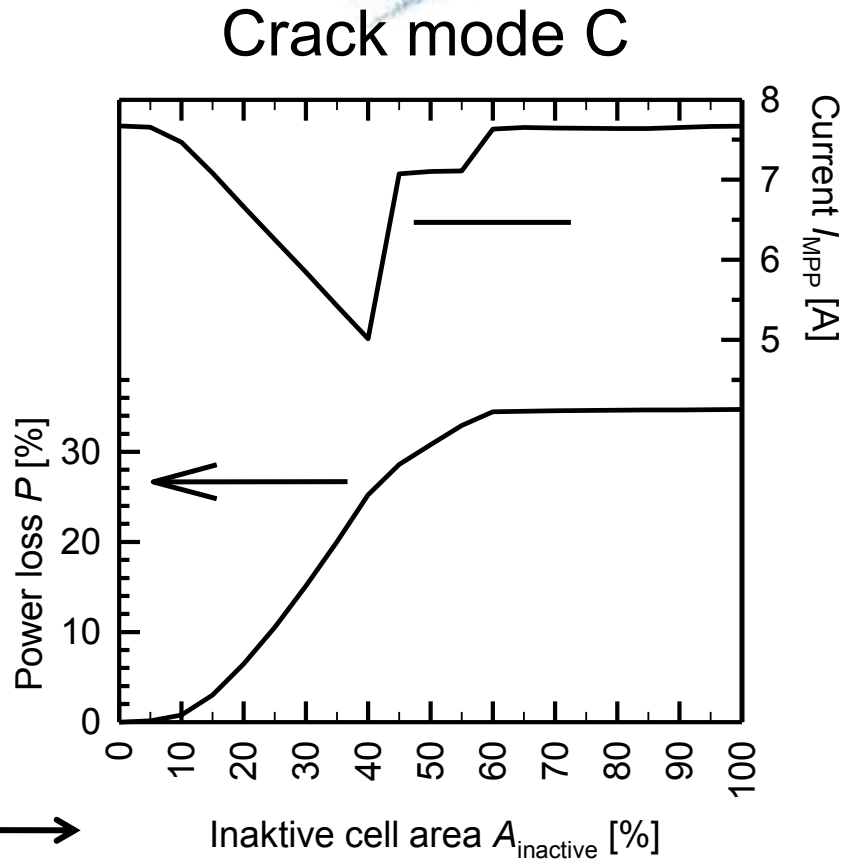
20s PV module array - series interconnected

Leibniz Universität Hannover

Scenario I single defective cell

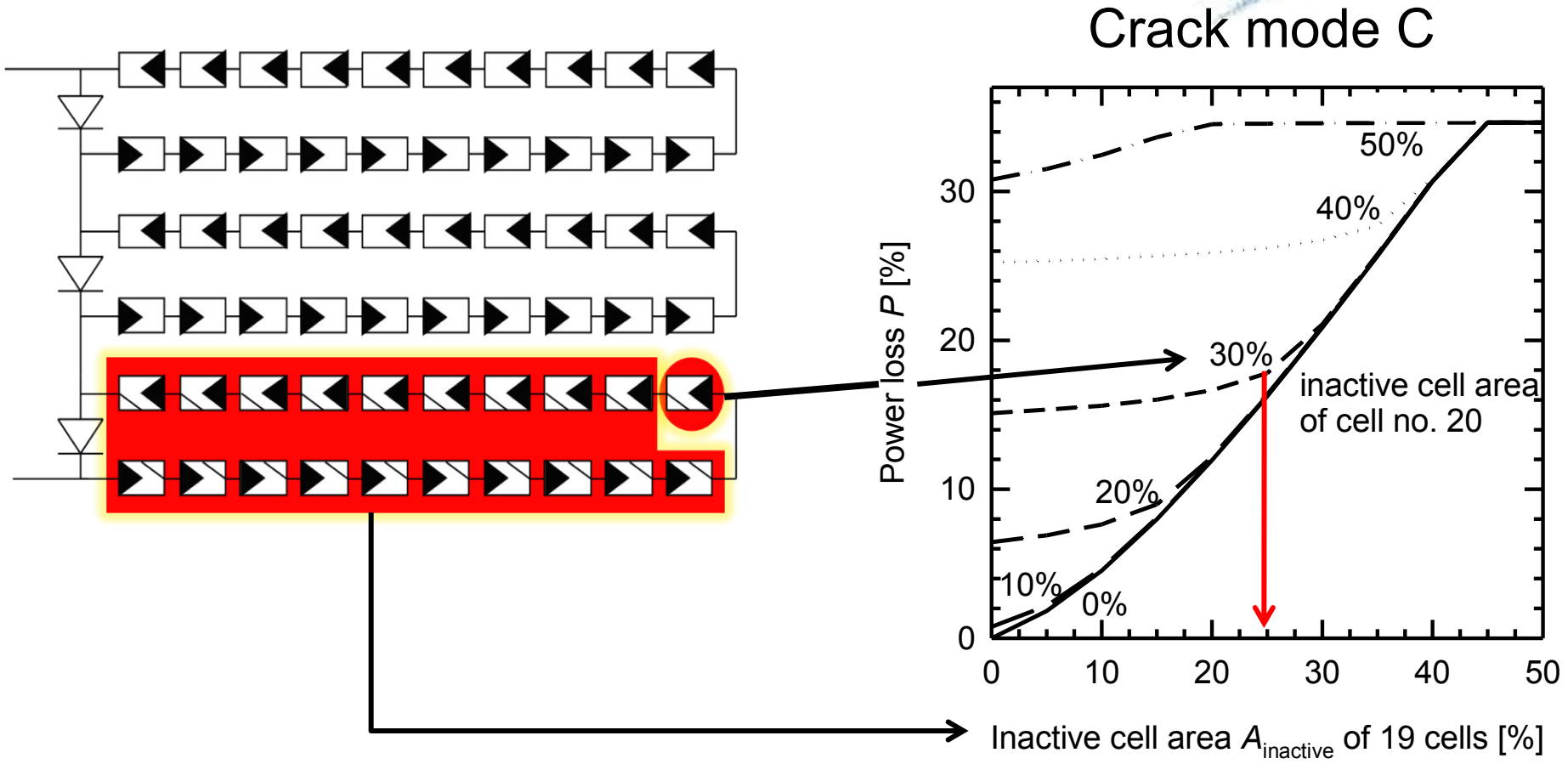


Inactive cell area



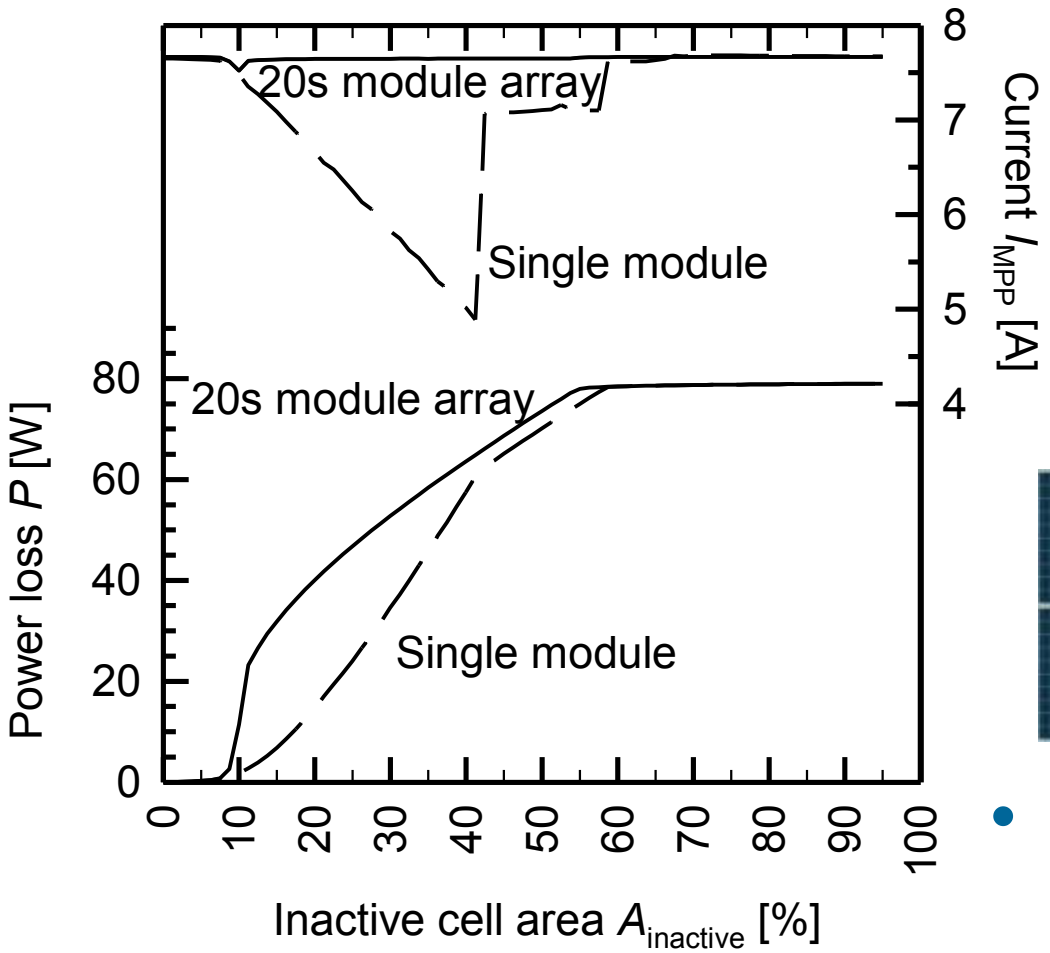
- 8% inactive cell area acceptable
- Huge inactive area rise risk of hot spots, power loss

Scenario II multiple defective cells



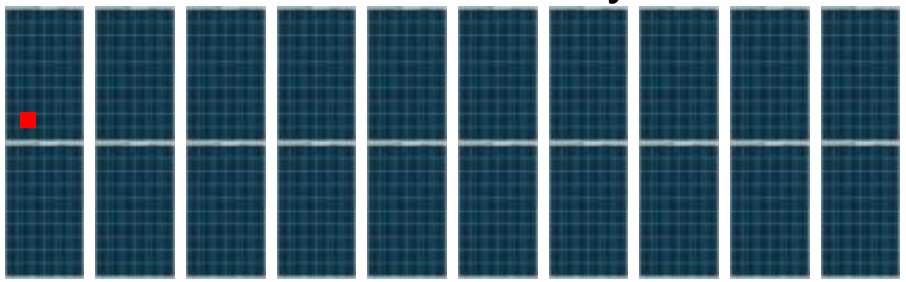
- Maximum inactive area in double string determines power loss

Scenario III PV module array





20s module array



- 8 % inactive area is acceptable for PV systems

Leibniz Universität Hannover

Origin of statistical distribution of cracks

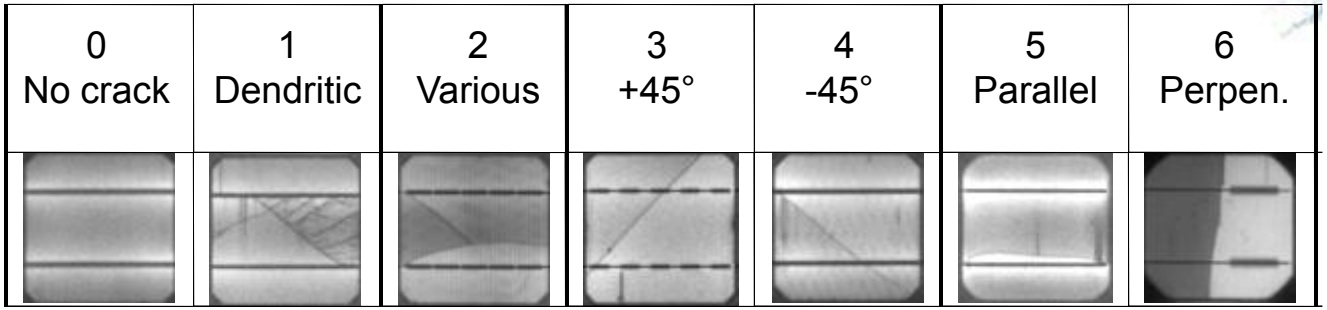
- IEC 61215 mechanical load

compare to

- transported PV modules

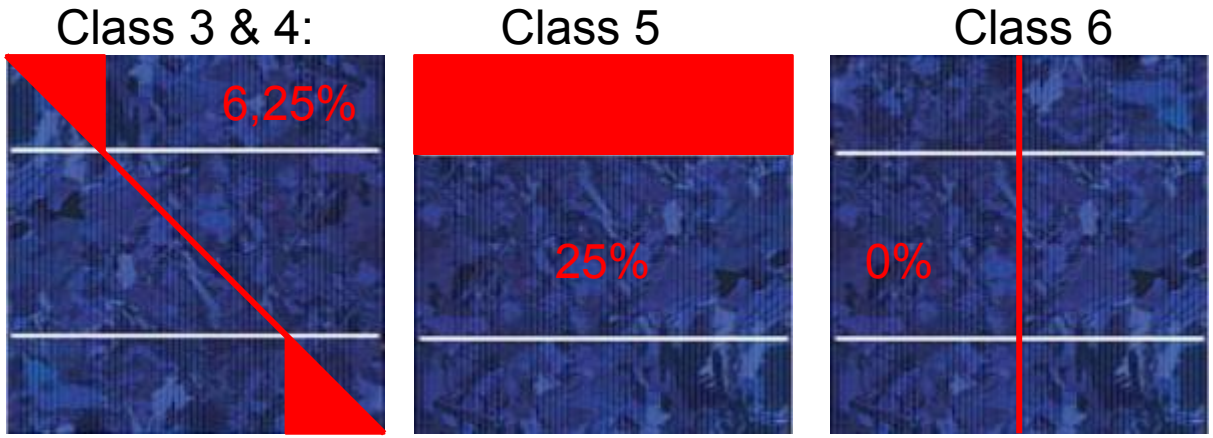
Transport simulation: F. Reil et al., 6. Workshop – „Photovoltaik-Modultechnik“, TÜV Rheinland Nov, 2009, Köln
Set up a transportation test standard: Poster from TÜV Rheinland at this Workshop

Crack classification



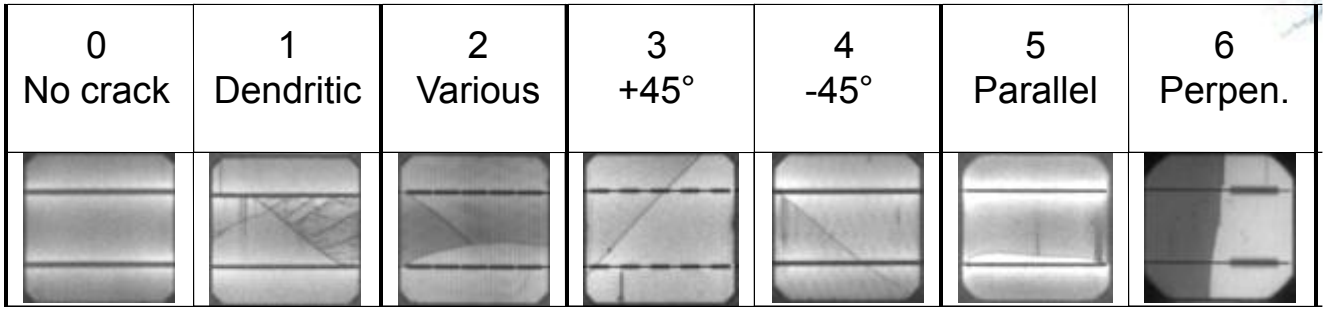
- Class 1,2 and 5: most area loss possible
- Class 3 and 4: medium area loss possible
- Class 6 : No area loss possible

Worst Case single crack



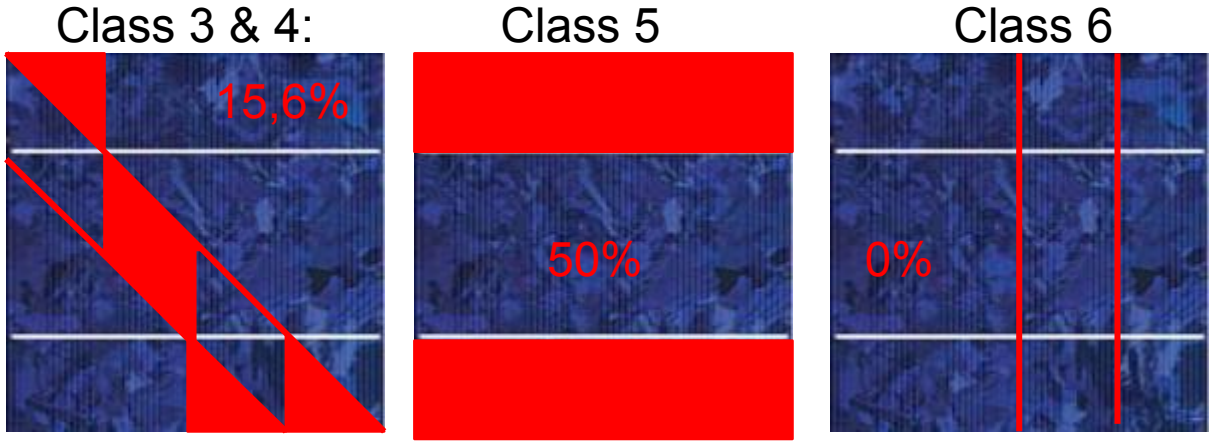
Leibniz Universität Hannover

Crack classification



- Class 1,2 and 5: most area loss possible
- Class 3 and 4: medium area loss possible
- Class 6 : No area loss possible

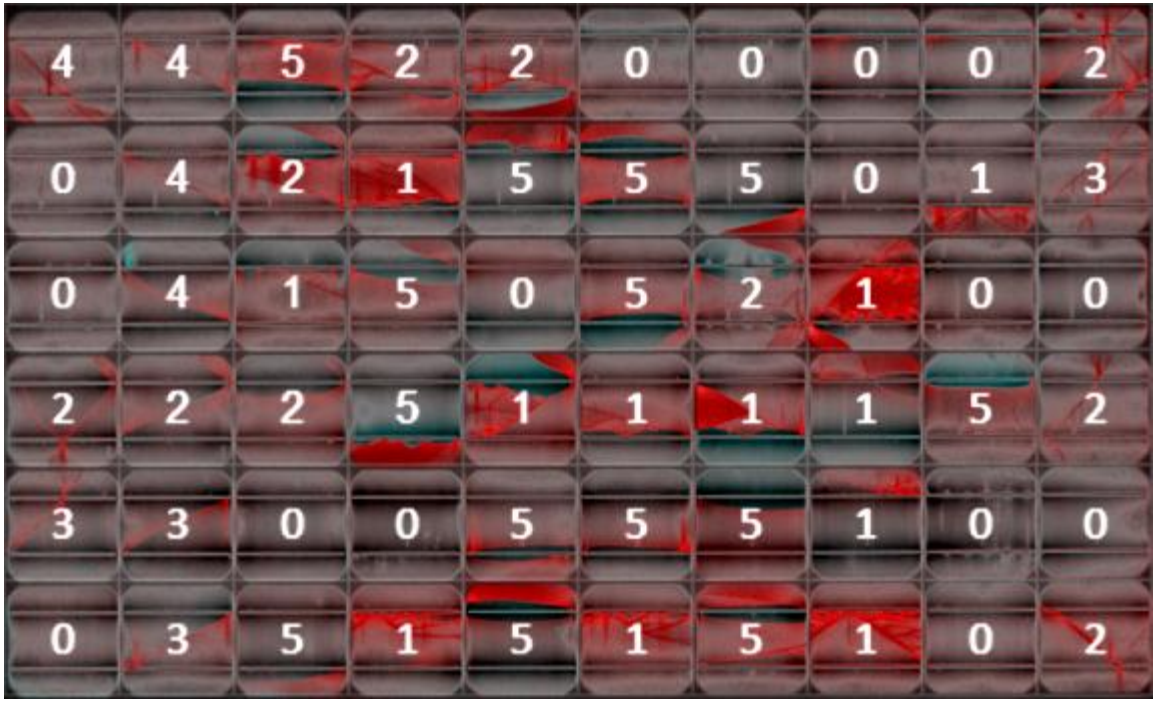
Worst case double cracks



Leibniz Universität Hannover

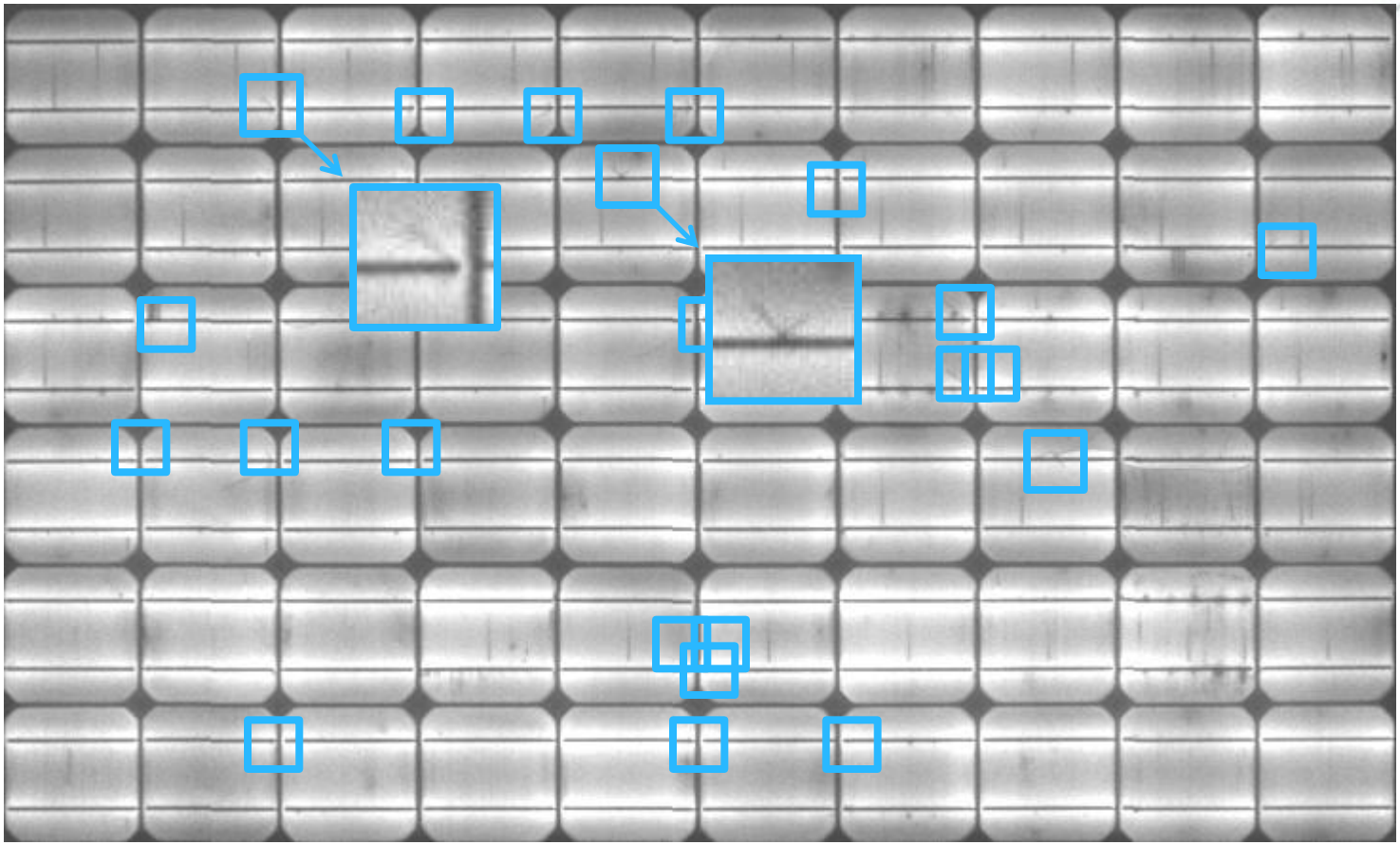
Classification for mechanical load

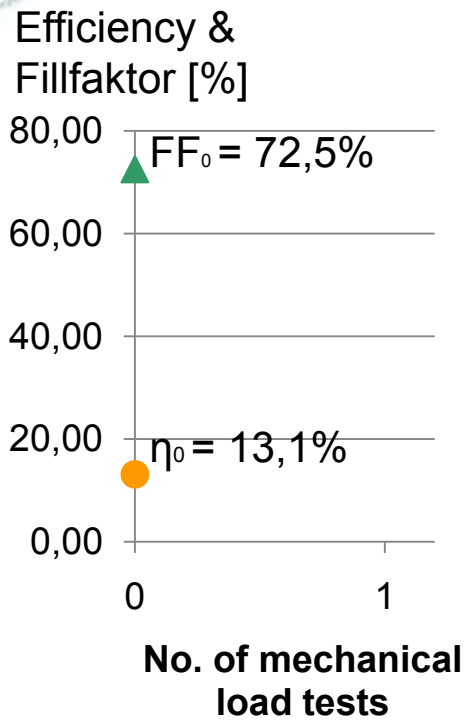
- Mechanical load 5400 Pa
- EL image before/after
- Mapping with image registration method
- Difference EL image
- Subjective classification



Red ➔ image becomes dark
Black ➔ image does not change
Green ➔ image becomes brigther

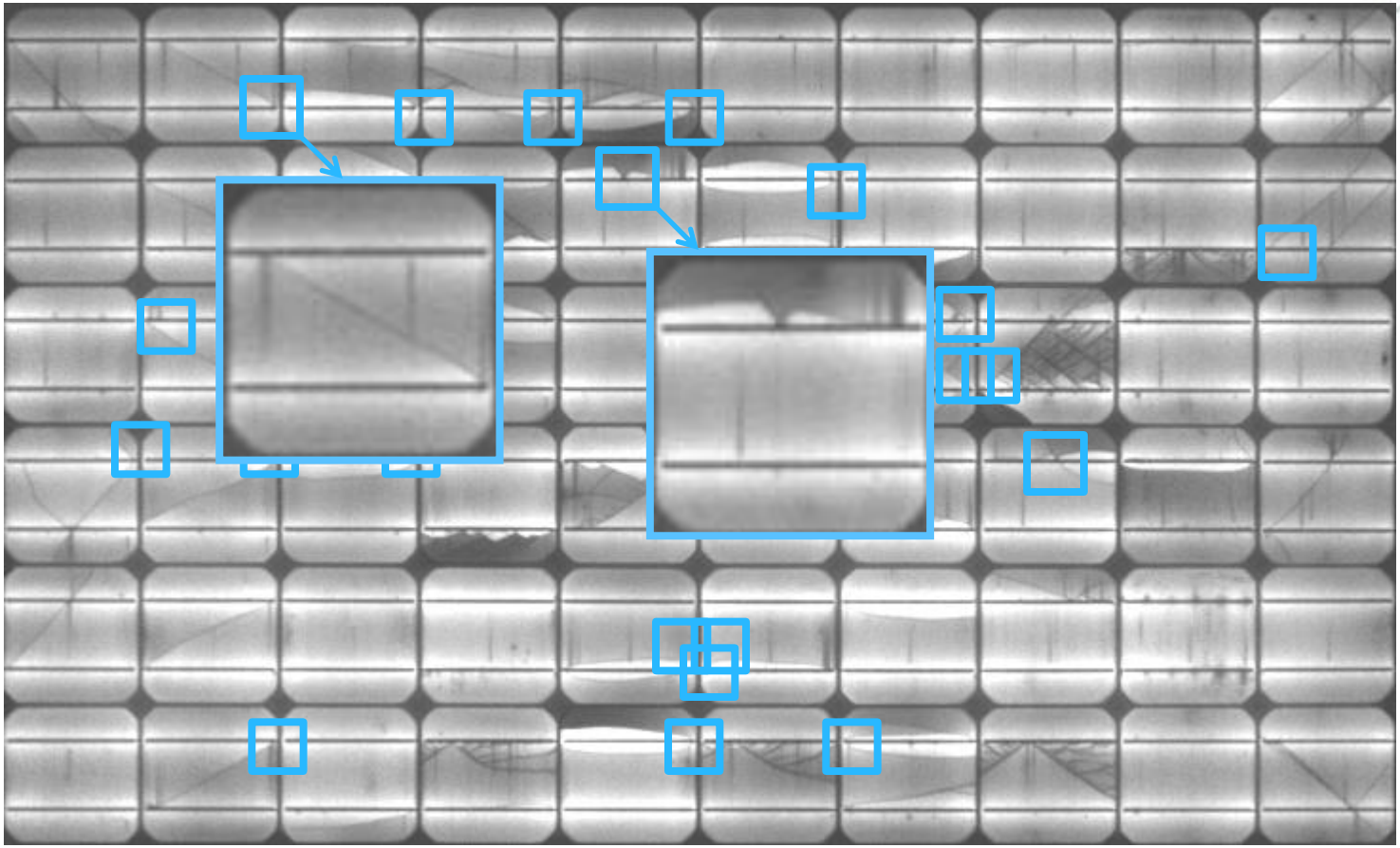
Initially precracked PV module

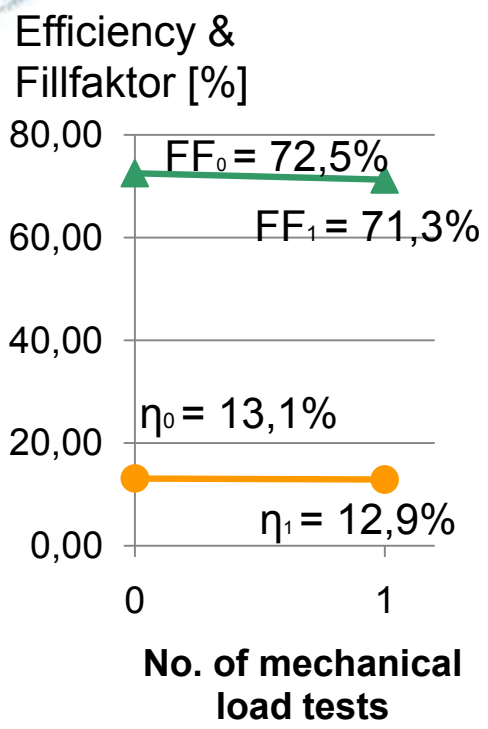




- Initial cracks at the busbars

5400 Pa mechanical load

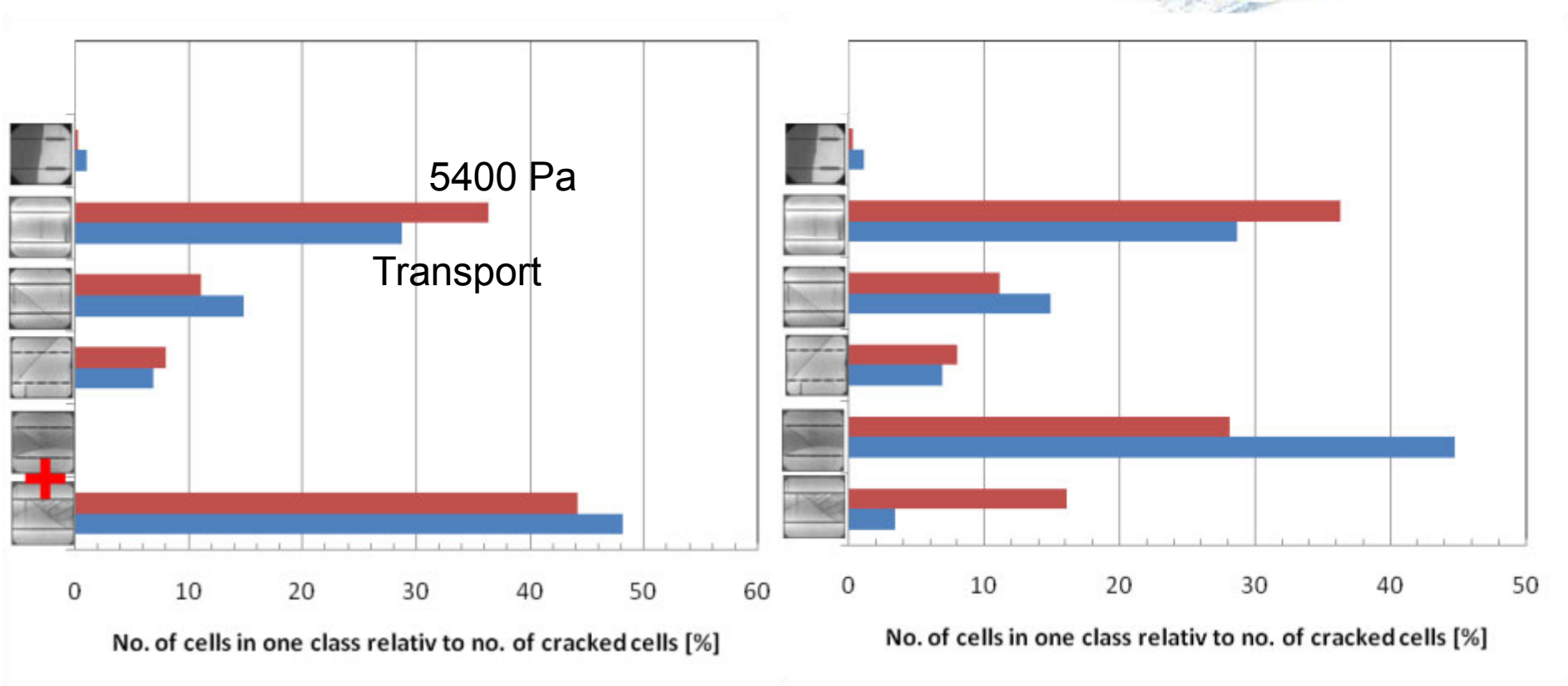




- Cracks do not always follow the initial crack or the preferred crystallographic crack orientation !

Leibniz Universität Hannover

Cracks of transported PV modules



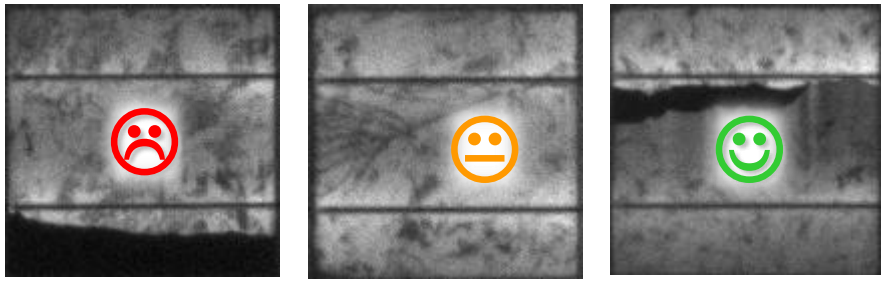
- Crack distribution of mechanical load test & transport is similar
- At 5400 Pa test shift from “Various” to “Dendritic” crack class
- Dendritic cracks occur at high strain
- High occurrence for worst case crack classes 1,2,5

Summary

- Crack distribution of mech. load is similar to transported modules
- Most real cracks are in most disadvantageous directions

Power loss due to

- mode A cracks is linear with no. of cells & less than 2.5%
- an mode C crack is acceptable as long as inactive part is less than 8% of cell area



Power loss is

- dominated by cell with maximum inactive area per double string

Funding was provided by the State of Lower Saxony and the German Federal Ministry for the Environment, Nature Conservation and Nuclear Safety with the support code 0325194C

Leibniz Universität Hannover



SOLON Corporation

Potential Induced Degradation

William Richardson

NREL PVRW, February 1th, 2011

SOLON

Don't leave the planet to the stupid

SOLON at a Glance



- One of the largest manufacturers of solar modules in Europe
- Large scale rooftop and greenfield installations
- Founded in 1997
- Production sites in Germany, Italy and the U.S.
- Employees: approx. 900

SOLON

SOLON Corporation at a Glance



- 80 MW of annual manufacturing capacity in Tucson, AZ
- Large scale rooftop and Utility-scale installations
- Founded in 2007
- Wholly-owned subsidiary of SOLON SE
  .
- Employees: approx. 150

Solar modules

Power plants

Industrial rooftops







SOLON

Content

- Introduction & Motivation
- Background & Approach
- Results
  - Cell level
  - Panel level
  - System level
- What's Next?
- Summary & Conclusion

SOLON

Motivation

Objective: To make Solar Energy even more competitive

→ Reduction of $/kWh

→ Two approaches:

1. Reduction of $/kWp

   → Become as cheap as possible!

2. Increase lifetime/ Decrease degradation

   → Become as stable/long-lasting as possible!

→ Both tracks have to be pursued in parallel …

SOLON

Potential Induced Degradation

- Power degradation due the exposure to an external potential

- External potential = Potential relative to ground

→ High Voltage Stress

= Power Degradation caused by the exposure to a potential relative to ground, and dependent on its magnitude and sign

→ Two cases: Reversible (Polarization)

Irreversible (Electro corrosion)

SOLON

Content

- Introduction & Motivation
- Background & Approach
- Results
  - Cell level
  - Panel level
  - System level
- What's Next?
- Summary & Conclusion

SOLON

Background

- First addressed by Hoffman and Ross (JPL) 1978: Impact of voltage-biased humidity exposure of solar panels on long term stability – “Bias Humidity test… as a candidate for module qualification”

- Prominent cases such as Sunpower’s Polarization effect

- More recently NREL: Degradation caused by HVS not covered by IEC or UL standards right now

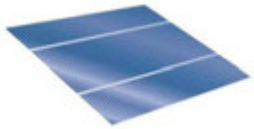
- Increasing importance because:
  - → Increasing need to push down overall degradation
  - → Increasing system voltages
  - → Increasing variety of solar cell technologies

SOLON

Approach

Objective: Minimizing / Avoiding PID

→ On cell level



→ On panel level



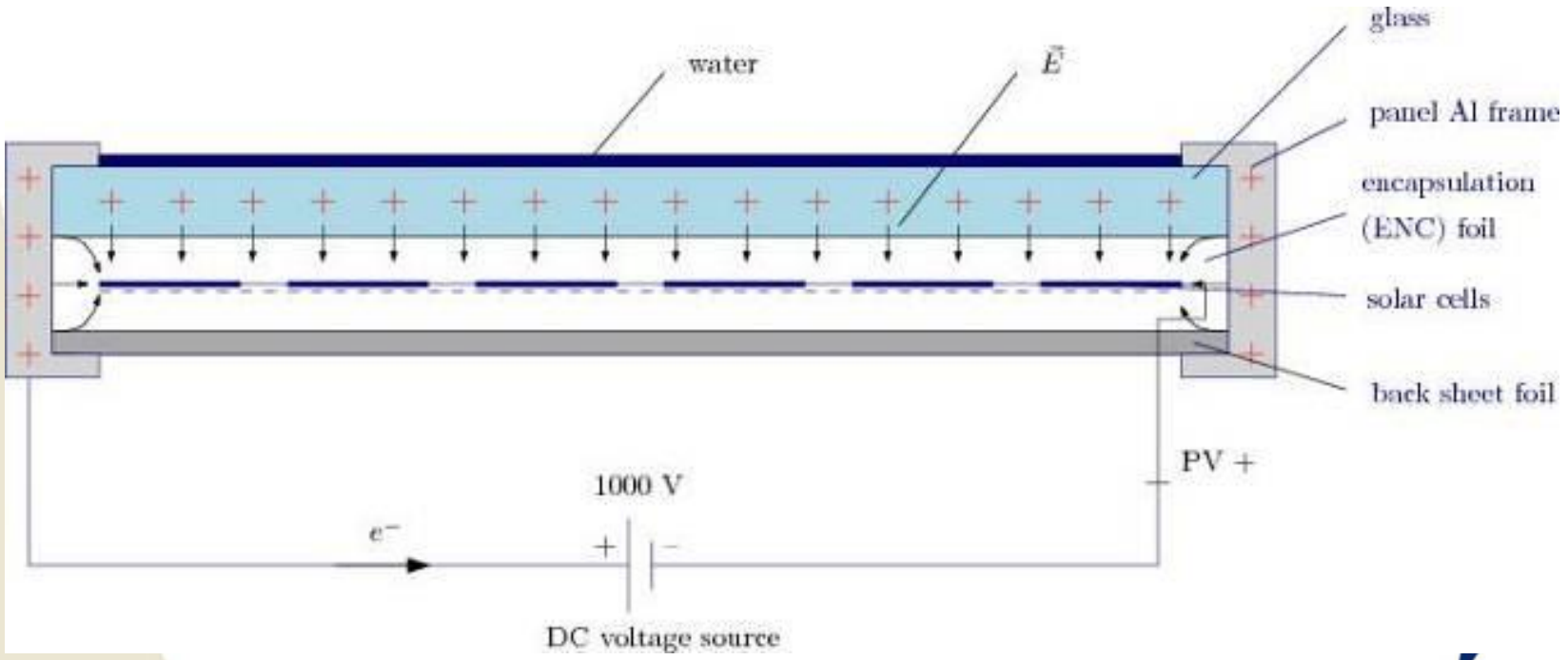
→ On system level



SOLON

Test Set up

- Worst case scenario
- Simulation of potential relative to ground

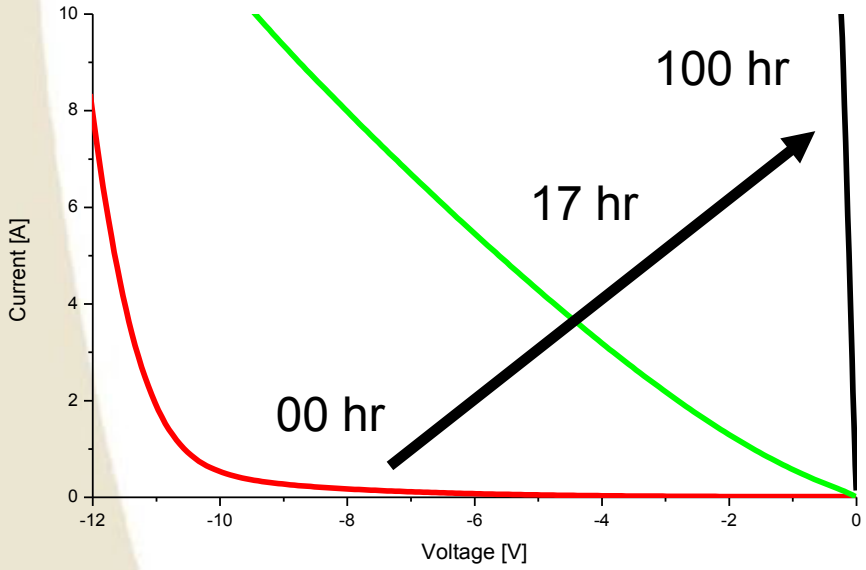


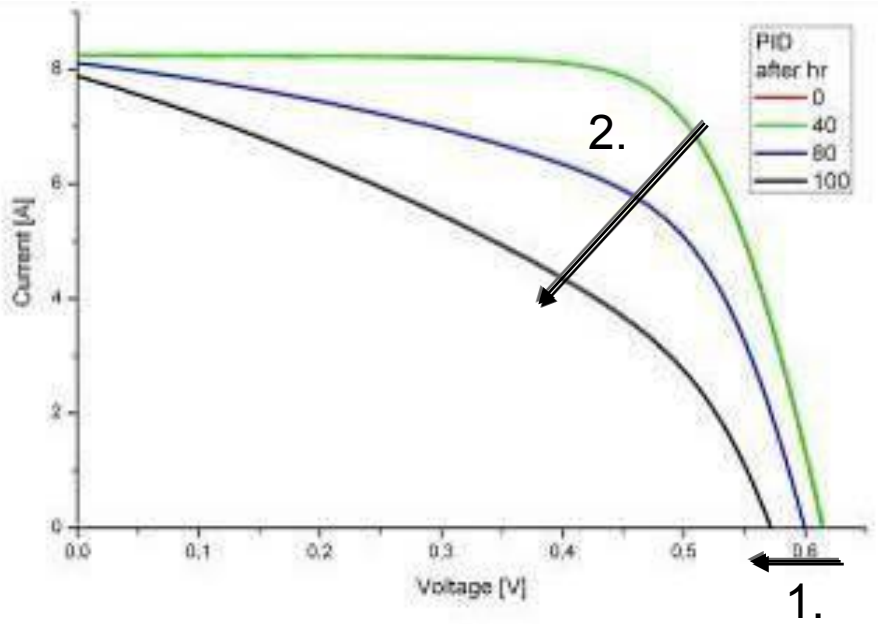
Content

- Introduction & Motivation
- Background & Approach
- Results
  - Cell level
  - Panel level
  - System level
- What's Next?
- Summary & Conclusion

SOLON

Cell Level

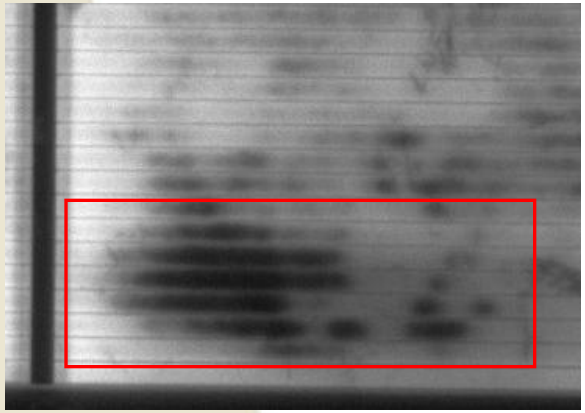




- Decrease of overall shunt resistance

→1. Loss FF

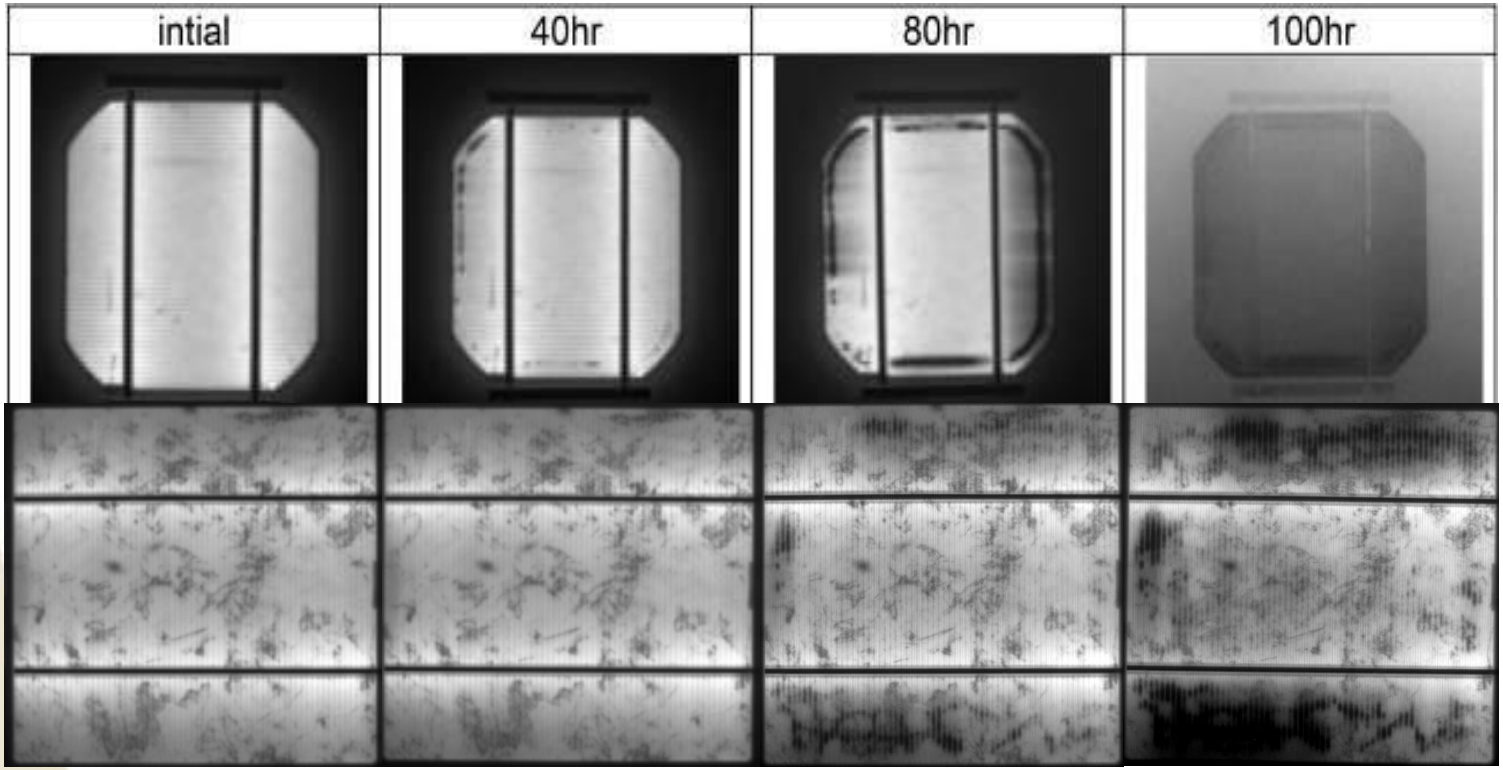
→2. Loss in open circuit voltage



→Local short circuit of the pn-junction

SOLON

Cell Level



EL images of a cell during PID test (1000V, 100h)

Tendency for PID very different for different cell manufacturers

→ Impact factors on cell level?

SOLON

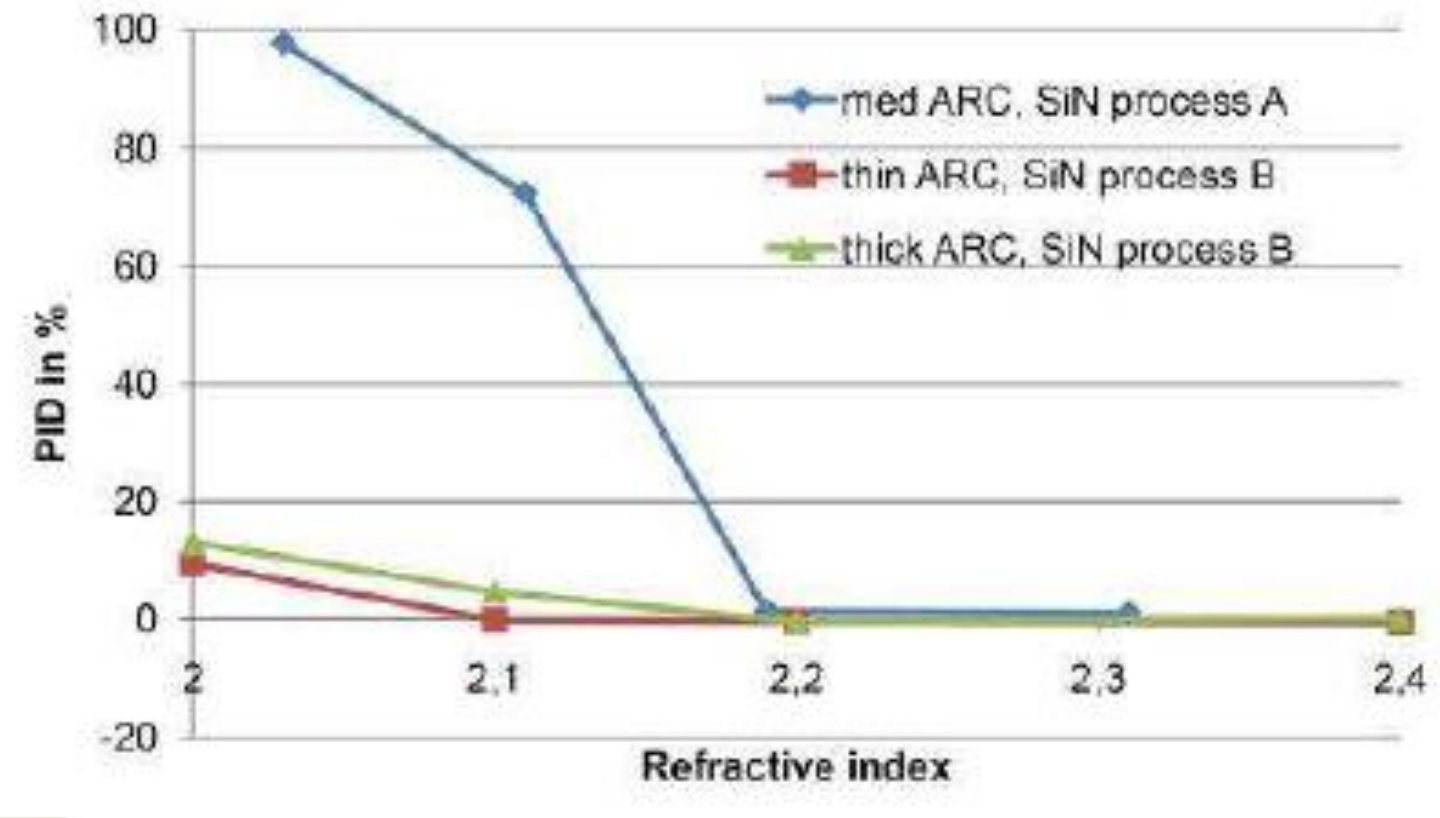
Cell Level

Impact factors:

- Base resistivity of wafer material → significant influence
- Emitter sheet resistivity → significant influence
- **ARC deposition → key feature**
  - Ratio of Si to N
  - Thickness
  - Homogeneity

SOLON

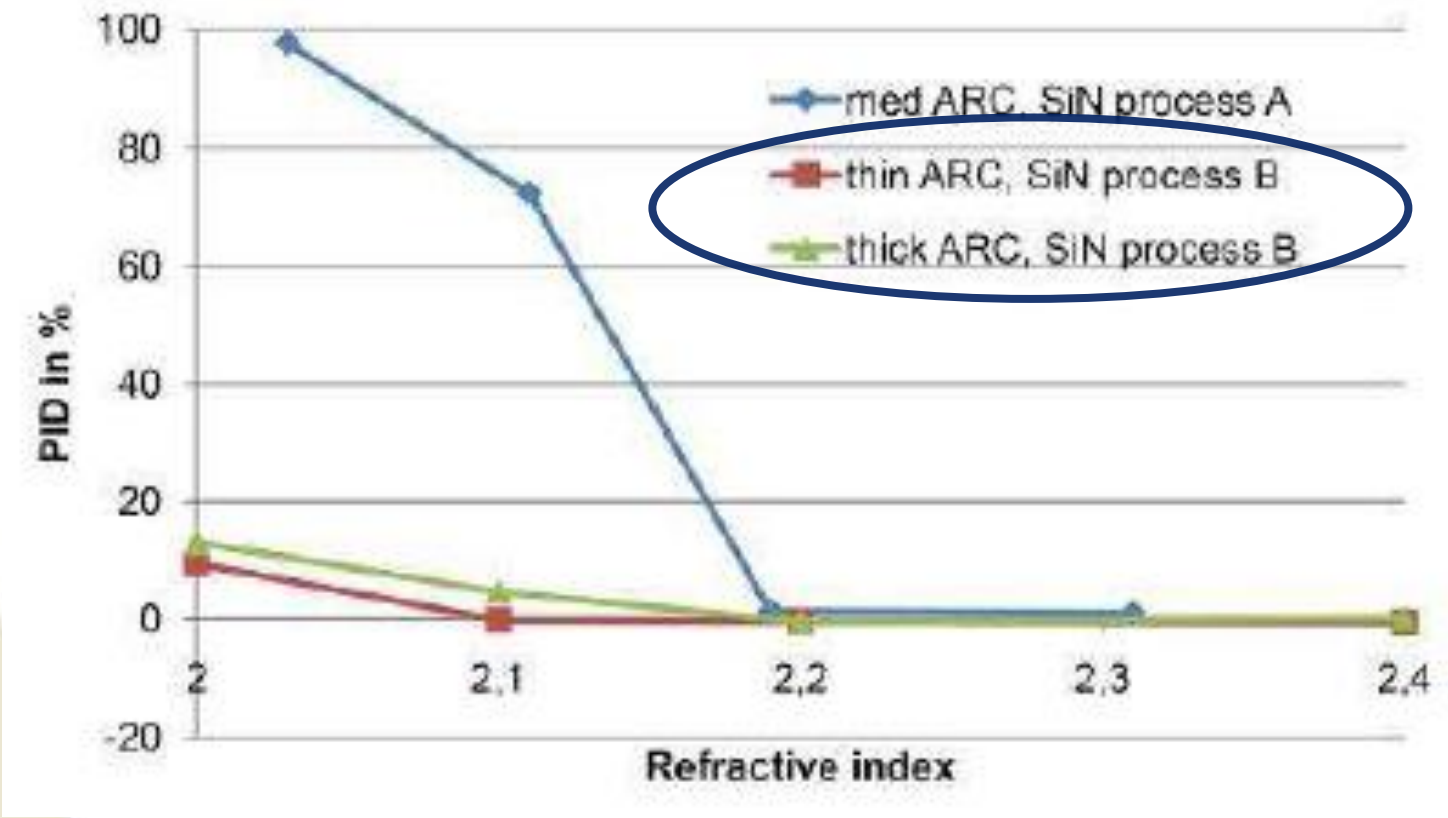
Cell Level



By choosing suitable parameters for ARC deposition PID can be minimized/ stopped on cell level

SOLON

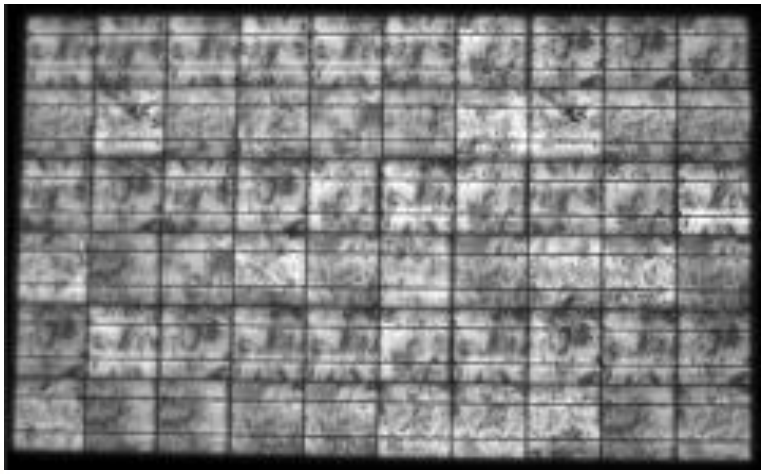
Cell Level



By choosing suitable parameters for ARC deposition PID can be minimized/ stopped on cell level

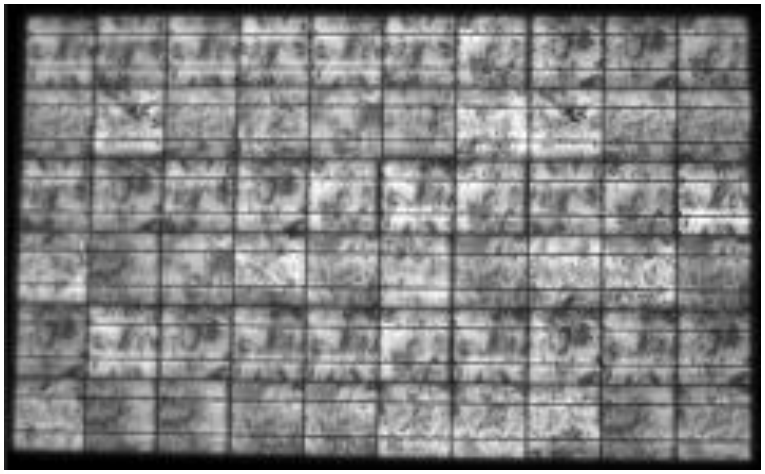
SOLON

Panel level

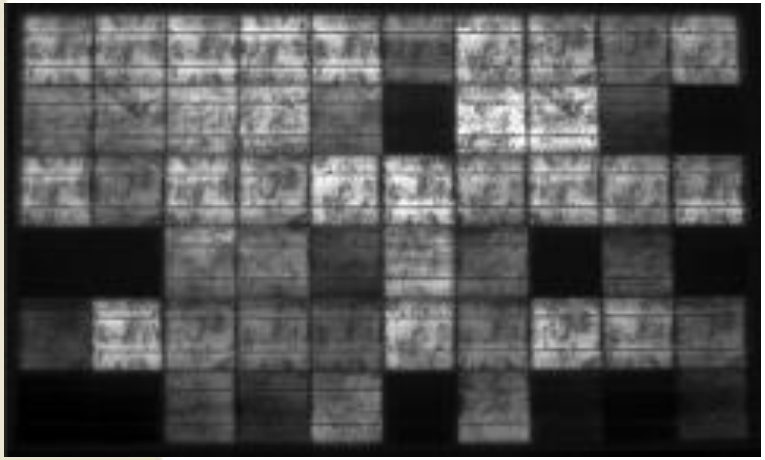


EL image of a panel before 100hr 1000V PID...

Panel level



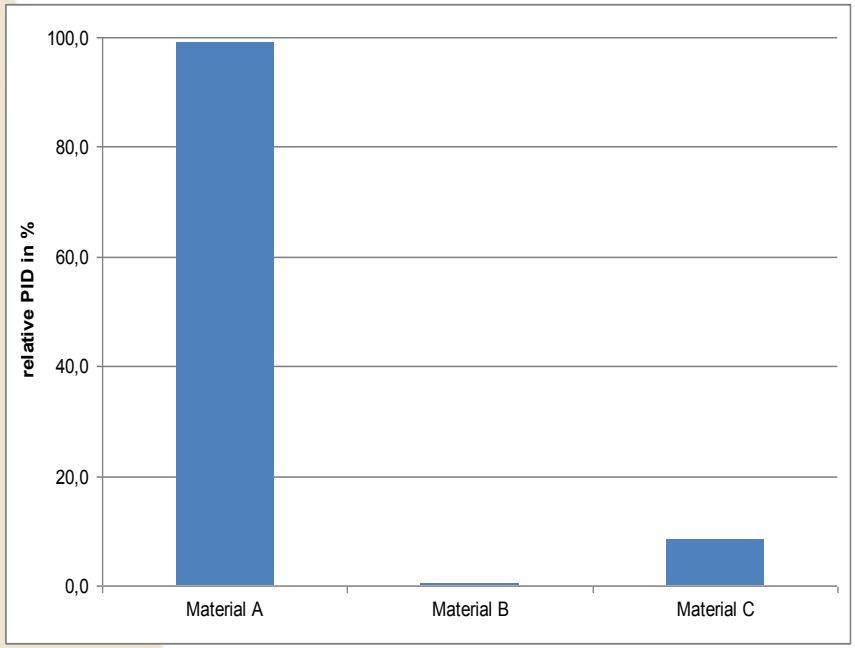
EL image of a panel before 100hr 1000V PID...

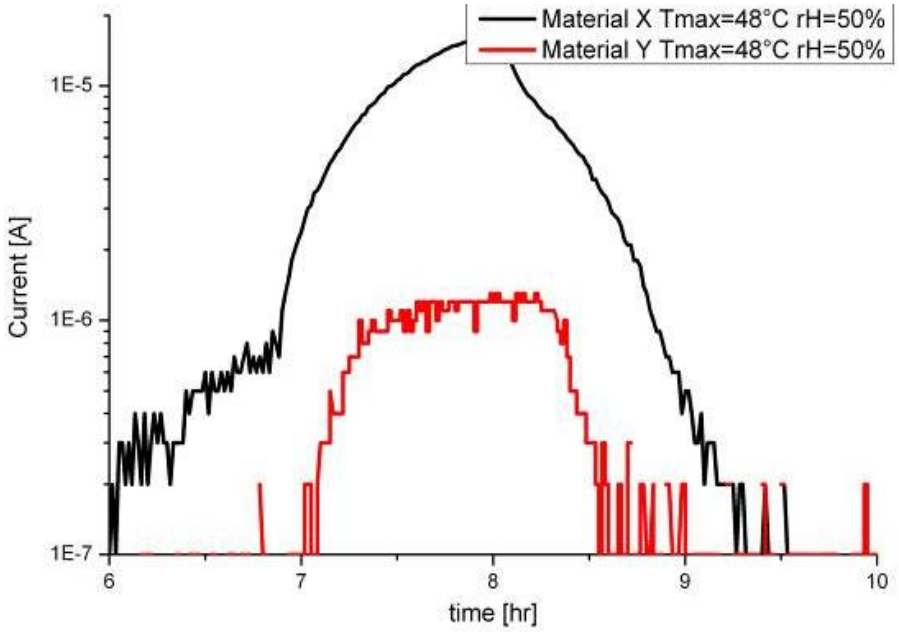


...and after.

Key feature: Leakage current

Panel level I

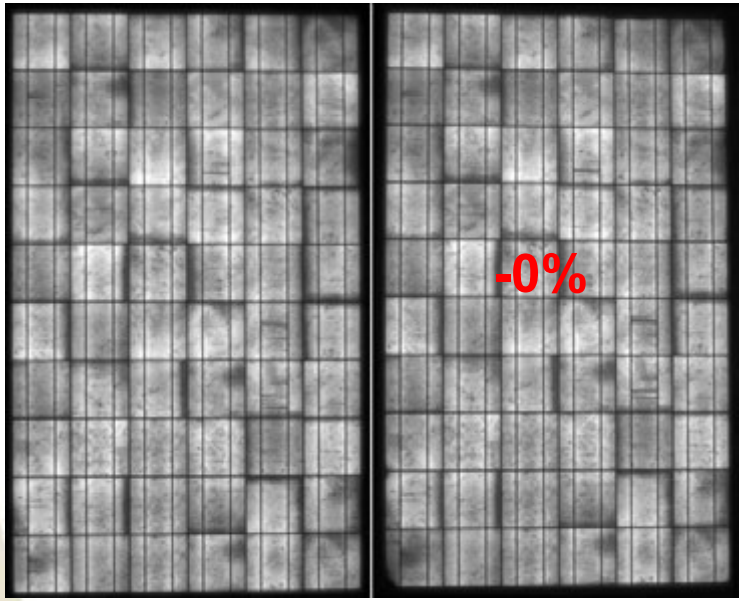




PID can be stopped/ minimized on panel level
by minimizing leakage current → Choice of suitable encapsulation

SOLON

Panel level II



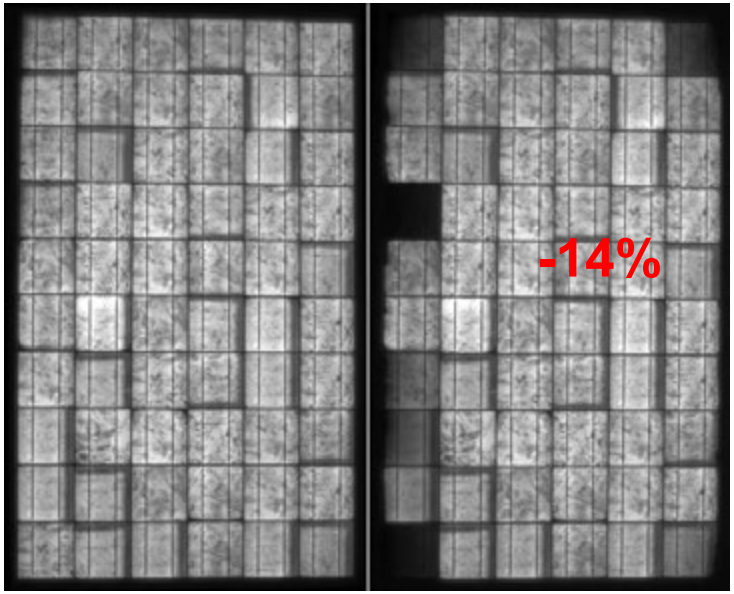
Time: 100h

Voltage: 1000V

Temperature: 48°C

Humidity: 50%

Material: X



Time: 100h

Voltage: 1000V

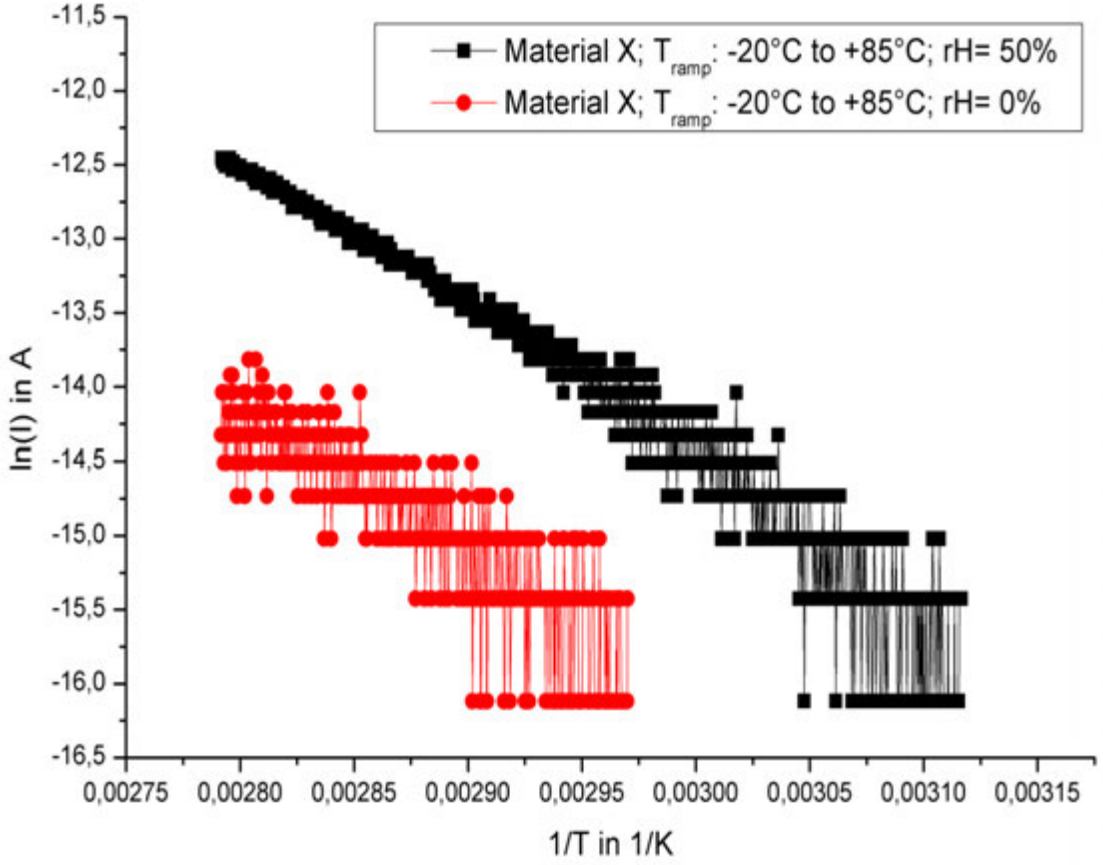
Temperature: 48°C

Humidity: 50%

Material: Y

SOLON

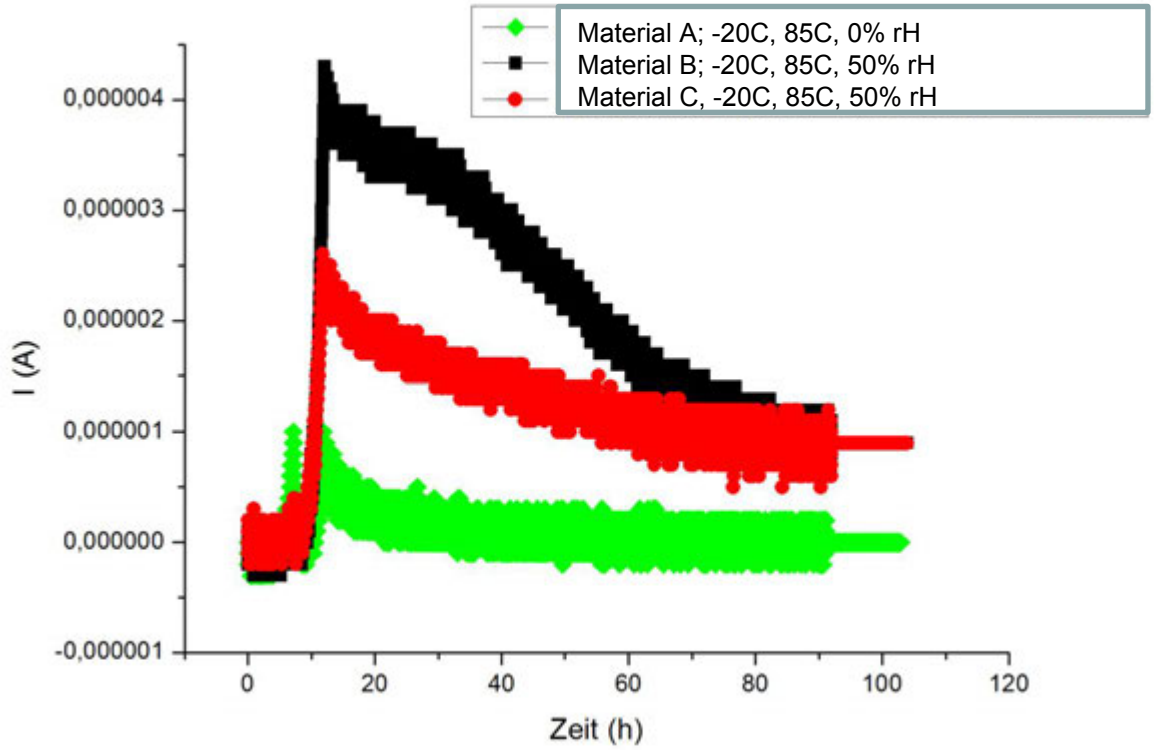
Panel level



Leakage current and cooresponding PID strongly dependent on temperature and humidity

SOLON

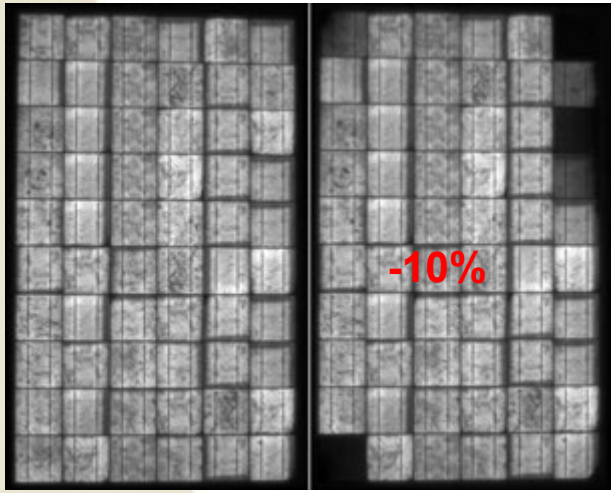
Panel level



Leakage current and cooresponding PID strongly dependent on temperature and humidity

SOLON

Temperature and humidity

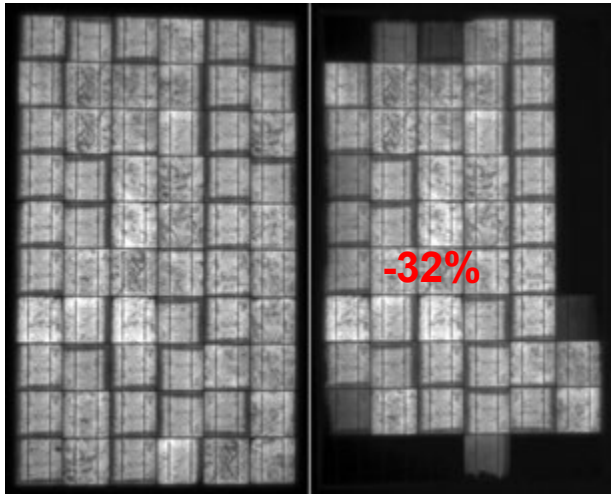


Time: 100h

Voltage: 1000V

Temperature: 85°C

Humidity: ≈ 0%

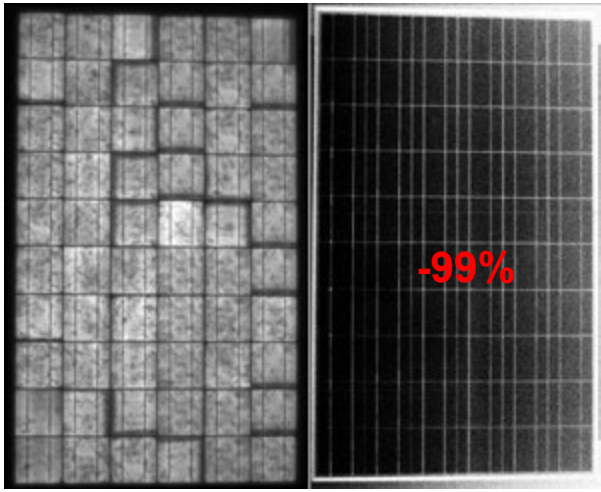


Time: 100h

Voltage: 1000V

Temperature: 85°C

Humidity: 50%



Time: 100h

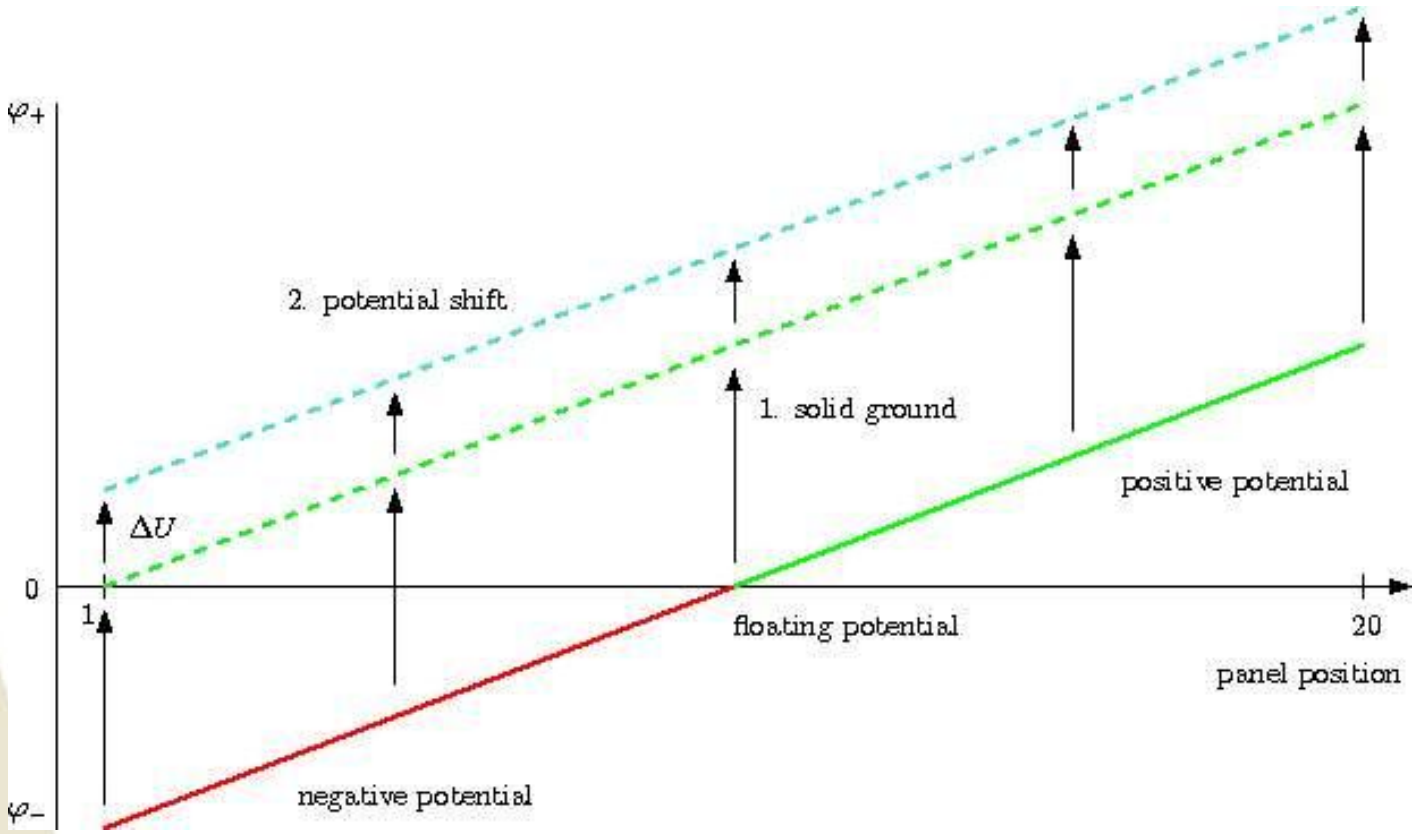
Voltage: 1000V

Temperature: 85°C

Humidity: 100%

SOLON

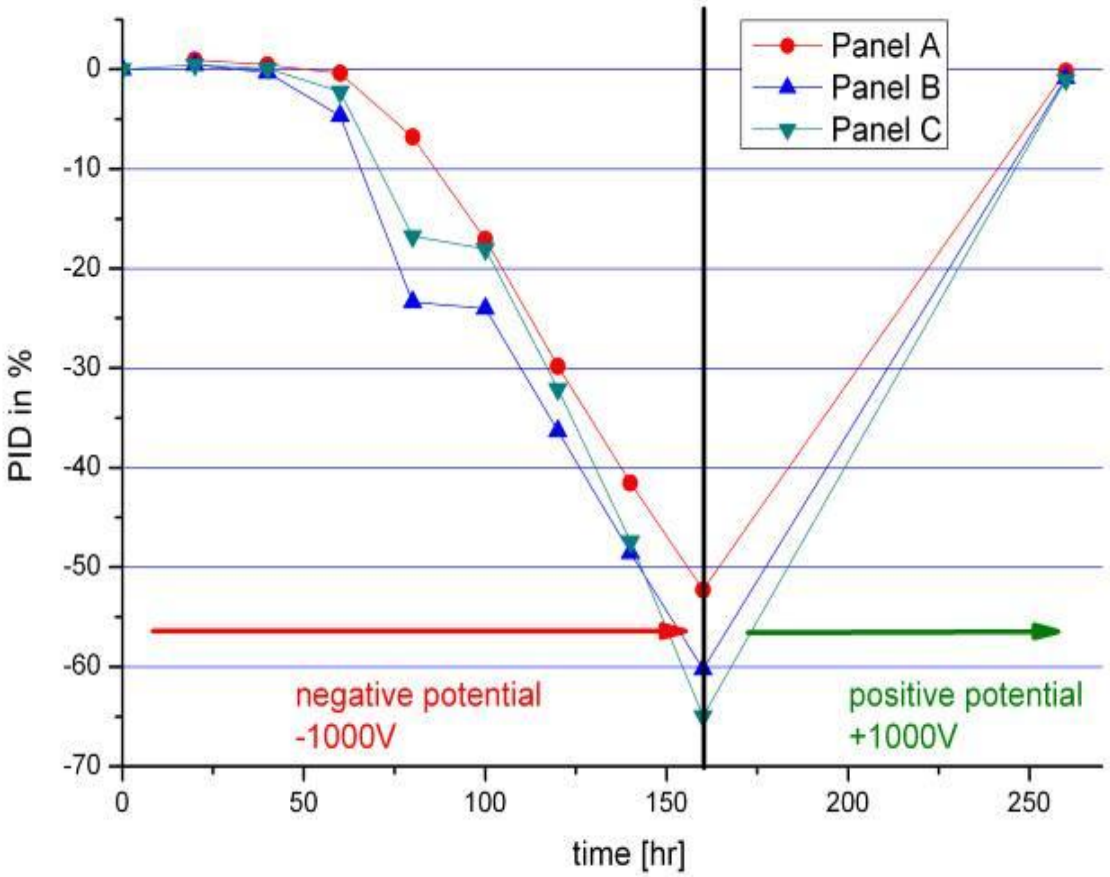
System level



→ Potential relative to ground is determinded by grounding configuration

SOLON

System level



Degradation and recovery of panels in the lab

PID can be stopped/ reversed by avoiding a negative potential
→ Suitable grounding configuration

SOLON

Content

- Introduction & Motivation
- Background & Approach
- Results
  - Cell level
  - Panel level
  - System level
- What's Next?
- Summary & Conclusion

SOLON

What's next?

How do laboratory results correlate to real life?

The concept:

- 2 different types of "laboratory proven" PID panels
  - High PID tendency
  - Low PID tendency
- 3 different climatic regions

The need:

- 3 identical test sites in 3 different regions

SOLON

Global Test Site Network



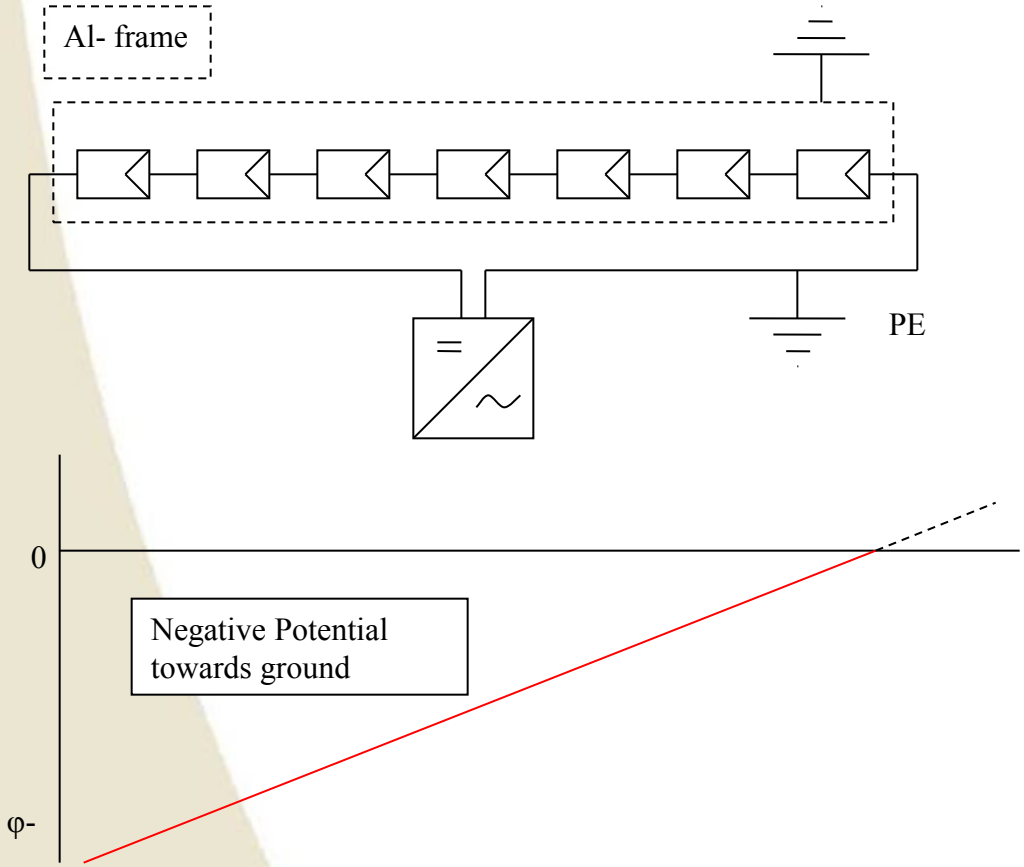
Global Test Site Network – The Locations



SOLON

What's next?

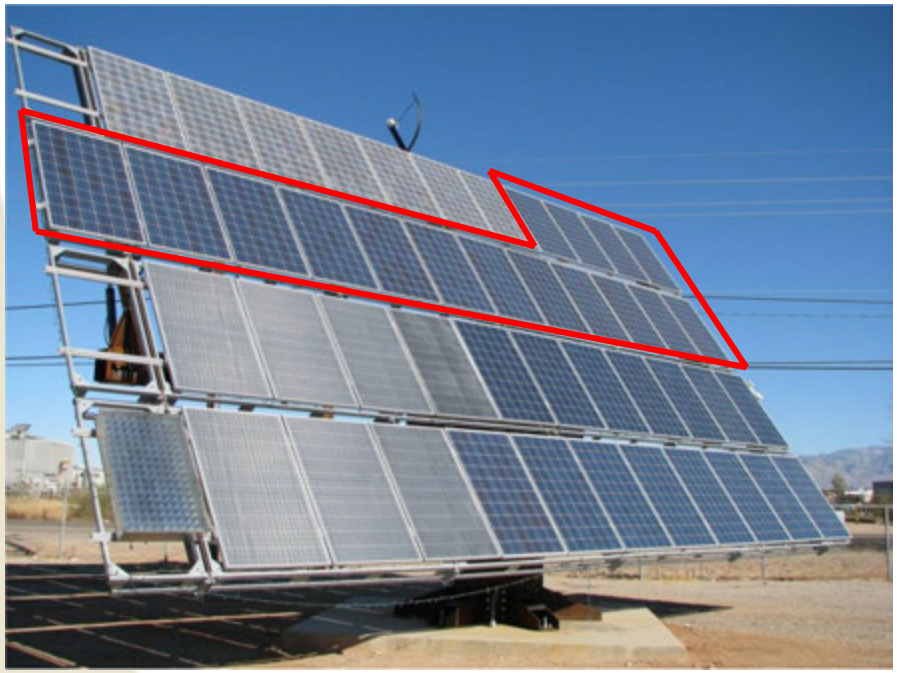
Setup on test sites:



- 3 test sites with identical system configuration and technology
- 2 strings of 7 modules each site – total 6 strings
- Two different materials (high and low PID tendency)
- Positive pole is grounded to simulate the worst case scenario
- Meteorological stations log environmental conditions at the different test sites

SOLON

What's next?



- 3 test sites with identical system configuration and technology
- 2 strings of 7 modules each site – total 6 strings
- Two different materials (high and low PID tendency)
- Positive pole is grounded to simulate the worst case scenario
- Meteorological stations log environmental conditions at the different test sites

SOLON

What's next?

Solar Cell Level

→ Cooperation with different cell suppliers to modify the ARC according to cell spec

Module Level

→ Electrical characterization of encapsulation foils with high and low PID prevention

System Level

→Evaluating suitable inverter suppliers and proposed solutions

SOLON

Content

- Introduction & Motivation
- Background & Approach
- Results
  - Cell level
  - Panel level
  - System level
- What's Next?
- Summary & Conclusion

SOLON

Summary and Conclusion

- Origin of PID: Properties of solar cell
  - → PID can be excluded/minimized on cell level
  - → ARC
- Leakage current on panel level key feature for PID
  - → PID can be excluded/ minimized on panel level
  - → Encapsulation
- Sign and magnitude of the external potential critical for PID
  - → PID can minimized on system level
  - →Grounding
- Avoiding PID on panel level favourable since
  - → Independent of cell technology
  - → Independent of system / grounding configuration

SOLON

Acknowledgements

Juliane Berghold

Sebastian Pingel

Oliver Frank

Markus Winkler

Henry Hoehne

& Different cell suppliers for providing us with specific test cells !!

SOLON



Thank you for your attention!

SOLON Corporation
6950 South Country Club Road
Tucson, Arizona 85756
www.solon.com

SOLON

FLORIDA SOLAR ENERGY CENTER

Creating Energy Independence

High Voltage Bias Testing of Specially Designed c-Si PV Modules

Neelkanth G. Dhere, Shirish A. Pethe, Ashwani Kaul

Florida Solar Energy Center,

1679 Clearlake Road, Cocoa, FL-32922, USA

e-mail: dhere@fsec.ucf.edu

A Research Institute of the University of Central Florida

Outline

- Introduction
- Earlier Generation a-Si:H PV modules
- Specially Designed c-Si PV modules
- Sister Projects
- Summary

Introduction

- Certification process currently employed for PV modules though reduces infant mortality does not duplicate the real time conditions completely.
- In grid connected PV systems the PV modules may be at voltage of as much as ±600 volts with respect to ground in USA and as high as ±1000 volts or higher with respect to ground in Europe and elsewhere.
- The voltage gradient between PV circuit and ground can cause the leakage current to flow.

Leakage Current

- Energy that dissipates from the PV circuit through the encapsulation to the ground is termed leakage current.
- Leakage current may be composed of charge carriers that move under the influence of voltage and concentration gradients through the insulation, reacting with it and cell and frame metals to produce corrosion products and can lead to electromigration and degradation.
- Leakage current levels are also determined in large part by the insulation electrical conductivity that varies greatly with temperature and relative humidity.

High voltage bias testing

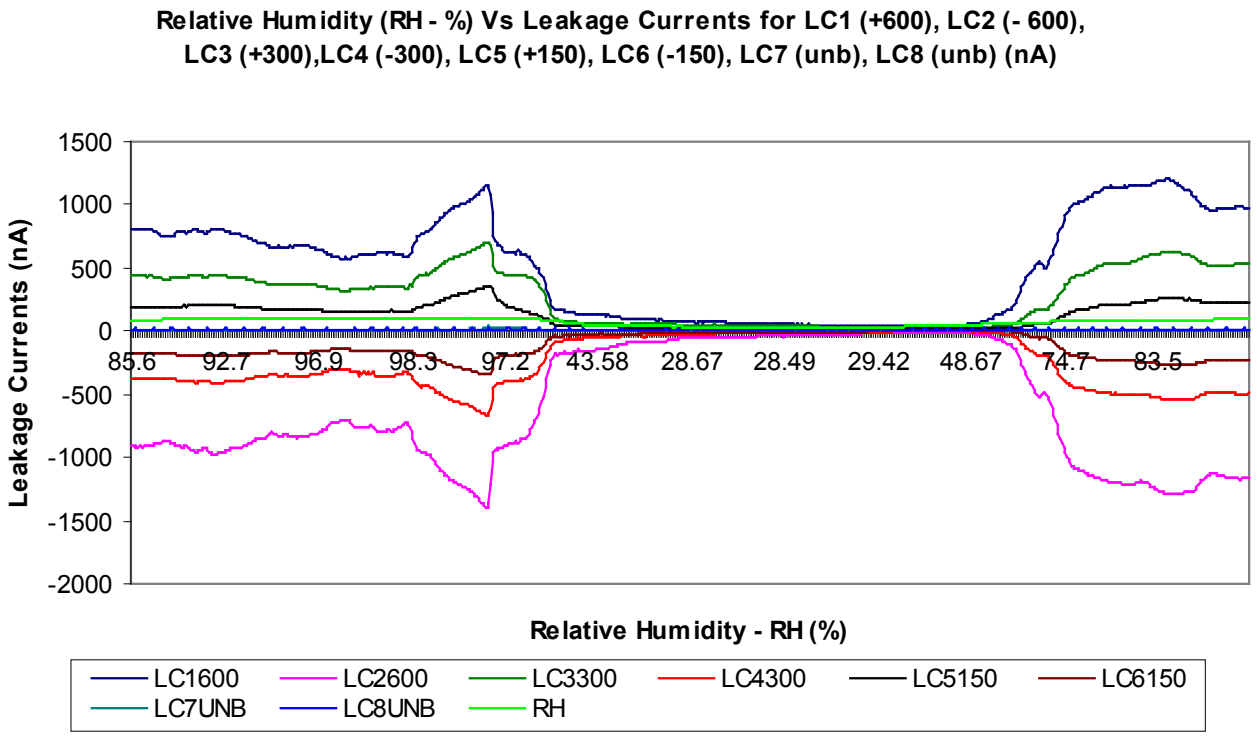
- Pioneering research by Joe del Cueto and colleagues
- The effect is considerably more prevalent in the hot and humid climate.
- Hence they encouraged and supported the initiation of the research plans at FSEC for high voltage bias testing in the hot and humid climate.
- Recent research on high voltage bias acceleration testing by Peter Hacke and colleagues.

Earlier Research at FSEC

- BP solar a-Si:H modules deployed in hot and humid climate of Florida
- Six modules at the following fixed bias voltages : +600 V, -600 V, +300 V, -300 V, +150 V, and -150 V, and two unbiased modules.

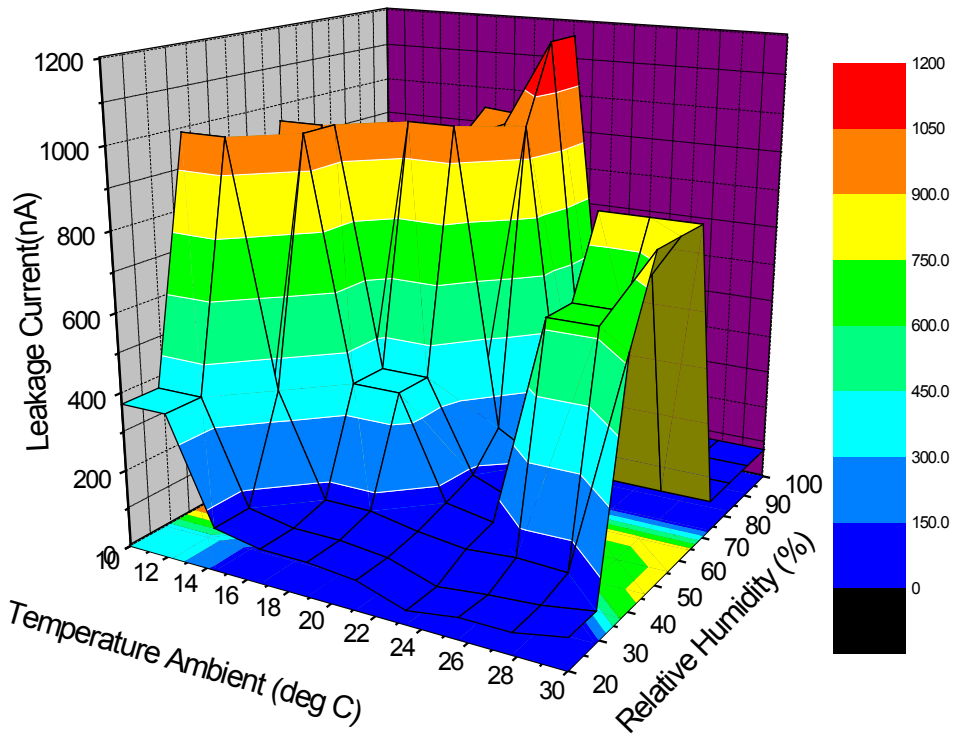


RH Vs Leakage Current



☼ Sunny Day

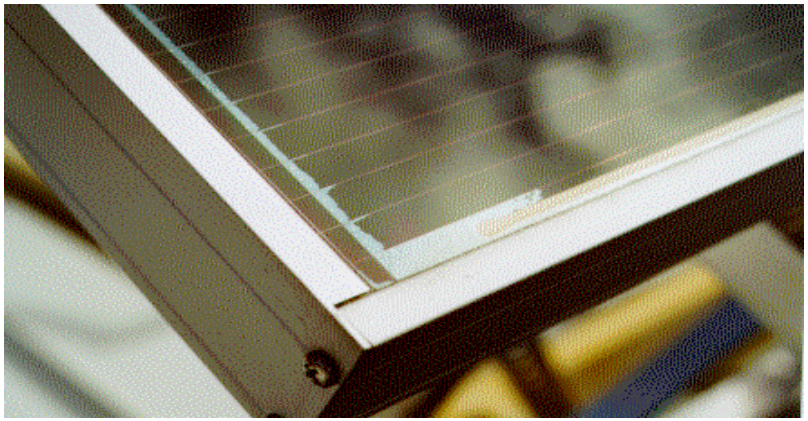
RH & T Vs Leakage Current



Degradation and Analysis

- *Delamination of SnO_2:F layer together with the a-Si:H cell from glass surface due to diffusion of sodium from sodalime glass.*
- *Thus sodium free glass as described by Dr. James Webb, Corning as well as low sodium, treated glass (described earlier in AFG, Siemens, FSC) will be valuable.*
- *Damage is caused by electrocorrosion*
- *Corrosion initiated near the bottom edges of individual cell strips and moved inwards.*

Degradation



-600 V Module – 8 months



-600 V – 27 months



-300 V – 32 months



-150 V – 32 months

Degradation and Analysis

- *Corrosion was not found in the positively biased modules.*
- *Some amount of corrosion was found in the unbiased modules.due to self bias.*





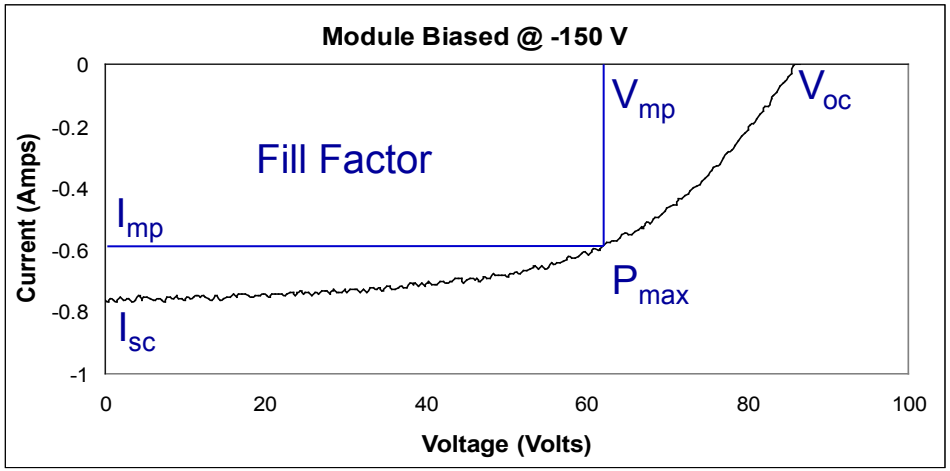
Degradation Process

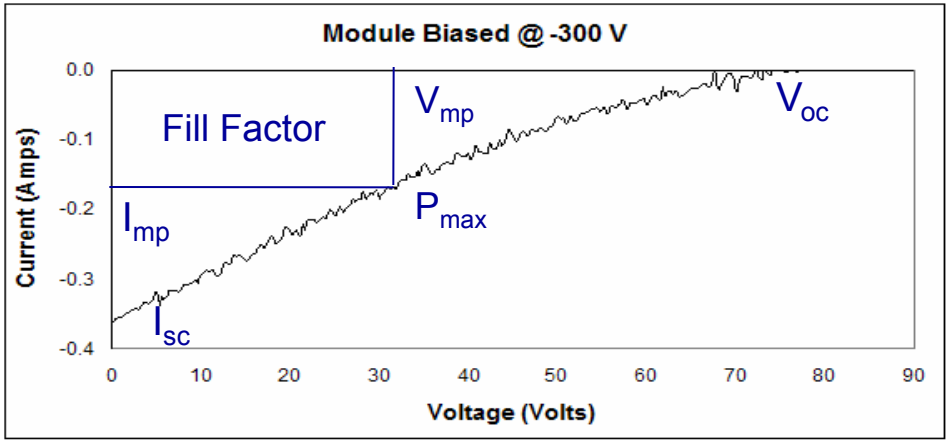
- *Initially no ingress paths hence incubation period.*
- *Damage initiated at lower edge and corners with the lattitude tilt*

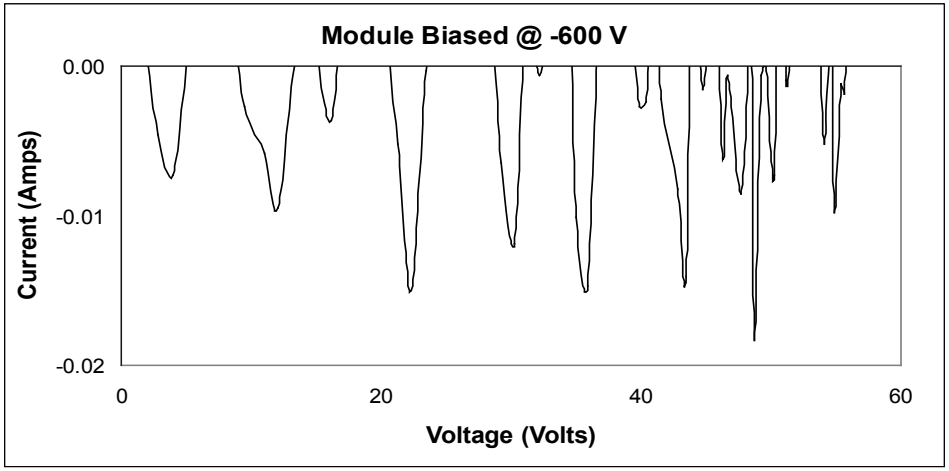


Degradation of -600 V with time

I-V Curves


Module Biased @ -150 V
Current (Amps)
0
-0.2
-0.4
-0.6
-0.8
-1
0
20
40
60
80
100
Voltage (Volts)
Fill Factor
V_{mp}
V_{oc}
I_{mp}
P_{max}
I_{sc}


Module Biased @ -300 V
Current (Amps)
0.0
-0.1
-0.2
-0.3
-0.4
0
10
20
30
40
50
60
70
80
90
Voltage (Volts)
Fill Factor
V_{mp}
V_{oc}
I_{mp}
P_{max}
I_{sc}


Module Biased @ -600 V
Current (Amps)
0.00
-0.01
-0.02
0
20
40
60
Voltage (Volts)

I- V Measurement Data Analysis

Power Reduction (%)

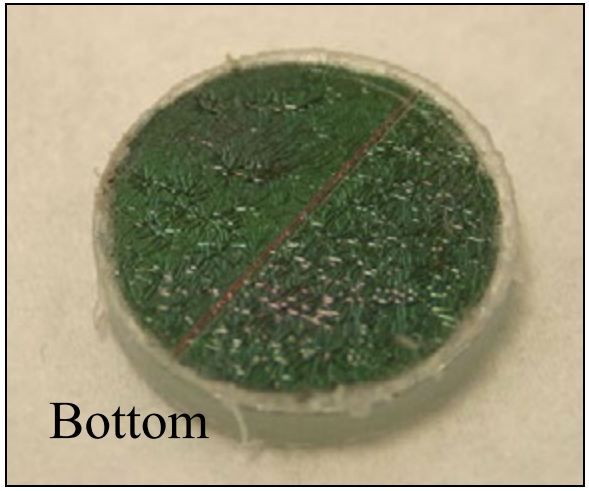
Bias	Oct - 2003	After Decommissioning
-150 V	11.4	21
-300 V	40.7	85.8
-600 V	NA	98
+600 V	NA	6
UB	NA	3.82
Control	NA	

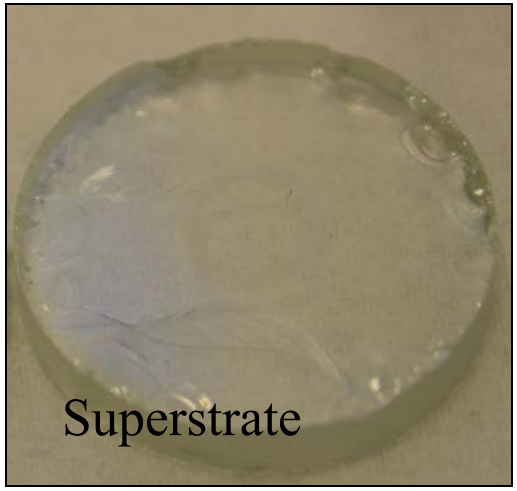
Series Resistance

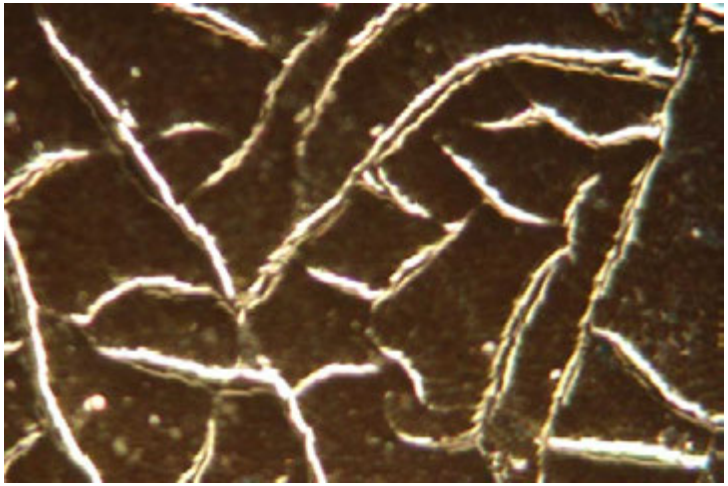
Bias	Control	-150 V	-300 V	-600 V
Series Resistance (Ω)	15	30	382	NA

Coring and Analysis

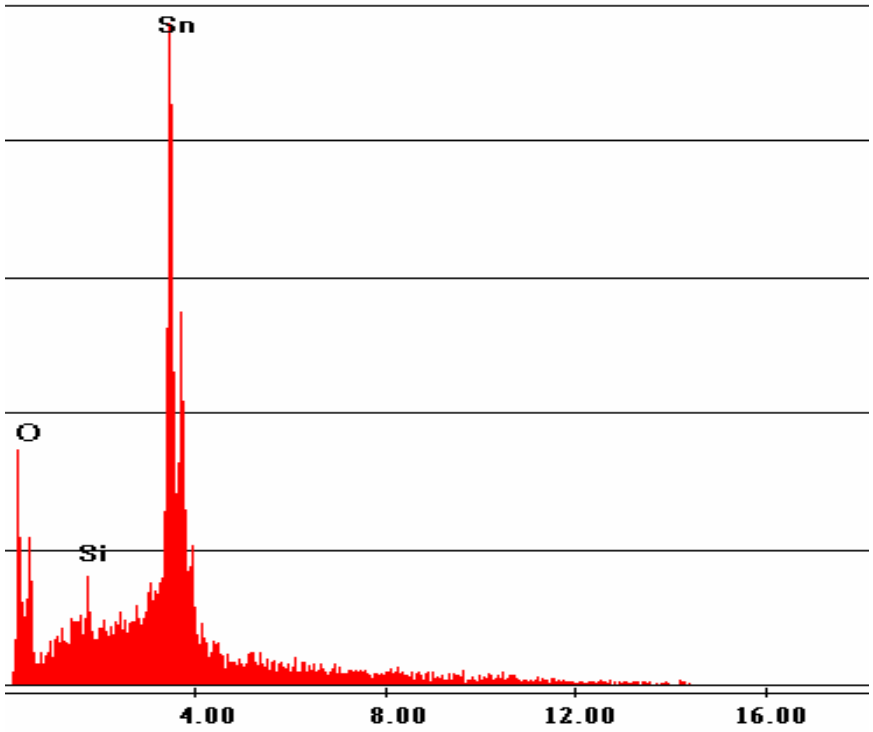
- *The a-Si:H cell delaminated and transferred itself entirely to the bottom glass/EVA surface.*
- *Adhesional strength was completely lost in the damaged area.*
- *Resistance above the range of measurement.*
- *The tendrils appeared as cracks*



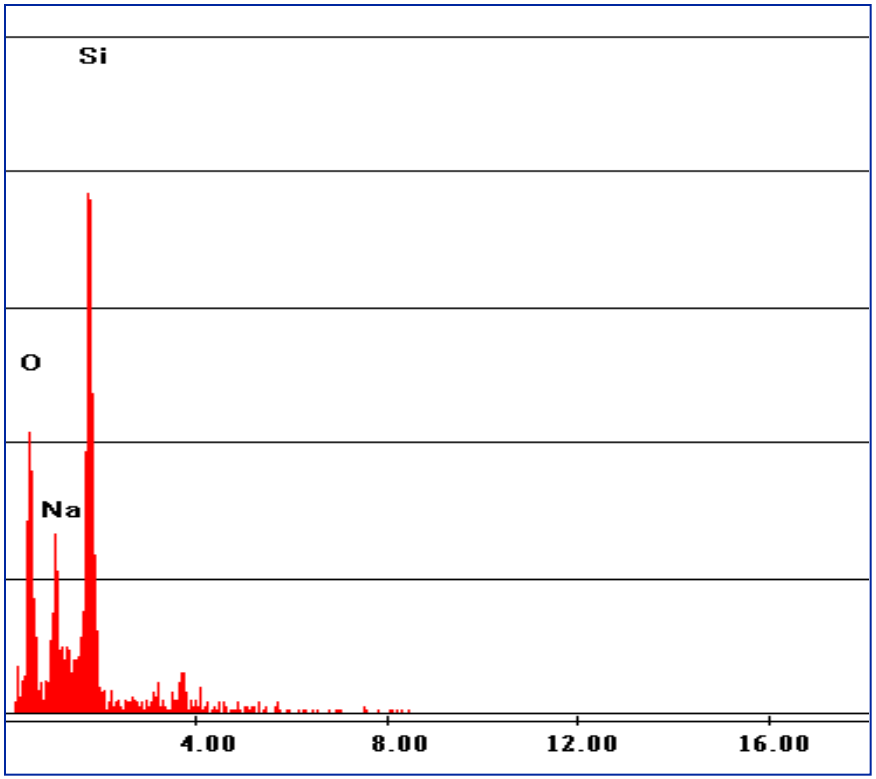




XEDS Analysis



Cell Sample



Superstrate Sample

Field deployed Thin Film PV Modules

- Side by side testing of thin-film PV module arrays self biased to voltages up to ± 600 V.
- Test bed designed and built by Graduate students



Continued work

- EPV and USSC continued the testing after the NREL project was over.
- USSC is very pleased with the work and is extending the Project for 3 more years
- Results are being submitted to IEEE PVSC, Seattle.

Advantages of this method

- Module are under real system bias
- Multiple voltages-different modules under different voltages, unbiased at night
- Reproduces real-time conditions and provides better statistics

Very High voltage bias testing of c-Si modules

- BP Solar/DOE supported project.
- The platform was designed with the participation of Graduate students.
- Especially meant for carrying out high voltage testing at voltages > than 600 V up to 3000 V.
- The design was certified by an engineering firm and approved by UCF EH&S.
- Satisfies the required NEC codes

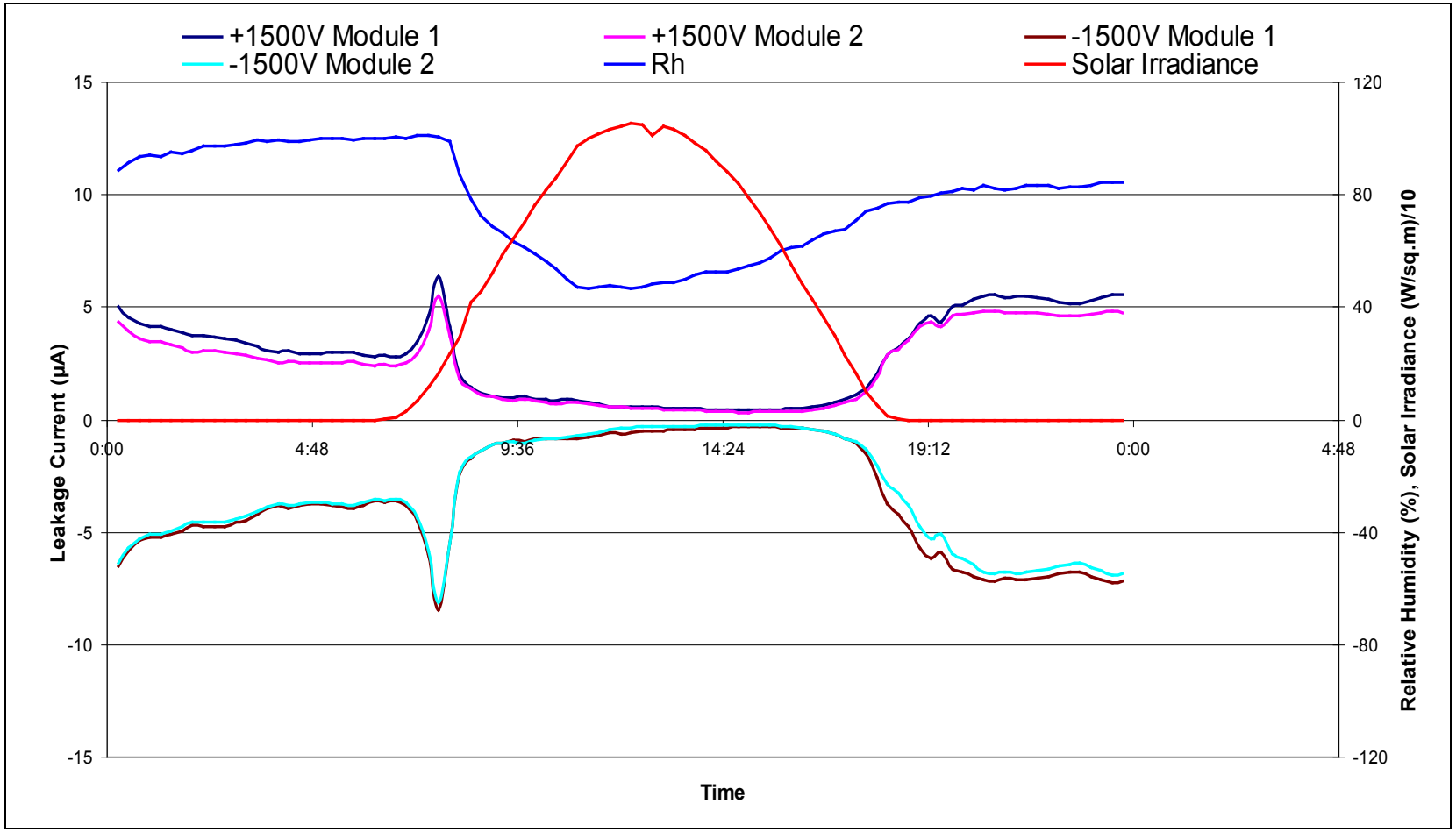
High voltage test bed



Specially Designed c-Si PV modules

- BP Solar c-Si modules specially designed for operation at the system voltage of 1000 V were tested in the hot and humid conditions of Florida. The modules were individually biased to +1500 V and -1500 V.
- One of the first observations made during this test was that the magnitude of leakage current for negatively biased modules was higher than that for positively biased modules.

Variation of leakage current in c-Si PV modules



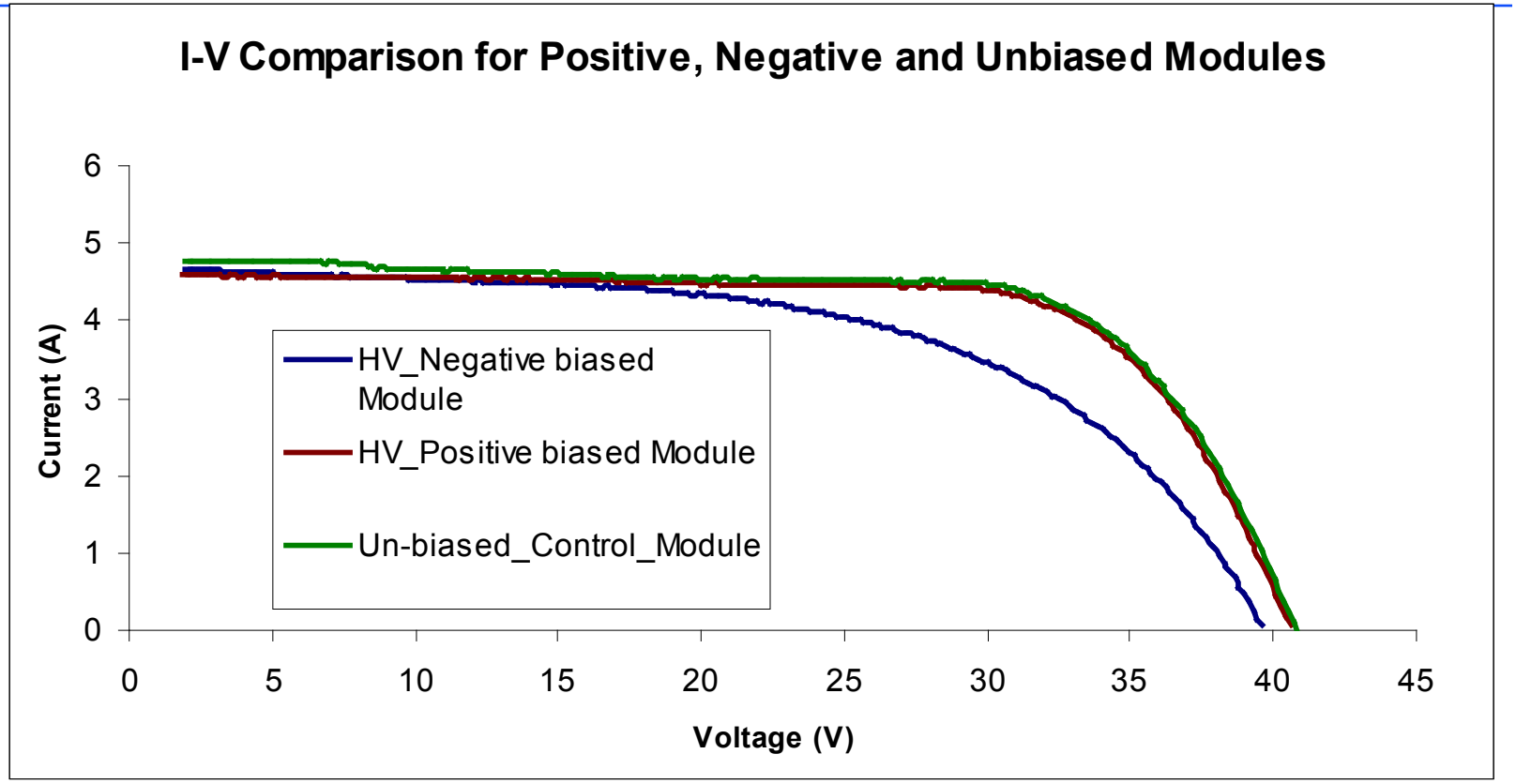
☼ Sunny Day

Specially Designed c-Si PV modules

- Periodic current-voltage (I-V) measurements were carried out on the high voltage biased modules.

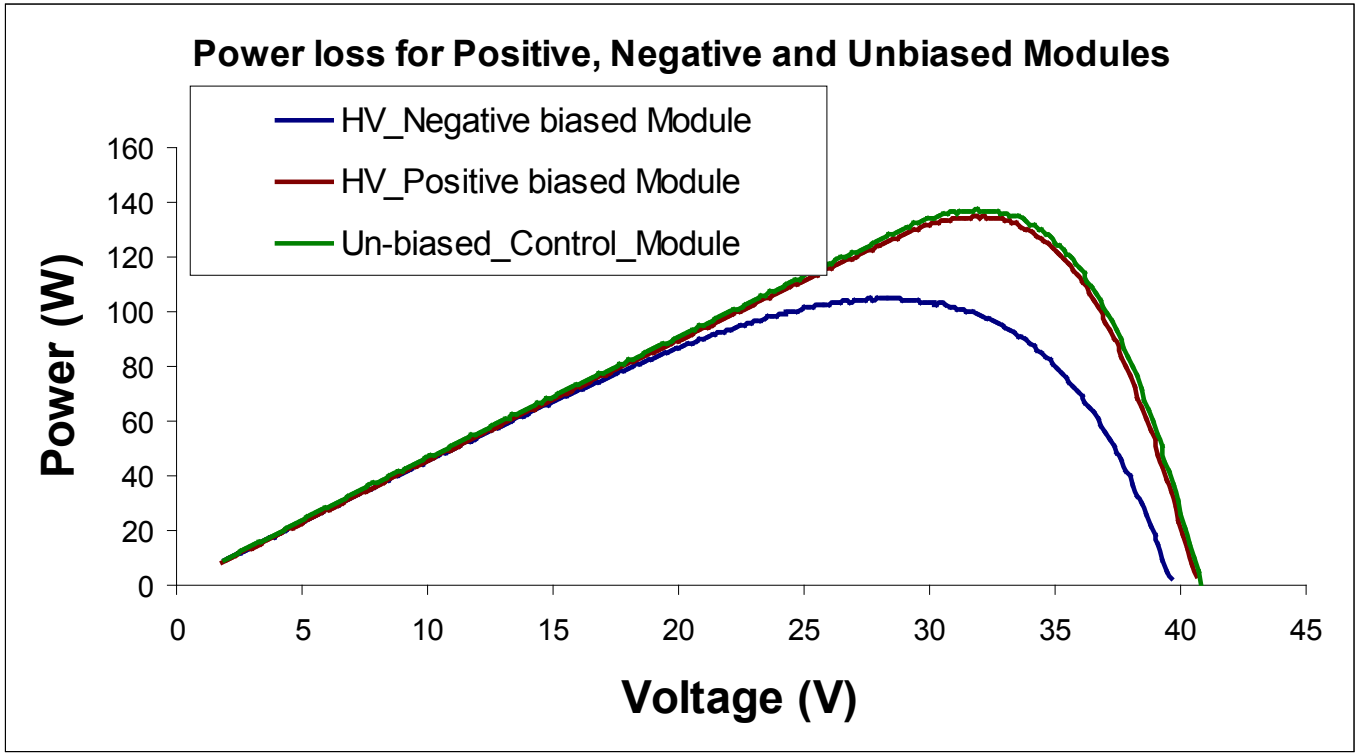
- Comparison of I-V, power-voltage characteristics, and calculations of the power loss, at the end of Year 1, are provided in the following Figures and a Table.

Current vs voltage I-V comparison



- Current versus voltage comparison of the control, positively biased and negatively biased modules.

Power loss comparison



- Power versus voltage comparison of the control, positively biased and negatively biased modules.

Power loss comparison

- As can be seen, at the end of Year 1, the control module, the two positively biased modules and the two negatively biased modules exhibited a power loss of 8.1%, 9%, 7.9%, 25.6% and 25.7% respectively with respect to their rated power.

Power loss Calculation

	Power loss (%)				
Module type	**Nov-08**	**Dec-08**	**Mar-09**	**Feb-11**	**SPIRE**
c-Si_P1	NA	12.2	9.0	9.8	6.9
c-Si_P2	9.0	10.7	7.9	9.3	5.9
c-Si_N1	30.9	30.1	25.7	NA	NA
c-Si_N2	29.3	29.2	25.6	21.5	18.6
c-Si_Control	NA	7.5	8.1	NA	NA

Comparison of PV Parameters

- Periodic current-voltage (I-V) measurements were carried out on the high voltage biased modules.
- Comparison of the normalized peak power and the photovoltaic parameters of the control, positively biased and negatively biased modules is provided in the following Table.
- Normalized peak power and PV parameters were calculated from the I-V curves.

Comparison of PV Parameters

PV Parameter	Unbiased Module	-1500 V biased module	+1500 V biased module
Normalized Peak Power	157.22 W	118.8 W	149.22
Fill Factor	70.4%	55.75%	70.6 %
Normalized O.C. voltage	46.17 V	44.63 V	44.83 V
Normalized S.C. current	5.16 A	5.11 A	5.0 A
Series Resistance	1.38 Ω	1.87 Ω	1.37 Ω
Shunt Resistance	175 Ω	68.5 Ω	161.3 Ω

Conclusion from Comparison of PV Parameters

- As can be seen from the Table, the power loss of the -1500 V biased modules is mostly due to the 15~% reduction in fill factor.
- Fill factor loss and power loss could be due to the increase of the series resistance and decrease of shunt resistance.
- One of the two degraded, negatively biased modules was sent back to BP Solar.

New c-Si modules

- Two new c-Si modules were received from BP Solar.
- One was negatively biased and other was deployed as control module in the field.

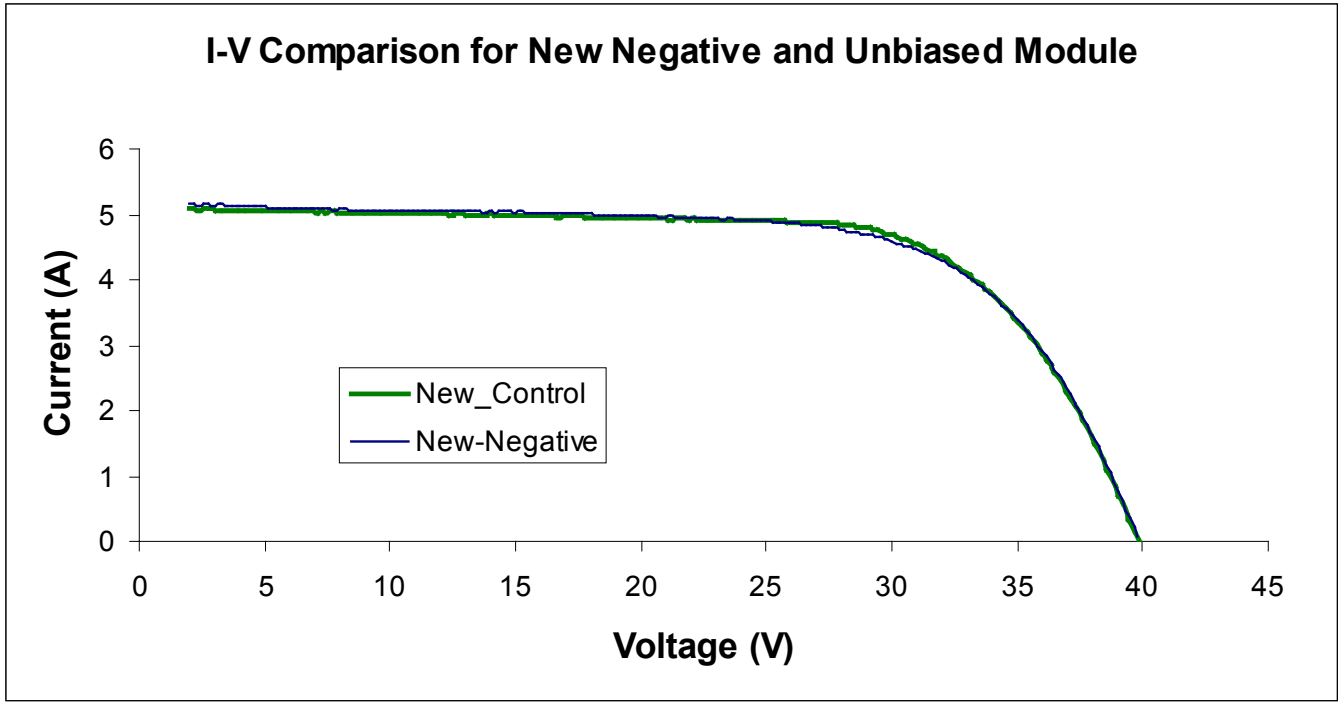
Important Clarification

- Here it must be stated clearly that all the results and any conclusions of the continued research must be considered as tentative and very preliminary because of the lack of opportunity to analyze the data systematically, as well as to carry out the essential and usual complementary measurements.
- It is planned to carry out the systematic analysis of the data as well as to carry out the essential and usual complementary measurements during the next few months.

New c-Si modules

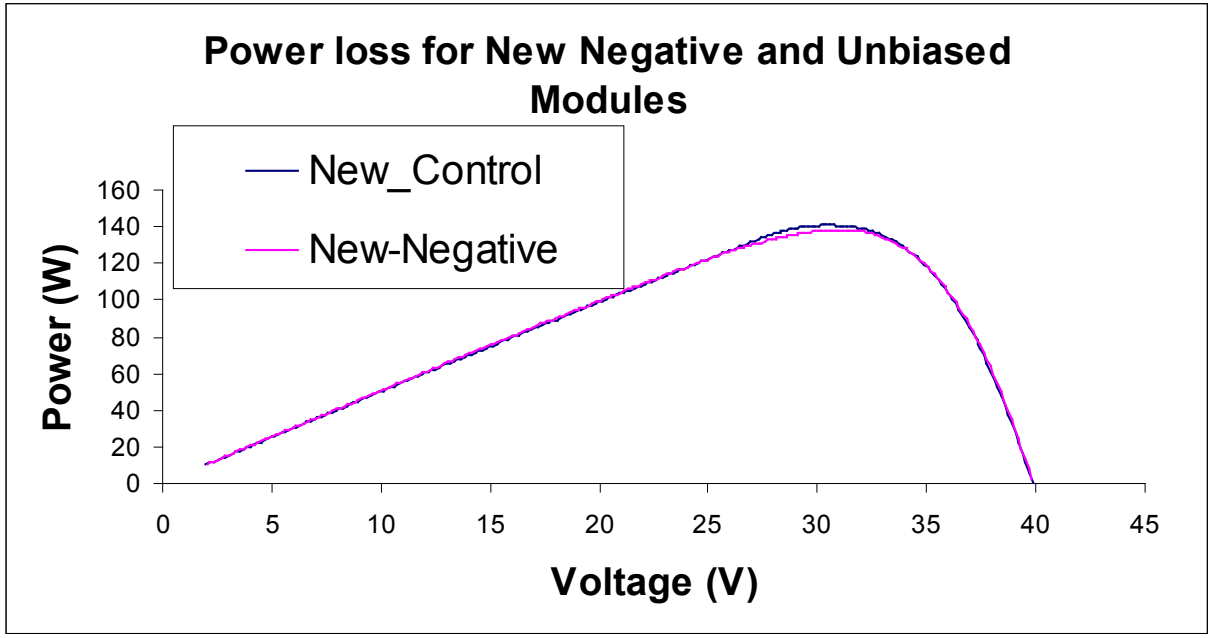
- Preliminary comparisons of current-voltage (I-V) and power-voltage characteristics after additional ~ 1 ½ years of field deployment in hot and humid climate are provided in the following Figures.

Preliminary I-V comparison



- Preliminary comparison of current-voltage (I-V) characteristics after ~ 1 ½ of field deployment in hot and humid climate.

Preliminary power loss comparison



- Power loss calculated based on the rated power of the c-Si modules.

Effect of hot and humid climate

- Both modules showed significant power loss calculated based on the rated power within a very short period
- There was only a 2% difference in power loss between unbiased and biased module.
- Apart from the negative bias the hot and humid climate itself had a significant impact on the module power loss within a period of 1 ½ years of field deployment.

Preliminary power loss calculation

	Power loss (%)				
Module type	**Nov-08**	**Dec-08**	**Mar-09**	**Feb-11**	**SPIRE**
c-Si_New_Negative	NA	NA	NA	11.9	9.6
c-Si_New_Control	NA	NA	NA	10.0	7.0

Preliminary power loss calculated from the I-V measurements with respect to rated power

Power loss Summary

	Power loss (%)				
Module type	**Nov-08**	**Dec-08**	**Mar-09**	**Feb-11**	**SPIRE**
c-Si_P1	NA	12.2	9.0	9.8	6.9
c-Si_P2	9.0	10.7	7.9	9.3	5.9
c-Si_N1	30.9	30.1	25.7	NA	NA
c-Si_N2	29.3	29.2	25.6	21.5	18.6
c-Si_Conrol	NA	7.5	8.1	NA	NA
*c-Si_New_Negative	NA	NA	NA	11.9	9.6
*c-Si_New_Control	NA	NA	NA	10.0	7.0

*Tentative and Preliminary

Comparison of PV Parameters for new c-Si modules

PV Parameter	New Unbiased Module (Control Module)	New -1500 V biased module
Normalized Peak Power	157.5 W	154.2 W
Fill Factor	69.85%	67.4%
Normalized O.C. voltage	43.0 V	43.1 V
Normalized S.C. current	4.98 A	5.0 A
Series Resistance (SPIRE)	0.95	0.98
Shunt Resistance (SPIRE)	162.84	173.68

Acceleration Factors (AF)

- Since the module are biased 24 hours a day preliminary calculations of the acceleration factors were carried out from the magnitude of the leakage current.

- The formula used is :

$$AF = \frac{\text{Total leakage current during day and night}}{\text{Total leakage current during the day}}$$

Acceleration Factors

Day	+1500 V P1	+1500 V P1	-1500 V N1	-1500 V N2
Cloudy Day	2.5	2.44	2.32	2.5
Clear Sunny Day	4.54	4.76	3.7	4.76

HV bias testing of Dow Chemical c-Si modules

- High voltage bias testing of c-Si modules with specially developed encapsulants of Dow Chemical Company.
- Modules with different encapsulation types biased individually to ± 600 V in hot and humid climate of Florida.
- Results from this research is being jointly submitted to IEEE PVSC Seattle conference (Currently awaiting approval).

Summary

- The results from the HV bias testing of c-Si modules have been presented.
- The tentative preliminary results from two new c-Si modules are also included after 1 ½ year of HV bias at -1500 V
- The acceleration factors have been calculated for a rainy day and clear sunny day.
- It can be inferred that the study of leakage currents in photovoltaic modules is effective in early detection of design, material, as well as process flaws.

Acknowledgement

- The research was supported by DOE/BP Solar project.
- The authors gratefully acknowledge encouragement by and useful discussions with Dr. John Wohlgemuth, Dr. Dan Cunningham, Dr. Rajeewa Arya, BP Solar and Dr. Joe del Cueto, Dr. Harin Ullal, Dr. Bolko von Roedern and Dr. Peter Hacke, NREL and Dr. James Webb, Corning.

Questions and Comments



Failure modes and degradation rates from field-aged crystalline silicon modules

Tony Sample

European Commission, DG JRC, Institute for Energy, Ispra, Italy

This presentation does not contain any proprietary or confidential information.

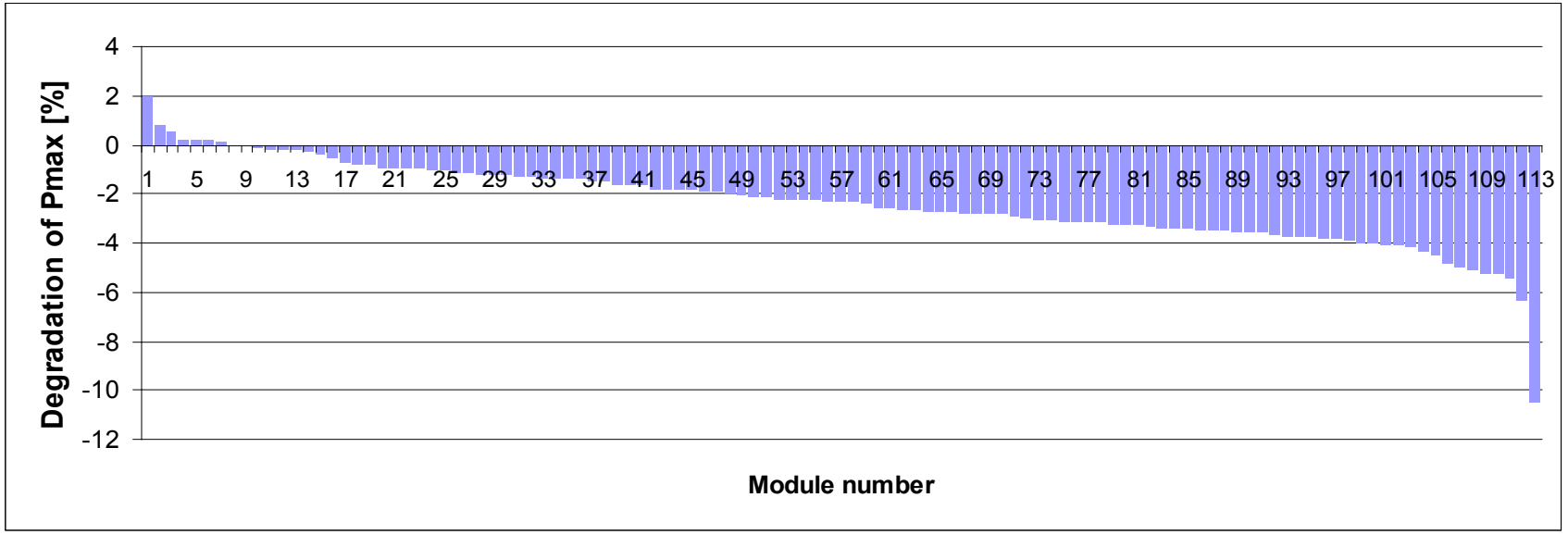
What we would like to know

- The **Degradation Mechanisms.**
  - One such source is the initial photon degradation related to a physical process in the solar cell itself, **short term**.
  - Other sources are related to **long term** weathering and degradation of the module package.
- The **Degradation Rates**. In order to understand the effect and relevance of each of these mechanisms on the total energy production of a PV module or array over its life time.
- The **Life Expectancy**. With this Life expectancy and knowledge of the degradation rates we can define the total energy output per lifetime of a PV module or array.

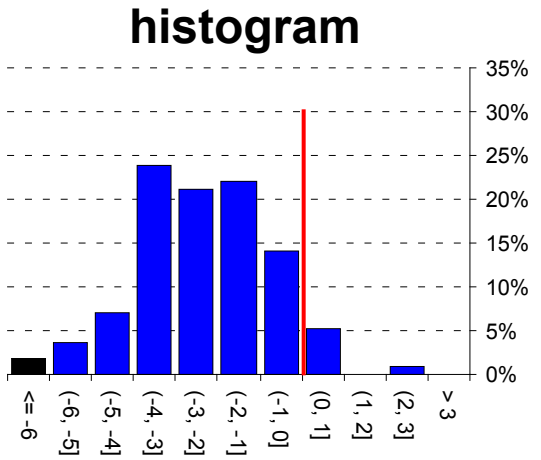
Examples of Initial Degradation

- During an IEC 61215 test procedure there is the requirement to perform a outdoor exposure (OE) test of 60kWh solar irradiance in short circuit conditions.
- At the JRC ESTI laboratory 113 modules types have been subjected to this test.
- Degradations observed range from zero to -6.3% with a correlation between the P_{max} degradation and the I_{sc} degradation.
- The average degradation observed is **2.4%** with deviation of ± 1.7%.

Degradation in OE Test



Summary of the degradation in P_{max} after the Outdoor Exposure Test for 113 module types tested at JRC Ispra.



The ESTI Outdoor Test Field, Operating Since 1982

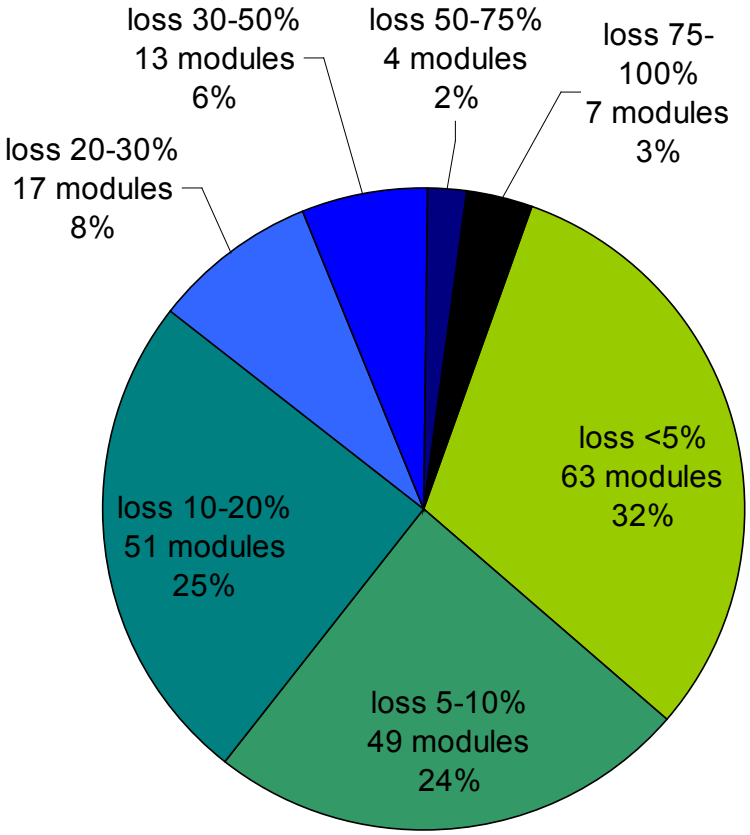


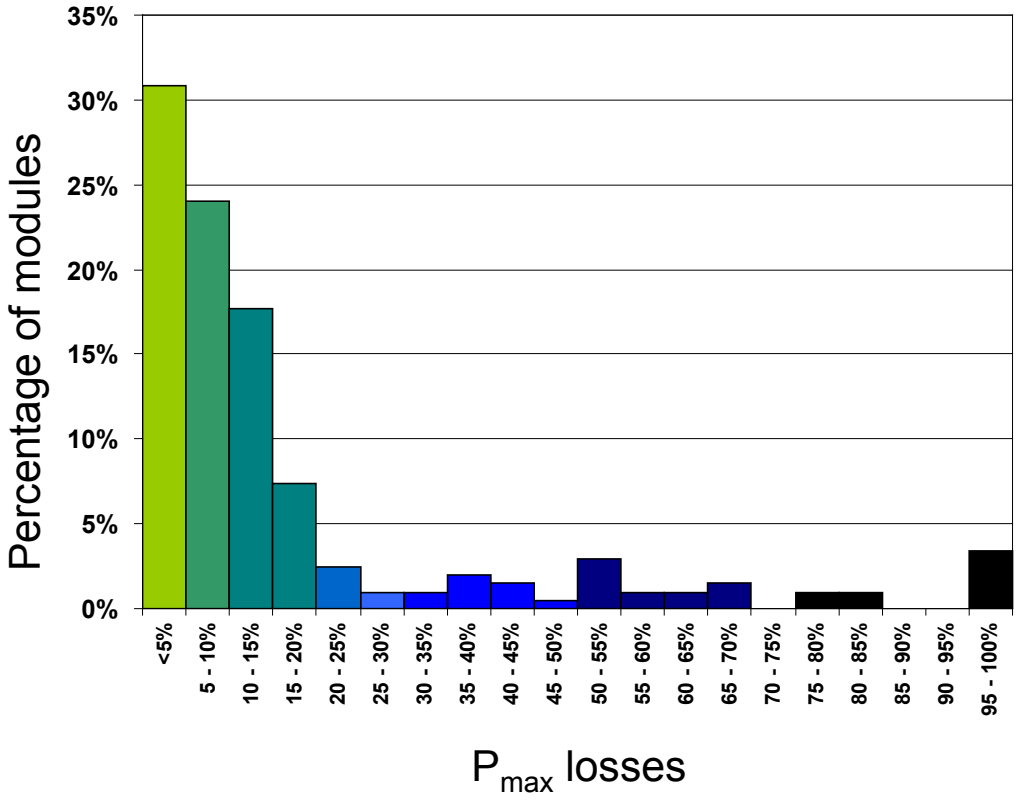
Long-term outdoor exposure

Long-term (18 - 24 years) outdoor exposure
Location: Ispra - moderate subtropical (-10º..+35º, >90% RH)

No of modules		**204**
No of producers		**20**
No of module types		**53**
Cell type	**Mono**	**123**
	Poly	**81**
Encapsulant	**PVB**	**59**
	Silicone	**40**
	EVA	**101**
	Other (unknown)	**4**
Substrate / Backsheet	**Glass**	**68**
	Tedlar, Tedlar/Aluminium/Tedlar	**62**
	Tedlar/Aluminium/Polyester	**8**
	Polyester/Aluminium	**20**
	Silicone	**20**
	Others, polyethylene, "plastic" Unknown	**26**

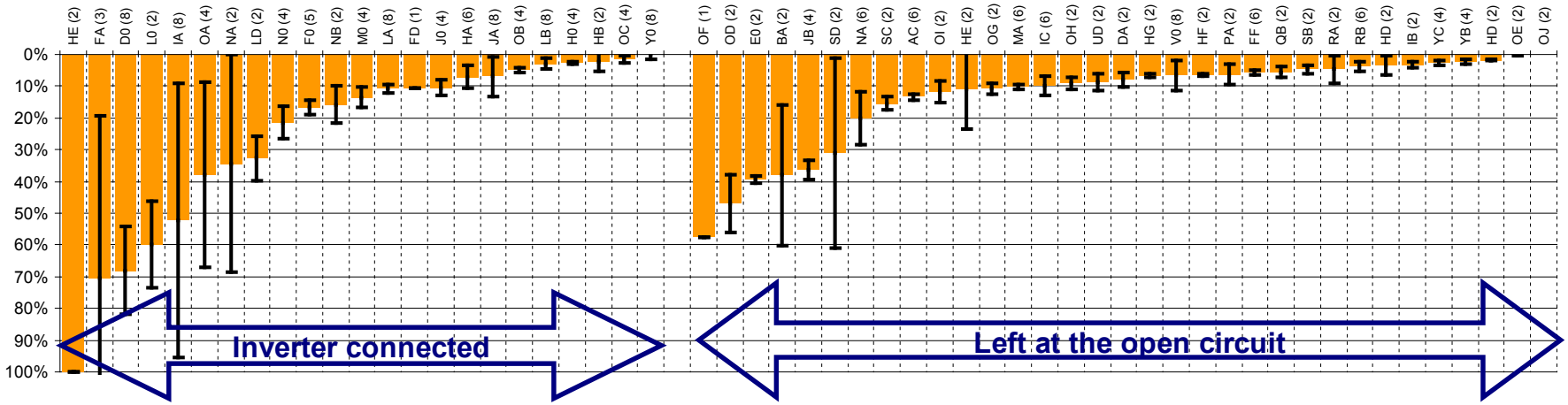
P_{max} losses from all 204 modules





Effect of electrical condition

Relative P_{max} losses of modules series grouped by module's test conditions

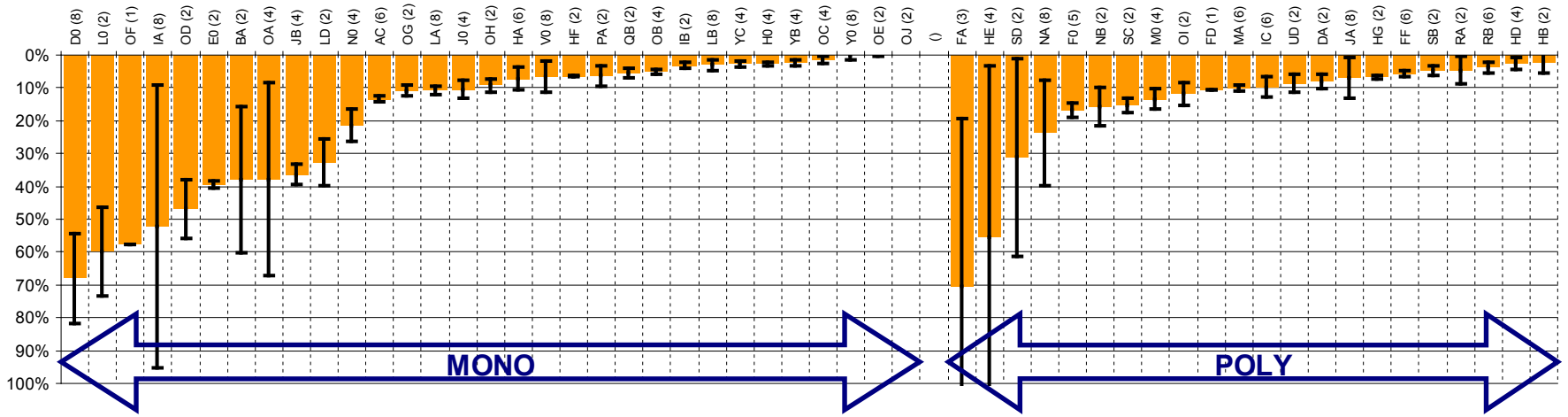


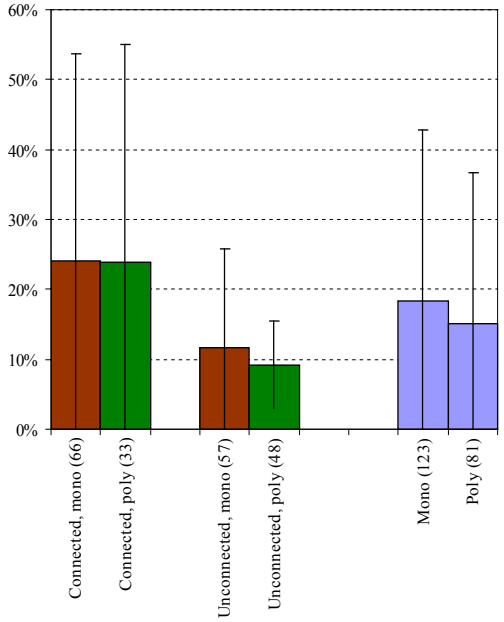
A statistical difference between modules initially connected to the inverter (charger) which exhibited approximately twice the average degradation in comparison to modules left in open circuit.

All of the modules (7) which exhibited total circuit breakage were connected to the inverter.

Impact of cell type

Relative P_{max} losses of modules series grouped by cell technology

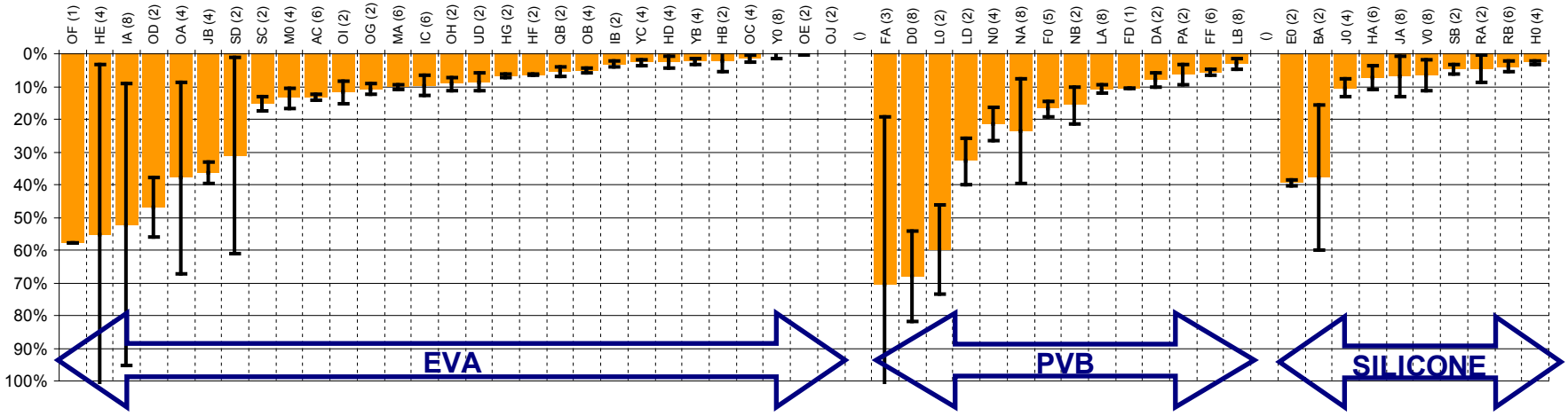


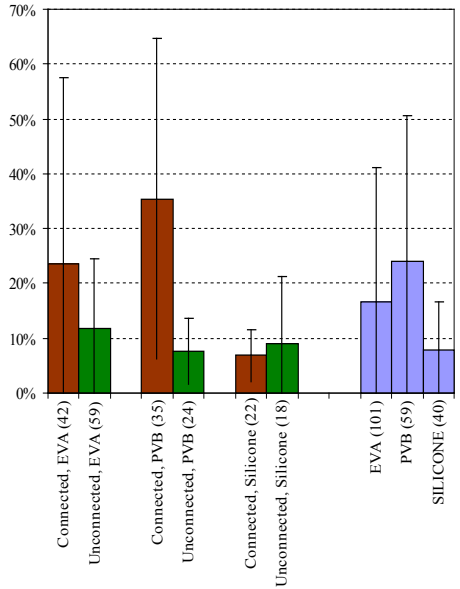


No statistical difference between modules incorporating monocrystalline or polycrystalline cells

Impact of the type of encapsulant

Relative P_{max} losses of modules series grouped by encapsulant

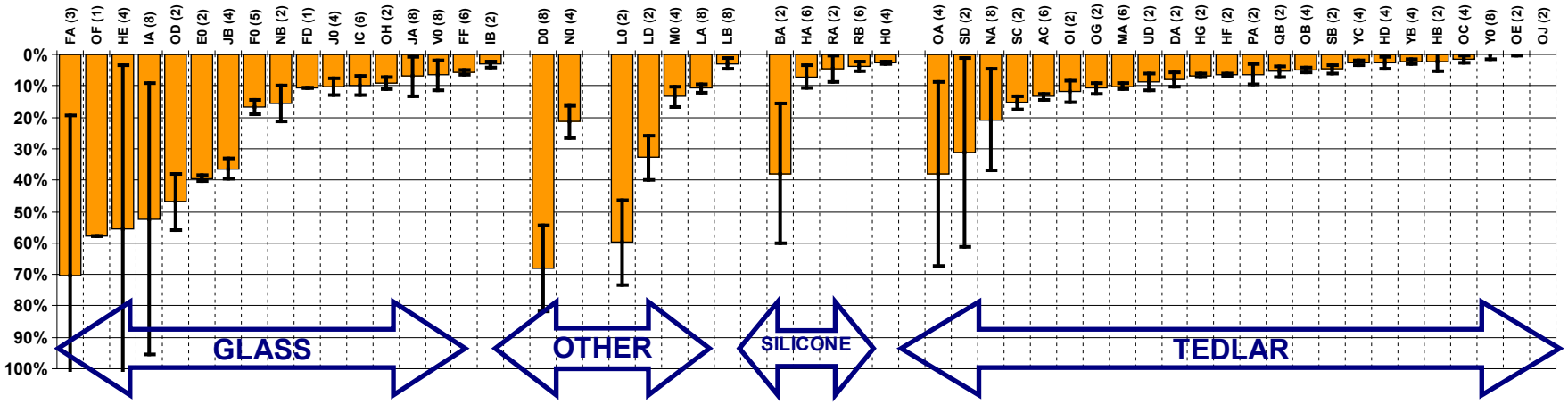


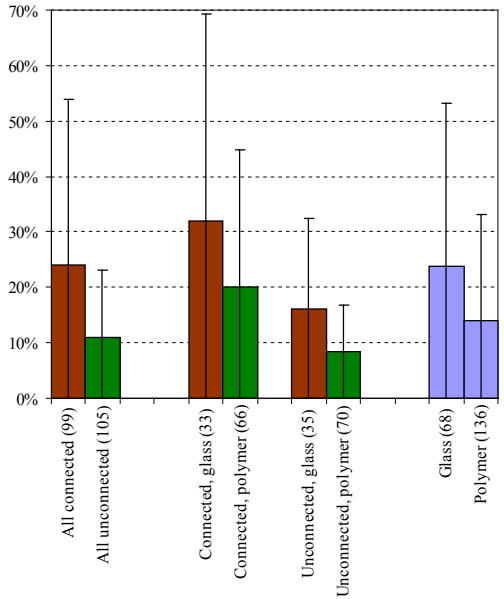


Modules incorporating silicone encapsulation generally exhibited lower degradation

Impact of the substrate

P_{max} losses of modules series grouped by back sheet

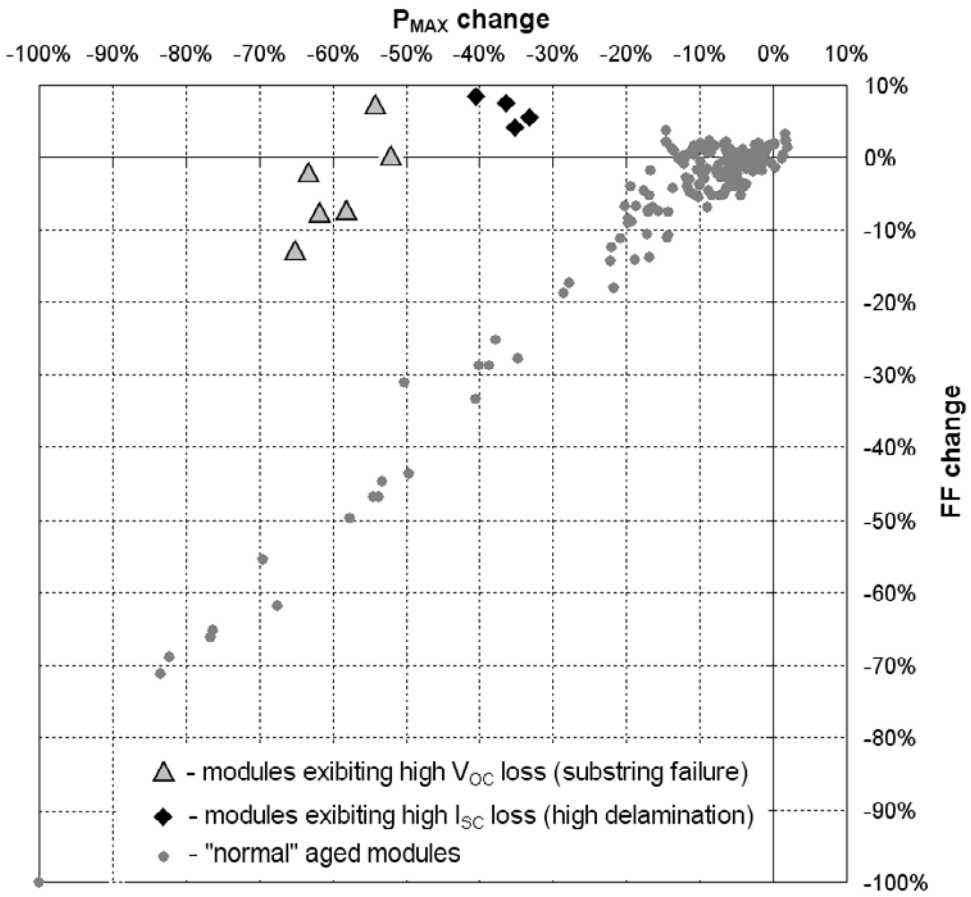




Glass-glass modules generally exhibited a greater degradation than glass-polymer construction

Correlation of P_{max} and FF

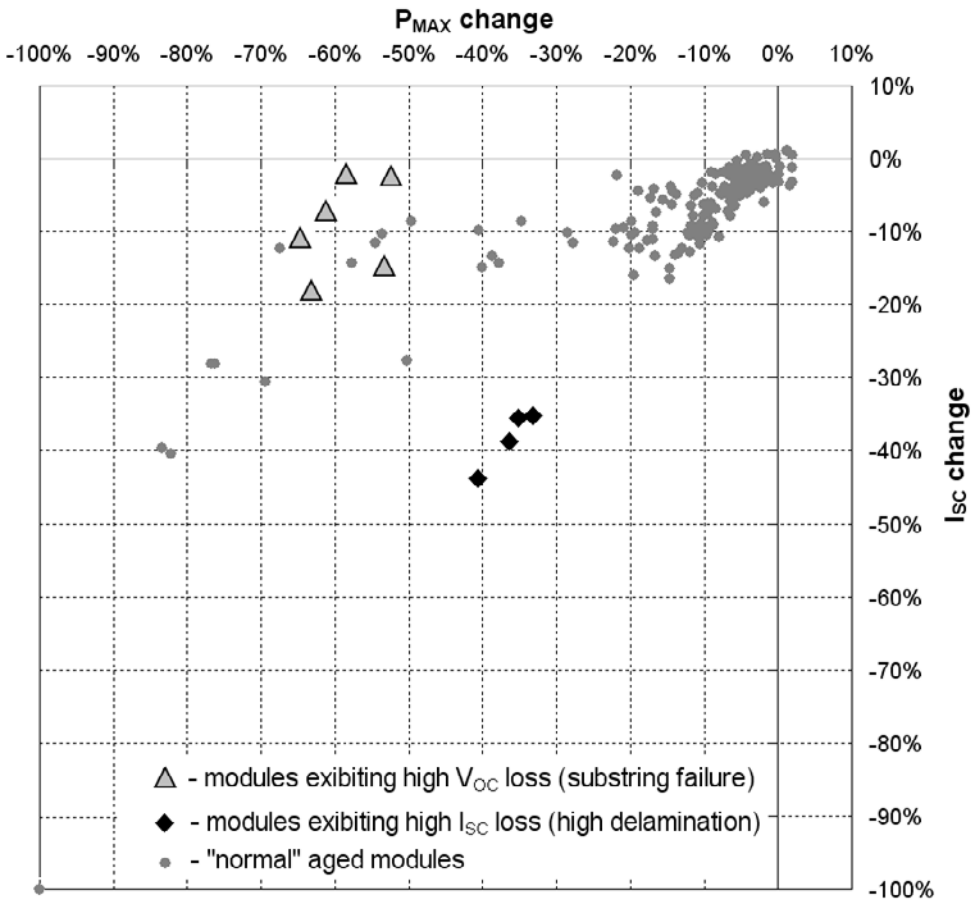
The scatter plot of the dependence of the P_{MAX} losses on the FF losses



Generally high P_{max} losses (>20%) are attributed to FF losses (series resistance increase)

Correlation of P_{max} and I_{sc}

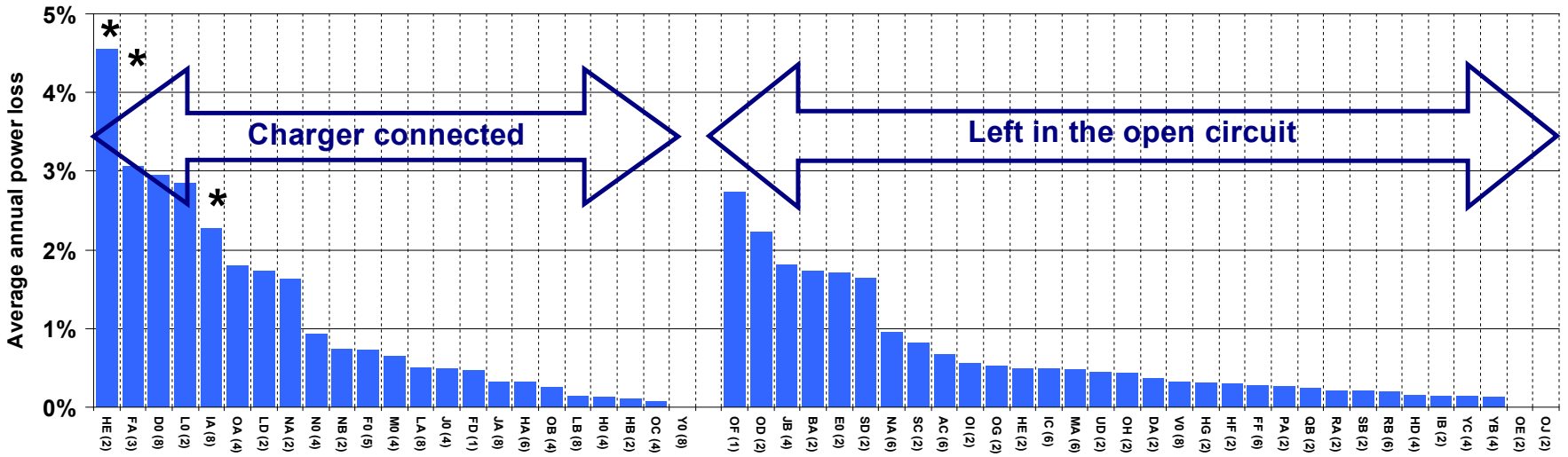
The scatter plot of the dependence of the P_{MAX} losses on the I_{SC} losses



Moderate P_{max} losses (<20%) can be attributed to I_{sc} losses (optical properties degradation)

-Changes in optical transmittance (glass or encapsulant)
-Delamination
-Light induced boron-doped silicon degradation

Annual degradation rates



* Average including total failures

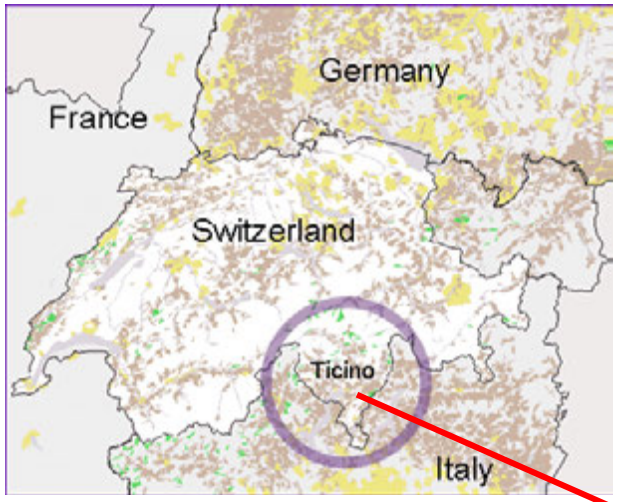
The average annual degradation for all of the connected modules **1%** (0.8% excluding total failures)

The average annual degradation for all of the modules left in open circuit **0.6%**

Field exposed modules summary

- No statistical difference between mono or polycrystalline cells
- Glass-glass modules generally exhibited a greater degradation than glass-polymer construction
- Modules incorporating silicone encapsulation generally exhibited lower degradation
- Generally high P_{max} losses (>20%) are attributed to FF losses (series resistance increase)
- Moderate P_{max} losses (<20%) can be attributed to I_{sc} losses (optical properties degradation)
- A statistical difference between modules initially connected to the inverter (charger) which exhibited approximately twice the average degradation in comparison to modules left in open circuit.
- The average annual degradation for all of the connected modules **1%** (0.8% excluding total failures)

10 kW PV plant study





252

(12 strings of 21 panels each)

Arco Solar

ASI 16-2300 modules

35 m-Si cells, PVB encapsulant, Tedlar/Al/Tedlar backsheet

Arco Solar, ASI 16-2300 m-Si Module power @STC: 37Wp

Construction

Monocrystalline cells, PVB Encapsulant, Tedlar/Aluminium/Tedlar backsheet

Initial Configuration 1982

288 Modules (24 strings of 12) (nominal 10.66 kWp)
200V operation (Abacus 10kW inverter)
Tilt array 65^{o}

Present Configuration since 1992

252 Modules (12 strings of 21) (nominal 9.32 kWp)
$\pm$ 350 V operation (Ecopower 15kW inverter)
Tilt array 55^{o}

1982: Initial aim

• To study technical and safety problems of a PV plant connected to the grid

2000-2003:

• Plant aging

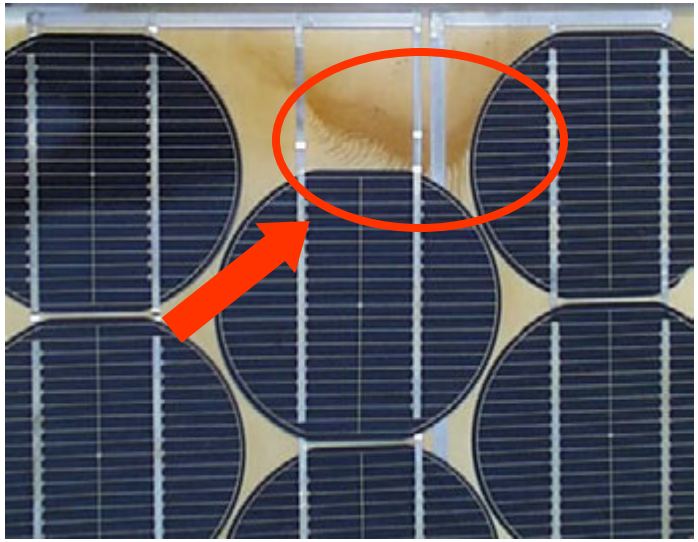
• Investigation of physical degradation mechanisms

• Field reliability/accelerated lifetime tests (CEI/IEC 61215) correlation

Investigation of the 10kW PV Plant

- Detailed visual inspection
- InfraRed analysis
- Indoor IV measurements
  - reference modules
  - all modules
- Repeated CEI/IEC 61215 Damp heat and Thermal Cycling

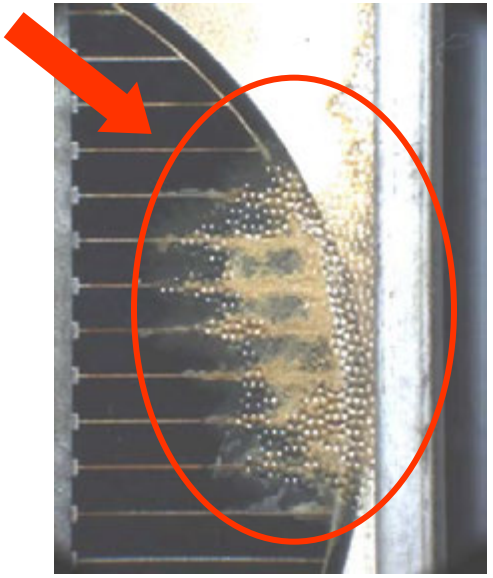
Visual defects: yellowing



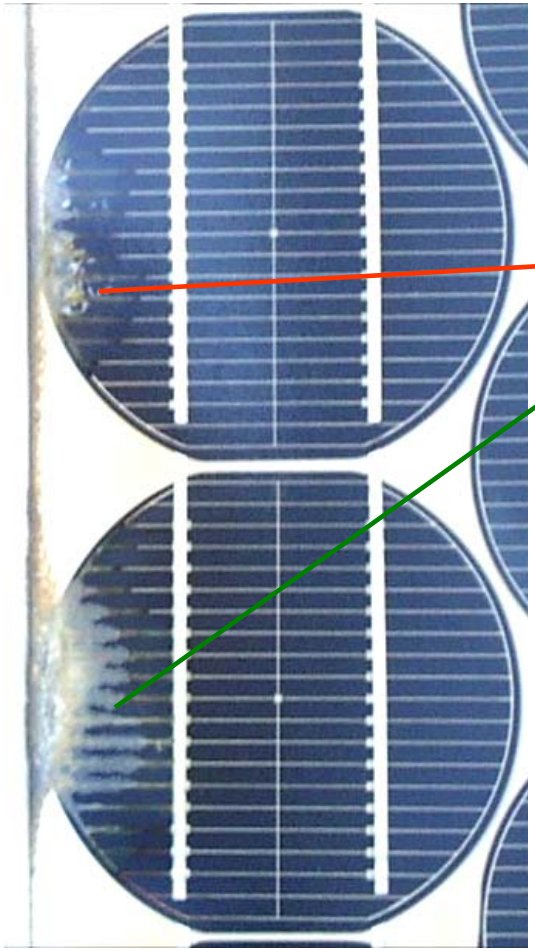
- 98% of modules (2003) (~50% in 1985)
- 78% exhibiting complete coverage of module (63% dark yellowing)
- Darker spots
- Practically no influence on encapsulant transparency (same spectral response for white and yellow modules)

Visual defects: delamination

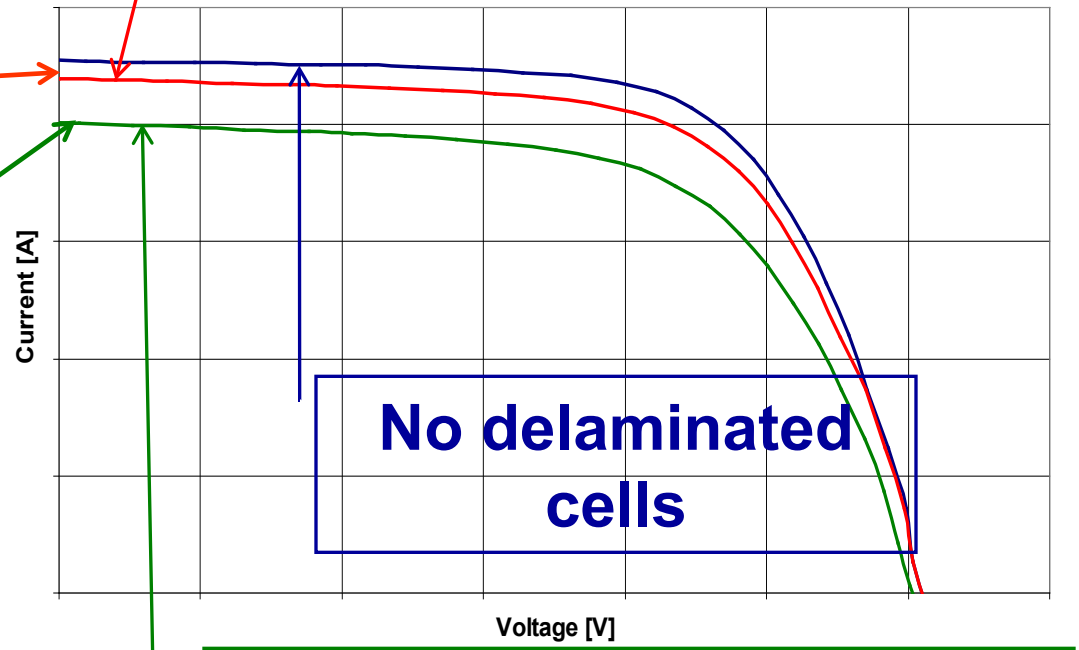
- 92% of modules (74% in 1996)
- 27% major defect according to IEC 61215
- No effects on modules insulation (dry & wet insulation tests)
- Effects on modules performance (delamination in front of cells) (cumulative total delaminated area)



Effect of delaminated areas



Delaminated area: 3.0%
ΔP_{max}: -6.5%, ΔI_{sc}: -3.4%



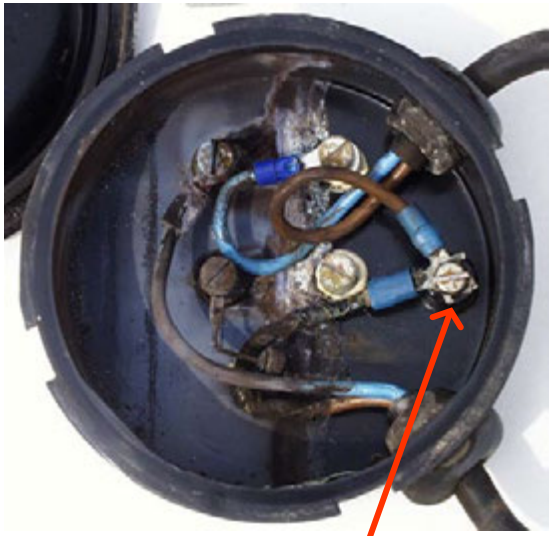
No delaminated cells

Delaminated area: 8.3%
ΔP_{max}: -18.3%, ΔI_{sc}: -11.7%

No great effect on module performance

Additional Visual defects:

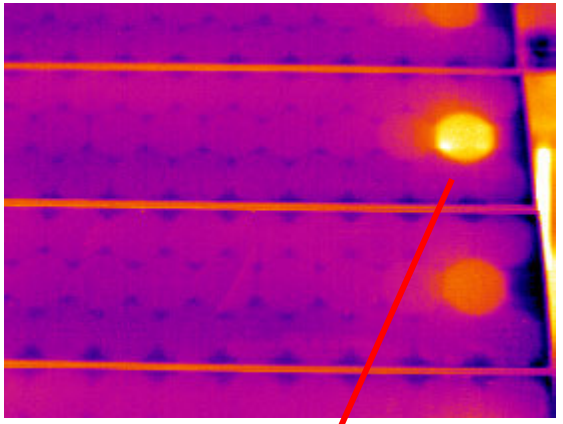
- Sealant infiltration
  76% of modules
- Cracked cells
  15% of modules
- Browning (oxidation) of gridlines
- Poor Junction box seal to backsheet tedlar
  risk of detachment; bad insulation
- Terminal oxidation
  problems when wiring

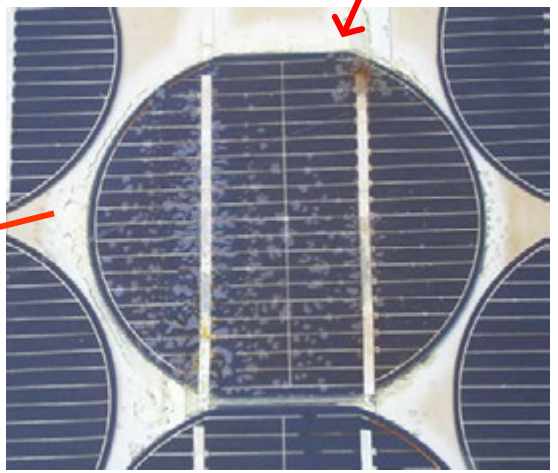


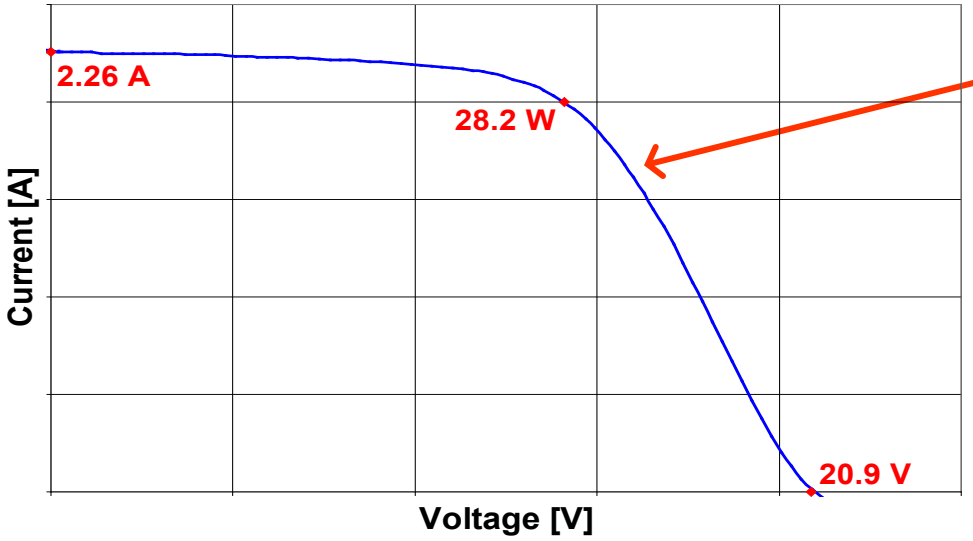
Infrared Analysis

- Noticeable Hot-spots: 24% of modules
  (22% in 1999)
  (Not just the effect of the junction box)

- Most degraded modules
  worst P_{max}: -29% vs P_n







P_{max}: -24% vs P_n
(-15% vs average actual P_{max})

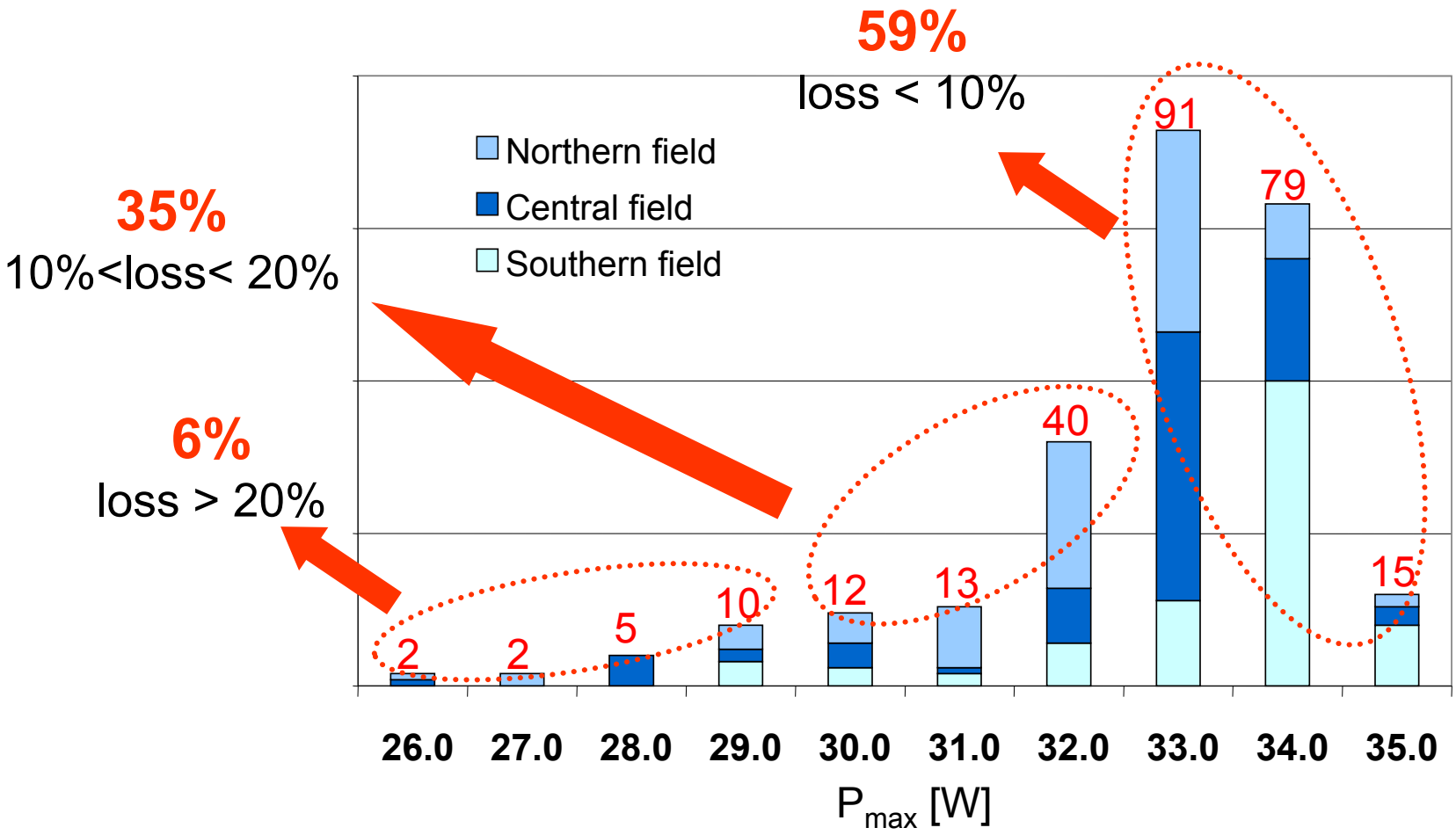
Indoor IV measurements

- **18 modules reference modules**
  ESTI laboratory IV measurements - since 1982

- **13 stable modules**
  power loss: -1.7% vs 1982 mean P_{max}

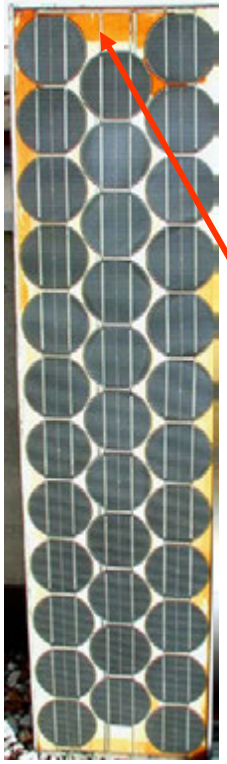
- **5 degraded modules**
  power loss: **-9.1%** vs 1982 mean P_{max}
  (2 hot-spot, 1 damaged cell)

IV measurement of the whole plant



Original Nominal Module power @STC: 37Wp

Testing of 20 year old modules



- 1220 Thermal Cycles:
  no major defects
  no measurable power losses

- 6000 hours Damp Heat:
  dark yellowing
  detachment of tedlar backsheet
  (not observed outside)
  no measurable power losses

Observed delamination outdoor, not reproduced through indoor tests



Conclusions for the 10kW TISO Plant

- **Good 20-year old technology**
- Not good looking, but perfectly functioning plant
- Hot-spots
- Delamination
- Remarkable modules resistance of old modules to repeated indoor Damp Heat and Thermal Cycling
- Good expectation for at least 30 year lifetime?

Currently at 29 years and still working well!

Examples of Degradation rates

Detailed analytical data of the progressive degradation of PV modules is not readily available.

Realini et. al. For a crystalline silicon array, with Arco Solar ASI 16-2300 modules. Indicates an average weighted degradation of 5.2%. Over the 19 years of operation or **0.3% per annum** including initial degradation.

Reis et. al. For a crystalline array, with Arco Solar M-75 modules. The array was installed in 1990 and indicates a degradation of 4.39% in 11 years or **0.4% per annum** including initial degradation.

Osterwald et al. Stated rates of between **0.5 and 0.8% per annum** (shorter term experiments which linked to total UV dose to degradation in I_{sc})

Granata et al. Concluded that only one of the eight arrays studied showed true power degradation beyond experimental error at **1.4 0.8% per annum**

"Comparison of PV module performance before and after 11-years of field Exposure" AM Reis, et al . Proceedings of the 29th IEEE PVSEC, New Orleans, USA, 2002; 1432–1435.

"Degradation analysis of weathered crystalline-silicon PV modules" C.R. Osterwald, et al Proceedings of the 29th IEEE PVSEC, New Orleans, USA, 2002; 1432–1435.

"Long-term performance and reliability assessment of 8 PV arrays at Sandia National Laboratories" J.E. Granata, et al. Proceedings of the 34th IEEE PVSEC, Philadelphia, USA, 2009; 1486–1491.

Summary: Degradation Mechanisms

Short Term Losses: have been shown to be in the order of **2.4%** ± 1.7%.

Long Term Losses: have been shown to in the order of 0.2% per annum up to 1% per annum.

May be skewed data towards low degradation rates, due to the types of systems studied

The effect on **Energy Life** can result in losses in the order of ~5% up to ~8% based on a 20 year operation.

Over the module lifetime this is dominated by the long term losses.

Acknowledgments

The ESTI laboratories module qualification team past and present

Artur Skoczek, Mike Field and Ewan Dunlop

Antonella Realini (LEEE-TISO)

The work was partially funded by the PERFORMANCE project of the European Commission under contract number SES-019718 within FP6.







Analysis of Hot Spots in Crystalline Silicon Modules and their Impact on Roof Structures

Daniel W. Cunningham, BP Solar
February 17th 2011

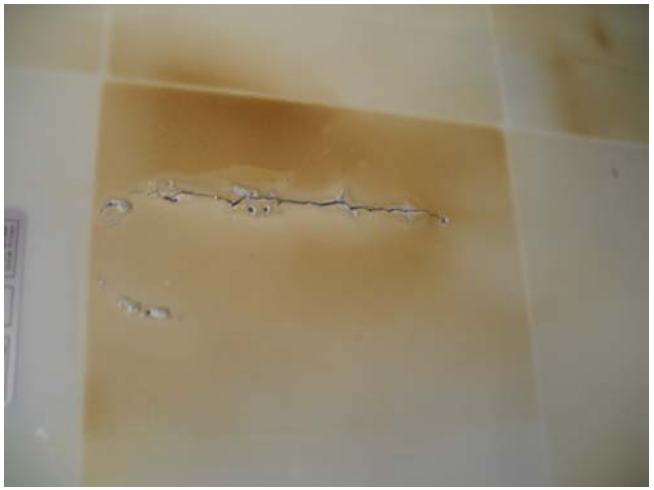
The information contained in this presentation is for informational purposes only. BP Solar specifically disclaims any implied or express warranty as to the accuracy or completeness of the information contained in the presentation. No third party may rely on such information.

Acknowledgements

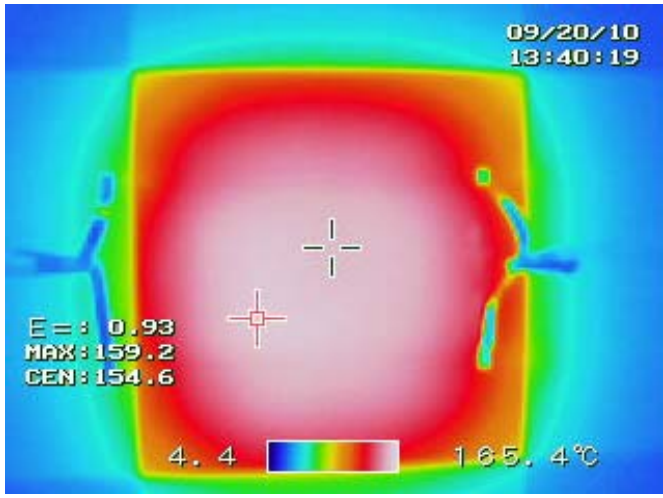
- **W. Anderson, G. Kelly, W. Nasse, BP Solar, Germany and USA**
- **M. Köhl, D. Philipp; Fraunhofer ISE, Germany**
- **A. Roth; VDE Institut, Germany**

BP Solar Proprietary

Introduction

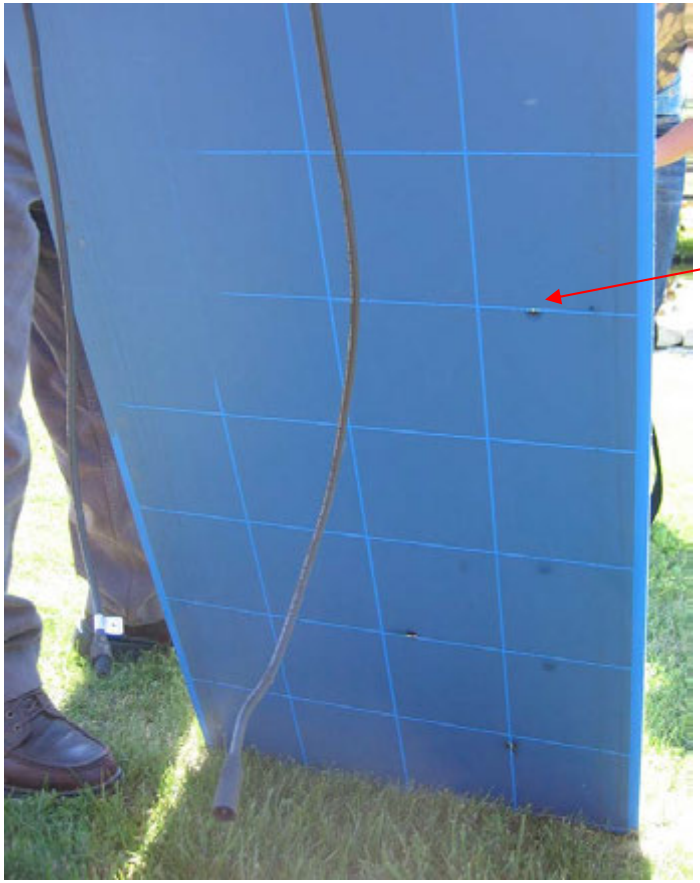


- **What are hot spots?** What the standards say:
- **IEC definition:** “Hot-spot heating occurs in a module when its operating current exceeds the reduced short-circuit current of a shadowed cell or group of cells within it”
- **UL definition:** “This reduced short-circuit current capability can be the result of a variety of causes including:
  - non-uniform illumination of the module (local shadowing)
  - individual cell degradation due to cracking
  - ..or loss of a portion of a series-parallel circuit due to individual interconnect open circuits.”
- These hot spot mechanisms are the result of reverse biasing of cells which can lead to localized p-n junction breakdown
- **Not all hot spots are the results of the p-n junction effect**



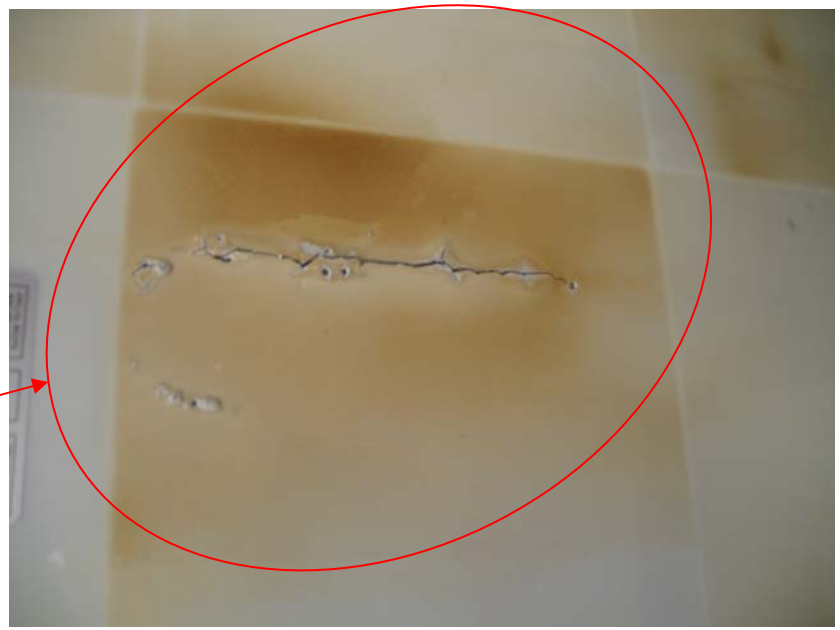
BP Solar Proprietary

Example: By pass diode failure



Localised hot spot

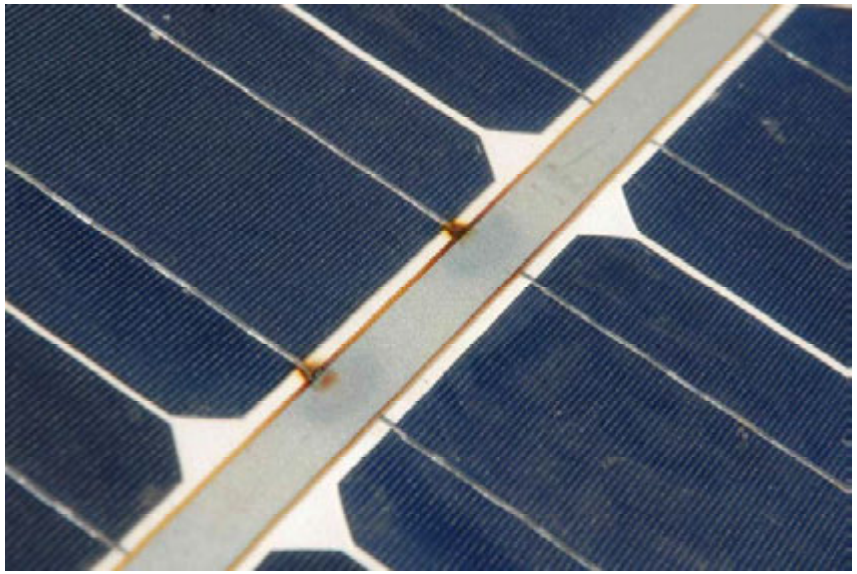
More uniform hot spot



- Loss of protection from a faulty by pass diode during periods of shading can lead to hot spots
- The highest temperature occurs where current density is highest. This can produce non uniform heating
- Cell shunt resistance influences hot spot formation on shading. Shunt limits have increased as a result

BP Solar Proprietary

Example: Non cell hot spots

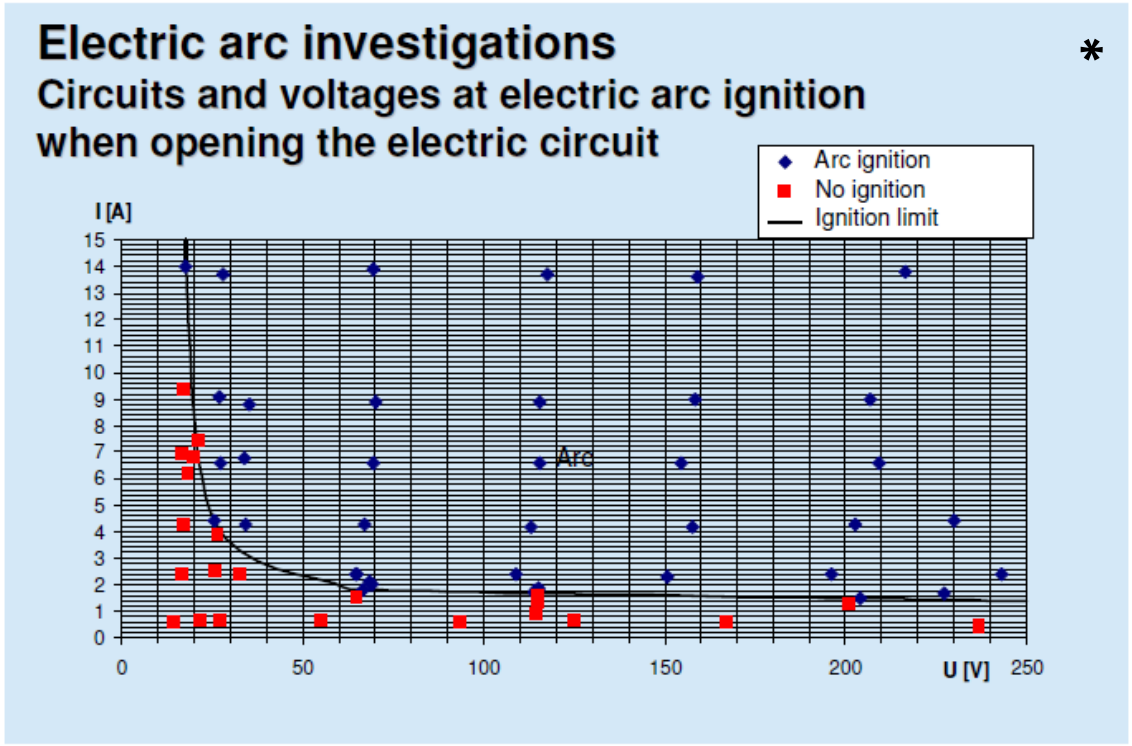




- Resistive heating is <u>not</u> associated with reverse bias conditions
- The heating is localized at the defect and can discolor the encapsulant and back sheet
- Poor workmanship can lead to soldering defects. These are not seen at the solar simulator
- The hot spot can be stable, does not increase in temperature
- In some cases, the contact will open

BP Solar Proprietary

Arc effects

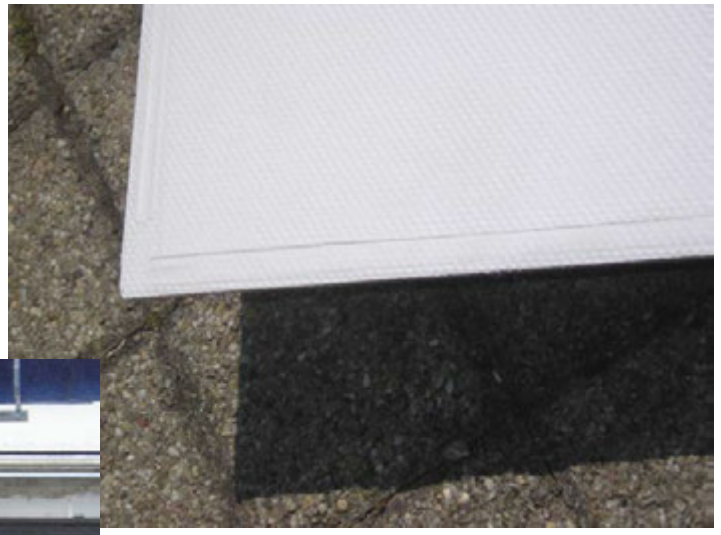


- DC arcs are another non reverse bias hot spot phenomenon
- Initiated under specific voltage/current conditions with a gap between conductors
- Current / Voltage ignition limits are well known
- The impact from this type of hot spot can be severe

* **Author acknowledges W Vassen of TUV Rhineland for permission to use the above chart**

Example: Structural interference



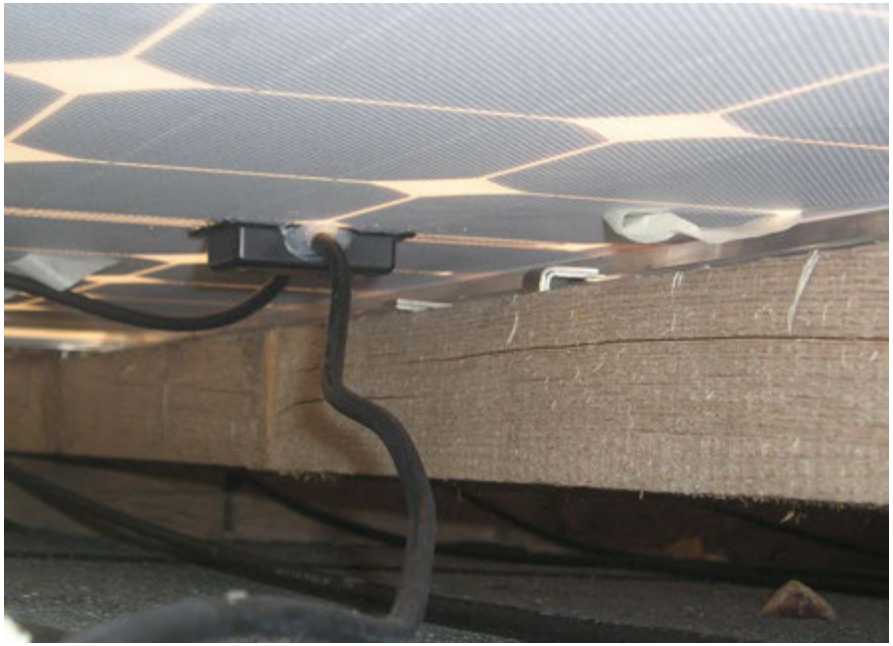




- Root cause is DC arc generation due to back sheet damage
- US systems: Negative ground needs single short
- EU systems: Typically need 2 shorts due to double isolation approach

BP Solar Proprietary

Impact of roof structure proximity





- BIPV designs often require close proximity of the module to the roof structure
- The study performed between BP Solar and the Fraunhofer Institute was initiated to better understand and quantify the risks and behavior

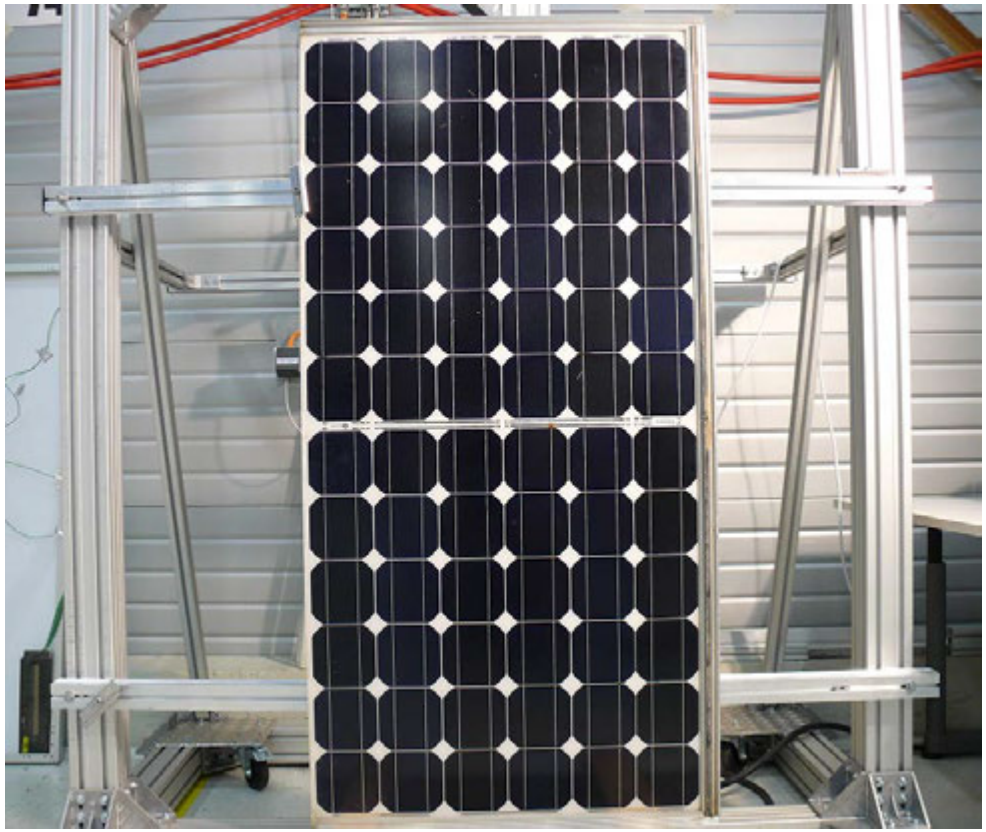
BP Solar Proprietary

2010 F-ISE/BP Solar hot spot study

- **Scope of the study:**
  - Perform a statistical evaluation on a sample of modules exhibiting hot spots.
  - Quantify the occurrence and temperature range/severity of hot spots
- **Characterization included**
  - Categorise the hot spots into specific root cause; cell contact, cell mis-match, cracked cell, etc
  - Determine highest temperature for hot spots
  - Perform electroluminescence and infra-red thermography
  - Effect of thermal cycling & mechanical load on hot spots
  - Heating influence on adjacent/close proximity structures with limited ventilation
  - Evaluate effect of rear side module damage at high voltages

BP Solar Proprietary

Module samples used in study



- BP Solar supplied 28 modules with varying degrees of hot spots
- Tests were performed at F-ISE, Freiburg
- Structures were custom built to replicate real field conditions
- Test protocols were followed according to IEC61215 & UL1703

BP Solar Proprietary

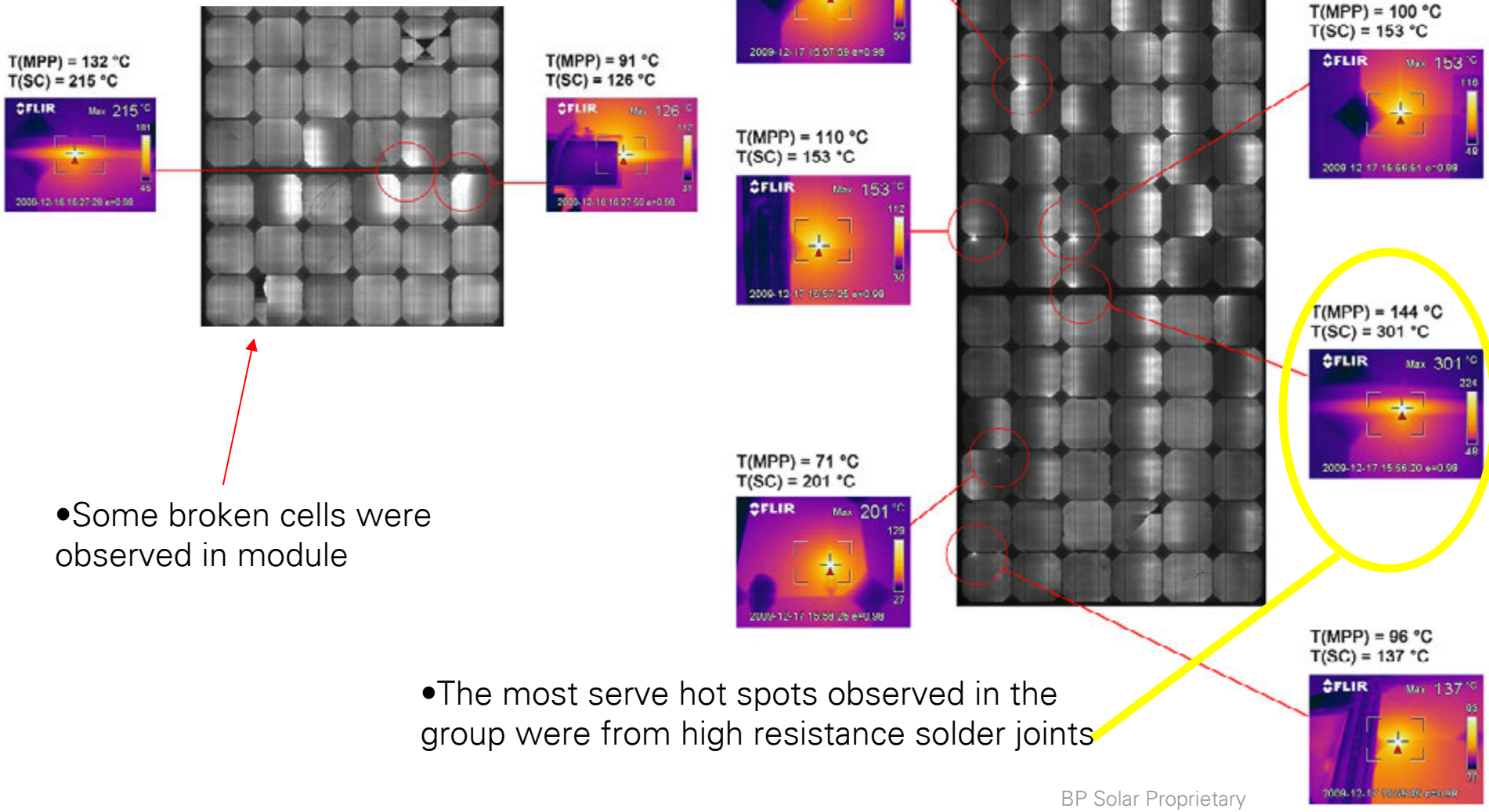
Hot spot characterization

- Full visual inspection, EL, & IR images was made on all modules
- Hot spot temperatures were measured under illumination (Class B-B-A solar simulator at 1000W/m^2).
- Both Isc and Imp current condition were investigated
- Initial condition: Ambient temperature was 20^{o}C and ventilation was not limited
- Table below shows the 5 highest hot spot temperatures found in the study

		Maximum hot spot temperature measured	
Sample	Isc (A)	T(C) @ Isc	T(C) @ Imp
A	4.9	301	144
B	5.1	312	267
C	5.0	272	147
D	4.9	296	210
E	4.6	287	172

BP Solar Proprietary

EL and IR images



- Some broken cells were observed in module

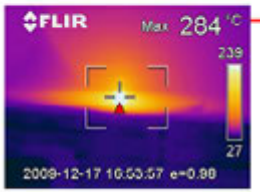
- The most serve hot spots observed in the group were from high resistance solder joints

BP Solar Proprietary

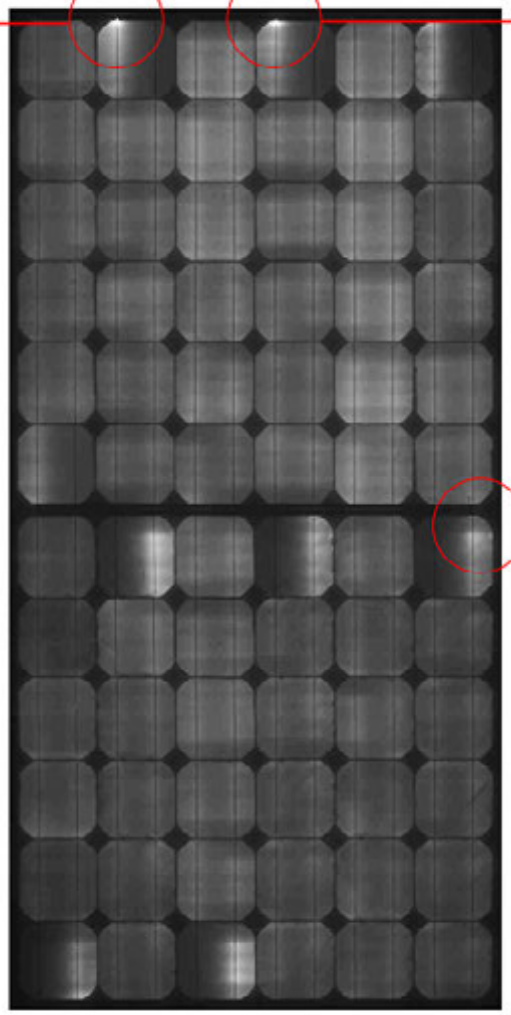
EL and IR images continued



T(MPP) = 190 °C
T(SC) = 285 °C



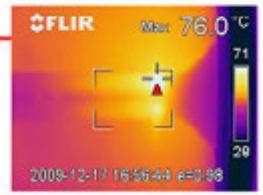
Sample B



T(MPP) = 267 °C
T(SC) = 312 °C



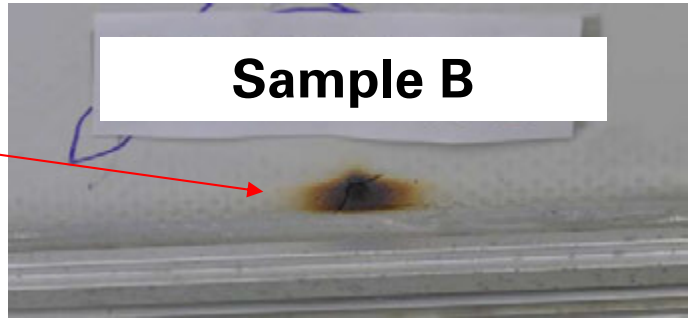
T(MPP) = 69 °C
T(SC) = 76 °C



Hot spot with restricted ventilation

- Rear side of the module (samples A thru E) was closed off using a wooden panel
- Air gap: 38mm
- Ambient raised to 40^{o}C with modules held at Isc
- Top 5 highest hot spot temperatures are shown below
- Temp trend was not consistent; 3 increased in temperature, 1 decreased, 1 unchanged
- Suggests that the hot spot source and properties can vary
- The module with the highest temperature hot spot was chosen for a “worse case” test
- This worse case test was designed to measure temperature rise in very proximity

Maximum hot spot temperature measured		
Sample	Isc (A)	T(C) @ Isc
A	5.2	300
B	5.2	343
C	5.2	283
D	5.0	251
E	4.7	332

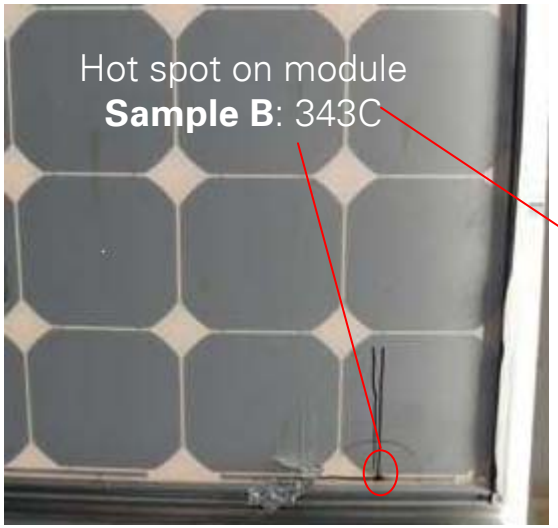


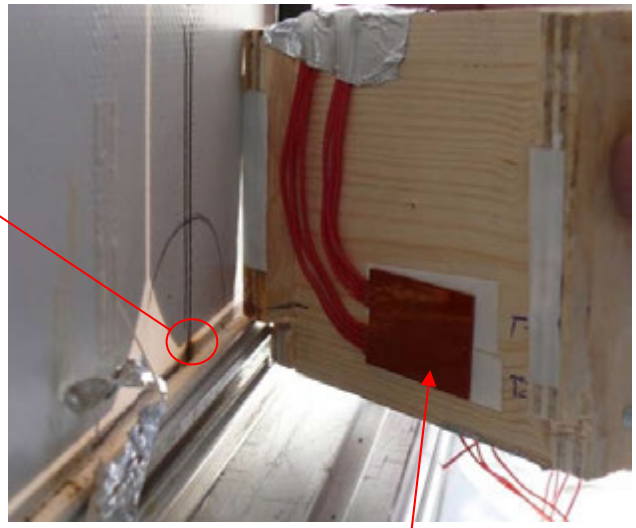
BP Solar Proprietary

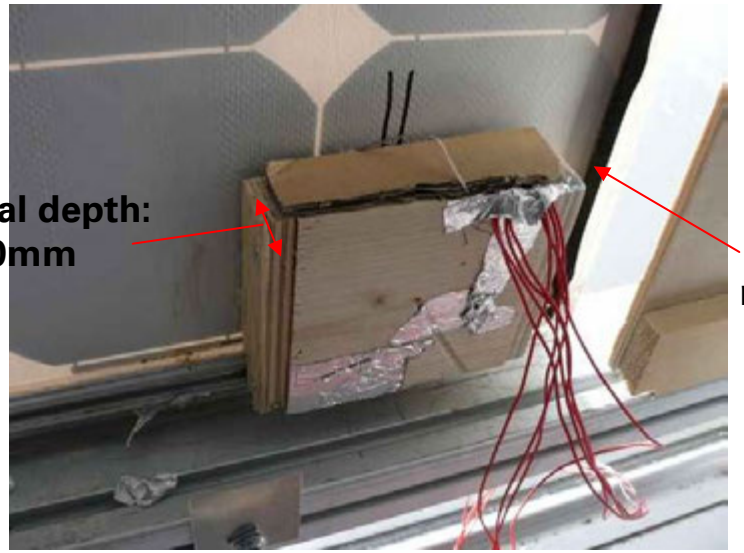
Worse case experiment
Hot spot behavior in 10mm enclosure



Back of module (**Sample B**) **completely enclosed** before start of test

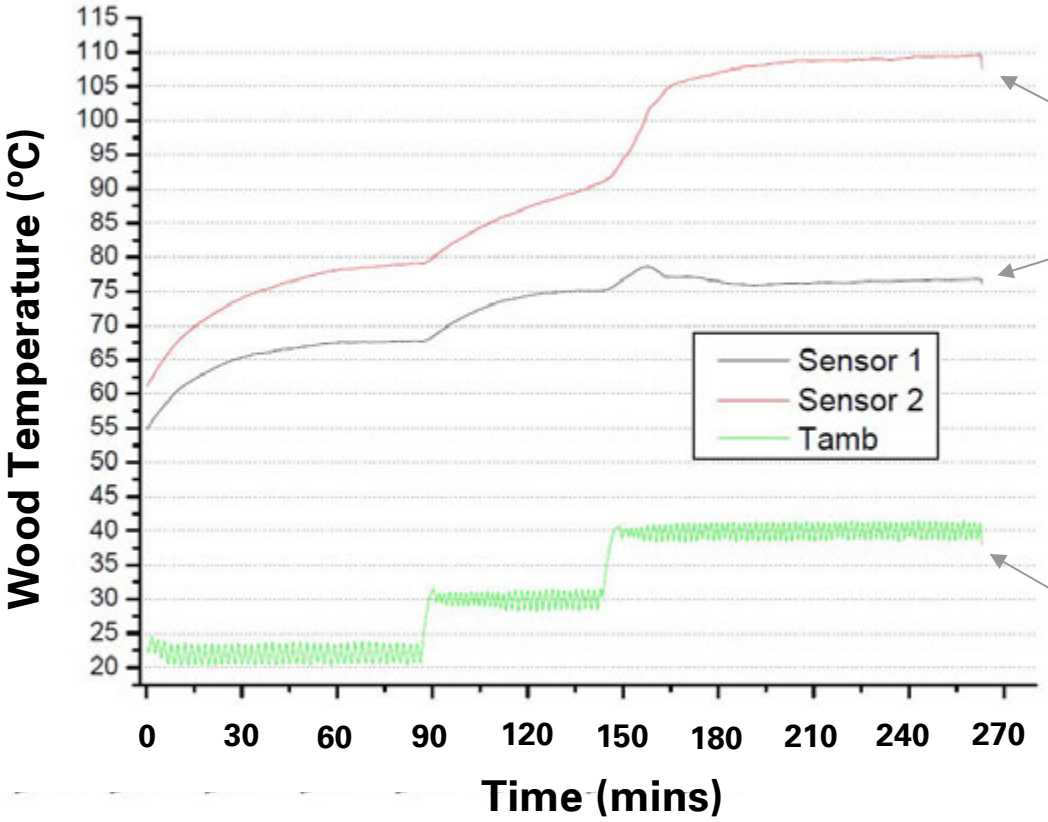






BP Solar Proprietary

Max temp at 10mm from structure



Auto ignition temperature of wood: 300°C

Sensor 2: max 109°C

Sensor 1: max 76°C

Secondary heating from hot spot low for such an extreme condition!

~120 mins soak time at 40°C ambient

- Ambient temp stepped from 25°C to 40C° while module illuminated to produce Isc current
- Maximum temperature range at wood surface by end of test: 76°C to 109°C
- **While absolute temperature of hot spot is high, the dissipated energy from it is very small**
- This accounts for the relatively low temperatures of adjacent surfaces

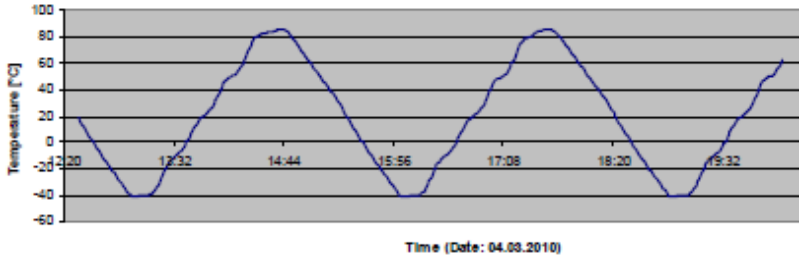
BP Solar Proprietary

Thermal & mechanical loading

- As part of the study, the effect of thermal and mechanical cycling of hot spot propagation was investigated
- IEC 61215ed2, 10.11 and 10.6 (thermal & mechanical cycling respectively) procedures were followed
- Thermal cycling: -40°C to +85°C, 200 cycles
- Mechanical cycling: 2400Pa and 1500Pa, cycling front & rear, 1 hour period

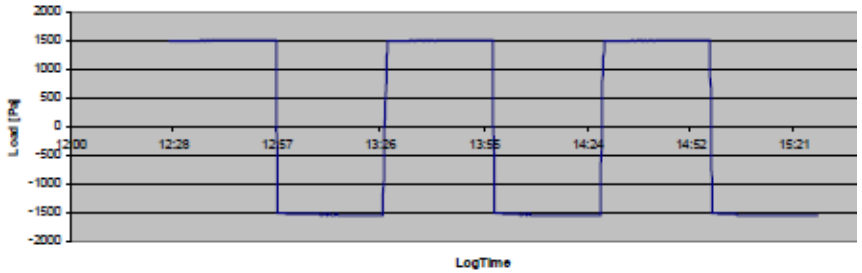
1) Thermal cycling





2) Mechanical cycling



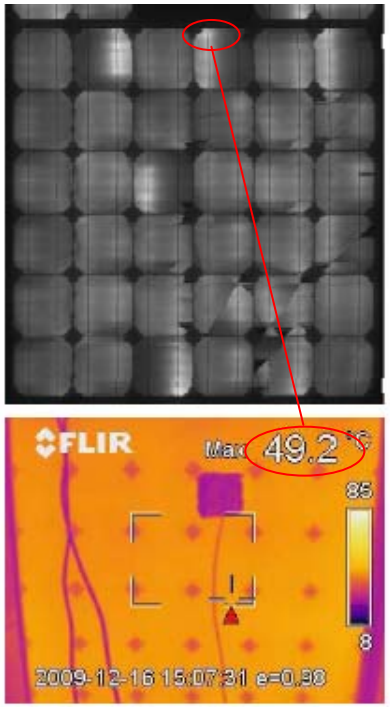


BP Solar Proprietary

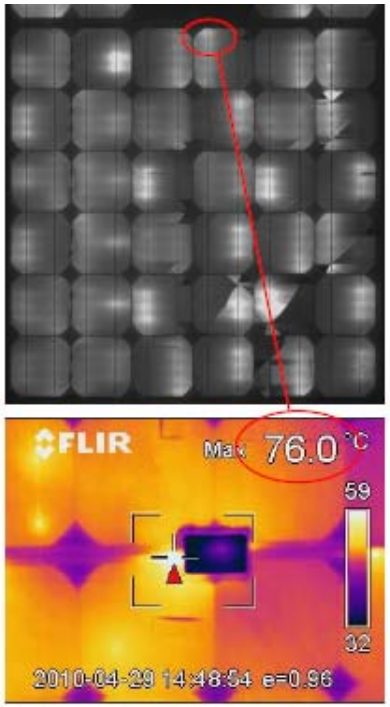
Thermal cycling effect

Sample 1: Thermal cycling

Initial

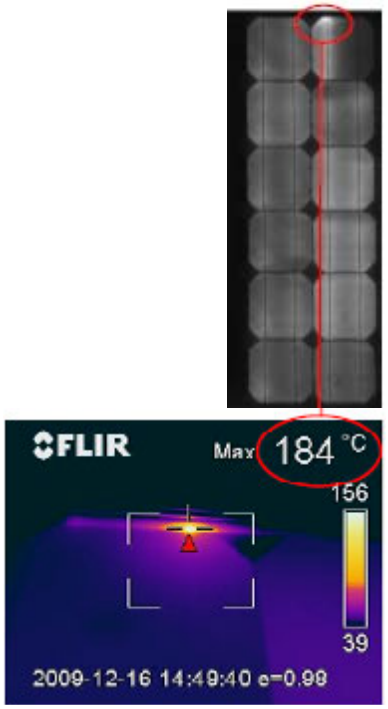


Post TC200



Sample 2: Thermal cycling

Initial



Post TC200



- For the examples used in the study, there was not a strong influence of thermal cycling on the propagation hot spots
- In the case above, the hot spots were located at interconnect to bus bar interface

BP Solar Proprietary

Mechanical cycling effect: Results

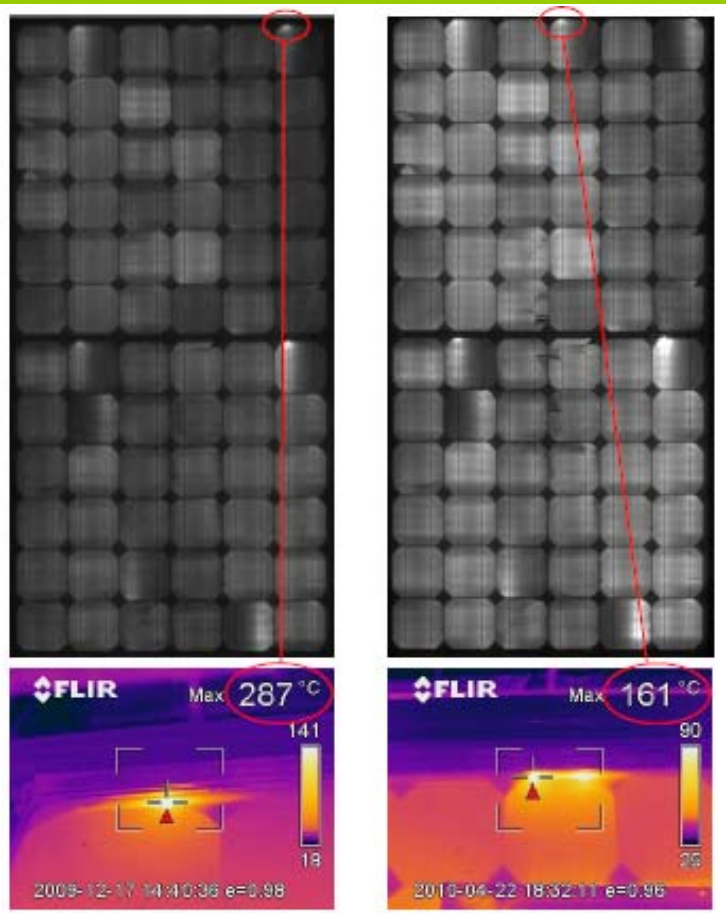
Sample 3

Mechanical cycling

3 front/rear cycles to 1,500Pa

Initial EL & IR images

Final EL & IR images



- Nature and severity of hot spot in this sample changed after repetitive load cycling
- Suggests that this type of stress could be a factor in perturbing the extent of hot spots
- Dependant on weather conditions including local wind and snow conditions
- This could take many years in the field

BP Solar Proprietary

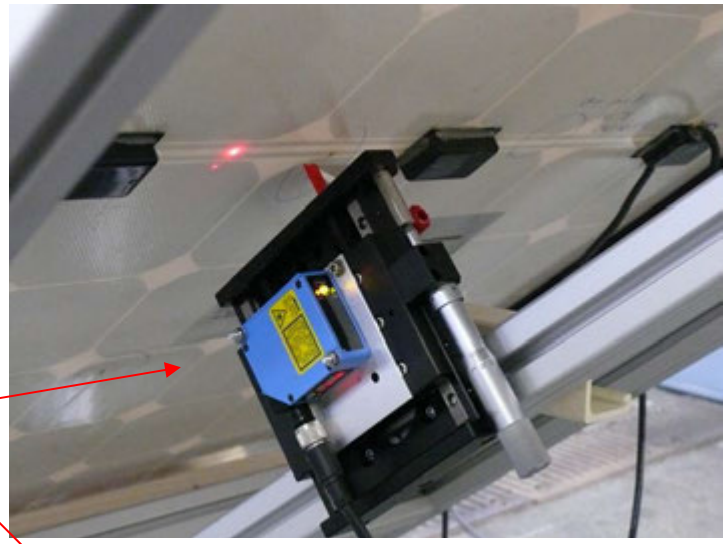
Simulated rear side damage at high voltages



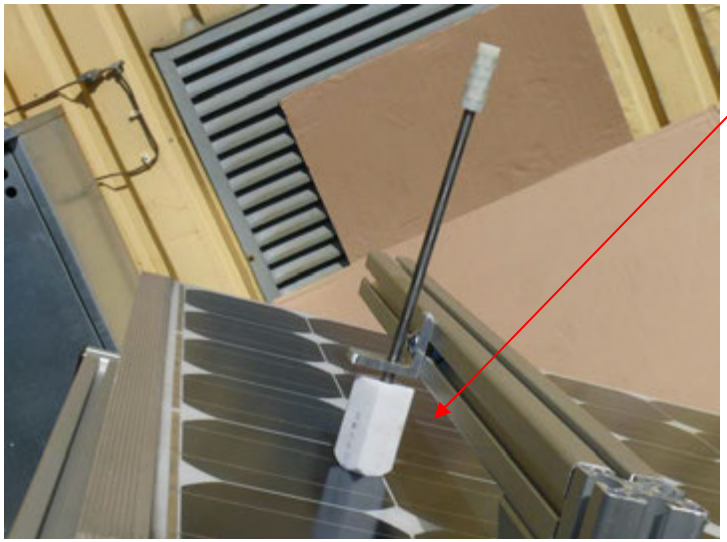
Isolated structure with metal probe at -1000V

+ve to output cables

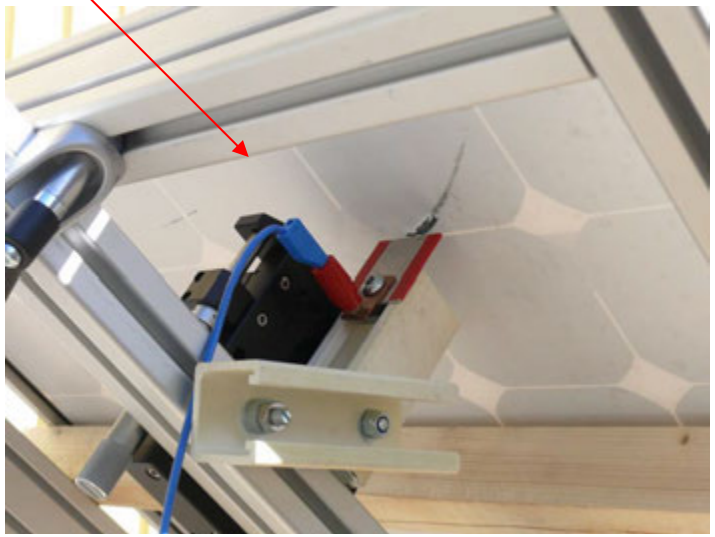
Current limit: 1A



Sensor measures the distance to the back sheet: 0 to 20mm

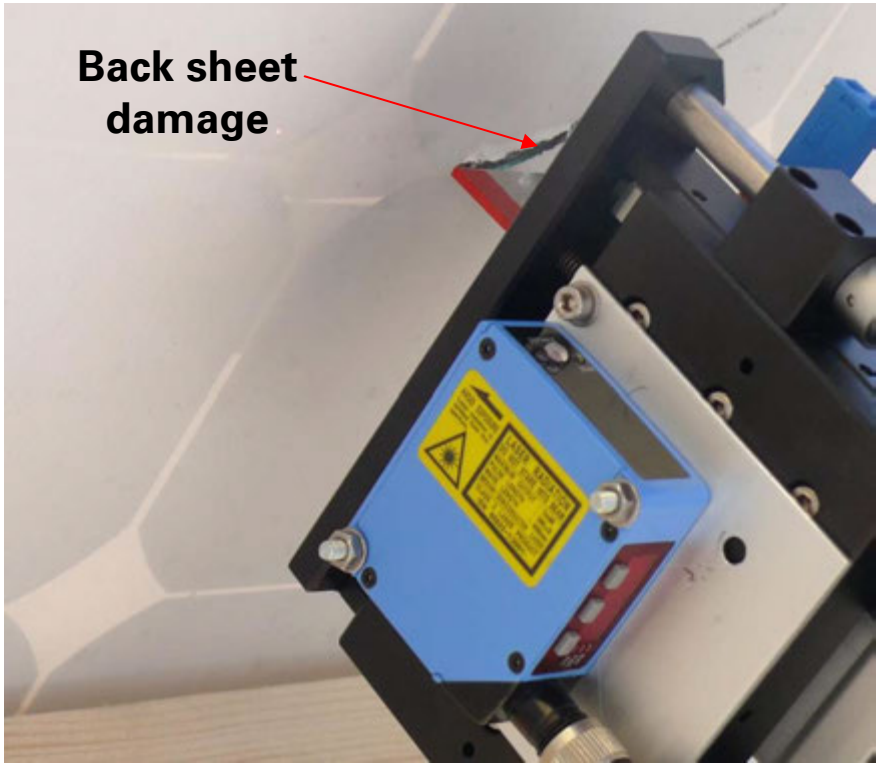


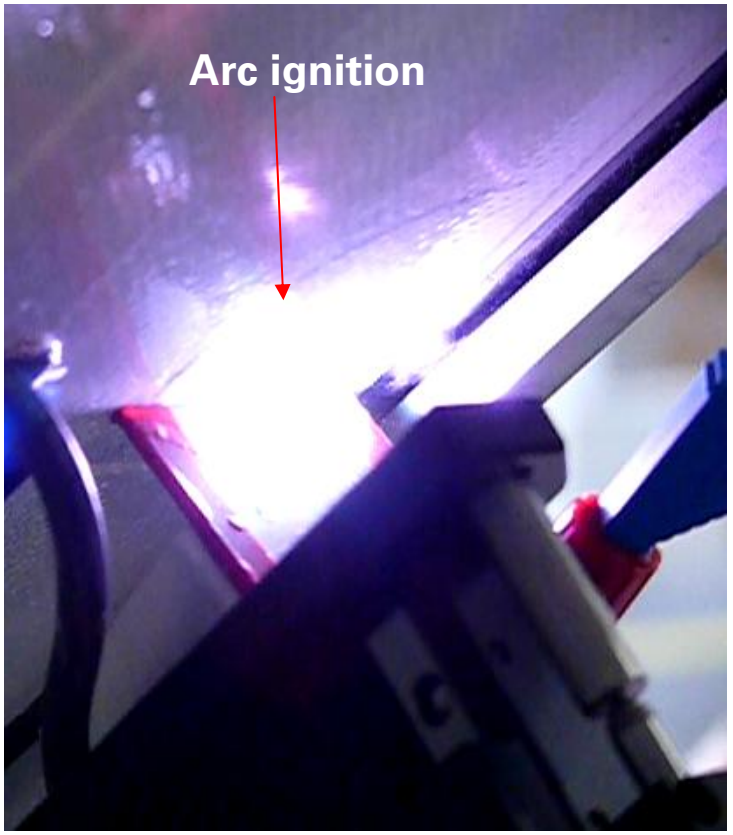
Pressure applied to front of glass to generate deflection



BP Solar Proprietary

Simulated back sheet damage
Arc initiation





- **Flash over occurred when the probe was in close proximity (<2mm) or direct contact**
- **Flash over occurred in dry environments but the presence of water greatly increased the chance for occurrence**
- **For these conditions, flash over was detected at voltages of 300V or higher**
- **<u>Undamaged back sheets</u> did not lead to leakage current or arc initiation**

BP Solar Proprietary

Summary

- Many different failure modes can create a hot spots not just p-n junction effects from shading
- A study between BP Solar, Fraunhofer Institute, and VDE examined 28 modules with examples of hot spots
- Broken cells were present but the most common root cause was resistive heating due to defective solder joints
- Maximum temperature measured was 343^{o}C, however the heating effect on the adjacent wooden structure was low
- This is due to the small physical size of the hot spot and low energy dissipation
- Stress testing showed a greater effect from mechanical cycling compared to thermal cycling
- However, this did not significantly increase the hot spot temperature
- By far the biggest risk for secondary damage from hot spots is if their source is a DC arc
- This was demonstrated by simulated back sheet damage at high voltage

BP Solar Proprietary

PV Module Arc Fault Modeling and Analysis

Presented to the NREL PV Module Reliability Workshop

Jason Strauch, PE

jestrau@sandia.gov, 505-284-6114

Microsystems & Engineering Sciences Applications (MESA)

Sandia National Laboratories

Sandia is a multiprogram laboratory operated by Sandia Corporation, a Lockheed Martin Company, for the United States Department of Energy's National Nuclear Security Administration under contract DE-AC04-94AL85000. SAND2009-2801P

This presentation does not contain any proprietary or confidential information

Module Failure Analysis

Jason Strauch
Michael Quintana
Jennifer Granata
Scott Kuszmaul
Jay Johnson

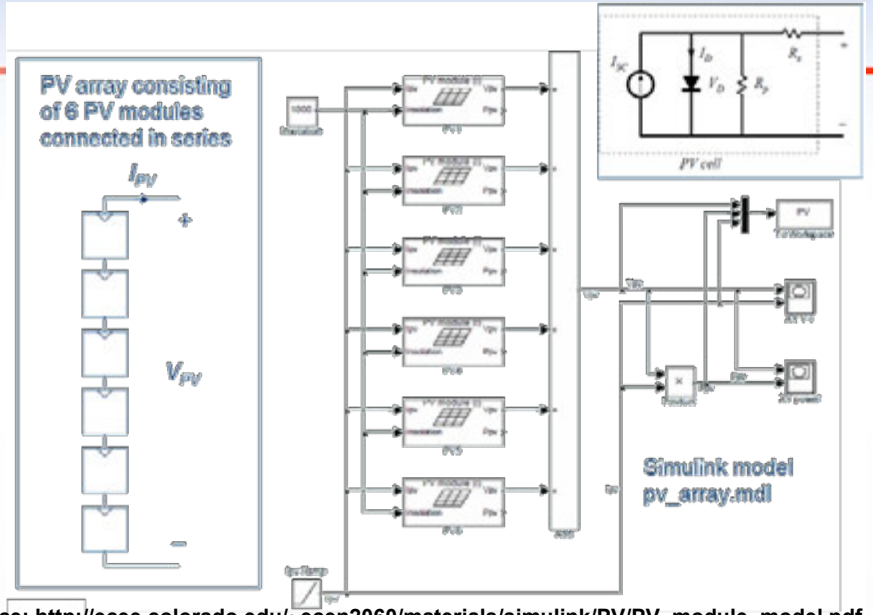
This presentation will help to answer the question of the potential for electrical arcing in the ubiquitous module busbar solder joint failures, as well as provide insights into the time domain of these failures and material effects.

Topics:

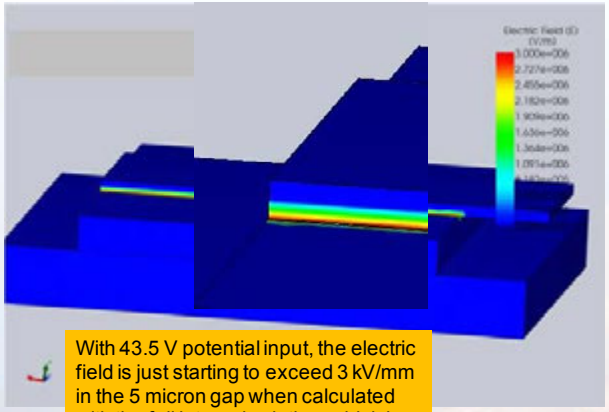
- Background and testing
- Description of observed failures
- Description of model and assumptions
- Model of electrical conditions to cause arc
- Analysis of glass breakage conditions
- Analysis of busbar connector ribbon deformation
- Conclusions

Arc Fault Modeling

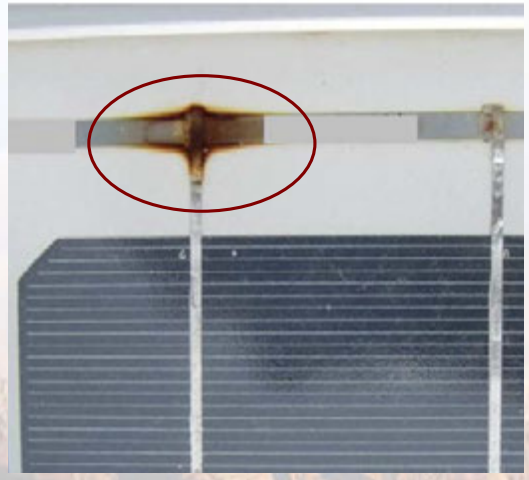
- **Frequency modeling**
  - Development of cell, module, and array models for AC studies
  - Studies investigate attenuation effects of PV components
- **Electrical modeling**
  - Simulation of current, voltage, and resistance changes preceding and for the duration of the arcing event

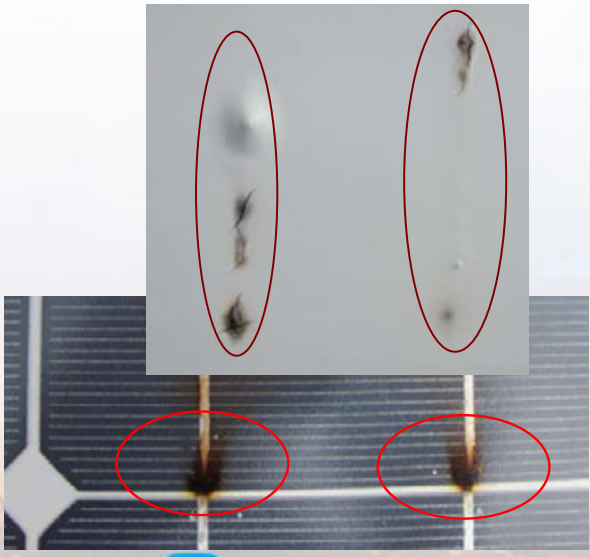


Source: http://ecee.colorado.edu/~ecen2060/materials/simulink/PV/PV_module_model.pdf



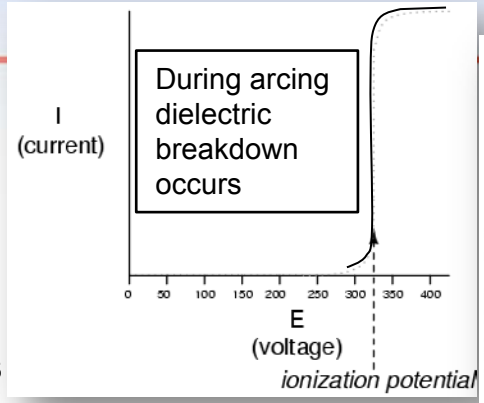
With 43.5 V potential input, the electric field is just starting to exceed 3 kV/mm in the 5 micron gap when calculated with the full integral solution, which is lower than the linear $\frac{43.5\text{V}}{5\text{micron}} = 8.7\frac{\text{kV}}{\text{mm}}$

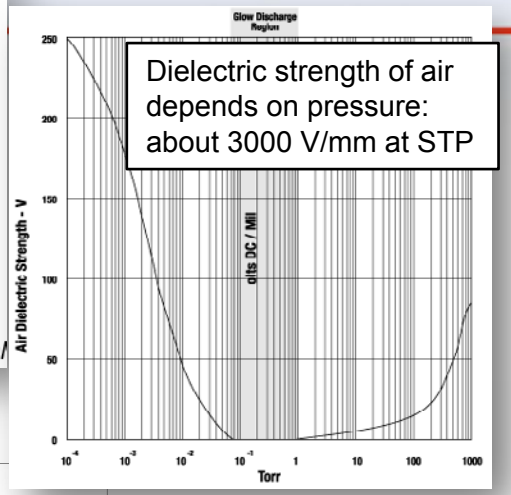


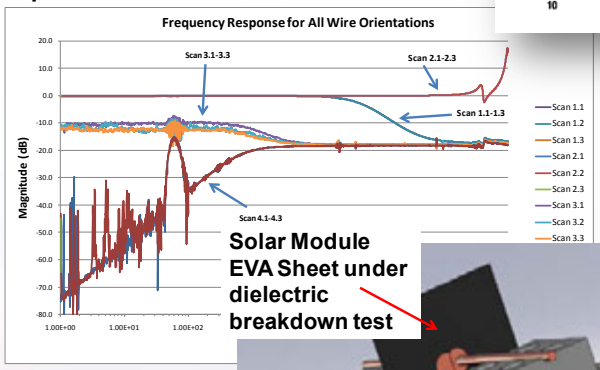


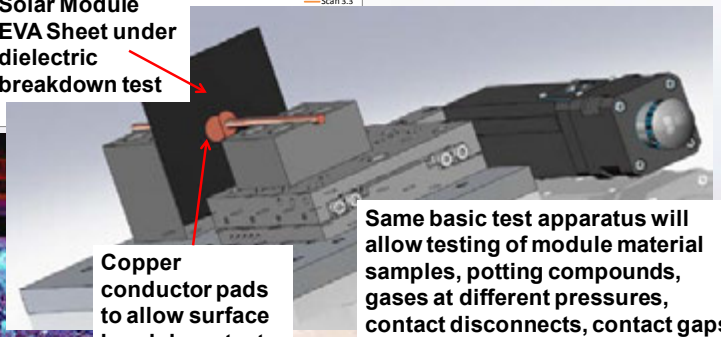
Arc Fault Testing

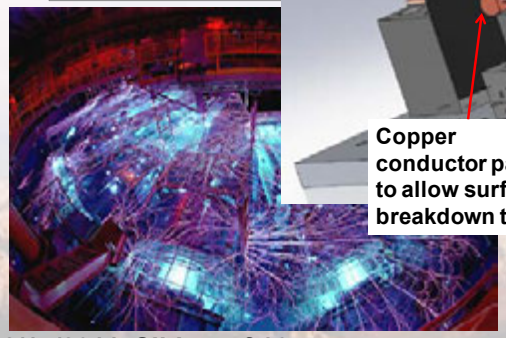
- **Testing includes**
  - Conditions that allow arcing
    - Materials for dielectric strength
    - Geometry
    - Voltages/potentials, boundary conditions
  - Introduction of simulated arcs into PV systems
    - Measure electrical frequencies present during arcing events
  - Filtering created by PV modules and other components
- **Testing facilities**
  - Manufacturers' laboratories
  - Standard developers' labs
  - National labs
- **Sandia National Laboratories facilities:**
  - PSEL: Photovoltaic Systems Evaluation Lab
    - Tests for module and cell manufacturers
  - Pulsed Power, Z machine
    - The big 'daddy' of man made arc generators
    - Understanding of the physics of arcs
  - DETL: Distributed Energy Testing Lab











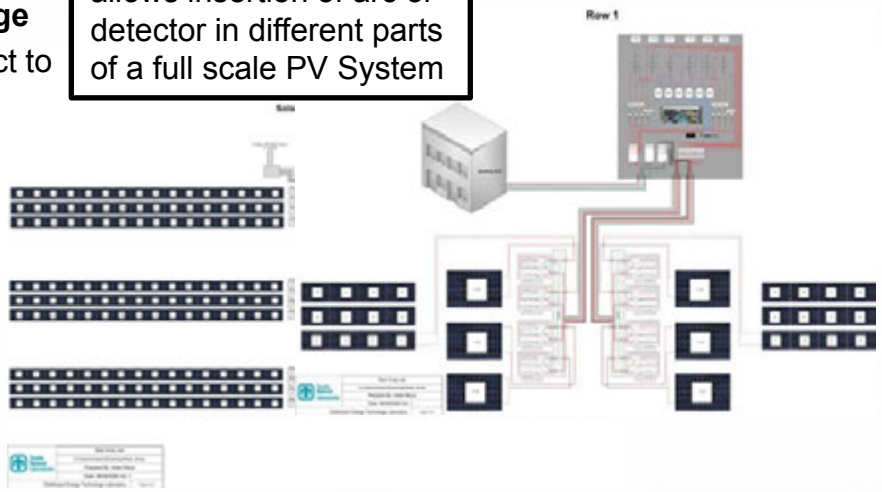
Same basic test apparatus will allow testing of module material samples, potting compounds, gases at different pressures, contact disconnects, contact gaps, parallel path arcs and be used with the solar simulator and in the field hooked up to various locations.

Arc Fault Testing, Sandia DETL Facility

Distributed Energy Testing Lab, DETL:

- **Many combinations of grid tied generation, loads and storage**
  - Inverter, AFCI and component manufacturers able to connect to PV arrays at any number of insertion points
- **Advanced R&D**
  - System level performance and reliability testing
  - Component interoperability testing
- **Advanced Power Electronics Components and Systems**
  - Solar Energy Grid Integration Systems (SEGIS)
  - Controllers for distributed grid equipment based on new and existing standards
  - Advances in inverter design, integration and manufacturing through partnerships with Industry
  - Long-term inverter performance characterizations
- **Technology Solutions for Communications and Security**
  - Secure Supervisory Control and Data Acquisition (SCADA) applications
  - Technology development and applications capable of supporting multiple communications protocols
- **Solar Standards and Codes**
  - Development of new procedures for performance and reliability testing
  - Assuring accountability, applicability and metrics of new standards development

Sandia DETL Facility allows insertion of arc or detector in different parts of a full scale PV System

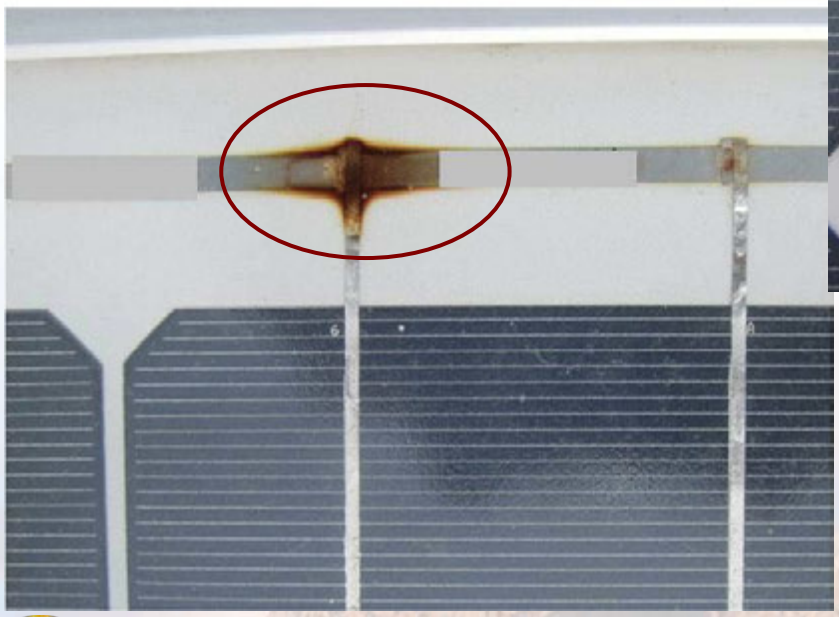


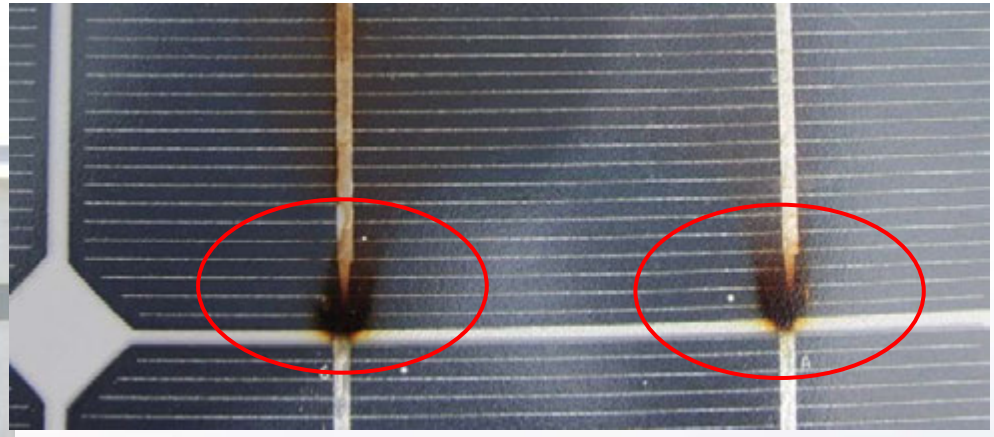


Module Failures and Discussion

- **Three primary failures can be seen:**
  1. Busbar discoloration, most common, seen in multiple locations and modules. Also busbar shifting and bending.
  2. Collector ribbon discoloration at location ribbon goes from cell back contact to front grid, also common
  3. Discoloration in the middle of the topside grid collector ribbon
- **All 3 of these failure modes have charring, burning and backsheet bubbling on the backside of the modules.**
- **The busbar discoloration appears to be linked to the front side glass fracture in one case**

Busbar discoloration shown below. Collector ribbons appear to be shifted to the right and the solder joint between the ribbons and busbar appears to be broken.





Discolored collector ribbon as they pass from the top of the PV cells to the backside contact.

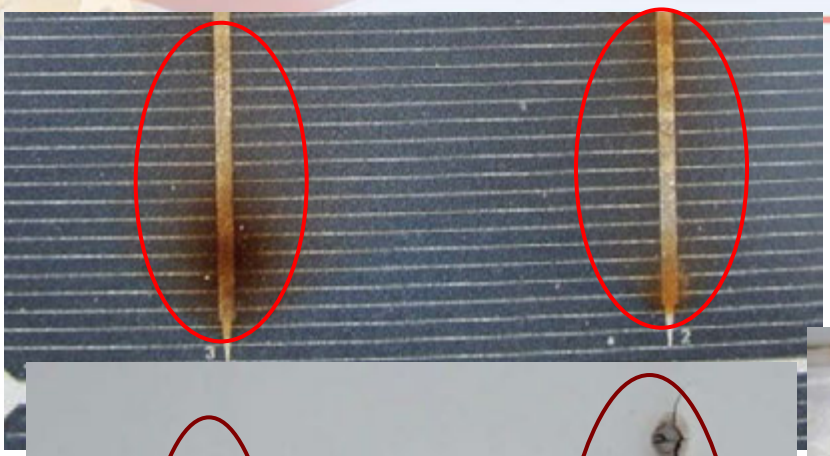
Some of the melting, boiling and maximum use temperatures of module materials are shown below.

$Tmelt_{Si} := 1687K$ $Tboil_{Si} := 3538K$ $Tmax_{Tedlar} := 200\,°C$

$Tmelt_{Cu} := 1358K$ $Tboil_{Cu} := 2835K$

$Tmelt_{Sn} := 505K$ $Tboil_{Sn} := 2875K$

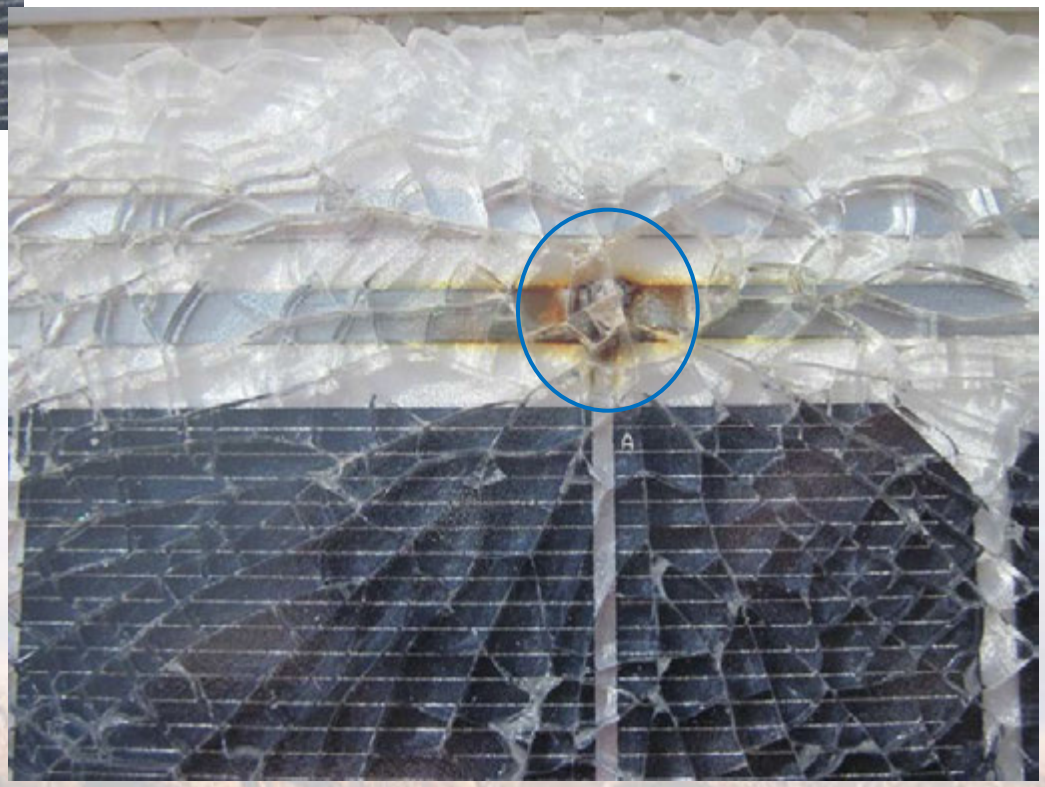
Module Failure Types and Discussion





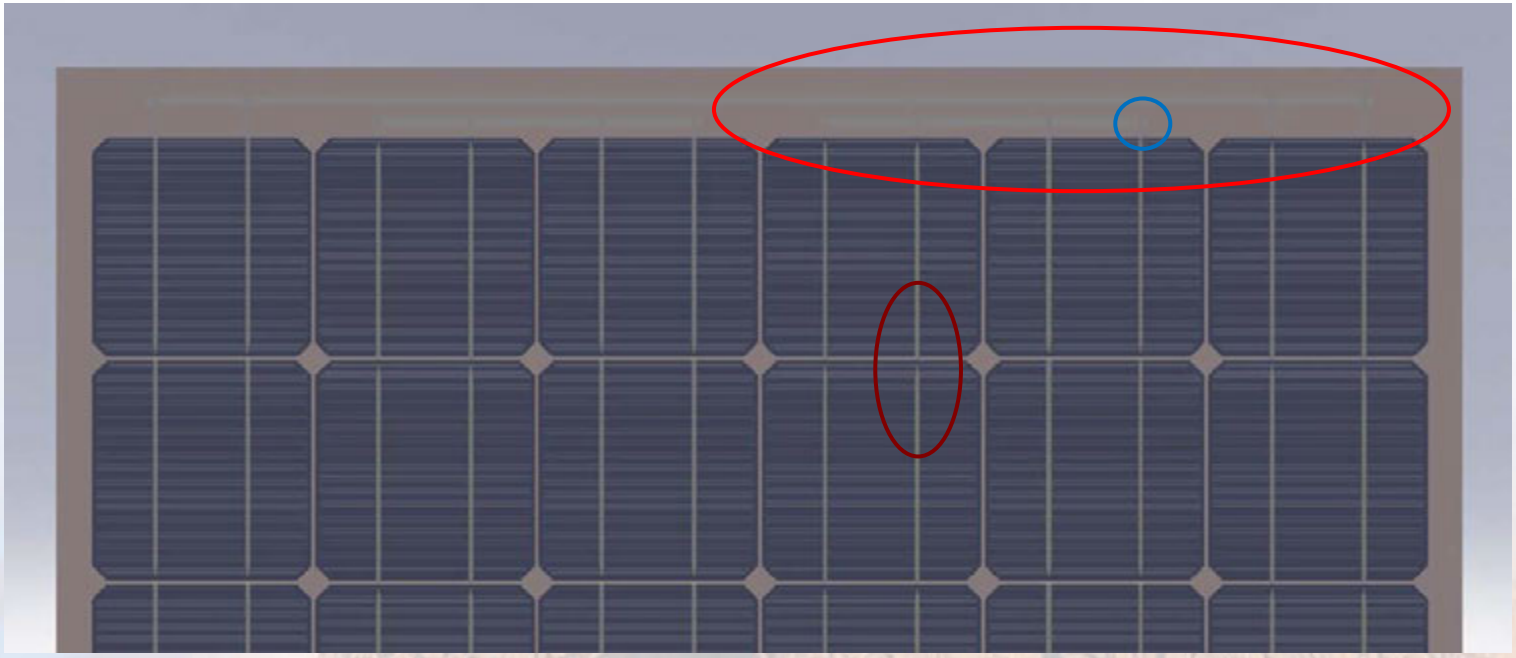
3. Discoloration in the middle of the topside grid collector ribbon

- **All 3 of these failure modes have charring, burning and backsheet bubbling on the backside of the modules.**
- **The busbar discoloration appears to be linked to the front side glass fracture in one case**
  - Note radial fracture pattern in glass, centered at busbar color



Description of model and assumptions

- **Complete module model developed:**
  - Full size with accurate geometry and materials, *except* tin plating on busbars and connector ribbons and backside contact aluminum, both of which are single micron thickness range
- **Small sections of the module model analyzed for arc generated thermal and thermo-mechanical effects**
- **Small sections of the module are analyzed for other effects.**
- **Due to the high temperature of an arc, published at minimum levels around 6000C, other heat transfer mechanisms are all neglected.**
- **Arc area of just 0.38 mm^2 at 6000K is modeled to determine if it could have resulted in glass breakage due to thermal expansion stress.**



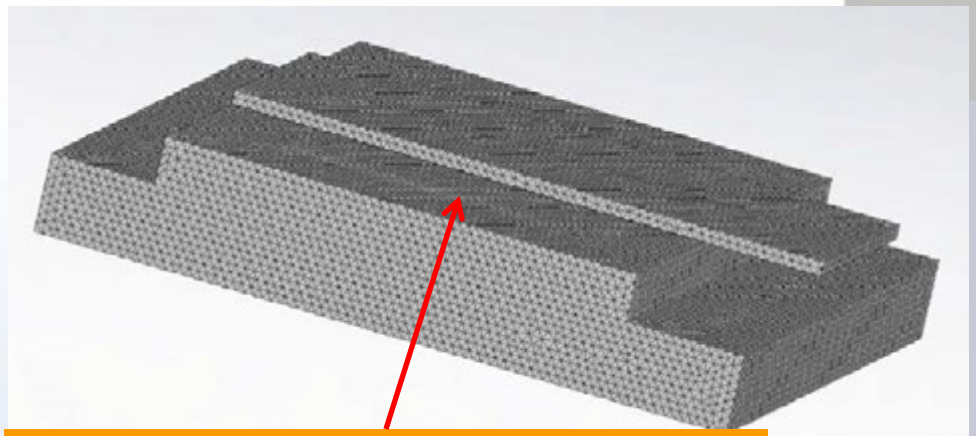
Module

- **72 125 mm cells**
- **160 W, 4.9 A Isc, 43.5 Voc**
- **54 50 x 250 micron grid lines per cell**
- **Two 2.54 mm x 150 micron collector grids per cell**
- **Large end busbars are 5.08 mm x 200 micron**
- **Areas analyzed**

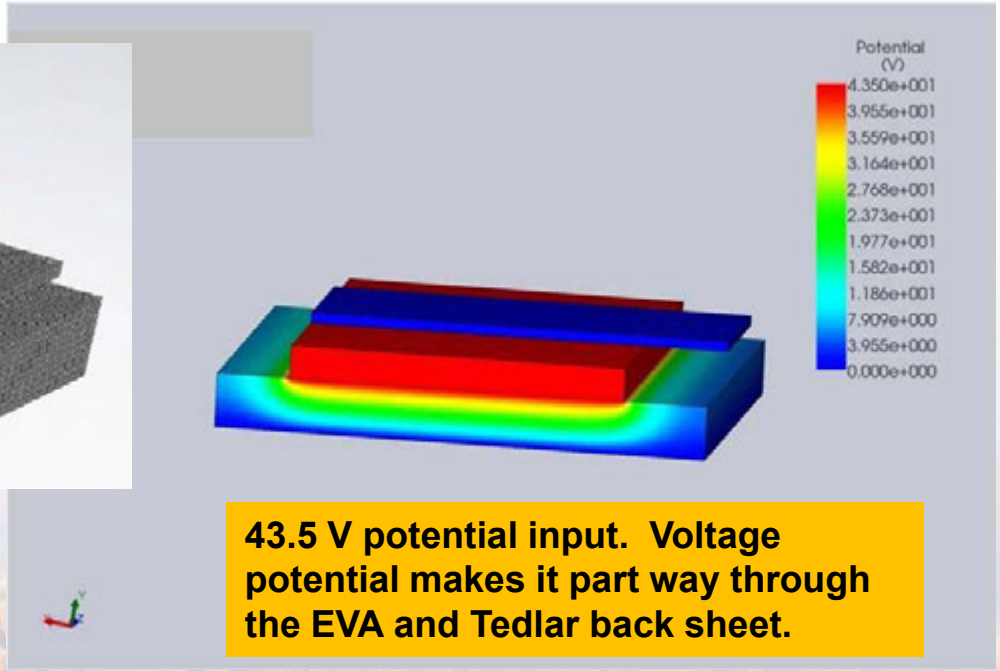
1. **Glass Break above Busbar**
2. **Busbar shifting**
3. **Ribbon between bottom and top of cells**

Electrical conditions to cause arc in busbar failures

- **To investigate the likelihood of an arc occurring at the junction between the collector bus and busbar, an electrical dielectric breakdown and discharge study was performed.**
  - Domain was reduced to 6.5 mm wide by 7.5 mm tall, and the non-electrical components, such as the top glass were removed. Air assumed to be in electrode gap.
  - A 5 micron gap was introduced between the two electrical contacts, which have an area of 2.54 mm x 5.08 mm = 12.9 mm^2 , and the potential of all the cells in the string, 43.5 V, was used to see if breakdown would occur.

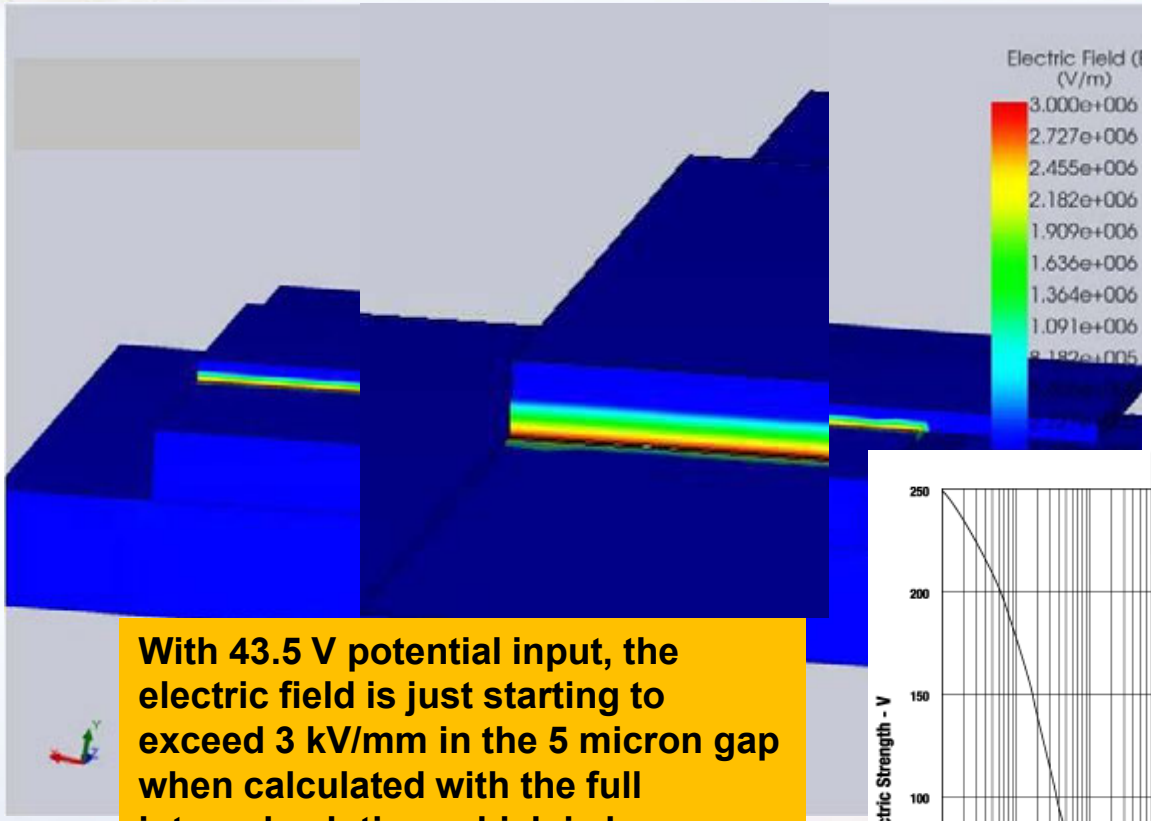


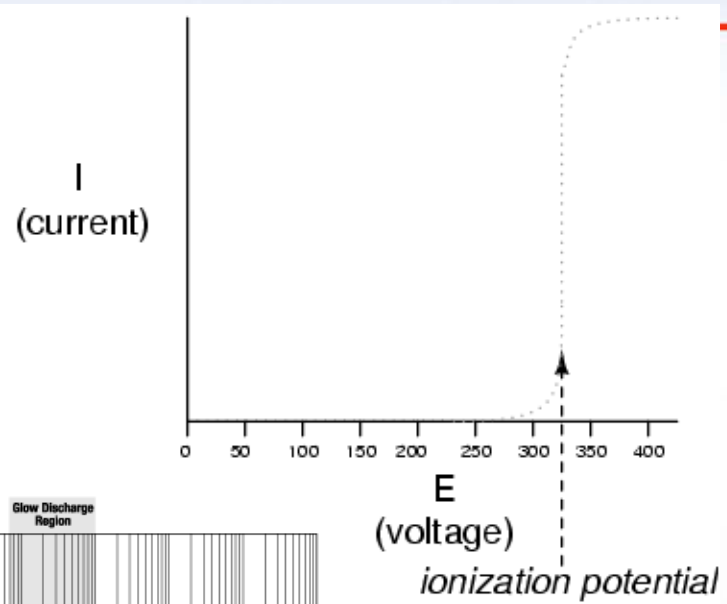
Greatly reduced domain for electrical discharge study. Mesh accounts for 5 micron air gap between parts.

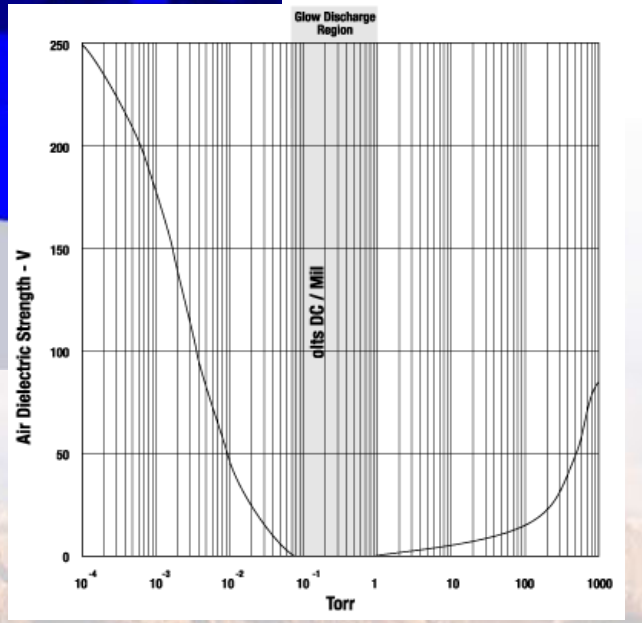


43.5 V potential input. Voltage potential makes it part way through the EVA and Tedlar back sheet.

Electrical conditions to cause arc in busbar failures, results







With 43.5 V potential input, the electric field is just starting to exceed 3 kV/mm in the 5 micron gap when calculated with the full integral solution, which is lower than the linear

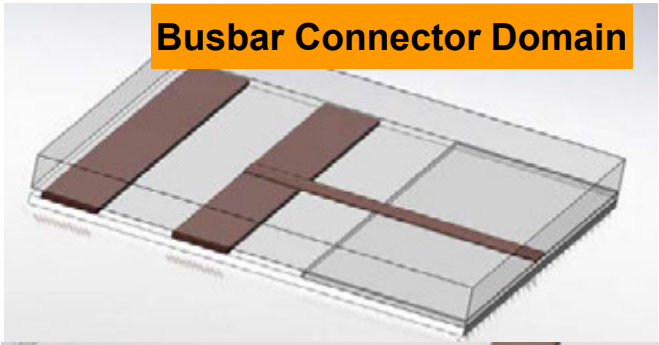
$$\frac{43.5\text{V}}{5\text{micron}} = 8.7\frac{\text{kV}}{\text{mm}}$$

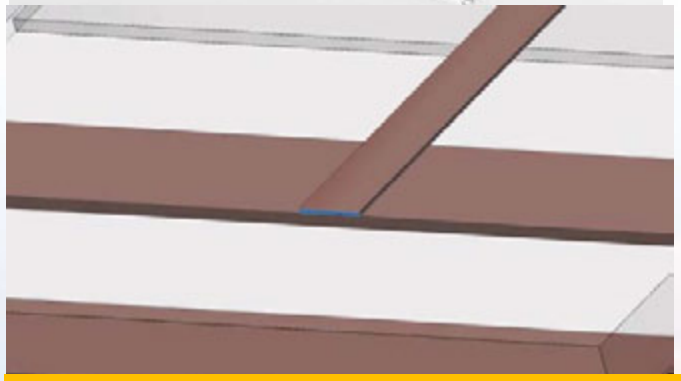
At 1 atm pressure, air dielectric strength is about 3 kV/mm, or 75 V/mil. Above this electrical potential, the air stops acting like a perfect insulator, and conducts very well.

Temperature and Time to Fracture Front Glass

- To investigate the glass fracture, a small 40 mm by 40 mm domain, including the module stack and collector grid to busbar interface was analyzed, as shown in the graphic: 6000K applied along end of grid.

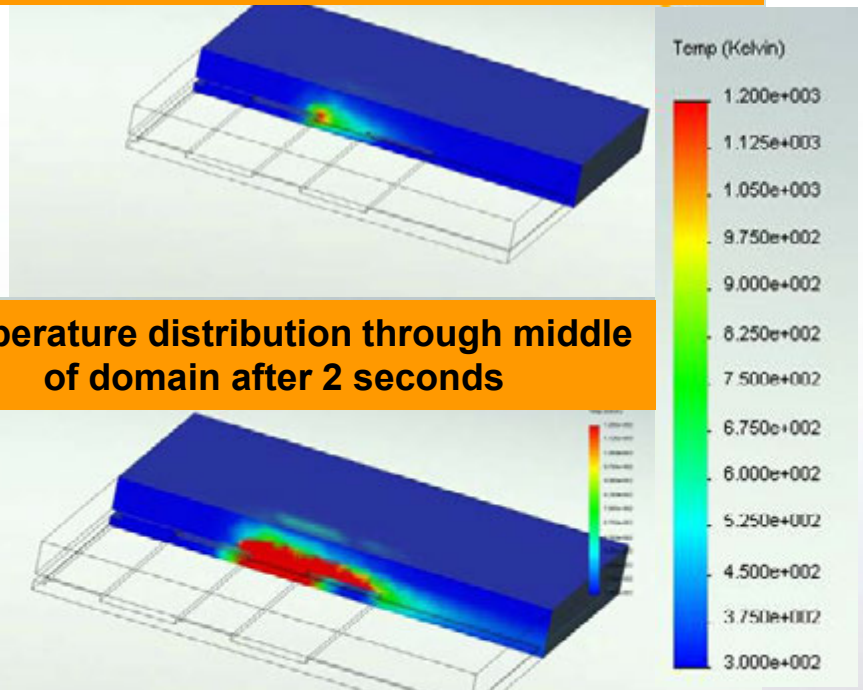
Busbar Connector Domain



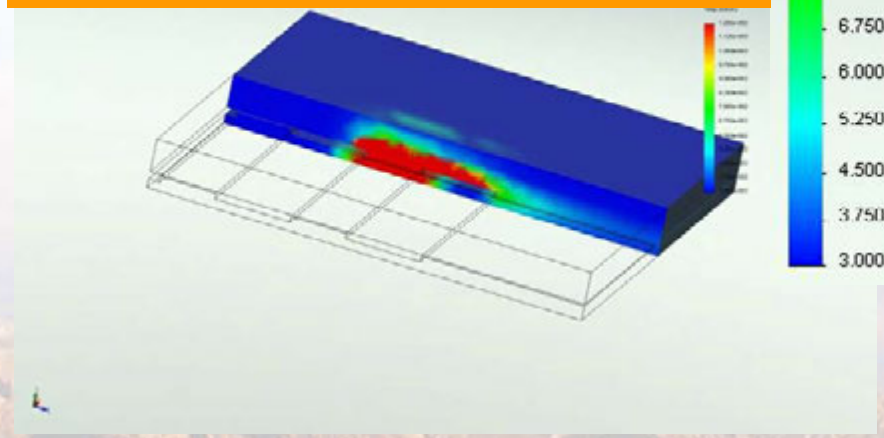


Busbar Connector Detail showing 0.381 mm^2 Arc Fault Initiation Area in blue

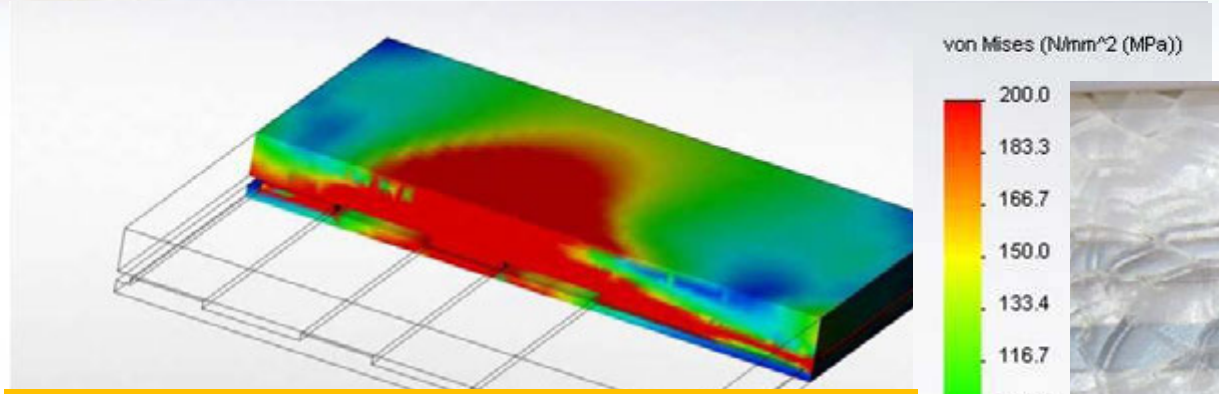
Temperature distribution through middle of domain after just 0.2 seconds



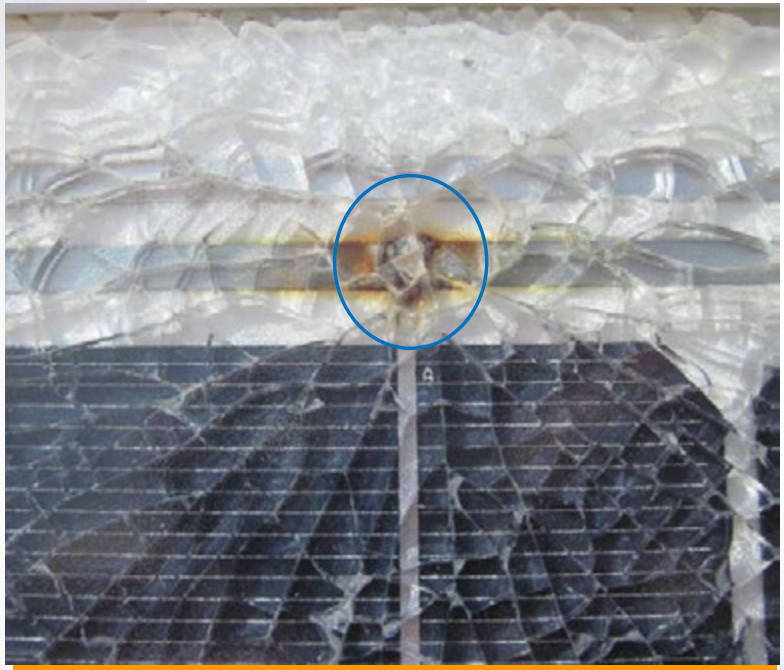
Temperature distribution through middle of domain after 2 seconds



Temperature and Time to Fracture Front Glass, cont.







State of thermal expansion stress after 2 seconds of arcing on the ~0.4 mm^2 area. Heat tempered glass has a modulus of rupture of *at most* 160 Mpa, and near 100 Mpa is more likely for glass that has a texture or pattern, as the module does. Conclusion: Glass fractured into small pieces from this temperature.

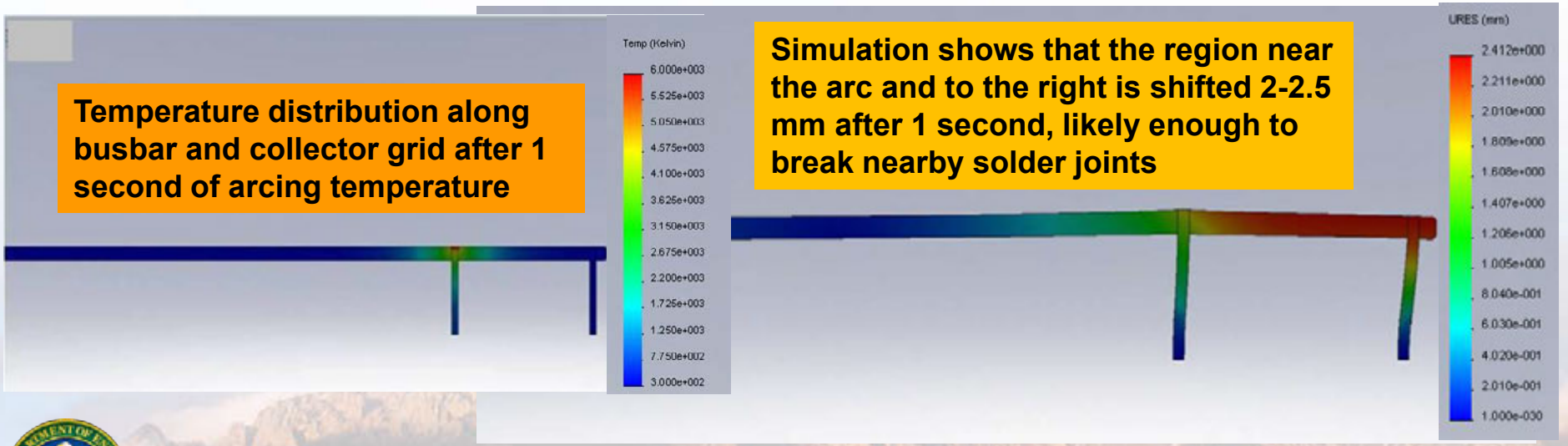
Glass Modulus of Rupture Properties:
Float 27-62 MPa
Tempered Float 160 MPa
Also from Flabeg Solar Glass
Specifications:
Fully Tempered: 120 MPa, 90 MPa with pattern and
Heat Strengthened: 70 MPa and 55 MPa patterned.
Also annealed at 6000 psi = 41 MPa
and tempered at 24,000 psi=165 MPa

The thermal expansion of the area above the arc puts the surrounding areas into tension, which is the weaker direction for glass and ceramics, resulting in fracture centered at the heat source, with the small size pieces being typical for tempered glass.

Busbar shifting and connection damage

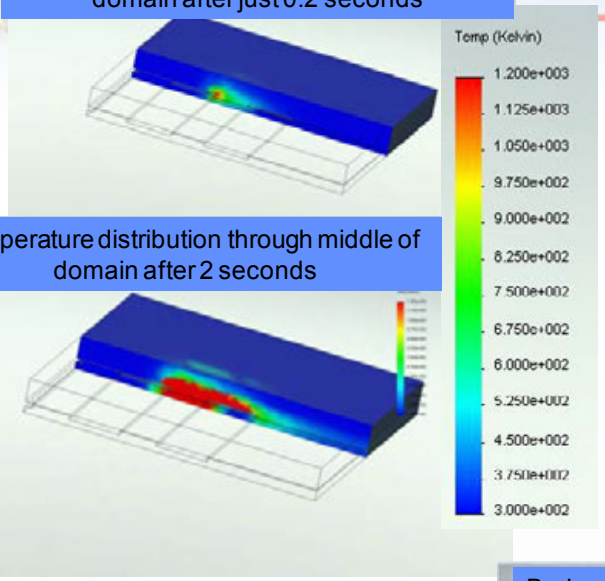
- **To investigate if arc temperatures could have caused the busbar shifting and broken collector to busbar connection, the thermal study of applying 6000K to just 0.38 mm^2 at the end of the connector was performed.**
  - Assumed busbar was restrained in the x direction at the module center, and restrained in the z direction by the module lamination.





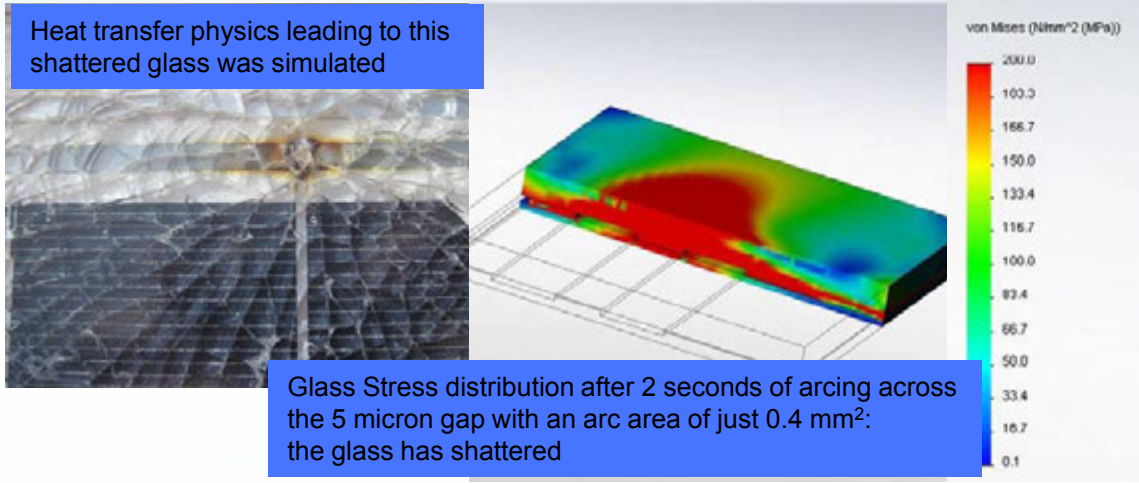
Arc Fault Modeling Summary

Temperature distribution through middle of domain after just 0.2 seconds



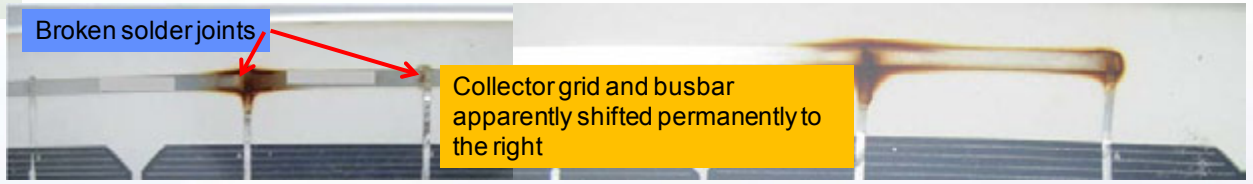
Temperature distribution through middle of domain after 2 seconds

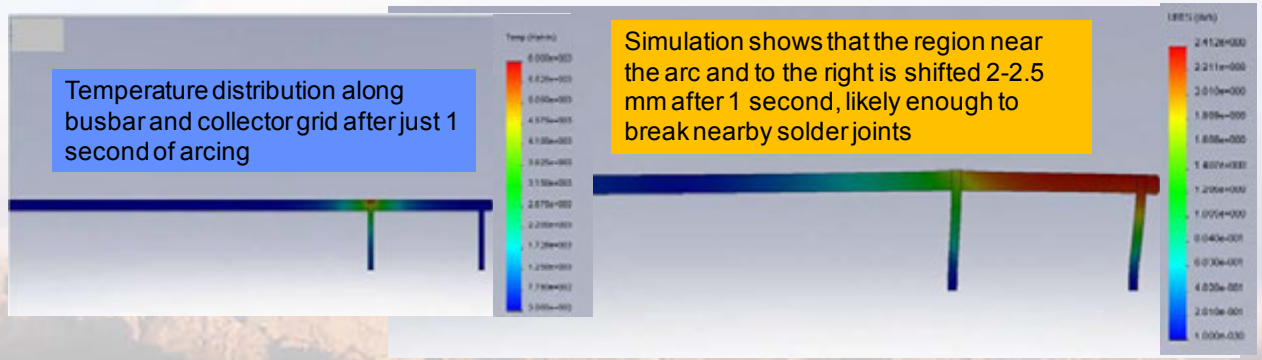
Heat transfer physics leading to this shattered glass was simulated



Glass Stress distribution after 2 seconds of arcing across the 5 micron gap with an arc area of just 0.4 mm^2: the glass has shattered

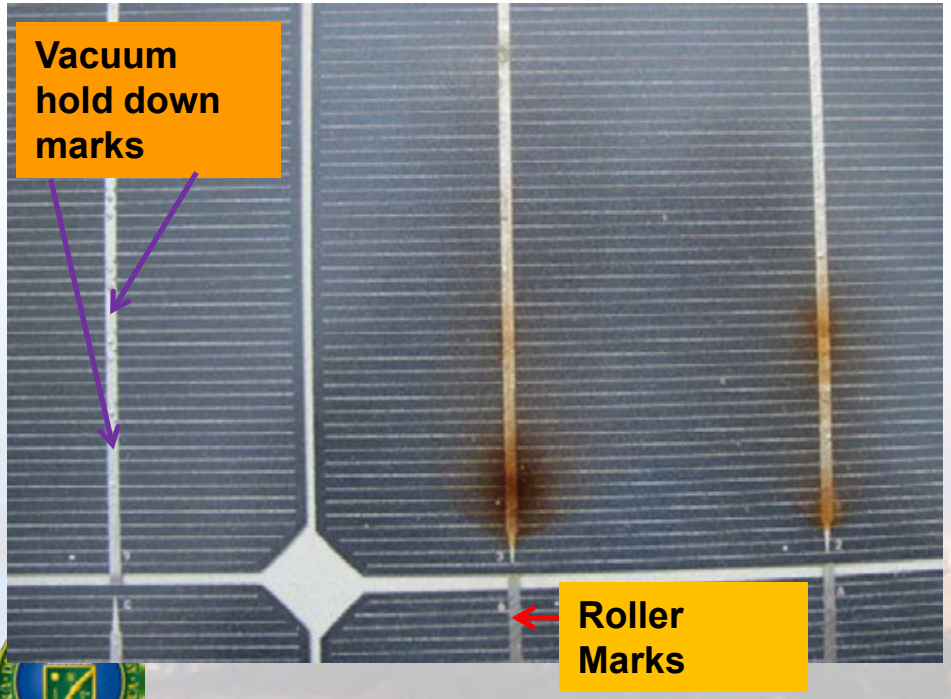
- **Thermo-mechanical modeling**
  - Simulation and prediction of temperature and mechanical stress effects of arcing given boundary conditions, material properties and geometry
  - Simulations provide insights into time scales for arc detection and material selection

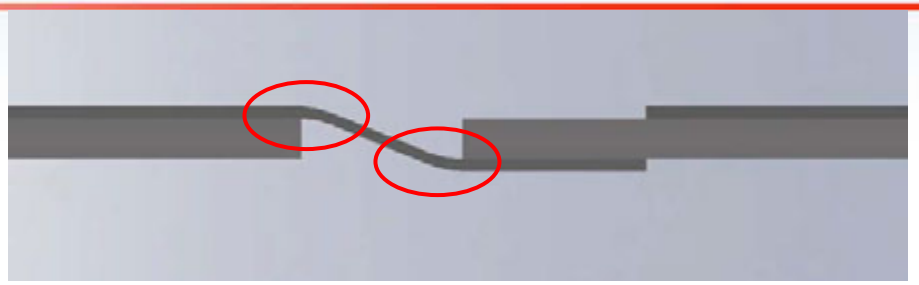




Conclusions

- It appears likely that some or most of the failures observed in the modules are due to high temperatures at (relatively) short durations, such as would be seen in an arcing event.
- It also appears that areas of the module that were under vacuum hold down were less susceptible to failure than those areas that were rolled, as shown below.





- Side view of ribbon from back contact to top of cells.
- Diurnal temperature shifts could have strained and broken the ribbon at either bend, leaving a tiny gap that could have arced any day the module is in the sun afterwards, leading to a common failure observed: burned collector ribbon between cells.
- Studies of Joule heating in oxidized backsheet to ribbon connections show insufficient temperatures to cause all observed effects.
- Future studies on thermal strain due to diurnal temperature fluctuations on the failed ribbons will be performed.
- Future study on limits of the current generation of Tyco Junction Boxes as well as effects of new connector materials to be performed as well.

THANK YOU!

From the Sandia PV ARC Fault Team

Questions?



Sandia National Laboratories

Life Prediction for CIGS Solar Modules

D.J. Coyle, H.A. Blaydes, R.S. Northey, J.E. Pickett, K.R. Nagarkar,

R.A. Zhao, and J.O. Gardner

GE Global Research

Niskayuna, NY, 12309

DOE PV Module Reliability Workshop

Denver, CO

February 16-17, 2011

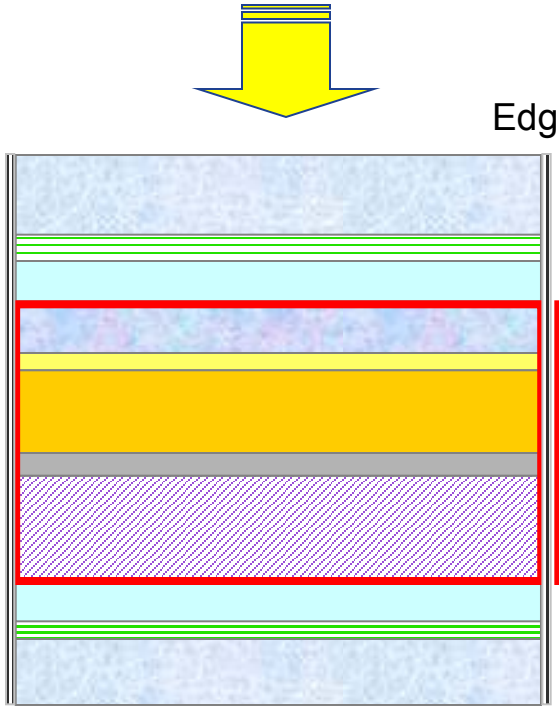
One can use accelerated testing data to predict real-world module failures only if the degradation mechanisms are known and their dependence on environmental factors measured. The moisture-induced degradation rate of flexible CIGS solar cells has been measured as a function of temperature and humidity and fit to a kinetic rate expression. This expression is coupled to a model of moisture diffusion into a package and typical meteorological input data to create a cumulative damage model to predict lifetime of packaged cells versus outdoor exposure and package construction. Estimated acceleration factors for damp heat (85C/85%RH) vs. Miami range from 15X to 50X, depending on the package, since diffusion through the package is accelerated differently than the cell degradation kinetics. The degradation rates are strongly dependent on the transparent conductive oxide used for the window layer and the electrically-conductive adhesive used for the contacts. The dependence of degradation on encapsulant materials is fundamentally different than is often assumed in the literature.



Prototype Flexible CIGS Module



Flexible Thin-Film PV Package



Top Sheet
- Transparent
- UV Stable, UV block
- Electrical insulation
- Mechanical (cut, hail)
- Moisture barrier

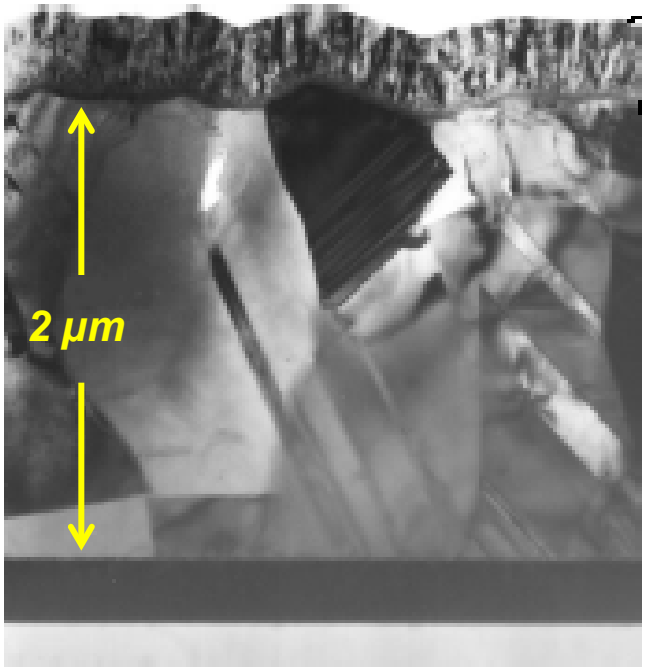
Encapsulant
- Low T_g compliant "glue"
- Transparent
- Adhesion

Backsheet
- Electrical insulation
- Mechanical (cut)
- Moisture barrier

Edge Seal
- Barrier
- Adhesion

$Cu(InGa)Se_2$ Device Environmental Stability

Moisture-induced degradation



ZnO/ITO ← Increased Series Resistance Rs

CdS ← i-ZnO Buffer Layer

Decreased Shunt Resistance Rsh

$Cu(InGa)Se_2$ ← Increased Recombination
1. Quasi-neutral region
2. Depletion region

Mo ← Increased Series Resistance Rs

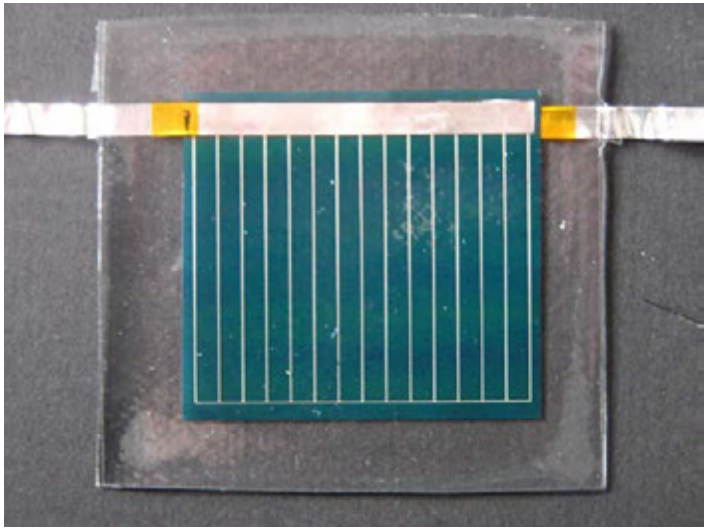
(W. Shafarman & L. Stolt, *Handbook of Photovoltaic Science and Engineering*, Ed. A. Luque & S. Hegedus, Wiley, 2003)

Test Cells:

1. Global Solar Test Cells (ITO)
2. AZO

GSE test cell

tabbed and encapsulated



~ 36 x 46 mm exposed

Stainless steel foil

Mo coating

ECA – Tabs/ribbons

Efficiency ~ 12 – 13.5%

V_{oc} ~ 600 - 610 mV

J_{sc} ~ 33-36 mA/cm^2

FF ~ 60 - 62%

A ~ 16.5 cm^2

Factors for prediction of lifetime (moisture degradation):

1. Cell construction
    - ITO vs AZO window layer
    - Type of ECA for interconnect
    - Other
2. Exposure
    - Accelerated testing (ovens with various temp, RH)
    - Real-world exposure (Miami, Phoenix, …)
3. Package
    - Barrier properties of topsheet and backsheet
    - Encapsulant
    - Edge seals
    - other

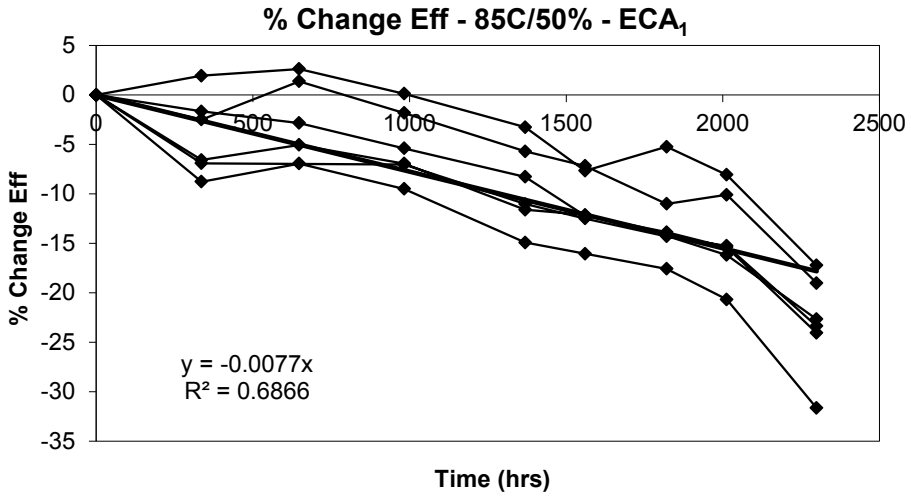


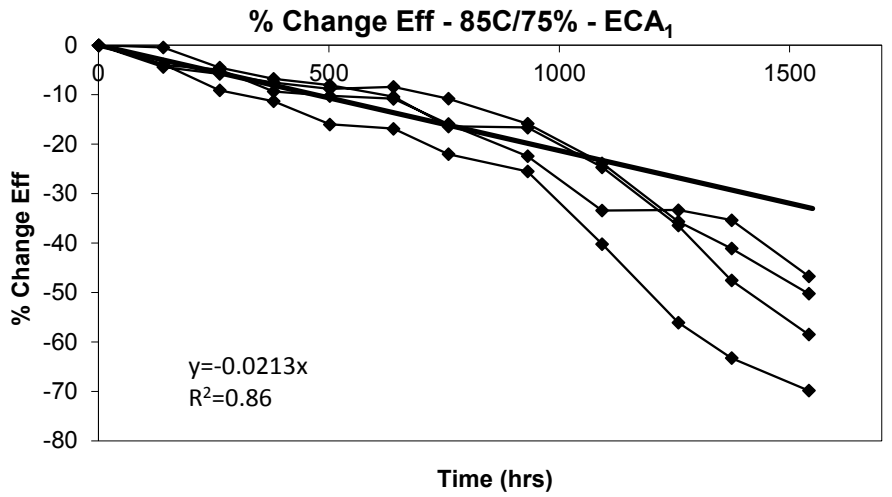
Life Model – Moisture Sensitivity

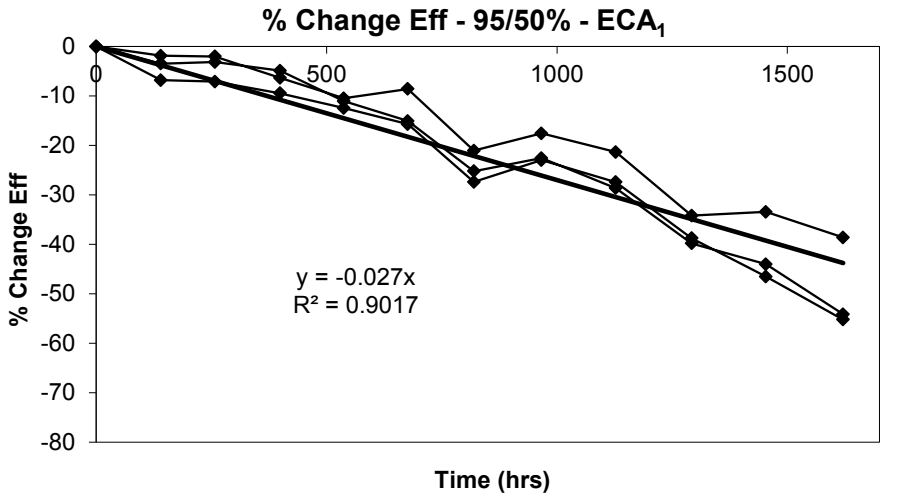
1. CIGS Degradation Kinetics - *Measure*
   - Degradation rate vs. Temp, humidity
   - ITO vs AZO
   - ECA - Interconnect degradation can play a role
2. Moisture Diffusion into Package - *Model*
   - Meteorological data – TMY3 from NSRDB
     - Hourly irradiance, air temp, ground temp, humidity, wind speed
   - Heat transfer model of module
     - Radiation, free & forced convection
   - Diffusion through barrier film, Saturation of encapsulant, no edge effects
3. Coupled Model - *Predict*
   - Cumulative degradation and average life vs. location and package design
   - Tradeoffs between CIGS sensitivity and package design/cost
   - Interpretation of accelerated tests results

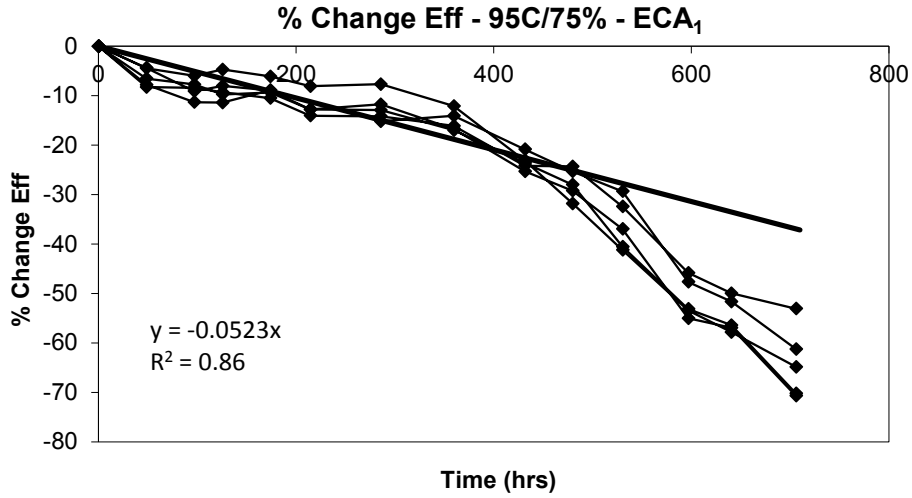


Degradation Data - Examples



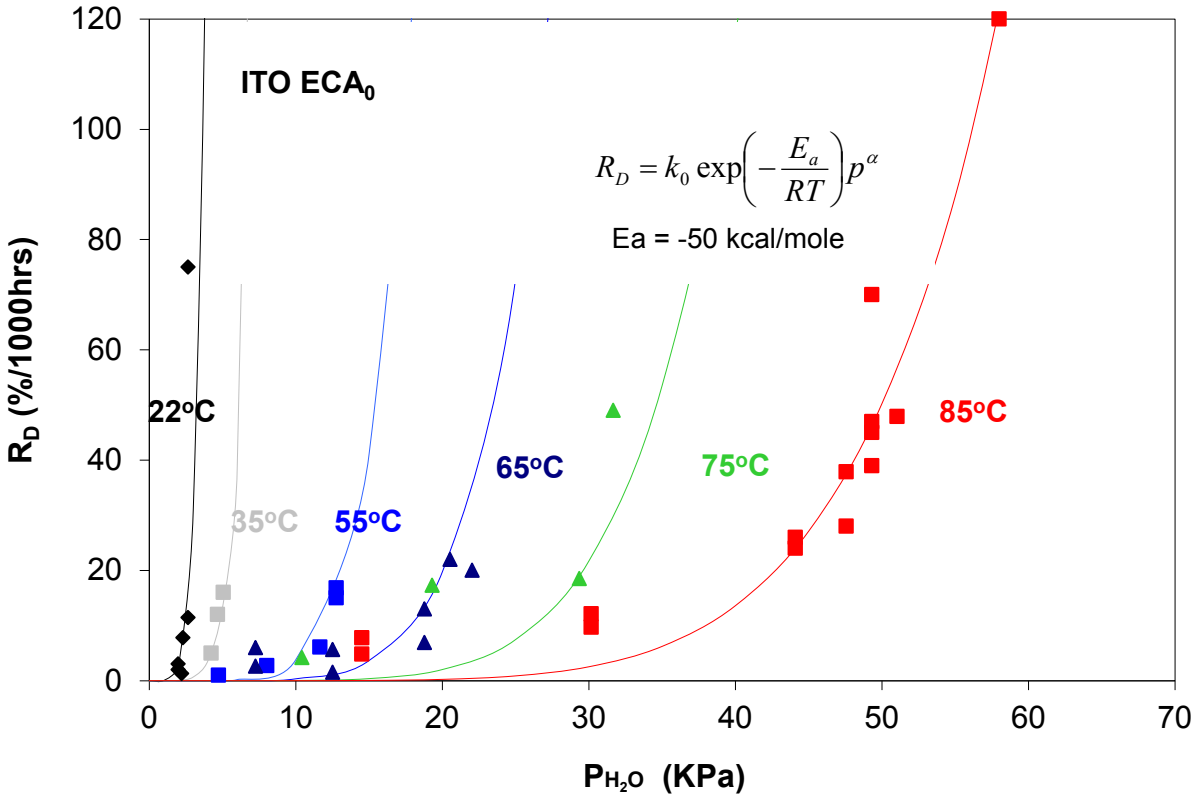






- High temperature, humidity faster
- Driven by FF loss due to R_{oc} and some shunting

Scaling with partial pressure water



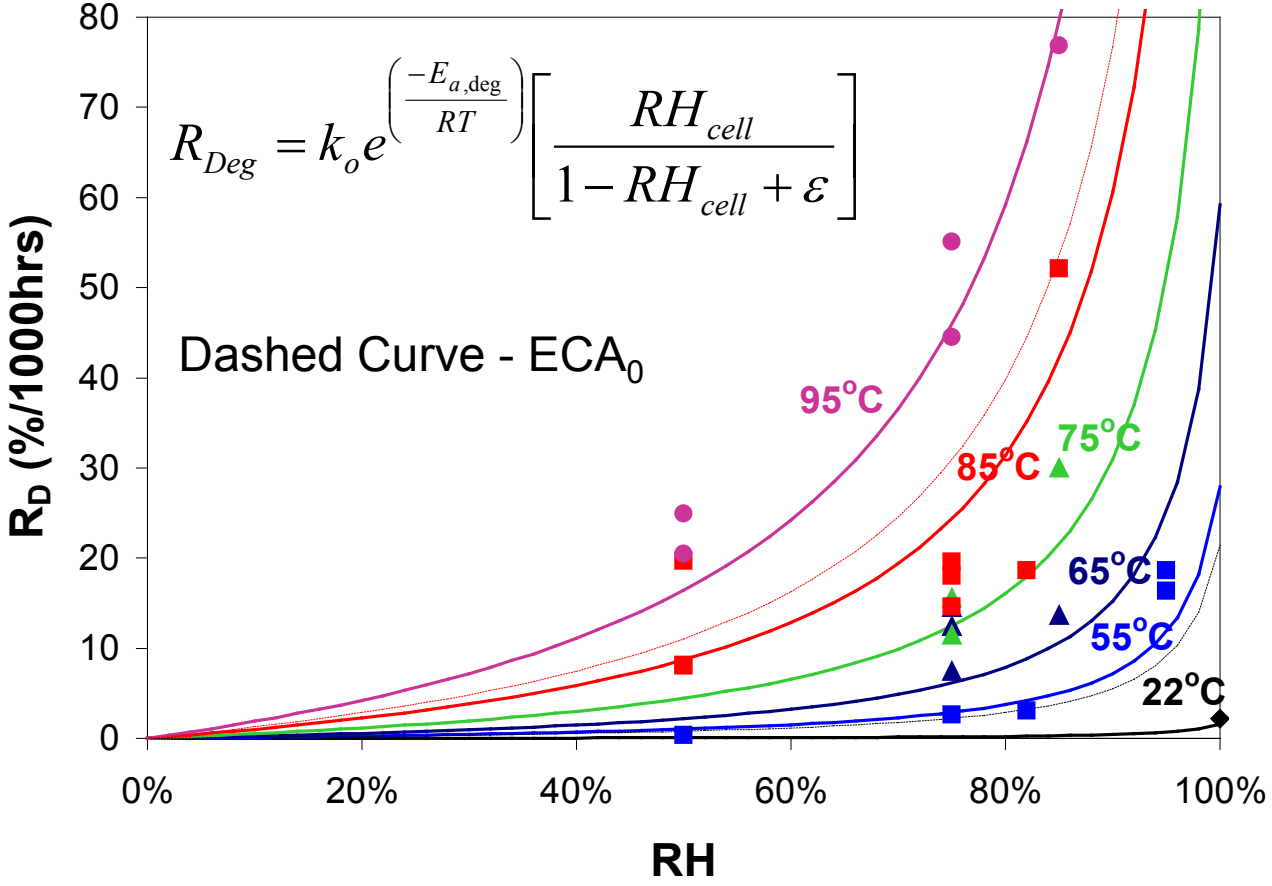
Negative activation energy!

Need to scale with % saturation (RH)

Interfacial equilibrium (Henry's Law) $\frac{C_a}{S_a} = \frac{C_b}{S_b} = RH$

CIGS Degradation Kinetics (Global Solar test cells)

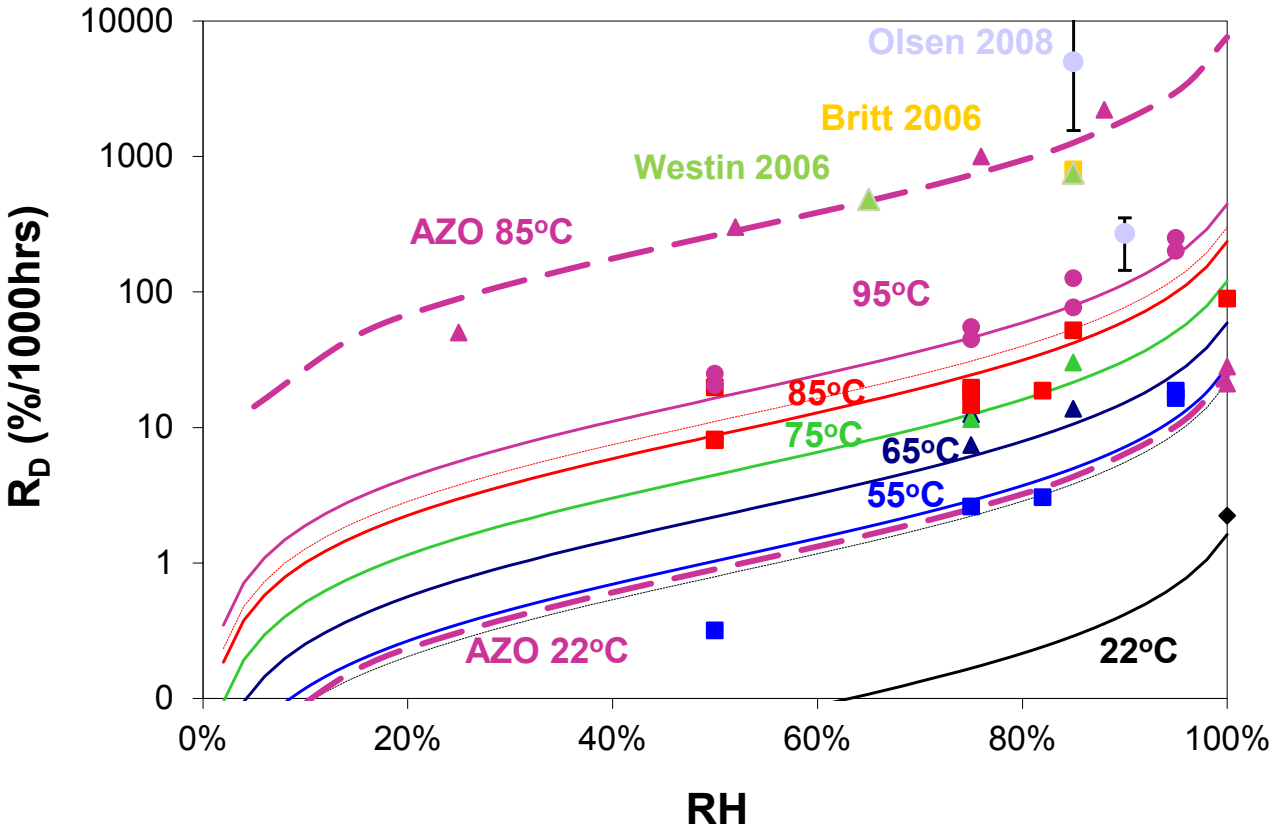
- For every Temp & RH, fit data to linear degradation rate (1st 20% of degradation)
- Fit rate of degradation vs Temp, RH to kinetic model



- Strong RH dependence at high RH
- ECA affects temperature dependence

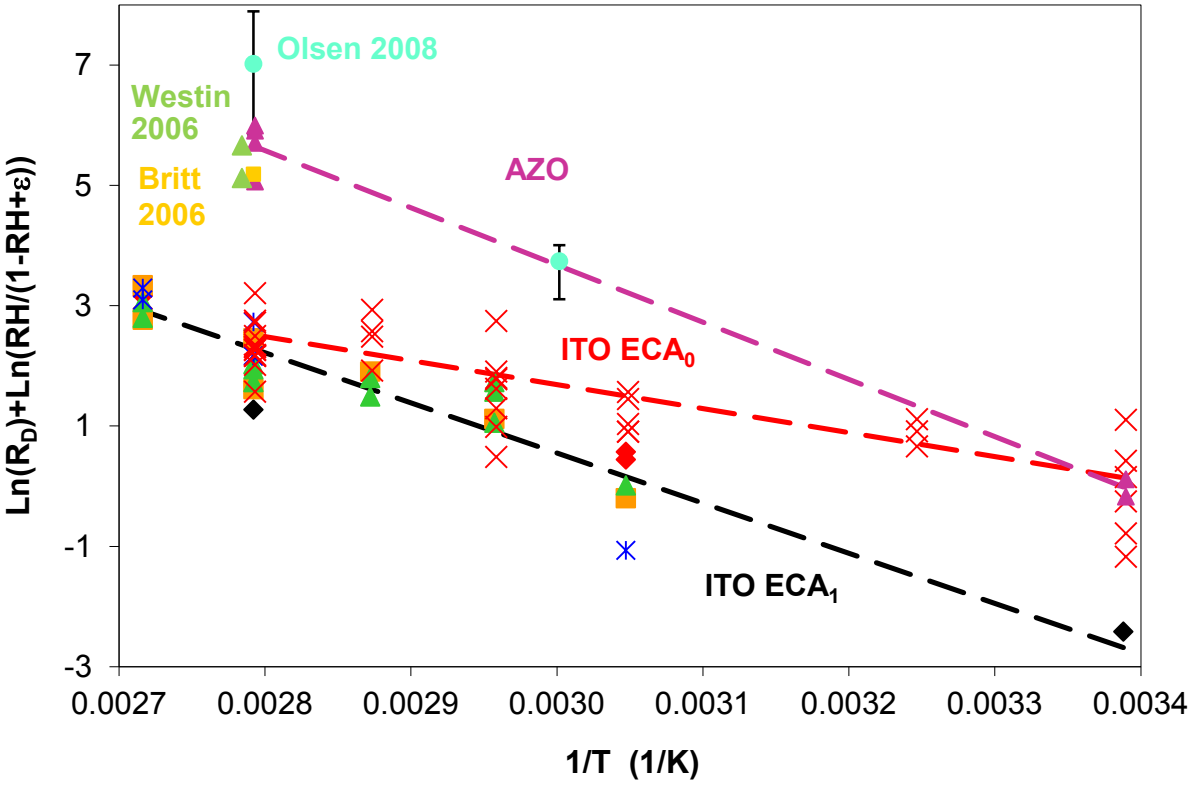
(Klinger, D. J., *"Humidity acceleration factor for plastic packaged electronic devices"*, Quality and Reliability Engineering International. Vol. 7, 965-3711, 1991).

CIGS Degradation - AZO vs ITO



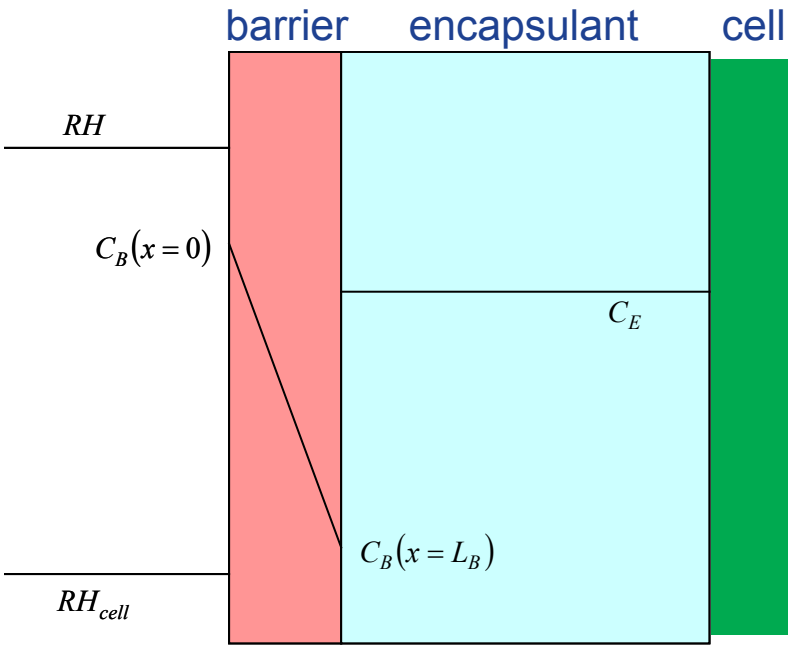
- AZO ~ 25X ITO
- Comparable to published data

Arrhenius Plot



- ECA_0 very low activation energy

Package Diffusion Model



Mass Balance, Interfacial Equilibrium, Fickian Diffusion, $D_{barrier} << D_{encapsulant}$

$$\frac{\partial C_E}{\partial t} = \frac{S_E RH - C_E}{t_c}$$

$$t_c = \frac{L_E S_E}{WVTR_{\max}}$$

If initially dry:

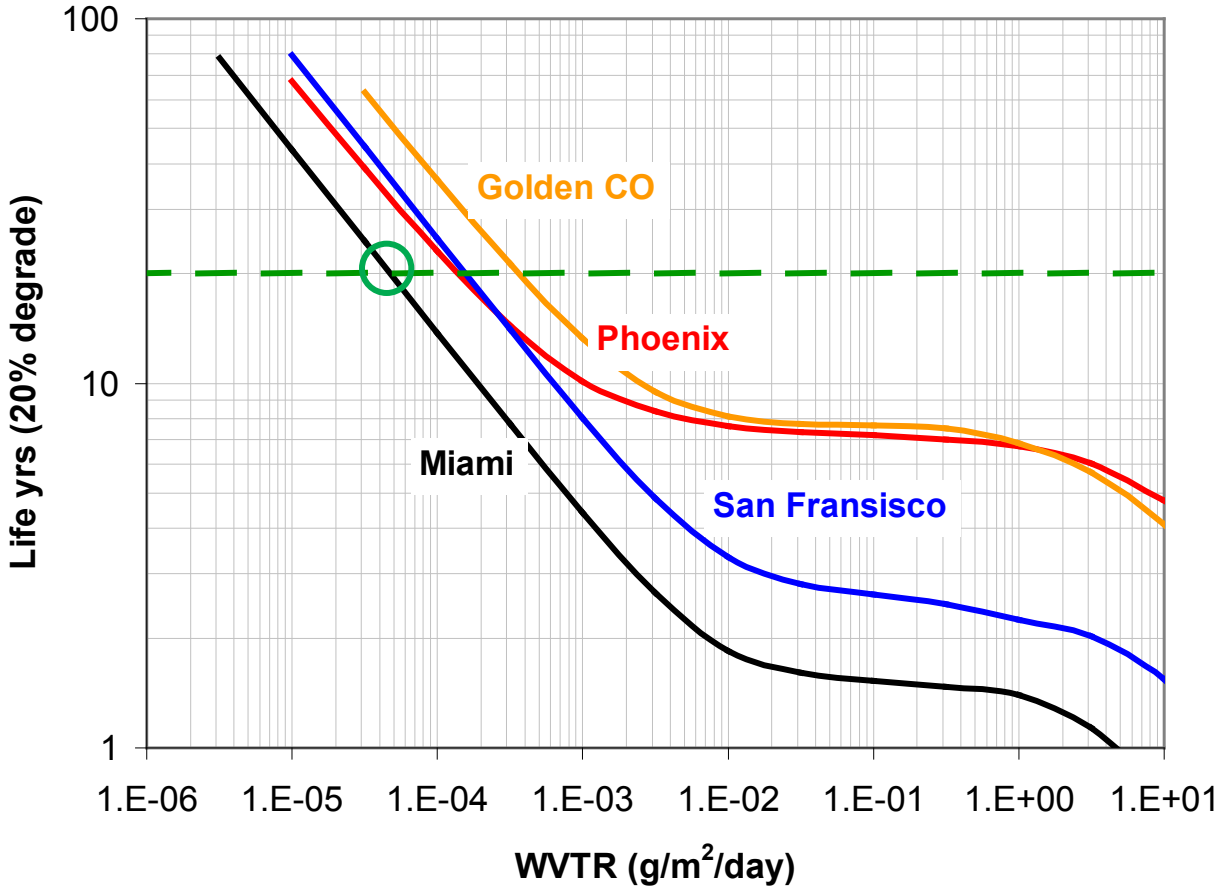
$$\frac{C_E}{S_E} = RH\left[1 - e^{\left(-t/t_c\right)}\right]$$

Integrate moisture ingress with hourly weather data (TMY3)



(Kempe, M.D., *"Modeling of rates of moisture ingress into photovoltaic modules,"* Solar Energy Materials & Solar Cells, Vol 90 (2006) pp. 2720–2738).

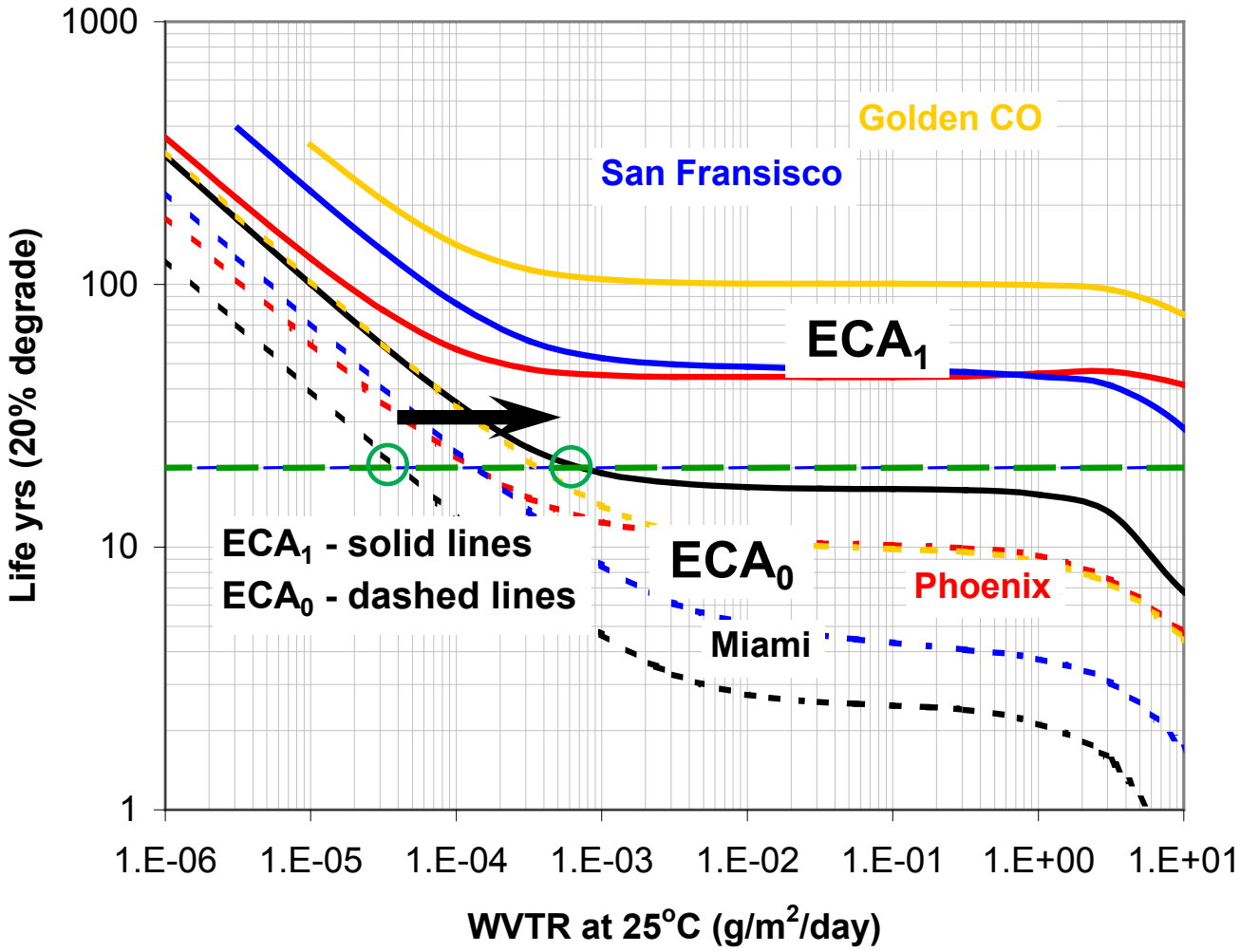
Life vs. Barrier: ITO-ECA$_0$



Need ~ 4x10^{-5} g/m^2/day package ~ 20 yr life

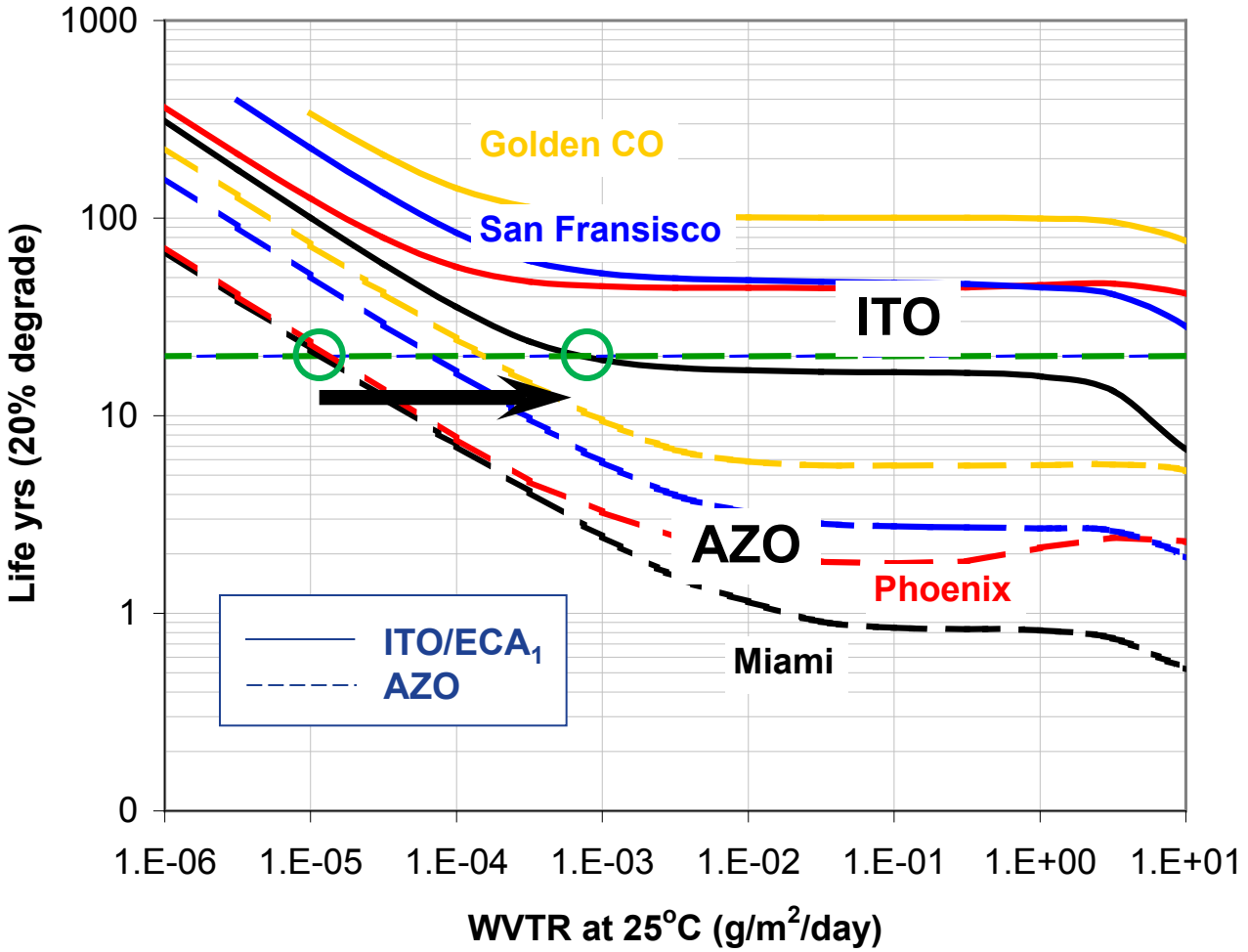
DJ Coyle
GE Global Research
16-February 2011

Life vs. Barrier: ITO-ECA$_1$



Need ~ 8x10^{-3} g/m^2/day package ~ 20 yr life

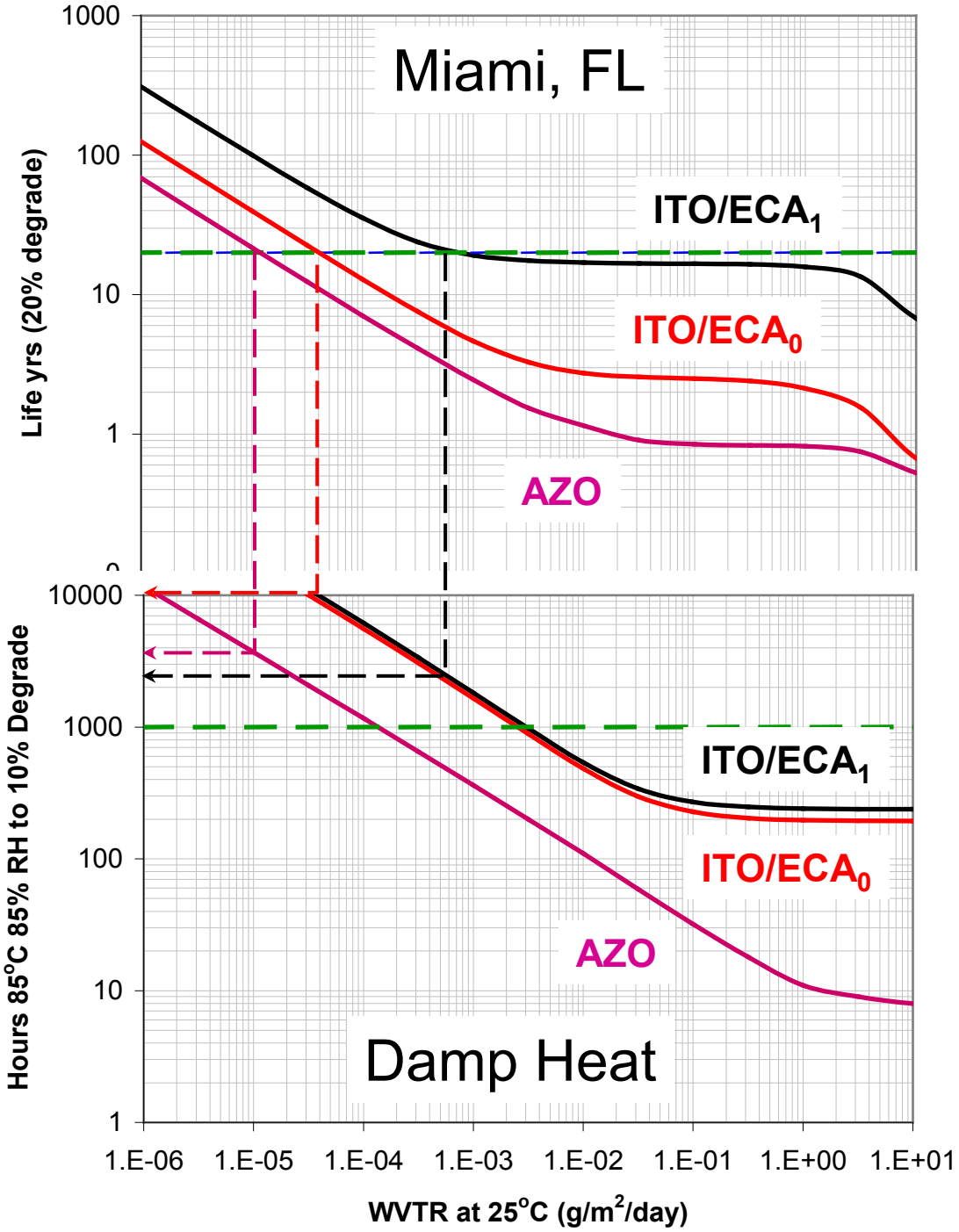
Life vs Barrier – ITO vs AZO



ITO Life 5-25x AZO Life

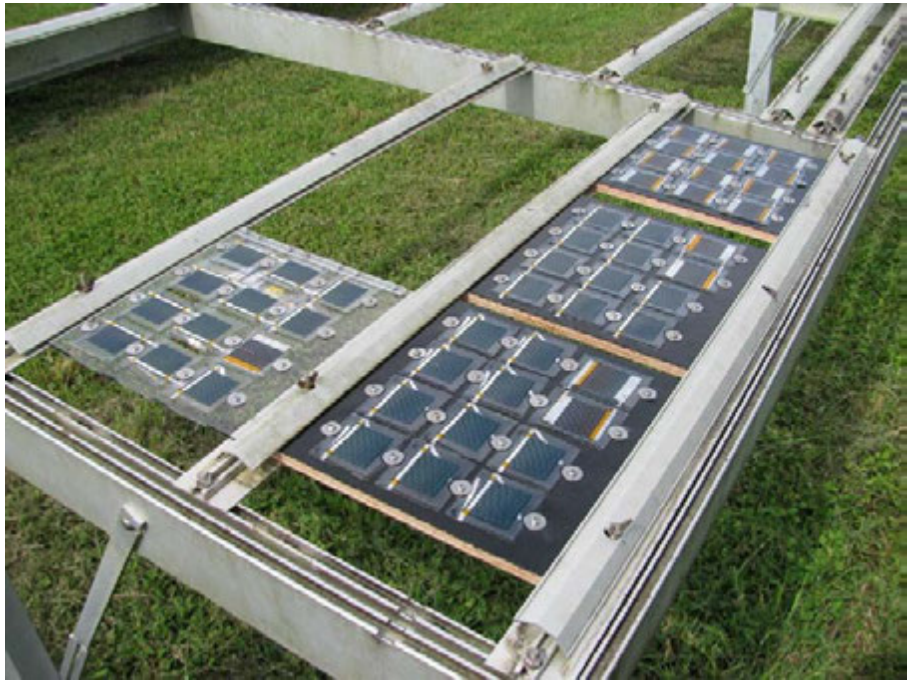
Accelerated Testing

- Nonlinear relationship
- No simple scaling
- Depends on details of kinetics and package



FL, AZ Testing

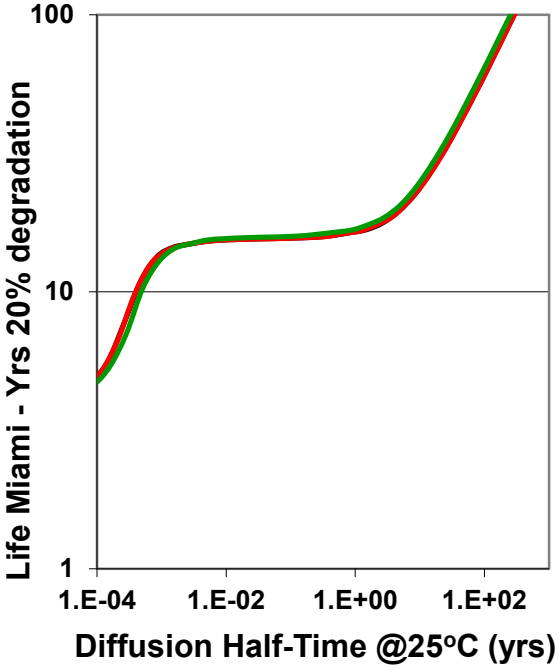
	Calc P_{max} change	Measured P_{max} change
Phoenix ECA_1	-0.1%	-1% +-2%
Miami ECA_1	-0.5%	-1% +-2%
Miami ECA_0	-4.1%	-5% +-2%

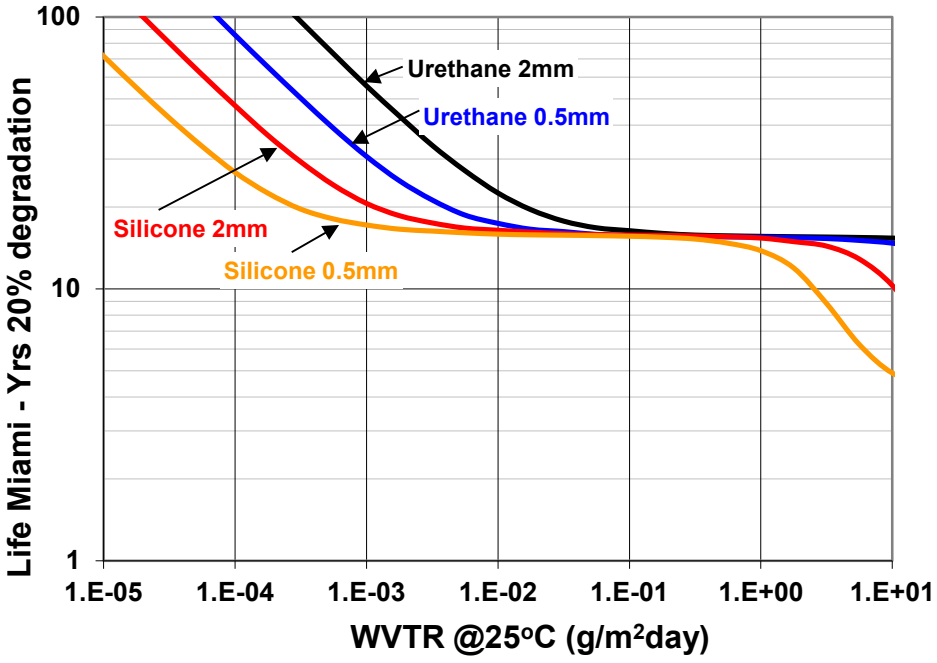


Results as expected after 3 months

- ITO/ECA_1 no measureable degradation
- ITO/ECA_0 ~ 5% down as expected

Encapsulant Effect



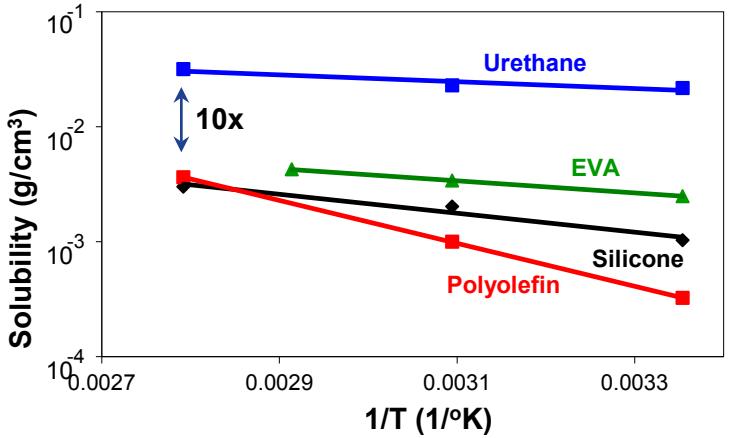


$$t_c = \frac{L_E S_E}{WVTR_{\max}}$$

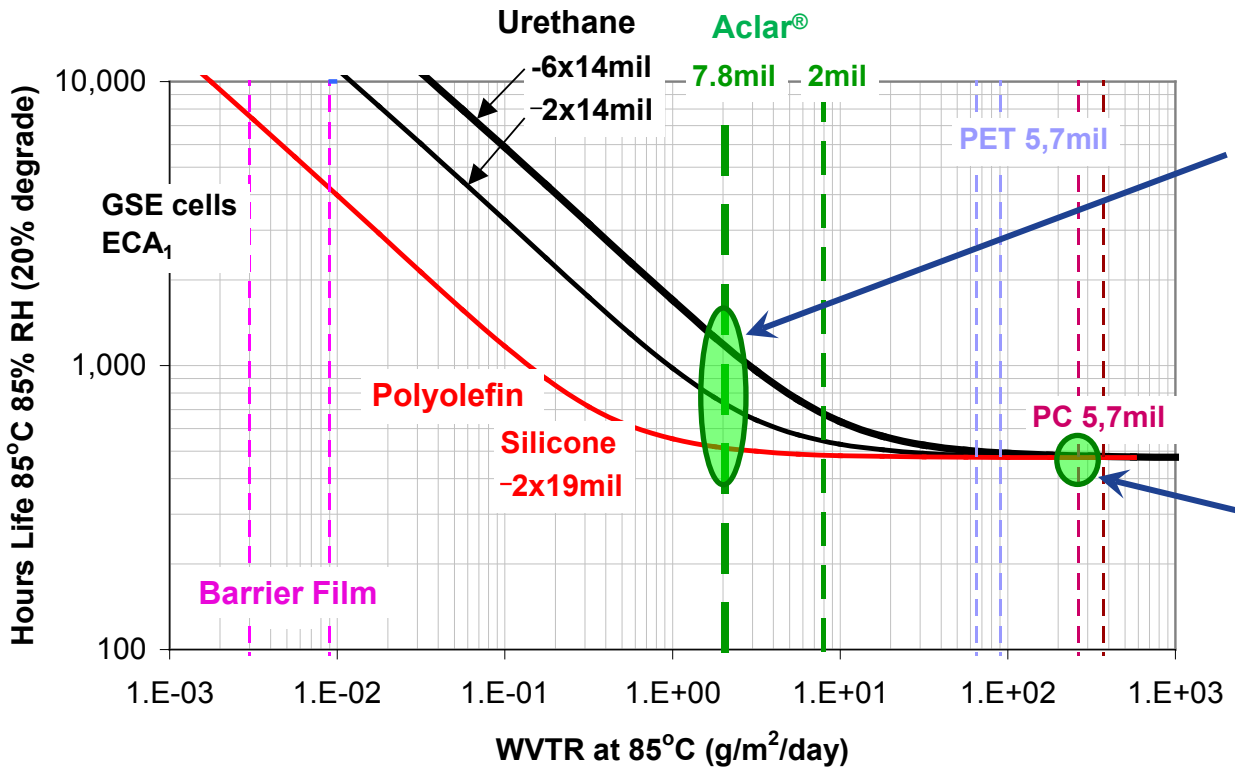
$$\frac{C_E}{S_E} = RH\left[1 - e^{\left(-t/t_c\right)}\right]$$

- Low solubility encapsulants become saturated faster => BAD!!

Encapsulant Experimental Plan (85°C, 85%RH)



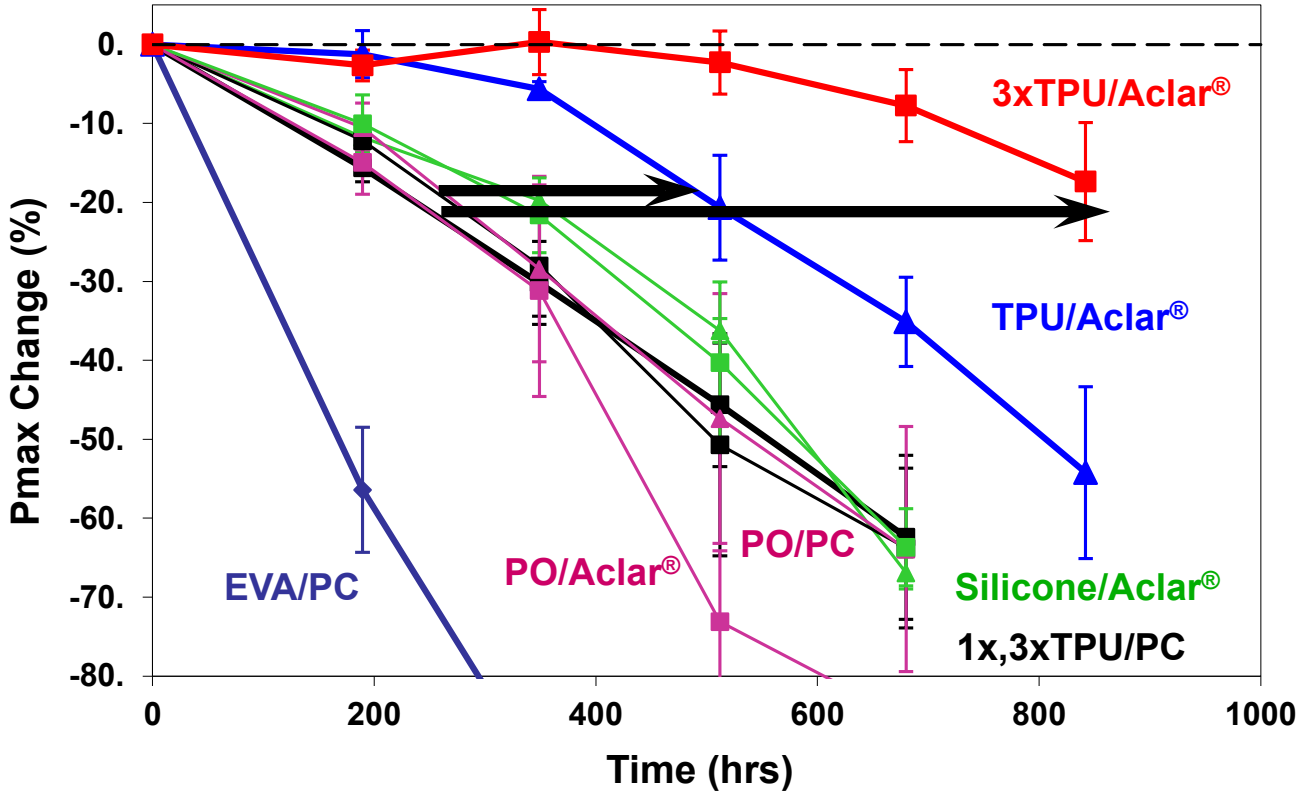
Material		Thickness (mm)	Solubility @85C g/cm³	$t_{1/2}$ Hrs @85C
Encapsulant	Urethane	0.355	3.0E-02	89
	Urethane	1.065	3.0E-02	268
	Silicone	0.480	3.1E-03	12
	Polyolefin	0.400	3.6E-03	12
Barrier	Aclar®	0.307	WVTR @85C g/m²day 2.0	



Thick, high S_E encapsulants better

All encapsulants the same

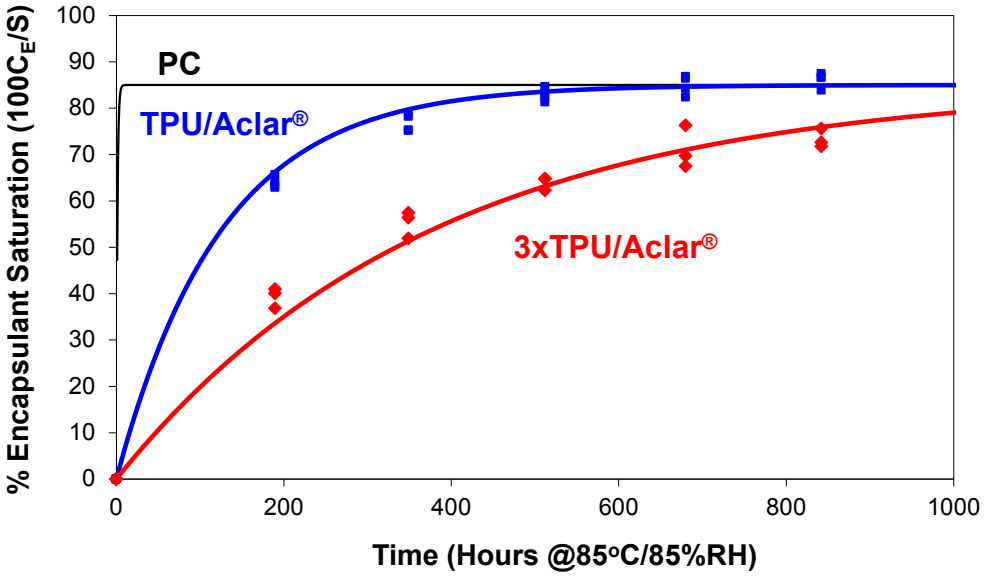
Encapsulant Confirmation Experiment



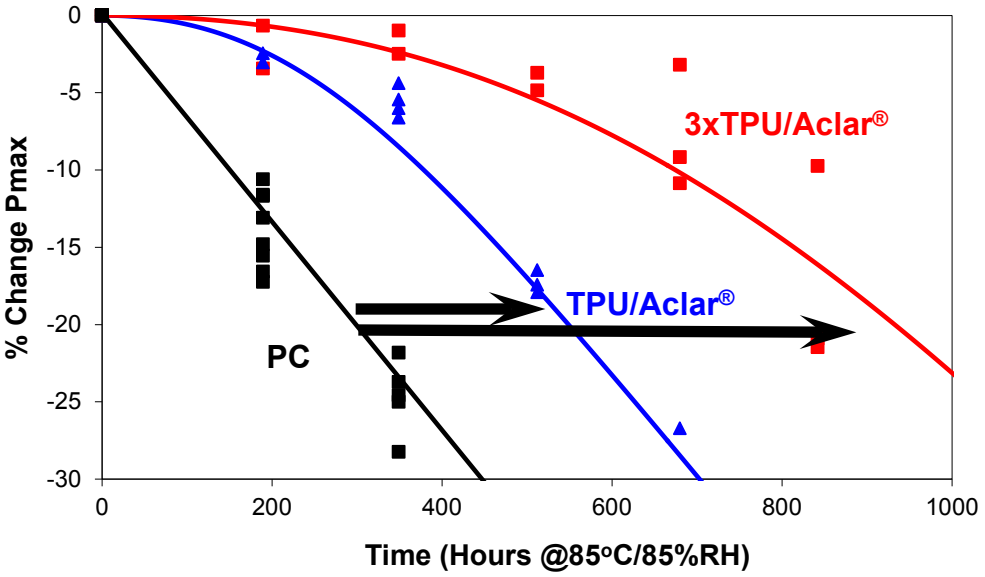
- EVA outlier – unusually fast degradation
- Urethane (TPU), silicone, polyolefin same, latter two even with Aclar®, as expected
- Barrier (Aclar®) makes no difference for silicone & polyolefin, as expected
- Barrier (Aclar®) improves TPU life, especially thicker, as expected

Comparison of Experiment & Model

Saturation



Degradation



Conclusions

1. Life model and accelerated test scaling developed
   – ***Relative humidity*** and ***% saturation*** of encapsulant are key
2. Moisture sensitivity of CIGS almost independent of encapsulant type
3. Module lifetime longer for ***thick encapsulants*** with ***high*** water solubility
4. AZO vs ITO CIGS degradation kinetics quantified ~25X
5. ECA can also be a strong factor in degradation
6. Diffusion-controlled: Life ~ $(t_c/R_D)^{1/2}$ ~ (diffusion-time*degrade-time)$^{1/2}$
7. Significant moisture barriers required for 20 yr life – even for ITO
8. Acceleration factor for damp heat smaller than assumed, highly nonlinear!
9. Methodology can predict life for any moisture-sensitive module (once kinetic constants are measured)



Acknowledgements

Mike Kempe	NREL
Jeff Britt	Global Solar Energy
Steve Hegedus	IEC

This work was supported by:

U.S. Department of Energy Award DE-FC36-07GO17045

GE Global Research

GE Energy



Systems Approach to High Performance CIGS Material Set Including Flex Ultra-Moisture Barrier and Hi-Temp MLI Substrate

K. W. Leffew, S. Boussaad, D. Reardon, H. Tate, N. Glassmaker, D. Dean, G. Nunes, C. Q. Zhao, S. L. Samuels, J. Schneider, P. Carcia, R. Mclean
DuPont Research & Development
Feb. 17, 2011



Flexible CIGS modules can accelerate advancement to grid parity

Copper Indium Gallium Diselenide (CIGS) has the highest efficiency of all thin-film PV technologies

- 19.9% cell in the lab (NREL)
- 13% in a module

Flexible modules can drive lower system cost

- Lower manufacturing cost
  - — Potential for high productivity with roll-to-roll processing
- Lower installation cost
  - — Lighter modules, no frames

However, moisture accelerates CIGS cell degradation



A flexible, transparent ultra barrier is needed

This presentation does not contain any proprietary or confidential information

DuPont's Growing Portfolio of Solutions for the PV Industry

A Frontsheet Materials
Lighter and less fragile than glass, durable DuPont frontsheet materials deliver high performance to help increase power output and offer more design options for BIPV applications.

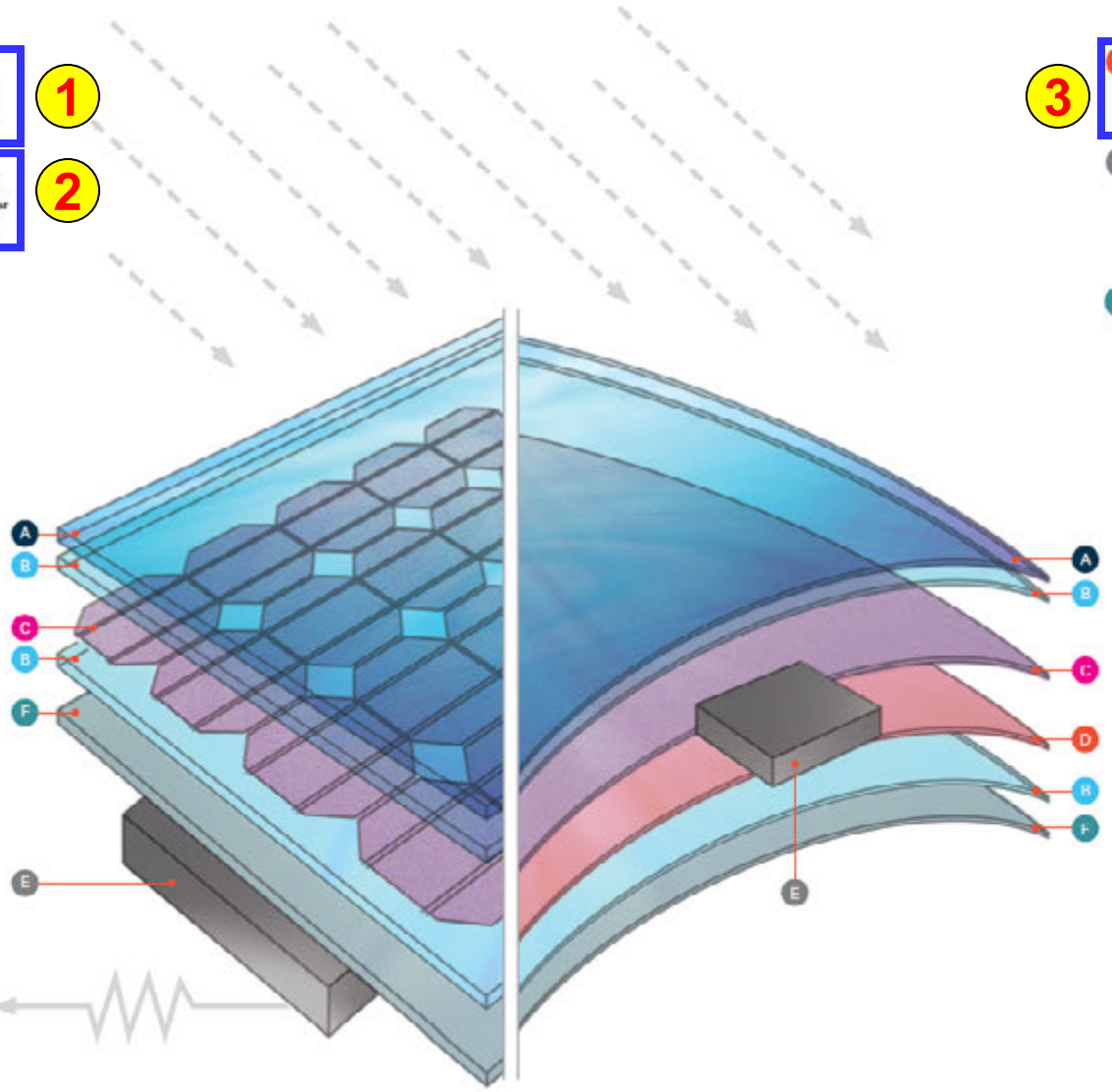
1

D Photovoltaic Encapsulants
With a broad portfolio of innovative solutions, DuPont encapsulation materials deliver long-term protection for the most sensitive portions of photovoltaic modules.

2

C Photovoltaic Metallizations
DuPont is raising the bar for PV cell metallizations. With a broad range of characteristics, these high performance metallization compositions help lower the overall cost per installed watt.

THE DUPONT PORTFOLIO
OF INNOVATIVE MATERIALS
FOR CRYSTALLINE SILICON
PHOTOVOLTAIC MODULES



energy for a thriving world™

3

D Thin Film Substrates
DuPont substrate materials deliver robust processing for both CIGS and a-Si modules with high temperature tolerances and low CTE capacity to minimize stress and increase productivity.

E Junction Box and Structural Component Materials
With a broad range of UL recognized solutions, DuPont materials can help increase safety, eliminate corrosion and provide long lasting performance for junction boxes and structural components in harsh environments.

F Backsheet Materials
For superior, long lasting backsheet protection against the elements, choose the products industry leaders trust.

THE DUPONT PORTFOLIO
OF INNOVATIVE MATERIALS
FOR PHOTOVOLTAIC
THIN FILM MODULES

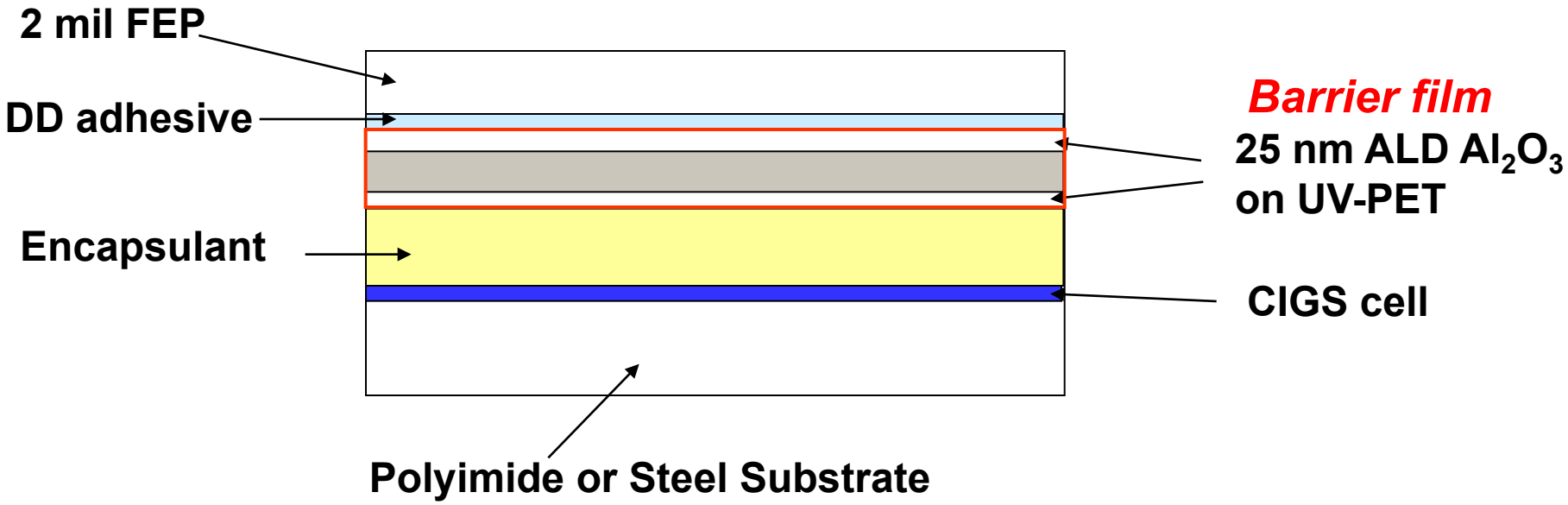
Sodium Metal for Poly-silicon Manufacturing
DuPont sodium metal enables alternative low cost manufacturing processes for poly-silicon.

Wet-Etch Additives for PV Manufacturing
DuPont fluorosurfactants provide unrivaled wetting aids in semiconductor texturing, offering etch control, reduced waste and improved cell efficiencies.

High Performance Parts
For improved solar cell manufacturing productivity, choose DuPont high performance parts that help increase throughput and equipment uptime.

This presentation does not contain any proprietary or confidential information

Frontsheet barrier/encapsulation of PV cell with Ultrabarrier:

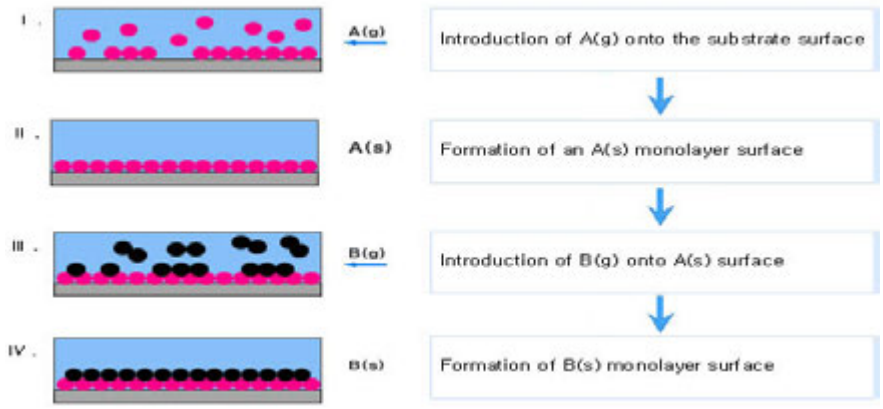


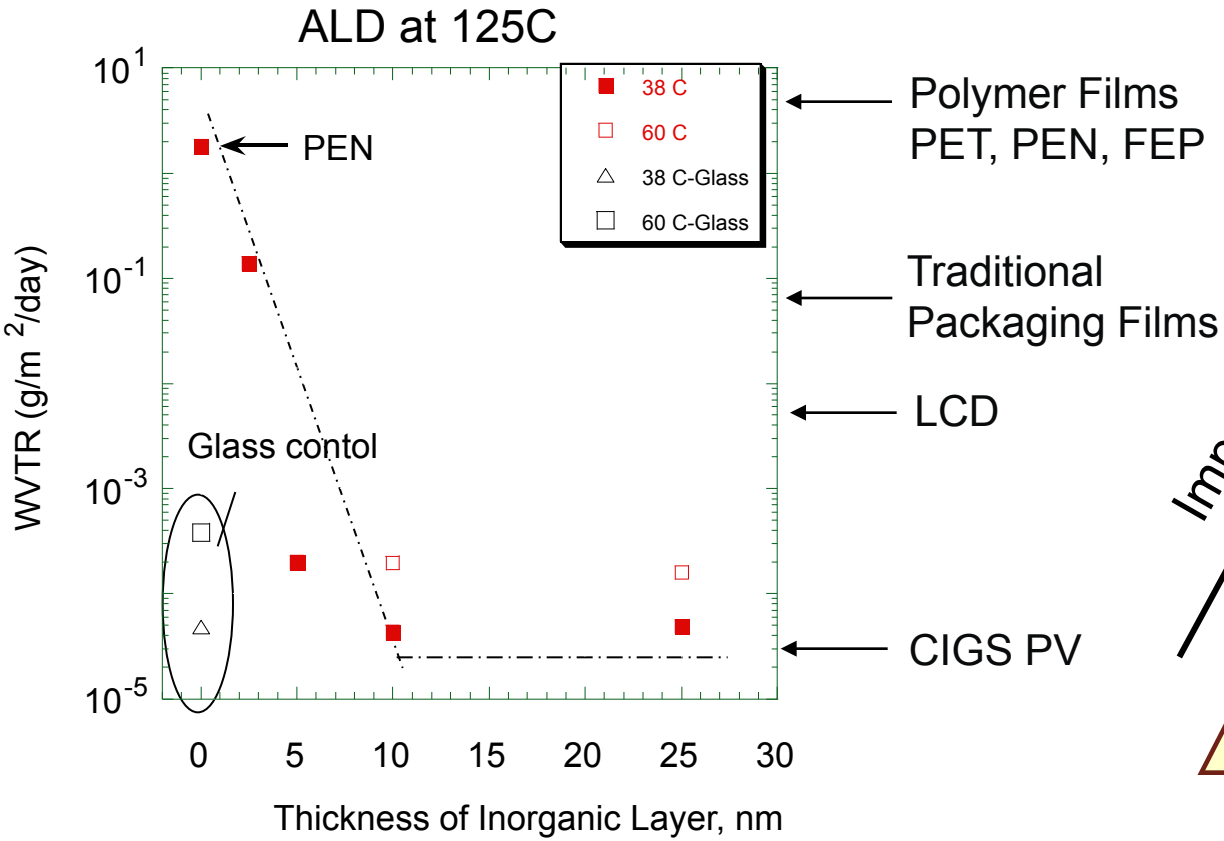
Performance Targets

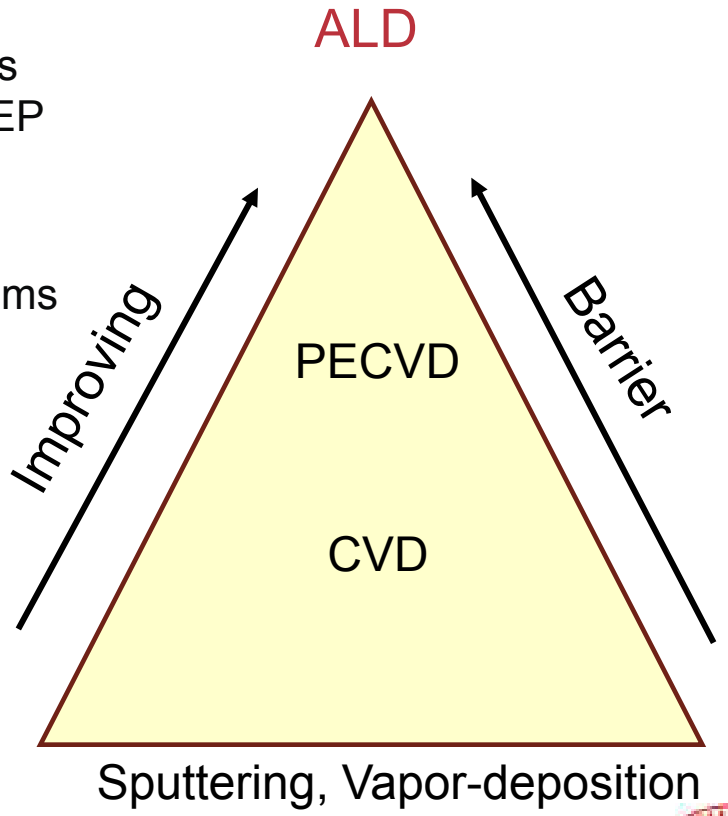
- Simple manufacturing process
- Compatible with plastics
- Barrier film that is transparent and flexible
- Water Vapor Transmission Rate (WVTR) < 10^{-4} $gH_2O/m^2/day$

Approach - Atomic Layer Deposition (ALD) on plastic

- Simple process
- Compatible with plastics
- Final film product is transparent and flexible
- WVTR < 10^{-4} $gH_2O/m^2/day$





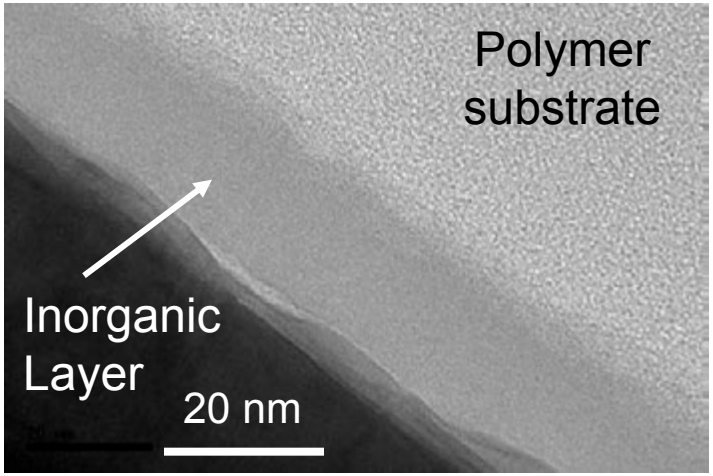


This presentation does not contain any proprietary or confidential information

ALD Can Provide a Uniform, Pinhole-free, Flexible Barrier Layer

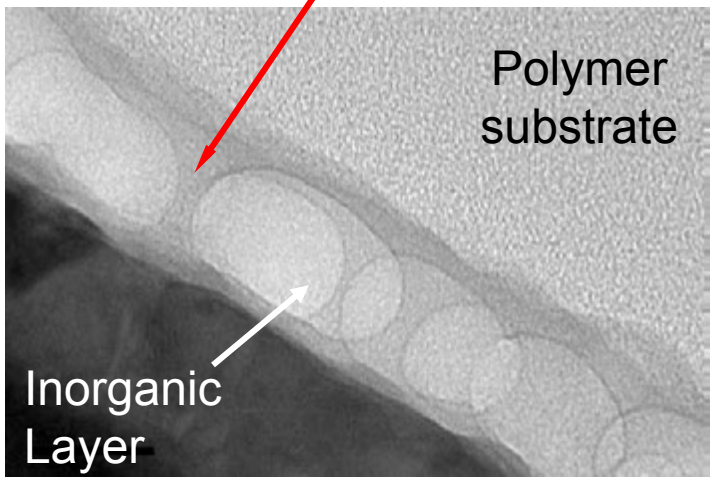
Transmission Electron Microscopy (TEM) images

ALD inorganic layer on polymer



Grain boundaries which can lead to water transmission

Vapor deposited inorganic layer on polymer

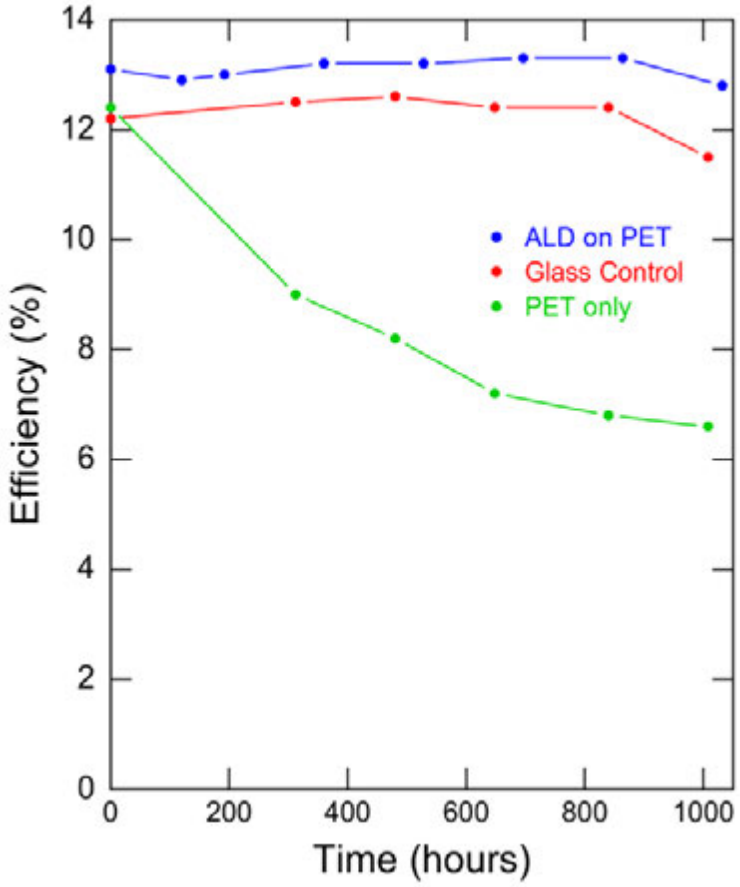


This presentation does not contain any proprietary or confidential information

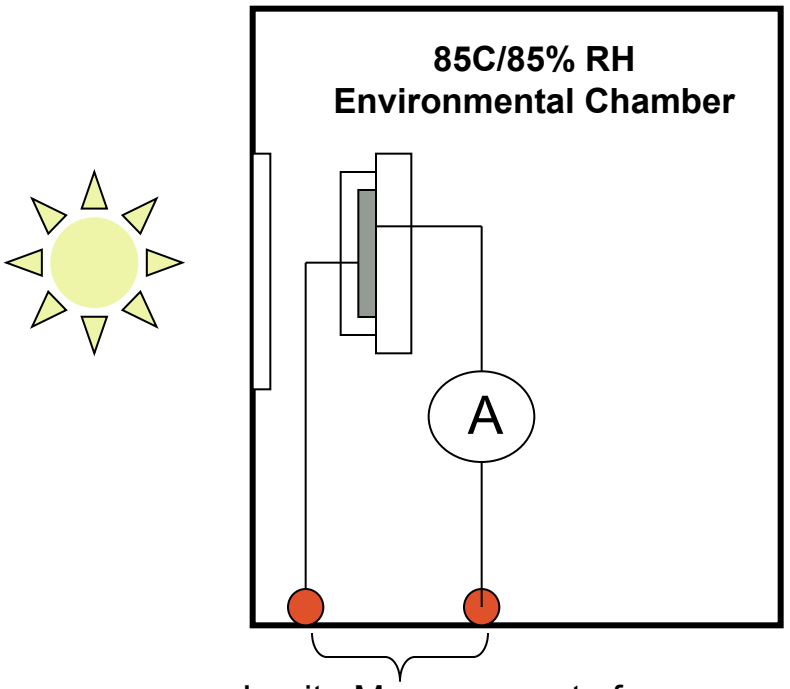
A Flexible UltraBarrier Layer Can Enable CIGS on Flex

- Our initial lab results indicated that ALD-on-plastic could effectively protect CIGS cell with accelerated aging performance comparable to glass
- Program objective now is to demonstrate manufacturing feasibility of ALD-on-plastic with water vapor transmission rate below 10^{-4} g/m^2/day at "low" cost

85C/85 % RH with illumination for 1032 hr

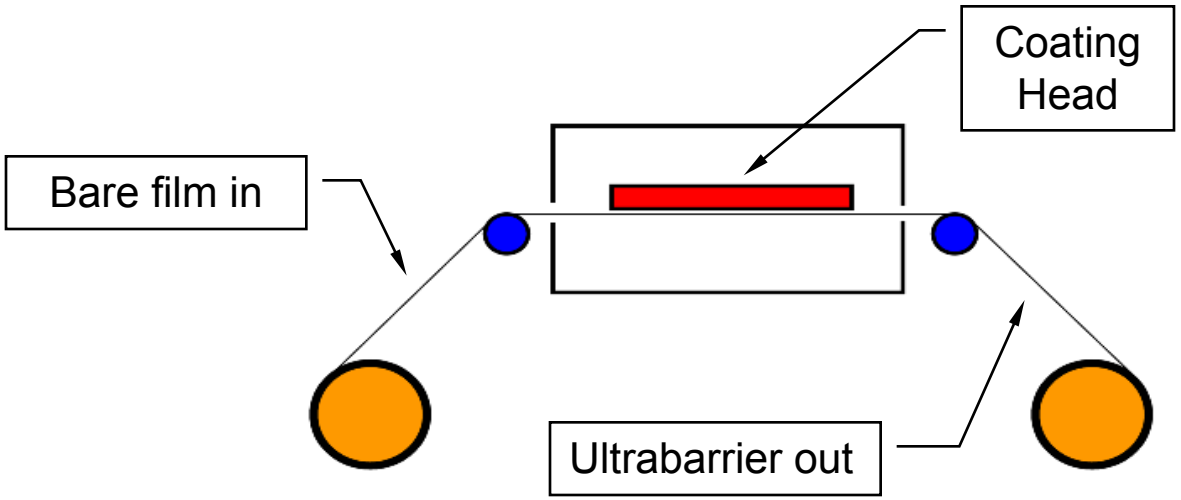


Measured at partner institute

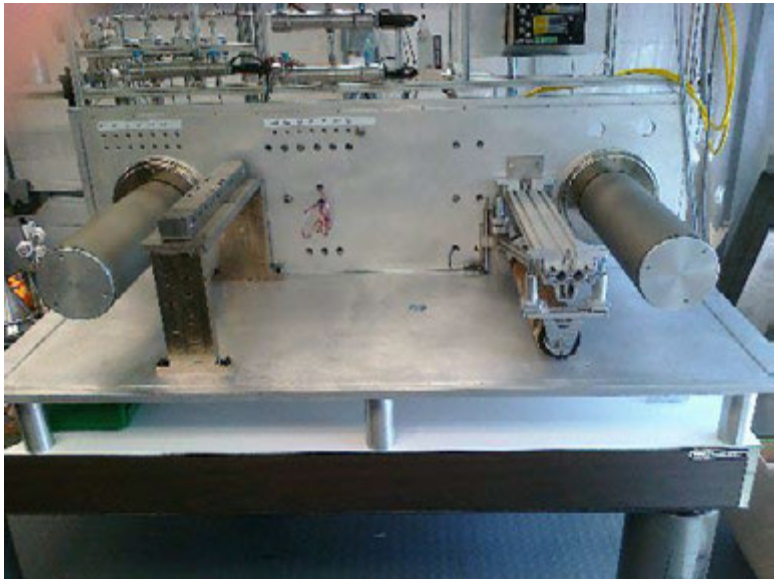


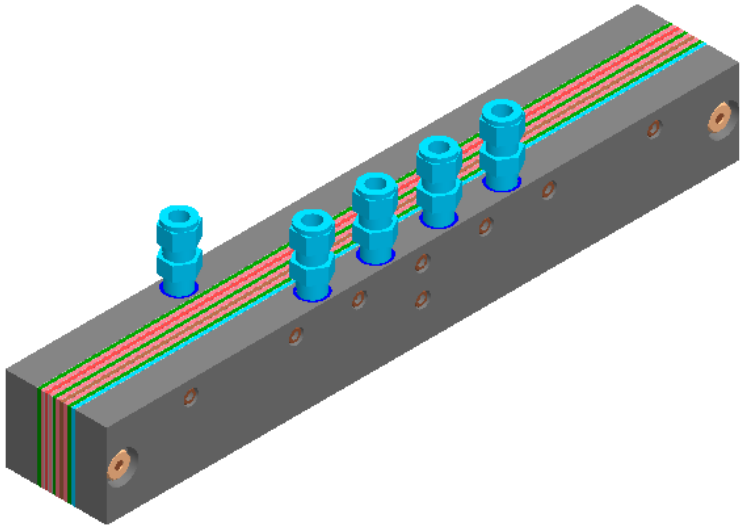
This presentation does not contain any proprietary or confidential information

Building prototype roll-to-roll equipment for ALD



- Prototype will demonstrate high throughput and low cost feasibility
- Funded in part by DOE





This presentation does not contain any proprietary or confidential information

Results – Modeling & Design

Proprietary coating head enables roll to roll manufacturing

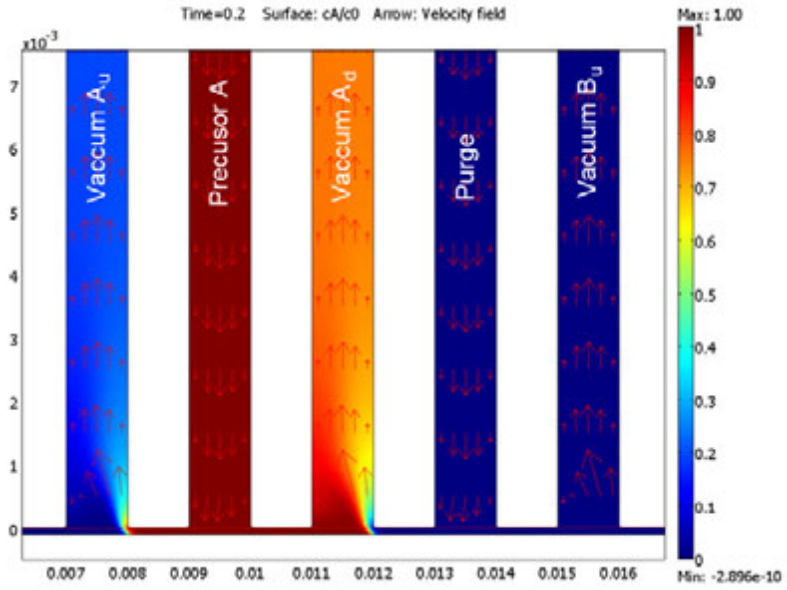
- Design confirmed by computational fluid dynamics & numerical modeling

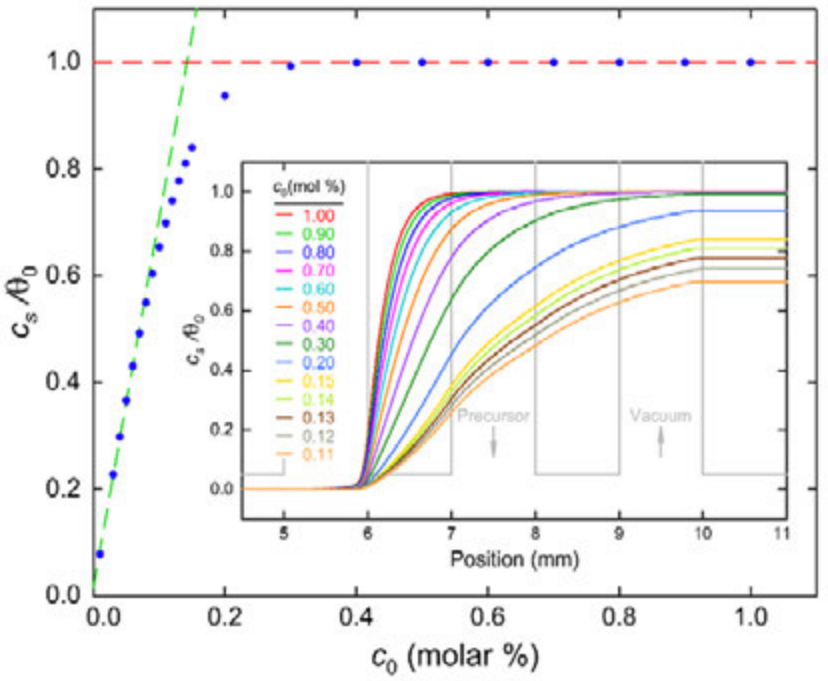
Model indicates feasibility of 1 m/sec web speed

- Initial target is 0.1 m/sec
- Process self-stabilizes in ~0.1 sec
- Negligible cross-talk between precursors

Optimization from model

- Shown process stable against expected variations in head to web gap
- Explored materials efficiency: precursor concentration can be reduced to 0.4%





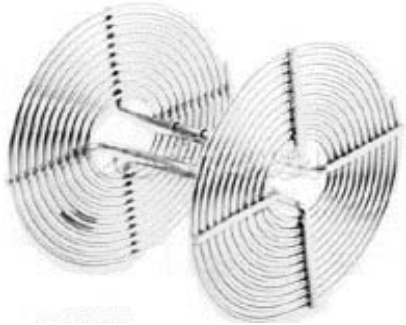
Take-home message: Modeling predicts feasibility

This presentation does not contain any proprietary or confidential information

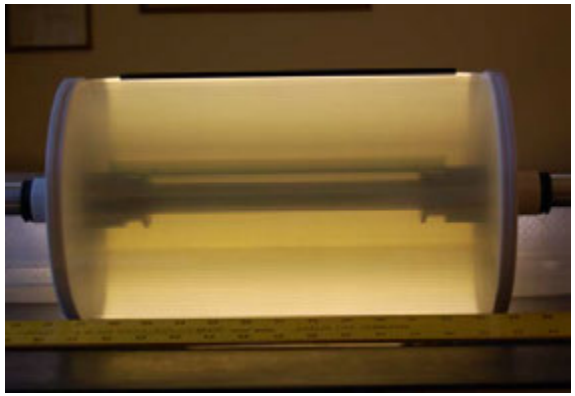
Batch ALD Coating Process

Cassette in batch chamber approach

- Technical challenges:
  - Cassette fabrication
  - Film loading/unloading
  - Process control
  - Scale-up plan
  - Batch ALD process modeling



Empty Cassette



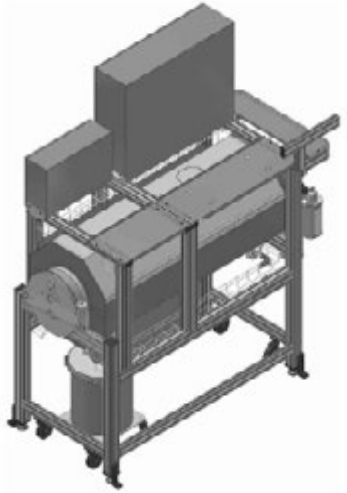
Cassette with UB Film Loaded

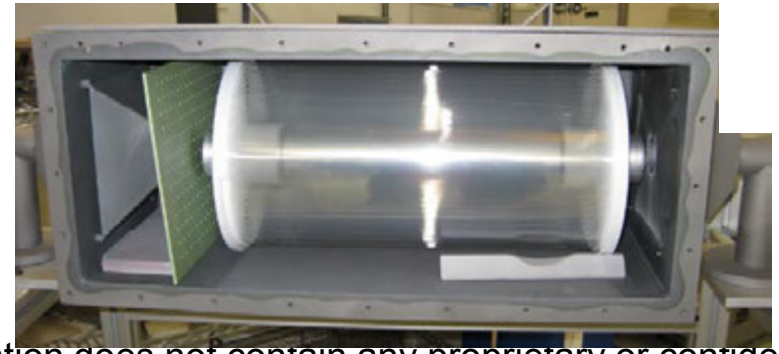
A number of cassettes (polycarbonate and aluminum metal) were fabricated and used in about 500 ALD batch depositions resulting in films with WVTR consistently below $5x10^{-4}$ (detection limit)

Detailed economic modeling concludes that R2R likely will still be the preferred commercial process

Batch process has been key to product validation and market development while continuous process is developed

VIEWS OF THE TOOL FRAME





Cassette inside ALD Batch Chamber

This presentation does not contain any proprietary or confidential information

Remaining Technical Hurdles for Ultrabarrier Frontsheet Development

- Optimization of frontsheet lamination process that fully retains the barrier performance of the barrier film
- WVTR measurement capability that will allow for accelerated process development and resolution in targeted product performance range ($<10^{-6}$ g/m^2/day)
- On-line measurement capability to predict WVTR and/or product-by-process control strategy to ensure performance of film over large area
- Confirmation of model that relates frontsheet WVTR to CIGS module lifetime
- Demonstration of continuous ALD process prototype to generate basic data for pilot and/or commercial-scale

This presentation does not contain any proprietary or confidential information

Summary and Next Steps for Ultrabarrier Frontsheet

- Transparent, flexible ALD-coated polymer protects CIGS cells against moisture and degradation
- Batch ALD process operated at scale that supports market and product development consistently generates film with WVTR < $5*10^{-4}$ $g/m^2/day$
- Modeling predicts that ALD-on-plastic can be produced at high throughput
- Prototype roll-to-roll equipment fabrication complete and ALD coating trials underway
- Partnering with academic, industrial, market and government partners
- Making progress against plan for further scale-up

  (pilot plant/commercial)

This presentation does not contain any proprietary or confidential information

Moisture ingress can affect module lifetime

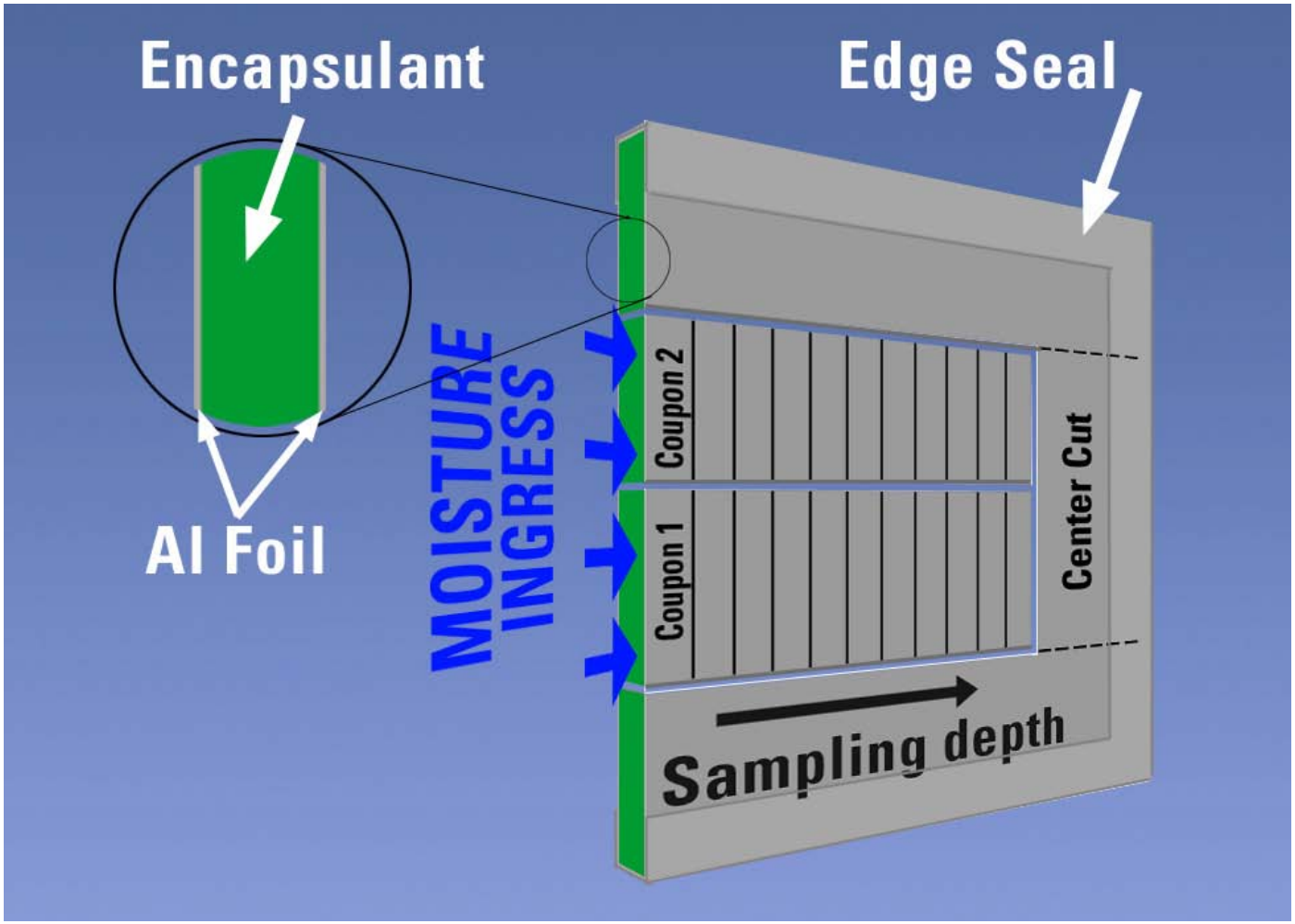
• Water permeability and equilibrium moisture content in the encapsulant may degrade module performance by metal corrosion or other adverse interactions, e.g. TCO degradation.

• Various other defects, such as delamination, bubble formation and edge cloud, are also known to be influenced by the presence of moisture.

• Using accepted methods to measure moisture ingress, we have quantified performance of commercial encapsulants and are developing new ones for moisture-sensitive technologies.

This presentation does not contain any proprietary or confidential information

Measuring moisture ingress via RH sensor method ASTM D7191

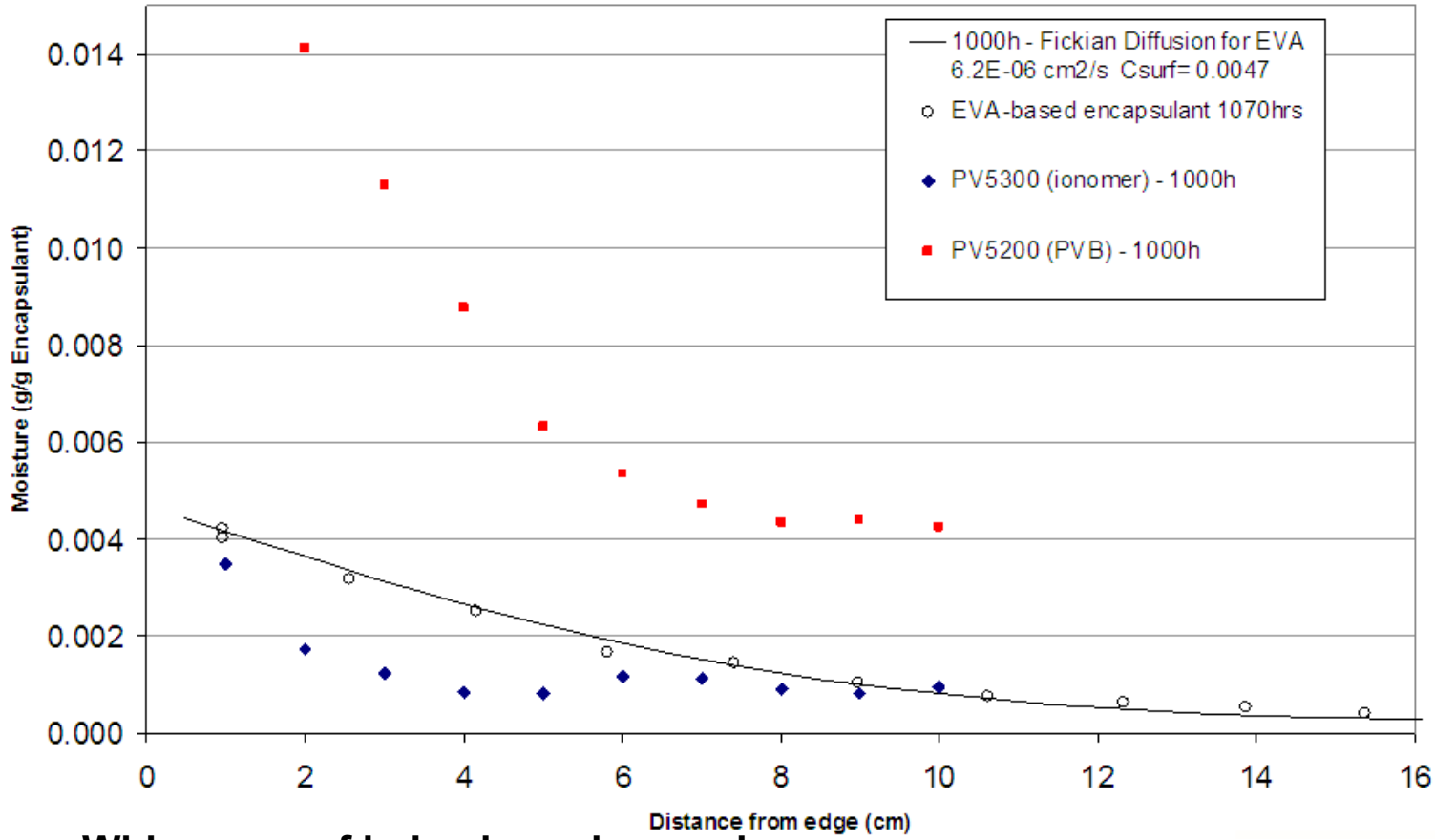


"One dimensional" foil-clad moisture intrusion specimens are laminated as shown.

After DH exposure, coupons are die cut for each measurement. Coupons are cut into thin strips & placed in vial for moisture analysis.

This presentation does not contain any proprietary or confidential information

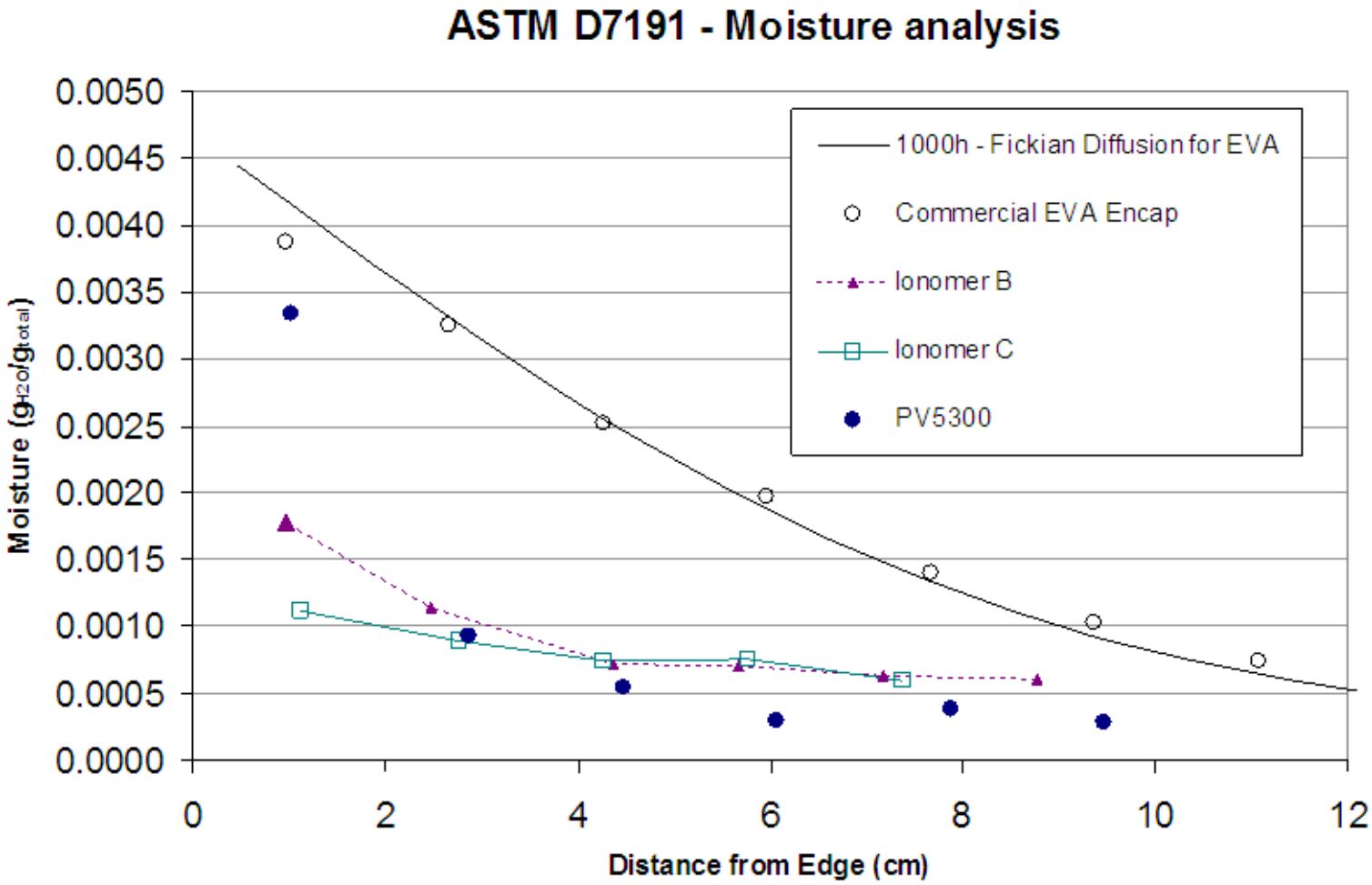
Moisture Ingress to Commercial Encapsulants after 1000hr DH exposure



- **Wide range of behaviors observed**
- **Equilibrium moisture content (at the exposed edge) and moisture transport rate through PVB is much greater than EVA**
- **Ionomer has lower rate of moisture transport rate than EVA**

This presentation does not contain any proprietary or confidential information

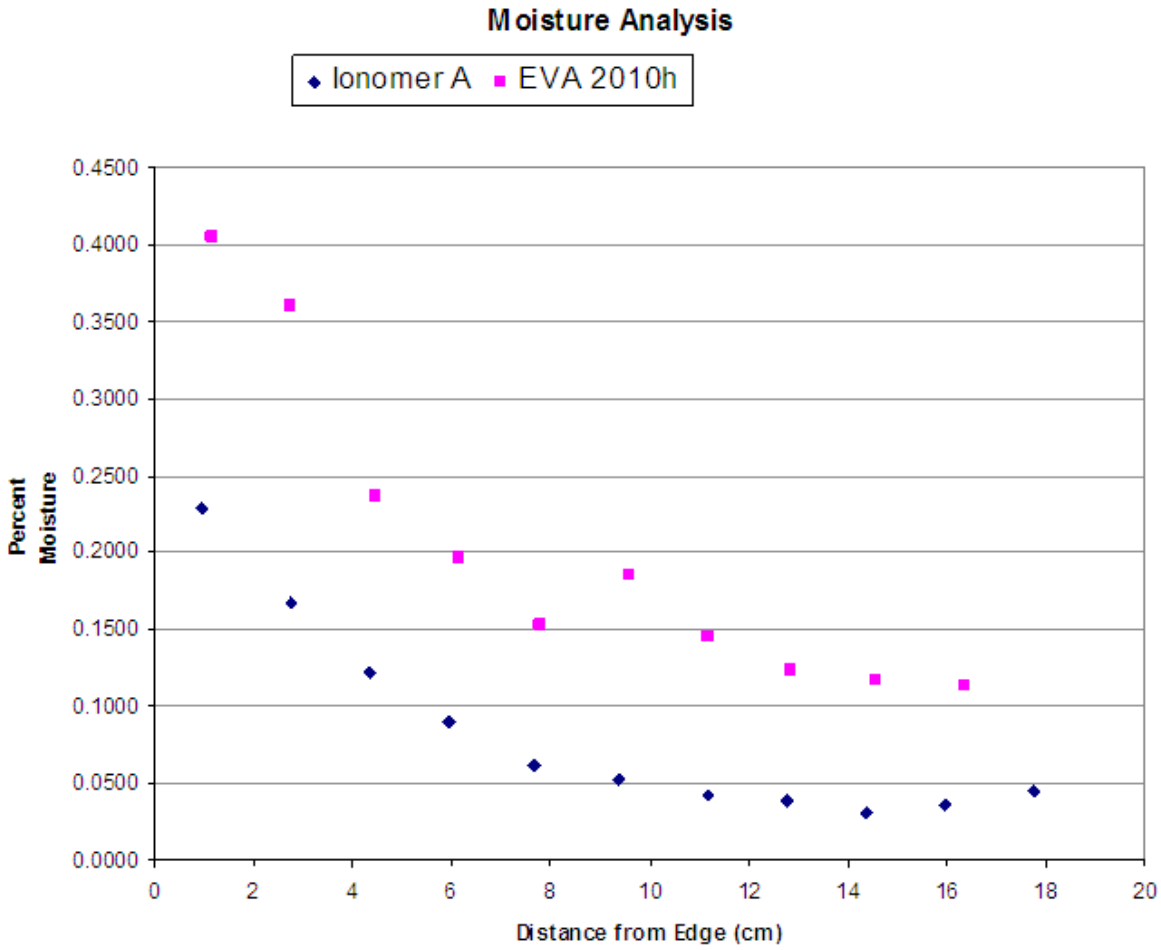
Moisture Ingress of EVA and Developmental Ionomer Encapsulants after 1000 hr DH



- **Encapsulants with even lower equilibrium moisture content (exposed edge) are being developed for moisture sensitive PV technologies**

This presentation does not contain any proprietary or confidential information

Moisture Ingress of EVA and Developmental Ionomer Encapsulants after 2000 hr DH



- **Even after 2000 hr DH exposure, developmental encapsulants retain desireably low moisture ingress characteristics.**

This presentation does not contain any proprietary or confidential information

Summary and Next Steps for CIGS encapsulant

• A methodology for evaluating moisture transport through encapsulants has been developed.

• Encapsulants with reduced equilibrium moisture content and moisture transport rates have been developed.

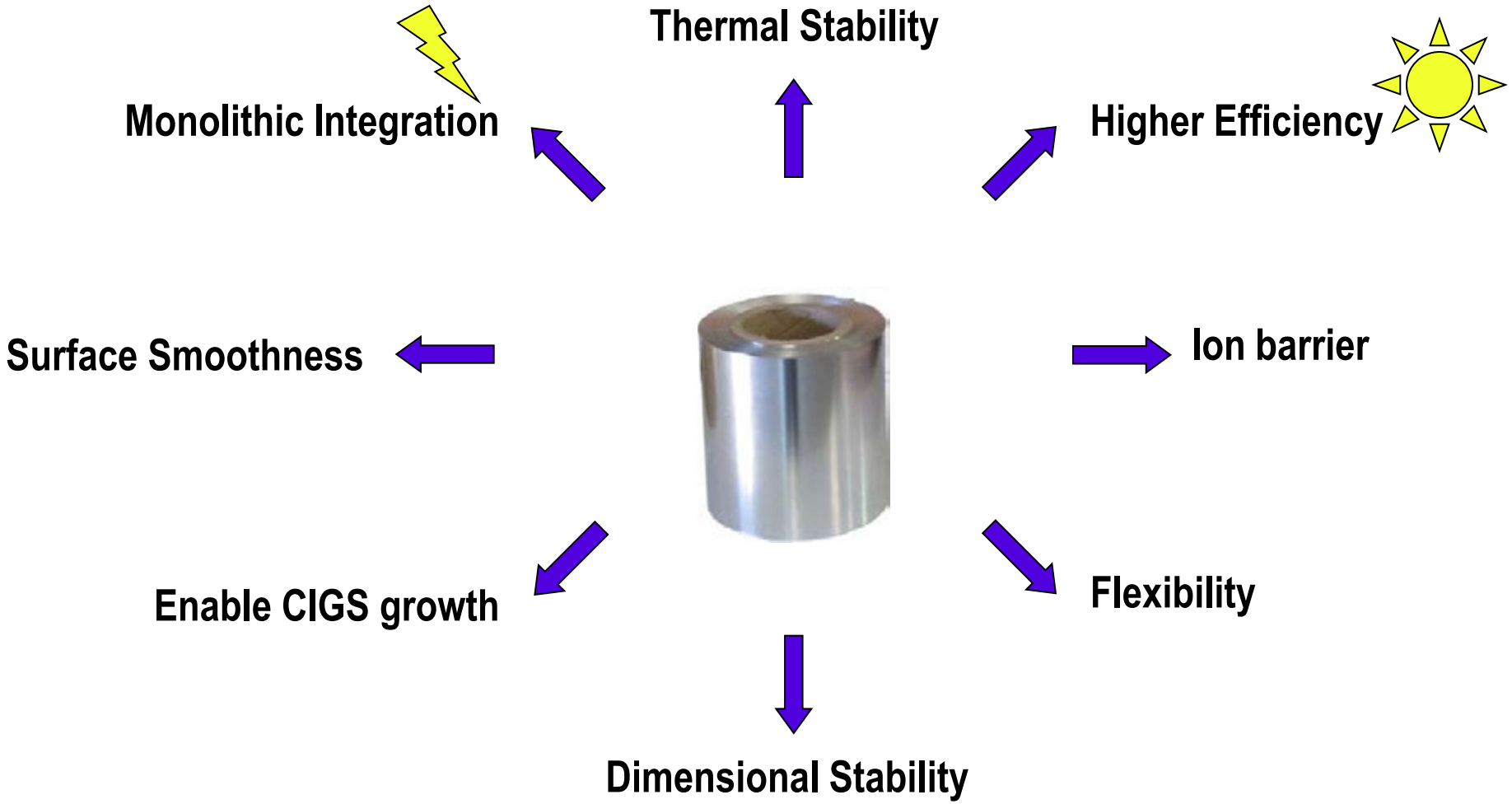
• A new ionomer encapsulant with reduced moisture sensitivity and transport has been scaled up and is being evaluated in thin film applications.

• Continue to develop and introduce encapsulants with enhanced properties needed for future generation PV module designs, e.g.

- Transmission
- Environmental stability (UV, temperature, moisture)
- Adhesion
- Moisture Transport
- Other interactions with module components

This presentation does not contain any proprietary or confidential information

Glass Coated Stainless Steel Characteristics



This presentation does not contain any proprietary or confidential information

Adding Functionality to Stainless steel

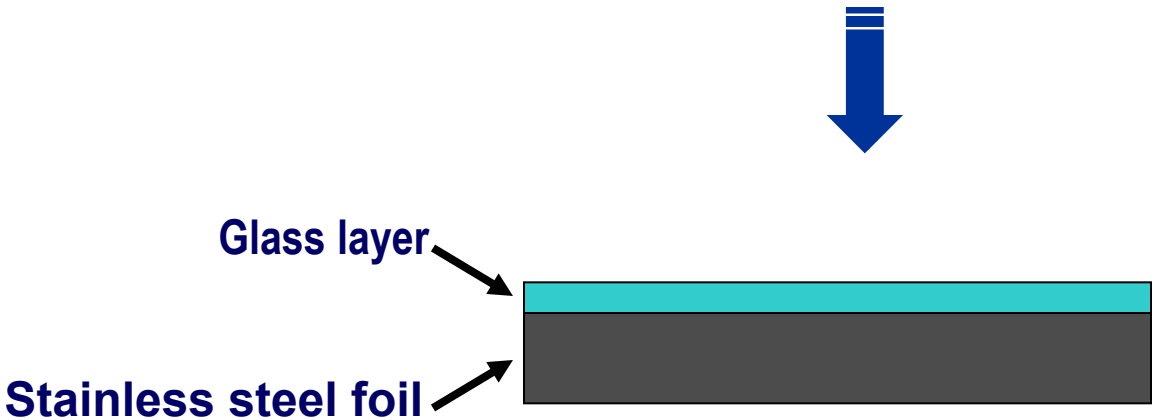
Stainless Steel

- Roll to roll processing
- High tensile strength
- High tear strength
- High temperature capability
- Currently used in manufacturing
- Electrically conducting

+

Glass

- Solution deposition
- Film thickness from up to 5μm
- Dielectric strength
- Ion barrier
- Enable sodium doping
- Smooth surface



This presentation does not contain any proprietary or confidential information

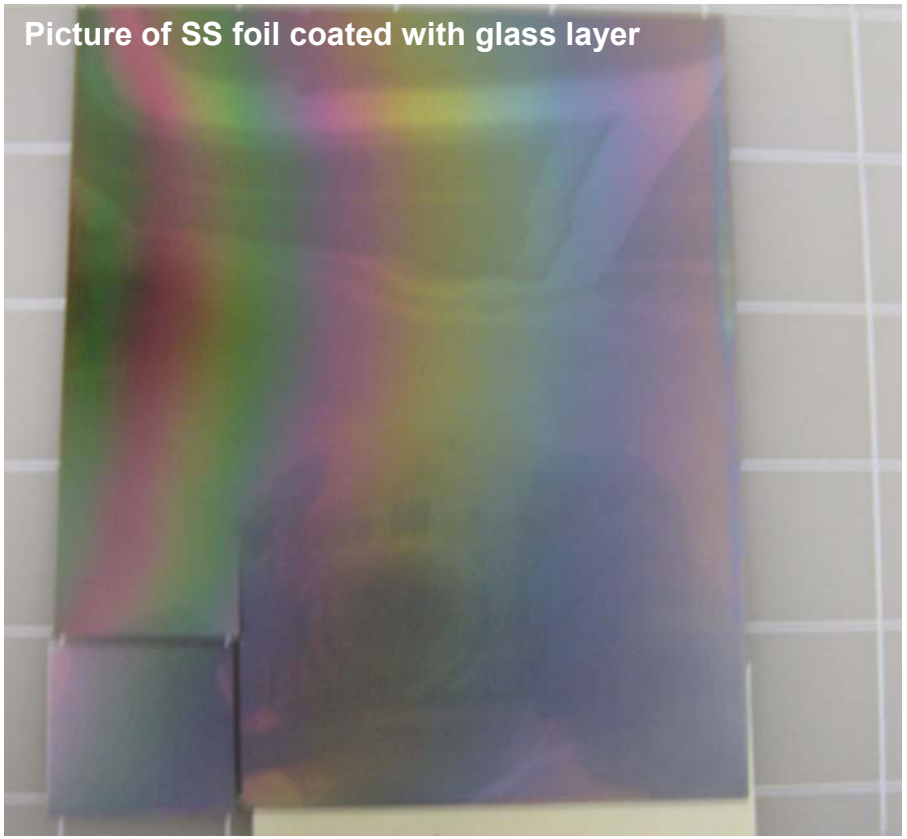
Coating Stainless Steel foil with Thin Glass Layer

Substrate:
2mil SS430

Solution:
Tunable composition in aliphatic alcohol

Film:
Drying

Firing



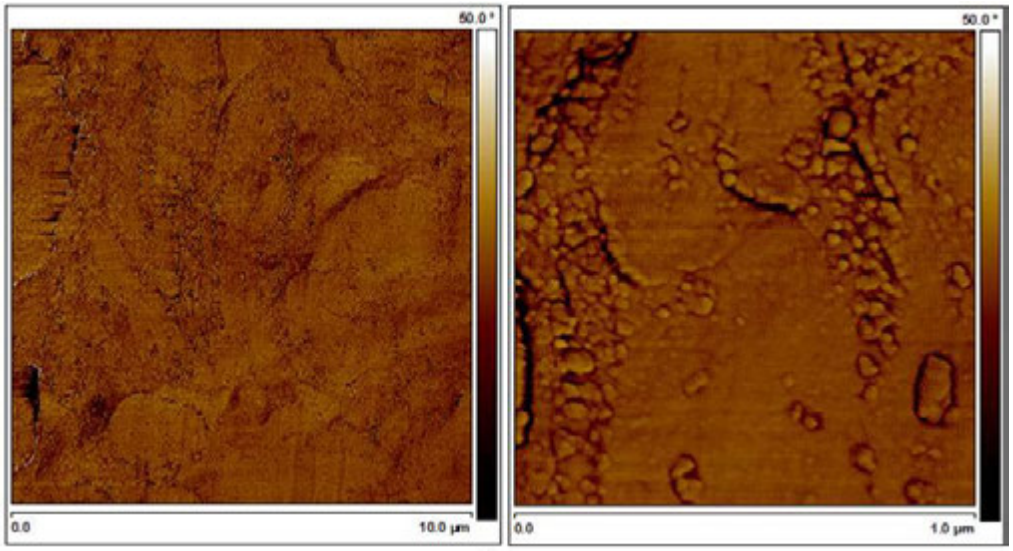
Stainless steel foil coated with 0.5μm glass layer

This presentation does not contain any proprietary or confidential information

Impact of glass coating on roughness of stainless steel

AFM – Surface topology

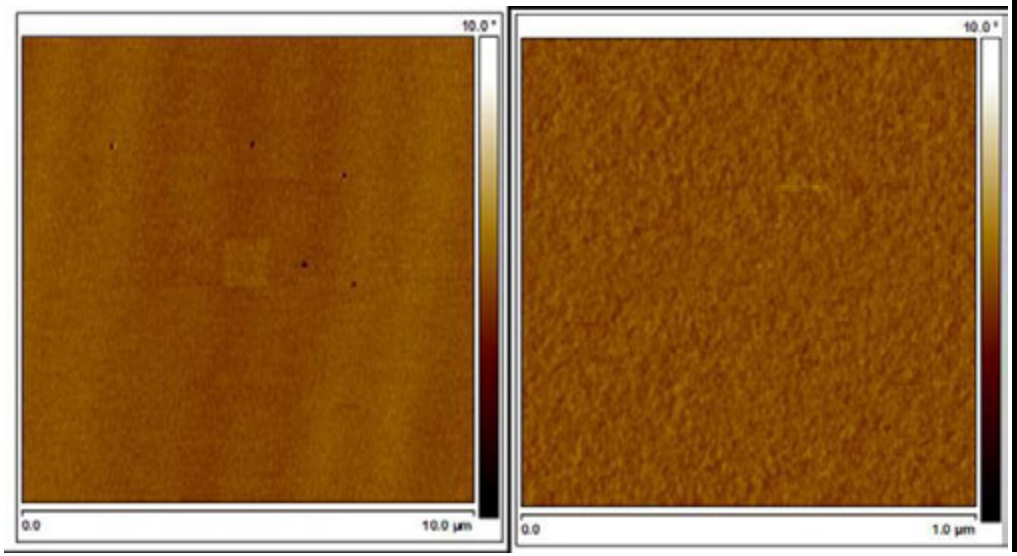
Stainless Steel



SS 2 mil	10 x10 (um^2)	1 x 1 (um^2)
Location 1 (nm)	81.0	6.6
Location 2 (nm)	87.0	8.0
Location 3 (nm)	91.8	5.6
Average (nm)	86.4	6.7

Avg. Ra =86.4nm

Glass coated stainless steel



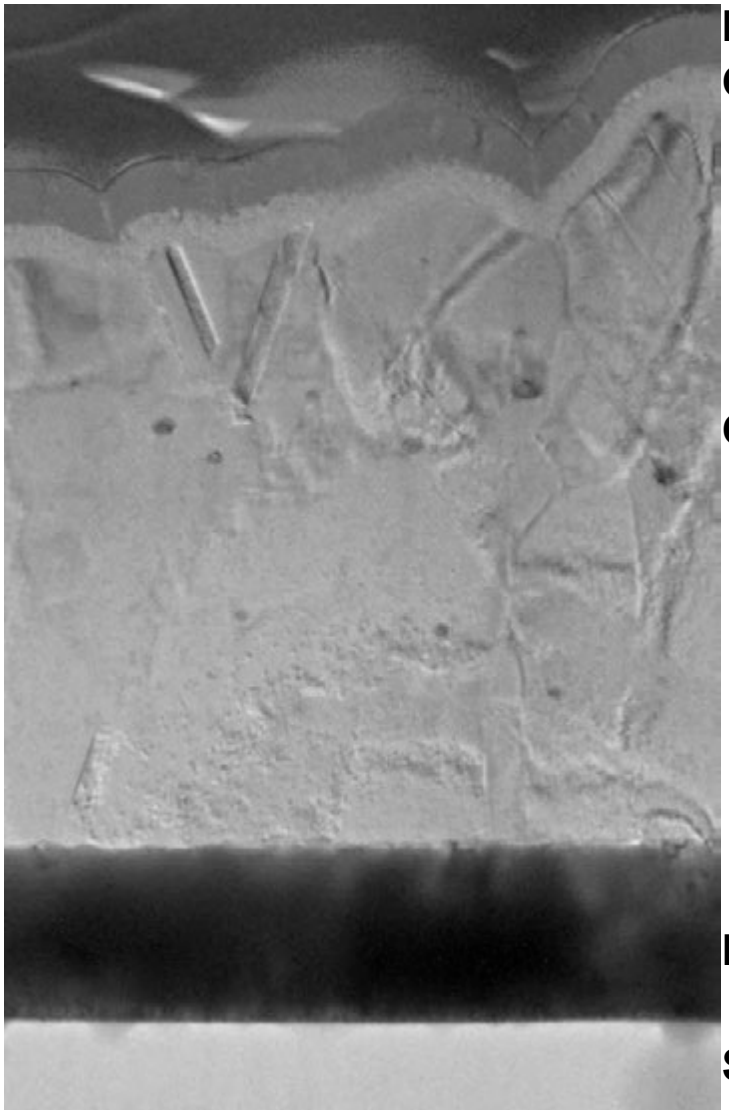
Coated SS	10 x10 (um^2)	1 x 1 (um^2)
Location 1 (nm)	6.9	0.19
Location 2 (nm)	6.3	0.13
Location 3 (nm)	6.6	0.16
Average (nm)	6.6	0.16

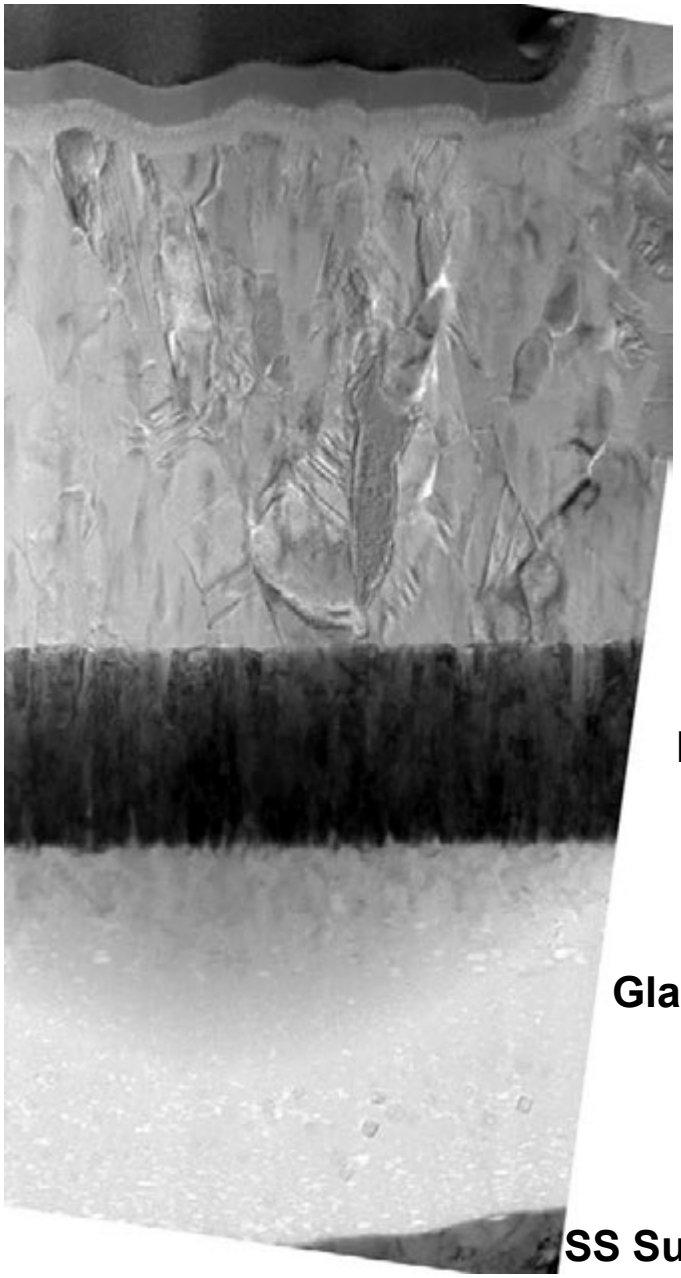
Avg. Ra =6.6nm

Glass layer reduced surface roughness of stainless steel

This presentation does not contain any proprietary or confidential information

TEM cross-section by FIB: Gen#3 vs. Soda lime glass



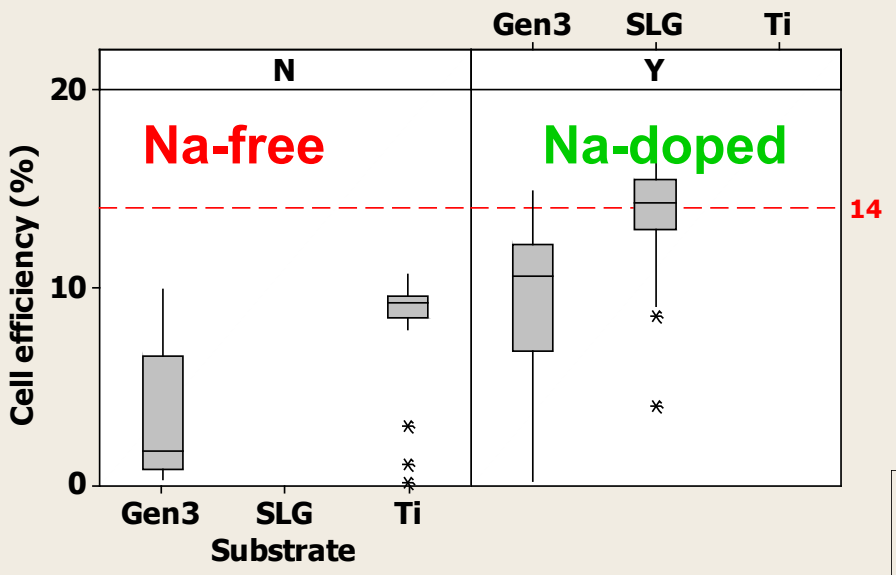


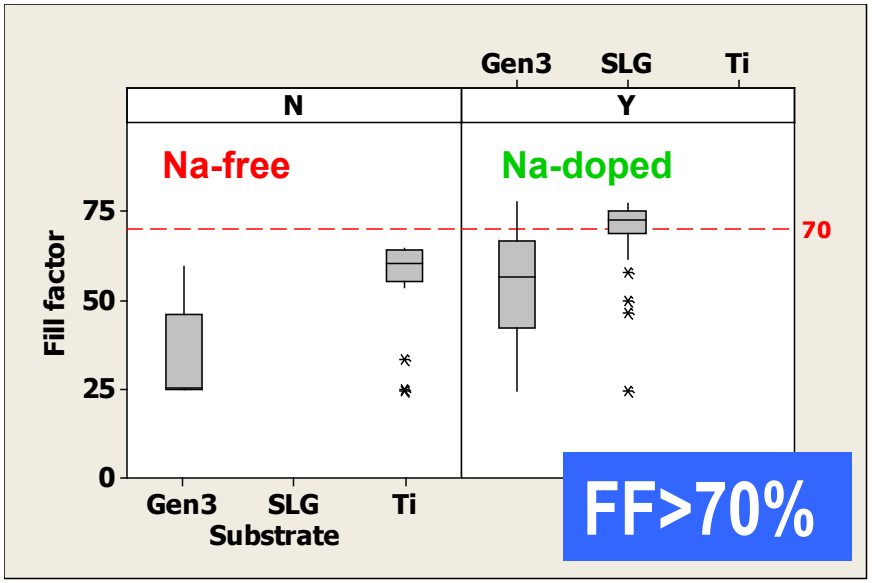
This presentation does not contain any proprietary or confidential information

†TEM: Transmission Electron Microscopy, FIB: Focused Ion Beam

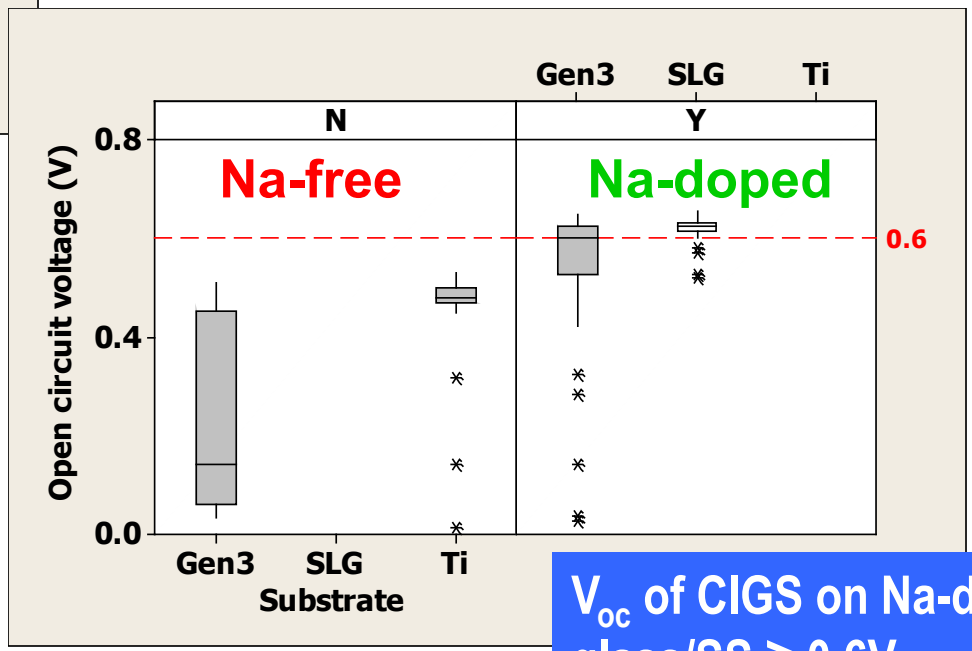
Performance of CIGS Solar Cells on Gen#3

SLG is the Na-doped reference and Ti foil is the Na-free reference to Gen3





FF>70%



V_{oc} of CIGS on Na-doped glass/SS ≥ 0.6V

Best device efficiency on Gen#3 is ~14.9% (without AR coating)

Best device efficiency on SLG is ~15% (without AR coating)

This presentation does not contain any proprietary or confidential information

Summary for Glass Coated Stainless Steel Substrate

Developed a glass coating as integrated solution with key features:

1- Barrier to ion migration

2- Na delivery to enable CIGS doping

3- Smooth surface

4- Match SLG cell efficiency

This presentation does not contain any proprietary or confidential information

Summary

DuPont's strategy in support of the CIGS thin film, flexible PV industry:

- Build on our existing portfolio of product materials for PV
- Utilize our core competencies in material science and engineering, polymer films, fluoropolymers, process development and advanced process control to generate new products including:
  - Flexible, robust frontsheets that provide ultrabarrier to water vapor transport
  - Encapsulents with property sets that are optimized for CIGS modules
  - Flexible substrate systems that provide key features of importance to CIGS

This presentation does not contain any proprietary or confidential information

Durability of Ultra Barrier Solar Films for Flexible PV Applications



Mark Roehrig
Mark Weigel
Tracie Berniard
Alan Nachtigal
Bill Murray

2011 PV Module Reliability Workshop

NREL, Golden Colorado

February 16th – *17th , 2011*

3M

Outline

- Flexible Solar Modules & Barrier Needs
- Flexible WVTR Requirements
  - Performance & Measurements
- Reliability Testing Ultra Barrier Films
  - Framework for 25 years
  - Test results to date
- Summary

Advantages of Flexible Solar Modules

Light weight →1/8th compared with glass-on-glass

Lower Balance of System costs → less labor and no mechanical racking

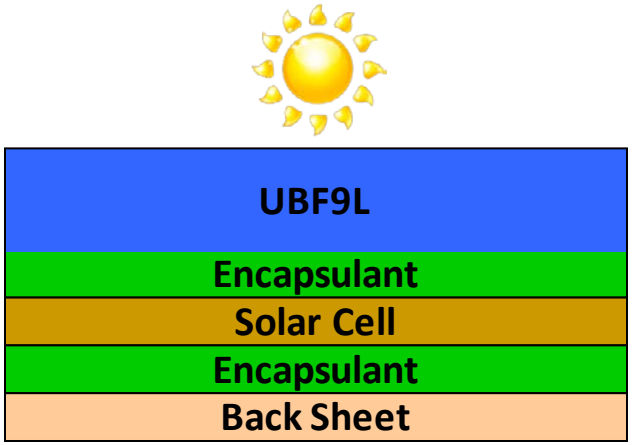
Higher packing density → Significantly more kW per shipping container

Higher energy output → Better transmission and off-angle performance

Large area modules → Lower relative “fixed” module costs

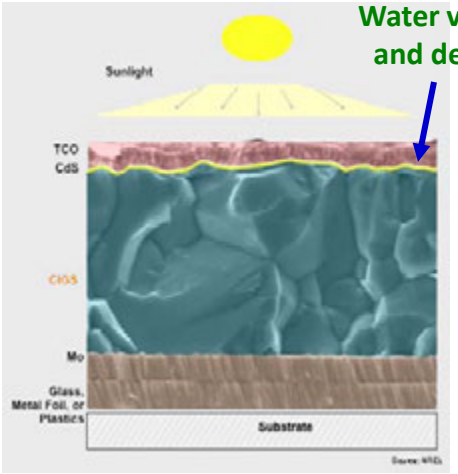
Lower manufacturing cost → Fully automated roll to roll processing





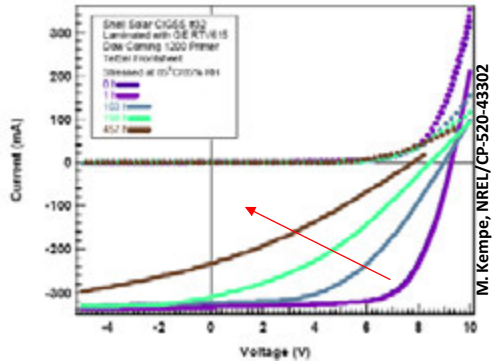
Thin Film Solar Barrier Needs

Failure Mode & CIGS Degradation Modeling



Degradation in Efficiency in CIGS

Exposure to Water (85%RH & 85°C)



CIGS Lifetime Model for Free Standing and Roof Mounted Modules , Time to 20% loss in Pmax

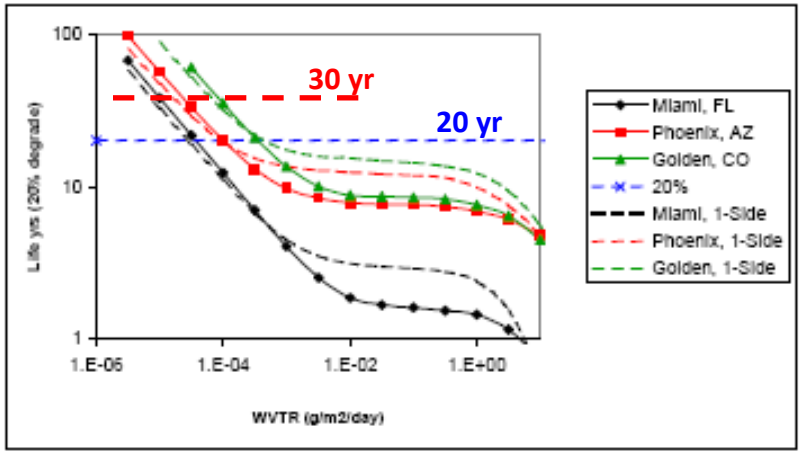


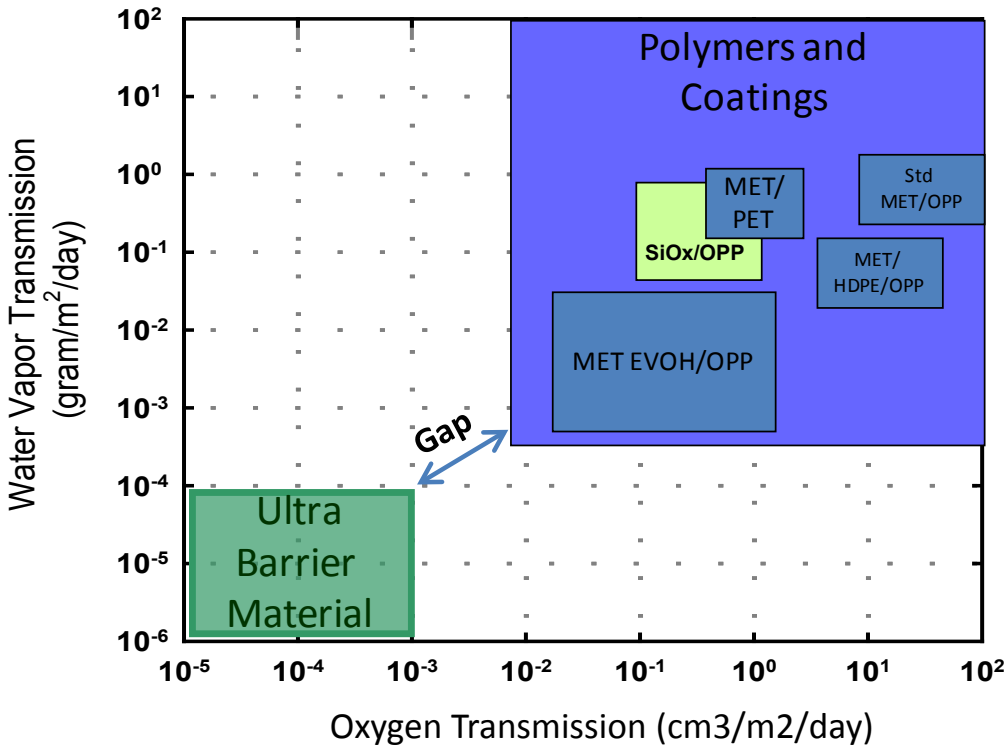
Figure 8. Module life for 2-side cooled (with symbols) and 1-side insulated (dashed) modules.

D.J. Coyle, etal , 2009 34th IEEE, pg. 001943 (2009)

Ultra-Barrier Requirements: 10^{-6} to 10^{-4} g/m^{2}day for 25 year

Ultra Barrier Films

- Ultrabarrier technology in development for over a decade
- Proprietary vacuum roll-to-roll process
  - Over 50 applications and 20 granted patents
- Challenge to actually measure < 10^{-3}g/m^{2}day



Ultra Barrier Film WVTR Measurement

Methods Overview

Scavenger Methods (Indirect)

Detection Level g/m²day

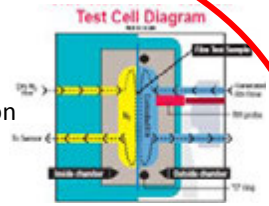
Permeation Cell (Direct)

Gravametric:
(ASTM E96) 1 to 1000g/m²day



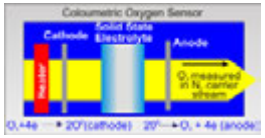
1

Mocon



Permatran: IR detection

Aquatran: Coloumbic detection



Ultra-Barrier Below this line

0.001

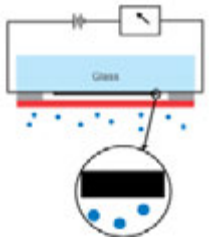
Calcium Test

$Ca + H_2O \rightarrow CaO + H_2$

$Ca + 2H_2O \rightarrow Ca(OH)_2 + H_2$

Optical Density

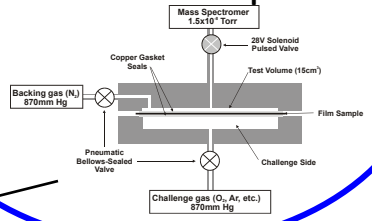




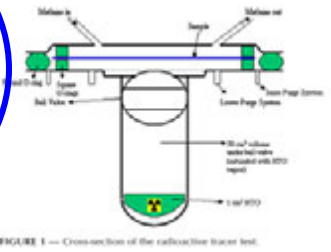
NREL Electrical Conductivity

Flex Solar

Mass Spec Under Development



HTO: Radioactivity



0.000001

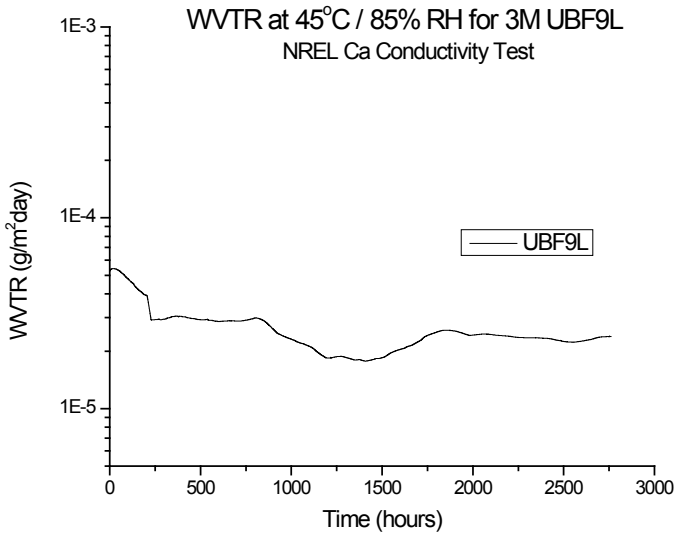
Arrelaine Dameron, NREL PVMRWS 2010

WVTR Measurements

Initial WVTR Performance of UBF9L by various Methods

Method	Detection Limit (g/m^2day)	Temperature (^oC)/RH(%)	UBF9L (g/m^2day)
MOCON Permatran	0.005	50/100	<0.005
MOCON Aquatran	0.0005	50/100	<0.0005
NREL Ca Test	10^{-6}	45/85	$5\pm3 \times 10^{-5}$

NREL Electrical Ca WVTR Test*



*Michael Kempe, Arrelaine Dameron, and Matthew Reese, "NREL Electrical Ca WVTR Test", *manuscript in preparation, 2011*.

- UBF9L still holding after 2750hr
- Variable temperature
- Size: 5cm2 to 50cm2
- Multiplexing for through-put
- Supported by NREL/3M CRADA CRD-08-293

Reliability Testing of Ultrabarriers

Key performance and safety properties need to be retained for 25+ years

- WVTR—one of a few key properties for flex solar
- Other key performance properties
  - Percent transmission—high output
  - Mechanical strength—robust module
- Key safety factors
  - Component & Module partial discharge
- Reliability and lifetime testing program needs to include all of these

Reliability Testing of Ultrabarriers

3 Weathering Resource Center

Historical products



Less direct sun exposure, shorter lifetimes

Products for Solar

More direct sunlight, longer lifetimes, under electrical load

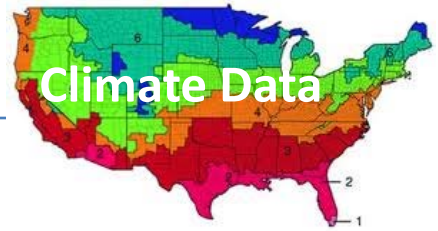


Technabob.com

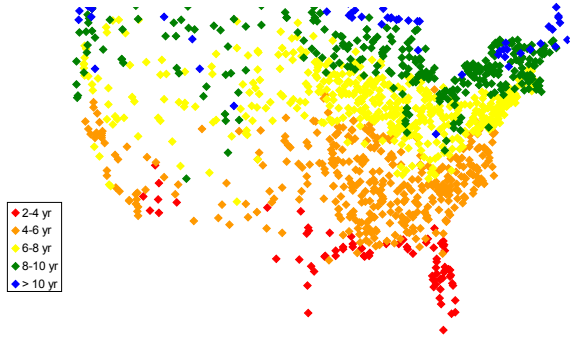
Mathematical models







Product Lifetimes





Successfully Used in Numerous Products

Reliability Testing of Ultrabarriers

3M Weathering Testing Plan for 25 year Lifetime

Natural Outdoor Exposure

Multiple Locations and Environments



Static Racks (5° or latitude w/ backing)

Accelerated Outdoor Exposure

2x to 5x UV range acceleration



Mirrored Enclosure



G90-type

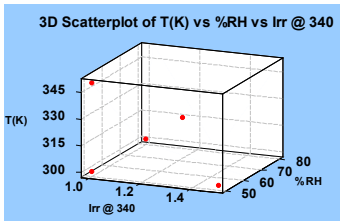


Large area G90-type

Accelerated Indoor Exposure & Lifetime Modeling



Controlled
- Irradiance
- %RH
- Temperature



SWAT Exposure

Sequential **W**eathering **A**ccelerated **T**est



Accelerated Outdoor

+ Damp Heat
+ Humidity Freeze
+ …

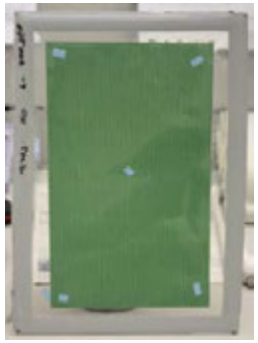
Reliability Testing of Ultrabarriers

UBF9L Film and Module Testing Plan

Multiple Testing Modes
for 25 Year

Film Performance

WVTR <10^{-4}g/m^{2}day
T>90%
Mechanical

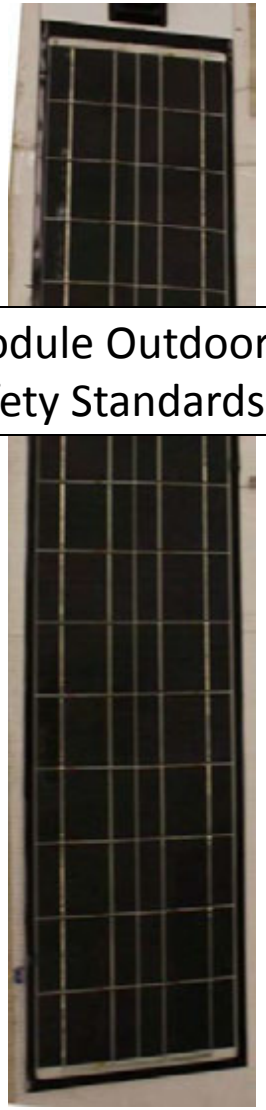


Mini Module Performance

Solar module output
Controlled environments



Full Module Outdoor UL Safety Standards



Reporting on UBF9L initial results

Reliability Testing of Ultrabarriers

Preliminary Accelerated Indoor Testing Baseline

Weathering Cycle Information		
Cycle	Light Source	Cycle
Damp Heat (DH)	n/a	n/a
Full Spectrum Dry	Xe-arc	ASTM G155 (mod)
Full Spectrum Wet	Xe-arc	ASTM G155 (mod)
UV Spectrum Wet	UV fluorescent	ASTM G154 (mod)

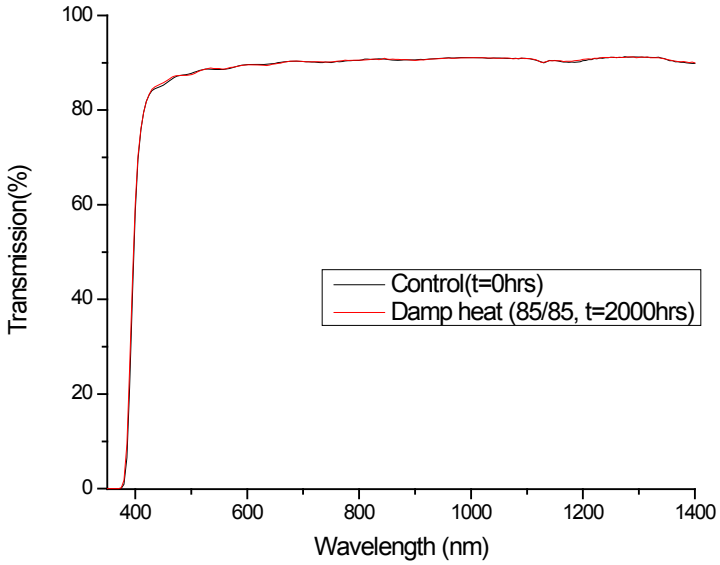
- Test results so far
  - WVTR and Optical Transmission

Damp Heat (85ºC/85%RH)

WVTR and Optical Transmission Results

Permatran measurements

Time in Damp Heat (hrs)	WVTR (50C/100%RH) (g/m2day)
0	<0.005
1000	<0.005
2000	<0.005



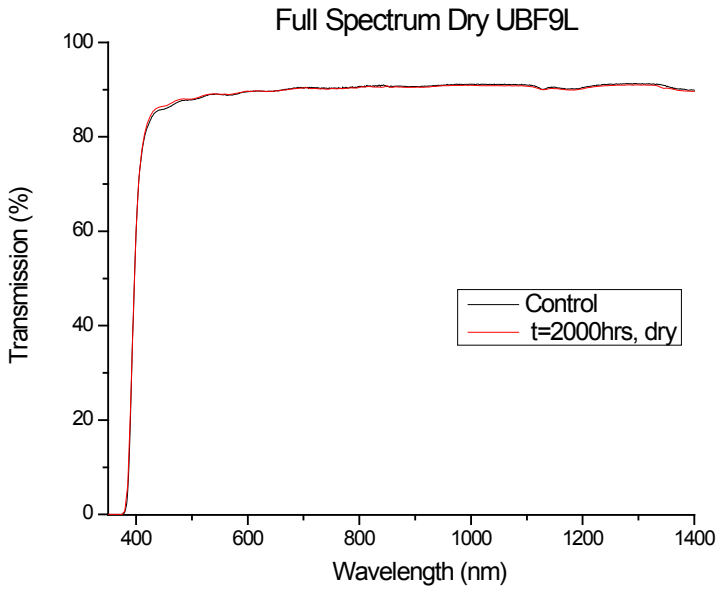
Full Spectrum Dry

Xe-Arc Lamp, Modified ASTM G155

WVTR and Optical Transmission Results

Permatran measurements

Time in Damp Heat (hrs)	WVTR (50C/100%RH) (g/m2day)
0	<0.005
1000	<0.005
1500	<0.005

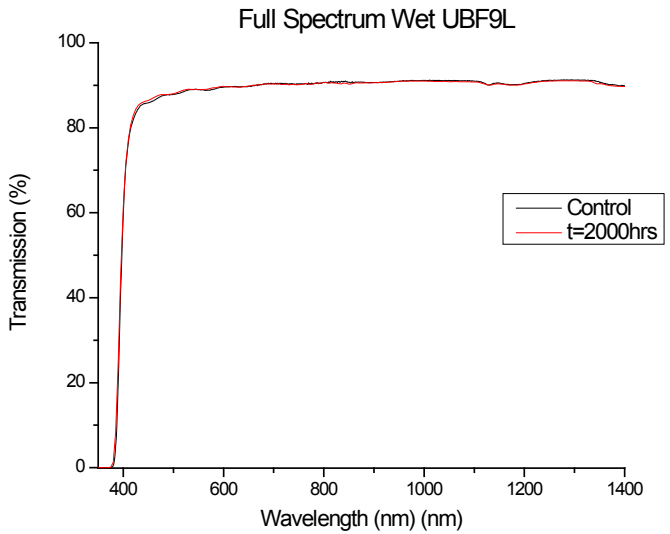


Full Spectrum Wet

Xe-Arc, Modified ASTM G155

WVTR and Optical Transmission Results

Time in Damp Heat (hrs)	WVTR (50C/100%RH) (g/m2day)
0	<0.005
1000	<0.005
1500	<0.005



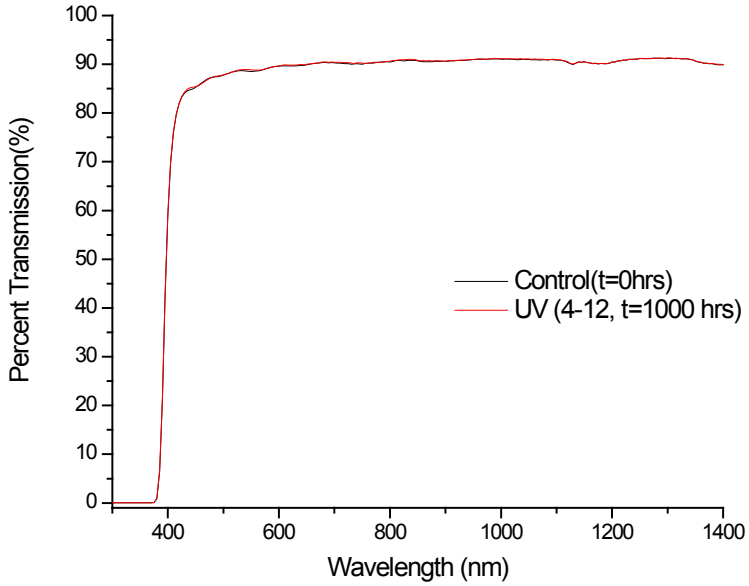
UV Spectrum Wet

UV Fluorescent, Modified ASTM G154

WVTR and Optical Transmission Results

Permatran measurements

Time in Damp Heat (hrs)	WVTR (50C/100%RH) (g/m2day)
0	<0.005
1000	<0.005
1500	<0.005



Next Step for WVTR: NREL Ca test values for aged samples

Reliability Testing of Ultrabarriers

Safety of UBF9L

- UL certified front sheet component
- UL and TUV front sheet partial discharge rating of 1,000V
- Solar Modules with our film have passed UL 1703 and IEC 61646/61730 certifications.

Reliability Testing of Ultrabarriers



The goal of this project is to develop and commercialize a flexible, highly transparent Ultra Barrier Topsheet that will enable successful commercialization of flexible photovoltaic modules.

3 **Renewable Energy Division & Corporate Research Lab**

Barrier Film Development & Scale-up, Accelerated Weathering, Lifetime Modeling



Module Reliability
Ca Conductivity WVTR Testing

Summary

- Ultra Barrier Solar Film for flexible modules
  - WVTR $5\pm3x10^{-5}$ g/m^{2}day after 2750 hrs at 45^{o}C/85%RH (NREL Ca Cond. Test)
- Preliminary accelerated aging results, *need many more hours*
  - No WVTR (MOCON) degradation after 1500hrs exposure full spectrum (wet/dry), 1000hrs UV wet
  - No degradation of optical transmission after 1500hrs of full spectrum (wet/dry)
  - No WVTR (MOCON) degradation after 2000 hrs of damp heat (85/85)
- 25 year lifetime plan
  - Leveraging internal 3M weathering resources/expertise
  - Indoor accelerated + outdoor acceleration → validation with outdoor
  - Looking at possible combination of in/out-door accl. Testing→SWAT
  - DOE SunShot Award: Reliability and scale up of ultra barrier films for flex solar

NREL
NATIONAL RENEWABLE ENERGY LABORATORY

Innovation for Our Energy Future

Calcium Based Test Method for Evaluation of Photovoltaic Edge-Seal Materials



Michael Kempe,
Arrelaine Dameron,
Matthew Reese

2011 NREL PV Module Reliability Workshop

February 16, 2011

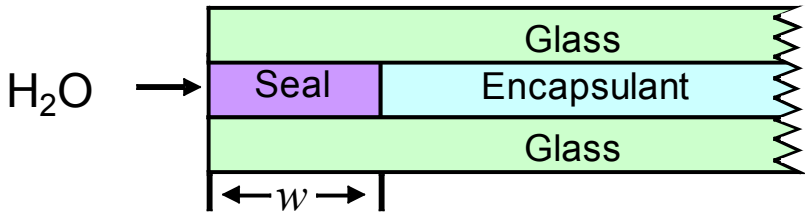
NREL is a national laboratory of the U.S. Department of Energy, Office of Energy Efficiency and Renewable Energy, operated by the Alliance for Sustainable Energy, LLC.

Experimental Objectives

Many PV technologies are sensitive to moisture. Even with impermeable front- and back-sheets, moisture can penetrate from the sides. Edge seals are incorporated around the perimeter to prevent this ingress.

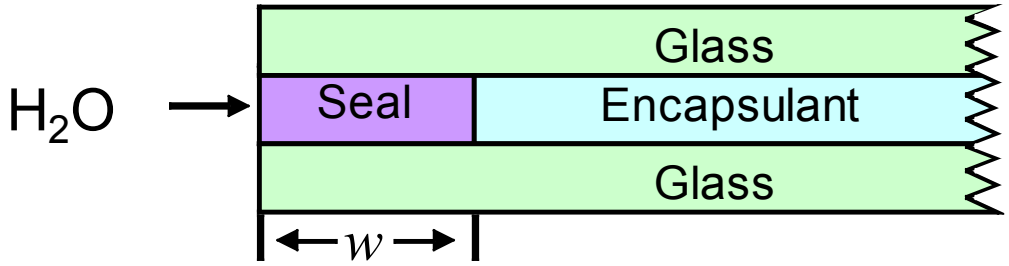
Here we use a Ca-based method to evaluate the moisture ingress time for edge seal materials.

Then we use this data to model the performance when deployed outdoors.

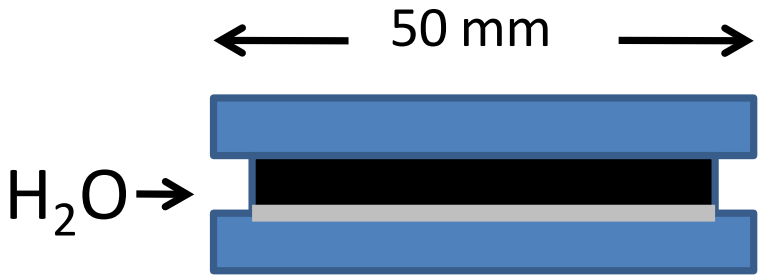


Test Sample Designed to Mimic Module Edge

Module Edge



Test Sample



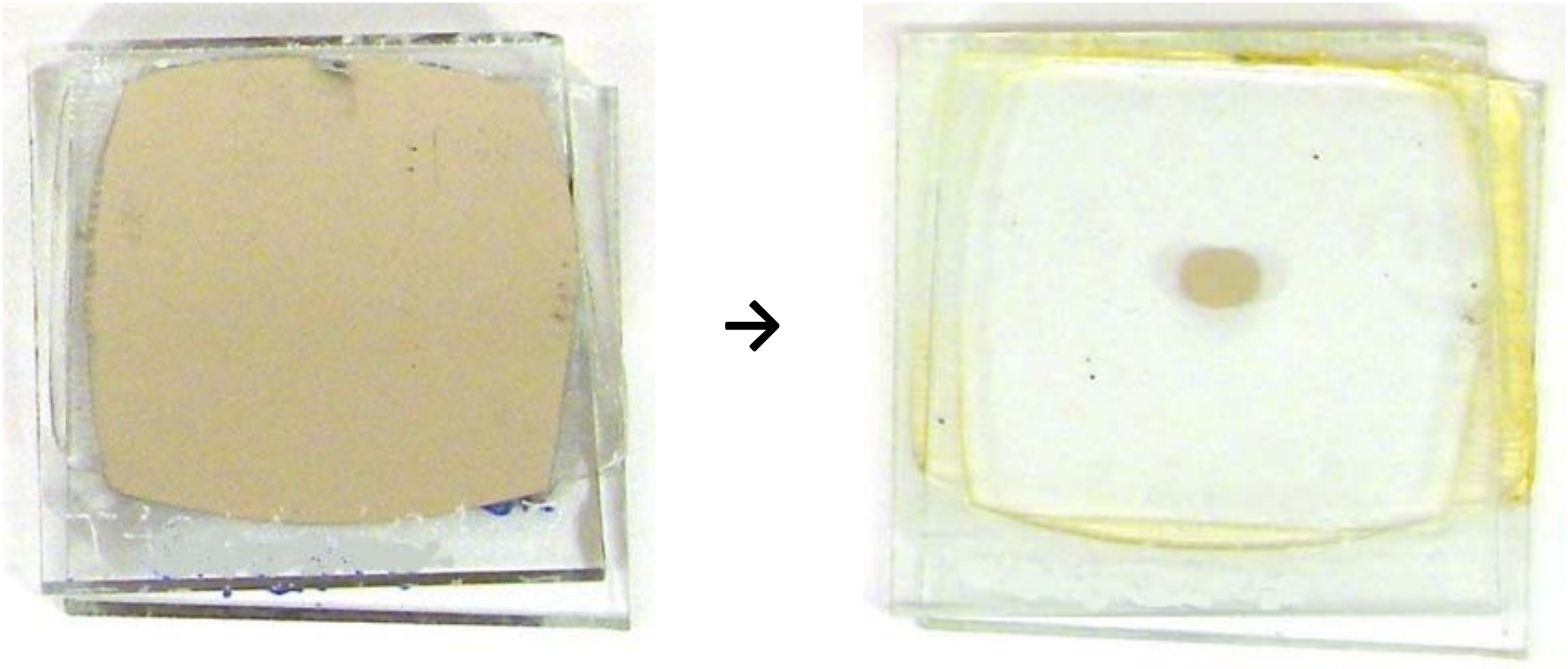
Glass (3.18 mm)
Polymer Film (~0.5 mm)
Ca (100 nm)
Glass (3.18 mm)

$$Ca + 2\ H_20 \rightarrow Ca(OH)_2 + H_2$$

Oxidation of Ca Indicates Moisture Ingress

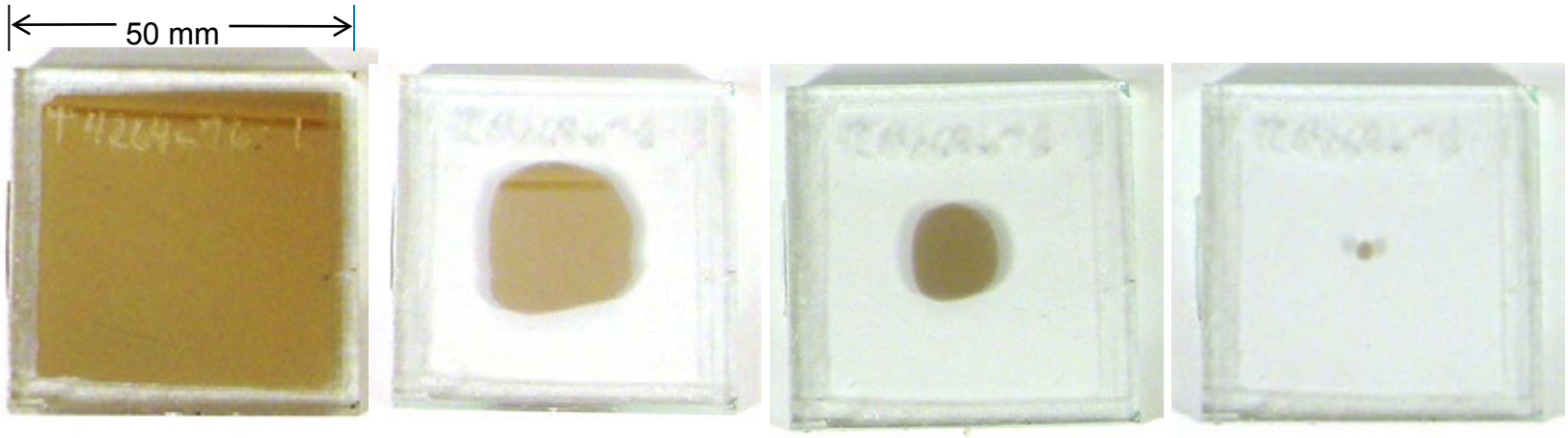
$$Ca + 2\ H_20 \rightarrow Ca(OH)_2 + H_2$$

Mirror-Like → Transparent



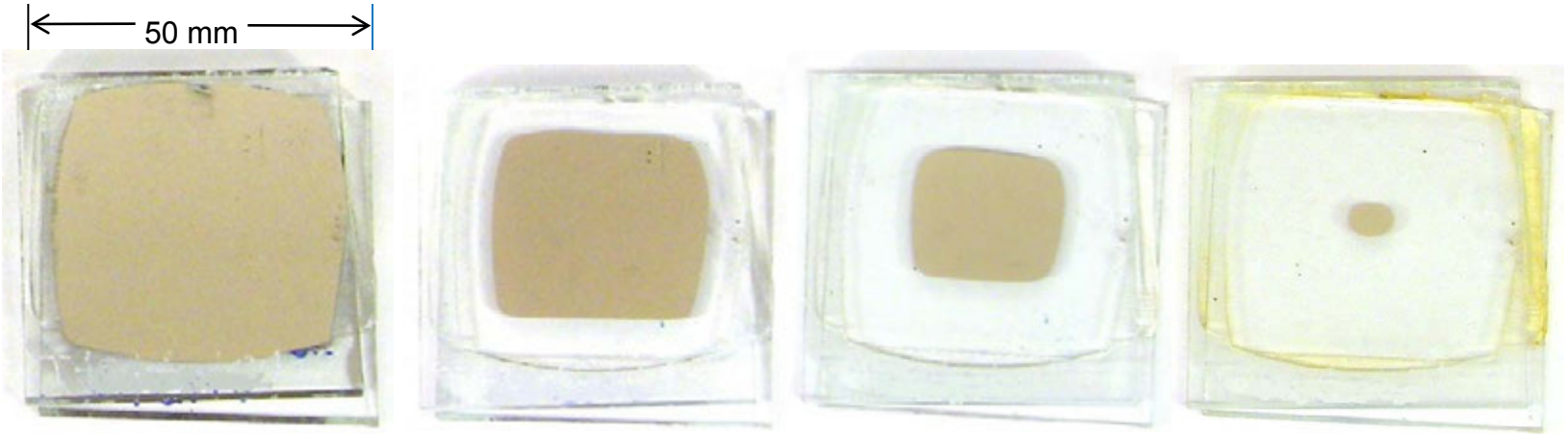
Moisture Ingress Varies Greatly in Encapsulants

PDMS



0 h | 1.5 h | 3 h | 4.5 h

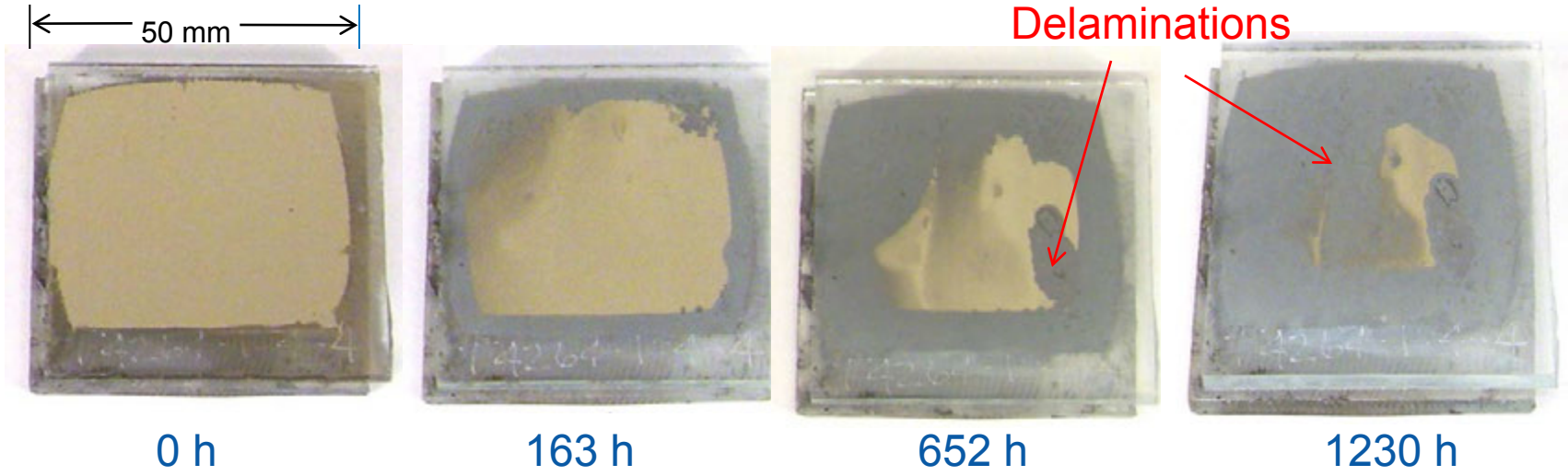
Ionomer #1

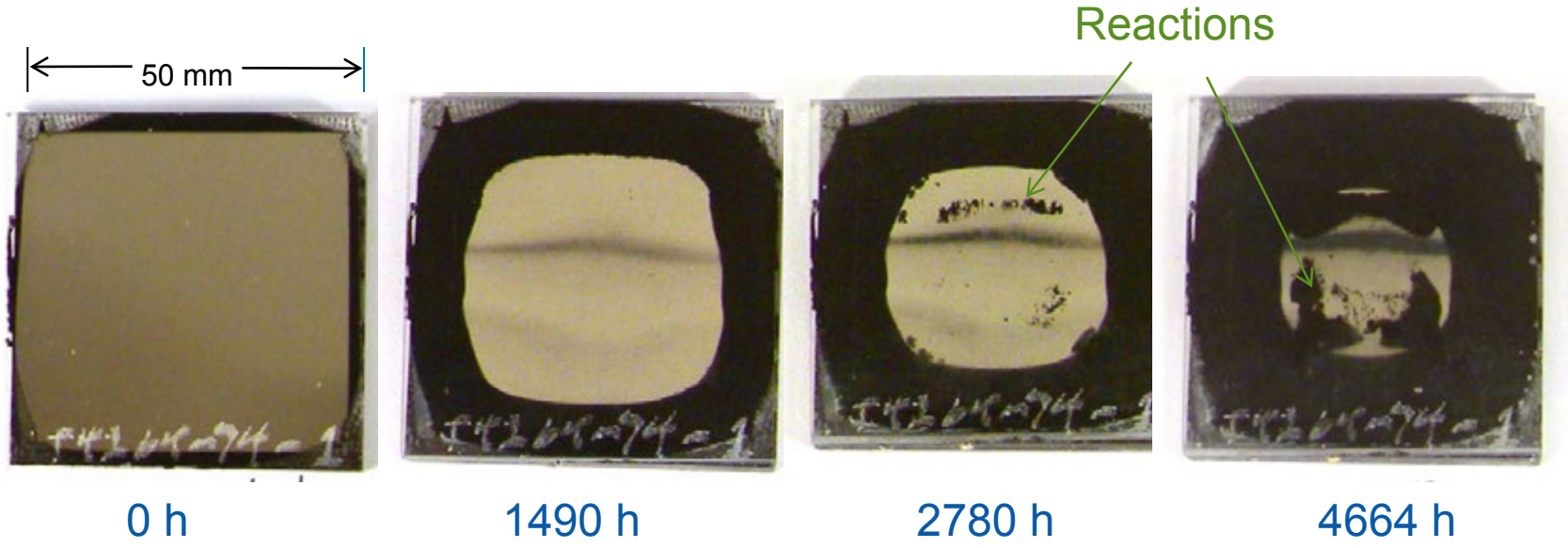


0 h | 67 h | 240 h | 652 h

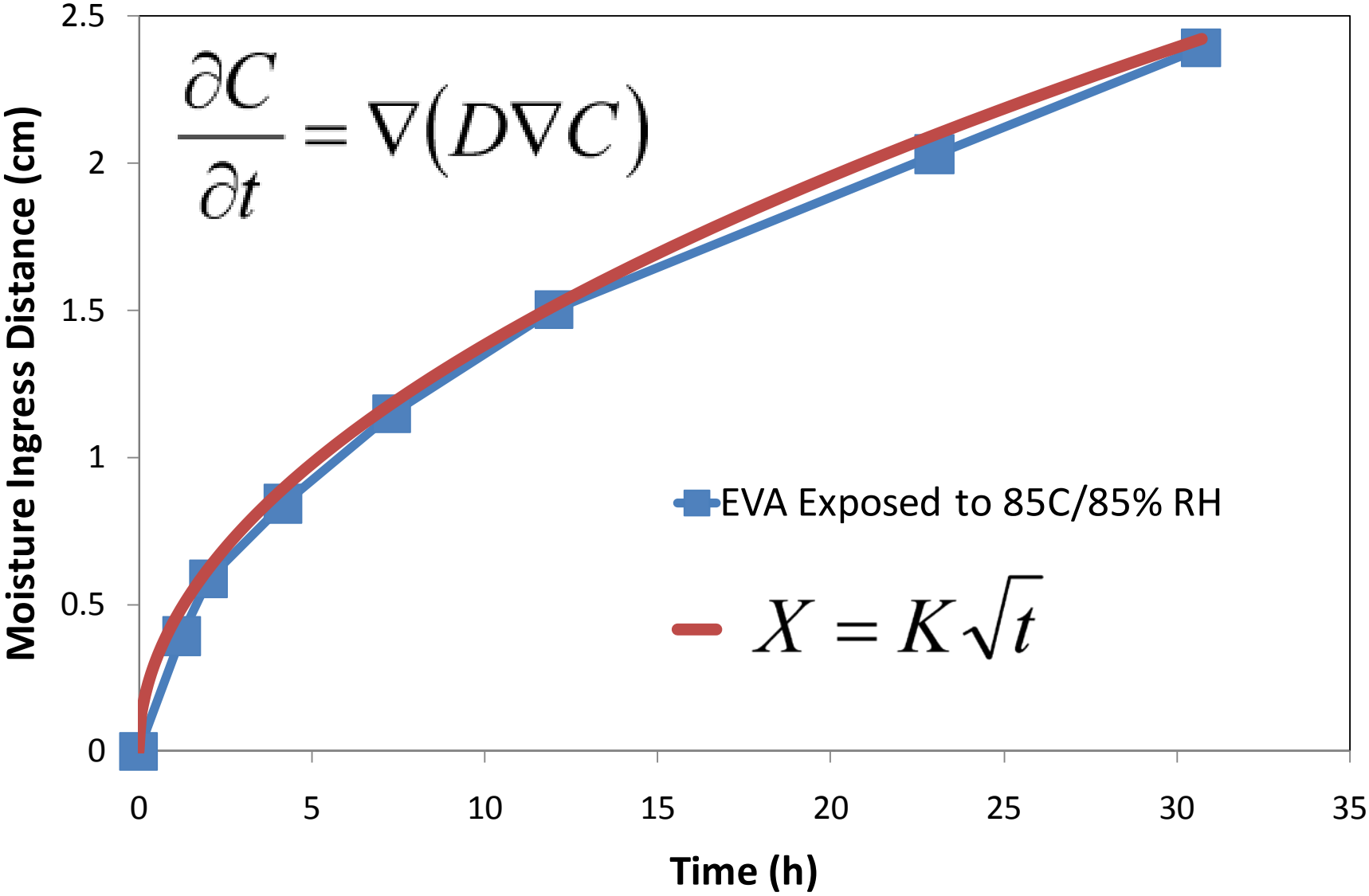
Exposed to 85°C and 85% RH

Polyisobutylene Edge Seals Slow Ingress

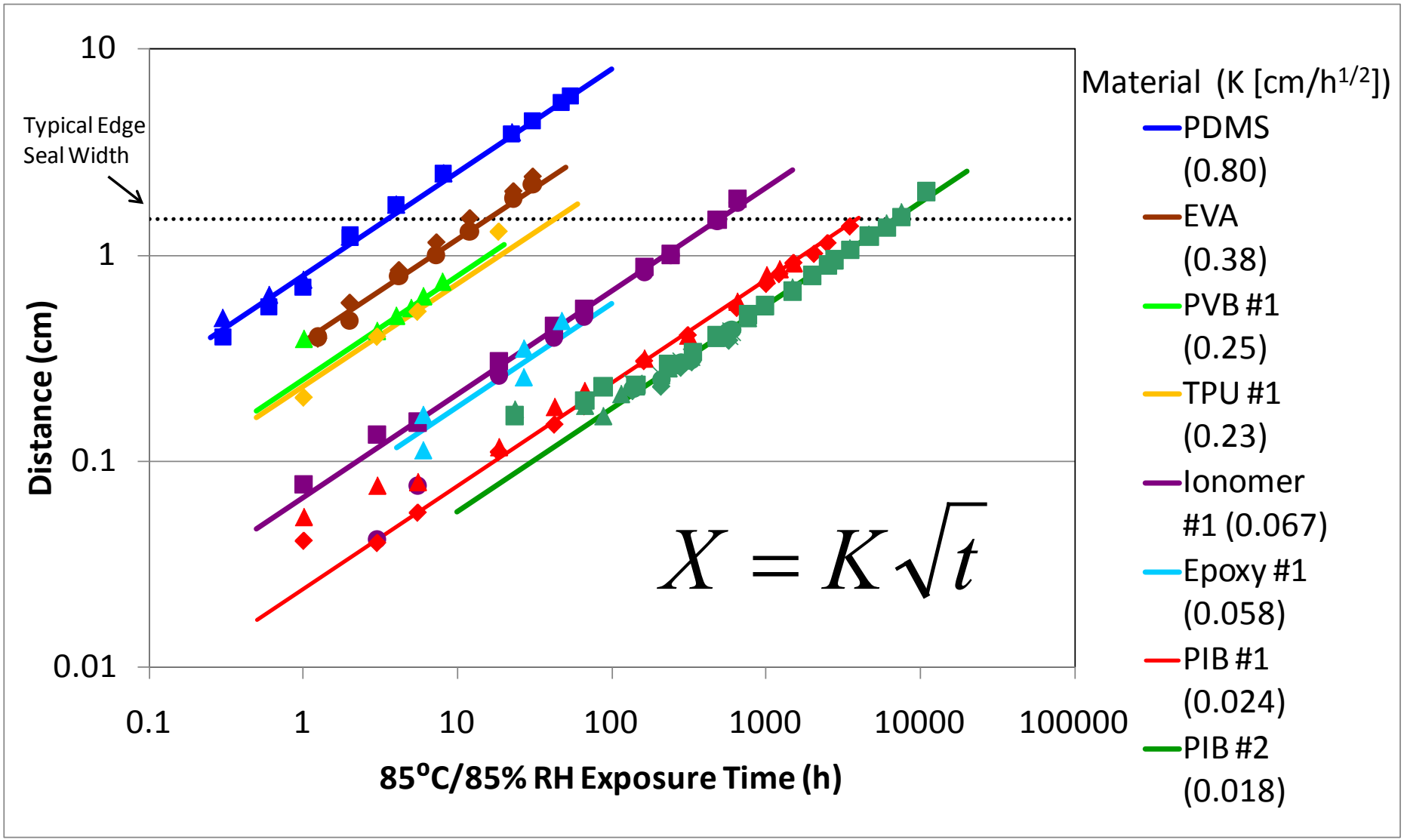




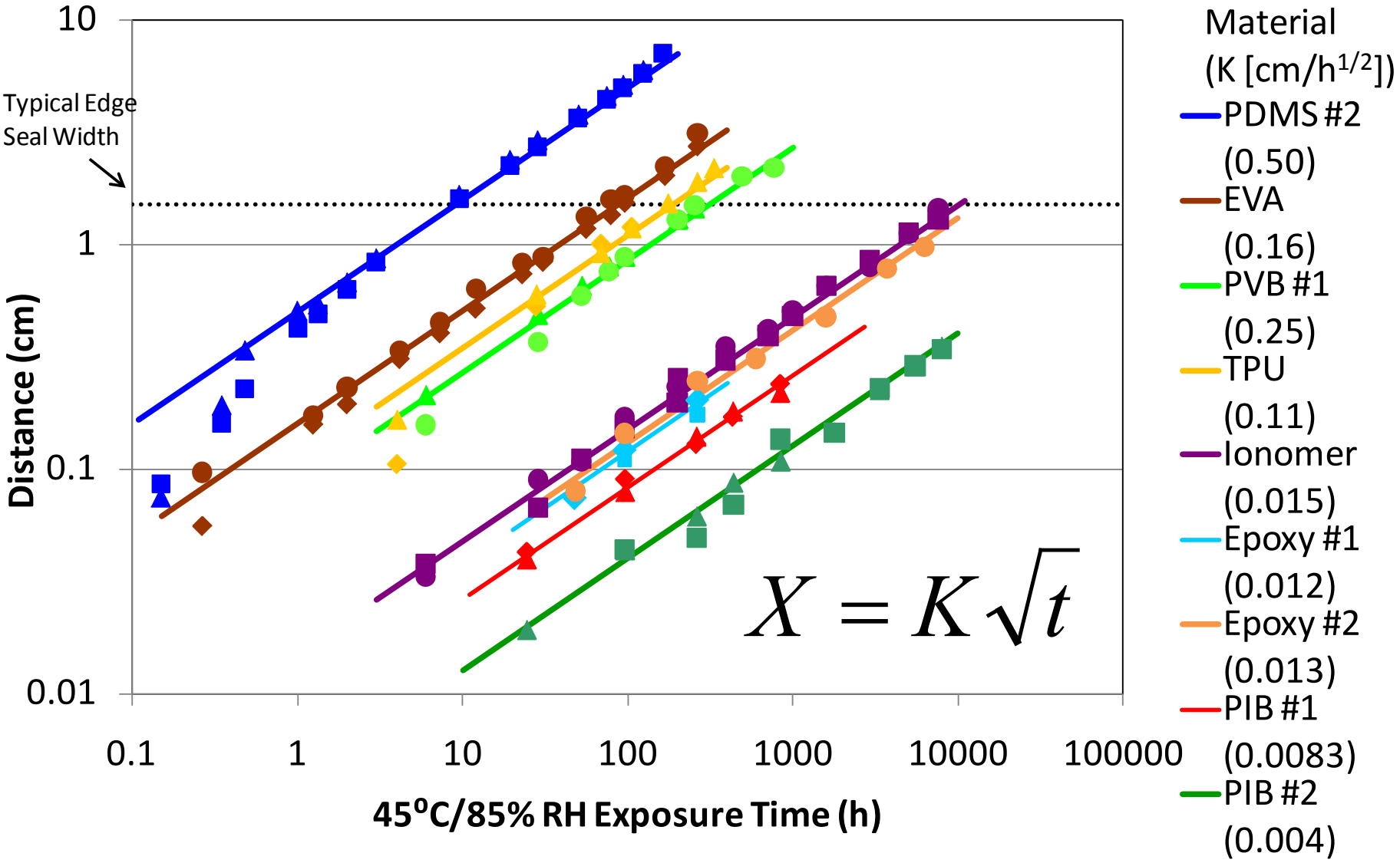
Moisture Ingress Rate Governed by Diffusion



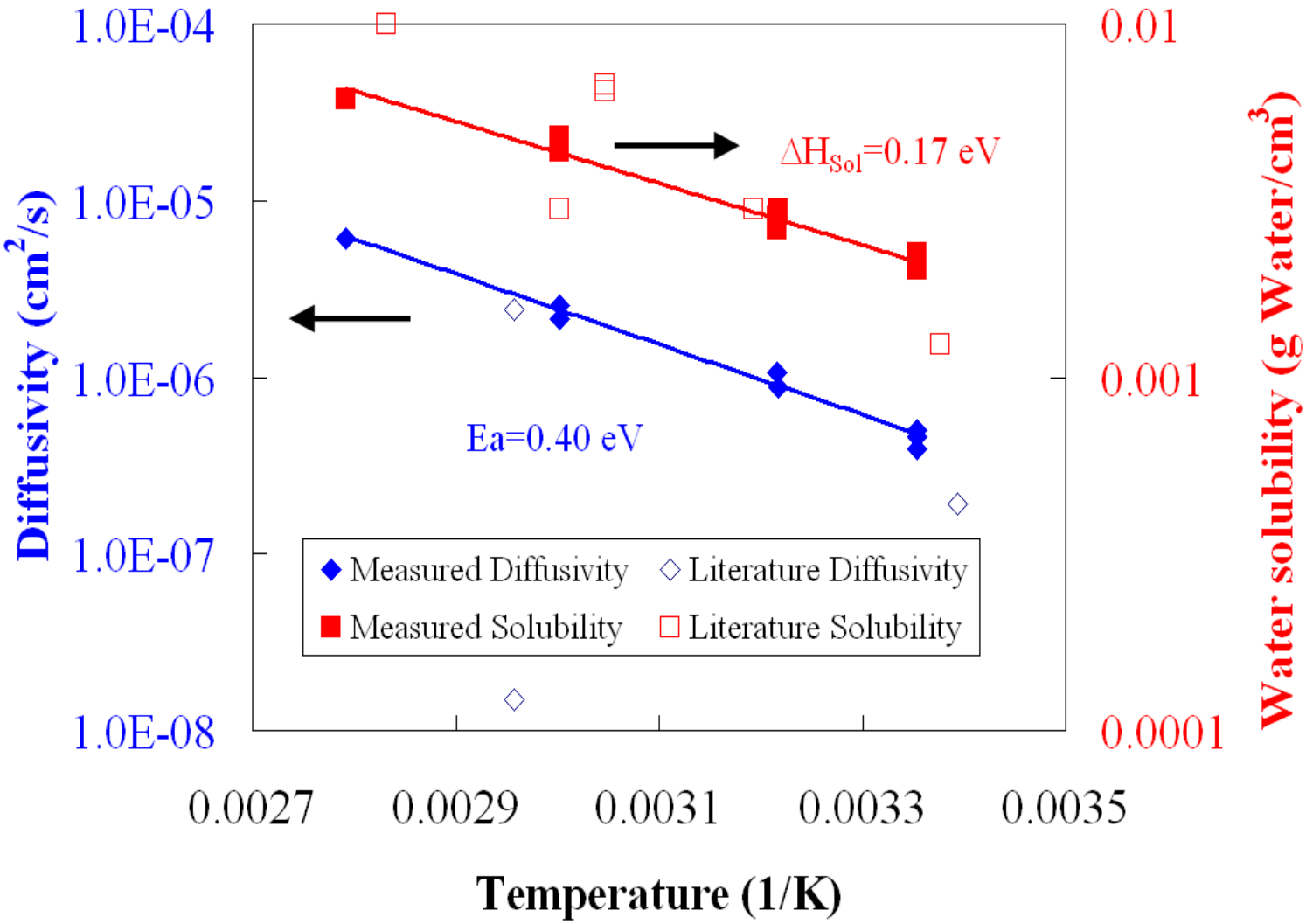
Ingress Rates Vary Greatly (85°C)



Ingress Rates Vary Greatly (45°C)

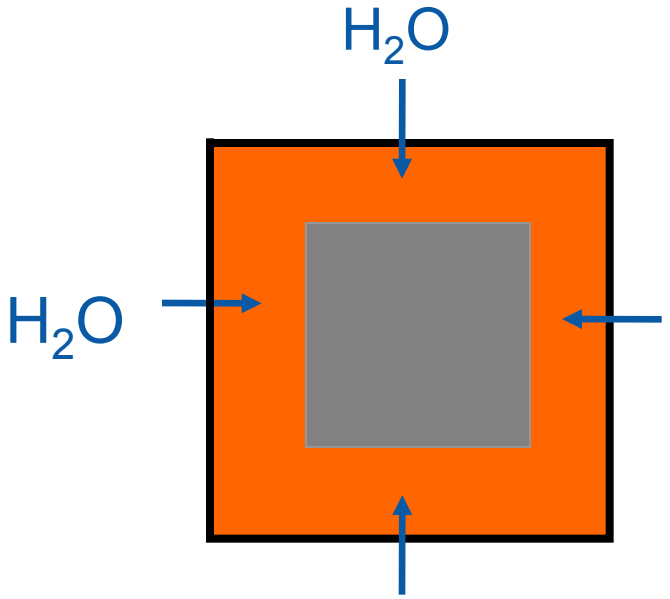


EVA Water Permeation Parameters



Moisture Ingress Rate Governed by Diffusion

$$\frac{\partial C}{\partial t} = \nabla(D\nabla C)$$



1-D Semi-Infinite Solid

$$C(x,t) = C_{eq}\left[1 - erf\left(\frac{x}{2\sqrt{Dt}}\right)\right]$$

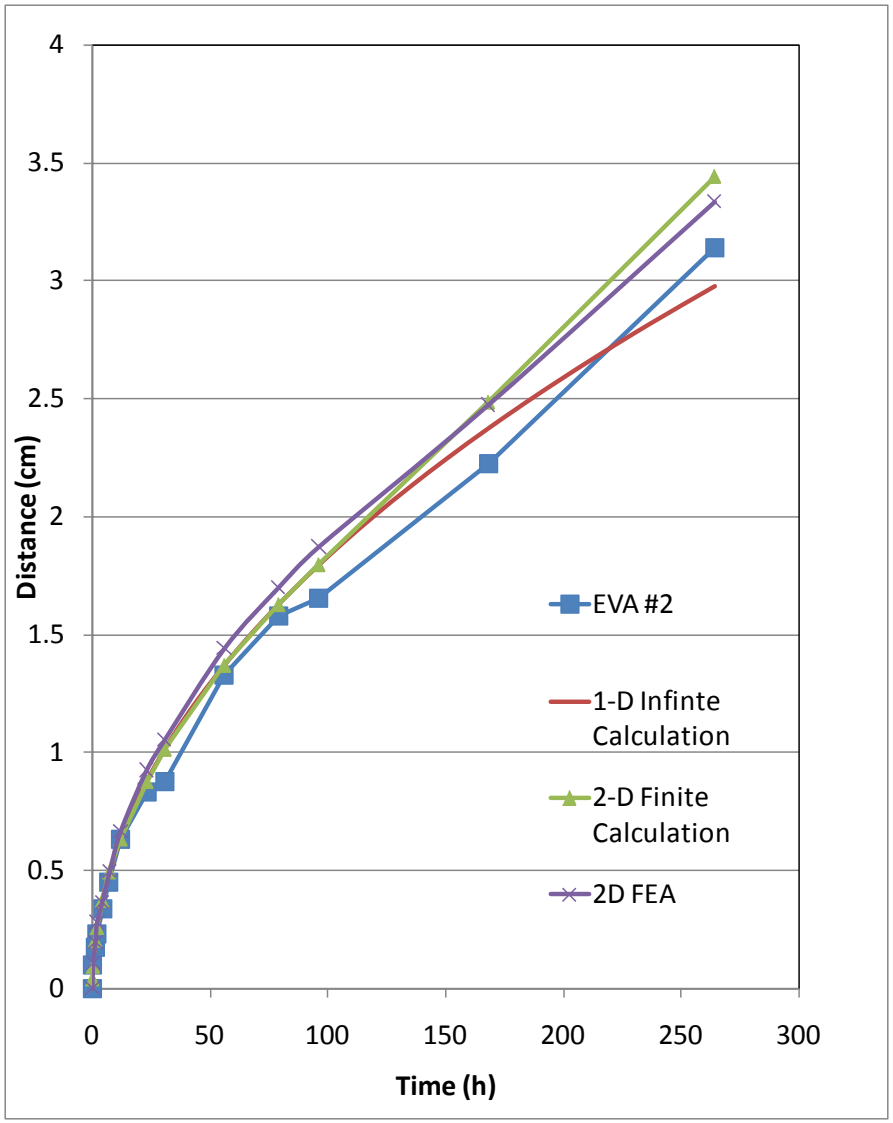
2-D Ingress, Infinite rectangular bar

$$\frac{C_{eq} - C(X,Y,t)}{C_{eq}} = \frac{16}{\pi^2}\sum_{m=0}^{\infty}\frac{1}{2m+1}\sin\left[\frac{(2m+1)\pi X}{l_x}\right]e^{\left[-\frac{D(2m+1)^2\pi^2 t}{l_x^{\,2}}\right]}\sum_{n=0}^{\infty}\frac{1}{2n+1}\sin\left[\frac{(2n+1)\pi Y}{l_y}\right]e^{\left[-\frac{D(2n+1)^2\pi^2 t}{l_y^{\,2}}\right]}$$

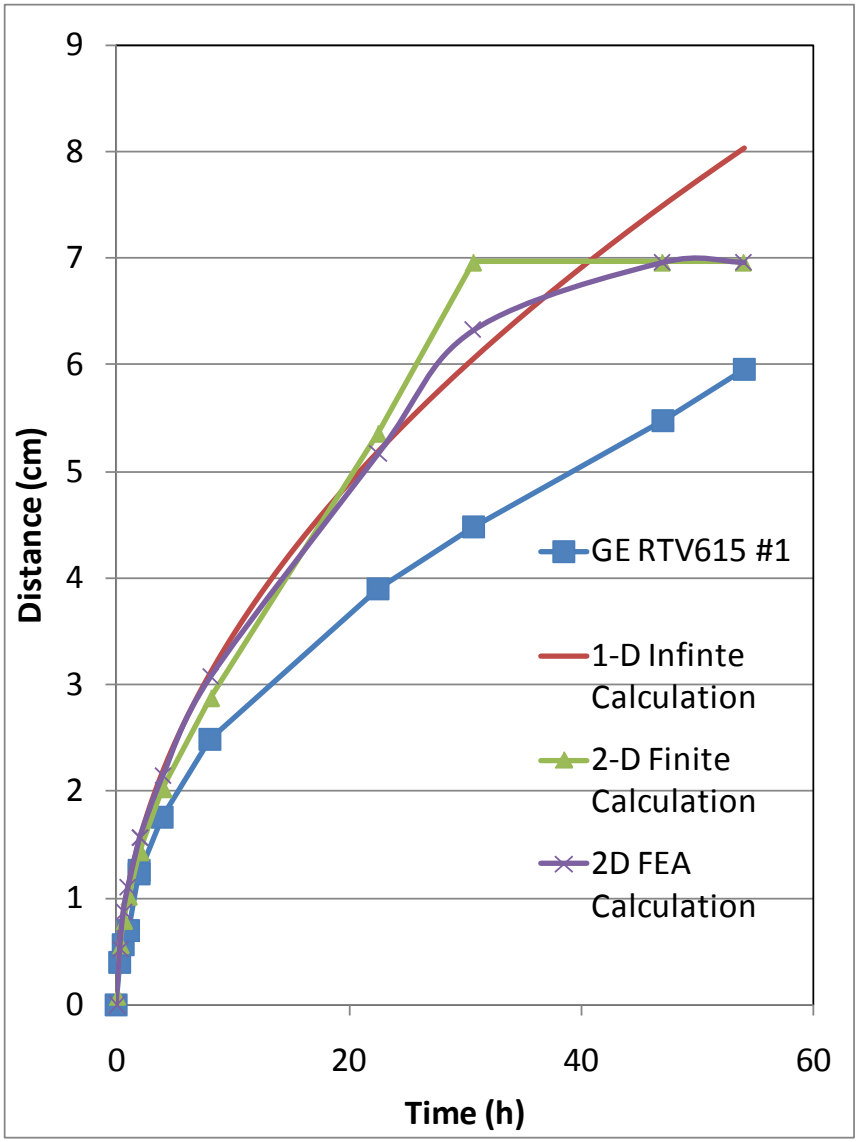
2-D Finite Element Analysis with Ca-H_20 Reaction

$$C_{m,n}^{P+1} = \frac{D\Delta t}{(\Delta X)^2}\left(C_{m+1,n}^{P} + C_{m-1,n}^{P} + C_{m,n+1}^{P} + C_{m,n-1}^{P}\right) + \left[1 - 4\frac{D\Delta t}{(\Delta X)^2}\right]C_{m,n}^{P} - (Calcium)$$

D and S allow for Modeling of Performance



EVA



Silicone

Edge Seal Modeling

The use of fillers, pigments, and desiccants makes the determination of modeling parameters much more difficult.

$$S_m = S_o e^{\left(-\frac{Ea_s}{kT}\right)} \frac{RH\%}{100\%}$$

Mobile phase water absorption is split between the polymer matrix and the mineral components. Assume linearity with relative humidity.

$$D_{eff} = D_o e^{\left(-\frac{Ea_D}{kT}\right)}$$

Mobile phase water diffusivity is an effective diffusivity. This accounts for a rapid equilibration between adsorbed and dissolved water.

$$R_{H_2O}$$

A non-reversible reaction with water.

Getting the Modeling Parameters

R_{H_2O}

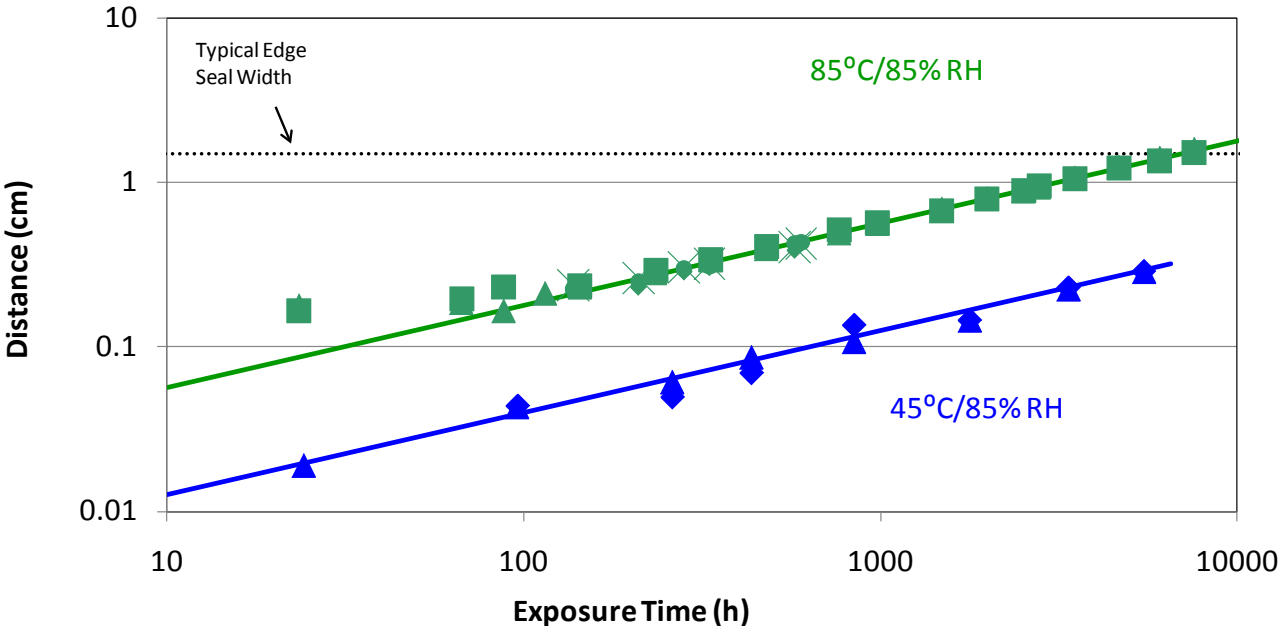
Measured by weighing samples before humidity exposure, after humidity exposure, and after drying.

S_o , Ea_S

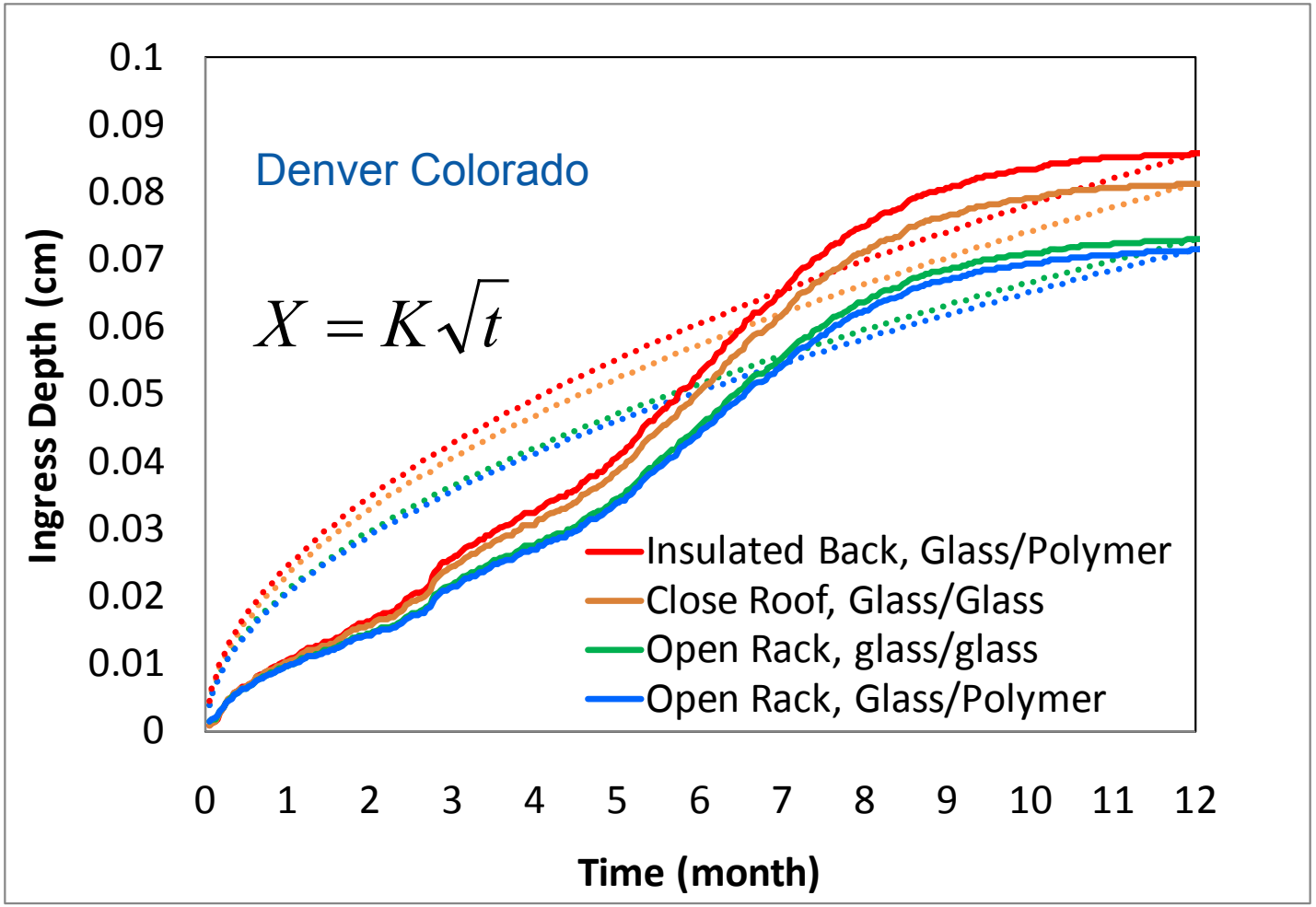
In progress: Measured by exposing to controlled humidity then drying in a TGA to determine moisture loss. Currently assuming Ea_S of 16 KJ/mol.

D_o , Ea_D

Estimate from other parameters and fit to Ca data.

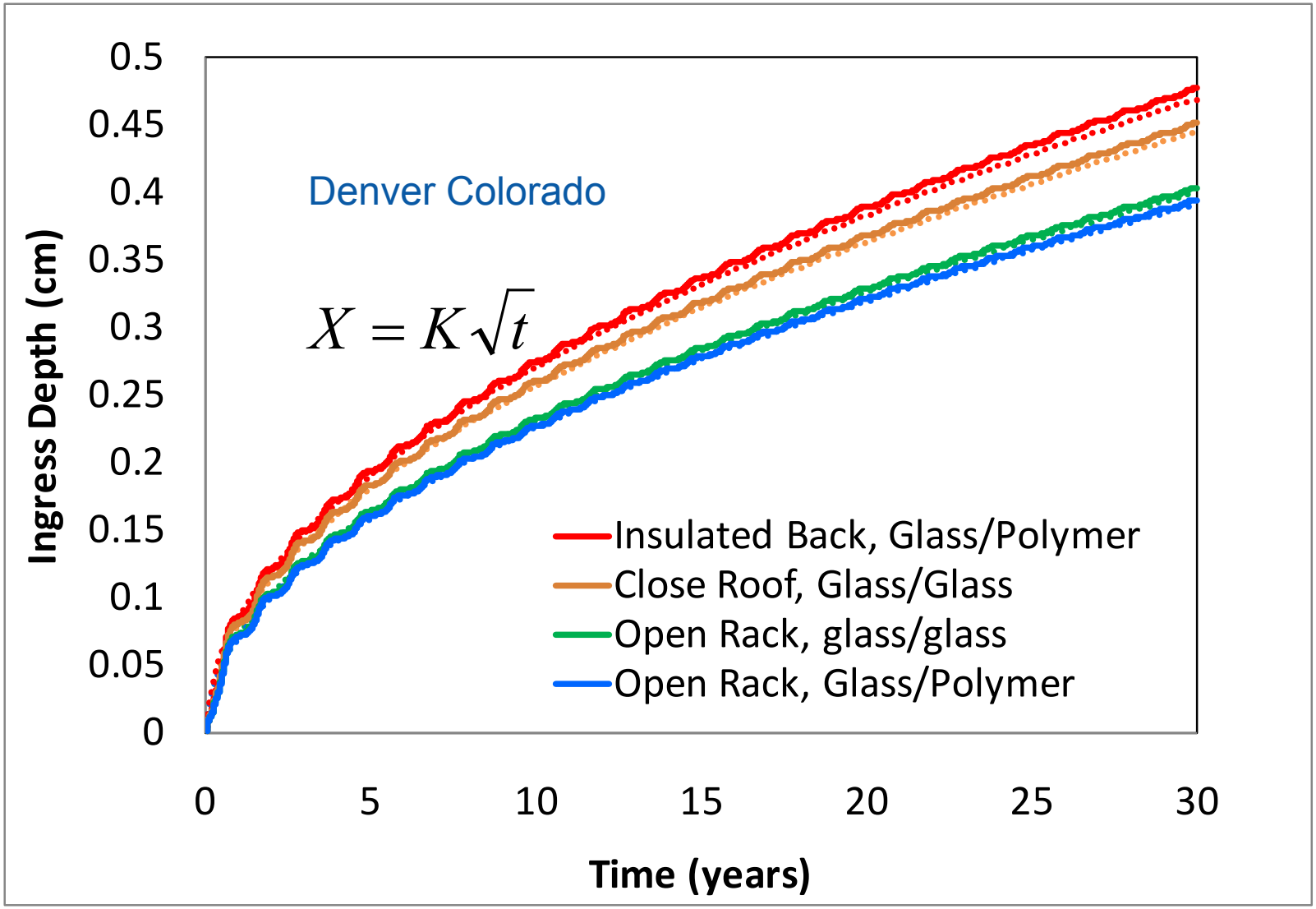


Ingress Estimated Using Finite Element Analysis



Used TMY3 Data and Temperature estimates similar to King et al, and Kurtz et al.

Square Root Relation Works to Longer Times



Used TMY3 Data and Temperature estimates similar to King et al, and Kurtz et al.

Preliminary Results for Different Climates

D_o (cm^2/s)=		9.22				
Ea_D (kJ/mol)=		56				
S_o (g/cm^3)=		7.77				
Ea_S (kJ/mol)=		16				
Reactive Ca absorption (g/cm^3)=		0.0327	K	20 y required width	20 yr equivalent at 85°C/85% RH	20 yr equivalent at 45°C/85% RH
			($cm/h^{1/2}$)	(cm)	(h)	(years)
DENVER/CENTENNIAL [GOLDEN - NREL]	Open Rack, Glass/Polymer		0.00076	0.32	**316**	0.7
	Open Rack, glass/glass		0.00078	0.33	330	0.8
	Close Roof, Glass/Glass		0.00087	0.36	408	0.9
	Insulated Back, Glass/Polymer		0.00092	0.38	454	1.0
MUNICH	Open Rack, Glass/Polymer		0.00081	0.34	353	0.8
	Open Rack, glass/glass		0.00082	0.34	364	0.8
	Close Roof, Glass/Glass		0.00089	0.37	432	1.0
	Insulated Back, Glass/Polymer		0.00093	0.39	471	1.1
RIYADH	Open Rack, Glass/Polymer		0.00099	0.41	525	1.2
	Open Rack, glass/glass		0.00101	0.42	551	1.3
	Close Roof, Glass/Glass		0.00114	0.48	705	1.6
	Insulated Back, Glass/Polymer		0.00121	0.51	795	1.8
PHOENIX SKY HARBOR INTL AP	Open Rack, Glass/Polymer		0.00119	0.50	767	1.8
	Open Rack, glass/glass		0.00122	0.51	805	1.9
	Close Roof, Glass/Glass		0.00138	0.58	1,029	2.4
	Insulated Back, Glass/Polymer		0.00146	0.61	1,161	2.7
MIAMI INTL AP	Open Rack, Glass/Polymer		0.00168	0.70	1,520	3.5
	Open Rack, glass/glass		0.00171	0.72	1,580	3.7
	Close Roof, Glass/Glass		0.00187	0.78	1,889	4.4
	Insulated Back, Glass/Polymer		0.00195	0.82	2,062	4.8
BANGKOK	Open Rack, Glass/Polymer		0.00198	0.83	2,115	4.9
	Open Rack, glass/glass		0.00201	0.84	2,192	5.1
	Close Roof, Glass/Glass		0.00220	0.92	2,625	6.1
	Insulated Back, Glass/Polymer		0.00230	0.96	**2,867**	6.6

A sensitivity analysis gave about 15% on K and Width, and 30% on 20 yr equivalent time.

What edge seal parameters are important?

1. Adhesion is the most important parameter.
   a) Must be maintained after environmental exposure.
   b) Residual stress in glass may affect adhesion.
   c) Material may expand as it absorbs water.
   d) Good surface preparation is necessary.
2. Breakthrough time is the next most important.
   a) The 12 mm edge delete perimeter should be wide enough to keep moisture out.
3. Module mounting configuration is not important.
   a) Hotter installations tend to dry out the module partially countering the effects of increased diffusivity.
4. The steady state transmission is less important.
   a) The amount of permeate is very low.
   b) Ideally one will not reach steady state.

Conclusions:

1. An edge seal width of 1 cm can be capable of keeping moisture out for 20 years in almost any climate.
2. The mounting configuration is not a significant factor for determining the diffusion based lifetime of an edge seal.
3. The climate a module is deployed in very significantly impacts edge seal performance.
4. Exposure to between 500 h and 3000 h of 85C and 85% RH will equate to about 20 years of moisture ingress through an edge seal.

Reliability and Application Challenges for Flexible Thin-Film (BIPV) Modules

Samir Sharma & Doug Herron

United Solar Ovonic LLC

PV Module Reliability Workshop

Golden, CO

February 17, 2011

This presentation does not contain any proprietary or confidential information.

Flexible BIPV Thin-Film PV Modules and their applications

United Solar Ovonic amorphous silicon-based flexible thin-film module



Advantages:

- Requires no roof penetrations
- Lightweight, durable, flexible
- Ideal for Building Integrated (BIPV)
- Easy to install
- Tested and proven products in real-life conditions since 1983

BIPV application for United Solar Ovonic modules (attached to metal and various roofing membranes/substrates)







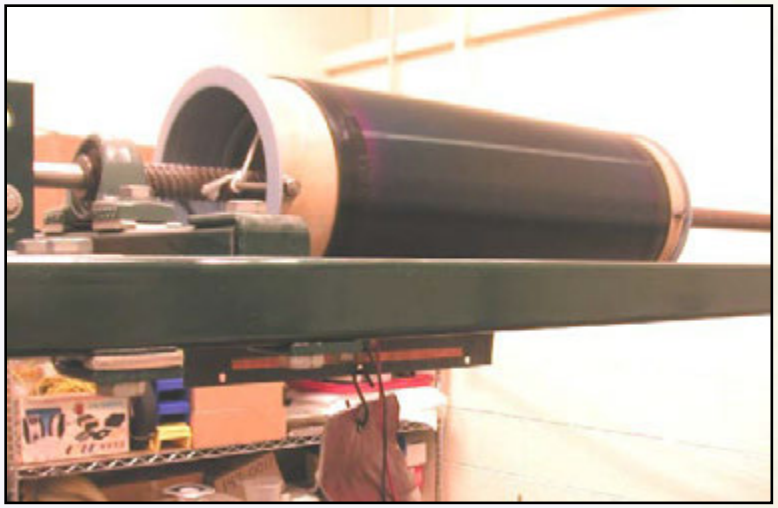
Product Development Process – Reliability

UNI-SOLAR

	GATE 1 CONCEPT	GATE 2 DEVELOP	GATE 3 VALIDATION	GATE 4 AUDIT
Marketing	Business Case	Update Business Case	Update Business Case including Roadmap	Audit Business Case and Roadmap
	Market Size and Pricing	Update Market Size, Price	Update Market Size, Price	Audit Market Size, Price
	Channel Strategy	Update Channel Strategy	Prepare Channel for Launch	Audit Channel Performance
Engineering	Product Specification (Prelim)	Detailed Product Specification	Finalize Product Specification	Verify Performance to Product Specification
	Product Layout (Concept)	Detailed Product Design and BOM	Finalize Product Design	Develop Continuous Improvements
	FMEA and Risk Reduction	Perform Internal Qualification	Perform External Qualification and Beta Tests	Reliability Audit with Corrective Actions
Operations	Preliminary Mfg Concept	Detailed Mfg and Quality Plan	Demonstrate Mfg Plan and Quality System	Audit Mfg Performance and factory quality
	Sourcing	Detailed Sourcing Plan	Production Suppliers under contract	Audit Supplier performance and quality
	Mfg Cost Estimates	Detailed Cost Estimates	Validate Cost Estimates	Confirm cost actuals meet business case
Field Service	Install and Field Support Concept	Detailed Install and Field Support Plan	Demonstrate Installation, maintenance procedures	Audit installation and maintenance procedures
	Installation and O&M cost estimate	Detailed Installation and O&M estimates	Validate Install and O&M cost estimates	Audit Install and O&M costs, warranty issues.
Legal	IP Search and Filing	Update IP Search and Filing	Update IP Search and Filing	Check for infringement

Unique Reliability Testing – Flexible PV

Cyclic Flex Test (Fatigue test): Useful for evaluating interconnect and bus bar designs, thin-film and encapsulant mechanical integrity. Flexible modules are subjected to flexing and coiling conditions





Hot water immersion is used for down-selection testing of polymeric materials; Inexpensive technique with high sample throughput and comparative analysis. Voltage/current biasing can be used for highly accelerated comparative testing

Application Challenges for BIPV Products

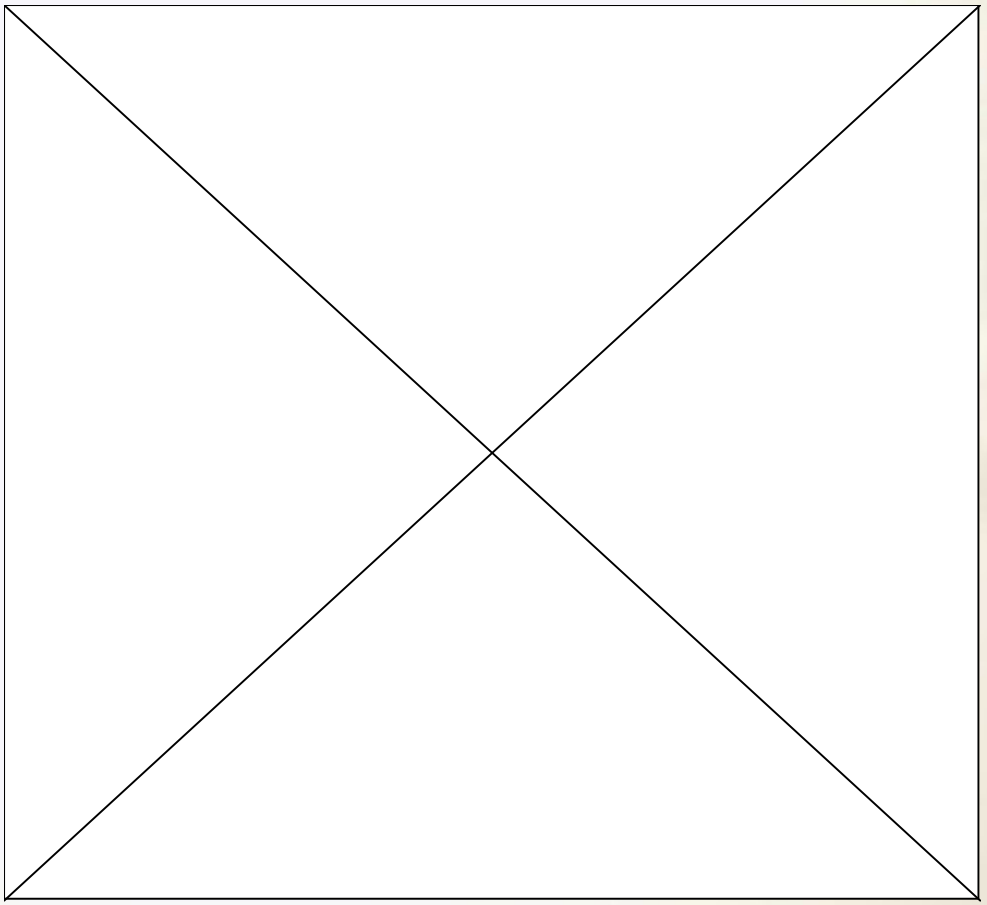
UNI-SOLAR

- BIPV/BAPV modules are integrated or attached to roofs or other part of the building (flexible membranes, metal etc), so it's critical to evaluate the application reliability of the BIPV module
  - BIPV modules are not only required to meet PV standards but also roofing/building material requirements and codes
- Several organizations are working on creating effective standards for BIPV modules, e.g. IEC TC82 (WG3), FM global and ICC-ES
- Several building/roofing material requirements, applicable to BIPV
  - Higher wind pressures for coastal regions (up to 150 mph),
  - Requirements for Hail Resistance
  - Heat aging requirements
  - Fire classification requirements per *2009 International Building Code® (2009 IBC)*
  - Wind-driven Rain test, *per Florida Building code*
  - Ultraviolet Exposure- up to 2000 hrs of exposure, *per International Building code (Double of UL/IEC requirements)*
  - Roof penetration test – *per ICC-ES, AC -07*
  - Resistance to Foot Traffic Test – *per FM 4470*

Basic Roof Construction and Application of BIPV

- BIPV modules can be attached to the roof membrane or uppermost layer of the roof

- BIPV modules must meet building and roofing codes and standards
  - *International Building Codes* (IBC)
  - US building codes published by *American Society of Civil Engineers* (ASCE)
  - Local code requirements (e.g. Miami-Dade), Factory Mutual (FM), *National Building Code* (BOCA), *the Standard Building Code,* (SBCCI); and the *South Florida Building Code* (SFBC), *ICC-ES* etc

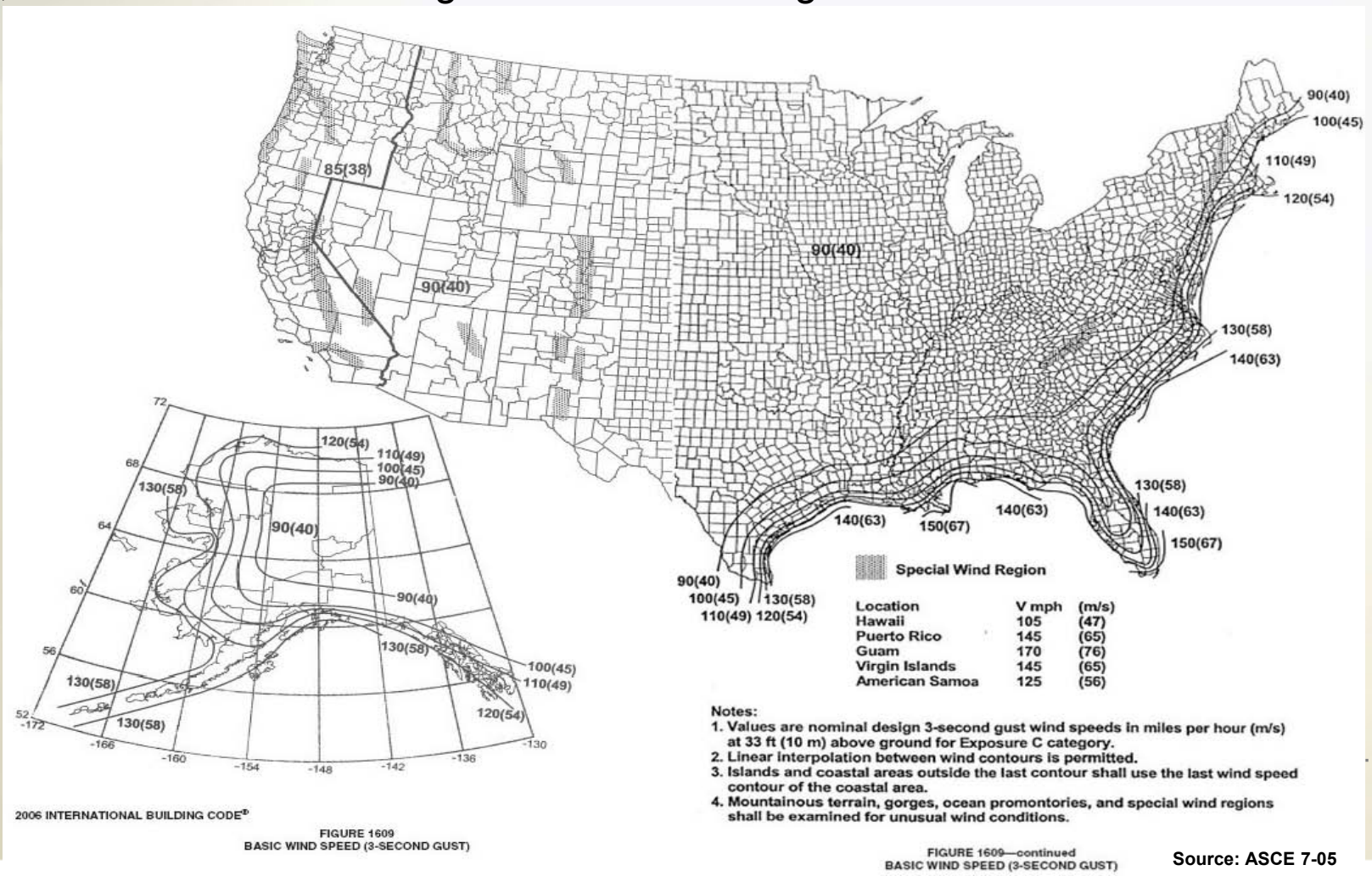


Courtesy: Carlisle SynTec

Heavy Wind Effects and Code Requirements

Certain parts of the US face heavy hurricanes, tropical storms, thunderstorms and high winds, so there are specific requirements set by regulatory bodies for building structures

US building codes use the engineering standard published by the American Society of Civil Engineers, ASCE7 “Minimum Design Loads for Buildings and Other Structures”



2006 INTERNATIONAL BUILDING CODE®

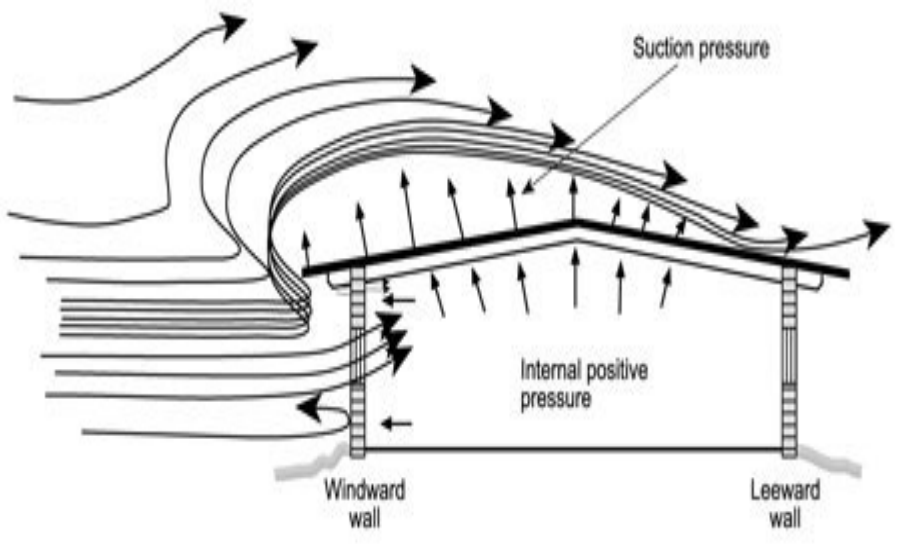
FIGURE 1609
BASIC WIND SPEED (3-SECOND GUST)

FIGURE 1609—continued
BASIC WIND SPEED (3-SECOND GUST)

Source: ASCE 7-05

Wind Uplift Resistance

- Roof /PV damage occurs when wind pressure directly above the roof is lower than below
- The result is a net upward force on the roofing system. This force is referred to as **wind uplift**.
- For hurricane zone areas the requirement for wind uplift resistance is very high
- *Standard Building Code,* (SBCCI); the *South Florida Building Code* (SFBC) and FM set the requirements for wind uplift resistance and BIPV systems. Other building/roofing materials must also comply with these codes/requirements .



BIPV System Design for Wind Uplift Resistance

- BIPV system must be designed to withstand heavy wind uplifts
- ANSI/FM 4474 standard provides a test for wind uplift resistance. The ratings are measured in psf, which correlates to wind speed using various parameters (multipliers):
  - The building's overall height
  - The terrain surrounding the structure
  - The type of roof deck on the building
  - Roof slope
  - Location of the building (city/state)
  - Usage of building
  - Location of BIPV on the roof deck/structure

(test rig – 12'x24'x4')



Uni-Solar modules tested for wind-uplift

- Solar roof (BIPV) samples are tested for wind uplift resistance using the 12' x 24' Simulated Wind Uplift Pressure Test
- Air pressure applied in 15 psf increments for one minute until failure occurs (or the limit of test equipment), ratings are given in 1-60, 1-90 or 1-120 (psf)
- All membranes and photovoltaic modules shall:
  a) not tear, puncture, fracture or develop any through openings
  b) not delaminate or separate from adjacent components

BIPV System Design for Wind Uplift Resistance

UNI-SOLAR

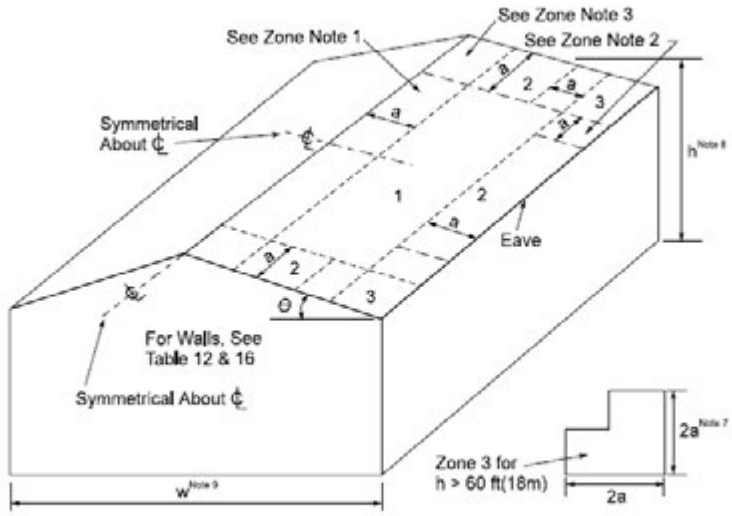
Table 5. Roof Field Area (Zone 1) Uplift Design Pressure, p, for Exposure D, Flat or Gable Roof, Θ ≤ 7° slope (For 60 ft (18 m) < h < 90 ft (27 m), limited to h/w ≤ 1); Enclosed Building

$p = 0.00256\ K_z\ K_{zt}\ K_d\ V^2\ I\ [(GC_p) - (GC_{pi})]$ *in pounds per ft² (psf)*

Enclosed Building; Roof Zone 1 (Field Area), Effective Wind Area 1 to 10 ft²;
K_{zt} = 1.0; z = h; (GC_p) = - 1.0 for h < 90 ft and (GC_p) = - 1.4 for h ≥ 90 ft; (GC_{pi}) = 0.18

Mean Roof Height h (ft)	Basic Wind Speed, V, 3-sec gust, (mph)											
	≤ 85	90	100	110	120	130	140	145	150	160	170	185
	Roof Field Area Uplift Design Pressure, p, Exposure D (psf)											
0-15	22	25	31	37	44	51	60	64	68	78	88	104
30	25	28	34	42	49	58	67	72	77	88	99	117
60	28	31	39	47	56	65	76	81	87	99	112	133
89	30	34	42	50	60	70	81	87	93	106	120	142
90	40	45	56	67	80	94	109	117	125	142	161	190
100	41	46	57	69	82	96	111	119	127	145	164	194
200	46	52	64	77	92	108	125	134	144	164	185	219
300	50	56	69	83	99	117	134	144	154	176	198	235
400	52	58	72	87	104	122	141	152	162	185	208	247
500	54	61	75	91	108	127	147	158	169	192	217	257

Source: FM Global Property Loss Prevention Data Sheets



Roof Design Negative Pressure Multipliers Zones 1, 2, 3 for Flat and Gabled Roofs

Apply multipliers to pressure values in Tables 3, 4, and 5, as appropriate.

Mean Roof Height, h	Roof Slope	Enclosed Building			Partially Enclosed Building[6]		
		Zone 1	Zone 2	Zone 3	Zone 1	Zone 2	Zone 3
h ≤ 60 ft (18 m); and when h/w ≤ 1 for 60 < h < 90 ft (18 < h < 27 m)	Θ ≤ 7°	1.0	1.68	2.53	1.31	1.99	2.85
	7° < Θ ≤ 27°	0.92	1.59	2.36	1.23	1.91	2.67
	27° < Θ ≤ 45°	1.0	1.17	1.17	1.31	1.48	1.48
when h/w > 1 for 60 ft < h < 90 ft (18 < h < 27 m) See Note 6 below	Θ ≤ 10°	1.34	2.10	2.86	1.65	2.42	3.18
	10° < Θ ≤ 27°	0.92	1.59	2.36	1.23	1.91	2.67
	27° < Θ ≤ 45°	1.0	1.17	1.17	1.31	1.48	1.48
h ≥ 90 ft (27 m) See Note 6 below	Θ ≤ 10°	1.0	1.57	2.14	1.23	1.80	2.37
	10° < Θ ≤ 27°	0.68	1.19	1.76	0.92	1.42	1.99
	27° < Θ ≤ 45°	0.75	0.87	0.87	0.98	1.11	1.11

Zone Notes:
1. Zone 1 except Zone 2 if Θ > 7°.
2. Zone 2 except Zone 3 if Θ ≤ 7° and h > 60 ft (18 m).
3. Zone 2 except Zone 3 if Θ > 7° and h ≤ 60 ft (18 m).
4. If a parapet height ≥ 3 ft (1 m) is provided around the perimeter of the roof with Θ ≤ 7°, treat Zone 3 as Zone 2.
5. 7° = 1½ in./12 in. (125 mm/m); 10° = 2 in./12 in. (167 mm/m); 27° = 6 in./12 in. (500 mm/m); 45° = 12 in./12 in. (1 m/m).
6. Partially enclosed building multipliers for roofs are based only on openings affecting the top story.
7. Value of "a":
   a) For h ≤ 60 ft (18 m), "a" is the smaller of 0.1 times the building lesser plan dimension or 0.4 times h, and never less than 4% of the least horizontal dimension, or 3 ft (0.9 m). Zone 3 is a square with dimensions "a".
   b) For h > 60 ft (18 m), "a" is 0.1 times the building lesser plan dimension, but not less than 3 ft (0.9 m). Zone 3 is an ell with dimensions ""2a".
8. Value of "h":
   a) For slopes ≤ 7°, h = eave height
   b) For slopes > 7°, h = mean roof height
9. Value of "w" is based on the lesser plan dimension.

BIPV System Design for Heavy Wind Resistance

- BIPV systems must also be designed to resist higher direct wind pressures

- ASTM D 3161: *Standard Test Method for Wind-Resistance of Asphalt Shingles (Fan-Induced Method) at a wind velocity of 160mph;* this method is primarily used for evaluating wind resistance of roofing Shingles and is also applicable to BIPV roofing systems

Test conditions:
Test time: 120 minutes
Wind speed: 160 mph at 75 ± 5°F
Roof slope: 2:12 or as applicable

Pass criterion:
No damage to roofing material/system

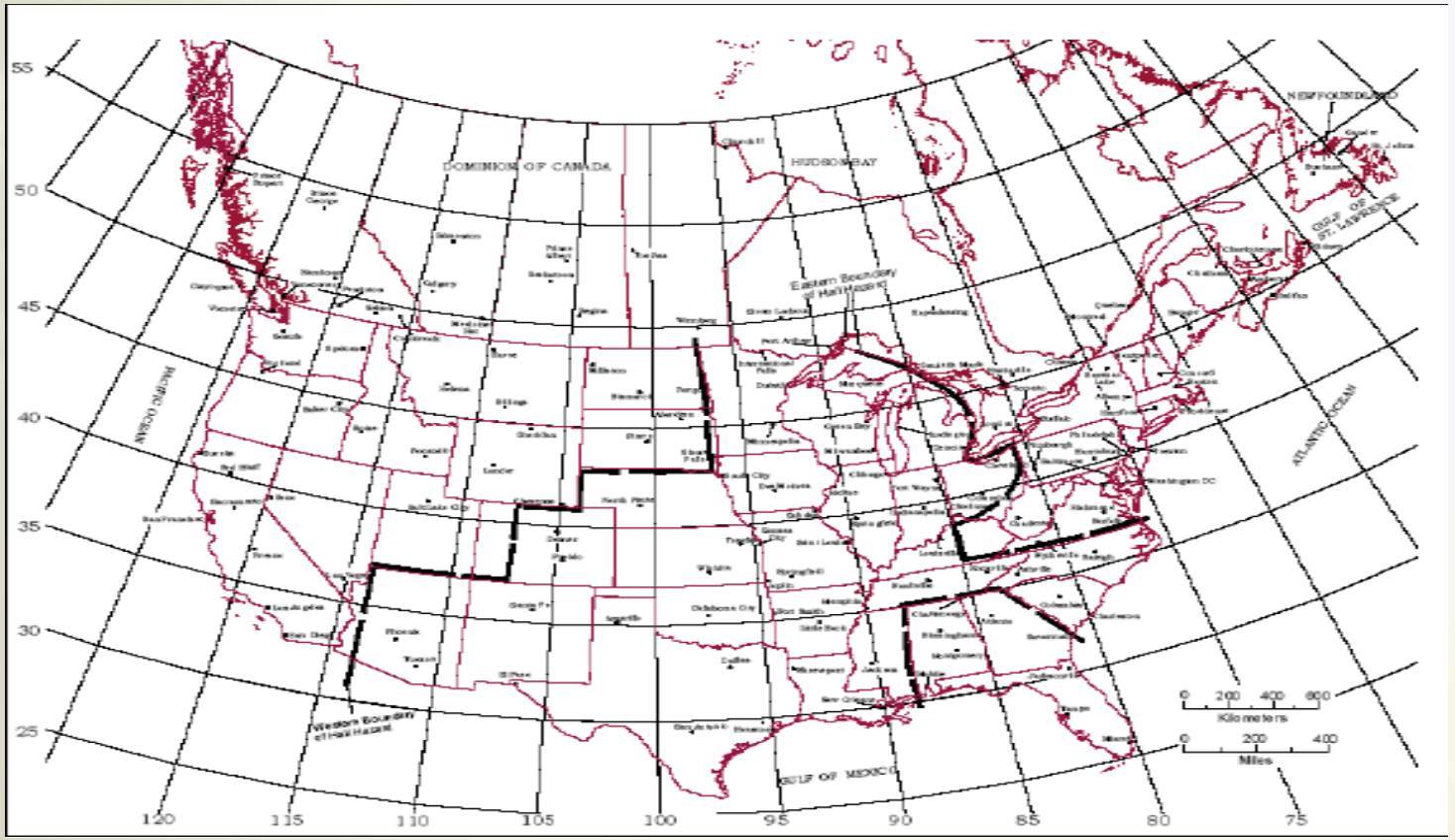


Uni-Solar laminates (performance test at **170mph)**

Effects of Hail and Code Requirements

UNI-SOLAR

- The most likely single cause of roof damage is hail; the U.S. sees about 4800 hailstorms every year
- Hail accounts for an estimated **1 billion dollars** per year in property damage in the US
- International Building Code (Chapter 38 in NFPA 5000) and FM 4470/4476 address the requirements for roof coverings/BIPV



Hailstorm Hazard Map for United States (ref: FM 4476)

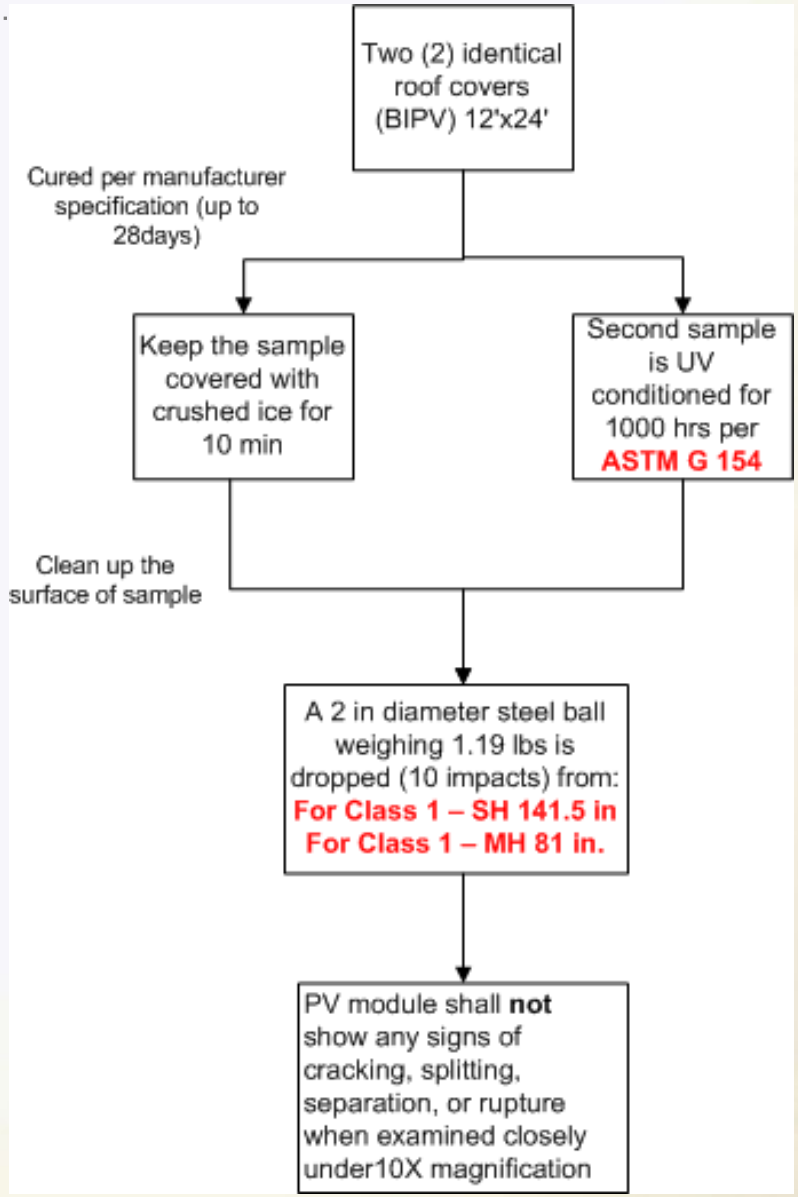
Susceptibility to Hail Damage for BIPV Systems

- **FM 4476** (Approval standard for Flexible PV modules) proposes tests to determine the susceptibility to Hail Damage for PV modules:

  Hail damage ratings:

  1. Class 1 – **SH** (Severe), impact energy 14 ft lb acceptable to use in most southern regions
  2. Class 1 – **MH** (Moderate), impact energy 8 ft lb used in rest of the country

- **UL 2218** (Impact Resistance for roof covering materials) provides a method to determine the Impact Resistance, but is not a standard for BIPV!



Retention of Adhesion for BIPV Systems

- BIPV modules can be applied to roofing membranes using an adhesive, so it is critical to have reliable adhesion strength of the membrane to PV module
- ICC –ES AC365 defines the test for Retention of Adhesion after Temperature Cycling
- This test primarily compares the adhesion strength before and after the environmental stress

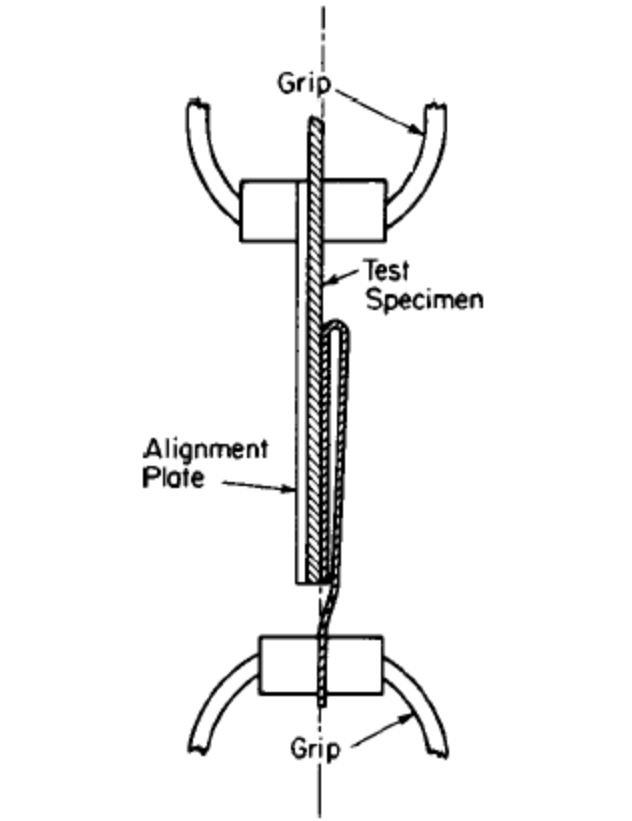
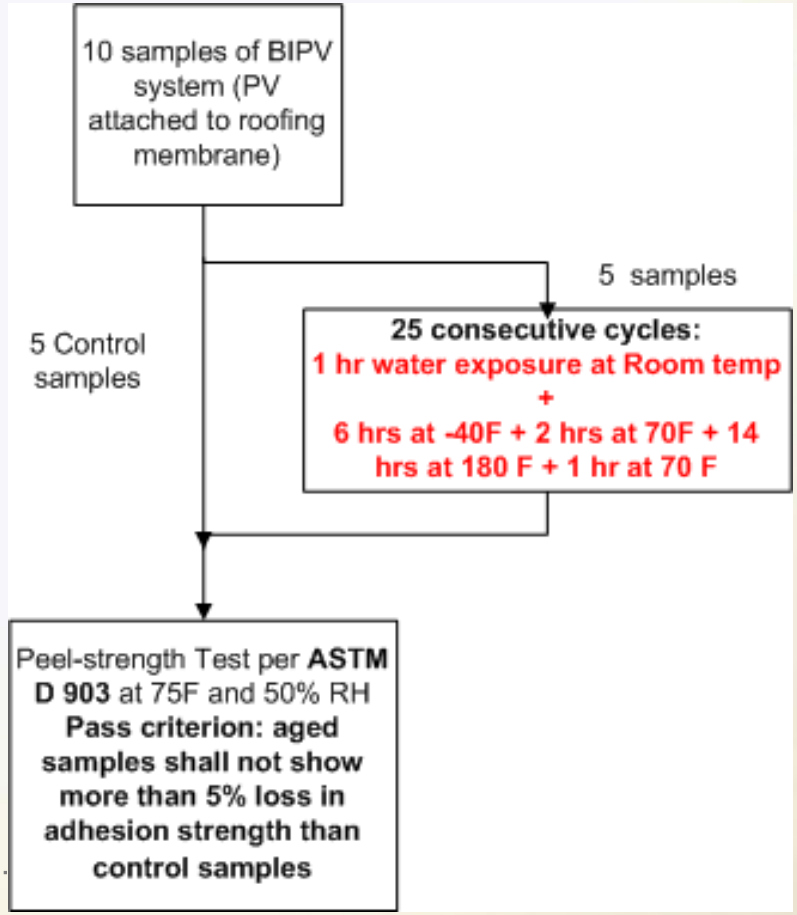


Fig: Specimen under test, per ASTM D 903



Laminate Mechanical Integrity Evaluation

The following tests can be used to evaluate mechanical integrity of the BIPV module with respect of performance of the adhesives and polymer/module interfaces

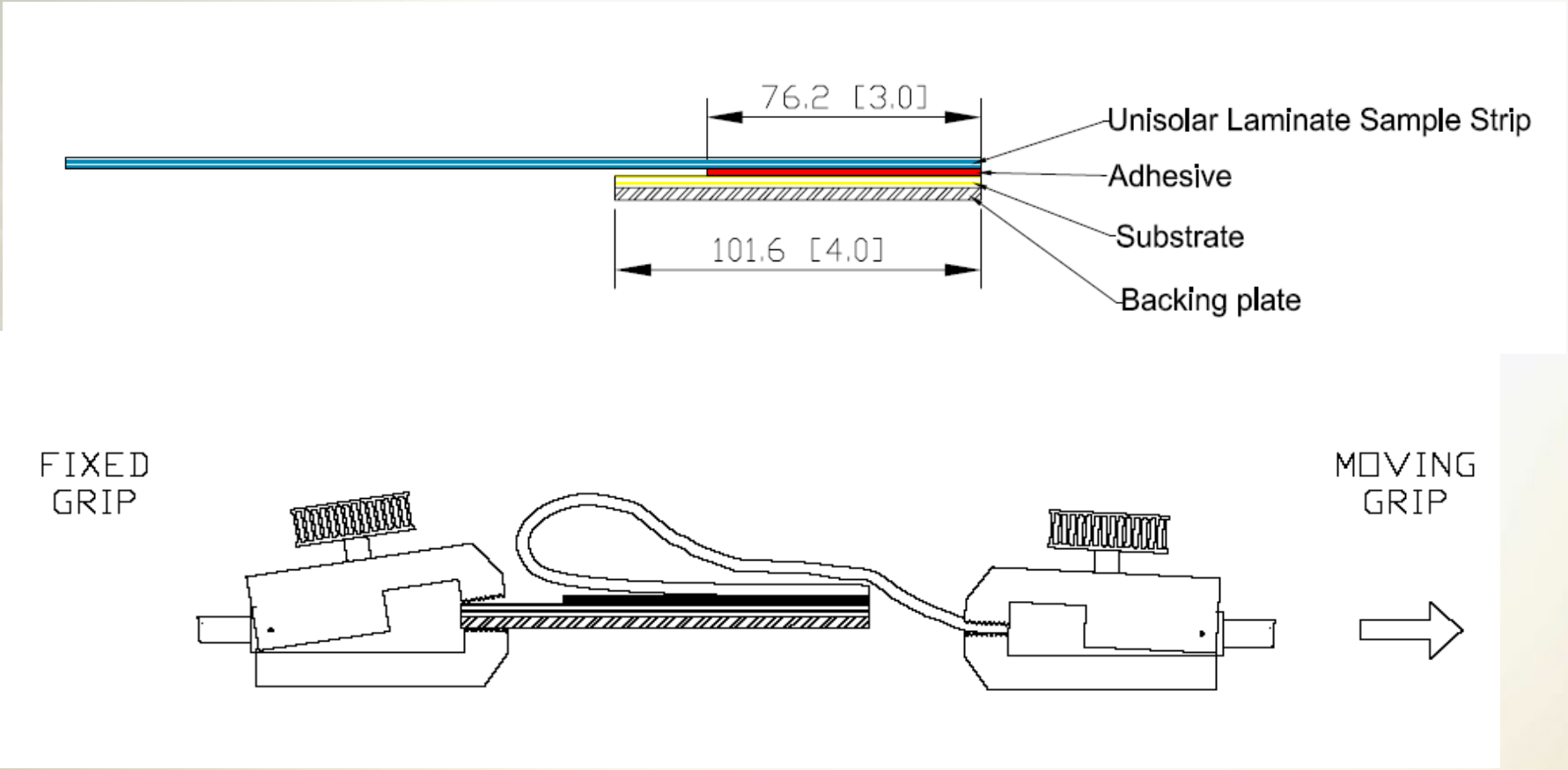
Uni-Solar Test Protocol for substrates

TEST	ASTM Test Protocol
Shear Test	ASTM D1002-05
Peel test	ASTM D 903-98(2004)
Environmental Aging	ASTM E1171 (2004)

TEST PHASES	Pre-Test		Test	Temperature Tested	Sample Size
Initial	Non Aging Test		Peel	- 40°C, RT and 85°C	5 samples/TEMP
			Shear	- 40°C, RT and 85°C	5 samples/TEMP
Final	After Environmental Aging	200 Thermal Cycles (30 days)	Peel	- 40°C, RT and 85°C	5 samples/TEMP
			Shear	- 40°C, RT and 85°C	5 samples/TEMP
		10 Humidity Freeze Cycles (10 days)	Peel	- 40°C, RT and 85°C	5 samples/TEMP
			Shear	- 40°C, RT and 85°C	5 samples/TEMP
		Damp Heat 1000 hrs (42 days)	Peel	- 40°C, RT and 85°C	5 samples/TEMP
			Shear	- 40°C, RT and 85°C	5 samples/TEMP

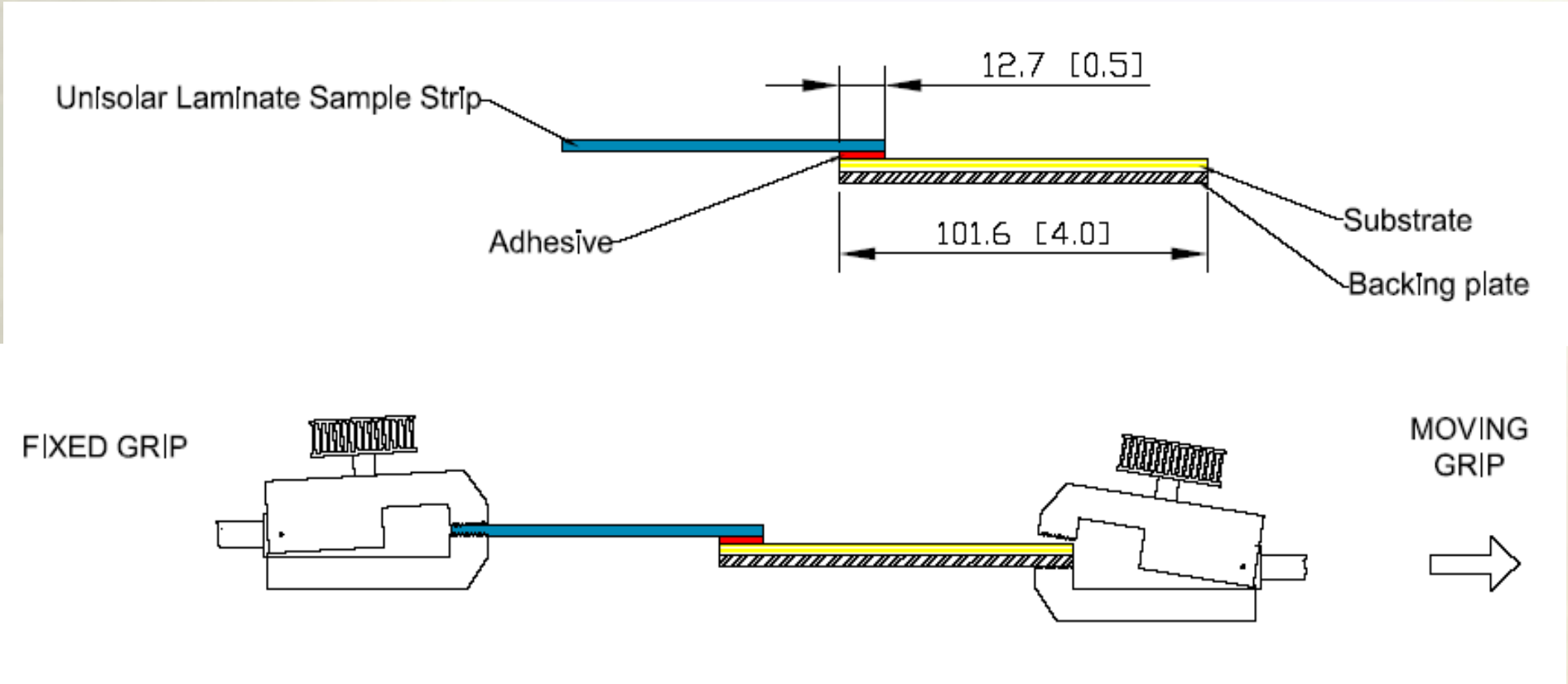
Laminate Mechanical Integrity Evaluation

Peel Samples as per ASTM-903



Laminate Mechanical Integrity Evaluation

Shear Test sample and setting as per ASTM D1002-01



Other Requirements for BIPV Systems

UNI-SOLAR

Fire

- Fire test per ASTM E108, Fire test for roof coverings or UL 790 (spread of flame and burning brand test)
- Roof slope dependent BIPV system classifications
- Various regions/states require BIPV systems to have **class A** fire rating

UV Exposure

- BIPV modules/materials are required by IBC to meet 2000 hrs of UV exposure, which is **double** the exposure that's required by UL 746C for **f1 rating** (polymer materials)

Resistance to Foot Traffic

- FM standard for BIPV, FM4470:
  - A simulated test to evaluate the performance of the roof covering when subjected to a 200 pound load a minimum of 5 times over the same area, using a 3 inch (76 mm) square steel plate
  - Sample size 12 inch (305 mm) square horizontal panel
  - Failure results if cracking, puncturing or tearing occurs

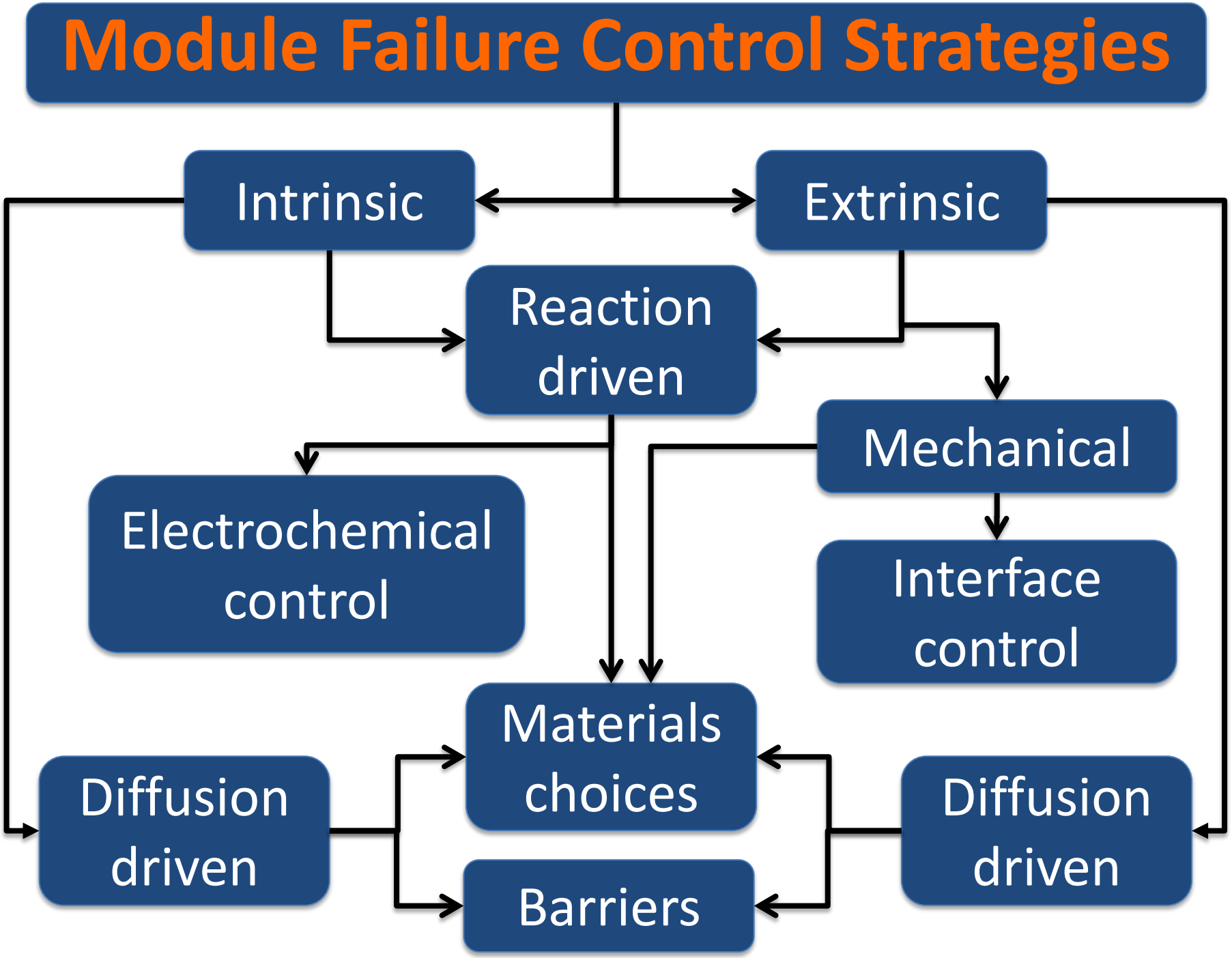
Summary

- Reliability evaluation of BIPV product is relatively challenging because of both product design and variety of applications
- Building industry codes are mature, proven and very stringent; matching with building roofing standards is a significant challenge that BIPV manufacturers must deal with and overcome
- Different regions set specific requirements, based on demographic location and environmental conditions
- Long term - Need specific tests and uniform standards for BIPV

Intrinsic Chemical Instability and Metastability in Photovoltaic Devices

Angus Rockett
Department of Materials Science and Engineering, University of Illinois
1304 W. Green St., Urbana, IL 61801
arockett@illinois.edu

This presentation does not contain any proprietary or confidential information.


Module Failure Control Strategies
Intrinsic
Extrinsic
Reaction driven
Mechanical
Electrochemical control
Interface control
Materials choices
Diffusion driven
Barriers
Diffusion driven

Module Failure Control Strategies

Intrinsic or extrinsic

Interdiffusion

Eg: SnO_2/CdS or Cu/CdTe

Thermodynamically stable interfaces

Diffusion barriers

Ti, Ta, TiN, TaN,…

Scavangers

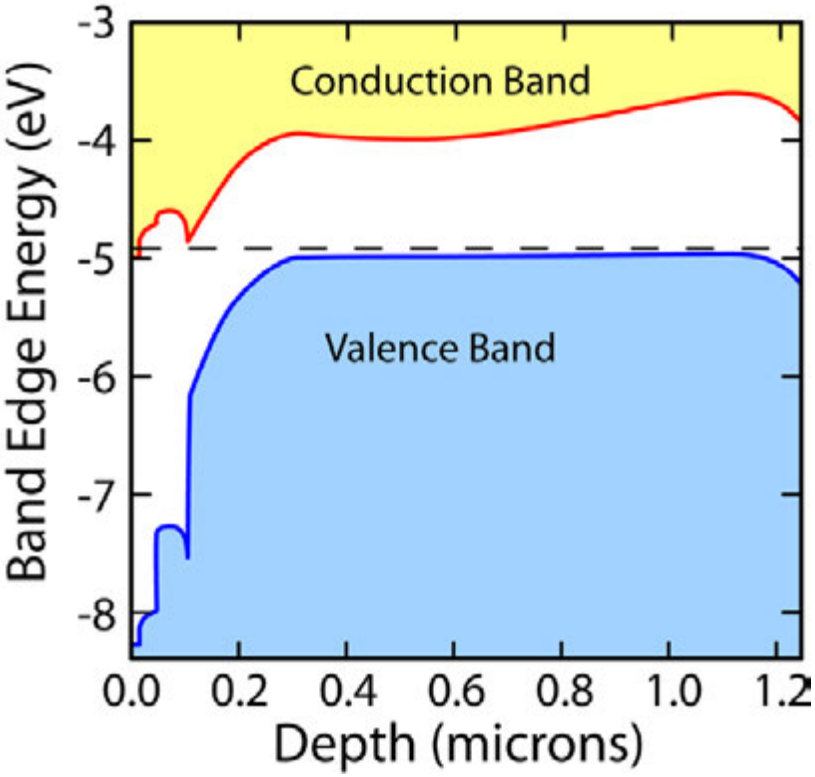
Require: 100% dense, conformal, chemically unreactive, electrically acceptable

Driven diffusion

There is a large electric field in the depletion region, which changes with forward bias. This leads to expectation of instability during operation.

May result in metastable changes in defect concentrations.

Could drive back-contact impurity diffusion in CdTe devices over time too.



Driven diffusion

Some diffusing species are charged and can respond to electric fields.

Theory shows that field driven diffusivity only increases by a factor of two. However vacancy formation energy is often chemical-potential driven. This can result in orders of magnitude changes in diffusion rates.

Vacancy formation enthalpy changes linearly with Fermi energy. Vacancy concentration changes exponentially with formation enthalpy so Fermi energy is pinned by vacancy formation.

$$\Delta E_d(q, E_f) = \Delta E_0(q) - q\Delta E_f$$

Driven diffusion

Fermi level pinning defines which defects would change near the junction.

CdTe and CIGS are both intrinsically p-type and are hard to dope n-type. Therefore when the Fermi energy rises (for example near the junction) we can expect formation of extra cation vacancies.

$$D_{impurity} = D_{q=0} + \sum_{q \le -1} D_{-q} \left(\frac{n}{n_i} \right)^{-q} + \sum_{q \ge 1} D_{+q} \left(\frac{p}{n_i} \right)^{q}$$

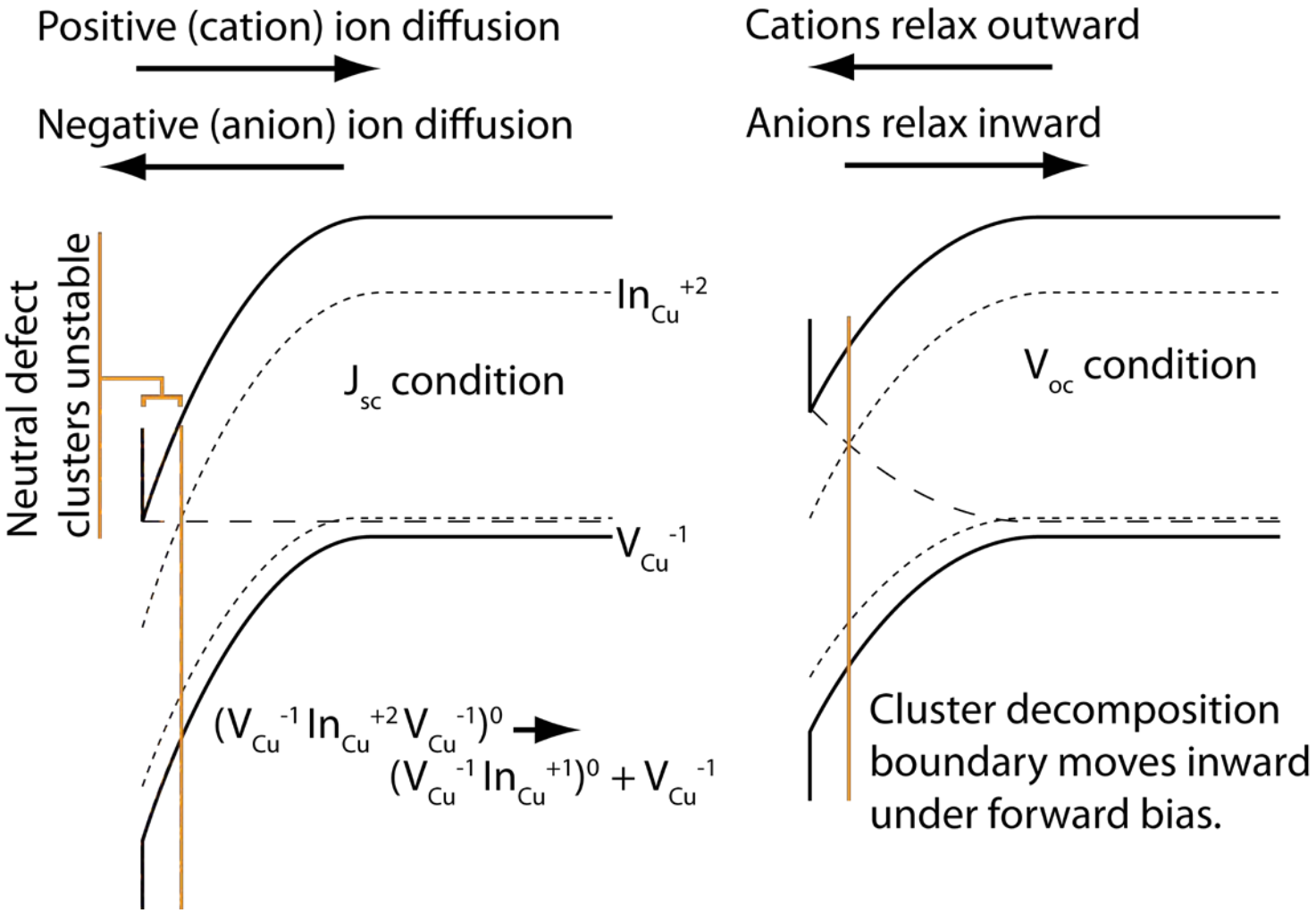
Diffusivity of species diffusing by cation vacancies (presumably the cations in the ionic material) would be expected to increase rapidly near the junction.

The vacancy gradient can drive diffusion more effectively than the field. This may be the most important factor for Cu diffusion in CdTe.

Kinetics probably limits diffusion in CIGS modules.

Metastability in CIGS Devices

Consider the electric field around the CIGS device junction:

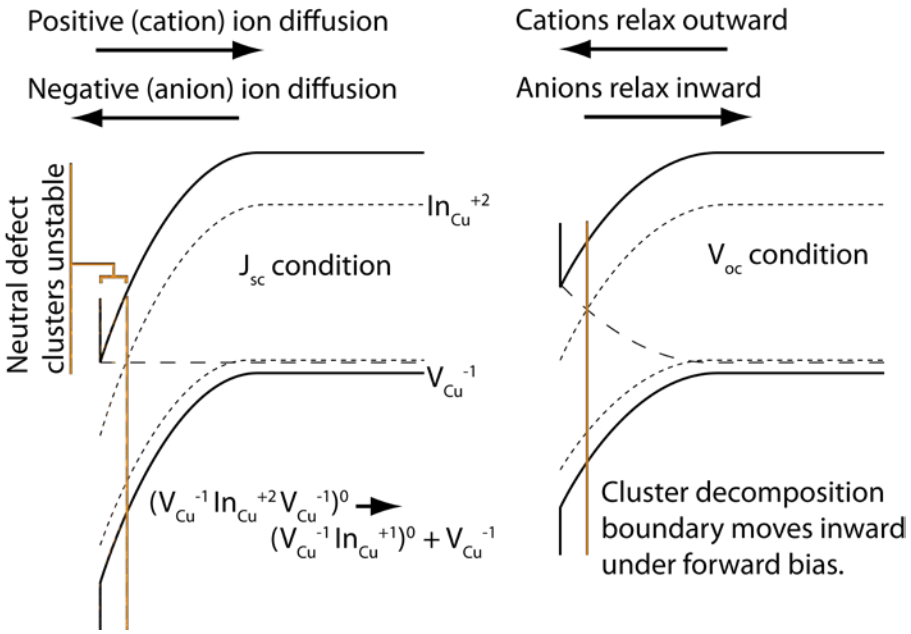


Possible moving species: Na^+ (grain boundaries only), vacancies (probably Cu)

Metastability in CIGS Devices

The neutral defect cluster is unstable in n-type material and can release a large number of Cu vacancies. This could significantly alter atomic mobility.

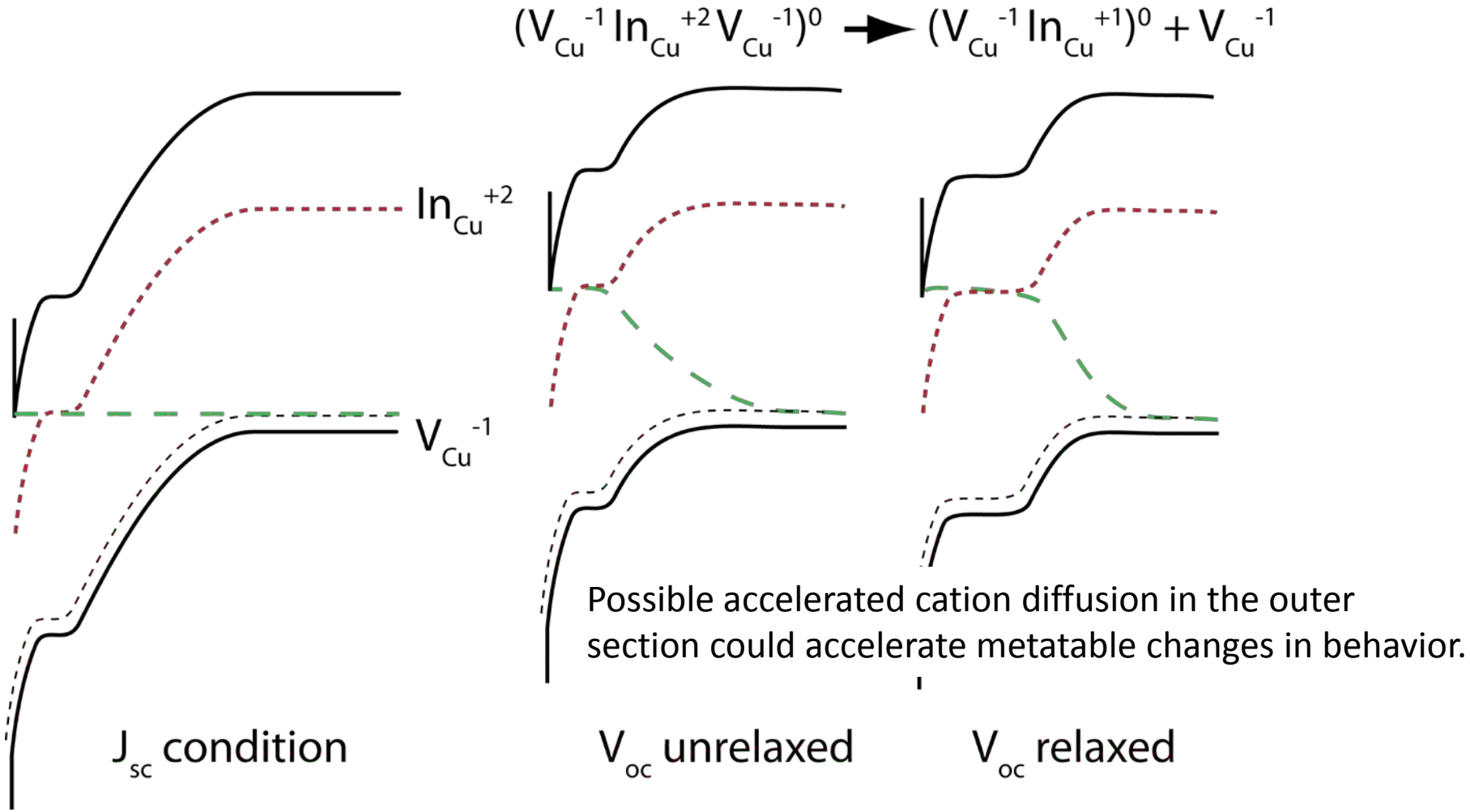
Of course at <100°C it is unlikely that the system is in equilibrium. Kinetics for long-range (nm) atomic transport seems likely too slow to explain metastability data.



Large numbers of defects can pin the Fermi level (at least over a range of depths). This may account for the metastable behavior.

Metastability in CIGS Devices

An example of metastable changes in a device due to forward bias, not requiring long range atomic transport.



Possible accelerated cation diffusion in the outer section could accelerate metatable changes in behavior.

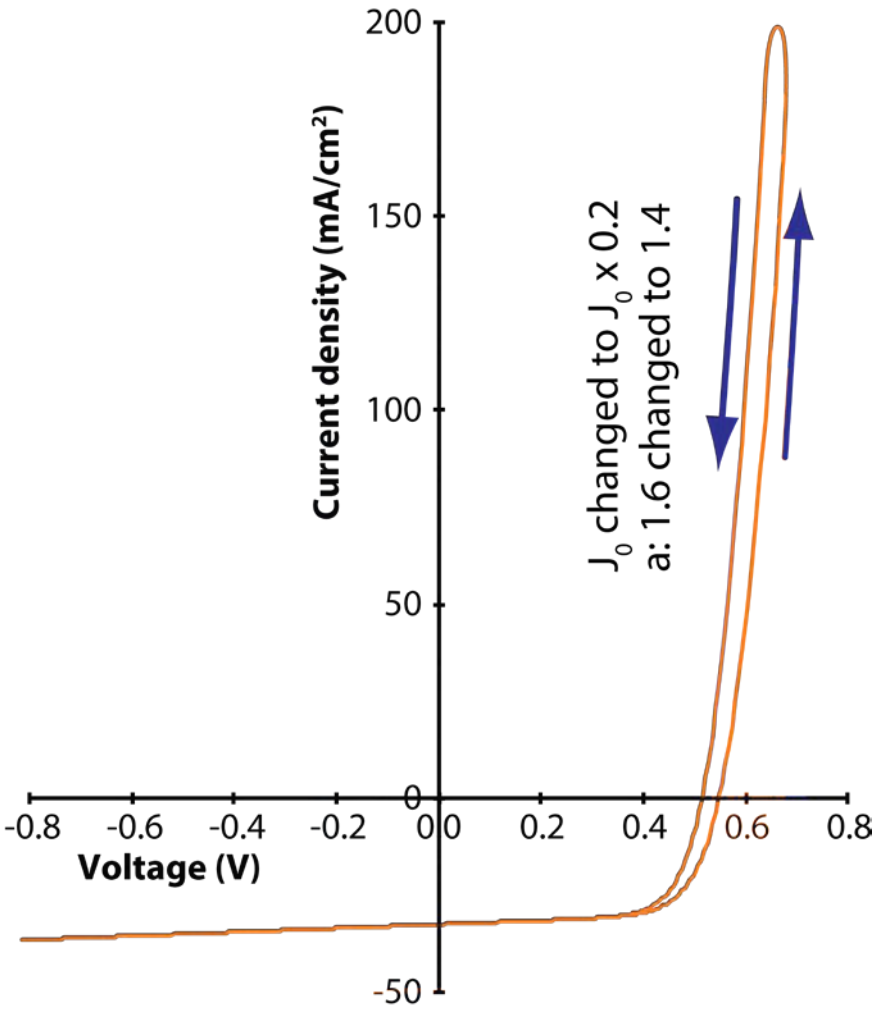
Short term metastability

j/V measurements (for example in CIGS cells) can show hysteresis, typically with sweep up showing a larger ideality factor and dark current.

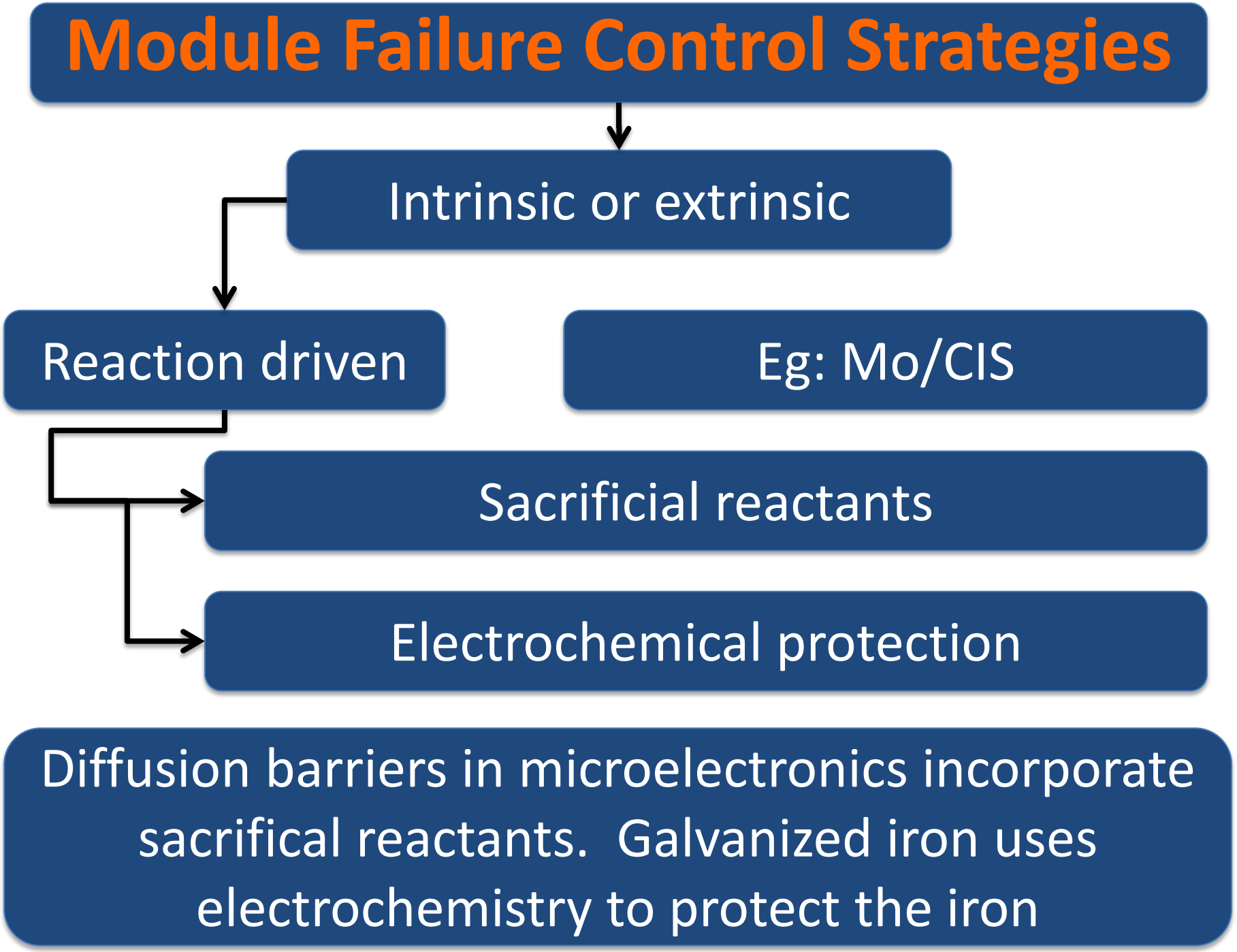
This represents metastable filling of trap states in the base by emitter injection current. **There is no atomic motion in this case.**

Sweep frequency can give information on trap depth based on the magnitude of hysterisis vs. sweep frequency.

Simulated metastable response

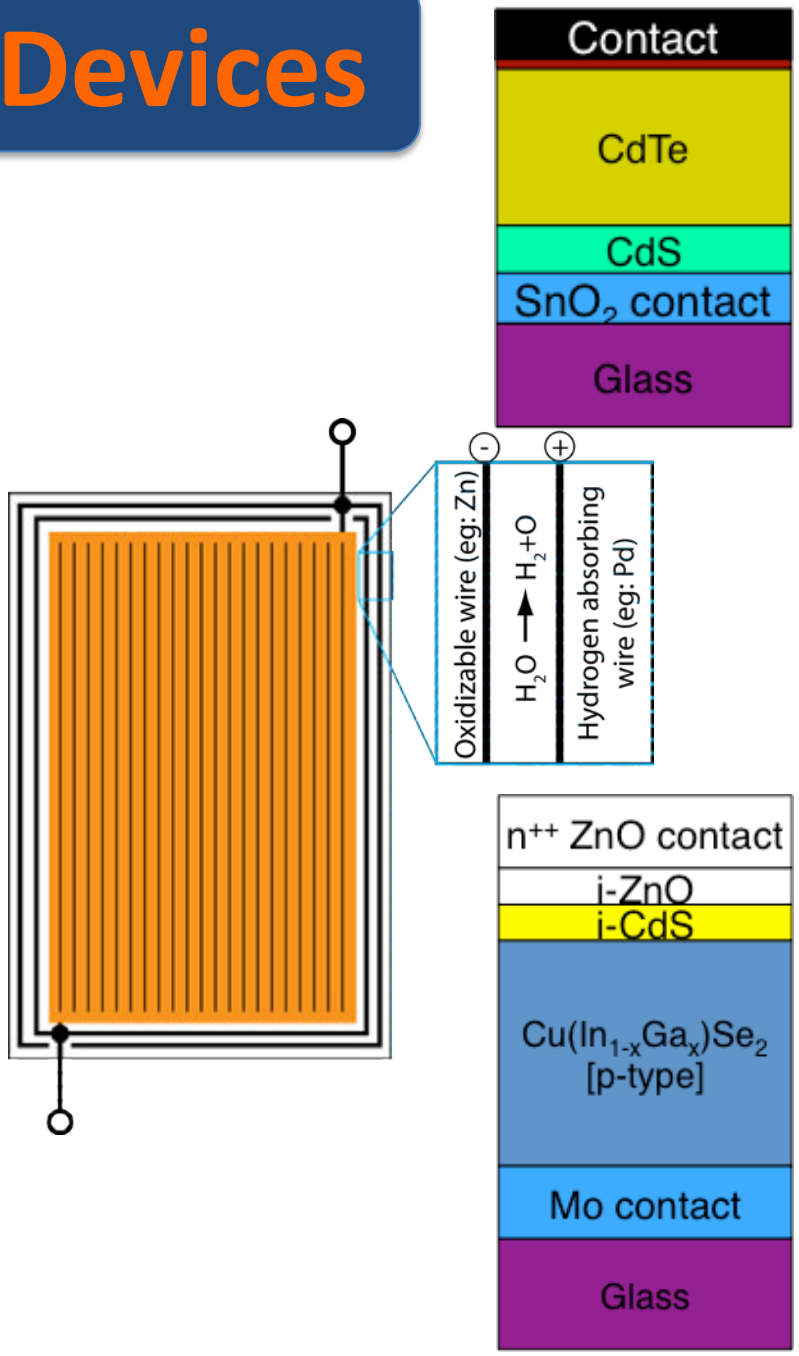


Module Failure Control Strategies



Water in Thin Film Devices

- TCO degradation: reaction with water.
- Consider active electrochemical control.
- Electrolyze the water in the module. Scavange the oxygen and hydrogen.
- Sacrificial wires integrated into module boundaries coupled to the output electrodes to drive electrolysis.



Module Failure Control Strategies

Intrinsic or extrinsic

Reaction driven → Encapsulant yellowing

Any organic (or amorphous network) that absorbs a photon breaks a bond. That bond may not reform if it has alternatives.

Selective absorbers

Molecular scavangers

Stable molecules

Module Failure Control Strategies

Intrinsic or extrinsic

Mechanical

Eg: tab & string failures

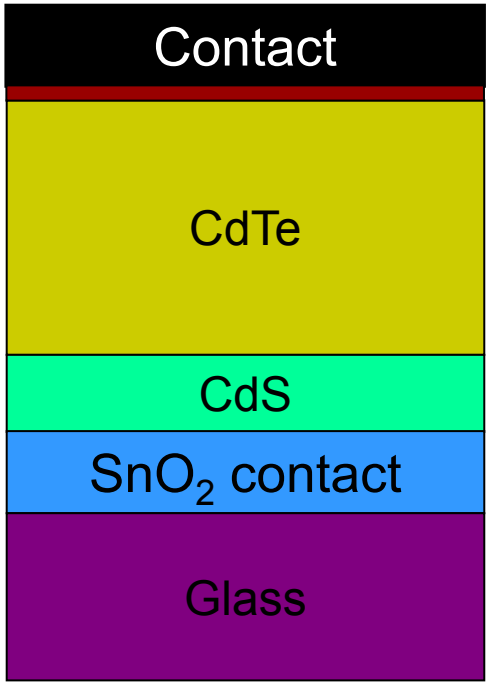
Soft inclusions in laminant

Lubrication of interfaces with laminant

The interface between the device/interconnect and the laminant can be adjusted. This can reduce mechanically-driven failures.

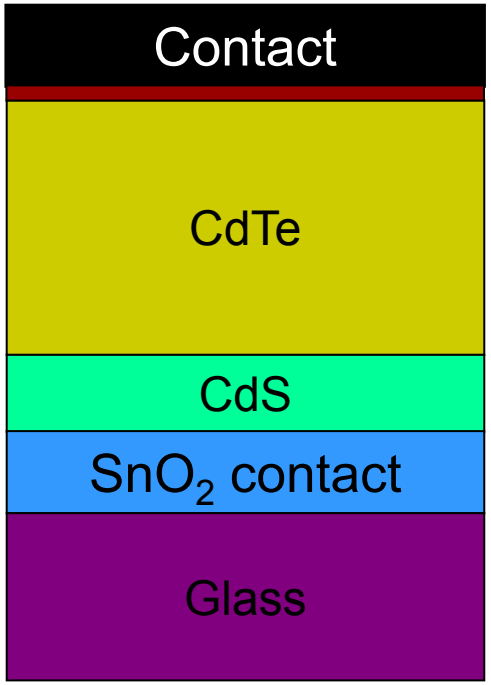
CdTe Thin Film Devices

- Thermodynamically unstable:
- SnO_2/CdS
- CdS/CdTe
- CdTe/[Cu_2Te]/C:Cu



CdTe Thin Film Devices

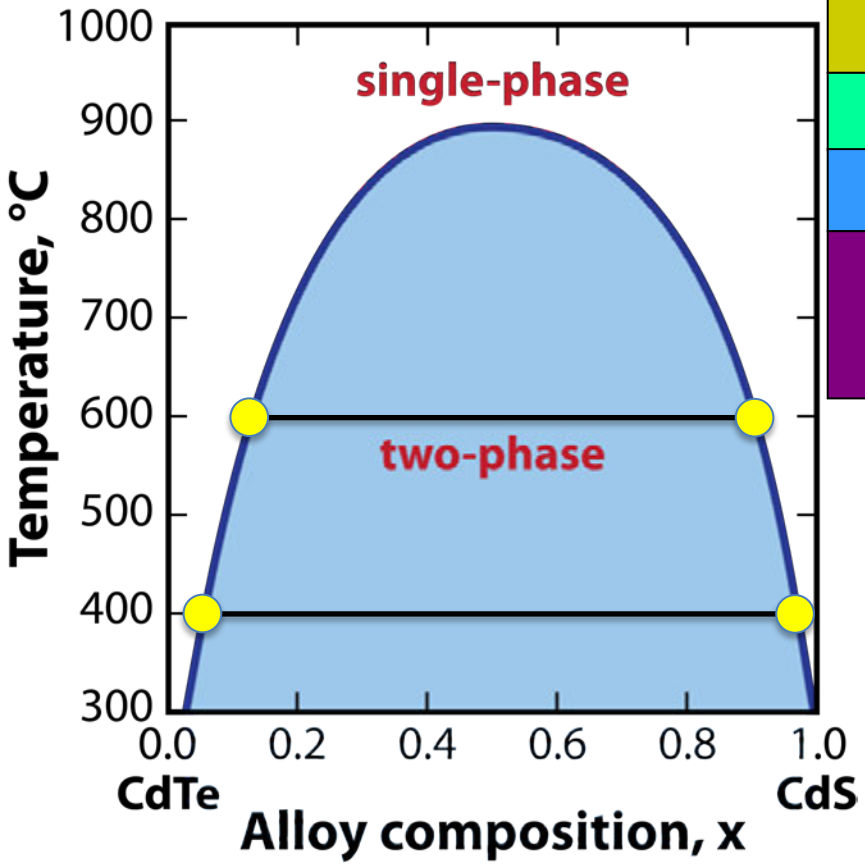
- CdS/CdTe interface: intrinsically stable if in equilibrium (but it is not). However, kinetics probably makes it adequately metatstable.



Heat-up: mutual dissolution

Cool-down: precipitation of alloy resulting in regrowth of a graded junction

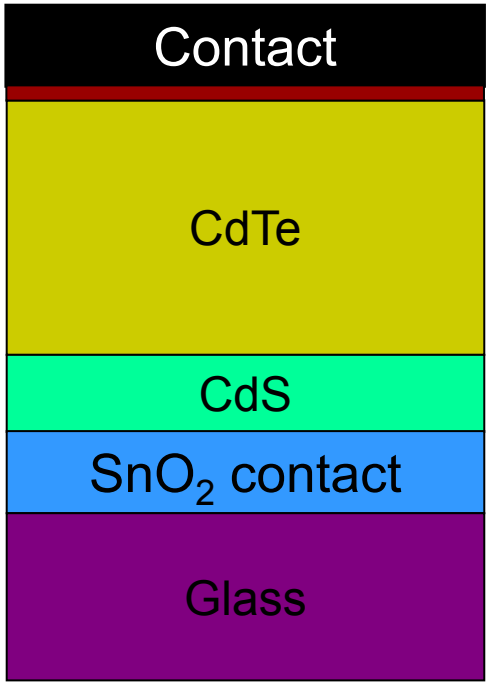
When transport freezes out local second phase preciptiation is possible.



At some temperature transport freezes out. That determines the composition grading at the heterojunction.

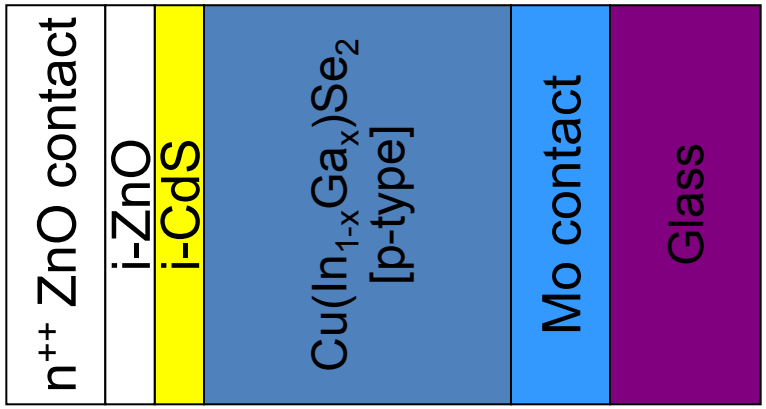
CdTe Thin Film Devices

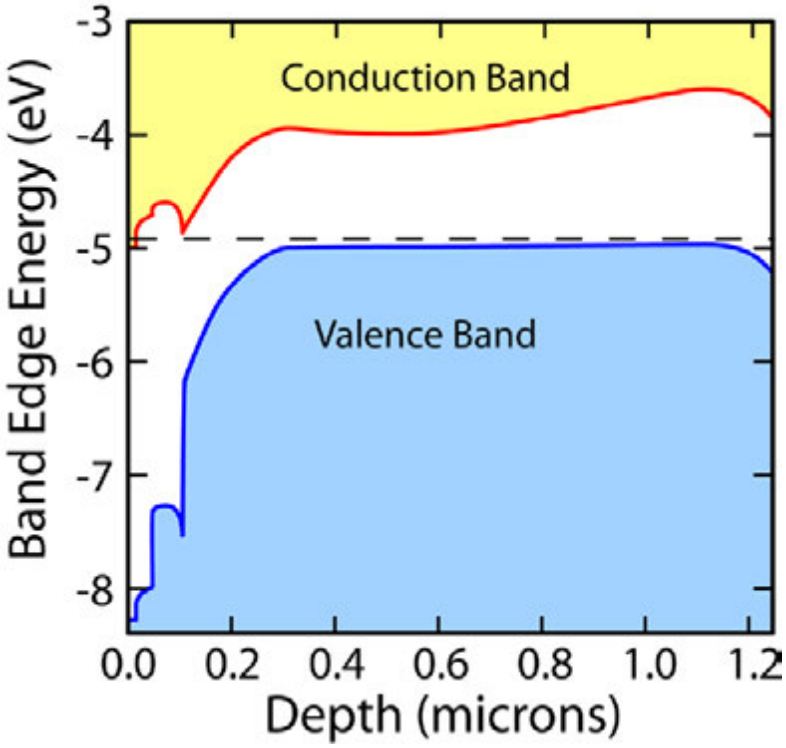
- SnO_2/CdS interface: Interdiffusion can be expected (thermodynamically favored, kinetically limited).
- Interdiffusion in this case yields Cd_2SnO_4 (cadmium stannate), an excellent TCO, comparable to or better than SnO_2.
- As long as the CdS is not consumed you should not be sensitive to interdiffusion.
- Diffusion kinetics is by far the fastest during CdTe deposition so further degradation is unlikely during operation.



CIGS Thin Film Devices

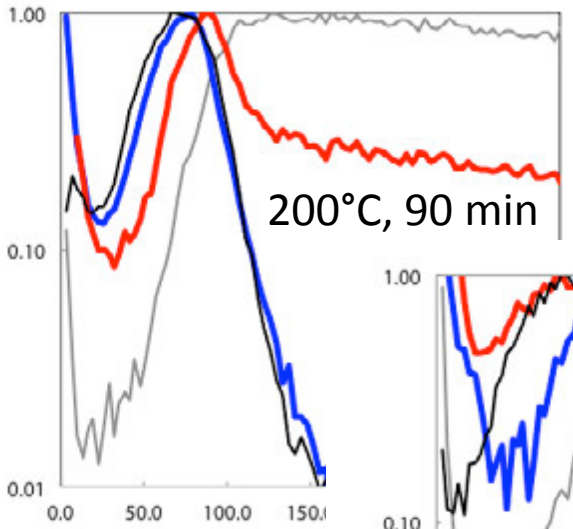
- Thermodynamically unstable:
- TCO: see I. Repins talk.
- ZnO/CdS
- CdS/CIGS
- CIGS point defects
- CIS/CGS (gradient)
- CIS/[$MoSe_2$]/Mo

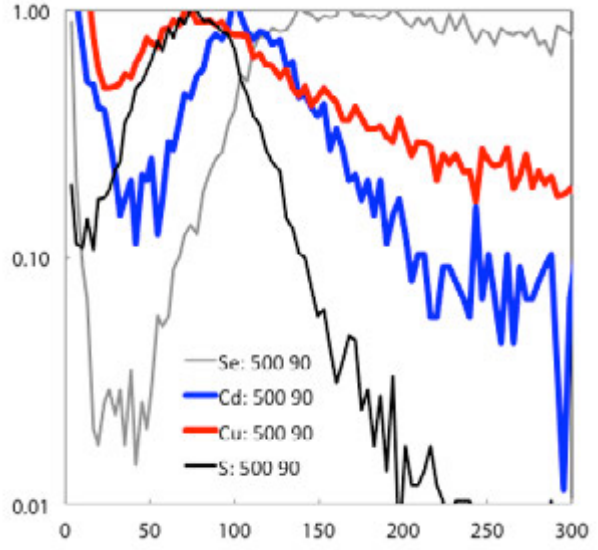




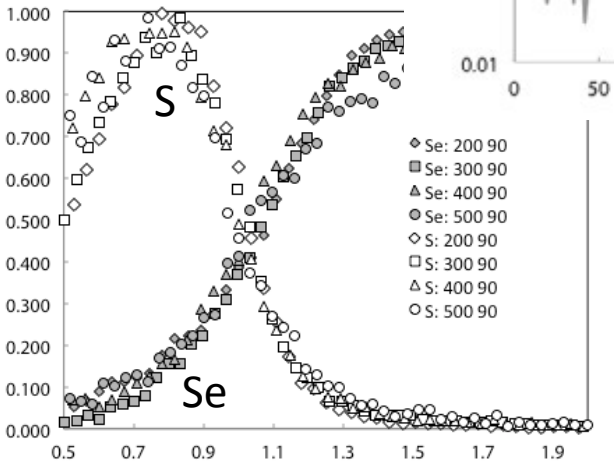
CIGS Thin Film Devices

- **CdS/CIGS Interface:**
- We measured CdS/CIS interdiffusion by SIMS on epilayers and polycrystals as a function of anneal temperature.
- Diffusion turns on around 400°C.
- Some evidence of a $Cd(CuIn)(S,Se)_2$ compound.
- No group VI movement.
- Diffuses rapidly in grain boundaries.
- Probably not much going on under operating conditions.





500°C, 90 min



CIGS Thin Film Devices

- **Mo/$MoSe_2$/CIGS:**
- Reaction with water similar to Al/Se reaction with water (but slower).
- Se loss would reduce p-type doping at the back contact, increasing resistance.
- $MoSe_2$ loss could result in a Schottky rather than an ohmic contact.

$$MoSe_2 + 2H_2O \rightarrow MoO_2 + 2H_2Se$$

Endothermic but if H_2Se is lost as a gas the law of mass action will drive it to products.

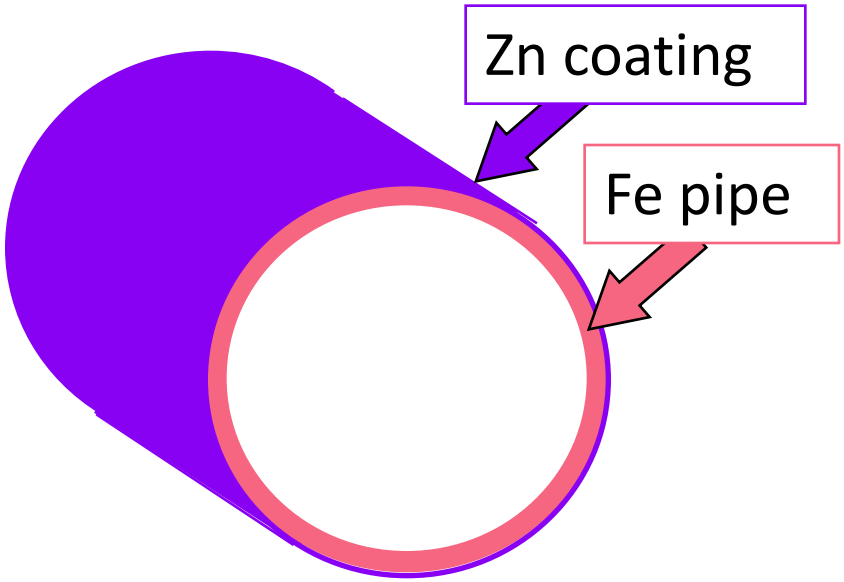
ΔH_f $MoSe_2$: -234 kJ/mol
ΔH decomposition $MoSe_2$ to Mo + Se_2(g): 378 kJ/mol
ΔH_f MoO_2: -586 kJ/mol
ΔH_f H_2Se: -29 kJ/mol
ΔH_f H_2O: -242 kJ/mol

Conclusions

- Module failures can be divided into diffusion-based, reaction/chemistry based, and mechanical failures.
- Barriers and sacrificial materials may help but choice of materials for slow kinetics may be the only real solution.
- Metastable phenomena may occur driven by changes in the Fermi level in the solid. However, kinetics makes long-range transport unlikely.
- Transient effects probably due to change of charge state of deep defects or clusters.

Electrochemistry:
Application -- corrosion protection

Electrolytic protection controls where corrosion occurs
Example: Zn protection of Fe



Because the Zn is higher on the electrochemical series than Fe, it corrodes in preference to the Fe.

Most of the available oxidizing species react with the Zn.

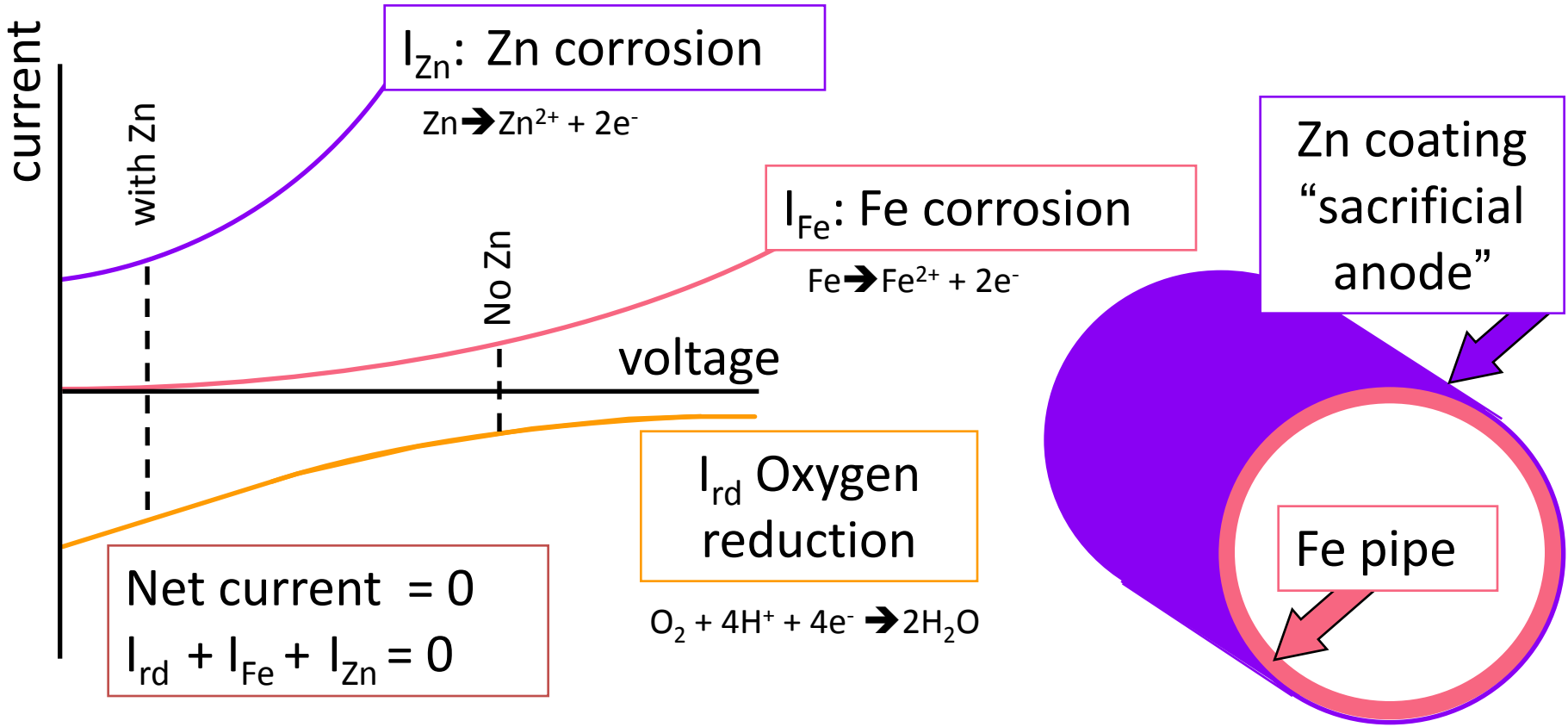
Until the Zn is completely gone it protects the Fe.

The electrochemical series:

$Mg \rightarrow Mg^{+2} + 2e^-$	+2.37	V
$Al \rightarrow Al^{+3} + 3e^-$	+1.66	V
$Zn \rightarrow Zn^{2+} + 2e^-$	+0.76	V
$Fe \rightarrow Fe^{2+} + 2e^-$	+0.44	V
$H_2 \rightarrow H^+ + e^-$	0.00	V
$Cu \rightarrow Cu^{2+} + 2e^-$	-0.34	V

Electrochemistry:
Application -- corrosion protection

The protection reaction can be quantized by looking at the current/voltage curve (voltammogram) for the reactions:



NREL
NATIONAL RENEWABLE ENERGY LABORATORY

Analysis of Alternate Methods to Obtain Stabilized Power Performance of CdTe and CIGS PV Modules



J.A. del Cueto, C.A. Deline, Steve Rummel

February 17, 2011
Reliability Workshop
Denver West Marriott

Testing, Evaluation and Reliability Team, Outdoor Test Facility (OTF)

NREL/PR-5200-51046

NREL is a national laboratory of the U.S. Department of Energy, Office of Energy Efficiency and Renewable Energy, operated by the Alliance for Sustainable Energy, LLC.

Outline

- Challenge: Transitory performance of CIGS & CdTe PV
- Study plan to probe metastable behavior
  - comprising preconditioning, thermal stress, indoor light or current soak in dark at 65° C, subsequent long-term outdoor exposure
- Modules used in study:
  - Group 1 – ended beginning of last year
  - Group 2 – finished end of last year
  - Group 3 – started end of last year, currently ongoing indoor exposures
- Cursory review of earlier Group 1 data
- Analysis of Group 2 data
- Update Status of Group 3 data
- C-V profiling data possible signature or metastability
  - carrier concentrations, depletion widths on CIGS & CdTe modules
- Summary

Issue: Transitory Electrical Behavior

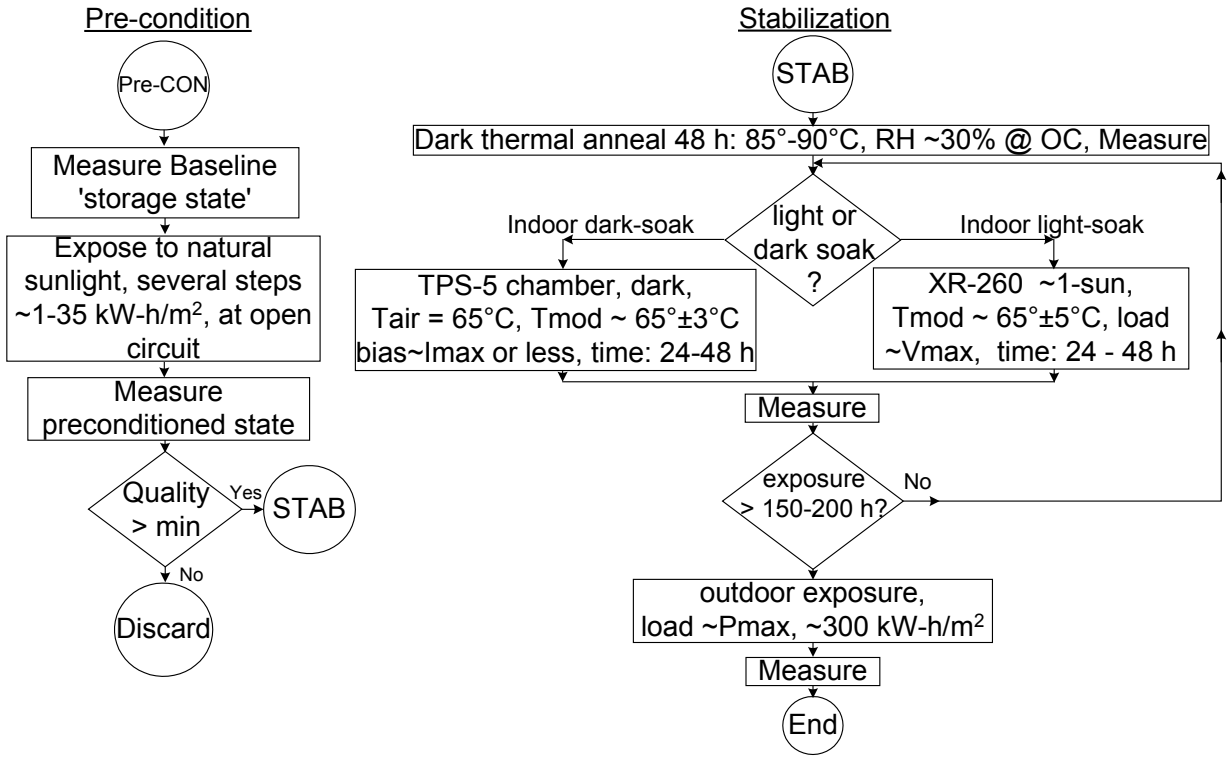
- High efficiency CdTe & CIGS thin-film PV devices exhibit transitory changes in electrical performance (I-V) at rapid (secs) & longer-term (hrs-weeks) time scales, specially after dark thermal stress or bias/light exposures
  - presents challenge assessing performance if I-V traces not consistent
  - prior history makes time between exposure and I-V measurement critical
- IEC 61646 certification standard for stabilizing thin-film PV calls for light-soaking until changes in power ≤ 2% achieved, in successive intervals of ~43 kW-h/m^2 of integrated irradiance
  - designed for a-Si, where defect mechanism is creation of dangling-bonds via light-induced Staebler-Wronski effect (SWE),
  - probably inadequate for CIGS or CdTe as these devices have different defect mechanisms
  - may even be inadequate for a-Si, because to get past SWE one really needs at least 400 h light exposure before testing for power changes between small intervals(43 kW-h)

Solution: practical preconditioning/stabilization steps

- Stabilization procedure is better if it addresses:
  - Reduced error assessing performance & measurement of temperature coefficients
    - impacts accuracy of models for long-term energy yield, and/or reliability
  - Feasibility questions: How long does it take? Resources & costs involved?
  - May need to dissect 'transitory' behavior into parts, reflecting time:
    - Metastable: addressing slower (maybe reversible) changes (occurring over days/weeks) that saturate to and correlate with actual field performance
    - Transients: rapid changes occurring on time scales: seconds to minutes
      - ✓ Short preconditioning step may stabilize fast/large transients & allow for manufacturers to (who must) count Watts-out per unit time from production
      - ✓ May be possible to establish correlation factor between performance assessed after preconditioning & that after stabilization steps,
        - thereby providing more accurate watts-out/time count from preconditioned state measurements
    - Instability: longer time scale, likely mostly irreversible change

Preconditioning /Stabilization Study Plan

- Preconditioning steps:
  - Wring out rapid transients, outdoor exposure at open circuit (OC) w/o temperature control
- Main Stabilization Sequence:
  - dark thermal anneal, emulates short version of stress tests in IEC certification
  - Studied two branches: 1) light soak & 2) current-soak in forward-bias in dark, ~65° ±5° C
  - Current-soak in dark is advantageous because of ease and lower cost of implementation
  - Final Outdoor exposure ~ 300 kW-h/m2 to correlate and validate indoor & outdoor stabilization



Modules Studied Groups 1, 2 and 3

- Group 1: diverse set of CdTe & CIGS mostly older modules
  - Some stored previously as controls, un-exposed; some pre-exposed outdoors; some light-soaked indoors; some new
- Group 2: 6 CIGS & 6 CdTe, identical models each type
- Group 3: 6 CdTe identical modules

Module Type	Group	Quantity	Configuration	Pre-existing exposure conditions
CdTe A	1	2	Glass-superstrate-glass laminate, monolithically interconnected	Yes, outdoors 3 years
CdTe B	1	2	Glass-superstrate-glass laminate, monolithically interconnected	Unexposed
CdTe C	1	1	Glass-superstrate-glass laminate, monolithically interconnected	Yes, indoor light-soak, 1130 kW-h in 2002
CIGS A	1	4	Glass-substrate-glass laminate, monolithically interconnected	Unexposed, 3 controls from 2003
CIGS B	1	2	Glass-flexsubstrate-glass laminate, solder bond interconnect	Unexposed, new
CdTe U	2	6	Glass-superstrate-glass laminate, monolithically interconnected	Unexposed, new
CIGS X	2	6	Glass-substrate-glass laminate, monolithically interconnected	Unexposed, new
CdTe W	3	6	Glass-superstrate-glass laminate, monolithically interconnected	Unexposed, new

Module Groups 1, 2 & 3: Prior & Present Exposure Steps

- Group 1
  - Initial CdTe A, C or CIGS A performance 5-6 years prior to baseline, was higher due to exposures outdoor or indoor
  - Phase I: part of the modules went through light soaking, part went into current soaking in dark forward-bias in;
  - Phase II: swapped modules, e.g., those previously in light-soak went to through dark current-soak and vise versa
  - Final outdoor exposure ~ 295 kW-h (after phase II) under load

- Groups 2 & 3
  - No prior exposures
  - Preconditioning, thermal anneal
  - Indoor chambers: start 3 in Light soaking, 3 in forward-bias current soaking in dark consisting of 5 steps (24-h, 48-h, 48-h, 48-h, 48-h)
  - Group 2, has final outdoor exposure 292 kW-h
  - Group 3 data up to 5th indoor increment, outside stabilization in progress

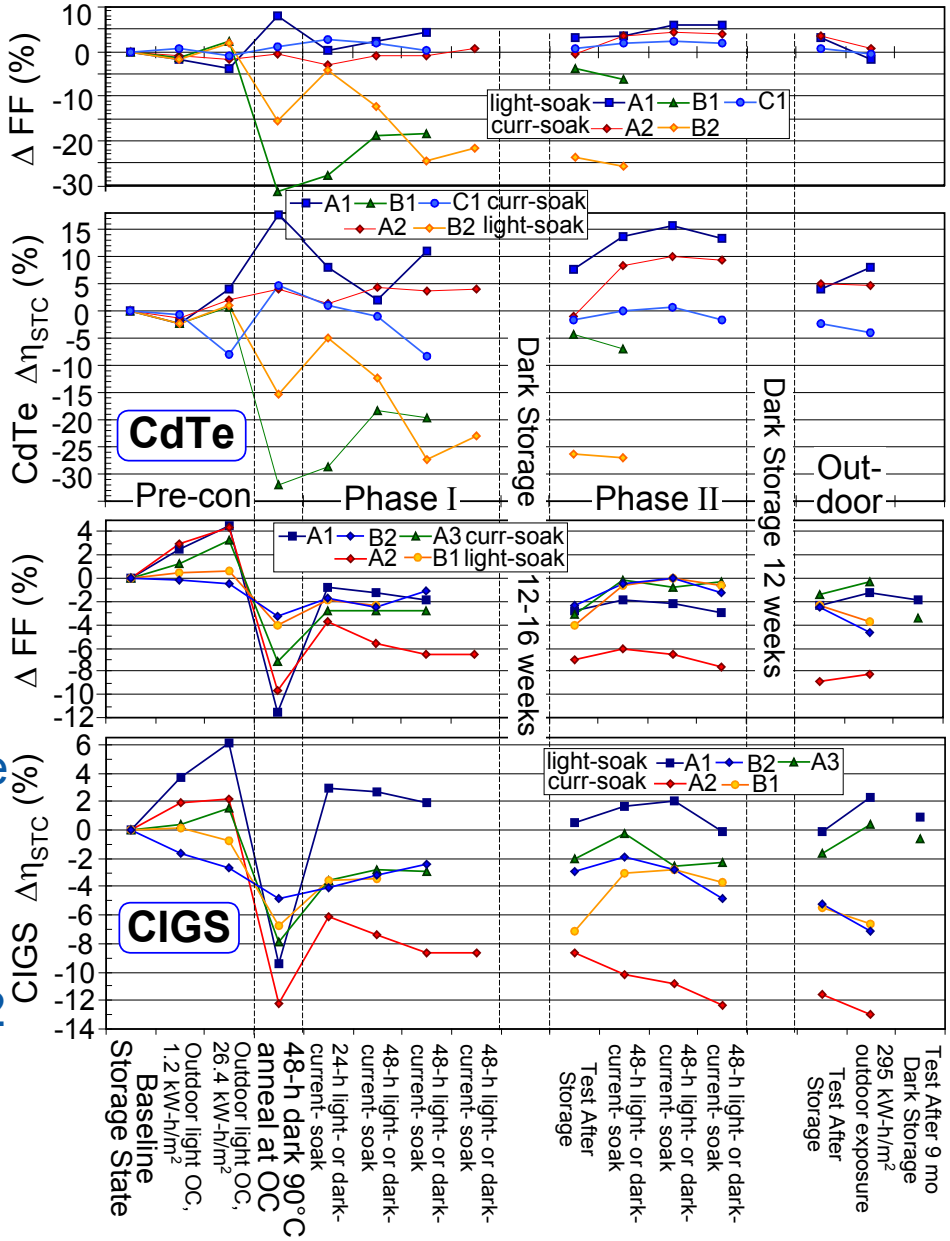
Module characterization tests

- Current-Voltage (I-V)
  - used 3 test-beds SPIRE, LACSS & SOMS outdoor for baseline performance at standard test conditions (STC)
  - used large area continuous solar simulator (LACSS) test-bed for incremental I-V performance tests; estimate Isc accuracy ~ ±1%
  - power parameter changes depicted $\Delta = X_t/X_0 - 1$, where X_0 , X_t = parameter at baseline, or time t
  - dark / light (STC), power parameters plus 2nd metrics from diode eqn. analysis (e.g., dV/dJ vs. 1/J for series Rse & diode A, dJ/dV for Gsh)

- C-V profiles measured exhibit correlations with performance changes, cursorily presented if time allows

Group 1 CIGS & CdTe Module Performance: Efficiency & FF changes vs. exposure relative to baseline

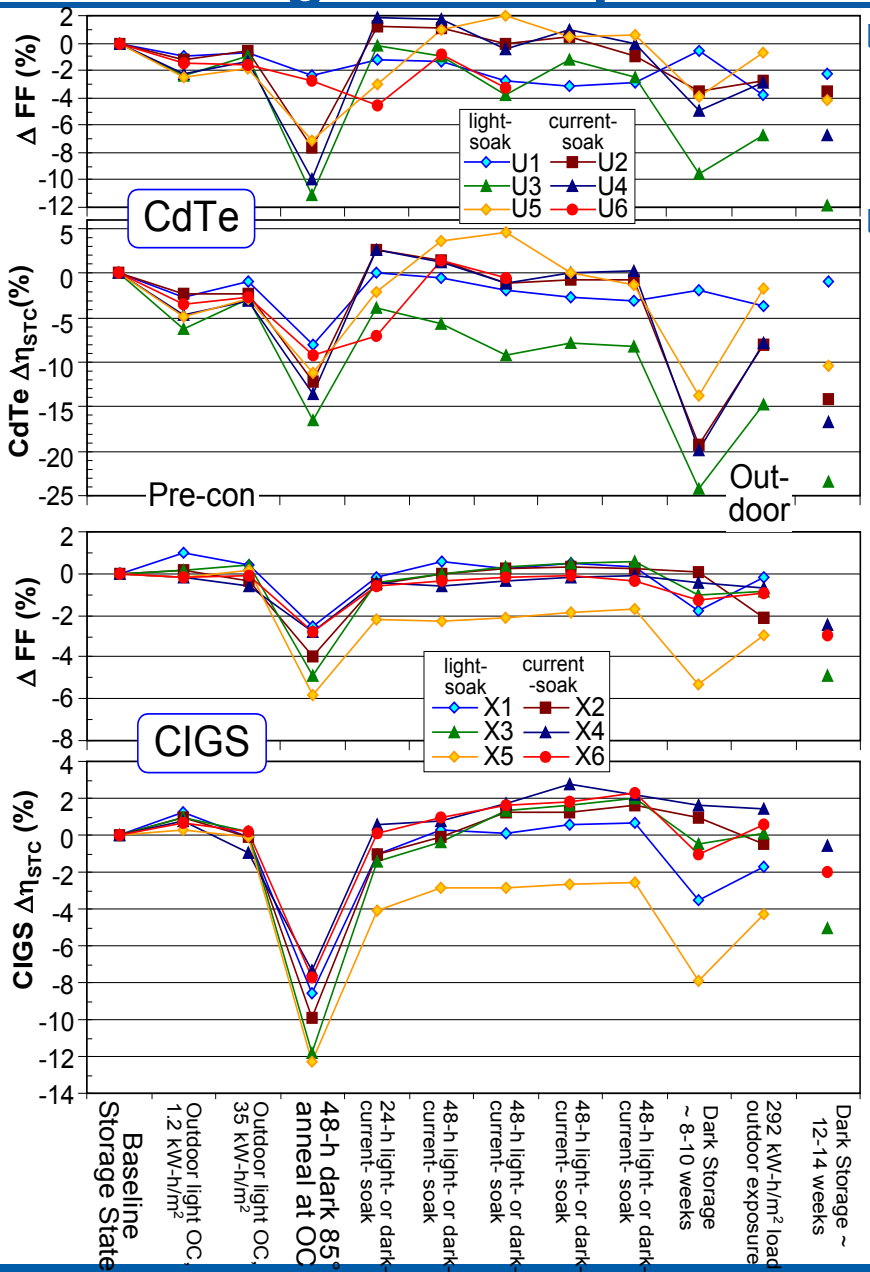
- precondition outdoor for 1, 26 kW-h/m^2
  - η_{STC} slight to moderate changes, but changes seen after 1kW-h precondition
- after dark thermal anneal , $\Delta\eta_{STC}$
  - All CIGS + CdTe B drop ⇨ FF
  - CdTe A & C improve
- Phase I steps: 4 light /3 dark soak
  - CIGS stabilize ($\Delta\eta \leq 2\%$) in light or dark
  - CdTe mixed, some stabilize (B1, A2)
- dark storage: CdTe's change 3%-5%, CIGS less ~1%-2%
- Phase II swap: 3 light/dark steps 48 h ea.
  - CIGS change some, most close to stabilize
  - CdTe: A stabilize per pre-existing prior to baseline, C stabilizes near baseline, Bs fail
- Final outdoor 295 kW-h exposure, loaded
  - CIGS appear stabilized $\Delta\eta$~2%, but A2 shows continuing $\Delta\eta$ loss ~2%
  - CdTe A2, C1 stabilize, not A1



Important summary of group 1 exposures & performance changes

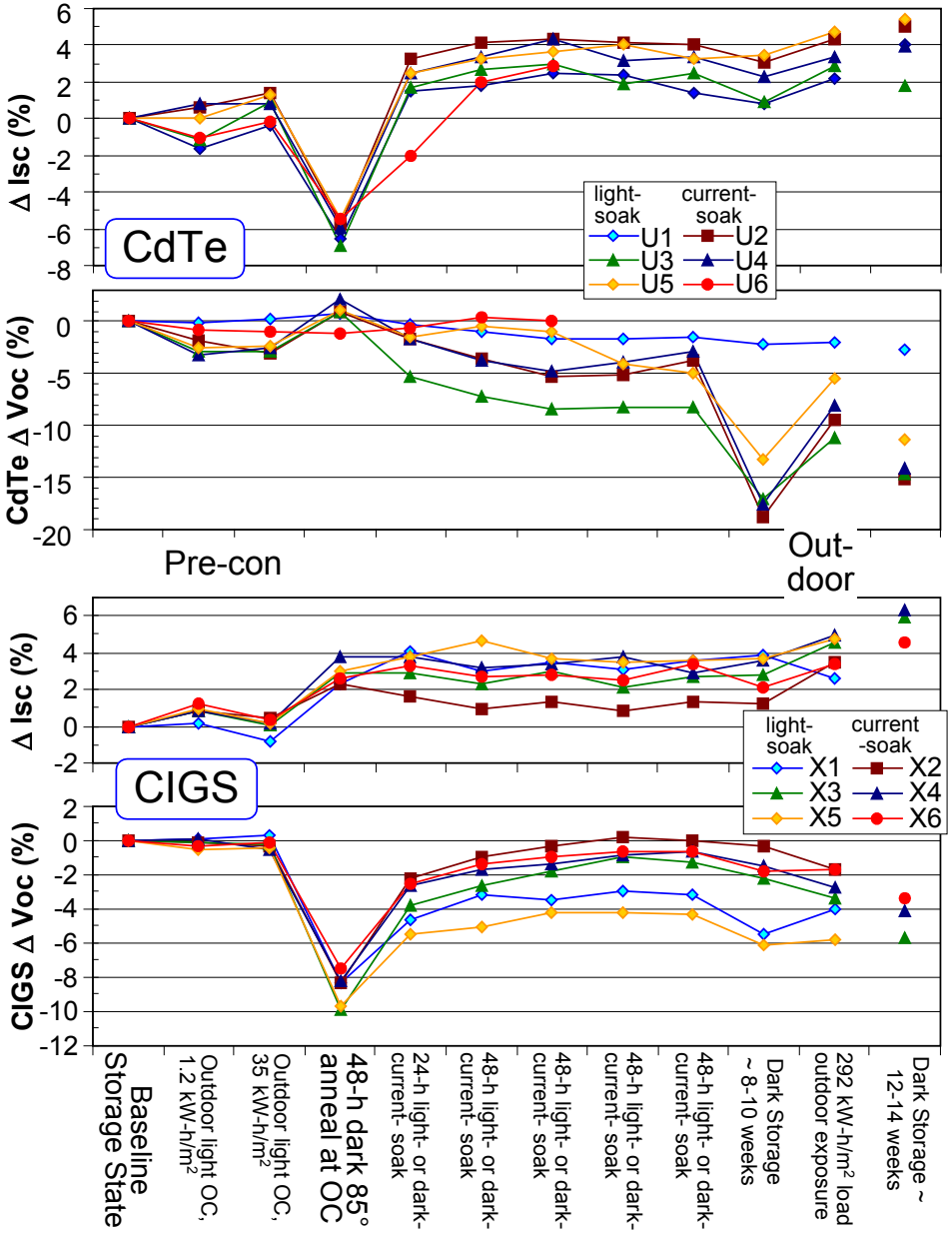
- dark thermal (85°C -90°C, 48h OC) anneal
  - Typically see FF loss as largest source of degradation
  - Voc changes: all CdTe improve ~ 2%-8%, All CIGS ~ 2%-3%
- chamber current-soaks in forward bias in dark
  - phase I
    - V_{bias} chosen ~ halfway between Vmax & Voc, I_{bias} <20% I_{max},
    - might have stifled stabilization
  - phase II
    - V_{bias} closer to Voc than phase I, I_{bias} ~ 80%* Imax
    - probably accelerated stabilization & changes
- dark storage intervals between phases
  - Improve Voc in CIGS A by 2%, diminish Voc in CdTe A 3%-5%
- outdoor exposure
  - CIGS A stabilize near levels after phase II, light soaking or current-soak appear to work equally well
  - CIGS B met stabilization criteria~ 2% light/dark-soak, but trends in same direction as changes in phase II so may not have stabilized
  - CdTe A,C mixed: light soak may work better, but sizable changes in Voc appear after dark

Group 2 CIGS X & CdTe U Module Performance: Efficiency & FF changes vs. exposure relative to baseline



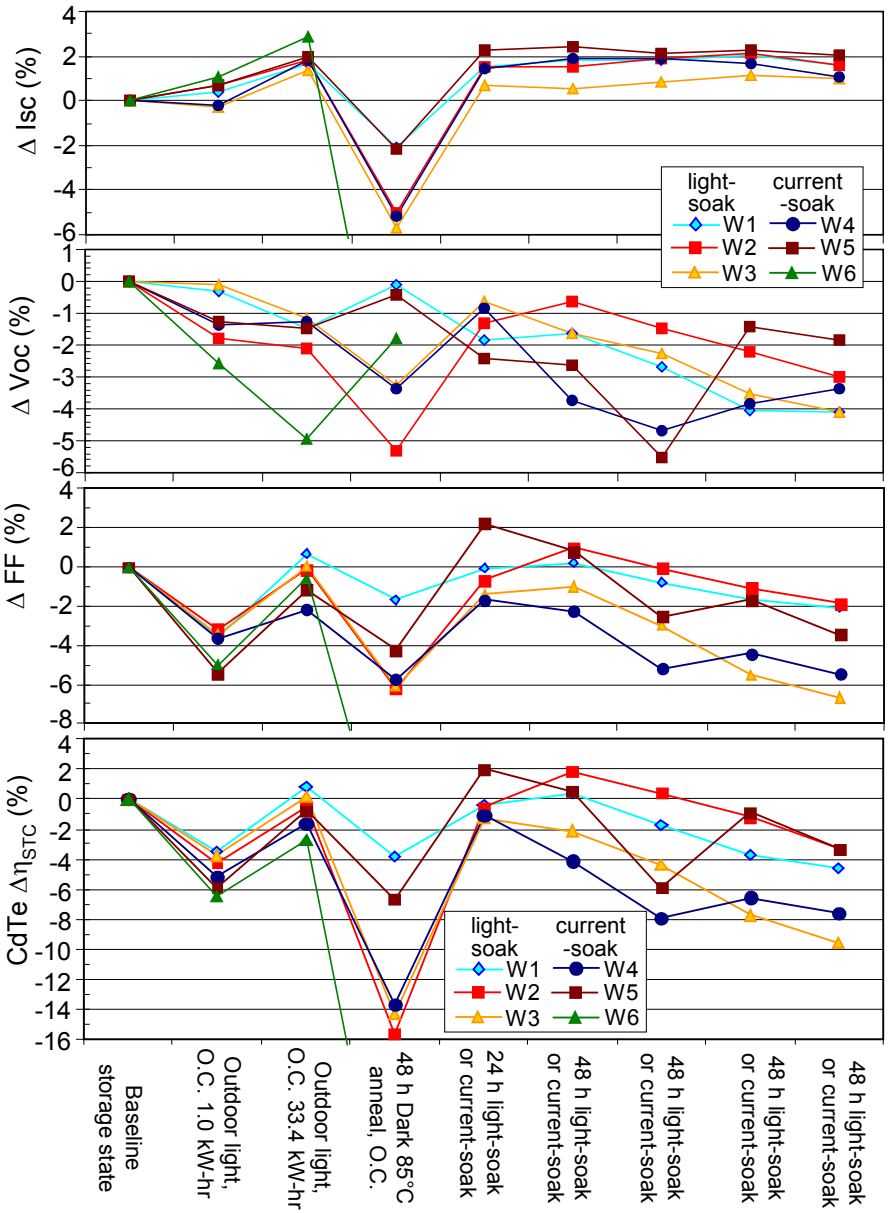
- Preconditioning 1, 35 kW-h lowers η_{STC} slightly ~ 0%-1% in CIGS X, moderately ~1%-5% in CdTe U
- Dark anneal degrades η_{STC}
  - CIGS X by 8%-12%, CdTe U by 8%-17%
  - FF loss accounts for half the loss in CIGS
  - Similar FF loss in CdTe U except for 1 & 6
- subsequent light or dark current soaks
  - 1st 24-h incr. recovers η_{STC} loss in CIGS to within 4%, in CdTe to +2% to -4%
  - either stabilize equally η_{STC} & FF in CIGS <1% after 96 h or CdTe after 200 h
- Dark storage drops performance
  - In CIGS X: modestly 1%-5% largely FF
  - In CdTe U: 13%-20%, some by FF
- Outdoor exposure validates stabiliz'ng η_{STC} using either light/current soak for CIGS, may indicate light-soak more effective for CdTe
- Changes still observed in dark storage at end

Group 2 CIGS X & CdTe U Module Performance: Voc & Isc changes vs. exposure relative to baseline



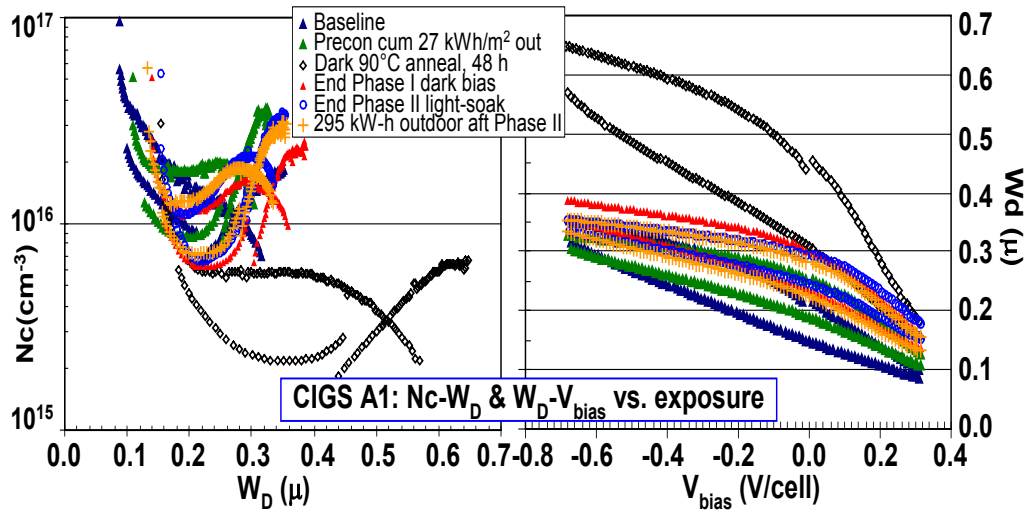
- Preconditioning 1, 35 kW-h: slight changes in Voc in CIGS X but larger ΔVoc in CdTe U; slight ΔIsc both
- Dark thermal (85° C) anneal
  - CIGS X , drops Voc by 8%-10%, bumps Isc up by 2% to 4%
  - CdTe U, drops Isc by 5%-7%, Voc ±1%
- sequel light or current soaks:
  - both seem to stabilize Voc & Isc
  - current-soak recovers more Voc in CIGS, less in CdTe, Isc responds to both
  - CdTe recovers slight better in light soak
- Dark storage diminishes Voc:
  - for CdTe ~12%-18% except U1;
  - for CIGS ~1%-2%
- Outdoor exposure
  - recovers Voc loss in CdTe U
  - Bumps Isc in both CIGS & CdTe by 2%,

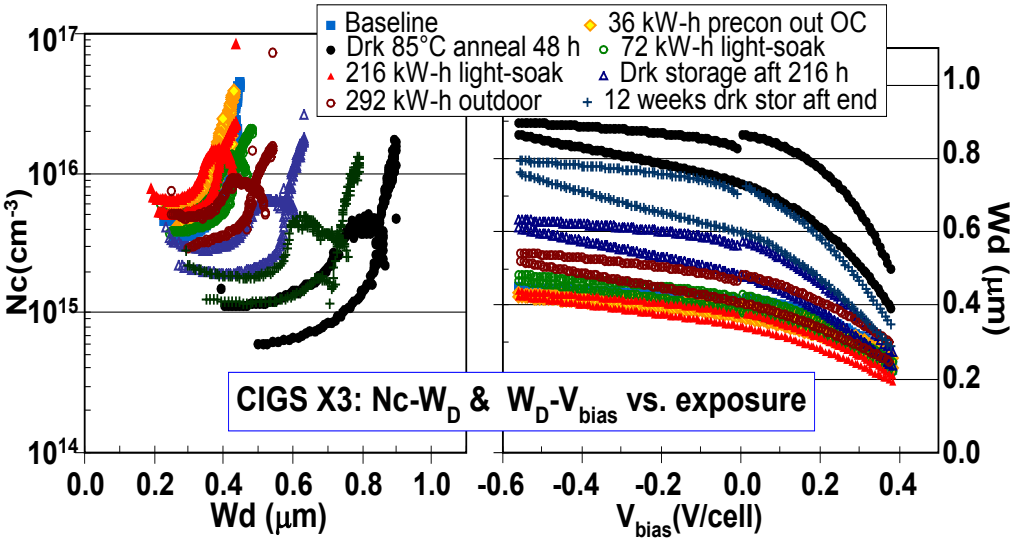
Group 3 CdTe W Module Performance: η_{STC}, FF Voc & Isc changes vs. exposure relative to baseline



- Preconditioning 1, 33 kW-h/m^2
  - 1st incr. drops η_{STC} ~3%-7%, then mostly thru FF & Voc loss
  - 2nd incr. recovers loss for total change -5% to +1% largely due to FF or Isc, not Voc
- Dark thermal anneal drops η_{STC} ~5-15%,
  - thru various combination FF, Voc, Isc loss
  - Isc loss in all, quite large (10%) for W2,W3
- post-thermal anneal light/current soaks incrs.
  - 1st 24 h recover most η_{STC} loss via FF, Isc
  - 2nd 48 h $\Delta\eta_{STC}$ ~ ±2% ambiguous due to opposing FF, Voc changes
  - 3rd 48-h $\Delta\eta_{STC}$ range -2% to -6%, mostly via Voc, FF losses in either light/current soak,
  - 4th 48-h $\Delta\eta_{STC}$ ~ +2% to +6% in current soak, but -2% to -3% loss in light-soak
    - Gains in current-soak from Voc
- 5th 48-h $\Delta\eta_{STC}$ ~1%-2% further losses maybe stabilization reached

Sample C-V profile data: CIGS A & U modules derived depletion widths (W_D) and Carrier densities (Nc) data

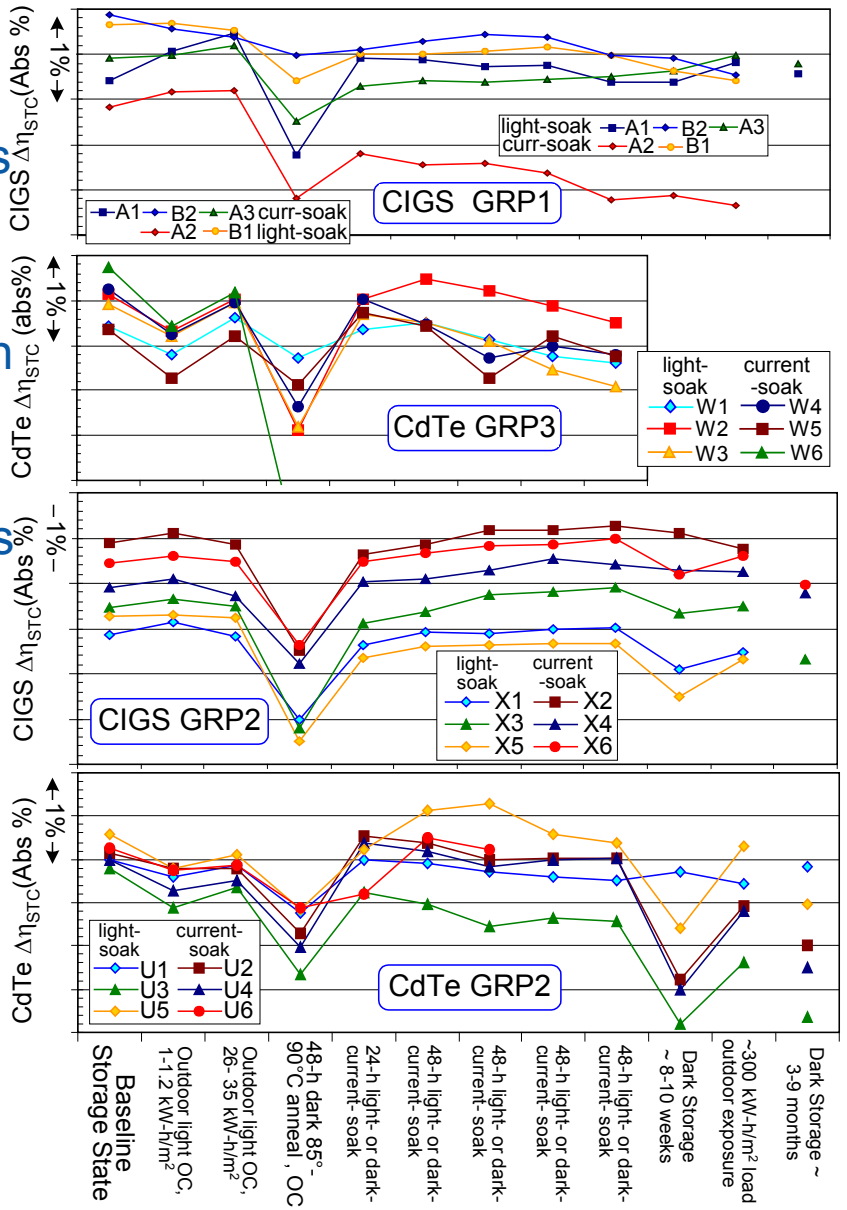




- CIGS A1 top, X3 at bottom
- Baseline W_D : similar ranges 0.1-0.3 µ for A1, 0.2-0.4 µ for X3
- Preconditioning has slight: widening on W_D ; lowers max Nc
- Dark thermal anneal large effect:
  - displaces W_D up by 2X to 3X & increases hysteresis
  - Drops Nc by factor 5 -10 to 10^{15}
- Indoor exposures drive W_D & Nc profiles to levels @ precon or base
- Outdoor exposure shifts A1 profiles closer to precon/baseline

Group 1, 2, 3 module absolute changes Eff η_{STC} plotted

- Plots vs. precondition, stress & exposures
  - grp 1 CIGS A & B at top, grp 3 CdTe 2nd from top panel, grp 2 CdTe & CIGS bottom 2 panels
  - groups begin with range $\Delta\eta_{STC} \leq 1\%$ abs., end with range $\Delta\eta_{STC} \leq$ ½% - 1½%
  - Preconditioning should be > 10 kW-h to quench transients, 1 kW-h does not seem enough
  - Dark thermal anneal drops most η_{STC} 1%-2% that seems recoverable after light/current soaks for most but not all, specially CdTe
  - Some modules (CIGS A2, CdTe U3) exhibit longer-term instability beyond metastability, which challenges notion that longer term outdoor exposures reflect performance better
  - Stabilizing w current soak in dark bias seems
    - as good as light soak in CIGS
    - feasible in CdTe but not as good as light
  - dark storage alters η_{STC} ~½% after outdoor stabilization past end or between exposures



Summary

- Thin-film CIGS & CdTe PV show transitory electrical performance ranging from fast (secs) transients to long (hours-days) time scales
  - Specially after dark thermal stress (85° C or more) or exposure
- Fast transients, may be quenched by preconditioning (20-30 kW-h) using outdoor light exposure, less may be possible, but need more than 1 kW-h
- For newer CIGS: preconditioned η_{STC} values are close to end-of-exposure levels; seem to stabilize after 100-150 h exposures at 65° C
- CdTe modules exhibit more variation in stabilization behavior than newer CIGS, thru variations in all power parameters, may need more like 200+ h exposure to stabilize
  - It's possible that we don't yet know what a representative sample size for CdTe modules is (to determine stabilization behavior).
  - To determine more representative sample size for CdTe, it may be better to deploy and monitor I-Vs in larger set, perhaps ~25-100 outdoors
- Time between measurement of I-V characteristics after stabilization procedures should be kept as short as possible, at least less than 1-2 hours

Summary

- Implemented two types stabilization procedures using : 1) light soak at 1-sun and 2) current-soak (forward bias dark), 65° ±5° C
- if current stabilization criterion used, $\Delta\eta \leq 2\%$ between successive intervals:
  - Current- or light-soaks capable of stabilizing CIGS modules, after ~150 h at 65° C
    - current-soak in dark should be performed with I_{bias} ~80%-90% I_{max} for acceleration
  - light soak may be more efficient than current soak for stabilizing CdTe, but higher temperature or larger current bias (in dark) may speed it up
  - CdTe probably needs even longer exposure than CIGS to stabilize

- Recommend IEC stabilization protocol be refined to require minimum ~150-200 h exposure for all thin-film modules,
  - specially if they are poly-c thin film & undergo dark thermal exposure
  - avoid successive steady low relative loss trends from biasing stabilization

- Will soon deploy group 3 CdTe set outdoors for 6-10 weeks to validate efficacy of light- or dark current- exposures against outdoor stabilized performance…Will next start testing newer CIGS (group 4) module set

Acknowledgements

- Dave Albin, for discussions & insight
- Kent Terwilliger, David Trudell, Ed Gelak for technical assistance with indoor weather/climate chamber
- Allan Anderberg IV measurements

Quantify degradation rates and mechanisms of PV modules and systems installed in Florida through comprehensive experimental and theoretical analysis

FSEC

Nicoleta Sorloaica-Hickman, Kris Davis, Florida Solar Energy Center - UCF
Sarah Kurtz, Dirk Jordan, National Renewable Energy Laboratory

NREL

Introduction

The economic viability of photovoltaic (PV) technologies is inextricably tied to both the electrical performance and degradation rate of the PV systems, which are the generators of electrical power in PV systems.

Over the past 15 years, performance data has been collected on numerous PV systems installed throughout the state of Florida. The following parameters are recorded using various data monitoring instruments:

- Array current and voltage (DC) - electrical power produced directly from incident sunlight by electrically connected modules
- Inverter power (AC) – power converted to AC by inverter and sent to home, building, or utility grid
- Plane-of-Array irradiance – amount of light (flux) incident on array
- Module temperature – measured from the back of modules







Photovoltaic Systems Characteristics

PV System	Location	Size (W)	Technology	Inverter	Years	Azimuth and Tilt
MMS	Florida	3960	multi crystalline Si	2500U	5	180 °South; 25 °
KMS	Florida	1680	mono crystalline Si	2500U	5	180 °South ; 17°
DW	Florida	2840	amorphous Si	2500U	5	180 °South ; 17°

Research strategy

Field Experience
Performance and metrological tests (5 or more years)

↓

Real Time measurements
Performance and metrological tests, visual inspection, IR pictures

↓

Life time Prediction

REFERENCES

1. Dunlop, Photovoltaic Systems, 2007
2. Marion et al, "Performance Parameters for Grid-connected Photovoltaic Systems", 31st IEEE Photovoltaic Specialist Conference, 2005
3. Ruther, Livingston, "Seasonal variations in amorphous silicon solar module outputs and thin film characteristics", Solar Energy Materials and Solar Cells, **36**, 29, 1994

PVUSA power rating analysis (AC, DC)

$$P = I_{POA}(a + bI_{POA} + CT_{amb} + dW)$$

Collect $T_{Ambient}$, Irradiance, DC and AC Power on all PV Systems data one-month blocks of 15-minute intervals

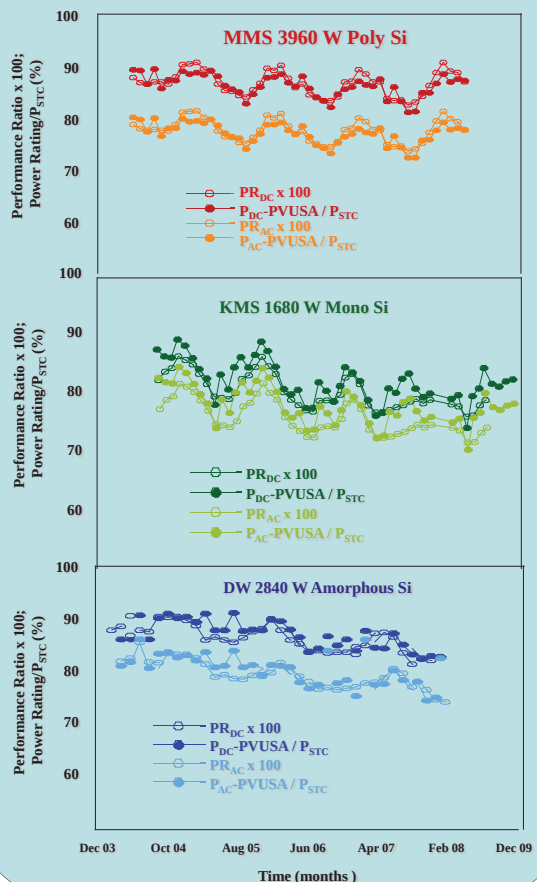
500 W/m²<Irradiance<1200 W/m²
-10 °C <T_a<60°C
P_{AC}>(75% of the P_{STC}) *Irradiance

Ignore Data

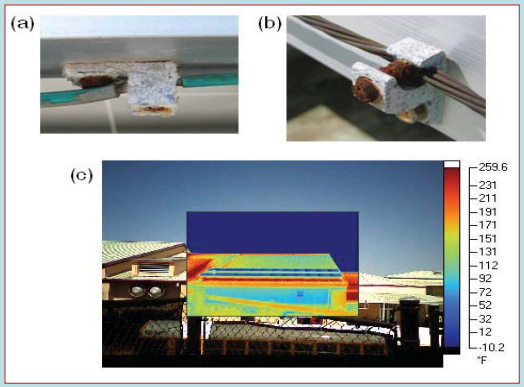
Calculate the regression coefficients and the Power Rate (W) at Illumination of 1000 W/m² and temperature of 20°C

Performance ratio analysis

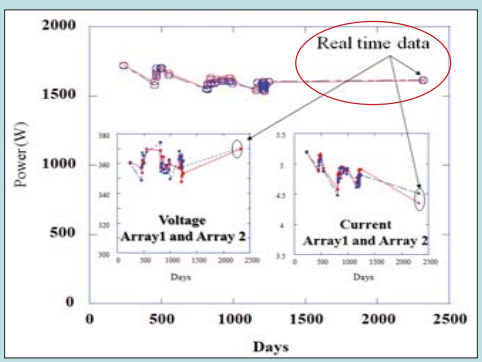
$$Y_f(\frac{kWh}{kW}) = \frac{E_{out}(kWh)}{P_{STC}(kW)}; \quad Y_r(hours) = \frac{H_{POA}(kWhm^{-2})}{G_{STC}(kWm^{-2})}; \quad PR = \frac{Y_f}{Y_r};$$



MMS 3960 W PV System Real time Measurements (2010) and inspections



(a) and (b) corroded grounding lungs; (c) zoomed out IR image



Conclusions

PVUSA Uncertainty

syst em	Array Degradation (DC) / year PR	PVUSA	Estimated DC Energy Production (20 years)	Array Degradation (AC) / year PR	PVUSA	Estimated AC Energy Production (20 Years)	PVUSA AC (500 - 1200 W/m²)	PVUSA DC (500 - 1200 W/m²)	PVUSA AC (800 - 1200 W/m²)	PVUSA DC (800 - 1200 W/m²)
DW	-0.57%	-0.40%	449.42 kWh	-0.68%	-0.69%	409.80 kWh	±100.36 W	±152.61 W	±108.96 W	±229.71 W
KMS	-1.14%	-1.26%	272.91 kWh	-1.16%	-1.13%	262.00 kWh	±67.240 W	±68.971 W	±63.510 W	±65.802 W
MMS	-0.33%	-0.75%	626.74 kWh	-0.40%	-0.82%	505.74 kWh	±142.19 W	±161.00 W	±139.77 W	±159.96 W

Acknowledgements

- NREL for funding this project
- Kevin Lynn, William Wilson, Steve Barkaszi, and all our colleagues from the Solar Energy Division at FSEC involved in systems installing and data collections.

Estimating the Degradation Rate of Photovoltaic Arrays Using a Two Component Nonlinear Model

Christopher Gotwalt
JMP Division, SAS Institute

Introduction

Modeling the degradation rate of the output of photovoltaic (PV) arrays over time is challenging because the degradation path can be clearly nonlinear, especially early in the life of the array. Identifying a nonlinear model for PV data is made more complicated because large solar seasonal effects mask the degradation path.

We model PV array output degradation data collected over 6 years and supplied to us by Dr. Dirk Jordan of NREL. We use the estimated degradation model to obtain the rate of degradation. The model fits very well, and modeling only the 1st 12 months of data leads to very similar results. This suggests that the same approach can be used to obtain earlier estimates of the life of arrays in general.

Initial Model

We proposed an exponential decay model for the degradation component. An cursory analysis suggested that a transformation on time would be needed. To accommodate this , a power parameter on time was added. An empirical seasonal model that was motivated as a two term sine series with unknown amplitudes and phase was also proposed.

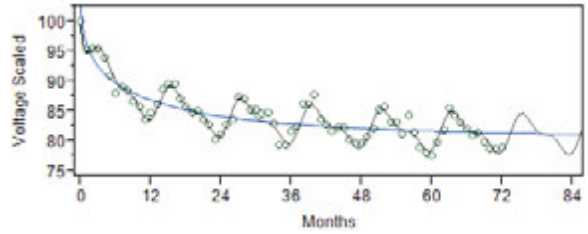
We use nonlinear least squares with a structural seasonal component rather than a nonlinear model with a seasonal ARIMA errors because our approach is easier in that it can be done using standard statistical software, and because a structural seasonal model will lead to more accurate predictions if it is close to correct.

Complete Data Model Fit

We fit the model using the nonlinear regression tools in JMP9 software. The parameter estimates and confidence intervals are below. The power parameter on time in the decay component is consistent with one half, which we assumed for the rest of the analysis. Notably a_2=.5*a_1 is also consistent with the data, though we did not take advantage of this later. Removing the second sine term of the seasonal model seriously degrades the fit and led to residuals with a large seasonal effect remaining. The model had an R^2 of .9, indicating an excellent fit.

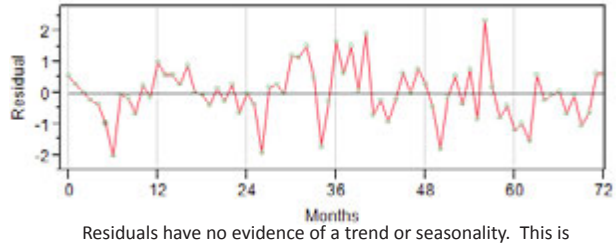
$$
\begin{aligned}
V(T) &= D(T) + S(T) \\
D(T) &= 80.2 + 22.2e^{-.35\sqrt{T}} \\
S(T) &= 2.7\sin(\tfrac{\pi}{6}(T-1.3)) + 1.3\sin(\tfrac{\pi}{3}(T-1.3))) \\
\dot{D}(T) &= 3.9T^{-\frac{1}{2}}e^{-.35\sqrt{T}}
\end{aligned}
$$

Six Years of PV Array Voltage Data



Green dots represent the monthly voltage measurements. Black line is the overall model, D(T)+S(T), blue line is D(T). Both lines fit to complete data.

Residuals



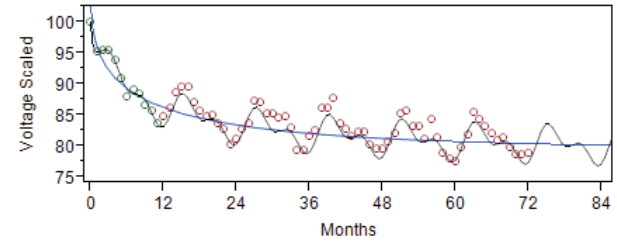
Residuals have no evidence of a trend or seasonality. This is evidence of a good model.

First Year of Data Model Fit

Because the model fit to the complete data was excellent, we sought to find how early one could obtain reasonably accurate estimates of the degradation path and rate. For this dataset, one year of data appeared to be enough, as can be seen by comparing the model coefficients below to the ones from the complete data fit to the lower left.

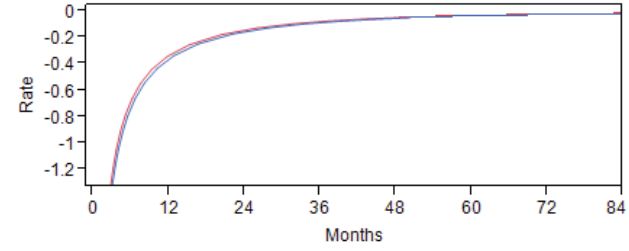
$$
\begin{aligned}
V(T) &= D(T) + S(T) \\
D(T) &= 79.2 + 23.8e^{-.35\sqrt{T}} \\
S(T) &= 2.2\sin(\tfrac{\pi}{6}(T-1.3)) + 1.6\sin(\tfrac{\pi}{3}(T-1.3))) \\
\dot{D}(T) &= 4.2T^{-\frac{1}{2}}e^{-.35\sqrt{T}}
\end{aligned}
$$

One Year of PV Array Voltage Data



Overall and degradation model fit to only the 1st year of data (green dots). Note how well the fit to the first year predicts the next five years of data.

Comparing the Rate Estimates



Red line is the 72 month rate estimate, blue line is the 12 month estimate. The rate function estimates are quite similar.

Conclusions

The two component model yields an excellent fit to the data, even when only using the first year's worth of data. This suggests that this exponential decay model in the square root of time with a two term trigonometric seasonal model can be used to obtain early, yet accurate estimates of the life of PV arrays.

NREL
NATIONAL RENEWABLE ENERGY LABORATORY

Requirements for a Standard Test to Rate the Durability of PV Modules at System Voltage



Peter Hacke
Kent Terwilliger
Steve Glick
Michael Kempe
Sarah Kurtz
Ian Bennett*
Mario Kloos*

***ECN, Petten, The Netherlands**

This presentation does not contain any confidential material

Presented at the 2011 Photovoltaic Module Reliability Workshop
February 16-17, 2011
Golden, Colorado

NREL/PR-5200-51099

NREL is a national laboratory of the U.S. Department of Energy, Office of Energy Efficiency and Renewable Energy, operated by the Alliance for Sustainable Energy, LLC.

Motivation

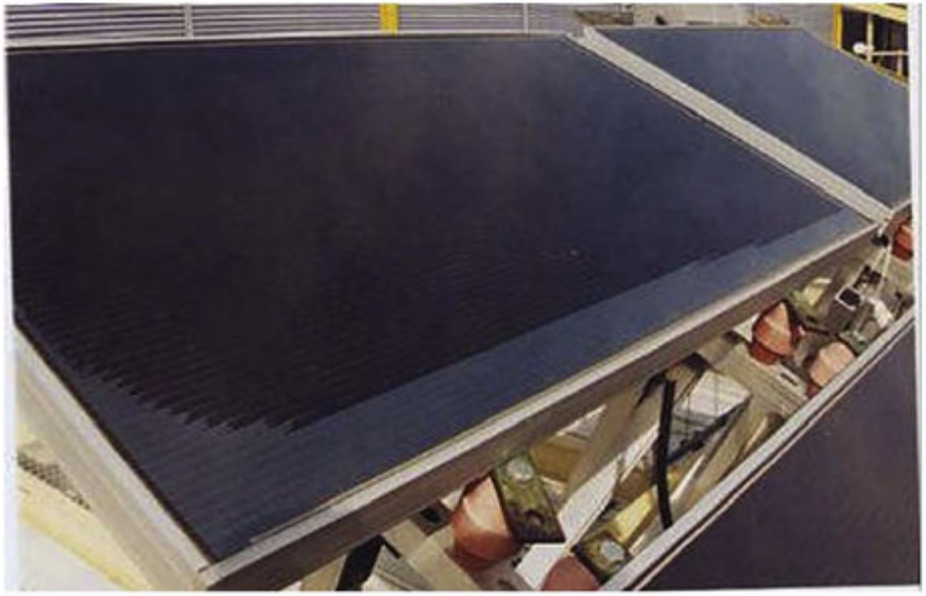
Over the past decade, there have been observations of module degradation and power loss because of the stress that system voltage bias exerts. This results in part from qualification tests and standards not adequately evaluating for the durability of modules to the long-term effects of high voltage bias that they experience in fielded arrays.

> "*Oh no! our modules are down 40%, we think it is potential–induced degradation*"
>
> *-anonymous module manufacturer, 2010*

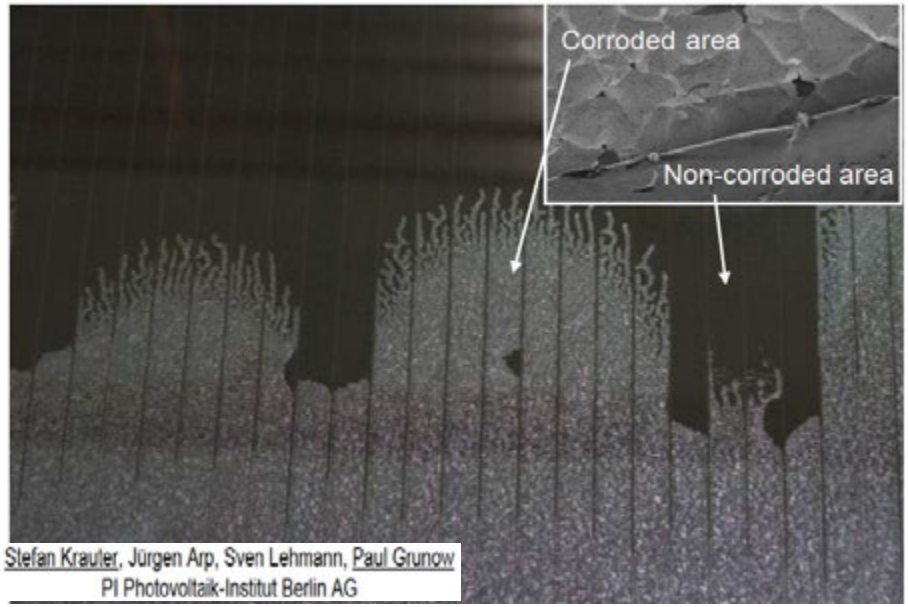
Three degradation modes - overview

1. Ionic motion in the packaging of the active layer leads to accumulation of charge or charged ions over the semiconductor surface
   - Charge influences surface field of semiconductor active layer
   - In severe cases, accumulation of mobile ions such as Na in the glass leads to delamination
2. Ionic motion also takes place within the active layer, degrading semiconductor junction properties and causing shunts
3. Usually in the presence of humidity in the packaging, electrolytic corrosion occurs and macroscopic transport of ionized conductor metal is observed.

Mode 1 : Na ions moving to glass TCO interface



J. H. Wohlgemuth et al. "LONG TERM RELIABILITY OF PHOTOVOLTAIC MODULES", WPSEC-4 (2006) p. 2050



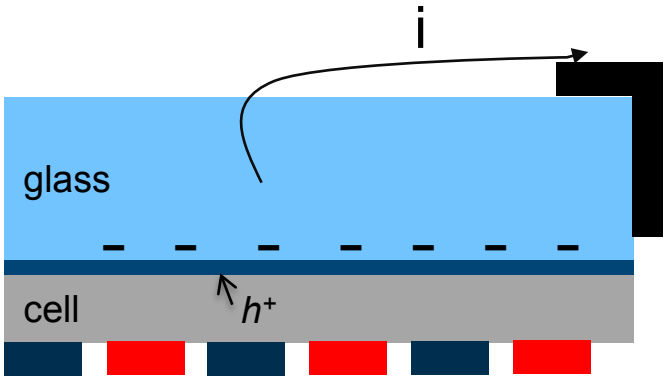
Reported by BP Solar…

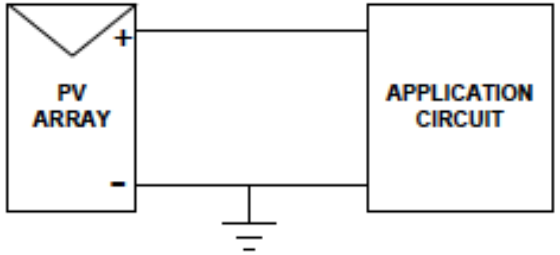
- a-Si modules
- - 600V bias
- 12 mo. in the field

- Sodium ions migrating to the TCO/glass interface causes delamination of the TCO, electrochemical corrosion
- Key drivers are:
  - *Negative cell polarity* vs. ground
  - Moisture ingress
  - Temperature
  - Na content in glass

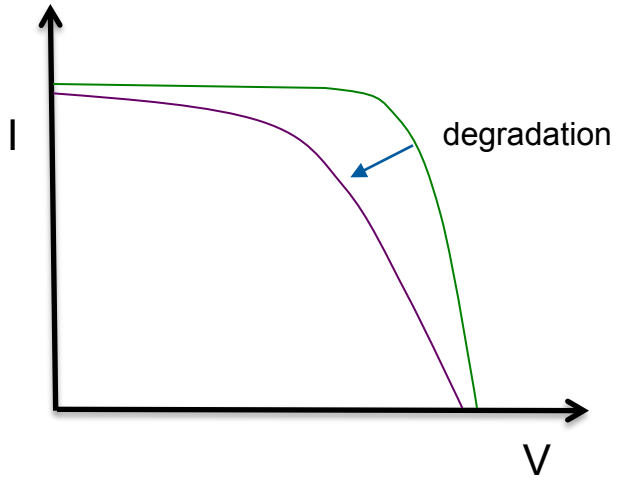
Mode 1 : Na ions moving away from active layer

SunPower reports 'surface polarization' in modules in 2005

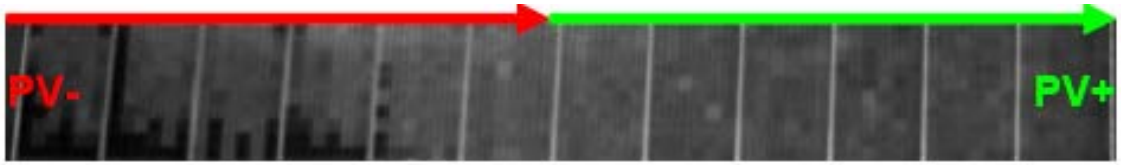




- *Positive bias* string leads to leakage current through glass to ground, leaving negative charge on cell surface, degrading effectiveness of the n^+ front surface field of the n^+/n structure
- Minority carriers (holes) recombine at front surface, leading to degraded cell performance

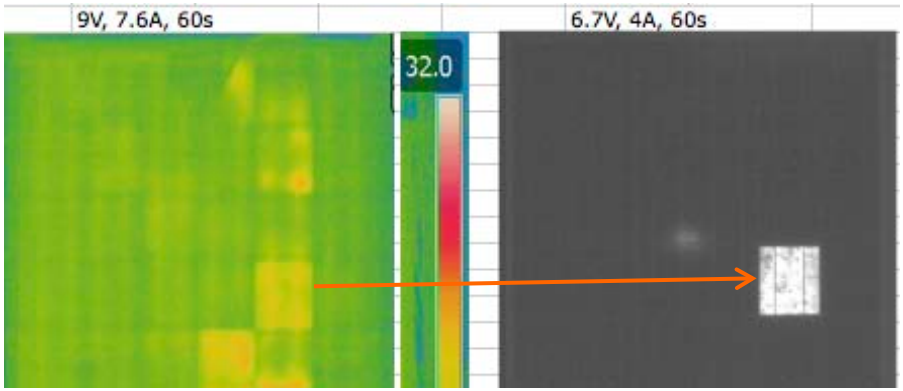


Mode 2: Ionic motion into active layer – pn junction shunt



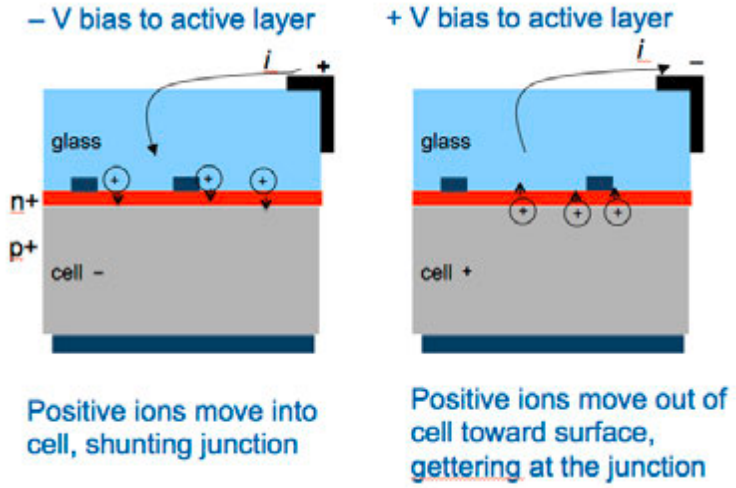
- Electroluminescence of mc-Si module strings indicating shunting in the negative portion of a center mounted or floating string *

Shunting indicates junction degradation



Thermography EL

Proposed model

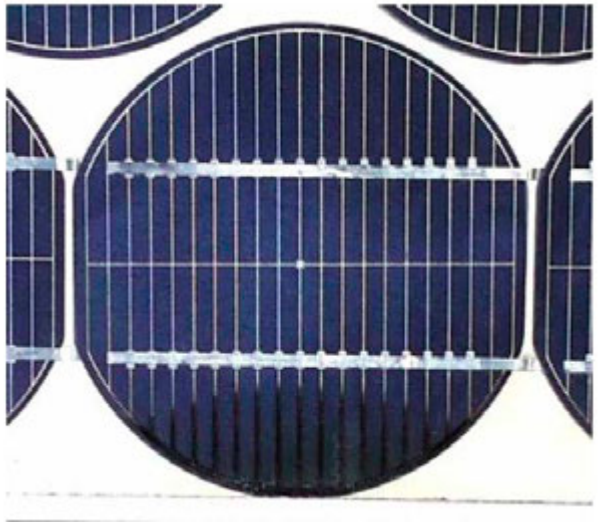


ionic motion within active layer of thin film devices also active

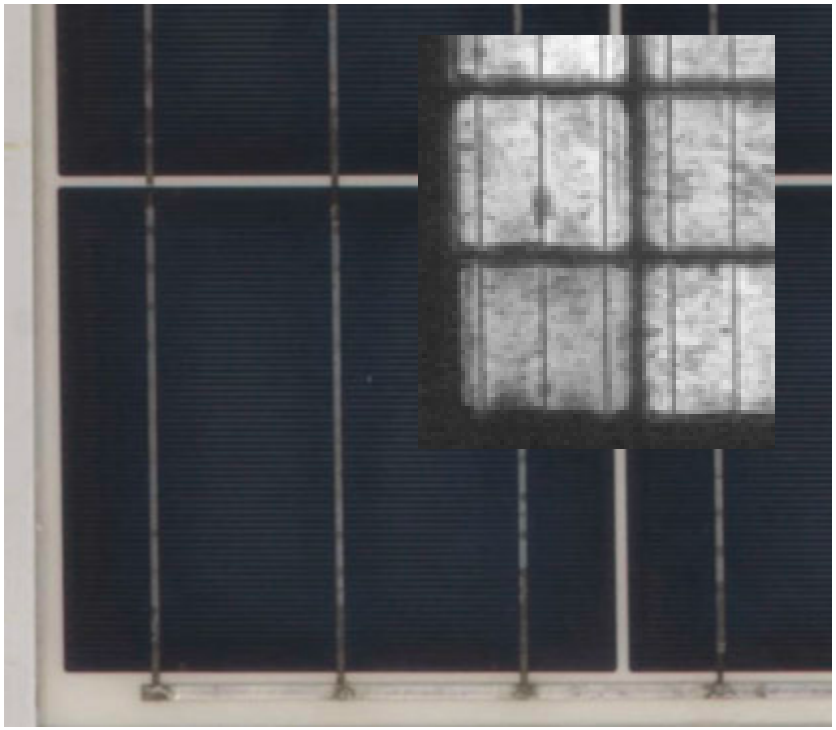
* S. Pingel, O. Frank, M. Winkler, S. Daryan, T. Geipel, H. Hoehne and J. Berghold SOLON SE, Presented at 35th IEEE PVSC, 2010

Mode 3 corrosion and macro - transport

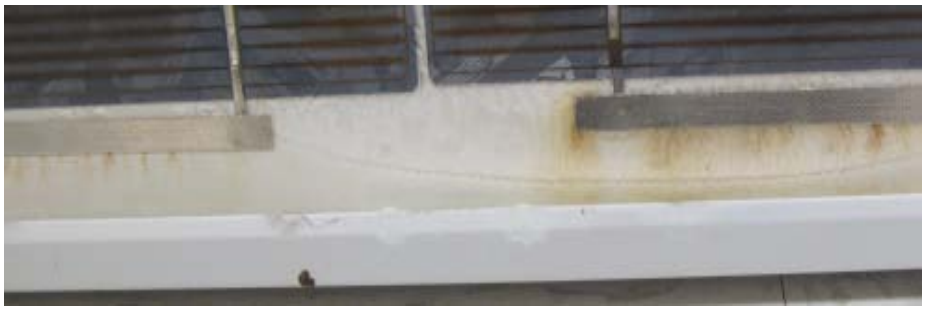
Corrosion of gridlines and Si-grid interface leading to higher series resistance evident visibly, in electroluminescence, and I-V curves



Realini (TISO)



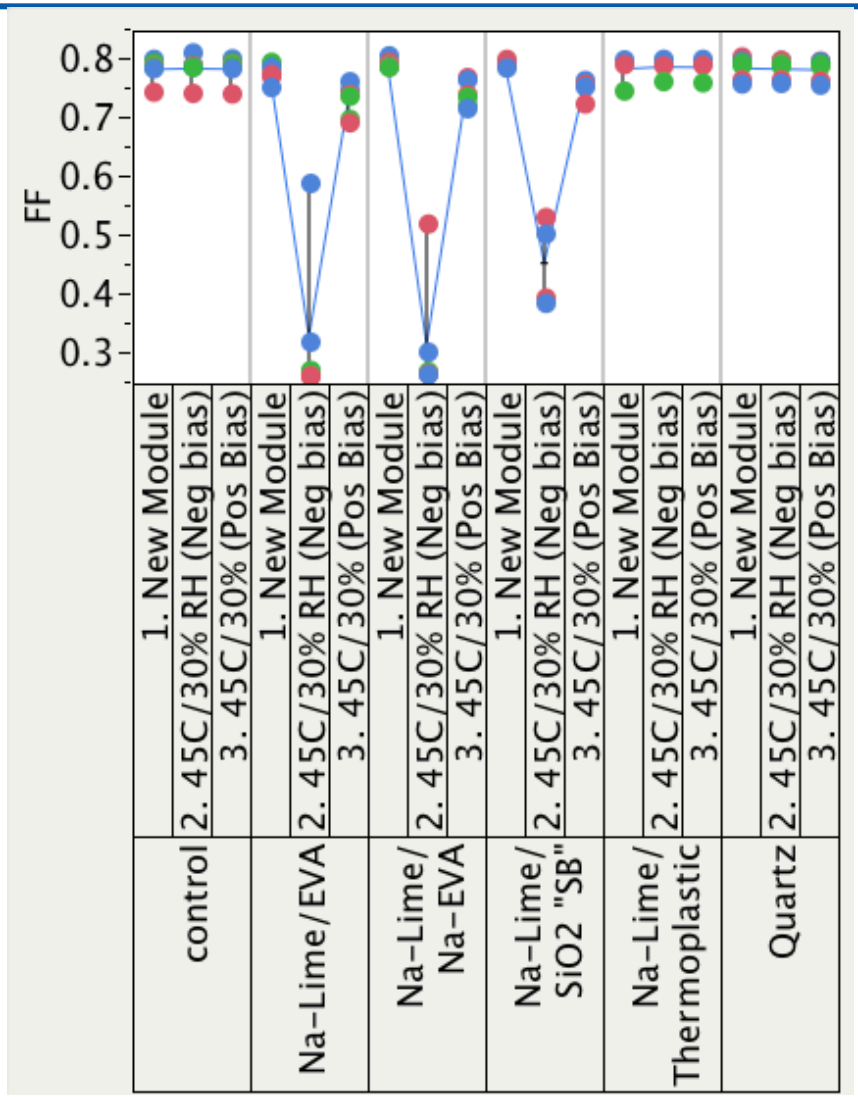
Corrosion and ionic transport at bus ribbons toward frame (positive string)



Testing methods – low T & RH regime

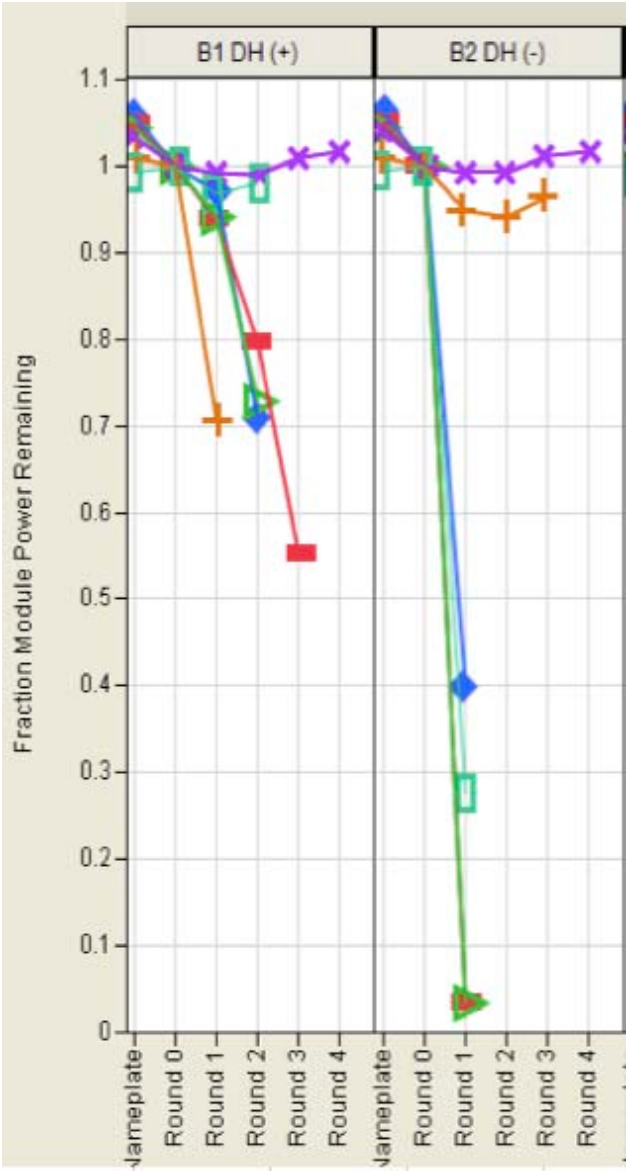
Near ambient temperature tests applying system voltage

- Saline water film, wet towel, or carbon paste act as the ground electrode to simulate wet surface, salt mist, or conductive dirty surface
- Degradation generally reversible by reversal of ionic motion
- No visible damage
- Degradation modes 1 & 2 active



1 cell mc-Si mimos, ± 1000 V bias applied to shorted leads; the module face grounded with C-paste, 120 h stress tests at 45 ° C, 30% RH

Testing methods – high T & RH regime



- 6 commercial module designs
- 85° C/ 85% RH
- 600 V system voltage

Activates modes 1,2 and 3, including corrosion, series resistance

Strongly differentiates modules' durability to system voltage bias potential-induced degradation

Summary

- Three modes of system bias potential-induced degradation
- Fielded systems showing system bias potential degradation
- Modern higher system voltages are more stressful on modules
- Increasing need to push down overall degradation rate
- Increasing variety of solar cell technologies sensitive to system bias potential (*e.g.*, selective emitter with junction closer to cell surface)
- Long-term degradation by system bias voltage is not presently captured in IEC 61215 and IEC 61646
- Tests around ambient temperature succeed reasonably well at elucidating 2 of 3 degradation modes, but higher temperature and humidity required to show durability to corrosion
- Exact, most appropriate level of stress is yet to be determined, but we shouldn't wait to implement some screening test



Plextronics OPV Outdoor Testing

Mike Pannone, Eric Karplus*, Darin Laird, Min Xiao

** Science Wares, Inc.*

Acknowledgement:

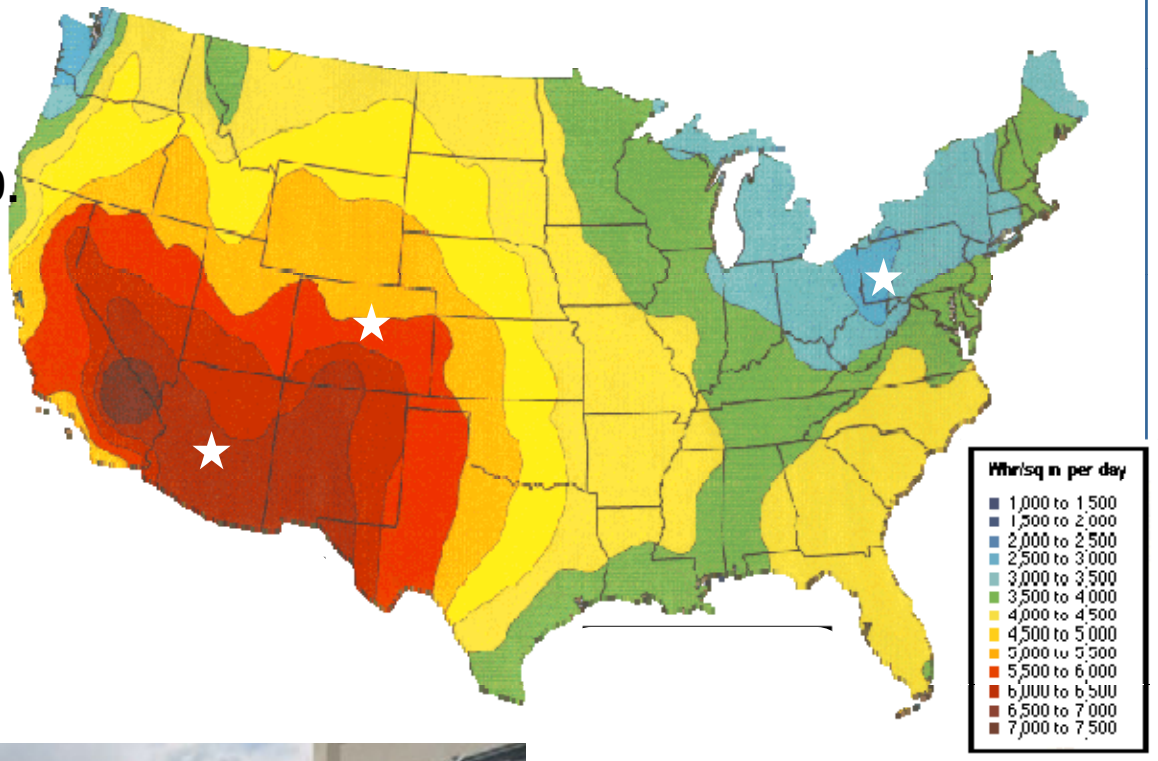
Joseph Del Cueto, Jose Rodriguez

PV Reliability Workshop, Feb. 16-17, 2011

This presentation does not contain any proprietary or confidential information.

Overview

- Plextronics started OPV outdoor testing since mid-2009.
- In Dec. 2009, 30 R&D modules were placed at three outdoor stations.
- We report here the results of these modules and lessons learned.







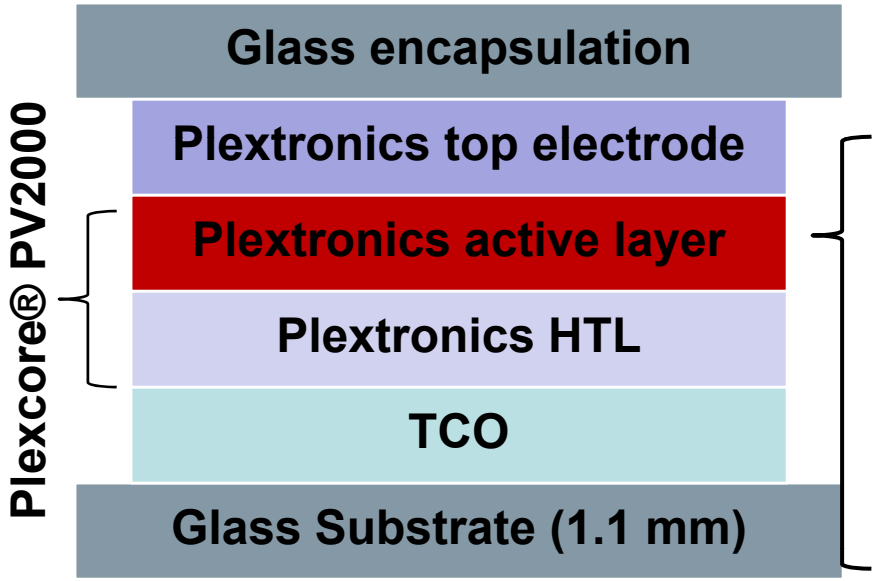


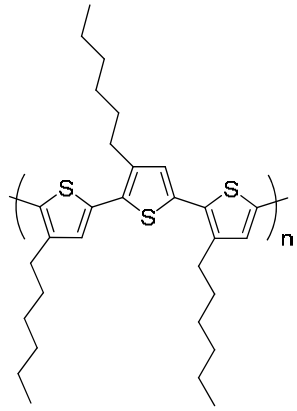
Device Description

- R&D modules
- Size: 6” x 6”
- 9 cells in series per column
- 6 columns in parallel

Initial Performance	Average	Range	
Jsc (mA/cm^2)	7.75	7.19	8.19
Voc (V)	6.82	6.2	7.0
FF	0.55	0.33	0.63
Efficiency (%)*	3.13	1.81	3.73

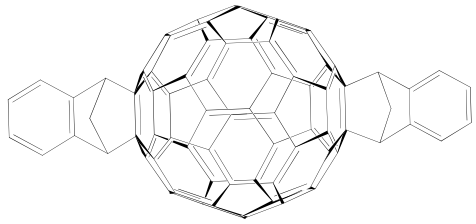
*Efficiency based on active area.





HT RR-P3HT

+

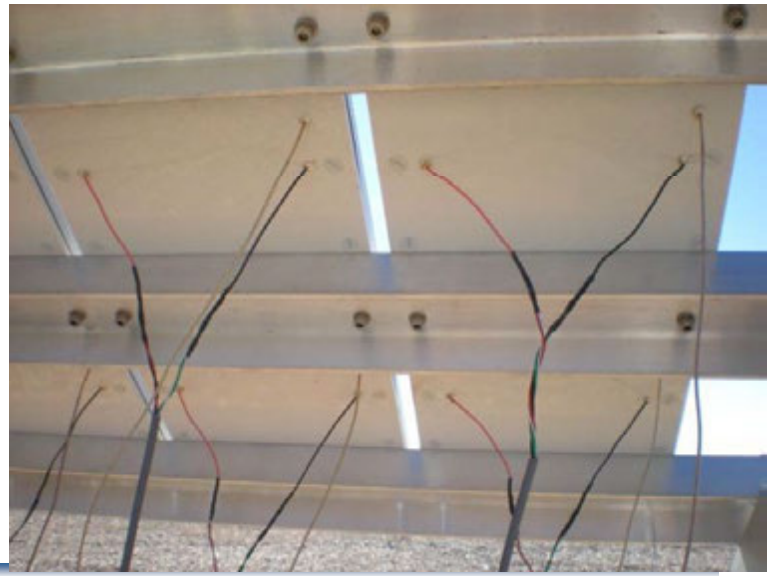


bis-indene[C60]

Laird, D. W.; Stegamat, R.; Richter, H.; Vejins, V.; Scott, L.; Lada, T. A. Patent WO 2008/018931 A2.

Outdoor Station Construction

- Custom module holders
  - Water-tight seals
  - Thermocouple on module back
- Custom tester
  - 16 channels
  - 1 pyranometer, 5 photodiodes
- Custom software
  - MPP maintained
  - IV curves taken every 10-15 minutes from sunrise to sunset.



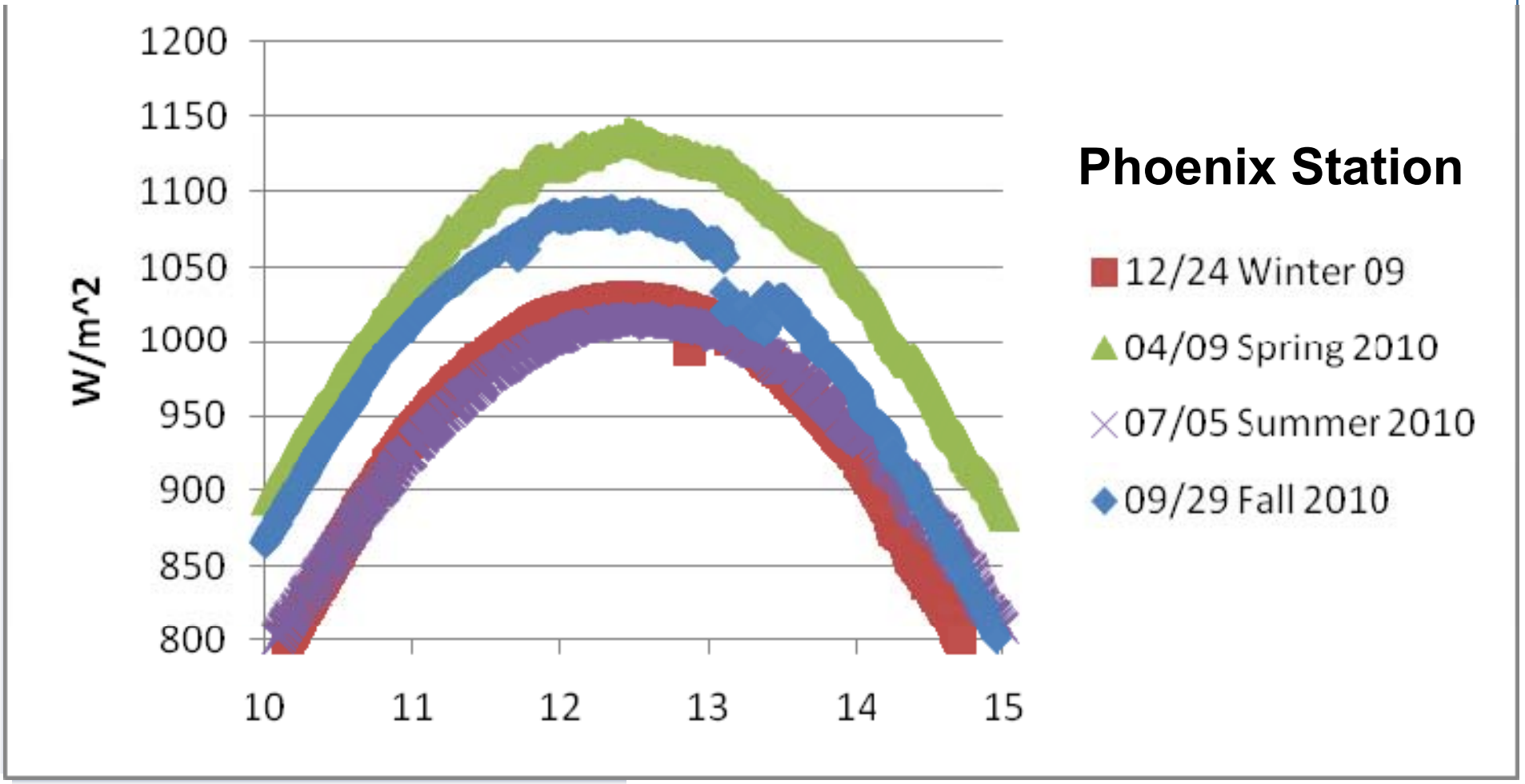


Data Analysis

- Goal: Track key parameters (Isc, Voc, MPP, FF, efficiency) as a function of time.
- Challenge: Extract data at fixed light intensity (close to “one sun”) and fixed light incident angle.
- Methods for setting filter criterion
  1. Peak intensity
  2. Fixed intensity range throughout the day
  3. Fixed intensity range over fixed hours of the day

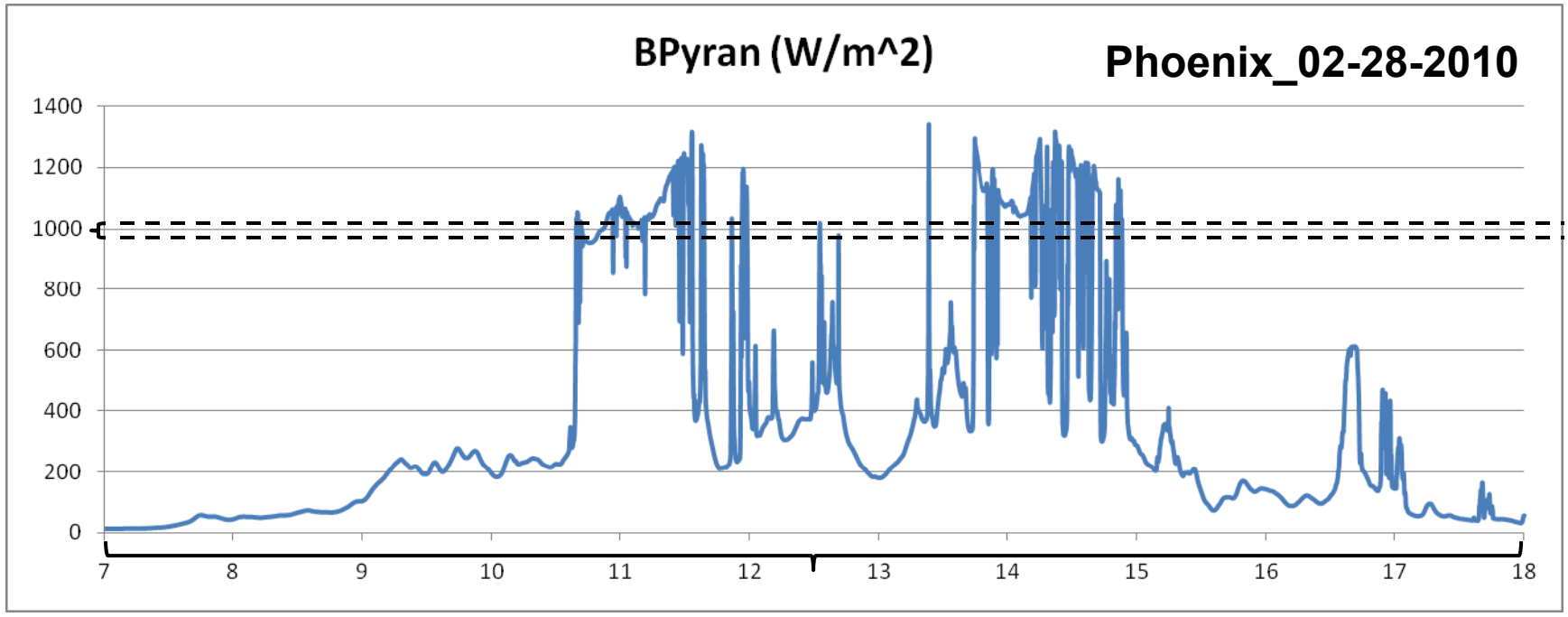
1. Peak Intensity Method

- This method uses peak value of pyranometer as criterion to select key parameters.
- However, peak intensity$_{chan}$ ges over the course of the year.



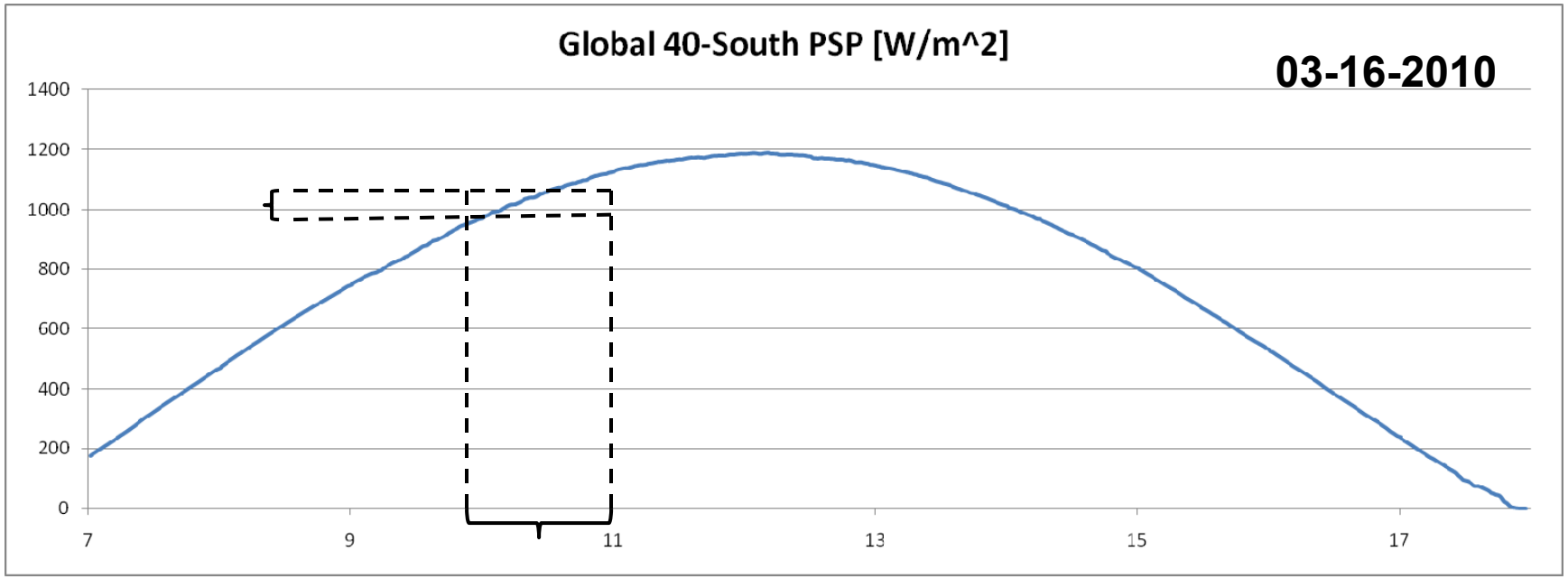
2. Fixed Intensity Range Throughout Day

- This method picks a fixed intensity range over the entire day.
- If the range is too large, qualified data can cover several hours, where the angle of incident also changes.
- If the range is too narrow, there may not be any qualified data for days.
- Data on cloudy or hazy days could also be challenging.

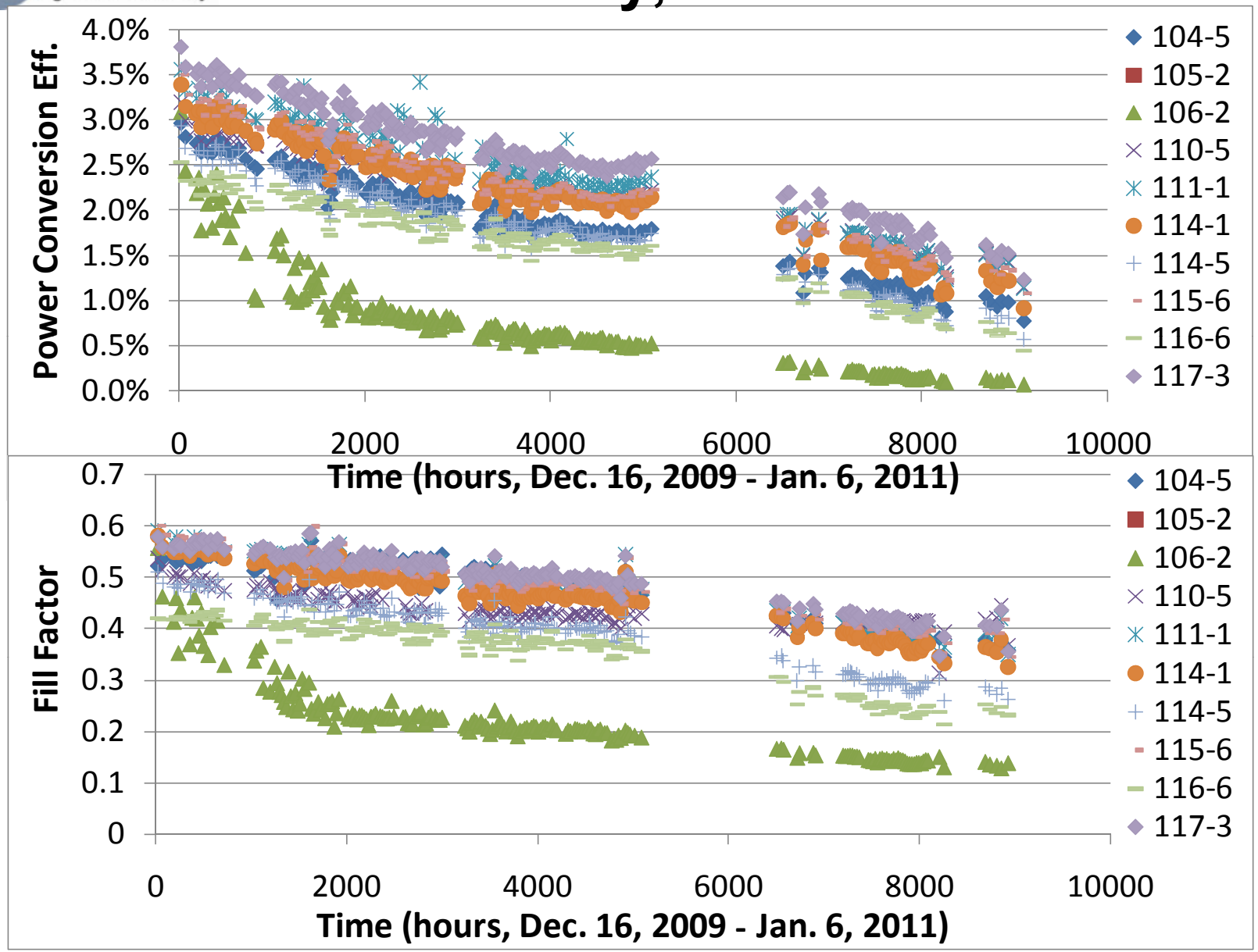


3. Fixed Intensity Range Over Fixed Hours of the Day

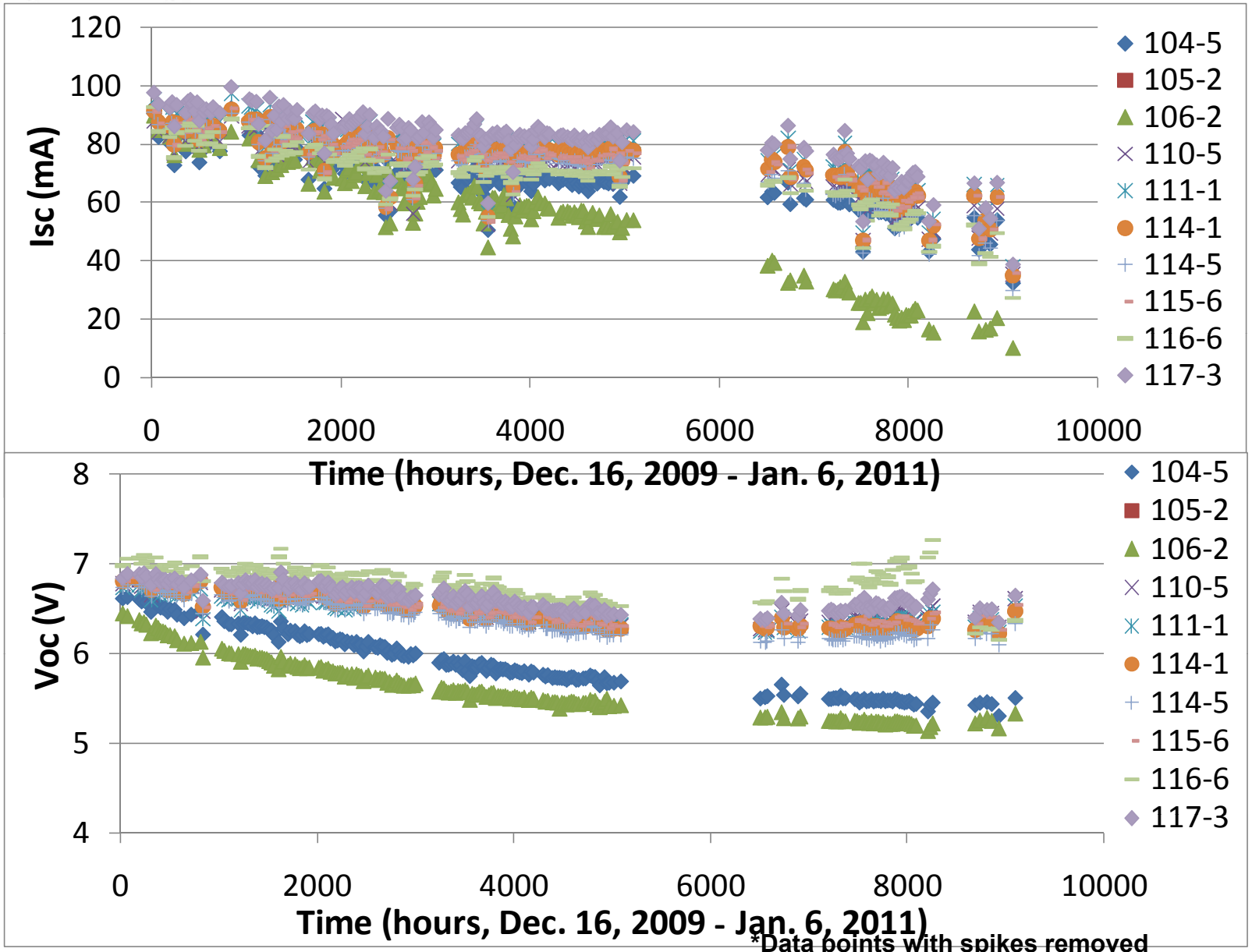
- This method was developed by Mike Pannone at Plextronics and used in our analysis. It chooses a particular irradiance and time window.
- A very tight intensity range was chosen centered around 1000 W/m^2.
- Data is captured in the morning only, generally between an hour interval to minimize changes of the solar incident angle.



Results of Modules in Phoenix: Efficiency, Fill Factor

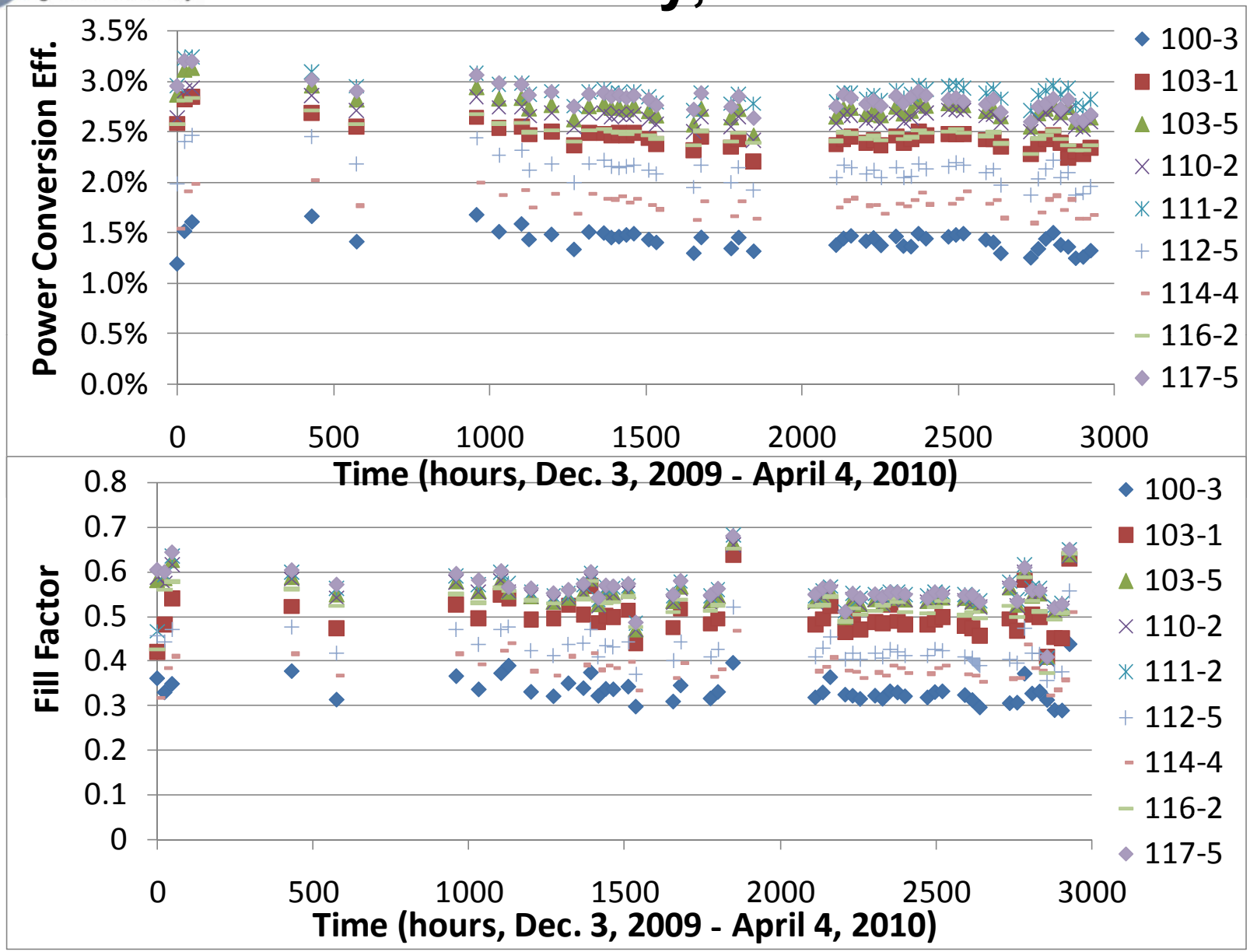


Results of Modules in Phoenix: Isc, Voc

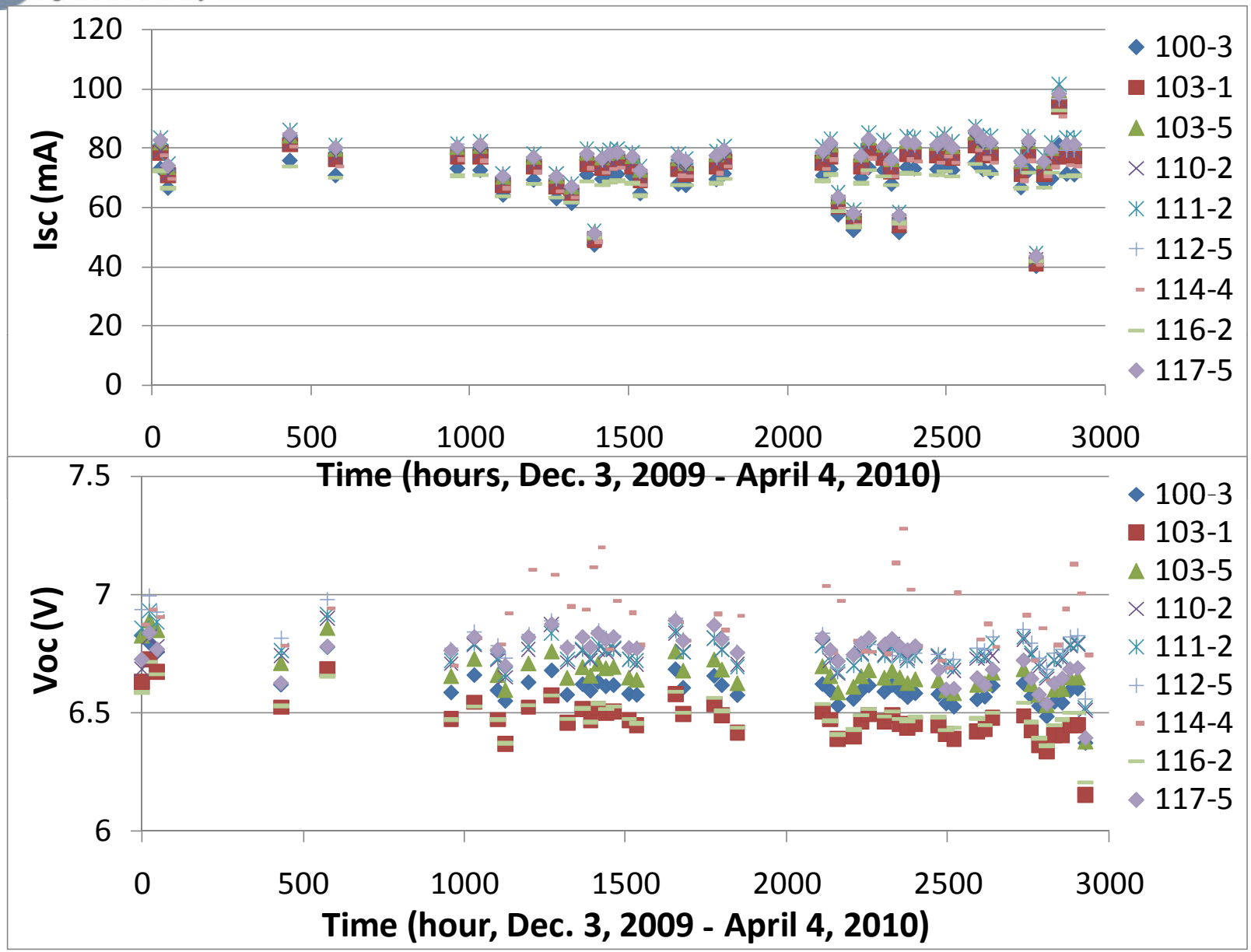


*Data points with spikes removed

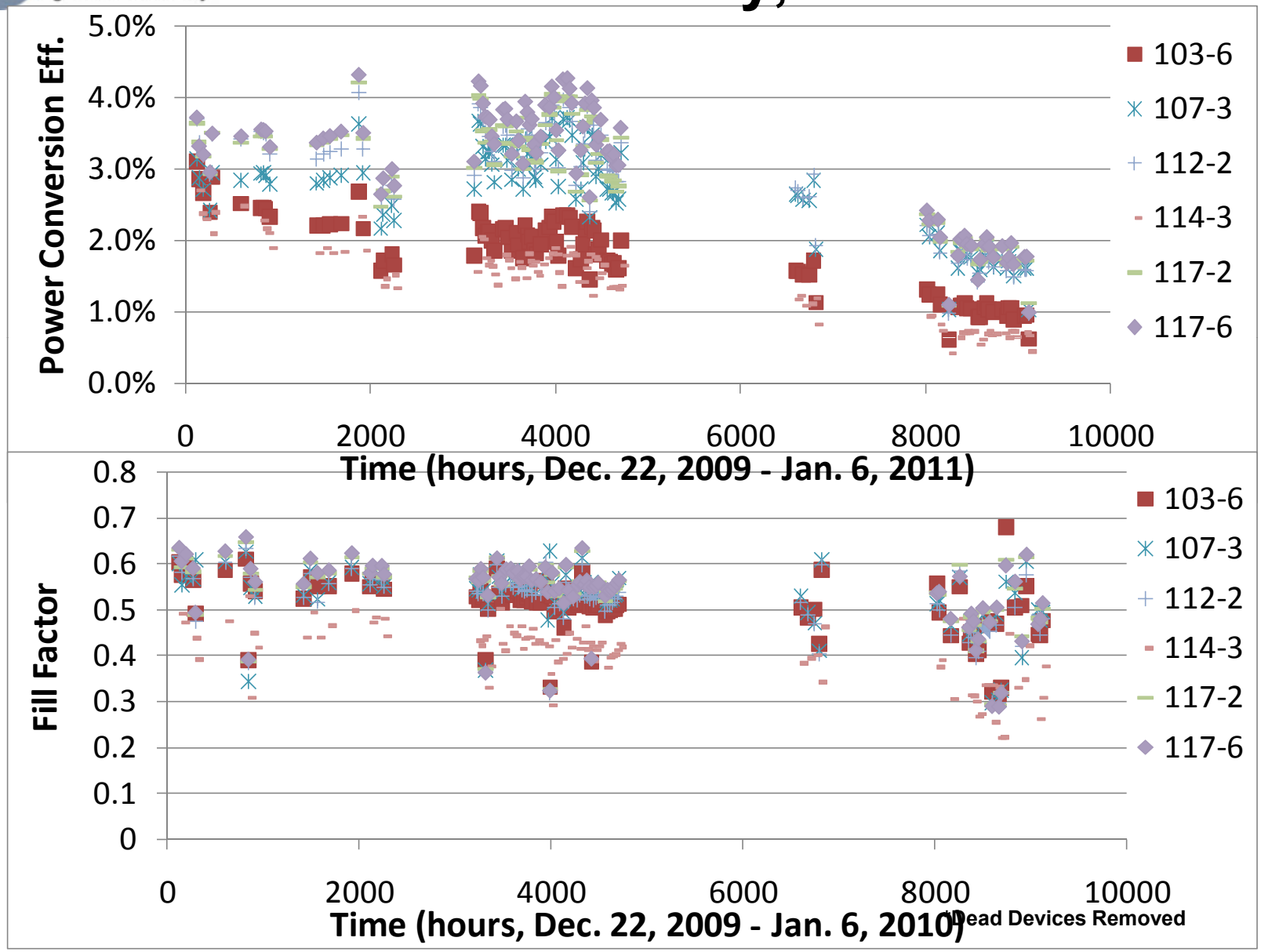
Results of Modules in Golden: Efficiency, Fill Factor



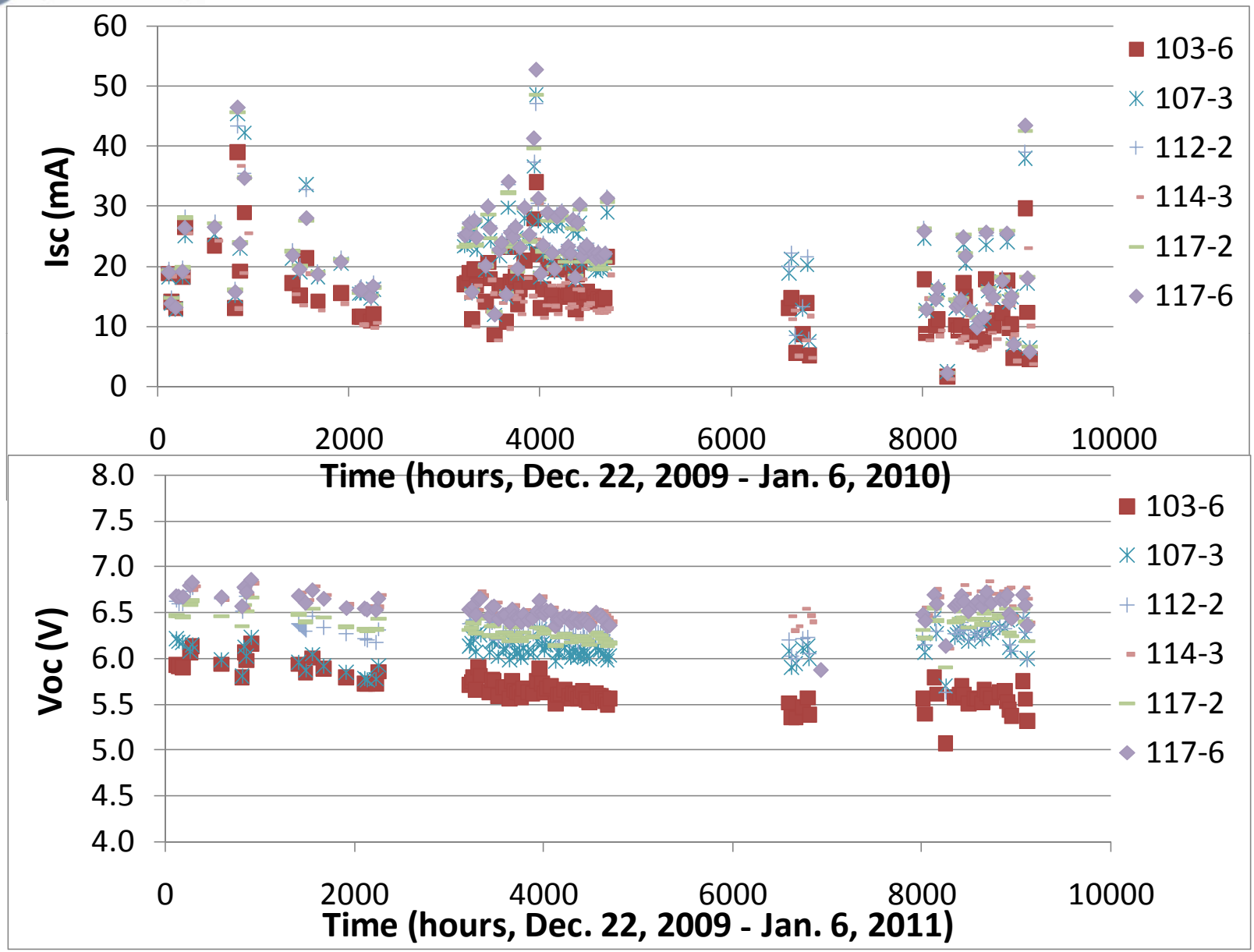
Results of Modules in Golden: Isc, Voc



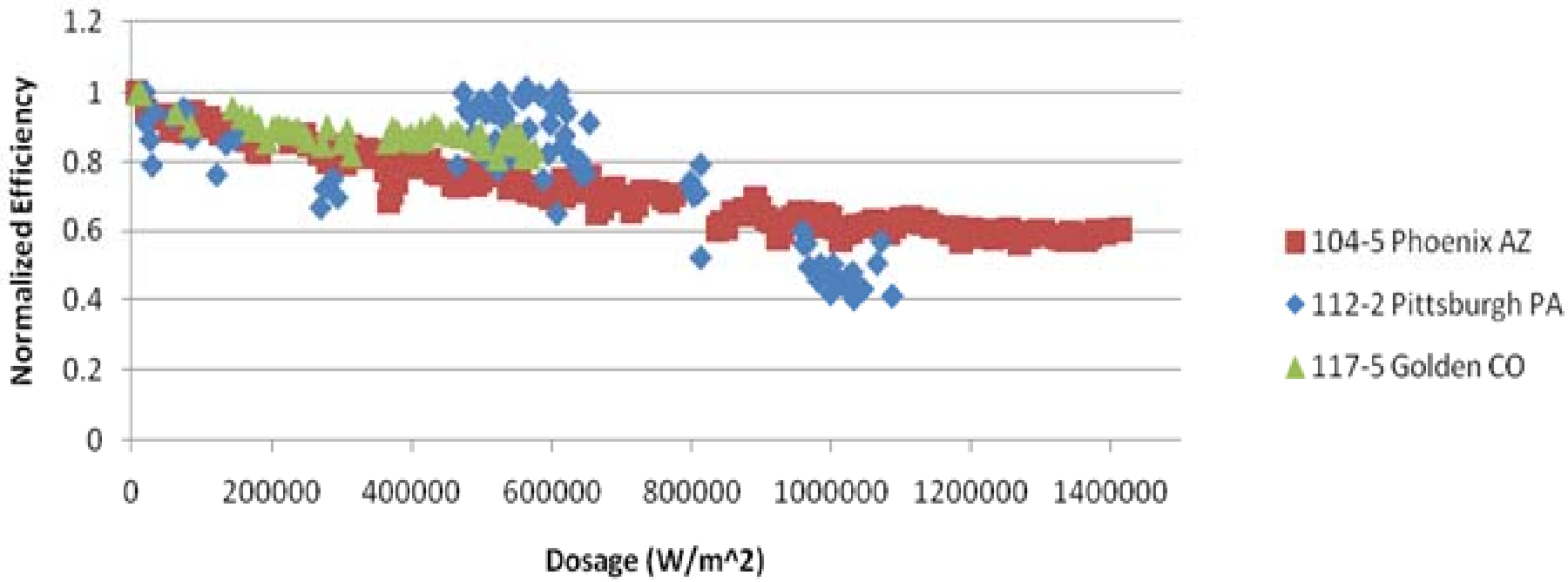
Results of Modules in Pittsburgh: Efficiency, Fill Factor



Results of Modules in Pittsburgh: Isc, Voc



Comparison Across Different Locations



After taking dosage into consideration, the decay trend at three different locations appears to be similar.

Lessons Learned

	Challenges	Solutions
Weather	Hail storm on June 11, 2010 in Golden, CO destroyed 7 out of 10 modules.	Acrylic cover. Thicker substrate.
	Modules at Atlas were covered in dirt.	Subscribe service to wash weekly.
	Pyranometer had different snow coverage from modules.	
Robustness of Parts	Glass cracking, resulting in catastrophic failure.	Treat glass edges.
	Pyranometer failure.	Use photodiode as backup.
Data Analysis	Power outages causing missing data.	Install backup power supply.
	Malfunctioning of software causing missing data.	pgrade software.
	Data spikes. U	
	Daylight savings not observed on NREL tower and in Arizona.	Analyze data based on local time instead of relying on Windows OS system clock.

Summary

- 30 R&D modules were placed at three custom outdoor stations in Dec. 2009: Pittsburgh, PA, Phoenix, AZ, Golden, CO. Data analysis methods were developed.
- Phoenix, AZ
  - 9 out of 10 modules showed gradual degradation during 12 months.
  - Most of the degradation was in current.
- Pittsburgh, PA
  - 4 modules showed catastrophic failure due to glass cracking.
- Golden, CO
  - No appreciable degradation in the first four months.
  - 7 out of 10 modules destroyed in a hail storm in June, 2010.
- Decay trend vs. dosage similar across three stations.
- Valuable experience gained in testing OPV outdoors.

the standard in safety

Photovoltaic DC Arc-Fault Circuit Protection and UL Subject 1699B

Tim Zgonena, Liang Ji, Dave Dini
Underwriters Laboratories Inc (UL)

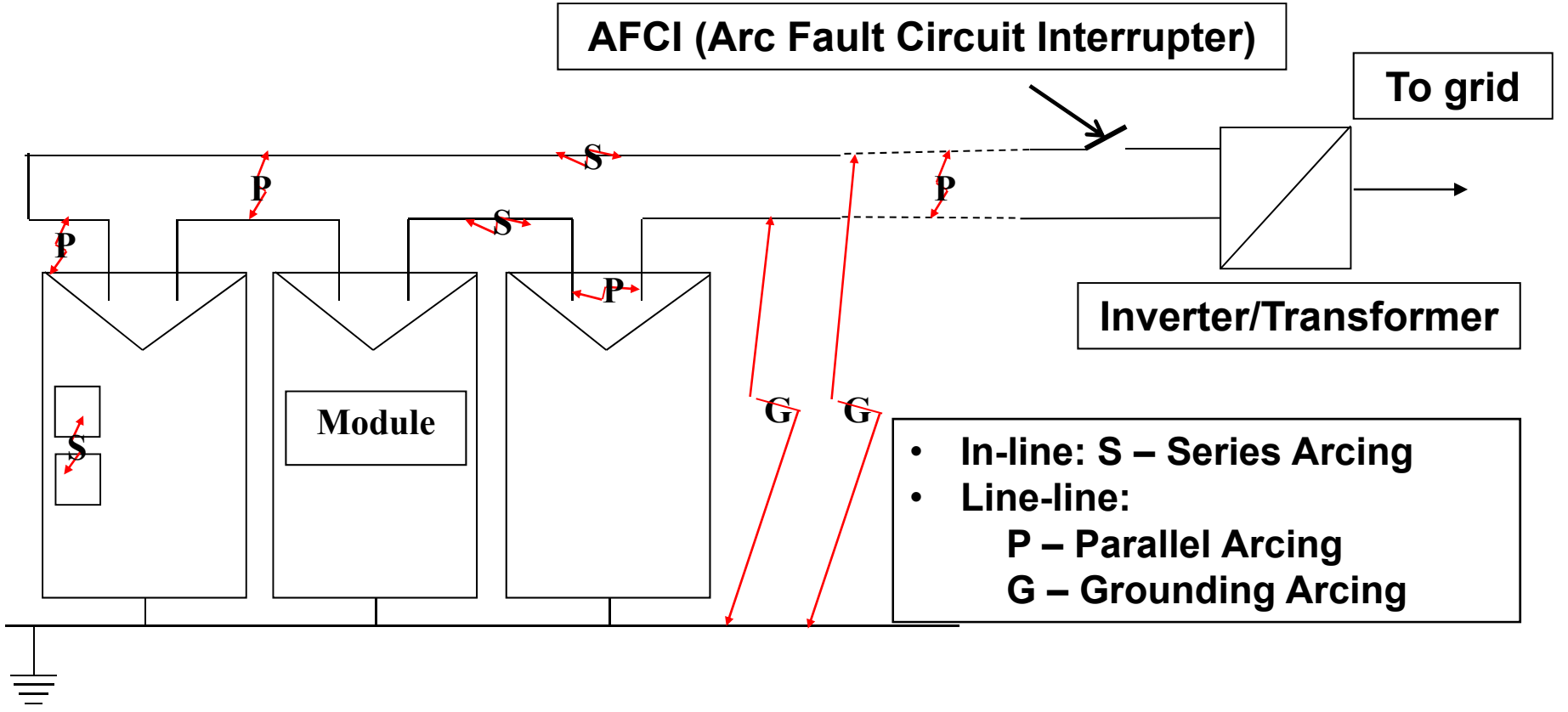
February 2011

Copyright© 1995-2007 Underwriters Laboratories Inc. All rights reserved. No portion of this material may be reprinted in any form without the express written permission of Underwriters Laboratories Inc. or as otherwise provided in writing.

PV Systems

- Unlike traditional electrical products PV modules and wiring **do not** have an overall enclosure to contain arcs and fires resulting from component or system faults.
- Are being installed in great numbers world wide.
- Are most often configured in high voltage series DC circuits.
- High voltage DC arcs are difficult to extinguish while energized.
- The number of PV system fires is increasing each year.
- PV systems need a mitigation means to protect from high voltage PV arcing faults.
- Solar ABCs, UL, PV BOS mfrs and AC AFCI mfrs are working to develop a solution.

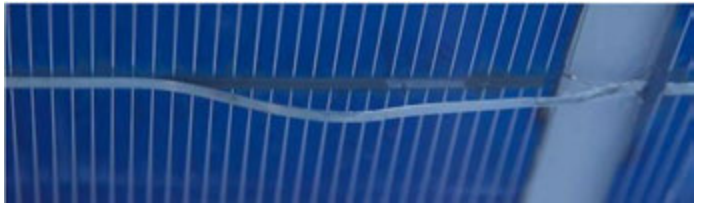
PV Arcing



On this chart, AFCI only works for series arcing, if installed on modules, it can protect from parallel or grounding arcing.

Los Angeles/USA, 2009-02







Early failure

system: 2kW (8 X 250W)

One week operation/one week rain/hours sun shine/fire

Not meet standard
No certification

Semi Valley/USA, 2009-03



Operated: 1.5yrs
Fire: 3:25pm

Meet standard
Have certification

BIPV standard improvement







Underwriters Laboratories

Bakersfield/USA, 2009-04











Bakersfield/USA, 2009-04



Metal conduit heat expansion







NEC 690.11 Is a New Requirement in the 2011 NEC

- It requires all PV systems with DC circuits operating at 80 volts or greater on a building to be protected by an AFCI, PV type, or other system components listed to provide equivalent protection.
- In parallel with this new NEC requirement, UL formed a PV AFCI Ad Hoc Working Group to develop requirements for the PV AFCI.
- UL Outline of Investigation, Subject 1699B, for PV AFCI equipment.

690.11 Arc-Fault Circuit Protection

Required by NEC for:

•Photovoltaic systems with dc source circuits and or dc output circuits

•On or penetrating a building

•Operating at a PV max system voltage of ≥ 80 volts.

Compliance Criteria:

•Shall be protected by a **Listed**

- PV/DC arc-fault circuit interrupter,
- PV system components **Listed** to provide equivalent PV arc-fault protection

NEC - PV AFCIs shall comply with the following

(1) The system shall detect and interrupt arcing faults resulting from a failure in the intended continuity (Series Arc Faults) of a conductor, connection, module, or other system component in the dc PV source and output circuits.

(2) The system shall disable or disconnect one of the following:

- a. Inverters or charge controllers connected to the fault circuit when the fault is detected
- b. System components within the arcing circuit

(3) The system shall require that the disabled or disconnected equipment be manually restarted.

(4) The system shall have an annunciator that provides a visual indication that the circuit interrupter has operated. This indication shall not reset automatically.

PV AFCI Subject 1699B Update

- Well balanced Ad Hoc Working Group developing Subject 1699B Draft PV DC Arc-Fault Circuit Protection AFCI
- Most recent Ad Hoc Meeting at UL on Nov 30 and Dec 1, 2010.
  - Revise document to address Ad Hoc comments
  - Better address PV BOS equipment such as inverters or combiner boxes that include PV AVCI functionality
  - Upcoming publication in 2011.

SU 1699B - PV DC Arc-Fault Circuit Protection AFCI

- Scope Includes:
  - Requirements cover DC photovoltaic arc-fault circuit protection devices for use in PV systems as described in Article 690 of the NEC.
  - Protection is intended to mitigate the effects of arcing faults that may pose a risk of fire.
  - Covers PV dc arc-fault circuit-interrupters (AFCI), arc-fault detectors (AFD), interrupting devices (ID) and
  - inverters, converters, and charge controllers with integral arc-fault circuit interrupter protection.
  - Rated up to 1000V dc.
  - Includes optional parallel tests but not required by 690.11

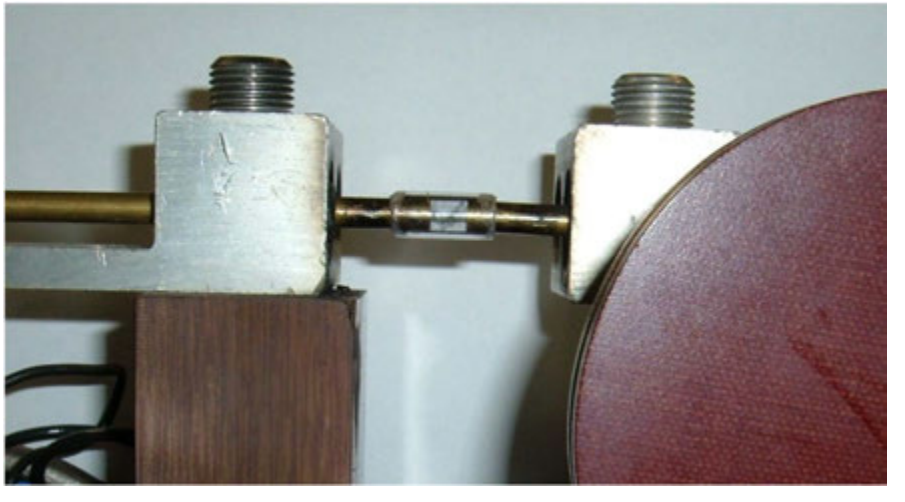
Subject 1699B Tests

Humidity	**Corrosion Test**
Leakage	**Crushing**
Voltage surge	**Strain relief**
Environmental sequence	**Mechanical**
Arc fault detection	**Resistance to Environmental Noise**
Unwanted tripping	**Electrostatic discharge**
Inhibition	**Radiated EMI**
Temperature	**Fast transients**
Overvoltage	**Voltage surge**
Overload	**Induced RF fields**
Endurance	**Voltage dips**
Dielectric Withstand	**Surge current**
Abnormal	**Abnormal overvoltage**
Short circuit	

Table 14.3 Arcing Tests and Clearing Times

Current (Amps)	Arcing Volts (Volts)	Arcing (Watts)	Electrode Gap (Inches)	Clearing Time (Seconds)
7	43	300	1/16	2
7	71	500	3/16	1.5
14	46	650	1/8	1.2
14	64	900	¼	0.8





Hey Wait a Minute!
PV AFCIs Are Not Here Yet!

- NEC 90.4 Enforcement
- The NEC includes a protection clause for new requirements when new protection products are not commercially available at the time of publication.

  – 90.4 This Code may require new products, constructions, or materials that may not yet be available at the time the Code is adopted. In such event, the authority having jurisdiction may permit the use of the products, constructions, or materials that comply with the most recent previous edition of this Code adopted by the jurisdiction.

PV AFCIs are on the way!

- PV AFCIs and related components are being developed by many manufactures.
- In addition to stand alone PV AFCI products, the functionality is being built into many PV system components
  - Inverters
  - PV modules mounted electronics
  - PV DC/DC converters
  - Combiner Boxes

UL Subject 1699B

- First step: UL Subject 1699B OOI (Outlines Of Investigation) will be used to evaluate and certify PV AFCI equipment.
- UL is starting a new Standards Technical Panel (STP) for ANSI UL 1699B.
  - PV Industry, AFCI industry, Mfrs, AHJs, Test Labs, National Labs, Industry Experts, and General Interest.
- UL Subject 1699B is going be developed through the ANSI consensus standards writing process into ANSI / UL 1699B.

For Further Information

Dave Dini
<David.A.Dini@us.ul.com>

Tim Zgonena
<Timothy.Zgonena@us.ul.com>

Liang Ji
<Liang.Ji@us.ul.com>



Photovotaic modules EDF EN quality control

Khalid Radouane♦, Pierre-Guy Therond, Françoise Evin* and Didier Binesti*
EDF Energies Nouvelles, Cœur Défense – Tour A – La Défense 4, 100, Esplanade du Général de Gaulle - 92933 Paris La Défense Cedex, France www.edf-energies-nouvelles.com
*EDF R&D, Avenue des Renardières – Ecuelles, 77818 Moret sur Loing Cedex, France www.edf.fr
♦Contact: khalid.radouane@edf-en.com

Abstract: The present document summarizes the procedure set-up by EDF EN to control the quality of the modules to be installed in EDF EN PV power plants (*crystalline and thin film technologies*) for a total volume larger than 500MW net capacity installed before 2012. Indoor and outdoor measurements have been initiated for initial power evaluation, long-term degradation and reliability. This allows to:

- *Minimizing the risk of failure during operation, assuring the investors and lenders about the robustness of the installed field,*
- *Evolving a business plan which can reflect more the reality of the field behavior*

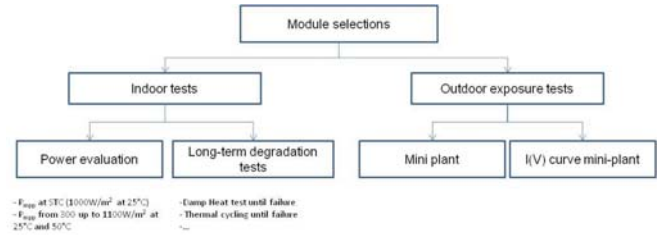
A statistical method is defined by Fraunhofer Institute (ISE) or Certisolis[1] laboratories to select a small amount of module representative of all purchased modules. The quality control procedure is defined according to some selected tests from IEC standards.

1- Introduction

The objective of this note is to give an overview about the quality control procedure and results for photovoltaic modules as defined and applied by EDF EN. Two test categories were followed:

- The first tests are from IEC standards (*IEC 61646 and IEC 61215*). This procedure permits to evaluate modules quality in terms of power estimation.
- The second set of tests is set-up to evaluate module robustness by performing complementary test to the IEC standards.

Both tests can be used to evaluate module quality for existing or new module manufacturers in EDF EN sourcing.



2- Power Estimation

a. Module sampling

A fraction of modules is taken randomly, by using a statistical method, from all modules flash lists for a corresponding lot or from a production batch. The module fraction and sampling is selected according to the maximum power at STC, to the production date and the acquired experience of the manufacturer. Finally, the distribution of the selected modules is checked visually with respect to the serial numbers or the date of production. Selection is made by ISE or Certisolis by defined statistical methods.

b. Electrical characteristics : Incoming indoor tests

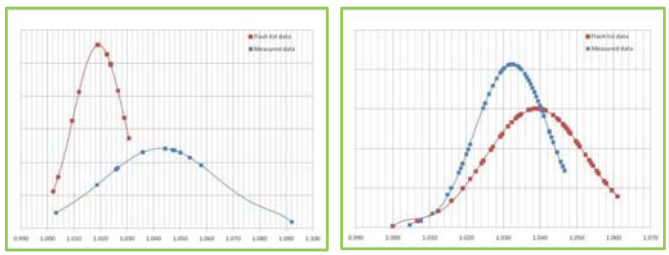
The indoor test for incoming modules is undertaken to verify module power before outdoor exposure or installation in the field. In fact, to determine the current-voltage characteristics I(V) of the module in accordance with IEC standard at the following conditions: *STC conditions: 1000 W/m², at module temperature of 25°C and at different irradiance from 200 up to 1100 W/m², at module temperature of 25°C and 50°C to verify low irradiance behavior of the modules*.

The pre-conditioning procedure corresponds to the one given by the manufacturer in the case of thin film technology modules.

The main results compared to the flash list data given by manufacturer are:

- The maximum power (P_{mpp}): should be in the tolerance range of module manufacturer
- The Fill Factor (FF %): need to have the same value as manufacturer one.

MPPT power comparison of CdTe (*by using the preconditioning procedure developed by the manufacturer*) and crystalline modules is presented below:



CdTe modules *Cristalline modules*

Comparison of Indoor power measurements between Flash list (Red) and measured one (Blue) by using pre-conditioning procedure from CdTe manufacturer

3- Long term behaviors

a. Long-term degradation : Indoor test

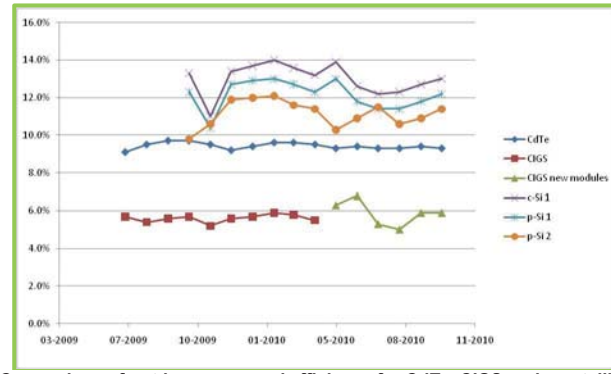
Additional tests with modules selected randomly, such like damp heat and thermal cycling, are also undertaken to determine and understand failure modes for crystalline silicone and thin film modules. These tests are performed longer than IEC standards. The results of some manufacturer were surprising. The performance full down quickly after IEC limits. More details are presented in the paper "*Damp Heat Testing Longer than IEC Standards*" presented by *Mike Van Iseghem et al.* EDF R&D.

b. Outdoor exposure test

To make a preliminary assessment of the ability of the module to withstand exposure to outdoor conditions and to reveal any synergistic degradation effects which may not be detected by laboratory tests. A significant amount of modules is taken from a random position from all flash lists for a corresponding lot or from a production batch. The modules are mounted in a small plant as recommended by the manufacturer. An irradiation measuring device is installed with the same orientation of the modules.

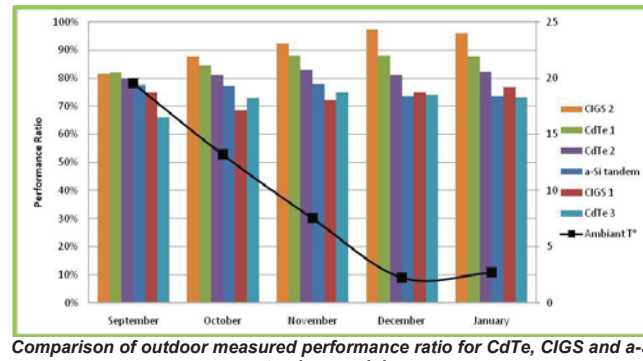
Two kind of installation are made:

- 3 modules per technology (CdTe, CIGS, a-Si and c-Si) are connected to a resistive load sized, such that at STC the modules will operate near the maximum power point via Papendorf software solution system. The I(V) curve is recorded every minute. The information is collected since more than one year.



Comparison of outdoor measured efficiency for CdTe, CIGS and crystalline modules

- 1 up to 100 kW_p equivalent modules are connected to different inverters by mean of PADCON system permitting to measure more precisely *DC and AC current and voltage*. The information is recorded since August 2010.



Comparison of outdoor measured performance ratio for CdTe, CIGS and a-Si tandem modules

4- Conclusion and perspectives

Flash test and long term degradation experiment undertaken by EDF EN help understanding the long term behavior of crystalline and thin film modules with collaboration with the manufacturer. All the information is shared with each manufacturer in order to improve their quality and assure good performance stability for our core business.

Statistical Modeling of Photovoltaic Reliability Using Accelerated Degradation Techniques

Jinsuk Lee, Ryan Elmore, and Wesley Jones

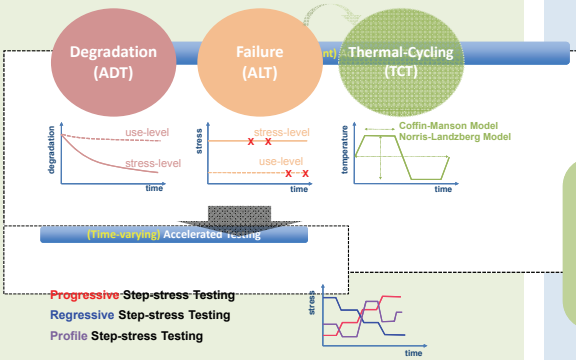
Computational Science Center, National Renewable Energy Laboratory, Golden, CO, USA

Presented at the 2011 PV Module Reliability Workshop, 16-17 February 2011, Golden, Colorado

Introduction & Objective

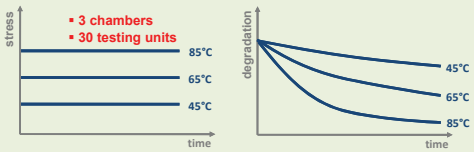
- Introduce cutting-edge life-testing technique, accelerated degradation testing (ADT), for PV reliability testing
- Apply two common types of ADT for life-time prediction of PV modules: multiple constant-stress ADT (MCSADT) and step-stress ADT (SSADT)
- Develop statistical models for use of SSADT with the thermal-humidity stress condition through the cumulative damage model (CDM)
- Provide quantitative models for prediction of PV module life-time including mean-time-to-failure (MTTF), warranty time and failure/degradation rates
- Estimate accelerated testing parameters, such as activation energy, acceleration factors, upper limit condition of stress via statistical inference procedure

Accelerated Testing



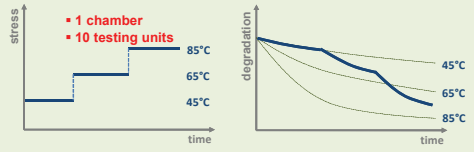
Multiple Constant-Stress ADT (MCSADT)

- The accelerated life testing (ALT) technique may offer little help for high reliable products which are not likely to fail during a rather short period time
- ADT collects the degradation data instead of failure data when it is more difficult to obtain sufficient failure data for ALT
- Single constant-stress testing (e.g, Damp-Heat Test) can be used for qualification testing with a specific durability criteria
- MSCADT can be used for life-time prediction of products



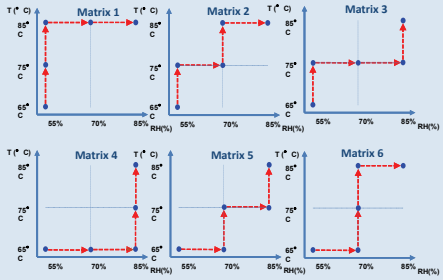
Step-Stress ADT (SSADT)

- Step-stress testing is one of the most basic time-varying stress tests. In a step-stress test, multiple samples in one or more sets are exposed to several stress conditions over time.
- Step-stress testing is an advanced reliability testing technique for high reliability products
  - **Economical:** suitable for limited test facility and condition
  - **Flexible:** useful for new developing products where there is not enough knowledge for test conditions
- SSADT can be constructed based on the cumulative damage model (CDM), which assumes that the remaining test units are failed according to the cumulative density function of current stress level regardless of the history on previous stress levels.



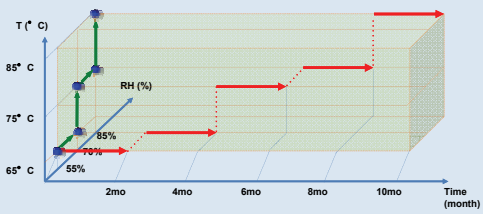
Statistical Models for SSADT

Test Matrix



- The thermal-humidity condition
  - Temperature (T): 3 levels (65°C, 75°C, 85°C)
  - Relative Humidity (RH): 3 levels (55%, 70%, 85%)
  - **No interaction** between T and RH
- 6 possible test matrices can be considered for the SSADT plan

Test Design



- This plot depicts a test design based on "Test Matrix 5" which has five stress levels
  - Level 1 (s_1): 65°C & 55%RH
  - Level 2 (s_2): 65°C & 70%RH
  - Level 3 (s_3): 75°C & 70%RH
  - Level 4 (s_4): 75°C & 85%RH
  - Level 5 (s_5): 85°C & 85%RH

Degradation Model

Stage 1: Defining a degradation pattern

- Linear: $L(t) = a \cdot t + b(s)$
- Exponential: $L(t) = b(s) \cdot \exp[a \cdot t]$
- Power: $L(t) = b(s) \cdot t^a$
- Logarithmic: $L(t) = a \cdot \ln t + b(s)$
- And some used: $L(t) = \exp[-b(s)t^a]$ (Tseng and Wen, 2000); $L(t) = \left(1 + b(s) \cdot t^a\right)^{-1}$ (Mitsuo, 1991)

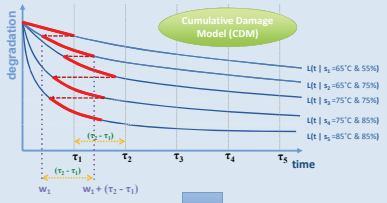
Stage 2: Defining a physical model for stress

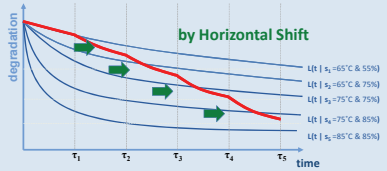
- Temp: $b(s;\ T) = \exp\left(c - \frac{E_a}{k \cdot (273+T)}\right)$
- Temp & RH: $b(s;\ T, RH) = c \cdot \exp\left(-\frac{d}{RH}\right) \exp\left(\frac{E_a}{k \cdot (273+T)}\right)$; $b(s;\ T, RH) = c \cdot \exp(-d \cdot RH) \cdot \exp\left(\frac{E_a}{k \cdot (273+T)}\right)$
- Other two stresses
- Three stresses

SSADT Model

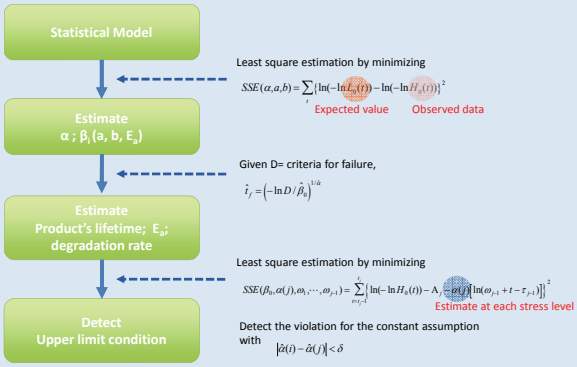
- Expected degradation for SSADT

$$L(t) = \begin{cases} L(t \mid s_1) & \text{if } 0 \le t < \tau_1 \\ L(t + w_1 - \tau_1 \mid s_2) & \text{if } \tau_1 \le t < \tau_2 \\ L(t + w_2 - \tau_2 \mid s_3) & \text{if } \tau_2 \le t < \tau_3 \\ L(t + w_3 - \tau_3 \mid s_4) & \text{if } \tau_3 \le t < \tau_4 \\ L(t + w_4 - \tau_4 \mid s_5) & \text{if } \tau_4 \le t < \tau_5 \end{cases}$$





Statistical Process for Lifetime Prediction



References:

[1] J. Lee and R. Pan, "Analyzing Step-Stress accelerated Life Testing Data Using Generalized Linear Models," *IIE Transactions*, 42, 2010, pp589-598.

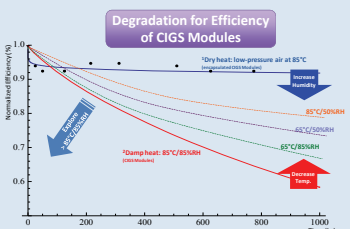
[2] S.-T. Tseng and Z.-C. Wen, "Step-Stress Accelerated Degradation Analysis For Highly Reliable Products, *Journal of Quality Technology*, 32, 2000, pp209-216.

[3] W. Nelson, Accelerated Testing – Statistical Models, Test Plans, and Data Analysis, Wiley & Sons, New York, 1990.

Measurement for Degradation of PV Modules

- **J-V measurement System**
  - Open-circuit voltage (Voc)
  - Short-circuit current (Isc)
  - Fill factor (FF)
  - Conversion efficiency of the device (η)
  - Series resistance (Rs)
  - Shunt resistance (Rsh)

Degradation for Efficiency of CIGS Modules



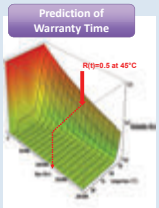
[1]Data source: J. Wennerberg, "Design and Stability of Cu(In,Ga)Se2-Based Solar Cell Modules," Dissertation, ACTA Universitatis Upsaliensis, 2002.

[2]Data source: J. Wennerberg et al., "Cu(In,Ga)Se2-Based thin-film photovoltaic modules optimized for long-term performance," Solar Energy Materials & Solar Cells, 75, 2003, pp47-55.

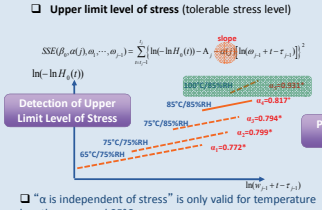
Outputs from SSADT

- **Product lifetime parameters** at various use-conditions
  - Mean time to failure
  - Reliability (Warranty) time
  - Failure rate
- **Degradation rate** at various use-conditions
- **Activation Energy** (E_a)
- **Upper limit level of stress** (tolerable stress level)

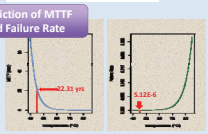
Prediction of Warranty Time



Detection of Upper Limit Level of Stress



Prediction of MTTF and Failure Rate



- "α is independent of stress" is only valid for temperature less than or equal 85°C
  - The issue of "over-stress" can lead to misleading results

Note, + : estimated value from Wennerberg et al. (2003)
* : assumed value

References:

[2] S.-T. Tseng and Z.-C. Wen, "Step-Stress Accelerated Degradation Analysis For Highly Reliable Products, *Journal of Quality Technology*, 32, 2000, pp209-216.

NREL NATIONAL RENEWABLE ENERGY LABORATORY

The Alliance for Sustainable Energy, LLC (Alliance), is the Manager and Operator of the National Renewable Energy Laboratory. Employees of the Alliance for Sustainable Energy, LLC, under Contract No. DE-AC36-08GO28308 with the U. S. Dept. of Energy have authored this work. The United States Government retains and the publisher, by accepting the article for publication, acknowledges that the United States Government retains a non-exclusive, paid-up, irrevocable, worldwide license to publish or reproduce the published form of this work, or allow others to do so, for United States Government purposes. NREL is a national laboratory of the U.S. Department of Energy, Office of Energy Efficiency and Renewable Energy, operated by the Alliance for Sustainable Energy, LLC. NREL/PO-2C00-50738 • February 2011

THE DURABILITY OF POLYMERIC ENCAPSULATION MATERIALS FOR CONCENTRATING PHOTOVOLTAIC SYSTEMS

David C. Miller [1*], Michael D. Kempe [1], Kenji Araki [2], Cheryl E. Kennedy[1], and Sarah R. Kurtz[1] *David.Miller@nrel.gov

[1] National Renewable Energy Laboratory (NREL), 1617 Cole Blvd., Golden, CO, USA 80401
http://www.nrel.gov/pv/performance_reliability/

[2] Daido Steel Co., Ltd. 2-30 Daido-cho, Minami, Nagoya 457-8545, Japan

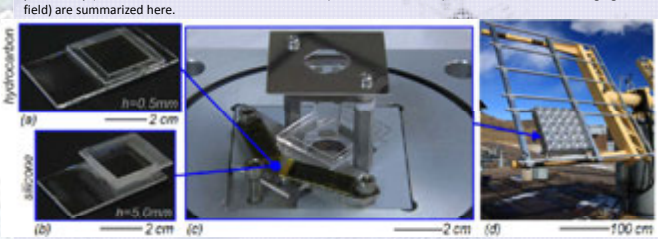
Presented at the PV Module Reliability Workshop, February 16-17, 2011, Golden, Colorado

Introduction

Polymeric encapsulation materials are typically used in concentrating photovoltaic (CPV) modules to protect the cell from the field environment. Because it is physically located adjacent to the cell, the encapsulation is exposed to a high optical flux, often including light in the ultraviolet (UV) and infrared (IR) wavelengths. The durability of encapsulants used in CPV modules is critical to the technology, but is presently not well understood. This work seeks to identify the appropriate material types, field-induced failure mechanisms, and factors of influence (if possible) of polymeric encapsulation. These results will ultimately be weighed against those of future qualification and accelerated life test procedures.

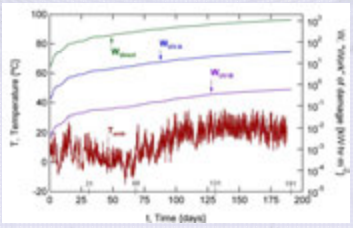
Background

Test specimens, including: ethylene-co-vinyl acetate (EVA), polyvinyl butyral (PVB), poly(ethylene-co-methacrylic acid metal salt) (ionomer), polyethylene and polyoctene copolymer ("polyolefin", PO), thermoplastic polyurethane (TPU), poly(dimethylsiloxane) (PDMS), and poly(phenyl-methyl silane) (PPMS) were formed between quartz slides. (Some of the test materials come from the existing flat-panel PV field and were not specifically formulated for use in CPV. Hydrocarbon formulations often contain a UV stabilization system whereas the silicones typically do not). Hydrocarbon-based materials were laminated to be 0.5-mm thick (as popular in existing film products) whereas silicones were molded to be 5.0-mm thick (to distinguish between these exceptionally optically transmitting materials). Specimens were situated between a secondary optic and then inserted in a contemporary CPV module product (nominally 500x concentration). The module uses a domed Fresnel lens as its primary optical element, and is mounted on a tracker in Golden, CO. Measurements (including hemispherical transmittance, direct transmittance, mass loss, and visual appearance) were/will be performed periodically (0, 1, 2, 4, 6, 12, 18, 24, 30, 36 … months). The initial results (for 6 months cumulative aging in the field) are summarized here.



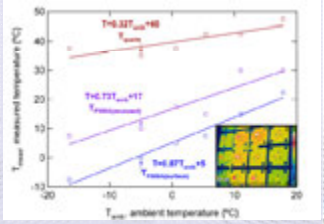
ABOVE: Photographs of representative (a) hydrocarbon and (b) silicone test specimens, are inserted (c) behind a secondary optic element and then (d) into a CPV module. The tracker-mounted module can accommodate 25 separate specimens (no duplicate formulations are used here).

Environmental conditions at the test site are logged using a plethora of instruments, including module-located thermocouples. Instruments not immediately present at the Outdoor Test Facility (OTF) are supplemented by those at the Solar Radiation Research Laboratory (SRRL), located on top of South Table Mountain.



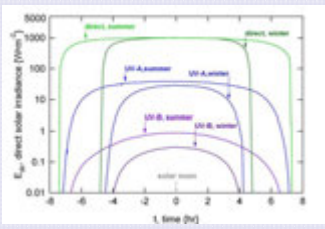
LEFT: Temperature and dose data from the OTF. The maximum and minimum temperatures of 36°C and -15°C, respectively, were observed during the first 6 months in the field. The damaging dose of solar radiation (note logarithmic scale) is distinguished here between "UV-B " (from 280-320 nm), "UV-A" (320-400 nm), and "direct"(285-2500 nm) wavelengths. Seasonal (winter) cloudiness is evident in the lesser slope during the first month relative to that encountered during the sunny summer months (the latter half of the data). The raw dose of radiation incident on first surface of the lens is shown in the figure. The dose at the encapsulation may be analyzed from the measured transmittance of the CPV optical system; its damaging effect may be further understood using the specimen's action spectrum .

Specimen temperature was determined using infrared thermography. For the purpose of the work here, it is critical that the specimen temperature be representative of CPV module products. For example, excessive temperature (because the cell and heat sink are not present) may motivate spurious failure modes.



RIGHT: The temperature of the quartz substrate is shown relative to that of the ambient and the poly(methyl methacrylate) (PMMA) lens. A thermal image of the back of the module is shown in the inset. From the temperature rise for the quartz (+40°C), the existing data suggests the specimen temperature of 75°C during the hottest summer days (36°C). The data for the lens indicates that its surface is cooler than the sites where it is attached to the module. A more advanced model may be used to account for the solar irradiance and wind.

The direct solar resource at the test site (elevation of 1.79 km) includes greater UV radiation than that found at other locations. Furthermore, the steppe climate typically features at least 300 half-days of sunshine. Seasonal differences between the duration and magnitude of the solar radiation, however, do arise based on the site location (latitude of 39.740 °N). A 4.2x, 2.3x, and 1.6x difference exists between the raw dose (integral) of radiation present during the summer and winter months based on duration, for the UV-B, UV-A, and direct wavebands, respectively. Another 2.9x, 1.3x, and 1.0x difference exists between the magnitude of radiation present during the summer and winter months based on magnitude, for the UV-B, UV-A, and direct wavebands, respectively. The damaging dose of UV-B radiation (which scales with both duration and magnitude) is therefore at least 10x greater in the summer months. For polymeric materials, radiation induced damage may be coupled to the temperature, further complicating seasonal differences.

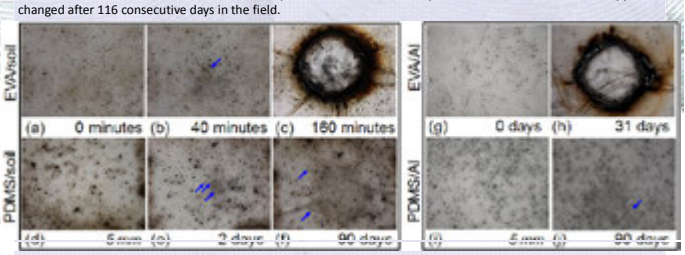


ABOVE: Irradiance data (note logarithmic scale), measured on cloudless days at the OTF . The differences in the duration and magnitude of radiation present are readily distinguished in the figure.

Experimental Results

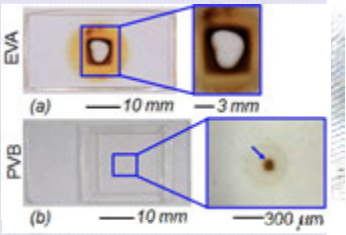
Discovery experiments using EVA and PDMS specimens were conducted to become familiar with the CPV environment and to understand the effect of contamination embedded in the specimens. Catastrophic failure (thermal runaway followed by material decomposition) may be quickly observed (within minutes or days) in CPV modules (geometric concentration ≥ 500x), if no homogenizing optic is used. The optical concentration at localized sites within the focus of a single optical element can easily be 1-3 orders of magnitude greater than the nominal geometric concentration. Such localized hot points are believed to have facilitated the destruction of EVA and PDMS specimens.

Soil, aluminum filings, polymer filings (black polyethylene), and voids (bubbles) were intentionally added to separate sets of EVA and PDMS specimens. Soil, aluminum, and polyethylene (PE) facilitated the thermal decomposition of EVA within 2, 31, and 2 days respectively. Like the earlier specimens, indicators of significant stress (including voided regions, localized delamination, and cracked glass) were observed in failed specimens. Only PE facilitated the thermal decomposition of PDMS; however, the soil and aluminum filled specimens became cracked within 2 days in the field. No primer was applied to the contamination, which may have facilitated the cracks in the PDMS. While voids reduce the optical transmittance, the specimens with bubbles did not appear changed after 116 consecutive days in the field.

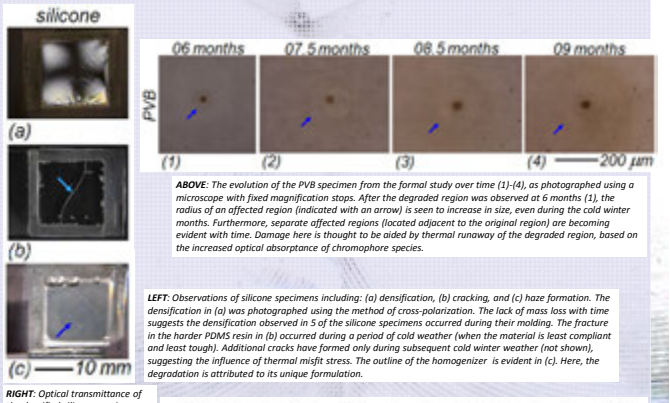


ABOVE: The visual appearance of soil-contaminated EVA [(a)-(c)], soil-contaminated PDMS [(d)-(f)], aluminum-contaminated EVA (g) & (h), and aluminum-contaminated PDMS (i) & (j). Discoloration and voiding (arrow) are evident in (b). The failed EVA specimens contain a voided central region, surrounded by charred, decomposed, and degraded material (c) and (h). The PDMS was prone to cohesive failure (crack formation, [arrows in (e), (f), and (j)]).

The formal experiment is presently examining (6) EVA, (2) PVB, (2) ionomer, (1) PO, (1) TPU, (11) PDMS, and (2) PPMS specimens. A queue of candidates exists to follow any failed specimens.



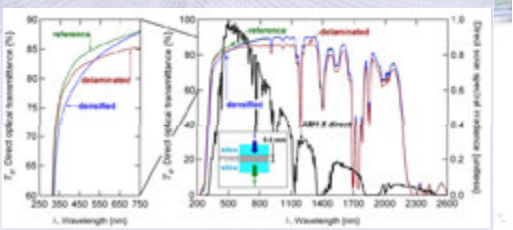
RIGHT: The square outline of the homogenizer is clearly evident in an EVA specimen. The discovery experiment in (a) used a custom UV-transmitting test fixture (nominal concentration of 500x). Similar behavior is anticipated in the formal experiment for a PVB specimen (b). The locally degraded region near the center of the concentrated spot appears similar to those seen to precede failure in the discovery experiments.



ABOVE: The evolution of the PVB specimen from the formal study over time (1)-(4), as photographed using a microscope with fixed magnification stops. After the degraded region was observed at 6 months (1), the radius of an affected region (indicated with an arrow) is seen to increase in size, even during the cold winter months. Furthermore, separate affected regions (located adjacent to the original region) are becoming evident with time. Damage here is thought to be aided by thermal runaway of the degraded region, based on the increased optical absorptance of chromophore species.

LEFT: Observations of silicone specimens including: (a) densification, (b) cracking, and (c) haze formation. The densification in (a) was photographed using the method of cross-polarization. The lack of mass loss with time suggests the densification observed in 5 of the silicone specimens occurred during their molding. The fracture in the harder PDMS resin in (b) occurred during a period of cold weather (when the material is least compliant and least tough). Additional cracks have formed only during subsequent cold winter weather (not shown), suggesting the influence of thermal misfit stress. The outline of the homogenizer is evident in (c). Here, the degradation is attributed to its unique formulation.

RIGHT: Optical transmittance of the densified silicone specimen, shown relative to a reference specimen (composed of the same material, but with no visible densification) and a separate specimen containing a delaminated region. Densification is clearly different from delamination - where a uniform optical loss results from reflections at the glass/void interfaces. Densification reduces the direct transmittance, particularly at shorter wavelengths. Such loss would be detrimental in a CPV module, possibly creating a current-limited condition in a multijunction cell.



Future work is planned to include chemical (FTIR, RAMAN, XPS, NMR) and polymer [differential scanning calorimetry (DSC)] analysis techniques. Traditional indicators (such as yellowness index) lack early warning (or predictive) capability, particularly in the case of thermal runaway. It is hoped that other methods (such as fluorescence spectrometry or chemical analysis) can provide predictive capability as well as insight into the mechanisms of degradation. Once a sufficient knowledge base is generated (including NREL's outdoor data as well as that shared by CPV researchers), NREL will work towards the development of indoor accelerated test methods. We hope to incorporate such methods into the CPV qualification standard(s) and use them to predict material lifetime in the field.

Acknowledgements

The authors are grateful to: Dr. Keith Emery, Mr. Matt Muller, Dr. Daryl Myers, Dr. John Pern, Matt Beach, Christa Loux, Tom Moricone, Marc Oddo, Bryan Price, Kent Terwilliger, and Robert Tirawat of the National Renewable Energy Laboratory for their discussion/help with the solar spectrum, experimental methods, and optical measurements, respectively. The authors would also like to thank Mr. Marc Gagnon of Bixby International Corp. for participation and help with specimens and related understanding. This work was supported by the U.S. Department of Energy under Contract No. DE-AC36-08GO28308 with the National Renewable Energy Laboratory.

Summary

The durability of polymeric encapsulation materials is being examined for the CPV application, using test coupons under the optics of a CPV module product. An assortment of popular encapsulants is presently under study. The monitoring of field conditions and diagnosis of specimen test conditions is essential to the work here. Discovery experiments identified the importance of optical flux uniformity and control of contamination. The initial field failures observed during the formal experiment include thermal decomposition (facilitated by thermal runaway), fracture (facilitated by thermal misfit), and haze formation (facilitated by the formulation chemistry). The work here will ultimately be applied towards test standards and lifetime prediction.

For More Information, refer to the publications:

D.C. Miller, M.D. Kempe, C.E. Kennedy, S.R. Kurtz, "Analysis of Transmitted Optical Spectrum Enabling Accelerated Testing of Multi-Junction CPV Designs", *Optical Engineering*, **50** (1), 2010, 013003.

D.C. Miller, M.D. Kempe, K. Araki, C.E. Kennedy, S.R. Kurtz, The Durability of Polymeric Encapsulation Materials for Concentrating Photovoltaic Systems", Proceedings of the 7th International Conference on Concentrating Photovoltaic Systems (Las Vegas, Nevada), 2011.

NREL is a national laboratory of the U.S. Department of Energy, Office of Energy Efficiency and Renewable Energy, operated by the Alliance for Sustainable Energy, LLC. NREL/PO-5200-50159 • February 2011

Linking Accelerated Laboratory and Outdoor Exposure Results for PV Polymeric Materials

Polymeric Materials Group
Engineering Laboratory

Xiaohong Gu, Kaipeng Liu, Tinh Nguyen, and Joannie W. Chin*

INTRODUCTION

Linking accelerated laboratory test results to field performance and predicting service life for polymeric materials are being investigated at the National Institute of Standards and Technology (NIST). In 2007, we successfully linked the laboratory and field exposure data for a model polymeric coating material, i.e., an amine-cured epoxy, using the reliability-based methodology.

Currently, we apply the same methodology to the polymeric materials used in PV modules and systems. The laboratory accelerated tests of PV polymers (frontsheet, backsheet, encapsulants, etc) were conducted on the well-controlled NIST SPHERE environmental chamber using a 4-factoral experimental design. The outdoor exposure was carried out in Gaithersburg, MD. Multiscale chemical, optical, mechanical and morphological measurements were carried out to follow changes during accelerated and outdoor exposures. The degradation mechanism and failure mode of PV materials and components were studied. Models for linking laboratory and outdoor results and predicting service life of PV materials are being developed.

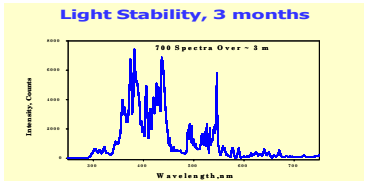
ACCELERATED LABORATORY EXPOSURE DEVICE

NIST Integrating Sphere-based UV Chamber



NIST-Patented 2-meter SPHERE

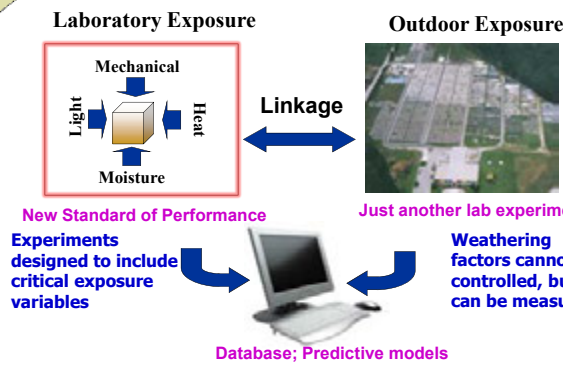
(Simulated Photodegradation via High Energy Radiant Exposure)



- 8400 W UV → 22 "SUNS"
- 95% exposure uniformity
- Visible and infrared radiation mostly removed
- Temperature and relative humidity around specimens precisely controlled (25-75 °C ± 0.1°C; 0-95 % ± 0.2 % RH)
- Capability for mechanical loading
- Exposure conditions of 32 chambers can be individually controlled (UV, RH,T)

• *Chin et al, Review of Scientific Instruments (2004), 75, 4951; Martin and Chin, U.S. Patent 6626053*

Reliability-based Methodology for Linking Laboratory and Outdoor Exposure Results



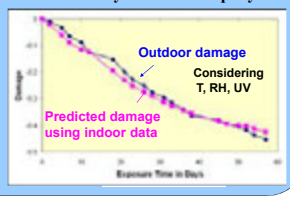
Total Effective Dosage Model

$$D_{total}(t) = \int_0^t \int_{\lambda_{min}}^{\lambda_{max}} E_o(\lambda,t)(1-e^{-A(\lambda)})\phi(\lambda)\,d\lambda\,dt$$

Cumulative Damage Prediction Model

$$Damage_{CUM}(t) = \sum_{t=0} \Delta D(t)$$

Successfully Linking Field and Laboratory Results for Epoxy

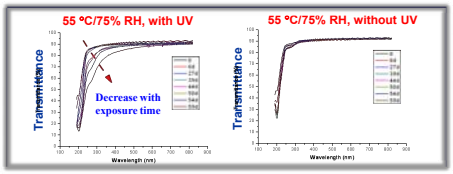


- There is a general agreement that field results are neither repeatable nor reproducible. A new methodology---reliability-based methodology--- is being used to predict the outdoor performance from laboratory exposure for PV polymers.
- The parameters of predictive models are estimated solely from laboratory experiments; outdoor exposure results are used to verify the models using field exposure conditions as input.

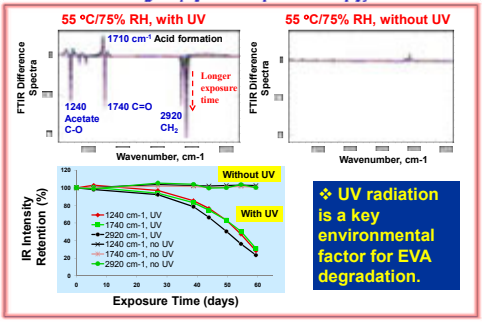
RESULTS FROM LABORATORY EXPOSURE

Effect of UV Irradiation on Degradation of EVA

➢ *Optical Property Changes (by UV-visible Spectroscopy)*

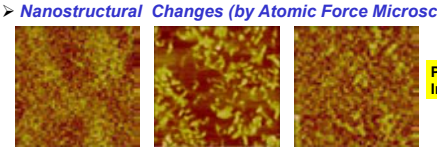


➢ *Chemical Changes (by FTIR Spectroscopy)*

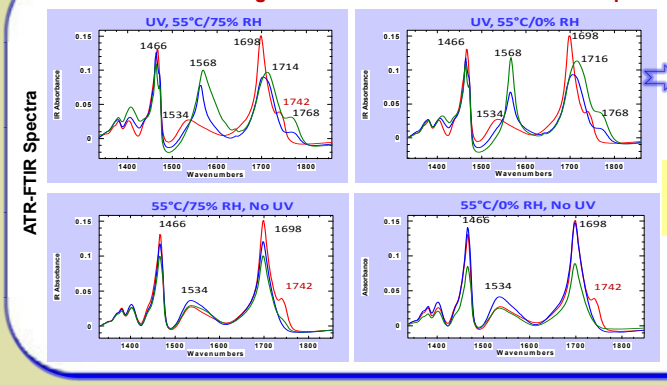


❖ UV radiation is a key environmental factor for EVA degradation.

➢ *Nanostructural Changes (by Atomic Force Microscopy)*



Chemical Changes of PV Ionomers Under Different Exposure Conditions

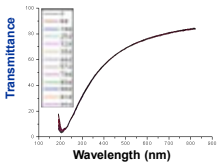


1466 cm-1: -CH2
1534 -1568 cm-1: C=O, carboxylate ions
1698 cm-1: C=O, carboxylic acids (H-bond)
1768 cm-1: C=O, anhydrides or lactones

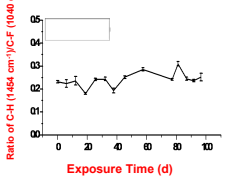
❖ UV radiation has shown a strong effect on chemical changes of PV ionomers, but humidity does not.

Photostability of Fluoropolymers (UV, 55 °C/75%RH)

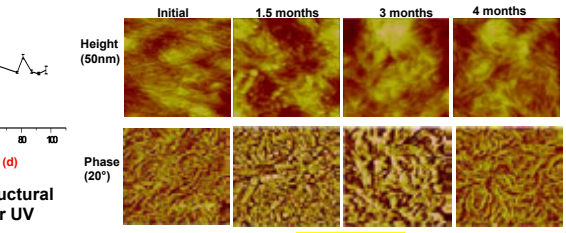
UV Transmittance Spectra



ATR-FTIR Relative Intensity



Surface Nanostructures of A Fluoropolymer Film Exposed on SPHERE for Different Times (AFM)



❑ Essentially, no chemical, optical or nanostructural changes are observed for fluoropolymers after UV exposure for 4 months on the SPHERE.

SUMMARY AND FUTURE WORK

➢ NIST SPHERE is a highly efficient UV weathering device for both rapid screening and fundamental study of reliability of PV materials and components.

❑ The SPHERE exposure results will be quantitatively correlated with outdoor data using mathematical predictive models and reliability-based methodology.

NREL 2011: Photovoltaic Module Reliability Workshop

Reliability of SOG for CPV Primary Optics



Edward Philips[1], Steve Scott[1], Stefan Gaebler[2], Maik Jacob[2], Juergen Zosel[2], Martin Bitzer[2]
[1] Reflexite Corporation, 120 Darling Drive, Avon, CT 06001 USA
[2] Fresnel Optics GmbH, Flurstedter Marktweg 13, 99510 Apolda, Germany
Inquiries to: steve.scott@reflexite.com



Figure 1 Scheme of the concentration principle in CPV (Courtesy of Concentrix Solar GmbH)

Motivation

Silicone on Glass (SOG) primary optics have been introduced into concentrator photovoltaic (CPV) for a few years only. As Figure 1 shows, a plane surface (i.e. the glass substrate) is exposed to the weather side while the micro-structured fresnel lens (made of silicone) lies safely on the inside. This hybrid material approach promises several advantages. Nevertheless before making a decision in favor of SOG, the concept needed to prove its long-term reliability. To shorten test durations of 20-30 years several ISO, EN, IEC and ASTM standards, commonly applied to PV components, define accelerated testing conditions. Corresponding tests were applied to SOG samples out of which a selection is shown on this poster.



Figure 2 Atlas Ci5000 Weatherometer from the outside and inside

Experimental

Unstructured SOG specimen were used for tests requiring transmission measurements. Original micro-structured lenses/lens arrays of several custom designs where used, where functional or cosmetic issues are rated. Weatherability in this context means a cyclic exposure comprised each of 102 minutes of UV-light irradiation at constantly 63° C (dry) and 18 minutes of irradiation combined with water spray (while air temperature is not controlled) as defined in ASTM G155 [1]. Tests were carried out in an Atlas Ci5000 Weatherometer (see Figure 2) with Boro S inner and outer filters. Transmission spectra were measured on plane test samples using a Varian Cary 500 Scan UV-VIS-NIR Spectrophotometer including baseline and zero correction. Yellowness indices were read on a HunterLab ColorFlex 45°/0° Spectrophotometer in accordance with ASTM E313 [3].

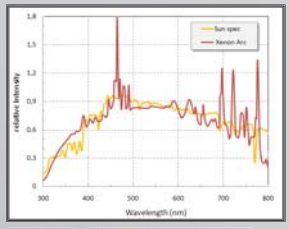


Figure 3 Relative intensities of Xenon Arc compared to the sun spectrum [2]



Figure 4 SOG weatherometer samples (unexposed vs. 7500h XWOM)

Results

Weatherometer conditions from ASTM G155 give an accurate accelerated view of photochemical, oxidative, and thermal degradations that may occur in a material in the field. Still the filtered Xenon Arc radiation at few wavelengths substantially differs from the sun spectrum (see Figure 3). Knowing that the rate that degradations occur and the stimulating wavelengths triggering them are entirely material specific, it is impossible to directly correlate transmission changes from such testing to a specific exposure time in the field. Nevertheless SOG material virtually showed no visual changes (esp. "yellowing", cracking) over a testing time of 7500h as can be seen in Figures 4 and 5. Figure 6 shows, that transmission losses are small and that highest losses occur between 300-400nm - a spectral range, not visible for the human eye in which the solar energy is low as well.

Figure 7 plots the spectral energy transmission of plane SOG samples normalized on AM 1.5 [5]. In initial state 91,4% of the Energy between 280-1700nm are transmitted through SOG. After 7500h of XWOM-Exposure that percentage drops no more than 0,8% without any cleaning of the samples. SOG lens-arrays also passed testing after IEC 62108 [4] without remarkable phenomena.

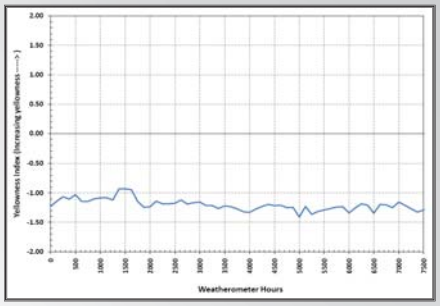


Figure 5 Progression of Yellowness Index [3] of SOG weatherometer samples

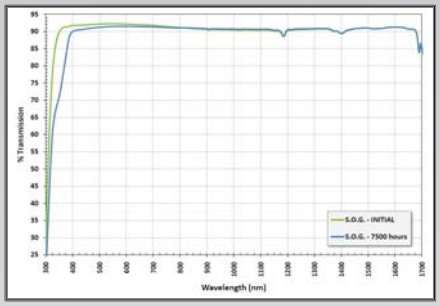


Figure 6 Transmission spectra of SOG weatherometer samples (unexposed vs. 7500h)

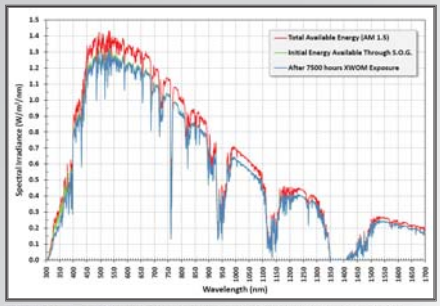


Figure 7 Energy transmission of plane SOG weatherometer samples [5]

Conclusions

It was shown that Silicone on Glass offers outstanding long term performance in commonly used accelerated tests. Its high initial energy transmission is nearly retained the same after 7500h of XWOM radiation. At the same time no relevant mechanical or chemical degradation such as yellowing, cracking and delamination could be observed. Although testing results cannot yet be correlated directly to lifetime in the field, the testing results create a strong confidence in the long term reliability of SOG primary optics.

References

1. ASTM G155 - 05a *"Standard Practice for Operating Xenon Arc Light Apparatus for Exposure of Non-Metallic Materials"*
2. Reproduced from Atlas Weatherometer Ci5000 brochure; http://www.atlas-mts.com/shopdownloads/4/Ci5000_E.pdf [2011-01-24]
3. ASTM E313 - 10 *"Standard Practice for Calculating Yellowness and Whiteness Indices from Instrumentally Measured Color Coordinates"*
4. IEC / DIN EN 62108: 2008-07 *"Concentrator photovoltaic (CPV) modules and assemblies - Design qualification and type approval"*
5. ASTM G173 - 03 *"Reference Spectra Derived from SMARTS v. 2.9.2"*

This poster does not contain any proprietary or confidential information.

PV Arc Fault Detector Challenges due to Module Frequency Response Variability

Jay Johnson, Scott Kuszmaul, Jason Strauch, Ward Bower - Sandia National Laboratories

Introduction

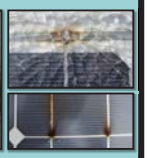
PV system arc faults have led to a number of rooftop fires which have caused significant property damage and threatened the safety of building occupants. In response, Article 690.11 was approved for the **2011 National Electrical Code** which **requires new PV systems on or penetrating a building to include a listed arc fault protection device**. Sandia National Labs is researching the electromagnetic phenomena of PV arcs and the propagation characteristics of arcing signals through PV arrays in order to inform arc fault detector designers of frequency-dependant PV attenuation, electromagnetic noise, and radio frequency effects within PV systems.



Arcing at the combiner box [1].



PV arc fault-initiated fire on a warehouse in Buerstadt Germany.



Discoloration indicating arcing at the busbar and collector ribbon.

Purpose

In order to prevent arc faults and fires in PV systems, Sandia National Laboratories is researching electrical signal propagation through PV modules to help design robust Arc Fault Circuit Interrupters (AFCIs).

Research Goal

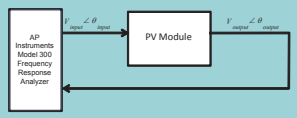
Arc fault detectors utilize frequency content on the string to determine if an arc is occurring. Due to filtering in PV components (e.g., modules, connectors, bypass diodes) and noise in the form of inverter switching, electromagnetic coupling (crosstalk), and other radio frequency (RF) effects, it is possible that arcing could go undetected. To better ascertain the potential for missing a faulting condition, Sandia National Labs is investigating if module degradation alters arcing frequency content measured by a remotely located detector.

Setup

Experimental Procedure: A frequency response analyzer was used to measure the AC response of an intermittent module from 1 Hz to 10 MHz. The attenuation of the AC signal is determined by the magnitude of the output voltage.

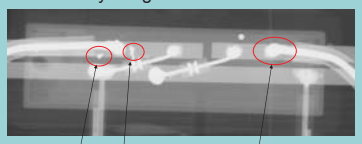


The experimental setup for the module scans. The scans were performed without irradiance.



Sinusoidal AC input voltage signal is driven into the PV module and the Frequency Response Analyzer calculates the attenuation from the output magnitude.

Test Module: An intermittent 80 W polycrystalline module had conductivity issues depending on the angle the external line made with the junction box. The continuity of the soldered junction box connection could be manipulated by twisting the line. The junction box is shown in the x-ray image below.



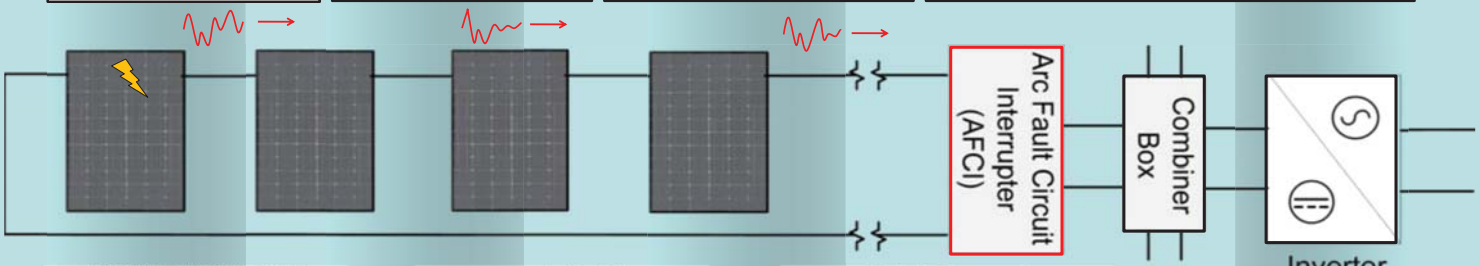
Arc Fault Signal Propagation and Remote Detection Challenges

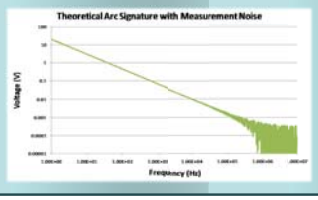
1. An arc fault initiates at a connector, junction box, or within a module and generates pink AC noise on top of the DC current. This signal travels down the line through the system.

2. As the signal passes through the modules and connectors, some of the frequency content of the electrical AC arc noise is attenuated (or potentially amplified).

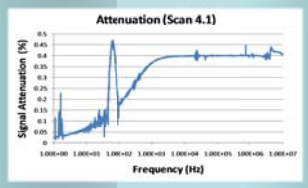
3. Depending on the system line lengths and antenna effects, RF phenomena can change the signal characteristics further. In some cases, crosstalk in the system will amplify certain frequency content.

4. The modified arcing signal reaches the arc fault detector within the AFCI. Depending on the cell technology, system topology, meteorological conditions, and health of the modules, the signal reaching the AFCI will be significantly different than the original arcing signal—possibly allowing an arcing condition to go undetected.

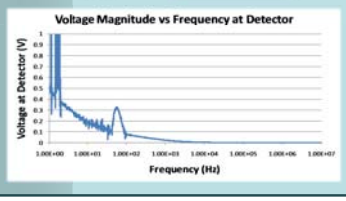




X



=



5. Inverter switching generates additional noise in the system at a few kHz to 100 kHz .

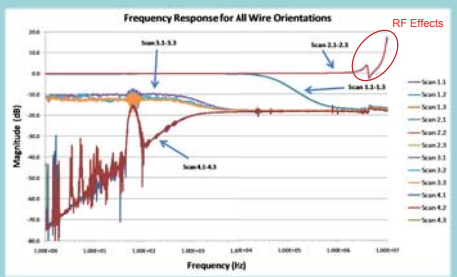
1/f noise is produced when the arc event occurs. The noise floor is reached at higher frequencies.

The signal is attenuated as it passes through an intermittent module.

Although this model ignores RF effects and crosstalk, the frequency content of the arc reaching the detector is affected by the intermittent module.

Results

The intermittent module was scanned three times with the loose connection in four different orientations. The 2nd orientation (Scans 2.1-2.3) made a good connection in the junction box. The odd behavior above 300 kHz is from RF effects in the line and the connections. Scans for the 1st and 3rd orientations show the module behaving as a low pass filter, whereas orientation 4 strongly attenuates low frequencies. The **variation in the frequency responses implies that conditions which cause arcs (i.e. an electrical discontinuity), could also cause detectors to miss the arc.**



Frequency response of a single intermittent module configured with a loose junction box wire held in four different orientations.

Conclusions

Sandia National Labs is testing electrical propagation through PV strings by characterizing different filtering and RF effects in individual components. Frequency analysis showed RF effects were present at higher frequencies and modules could act as filters on the line. **One intermittent module was capable of acting as either a high pass or low pass filter** depending on the orientation of the junction box wire. This could have grave implications for a remotely located arc fault circuit interrupter because if the AFCI uses sufficiently filtered frequencies for detection, the **AFCI would not trip and the arcing event would not be extinguished**.

Sandia is a multiprogram laboratory operated by Sandia Corporation, a LockheedMartin Company, for the United States Department of Energy's National Nuclear Security Administration under contract DE-AC04-94AL85000.
This work was funded by the US Department of Energy Solar Energy Technologies Program.

This poster does not contain any proprietary or confidential information.

National Nuclear Security Administration

LOCKHEED MARTIN

Sandia National Laboratories

CPV Module Acceptance Angle Characterization

Sandheep Surendran
290 Division St, Suite 401, San Francisco, CA 94103, USA

Introduction

While angle of incidence effect on flat plate PV modules can be modeled as a simple cosine response, CPV modules have a much greater sensitivity to misalignment. Presently there are no standard methods for measuring the acceptance angle of CPV modules. Not even a standard, CPV-specific definition for acceptance angle exists. Nameplate power ratings for CPV modules are essentially meaningless without an understanding of how misalignment will affect module performance. The expression of acceptance angle as a single value provides only a mere glimpse into the much more complicated quantification of misalignment sensitivity.

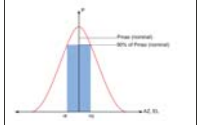
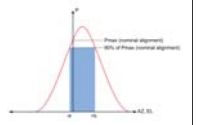
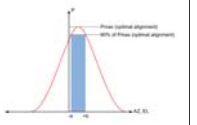
The Current Situation

The generally accepted definition for acceptance angle is:

"The angular misalignment that a module can tolerate while still delivering at least 90% of its maximum power"

There are some problems with this definition:

- What is maximum power? Is it:

A Nominal Value	Max Power at Nominal Alignment	Max Power at Optimal Alignment
		
A module vendor may wish to "de-rate" their power rating to inflate their acceptance angle. E.g a 100W module with ± 0.2° acceptance angle could be re-stated as a 80W module with ±5° acceptance angle.	For a customer to achieve the stated performance in this case, they would have to individually align every module on their tracker.	In this case, the customer need not align each module—the modules can simply be installed onto a tracker. However, the power output may be in excess of the stated max power.

- A single value does not communicate the asymmetry of misalignment sensitivity between the module's axes (and all angles in between).
- Misalignment sensitivity at other percentages of max power can affect tracker and inverter selection and configuration.

Proposed Procedure

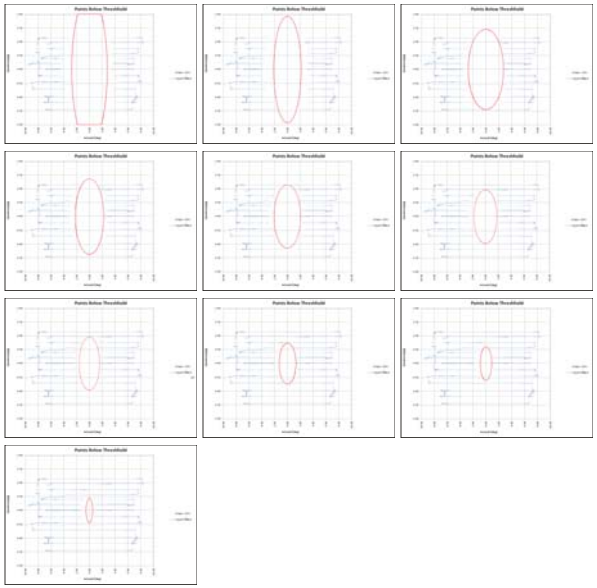
Measurement

1. Mount module and instruments on tracker per respective manufacturers' recommendations
2. Allow module to thermally equilibrate while tracking sun
3. Snap IV curve, determine V_{mpnom}
4. Intentionally misalign module in various orientations while synchronously sampling environmental conditions, tracker orientation, and module output (P_{max} or I @ V_{mpnom})

Analysis

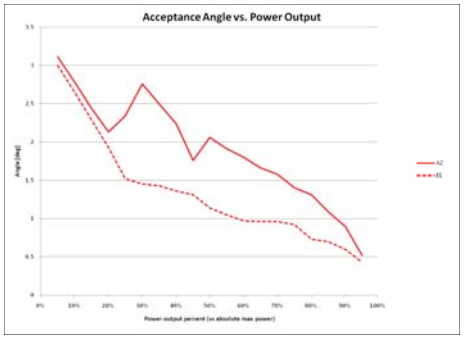
1. Correct data for movement of sun (if necessary) and variations in environmental conditions
2. Plot points on axis 1 vs. axis 2 (e.g. AZ vs. EL)
3. Filter out points with P_{max} greater than various thresholds
4. Inscribe largest ellipse possible not containing plotted points
5. Plot ellipse semi-axis lengths vs. various thresholds

Sample Data & Analysis



Data courtesy of SolarMation

Sample Results



Outstanding Questions

- What is the algorithm for maximizing the ellipse size?
- How to ensure sufficient point density?
- How to communicate results?
  - Acceptance Angle = f(Power Out)
  - Power Out = f(Acceptance Angle)

Conclusions

This is a simple and effective method for assessing the complete characterization of a CPV module's acceptance angle. In doing so, it defines acceptance angle as:

"The relationship between a module's output power and its misalignment to the sun vector"

Knowing this relationship will be critical for CPV integrators to know which modules have acceptance angles that are not just *sufficiently*, but *optimally* accommodated by which trackers.

This poster does not contain any proprietary or confidential information.

surya design

Performance of a Low-cost, Low-concentration Photovoltaic System

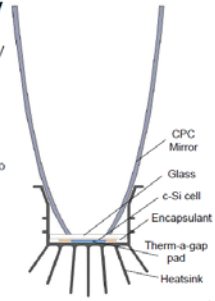
K.A. Shell[1], S.A. Brown[1], M.A. Schuetz[1], R.J. Davis[2], R.H. French[3]

[1] Replex Plastics, 11 Mount Vernon Ave, Mount Vernon OH 43050
[2] Nanotech West Lab, The Ohio State University, 1381 Kinnear Road, Columbus OH 43212
[3] Materials Science, Case Western Reserve University, 302 White Hall, 10900 Euclid Ave, Cleveland OH 44106

Introduction: LC2PV

Low-cost, Low-concentration PV
- 10x Geometric Concentration
- Asymmetric Dual-axis compound parabolic concentrating reflector

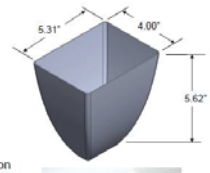
Benefits of low-concentration:
- Wide acceptance angles collect larger portion of circumsolar radiatio
- Reduce tracking accuracy requirements, lowering Balance of System costs
- Less risk for material degradation caused by concentrated UV exposure
- Can use more standard materials and manufacturing methods

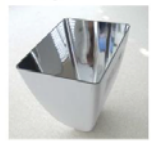


1

Optical Design

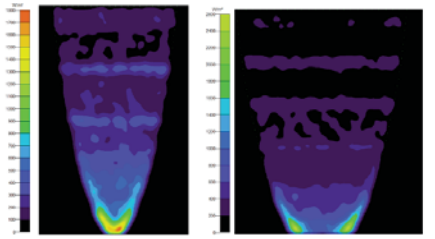
- Acrylic CPC
- Second surface mirror
- Designed for 1-axis inclined tracking
  - Non-tracking direction
    - θ_{ha}= 23.5°
    - Allows for seasonal variation in the angle of the sun
  - Tracking direction
    - θ_{ha}= 12.1 °
    - Allows for inaccuracies in tracking
- Geometric Concentration = 10.3





2

Expected Irradiance on CPC Reflector



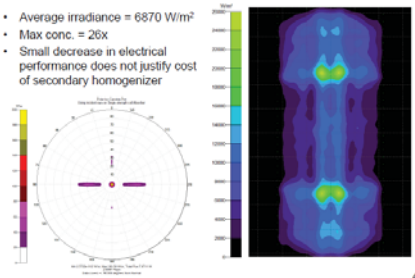
Non-tracking N/S direction
Max irradiance = 1800 W/m²

Tracking E/W direction
Max irradiance = 2800 W/m²

3

Expected Irradiance on Encapsulated Cell

- Average irradiance = 6870 W/m²
- Max conc. = 26x
- Small decrease in electrical performance does not justify cost of secondary homogenizer



4

Heat Dissipation Requirements

Designed a custom extruded aluminum heatsink to dissipate the heat and optically align the reflectors.

R_{th} = thermal resistance of heat sink

$R_{th} = \frac{T_{cell} - T_{air}}{P} = 1.9°C/W$

Desired $\Delta T_{cell-air}$ = 20°C

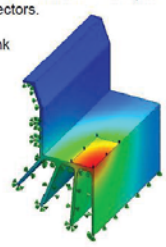
$P = I \times (1-\eta) \times CF \times A_{cell}$

I = solar irradiance, W/m²

η = cell efficiency

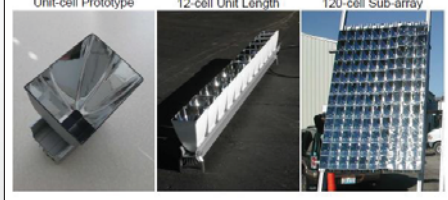
CF = concentration factor

A_{cell} = cell area, m²



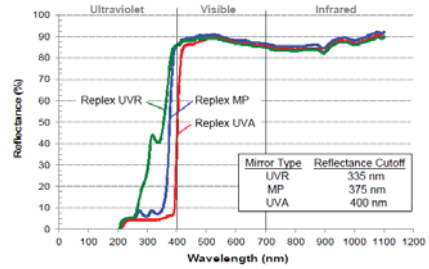
5

Prototypes



6

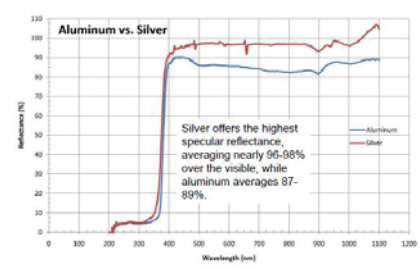
Replex UV Selective Mirrors



Mirror Type	Reflectance Cutoff
UVR	335 nm
MP	375 nm
UVA	400 nm

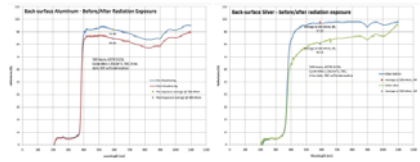
7

Optical Efficiency: Al vs. Ag



8

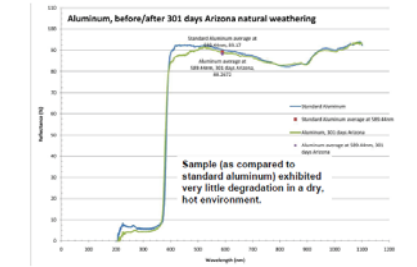
Mirror Durability: Accelerated Testing



- Conditions most closely resemble a Florida-type environment. Addition of moisture + heat in addition to UV changes the rate of degradation as compared to Arizona-type conditions.
- Aluminum: average 7% reduction in specular reflectance
- Silver: Average 17% reduction in specular reflectance
- Aluminum shows greater durability under adverse conditions.

9

Mirror Durability: Arizona Outdoors



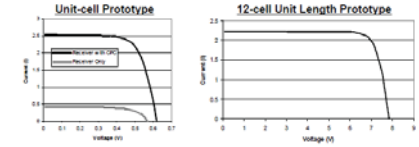
10

Manufacturability

- Front Surface Mirror:
  - Higher overall spectral response.
    - Depending on cell technology, may not be relevant. ie: III-V vs c-Si
  - Higher accuracy (no refractive effects).
  - Substrate flexibility.
  - Lower durability, higher cost (coatings, tie layers).
- Back Surface Mirror (chosen for Gen 1 design):
  - Similar reflectance in visible.
  - Refractive effects must be accounted for.
  - Proper substrate selection important.
  - Good durability, low cost.
  - Able to reduce UV exposure to receiver through Replex' UV selective mirror.

12

LC2PV Gen1 Prototype Performance



Unit-cell Performance	Receiver Only	With CPC
I_{sc}	0.43	2.53
V_{oc}	0.56	0.56
P_{max}	0.17	1.11
Fill Factor	0.69	0.77
Conc. Factor	-	6.6
Efficiency	15.0%	7.9%

12-cell Length Performance	With Glass
I_{sc}	2.29
V_{oc}	7.78
P_{max}	14.7
Fill Factor	0.83
Conc. Factor	7.1
Efficiency	10.0%

13

LC2PV Performance Over Time

- Glass Breakage
  - PV glass was not available to fit the form factor needed (2" width).
  - Almost all modules exhibited significant cracks in the cover glass.
- Moisture Intrusion
  - Pockets of moisture or voids between cover glass and cells, both at cracks and near the ends of the laminations.
- Delamination
  - Which occurred first: Glass breakage, moisture intrusion, or delamination?
  - Did Glass breakage or moisture intrusion cause delamination?
  - Potentially result of improper glass cleaning
- Significant decrease in power output
  - From material degradation or optical losses from glass breakage, voids and moisture intrusion?

14

Conclusions

- Low-concentration PV with inexpensive acrylic mirrors works
- Form factor unsuitable for cost-effective installation
  - Heat sink design complicated mounting procedure to tracker racking
  - Too many junction box leads increases installation time
  - Too heavy
  - Difficult to manufacture using standard equipment
- Next generation receiver design must be simplified to improve cost, manufacturability, and durability
  - Allow for use of PV glass in available sizes
  - Able to utilize industry-standard equipment
  - Simplify installation
  - Reduce weight

15

This poster does not contain any confidential information.

This work has been supported by the Ohio Third Frontier Photovoltaics Program under grant numbers 08-038 and TECH 10-051 in collaboration with the Ohio Wright Center for Photovoltaics Innovation and Commercialization (PVIC).







ACRYLITE®

acrylics for reliable long-term performance

Evonik acrylics offer:

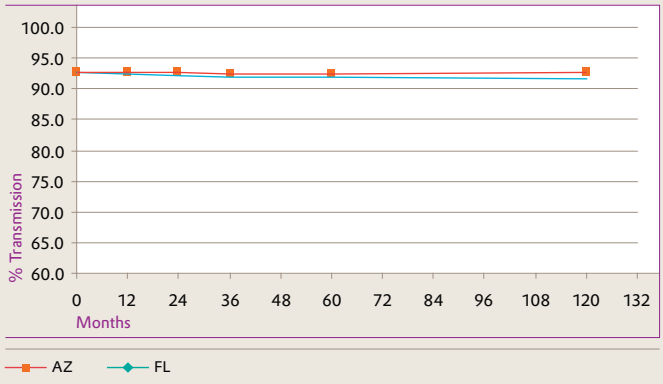
- proven UV stability
- very low residual monomer
- outstanding control of molecular weight

Evonik processes provide:

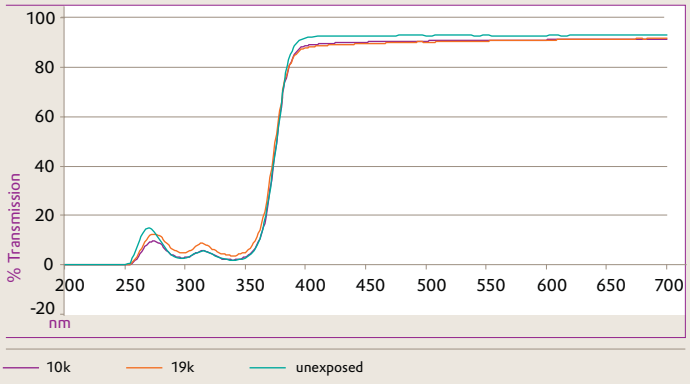
- advanced, selective UV stabilizers and additives
- flexibility in formulation and design
- no internal material stress minimizes lens bowing over product lifetime
- proprietary process optimization for dimensional stability

Transmission losses < 0.10% per year average

Light Transmission after Natural Weathering
3 mm ACRYLITE® FF acrylic sheet



Xenon Arc Weathering Performance
of ACRYLITE® acrylic sheet



ACRYLITE® ending transmission >glass starting transmission (91%)

Lens flatness ensured in variable moisture and temperature conditions

25 year warranty

Reliability poster
DRAFTv4 2-2-11

Evonik. Power to create.

EVONIK INDUSTRIES

On the development of accelerated aging tests based on thermal stress impact to assess the reliability of 1000 suns CPV modules

G. Fleury, S. Colasson, T. Baffie, M. Mariotto, J.L. Martin*, C. Mangeant*, L. Mabille*, J.E. De Salins**

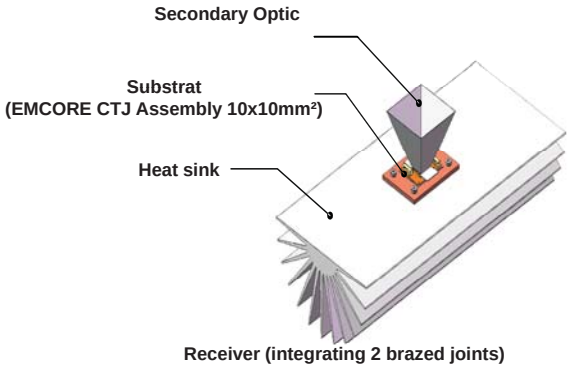
CEA-LITEN, 17 rue des Martyrs-38054 Grenoble
* INES, 50 av. du Lac Léman, Parc Savoie Technolac, 73375 Le Bourget du Lac
** HELIOTROP SAS, Paris Innovation, 5 rue d'Uzès, 75002 Paris, France
gatien.fleury@cea.fr, Tel: +33 4 38 78 01 05

Background

- Development of CPV systems by the French company HELIOTROP
- Technical and research support by CEA
- Reliability assessment of modules and receivers is performed according to the IEC 62108:2007, whereas sub-components follow other suitable qualification standards (MIL-STD-883H, IEC 60068-2-21…)

Technology

- CPV system with a concentration factor of 1000 suns
- First generation module based on EMCORE Solar triple junction cell receiver
- Developed modules are mounted on a commercial tracker



Receiver (integrating 2 brazed joints)



Module (concentration of 1000 suns)



Tracker installed in CEA-Cadarache (south of France)

Issues

Accelerated aging tests are needed to assess the design 's robustness of the whole module during product's life

=> How to develop simple but pertinent accelerated aging tests reflecting the real environment?

Methodology

- A special Instrumented Module (IM) is developed with precise measurements of temperature, relative humidity, pressure, surrounding air velocity and I(V) characteristics

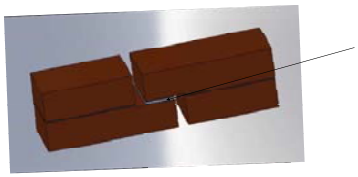
- Data from a weather station is used to link the conditions measured inside the IM with global weather data
  ⇒ Aim is to link the climate of CEA-Cadarache (sunny place in the south of France) with the temperature repartition inside the module (especially the receiver) during a long period of time
  ⇒ Measurements are used to check the thermal model of the module developed in parallel
  ⇒ Experimental data obtained at the module level allow a better prediction of the climate stress (duration and number of cycles) accumulated during products' life

- Aging of polymer (encapsulants and Fresnel lens) is studied apart (UV, humidity, temperature aging and cycling)

- Aging of the braze (that is integrated in the receiver) is studied by means of analytical tests (composite Double Notches Specimens are fabricated and submitted to thermal aging and thermomechanical cycling aging)

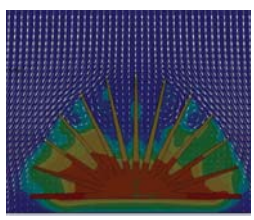
- Thermomechanical calculations are used to compare the design of the different receiver generations and orient the design in order to reduce the mechanical stress inside braze and cell

- A Special testing bench (receiver level) is being developed to reproduce the thermal map around the receiver for better simulate the transient thermal behavior of the receiver during thermal cycling.

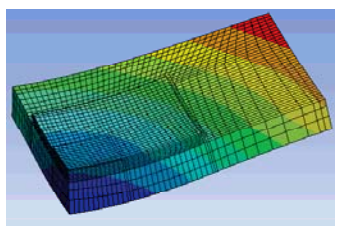


Braze + specimen representative of a cell

Composite Double Notched Specimens used to evaluate the aging of the braze



Air velocity and temperature repartition around the heat sink placed outside the module (Vz = 3 m/s)



Deformation of the brazed assembly (Cell + DBC + copper heat sink) during brazing operation

This poster does not contain any proprietary or confidential information

Correlations in Characteristic Data of Concentrator Photovoltaics

Cassi Sweet, Nick Bosco, Sarah Kurtz

Presented at the 2011 Photovoltaic Module Reliability Workshop, 16-17 February 2011, Golden, Colorado

Introduction

- This study is motivated by reports of immediate on-sun degradation or failure in concentrator photovoltaic cell assemblies for ~1% parts.
- Over 500 bare III-V multi-junction cells were initially characterized, put on-sun, and evaluated.
- Correlations between initial characterization and immediate degradation are discussed.

Procedures

- Light and dark current-voltage traces (IV) and EL images were recorded for over 500 bare cells before packaging. High and low pass filters are used to image GaInP and GaAs junctions.
- IR images were taken of cells lacking adequate EL emission (at 50mA).
- Bare cells were then packaged into receiver assemblies and the voltage response at 10mA was recorded (Figure 1).
- Cell assemblies were fit into modules and exposed to outdoor solar stress of at least 750DNI for a minimum of 4 hours.
- Voltage response at 10mA was also recorded after exposure.

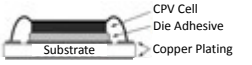


Figure 1. Cross sectional diagram of CPV receiver

Results - Initial IV and cell change due to on-sun exposure

Representative bare cell dark IV curves are presented in Figure 2. Current data at 1.5V bias is plotted against the change in voltage (recorded at 10mA) between pre and post on-sun exposure (Figure 3). This produces a distribution of points comparing the cells' initial IV condition to the change after solar stress.

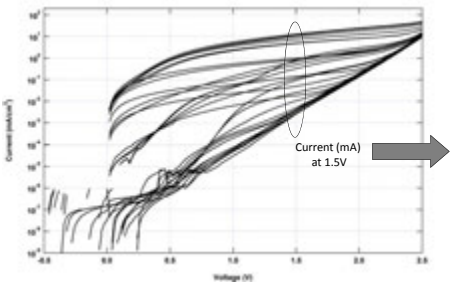


Figure 2. Initial Bare cell dark IV plots of several samples tested. Current information at 1.5V is recorded for comparison.

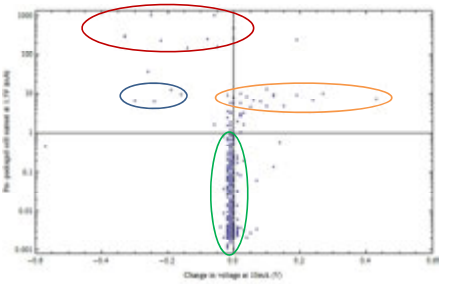


Figure 3. Current (mA) data from bare cell dark IV traces at 1.5V is plotted with the change in packaged cell voltage response to 10mA due to solar exposure.

Approximately 500 bare cells are shown in a current point plot (Figure 3). Areas of the graph are highlighted for further review. Highlighted colors correspond to graphs and images throughout this poster.

The majority of all cells showed an initial response of less than 1mA at 1.5V (highlighted in green, Figure 3). These cells experience minimal change due to solar exposure, with a voltage change between -0.04V and 0.04V at 10mA, if any.

Cells with pre-exposure IV tests above 100mA (at 1.5V) are severely shunted. These cells, highlighted in red, had no detectable electroluminescence emission.

The region between 1mA and ~10mA includes a large number of cells that experience positive change where Vf>Vi, highlighted in orange, or negative change Vf<Vi, highlighted in blue (Figure 3).

Analysis of light IV curves suggest that the change in cell response is primarily due to a change in shunt resistance, while negative or positive change corresponds to a decrease or increase, respectively. It is suspected that all cells in the orange highlighted region experienced shunt improvement due to solar exposure.

Results - Initial IV, EL and cell change correlations

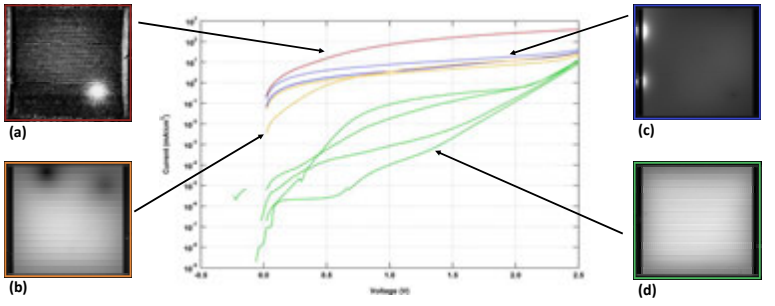


Figure 4. Initial bare cell dark IV trace curves are plotted on log scale for various cells that reside in highlighted regions of Figure 3. Each unfiltered EL image is representative of a typical cell in each region. Colors correspond accord-

All cells in the red region of the current point plot (Figure 3) are shunted and did not sufficiently emit at 50mA for EL imaging. An IR image of a severely shunted cell shows the shunt location where high current density produces excess heat (Figure 4a). The shunt location varies from cell to cell in this region.

Samples in the orange highlighted region have two distant dark IV shapes (shown in orange, Figure 4) with some variation in the EL images artifacts. An example of such is shown in Figure 4b.

All samples in the blue region of the current point plot (Figure 3) have a shunt that produces an EL image with bright spots on the edge of the cell near the bus bar (Figure 4c). This is due to manufacture probe damage for all cells in this region. Additionally, all cells share a similar IV shape as in the blue dark IV curve (Figure 4).

Cells in the lower current point IV range experience minimal change due to solar exposure (green region, Figure 3) and produce clean initial bare cell EL images (Figure 4d).

Results - Filtered EL Images

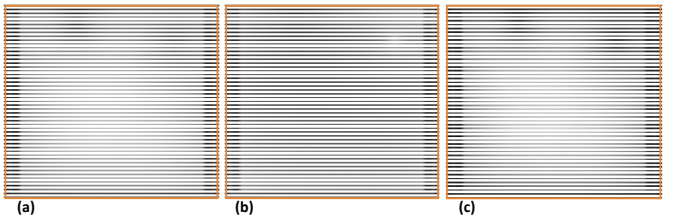


Figure 5. Initial bare cell images of one cell unfiltered (a) that display two types of artifacts seen in multiple cells in the orange highlighted region of Figure 3. Low and high pass filters are used to obtain images of the GaInP (b) and GaAs (c) junctions.

Shunts primarily affecting the GaAs layer may appear as a bright spot in the GaInP layer (Figure 5b) with a corresponding dark area in GaAs layer (Figure 5c). The bright spot is due to current crowding in the GaInP area adjacent to the GaAs shunt. Greater shunting in the GaAs compared to GaInP layer is confirmed by analysis of filtered light IV curves.

Conclusions

A large majority of cells that experienced change due to immediate solar exposure, tested above 1mA at 1.5V in current-voltage bare cell analysis before packaging and solar exposure. Functional cells experiencing change due to exposure predominantly show ~10mA response at 1.5V in bare cell IV tests.

Correlations exist between the initial dark IV characteristic and artifacts found in the bare cell EL images. Results suggest that artifacts observed in the bare cell may serve as an indicator for early on-sun degradation. It is suspected cells experiencing short term change due to solar stress may be correlated to a change in shunt resistance.

This poster does not contain any proprietary or confidential information. NREL is a national laboratory of the U.S. Department of Energy, Office of Energy Efficiency and Renewable Energy, operated by the Alliance for Sustainable Energy, LLC. NREL/PO-5200-51246 • February 2011

NICE Modules Certification According to IEC-61215 and 61730

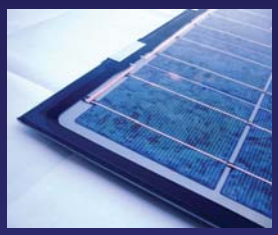
J. Dupuis[1]*, E. Saint-Sernin[1], K. Bamberg[1], R. Einhaus[1], E. Pilat[2], A. Vachez[2], D. Bussery[3]
[1]Apollon Solar, Lyon, France [2]CEA-INES, Le Bourget du Lac, France, [3]Vincent Industrie, Brignais, France
*Corresponding Author: Tel: +33 681 108 156, dupuis@apollonsolar.com

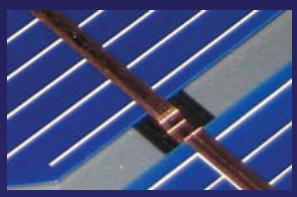
Apollon Solar's NICE Module Technology

Objectives:
- Production costs <0,30 €/Wc Module Cost
- Module Lifetime: 30 years

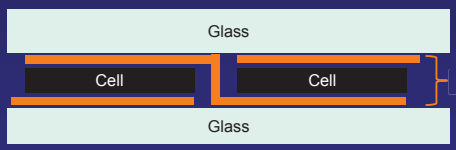


- No EVA
- No Lamination
- No Soldering





- Under pressure inside the module for electrical series connection of cells
- High module fill factors and low series resistances



- Air and humidity tight sealing around module perimeter
- 100% automatic in-line operation



- Prototype Line at INES for Process Optimization (since 2008)
- TÜV Validation (June 2010)
- 2 Industrial Lines under Tuning and Optimizing (2011)

Certification Process by TÜV Rheinland: NICE-80X Modules passed all relevant tests according to IEC-61215 and 61730

Test-modules: 36-cells NICE modules produced on the prototype line (125x125 mm² cells)

Humidity Freeze	-0.22
	-0.31
Thermal Cycling 200	-2.01
	-1.20
Damp Heat	-0.92
	+2.26
Mechanical Load (2400 Pa)	+1.61

Bypass Diode Thermal test	+0.48
Hot-spot endurance test	+0.64
UV preconditioning test	+1.42
	+1.83
Robustness of terminations	+0.48
Hail Impact	-1.60

Module ID	Power Variation (%)
1	+0.16
2	+1.23
3	+1.37
4	+0.70
5	-2.01
6	-1.20
7	+0.71

- **Ageing Tests : Power Variation (%) Maximum Power Decrease: 2.01%**
- **Normalized Tests: Power Variation (%) Maximum Power Decrease: 1.60%**
- **Maximum Power Decrease after Complete Certification Process: 2.01%**

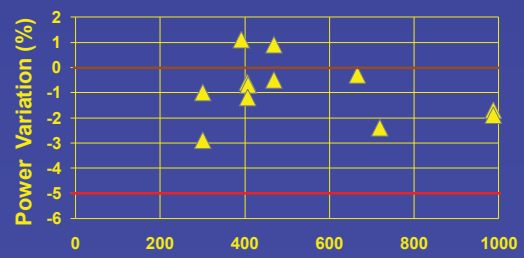
Highly Extended Ageing Test

Outdoor Exposure



- 24 modules monitored on the INES rooftop
- Consistent energy production
- No resistance degradation after 7 months
- NOCT: 42.6 (Source: TÜV)

Thermal Cycling (-40°C to +85°C)



- Despite under-pressure variation : no significant losses
- **1 000 Cycles with Power Degradation <2%**

Alternative Mechanical Loads ± 2 000 Pa

	Tensile load	Pressure load
Maximum bending at module centre (mm)	10	6
Circuit interruption	No	
Power Variation	-0.57 %	

- 100 Cycles
- Performed by TÜV



Resistance to wind load" – DIN-12210 & DIN-12211

Conclusion:

- Contrary to EVA-laminated modules, damp heat test = No difficulty for NICE modules (PIB=excellent barrier)
- Hardest Ageing Test for NICE: Thermal Cycling and 1000 Cycles achieved according to IEC 61215
- Next Step in Hard Ageing Test: Test-To-Failure Protocol at NREL with industrial 60-Cells Modules (2011)

NICE New Industrial Cells Encapsulation TECHNOLOGY

Acknowledgements : This work was supported by the Rhône-Alpes Region and is in the framework of the French Solar Nano Crystal project financed by OSEO. The authors are grateful to all its industrial and labs partners: INES, Kömmerling, CentroSolar Glas, Suntech, Lisec.

Fraunhofer CSP

FRAUNHOFER CENTER FOR SILICION PHOTOVOLTAICS CSP

MECHANICAL ISSUES ON SOLAR MODULES AND ENCAPSULATED COMPONENTS

S. Dietrich, M. Pander, R. Meier, S.-H. Schulze, M. Ebert
Fraunhofer - Center for Silicon-Photovoltaics CSP, Walter-Hülse-Straße 1, 06120 Halle (Saale)
Telefon +49 (0) 345/5589-408
matthias.ebert@csp.fraunhofer.de

Bundesministerium für Bildung und Forschung
SOLARVALLEY Mitteldeutschland

Motivation

- demand on solar modules:
  - operation for a long period
  - low performance loss (typically less then 20 % in 25 years)
  - resist thermo-mechanical and mechanical loads
- loads on solar modules
  - mechanical (wind, snow)
  - thermal-mechancial (production process, day/night shift, seasons)
  - dynamic-mechanical (wind squall, hail)
- typical mechanical failures:
  - glass breakage
  - cell breakage
  - broken interconnector
  - delamination

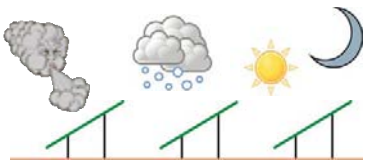




Fig. 1: broken copper ribbon [1]

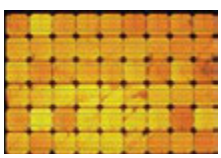


Fig. 2: EL image of a mono-Si solar module with microcracks due to thermal cycling [2]

Material Characterization

- solar module consists of various materials
  - → widely different CTE and Young's Modulus
  - → origin of thermal stresses due to mismatch of CTE
- properties of encapsulant exhibit a strong dependence on temperature
  - → distinct change in mechanical properties around glass transition
  - → strong influence on the amount of external loads, which is transferred to the solar cells

Material	Youngs Modulus [GPa]	CTE [10^{-6} K^{-1}]
Silicon	162 (multi)	2.6
Glass	70	8.5
Copper	86	16.65
EVA	0.07 – 0.001	90 – 360

Tab. 1: mech. properties of solar module components

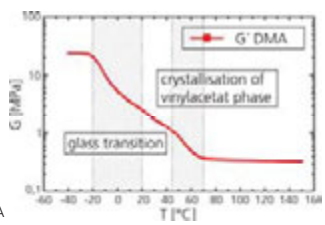


Fig. 3: characteristic development of shear modulus over temperature for an EVA

Simulation of Lamination Process

- stress free state at lamination temperature (150 °C) is assumed
- contraction of the materials leads to a change in the gap between solar cells
- plastic strain is induced into copper ribbons → pre-damage that influences lifetime
- enlarged initial cell gap reduces the amount of plastic strain

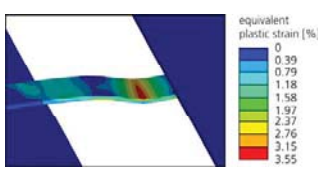


Fig. 4: plastic strain of copper ribbon after lamination

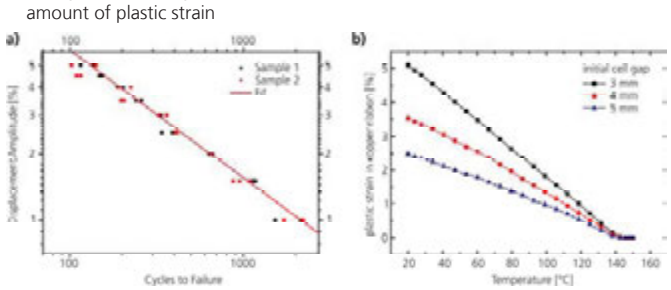


Fig. 5: a) lifetime model for copper ribbon under given geometric constraints [3]
b) plastic strain of copper over temperature for different initial cell gaps

Simulation of Mechanical Loads

- investigation of a module laminate with 3 cells under wind load
- deflection influenced by cells and temperature dependant polymer stiffness
- polymer mainly under shear deformation → amount of strain compensation depends on shear stiffness and thickness of polymer
- stress in solar cell considerably higher for low temperatures and thin polymer
- reduction of cell thickness leads to higher deformation and stress

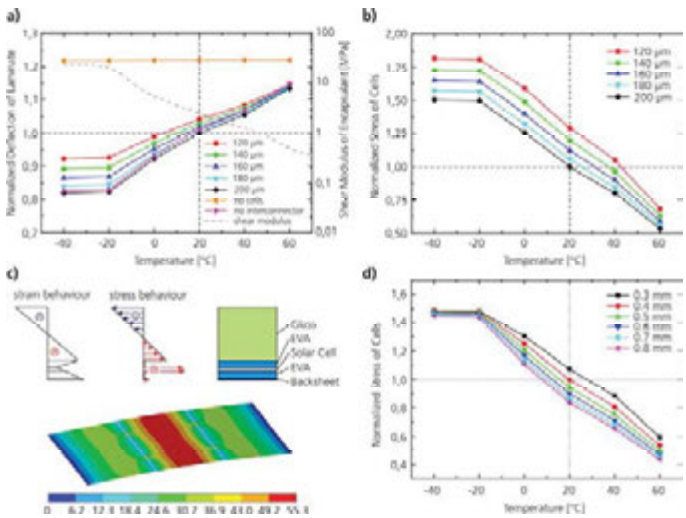


Fig. 6: a) Influence of deflection of module laminate on temperature → encapsulant [3]
b) Influence of normalized stress with respect to temperature/polymer stiffness [3]
c) strain and stress behavior of the laminate under a mechanical load, characteristic stress plot
d) Influence of normalized stress with respect to polymer stiffness and thickness [3]
Reference for all graphs: 200 µm, 20 °C, 0.4 mm

- reduction of glass thickness leads to higher deformation and strain in glass → increased strain is transferred to cells and induces higher stresses
- effect also applies to manufacturing tolerances → more than 10 % stress variation possible
- variation of shear modulus of encapsulant due to inhomogeneities
  → variation of shear modulus up to 60 %
  → low impact on deflection
  → effect on stress up to 20 %

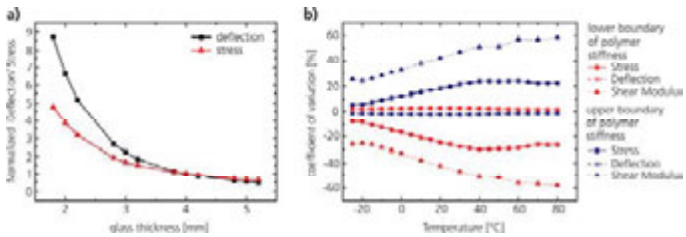


Fig. 7: a) impact of glass thicknesses including tolerances (± 0.2 mm) on stress and deflection, Reference: 4 mm glass, 200 µm cell, 20 °C
b) influence of the variation of the shear modulus of the encapsulant on deflection and stress

Acknowledgement

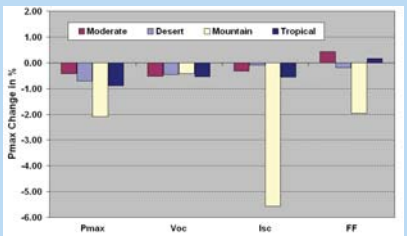
This work was supported by the Federal Ministry for Education and Research (BMBF) within the "Excellence Cluster" project "xµ-Module" (project no. 03SF0337A)

[1] Meier, R. et al.; Thermo-Mechanical behaviour of copper-ribbon materials, Proc. 24th EUPVSEC (2009), Hamburg
[2] Sander, M. et al.; PV Module defect detection by combination of mechanical and electrical analysis, Proc. 35th IEEE (2010), Hawaii
[3] Dietrich, S.; Mechanical and Thermo-Mechanical Assessment of Encapsulated Solar Cells by Finite-Element-Simulation, Proc. SPIE 7773, 77730F (2010); doi:10.1117/12.860661

Outdoor weathering of c-Si PV modules in various climates
- measurement and transfer of module data of PV-modules via GPRS -

Nicolas Bogdanski, Werner Herrmann

[1] TÜV Rheinland Energie und Umwelt GmbH, Am Grauen Stein, 51105 Köln, Germany, Phone: + 49 221 806 4741, Mail: nicolas.bogdanski@de.tuv.com



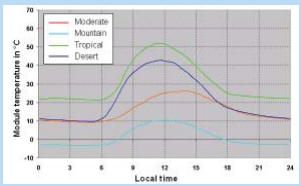
Change of STC Performance after 3 years:
Averaged parameters of 7 modules from 4 test sites

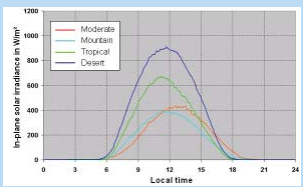
Moderate City Climate	→	Cologne, Germany
Desert Climate	→	Sede Boqer, Israel
Tropical Climate	→	Serpong, Indonesia
Mountain Climate	→	Zugspitze, Germany

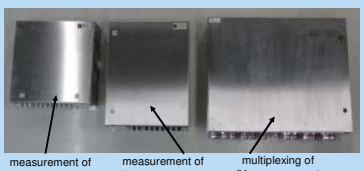
Previous results

- Average power degradation in the first year for all locations is -0.6%, 3.8% after 3 years (0.7% without Zugspitze)
- Max. power degradation of -6.3% could be explained by cell breakage (location Zugspitze)
- No evidence of deterioration of electrical contacts in the interconnection circuit of the module (indicator = internal series resistance)
- Effect of soiling < 0.5% for Cologne and Zugspitze, but 2.3% – 4% for Indonesia (modules from Israel received in cleaned condition)
- Reliability criteria are fulfilled for all module types
- Impact of transport on module degradation not clear
- None of the modules failed during isolation testing
- Comparability of yearly re-measurement results is limited since the modules constructed equally but are not identical

→ **on-site measurement may be beneficial**







Compact on-site Monitoring Programme

IV-curve measurement 1 per hour (12 modules multiplexed)

loading settings → small fluctuation of G? → parallel measurement of V, I and reference → data transfer

weather data measurement

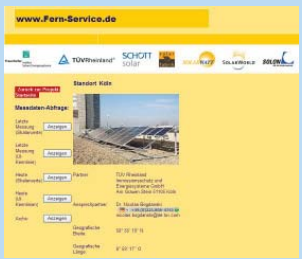
continuous measurement of all parameters → 5 min averages → data transfer

evaluation of data through database

continuous measurement of all parameters ← definition of filter settings ← data download and import

measured data consisting of:

- global irradiation	- ambient temperature	- relative humidity
- UV-A,UV-B irradiation	- module temperature	- module deflection
- calibrated ref. cell	- 2D wind	- rain intensity



Data available via internet platform

Test locations

Moderate City Climate

Cologne, Germany
- Moderate temperatures
- Moderate humidity
- Moderate UV irradiation
- Moderate wind and snow load

Local partner:
TÜV Rheinland Group



Desert Climate

Tempe, USA
- high temperatures
- high day/ night temperature gradients
- high UV irradiation
- high global irradiation

Local partner:
Ben-Gurion University of the Negev



Tropical Climate

Serpong, Indonesia
- high temperatures
- high humidity
- high UV irradiation
- high global irradiation

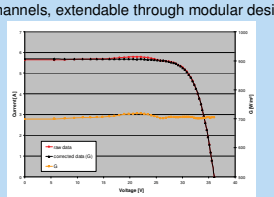
Local partner:
Agency for the Assessment and Application of Technology (BPPT)



Multiplex IV-measurement

- 12 channels, extendable through modular design -

- irradiation is measured by pyranometer and calibrated reference cell
- measurement of IV-characteristic hourly if fluctuation < 2% (configurable)
- data points for irradiation (ref. cell), voltage, current are measured simultaneously → fluctuations of G can be corrected subsequently
- measurement of module temperature enables temperature correction



- irradiation correction with respect to first value measured
- duration of one IV-measurement 30s
- configurable number of data points
- start of measurement 10/10 in Cologne
- fluctuation and minimum irradiance demands limit number of IV-curves collected to app. 2-3 per day

→ degradation not yet detectable

Results

- change of PV-module parameters can be detected on site, lengthy interruption of exposure period due to yearly shipment for re-measurement can be omitted
- modular design and wireless data transfer enables the measurement in remote areas
- on-site measurement allows to detect soiling effects throughout the year
- to collect all degradation parameters re-measurement at the end of the measurement campaign should still be conducted

Acknowledgements

Support by the Bundesministerium für Umwelt, Naturschutz und Reaktorsicherheit (Federal Ministry for the Environment, Nature Conservation and Nuclear Safety, FKZ 0329978C) and partial funding by the industrial project partners has been greatly appreciated.

2011 NREL Photovoltaic Module Reliability Workshop, Golden Colorado

Fraunhofer ISE · solar fabrik · SOLARWATT · SolarWorld · SOLON AG für Solartechnik · SCHOTT solar · solar glass · Scheuten · TÜVRheinland® Precisely Right.

© TÜV, TUEV und TÜV sind eingetragene Marken. Eine Nutzung und Verwendung bedarf der vorherigen Zustimmung.

阿特斯

The Super Highway to Grid Parity

Progress on e-Modules Research and Production

Genmao Chen, Shawn Qu, Jiang Peng, Xusheng Wang, and Wenda Zheng
Canadian Solar Inc.

PV Modules Reliability Workshop, Golden CO, Feb. 2011

OUTLINE

Abstract

SoG-Si vs. conventional Si

Ingot growth and e-Wafers

e-Cells and reverse breakdown voltage

e-Modules performance

Summary

Selected projects of e-Module PV power plant

阿特斯

ABSTRACT

Low cost, high conversion efficiency and fast energy payback time are the key focusing directions for PV industry. Since Canadian Solar first introduced e-Modules that made from 100% low cost solar grade Si (SoG-Si) into PV market in the middle of 2008, great progresses in the production improvement have been achieved in the past two years. This presentation reports the results of an average e-cell conversation efficiency of 15.93%, an high yield of SoG-Si ingot growth and wafering comparable to conventional Si ingot growth and wafering, a less than 2% of light induced degradation and an average of 0.56% annual long term degradation for e-modules.

阿特斯

Solar Grade Si vs. Conventional Poly Si

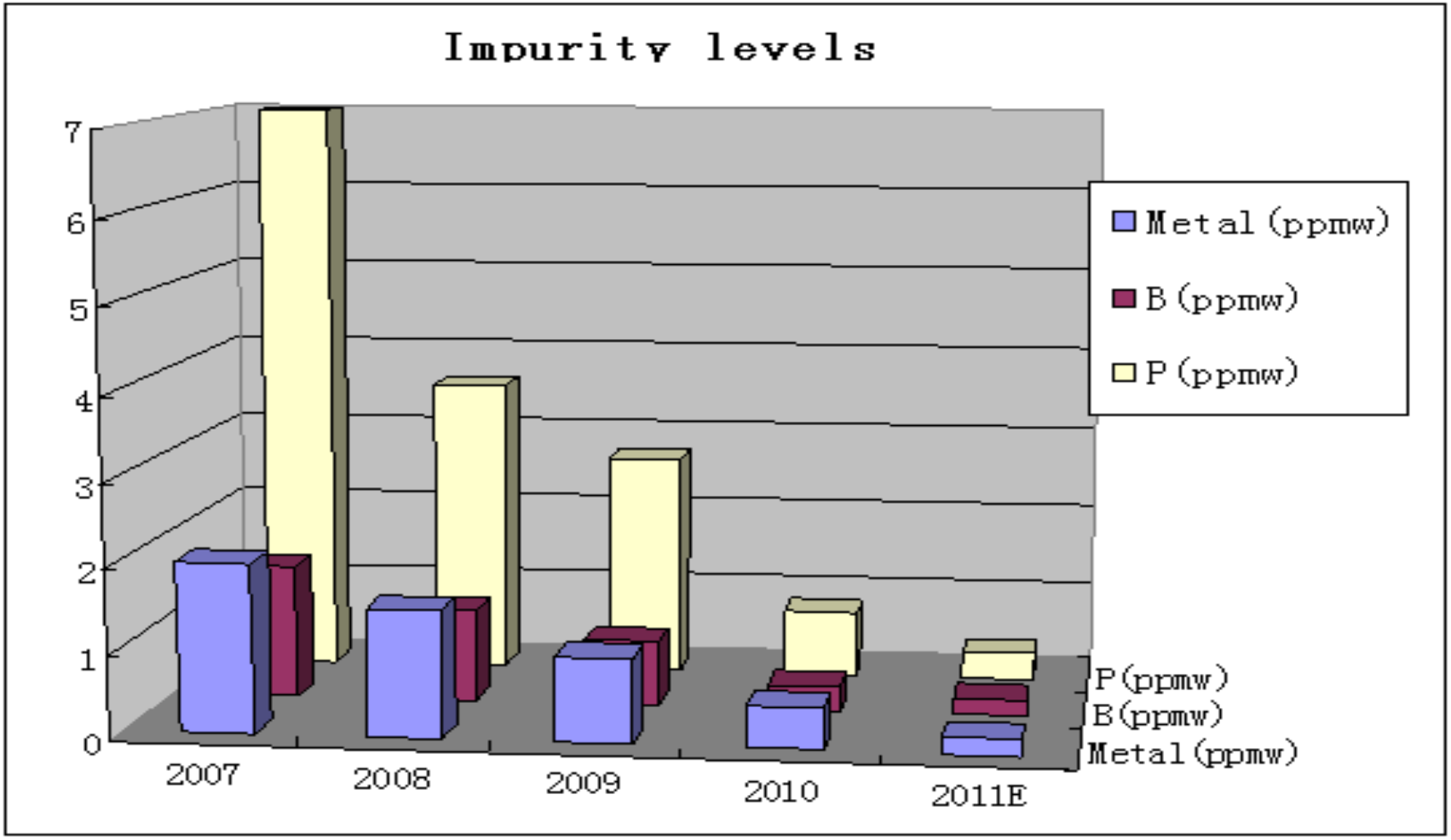
	Conventional poly-Si	Solar grade Si
Energy consumption (KWh/kg)	80-200	10-20
Environmental impact	High	Very low
Impurity levels* of currently available commercial supply	1) 7N-8N; 2) 8N-9N; 3) better than 9N	~6N
Product cost ($/kg)	25-50	15-25
Investment $(USD)M/1000MT	~100	~15
Factory construction period	~2Years	<1Year
Typical multi-crystalline cell efficiency	15.5-16.5%	15-16%

Solar grade Si: Low cost, fast energy payback, environmentally friendly

* Not including O and C

阿特斯

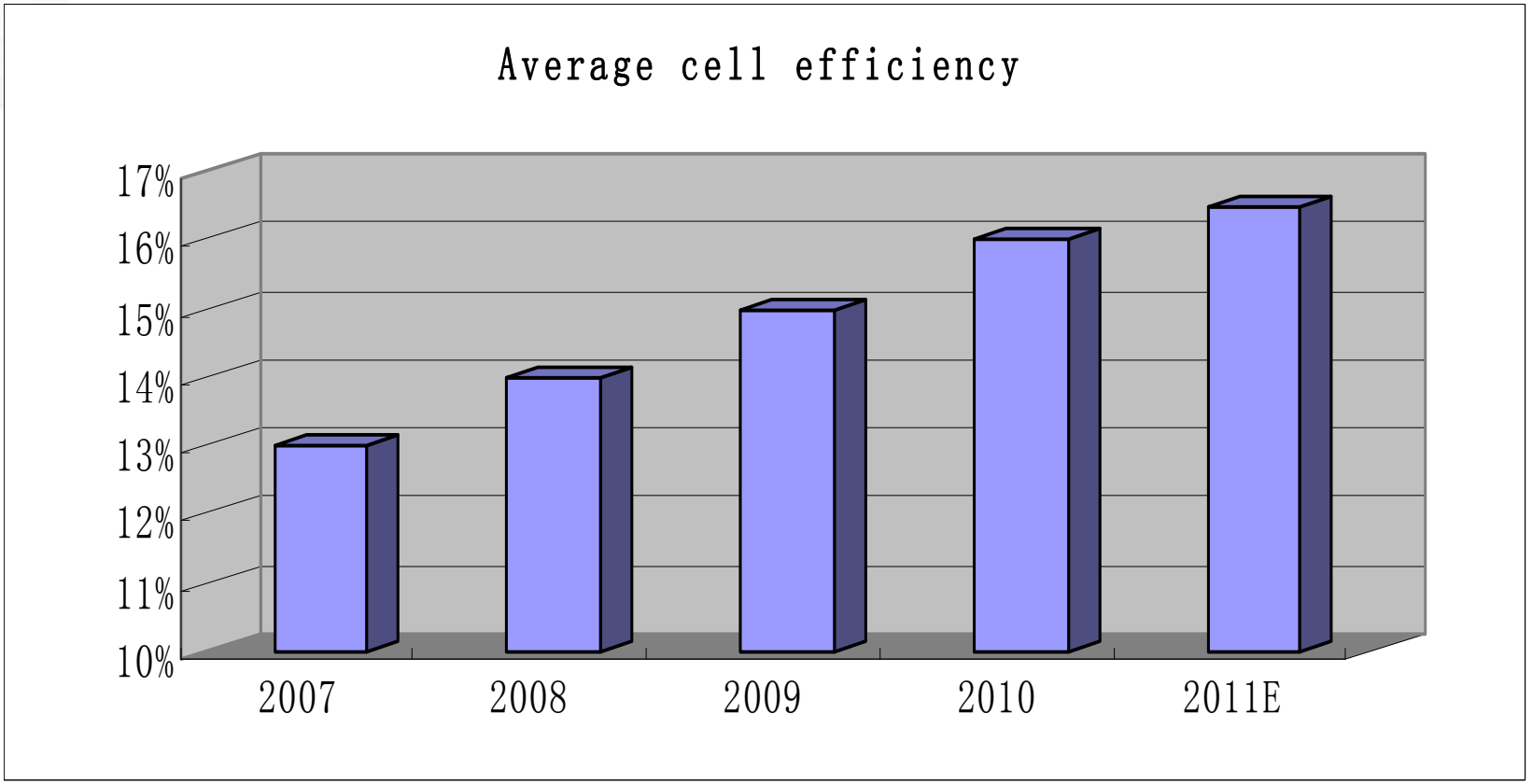
UMG/SoG Si Impurity level Footprint



UMG-Si (5-6N) has improved into SoG-Si (better than 6N)

阿特斯

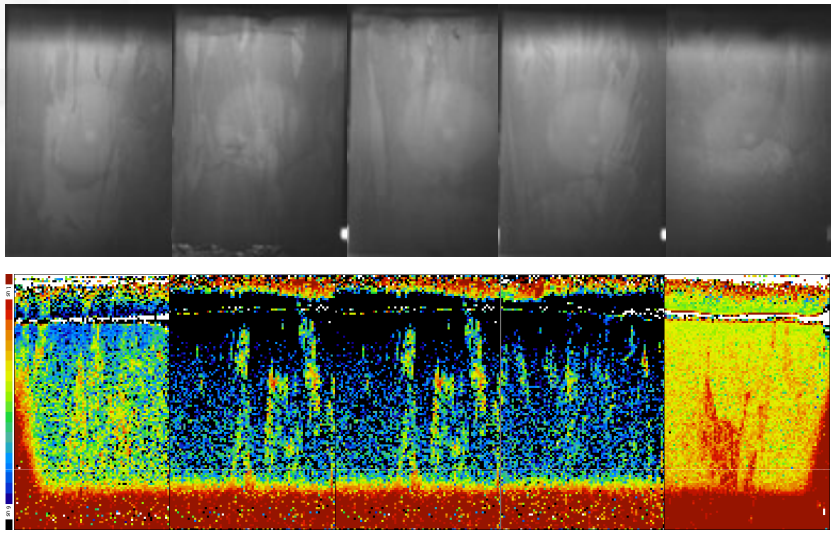
e-Cell Efficiency Footprint & Roadmap

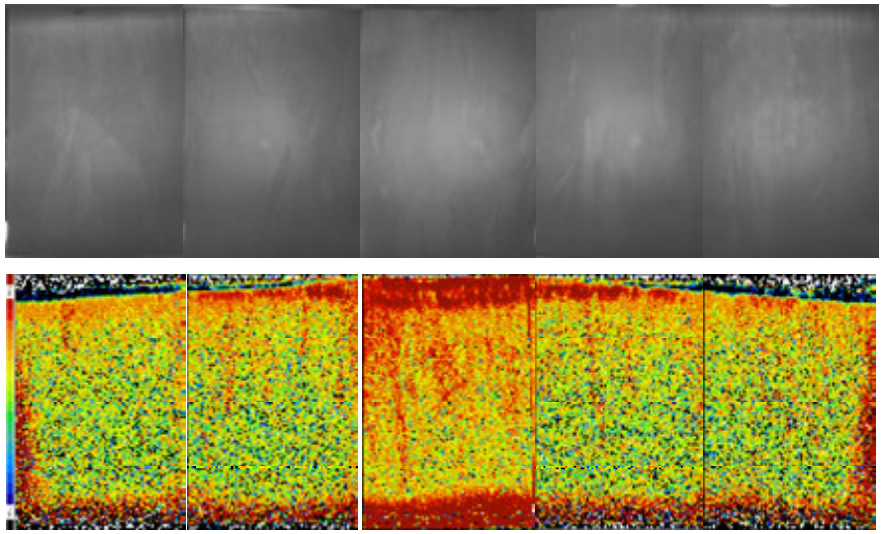


e-Cell efficiency will catch up the conventional Si cell efficiency in next 1-2 years

阿特斯

Brick IR Images and Lifetime Mapping





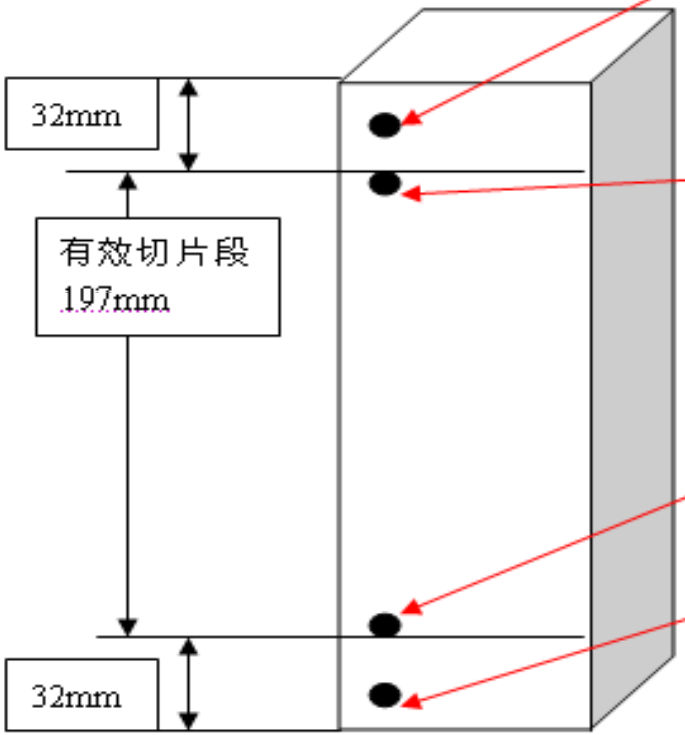
SoG-Si from supplier A:
B and P high
Effective ingot length low
Metals impurity low
Brick lifetime high (>3us)

SoG-Si from supplier B:
B and P lower,
Effective ingot length high
Metals high
Brick lifetime low (>2us)

阿特斯

SIMS Analysis of Brick Impurity

Ingot grown from Supplier B
SoG-Si with relative high metals



距顶部 15mm 处，

C： 5.71E+17 (atoms/cm3)　　O： 5.12E+16 (atoms/cm3)

Cr：< 2.00E+13 (atoms/cm3)　　Fe：< 1.00E+14 (atoms/cm3)

Ni： < 2.00E+14 (atoms/cm3)　　Cu：< 1.00E+14 (atoms/cm3)

Zn：< 5.00E+14 (atoms/cm3)　　Al： 2.04E+15 (atoms/cm3)

有效切片段顶部处，

C： 3.97E+17 (atoms/cm3)　　O： <5.0E+16 (atoms/cm3)

Cr：< 2.00E+13 (atoms/cm3)　　Fe：< 1.00E+14 (atoms/cm3)

Ni： < 2.00E+14 (atoms/cm3)　　Cu：< 1.00E+14 (atoms/cm3)

Zn：< 5.00E+14 (atoms/cm3)　　Al： 9.86E+14 (atoms/cm3)

有效切片段底部处，

C： 3.41E+17 (atoms/cm3)　　O： 1.85E+17 (atoms/cm3)

距底部 10mm 处，

C： 3.27E+17 (atoms/cm3)　　O：3.70E+17 (atoms/cm3)

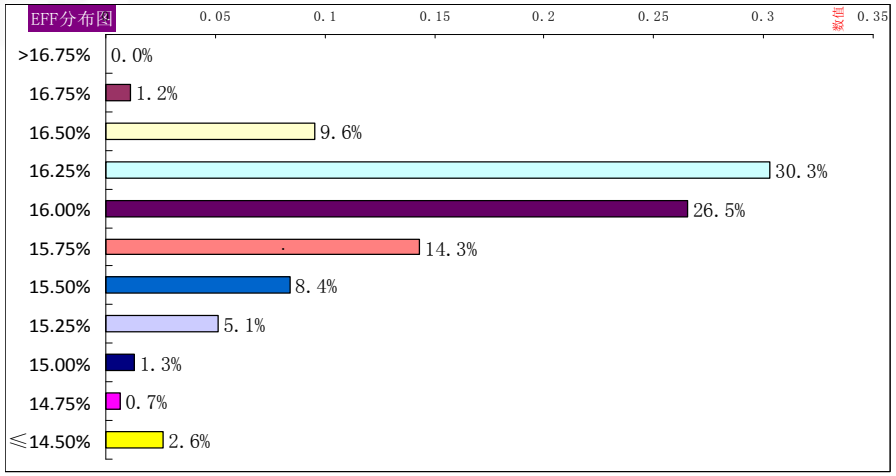
SoG-Si ingot effective length (197mm) has achieved 97.5%
of conventional ingot effective length (202mm)

阿特斯

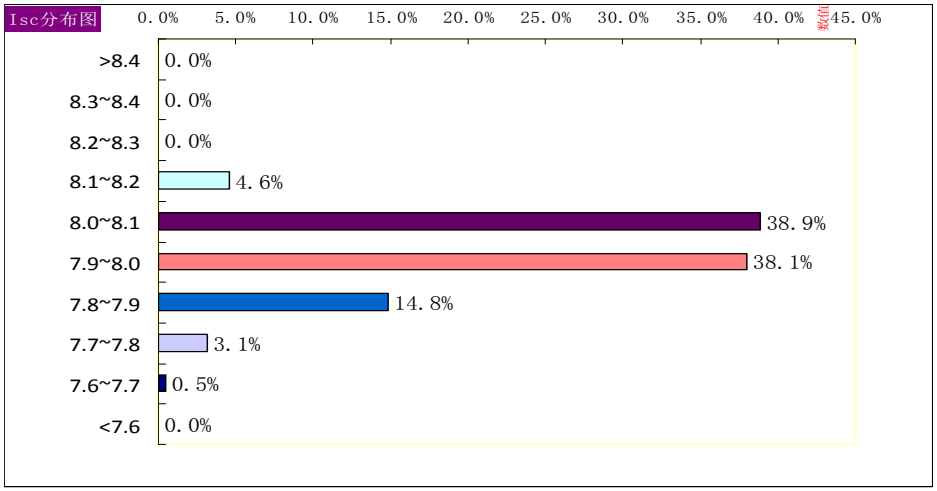
e-Cell Process Results

Uoc	Isc	Rs	Rsh	FF	EFF
0.632	7.98	0.00387	21	76.87	15.93%

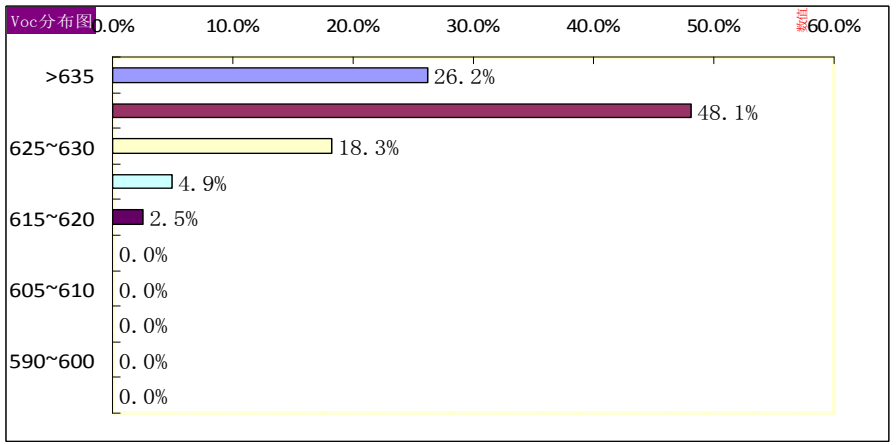
EFF



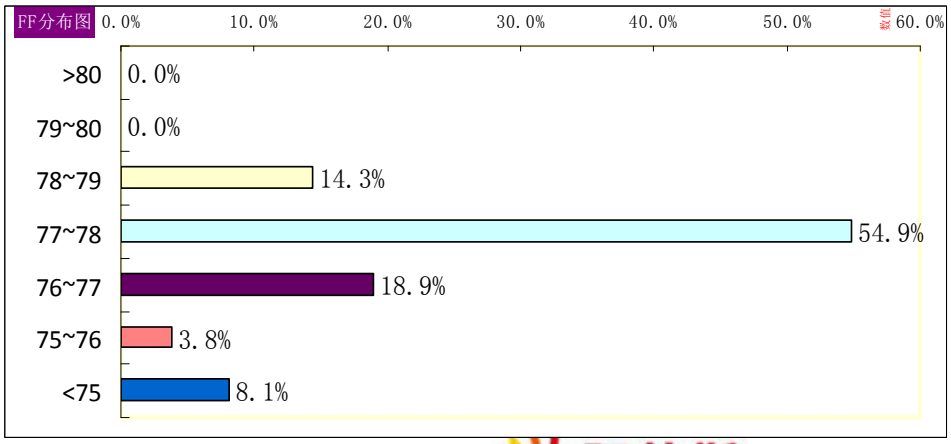
Isc



Voc

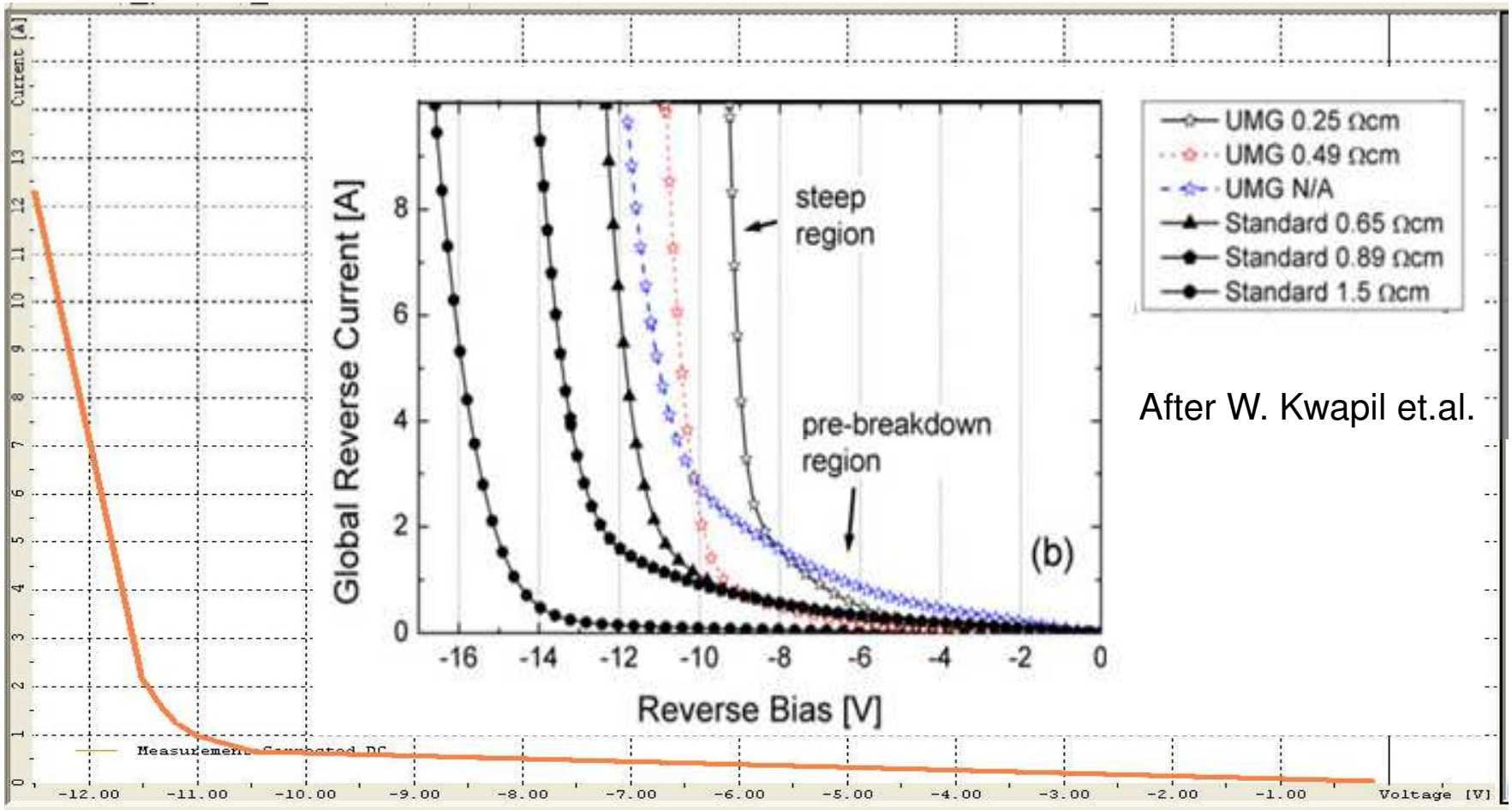


FF



阿特斯

e-Cell Reverse Breakdown Voltage



After W. Kwapil et.al.

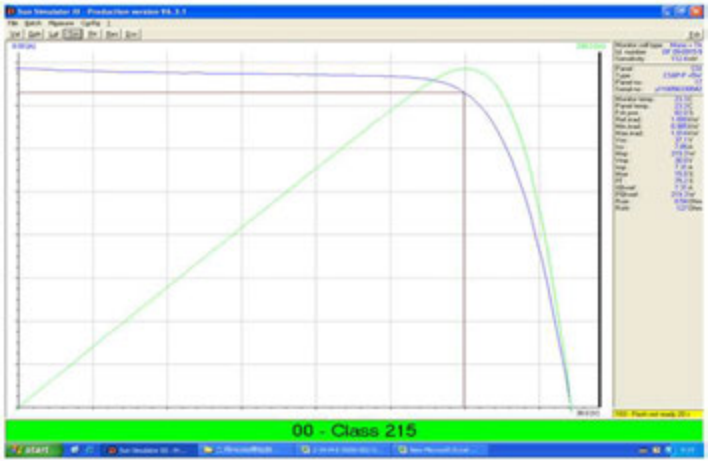
With similar wafer resistivity, e-module has achieved a comparable breakdown voltage

阿特斯

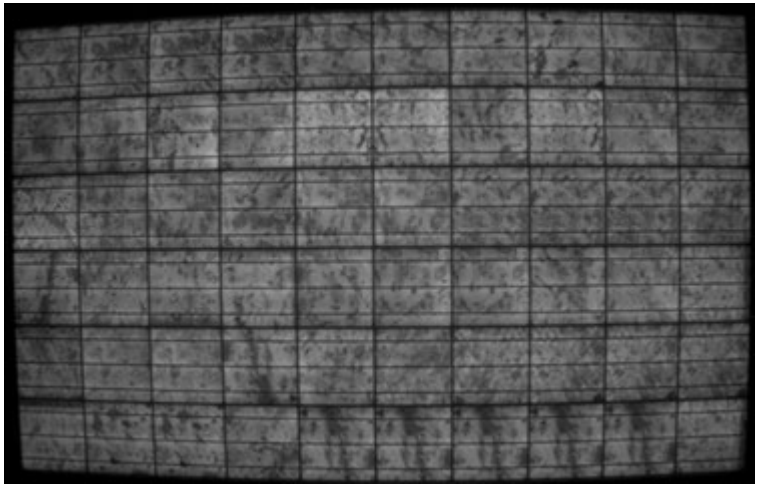
e-Module I-V Testing and EL Image

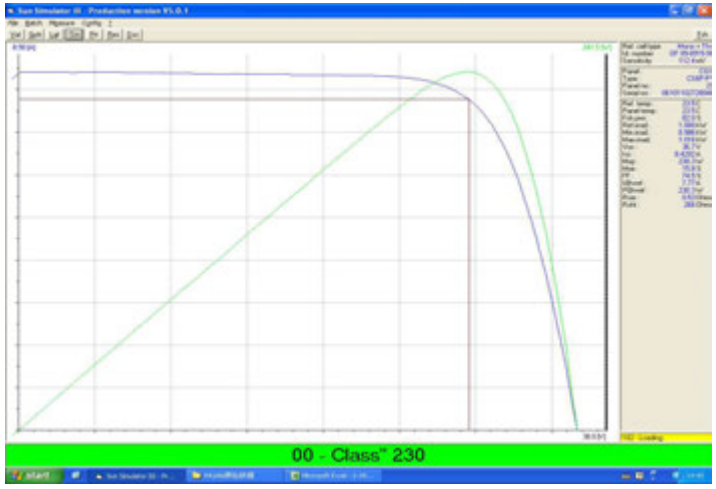
E-module(cell Eff. 15.5%)





P-module(cell Eff. 16%)

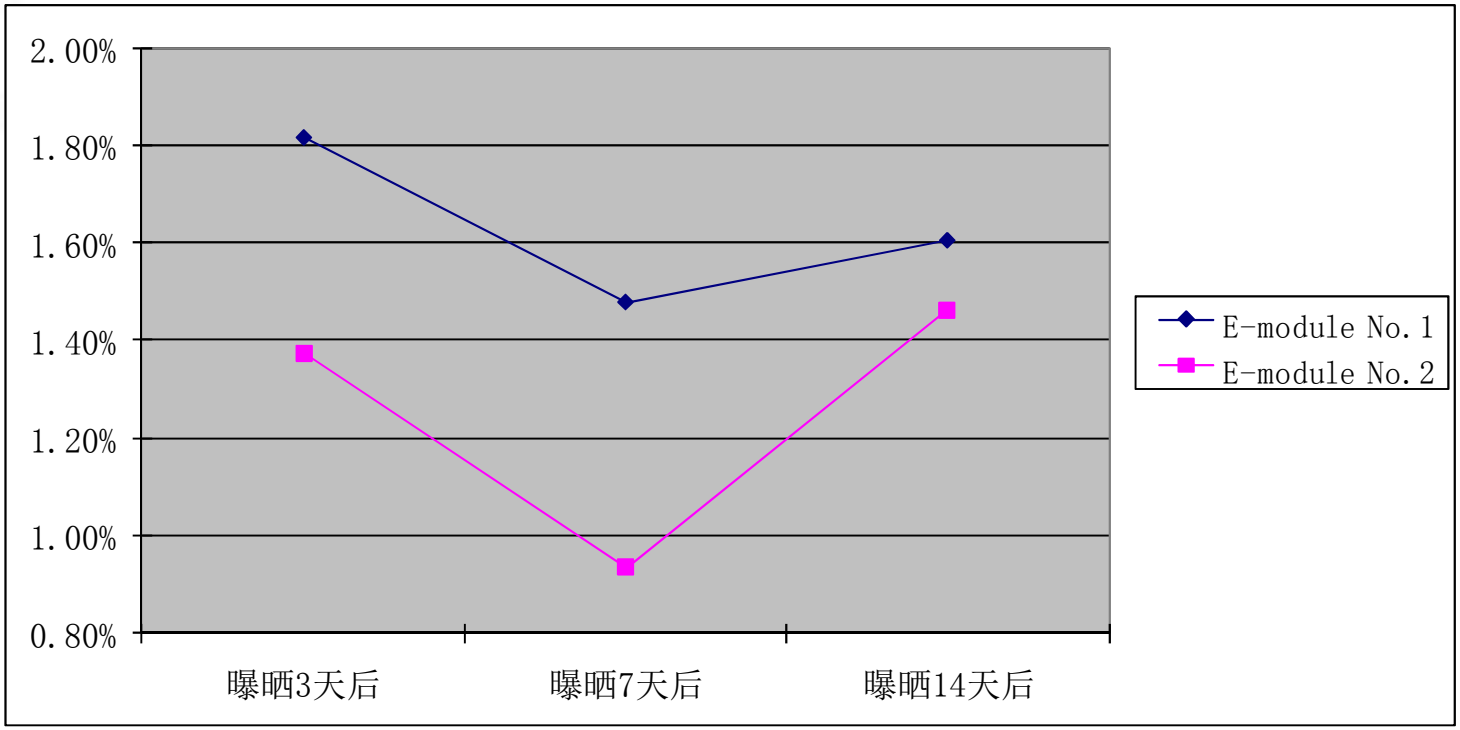




Compared with conventional module, e-module has a similar EL image although slightly lower Eff.

阿特斯

Performance of e-Modules



Initial performance results:

- **Typical LID for e-Modules is less than 2%, which is comparable with the conventional crystalline Si module; stabilized after 3-4 days**
- **LID mainly caused by B-O complex; LID results in a reduction of Isc**
- **New generation of e-Module without LID will be in production soon**

阿特斯

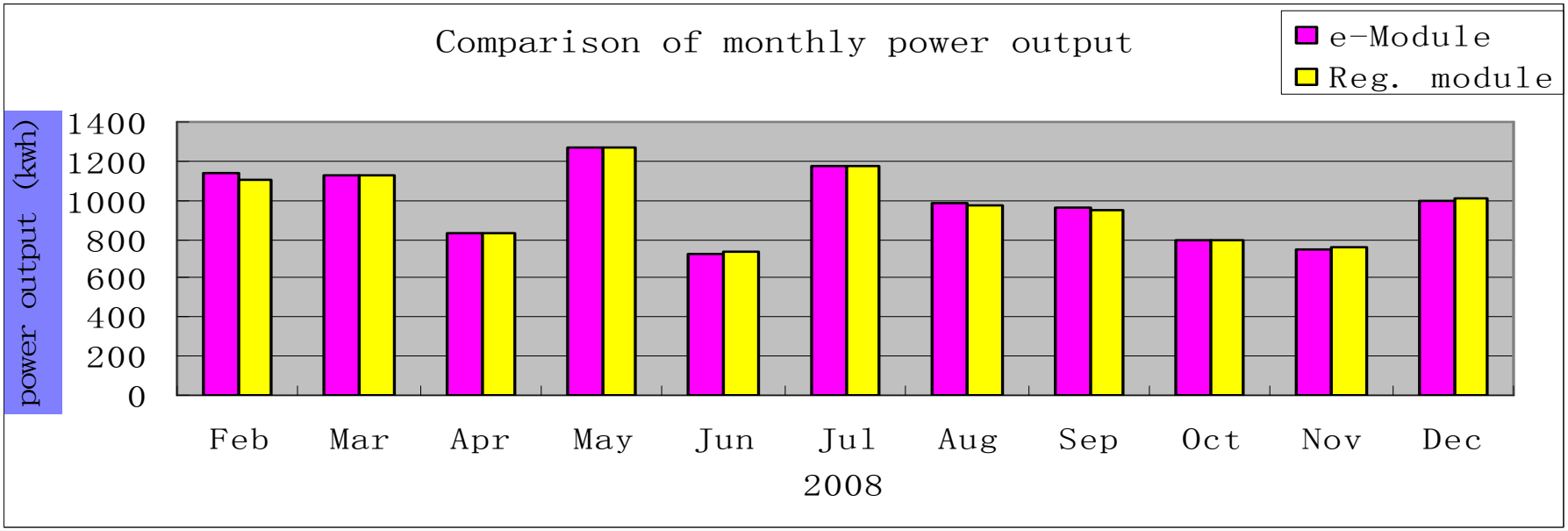
Performance Comparison

e-Modules



Conventional Modules

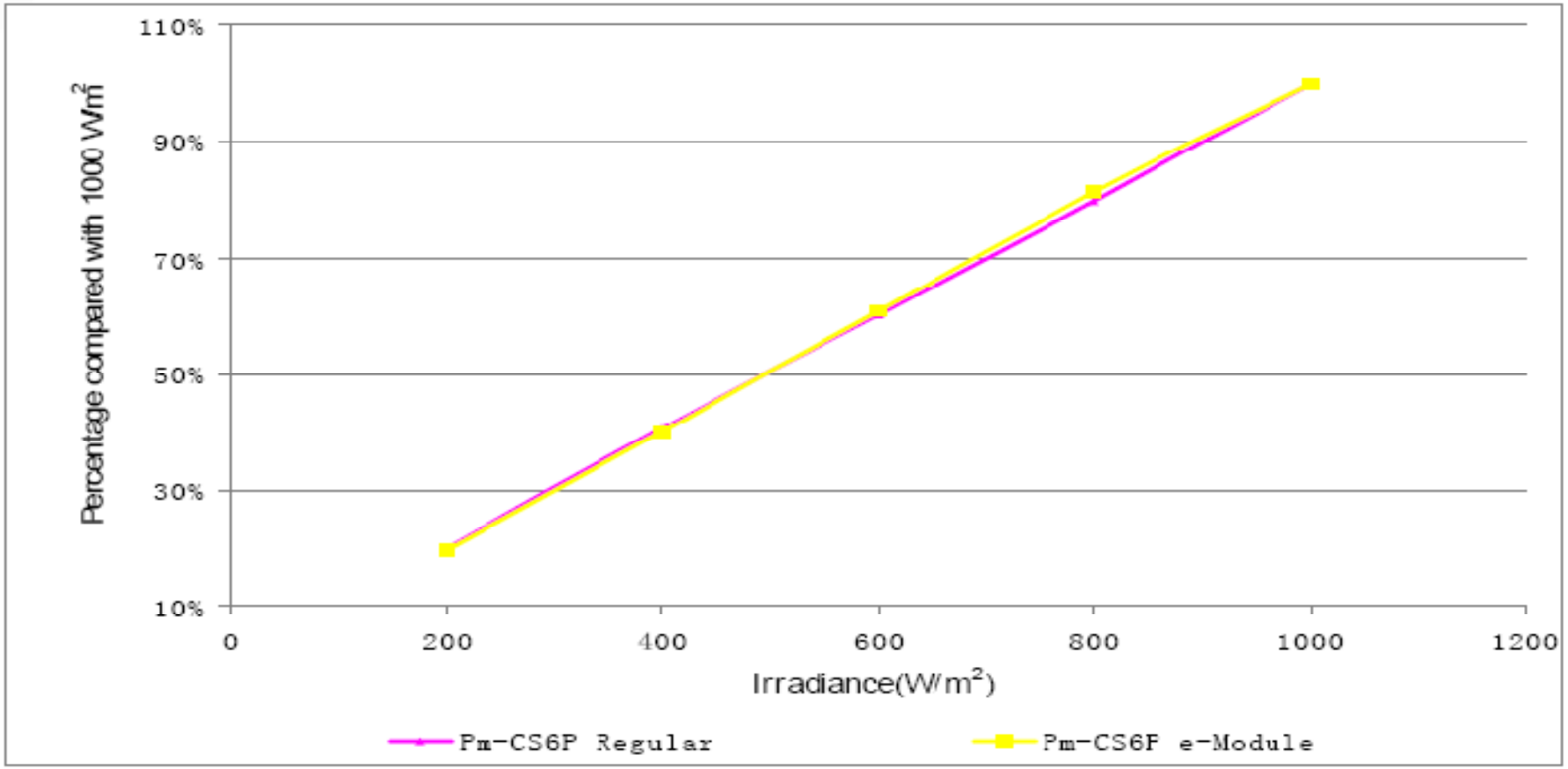




- **Equal performance to conventional modules, better at high temperatures (peak pricing periods)**
- **long term degradation is about 0.56% per year both of these values are comparable with conventional modules**

阿特斯

System Output vs. Irradiation

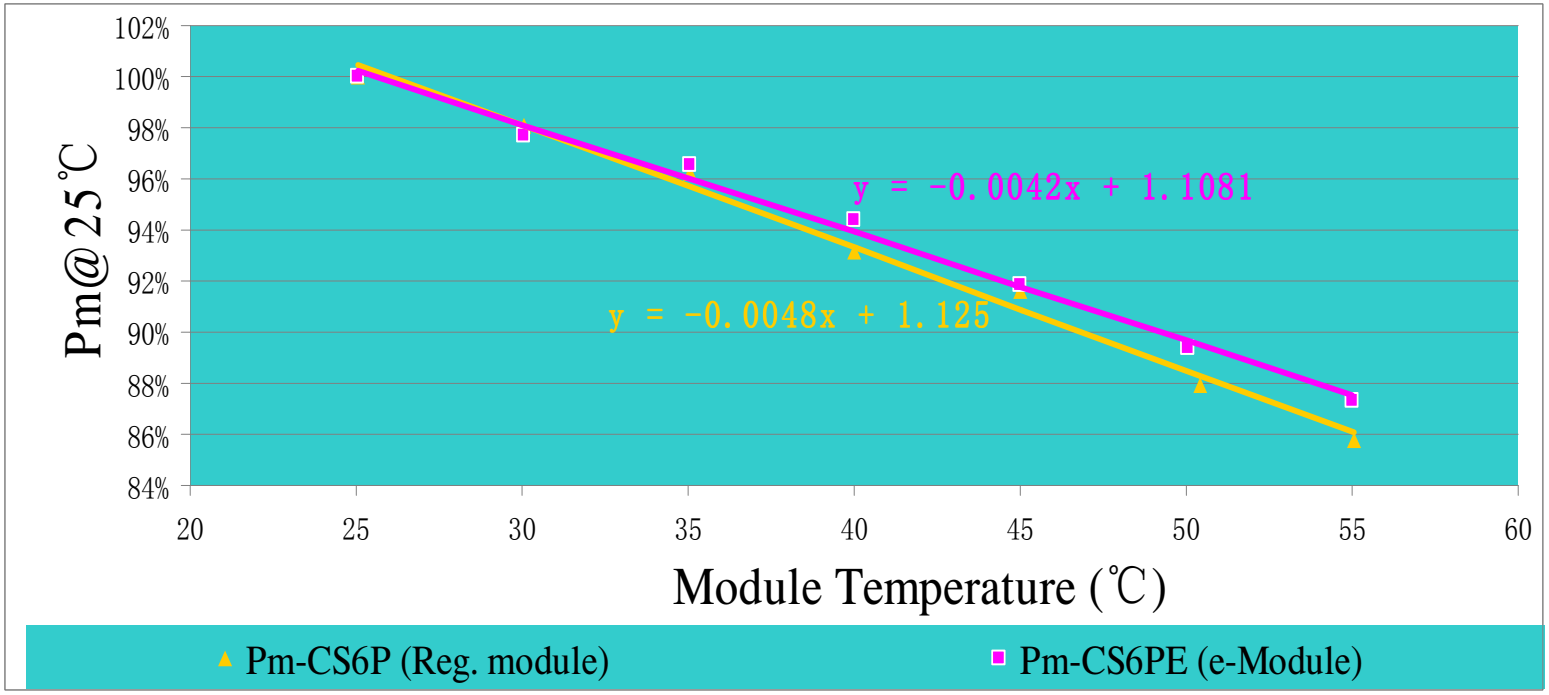


Equal performance to conventional modules

阿特斯

Modules Temperature Coefficients

	α-Isc(%/℃)	β-Voc(%/℃)	γ-Pm(%/℃)
CS6P Reg. module	0.073%	-0.356%	-0.494%
CS6PE e-Module	0.107%	-0.378%	-0.438%



A lower peak power temperature coefficient

阿特斯

Summary

- SoG Si: low cost, fast energy payback time, and environmental friendly
- CSI's SoG-Si ingot growth and wafering have achieved the similar yield to conventional Si ingot growth and wafering.
- e-Cells average efficiency has reached ~16%, and reverse breakdown voltage has achieved 11.3V
- e-Modules have demonstrate a LID of less than 2% and long term degradation of about 0.56% annually, both values are comparable with conventional modules.
- e-Modules demonstrate excellent potential for fast-pace efficiency improvement and cost reduction
- e-Modules will lead the crystalline modules toward the grid parity.

阿特斯

Minturn Huller



Location: California, US
Module: CS6P-200PE e-Module

System Size: 540 kW
Activated: Dec. 2009

阿特斯

Person County Solar Park



Location: North Carolina, US
Module: CS6P 190PE e-Module

System Size: 650 kW
Activated: Aug. 2009

阿特斯

Concord Truss Company



Location: New Jersey, US	System Size: 117.6 kW
Module: CS6P PE e-Module	Activated: Oct. 2009

阿特斯

e-Module Project in USA



Project Details			
Location	Visalia, CA	Module Type	e-Module CS6P-PE
System Size	392.645 kWp	Completion	August 2008

阿特斯

e-Module Project in Germany



Project Details			
Location	Ostfriesland, Germany	Module Type	e-Module CS6A-PE
System Size	111 KWp	Completion	September 2008

阿特斯

e-Module Project in Korea



Project Details			
Location	Jeong Up-si, Korea	Module Type	e-Module CS6P-PE
System Size	300 KWp	Completion	September 2008

阿特斯

Thank You !

Development of a New Standard for Transport Simulation on Complete PV-Module shipping units in Combination with Thermo-Mechanical Stress

Jörg Althaus, Florian Reil, Konstantin Strohkendl, Nicolas Bogdanski

TÜV Rheinland Energie und Umwelt GmbH, 51101 Cologne, Tel.: +49 221 806-2794, Fax: +49 221 806-1350,

Mail: florian.reil@de.tuv.com, Internet: www.tuv.com/pv

In the IEC standards for type approval testing of photovoltaic modules IEC 61215 and IEC 61646 it is noticeable, that mechanical load testing (clause 10.16) is only considering static loads. To estimate and characterize also the performance and lifetime behavior of PV modules in regard to dynamic loads, additional tests need to be carried out under different load parameters. A variety of mechanical stresses has to be expected during the life-time of a PV module. The stresses are caused by vibration e.g. during transportation, by wind and from thermo-mechanical loads.
Since different scientific work has been published by several institutes and companies dealing with the examination of PV modules under the influences of transport impacts, a joint sub group within Working Group 2 of the Technical Committee of IEC (IEC TC82/WG2) started to elaborate a draft standard for these relevant product-specific issues.

Approach

- PV modules are generally exposed to different kinds of mechanical and thermo-mechanical impacts in nature (wind, humidity, temperatures, snow etc.)
- In general mechanical loads influence the properties and quality of the solar cells, encapsulation, conductors, glass, frames, etc.
- The standard draft is designed so that its test sequence can co-ordinate with those of IEC 61215 or IEC 61646
- The standard draft shall describe methods for the simulation of transportation of stacks of modules and describe subsequent environmental tests; it is not part of the type approval testing

Therefore, the following standard draft focuses on vibration tests, shock tests and subsequent environmental stress testing





Figure 1 & 2: A complete shipping unit exposed to transport-like vibrations and handling induced shocks (rotational flat drop test)

Test Item

It is recommended to use regular shipping units as marketed by the manufacturer.

A minimum of 10 modules shall be included in the shipping unit. B or C grade modules or module dummies can be used to fill the stack.

The subsequent environmental tests are performed on selected modules (see figure 3 – test sequence)

Transport Simulation

The state of the art test method for transport simulation is based on a broadband random noise acceleration (see PSD diagram).

To achieve a broadly accepted standard the applied test profile is not fixed to one special test profile. But for comparability reasons some requirements are needed:

- Minimum Frequency range: 5 – 200 Hz
- Minimum Test severity (between 5 – 200 Hz): 0,49 g_{RMS}
- Minimum Test duration: 180 minutes
  - ► Main reference: ASTM D 4169

For the reproduction of typical handling induced stress, the complete shipping unit will be exposed to shocks and rotational flat drop tests.

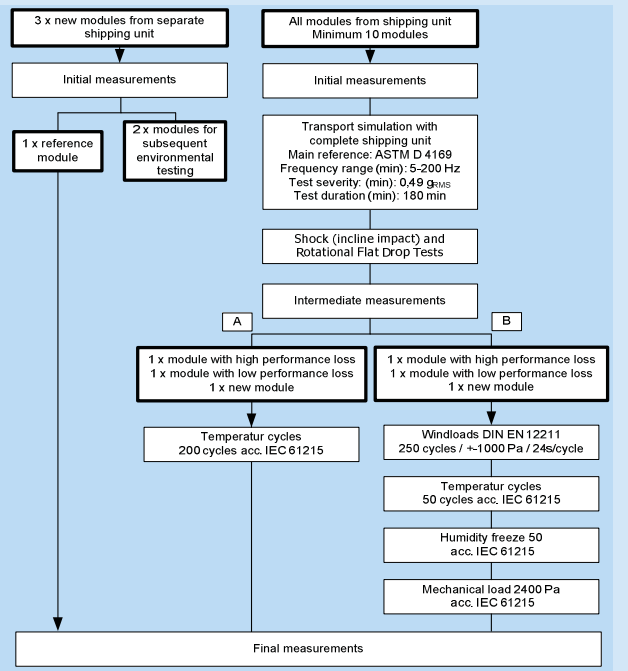


Figure 3: Test plan for transport simulation on complete shipping units and further single module tests

Environmental Tests

Six selected modules will be exposed to two different test sequences (A & B).

Path A can be integrated into the IEC 61215 certification process of a PV module type family.

Path B is a combination of thermo-mechanical stresses which represent different kinds of mechanical and thermo-mechanical impacts in nature.

Results

- This draft shall guide and support the manufacturer of PV modules to assess the risk of impacts on shipping goods and to evaluate the applied packing concept.
- Through the standardization a comparability and quality estimation of packaging is given

Further Tasks

An extended approach shall be realized in a separate part to the future standard (Part 2: Rough handling of individual PV modules). Part 2 shall support installers as a guideline and help manufacturers getting a 'feeling' about the risk for their modules.

Previously performed tests revealed that in handling or mounting situations defects occur on cell level. These may influence relevant safety aspects in a long-term perspective.

Transport task group members : NREL, Westpack, VDZ, TÜV Rheinland

© TÜV, TUEV und TÜV sind eingetragene Marken. Eine Nutzung und Verwendung bedarf der vorherigen Zustimmung.

Photovoltaic Module Reliability Workshop - 2011 February 16-17, Colorado, USA

The work presented has been elaborated in the course of the project "InnoPV" (EN/1022 A) funded by the European Union and the German Federal State of North-Rhine Westphalia.

EUROPÄISCHE UNION
Investition in unsere Zukunft
Europäischer Fonds
für regionale Entwicklung

Ministerium für Wirtschaft, Mittelstand und Energie des Landes Nordrhein-Westfalen

TÜVRheinland®
Precisely Right.

PV Module Reliability Workshop @ Golden, CO
Feb. 16th-17th, 2011

Mitsui Chemicals Group

Volume Resistivity of EVA Encapsulant Sheet

Tsuyoshi SHIODA

Mitsui Chemicals, Inc.

Background and Motivation

Potential-induced electrical corrosion of PV module

PVB vs EVA

	PVB	EVA
Volume Resistivity @23^{O}C[Ωcm]	10^{11}	10^{14}
Rate of electro-corrosion between cell and frame	fast	slow

G. R. Mon and R. G. Ross, Proc. 18th IEEE PV Specialists Conference, Las Vegas, 1985, pp. 1142-1149.

EVA vs Ionomer-blend

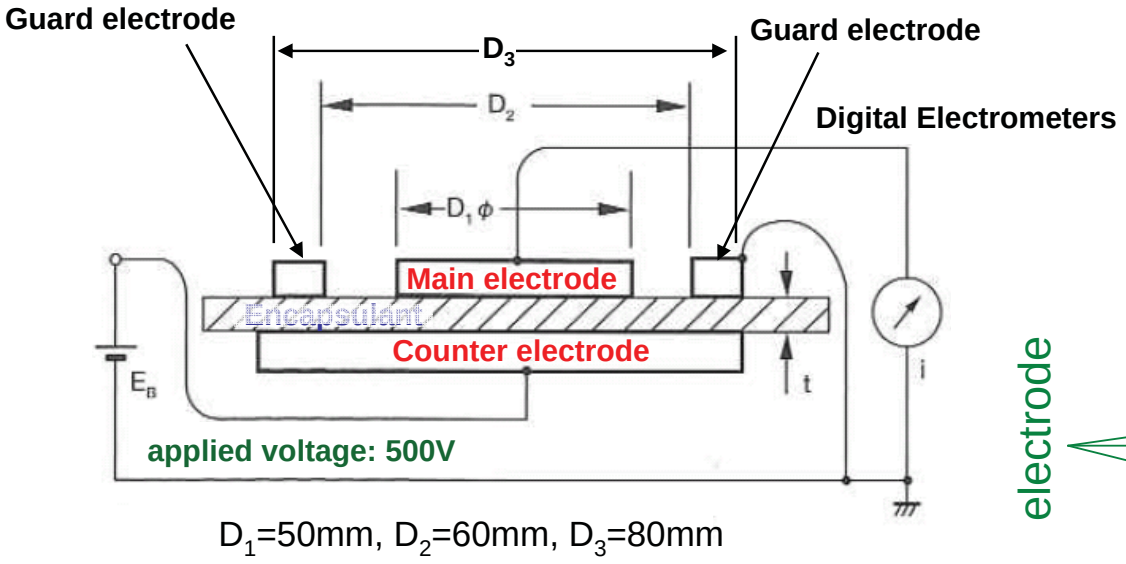
	EVA	Ionomer-blend
Volume Resistivity @23^{O}C[Ωcm]	10^{14}	10^{16}
Rate of electro-corrosion at AR film on cell	fast (Na-ion diffusion?)	slow

P. Hacke *et al*. Proc 25th EU PVSEC, Valencia, 2010.

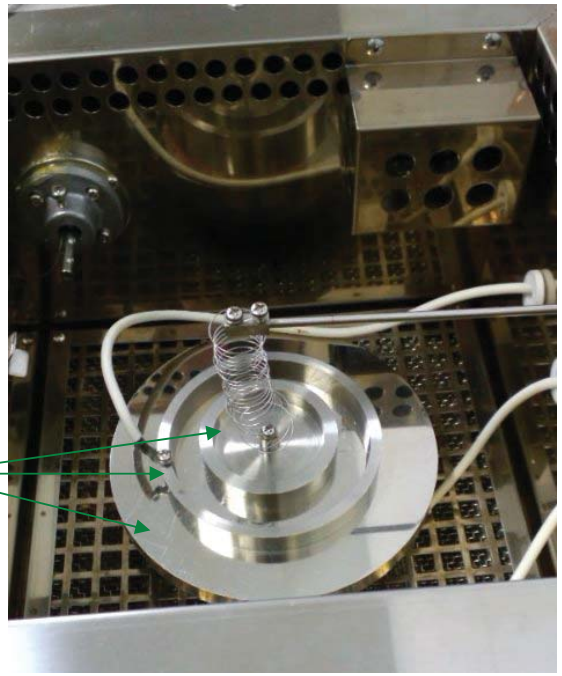
✓**Our goal is to make clear the relationship between rate of electrical corrosion and volume resistivity of EVA or its formulation.**

✓**Our first step is to know volume resistivity of EVA sheets with different VA content and formulation**

Measurement according to IEC 60093



D_1=50mm, D_2=60mm, D_3=80mm

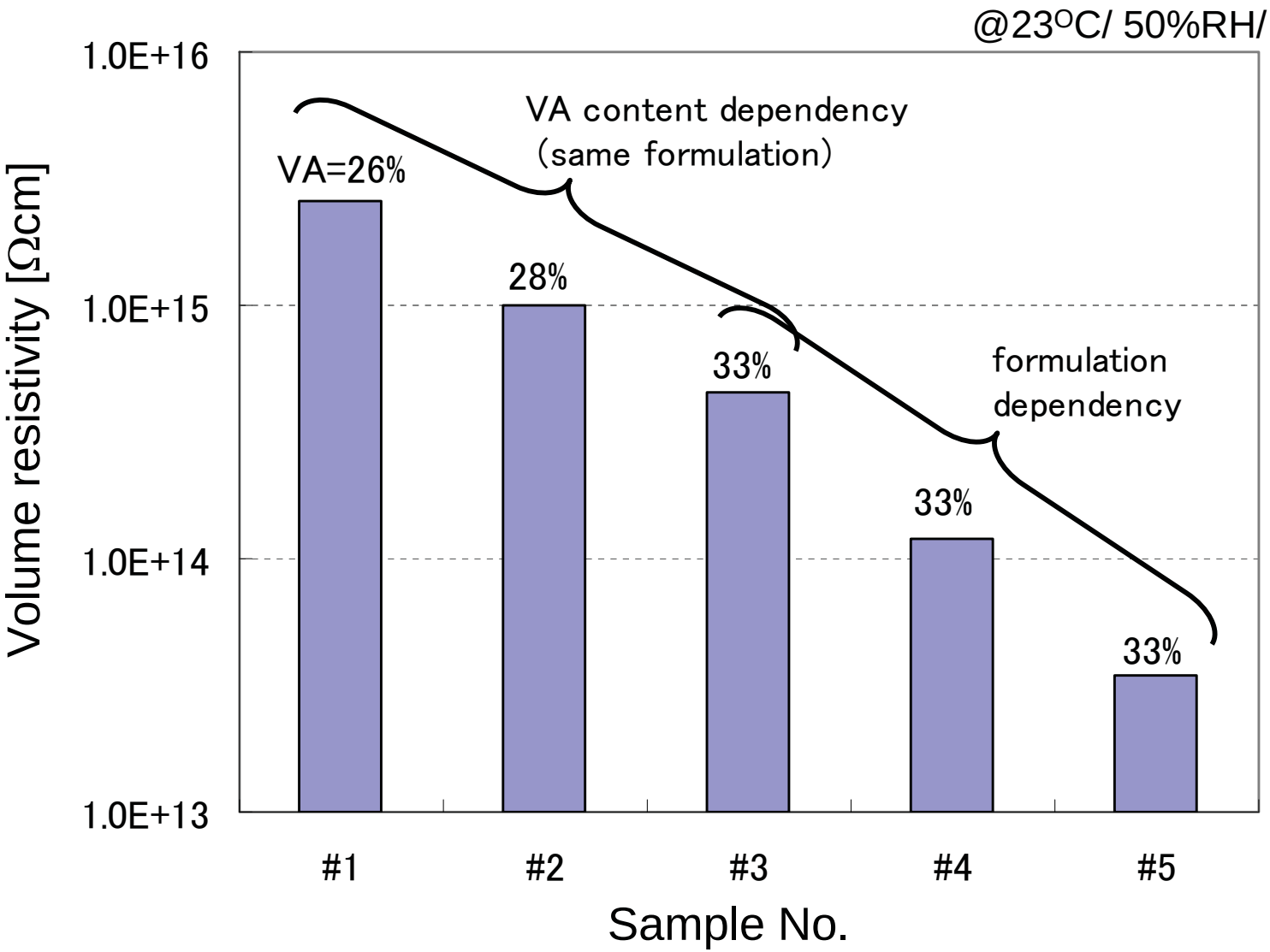


electrode

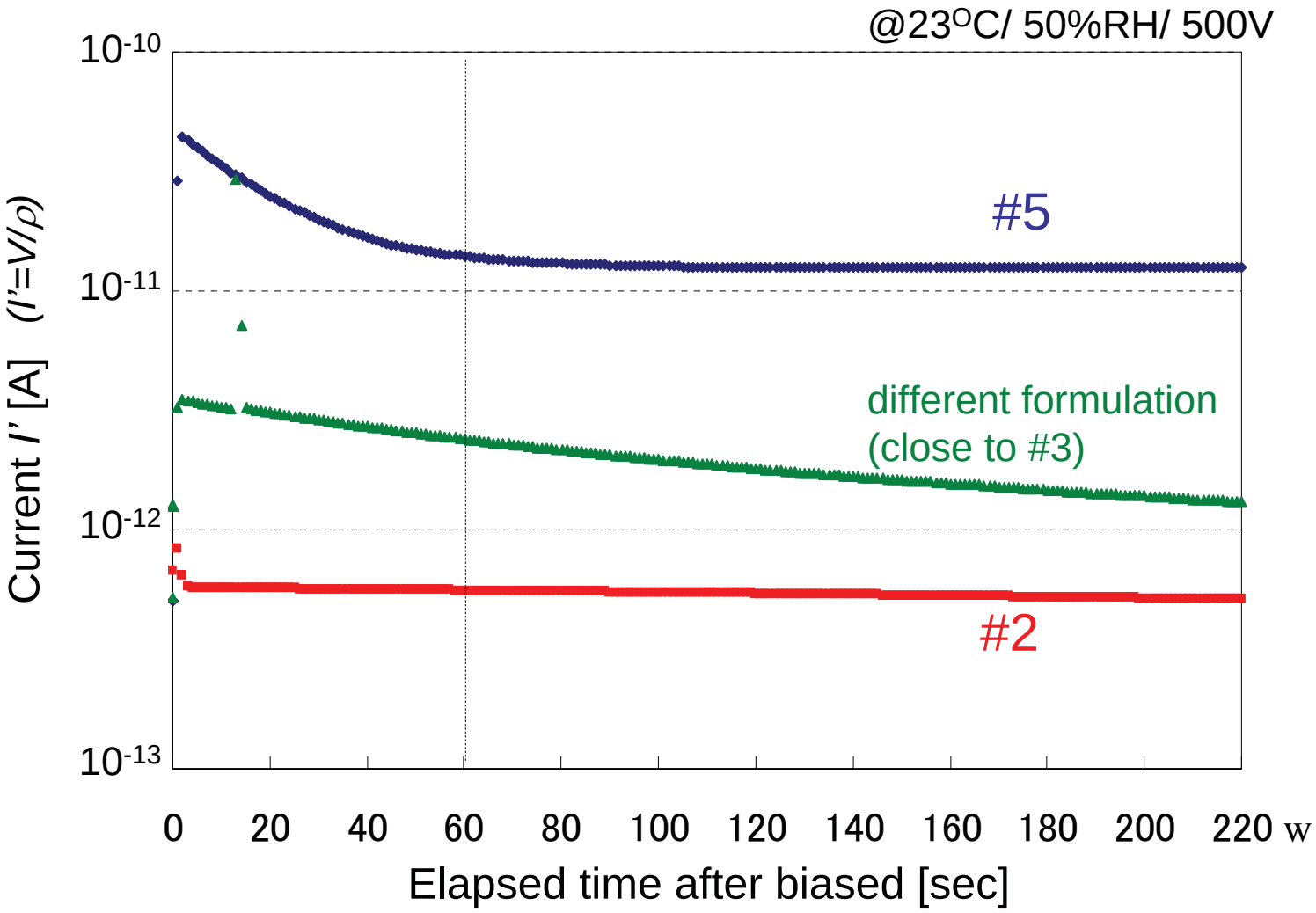
Photo of electrodes for measurement of volume resistivity

Sample size (W x L x T) : 10 x 10 x 0.045 [cm]
The number of measured specimen : 5
Measurement environment : 23 ^{O}C / 50% relative humidity (RH)

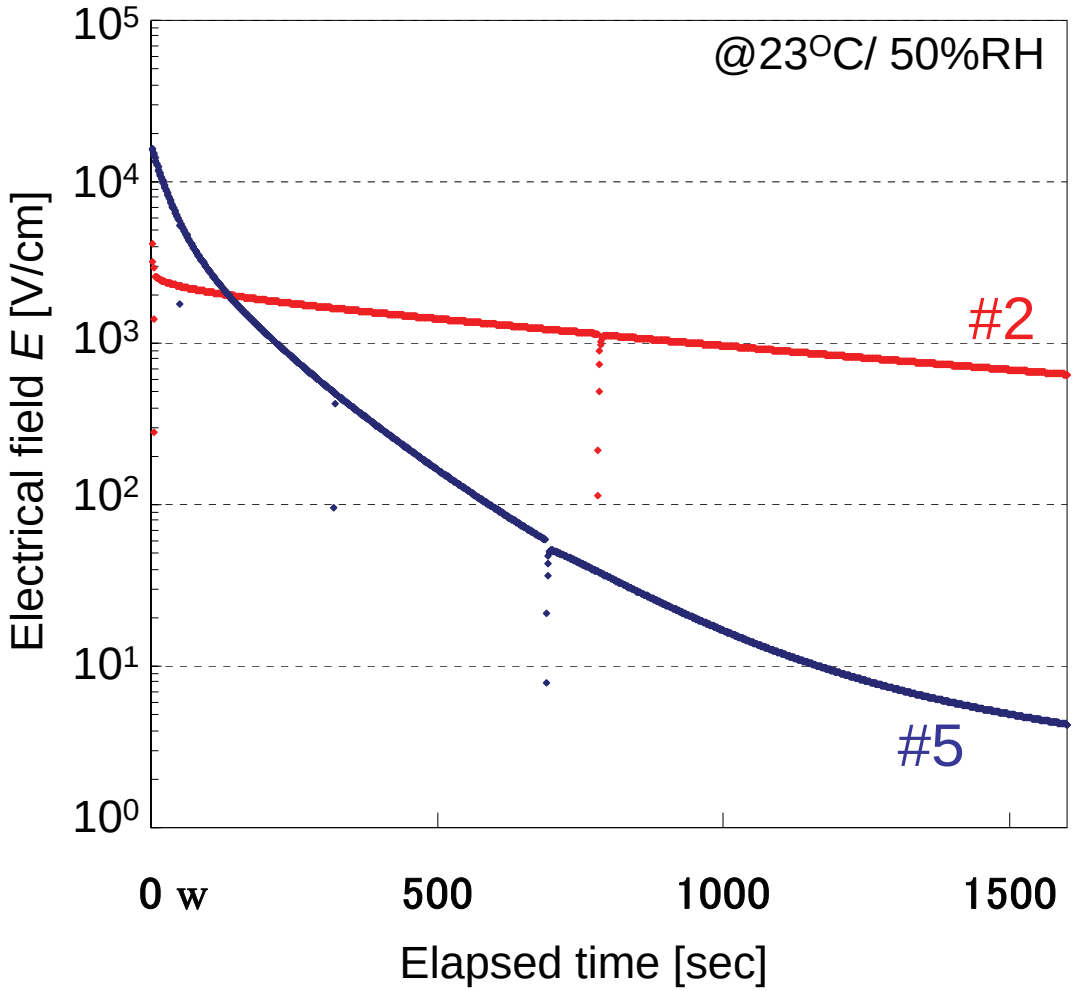
Volume resistivity of EVA sheet

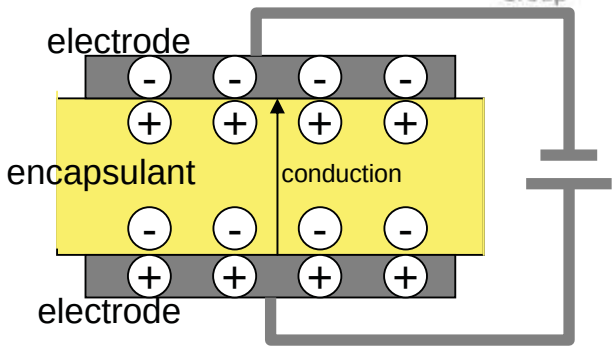


Transient Phenomena during measurement



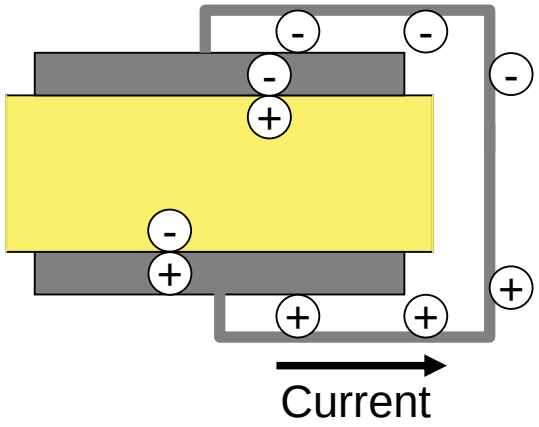
Discharge after measurement





Charge-up & conduction

Short-circuit



discharge

Summary and Future works

✓Volume resistivity of EVA ranged from 10^{13} to 10^{15} [Ωcm], even though these are called as “EVA encapsulant sheet.”

✓We found the slow transient change in current for some types of formulation during measurement of volume resistivity.

✓We can observe discharge phenomena depending on its formulation after measurement and then short-circuit.

✓We have been conducting research related to electrical corrosion using these EVA samples with different volume resistivity. We will share some data near future.

RELIABILITY FACTORS FOR SALVAGE VALUE OF PHOTOVOLTAICS

Joseph McCabe, P.E.

ABSTRACT

As photovoltaic (PV) system prices become less expensive, the salvage value can be increasingly important in life cycle economic calculations. This poster examines data from historic utility salvage sales and reliability perspectives. From 2005 to 2010, large volume PV modules sold at salvage for a variety of pricing dependent upon strength of glass, amount of easily recycled aluminum, industry reduced average selling price (ASP) of new modules and expectations for future energy production. Reliability of product, both real and perceived, are important factors in resale valuations.



Photo 1: 2006 Stacked single crystal silicon salvage sales PV panels.

LARGE SCALE SALVAGE SALES

The Sacramento Municipal Utility District (SMUD) has been re-selling salvaged PV equipment since 2005. The table presented includes the technology based dollar per nameplate watt prices. Over 0.9 megawatts of nameplate modules were sold during this period.

Winning bids ranged from $0.04 to $1.26 / watt. The table shows minimum, maximum, average $/watt winning price for individual lots and approximate nameplate wattage sold that year. Modules sold included tandem amorphous silicon (a-Si), single crystal (Single) and polycrystal (Poly) PV. Model numbers included: Solarex MST 43 and MSX 60, Shell SQ 75/80, Solec SP-102 and SQ-80, and Siemens M55's. Some modules had been panelized, as shown in Photo 1.

Winning Bids from 6 Years of Surplus Photovoltaic Sales at SMUD

	2005		2006		2007		2008		2009		2010	
Bid Lot	Type	Price Per watt	Type	Price Per watt	Type	Price Per watt	Type	Price Per watt	Type	Price Per watt	Type	Price Per watt
1	a-Si	$0.46	a-Si	$0.46	Single	$0.78	a-Si	$0.53	a-Si	$0.07	a-Si	$0.09
2	a-Si	$0.46	a-Si	$0.31	Single	$0.66	a-Si	$0.50	a-Si	$0.06	a-Si	$0.13
3	a-Si	$0.46	a-Si	$0.20	Single	$0.77	a-Si	$0.97	a-Si	$0.04	a-Si	$0.07
4	Poly	$0.98	a-Si	$0.22	Single	$0.82	Poly	$0.44	a-Si	$0.06	Poly	$0.23
5	Poly	$0.75	a-Si	$0.24	Single	$0.73	Poly	$1.15	a-Si	$0.04	Single	$0.13
6	Single	$0.51	Single	$0.66	Single	$0.82	Single	$0.54	a-Si	$0.04	Single	$0.13
7	Single	$0.51	Single	$1.04	Single	$0.72	Single	$0.83	Poly	$0.17	Single	$0.18
8	Single	$0.61	Single	$1.26	Single	$0.48	Single	$0.88	Poly	$0.48	Single	$0.19
9	Single	$0.61	Single	$0.77	Single	$0.66	Single	$0.76	Poly	$0.24	Single	$0.33
10	Single	$0.61	Single	$0.77	Single	$0.82	Single	$0.88	Poly	$0.29	Single	$0.04
11			Single	$0.92	Single	$0.78	Single	$0.91	Poly	$0.21	Single	$0.24
12					Single	$0.82	Single	$0.72	Poly	$0.17		
13					Single	$0.52	Single	$0.56	Poly	$0.23		
14							Single	$0.72	Single	$0.25		
15							Single	$0.65	Single	$0.24		
16									Single	$0.17		
17									Single	$0.30		
18									Single	$0.16		
Min		$0.46		$0.20		$0.48		$0.44		$0.04		$0.04
Max		$0.98		$1.26		$0.82		$1.15		$0.48		$0.33
Total kW		150		69		177		136		212		160

Table 1: 2005 – 2010 Salvage Values for various technologies; 0.9 MW total original capacity. .

RESALE MARKETS

Used or salvaged modules are bought and sold in a number of ways. In some cases, they can be installed into non-incentivized systems like off grid markets. Or they might be showing up in resale channels like on E-Bay, Craigslist or classified section of Home Power Magazine.

It is possible individual modules are being sold into existing systems where a component has broken. All modules in a system should perform at exactly the same level, thus avoiding miss match conditions that reduce overall system performance. Similar to a fine china dinner set that has a broken plate; specific modules have a high replacement value, even if they are a used module. If an existing PV system has a problem with an individual module, replacing that module could have a very high system level value.

Used modules could be sold into a wholesale green power generator; however a tax credit for the installation would not be allowable because the PV materials are not new.

Scrap markets can utilize crystalline cells, as well as the aluminum frames, thus non-working crystalline modules can have an attractive scrap value. Various PV recycling programs have begun around the world including PVCycle headquarted in Phoenix Arizona with additional collection points in Tucson Arizona and San Jose CA.

ENERGY and GLASS

Most PV technologies lose 1% per year in performance consistent with typical 20 year, 80% power warranties. A module with an original standard test condition (STC) power output rating of 100 watts will probably be producing 90 watts at STC after ten years, 80 watts after 20 years. Used modules can be tested for their performance using a max power point current / voltage meter, correcting for module temperature and actual solar radiation normalized to the STC conditions of 1,000 watts per square meter and 25 degrees centigrade cell temperature.

It is important to note that the SMUD salvage sales illustrates a-Si on breakable float glass has considerable less salvage value than single or poly silicon technologies using tempered glass. CdTe might have similar issues with removability and transportability of the more fragile glass compared with tempered glass of crystalline PV. Even tempered glass is subject to breakage during decommissioning, removal transportation and storage activities. If flexible PV like United Solar or other newer flexible PV players in the market were designed for removability, it is possible the salvage value would be even higher than glass based PV.

Visual factors including browning of EVA was an important factor for resale, with large amounts of browning, as shown in the 15 year old single crystals cells of Photo 2, reducing the resale value dramatically.

PHOTOS OF SALVAGED PV MODULES





Photo 2 & 3: 1995 Solec SP-102's piled up in 2010, EVA discoloration

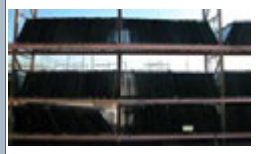




Photo 4 & 5: Bid of panelized single crystalline modules.



Photo 6: Panorama of poorly handled float glass a-Si for bid 2005.



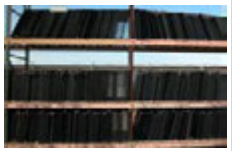


Photo 7 & 8: Well stacked float glass a-Si for bid in 2009.





Photo 9 & 10: Broken tempered glass and j-boxes w/wires in 2009.





Photo 11 & 12: Nicely handled salvaged PV modules in 2010.

PHOTOS OF SALVAGED PV MODULES



Photo 12: Well cared for and stacked modules obtain best resale bid price.

CONCLUSION

There is a healthy resale market for PV modules that should be recognized in project level economic calculations. As systems costs become lower and lower, salvage value have more significant ramifications. Functioning modules will have a revenue value based on life/performance expectations with the additional shipping and handling costs in comparison to other alternative to electric generation costs. The fragility due to glass used in PV modules has important resale value ramifications. Non-glass modules should have greater resale values because of no potential breakage during removal, and resale. There will continue to be a healthy used PV module market for years to come.

ACKNOWLEDGMENTS / REFERENCES

Thanks and appreciations are extended to Brian Robertson, Jigar Shah, Daniel Shugar, ASES and SMUD (Jon Bertolino and Lynne Valdez).

Personal Communication, January 26, 20009, Dan Shugar.

Personal Communication, January 25, 20009, Jigar Shah.

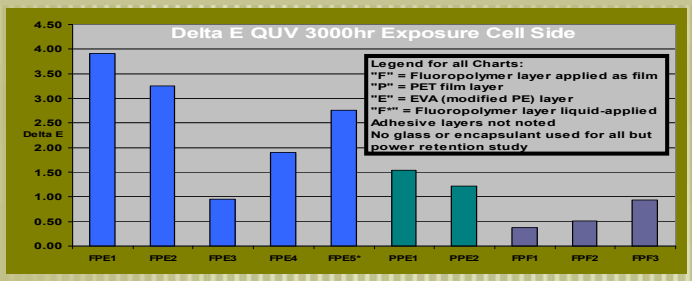
Personal Communication, January 26, 20009, Brian Robertson.

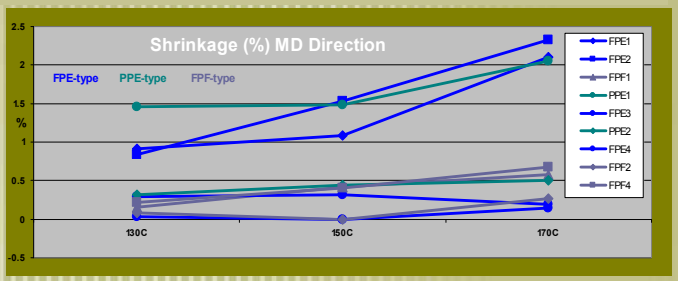
SMUD Salvage Sales, 2005 – 2010 (http://www.smud.org/).

NREL PVRW 2010 BP Ssolar presentation pvrw2010_wohlgemuth.pdf

Material Considerations for Crystalline Silicon PV Module Backsheets

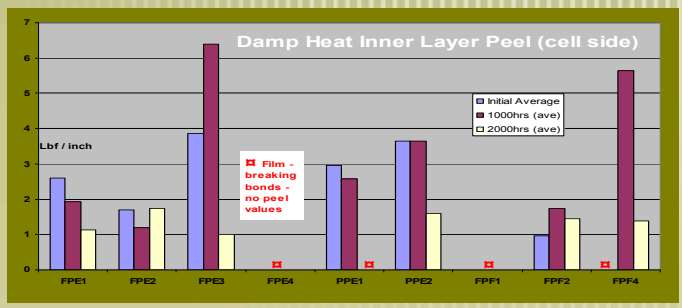
Purpose of Work: In response to market growth and drive to grid parity, PV module producers have a number of new backsheet offerings to consider for cost-effective performance and supply assurance. Many share similar generic descriptions and components. This study attempts to gain insight to any significant impact with respect to module reliability and critical performance areas such as power retention from various generic backsheet structures.

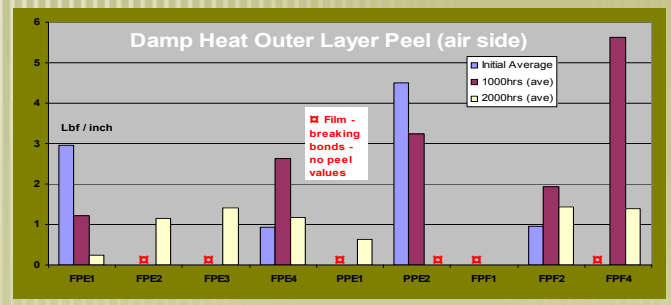




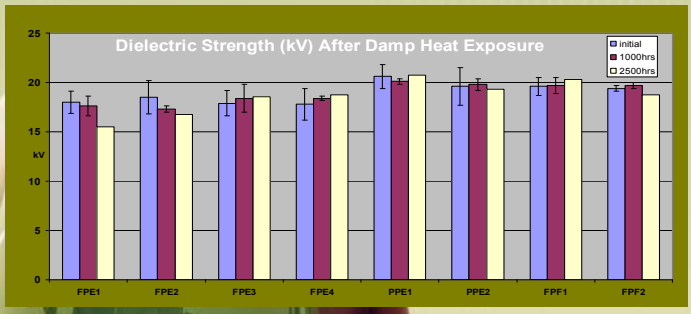
Sun-facing layers appearing more color-fast than others could maintain prolonged reflectivity and stable (1 – 2 unit ΔE) BIPV esthetics.

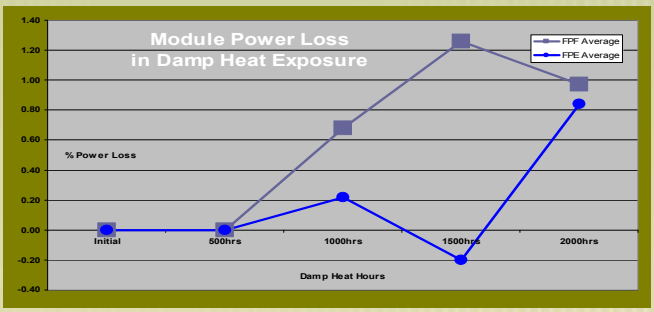
Shrinkage in excess of 1% may induce module stress and results from degree of orientation and heat stabilization of thick PET film layer(s).





Relative comparisons of backsheet long-term inter-laminar bond strengths can become much more revealing beyond 1000 hours damp heat exposure. Also, destructive bonds must be interpreted for adhesive bond strength vs. tear strength or embrittlement of film layer(s) .





Damp heat appears to have little effect on dielectric strength of various structures tested out to 2500 exposure hours.

Modules using single or double side fluoropolymer backsheet displayed good power retention after 2000 hours damp heat exposure.

Conclusion: While many of today's available backsheet offerings for c-Si modules often are described with similar constructions and components, it appears there can be considerable differences in certain properties and their retention over time. This implies that not all products with/without equivalent constructions perform equally over time and therefore may have varying degrees of impact on module reliability and power retention. Testing beyond 2000 hours and adding more structures will continue.

This presentation poster does not contain any proprietary or confidential information.
This data is generated from preliminary testing only. Additional tests will need to be conducted to verify these results. While Honeywell International Inc. believes that the information presented is accurate, we makes no representations or warranties (either expressed or implied) of any kind to the reliability of this data as incorporated into any specific product design. A number of factors may affect Performance of any specific photovoltaic module, such as design, components, construction and manufacturing conditions, all of which must be taken into account by the customer in manufacturing its product. Information provided herein does not relieve the user from the responsibility of carrying out its own tests and experiments and the user assumes all risks and liability (including, but not limited to, risks relating to results, performance, patent infringements and health, safety and environment) for the results obtained by the use of this information.

Honeywell

Automated Extraction of Cell Parameters in a Fully Packaged Solar Module

G. B. Alers, J. Olsen, N. Green
Department of Physics, University of California, Santa Cruz, CA 95066
APV Research, UCSC/NASA ASL, Moffett Field, CA 94035
*Contact: galers@ucsc.edu

Abstract

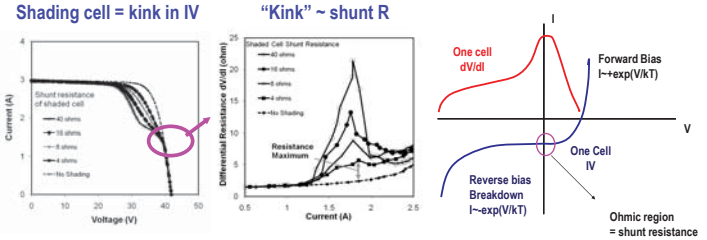
A fully automated methodology is developed for the extraction of cell level parameters in a fully packaged solar module using a computer controlled partial shading screen. The shading screen uses smart window technology to selectively shade individual cells of a module, leaving all other cells clear for full illumination. Under illumination, the partially shaded cell becomes the current limiting cell in the string allowing performance parameters of the individual cell to be extracted from the current-voltage curves and differential impedance analysis of the module. The shunt resistance, short circuit current and peak power output of each cell is extracted from the IV curves in less than ten seconds / cell.

Purpose

- Identification of shunted or low performing cells in module
- Improved statistics on module after reliability / field testing
- Quantitative determination of variation in cell performance

Technique: Simulations of 50% shading of one cell

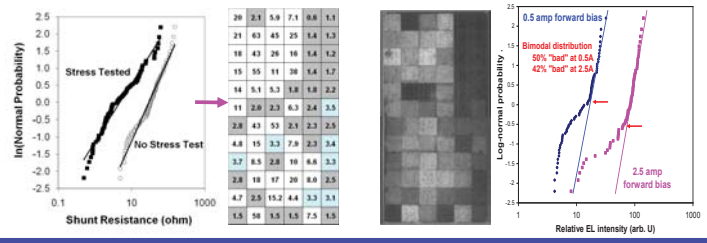
Shading cell = kink in IV "Kink" ~ shunt R



Shunt resistance of shaded cell = (peak dV/dI) – (Module resistance)

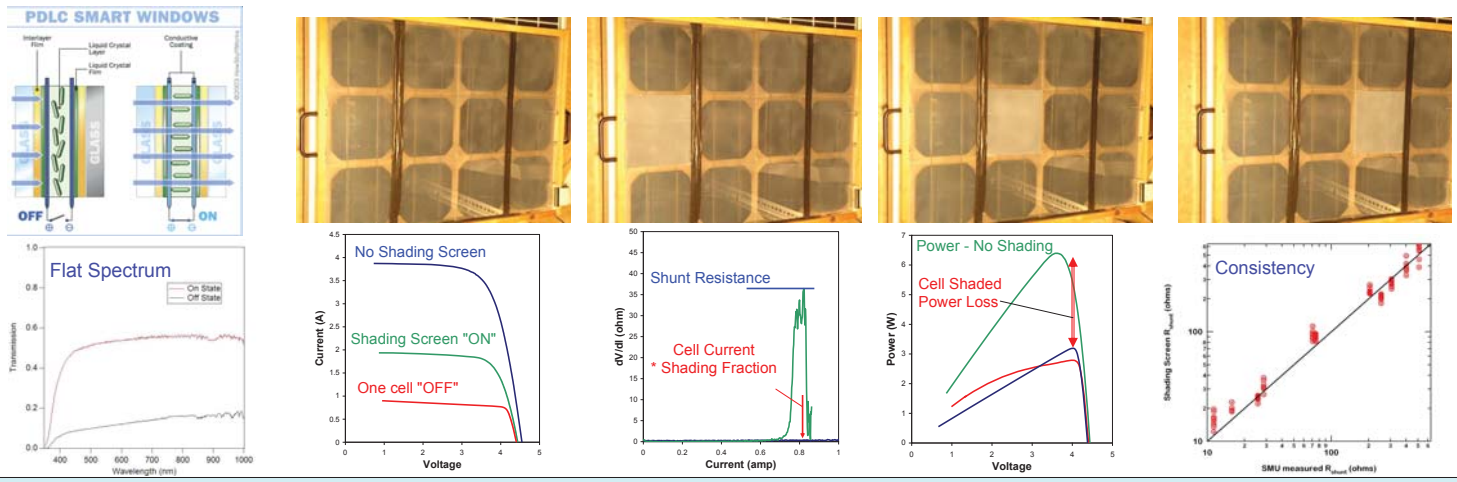
Application to accelerated lifetime test

Module after 85% RH / 85°C / 600V Electroluminesence



Quantitative mapping of cell shunt resistance consistent with EL image

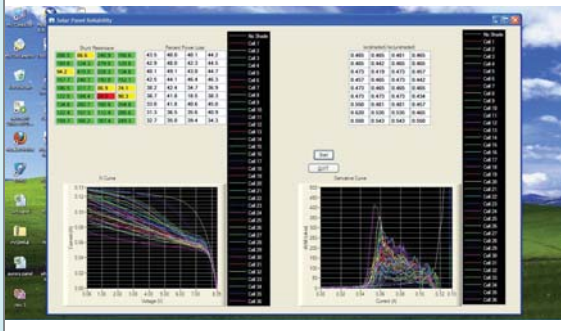
Automation of process

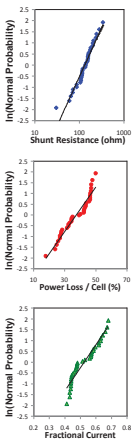


Application to commercial 36 cell module



Shunt resistance
Screen layout: Power loss / cell
Short Circuit Current / cell





Application to commercial 36 cell module

- Automated shading screen for extraction of cell parameters
- External illumination

Environment & Energy Development Center

Durability test of Poly-Ethylen-Terephthalate (PET) film for Backsheet

Kusato Hirota, Masanori Miyashita, Takao Amioka,

Toray Industries, Inc.
Environment & Energy Development Center
, 1-1, Oe 1-chome, Otsu, Shiga 520-2141 JAPAN

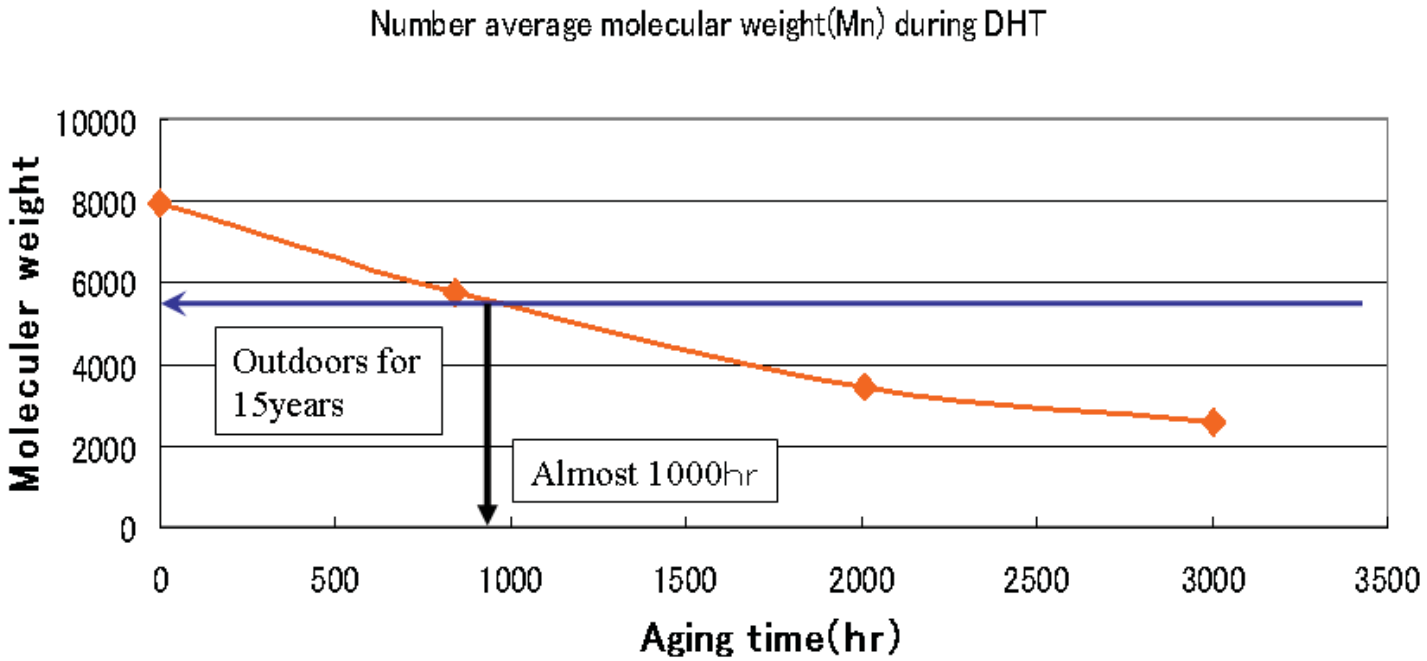


Fig.1 Molecular weight of typical PET film after DHT
Test conditions; 85deg.C 85%RH

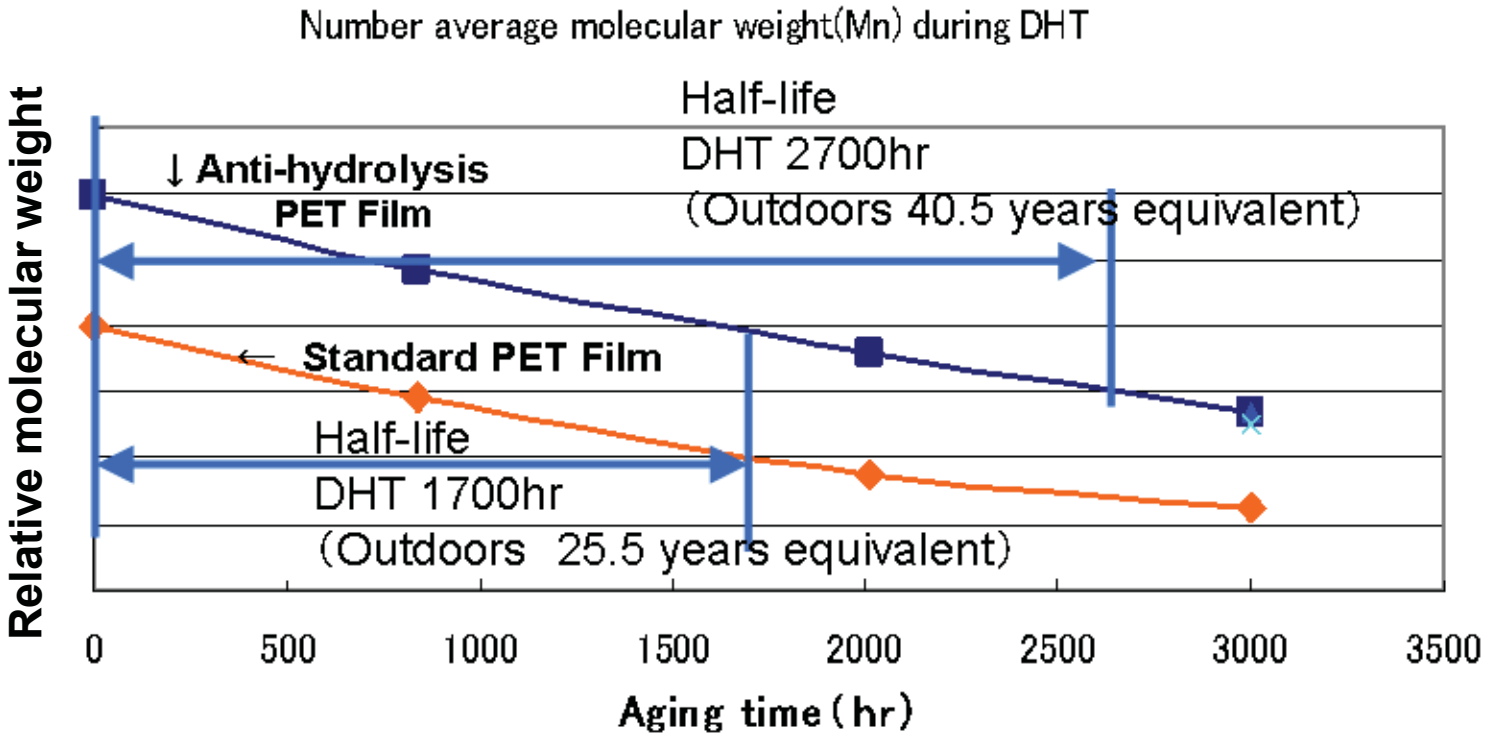


Fig.2 molecular weight half-life model for PET films

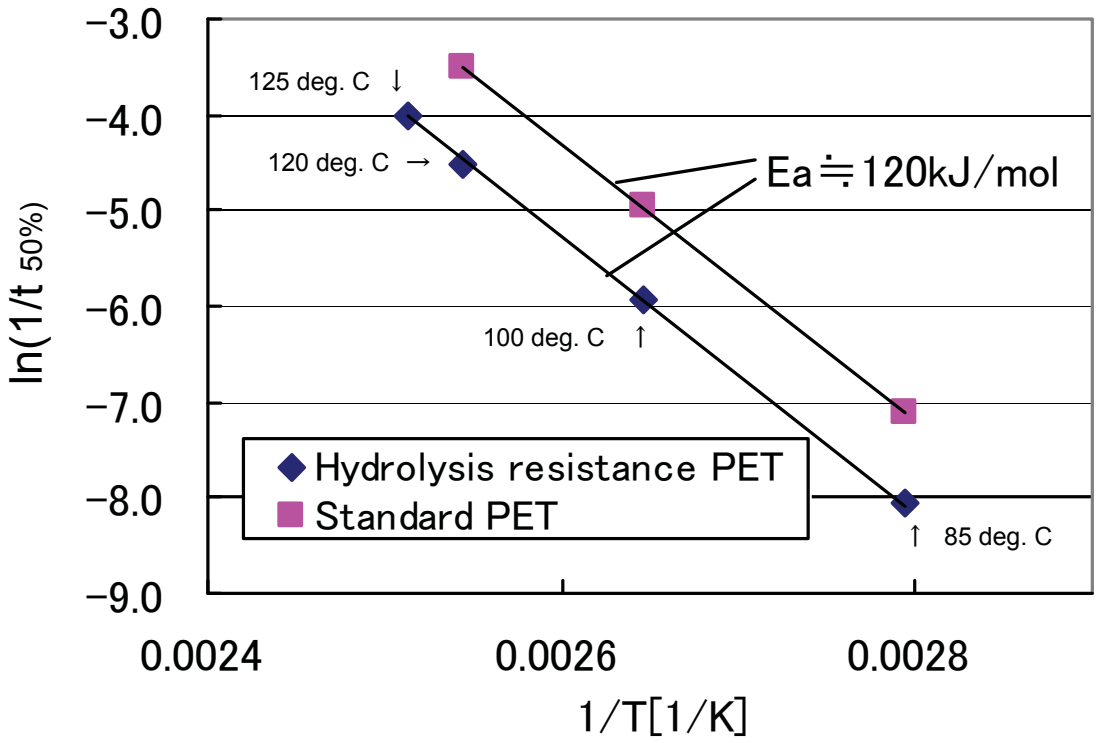


Fig.3a Arrhenius plot of elongation at break (Half-life) of PET films

DHT：85deg. C 85%RH ,

PCT：105deg, C 100%RH, 120deg.C 100%RH and 125deg. C 100%RH

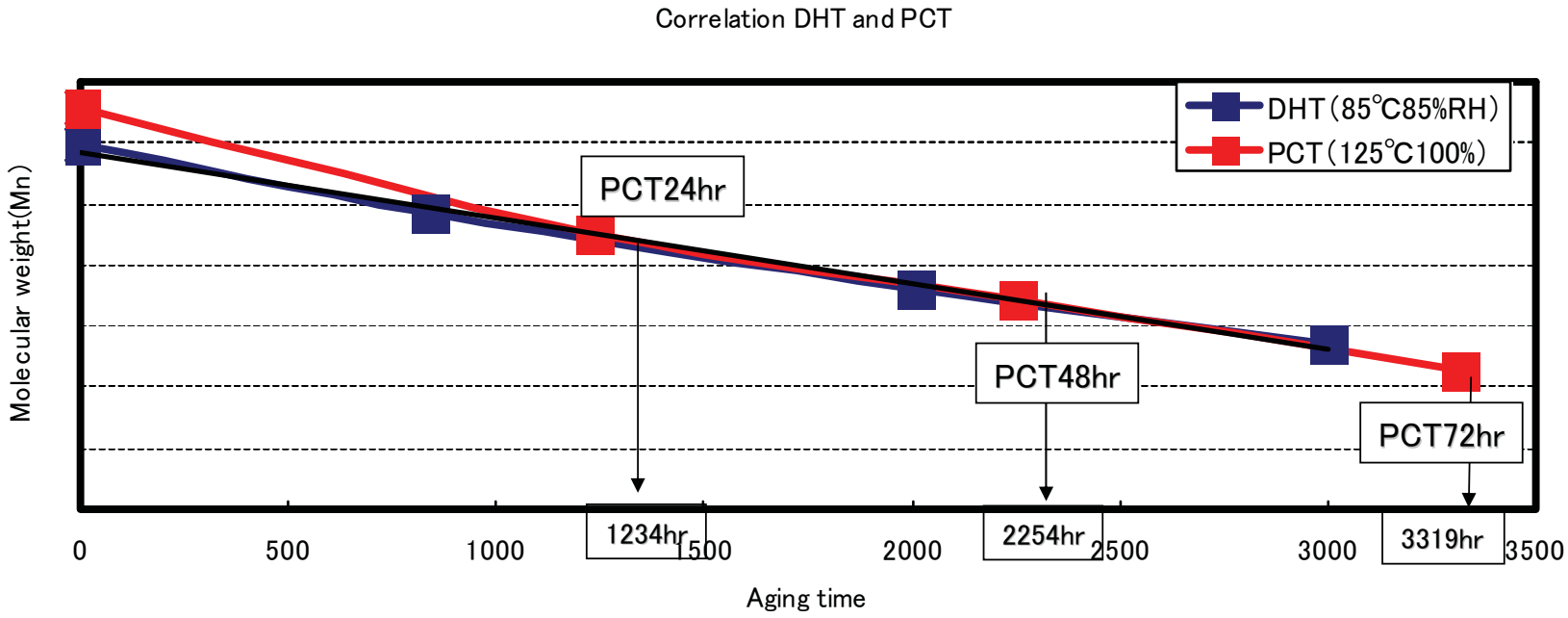


Fig.3b Correlation between DHT and PCT

Conditions; DHT : 85deg. C 85%RH ,
PCT : 125deg. C 100%RH in 2.5atm.

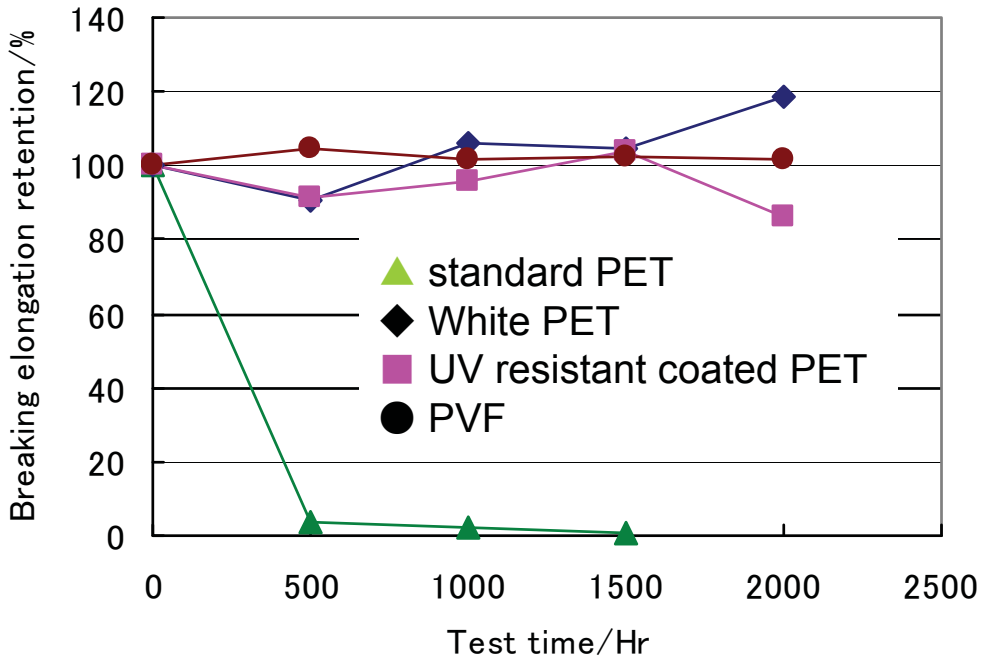


Fig.4. Elongation at break after xenon lamp irradiation

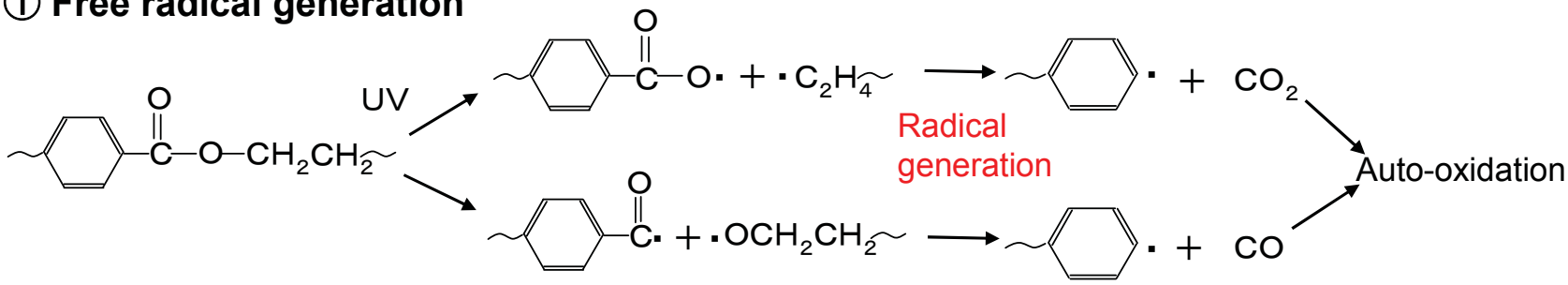
Light Intensity 60W/m2
Black Panel temperature 60deg. C
Relative Humidity 50%RH

TORAY
Environment & Energy Development Center

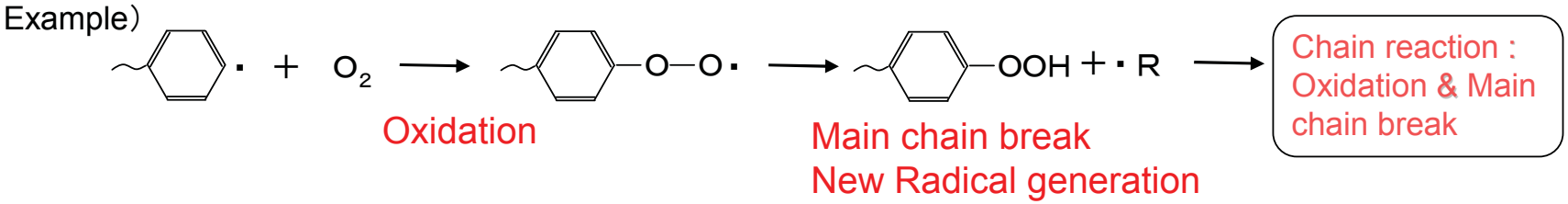
Degradation mechanism by UV light

【Norrish Ⅰ Type】 ～ Free radical generation & Auto-oxidation ～

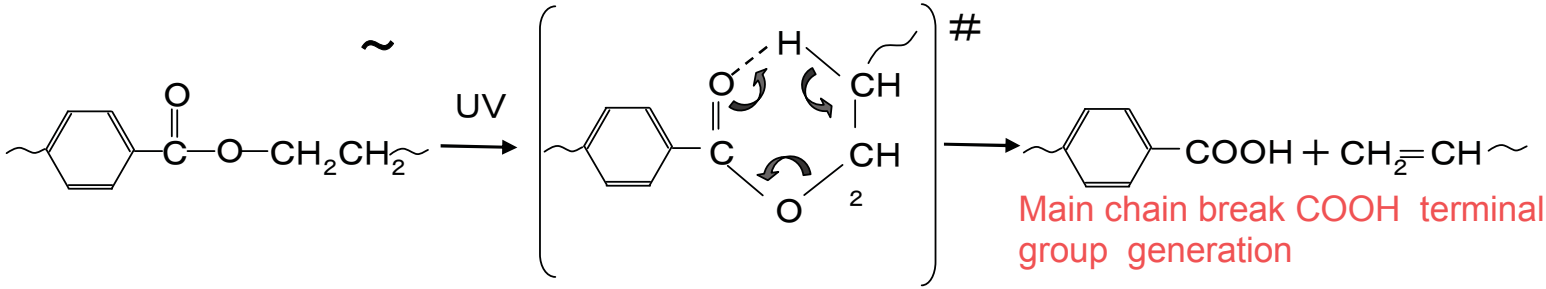
① Free radical generation



②Chain reaction of oxidation : Auto-oxidation



【Norrish Ⅱ Type】 ～ COOH terminal group generation



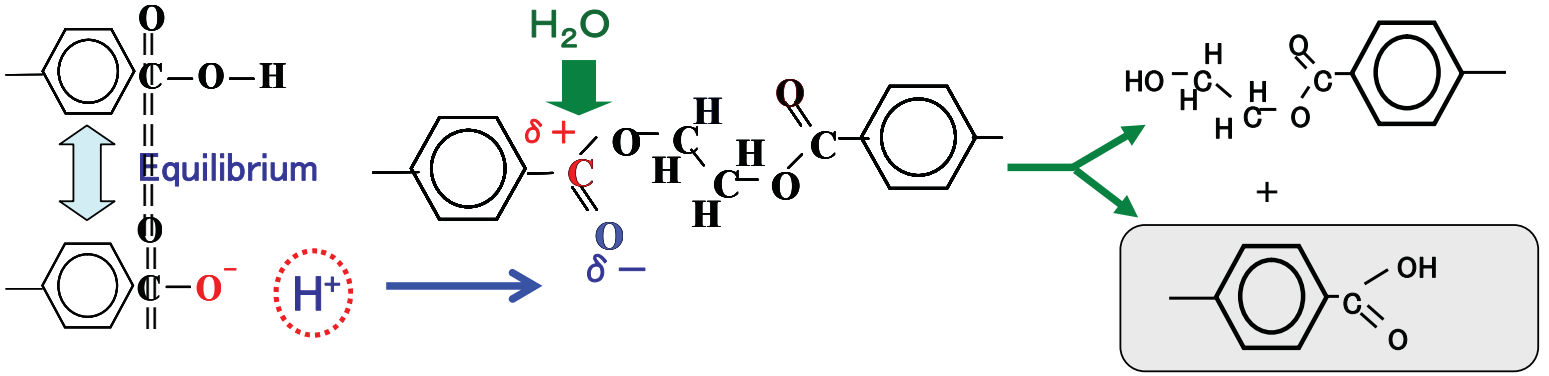
'TORAY'
Environment & Energy Development Center

Hydrolysis mechanism of the PET

【Proton dissociation of the terminal group 】w

【Hydrolysis reaction】

【New terminal group generation 】w



Junction box qualification at REC Solar

Frøydis Oldervoll*, Børge Bjørneklett*, Teck Cheng Tan**
*REC Solar, Kjørboveien 29, 1337 Sandvika, Norway
**REC Solar, 20 Tuas, South Ave. 14, 637312, Singapore

Introduction

The junction box is a very critical component in a PV module. A poor contact in the JB can give rise to temperature increase and potentially lead to hot spots or arcing. Poor adhesion between box and backsheet can cause the JB to detach from the module which again can give rise to numerous problems such as leakage to ground, risk of electrical shock, corrosion of contacts etc. The JB also contains the protective by pass diodes and a failure in one of these diodes can cause hot spot development in shaded cells.

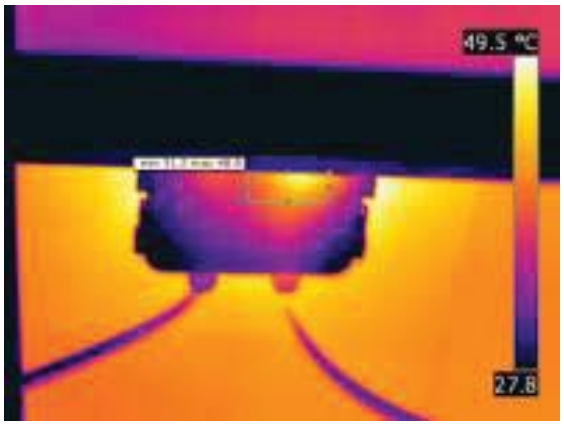


Figure 1: IR image of a junction box with high contact resistance.

Test program

Due to the major impact of the JB on module reliability, REC Solar runs an extensive qualification program before approving a new JB.

- Double IEC 61215 testing (DHT 2000, TC 400, HF 20)
- Adhesion, wet leakage, contact resistance
- Solder joint reliability
- Contact and connector fatigue testing
- Arcing test
- Diode temperature test

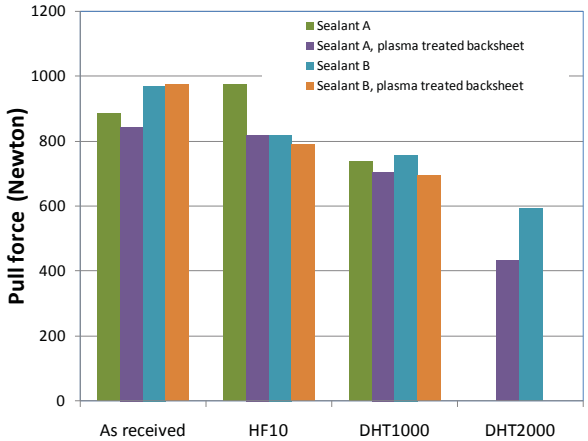


Figure 2: JB pull force after climate chamber ageing at 85°C/85%RH. The adhesion strength decline , but even after 2000 hours it is well above the 160 N limit specified by UL 1703. Plasma treatment of backsheet was found to have little effect on the long term performance.

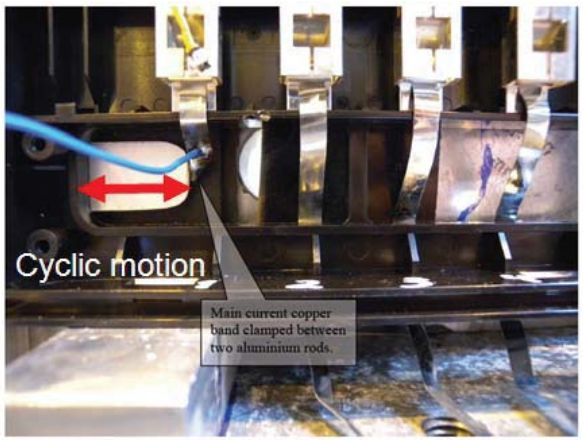


Figure 3: Fatigue testing of junction box terminals. The imposed motion of cross connectors reflect the thermal expansion/contraction that may arise from thermal fluctuation between day and night. Several 10^5 cycles at 1Hz. Failure mechanisms may be fretting corrosion in mechanical clamps or creep/fatigue of soldered terminals in situations with poorly designed stress relief.

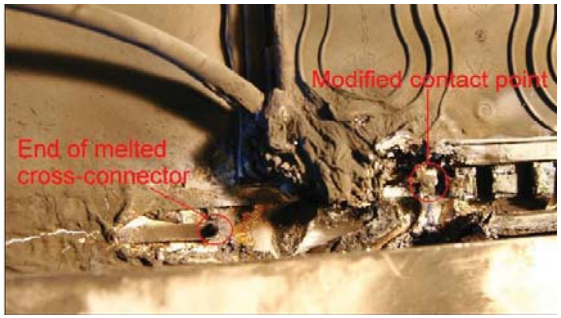


Figure 4: Artificial arc test. Controlled contact resistance of 50 kΩ. The applied voltage was 340 Volt and a short circuit current of 8 A was running through the contact. Arcing and flaming was visible for about 1 minute, after this only a slight smoke indicated heat development. The power was disconnected after 4 minutes.

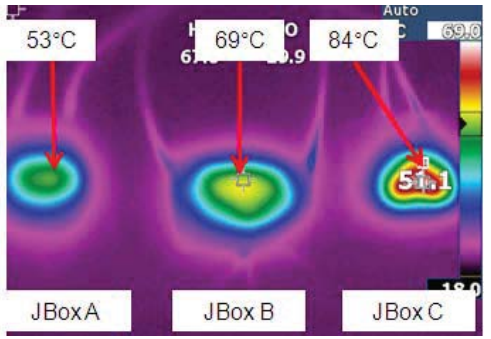


Figure 5: Apply a current equal to the expected current during module field operation. The diodes dissipate a certain power and requirements must be met for diode junction temperature, junction box temperature, and Backsheet temperature.

Conclusion

As part of the reliability testing at REC the junction box is subjected to multiple accelerated tests in order to avoid adverse long term degradation effects. Sound electrical and mechanical integrity is vital for securing PV module longevity. A comprehensive test program has been successful in identifying favorable combinations of materials and components. Future test methods may include shaded module effects on EVA degradation.

This poster does not contain any proprietary or confidential information

Comparison between Outdoor Performances and Manufacturers' Flash Test Results of Crystalline Si PV Modules

Yuzuru UEDA and Kosuke KUROKAWA, Tokyo Institute of Technology
Mitsuru KUDO and Hiroo KONISHI, NTT FACILITIES, INC.

Overview











Type	Manufacturer	Capacity [kW]
single-crystalline silicon	SHARP	30
	SANYO	30
multi-crystalline silicon	SHARP	30
	KYOCERA	100
	Mitsubishi electric	30
amorphous silicon	KANEKA	30
	KANEKA	10
	Mitsubishi Heavy Industries	10
	Fuji Electric Systems	10
spherical	SST	20
compound-semiconductor	Showa Shell Solar	30
	Honda Soltec	3
single-crystalline silicon	MOTECH	10
	KPE	10
	E-TON	10
	Isofoton	30
	GE	30
	Sun Power	50
multi-crystalline silicon	Q-Cells	10
	ErSol	10
	Suntech	30
	BP Solar	10
	Day4Energy	30
	Schott Solar	30
Systems	SHARP	3
	DAIDO METAL	3

Different PV technologies have different characteristics, i.e. different temperature coefficient, different spectral response and so on. "HOKUTO Mega-Solar Project" has been conducted by NEDO in Hokuto city, Japan since 2006 for the evaluation of the advanced PV technologies.

Rating of the PV module in Japanese industrial standards allows +-10% tolerance of nameplate peak power to its actual peak power. Most manufacturers measure each module's output by using flash tester before shipment and confirm whether modules meet the JIS requirement. This paper summarizes single and multi crystalline silicon PV modules' flash test results and their outdoor performances.

Approximately 2MW PV systems are constructed in this project. Because of the availability of the flash test data, twenty four 10kW systems which consist of twelve different module types are chosen for the analysis.



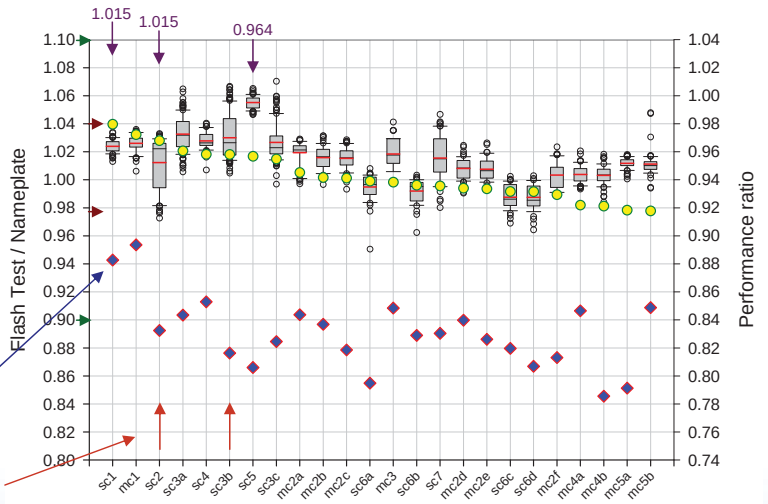
Commissioned by New Energy and Industrial Technology Development Organization (NEDO)

Results

- The STC output of each one sample for twelve types is measured prior to the outdoor exposure in indoor testing facility.
- Adjusted averages are calculated using the following equation.

$$Adjusted\ average = \frac{\sum flash\,test}{\sum nameplate} \cdot \frac{STC(sample)}{Flash\,test(sample)}$$

- All the modules met the JIS requirement.
- Adjusted averages of the normalized flash test results for each 10kW systems scattered between 1.040 and 0.978.
- Ratios of the STC measurement to flash test result of each samples varied from 1.015 to 0.964.
- The systems with the higher adjusted average showed relatively higher performance ratio.
- Some of the systems with the wider deviation of the flash test values resulted slightly lower performance ratio than others.



"sc" stands for single crystalline and "mc" stands for multi crystalline.

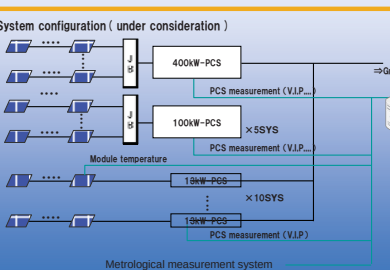
Future plan

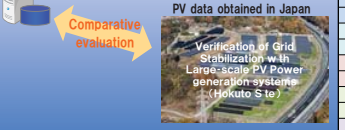
The Japan-U.S. Smart Grid Collaborative Demonstration Project

being conducted in the State of New Mexico of the United States.

•Evaluation of distributed power systems.
Evaluate the performance of PV modules (about ten different types totaling 1 MW capacity will be installed), and compare with other performance evaluation results obtained in Japan.

■ System configuration (under consideration)





■ PV modules (under consideration)

No.	Type	Manufacturer
1	single-crystalline silicon	SHARP
2	single-crystalline silicon (HIT)	SANYO
3	single-crystalline silicon	Sun Power
4	multi-crystalline silicon	KYOCERA
5	multi-crystalline silicon	SHARP
6	amorphous silicon (single)	KANEKA
7	amorphous silicon (tandem)	KANEKA
8	CIGS	Honda Soltec
9	CIS	SOLAR FRONTIER
10	CdTe	First Solar

This poster does not contain any proprietary or confidential information.

Study on Anti-reflection Coated Glass for Photovoltaic Modules

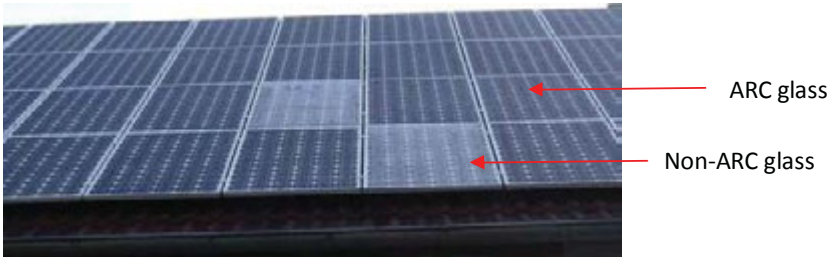
B. Yin, Y. Tang, G. Wang, J, Liu, R. Gao, Q. Guo, J. Wen, G. Zhang
Suntech Power Co., Ltd, 16 Xinhua Road, New District, Wuxi, Jiangsu, China 214028

Photovoltaic modules with higher power are pursued by both module manufacturers and end users. In order to increase modules' power output, anti-reflection coated (ARC) glass as one of many technical methods, has been studied at Suntech since 2006 with a dedicated partner. This paper reported Suntech's work on ARC glass.

(1) Verification of Power Gain

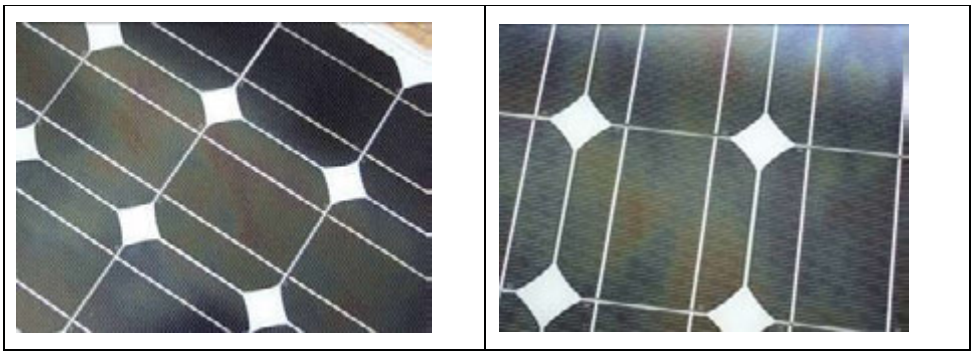
A certain percentage of power gain from using ARC glass for photovoltaic modules is critical to cover the cost on the coating process. In past 5 years, the percentage of power gain increased from about 0.8% to 1.5%, 2.5%, and to about 3% now, based on transmittance measurement of ARC glass and indoor I-V measurement of modules.

In order to verify that ARC glass works in the field, module arrays were installed outdoor for long-term purpose. Actual electricity generation indicated that ARC modules performed well as expected. Normalized output indicated modules with ARC glass even performed better than non-ARC modules because of better self-cleaning and low-angle effect of ARC glass. It should be pointed out that modules with ARC glass would be visually different from modules with non-ARC glass in the field as shown below. It is not recommended to mix using them in the same application.



(2) Coating Uniformity

Uniform coating is very important both visually and functionally. Modules with uniform ARC glass were shipped worldwide by Suntech. However, the coating uniformity was not acceptable at the very beginning as shown below.



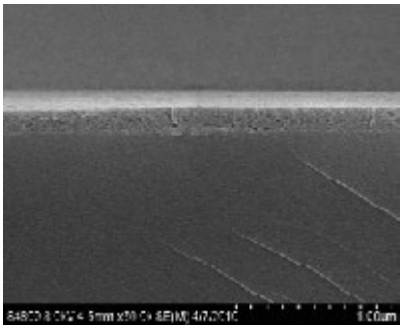
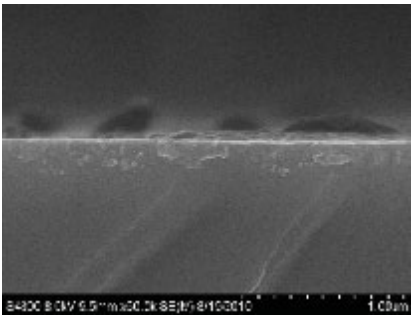
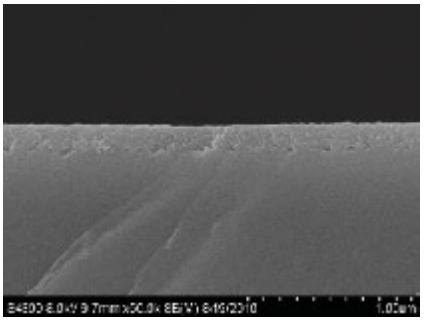
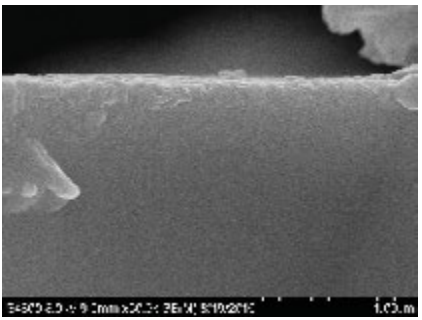
(3) Self cleaning capability

It's hoped that ARC glass can offer better self cleaning than non-ARC glass. Test shown in following pictures indicated that ARC glass has better self cleaning capability than non-ARC glass.

ARC glass	Non-ARC glass
	
Dust applied to ARC glass	Dust applied non-ARC glass
	
After cleaning of ARC glass	After cleaning non-ARC glass

(4) Indoor Reliability Test

- Modules with ARC glass passed nicely DH1000, TC200, UV, HF10 and salt spray tests per IEC and UL standards.
- Beyond standard tests, acid test, adhesion test, pencil hardness test, scratch test and SEM analysis were carried out to ARC glass. Results indicated that anti-reflection coating survived well after these tests.

 Pencil hardness test	 Scratch test
 Cross section before test	 After acid test
 After salt mist test	 After damp heat test

(5) Conclusion

Based on our indoor reliability testing, outdoor measurement in house, and feedback from field applications, it is concluded that ARC glass is reliable, while it helps increasing power output of photovoltaic modules. The study is being continued.

Qualification and Lifetime Testing Protocols for Gen II Back Contact Solar Cells/Modules

Bethanne Felder/ Sonya Xu

Applied Materials

2011 PV Module Reliability Workshop

February 16- 17, 2011

This poster does not contain any proprietary or confidential information.

Front Contact vs. Back Contact Technologies

- Current front contact module (Gen I) technology is highly reliable
  - Proven with accelerating aging results and field performance (30 years)
  - Most failure modes and mechanisms have been identified and are well understood

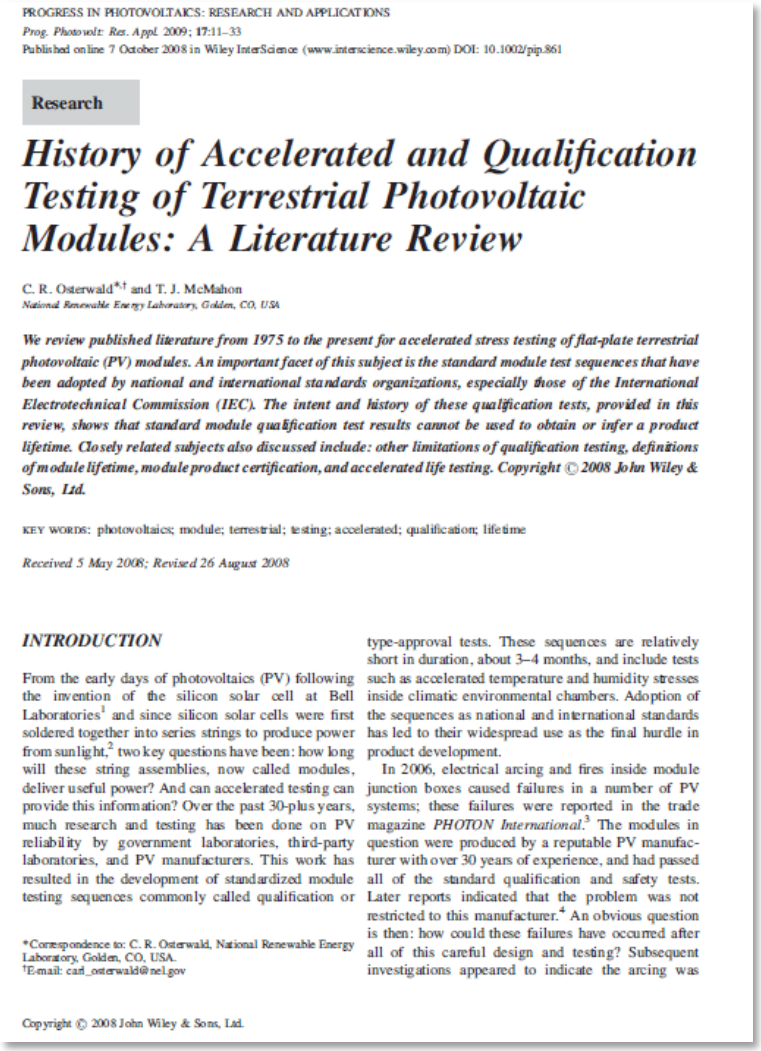
- Second Generation Back Contact (Gen II) Modules have:
  - New designs
  - New materials and material combinations
  - New methods of construction
  - **Potentially new failure mechanisms**

Adoption of Gen II Back Contact Modules requires proof of equal or better reliability than Gen I Front Contact Modules

This poster does not contain any proprietary or confidential information
APPLIED MATERIALS®

Gen I Front Contact Qualification is Proven

- Carl Osterwald and Tom McMahon from NREL published an excellent history of how the current set of accelerated and qualification tests were established[1]
- IEC 61646, 61730 and 61215 along with UL 1703 are the industry standards for certifying and baseline testing of modules
- Many manufacturers have extended testing beyond the 200 thermal cycles and 1000 hours of 85 C, 85% RH called for in the above standards to further demonstrate the reliability of their modules



PROGRESS IN PHOTOVOLTAICS: RESEARCH AND APPLICATIONS
Prog. Photovolt: Res. Appl. 2009; **17**:11–33
Published online 7 October 2008 in Wiley InterScience (www.interscience.wiley.com) DOI: 10.1002/pip.861

Research

History of Accelerated and Qualification Testing of Terrestrial Photovoltaic Modules: A Literature Review

C. R. Osterwald*,† and T. J. McMahon
National Renewable Energy Laboratory, Golden, CO, USA

We review published literature from 1975 to the present for accelerated stress testing of flat-plate terrestrial photovoltaic (PV) modules. An important facet of this subject is the standard module test sequences that have been adopted by national and international standards organizations, especially those of the International Electrotechnical Commission (IEC). The intent and history of these qualification tests, provided in this review, shows that standard module qualification test results cannot be used to obtain or infer a product lifetime. Closely related subjects also discussed include: other limitations of qualification testing, definitions of module lifetime, module product certification, and accelerated life testing. Copyright © 2008 John Wiley & Sons, Ltd.

KEY WORDS: photovoltaics; module; terrestrial; testing; accelerated; qualification; lifetime

Received 5 May 2008; Revised 26 August 2008

INTRODUCTION

From the early days of photovoltaics (PV) following the invention of the silicon solar cell at Bell Laboratories[1] and since silicon solar cells were first soldered together into series strings to produce power from sunlight,[2] two key questions have been: how long will these string assemblies, now called modules, deliver useful power? And can accelerated testing can provide this information? Over the past 30-plus years, much research and testing has been done on PV reliability by government laboratories, third-party laboratories, and PV manufacturers. This work has resulted in the development of standardized module testing sequences commonly called qualification or type-approval tests. These sequences are relatively short in duration, about 3–4 months, and include tests such as accelerated temperature and humidity stresses inside climatic environmental chambers. Adoption of the sequences as national and international standards has led to their widespread use as the final hurdle in product development.

In 2006, electrical arcing and fires inside module junction boxes caused failures in a number of PV systems; these failures were reported in the trade magazine *PHOTON International*.[3] The modules in question were produced by a reputable PV manufacturer with over 30 years of experience, and had passed all of the standard qualification and safety tests. Later reports indicated that the problem was not restricted to this manufacturer.[4] An obvious question is then: how could these failures have occurred after all of this careful design and testing? Subsequent investigations appeared to indicate the arcing was

*Correspondence to: C. R. Osterwald, National Renewable Energy Laboratory, Golden, CO, USA.
†E-mail: carl_osterwald@nel.gov

Copyright © 2008 John Wiley & Sons, Ltd.

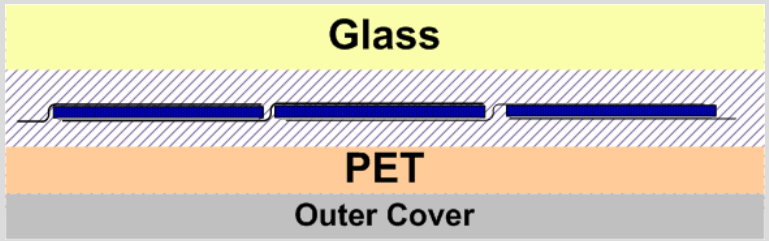
[1] History of Accelerated and qualification Testing of Terrestrial Photovoltaic Modules: A literature review, Progress in Photovolt: Re. Appl 2009

This poster does not contain any proprietary or confidential information

APPLIED MATERIALS®

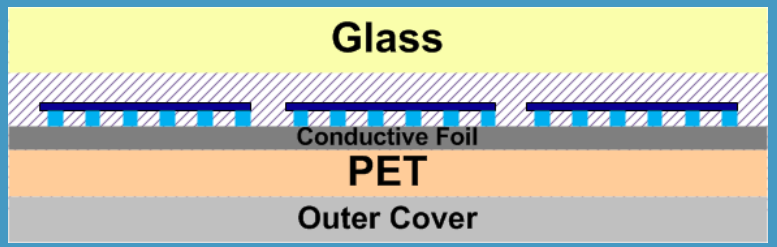
Front Contact is Different than Back Contact

Generation I Front Contact



- Flat Cu wire interconnects weaved from front to rear surface of adjacent cells requiring space between the cells for stress relief
- Aligned Cu interconnects on front and rear of cells produce balanced stress
- Soldered interconnects
- Permeable backsheet construction
- Industry standard EVA encapsulant

Generation II Back Contact



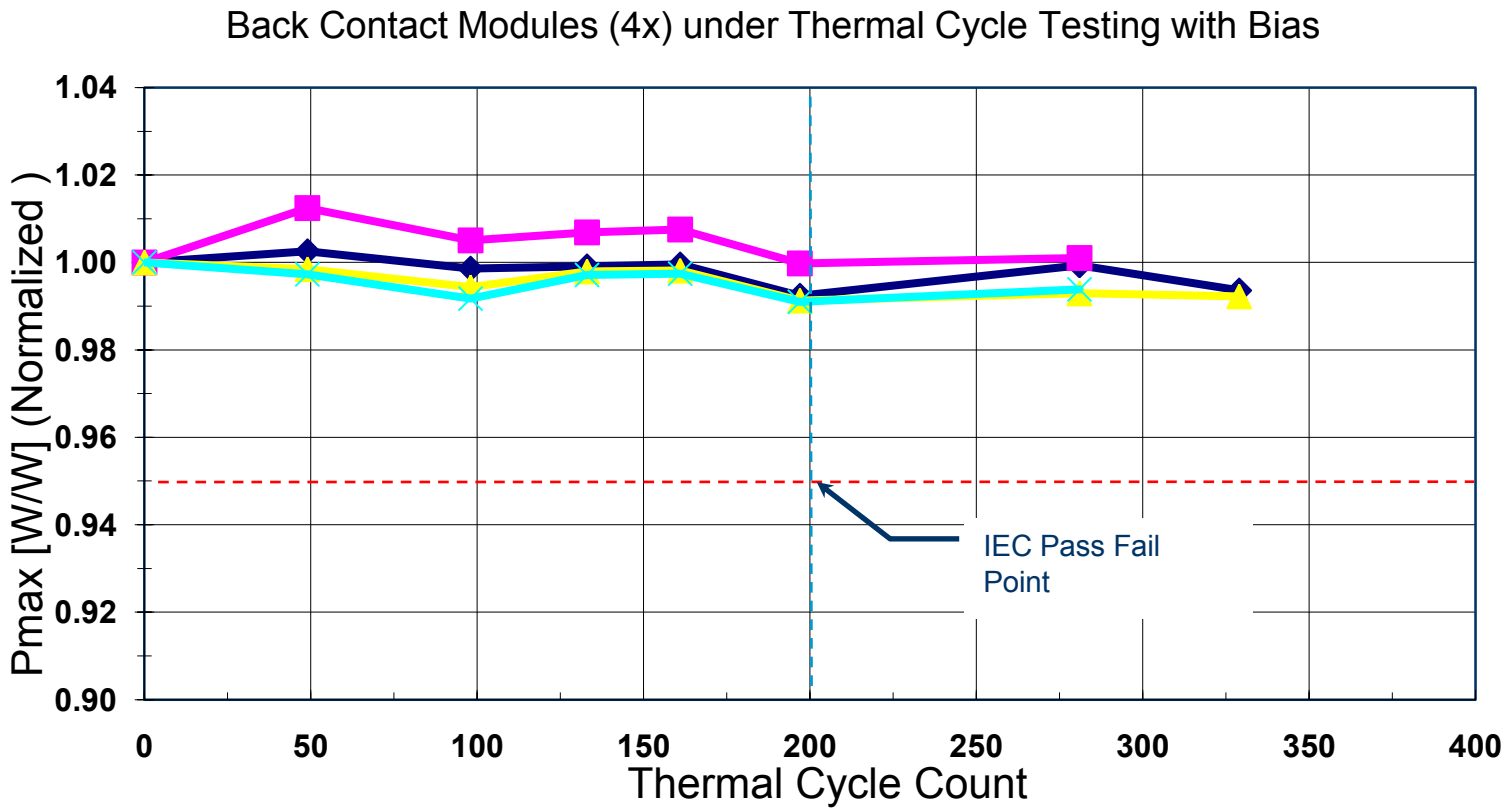
- Interconnects solely on the rear surface
- Reduced spacing between cells
- New materials and new interfaces
- Interconnects are no longer balanced
- Alternative circuit interconnects (electrically conductive adhesives, low temperature solder, etc.)

This poster does not contain any proprietary or confidential information

APPLIED MATERIALS®

Gen II Back Contact Module Qualification

Current Status – Example 1

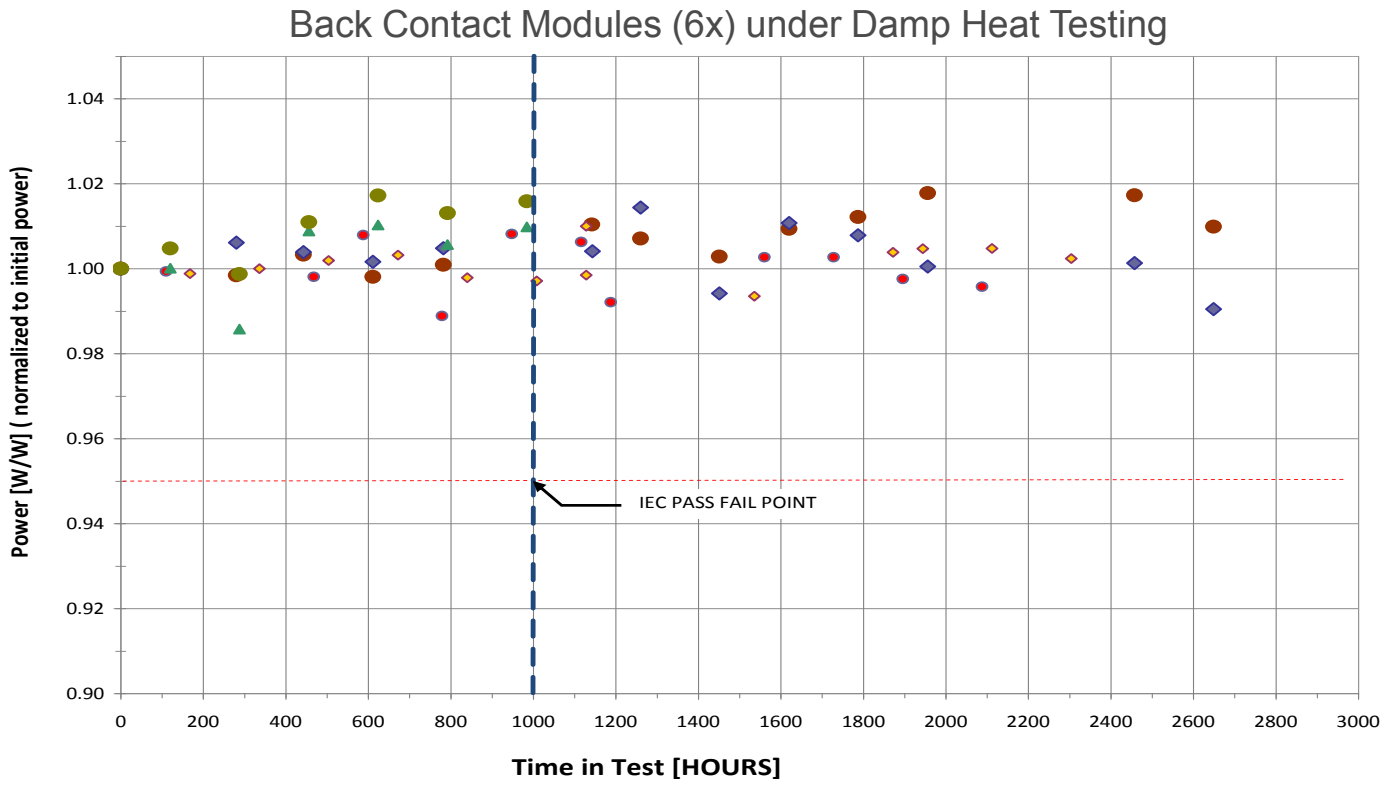


- An example of the use of extended testing to characterize reliability properties of new designs
- **Consistently passes industry standard tests, but is this sufficient?**

This poster does not contain any proprietary or confidential information
APPLIED MATERIALS®

Gen II Back Contact Module Qualification

Current Status – Example 2



- An example of the use of extended testing to characterize reliability properties of new designs
- **Consistently passes industry standard tests, but is this sufficient?**

This poster does not contain any proprietary or confidential information

APPLIED MATERIALS®

Advancing Gen II Back Contact Technology

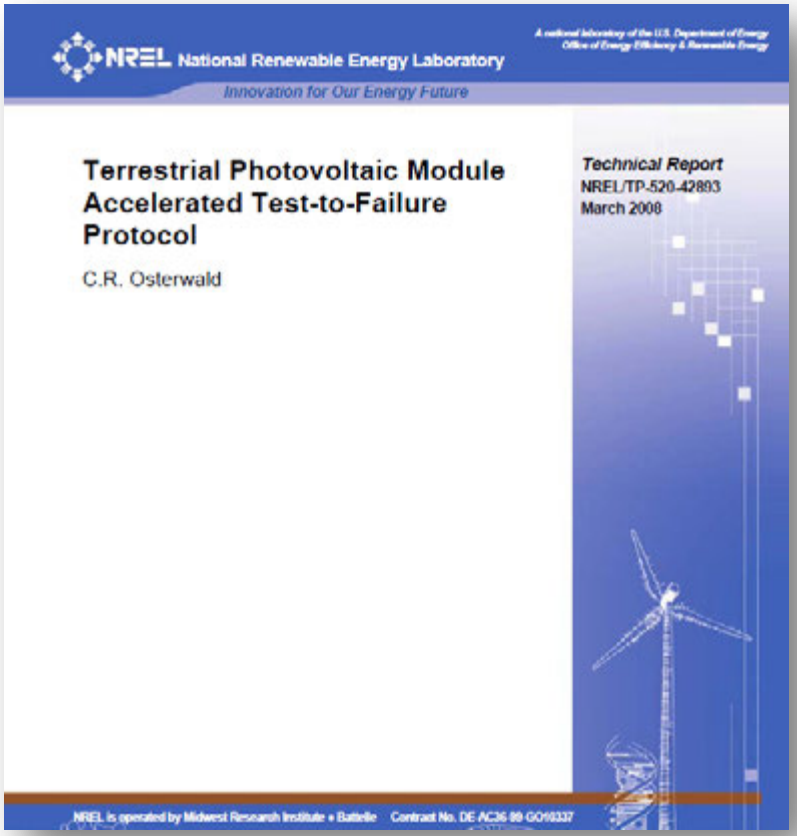
- Industry standard accelerated aging tests will detect common failure modes such as those in Gen I Front Contact modules

- **Collaboration** between material suppliers, module manufacturers and National Labs is required **to define and conduct accelerated testing** that is necessary to **prove reliability** of Gen II back contact modules **enabling** expedited market acceptance

This poster does not contain any proprietary or confidential information
APPLIED MATERIALS®

Approach – Exceed Front Contact Standards

- Our proposal is to use comparative testing that expands on current IEC 61215 standards to include protocols recommended by Carl Osterwald[2]
- A Gen I front contact module with a proven 25 year life will undergo selected accelerated tests side by side with Gen II back contact modules. This will reduce uncertainty and provide the required comparative measure
- Gen II back contact modules must perform as well or better than the conventional module under extended life time tests to failure



[2] **Terrestrial Photovoltaic Module Accelerated Test-to-Failure Protocol** C.R. Osterwald ,***Technical Report,*** **NREL/TP-520-42893 ,March 2008**

This poster does not contain any proprietary or confidential information

Proposed Testing Protocols for Gen II Back Contact Modules

Recommended Test	Origin	Failure to be Detected
TC (-40 to +85 or 90ºC) cycle; 4x daily, under 1.25 I_{sc} forward bias; Test to Failure	IEC 61215	CTE mismatch failure, excessive heating due to poor interconnect bonding, soldering issues
HF (-40 to + 85ºC) cycle; 1x daily; Test to Failure	IEC 61215	Failure of bonds at surfaces
HF (-40 to + 85ºC) cycle; 1x daily; Test to Failure	IEC 61215	Failure of bonds at surfaces
Mechanical Load and Hail Test	IEC 61215	Mechanical integrity of module design
DH under 1000 volts; Test to Failure	New	Galvanic corrosion, yellowing, electro migration
DH 1000 followed by HF; Test to Failure	New	Failure of bonds at surfaces; moisture ingression

Additional Ideas are Welcome!

This poster does not contain any proprietary or confidential information

APPLIED MATERIALS®

Advantages

- This combination of extended industry standard test protocols with additional stresses of electric field on DH and current load in TC is likely to identify most of the failure modes
- By extending all protocols to be test to failure and comparing to the performance of a standard reference module provides confidence in the reliability performance of new module designs

Risks and Mitigations

- No method in any HALT approaches to reliability testing can guarantee that all failure modes will be found
- Early field testing is required to gain complete confidence that the majority of failure modes are found
- Reliability engineering and physics studies must also be conducted to analyze the reliability properties of designs

This poster does not contain any proprietary or confidential information
APPLIED MATERIALS®

Moving Forward

The solar industry and the National Labs, building on our experiences from the last 30 years, need to have a collaborative effort to define and conduct the accelerated testing required to prove the reliability of these Gen II back contact modules enabling expedited market acceptance.

This poster does not contain any proprietary or confidential information
APPLIED MATERIALS®



Turning innovations
into industries.™

Characterization and Aging Study of Encapsulant (EVA) and Backsheet for PV Modules

Shuying Yang, Abhay Maheshwari, Shirish Shah,
Junaid Fatehi and Kent Whitfield

6200 Paseo Padre Parkway, Fremont, CA94555

SOLARIA™

1-13-2011

Abstract

- Given the warrantee and customer expectation for a 25 to 30 year product, all components used with PV module must exhibit very high durability in a multitude of climates. This study focuses specifically on EVA encapsulant and polymer backsheet that are relatively standard components for crystalline silicon PV modules.
- Durability is considered from the standpoint of stress aging via UV exposure, damp heat and thermal exposure.
- Durability characterization utilized FTIR, TGA and spectrophotometer measurement.
- Relative performance of EVA and backsheet from different commercial vendors are presented.
- Based on failures observed, recommendations are given to further improve the quality of these two key components for the industry.
  - EVA - improve for the UV stability;
  - Backsheet – improve UV stability, hydrolysis resistance and interlayer adhesion strength.

Characterization Techniques for EVA and Backsheet

- FTIR (Fourier Transform Infrared)
  - Chemical Compositions
  - Easy Technique for IQA;
- DSC (Differential Scanning Calorimetry)
  - Melting Points, Degree of Curing and Crystallization Behavior
  - Quick and Easy Technique for Production Control
- TGA (Thermo gravimetric Analysis)
  - Thermal stability
- Spectrophotometry
  - Transmission, Reflection, Haze, Yellow Index

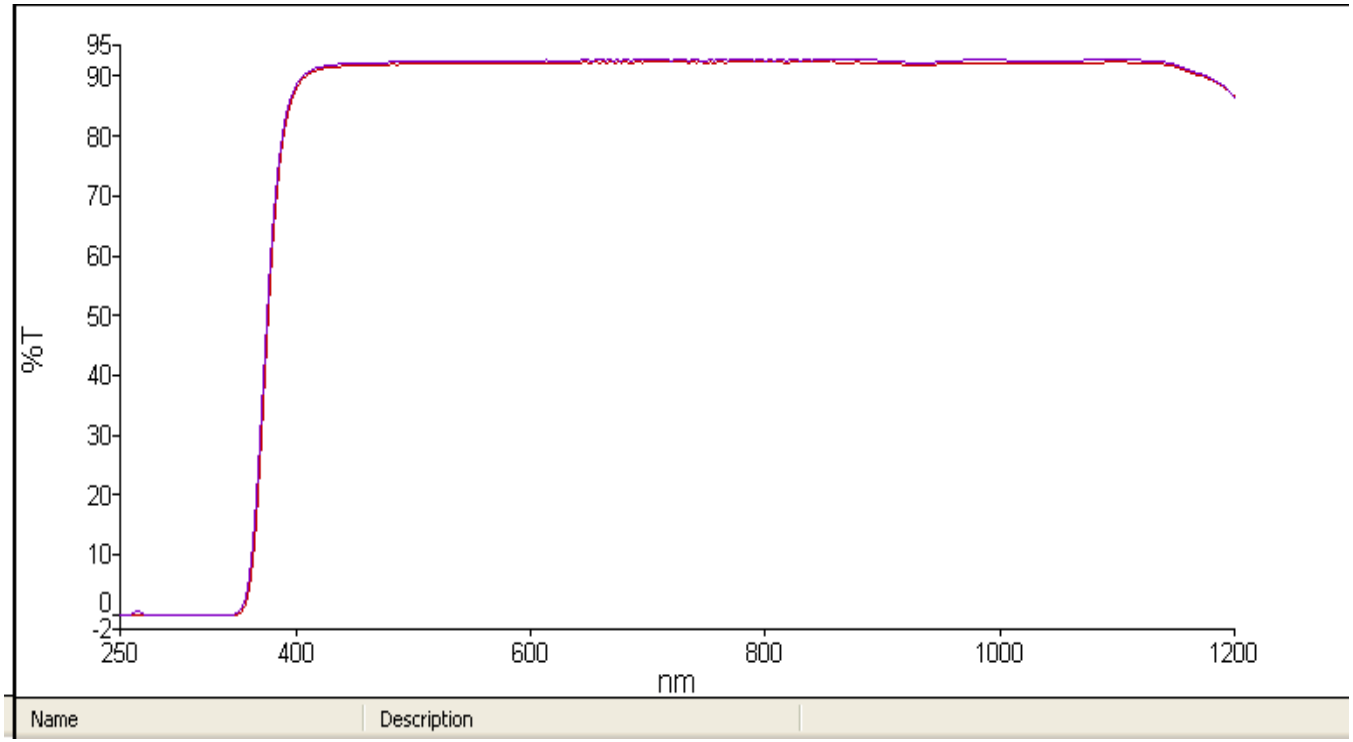
Aging Study of EVA/Backsheet

- UV Dosage: 0.72 W/m^2/nm at 340nm (37W/m^2) for 1030hrs at 60°C
- Damp Heat: (85%RH/85°C, 1030hrs)
- Thermal oven aging: 105°C 1176hrs/49days)
- Thermal stability by TGA (ramp rate: 10C/min)

EVA Durability/Aging Summary

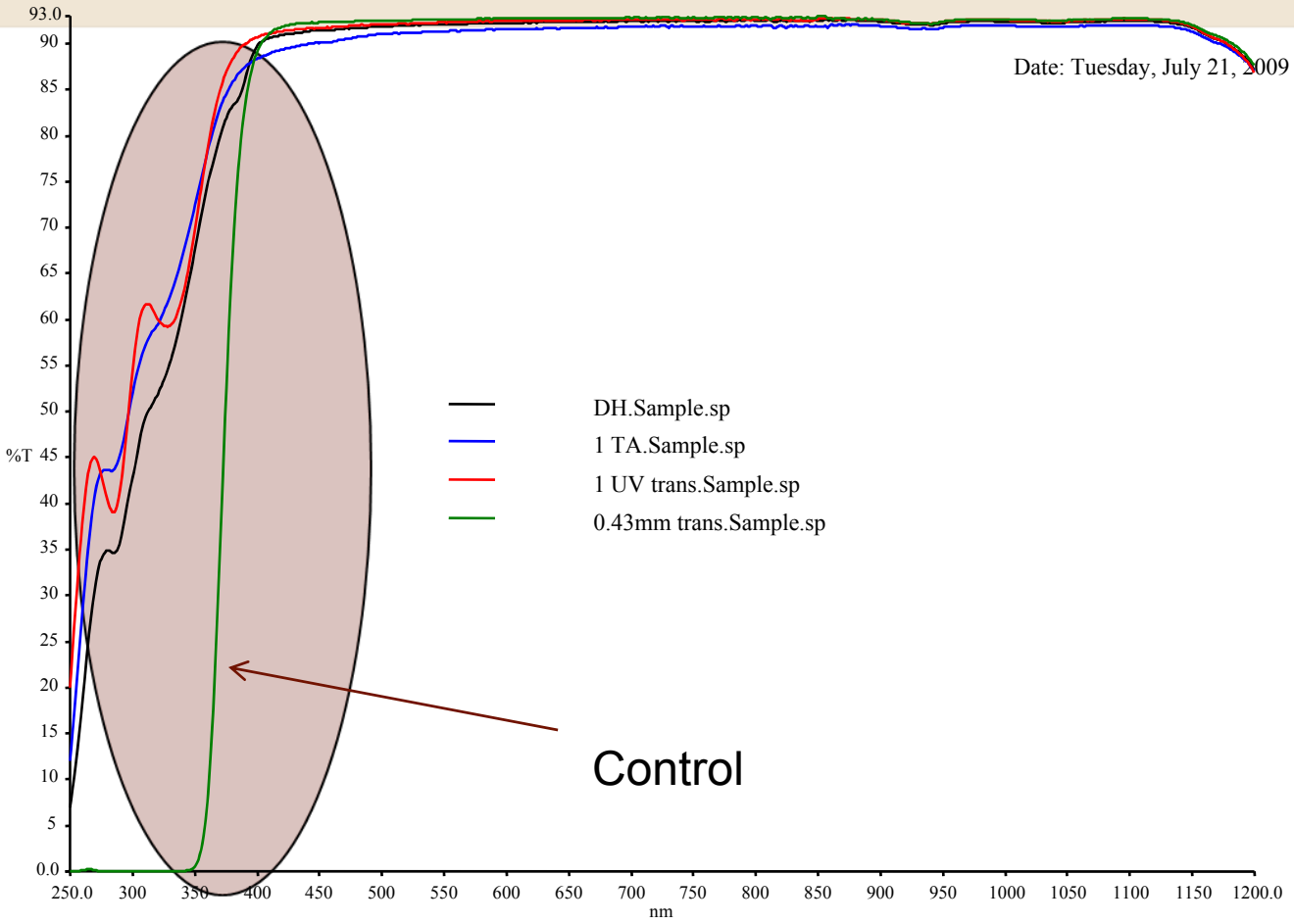
- Transmission/FTIR/Yellowness Index/Refractive index were characterized
- **Significant Changes**
  - **Transmission-wise, very obvious difference between vendors upon aging, especially in UV range**
  - **The degradation of EVA is detectable in FTIR and different vendor shows different level of degradation for the different aging**
- Minor Changes
  - YI (Yellowness Index) showed minimal change, indicating color change is small
  - Refractive index change is also minimal, guarantees good optical coupling without risk of increasing of reflection loss to PV cells

Transmission of as-built EVA



* Very similar transmission curve; 350nm UV cutoff

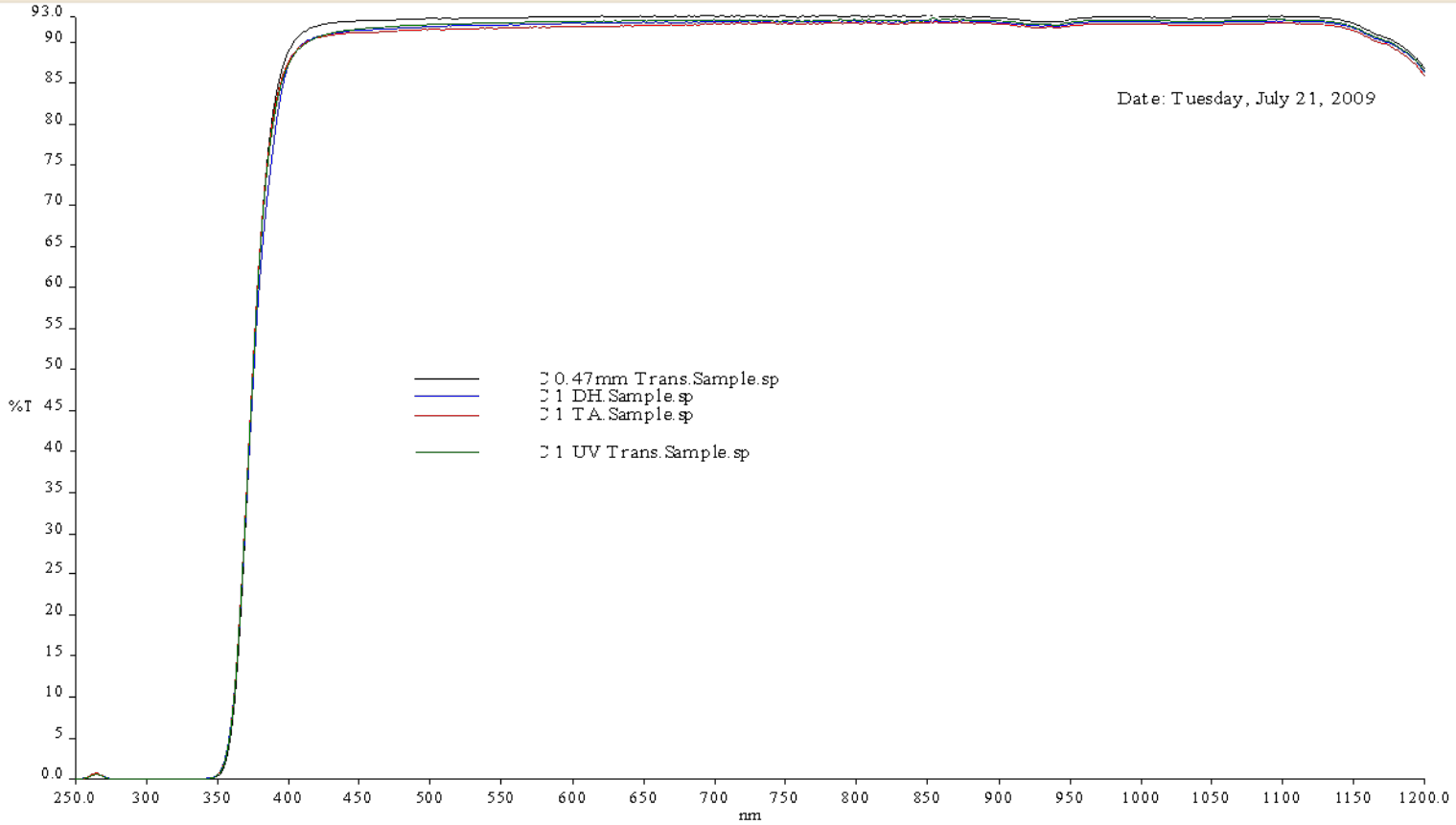
Transmission of Sample 1 Aged



- Very obvious transmission behavior change, especially in UV range. UV package loss

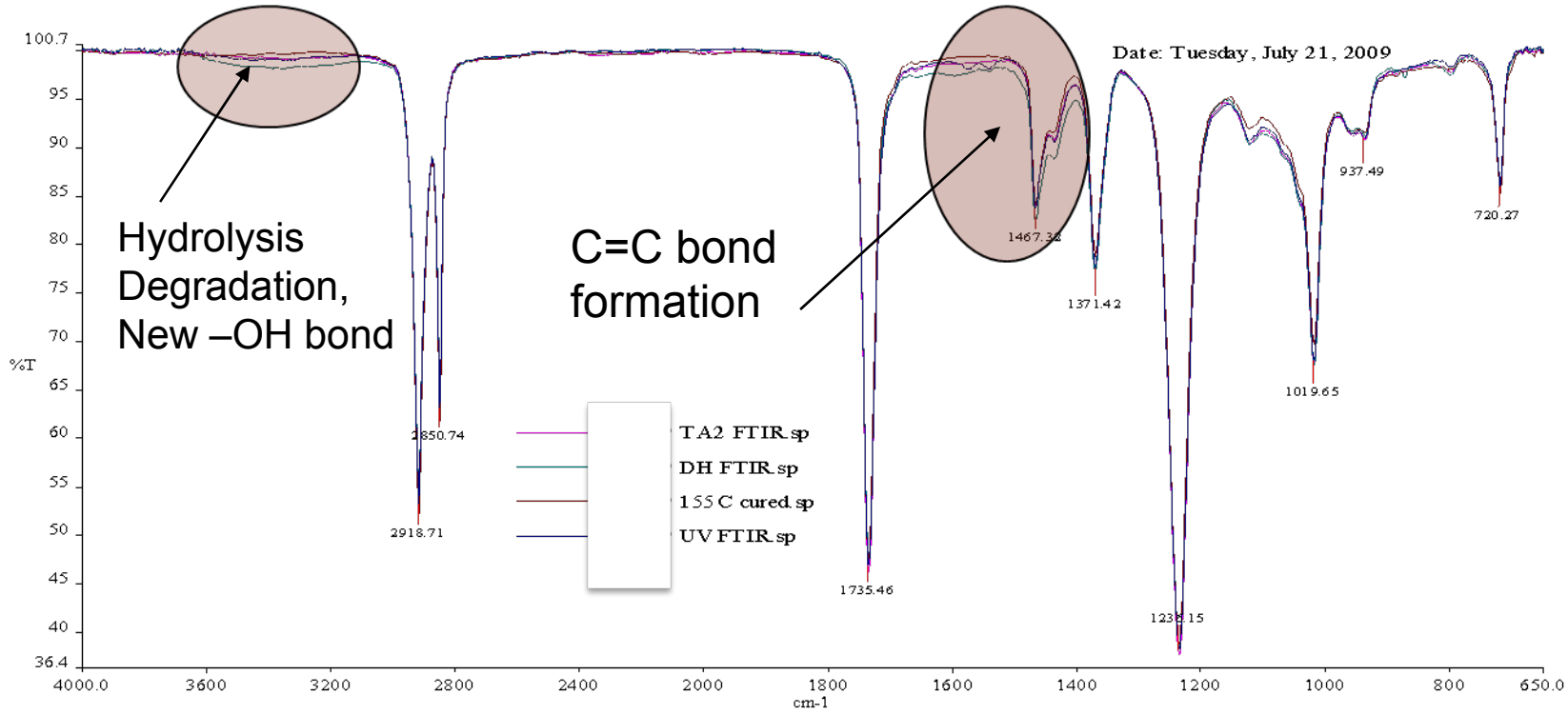
SOLARIA

Transmission of Sample 2 Aged



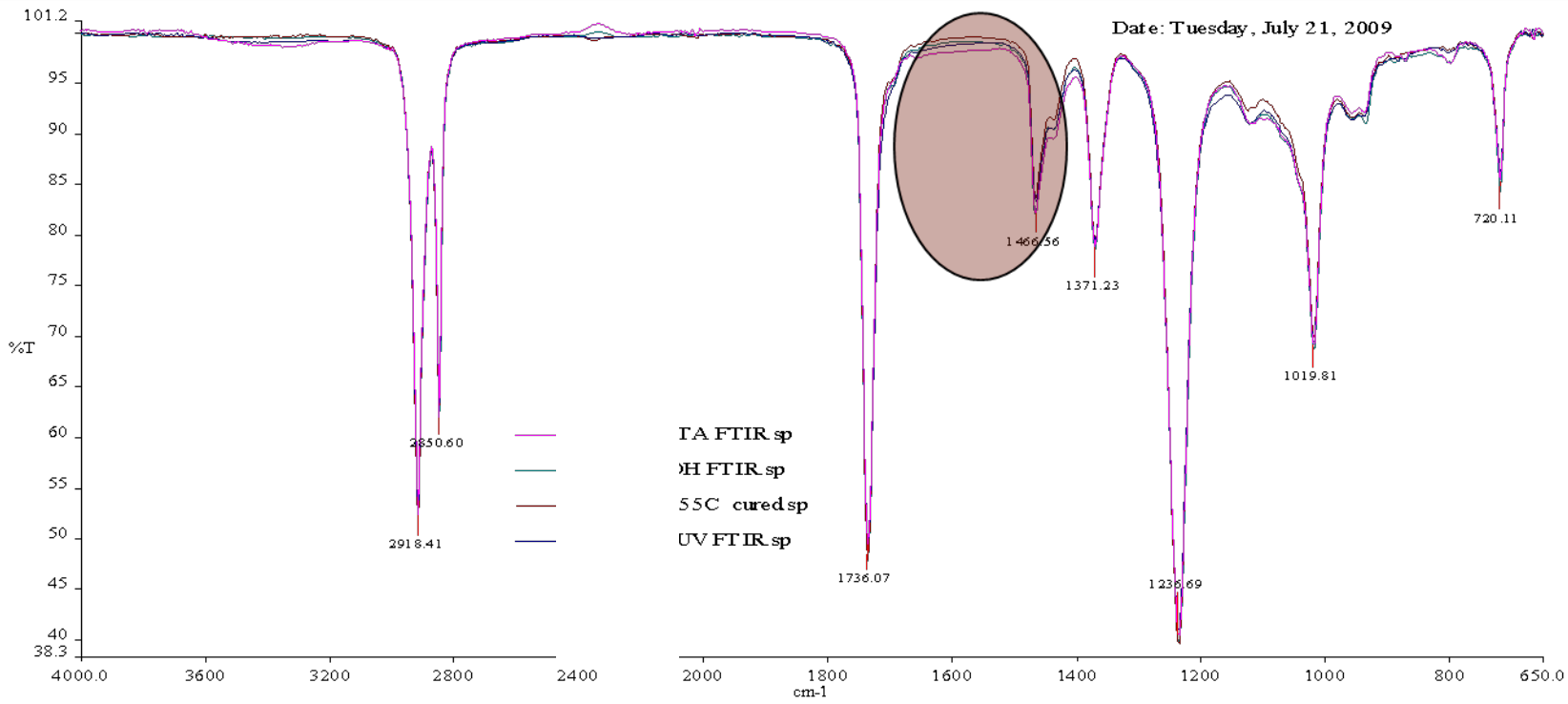
* Extremely stable compared to sample 1

FTIR of Sample 1 Aged



* Noticeable peak change observed due to aging: New –OH and C=C bond

FTIR of Sample 2 Aged



- Chemical composition change observed, but less compared to Sample 1, thus sample 2 is more stable than Sample 1

Yellowness Index of Aged Samples

- Yellowness index (YI): number calculated from spectrophotometric data that describes change in color of a sample from clear/white toward yellow
- The YI change of the aged samples are quite minimal, indicating the materials' resistance to color change is quite good.

	Fresh Cured	UV 1030hrs	DH 1030hrs	105C/1176hrs
Sample 2	0.88	1.29	1.46	1.01
Sample 1	0.81	1.14	1.21	1.41

Refractive Index (RI) of Aged Samples

- Negligible RI change
- This is important that the encapsulant EVA is in the optical path, minimal refractive index change is critical for power stability, especially with low concentration PV.

	Fresh Cured	UV 1030hrs	DH 1030hrs	105C/1176hrs
Sample 2	1.482	1.483	1.484	1.483
Sample 1	1.482	1.481	1.482	1.482

Key EVA Aging Summary

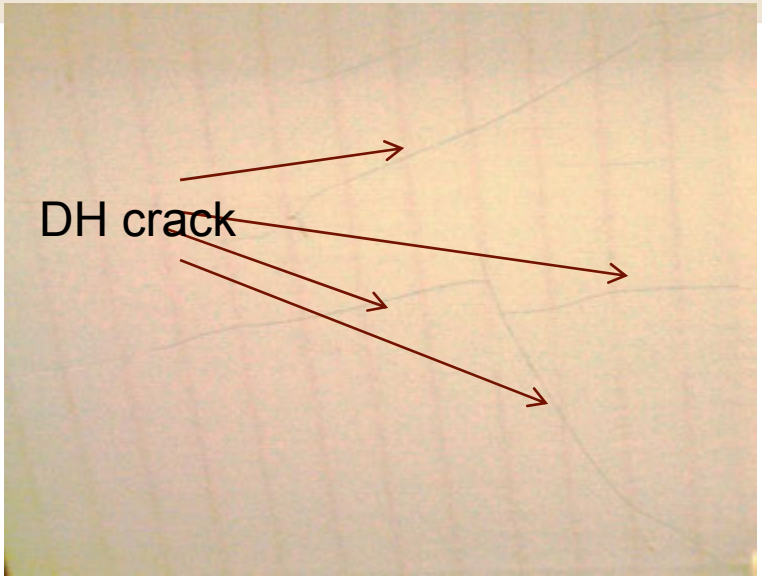
- Aging effect on transmission in visible range: thermal aging>DH>UV
- Resistance to aging: Sample 2 better than Sample 1
- Sample 1 needs to improve the UV stability package for the additives to last longer in the material

Backsheet Aging Summary

- Characterization
  - TGA
  - FTIR
  - Reflection

Common backsheet failure modes

- **Backsheet crack** due to hydrolysis. The middle PET layer provides mechanical strength and electrical insulation. However, PET is very prone to hydrolysis.
- **Delamination** due to poor inter-layer adhesion quality
- **Yellowing/crack of inner EVA** layer due to the poor UV package for the material.

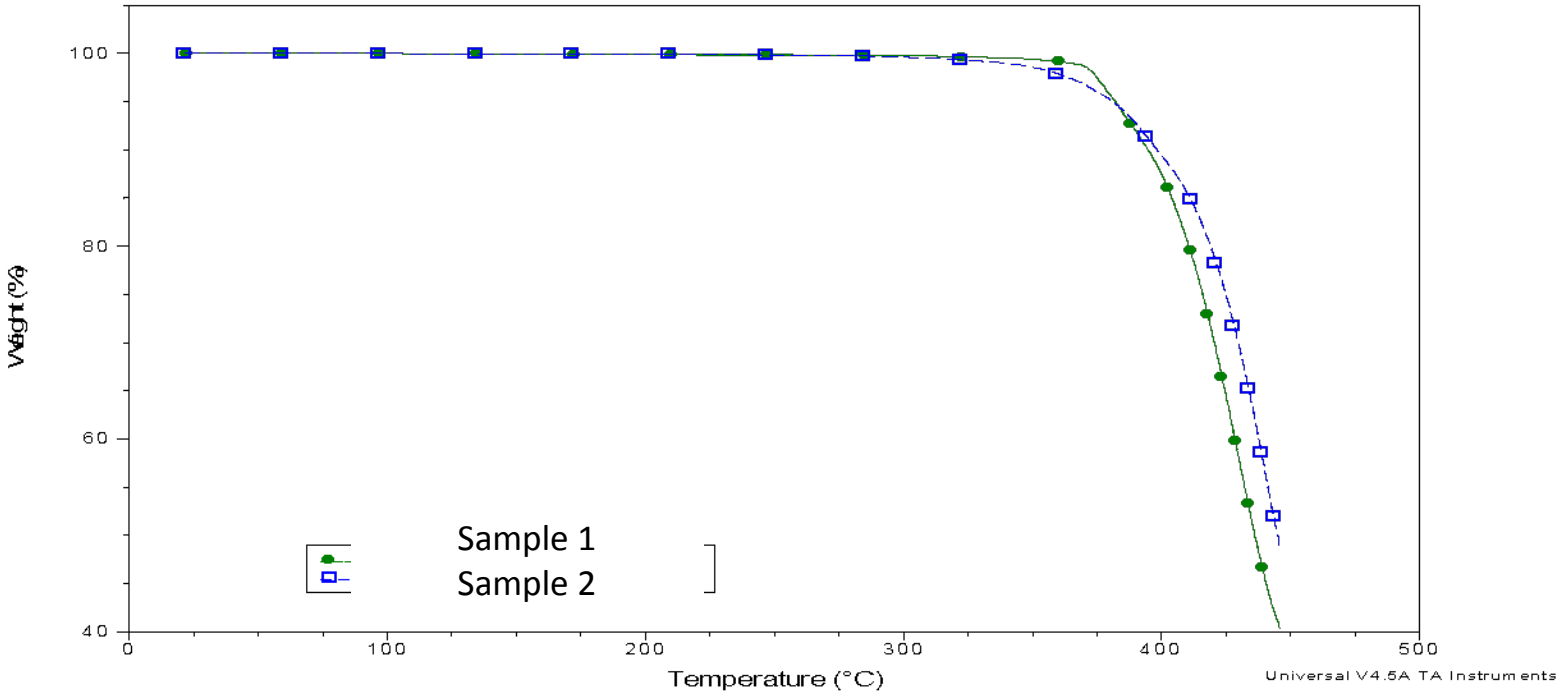




Thermal Stability

- Normal modules' operating temperature is about 50°C. It is important for the backsheet to be thermally stable at or above this temperature for 25 year service life
- TGA is a simple way to characterize the thermal stability of the backsheet

TGA Sample Curves:

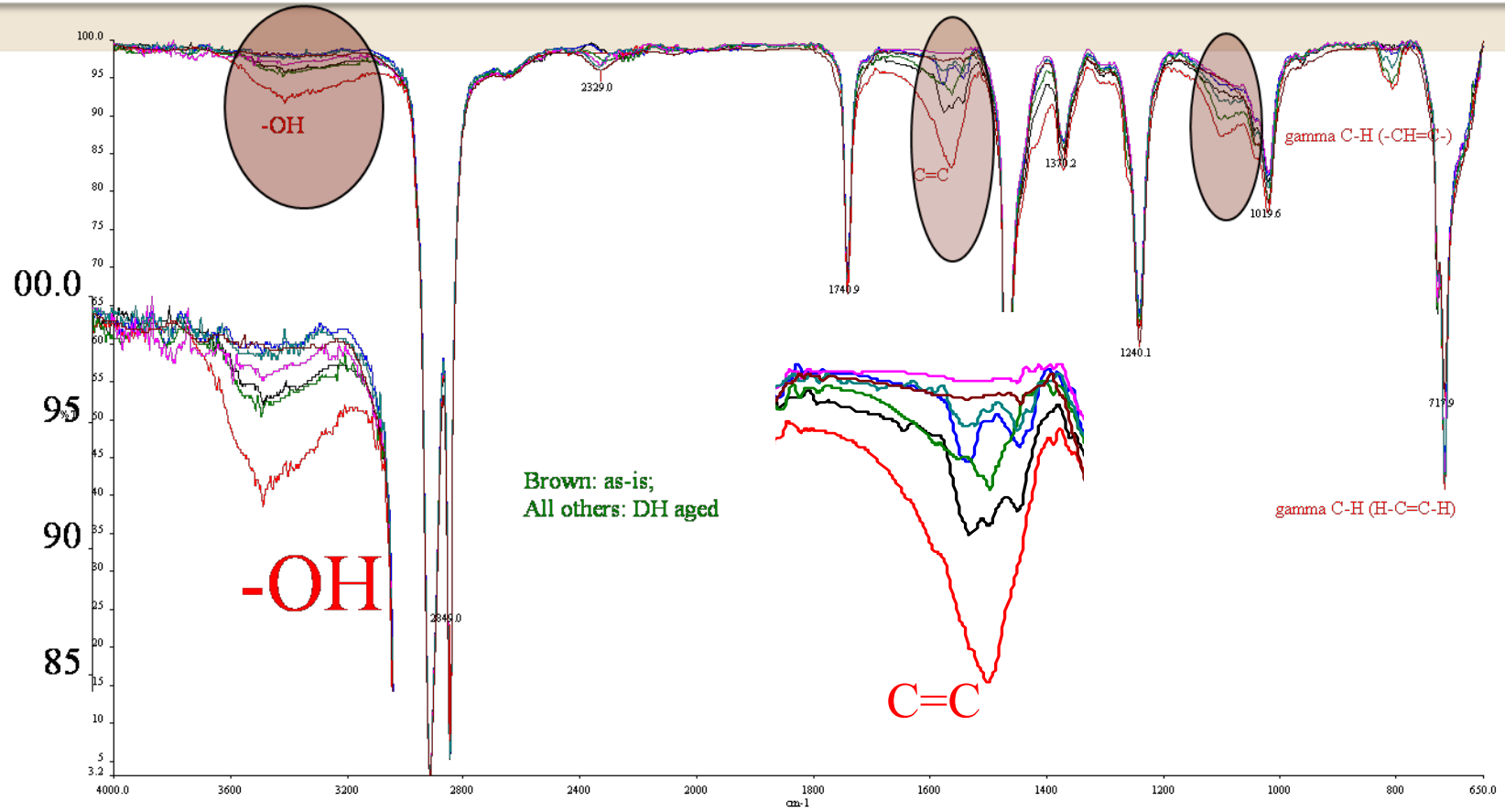


• Generally similar behavior, however, Sample 2 showed earlier degradation onset

Damp Heat aging

- A common polymeric backsheet structure is a 3-layer composite film: EVA(or alternative)/PET/Fluoro layer
- Fluoro layer's weatherability well characterized
- PET, however, can suffer **hydrolysis failure**

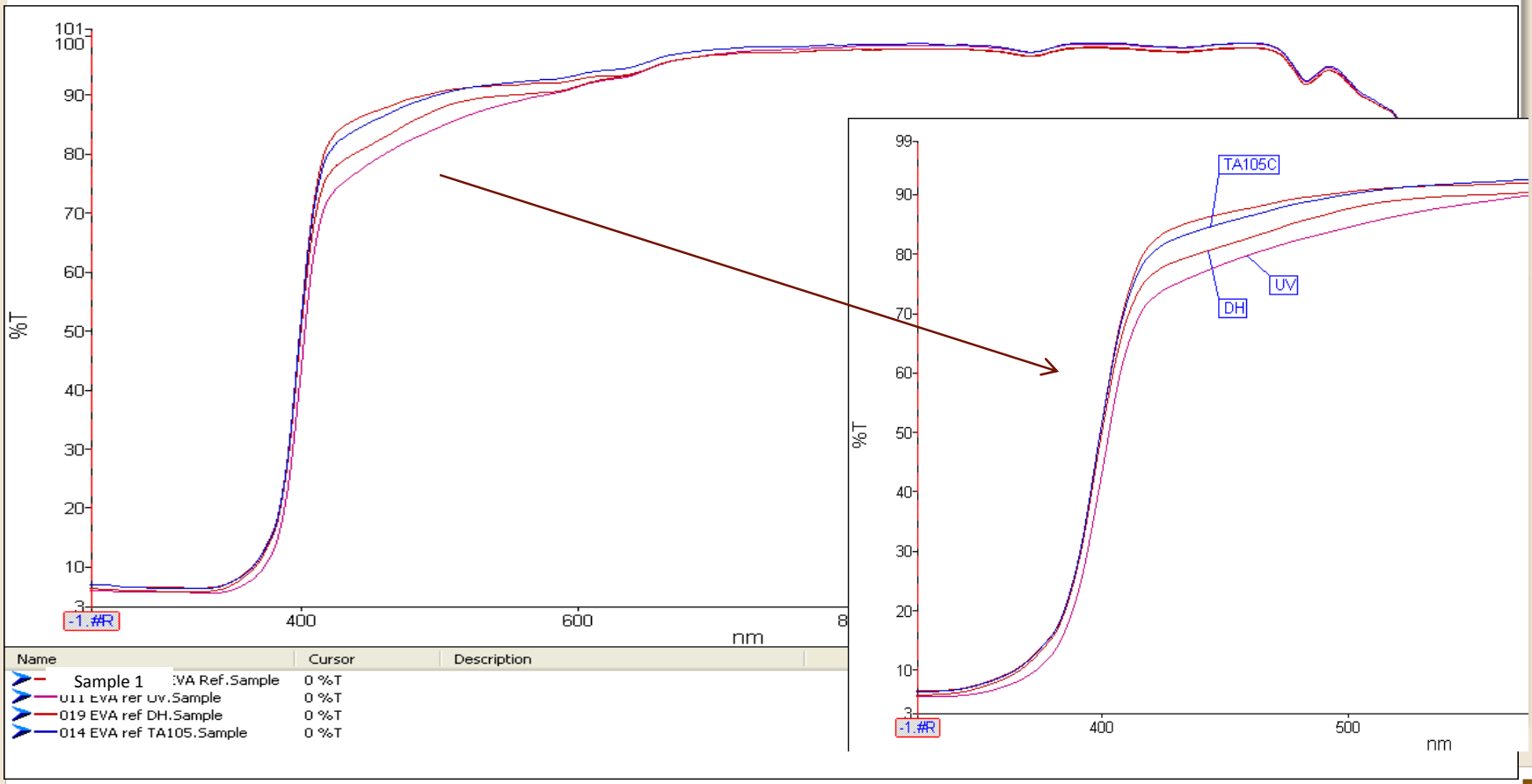
DH Aged Sample 1, EVA side



* Obvious hydrolysis: More –OH, C=C, C-H

Sample 1 Reflection: UV aging showed most loss

Higher reflection of inner side of backsheet helps to redirect more leaked Light back to PV cell service thus higher power gain



SOLARIA

Backsheet Aging Summary

- Damp Heat Resistance (Hydrolysis Resistance of the PET layer) is a major failure to many backsheets, visual backsheet crack were observed in DH chamber testing. Also the failure is obvious in FTIR characterization.
- The UV resistance of inner layer is also important. 2X IEC61215 precondition UV aging showed yellowing/browning/cracking of EVA layer. Much more effort is needed for UV stability

Conclusion

- EVA
  - Though in the past 30 years, EVA formulation has improved a lot, especially for UV stability. Still there is room to improve to keep the EVA as transparent as possible for the service life. Some suppliers' materials tend to turn hazy after aging.
- Backsheet
  - Different supplier's material varies a lot in regard to UV resistance, hydrolysis resistance, inter-layer adhesion strength and reflectivity. No perfect material is available in the market. A lot more effort is needed to develop quality material to meet the demand of the world's growing solar market.

Demonstration of the Benefits of Silicone Encapsulation of PV Modules in a Large Scale Outdoor Array

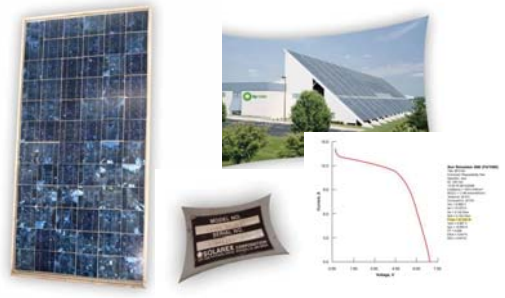
Barry Ketola[1], Chris Shirk P.E.[1], Philip Griffith[1], Gabriela Bunea.[2]

1 Dow Corning Corporation, Midland, Michigan USA

2 SunPower Corporation, San Jose, California, USA

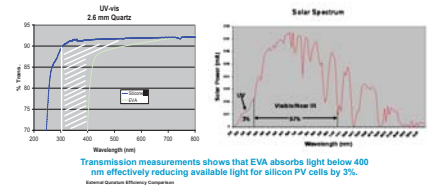
Abstract: Based on the historical performance of silicones in both the construction and electronic industries, silicones are known for their superior performance in outdoor applications. This performance makes silicone materials well suited for solar photovoltaic (PV) modules in their application as a semiconductor device made for outdoor use. Silicone applications within the module include encapsulants, potting materials, and junction box and frame sealants. Dow Corning has developed a number of silicone-based products for use in PV module construction including the Dow Corning® PV-6100 Cell Encapsulant Series product line launched in 2009. To demonstrate the product line performance in real-world conditions, 15 kilowatts of mono-crystalline matrices were purchased from SunPower Corporation, San Jose, California, USA under the United States Department of Energy Solar America Initiative Program. The matrices were encapsulated on the Pilot Line in Dow Corning's USA Solar Application Center in Freeland, MI USA. The silicone-encapsulated modules were installed as part of a 30 kW PV array at the Dow Corning corporate headquarters in Auburn, Michigan in 2009. The balance of the array was constructed using 15 kW of EVA modules purchased from SunPower Corporation, using identical cell and glass technology to compare efficiency and durability.

Proven Durability Using Silicone Encapsulants

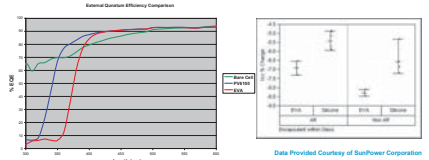


Silicone encapsulated crystalline silicon PV modules have been in service in large scale arrays for over 25 years.

Measurements for Efficiency Gains



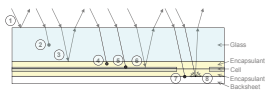
Transmission measurements shows that EVA absorbs light below 400 nm effectively reducing available light for silicon PV cells by 3%.



External Quantum Efficiency measurements indicate silicones superior performance at wavelengths below 400 nm.

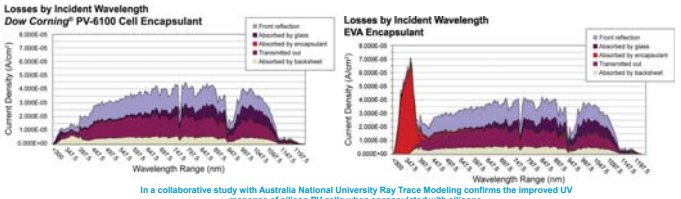
Comparative flash test measurements at STC of encapsulated SunPower Cells shows superior silicone improved Isc response

Modeling Efficiency Gains
Australia National University Ray Trace Modeling



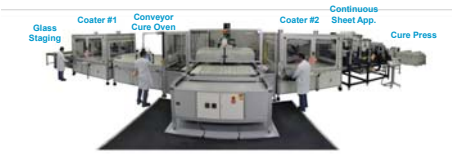
Optical loss mechanisms in a PV module

Loss mechanism	Main dependence
1. Reflection from glass	n_{glass}
2. Absorption in glass	α_{glass} & t_{glass}
3. Refl at glass-encapsulant & escape	n_{glass} & n_{encaps}
4. Absorption in encapsulant	α_{encaps} & t_{encaps}
5. Absorption in ARC	n_{encaps}; n_{ARC}, k_{ARC} & t_{ARC};
6. Reflection from ARC and escape	$n_{silicon}$ & $k_{silicon}$; morphology
7. Absorption in backsheet	$R_{backsheet}$ (when encapsulated)
8. Reflection from backsheet and escape	$R_{backsheet}$ & t_{encaps}



In a collaborative study with Australia National University Ray Trace Modeling confirms the improved UV response of silicon PV cells when encapsulated with silicone.
Originally Presented at 24th © 2009 IEEE PVSEC - AN OPTICAL COMPARISON OF SILICONE AND EVA ENCAPSULANTS FOR CONVENTIONALSILICON PV MODULES: A RAY-TRACING STUDY
Keith R. McIntosh, James N. Cotsell, Ann W. Norris, Nick E. Powell, and Barry M. Ketola

Module Production, Installation and Observations



Automated Cell Press

To demonstrate the *Dow Corning*® PV 6100 Cell Encapsulant Series improved manufacturing throughput at an industrial scale, a pilot line was designed and installed in Freeland, Michigan USA.



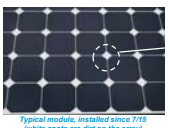
Silicone array being installed



Fronius Invertors (4)

Array erected in two halves in same location, 45° angle, no shading, East (EVA): Inv #1: 4x9 modules; Inv #2: 4x8 modules, West (Si): Inv #3: 4x8 modules; Inv #4: 4x9 modules, Four Fronius 7.5 kW Inverters
Data acquisition using Fronius software.





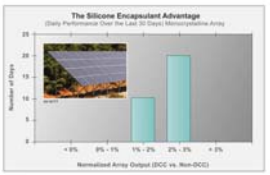
Typical module, installed since 7/15 (white spots are dirt on the array)



Close-up of "diamond" showing no delamination or bubbles

- Modules have experienced temperatures of ~ 95ºF to -10ºF, sun, rain and snow
- Appearance of all Silicone modules is "excellent"
- No evidence of delamination or yellowing for either Silicone or EVA

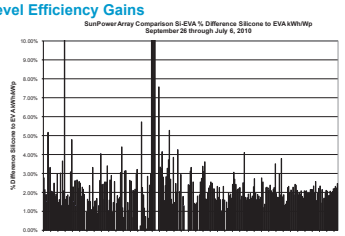
Array Level Efficiency Gains



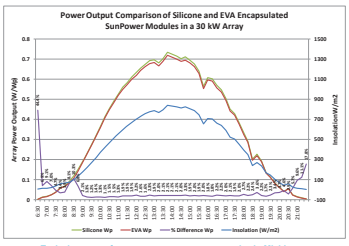
	Dow Corning	Non-Dow Corning	System
Watts produced at 2:45 PM	7,312W	7,130W	14,442W
Yesterday's KWh Produced	63.8 kWh	63.1 kWh	126.9 kWh
Total KWh Produced			29,533 kWh
Normalized KWh/Wp	0.1629	0.1596	
Total Advantage	2.08%		

Monocrystalline Array at Dow Corning Corporation, Midland, Michigan

Summary of Efficiency Gains over a 30 day period.



Consistent Efficiency Gains Demonstrated over all seasons.



Typical array performance on a sunny summer day in Michigan.

SunPower Corporation makes no warranties, express, implied or otherwise, regarding the sufficiency, accuracy or completeness for any data it has provided herein.

Conclusions: A 30 kW array to compare the performance of EVA to Silicone encapsulated modules was constructed at Dow Corning Corporation at the Corporate Center in Auburn Michigan USA using EVA modules and matrices purchased from SunPower Corporation under the United States Department of Energy Solar America Initiative program under Award Number DE-FC36-07GO17043. The silicone modules were encapsulated using Dow Corning® PV-6100 Cell Encapsulant Series at Dow Corning's pilot line in Freeland, Michigan, USA. The array was installed in July of 2009. Data collection on the array has been underway from September 2009. The data collection has shown silicone encapsulated modules outperform EVA encapsulated modules at greater than 2% kW/kW_p relative efficiency gain. The modules have been exposed to all seasons experiencing temperatures from approximately 95ºF to -10ºF, and sun, rain and snow. Regular inspections have shown that the appearance of the Silicone and EVA modules continues to be very good. The array continues to be monitored for performance and appearance.

DOW CORNING

Solar Solutions

Unleash the power OF SILICON

www.dowcorning.com/solar

"The information provided in this presentation does not constitute a contractual commitment by Dow Corning. While Dow Corning does its best to assure that information contained in this presentation is accurate and fully up-to-date, Dow Corning does not guarantee or warranty the accuracy or completeness of information provided in this presentation. Dow Corning reserves the right to make improvements, corrections and/or changes to this presentation in the future."

Evaluation and Analysis of 15 years exposure PV module

We conducted various analyses on 15 years exposure modules and investigated the relationship between the exposure year and Damp heat test from material evaluation by molecular weight analysis of the backsheet.

Yoshihito Eguchi
SOLAR SYSTEMS GROUP
ENGINEERING DEPARTMENT
Feburary 16th and 17th, 2011

Acknowledgements
This work was supported by the New Energy and Industrial Technology Development Organization in Japan.

Visual Inspection

Crystalline silicon type modules in the order of mass, are composed of glass, aluminum frame, EVA resin, solar cell, terminal box, back film, tapping screws, etc. Among these, those which are continuously exposed to external atmosphere are glass, aluminum frame, tapping screws, terminal box, and back film. The below table shows the results of visual observation of modules made by three companies with a focus on these items. The modules made by the three companies had in common that EVA had turned yellow somewhat. It seems that the companies used the same EVA at that time and therefore the same slightly yellowing resulted. In respect to other parts, materials involving the designing concept of the respective companies were used and the conditions are as shown in the below table.

Model No.	A	B	C
Cell type	Mono-crystalline	Multi-crystalline	Mono-crystalline
Front Appearance	Good	Good	Not Good
Back Appearance	Good	Good	Not Good
Al Appearance	Good	Good	Good
Screw Appearance	Good	Good	Good

This document does not contain any proprietary or confidential information

Material evaluation by molecular weight analysis of the backsheet

- In conducting analysis of the back film, measuring of back film material and molecular weight were made by Gel Permeation Chromatography (GPC). In regard to the product of A type module, the correlation of material deterioration was examined by comparing with the test piece on which JIS reliability test had been conducted.
- The analyzed back film of modules may be roughly divided into two types, one structured with PET type materials as the base material and the other with PVF type materials as the base material. module type A used PET type while module type B and C used PVF type. All three types of modules used a three layer structure of film/ aluminum foil/film. In regard to PET of module type A, the data are all shown in known PET reference standard values of absolute molecular weight and therefore the figures approximate absolute figures. On the other hand, PVF is shown in relative values of polyethylene glycol reference standard and therefore the disparity with absolute values is seen. By comparison with initial stage samples, it was found that the “high temperature, high humidity sample” had shifted more to the low molecular weight side than the “long-term exposure sample.” Therefore it may be judged that JIS high temperature, high humidity conditions are more severe to PET for back film material than long-term exposure conditions.

	Material	Number Average Molecular Weight [Mn]	Weight Average Molecular Weight [Mw]
Module Type B (15 years)	PVF	5860	232,000
Module Type C (15 years)	PVF	6130	214,000
Module Type A (15 years)	PET	6910	25,300
Initial	PET	7350	28,500
After Thermal cycling test	PET	7510	28,800
After Humidity Freeze test	PET	7670	28,900
After Dam Heat test	PET	4500	16,100
After Dry heat test	PET	6910	25,300

This document does not contain any proprietary or confidential information

Material evaluation of Ethylene Vinyl Acetate

Composition analysis, analysis of additives and measuring of gel fraction of EVA resin sealing the solar cell were conducted and the condition of the EVA after 15 years of exposure was examined. As shown in the below table, the VA value for EVA sheets of the respective companies was 31～32%. From the results of analysis of additives, it was found that although fair amount of light stabilizer and ultra violet ray absorbent were consumed, such still remained in the EVA. Since the amount decreased from initial values, it is thought that the above mentioned two types of light stabilizers functioned as prevention sufficiently. Also, the gel fraction which was around 80 - 85% prior to use of the solar battery had increased. It is believed that this increase was caused by progressing of EVA cross-linking reaction by factors such as temperature increase by long-term exposure

	VA [%]	Crosslinking Agent	Light Stabikizer	UV Ray Absorbent	Gel Fraction [%]
Before Crosslinking	-	100	100	100	-
After Crosslinking	-	40	Over 90	Over 90	80-85
15 years Type A	32	0	37	27	91
15 years Type B	31	0	21	6	93
15 years Type C	32	0	29	37	93

This document does not contain any proprietary or confidential information

Evaluation of electrical characteristics

The below table shows the electrical performance evaluation of the modules made by the three companies and introduced on the market for 15 years. Comparing the maximum output shown in the Table with the values given on the nameplate, it was found that 90% or more output was maintained. Also, withstand voltage test and measuring of insulation resistance values as specified by JIS were conducted, and no problem was seen on the modules made by the respective companies.

Model No.	A	B	C
Voc [V]	27.8	25.58	17.85
Isc [A]	2.6	2.89	3.19
Pmax [W]	54.64	54.22	40.31
F.F.	0.756	0.732	0.708
Power ratio compared with Type label	0.923	0.972	0.96
Dielectric Voltage Withstand test (2200V, 1min)	OK	OK	OK
Insulation-Resistance test (Applied voltage:1000V)	1200MΩ	1000MΩ	850MΩ

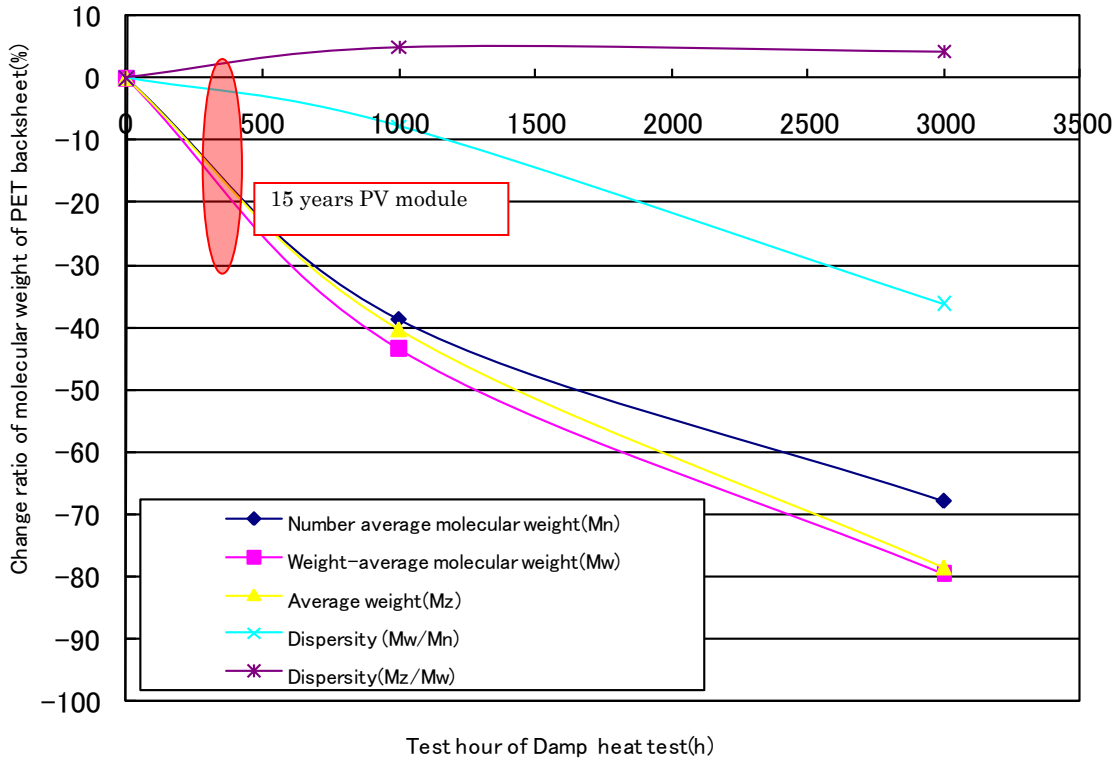
This document does not contain any proprietary or confidential information

Comparison between exposure year and Damp heat test

From the result of comparison the change ratio of molecular weight of PET backsheet, the condition of outdoor exposure at Rokko is almost same as 300 hours of Damp heat test. Therefore, we assume that the test condition of Damp heat 1000 hour is equivalent for 45 years at Rokko.

		Change ratio (%)				
		Number average molecular weight(Mn)	Weight-average molecular weight(Mw)	Average weight(Mz)	Dispersity (Mw/Mn)	Dispersity (Mz/Mw)
Damp heat test	Initial	0	0	0	0	0
	After 1000h	−38.78	−43.51	−40.43	−7.73	5.00
	After 3000h	−67.96	−79.64	−78.75	−36.29	4.26
15 years exposure	Initial	0.00	0.00	0.00	0.00	0.00
	After 15 years	−5.99	−11.23	−9.57	−5.67	1.67

Figure 1 Change ratio of Molecular weight of PET backsheet after Damp heat test



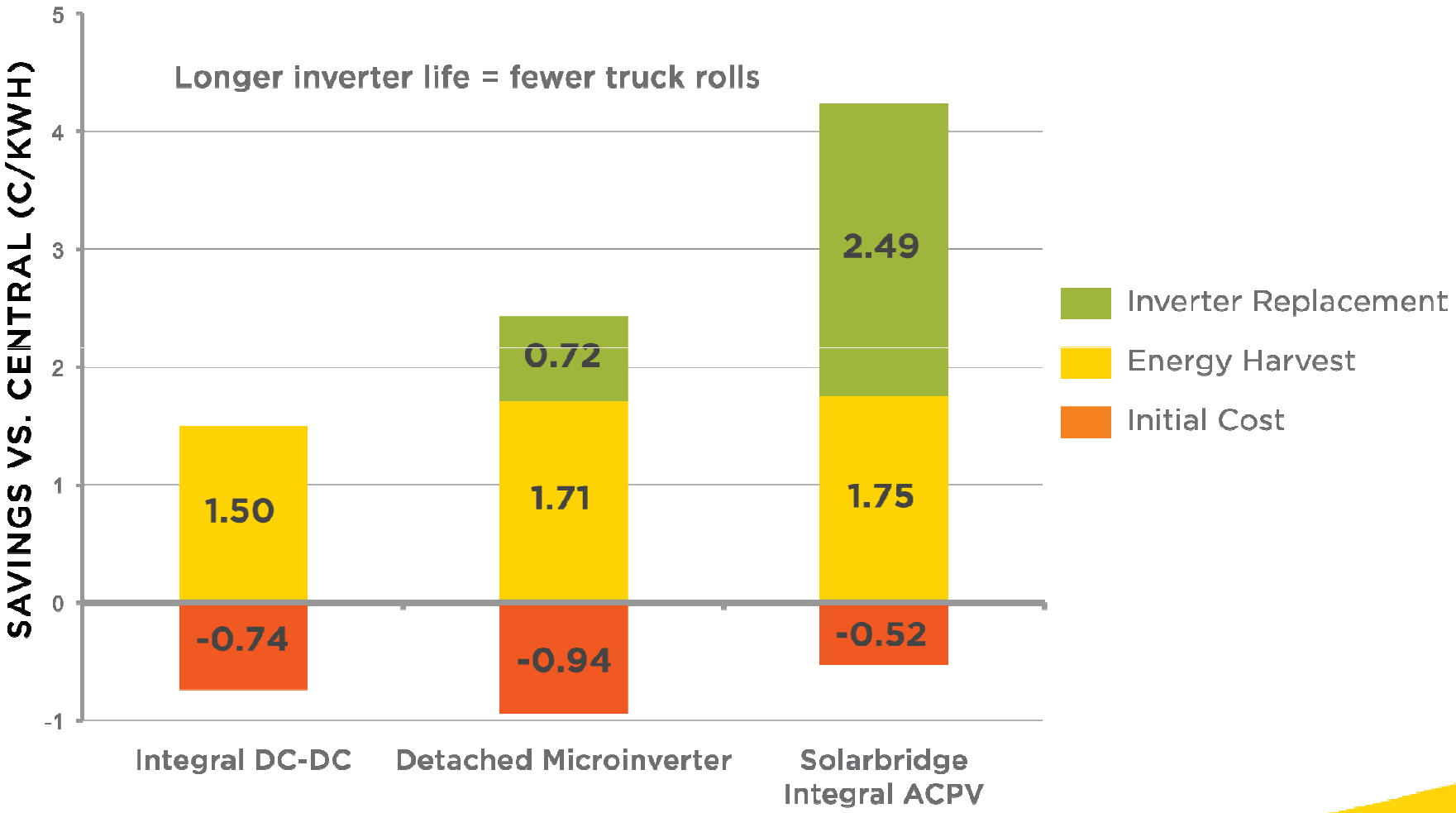
This document does not contain any proprietary or confidential information

PV-INTEGRATED MICROINVERTERS IN HIGH-RELIABILITY ROOFTOP APPLICATIONS

T. Paul Parker, Director of Product Qualification and Reliability

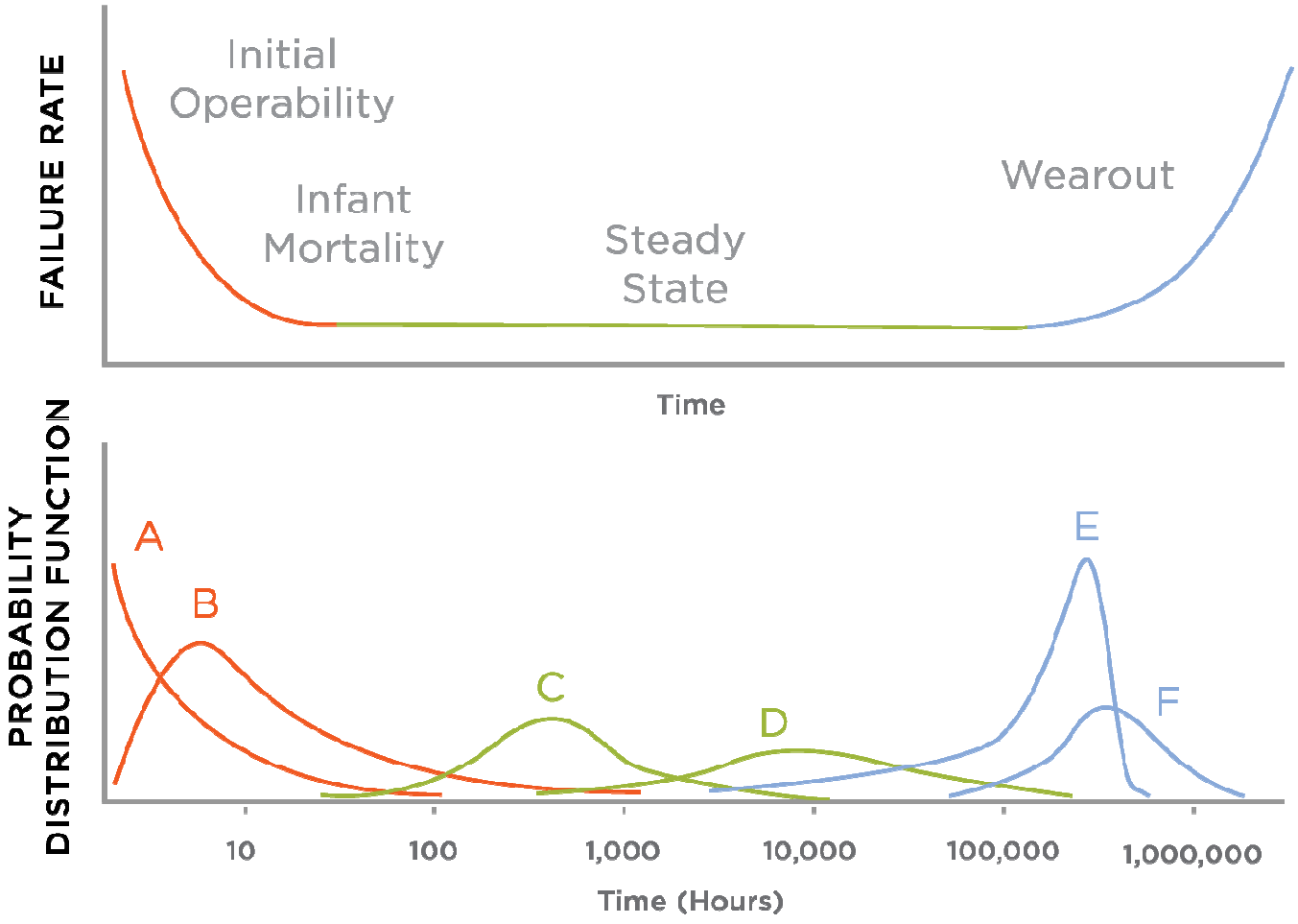
SOLARBRIDGE TECHNOLOGIES

INTEGRAL ACPV: HIGHER RELIABILITY, LOWER LCOE



SOLARBRIDGE TECHNOLOGIES

THE TRADITIONAL BATHTUB CURVE



Infant Mortality:
A. Weak Solder Joints
B. Cracked Ceramic Capacitor

Steady State:
C. FET Single Event Burnout
D. Corrosion

Wearout:
E. Electrolytic Capacitor Degradation
F. Non Compliant Solder Joints (BGA,etc.)

SOLARBRIDGE TECHNOLOGIES

DEFINING RELIABILITY: MTBF HAS NOTHING TO DO WITH LIFETIME

- MTBF only applies to useful life/steady state
- MTBF does not predict product wearout
- MTBF does not account for harsh use environments
- MTBF does not consider manufacturing variation

MTBF ≠ Lifetime

SOLARBRIDGE TECHNOLOGIES

ACHIEVING 25-YEAR RELIABILITY

- Design For Reliability
- Test For Reliability
- Manufacture For Reliability

DESIGN FOR RELIABILITY: ELIMINATE TOP 5 RELIABILITY RISKS

Do not use:

- Electrolytic Capacitors (E-Caps)
- Optical-isolators
- Tantalum Capacitors

Minimize stresses on:

- Printed Circuit Board Vias
- Solder Joints

E-CAPS FAIL TO MEET PV RELIABILITY STANDARDS

CAPACITOR OPERATING LIFE

		T operating (Cap Core)	
Capacitor Description	**End of Life Failure Criteria**	**60**	**70**
5,000 Hour, 105C Rated e-caps	20% drop in Cap or 2x ESR	**8 Years**	**4**
10,000 Hour, 105C Rated e-caps	20% drop in Cap or 2x ESR	**16**	**8**
Film Capacitor (Industry Model)	20% drop in Cap	**1540**	**770**
VOLTAGE DERATING = 80% in all cases			

STEADY STATE FAILURE RATE (FIT)

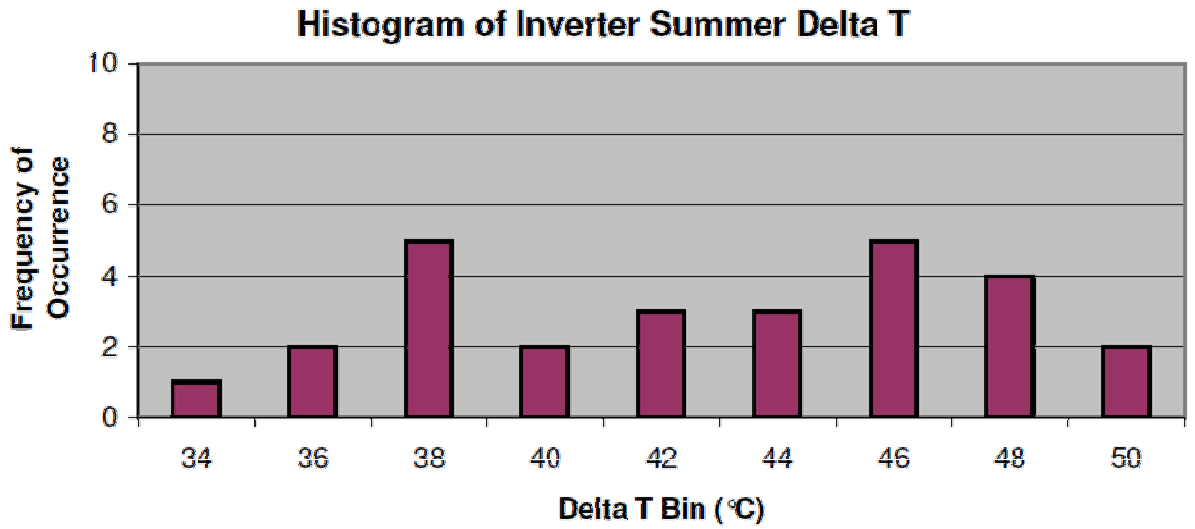
Capacitor Description	Bellcore	CNET	HRD4	M217	Siemens
Aluminum Electrolytic Capacitor	**210**	**22**	**120**	**16**	**120**
Film Capacitor	**17**	**4**	**6**	**1**	**14**
FIt Ratio E-Cap / Film	**12.4**	**5.5**	**20.0**	**16.0**	**8.6**

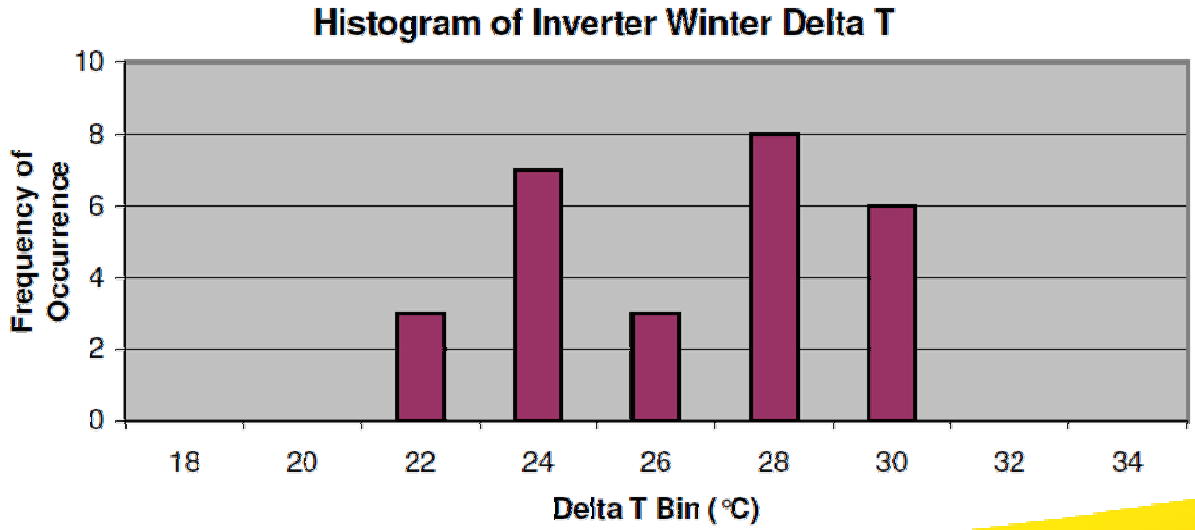
Bellcore: Similar to Telcordia SR-332
CNET: National Center for Telecommunications Studies
HRD4: Handbook of Reliablity Data – Issue 4
M217: MIL HDK-217
Siemens: SN29500

Ref: Jones, et.al., “A comparison of Electronic Reliability Prediction Methods”, IEEE Trans. On Reliability, June 1999, p. 127-143.

SOLARBRIDGE TECHNOLOGIES

SUMMER/WINTER DESERT TEMPERATURE DATA

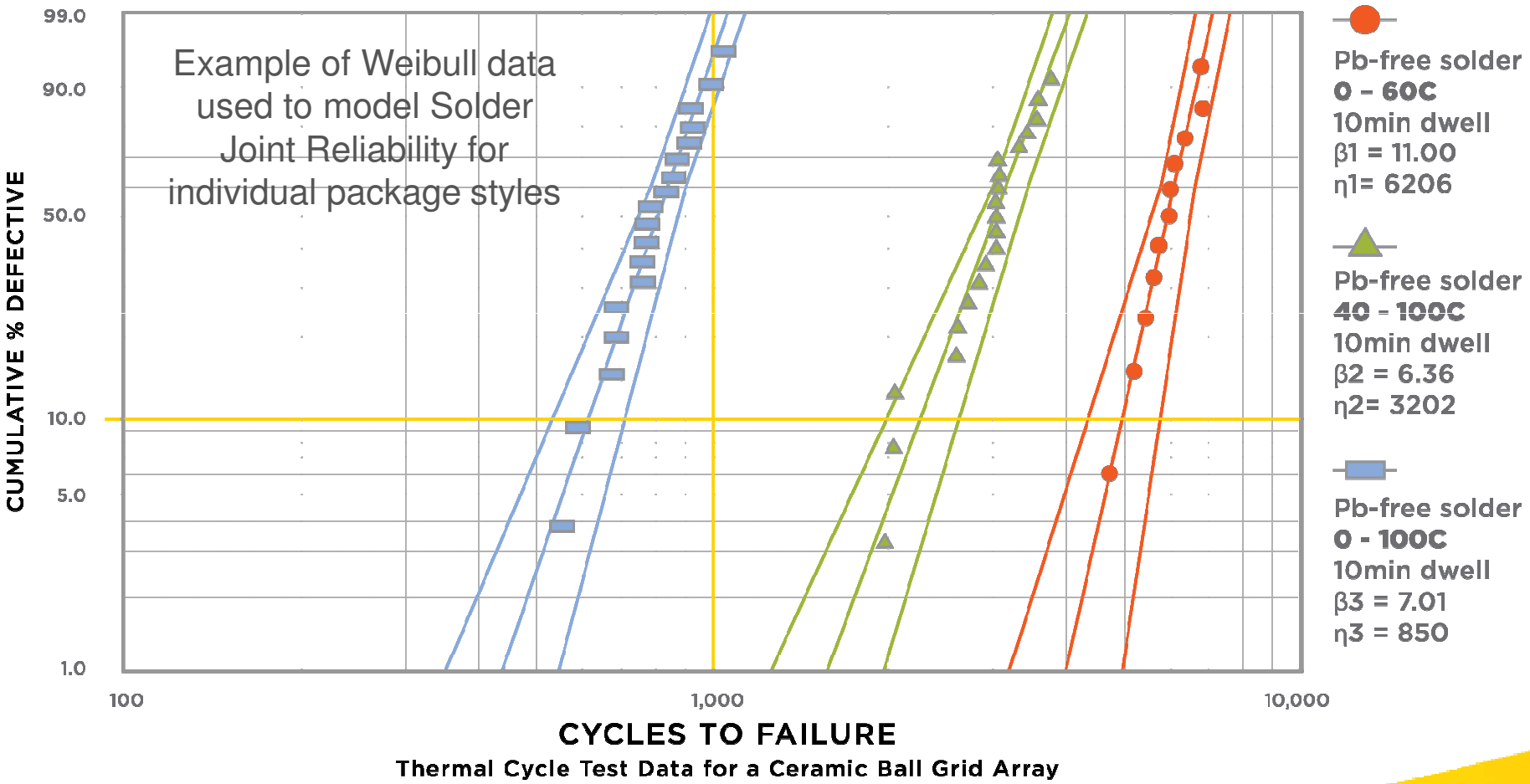




Component Daily ΔT statistics are applied to fatigue models to predict time to wearout

SOLARBRIDGE TECHNOLOGIES

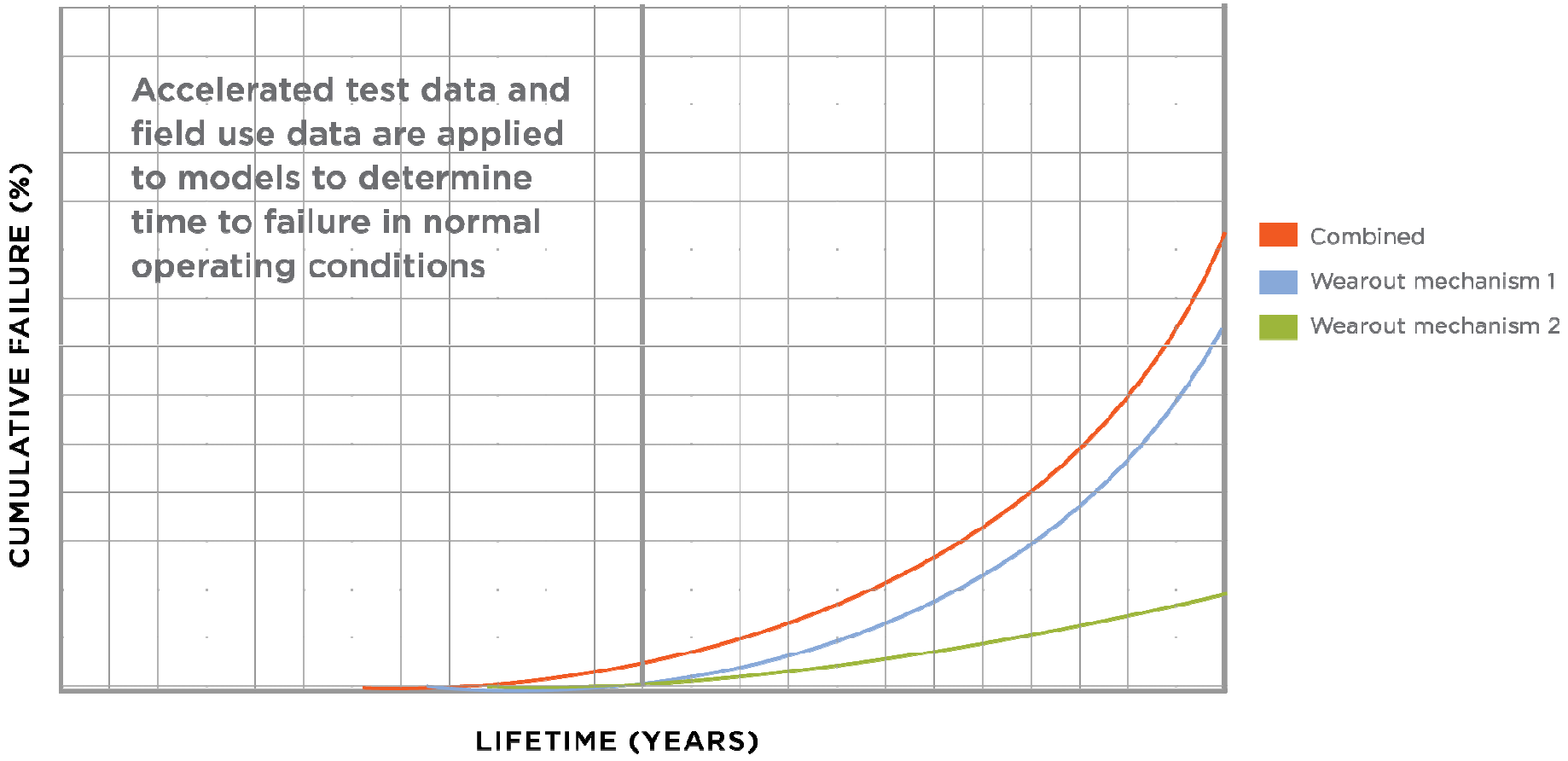
ACCELERATED TESTING: SOLDER JOINT RELIABILITY ACCELERATED WEIBULL ANALYSIS



Pan, et.al.," An Acceleration Model for Sn-Ag-Cu Solder Joint Reliability Under Various Thermal Cycle Conditions.", 2005 SMTAI, pp. 876-883.

SOLARBRIDGE TECHNOLOGIES

PREDICTING TIME TO WEAROUT



Damp Heat Testing Longer than IEC Standards

EDF R&D : Mike Van Iseghem, Antoine Plotton, Didier Binesti - Moret-sur-Loing (France)
EDF Energies Nouvelles : Khalid Radouane, Pierre-Guy Therond - Paris La Défense (France)

INTRODUCTION

Indoor and outdoor measurements have been initiated for degradation monitoring and analysis: a new test laboratory has been equipped with climatic chambers and a PASAN 3 x 3 m flasher of **AAA quality**.



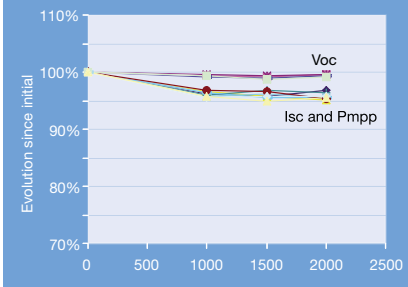
TEST CONDITIONS

Recently, 2000h of "IEC-like" Damp Heat at 85°C 85% RH has been completed on 3 types (A, B and C) of crystalline Silicon modules, **3 modules of each type have been aged, while one module is kept for reference.**

- Type A is mono-crystalline Silicon based. It has no aluminium frame. This is meant for fully integrated BIPV; indeed maximum French feed-in-tariff is obtained when the top surfaces of tiles/shingles and modules are coinciding (max 2 to 6 cm, for more information see ***www.ceiab-pv.fr***) so the PV system on the roof needs to be very thin.
- Type B and C modules are regular commercially available poly-crystalline Silicon modules, with frame.

RESULTS

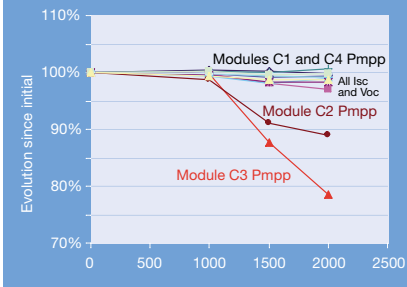
Type A mono-c Si modules, **without aluminium frame**



Type B poly-c Si modules



Type C poly-c Si modules



In both A and B type modules :
- the reference module and the aged modules have evolved in the same way :
- therefore there is no influence of 2000 h of DH8585 on the measured electrical properties.

Module C3 lost 23% on Pmpp.
Module C2 lost 12% on Pmpp.
Modules C1 and "non-aged" C4 stable.

CONCLUSIONS

After 2000 h of IEC like DH 85 85:

- A and B type modules are not degraded significantly (reference and aged modules have evolved in the same way).
- C type modules degrade
  - After 1500 h, 2 out of 3 type C modules have degraded about 10%.
  - After 2000 h these 2 modules continue to degrade "way over" 10%.

PERSPECTIVES

- Investigation on possible degradation mechanism(s) on C type modules due to DH 85 85.
- Comparison of indoor and outdoor measurements, see poster by Khalid Radouane *et al.* (EDF EN) also presented at this workshop.

This poster does not contain any proprietary or confidential information

CONTACT EDF R&D :
Mike VAN ISEGHEM, mike.van-iseghem@edf.fr +33 (0)1 60 73 61 36

energies EDF nouvelles

EDF
LEADING THE ENERGY CHANGE

Improvement of reliability using four bus bar cell

Masashi Nakamura
Mitsubishi Electric Corporation, 1-3 Komanba-cho, Nakatsugawa-city, Gifu-pref., Japan

1. Background

Reliability of PV module becomes important increasingly as PV modules are expected to operate for more than 25 years, compared with previous market of 20 to 30 years ago. Especially, as PV modules are installed outside and are subjected to external forces from wind, snow and daily/seasonal temperature cycle, cell strength is one of the key points to maintain PV module output for a long term. Mitsubishi Electric has introduced PV modules using 4 bas bar cells in 2010, and is shifting to manufacturing them from previously standard two bas bar cells to improve reliability of PV modules in addition to increase of cell efficiency by 3%.

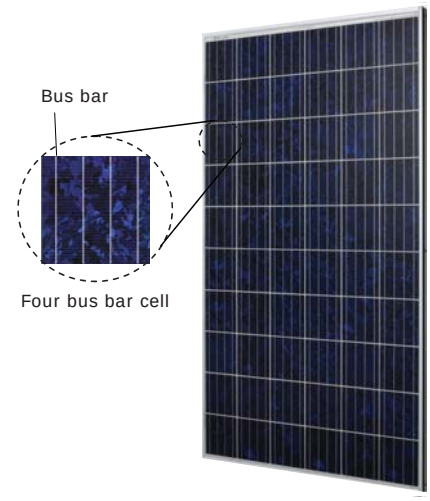


Fig.1 PV module, PV-UJ235GA6

2. Advantage of Four bus bar cell

1) Reduction of residual stress peaks

Four bus bar cells use finer interconnectors and front electrodes which have 1 mm width than two bus bar cells whose interconnectors and front electrodes have 2 mm width to maintain same light receiving area as two bas bar cells. Using finer interconnector and electrode can reduce residual stress peaks along interconnectors which occur when interconnectors are soldered on the electrodes. Figure 2 shows the simulation result of residual stress peaks of a four bus bar cell and a two bus bar cell after assembling interconnectors on a cell. The stress peaks of the four bus bar cell along interconnectors are approximately 3/4 of the two bus bar cell peaks. The decrease makes PV modules more robust to external forces and can keep more output. In addition, the yields of four bus bar cells also improve and material waste can be reduced during manufacturing.

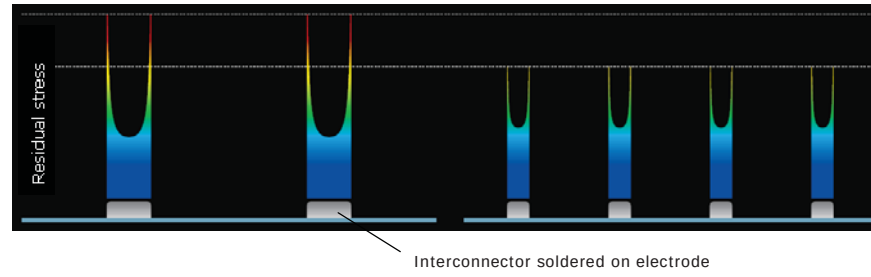


Fig. 2 Stress distribution of two bas bar cell (left) and four bus bar cell (right)

2) Robustness of output

Four bus bar cells can reduce power loss compared with two bus bar cells, in case that cell breakage occurs by unexpected force,. Figure 2 shows that current path of the four bus bar cell is shorter than the two bus bar cell's one under cell breakage occurrence. As the current path is shorter, then the four bus bar cell can reduce output loss compared with the two bus bar cell.

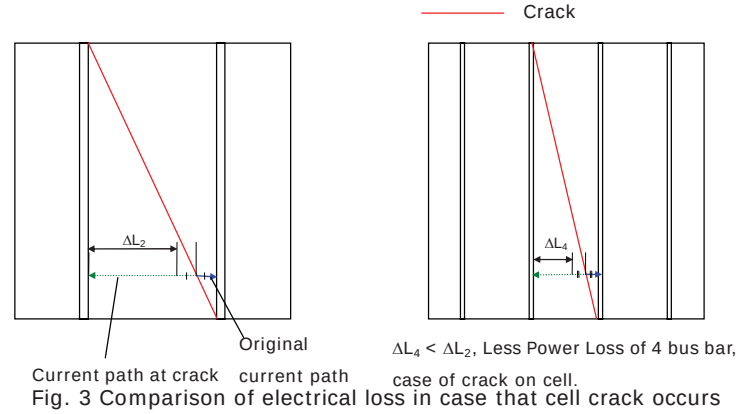


Fig. 3 Comparison of electrical loss in case that cell crack occurs

3. Technologies to use four bus bar cell

As described above, the four bus bar cells need to have finer interconnectors and electrodes. Therefore it is necessary to align and solder them precisely. Mitsubishi Electric has introduced the new alignment system employing the image processing unit and achieved +/- 0.1 mm accuracy. In addition, the introduced system inspects alignment accuracy between the electrodes and the interconnectors and it prevents cells with deviation errors from passing through to next process.

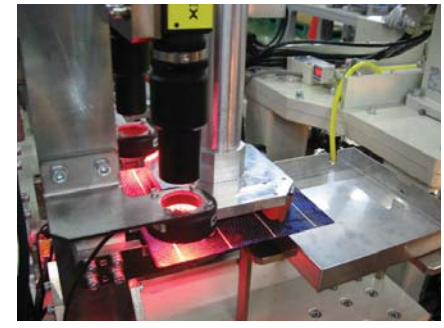


Fig.4 The new alignment system employing the image processing unit.

4. Conclusion

Four bus bar cells have achieved:

1) More robustness to external forces reducing residual stress peaks

2) More reliability against unexpected cell breakage.

Developments in weatherable Polyester Films For Photovoltaic Applications

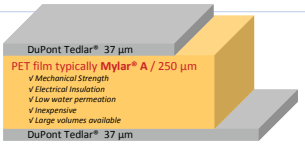
DuPont Teijin Films

William J. Brennan ,
Wilton Centre, Middlesbrough,
TS10 4RF, United Kingdom
Bill.j.brennan@gbr.dupont.com

Simon J Shepherd,
3600 Discovery Drive, Hopewell
Virginia, USA, 23120
Simon.j.shepherd@usa.dupont.com

Polyester films have been used in c-Si PV module backsheets for many decades
E.g TPT ™ is a three-layer laminate of a poly(ethylene terephthalate) (PET) film such as Mylar® or Melinex® between two Tedlar® poly(vinyl fluoride) films:
PET chosen technically due to its excellent electrical insulation, low moisture permeation and high mechanical strength
PET chosen commercially because it is available in large volumes and relatively inexpensive vs other engineering polymers
PET restricted in the past to role as passive central layer due to standard grades having low hydrolysis and uv resistance

The fast growth of the PV market has been matched by the development of polyester films which are much more resistant to hydrolysis and uv degradation

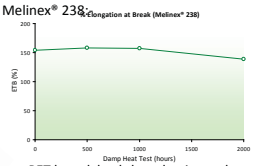


PET film in TPT™ laminate structure

DuPont Teijin Films

Hydrolysis Resistant PET Films

Chemistry dictates that standard PET film grades hydrolyse and therefore lose their mechanical properties when exposed to environments used for PV module testing eg the 85 Deg C /85% rh damp heat test . However PET films are now available which far exceed the 1000hr DHT eg Melinex® 238:-

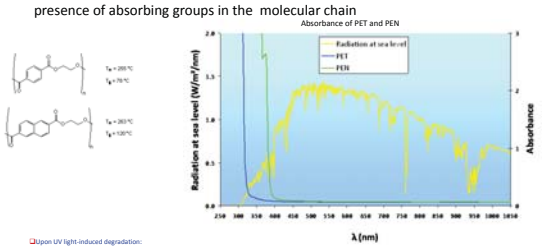


PET based backsheet laminates have been announced which go beyond even 3000 hours in the DHT

DuPont Teijin Films

UV performance of PET and PEN polyester films

Unstabilised polyesters are chemically prone to uv degradation due to the presence of absorbing groups in the molecular chain



Upon UV light-induced degradation:

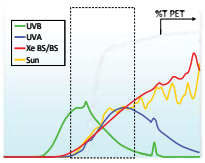
- Yellowness increases
  - formation of new light-absorbing chemical species
- Haze increases (clear films)
  - bulk + surface scattering
- Gloss decreases
  - surface roughens
- Light transmittance decreases
  - more absorption and scattering
- Mechanical properties i.e. %ETB, UTS decrease
  - chains break down

Off-the shelf polyester films would not be expected to pass comfortably standard PV qualification tests, but significant advances in polyester chemistry and polyester film production engineering have allowed the development and commercialisation of highly uv durable polyester films

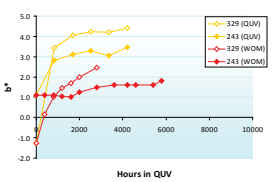
DuPont Teijin Films

Choice of weathering radiation source

Material durability is usually evaluated by accelerated weathering techniques. It may be tempting to use high energy light sources to accelerate aging.



Radiation with λ < 300 nm, which occurs very little at sea level, will unnaturally age polymers and results will not correlate well with outside tests. UVB ageing is still used as a cheap but rather unreliable method to predict polymer lifetime. UVA also only emits in a specific portion of the UV light range and can be highly misleading since photooxidation of the initially generated yellow species happens upon exposure to the 370-430 nm range, a process known as photobleaching. Thus using a UVA lamp PET can appear yellower after UVA testing despite not much degradation having occurred.

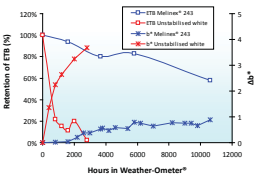


DuPont Teijin Films

White PET PV backsheet films

Weatherometer data again shows the effect of uv stabilising a white polyester film. The data below is for two films, Melinex® 329, a 50um thick standard white film and Melinex® 243, a stabilised 50 um film used for c-Si backsheets. After 10,600 hours Melinex®243 shows excellent retention of elongation to break and very little increase in yellowness, hardly noticeable by visual inspection.





Estimation of PET backsheet lifetime

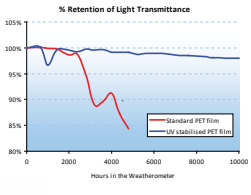
From intensity of lamp 1 year in Florida direct sunshine is 1637 hours in WOM
Back sheet not directly exposed to sunlight

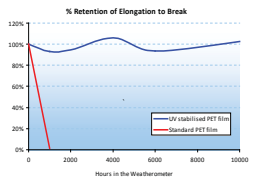
- Most of irradiation typically by reflectance
- Most surfaces will typically have 10 – 20 % reflection in wavelength range that causes degradation to PET
- So use 15 % reflection ie multiply exposures by factor of 1/0.15 = 6.7
- For 1637 hours in weatherometer = 1year in Florida direct sunlight
- 1637 hours = 1x 6.7 years in Florida diffuse reflected
- 25 years given by 25x1637/6.7= 6100 hours in weatherometer
- So 10000 hours sample above should safely simulate 25 years

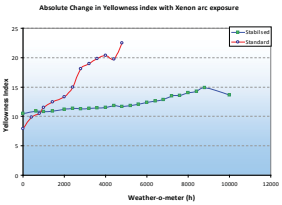
DuPont Teijin Films

UV stabilised polyester films

DTF has marketed uv stabilised PET films for over 20 years . Xenon arc lamp ageing in an Atlas Ci5000 Weather-Ometer® (calibrated at 0.55 W/m2/nm at 340 nm, according to ISO 4892-2) was used to age DTF UV-stabilised grades . Results for clear 175 um films are shown for the three main properties mentioned to be degraded by uv exposure in standard PET films in comparison with non uv stabilised films







This technolgy has been used in external applications for 20 years now and has recently been applied to white and black films used in PET/PET/EVA laminates for PV backsheets

DuPont Teijin Films

Fraunhofer USA

Center for Sustainable Energy Systems (CSE)

25 First Street, Cambridge, MA 02141

Effect of Temperature on the Response of PV Modules to Mechanical Stress

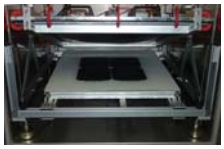
John Lloyd, Matthias Winter, Adam Stokes, Dan Doble, Rafal A. Mickiewicz

MOTIVATION

The crystalline silicon photovoltaic (PV) module is a laminate assembly composed of materials with widely varying mechanical and thermal properties. The properties of these materials are important factors influencing the performance and reliability of modules following exposure to external mechanical stress. In particular, a key role of encapsulation is to protect the solar cells from external stresses, yet some encapsulant mechanical properties can vary with temperature. Since current mechanical loading tests for certification of PV modules are performed at room temperature, these tests may not adequately simulate or accelerate in-field mechanical stresses and failures. This work examines the impact on module performance and cell integrity of dynamic and static load testing at both high and low temperature using a custom-built mechanical testing rig capable of operating inside a climate chamber. The loading conditions were based on relevant qualification test standards and test modules were characterized for performance and damage using a solar simulator and electroluminescence imaging .

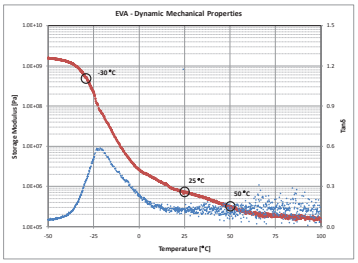
EXPERIMENTAL



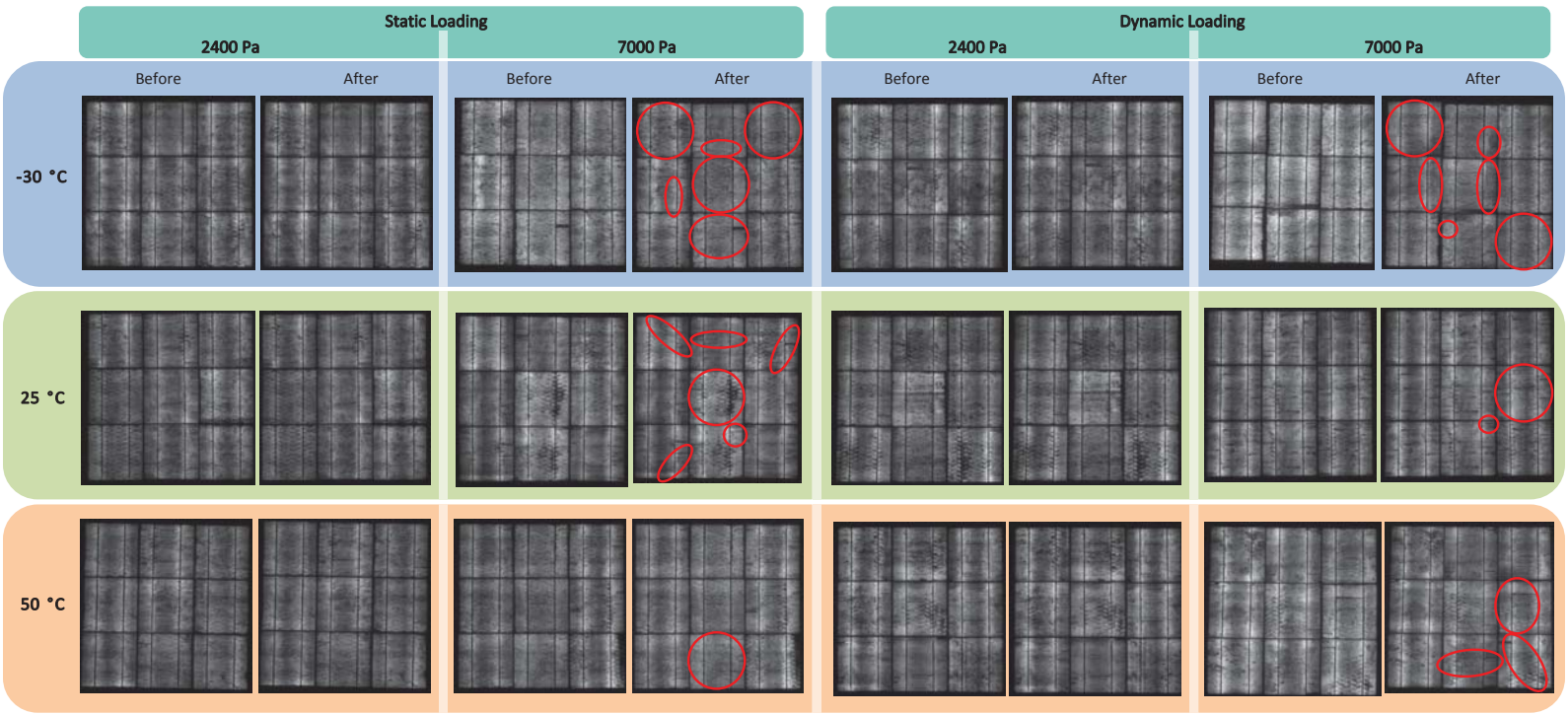


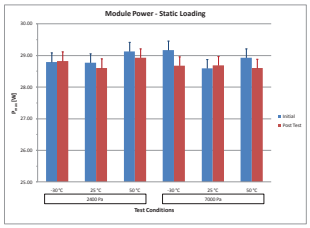
- Mechanical test stand designed and built to fit inside a climate chamber
- Elastomeric bladder applies uniform load from 2,400 Pa to 10,000 Pa
- Test modules with maximum dimension of 550 mm x 550 mm
- Flexibility in mounting configuration
- Deflection measurements using LVDT
- Static and dynamic loads (up to1 Hz)

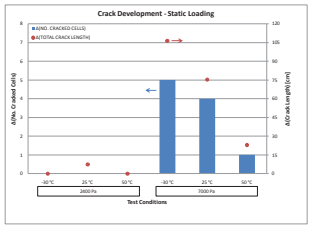
Experimental Test Parameters		
Modules	**Temperatures**	**Applied Loads**
Encapsulation:	-30 °C	Static:
EVA	25 °C	3 x 1 hr @ 2400 Pa
Backsheet:	50 °C	3 x 1 hr @ 7000 Pa
TPE		Dynamic (0.5 Hz):
Strings:		10 000 cycles @ 2400 Pa
3 x 3 -cell mc-Si		10 000 cycles @ 7000 Pa

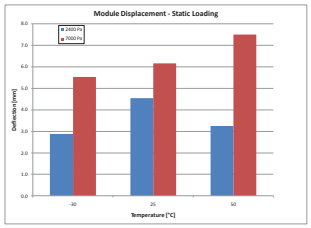


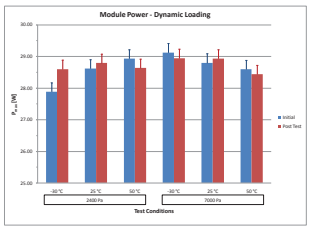
- Module behavior was characterized before and after loading using electroluminescence and solar simulator
- EVA modulus changes by several orders of magnitude in the operating temperature range due to glass transition at around -20 °C

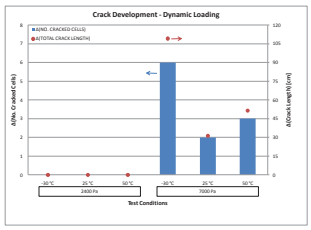


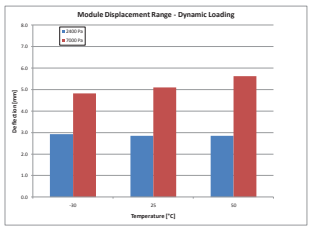












RESULTS

- All modules passed the standard qualification requirement of less than 5 % power decrease after testing
- Low pressure loading (2400 Pa) did not cause visible cracking of the cells in the test modules
- High pressure loading (7000 Pa) caused significant damage to the cells in the test modules under both static and dynamic conditions
- High pressure loading at sub-ambient temperature causes the most cracking in the cells, consistent with the increased modulus of the encapsulation, which transmits the loading stress to the cells
- Module deflection decreases with decreasing temperature, as a result of the stiffening of the encapsulation

CONCLUSION

- Temperature plays an important role in the response of PV modules to applied mechanical stress at high loading pressure

© 2011 Fraunhofer Center for Sustainable Energy Systems (CSE)

SEMPRIUS
High performance semiconductors anywhere

Silicone Yellowing Due to Material Interaction in a CPV Application

Steve Seel*, Wolfgang Wagner, and Scott Burroughs

Feb 17th, 2011

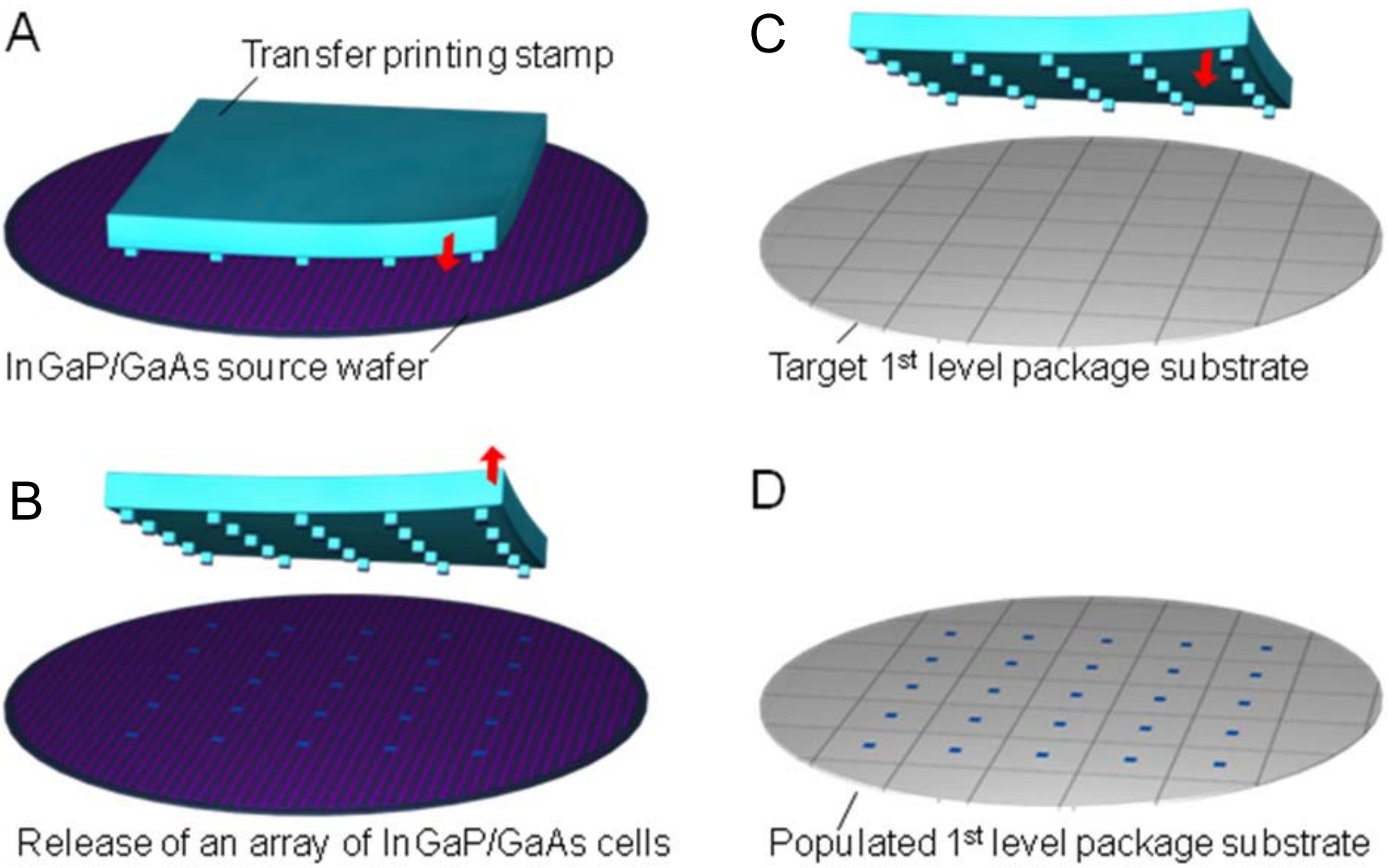
*steven.seel@semprius.com, 919-314-7708

Semprius Background

- Semprius is developing low cost, high performance concentrator photovoltaic (CPV) modules to make solar power generation economically viable in sunny, dry climates. The company's unique micro-transfer printing technology enables CPV modules with high performance, high reliability and low cost with scalability to high-volume production.

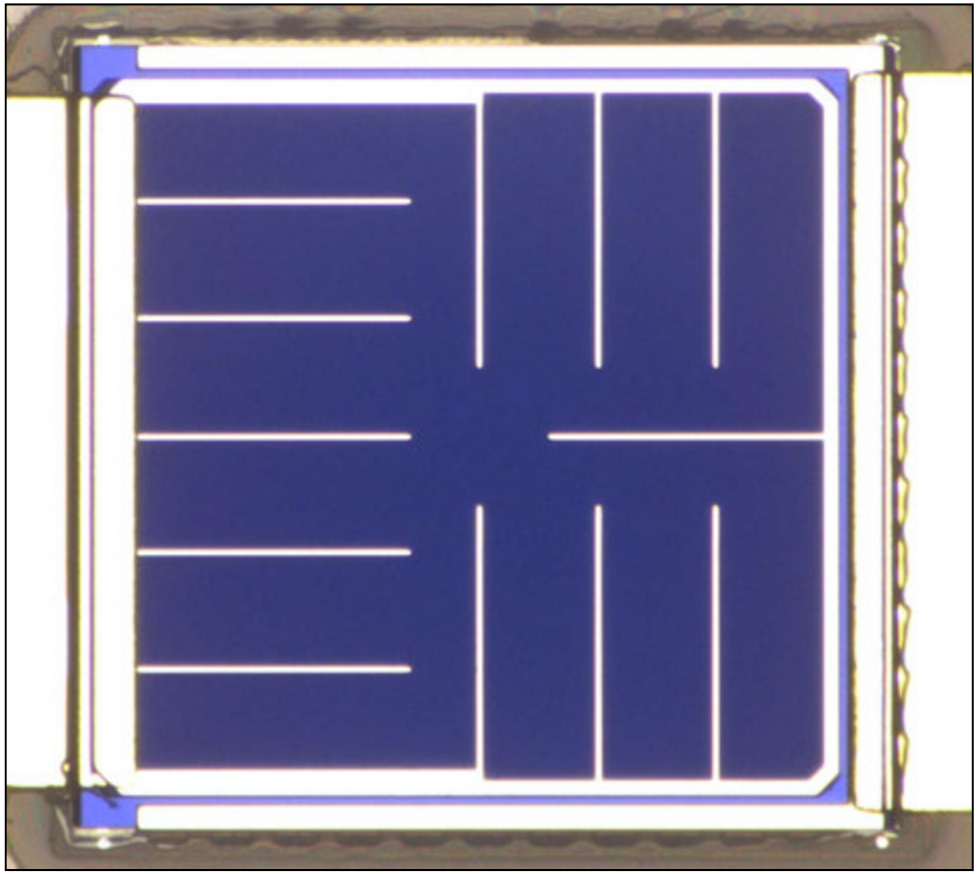
- Semprius is also licensing its micro-transfer printing technology for non-solar applications to enable a wide variety of new products requiring large-area, thin, lightweight form factors, unprecedented performance, high reliability and low cost. Applications include flat-panel displays, flexible electronics, large-area sensors, RF devices and other applications requiring heterogeneous integration of high-performance semiconductors.

Transfer Printing Process



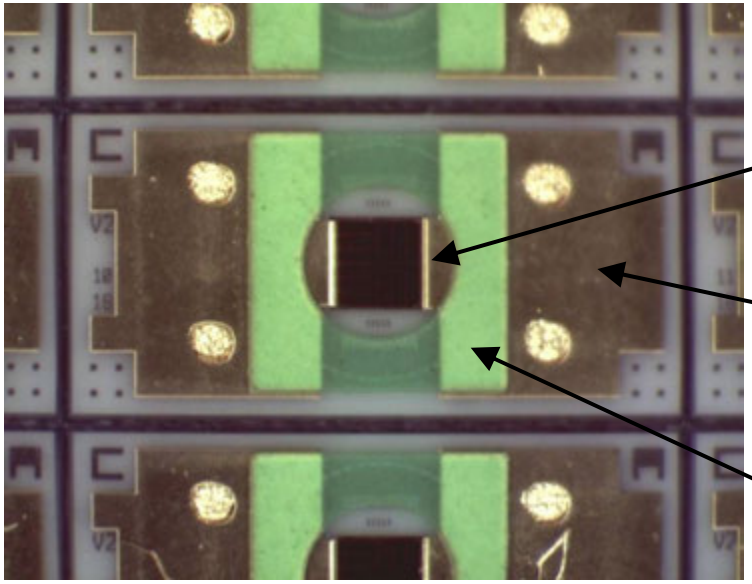
Transfer printing allows for epi source wafer reuse

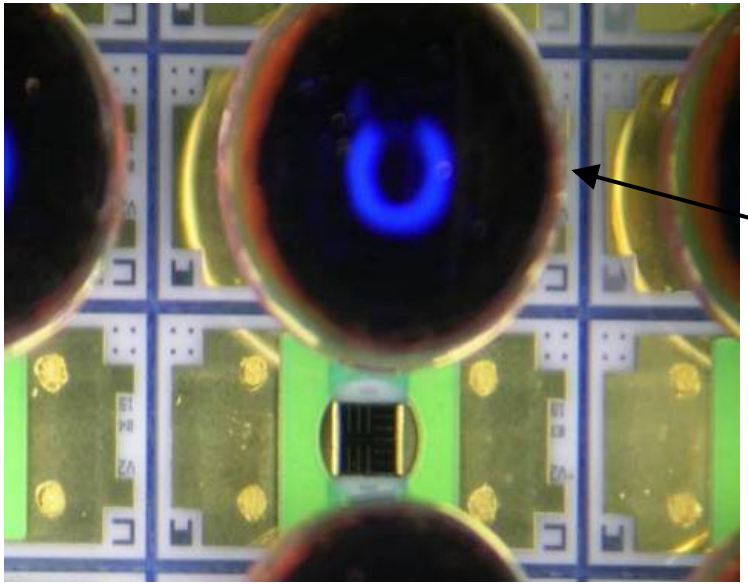
Cell Geometry & Interconnection



- 650um triple-junction unifacial solar cell with +40% efficiency
- Thin film metallization creates anode/cathode interconnection
- Residual heterogeneous anchors from printing process around perimeter of solar cell

Packaging and Secondary Optic





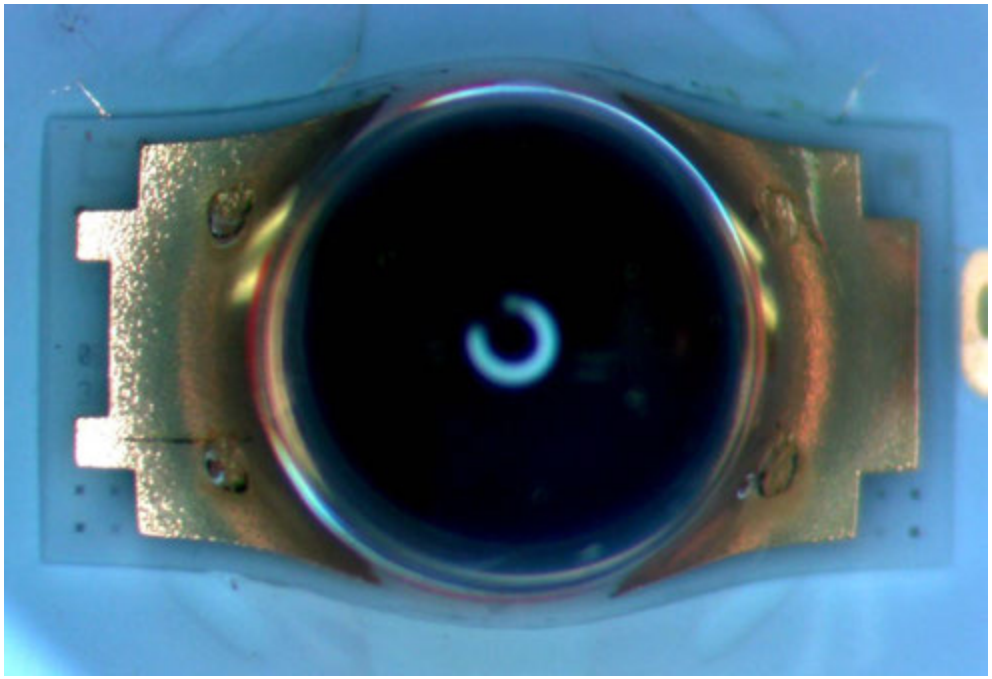
Cell printed onto thin epoxy on ceramic interposer with vias

Evaporated + plated thin film interconnection to solar cell

Photoimageable soldermask used as spacer to control position of glass secondary optic relative to solar cell

Secondary optic provide uniform illumination on cell and 0.9 degree acceptance angle

Silicone Underfill and Overcoat



*Distortion due to refraction by silicone

- Silicone dispensed onto packaged solar cell then ball lens cured in place
- Elimination of air gap between glass ball lens and solar cell reduces Fresnel losses
- Silicone encapsulated solar cell, metallization, and solder joint improves reliability

Failure Mode Discovery

- Long-term damp heat testing was being performed to evaluate effectiveness of silicone encapsulation to protect solar cell
- No secondary optics in place since only darkIV being measured
  - DIV more sensitive to shunts and series resistance changes
  - Easier to measure since no optics involved
- After 1000 hrs at 85C and 85%RH, the silicone encapsulation appeared to be discolored but impossible to measure impact without secondary optics in place
- Lesson Learned: Short cut in testing protocol (no lightIV recorded) means that potential failure mode could have been missed

Silicone-Soldermask Interaction



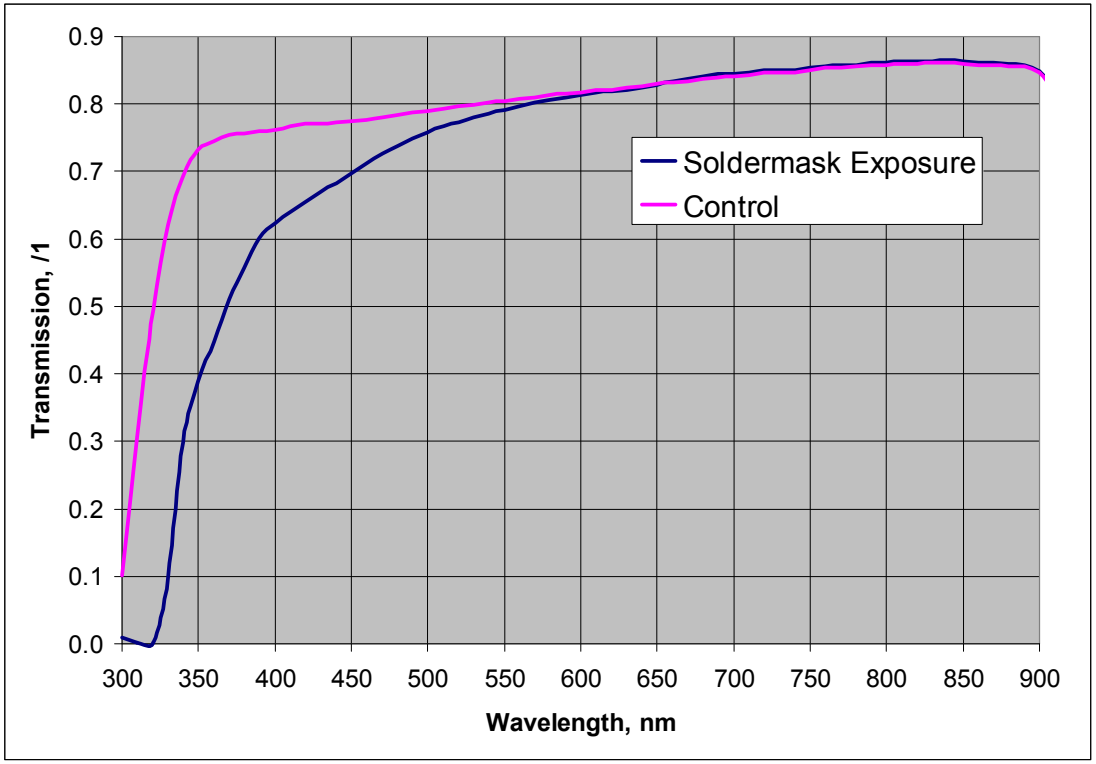
- Sample Coupon Generation

-Cast silicone onto large area of soldermask

-Expose sample to damp heat (85C and 85%RH)

-Peel off silicone from soldermask, attach to glass

-Measure optical transmission of silicone on glass

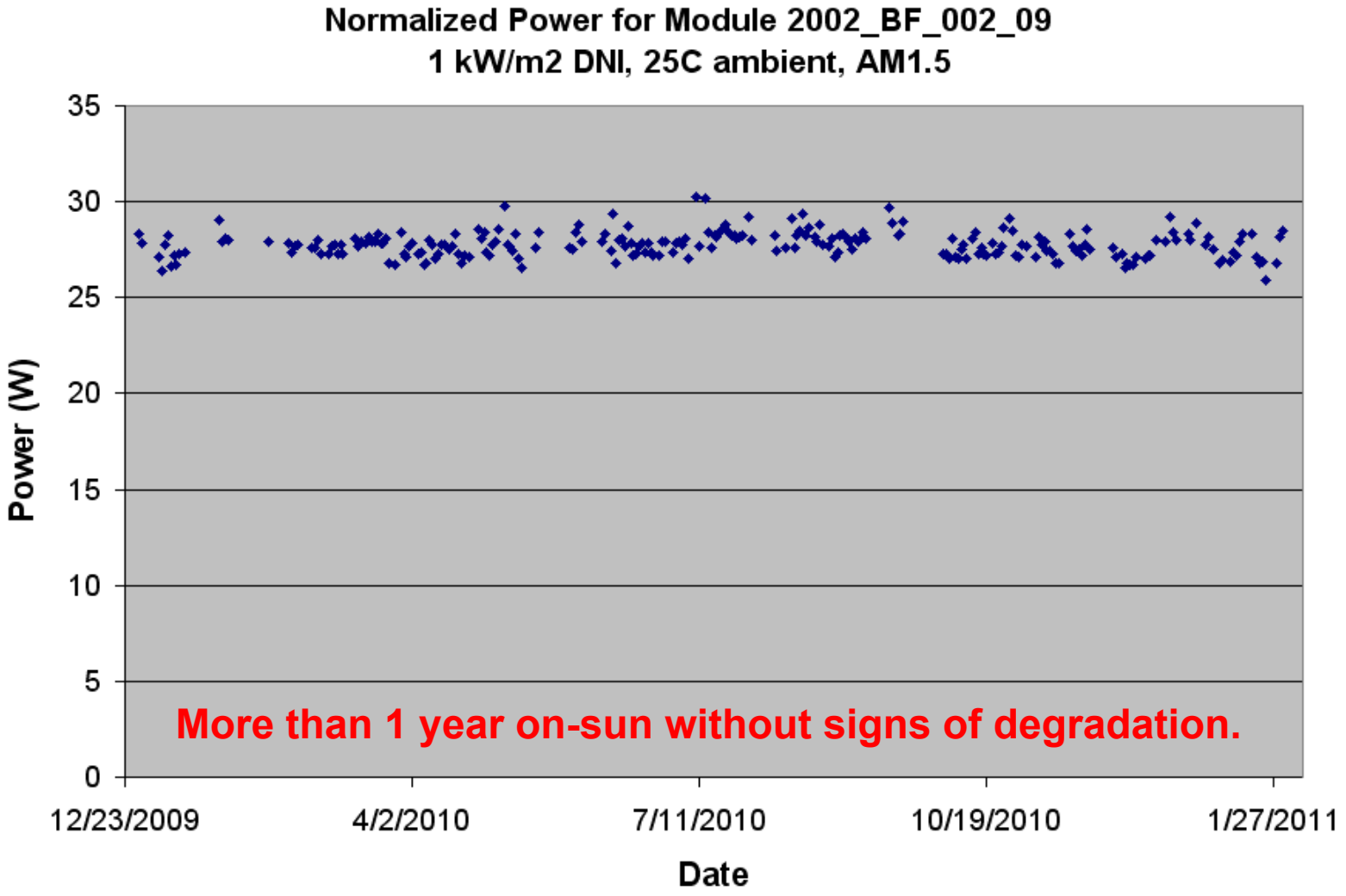


Root Cause of Failure

- Heat and humidity exposure of silicone alone not root cause since control sample shows no signs of degradation
- Tests at 85C without moisture showed same undesirable silicone-soldermask interaction
- Silicone discoloration likely due to fast diffusion of mobile green dye in soldermask into “porous” silicone at temperature
- Alternative soldermasks with brown dye **did not** show any signs of interaction with silicone through damp heat testing
- Classic case of interactions between reliable components causing problems only observed once full product assembled

Long-Term Module Reliability

Module **without** silicone-soldermask issue



Multi-Crystalline Silicon Solar Cell Modules: Crack Formation and Development due to Climate Chamber Thermal Cycle Testing

A.F. Dethlefsen
SCHOTT Solar AG, Global R&D, Testcenter, Carl-Zeiss-Str. 4, 63755 Alzenau, Germany

1 Abstract

In the previous years more and more interest is shown in the investigation of photovoltaic (PV) modules by means of electroluminescence (EL) imaging. This holds not only for the manufacturers but also for their distributors and/or customers.
Being confronted with the assessment of EL-images several questions arise: How do EL-visible failures influence the degradation of PV-modules? Is it possible to do a forecast about the module degradation from the initial EL-image? There is still a lack of direct correlation between reliability testing in a laboratory and the lifetime of a PV module in field. Nevertheless we know that certain failure mechanisms can be accelerated by means of climate chamber testing.

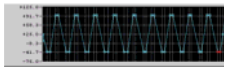
We like to present a study in which we used 40 multi-crystalline glass-foil silicon solar cell modules. The modules have been produced during the last two years. They have been part of the routine quarterly year climate chamber tests performed at SCHOTT Solar. A database has been set up containing the number of cracks before and after stress testing and the power degradation of the modules due to the TC testing.
Furthermore the development of cracks has been assessed during the tests with means of intermediate EL imaging

2 Experimental Setup

40 glass-foil modules with 5" (40 %) and 6" (60 %) multi-crystalline solar cells have been under investigation.

The modules have undergone 400 thermal cycles (TC) in a temperature range from - 40 °C to + 90 °C which is equivalent to double the DIN EN (IEC) 61215 testing time with a slightly higher temperature range (according to UL 1703).

- Intermediate tests every 100 thermal cycles
- Measurement of the module power by a AAA Halm flasher with a reproducibility of +/- 0,1 % in module power for repeated measurements at standard test conditions.
- Electroluminescence setup equipped with a CoolSamBa Camera from Sensovaton. Exposure time was 10 s at a current of 7,5 A or 40 s and 15 A respectively
- 400 Cycles (200 % IEC): -40 °C ⇒ +90 °C



Crack Counting:

- A cell with multiple cracks counts as one
- Fingerpeeling is not counted as a crack
- The size of the crack is not taken into account

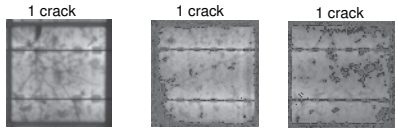


Fig. 1: Examples for crack counting

3 Results

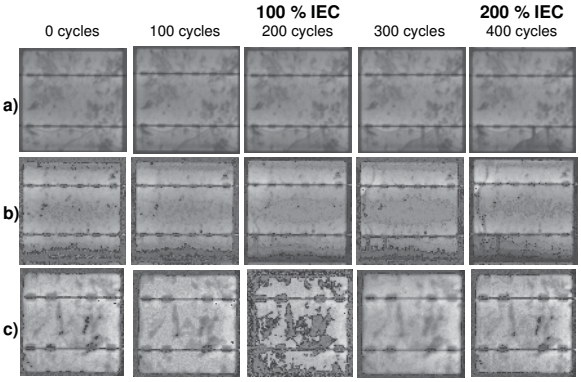


Fig. 3: Different development of cracks during the thermal cycle test

a) Cracked cell at start with developing degradation

b) No cracked cell at start

c) Non developing crack

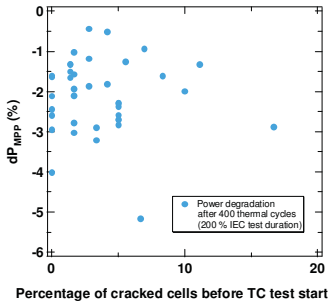
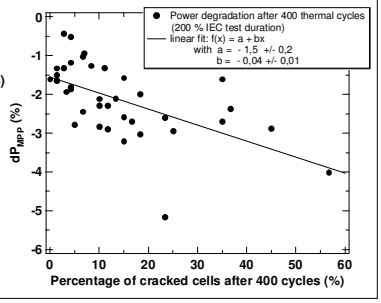


Fig. 5:
On the graph to the right the percentage of cracked cells after 400 thermal cycles versus the power degradation after 400 thermal cycles is shown (200 % IEC).
As expected it can be seen that the power degradation rises with the number of cracked cells (linear fit).

Fig. 4:
To the left the percentage of cracked cells before the thermal test start versus the power degradation after 400 thermal cycles is shown (200 % IEC). There is no visible correlation between those two sets of data.
The spread of the data points for a certain percentage of cracks is very high.



4 Discussion

The results show that it is not possible to do a forecast about the module degradation due to accelerated aging based on the number of cracked cells on the initial inspection by means of electroluminescence measurements. There are several reasons:

-The development of initially present cracks during stress testing is not clear without ambiquity. 38 % of the cracks were not developing during the tests (Fig. 3 c).

-The separation between degradation due to cracks and degradation due to other failure modes (e.g. finger separation) was impossible.

-A high number of cracks was either not present or not visible in the initial electroluminescence image (Fig. 3b).

-The spread of data points in case of the number of initial cracks before the test start and the resulting power degradation after 400 thermal cycles is very high (Fig. 4).

The study shows that even modules with a relatively high number of cracked cells do not give rise to a high degradation after double the IEC 61215 testing time. For further analysis in particular regarding the qualification of cracks in PV modules please see as well [1].

References:
[1] M. Köntges et al., Quantifying the risk of power loss in PV modules due to micro cracks, 25th PVSEC Valencia 2010

SCHOTT Solar AG, Carl-Zeiss-Str. 4, 63755 Alzenau, Germany, annelene.dethlefsen@schottsolar.com

This poster does not contain any proprietary or confidential information.

NREL PVMRW 2011, Feb. 16-17, Golden, CO, USA

Research Center for Photovoltaics

New Acceleration Test for PV modules Such as Burns or Interconnector failures

Takuya DOI
AIST-RCPV, AIST Central 2, Tsukuba, Ibaraki, 305-8568, Japan

Introduction

Motivation: Comparing to popular consumer electronics, longer lifetime and bigger size as sample make it difficult to estimate its lifetime; we have to develop the special lifetime evaluation technique for PV-modules.

Target: Interconnector failure and surroundings.

Goal: To develop new test method which evaluates PV module life in 30yrs over.

Conclusion

☆ Phenomena having analogies to the failure in the outdoor PV modules is observed.

☆ Confirm the possibility of cyclic test.

☆ Proposal of new acceleration method to PV module deterioration such as cell burn or interconnector failure.

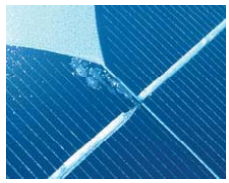
Future tasks: Expansion to full size modules, then study whether it is applicable to acceleration test.

Materials and Methods

Failures of PV modules



burnt edge of cell



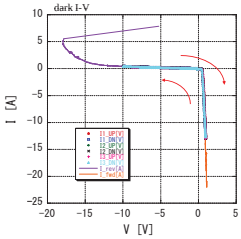
bubbles in EVA



burnt back sheet

These phenomena are observed in the AIST's mega solar system in 2009. It is a grid-connected system and has been operating since 2004. How do you think about these failures occurred within 5 years operation. I wonder why these failures occur and how to simulate this in acceleration test.

Proposal: concept of cyclic test



Supposing acceleration test: periodically changing (=cyclic) voltage, forward and reverse

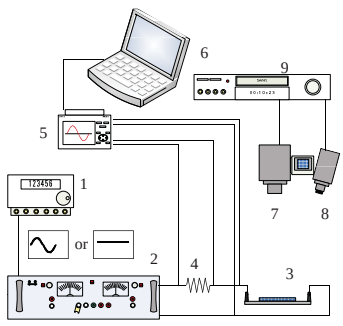
Goal = No breakdown test!

As the first step;
¤ reverse biased breakdown test
¤ wave voltage cyclic test

Samples: Single-cell PV modules

We intend to add cyclic voltage indicated in light blue curve.

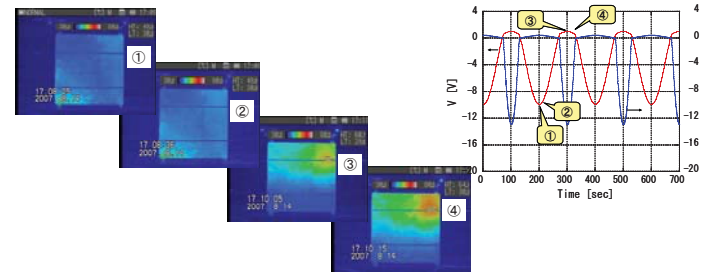
Experimental apparatus



1: DC or wave voltage source
2: Bipolar power supply
3: PV cell and sample stage
4: Resistance
5: Data logger
6: PC
7: IR thermographic camera
8: Visible Ray camera
9: Videocassette recorder

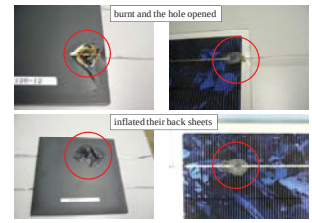
Results

Wave voltage cyclic test



Right graph shows the time changes of voltage and current. Red line is voltage and blue line is current. The numbers in pictures are corresponding to the same number in the graph. There are 4 points of two peaks of the voltage and two peaks of the temperature. It was observed that the peak of temperature delays 7 to 11 seconds from the peak of voltage. You can see the warm area is different according to the direction of the voltage. This is the skeleton of proposed method.

Reverse biased breakdown test

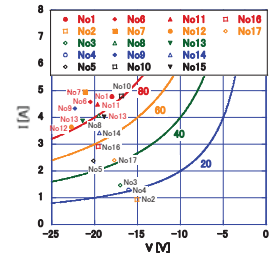


We used two type of EVA, that is, EVA-A and EVA-B. This breakdown test is so-called destructive test.

At the moment of the destruction, each sample group using different EVA has the following characters; all test samples of the EVA-A burnt and the hole opened (4 of 4), on the other hand, as for the EVA-B, 3 test samples inflated their back sheets and burst (3 of 5), one test sample burnt and the hole opened and one test sample only blew smoke out because the breakdown occurred at the edge of the single-cell module.

Phenomena having analogies to the failure in the outdoor PV modules

Wave voltage cyclic test



* Contour line indicates the level of power stress : S [w]
* Filled marks : breakdown occurred in certain experiment duration
* Open marks: breakdown not occurred in certain experiment duration
* V for forward was fixed at 0.6 [V].
* V for reverse was adjusted as the power stress S [W].

It was found that there are certain threshold levels around 80 watt for whether the breakdown breakage occurs or not.

From the IV measurement after the experiment, degraded samples had increased series resistance.

Proposed method is useful for new acceleration test to the cell and interconnector failure.

Acknowledgments This work is supported by NEDO as a part of the "Projects for New Energy Technology Development" under METI. The authors would like to thank them.

Solar Module Logistics
Current Packaging Methodologies & Considerations

WESTPAK, INC.
EXCELLENCE IN TESTING

MATERIALS

- Solar modules are likely produced in an area geographically distant from their destination.
- Packaging materials known to produce good results in one part of the world may be unavailable or overly expensive in another part of the world.
- Ability to use multiple or different materials that both result in acceptable package performance characteristics is critical to a globally integrated supplier of solar modules.





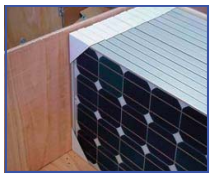





MODULE ORIENTATION

- Because of their large and flat structure, solar modules have very different response characteristics to mechanical vibration depending on the orientation of the module during excitation, that is, transportation.
- Example, module natural frequency in the z-axis is normally in the 15 Hz range which is precisely where input from truck vehicles is most severe.
- Changing the orientation for shipment to the X or Y axes may be justifiable based on product protection.





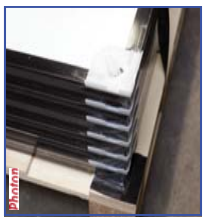


PRODUCT PROTECTION

- This is a **primary function** of the package system.
- A distribution environment is the most mechanically severe environment the product will experience during its entire lifecycle.
- The purpose of the package is to efficiently protect the product and prevent damage during this time.





INSTALLATION CONSIDERATIONS

- Without careful considerations of the requirements of the installation sites, a properly manufactured and delivered solar module may suffer damage during installation that can easily be avoided.
- Considerations include:
- Ability to remove modules easily from a package system.
- Ability to deliver modules to a job site in a pallet load configuration.
- Removing waste materials easily from the job site.
- Possibility of reverse logistics with reusable packaging.



COST EFFICIENCY

- Because of the size of typical solar modules relative to the size of distribution vehicles, the actual dimensions of the module has a great deal to do with the overall distribution costs and therefore of logistics.
- Products that are sized to be efficient in the distribution environment are far less costly to deliver than the same products that have lower efficiency in distribution.




RELIABILITY AND LONGEVITY

- The distribution environment is the most **mechanically active** environment that the product will likely experience during its entire lifecycle.
- Product ruggedness and the associated longevity of the product is highly dependent on isolating it from forces that are above its design.
- The packaging system must be designed to increase module reliability and longevity.




LOGISTICS

- The single largest identifiable cost of a delivered solar module anywhere in the world is the logistics necessary to get it from the point of its production to its ultimate destination.
- Without control of logistics, a module manufacturer does not have control of major product costs.
- Packaging is one of the single largest components of logistic costs.







THIS PRESENTATION DOES NOT CONTAIN ANY PROPRIETARY OR CONFIDENTIAL INFORMATION

HERB SCHUENEMAN, CEO, WESTPAK, INC.

Prediction of critical module hot spots caused by shunts in silicon solar cells using in-line thermography

Chris Stapelmann, Fabian Fertig^Δ, Benjamin Weiss˚, Robert Fritz**

SolarWorld Industries America, Hillsboro, OR, ^Δnow: Fraunhofer ISE, Freiburg, Germany, ˚now: Oregon State University, Corvallis, OR

Background and Motivation:

One of the critical failure modes of photovoltaic modules installed in the field is damage of the module due to hot spots. The effects of hot spots in the field range from degradation of the module power to complete loss of module performance. Hot spots in modules can be classified into two main groups as cell related (shunts) and non-cell related (arcing). This work focuses on cell related hot spots and their detection using in-line thermography in a high-volume crystalline solar cell manufacturing environment.

Shunts in solar cells can lead to hot spots and are either process or material induced. Process induced shunts can be due to insufficient edge isolation or metallization edge paste. Material related shunts in cells can be due to carbon inclusions or impurities at grain boundaries when these are located near the PN-junction.

Shunts across the PN-junction of a solar cell lead to an increase of current at a given reverse bias. While the reverse-bias current can be measured during IV-curve testing, it is not a good predictor of hot spots as the shunt area determines the dissipated power and subsequent Joule heating[1]. Figure 1 shows the correlation of the reverse-bias current measured by an IV-curve tracer to the temperature of the hot spot for a large amount of sample cells. Many of potentially critical hot spots would not be caught by mere reverse-bias current sorting of cells. On the other hand, not every cell with a high reverse-bias current displays significant hot spot behavior.

To solve this problem, SolarWorld is implementing an in-line thermography system for production monitoring in their cell testers. The thermography system uses an IR camera to detect hot spots on cells while applying a reverse bias and measuring the resulting localized temperature. Due to the required high throughput of the cell testers, the thermography measurement has to be limited to less than one second. The thermal mass of the solar cell and the varying degree of the shunting make it difficult to correlate this short measurement to the equilibrium temperature of the shunt or even potential module damage.

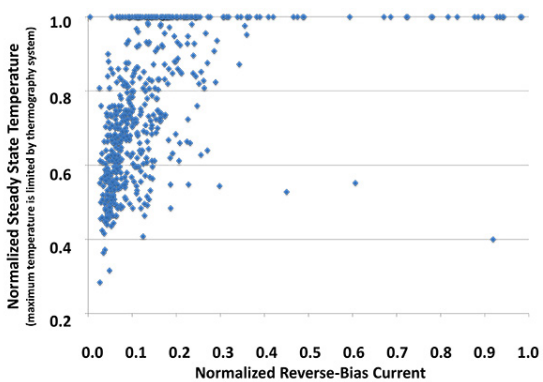


Fig. 1 – Correlation between reverse-bias current and steady state hot spot temperature

References:

[1] M. Kasemann *et al*, "Spatially resolved silicon solar cell characterization using infrared imaging methods," *Proc. 33rd IEEE PVSC*, San Diego, CA, 2008.

[2] F. Fertig, "Hot Spot Detection via IR Thermography in Crystalline Silicon Solar Cells", Masters Thesis, IPE, University of Stuttgart, 2009

Acknowledgements:

Ethan Good, Nestor Rigonan, Max Selahi, Paul Norum, Josh Yaskoff, Yiping Wang, Tom Wolf, Eric Schneiderlöchner* (SolarWorld Industries America, *SolarWorld Innovations)

Methodology:

In order to correlate the in-line thermography measurements to the hot spot behavior of modules, the methodology shown in Figure 2 was established.

A test set of about 1,000 solar cells with hot spot signatures was sorted out at the cell tester and characterized on an off-line thermography system (Fig. 3). The hot spot temperatures of these cells were measured at steady state equilibrium. The samples were then grouped into temperature bins of 10 °C steps and cells from each group were interconnected and encapsulated into modules.

These modules were exposed to sun irradiation >800 W/m² under short circuit conditions and the steady state temperatures of the resulting hot spots of shaded cells were measured using an IR camera (Fig. 4, Fig. 5).

In addition to the IR camera temperature measurements, any optical defects like bubbling, delamination, or discoloration of the back sheet or EVA arising from the hot spot were recorded with respect to the hot spot temperature. Figure 6 shows an example of delamination on the front and the back side of a module caused by a significant hot spot which was created specifically for this experiment.

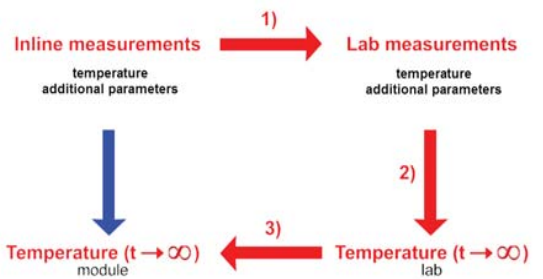


Fig. 2 – Methodology to correct in-line thermography measurements to module hot spot temperatures[2]



Fig. 3 – Off-line thermography measurement system

Results:

Based on these module test re
temperature (as measured on
potential for module damage
can occur is dependent on the

In the final step, multiple-regr
line thermography measuremen
sorting criteria.





Fig. 4 – Set-up of out

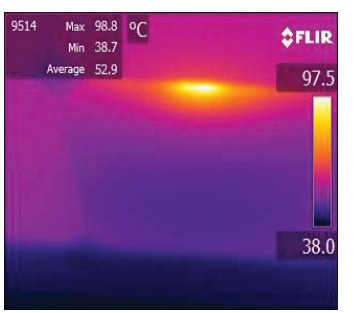


Fig. 5 –

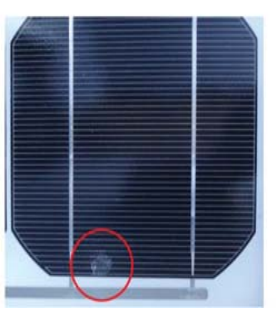




Fig. 6 – E

This poster does not contain any proprietary or confidential information.

Advanced Fluoropolymer-Free, High-Grade PET-Based Backsheet Reaching Over 3,000 Hours DHT*

M. Vannini[1,2], A. Palazzo[1], and T. Surek[3]
[1]Coveme SpA, Italy, www.coveme.com
[2] Corresponding Author: mvannini@coveme.com
[3] Surek PV Consulting, Denver, Colorado

INTRODUCTION:

- PV manufacturers design modules for long-term outdoor durability.
- Damp Heat Test (DHT) is the main differentiator for good quality backsheet.

We developed a methodology for fabricating high-grade PET and adhesives with our partners. This method resulted in the only PET-based backsheet to withstand 3,000 hours of DHT.

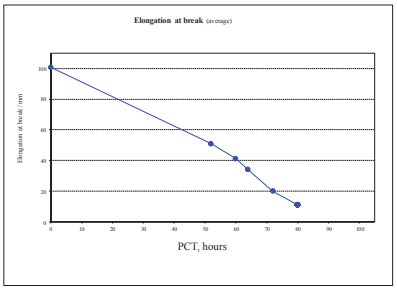
Sample Preparation – Pressure Cooker Test (PCT)



Duplex

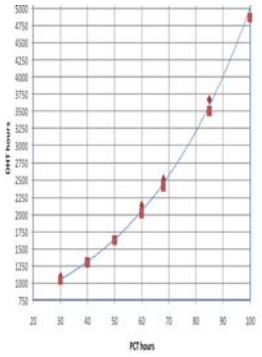
Two layers of high-grade PET were selected and laminated (Duplex) with a special adhesive. Duplex strips were then put into a Pressure Cooker chamber at 121°C and 100% Relative Humidity. After 80 hours of PCT, the Duplex still retains more than 10% of Elongation to Break (ETB). This is estimated to be equivalent 3,000 hours of DHT.







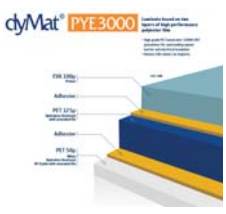
ETB is measured with an Electronic Dynanometer

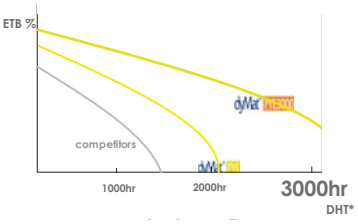


DHT vs. PCT based on Coveme experience with hydrolysis-resistant PET

CONCLUSIONS:

- Pre-selection of the right, high-grade hydrolysis-resistant PET films was key.
- Adhesive system development was also fundamental to achieve the desired product.
- Note that the proper selection of the high-grade hydrolysis-resistant PET films affects positively the adhesion value and overall performance.

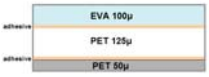


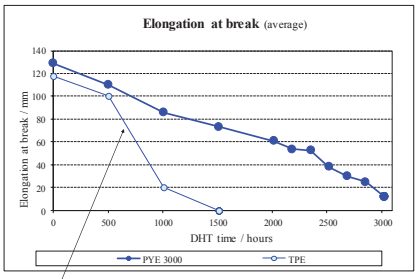


Standard PET-based backsheets show degradation around 1000-1300 hours of DHT.

DHT Verification

3,000 hours of DHT was also verified with the dymat PYE 3000 backsheet (Duplex with the EVA layer).

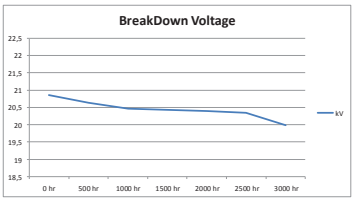


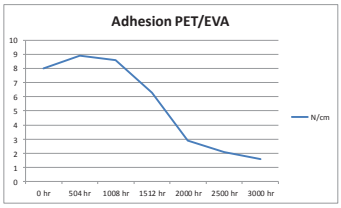


After 18 weeks or 3024 hours of DHT, the PYE 3000 still retained more than 10% of ETB.

TPE typical ETB curve

The quality of the selected films positively affected the adhesion.

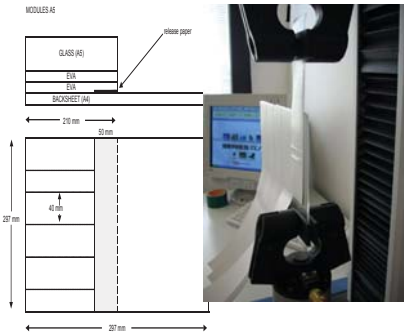




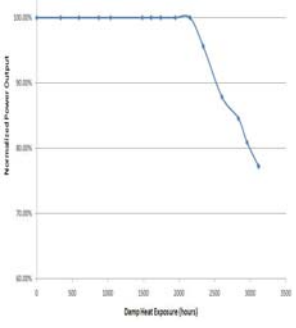
DHT on Module

The dyMat PYE 3000 was then laminated into A5-size dummy modules and put into the DHT chamber. After 3000 hours, the visual inspection was very positive. Adhesion tests were also carried out.





Our Customers' DHT Results



The dyMat PYE 3000 was then laminated into full-size modules by our customers, reaching over 3,000 hours DHT. Many customers are already using it, and the modules are UL and TUV certified.

*This poster does not contain any proprietary or confidential information.

Accelerated Test and Statistics Model Analysis of Degradation Performance for PV Module Lifetime Prediction

Yi-Hung Chou, Shih-Yu Huang, Rong-Sheng Cheng, Kuei-Chang Fan, Chung-Chin Lee, Delsolar Co., Ltd.
Yao-Tung Hsu, Yi-Ru Hsu, Cheng-Ban Chung, Institute of Nuclear Energy Research
Chien-Yu Peng, Institute of Statistical Science, Academia Sinica, Taiwan
Sheng-Tsaing Tseng, Chi-Chun Tsai, National Tsing-Hua University, Taiwan
Ethan Wang, Carl Wang, Underwriters Laboratories Taiwan Co., Ltd.

Introduction

The reliability of crystalline silicon PV modules has improved dramatically in recent years. Today, manufacturers are usually asked to provide their customers with reliability information about degradation rate of PV module power. However, module power degrades very slowly at the normally used condition. Accelerated degradation tests are used widely to obtain timely information on the reliability of module.

Accelerated degradation tests for assessing the long-term reliability and performance of photovoltaic modules were conducted as follows. The damp heat tests were run at high levels of temperature and relative humidity to accelerate the hydrolytic and corrosive action of hot, humid environments and obtain degradation data more quickly. In our tests, the 2 x 2 cell modules were fabricated in the same type of crystalline Silicon cells, glass and back sheet foil. Before the damp heat tests, the modules were exposed by UV 15 KWhr as the pre-test mentioned in IEC61215. Those small modules were tested as the process flow (as Fig 1.) which are then divided into five conditions (as Fig 2.). Damp heat test were plan to keep going non-less than 2000 hrs. The tests of IV-characteristics and a visual control were carried out, and measurements were made at specific times so as to obtain the degradation ration of power loss.

The performance of a degradation model depends strongly on the appropriateness of the model describing a product's degradation path. we propose a relationship between the product's lifetime and stress variables. The method can be used for highly reliable products.

Objectives

For PV module makers, we hope to have a cost effective way but accuracy method for lifetime prediction. In this study, a general linear degradation model was proposed . The unit-to-unit variation of modules can be considered simultaneously with the time-dependent structure in degradation paths. Based on the proposed degradation model, an implicit expression of a product's lifetime distribution, and its corresponding mean-time-to-failure (MTTF) was derived. By using the profile likelihood approach, maximum likelihood estimation of parameters, a product's MTTF can be obtained. In the illustrative example, we use the accelerated degradation data for PV module to address the proposed method.

Methods

The 2 x 2 cell modules were fabricated and every module is subject to UV and Damp Heat test as the process flow.

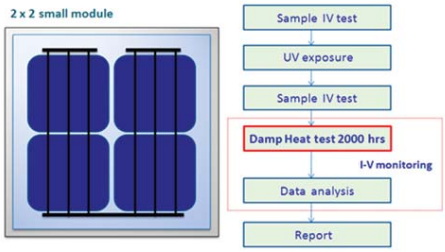


Fig 1. The 4 cells module and test flow

Five conditions of Damp and Heat accelerated degradation tests are conducted, and there are 15 test units for each test environment. In this study, the Run 1 tests had ended.

DOE	(°C, RH%)	k	l
Run1	85/85	n1=15	l1=168 l2=336 l3=504 l4=672 l5=840 l6=1008 . . . ln=2000
	95/70	n2=15	
	85/70	n3=15	
Run2	85/95	n4=15	
	90/90	n5=15	

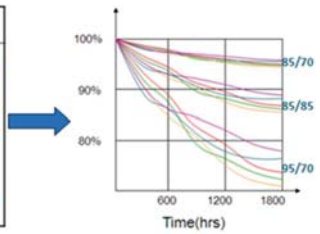


Fig 2. Five conditions of Damp Heat

Lifetime prediction of PV module was carried out by the linear degradation model. The analysis package (iDEMO: integrated degradation models) was used and it was developed by Cheng, Y. S. and Peng, C. Y. It could be downloaded freely at the website: http://www.stat.sinica.edu.tw/chienyu/demo.htm.

$$M_0: \begin{aligned} Y(t) &= L(t) + \sigma_\varepsilon \varepsilon, \\ L(t) &= \Theta t + \sigma_B B(t), \end{aligned}$$

where

- $Y(.)$ is an observed degradation path,
- $L(.)$ is a true degradation with stochastic path,
- ε is a measurement error,
- Θ is a random effect, $\Theta \sim N(\eta, \sigma_\theta^2)$
- $B(.)$ denotes the standard Brownian motion.
- The proposed degradation model is identifiable.

Results

We use the accelerated degradation data at Run 1 to illustrate the proposed method. By Nelder-Mead's optimization algorithm, the maximum likelihood estimations of model parameters can be obtained. Furthermore, by Akaike information criterion, the random effect model with measurement error is suitable for describing the accelerated PV module degradation data. Then, given 20% power loss ($\omega = 0.2$), the estimated MTTF of PV module under (85°C,85%), (95°C,70%), and (85°C,70%) were calculated to be 1.64, 1.37, 2.08 years, respectively. Then, we can extrapolate the estimated MTTF at specific environment conditions by the following equation:

$$T_{0.1}(\text{Temp},\text{RH}) = \frac{1}{24\times 365}\exp\left(\log(\omega) - \hat{a} - \frac{\hat{b}}{273.15+\text{Temp}} - \hat{c}\log(\text{RH})\right). \quad (1)$$

By using the experimental conditions and lifetimes, the estimates of *a*, *b*, and *c* can be obtained as $\hat{a}$ =–1.37, $\hat{b}$ = – 5466.41 and $\hat{c}$ = 1.23, respectively. Fig 3. shows the contour plot of the equation in (1) under the various combinations of temperature and humility. If the normally used condition is (50°C,70%), then the lifetime can be evaluated as follows:

$$T_{0.1}(50,70) = \frac{1}{24\times 365}\exp\left(\log(0.2) - \hat{a} - \frac{\hat{b}}{273.15+50} - \hat{c}\log(70)\right) = 10.86.$$

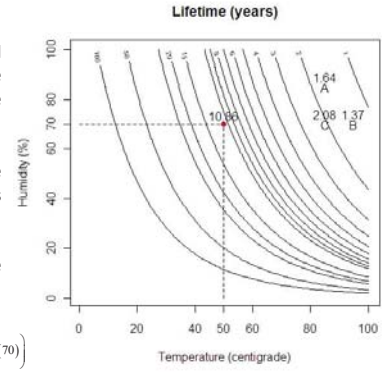


Fig 3. The contour plot of Temp and RH

Conclusions

In this study, motivated by the data of PV module power loss, a general linear degradation model which takes "unit-to unit variation", "time-correlated structure", and "measurement error" into considerations simultaneously was proposed. The product's lifetime under the normally used conditions can be obtained. The estimates are reasonable for practical condition from the experiences of engineering and the viewpoint of material property.

The following two issues are worthwhile for further research: (1). We will implement Run 2 tests with longer testing time around 3000 hrs for Damp Heat testing which will give more clearer accelerated degradation path. (2). We will develop a statistical degradation model for the outdoor testing of PV module.

References

1. Tamizh Mani (2008), "12 year's experience in PV module testing - expansion of testing services", *33rd PVSC*.
2. Meeker, W. Q. and Escobar, L. A. (1998), *Statistical Methods for Reliability Data*, New York: John Wiley and Sons.
3. Peng, C. Y. and Tseng, S. T. (2009), "Mis-specification Analysis of Linear Degradation Models." *IEEE Transactions on Reliability*, 58, 444-455.

Acknowledgements

The authors would like to thank the Dr. Meeker, W.Q, the Professor of Statistics Department of Iowa State University, and the Dr. Tang, Loon Ching, the Professor of Industrial & Systems Engineering Department of National University of Singapore for valuable comments that help to improve the design of experiments and model for data analysis.

Yi-Hung Chou, Delsolar Co., Ltd, No.2, R&D 2nd Road, Hsinchu 30076, Taiwan, ROC
Contact mail : ivan.chou@delsolarpv.com

SENSITIVITY OF PV SYSTEM DEGRADATION RATES TO DATA FILTRATION

Kenneth J. Sauer

2011 PV MODULE RELIABILITY WORKSHOP, NREL, Colorado.
February 16 – 17, 2011

1. Introduction

PROBLEM STATEMENT

- Photovoltaic (PV) project size and financing are governed – and potentially limited – by the confidence investors have in the projected energy production of systems over the terms of their power purchase agreements or planned asset lifetimes.
- Production estimates are largely a function of anticipated annual system degradation rates, which are known to significantly vary both within and across technologies and systems.
- Objectively mining accurate downward trends in system performance over time (commonly referred to as annual system degradation rates) from large sets of historical meteorological and production data is an essential but challenging task, as each step in degradation analysis (summarized at right) carries the potential to contribute uncertainty and error.
- The frequent presence of noise in such data sets, stemming from any number of possible root causes, makes the task all the more challenging.

STEPS IN DEGRADATION ANALYSIS

1. Data input
   - Raw meteorological and production data
     - Quantity – observation interval (hourly or sub-hourly) and time (years)
     - Quality – equipment measurement uncertainties and their evolution over time
   - Integrated external data
     - Incorporation of data from multiple sources (e.g., ambient temperature or wind speed data from nearby RMS)
   - PV module and system characteristics
     - Presence of light-induced degradation (extent and timeframe)
     - Agreement with module "datasheet" parameters (e.g., tolerances, temperature coefficients, NOCT, efficiency changes with temperature and irradiance)
     - Occurrence of downtime or climatic events
     - O&M procedures
2. Data transformation
   - Energy model
   - Thermal model (e.g., Martin Green "simple model", NOCT model, Fuentes, Sandia, CEC, BEW, IEC 61853-1, Dows)
3. Data cleansing
   - Statistical identification and processing of outliers and data shifts
   - Filtration method used to process noisy data that fail to meet user-specified upper and lower qualification limits
4. Data normalization
   - Power model (e.g., PVFORM, Myers, PVUSA, BEW, King, performance ratio)
5. Data evaluation
   - Statistical method (e.g., linear least squares fit, seasonal indexing, classical decomposition, ARIMA)

2. Approach

MODEL

- An Excel/VBA model has been built with a high degree of flexibility in all aspects of degradation rate analysis to enable research on the sensitivities of degradation rates to the numerous possible analytical approaches used to calculate them.
- In an effort to limit the potentially broad scope of investigation that the model allows, this study restricts each step of degradation analysis to one set of model configurations, as detailed in the sections that follow.

OBJECTIVE

- This particular study explores the application of the PVFORM power model as a possible data filtration tool for processing noisy raw input data that fail to meet user-specified upper and lower qualification limits. For global plane-of-array irradiances >125W/m², this model is more commonly referred to as either the single-point efficiency model (with temperature correction), or the power temperature coefficient model.

CASE STUDY

- A system with >1.5 years of continuous historical meteorological and production data is evaluated in this study.
- The chosen system experienced both inverter downtime and significant snow events, which are (thus) present in the raw input data set. Although these events contributed noise to the data that would influence the results of this sensitivity study, the occurrence of such events and presence of noise in raw data are not uncommon for large-scale PV systems. The selected system is therefore considered to be a realistic and not extreme case study.

DISCLAIMERS

- The effects of light-induced degradation, soiling, spectral shifts, sensor drift, and operations & maintenance (O&M) have not been analyzed at this time.
- Potentially sensitive project-specific details (e.g., equipment suppliers and owner information) are left undisclosed at this time.
- As this study is largely a work in progress, several future steps needed to further reduce analytical uncertainty and more objectively evaluate annual system degradation are outlined throughout the following sections.

3. Data Input

Raw Meteorological & Production Data

- 19 full months (1.6 years) of non-spectrally corrected 15-minute interval data were used in this case study. Longer-term (>4 year) data sets expected to yield more meaningful degradation rates will be explored in future work.
- Data for the chosen system included day, month, time, AC energy output (E_ac, kWh), global plane-of-array irradiance (G_poa, W/m²), module backsheet temperature (T_mod, °C), and ambient temperature (T_amb, °C).
- Initial uncertainties for G_poa, T_mod, and T_amb measurements were +/-5%, +/-0.5°C, and +/-0.3°C, respectively.
- Measured T_mod data (recorded for a small sample size of modules) were initially unavailable but eventually obtained.
- E_ac is a summed value, while G_poa, T_mod, and T_amb are instantaneous. It is hypothesized that the nature of the meteo readings as instantaneous (rather than averages or medians) may be contributing noise to the raw data.

Integrated External Data

- No data from external sources were incorporated at this time; however, wind speed data from a nearby reference meteorological and irradiance station (RMIS) will be incorporated in future work.

PV Module & System Characteristics

- The selected case study is a south-facing, ground-mounted, large-scale (>1MWac) system using multicrystalline silicon PV technology.
- The system is located in an area with snowfall and experienced snow events in months 6 (13.3"), 7 (1.7"), 8 (32.9"), 18 (24.5"), and 19 (17.4").
- One 250kWac inverter malfunctioned intermittently throughout month 1 and was offline during much of the latter half of month 12 and beginning half of month 13.

4. Data Transformation

Energy Model

Sandia Thermal Model

- Eq. (1) was used to convert between E_ac and AC power (P_ac, kW) as needed throughout the analysis [1].
- Cell temperature (T_cell, °C) values were required for input into the PVFORM power model (discussed below). As measured T_mod was initially unavailable for the chosen array, the Sandia thermal model was used to convert T_amb to T_mod (Eq. 2) and then T_mod to T_cell (Eq. 3) [2]. Coefficients "a", "b" and "ΔT" were derived using the PVModuleWizard tool provided by Maui Solar Energy Software Corporation, and based on EN 50380 module datasheet values. WS was assumed constant at 1 m/s, inevitably introducing some amount of error. T_mod data for a small sample size of (1) module were recently obtained and evaluated against the Sandia and also California Energy Commission (CEC) thermal models (see Fig. 1 and 2).
- In future work, measured T_mod values will be investigated; however, it is uncertain whether the sample size is large enough to adequately represent the module temperature distribution across the array.

$$(1)\ E_{ac} = \Delta T \cdot \sum P_{ac,i}$$

$$(2)\ T_{MOD} = G_{POA} \cdot \left(e^{(a+b\cdot WS)}\right) + T_{AMB}$$

$$(3)\ T_{CELL} = T_{MOD} + \frac{G_{POA}}{G_{STC}} \cdot \Delta T$$

Figure 1.

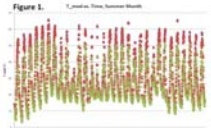
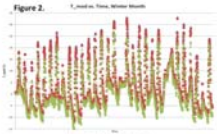


Figure 2.



5. Data Cleansing

Boxplot

(4) Lower limit = Q1 - 1.5 (Q3 - Q1)
(5) Upper limit = Q3 + 1.5 (Q3 - Q1)

- Boxplot analyses on P_ac values and PVUSA regression residuals were used throughout to statistically identify outliers per Eq. (4) and (5).
- Outliers in P_ac were present (and therefore processed) only when the PVFORM model (described below) was not used to filter out data.

PVFORM

For G_poa >125W/m²:

$$(6)\ LL \le \left[\frac{\left[1+\lambda\cdot\left(T_{CELL}-T_{STC}\right)\right]}{P_{ac,stc}}\right] \le UL$$

For G_poa <125W/m²:

$$(7)\ LL \le \left[\frac{P_{ac,i} - \left(\frac{G_{POA}}{G_{STC}}\right)\cdot k\cdot G_{POA}}{P_{ac,stc}}\right] \le UL$$

Table 1.

98%	2	102%
95%	5	105%
90%	10	110%
85%	15	115%
70%	30	130%
0%	100	∞

- The primary objective of this study was to test the sensitivity of degradation rates to filtration, using the PVFORM power model as a possible tool for removing noisy data that failed to meet user-specified upper and lower qualification limits (UL and LL). A successful tool would remove data recorded when inverters were malfunctioning or offline or when snow was covering all or part of the array. If the instantaneous nature of the irradiance and temperature readings truly added noise to the raw input data, this data would likewise be processed.
- For all data above a G_poa threshold of 500W/m² (as defined in the PVUSA section below), P_ac was normalized to Standard Test Conditions using the PVFORM model along with the EN 50380 module datasheet values for the temperature coefficient of P_max (γ) and k coefficient [3,4]. The normalized values were then divided by the total system size (kWp AC STC) and evaluated against the user-specified qualification (qual) limits summarized in Table 1. Whenever the criteria were not fulfilled, the data would be filtered out. The PVFORM-based filtration methods evaluated in this study are summarized in Eq. (6) and (7). Note that the investigated qual limits mostly fall well outside a range of what might be expected for annual system degradation.
- The PVFORM power model is customarily applied to DC (typically module) power. Because only AC data was available, this study is also used to investigate the suitability of the PVFORM model to the AC power of the selected system. It is often difficult to avoid the effects of, e.g., inverter peak power tracking when evaluating long-term system performance or degradation using production data from operational PV systems.

6. Data Normalization

PVUSA

$$(8)\ P_{PTC} = G_{POA} \cdot \begin{pmatrix} A + \\ B\cdot G_{POA} + \\ C\cdot T_{AMB} + \\ D\cdot WS \end{pmatrix}$$

- The multiple regression-based PVUSA power model (Eq. 8) was used to derive monthly system AC power ratings at PVUSA Test Conditions (PTC) from the filtered data set [5,6]. WS was assumed constant in this study as an approximation but will be integrated from a nearby RMIS in future work.
- PVUSA power ratings at PTC (P_ptc, kW) partly eliminate seasonal effects, as new sets of regression coefficients (A, B, C, and D) are generated for each month throughout the observation time. Variations in monthly PTC ratings can be used to indicate module, inverter, or climatic events if they exist in the raw data.
- Following Dows et al., G_poa values below a 500W/m² threshold were removed from the input data set. The effect of using other G_poa thresholds reported in literature (600, 700, 750, 800W/m²) – as well as time of day, P_ac, T_cell, T_amb, and WS thresholds – can conveniently be explored using the model that has been built.
- Additional regression-based models, including the simplified Dows, Myers, BEW, and King models, will be investigated in future work.

PVFORM

- The previously described PVFORM power model was used to derive monthly average P_stc values from the same post-filtered data set described above.

Performance Ratio

- The same data set was also used to derive monthly average performance ratio (PR) values. While the actual values of PR may be arbitrary due to filtration, decreasing trends may be useful for indicating system degradation.
- Although PR normalizes values with respect to solar radiation, monthly PRs are typically highest in winter months and lowest in summer months, resulting from module efficiency reductions at higher temperatures. Due to the pronounced seasonality effects present in monthly PR values, longer time spans are generally needed for deriving meaningful degradation analyses [7].

7. Data Evaluation

Linear Least Squares Fit

$$(9)\ y = m\cdot x + b$$

$$(10)\ R_{DEG}\left(\frac{\%}{yr}\right) = \frac{(m\cdot 12)}{b}\cdot 100$$

- The linear least squares fit method was used to generate trend lines described by Eq. (9) from normalized monthly values of P_ptc, P_stc, and PR.
- The y-axis intercept ("b"), indicating the normalized system power [kWp AC] at the beginning of the observation time, and the slope ("m") of the trend line were entered into Eq. (10) to yield degradation rates (R_deg) [8].
- A system experiencing no measureable annual degradation is expected to have a straight, horizontal trend line. Note that when evaluating the output of a linear regression model in degradation rate analysis, a low R^2 value can be expected due to the low signal-to-noise ratio caused by other sources of normal variation (e.g., spectral shifts). This is particularly true for shorter observation times.

Classical Decomposition

- Although the total observation time was less than the recommended two seasonal cycles, the classical time series decomposition (CD) method was applied for interest and comparison.
- Using the monthly normalized data sets as inputs, the CD method was used to extract the trend component – of most immediate interest in this investigation – from the seasonality and remaining irregular components [9].
- In CD, the trend component is obtained with a centered 12-month moving average applied to the normalized data. An additive model was chosen with a period of 12.
- Following CD, extracted trend values were evaluated using the linear least squares fit-based method described in Eq. (9) and (10) above.
- Future work (following at least two seasonal cycles) will further investigate the resultant seasonality and irregular components further.

8. Results: Data Filtration

Figure 3.

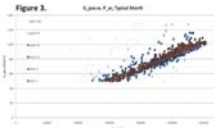
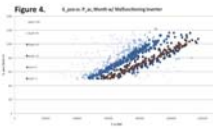


Figure 4.



- For typical months, such as that shown in Fig. 3, it was observed that tightening the qual limits mostly yielded a higher R^2 in the G_poa vs. P_ac trend line while making little or no difference to the fitted trend.
- Interestingly, the slope of the trend lines began to slightly increase for qual limits <5 (e.g., 98-102, 99-101). This may have been due to an overcorrection for T_cell in the PVFORM power model, stemming from the use of derived, rather than measured, T_mod values (where derived values exceeded measured, as previously shown). The relatively small effect was avoided by not exceeding a qual limit of 5 in the subsequent degradation rate evaluation.
- Note that a shift in the opposite direction for tighter qual limits could possibly indicate degradation. For official degradation rate reporting, qual limits and any data that are removed from the analysis should be statistically justified.
- Having applied a traditionally DC (module) power model to AC system power, there appears to be a strong correlation between module and system performance, at least during times of uninterrupted production. This may be indicative of proper inverter sizing and effective maximum power point tracking.
- Months with inverter downtime or snow events showed effects similar to that displayed in Fig. 4. As the qual limits tightened from 100 to 5, the trend line expectedly followed the cluster of data corresponding to higher P_ac values (for given values of G_poa).

9. Results: Data Normalization

Figure 5.

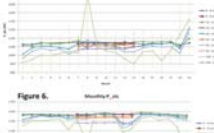


Figure 6.

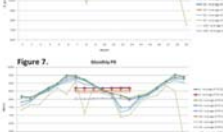


Figure 7.



- Figures 5, 6, and 7 display (as univariate time series) the monthly normalized P_ac values following PVUSA (P_ptc), PVFORM (P_stc), and PR analyses, respectively.
- The graphs seem to indicate the utility of the PVFORM power model as a filtration tool, at least in eliminating noisy data collected during inverter downtime (months 12 and 13) and significant (>12") snow events (months 6, 8, 18, 19). Note that normalized values converged for qual limits well outside an expected range of degradation.
- As expected, the relative standard error around P_ptc values (graphed in Fig. 5) decreased dramatically (from >30% to <2%) as the qual limits tightened from 100 to 5. It is important to note that model error – for all power models – is only one contributor to the total uncertainty associated with the normalized power values.
- As expected, the months with the lowest R^2 coefficients in the pre-filtered G_poa vs. P_ac plots (months 6, 8, 13, 18, and 19) shifted the most following filtration, while the months with the highest monthly R^2 (months 9, 10, 11, 15, 17) shifted the least (see Table 2 below). This helps statistically reinforce the utility of the PVFORM power model as a possible tool for removing noisy data.

10. Results: Data Evaluation

Table 2.

Month	1	2	3	4	5	6	7	8	9	10	11	12	13	14	15	16	17	18	19
R^2	0.37	0.43	0.51	0.40	0.45	0.21	0.51	0.19	0.79	0.56	0.56	0.35	0.15	0.42	0.63	0.29	0.52	0.13	0.50
Rank	12	9	6	11	8	16	7	18	1	3	4	13	17	10	2	14	5	17	16

Table 3.

Qual	PVUSA	ΔR_{deg}	PVUSA - CD	ΔR_{deg}
100	10.7%		6.3%	
30	6.4%	4.3%	3.8%	2.5%
20	6.1%	0.3%	3.6%	0.2%
10	1.7%	4.4%	1.1%	2.5%
5	0.1%	1.6%	-0.4%	1.5%
Qual	**PVFORM**	**ΔR_{deg}**	**PVFORM - CD**	**ΔR_{deg}**
100	-6.0%		-0.9%	
30	0.1%	6.2%	0.6%	1.5%
20	0.3%	0.1%	0.9%	0.3%
10	0.5%	0.2%	1.1%	0.2%
5	0.0%	0.5%	0.1%	1.0%
Qual	**PR**	**ΔR_{deg}**	**PR - CD**	**ΔR_{deg}**
100	0.6%		-0.7%	
30	3.0%	5.6%	0.5%	1.2%
20	3.2%	0.2%	0.9%	0.4%
10	3.4%	0.1%	0.9%	0.1%
5	2.8%	0.5%	0.0%	0.9%

- Table 3 reports the "degradation" rates calculated using both linear least squares fit and CD and following the PVUSA, PVFORM, and PR models. In Tables 3 and 4, differences in rates between the various investigated qual limits and statistical methods are displayed (ΔR_{deg}) for relative comparisons between the different approaches.
- The near-zero or slightly positive rates suggest that the signal-to-noise ratio is too low for a meaningful assessment of, and therefore sensitivity analysis on, the system degradation rate at this time. Any general observations made here will continue to be monitored in future work, given that the results are subject to change as additional data is collected. An evaluation of monitoring equipment may also be conducted to identify any possible lurking variables (e.g., soiling or drift of sensors).
- From the results in Table 4, it appears as if degradation rates calculated using the multiple regression-based PVUSA power model are most sensitive to data filtration, followed by PR and PVFORM.
- Sensitivities to filtration are considerably reduced between qual limits and across power models through the use of CD.
- It appears as if PR is most affected by the use of classical decomposition, followed by PVFORM and PVUSA.

Table 4.

Power Model - Stat Method	PVUSA	PVUSA - CD	Δ	PVFORM	PVFORM - CD	Δ	PR	PR - CD	Δ
Max ΔR_{deg}:	6.4%	2.5%	1.9%	6.2%	1.5%	4.7%	6.6%	1.2%	5.5%
Average ΔR_{deg}:	2.1%	1.3%	0.6%	1.4%	0.6%	0.8%	1.5%	0.5%	1.0%
St. dev. ΔR_{deg}:	2.1%	1.0%	1.1%	2.7%	0.6%	2.1%	2.9%	0.5%	2.3%
Overall (Qual: 100 -> 2) ΔR_{deg}:	10.6%	5.9%	4.7%	6.0%	0.9%	5.0%	6.4%	0.7%	5.6%

11. Summary

- Determining accurate PV system degradation rates is essential in yielding more favorable system production exceedance probabilities and improving the overall financial viability of PV. Such efforts can be challenging, however, particularly when handling large and oftentimes noisy sets of operational and meteorological data. Nearly every step in degradation analysis has the potential to contribute uncertainty and error to the calculated rates.
- An Excel/VBA model was built with a high degree of flexibility in all aspects of degradation analysis. The potentially broad scope of investigation was limited to focusing on the sensitivity of degradation rates to the quantity and quality of data that gets filtered out prior to data evaluation. Given the convenience of the model that was built, however, a number of additional aspects of degradation analysis can and will be explored in future work.
- It is important to note that the intention of this study was not to advocate any specific method of data filtration, but rather to gain experience with one possible approach (PVFORM) as applied to a real, operating PV system. In fact, careful consideration of qual limits would be needed when following this method for official degradation rate reporting. As a general rule of thumb, chosen qual limits and any filtration of data should be statistically justified.
- In this study, a system with >1.5 years of continuous historical meteorological and production data was selected for evaluating the sensitivity of degradation to filtration, using the PVFORM power model as a possible tool for eliminating noise from data sets prior to rate evaluation. The selected system had experienced both inverter downtime and significant snow events that contributed noise to the raw input data set.
- The PVUSA, PVFORM, and performance ratio models were used to normalize P_ac, after which the linear least-squares fit and classical decomposition methods were applied to extract degradation trends.
- As measured T_mod was initially unavailable, the Sandia model (with assumptions) was used to derive module and cell temperatures. Although the recently acquired measured T_mod data show a measureable difference from derived values, the difference seems to have had a relatively small effect following PVFORM-based filtration.
- The results indicated that the PVFORM power model effectively filtered noise (at least that which was caused by inverter downtime and snow events) out of the raw input data set for the selected case study.
- The PVUSA power model (no CD) appeared to be most sensitive to filtration. In all cases, sensitivities to filtration were reduced between qual limits and across power models through the use of CD, particularly for the PR model.
- The chosen system will be continuously monitored to see if and how additional data input affects the calculated degradation rates, as well as the general observations made on the sensitivity of those rates to data filtration.

12. References

1. C. Whitaker and J. Newmiller, Photovoltaic module energy rating procedure: Final subcontract report, National Renewable Energy Laboratory, Golden, CO NREL/SR-520-23942, 1998.
2. D. L. King, W. E. Boyson, J.A. Kratochvil, "Photovoltaic Array Performance Model", Sandia National Laboratories Publication #SAND2004-3535, August 2004.
3. B. Marion, "Comparison of Predictive Models for Photovoltaic Module Performance," in *33rd IEEE Photovoltaic Specialists Conference, NREL, 2008.*
4. STC: 1,000W/m² global POA irradiance, 25°C T_mod, AM1.5g spectrum according to EN 60904-3.
5. R. Dows, et al. PVUSA Procurement, Acceptance, and Rating Practices for Photovoltaic Power Plants, September 1995, PG&E R&D Report #953091000D.1.
6. PTC: 1,000W/m² global POA irradiance, 20°C T_amb, 1m/s wind speed.
7. Marion, B.; Adelstein, J.; Boyle, K.; Hayden, H.; Hammond, B.; Fletcher, T.; Canada, B.; Narang, D.; Kimber, A.; Mitchell, L.; Rich, G.; Townsend, T.; , "Performance parameters for grid-connected PV systems," *Photovoltaic Specialists Conference, 2005. Conference Record of the Thirty-first IEEE* , vol., no., pp. 1601- 1606, 3-7 Jan. 2005.
8. Dhere, N.G.; Pethe, S.A.; Kaul, A.; , "Comparative study of various PV technologies in terms of energy yield and annual degradation," *Photovoltaic Specialists Conference (PVSC), 2010 35th IEEE* , vol., no., pp. 002899-002903, 20-25 June 2010.
9. Jordan, D.C.; Kurtz, S.R.; , "Analytical improvements in PV degradation rate determination," *Photovoltaic Specialists Conference (PVSC), 2010 35th IEEE* , vol., no., pp.002688-002693, 20-25 June 2010.

This poster does not contain any proprietary or confidential information.

Yingli Americas

Fast and reproducible test method to investigate Hot-spot sensitivity of c-Si solar cells

B. Jaeckel, J. Novak, R. Won, and A. Krtschil
Q-Cells SE, Sonnenallee 17-21, 06766 Thalheim, Germany

Introduction

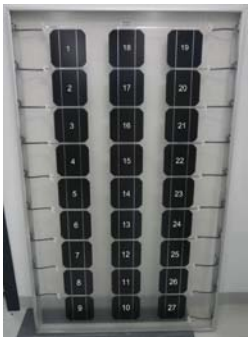
To guarantee the long term reliability of a PV-system it is important to investigate possible failure modes in a regular, easy to use and reproducible way. However, each failure mode might require an individual setup. Among them, the Hot-Spot effect is one of the major and most critical failure modes for PV modules.
We present a test station that enables the user to screen a high number of c-Si cells in dependence of string length in a very short time and very realistically way in terms of possible Hot-Spot failures. This approach provides an excellent statistics of cells from mass production.

Experimental Setup

The experimental setup requires first a sun-simulator of at least class C as a light source, second a specially constructed PV module that acts as a constant power source during the test and third, single cell samples made out of cells with different cell sorting parameters. Both sample and power source modules are kept at a temperature of about 50°C. The design of the source module allows the test expert to vary the maximal voltage depending on whether the product is attributed to 12, 16, 18, 20, 24 of 28 cells/bypass diode. The Hot-Spot test is performed following the procedure described in IEC 61215 ed.2 by varying the size of the shading tool. At critical high temperatures the test time has to be exceeded to more than 5 hours.



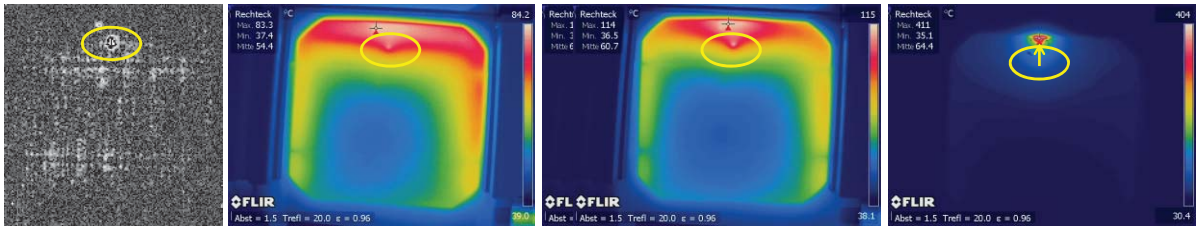




Experimental Results

The following sequence of images shows the cell temperature behaviour as a function on the number of serially connected cells. The black-white-picture of the cell-tester is a differential image with arbitrary units, indicating areas of high Hot-spot risk. The other images are taken with an infrared (IR) camera showing effective cell temperatures.

IR-cell-tester | **Cell in a 12cell-string Tm= 84°C** | **Cell in a 20cell-string Tm= 114°C** | **Cell in a 24cell-string Tm= 411°C**



By increasing the number of serially connected cells from 12 to 20 cells the temperature is increasing. Here the hottest spot in the IR pictures corresponds to the cell tester data. By crossing a certain voltage level (here at 24 cells with 0.6V from each cell), a new mechanism is getting active. This leads to a significant increase in temperature and a new hot spot mode arising at the cell edge. For that special cell (solar cells with damaged laser edge isolation) a maximum temperature of nearly 500°C was observed. These high temperatures lead to a full destruction of the laminate, but not of the cell as it can be seen in the EL-picture. Repeating this test with the same cell, pictures of 12 to 20 cell strings are reproducible, but not for 24 cells. Here the Hot-Spot moves to another region of the cell edge, dependent on the position of the shading tool.
The observed change in hot-spotting mechanism shows, that our test system allows the analysis of different Hot-Spot failures by varying the test conditions. This includes conventional Hot-Spot risks visible in the cell tester IR-images and, moreover, additional risks due to damaged edge isolation which are not visible there.

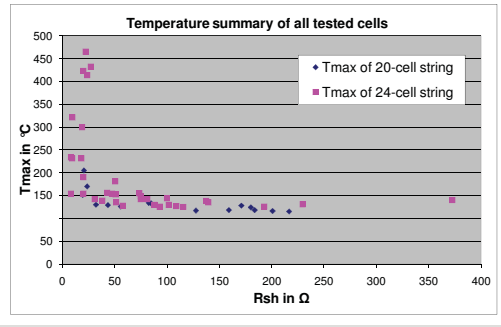
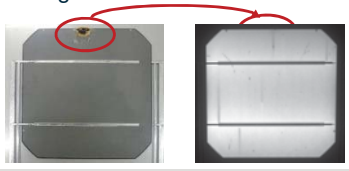


Photo after Hot-Spot Test with defective encapsulation



EL-picture after Hot-Spot Test

Conclusions

Using this setup it is easily possible to investigate and understand the influence of different Hot-Spot failure modes by means of critical temperatures, power dissipation and the size and position of a Hot-Spot.
The results also demonstrate that under more extreme test conditions additional Hot-Spot risks might appear which are difficult to detect in the cell tester IR-data before.

contact: b.jaeckel@q-cells.com

LightSwitch™ ETFE Frontsheet

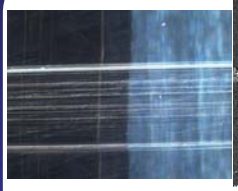
Robert Pleydon, N. Bhiwankar, Phoebe Kwan, Jessica McCoy

Northboro & Worcester Research & Development Center

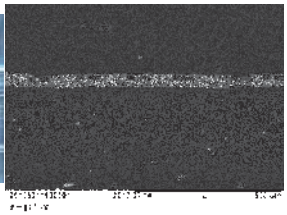
Cut Resistance, with EVA

IEC/UL standard testing

ETFE integrity and electrical resistance maintained



Optical microscope top view of cut test track on ETFE surface (50µ ETFE, over 0.45mm EVA on a steel substrate)



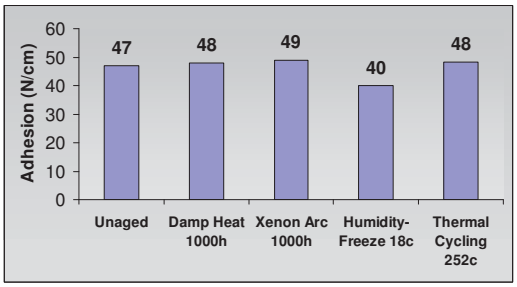
SEM cross section of cut track with ETFE thickness variation

Introduction

- LightSwitch™ ETFE is a fluoropolymer film from Saint-Gobain Performance Plastics
- Physical properties are ideal for a photovoltaic module frontsheet
- Properties are stable in standard climate conditioning processes, UV and outdoor exposure

Adhesion to EVA

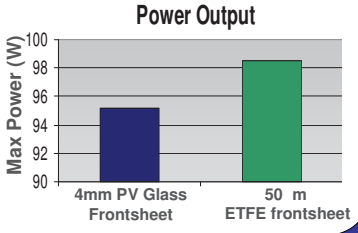
Laminate peel data



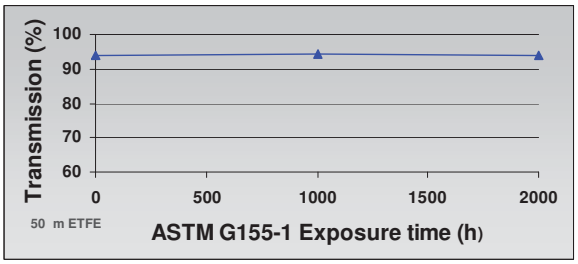
Power Output

Transmission and power output

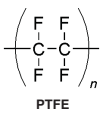
Product	% Transmission ASTM E424
ETFE	> 94%
PV Glass	> 91.5%



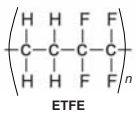
Stability of transmission in UV



Architectural Use



PTFE



ETFE

- PTFE and ETFE share similar chemical structures. Both materials exhibit excellent long-term weatherability
- PTFE has been used in fabric membrane roofing since 1973
- In recent years, ETFE used increasingly in outdoor building and roofing structures due to its high light transmittance and durability
- References: ETFE - The New Fabric Roof
  - *http://www.rci-online.org/interface/2009-01-wilson.pdf*

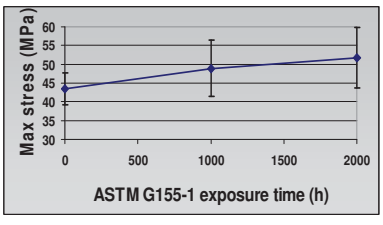


University of La Verne (1973)



Denver Airport

Tensile Strength



LightSwitch™

SAINT-GOBAIN

INNOVATIVE MATERIALS

February 2011

The Thresher Test

Crystalline Silicon Terrestrial Photovoltaic (PV) Modules Long Term Reliability and Degradation



General Test Requirements and Procedures Based on IEC 61215

SCOPE and OBJECTIVE

Currently in the c-Si PV module industry, there is no established and accepted accelerated test of a module's long term performance and reliability. Many manufacturers have proprietary testing regimens, and are using their in-house testing to ensure that their products will hold up well overtime (25+ years) as well as to privately test their competitors' modules for internal benchmarking.

Purchasers of tens of MW of modules spending considerable time working with banking institutions to access project financing are experiencing increasing module quality questions/hurdles/barriers during project financing diligence, as investors/lenders reevaluate long term investment risk due to module quality and performance assumptions.

Though PV module manufacturers strive to ship products that will survive or outlast their stated warranties, very little attention has been given to degradation pattern of those modules while in the field. Simple assumptions of a uniform and linear 0.5 - 0.7% degradation rate in module performance per year are being questioned carefully, especially when array sizes are increasing greatly and the impacts of non-linear, or non-uniform degradation on array performance are considered.

Many module manufacturers spend a considerable amount of time and money on quality, and are not able to monetize that quality given the perceived "commoditization" of the PV module market. Project developer/owner-operators are concerned about the dependability of their energy yield models in years 10-25 (the years beyond the IEC61215 testing schema). Although they want to buy quality, they have had no independent way to verify the proprietary test results shared with them under NDA.

Thus, a critical mass of manufacturers got together and jointly developed an agreed upon long term reliability and degradation testing protocol that can then be implemented by an independent testing authority/laboratory, called "The Thresher Test for c-Si PV", with the intention of bringing long-term performance test data to the market.

This proposed "Thresher Test" will describe a new long-term reliability test program that will not only help in differentiating products, but also in determining the degradation patterns of different c-Si solar modules..

This Thresher Test does not apply to modules used with concentrated sunlight.

CONTRIBUTORS & PARTICIPANTS

Sincere thanks and acknowledgement are given to the following Individuals who have participated in various ways to the development of the "c-Si Thresher Test":

* Hugh Kuhn, Solar Power Partners, - **Program Leader**
* Alelie Funcell, RETC - **Project Coordinator**
* Govindasamy Tamizh-Mani, ASU/TUV Rheinland
* Daniel Cunningham, BP SOLAR
* Matthew Blom, DuPont Photovoltaics Solutions
* Sunil Panda, DuPont Photovoltaics Solutions
* Keith Shellkopf, KYOCERA
* Glenn Tomasyan, MITSUBISHI
* Peter Hacke, NREL
* Sarah Kurtz, NREL
* Jenya Meydbray, PVEL
* Cherif Kedir, RETC
* David King, Sandia Labs
* Alex Marker, SCHOTT
* Paul Wormser, Sharp
* Michael Lasky, Sharp
* Bill Richardson, SOLON
* Neil Shey, SOLON
* Jan Carstens, SOLON
* Oliver Koehler, SUNPOWER
* Monali Joshi, SUNTECH
* Wei-Tai Kwok, SUNTECH
* Jon Haeme, TRINA Solar
* Anthony Chia, TRINA Solar
* Regan Arndt, TUV SUD
* Robert Puto, TUV SUD
* Kenneth Sauer, YINGLI SOLAR

SAMPLING

Eight modules (plus spares as desired) shall be taken at random by a Third Party from a production batch or batches, in accordance with the procedure given in IEC 60410.

The modules must have been fabricated based on manufacturer's BOM and in accordance with the relevant drawings, process specifications / inspections and quality control.

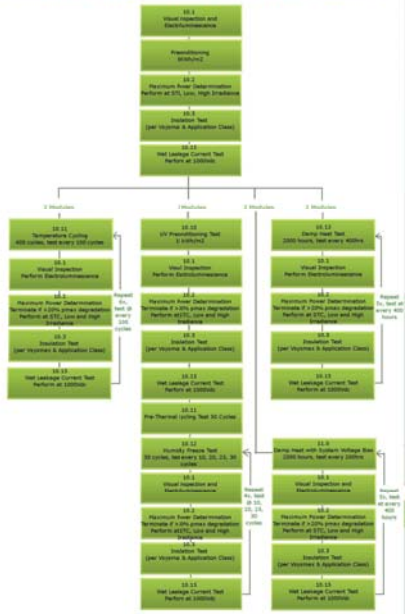
The modules shall be submitted together with manufacturer's Safety Installation Manual showing handling, mounting and connection instructions including maximum permissible system voltage, power rating, application class.

MARKING

All eight modules shall carry the following clear and indelible markings:

- Manufacturer's Name or Symbol
- Model Number
- Serial number
- Power Rating
- Maximum system voltage for which the module is suitable
- Traceability: date and place of manufacture

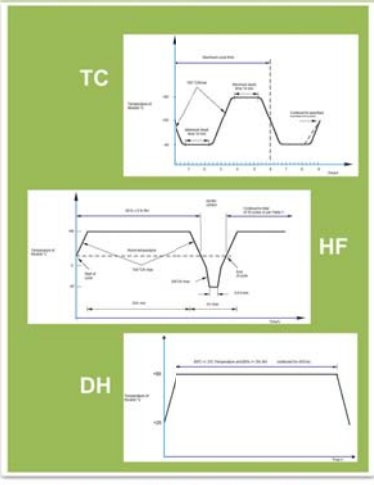
c-Si THRESHER TEST FLOW



TEST DESCRIPTIONS & CONDITIONS

Seq. Clause No.	IEC 61215 Ref. Clause	Title	Test conditions
10.1	10.1	Visual Inspection	See detailed inspection item 10.1.2
10.2	10.2	Maximum Power Determination	See IEC 60904-1
10.3	10.3	Insulation Test	Dielectric withstand at 1 000 Vdc twice the Maximum systems voltage for 1 min For modules with an area of less than 0.1 m2 the insulation resistance shall be not less than 400 MΩ. For modules with an area larger than 0.1 m2, the Measured insulation resistance times the area of the module shall be not less than 40 MΩ·m2 measured at 500 V or maximum systems voltage, whichever is greater
10.4	10.10	UV Preconditioning Test	15 kWh/m2 total UV irradiation in the wavelength range from 280 nm to 385 nm with 5 kWh/m2 UV irradiation in the wavelength range from 280 nm to 320 nm 10 and 600 cycles from -40 °C to +85 °C with 10 °C peak power current applied during the 600 cycles only Test at every 100 cycles increment
10.5	10.11	Thermal Cycling Test	200 cycles from -40 °C, 85 % RH to +85 °C Test at every 10, 20, 25, 30 complete cycles
10.6	10.12	Humidity Freeze Test	Test at every 10, 20, 25, 30 complete cycles
10.7	10.13	Damp Heat Test	1000 hours at +85 °C, 85 % RH Test at every 400 hours increment
10.8	10.15	Wet Leakage Current Test	See details in IEC 61215 clause 10.15 For modules with an area of less than 0.1 m2 the insulation resistance shall be not less than 400 MΩ. For modules with an area larger than 0.1 m2 the measured insulation resistance times the area of the module shall be not less than 40 MΩ·m2 to be measured at 500 V or maximum systems voltage, whichever is greater
10.9	Not included	Electroluminescence	10 Vdc, I= 1(2) Isc
10.10	Not included	Damp Heat with System Voltage Bias	2000 hours at 85C, 85% RH Test at every 400 hours increment

CHAMBER TEST PROFILES



DAMP HEAT w/ SYSTEM VOLTAGE BIAS

Purpose / Objective

Long term degradation by system bias voltage is not covered in IEC 61215 standards. This test is designed to determine the ability of the module to withstand the effects of long-term penetration of humidity with high temperature and system voltage bias. Studies in the industry have shown that in areas where it is hot and humid, there is a greater sensitivity of mc-Si PV modules to system voltage bias degradation. In such environments, damp heat with System Voltage bias enable greater ionic current flow through the module resulting to Sodium ions (Na+) migrating to the TCO / glass interface causing delamination of the TCO, an electro-chemical corrosion. - Some known key drivers are negative cell polarity, moisture ingress, temperature, sodium content in glass and from the atmosphere. (Reference: Peter Hacke, NREL "System Bias Voltage Stress Effects in Multicrystalline Silicon Modules")

System Voltage Bias

- Module 1: Damp Heat with +Ve voltage bias (or as per manufacturer's grounding instructions)
- Module 2: Damp Heat with -Ve voltage bias (or as per manufacturer's grounding instructions)

- The magnitude and polarities of the system voltage should be in accordance to the manufacturers nameplate system voltage rating and applied to the shorted module leads with respect to the grounded module frame.

DATA and RESULTS

The "Thresher Test" goal is not a Pass / Fail test but rather a test designed to gather and report degradation through the course of the test sequences described in Table-1 and Test Flowchart

The Test cycles / hours are as follows:
-Temperature Cycle = 600 cycles at 100 cycles interim test points / puls

-Damp Heat with and without System Voltage Bias = 2000 h at 400h, 800h, 1200h, 1600h, 2000h interim test points / puls
Note: maybe increased to 2500h if 2kh does not provide sufficient degradation to differentiate and to reflect >10, <25 years performance warranty

-Humidity Freeze = 30 cycles at 10, 20, 25, 30 cycles interim tests points / pulls

Testing shall be terminated when one of the following is encountered or achieved:

A. the maximum power output power degradation reaches >20% from initial power rating test data
B. the maximum test sequence cycles / hours are completed

Record and report the following at the beginning and at the end of each test sequence pulls:
-power drop
-leakage current reading
-Visual observations / visual evidence of major defects as described in IEC 61215, Clause-7

DATA REPORTING

The "Thresher Test" data and results will be reported by the 3rd Party Testing Laboratory to the Manufacturer who may decide to publish it, as they see fit.

The Manufacturer can only publish their own data.

The data and results will ultimately be used by Buyers / Developers to enable them to set their own threshold and suit their own requirements.

REFERENCES

IEC 61215:2005, Crystalline silicon terrestrial photovoltaic (PV) modules – Environmental testing – Part 1: General and guidance

Peter Hacke, NREL "System Bias Voltage Stress Effects in Multicrystaline Silicon Modules"

IEC 60068-2-21:1999, Environmental testing

IEC 60068-2-78:2001, Environmental testing – Part 2-78: Tests – Test Cab: Damp heat, steady state

IEC 60410:1973, Sampling plans and procedures for inspection by attributes

IEC 60721-2-1:1982, Classification of environmental conditions - Part 2: Environmental conditions appearing in nature – Temperature and humidity

IEC 60891:1987, Procedures for temperature and irradiance corrections to measured I-V characteristics of crystalline silicon photovoltaic device. Amendment 1 (1992)

IEC 60904-1:1987, PV devices – Part 1: Measurements of PV current voltage characteristics

IEC 60904-2:1989, Photovoltaic devices – Part 2: Requirements for reference solar cells

IEC 60904-3:1989, Photovoltaic devices – Part 3: Measurement principles for terrestrial photovoltaic solar devices with reference spectral irradiance data

IEC 60904-6:1994, Photovoltaic devices – Part 6: Requirements for reference solar modules

IEC 60904-7:1998, Photovoltaic devices – Part 7: Computation of spectral mismatch error introduced in the testing of a photovoltaic device

IEC 60904-9:1995, Photovoltaic devices – Part 9: Solar simulator performance requirements

IEC 60904-10:1998, Photovoltaic devices – Part 10: Methods of linearity measurements

IEC 61853: Performance testing and energy rating of terrestrial photovoltaic (PV) modules 1

ISO/IEC 17025:1999, General requirements for competence of testing and calibration laboratories.

CONTACT INFORMATION

For further questions, please contact:

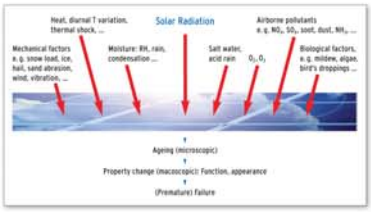
Hugh Kuhn
hkuhn@solarpowerpartners.com
Alelie Funcell
alelief@retc-ca.com

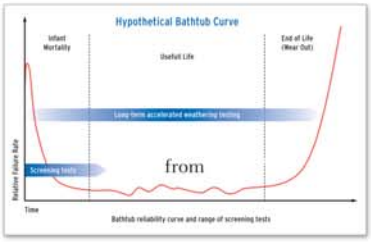
Accelerated Weathering Testing Principles to estimate the Service Life of OPV Modules

Authors: O. Haillant (Ph.D.), ohaillant@atlasmtt.de and Kurt P. Scott, kscott@atlas-mts.com

Reliability Testing of PV Modules ... vs. Long-term Durability Testing

- Outdoor testing necessary to understand failure modes of PV systems, but unacceptably long for decision making.
- Faster ways to predict the reliability of crystalline PV systems rely extensively on Highly Accelerated Life Testing (HALT).
- However HALT are screening tests meant to detect early life failures resulting from materials, design and processing issues that might happen after few years in the field.
- **Design qualification standards** for PV modules (using HALT) screen for **"infant mortality"** on bathtub reliability curve.
- In contrast to crystalline and thin-film PV technologies, OPV technologies do not benefit from standardized design qualification and safety protocols.
- While philosophy of IEC standards may be applicable to OPV, relevance of HALT protocols for polymer-made products needs to be investigated.





- By contrast to reliability testing, durability testing focuses on longer term in-service period where **repeated application of combined environmental stresses accumulates damage** which cause wear-out and eventual failure → Durability is a component of reliability.
- **Environmental durability** of materials impacted by combined effects of **solar radiation, heat, moisture, oxygen,** temperature and moisture cycles + secondary stressors.
- Accelerated weathering testing used for decades by established industries (automotive, plastics & coatings, building materials, etc. ...) to predict durability of polymer-based products.
- Typically addresses **useful life** and **end of life** on bathtub reliability curve.
- May prove highly beneficial for OPV testing and material qualification.

Procedure for Estimating Service Life of OPV Systems

Step 1 – Problem definition

- In-service performance requirements and criteria
- Characterize product, materials and end-use environments
- Run modified FMEA to identify failure modes, root causes and degradation mechanisms
- Understand type and range of degradation factors of importance
- Determine worst-case conditions in end-use environment

Step 2 – Pre-testing

To demonstrate that rapid changes in material properties can be induced by exposure to extreme levels of individual or combined degradation factors. Relies on HALT and HASS

- Supports (or rules out) assumptions/findings made during FMEA
- Determines order of importance for degradation factors
- Provides guidance on applicable levels of degradation factors

Step 3 – Design Test Program

- Test Program: set of test methods (existing or newly designed) intended to test response of product to specific or combination of environmental stresses. Include natural and accelerated laboratory weathering + other ALT
- Determine test specimen types, number and sizes
- Specify evaluation intervals and techniques

Step 4 – Validation of Test Program

- Initiate long-term outdoor exposure(s) at benchmark climates (e. g. hot humid, hot dry, coastal, cold temperate)
- Implement Test Program. May take several months
- Measure and compare property change rates and other criteria of laboratory and (when available) outdoor tests
- Determine correlation and acceleration factor

What makes an Accelerated Weathering Test Method predictive?

REALISTIC

Same stress factors, failure modes and degradation mechanisms as in real life

Correlation of change in properties between laboratory and real life / field results with statistical tools, analytical techniques to determine degradation mechanisms

ACCELERATED

To get answers as quickly as possible

Primarily obtained via controlled increase of stress factors levels. For composite products, cycling of test parameters recommended (temperature, and humidity mainly)

PRECISE

Acceptable repeatability and reproducibility

Precision affected by repeatability of the testing devices, operators skills, variations in test specimens production process. Monitored through using controls of known performance

ATLAS
MATERIAL TESTING SOLUTIONS
An AMETEK Company

From Rigid to Flexible: The Real Challenge of CIGS Module R&D

A. Reithe[1,2*], M. Wachsmuth[1,3], M. Münch[1], M. Meißner[1], S. Tegen[1], K. Heger[1]

[1]Solarion AG, Ostende 5, 04288 Leipzig, Germany
[2]Institut Aufbau- und Verbindungstechnik, Technische Universität Dresden, Helmholtzstraße 18, 01069 Dresden, Germany
[3]Hochschule Mittweida, University of Applied Sciences, Technikumplatz 17, 09648 Mittweida, Germany

Introduction

Solarion develops and manufactures solar modules in pilot stage, based on CIGS thin-film solar cells on ultra thin plastic substrate employing a proprietary ion beam-assisted manufacturing process, that deposits a thin layer of copper indium gallium diselenide (CIGS) at reduced deposition temperatures. The cell materials Molybdenum, CIGS, the buffer layer and ZnO front contact are manufactured in a continuous roll-to-roll process to the 25 micron plastic film substrate. A thin contact grid of silver conductive paste is printed on top of the cells. These will be converted to single cells and sorted to several power classes. These cells can be encapsulated in rigid glass-glass modules as well as in flexible encapsulation systems.

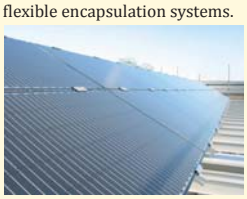


Fig. 1: View of our modules



Fig. 2: Front side view of interconnected cells

Since it is very difficult to predict the lifetime of solar modules using accelerated weathering methods for a defined and limited time, it is necessary to extend the tests beyond the advised limits. This approach leads to a deeper understanding of the development of single defects in the module system and their spreading in the module leading to complete failure.

Experimental Setup

A variety of accelerated weathering tests with scheduled measurements of the performance are carried out for the qualification of flexible or rigid solar modules. Our methods of internal module qualification meet international standards (IEC61646/61730) and go even further.
The modules have to withstand for example more than 400 temperature cycles from -40 to 85 °C as well as damp-heat testing for more than 2000 hours to pass our internal qualification. Also combined and sequential UV/moisture tests are applied to the modules.
Different module configurations with rigid glass barriers and several flexible barrier films have been investigated.
The modules encapsulated with different commercial and lab-stage barrier films were exposed to damp-heat (85% relative humidity, 85°C) for more than 2000 hours . Performance testing and electro-luminescence imaging were carried out in 600 hour intervals for rigid modules and in 100 hour intervals for flexible modules.
A standard AAA pulsed solar simulator according to IEC60904-9 was used for electrical characterization of the samples.
Electroluminescence imaging was performed with a 4 megapixel IR CCD–camera for failure identification .

Durability of Solarion's CIGS on Plastic: Solar Cells in a Glass-Glass Encapsulation System

Weathering tests under damp-heat exposure were performed at rigid glass-glass modules for more than 8000 hours.
In previous studies by Sample et. al. [1] modules using similar CIS technology showed at least 30% power loss relative to the initial value under 4000 hours of damp-heat exposure.
Significantly better results could be achieved in internal tests with our own rigid glass-glass module encapsulation technology. A light power loss of 3% could be observed after the first 1500 hours attributed to a light glass corrosion and water stains.
After intensive cleaning the module showed an increased performance due to the better transmission.
The module performance still remained above 96% of the initial value after 8000 hours in damp-heat testing. No signs of delamination could be found.
Additionally, the wet leakage test was done according to IEC 61646. The isolation resistance was three times higher than required even after such a long time of weathering and completely uncritical. CIS and CdTe modules tested by Sample et. al. [1] failed in this category between 3000 and 4000 hours damp-heat exposure.

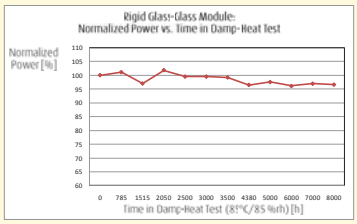


Fig. 3: Normalized maximum power peak (MPP) for rigid modules after damp-heat weathering

Durability of Solarion's CIGS on Plastic: Solar Cells in a Flexible Encapsulation System

Smaller samples with three cells per module were used for the investigation of the flexible barrier systems. These samples were exposed to damp heat for more than 2000 hours. Different encapsulation systems were used including industrial and lab-stage products.
Typically, flexible barriers show a wide range of results in their damp-heat behavior. Aside from complete failures due to moisture ingress after 250 hours of damp-heat exposure very stable barrier materials could be identified.
One lab-stage barrier has already been tested successfully for 4000 hours in damp-heat. The modules show a power loss of only 5% compared to its initial value.

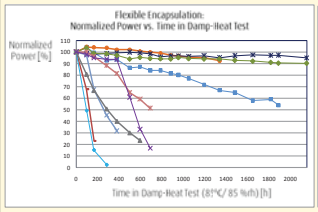


Fig. 4: Normalized maximum power for modules with different flexible barrier materials after damp-heat weathering

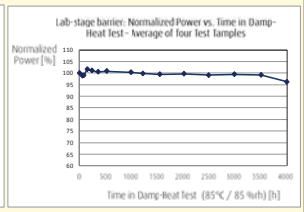


Fig. 5: Normalized maximum power for a module built with a flexible lab-stage barrier after damp-heat exposure of 4000 hours

Conclusion and Outlook

Solarion's rigid glass-glass modules internally tested show very stable behavior. The module performance remains above 95% of their initial power after 8000 hours of damp-heat exposure at 85°C and 85% relative humidity (Fig. 3). These results of the accelerated weathering tests exceed the IEC 61646 standard requirements for thin-film photovoltaic modules for eight times and demonstrate that long-term moisture stability for rigid modules can be achieved.
Also modules with different flexible barrier materials were tested. It was demonstrated that flexible module encapsulation and damp-heat stability for at least 2000 hours do not exclude each other. These results show the feasibility of reliable damp-heat stability for flexible CIGS modules.
Further studies regarding the reliability of barrier systems, including temperature cycling, dry UV and combined UV/damp-heat exposure are already performed or still ongoing and show promising results. Additionally, future works for investigating the mechanical behavior before and after accelerated weathering of flexible CIGS modules will complete our studies.

Acknowlegements

The work was partially funded by the German Federal Government under contract No.03SF0389C.

* Corresponding author contact: reithe@solarion.de

Literature cited

[1] Tony Sample, Artur Skoczek, Michael Field, Michael Köhl, Dieter Geyer, Werner Hermann: *Accelerated Ageing of seven different thin-film Modules by sequential Exposure to Damp-Heat or Damp heat with either additional applied Voltage or Ultraviolet Light*; Proceedings of 24th European Photovoltaic Solar Energy Conference, September 2009, Hamburg, Germany
[2] Thin-film terrestrial photovoltaic (PV) modules – Design qualification and type approval; (IEC 61646:2008)

A DECADE OF COMBINED CYCLE ACCELERATED TESTING

Stefan Jarnason, CSG Solar Pty Ltd, 82 Bay St Sydney, NSW, 2019, Australia
Phone: +612 9695-8148, email: stefanj@csgsolar.com.au

CSG Solar produces Crystalline Silicon on Glass (CSG) photovoltaic modules in its research line in Sydney and pilot scale 20 MW factory in Thalheim, Germany. Although CSG modules have been tested outdoors for over ten years, and have passed IEC 61646 and IEC 61730 qualification testing, CSG Solar conducts additional tests to provide confidence that this new thin-film technology will survive 25+ years in the field. To obtain this confidence two things are required: a) in-depth analysis, understanding and rectification of any failure mechanisms, and b) extended accelerated testing to simulate 25+ years outdoor exposure.

COMBINED CYCLE TEST SEQUENCE

Standard qualification testing simulates less than five years of outdoor exposure and is only intended to provide rapid feedback during product development[1,2]. Realising this limitation, in 1999 CSG Solar developed an extended accelerated testing regime, called "Combined Cycle" testing[3]. A single Combined Cycle consists of the standard IEC Qualification tests being applied sequentially to the same module(s), namely 200 temperature cycles from -40°C to 85°C, then 1000h of damp heat at 85°C and 85% RH, then 10 humidity-freeze cycles from -40°C to 85°C/ 85% RH (Figure 1). If these modules survive one such Combined Cycle, which takes about four months of continuous accelerated testing, the Combined Cycle sequence is repeated until the module output drops below 80% of its initial value. Linear interpolation is used to estimate when output drops to the 80% value, giving a numerical value for the modules durability performance in terms of number of Combined Cycles withstood. Multiple modules are tested to increase the statistical significance.

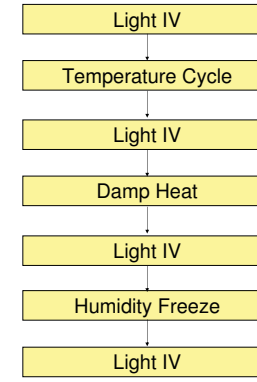


Figure 1: One Combined Cycle sequence.

Advantages of Combined Cycle Testing
- Standard environmental equipment utilised
- Individual exposures well accepted by PV community
- Environmental exposures are within the "normal operating and design conditions" for PV modules
- Continues standard qualification testing for efficient use of durability resources

Limitations of Combined Cycle Testing
- Long test time of 4-12 months required
- No UV or illumination stresses/exposure introduced
- Typically small number of modules under test

COMMERCIAL MODULE COMPARISONS

CSG Solar has more than a decade of results from performing the Combined Cycle sequence on its own modules, and in comparison with other commercially available thin-film modules and traditional crystalline silicon wafer modules. By comparing the results of CSG modules to standard crystalline silicon wafer modules, which have demonstrated their reliability for over 30 years, a relative comparison between the technologies can be obtained. Generally crystalline silicon wafer modules survive approximately 2 Combined Cycles, with remarkable reproducibility between modules from the same manufacturer (Figure 2).

Typically modules from all manufacturers lose some power due to current degradation, however the primary cause of degradation is an increase in the module's equivalent-circuit series resistance. The causes of this increase in series resistance vary between modules, and may be due to delamination, cell cracking, tabbing connections or hot-spots. Although the precise cause of the failure of a laminated module is difficult to diagnose, with the assistance of techniques such as Lock-In Thermography (DLIT)[4], and unique in-module test structures to identify degradation locations, CSG Solar has steadily improved the long term durability of its crystalline silicon on glass modules.

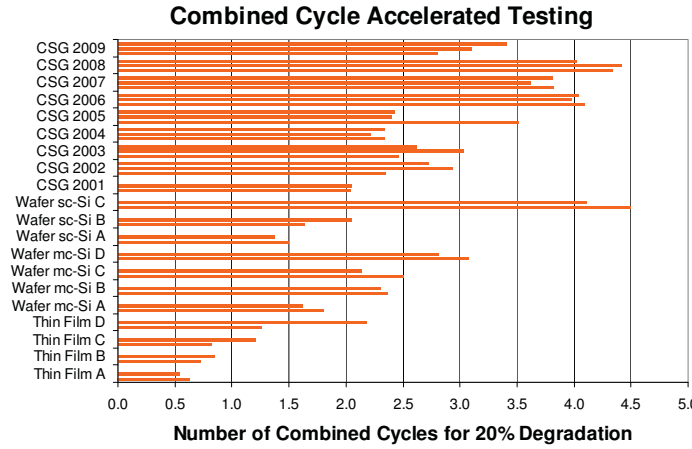


Figure 2: Comparison of commercial and CSG modules in combined cycle testing

DESIGNED EXPERIMENTAL RESULTS

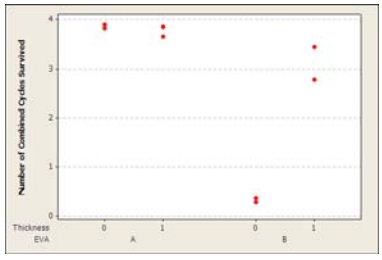


Figure 3: EVA type and thickness experiment

To improve durability a pro-active approach is required to initiate, investigate and test potential module material and process changes. CSG Solar uses a Design of Experiments approach to evaluate proposed module modifications that are based on the previous durability testing results and process advancements,. The results of a typical orthogonal designed experiment comparing two types of EVA in two different thicknesses is given in Figure 3. These results, which were also controlled for material batch, showed that thin EVA B was unable to survive a single combined cycle, while modules with either thickness of EVA type A or with thick EVA type B, were able to achieve 3-4 Combined Cycles before degrading by 20%. Based on this result, EVA type A was the preferred material since it has less susceptibility to thickness and was able to withstand almost 4 Combined Cycles.

Importantly even the poorly performing thin EVA B combination is able to pass the standard IEC 61215/61646 qualification testing, however this combination would be extremely unlikely to survive 25 years in the field. This result demonstrates the advantages of the prolonged Combined Cycle exposure in identifying longer term failure mechanisms.

CONCLUSION

Combined Cycle testing has become the mainstay of CSG Solar's long term durability testing. Over the previous decade this exposure sequence has been demonstrated to consistently identify module degradation that is not detected by the standard qualification testing. The Combined Cycle test sequence is an essential tool in the kit to assess and extend the module lifetime, and is considered a key test that needs to be passed to qualify any significant changes in module processing. The ambitious long term goal of CSG Solar's durability program is to produce modules that consistently achieve survive greater than 4 Combined Cycles, which is primarily achieved by identifying and resolving the identified failure mechanisms.

REFERENCES

(1) Hoffman AR, Ross RG. "Environmental qualification testing of terrestrial solar cell modules", 13th IEEE PV Specialists Conference, 1978, pp 835–842.

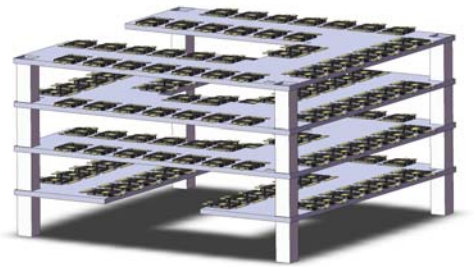
(2) McMahon TJ, Jorgensen GJ, Hulstrom RL, King DL, Quintana MA, "Module 30 year life: what does it mean and is it predictable/achievable?", National Center for Photovoltaics Program Review Meeting, 2000.

(3) MA Green, et al, "Crystalline silicon on glass (CSG) thin-film solar cell modules", Solar Energy 77, 2004, pp 857-863.

(4) Straube H, Wagner J, Breitenstein O, "Interpretation of lock-in thermography on thin film solar cells considering dissipative and Peltier contributions", 10th International Conference on Quantitative InfraRed Thermography, 2010, pp 221-227.

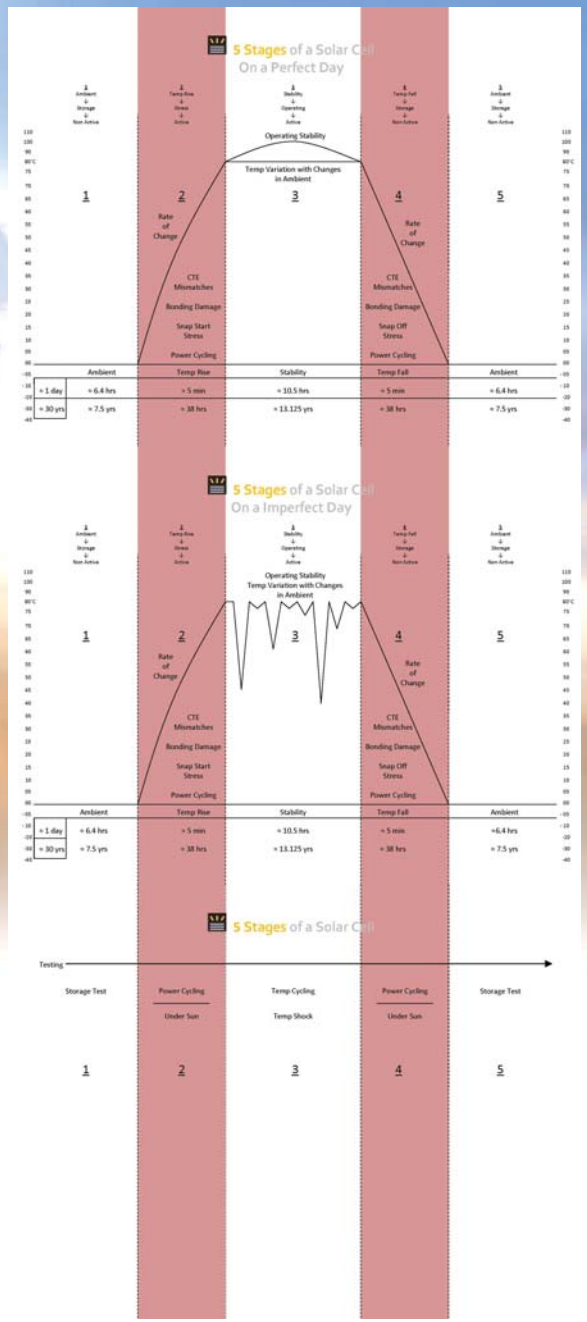
Solar Junction

Forward Bias Test Fixture



N.I.S.T. Cycling Chamber
-40°C to 110°C





- Rate of Change
- CTE Mismatches
- Extremes of Change
- Repetition Rate

High Temp Storage



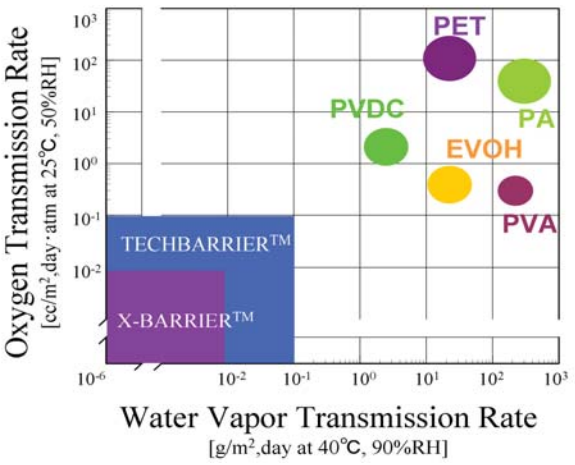




* This Poster Containd No Confidential Information

High Moisture Barrier Flexible Front Sheet for CIGS

O.Akaike, T.Aya, N.Ninomiya,Y.Mitsukura and S.Kanai
Gas Barrier Film Development Centre, Mitsubishi Plastics Inc. Japan

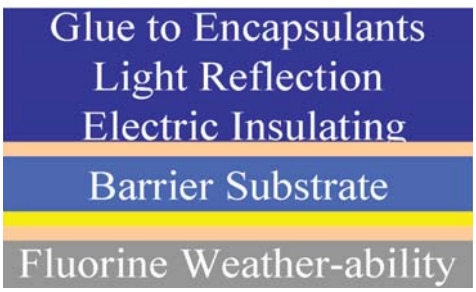


MPI established first toehold in food packaging market by transparent high gas barrier film 'TECHBARRIER™' at the begging of '90s. MPI has been major supplier in world wide for more than 20 years.

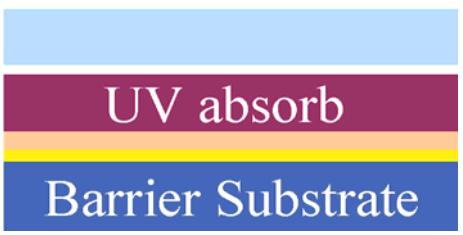
MPI launched the sales of the transparent super high barrier films 'X-BARRIER™' for the PV markets with supply reliability.

We have evaluated the 'X-BARRIER™' by several acceleration tests, damp-heat, fluorescent UV and we have found that the new developed 'X-BARRIER™' which are laminated with functional films via proper adhesives, have marked the highly durable performances through the acceleration tests.

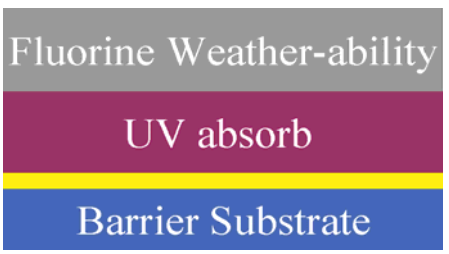
Features of X-BARRIER™ : PV Back Sheet & Front Sheet



Back Sheet :Thickness : 200 to 250 micron
WVTR : 10^{-2} to 10^{-4} [g/m² day] 23ºC

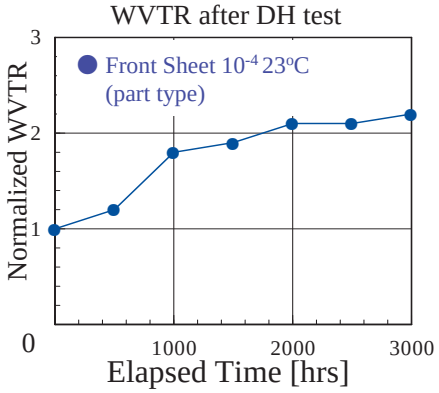


Front Sheet (Part Type)
Thickness : 75 to 150 micron
WVTR : 10^{-3} to 10^{-4} [g/m² day] 23ºC

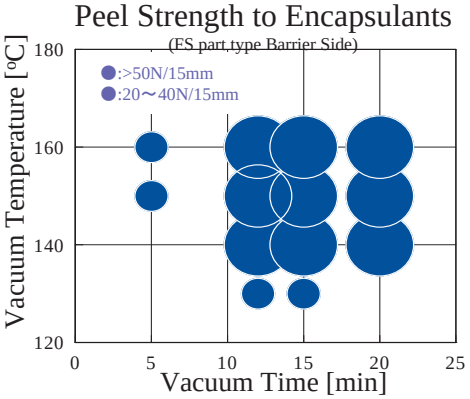


Front Sheet (Whole Type)
Thickness : 80 to 150 micron
WVTR : 10^{-3} to 10^{-4} [g/m² day] 23ºC

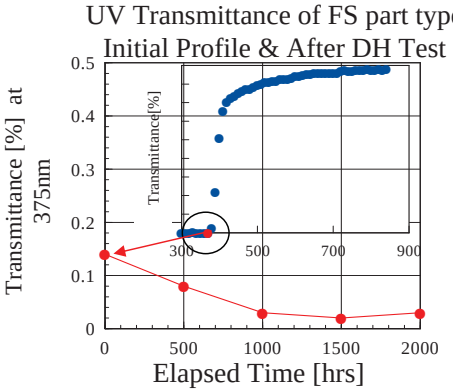
WVTR after DH test



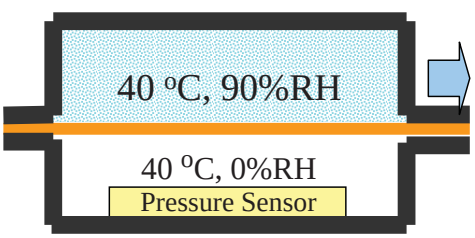
Peel Strength to Encapsulants

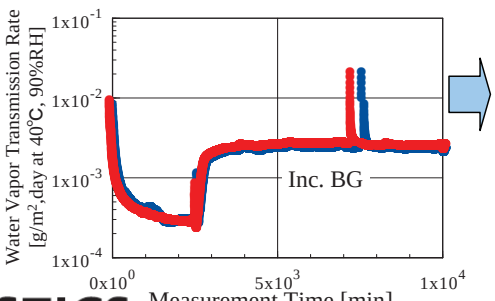


UV Transmittance of FS part type
Initial Profile & After DH Test

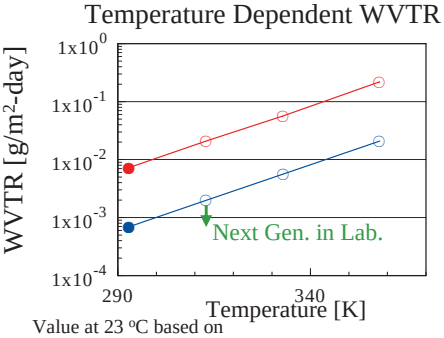


MPI Precise WVTR Measurements : Differential pressure method





Temperature Dependent WVTR



Value at 23 ºC based on
apparent activation energy

MITSUBISHI PLASTICS





Product Reliability Challenges due to Packaging in A-Si Thin Films Modules

Deepak Shivaprasad, Novasolar Technologies, Hayward Ca, USA

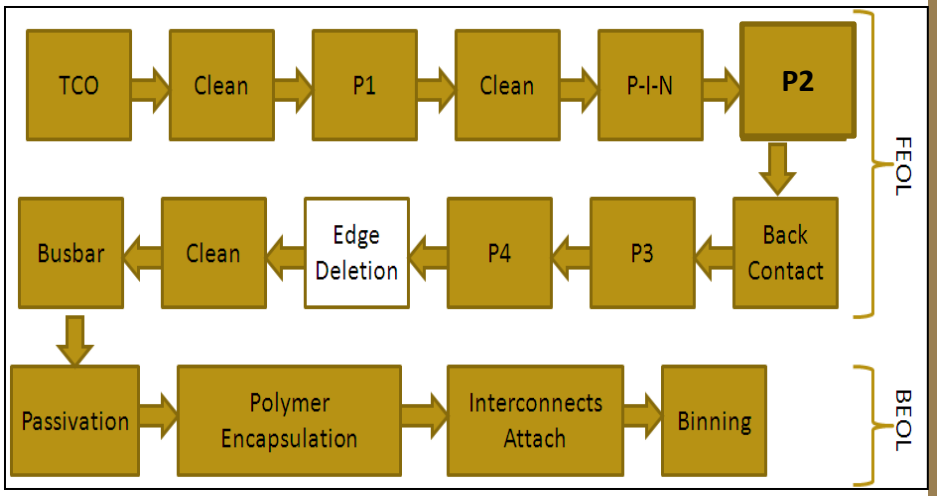
NovaSolar 新日能

Introduction

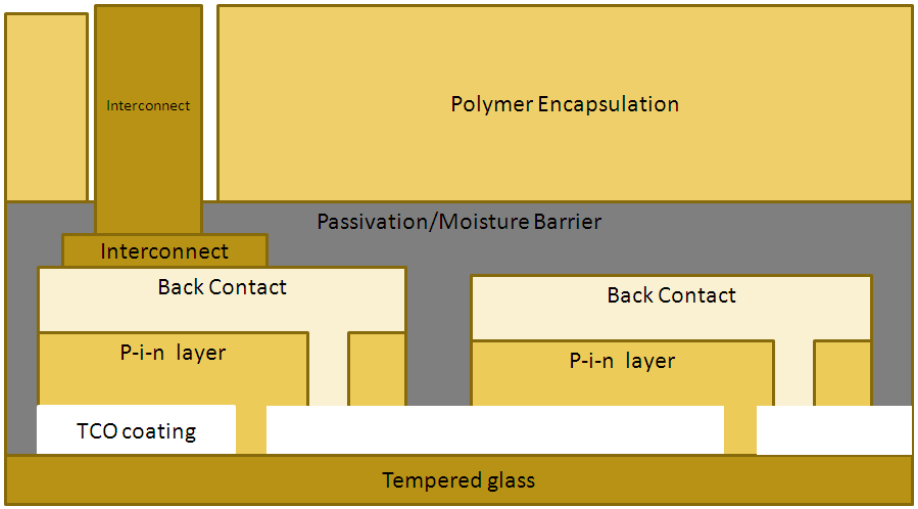
Packaging of the thin film modules is a significant contributor for the product reliability in the field.

We found that the contributions of the edge deletion methodologies on the module reliability is paramount and contributes to the long term performance of the module.

Effects of temperature, voltage, moisture, current, and were studied on the modules with edge deletion both Sand Blast Techniques and Laser Based Techniques



Novasolar's Continuous Module Production Process



Novasolar's Module Construction

NovaSolar 新日能

Key Reliability Challenges – Edge Deletion Using Sand Blasting

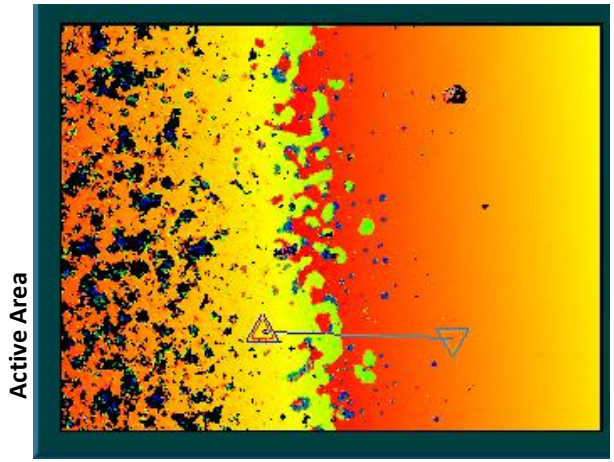
Novasolar found Sand Blasting Technique causing the

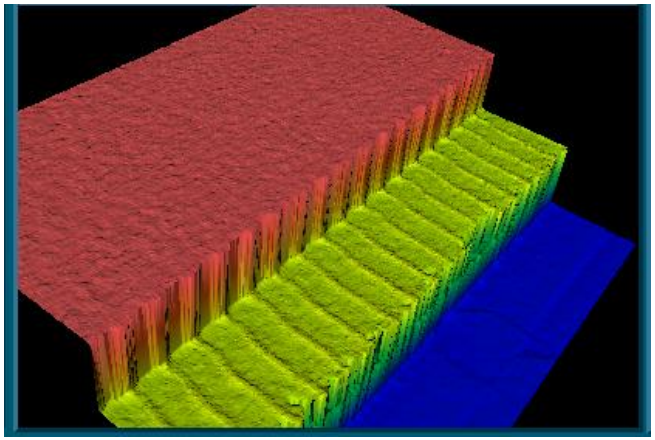
1. Delamination of Encapsulation during accelerated stress testing
2. Failures caused due to delamination of the encapsulation and moisture ingress
3. Field Failures caused due to delamination in the active area
4. Random module breakages in the field

NovaSolar 新日能

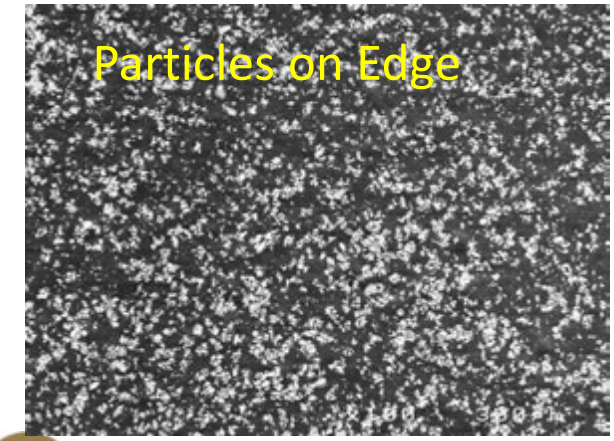
Edge Finish Comparison Sand Blast Vs. LED

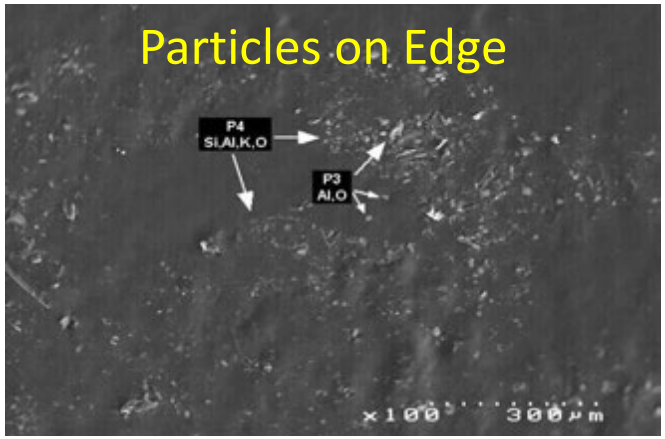
Sand blast ED Process	Laser ED Process





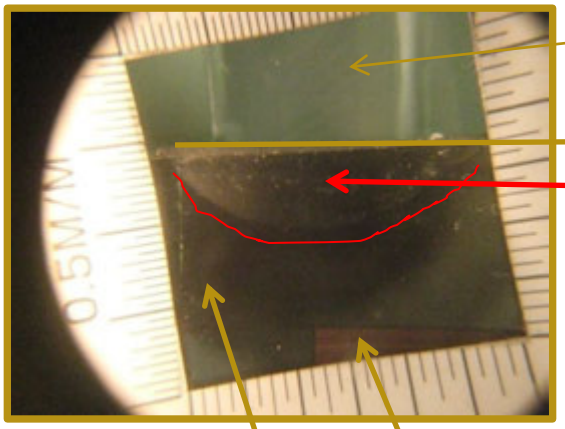
Sand Blast caused a very rough and contaminated edge unlike Laser Edge Deletion Method causing adhesion issues for the polymer encapsulation and causing Delamination

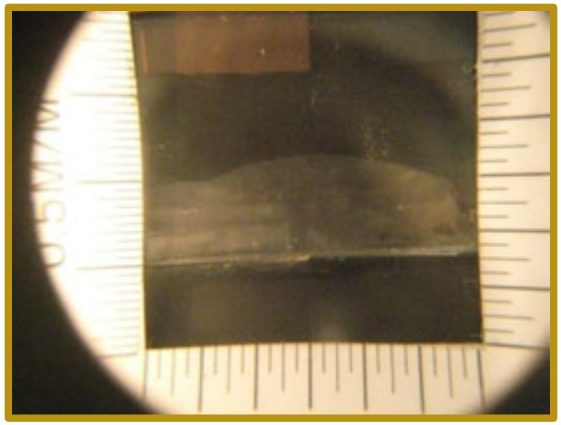


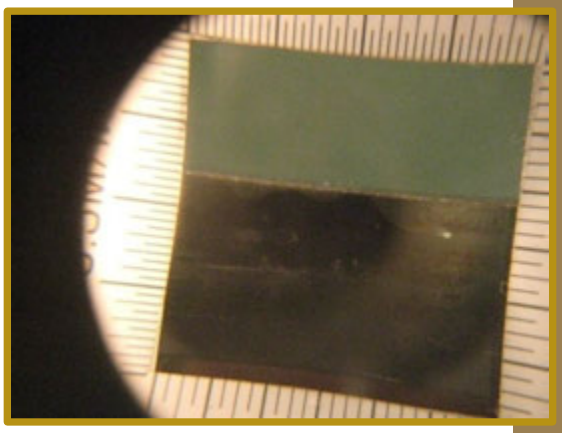


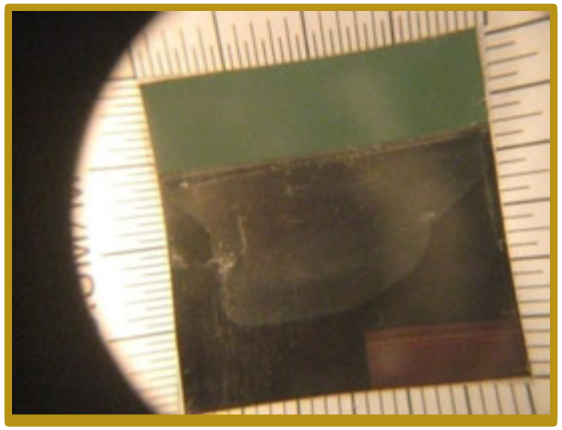
NovaSolar
新日能

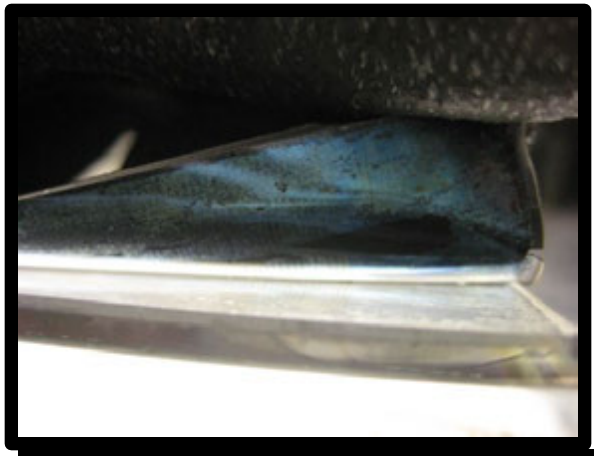
Edge Delamination Post Accelerated Testing



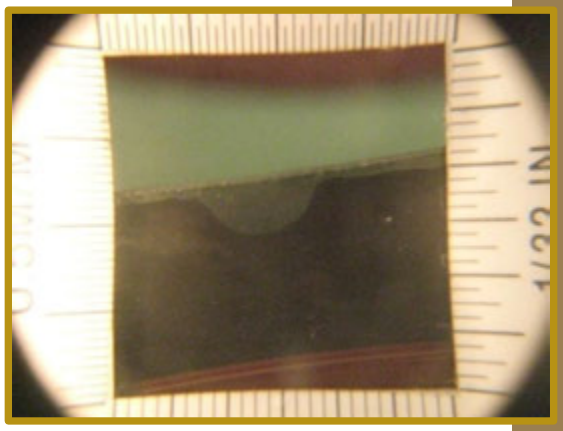








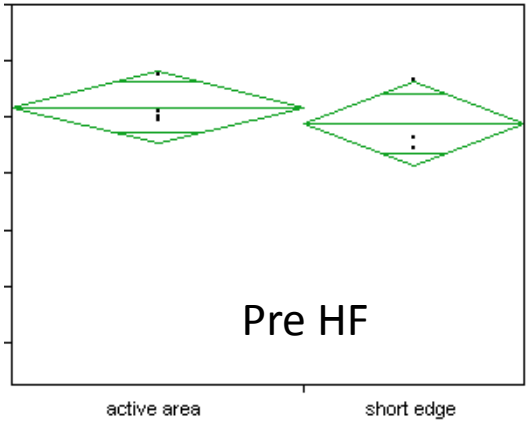
Polymer peel off due to poor adhesion & Contamination Post HF

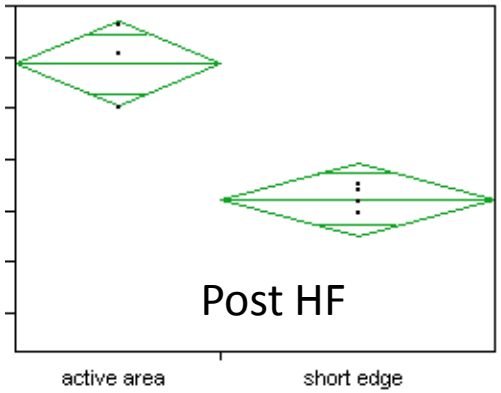


NovaSolar 新日能

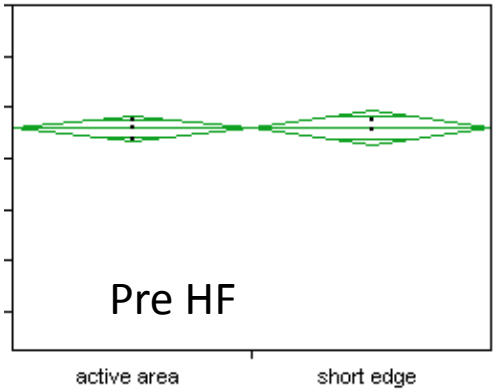
Adhesion of the Encapsulation to the Stack : Mechanical Pull Experiments

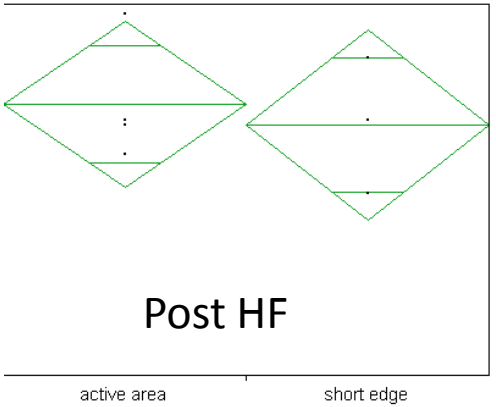
Sand blast ED Process





Laser ED Process





Lower Adhesion on the edge of the modules found caused due to the Sand Blast's rough and contaminated edges and the same effect amplified post accelerated stress testing

NovaSolar 新日能

Mechanical Testing : Rupture Test Results

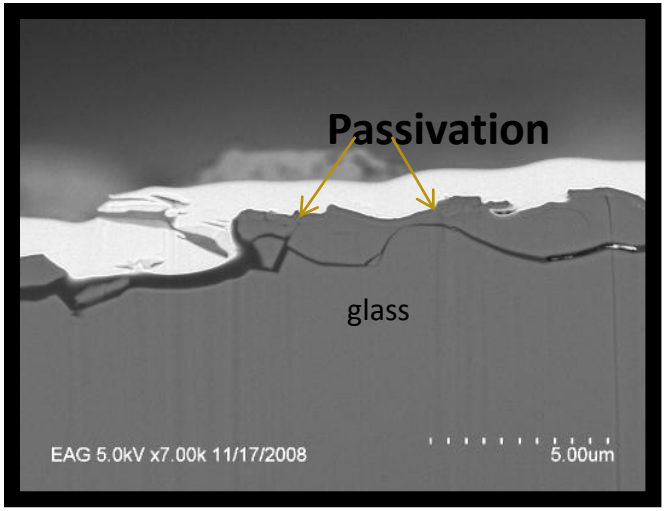


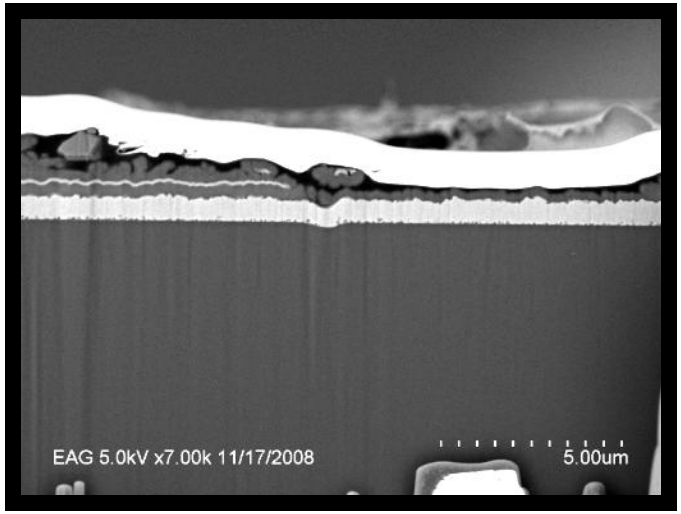
Sr. No.	Sample	Condition	Breaking Load (lbs)	Breaking Stress (lbs/cm^2)	Breaking Stress (lbs/in^2)
1	Sand Blast	Temp40_RH80	222	3088.02	19922.67
2	Laser Edge Deletion	Temp40_RH80	267	3713.97	23961.05
3	Sand Blast	Temp80_RH80	229	3185.39	20550.86
4	Laser Edge Deletion	Temp80_RH80	272	3783.52	24409.76
5	Laser Edge Deletion	Room Conditions	289	4019.99	25935.37
6	Laser Edge Deletion	Room Conditions	283	3936.53	25396.92
7	Sand Blast	Room Conditions	208	2893.28	18666.29
8	Plain Glass	Temp40_RH56	264	3672.24	23691.82

Glass Micro-cracks due to Sanblast Edge Deletion Causing Poor Adhesion and Lower Module Strengths

NovaSolar 新日能

Glass Micro cracks due to Sand Blasting





Glass Micro-cracks due to Sanblast Edge Deletion Causing Poor Adhesion and Random Module Breakages in the Field

NovaSolar
新日能

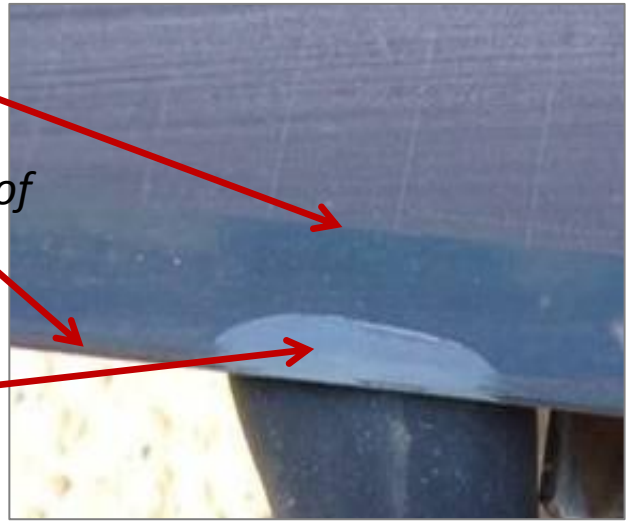
Delamination in Field Caused Due to Contamination from Sand Blast & Resulting Poor Encapsulation Adhesion

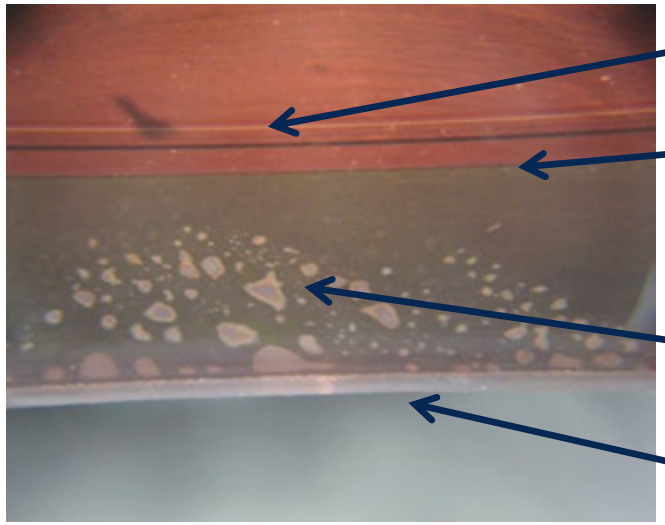
Gross Delamination

- Continuous from edge
- Large scale (> 10mm width)
  - Rarely more than 5mm deep

Bubble Delamination

- Not continuous
- Individually small (< 5mm)



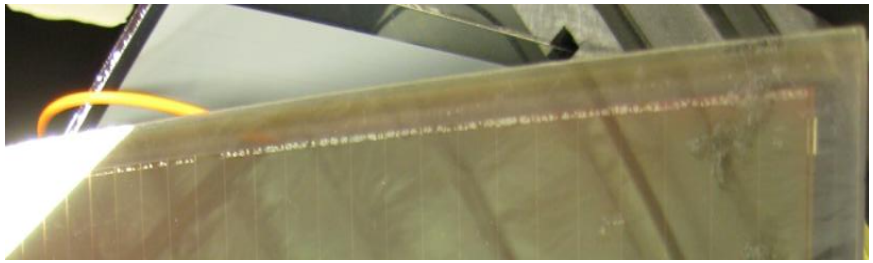


NovaSolar 新日能

Arcing Effects Due to Sand Blasting



Arcing effects observed across isolation scribe due to pockets of un-removed TCO in the edge area - Issue found in the field



Arcing effects observed across isolation Scribe due to pockets of un-removed TCO in the edge area – Issue Simulated in the Lab during Accelerated Stress Testing

NovaSolar
新日能

Conclusions

- Novasolar has found both by accelerated stress tests and field exposure tests that Sand Blasting used for Edge Deletion contributes negatively to the module reliability and long term performance

- Seeing the effects of Sand Blast Technique, Novasolar Technologies switched to Laser Based Techniques on the production lines and saw a significant improvement in the module reliability performance

NovaSolar 新日能



NovaSolar

新 日 能

NovaSolar
新 日 能

Light Soaking Effects on PV Modules: Overview and Literature Review

Michael Gostein and Lawrence Dunn
Atonometrics, Inc.
Austin, Texas 78757
www.atonometrics.com

Prepared for NREL PV Module Reliability Workshop
February 16-17, 2011

michael.gostein@atonometrics.com
lawrence.dunn@atonometrics.com

Abstract

- Light exposure of PV modules can produce a variety of effects including reversible metastable phenomena which influence the accuracy of PV module power output determination and long-term phenomena which affect power output stability of installed modules.
- We present a brief review of technical literature on the effects of light exposure on different PV module technologies, including a-Si/μc-Si, CdTe, CIGS, and c-Si, addressing: the physical mechanisms of light-induced changes in each PV technology; long-term light-induced degradation effects; and current literature knowledge on PV module preconditioning for accurate power output determination.
- Our poster is intended to provide an overview and to promote discussion on these subjects amongst workshop attendees.

a-Si / µc-Si

Amorphous Silicon

- Typical device structure, Ref [1][A]
- Light-induced degradation (LID) causes ~10-30% efficiency loss in first several hundred hours of light soak, Ref. [2][B]
- IEC 61646 qualification test introduced extended duration light soak requirement for module stabilization
  - Light soak until power varies <2% in successive 43 kW-hr/m^2 periods
- Microcrystalline silicon (μc-Si) shows increasing level of LID depending on amorphous content, Refs. [3],[4]

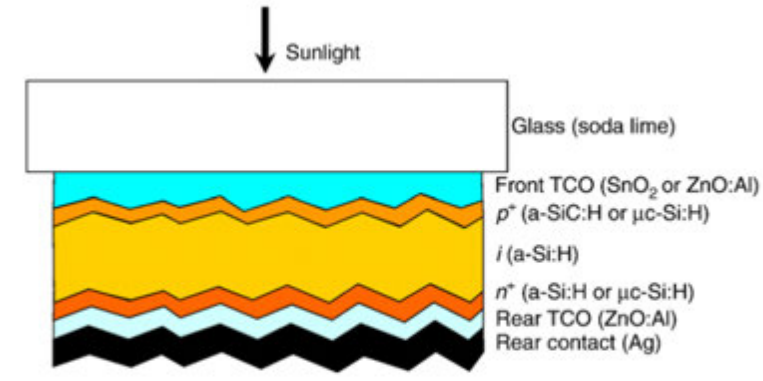
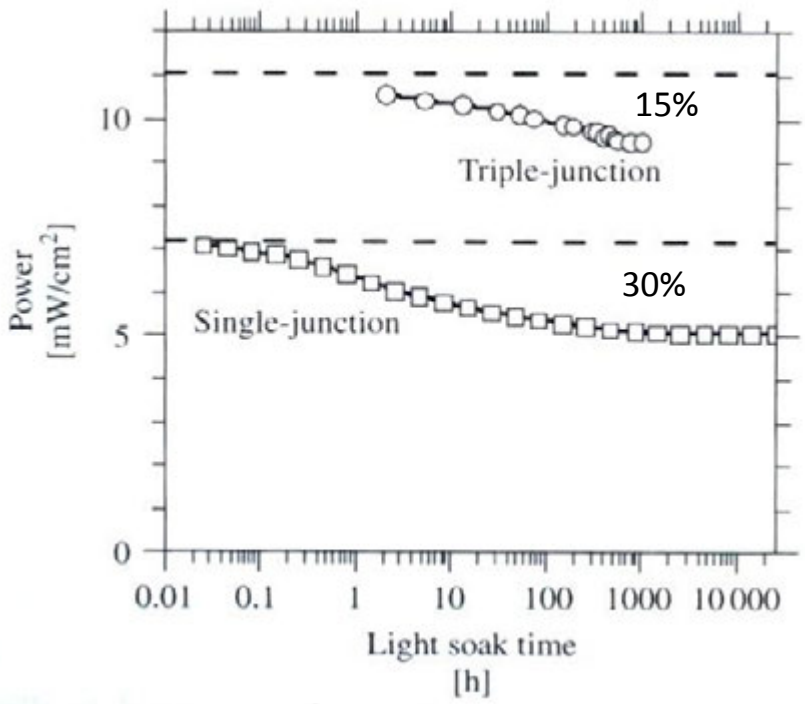


Fig. 1. Schematic of a state-of-art *p-i-n* a-Si:H solar cell on a glass superstrate.

From Ref. A



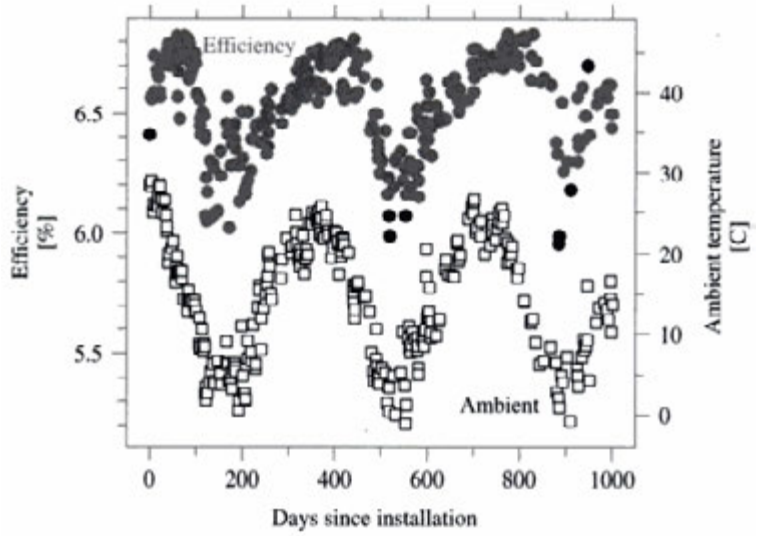
From Ref. B, page 511

Staebler-Wronski Effect in a-Si

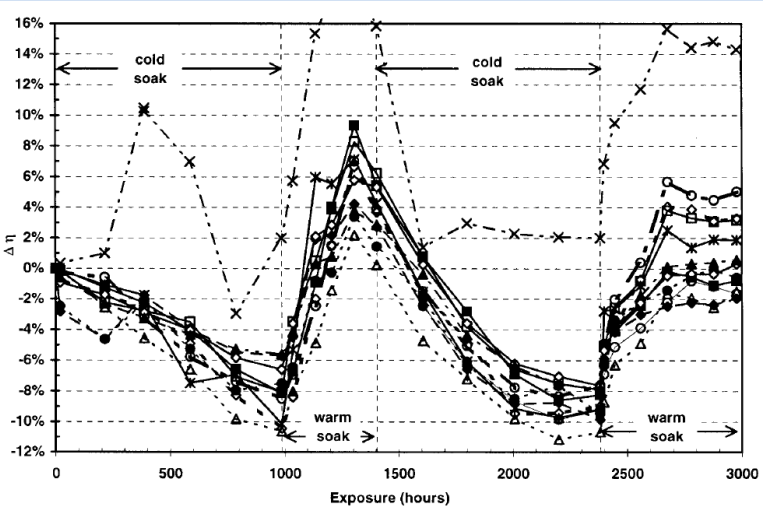
- Staebler-Wronski effect (SWE)
  - Staebler and Wronski, 1977, Ref. [5]
  - Reduction in dark conductivity and photoconductivity of a-Si:H after light exposure
  - Reversible by annealing >150 C
- Mechanism, Ref. [6]
  - Recombination-induced breaking of weak Si-Si bonds by optically excited carriers after thermalization, producing defect centers that lower carrier lifetime
  - Self-limiting effect
- Details
  - Many proposals, but exact microscopic mechanism not fully understood
  - Intrinsic effect – does not depend on impurities, Ref. [7]
  - Occurs in bulk of material, with additional surface contribution, Ref. [6]
  - Defects introduced by e.g. current injection produce different results, Ref. [6],[8],[9]
  - Accelerated testing possible using high-intensity pulsed light, while maintaining standard operating temperature, Ref. [8]
  - Annealing behavior correlated with H diffusion, Ref. [6],[7]
- Review of possible defect structure models and reaction mechanisms, Ref. [9]
- Recent theoretical analysis and proposed mechanisms, Ref. [7],[10]
- Simulation of a-Si:H device performance upon light exposure, Ref. [11]
  - Thinner cells show reduced light-induced performance degradation

Seasonal Effects in a-Si

- Seasonal effects
  - Correlation of a-Si performance with daily mean temperature, Ref. [2][A]
  - Due to partial annealing of defects causing SWE
  - 10-15% relative changes
- Temperature effects in light soaking
  - Stabilized efficiency depends on temperature during exposure, Ref. [12][B]
  - SWE degradation vs. annealing
  - Warm-soak = higher efficiency
- Stabilization of module performance correlated with temperature at installation site, 2008 study
  - Modules installed at higher-temperature locations have better performance, Ref. [13]
  - Similar for single, dual, triple-junction



From Ref. A, page 512

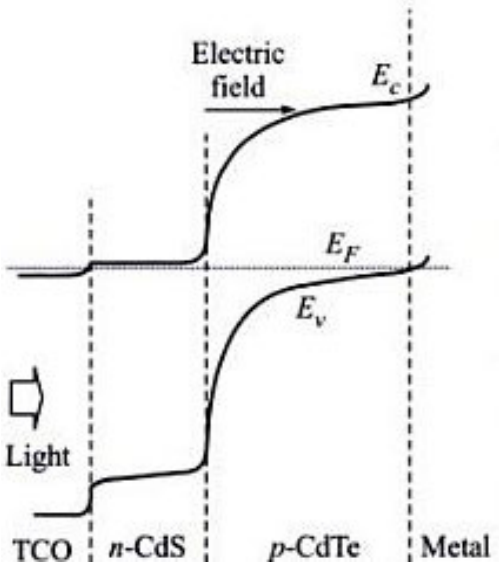


From Ref. B. Cold soak ~ 25 °C; Warm soak ~ 50 °C.

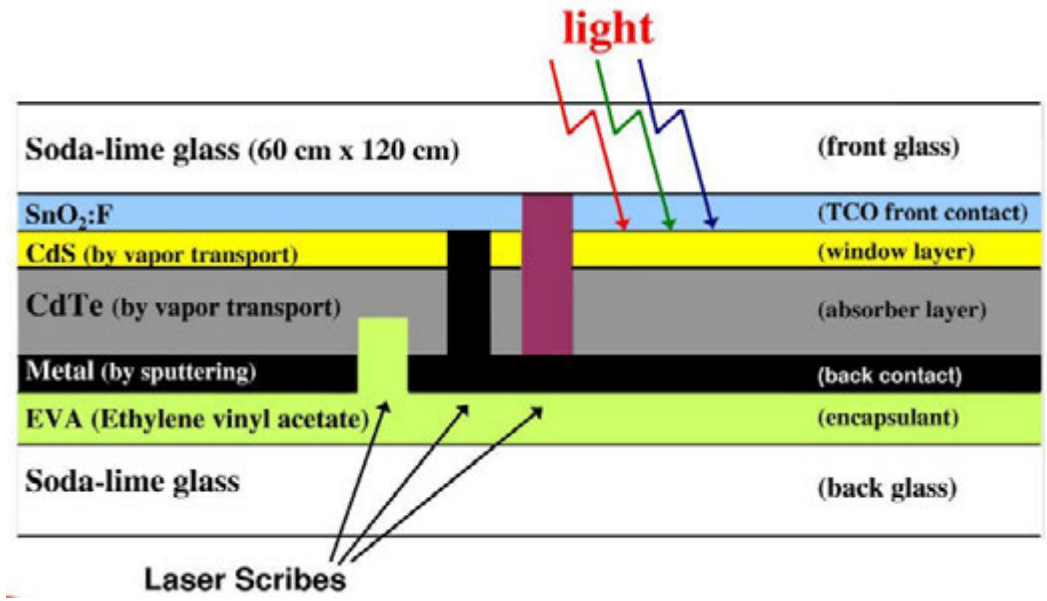
CdTe

CdTe Cell Structure

- CdTe device structure: TCO / n-CdS / p-CdTe / back-contact ([14][A], [15], [16], [17][B])
- Back-contact metallization problematic – requires high work function for ohmic contact
  - Various back-contact metallizations used (see e.g. [18]).
  - A Te-rich interfacial layer is beneficial. Ref. [18], [19]
  - A Cu component is beneficial, although Cu diffusion causes stability issues.



From Ref. A, page 209

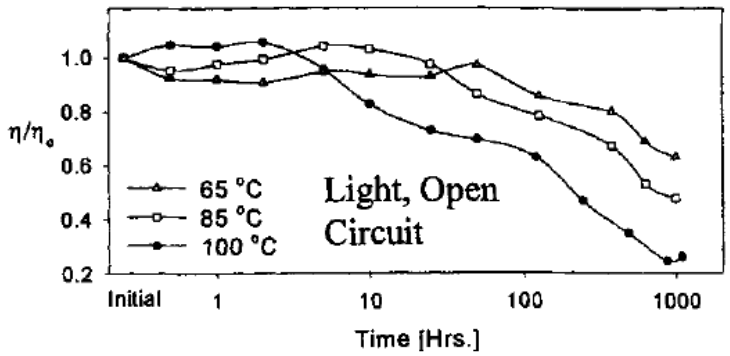


From Ref. B

Extended Duration Light Soaking of CdTe

- Extended duration studies of light soaking reveal need for long-term testing. [20][A]
- Accurate determination of long-term performance required >5000 hours of light soaking per sample.

- High temperature accelerates degradation [21][B]



From Ref. B

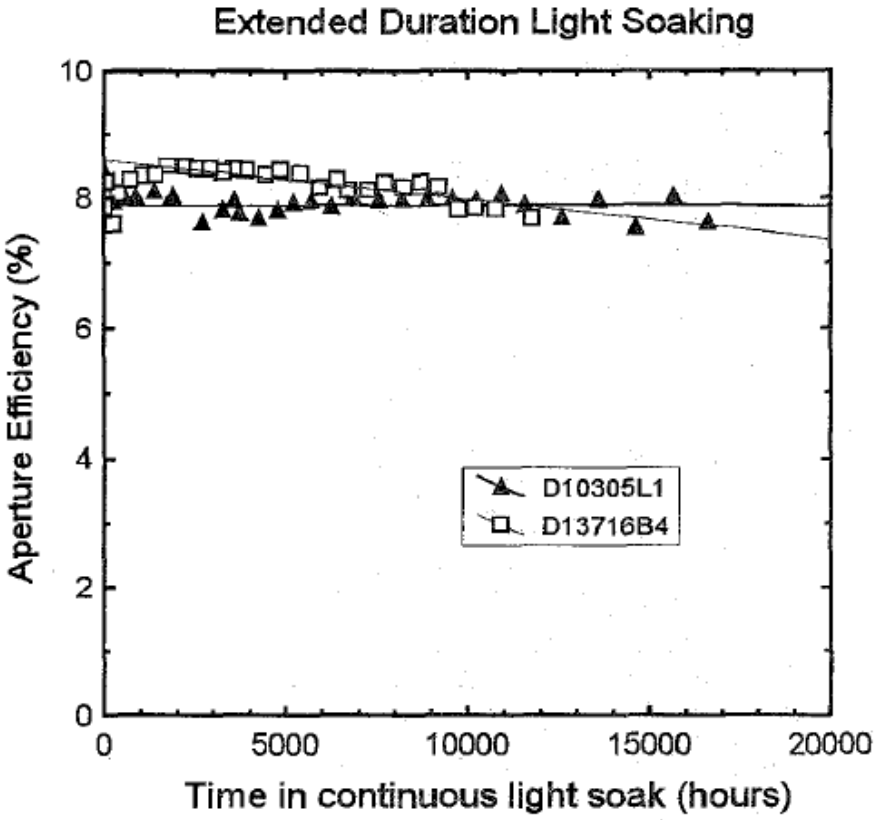
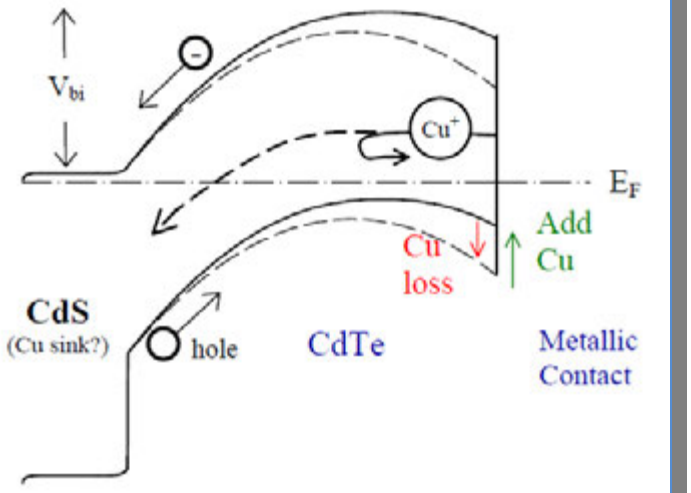


Figure 1. Performance history of two sub-modules fabricated using different recipes. The need for long term testing is apparent.

From Ref. A

Copper Diffusion from Back-Contact in CdTe

- Cu diffusion, Ref. [22][A],[23],[24][B]
  - Back contact in CdTe forms diode of opposite polarity, limiting performance
    - See e.g. modeling in [25]
  - Addition of Cu lowers back-barrier height and improves J-V performance [24]
- Cu loss via diffusion through CdTe (e.g. at high temperature) increases back-barrier height and reduces fill factor
- Light soaking stress leads to efficiency loss



From Ref. A

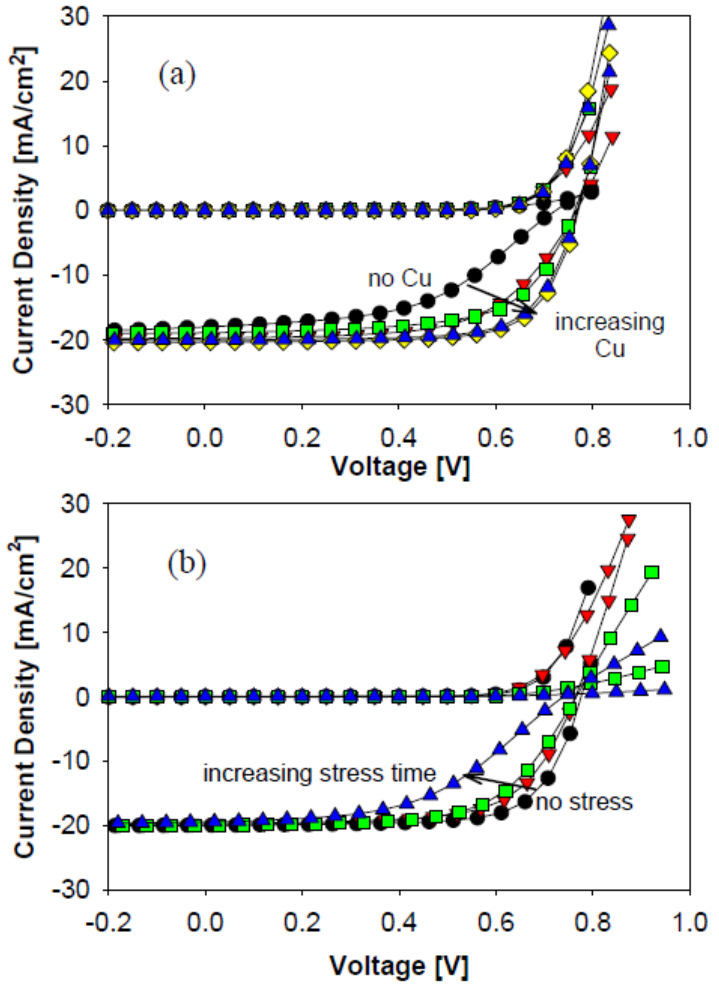
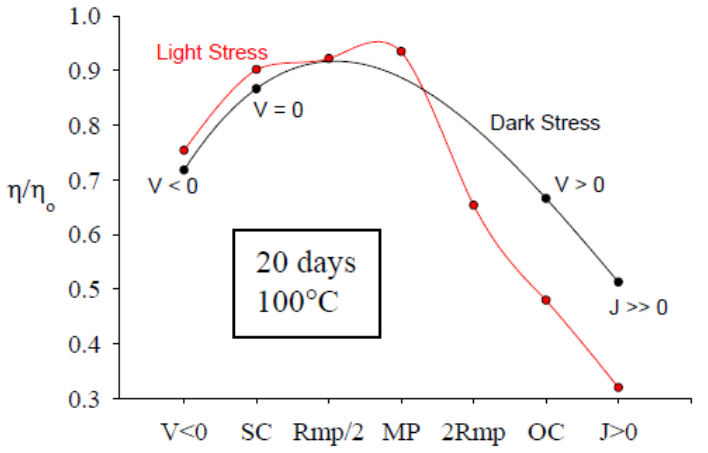


Figure 3. Variations in J-V curves with (a) amount of copper concentration and (b) stress time [from Ref. 5].

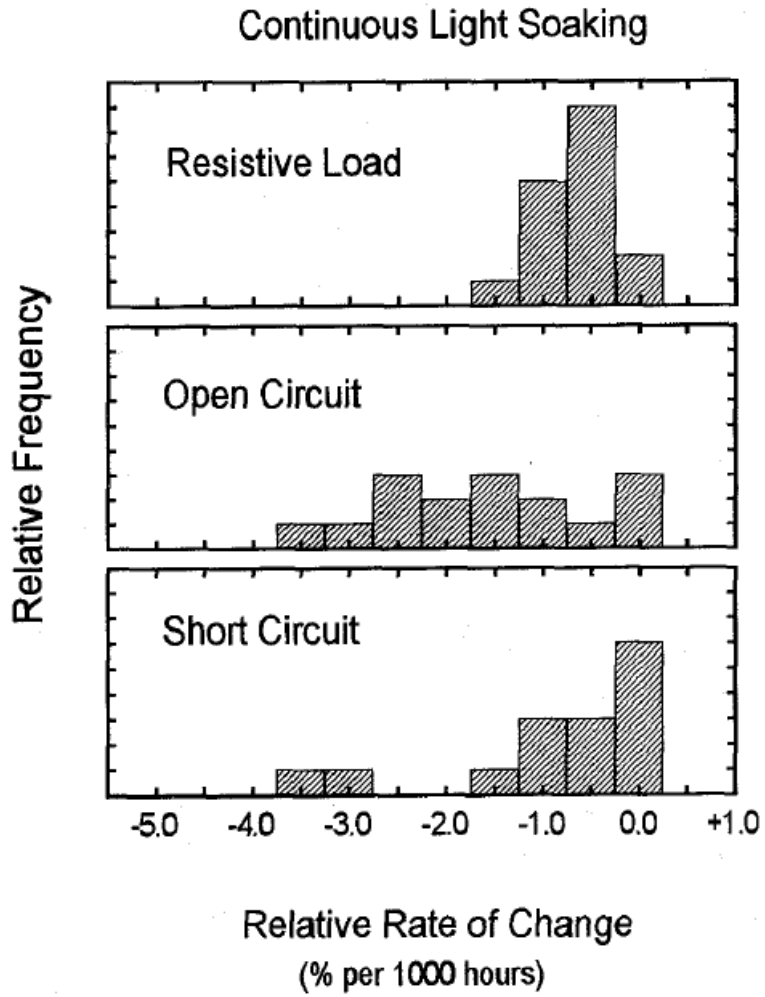
From Ref. A after B

Effect of Bias During Light-Soaking of CdTe

- CdTe degradation during extended light soaking is strongly affected by bias condition Ref. [22][A], [21][B],[20][C]
- Degradation rate increases with increased temperature, Ref. [21]
- Degradation significantly faster at 100C than in the field. Can use high temperature as accelerated test, Ref. [21]



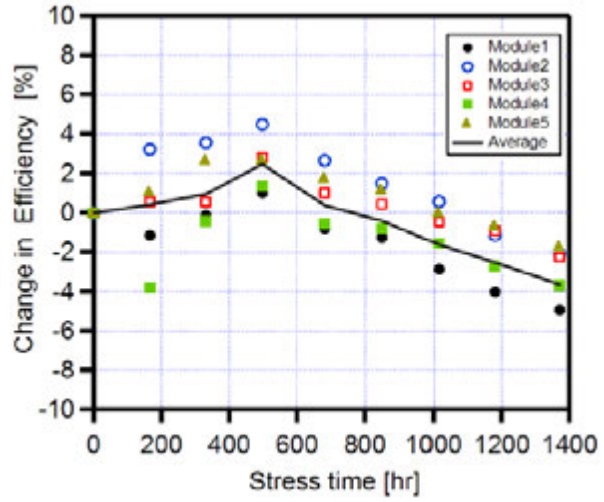
Efficiency drop during extended stress as function of bias condition. From Ref. A after B



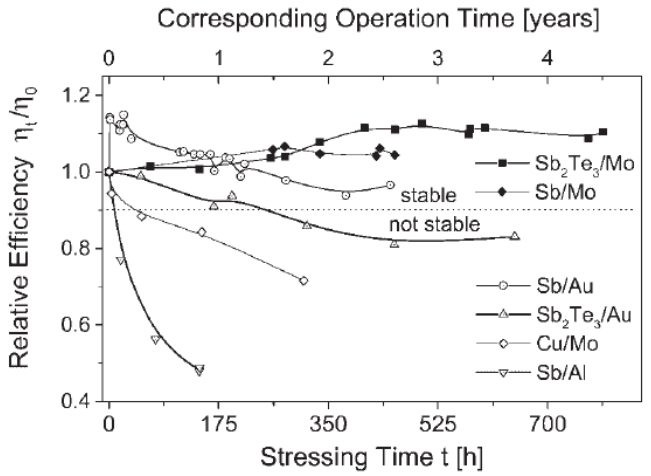
From C

Stability in Various CdTe Devices

- Stability of CdTe modules, Ref. [26][A]
  - Light soaking stress yielded initial efficiency improvement, followed by degradation
- Metastable effects in CdTe, Ref [27]
  - Measurements of I-V curves in-situ during extended light soaking of CdTe modules
  - Shifts in Isc, Voc, and FF versus light exposure
  - Voc could move either up or down with exposure, depending on fabrication details
  - I-V parameters depend on module stabilization
- Investigation of CdTe back contacts, Ref [28]
  - Without Cu: initial performance similar to devices with Cu following stress
- Degradation in CdTe with Sb-based back contacts
  - Back contacts based on Sb_2Te_3/Mo yielded stable cells, Ref. [18][B]
  - Sb_2Te_3-based back contacts, Ref. [29]
    - Outdoor testing of CdTe for 1.5 years
    - Degraded ~5% in Voc and 8-10% in FF



From Ref. A

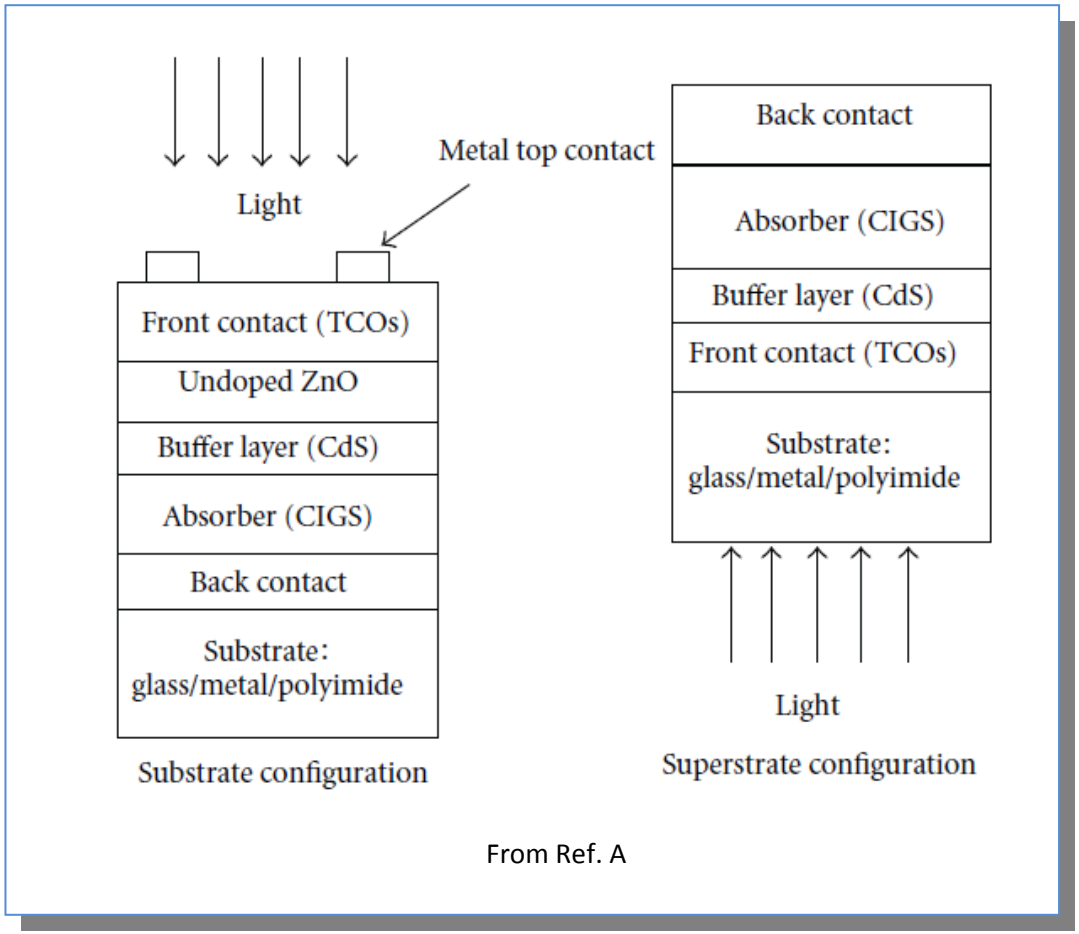


Stability vs. back contact materials. From Ref. B

CIGS

CIGS Device Structure

- CIGS = Copper Indium Gallium Selenide = $Cu(In,Ga)Se_2$
- Device structure, Ref. [30][A],[31], [18]
- Typically uses CdS buffer layer
- Typically formed in substrate configuration
  - If superstrate, undesirable CdS diffusion during CIGS deposition
- Desire for structures without CdS
  - Various approaches



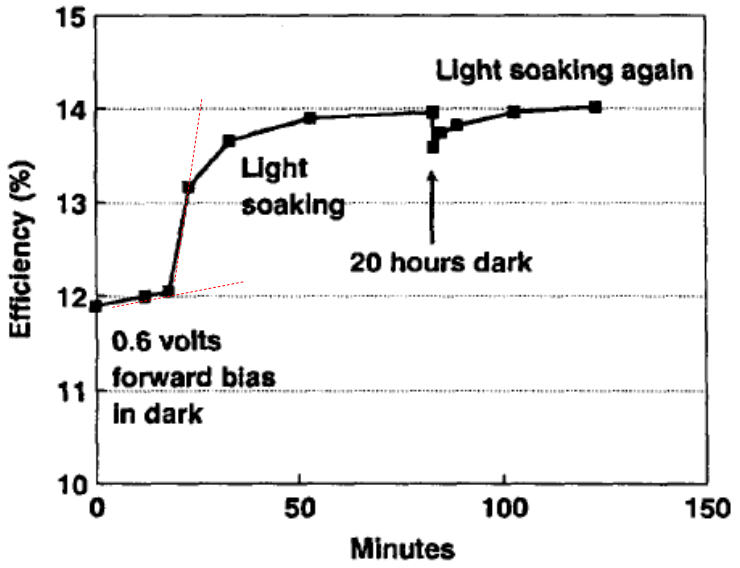
From Ref. A

CIGS Light Soaking Effects

- Reversible metastability of photoconductivity in CIGS films, Ref [32]
  - Annealing at 80 °C leads to decrease of dark conductivity by ~2x at room temperature
  - By exposure to light, the initial state can be re-established

- Voc of CIGS cells shifts reversibly with light exposure or bias, Ref [33]
  - CIGS Voc rises upon light exposure or forward bias in dark, with corresponding rise in efficiency of ~5%
  - Time scale ranges from minutes to hours; faster at higher temperature

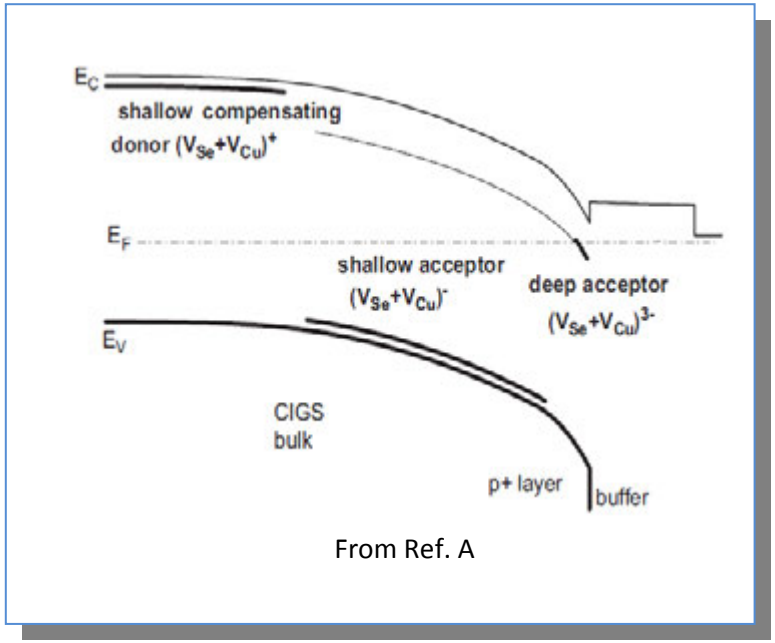
- Effects of sweep rate and voltage bias on CIS cells, Ref [34][A]
  - Light soaking produced 7-15% improvement in cell efficiency
  - Light soaking effect more pronounced and longer lived than effect of forward bias



From Ref. A

CIGS Metastability Mechanisms

- Three effects in CIGS metastabilities, Ref [35],[36]
  - Light soaking with white light may produce overall beneficial effect due to balance of beneficial and detrimental effects [36]
  - Red light: increase in Voc, due to increase in carriers in absorber
    - Similar effect from forward bias
  - Blue light: interface effect
  - Reverse bias: interface effect
- Proposed mechanisms, Ref. [36]
  - Metastable defects that trap carriers
  - Reversible migration of Cu
- Amphoteric Se-Cu divacancy (V_{Se}-V_{Cu}) complex
  - First principles calculations, Ref. [36]
    - V_{Se}-V_{Cu} complex can act as amphoteric (donor or acceptor) defect
    - Defect state converted by light absorption
    - Explains observed effects of red light, blue light, and reverse bias
  - Experimental support
    - Refs. [37], [38], [39], [40][A]



From Ref. A

Light Soaking in CIGS with Alternative Buffer Layers

- Light soaking effects vary greatly depending on the device structure and especially the buffer layer composition.

- Strong light soaking effect observed:
  - Superstrate CGS/CIGS cells grown with ZnO buffer instead of CdS, Refs. [41], [42]
  - ZnO/CIGS cells without CdS, Ref. [43]
  - $Zn_{1-x}Mg_xO$ buffer layers without CdS, Ref. [44]

- Minimal light soaking effect observed:
  - CIGS with ZIS (Zn-Indium-Se) buffer layer (alternative to CdS), Ref. [45]

Thin-Film Pre-Conditioning

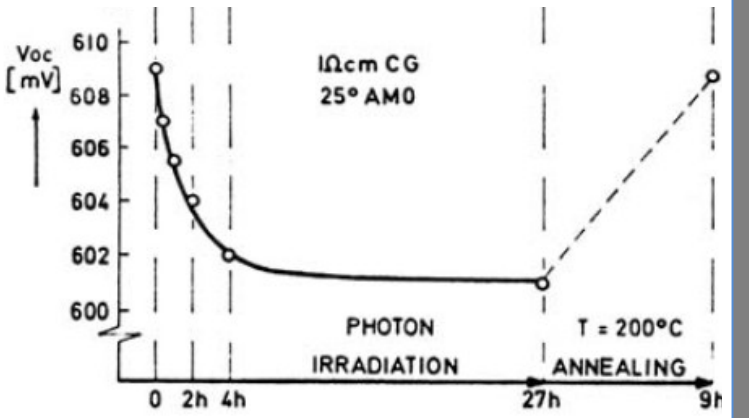
Thin-Film Pre-Conditioning

- Due to metastability phenomena, preconditioning is essential for accurate power output determination of thin film PV modules.
- However, due to the complexity of the phenomena and variability between different module technologies, reliable preconditioning methods are difficult to establish.
- Current standard for stabilization in thin-film PV modules is IEC 61646
  - <2% change after successive 43 kW/m^2 exposure periods
  - Designed primarily for a-Si where dominant degradation is via Staebler-Wronski effect
- Questions:
  - Can modules be stabilized via dark soaking (at bias? at temp?), without light soaking?
  - What are optimal temperatures and durations for stabilization?
- Recent CdTe preconditioning examples:
  - CdTe efficiency found to initially improve, then degrade, with light exposure, Ref. [26]
  - CdTe efficiency measurements depend strongly on pre-conditioning conditions, with various conditions yielding higher or lower efficiency results, Ref. [46]
- Recent NREL studies on pre-conditioning techniques for CdTe & CIGS, Refs. [47], [48], [49]
  - Comparing effects of light soaking and dark-bias-soaking
    - Some modules stabilized equally in light vs dark-bias, while others do not
  - Comparing indoor to outdoor stabilization

Crystalline Si

Light-Induced Degradation (LID) in Crystalline Silicon

- Boron-doped crystalline Silicon solar cell material includes:
  - Czochralski-grown monocrystalline silicon (Cz-Si)
  - Cast multicrystalline silicon (mc-Si)
- LID in Cz-Si solar cells, Ref. [50][A],[51],[52],[53]
  - ~4% power output degradation in B-doped Cz-Si cells during first 5 hours of light soaking
  - Recovers upon anneal or dark storage [51]
  - Due to activation of metastable boron-oxygen defect which lowers carrier lifetime
  - Greatly reduced using either Ga-doped Cz-Si or low oxygen content B-Cz-Si, [52]



Observation of LID in B-doped Cz-Si solar cells.
From Ref. A

- IEC 61215 preconditioning
  - Qualification for c-Si modules requires 5 hours of preconditioning at 1000 W/m^2 prior to power output measurement
- Statistical review of LID in different monocrystalline Cz-Si and mc-Si modules, Ref. [54]
- LID may also be present in upgraded metallurgical grade or low-cost silicon, Refs. [55],[56]

References

References

[1] A.G. Aberle, "Thin-film solar cells," *Thin Solid Films*, vol. 517, Jul. 2009, pp. 4706-4710.
[2] A. Luque and S. Hegedus, *Handbook of photovoltaic science and engineering*, John Wiley and Sons, 2003.
[3] Y. Wang, X. Geng, H. Stiebig, and F. Finger, "Stability of microcrystalline silicon solar cells with HWCVD buffer layer," *Thin Solid Films*, vol. 516, Jan. 2008, pp. 733-735.
[4] B. Yan, G. Yue, J.M. Owens, J. Yang, and S. Guha, "Light-induced metastability in hydrogenated nanocrystalline silicon solar cells," *Applied Physics Letters*, 2004.
[5] D.L. Staebler and C.R. Wronski, "Reversible conductivity changes in discharge-produced amorphous Si," *Applied Physics Letters*, 1977.
[6] M. Stutzmann, W.B. Jackson, and C.C. Tsai, "Light-induced metastable defects in hydrogenated amorphous silicon: A systematic study," *Physical Review B*, vol. 32, Jul. 1985, p. 23.
[7] R. Biswas and B.C. Pan, "Mechanisms of metastability in hydrogenated amorphous silicon," *Solar Energy Materials and Solar Cells*, vol. 78, Jul. 2003, pp. 447-467.
[8] M.C. Rossi, M.S. Brandt, and M. Stutzmann, "Accelerated stability test for amorphous silicon solar cells," *Applied Physics Letters*, vol. 60, 1992, pp. 1709-1711.
[9] H. Fritzsche, "Development in Understanding and Controlling the Staebler-Wronski Effect in a-Si:H," *Annual Review of Materials Research*, vol. 31, 2001, pp. 47-79.
[10] V. Nádazdy and M. Zeman, "Origin of charged gap states in a-Si:H and their evolution during light soaking," *Physical Review B*, vol. 69, Apr. 2004, p. 165213.
[11] A. Klaver and R. van Swaaij, "Modeling of light-induced degradation of amorphous silicon solar cells," *Solar Energy Materials and Solar Cells*, vol. 92, Jan. 2008, pp. 50-60.
[12] J.A. del Cueto and B. von Roedern, "Temperature-induced changes in the performance of amorphous silicon multi-junction modules in controlled light-soaking," *Progress in Photovoltaics: Research and Applications*, vol. 7, 1999, pp. 101-112.
[13] R. Ruther, J. del Cueto, G. Tamizh-Mani, A. Montenegro, S. Rummel, A. Anderberg, and B. von Roedern, "Performance test of amorphous silicon modules in different climates - year four: Progress in understanding exposure history stabilization effects," *Photovoltaic Specialists Conference, 2008. PVSC '08. 33rd IEEE*, 2008, pp. 1-5.
[14] Solanki, *Solar Photovoltaics: Fundamentals Technologies And Applications*, PHI Learning Pvt. Ltd., 2009.
[15] L.D. Partain and L.M. Fraas, *Solar Cells and Their Applications*, John Wiley and Sons, 2010.
[16] K.L. Chopra, P.D. Paulson, and V. Dutta, "Thin-film solar cells: an overview," *Progress in Photovoltaics: Research and Applications*, vol. 12, 2004, pp. 69-92.
[17] N. DeVoe and S. Hansen, "First Solar Company and Product Overview," *Thinfilm Workshop JRC-ISPRA*, 2005.
[18] A. Romeo, M. Terheggen, D. Abou-Ras, D.L. Bätzner, F. Haug, M. Kälin, D. Rudmann, and A.N. Tiwari, "Development of thin-film Cu(In,Ga)Se2 and CdTe solar cells," *Progress in Photovoltaics: Research and Applications*, vol. 12, 2004, pp. 93-111.
[19] R.A. Sasala, R.C. Powell, G.L. Dorer, and N. Reiter, "Recent progress in CdTe solar cell research at SCI," *AIP Conference Proceedings*, vol. 394, Feb. 1997, pp. 171-186.

[20] R. Powell, R. Sasala, G. Rich, M. Steele, K. Bihn, N. Reiter, S. Cox, and G. Dorer, "Stability testing of CdTe/CdS thin-film photovoltaic modules," *Photovoltaic Specialists Conference, 1996., Conference Record of the Twenty Fifth IEEE*, 1996, pp. 785-788.
[21] J.F. Hiltner and J.R. Sites, "Stability of CdTe solar cells at elevated temperatures: Bias, temperature, and Cu dependence," *AIP Conference Proceedings*, vol. 462, 1999, pp. 170-175.
[22] C. Jenkins, A. Pudov, M. Gloeckler, S. Demtsu, T. Nagle, A. Fahrenbruch, and J. Sites, "CdTe Back Contact: Response to Copper Addition and Out-Diffusion," 2000.
[23] C.R. Corwine, A.O. Pudov, M. Gloeckler, S.H. Demtsu, and J.R. Sites, "Copper inclusion and migration from the back contact in CdTe solar cells," *Solar Energy Materials and Solar Cells*, vol. 82, May. 2004, pp. 481-489.
[24] A. Pudov, M. Gloeckler, S. Demtsu, J. Sites, K. Barth, R. Enzenroth, and W. Sampath, "Effect of back-contact copper concentration on CdTe cell operation," *Photovoltaic Specialists Conference, 2002. Conference Record of the Twenty-Ninth IEEE*, 2002, pp. 760-763.
[25] S. Demtsu and J. Sites, "Effect of back-contact barrier on thin-film CdTe solar cells," *Thin Solid Films*, vol. 510, Jul. 2006, pp. 320-324.
[26] S. Demtsu, S. Bansal, and D. Albin, "Intrinsic stability of thin-film CdS/CdTe modules," *Photovoltaic Specialists Conference (PVSC), 2010 35th IEEE*, 2010, pp. 001161-001165.
[27] J.A. del Cueto and B. von Roedern, "Long-term transient and metastable effects in cadmium telluride photovoltaic modules," *Progress in Photovoltaics: Research and Applications*, vol. 14, 2006, pp. 615-628.
[28] S.S. Hegedus and B.E. McCandless, "CdTe contacts for CdTe/CdS solar cells: effect of Cu thickness, surface preparation and recontacting on device performance and stability," *Solar Energy Materials and Solar Cells*, vol. 88, Jun. 2005, pp. 75-95.
[29] T. Carlsson and A. Brinkman, "Identification of degradation mechanisms in field-tested CdTe modules," *Progress in Photovoltaics: Research and Applications*, vol. 14, 2006, pp. 213-224.
[30] U. Singh and S. Patra, "Progress in Polycrystalline Thin-Film Cu(In,Ga)Se2 Solar Cells," *International Journal of Photoenergy*, vol. 2010, 2010.
[31] S.R. Kodigala, *Cu(InGa)Se2 Based Thin Film Solar Cells*, Academic Press, 2010.
[32] U. Rau, M. Schmitt, J. Parisi, W. Riedl, and F. Karg, "Persistent photoconductivity in Cu(In,Ga)Se2 heterojunctions and thin films prepared by sequential deposition," *Applied Physics Letters*, vol. 73, 1998, pp. 223-225.
[33] R. Sasala and J. Sites, "Time dependent voltage in CuInSe2 and CdTe solar cells," *Photovoltaic Specialists Conference, 1993., Conference Record of the Twenty Third IEEE*, 1993, pp. 543-548.
[34] D. Willett and S. Kuriyagawa, "The effects of sweep rate, voltage bias and light soaking on the measurement of CIS-based solar cell characteristics," *Photovoltaic Specialists Conference, 1993., Conference Record of the Twenty Third IEEE*, 1993, pp. 495-500.
[35] P. Zabierowski, U. Rau, and M. Igalson, "Classification of metastabilities in the electrical characteristics of ZnO/CdS/Cu(In,Ga)Se2 solar cells," *Thin Solid Films*, vol. 387, May. 2001, pp. 147-150.
[36] S. Lany and A. Zunger, "Light- and bias-induced metastabilities in Cu(In,Ga)Se[sub 2] based solar cells caused by the (V[sub Se]-V[sub Cu]) vacancy complex," *Journal of Applied Physics*, vol. 100, 2006, p. 113725.
[37] M. Igalson, M. Cwil, and M. Edoff, "Metastabilities in the electrical characteristics of CIGS devices: Experimental results vs theoretical predictions," *Thin Solid Films*, vol. 515, May. 2007, pp. 6142-6146.
[38] S. Siebentritt and T. Rissom, "Metastable behavior of donors in CuGaSe[sub 2] under illumination," *Applied Physics Letters*, vol. 92, 2008, p. 062107.

[39] J.D. Cohen, *Identifying the Electronic Properties Relevant to Improving the Performance of High Band-Gap Copper Based I-III-VI2 Chalcopyrite Thin Film Photovoltaic Devices: Final Subcontract Report, 27 April 2004-15 September 2007*, 2008.
[40] M. Igalson, P. Zabierowski, D. Przado, A. Urbaniak, M. Edoff, and W.N. Shafarman, "Understanding defect-related issues limiting efficiency of CIGS solar cells," *Solar Energy Materials and Solar Cells*, vol. 93, Aug. 2009, pp. 1290-1295.
[41] F.-. Haug, D. Rudmann, H. Zogg, and A.N. Tiwari, "Light soaking effects in Cu(In,Ga)Se2 superstrate solar cells," *Thin Solid Films*, vol. 431-432, May. 2003, pp. 431-435.
[42] M.R. Balboul, A. Jasenek, O. Chernykh, U. Rau, and H.W. Schock, "CuGaSe2-based superstrate solar cells," *Thin Solid Films*, vol. 387, May. 2001, pp. 74-76.
[43] A.E. Delahoy, A. Ruppert, and M. Contreras, "Charging and discharging of defect states in CIGS/ZnO junctions," *Thin Solid Films*, vol. 361-362, Feb. 2000, pp. 140-144.
[44] J. Pettersson, C. Platzer-Björkman, and M. Edoff, "Temperature-dependent current-voltage and lightsoaking measurements on Cu(In,Ga)Se2 solar cells with ALD-Zn1-xMgxO buffer layers," *Progress in Photovoltaics: Research and Applications*, vol. 17, 2009, pp. 460-469.
[45] A.E. Delahoy, J. Cambridge, L. Chen, and Z.J. Kiss, *Thin Film CIGS Photovoltaic Technology: Final Technical Report, 16 April 1998 - 15 October 2001*, NREL, 2002.
[46] M. Propst, K. Goshia, and J. Hevelone, "Effects of Various Module Preconditioning Procedures on CdTe Pmax Measurements," *NREL PV Module Reliability Workshop 2010*, Golden, Colorado: 2010.
[47] Joseph A. del Cueto and C.A. Deline, "Comparison of injection of carriers through light soaking and forward bias in dark (In Stabilization of polycrystalline thin film photovoltaic modules)," *NREL PV Module Reliability Workshop 2010*, Golden, Colorado: 2010.
[48] J.A. del Cueto, C.A. Deline, D.S. Albin, S.R. Rummel, and A. Anderberg, "Striving for a Standard Protocol for Preconditioning or Stabilization of Polycrystalline Thin Film Photovoltaic Module," *SPIE 2009 Solar Energy & Technology Conference*, San Diego, California: 2009.
[49] J.A. del Cueto, C.A. Deline, S.R. Rummel, and A. Anderberg, "Progress Toward a Stabilization and Preconditioning Protocol for Polycrystalline Thin-Film Photovoltaic Modules," *35th IEEE Photovoltaics Specialists Conference 2010*, Hawaii: 2010.
[50] H. Fischer and W. Pschunder, *Proceedings of 10th IEEE Photovoltaic Specialists Conference*, 1973, p. 404.
[51] J.H. Reiss, R.R. King, and K.W. Mitchell, "Characterization of diffusion length degradation in Czochralski silicon solar cells," *Applied Physics Letters*, 1996.
[52] J. Schmidt and R. Hezel, "Light-Induced Degradation In Cz Silicon Solar Cells: Fundamental Understanding And Strategies For Its Avoidance," *12th Workshop on Crystalline Silicon Solar Cell Materials and Processes 2002*, Breckenridge, Colorado: 2002.
[53] J. Schmidt, "Light-Induced Degradation in Crystalline Silicon Solar Cells," *Solid State Phenomena*, vol. 95-96, 2004, pp. 187-196.
[54] M. Munoz, F. Chenlo, and M. Alonso-García, "Influence of initial power stabilization over crystalline-Si photovoltaic modules maximum power," *Progress in Photovoltaics: Research and Applications*, 2010, pp. n/a-n/a.
[55] R. Einhaus, J. Kraiem, F. Lissalde, S. Dubois, N. Enjalbert, and R. Monna, "Crystallisation of purified metallurgical silicon," *Photovoltaic Specialists Conference, 2008. PVSC '08. 33rd IEEE*, 2008, pp. 1-4.
[56] Z. Liang, D. Chen, X. Liang, Z. Yang, H. Shen, and J. Shi, "Crystalline Si solar cells based on solar grade silicon materials," *Renewable Energy*, vol. 35, Oct. 2010, pp. 2297-2300.

An Edge Sealing "Getter" Tape for Ultra-long Lifetime (up to 3000 hours) of Thin Film CIGS PV Modules

A. Bonucci, R. van der Wel, P. Gallina, M.Amiotti[1], S. Hiss[2], O. Salomon, W. Wischmann[3]
[1]SAES Getters SpA, Viale Italia 77, 20020 Lainate (Italy)
[2]Kuraray Europe GmbH, Division TROSIFOL, Mülheimer Str. 26, 53840 Troisdorf (Germany)
[3]ZSW Stuttgart, Industriestrasse 6, 70565 Stuttgart (Germany)

Background and Objectives

Long term stability, reliability and operational lifetime of PV modules are essential for their commercial success. This is especially true for modules based on thin film technologies like CdTe, CIGS and a-Si. Since both performances as well as yield may be strongly affected by environmental conditions, proper encapsulation architecture is important to obtain the desired long term outdoor stability.
We have focused on the moisture ingress along the edges of the module, which is believed to be the main cause of degradation over time.

B-Dry

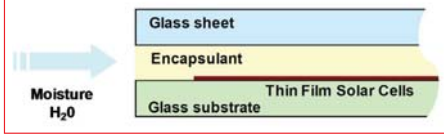
The joint action of low permeability thermoplastic polymer and SAES Getters proprietary powerful moisture absorbing materials makes B-Dry® the first edge sealant optimized as active barrier against moisture ingress which assures extra-long term stability to thin film PV modules. B-Dry has the ability to completely stop the moisture ingress, reducing the WVTR to values lower than 10^{-3} g mm / m^2 day until the chemical saturation of the moisture absorbing material after several thousand hours of Damp Heat testing time (85°C, 85% r.h.).

B-dry edge sealant

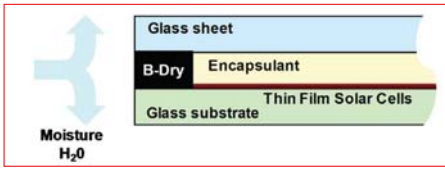


B-Dry® black thermoplastic edge sealant tape:
Thickness: 0.4 mm to 1.1 mm
Width: 7 mm to 12 mm.

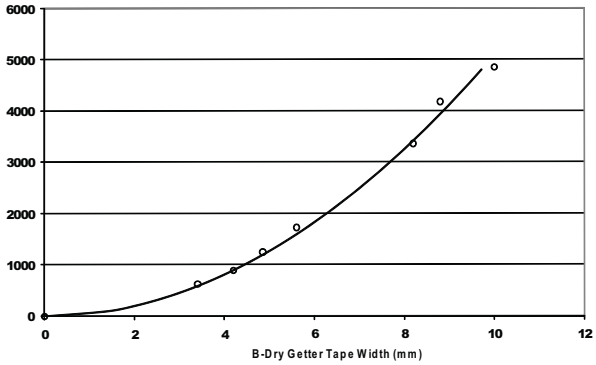
Moisture ingress without B-dry



B-dry edge sealant as an Active Barrier

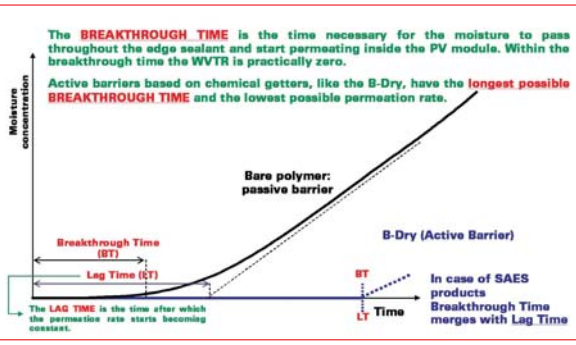


B-Dry® is compatible with most common PV module encapsulation processes and materials (EVA, PVB, TPO)
Process temperature range: 140°C to 170°C.

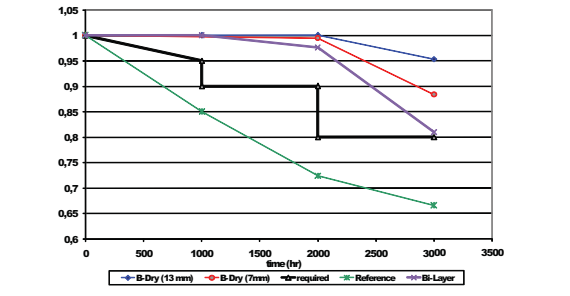


B-Dry® protects against moisture ingress with a relatively small tape width.

Features and Results

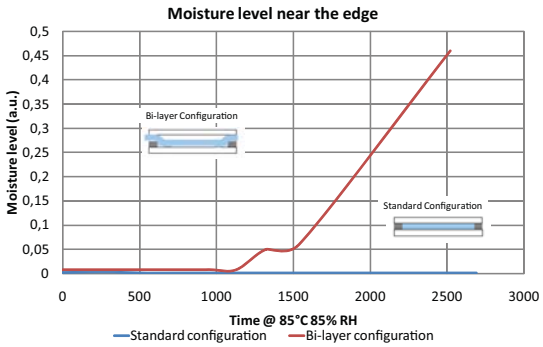


Damp Heat stability: Performed at ZSW



Relative efficiency after damp heat 85°C 85% R.H. for 30 cm x 30 cm CIGS modules.

Kinetic of moisture penetration during damp heat: Performed at Kuraray laboratories



Moisture penetration at 85°C 85% r.h. within the encapsulant (Kuraray PVB) after damp heat for 30 cm x 30 cm dummy modules. (Reflection Analyzer (PIER-ELECTRONIC) (B-Dry® is 10 mm wide)

Electrical isolation

Before DHT 1000 hours	Before DHT 1000 hours
B-Dry®: 0.20 µA	B-Dry®: 0.25 µA
No B-Dry®: 0.20 µA	No B-Dry®: 0.99 µA

Wet leakage current of 30 cm x 30 cm CIGS modules encapsulated with PVB before and after 1000 h of damp heat.

Conclusions

- B-Dry® shows a very high moisture barrier property
- B-Dry® ensures very good damp heat stability
- B-Dry® ensures high electrical isolation

we support your innovation

saes getters

www.saesgetters.com
photovoltaics@saes-group.com

This poster does not contain any proprietary or confidential information.

ELECTROLUMINESCENCE TO TRACK CELL AND MODULE CHANGES – FROM SMALL-AREA CELLS TO LARGE-AREA MODULES

M. Topič[1], K. Zaunbrecher[2], M. Bokalič[1], J.R. Sites[2]

[1] University of Ljubljana, Slovenia
[2] Colorado State University, Fort Collins, CO

University of Ljubljana
Faculty of Electrical Engineering

Introduction

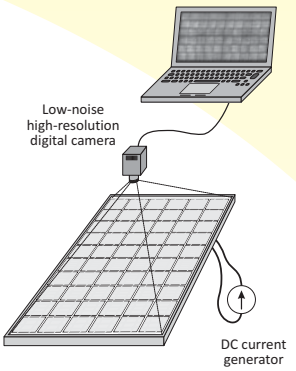
Small-area solar cell performance is always larger than the large-area PV module performance, primarily due to losses of series connection of cells into modules. In particular in thin film PV modules (a-Si, a-Si/mc-Si, CIGS, CdTe), front contact and monolithic contact losses often dominate. However, inhomogeneities distributed across the larger area can affect the cell or module performance.

Inhomogeneities do not origin from the production processes only, but they may evolve during the transport or installation and inevitably during their operation in the course of life.

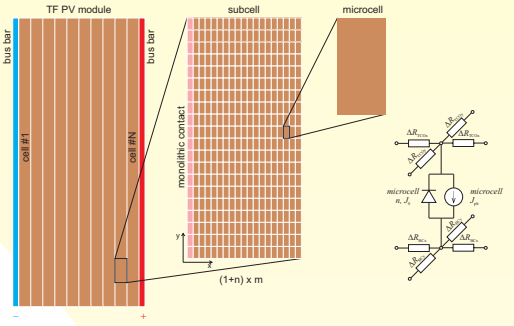
Electroluminescence (EL) systems have already proved to be fast and reliable inspection tool for detection and monitoring of inhomogeneities. Systems under development at both Ljubljana and Colorado State University aim at tracking small-area changes in thin-film cells and modules. EL is particularly attractive, because it can be directly related to cell performance, the field of view can be varied over two orders of magnitude with conventional optics, and the imaging time for large-area imaging is the order of seconds. Parallel to the system development, a joint program is in progress to expand the information acquired from the analysis of the recorded images.

SPICE simulations enable an evaluation of the impact of inhomogeneities from the microcell level to the subcell level with a focus on the type and strength of inhomogeneities and the consequent loss of sub-cell power. EL with SPICE simulations offers a powerfull platform for tracking changes and paths the way toward the degradation mechanisms throughout the life-time.

EL set-up



Thin Film PV module layout

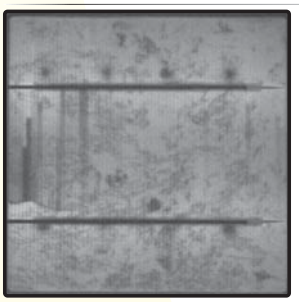


Shematic view of thin film PV module made of two bus bars and cells, which are divided into subcell. Each subcell consists of monolithic contact area and active area, which is divided/parcelled into microcells as the smallest unit. A model of microcell with adjacent discretized resistors (ΔR) of the front TCO and back contact.

Legend: naked eye visibilty; effect on performance

Defects in c-Si cells and modules

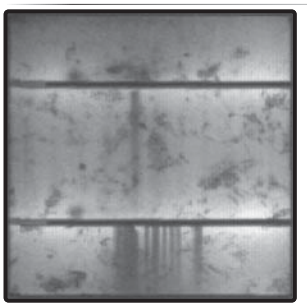
CRACKS



presence [%]

inactive	1.6
active	0.5

BROKEN FINGERS

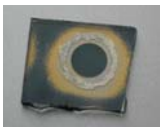


presence [%]

weak	15.5
strong	2.0
complete	0.2

Cracks and broken fingers on individual c-Si cells in strings occur during module production process, and they both affect performance of a PV module. These defects are important to inspect in production, because they decrease production line power yield.

Defects in thin-film CdTe solar cells

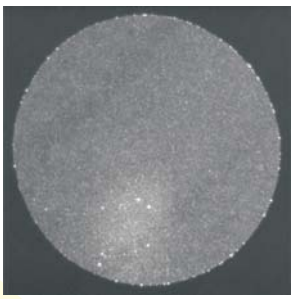


J_F = 2.4 mA/cm^2



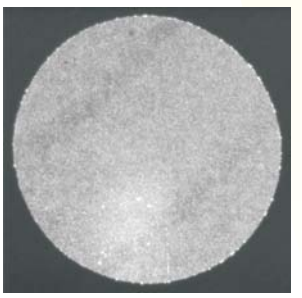
Low injection level with little EL response.

J_F = 4.9 mA/cm^2



Mid injection level generates bright spots. At the cell edge shunts can be identified, while in the inner part of the cell it is not clear whether they are shunts or regions of better performance .

J_F = 7.9 mA/cm^2



High injection level generates overall higher intensity with even brighter spots.

Conclusions

- EL is a fast and powerful method for inline cell and module inspection regardless the PV technology.
- Cracks and broken fingers arise in individual mc-Si solar cells during the module fabrication steps.
- In c-Si PV modules cracks and broken fingers are the most common drivers of the module power loss.
- EL increases roughly linearly with current; individual features, however, become more at higher currents.
- Field of view can range from 3 mm to 500 mm by changing lenses.

Acknowledgements

SLO-US/10-12 bilateral project
US National Renewable Energy Laboratory

Highly Accelerated Weathering of CIGS Photovoltaics

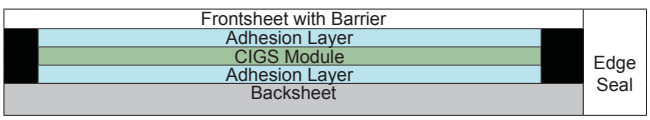
J. Cole Rickers, D. Garth Jensen
Ascent Solar Technologies, Inc.

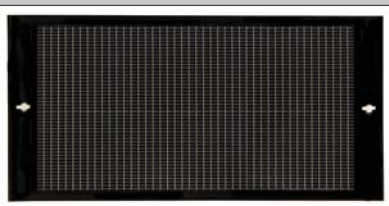
Introduction:

- Damp Heat (85°C/85% RH) is a widely accepted industry standard
- However, it is a very long test, taking up to 5 months
- Since WVTR increases exponentially with temperature, barrier layers can be evaluated more quickly by increasing the temperature and humidity beyond standard damp heat conditions
- Ascent Solar has developed a non-biased HAST (Highly Accelerated Stress Test) procedure to quickly evaluate lamination packages for flexible CIGS PV
- The HAST procedure was applied to flexible CIGS modules encapsulated using various package designs and material combinations and the results were compared to standard Damp Heat stressing

Test Sample Construction:

- Test samples consist of a backsheet, a front sheet with barrier, and two adhesion layers. An edge seal is applied around all four edges. Electrical feedthroughs are potted.





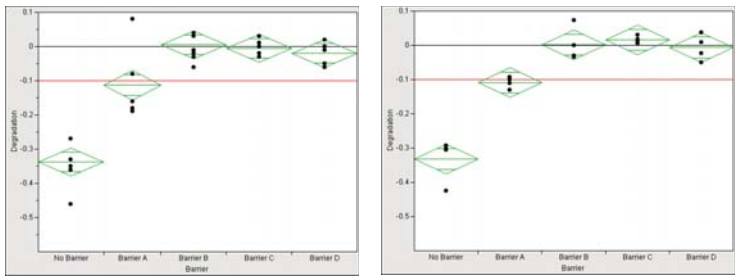
Summary:

- The HAST procedure was found to accelerate the effects of standard Damp Heat by a factor of around 15 for most of the package designs and material combinations evaluated
- Some modules experienced failure mechanisms which did not occur in standard Damp Heat, but these modules generally did not survive even 1000 hours in standard Damp Heat
- If modules performed well in HAST, the performance in standard damp heat was at least as good and often better
- Barrier layer performance can be evaluated in days with HAST instead of the weeks required with Damp Heat
- The HAST procedure also allows for rapid evaluation of a full package design including interactions of multiple materials
- Once a baseline for a module construction is established, it can be used to rapidly screen incoming material

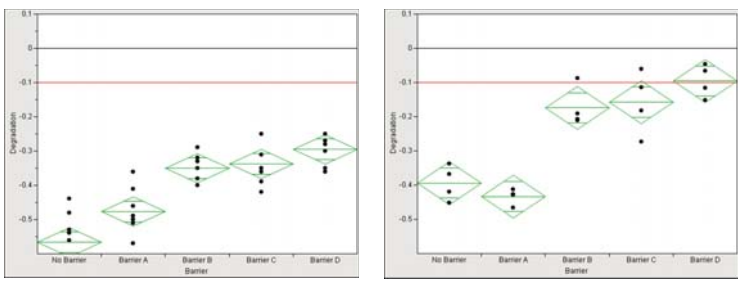
Results:

Power Degradation of CIGS Packaged using Various Barrier Frontsheets after 1 and 2 days of HAST Compared to 2 and 4.5 weeks in Standard Damp Heat

Highly Accelerated 48 hours → Standard 336 hours

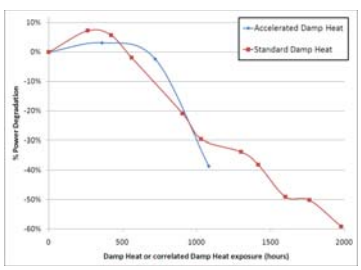


Highly Accelerated 48 hours → Standard 746 hours

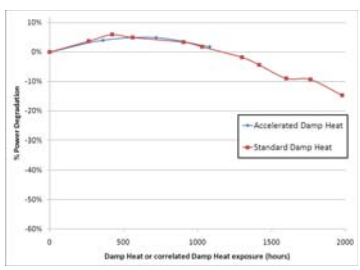


Correlation of HAST to Standard Damp Applying an Acceleration Factor of 15 to HAST

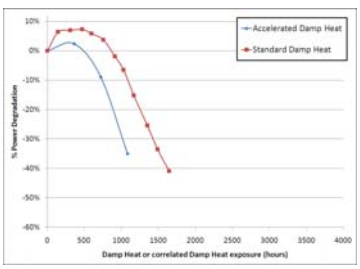
Backsheet A / Glass



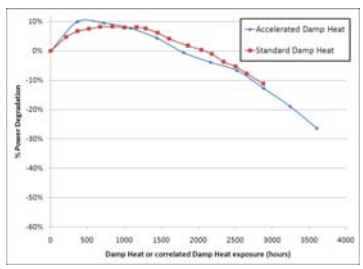
Backsheet B / Glass



Backsheet C / Flexible Barrier E



Backsheet C / Flexible Barrier E



This poster does not contain any proprietary or confidential information

Stress Testing and Failure Analysis Methods for Determining the Reliability of Metal Buss Tapes

Jason Hevelone*, Michelle Propst and Chris Richardson

Abound Solar

Background

The use of conductive metal buss tapes is widely used by thin film PV manufacturers. These tapes are key to providing a low resistance contact to the anode and cathode of PV cells and to conduct current within the PV module. The ability of these tapes to withstand the harsh environments created during the lifetime of a solar panel can be difficult to simulate and therefore accelerate in the lab. Existing industry certification tests such as thermal cycling, reverse current overload, damp heat, and humidity freeze often fail to detect what will ultimately become field reliability failures. Classical tape adhesion pull and shear tests are informational, but can be difficult to calibrate to actual product requirements as they don't effectively measure ohmic ampacity, the ability of a conductive tape to maintain a low ohmic contact / high current carrying capability.

Characteristics of Buss Failure

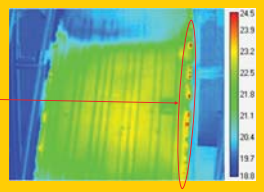
Buss failure typically begins with an increase in the series resistance between the tape and semiconductor back-metal that is induced by thermal fatigue and localized heating. The increased resistance is the result of decreased electrical contact surface area between the buss tape and back-metal resulting in the current being channeled through a diminishing amount of electrical contact points. This increased current density in turn generates more heat and continues to reduce electrical contact points creating a thermal runaway condition that ultimately results in sporadic or completely open buss tape to back-metal contact.



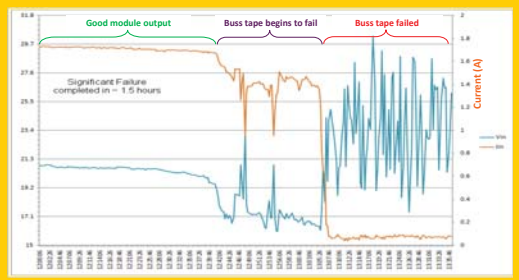
Buss tape failure resulting in film damage along length of thin-film cell



Buss tape failure as seen from the backside of the module



IR (Infrared) image showing poor ohmic contact areas along metal buss tape prior to failure



Voltage (blue) and Current (orange) characteristics at time of buss tape failure

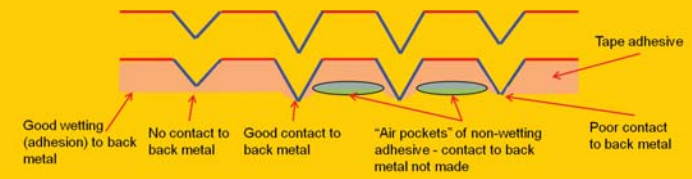
Lab Acceleration of Failure Mechanism

Industry certification tests failed to identify the metal buss tape failure mechanism primarily because they don't stress the failure mechanism adequately or are not performed for a long enough duration.

Stress Test	Catch Buss Failure Mechanism?	Reason
Temperature Cycling Test: UL1703, 35 (-40C to +90C, 200 cycles, small fwd bias current to assure continuity during cycle)	No	Failure mechanism requires both thermal fatigue and ***high current flow*** during cycles
High Temperature Bake (90C, 1000 hours, with and without high fwd bias current)	No	Failure mechanism requires both ***thermal fatigue*** and high current flow
Reverse Current Overload: UL1703, 28 (Fwd bias at 130% of fuse rating, 1 hour)	Rarely	Failure mechanism requires ***thermal fatigue***. Much higher current flow (>200% of fuse rating and longer stress duration increase chances of detecting failure mechanism)
Damp Heat: IEC61646, 10.13 (85C, 85% R.H., 1000 hours, unbiased)	No	Failure mechanism requires both ***thermal fatigue*** and ***high current flow***
Humidity Freeze: UL1703, 36 (-40C to +85C/85%R.H., 10 cycles, small fwd bias current to assure continuity during cycle)	No	Failure mechanism requires both thermal fatigue and ***high current flow*** during cycles. Ten cycles is insufficient to provide enough thermal fatigue.
Modified Temperature Cycling Test (-40C to +90C, test to failure, high fwd bias current, >2x I_{mp})	Yes	Failure mechanism requires both **thermal fatigue** and ***high current flow*** during cycles. Must test to failure in order to get to tape wear-out.

Buss Tape Adhesive Wetting

Cross-sectional representation of possible tape conditions prior to application. Due to embossing variability, not all emboss points are "cleared" of adhesive during embossing. Areas of higher emboss might not fully wet during application, leaving an air pocket between the back metal and the adhesive.





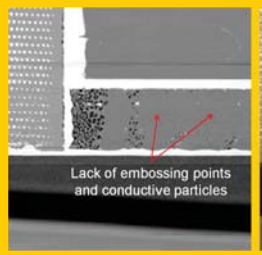


Top-down pictorial and acoustic image of buss tape specifically showing where embossed points make and don't make contact to the back metal and where adhesive wetting is both good and bad. The non-wetting regions are where air pockets exist between the back metal and the adhesive due to insufficient tape application.

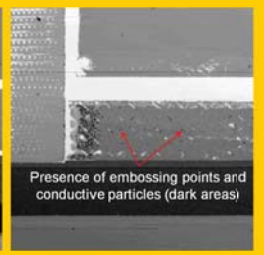
Buss Tape Application Considerations

- Roller force
- Roller durometer
- Speed of tape application
- Surface quality and cleanliness
- Back metal composition
- Embossed vs. smooth tape
- Adhesive properties
- Inclusion of conductive filler particles
- Composition of conductive filler particles

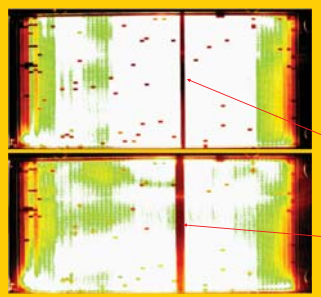
Failure Analysis Techniques



Acoustic image of poor tape application that results in buss tape failure



Acoustic image of good tape application that results in reliable buss tape



LBIC (Laser Beam Induced Current) image of a perpendicular, isolation laser-scribed module

Dark vertical line shows location where a 2 cm length of the metal buss tape is not making contact with the back metal

After additional stress testing, another 2 cm length of metal buss tape has failed

Conclusions

- Industry tests (UL1703, IEC61646/61730) are inadequate to detect thin-film buss tape reliability failures because they don't stress the failure mechanism adequately or are not performed for a long enough duration
- Creative use of failure analysis tools such as LBIC, IR and Acoustic Microscopy can be used to optimize tape application and observe incipient failure

Future Work

- Determine Coffin-Manson inverse power law relationship of various metal buss tapes
- Use Coffin-Manson relationship to project product lifetimes in various climates

Performance and reliability characterization of conductive inks for solar cell front grids and busbars

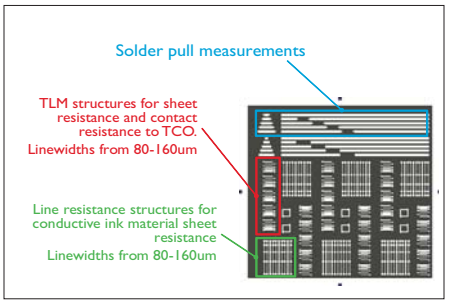
D.W.J.Harwood[1], S. Agaskar[1], S. Pirzada[2], S. Coughlin[2], L. Nguyen[2]
D2Solar, 2369 Bering Drive, San Jose, CA 95131[1]
AQT Solar, 1145 Sonora Court, Sunnyvale, CA 94086[2]

The temperature sensitivity of thin film CIGS cells and next generation crystalline silicon devices requires alternative metallization schemes for current collection and cell interconnection such as low temperature curable conductive inks. In addition to low contact and line resistance, ideally the conductive material should be solderable allowing serial connection of cells by tabbing and stringing of cells with solder coated copper ribbon. In comparison to traditional frit-fired silver pastes, silver filled conductive inks have both higher contact and line resistance due to the polymeric binder which can also reduce the metal surface available for soldering to the solder coated copper ribbon. In order to evaluate conductive inks for solar application, it is important to characterize both the electrical and mechanical characteristics pre- and post- reliability testing. In this study, a number of materials were characterized for their suitability as screen printed fingers and busbars both initially and as a function of reliability testing per IEC61646/61215 using non-encapsulated cells. Two materials were found as candidates for grid and busbar respectively that met the requirements for electrical and mechanical properties after reliability testing.

Electrical and mechanical characterization

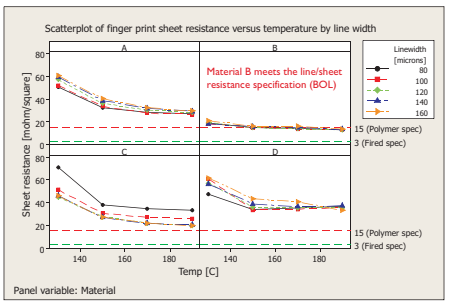
Conductive inks were evaluated for their suitability as both a conductor and interconnect surface using a screen printed test structure to evaluate the following parameters.

- Line resistance
- Contact resistance to surface e.g. TCO
- Print resolution - minimum line width
- Curing temperature
- Solderability - peel strength to cell surfaces



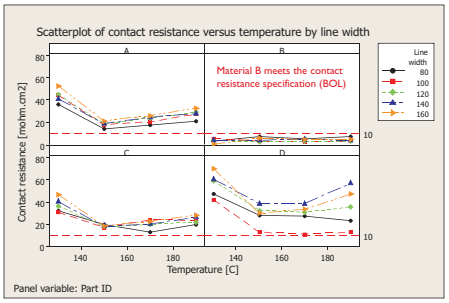
Line resistance versus curing temperature

As curing temperature increases, line resistance decreases. Print resolution issues at narrow line widths are revealed as higher sheet resistance when normalized to screen line width e.g. for material C 100um and 80um line show higher sheet resistance than expected.



Contact resistance vs curing temperature

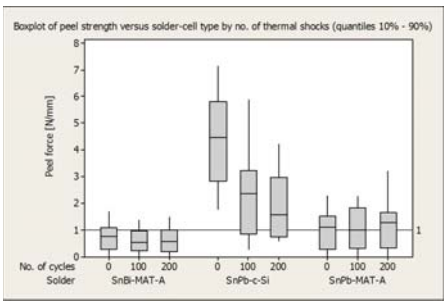
As curing temperature increases, contact resistance also decreases to a minimum but increases again as the conductive ink polymer binder begins to degrade. The maximum curing temperature is dictated by this minimum contact resistance value and the temperature sensitivity of the cell.



Based on the material and process evaluation for the conductive inks, material B was found to meet the requirements for sheet resistance of 15mohm/square and contact resistance of 10mohm.cm^2 at process temperatures below 200C.

Solder peel strength

Ideally, the material with the best electrical properties for grid (material B) would also be solderable allowing single step printing. However, this and many other materials were found to delaminate from the cell surface during soldering and only material A showed good solder peel values for both low temperature SnBi and conventional SnPb ribbon. Solder peel strength values are typically lower than a conventional fired contact but median values of 1N/mm were measured which remained stable over 200 thermal shocks in comparison to c-Si fired frits which start off higher but deteriorate with stress.



Reliability testing

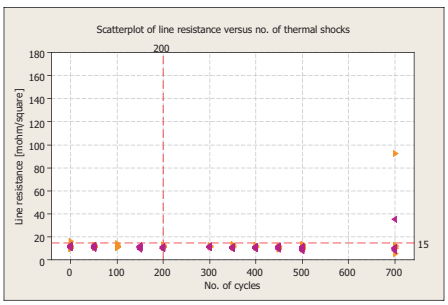
In addition to the solder peel strength of the busbars, the electrical characteristics of the grid materials were evaluated through reliability testing:

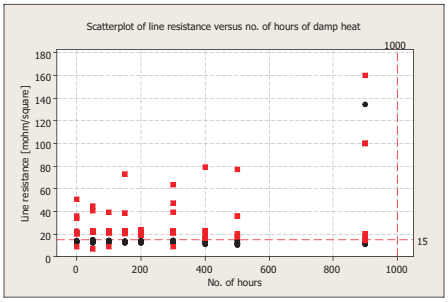
1. Thermal Shock (-40C to 90C)
2. Damp Heat (85C/85%RH)
3. Humidity Freeze (-40C to 85C/85%RH)

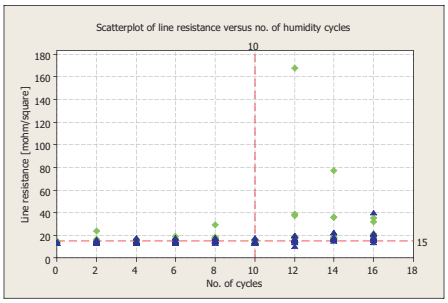
For worst case analysis, non-encapsulated test vehicles were used for these tests to determine the impact of both humidity and thermo-mechanical stresses on the materials. For edge sealed modules, moisture related failure modes e.g. damp heat, humidity freeze are eliminated but thermo-mechanical stresses are still present.

Line resistance versus reliability

Line resistance is seen to be very stable for thermal cycling stresses well in excess of IEC requirements but some degradation is observed in humidity tests for longer exposures on non-encapsulated samples.

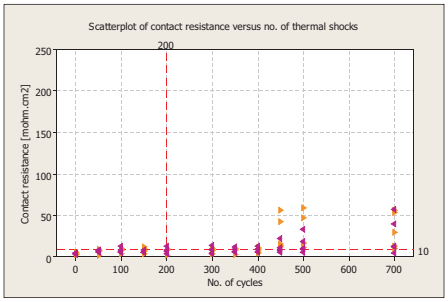


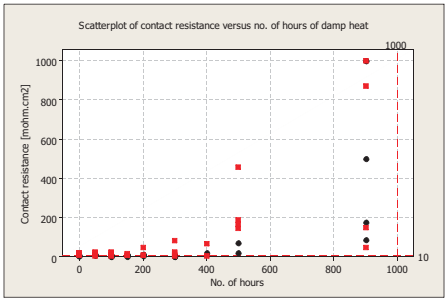


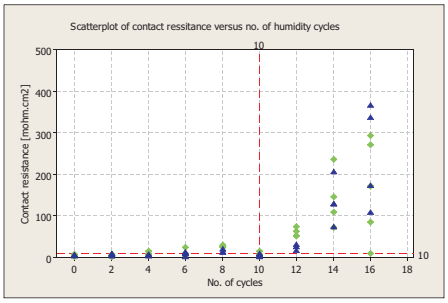


Contact resistance vs. reliability

Contact resistance on bare devices is more sensitive than line resistance to humidity exposure with similar increases seen in humidity cycle and damp heat testing.







Summary

Based on electrical, mechanical and reliability testing, two materials (A) and (B) were identified as promising candidates for application as busbar and grid materials.
A comparison of the performance of these materials and other candidates is summarized in the table below.

Property	Spec.	Material A	Material B	Material C	Material D	Material E
Line resistance [mohm/square]	<15	25	**15**	50	25	40
Minimum linewidth [microns]	<120	140	**100**	120	120	120
Contact resistance [mohm.cm2]	<10	30	**5**	100	25	35
Curing temperature [C]	<200	160	**130**	-	190	160
Median peel strength [N/mm]	>1	**1.1**	0.2	0.2	0	0.3
10th percentile peel strength [N/mm]	>0.2	**0.4**				

This poster does not contain any proprietary or confidential information.

Temperature Study on a-Si:H Solar Cell Degradation with Different Loading Conditions

Sang Hyun Park*, Yong Sun Kang, Jun-Sik Cho, Jeong Chul Lee and Kyung Hoon Yoon
Photovoltaic Research Center, Korea Institute of Energy Research (KIER), South Korea
*** e-mail: parksh@kier.re.kr**

Photovoltaic Research Center, Korea Institute of Energy Research

INTRODUCTION

The importance of predicting PV module lifetime reliable than previous trial is gaining significance with strongly growing PV industry.

There has been many researches mainly based on mathematical calculation for predicting PV module lifetime. However the results from these calculation have limitation to be practically applied to the commercial module evaluation and marketing.

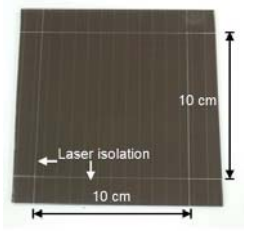
With many results and development in equipments for evaluating PV degradation characteristics, the practical test method which can predict PV module lifetime accurately are under research in many groups.

For relative reliable and accurate prediction of PV lifetime, detailed understanding in accelerating conditions and resultant degradation is essential.

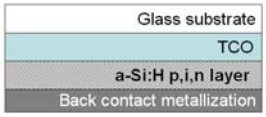
In this work, three different loading conditions and their effect on light degradation are compared for a-Si:H solar cell. Three loading conditions include open, short and maximum power point resistance. The maximum power point resistance has been calculated form the I-V characteristics before any light soaking.
The different degradation results from loading conditions has been analyzed by test cell temperature during the light soaking.

* The experiment in this work mainly focused on the degradation of a-Si cell itself. Other parts of complete module like back sheet, frame, soldering are not included in the analysis.

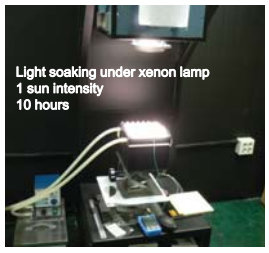
EXPERIMENTAL



(a)



(b)



(c)

Figure 1. (a) Amorphous silicon solar cell for indoor aging test with dimensions and (b) cross sectional view for cell structure and (c) 1 sun light soaking tester

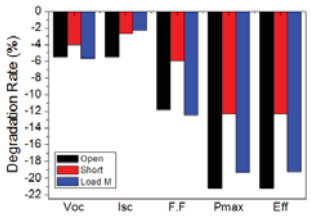


Figure 2. (a) Light degradation results depending on different loading. Light soaking intensity was full spectrum 1 sun (1kW/m^2) for 24 hours. Load M indicates resistive loading which has been calculated from the maximum power tracking point of I-V characteristics before light soaking.

Table. 1. The percentage change of electrical characteristics after 24 hours full spectrum light soaking. (%)

	Open	Short	Load M
Voc	-4.93	-3.92	-3.54
Isc	-3.72	-1.13	-3.29
F.F	-12.5	-3.94	-7.47
Pmax	-19.5	-8.89	-13.67
Eff.	-19.97	-8.78	-13.35

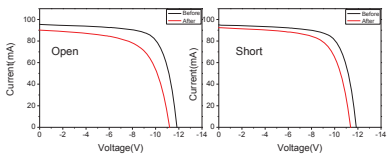


Figure 3. IV characteristics before and after 1 sun light soaking (24 hours) with different loading conditions.

Discussions

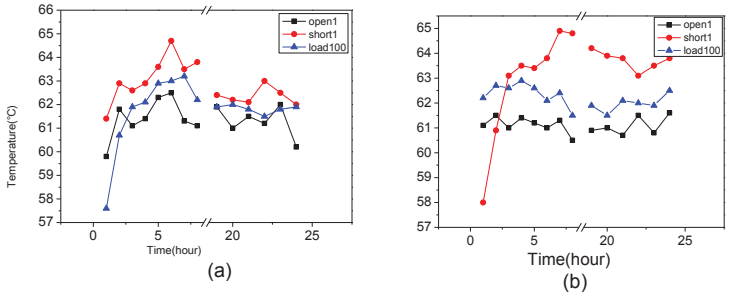


Figure 4. Two test sets of a-Si cell temperature during 24 hours 1 sun intensity light soaking. Both test shows opened load condition has higher cell temperature than other two load conditions during the whole light soaking test.

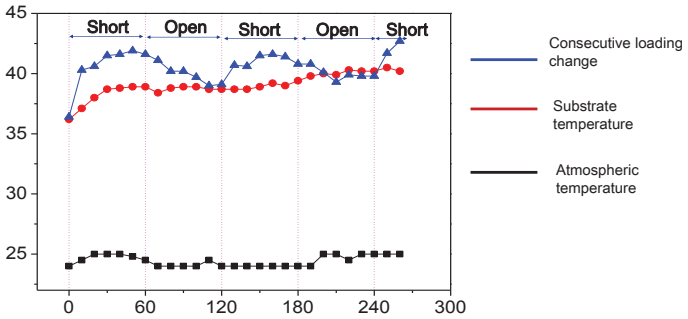


Figure 5. Consecutive loading variation between opened and shorted load conditions during the light soaking. This result indicates the temperature variation in Fig. 4 has been resulted from the loading condition itself.

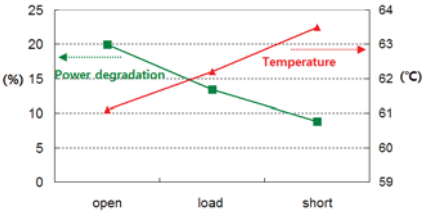


Figure 6. Comparison between a-Si cell temperature and power degradation after 24 hours light soaking with different loading conditions. This result shows different load conditions cause unexpected cell temperature difference with related power degradation rate.

Though the difference is small (few ℃s), different load condition shows clear relation to cell temperature during the light soaking and resultant output power degradation is almost twice different.
(Shorted test cell ⇒ - 8.78%, opened cell ⇒ nearly - 20%)

The electrical effects due to various load condition should be evaluated further for wider understanding of different load conditions in light soaking degradation

SUMMARY

- **Different load types resulted in different cell temperature during the light soaking which was not intended. This temperature difference would mainly be caused by the different amount of current flow through the a-Si cell.**
- **The output power degradation rate depending on different load conditions shows clear relation with test cell temperature resulted from load conditions. As generally known from Stabler-Wronski effect, higher temperature (short) suppressed output power degradation while lower temperature (open) showed most degradation with light soaking.**
- **For relatively accurate prediction of a-Si module lifetime, above degradation rate difference caused by different loading condition should be carefully considered.**

ACKNOWLEDGEMENT
This work was supported by the New & Renewable Energy of Korea Institute of Energy Technology Evaluation and Planning (KETEP) grant funded by the Korea government Ministry of Knowledge Economy (*No. 20093020010080*)

Accelerated Ageing and Reliability of CIGS Thin Film Solar Cells

Raymund Schäffler[1]

Th. Walter[2]*, Ph. Mack* [2]*, Th. Ott* [2]

[1]*:Würth Solar GmbH & Co KG,* [2]*:Univ. of Applied Science, Ulm*

Abstract:

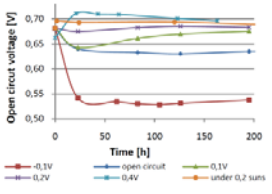
Solar cells based on CIGS play a significant role in thin film PV due to conversion efficiencies exceeding 20 % [1]*. However, not only the efficiency but also the long term stability is crucial for the assessment of a PV technology. Within the project "RECIS" (funded by the German Government) the reliability and long term stability of CIGS based solar cells have been investigated. The well known metastability of the CIGS material is addressed.*

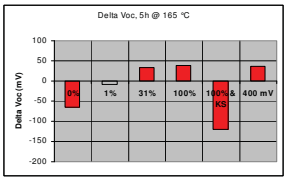
In order to assess the long term behavior of high efficiency solar cells (14 – 16 %) accelerated ageing experiments under different conditions were carried out. Parameter drifts of Voc, ff, reverse characteristics and luminescent (EL, PL) properties were monitored during high temperature operation (85 – 205 °C) and analyzed. From these parameter drifts activation energies were extracted allowing the extrapolation and prediction of parameter drifts under real field conditions. In a second step the physical reasons for the observed parameter drifts were investigated and operation conditions for an improved stability were established.

Results:

Voc parameter drifts:

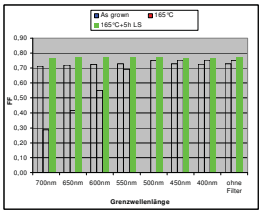
For a dark anneal we observed a Voc drop of about 5 -10 %. The activation energy for the initial drop ranges around 1 eV followed by a saturation of the parameter drift. This parameter drift can be associated to a decrease of negative charge in the absorber as a result of the dark anneal. An illumination intensity as small as 1-10 % of one sun (i.e. 10W/m² - 100W/m²) during the high temperature anneal is sufficient to stabilize or even enhance Voc slightly (lightsoak). Alternatively a positive bias of 100-200 mV applied externally to the device leads to a similar result indicating that rather the splitting of the quasi fermi levels than the light absorption seems to be responsible. It should be noted that the application of a negative bias leads to a drop of Voc. This drop seems to be reversible. Thus such *continuous* operation conditions should be avoided, consequences for reliability issues are further investigated.

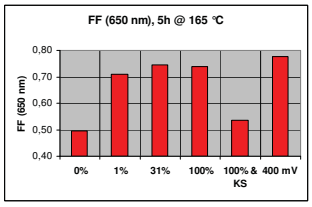




FF parameter drifts:

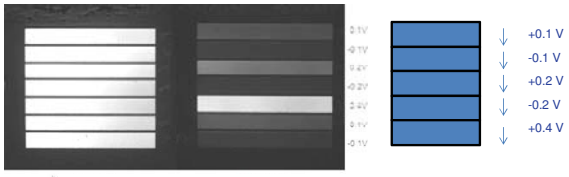
The parameter drift of the ff also exhibits a thermally activated behavior with a similar activation energy (~1eV), however, with a much higher prefactor, resulting in a significant slower ageing process compared to Voc. The drift of the ff can be associated to the so called "blue metastability" which is due to a change of interface properties probably related to the existence of negative interface charges. The expression "blue metastability" stems from the fact that hole generation in the CdS can cancel the ageing due to charge compensation at the interface. Therefore, compared to Voc the ff is a less relevant reliability parameter. Nevertheless, illumination or application of a positive bias further stabilizes and eventually enhances the ff.





Luminescence properties:

Ageing of CIGS Cells in general also affects EL and PL by interface and bulk properties (see above). Therefore, these imaging techniques are a suitable and fast method to assess the ageing state of CIGS-based devices.

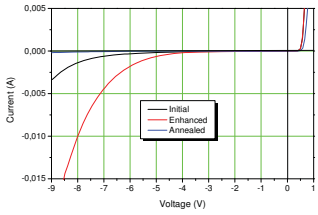


b) Initial

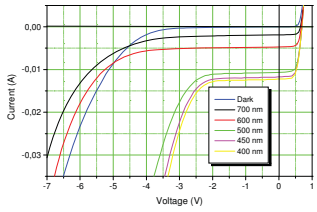
after 40 h @ 125 °C
under applied bias

Reverse characteristics:

The reverse characteristics play an important role for the partial shadowing in an interconnected module. These reverse characteristics are also strongly affected by the ageing – i.e. the conditioning status - of the devices as negative interface charges influence the field distribution in the junction under reverse bias and impact consequently breakthrough currents.



Impact of conditioning status of the cell



impact of spectrum

Illumination of window layer significantly reduces hot spot risk (close to "real life")

Summary:

In summary it can be stated that especially under illumination or application of a positive bias the investigated devices exhibit a high degree of stability. A critical parameter with respect to the reliability seems to be the existence of a permanent negative bias across the junction. Application of continuous negative operation conditions is under further investigation.

Energy Production Comparison of Four Representative Solar Cell Technologies: mc-Si, a-Si, CIGS and OPV

Dr. Richard Childers/Konarka

Elsa Kam-Lum/Total S.A.

NREL Reliability Workshop, February 2011

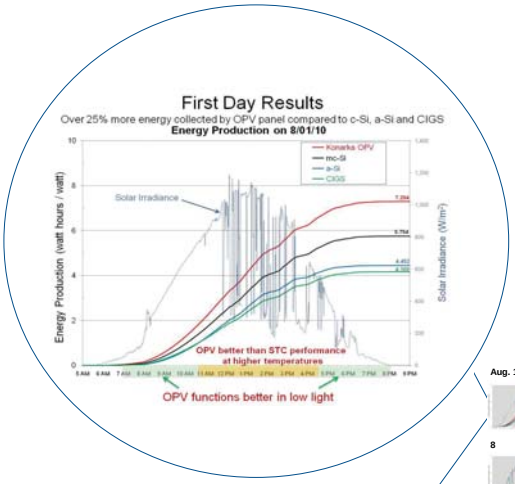
- This report summarizes the work from an initial scoping study at Konarka to compare energy production of four different PV technologies. Representative, commercially obtained PV panels from four types of solar technologies, mono-crystalline Si, a-Si, CIGS and OPV exposed to Boston Area (42° Latitude) outdoor conditions were monitored for daily energy production during August to November 2010. The OPV panel surpassed the energy production of mc-Si, a-Si and CIGS panels in watt-hrs per nameplate watt every day on all 4 months monitored.
- Comparison of the daily results are presented for the 4 month period (August to November 2010).

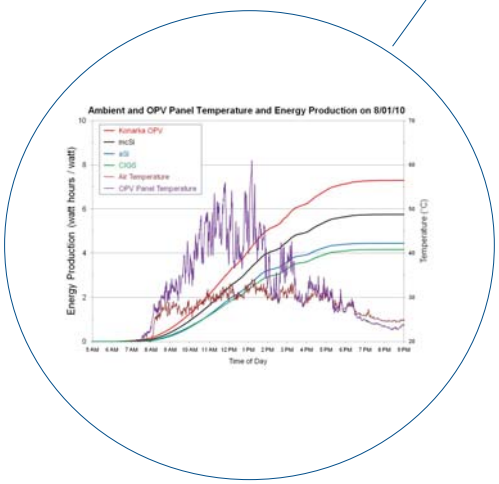
Methodology

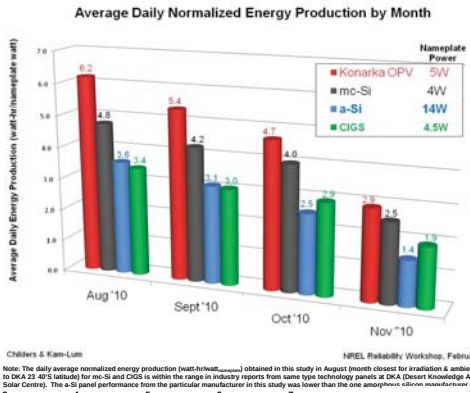
- Test Vehicles: PV test panels acquired commercially
- Test location: Konarka Headquarters - Boston, MA area
- Panels Orientation: due South tilted at 42° off horizontal (at latitude)
- Measurements:
  - •Parameters: voltage, current, temperature and irradiance
  - •Frequency: data acquired and stored every 1 minute from 5am to 9pm, every day over the 4 months reported.

•Data Acquisition Equipment:
- digital voltage and current meters
- microprocessor controlled maximum power point tracking (50 msec response time) for each panel under test
- ambient and OPV panel temperatures measured with type K thermocouples
- Eppley Model PSP pyranometer to measure solar irradiance

Outdoor Measurements, Boston, MA area, USA

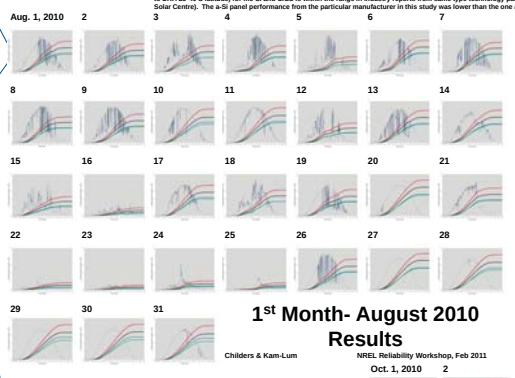


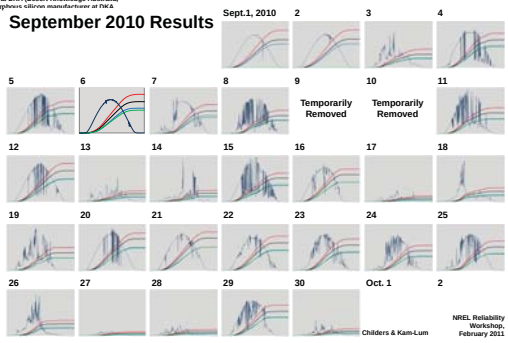


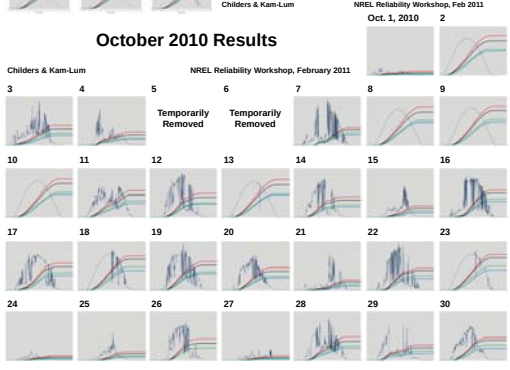


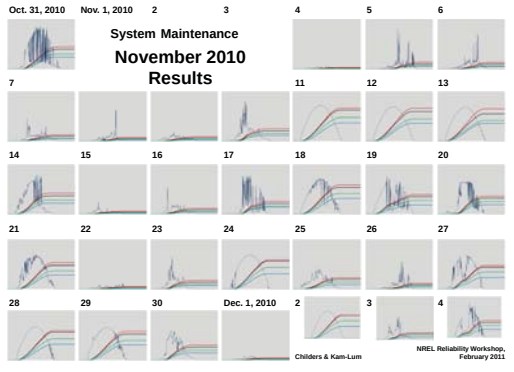
ENERGY PRODUCTION (in watt-hr)
POWER (Panel rating in watt)

Highest for Konarka OPV









Conclusions & Recommendations

- The OPV panel energy production surpassed the energy production of mono-crystalline Si, a-Si and CIGS commercially obtained panels every day during the 4 months of monitoring.
- •Decreasing energy production was observed for all panels over the four months. This is believed due to each technology's particular temperature coefficient properties and decreasing ambient temperature and irradiation between August to November at 42° latitude. Corresponding ambient temperature and irradiation data is being compiled.
- The daily average normalized energy production (watt-hr/watt$_{nameplate}$) obtained in this study during August for mc-Si and CIGS is within the range in industry reports from same type technology panels at DKA (Desert Knowledge Australia, Solar Centre).
- •This was a scoping study of energy production of four different solar photovoltaic technologies from commercially available panels when exposed to outdoor conditions at 42° latitude. A more in-depth study adding other PV technologies not included in this study, with more manufacturers and larger number of samples and longer duration is recommended.

Contact:
Richard Childers/Konarka
rchilders@konarka.com
Elsa Kam-Lum/Total S.A.
ekam-lum@konarka.com

This poster presentation does not contain proprietary or confidential information

Konarka – converting light to power – anywhere

nanosolar KEEPING THE WATER OUT FOR 25 YEARS

NANOSOLAR UTILITY PANEL



DESIGN FOR DAMP HEAT RELIABILITY

- Glass/glass package
- Water resistant junction-box
- Edge-seal embedded with desiccant

MODELING

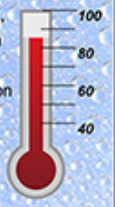
To define the appropriate width of edge-seal that would protect the CIGS from moisture degradation over the panel lifetime, a 1-D diffusion process has been used. Nanosolar edge-seal has been modeled as a finite volume of a Fickian material filled with a desiccant to immobilize water until it saturates. The results of this model have been validated against experimental data sets (Figure 1).

Using real environmental data, simulations of water penetration over 25 years can be run for various edge seal thicknesses and various climates. Based on the Nanosolar model, 7.5 mm is the absolute minimum edge seal width allowable for 25 year lifetime (Figure 2) but based on damp-heat experimental data, 9 mm is a more realistic width.

Therefore, after taking into account process variations and adding a 1 mm safety margin, Nanosolar edge-seal width specification has been set to 11 mm ±1 mm.

CONTEXT

From 2005 to 2007, 70% of the thin film panels and 28% of the crystalline silicon panels tested for qualification failed 1000 hours damp heat test. [1]



BACKGROUND

Damp heat exposure is particularly harmful to CIGS devices with humidity being the primary cause of degradation. The challenge for Nanosolar was to design and manufacture a robust package that could keep moisture out during 25 years.

Glass/glass packages which restrict potential moisture ingress to the edge of the panel and through the junction-box was an obvious choice but this design still has significant moisture ingress through its edges [2]. The preferred way to prevent moisture ingress over the lifetime of the panel is by adding a low-diffusivity edge-seal embedded with an active moisture absorber.

Water penetration in the edge-seal in HALT

No water breakthrough observed yet in panels after 6000 hours of damp-heat.

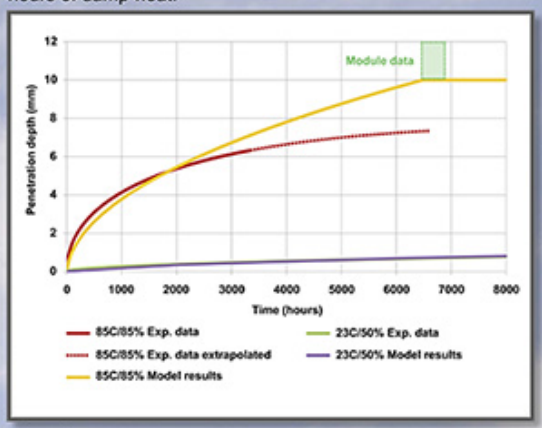


Figure 1

Damp Heat

Nanosolar panel withstands more than 3000 hours of damp heat with less than 5% change in power and no wet-leakage failures.

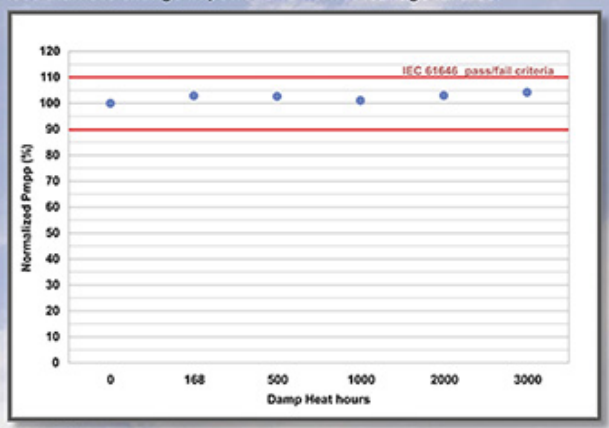


Figure 3

Water penetration in the edge-seal in Hawaii

Simulation of the water penetration depth for different edge-seal thicknesses in Honolulu, Hawaii.

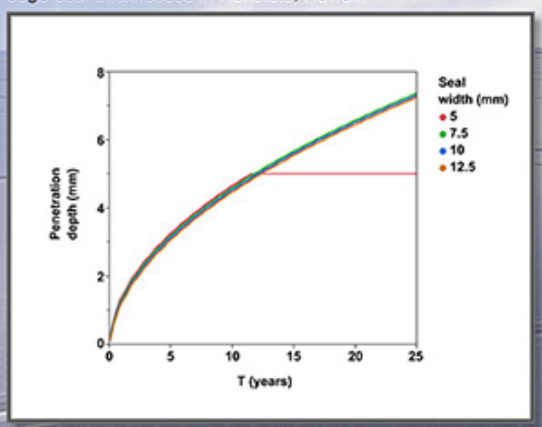


Figure 2

Damp Heat and High Voltage

Nanosolar panel withstands 1000 hours of damp heat and 1500V test with less than 5% change in power and without structural damage.

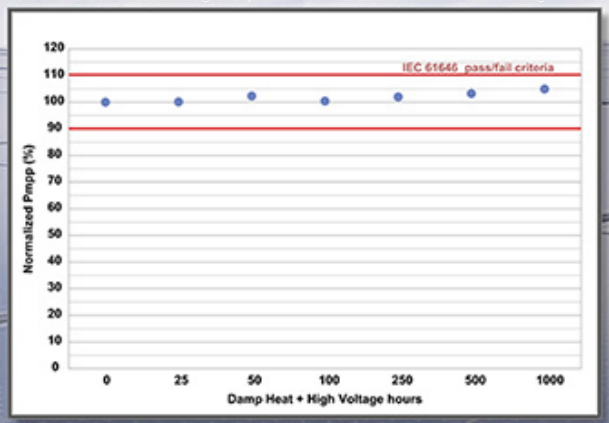


Figure 4

DAMP-HEAT TESTS

By choosing the right materials and the right design, the Nanosolar panel can withstand more than 3000 hours of damp heat test with less than 5% change in power (Figure 3) and without failure in the wet-leakage test.

As the Nanosolar Utility Panel has been designed for high-power and utility-scale applications, it was important to test its ability to withstand high voltage relative to ground. Therefore, in collaboration with ZSW Photovoltaic Department, Nanosolar performed a damp-heat test with high voltage. During the exposure time in the climate chamber, a voltage of -1500V is connected between the positive pole of the panel and the metallic structure that retains the panel.

As expected and reported in the literature [3], Nanosolar packaging blocked leakage current very effectively in the damp-heat test. After 1000 hours of damp-heat with high-voltage, Nanosolar panels have more than 4% power increase and no structural damage (Figure 4).

O. Suavet, E. Prather, D. Bayon

[1] G. TamizhMani; B. Li; T. Arends; J. Kuitche; B. Raghuraman; W. Shisler; K. Farnsworth; J. Gonzales; A. Voropayev; P. Symanski; Failure analysis of design qualification testing: 2007 VS. 2005; 2008 33rd IEEE Photovoltaic Specialists Conference (May 2008), 2008, pg. 1-4

[2] Kempe, M. D. 2006 "Modeling of Rates of Moisture Ingress into Photovoltaic Modules", Solar Energy Materials and Solar Cells, Vol. 90, pp. 2720-2738

[3] Hacke, P.; Terwilliger, K.; Glick, S.; Trudell, D.; Bosco, N.; Johnston, S.; Kurtz, S. R. (2010). Test-to-Failure of Crystalline Silicon Modules: Preprint. 10 pp.; NREL Report No. CP-5200-47755

Solar Attachment Adhesives for Building Applied Photovoltaic (BAPV) with Superior Bond Strength

Tim O'Neil and Samar Teli, ADCO Products Inc.

INTRODUCTION

Photovoltaic (PV) attachment adhesives are required to adhere to a wide array of substrates. These substrates include the roof/building surface and the PV back sheet. The attachment adhesive must exhibit superior bond strength to both the PV module and building material for their warranty lifetime while being able to withstand the harshest environmental conditions. Without an adequate attachment solution, long term reliability of BAPV arrays can be compromised.

REQUIREMENTS

- Heat Aging
- Environmental Stress Resistance
- Wind Uplift Resistance
- Hail Damage Resistance
- Electrical Safety and Performance
- Fire and Flammability

Reference Standard Documentation

• FM 4470	• IBC, IRC, UBC
• UL 1703, 2703	• Miami-Dade
• IEC 61730	• ASCE 7
• IEC 61646	• ASTM
• ICC (AC365)	• CAL Fire Code

MINIMUM REQUIRMENTS – ADCO RECOMMENDATIONS

Based on Extensive Knowledge and Experience in the Roofing Industry, ADCO Recommends Minimum Test Requirements For BAPV Attachment Adhesives:

- **Peel Strength -** ASTM D-903 (12"/minute)
- **Shear Strength -** ASTM D-1102 (0.2"/minute)
- **Aging and Test Conditions:**
  - 24 hours at 25ºC/50% RH
    - Pull at room temperature
  - 7 days at -40ºC
    - Pull at -40ºC and Room Temperature
  - 7 days at 25ºC/50% RH
  - 7 days at 85ºC
  - 1000 hours Damp Heat (85ºC/85%RH)
  - 200 Thermal Cycles (IEC61646, UL1703)
  - 10 Humidity Freeze Cycles (IEC61646, UL1703)
    - Pull at 85ºC and Room Temperature (All Above)

ADCO PVA 600BT - KEY PERFORMANCE ATTRIBUTES

- High bond strength
  - High peel and shear strength
    - Resists high wind loading
    - Resists up-curl and up-lifting
- Long term durability
  - Over 20 years of field history
- Ease of installation
  - Peel and stick speed and convenience
    - Reduced installation time
    - Purpose designed release liners
      - provides superior release
    - No primers needed
      - Reduced installation time
      - Reduced training requirements
      - No toxic or flammable solvents

PVA 600BT TYPICAL ADHESIVE STRENGTH PROPERTIES

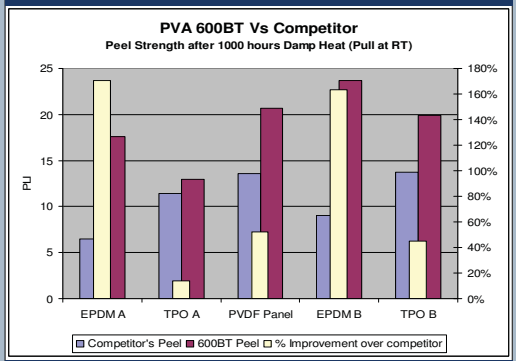
PVA 600BT Typical Adhesive Strength Properties

Flexible PVs were bonded to various substrates using PVA 600BT. Peel and shear values were then determined after exposure to the following conditions.

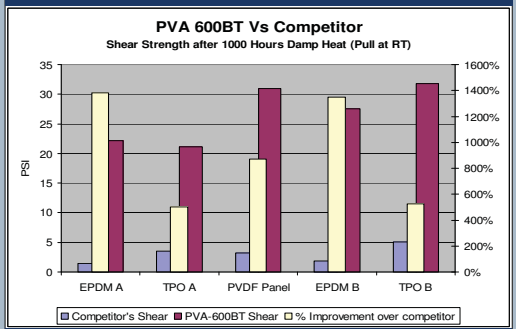
Time	Temperature	Test Conditioning	Typical Peel Values (ASTM D-903) TPO	EPDM	PVDF Painted Steel	Typical Shear Values (ASTM D-1102) TPO	EPDM	PVDF Painted Steel
			All results expressed in pli			All results expressed in psi		
24 hours	RT	RT	15	10	19	15	10	5
24 hours	70°C	RT	21	11	20	20	15	8
24 hours	70°C	70°C	3.5	3	7.5	6.5	6.5	2
24 hours	85°C	85°C	3.5	3.5	5	9	8	2.5
24 hours	-40°C	-40°C	15	15	24	30	30	10
7 days	RT	RT	15	20	20	15	13	6.5
7 days	70°C	RT	13	10	22.5	20	20	12
7 days	70°C	70°C	3.5	3	9	20	12	3
7 days	85°C	85°C	3.5	3.1	6.5	15	10	3.5
7 days	-40°C	-40°C	17	15	24	30	30	6
UL1703 & IEC61646 Conditions								
10 Humidity Freeze Cycles		RT	23	25	18	12	6	15
1000 Hours Damp Heat		RT	15	15	9*	20	20	30
200 Thermal Cycles		1 hr @ 85°C	2.5	1.5	1.5*	4	5	8
200 Thermal Cycles		RT	20	20	10*	13	8	15

*Superstrate failure.

PEEL STRENGTH – DAMP HEAT AGING



SHEAR STRENGTH – DAMP HEAT AGING

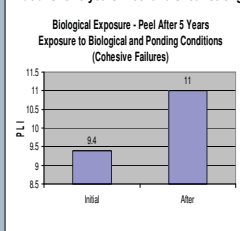


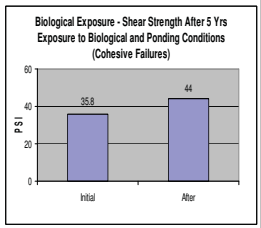
LONG TERM DURABILITY



BIOLOGICAL EXPOSURE

Samples of roofing membrane submerged in a water tank seeded with typical roofing debris for 5 years. Peel and shear strength were measured before and after exposure.





SUBSTRATES TESTED WITH

Materials Tested with PVA 600BT

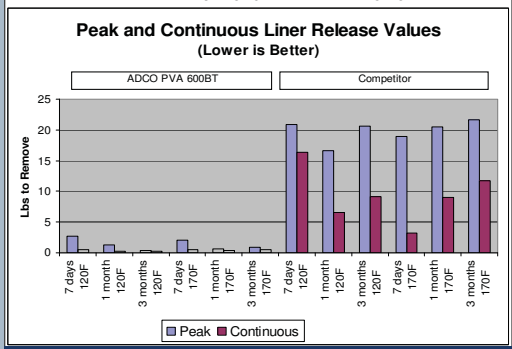
The materials listed below have been tested with or are being tested with the 600BT

Roofing Materials		PV Materials
Carlisle TPO	Johns-Manville Granulated Mod-Bit	LPL Backsheet
Firestone TPO	Garland Smooth Mod-Bit	PVDF film (Kynar)
GAF TPO	Garland Granulated Mod-Bit	Tefzel Adherable)
Stevens TPO	Garland Coated/Granulated Mod-Bit	Glass
Johns-Manville TPO	CertainTeed Mod-Bit	
		J-Box Materials
Carlisle EPDM	Eternalastic 911 (Tropical Asphalt)	Noryl (500-701 black)
Firestone EPDM	Siplast PC-227	Lexan (SE1-GFN2)
Mulehide EPDM	Pyramic 7467 White Coating	
	Garlabrite 7411 Silver Coating	**Other Materials**
PVDF coated steel (4 brands)		Stainless Steel
Galvaneal		Sealed concrete
Galvalume Plus		

PVA 600BT is not compatible with PVC materials.
If not listed above, testing of specific substrates is recommended to ensure satisfactory results.

EASE OF INSTALLATION

LINER RELEASE FORCE AFTER HEAT AGING



CONCLUSIONS

- **PVA 600BT is a high strength, thermoset butyl that offers a broad spectrum solution to long term BAPV attachment**
- **Superior adhesion properties to many types of roofing and BAPV substrates**
- **Over 20 years of field history in the roofing industry**
- **Superior adhesion performance after vigorous reliability tests including heat aging and thermal cycling**
- **Excellent performance after harsh rooftop biological exposure**
- **Easy installation for reduced installation costs**
- **Does not require primer, reducing costs and eliminating safety concerns**
- **Peel & Stick methodology is readily accepted by the roofing industry**
- **ADCO sets the standard in performing accelerated aging tests at levels beyond any standards available today for BAPV attachment adhesives**
- **ADCO will continue to work with NREL and building regulatory bodies to provide benchmarks and set minimum application requirements for BAPV**

Acknowledgements:

The Authors would like to thank Paul Snowwhite, Dennis Booth, Jim Wood, Justin Bates and Tom Springstead for their assistance.

This poster does not contain any proprietary or confidential information.

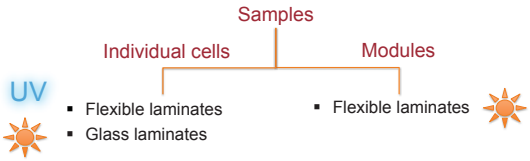
Effect of long-term light soaking on shunts and P_{max} in CIGS solar cells and modules

A. Kamer, S. Jayanarayanan, N. Staud, D. Nayak, B. Metin, E. Lee, M. Pinarbasi

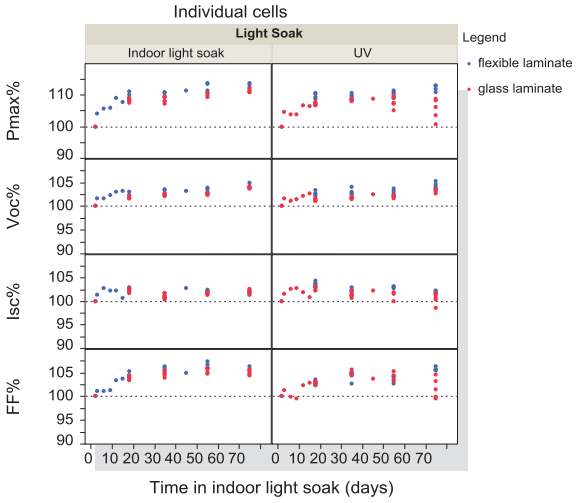
Solopower, 5981 Optical Ct., San Jose, CA 95138

Goal of the Study

- Understanding the effect of prolonged light soaking on P_{max}, V_{OC}, FF and J_{SC}
- Shunt generation with prolonged light soaking

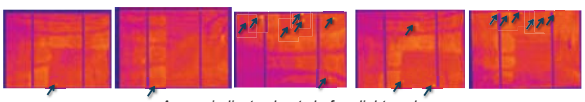


Effect of light soaking on P_{max}, V_{OC}, FF and I_{SC} and shunts of individual cells



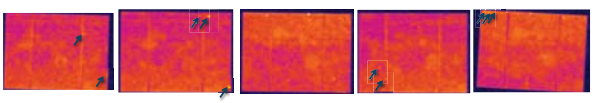
- The cells were loaded in the last 40 days
- Average dose per day was 14.4 kWhr/m²
- The total dose 75 days was 1080 kWhr/m²

Before light soak



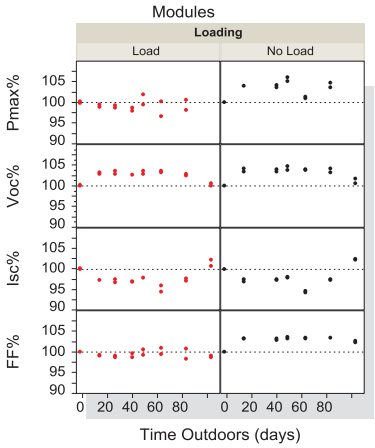
Arrows indicate shunts before light soak

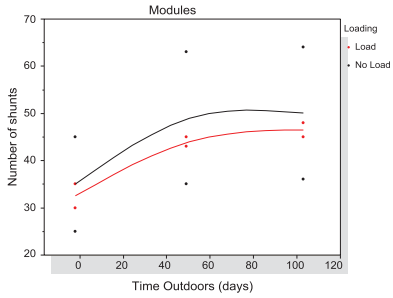
After 45 days indoor light soak



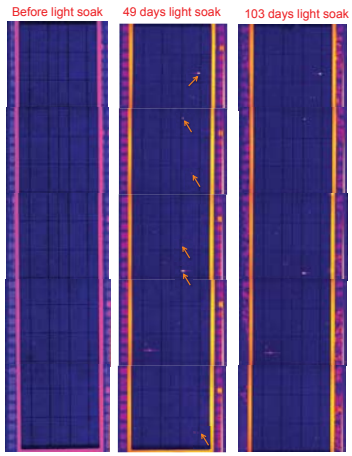
*Arrows indicate **new** shunts after light soak*

Effect of light soaking on P_{max}, V_{OC}, FF and I_{SC} and shunts of flexible modules

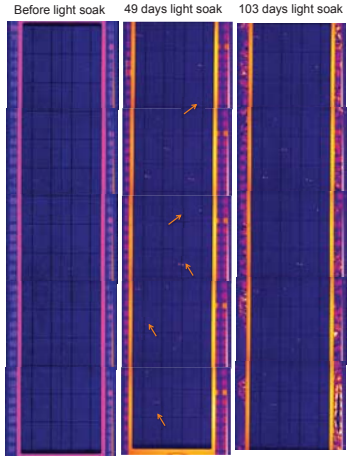




- Average dose per day was 3.4 kWhr/m²
- The total dose after 103 days was 348 kWhr/m²



Arrows indicate new shunts



Conclusion

Panels (100 days light soaking, 350 kWhr/m²)

- Light soaking of unloaded, flexible panels increased P_{max} by ~ 5%
- Loaded panels retained their initial P_{max} value within 3%
- New shunts were generated in the first few days of light soaking
- The number of shunts stayed constant for more than 3 months
- Shunt generation did not degrade panel performance

Individual cells (75 days light soaking, 1080 kWhr/m²)

- New shunts were created
- No performance degradation was observed with or without loading
- Individual cell data supported the results from the module light soaking data

This poster does not contain any proprietary or confidential information

Strategies For Developing Barrier Films For Photovoltaics

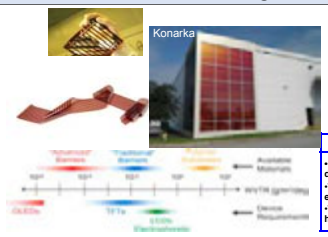
Yongjin Kim[1], Hyungchul Kim[1], Namsu Kim[1],and Samuel Graham[1,2]

[1]Mechanical Engineering, *Georgia Institute of Technology, Atlanta, GA 30332,*

[2]Materials Science and Engineering, Georgia Institute of Technology, Atlanta, *GA 30332*

Background

The development of barrier films is a critical technology to reduce the susceptibility of photovoltaic systems to environmental degradation. These barrier films, which have effective water vapor transmission rates (WVTR) less than 10^{-4} g/m^2/day, often consist of multilayer films deposited by vacuum deposition. Methods which can be used to improve barrier properties while maintaining mechanical durability are critical for the packaging of flexible organic electronics.



Barrier Issues

Barrier Layer WVTR	Barrier Layer Mechanical Performance
• Single layer vacuum deposited barrier films contain defects which limits their effectiveness. •The microstructure of the thin films controls their effective WVTR and is not well understood. •The impact of interfaces on the transmission properties has not received much attention.	•The mechanical properties of most barrier film are not known and are needed to model the stresses in the films. •Fracture toughness and adhesion are critical to mechanical reliability. •Methods to enhance mechanical reliability are needed.

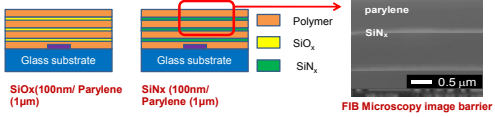
Research Objectives

• Investigate the nucleation of thin films and interfaces and its impact on barrier layer performance.

•Investigate the mechanical adhesion in barrier films.

• Investigate edge sealants for high performance laminated barrier systems.

Multilayer Organic/Inorganic Barrier Films



SiOx(100nm/ Parylene (1µm)

SiNx (100nm/ Parylene (1µm)

FIB Microscopy image barrier



Barrier films consisted of:

SiO_x/Parylene

SiN_x/Parylene

SiNx/ PMMA

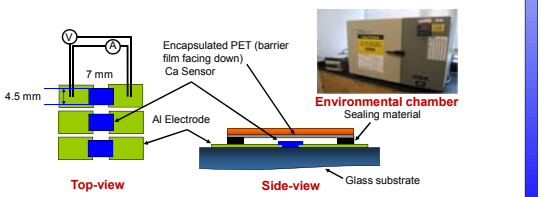
Al_2O_3/ Cytop

Al_2O_3, ZnO, or Al_2O_3/ZnO



Films were deposited on PET substrates at 110 C (flexible lids) or directly onto Ca samples for testing. Parylene, PMMA, and Cytop were deposited at room temperature and annealed at 110 C. Barrier films ranging from one to four dyads created and tested.

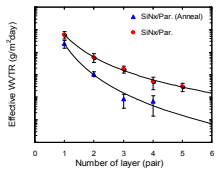
Ca corrosion test





$$WVTR[g/m^2/day] = 2\delta_{Ca} \times \rho_{Ca} \times \frac{dG_3}{dt} \times \frac{M(H_2O)}{M(Ca)} \times \frac{Ca_Area}{Window_Area}$$

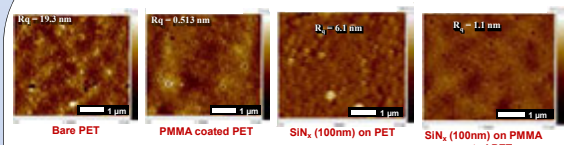
SiNx/ Parylene Results



No. of Layers [pairs]	WVTR [g/m²/day] Before annealing	After annealing	Decrease in WVTR [%]
1	4.3×10^{-3}	2.4×10^{-3}	44
2	4.4×10^{-4}	1.3×10^{-4}	70
3	1.3×10^{-4}	7.3×10^{-6}	94
4	4.4×10^{-5}	6.6×10^{-6}	85

Annealing of the polymer layer was found to result in an improvement in barrier performance.

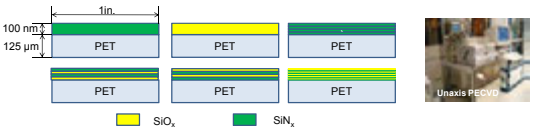
Nucleation Of Barriers on PET



Bare PET | PMMA coated PET | SiN_x (100nm) on PET | SiN_x (100nm) on PMMA coated PET

Surface treatments play a large role in the quality of the barrier film. Amorphous SiN_x layer are smoother when grown on a PMMA buffer layer and has a smaller grain-like structure. This results in improved barrier performance.

The Role of Interfaces: PECVD Nanolaminates



Nanolaminates were created using PECVD deposition film (SiO_x/SiN_x) on PET lids. The film thickness was held constant at 100 nm while alternating layers of SiO_x and SiN_x were deposited. By reducing the thickness of each layer, the number of interfaces in the barrier films was increased.

Barrier performance of PECVD films

Number of dyads	Film structure/composition	WVTR [g/m^2/day]
1	SiO_x(100nm)	$3.26 \ 10^{-2}$
1	SiN_x(100nm)	$2.03 \ 10^{-3}$
2	SiN_x(25nm)/SiO_x(25nm)	$1.94 \ 10^{-3}$
2	SiO_x(25nm)/SiN_x(25nm)	$1.04 \ 10^{-3}$
4	SiN_x(10nm)/SiO_x(10nm)	$1.94 \ 10^{-3}$
2	SiN_x(25nm)/SiN_x(25nm)	$2.27 \ 10^{-3}$

The Role of Interfaces: ALD Nanolaminates

AFM scan data of Thermal ALD films

	Al_2O_3	ZnO	Al_2O_3/ZnO nanolaminate
Roughness [nm]	0.236	1.07	0.488

Al_2O_3/ ZnO nanolaminate layers are deposited as 1:20 ratio with the total thickness of 100 nm. The Single Al_2O_3 and ZnO are also 100 nm.

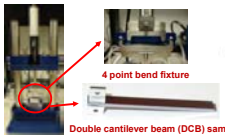
Comparison of ALD Nanolaminates to Organic/Inorganic Multilayers

Film structure/composition	WVTR [g/m^2/day]
Al_2O_3	4×10^{-4}
ZnO	7×10^{-4}
3 dyads of PMMA(400 nm)/SiN_x(100 nm)	$<5 \times 10^{-5}$
10 dyads of Al_2O_3(5 nm)/ZnO(5 nm)	$<5 \times 10^{-5}$
Commercial Barrier	$<5 \ 10^{-5}$
Glass Slides (sealant performance)	5×10^{-5}

Nanolaminates made from atomic layer deposition results in a synergistic effect which reduces the water vapor transmission rate beyond that of individual layers. This impact shows that ultrathin and ultrahigh barrier performance can be achieved.

Adhesion At Interfaces

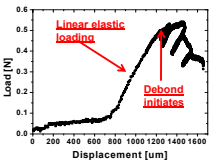
Delamination test with 4pt and DCB Samples



$$G < G_c \left[J/m^2\right]$$

Environment and stress accelerates defect evolution.

Test setup



Load vs. displacement curve with DCB sample



DCB experimental sample

$$G_c = \frac{12(1-\nu^2)P^2a^2}{Eb^2h^3}$$

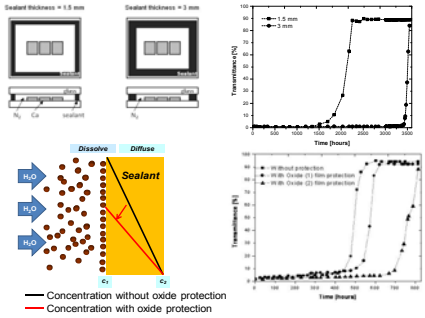
= 1.84 J/m²

a_c = 29.94 mm
P_c = 0.3747 N

•The adhesion within the barrier layers is important to ensure the mechanical robustness of these films.

•SiNx/Parylene layers were shown to have an interfacial fracure energy of 1.5 - 4 J/m^2.
•SiNx PMMA layers were shown to have 30-36 J/m^2 showing vastly improved adhesion.
•Interface modification can be used to improve adhesion and resist environmental degradation effects.

Edge Sealant Performance



•Desiccant filled polyisobutylene edge have shown excellent performance. (WVTR < 10^{-3}g/m^2/day).
•A thin oxide layer (30nm) can be used to improve the sealing performance, increasing the Ca lifetime by 60%.

Conclusions

The structure of barrier films can play a large role in their effective WVTR. The use of nanolaminate inorganic or organic/inorganic films both provide excellent barrier performance. Adhesion in inorganic/organic laminates may provide some concern in long term performance in solar environments and must be addressed. Finally, edge sealants which utilize desiccant materials show promise for creating high performance laminated packaging for PV cells.

Georgia Institute of Technology | NSF | MDITR | CIS:SEM Center for Interface Science : Solar Electric Materials | COPE | emrl Electronics Manufacturing And Reliability Laboratory

Understanding Degradation Pathways in Organic Photovoltaics

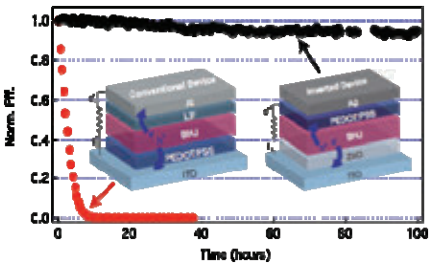
Matthew T. Lloyd,[1] Dana C. Olson,[1] Andres Garcia,[1] Isaac Kauvar,[2] Nikos Kopidakis,[1] Matthew O. Reese,[1] Joseph J. Berry,[1] David S. Ginley[1]

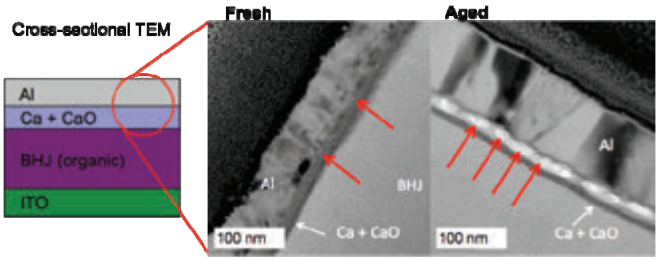
[1] National Center for Photovoltaics, National Renewable Energy Laboratory, Golden, CO 80401
[2] Materials Science and Engineering, Stanford University, Stanford, CA 94305

Presented at the 2011 Photovoltaic Module Reliability Workshop, February 16-17, 2011, Golden, Colorado

Enhanced Environmental Stability via Contact Selection

Organic photovoltaics (OPVs) require an offset in the work function of the anode and cathode in order to efficiently extract charge from the active layer. Conventional devices rely on low work function contacts, such as LiF/Al or Ca/Al, the chemical reactivity of which precludes fabrication or operation outside of an inert atmosphere glovebox. By employing ZnO as the electron accepting contact and using PEDOT:PSS to collect holes, the relative stability of these materials enables extended operation in air without an encapsulation layer.



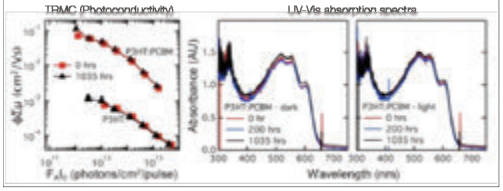


Lloyd et al., J. Mater. Chem., 19, 7638 (2009).

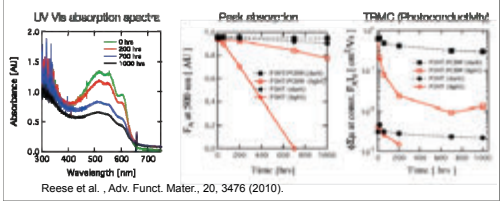
Impact of Oxygen and Moisture on the Active Layer

Contrary to conventional wisdom, in an inert atmosphere the electronic and optical properties of the polymer-fullerene blend prove to be inherently stable. After 1000 hrs illumination in an inert atmosphere there is is no change in the photoconductivity or the UV-Vis absorption spectrum for bare films of P3HT:PCBM on glass (i.e. not functional devices). Outside of the glovebox, however, there is an appreciable loss in light-absorbing chromophores in pristine P3HT. When blended with PCBM, photobleaching of the active layer system can be mitigated significantly.

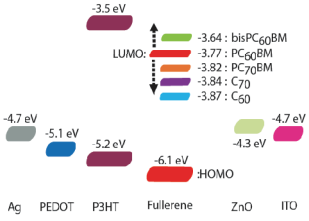
Inert atmosphere



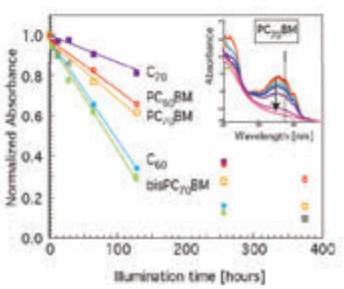
Ambient atmosphere

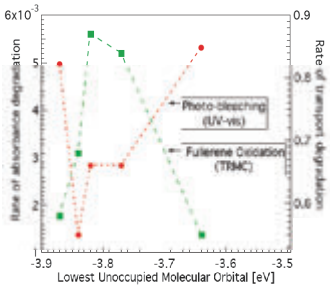


Reese et al. , Adv. Funct. Mater., 20, 3476 (2010).



The degree of stabilization imparted to P3HT by the electron acceptor is intimately related to the D/A morphology, exciton lifetime, and the energy levels that drive charge transfer. Preliminary data indicate that a smaller the LUMO-LUMO offset results in a higher rate of photobleaching in P3HT. We have also observed this trend in D/A systems where the LUMO level of the acceptor can be systematically tuned via molecular functionalization.





Routes of Ingress for Devices Under Operation

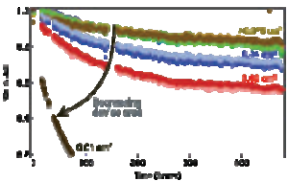
Using a combinatorial degradation system we are able to compare the relative performance of 360 diodes subjected to constant illumination. By varying the aspect ratio of the device active area we are able to observe an increase in device lifetime as the relative fraction for "unprotected edge" is decreased. For these small pixels, edge-in diffusion represents a significant route for degradation of the active layer. Generally, we find that the top contact acts as barrier to prevent oxygen and water vapor transport through the contact. Hence, most aged devices are photobleached around the active areas, but there is little color loss under the electrode.

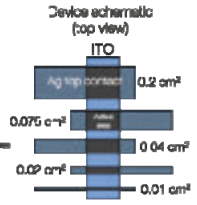


Combinatorial degradation system designed and fabricated by Matthew Reese.

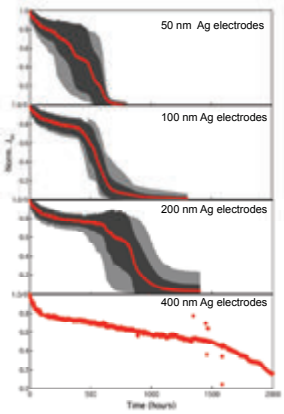
Unbleached active layer under electrodes



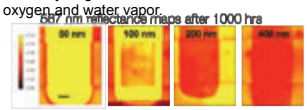


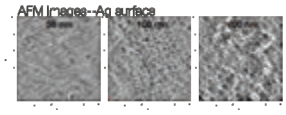


Device Lifetime Primarily Determined by Top Contact



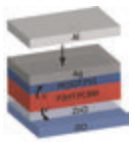
We find that the thickness of the top contact is the first-order, rate limiting factor in determining device lifetime. The average (red), standard deviation (dark grey), and max/min (light grey) behavior are shown (left) for devices with 50, 100, 200, and 400 nm electrodes. Reflectance maps indicate that the thinner electrode eventually become susceptible to oxygen or water vapor transport, indicated by loss of chromophores within the active layer. Tapping mode AFM images suggest that in addition to offering shorter diffusion lengths, thinner top contacts also display a greater density of grain boundaries that assist in the transport of oxygen and water vapor.

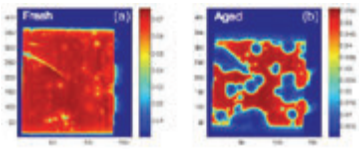


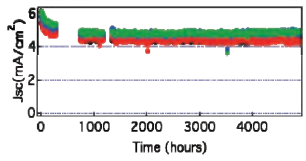


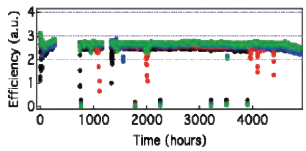
Nucleation and Island Growth Suggests Pinhole Ingress

Photocurrent mapping measurements display regions of zero photocurrent, which nucleate and grow radially as the device ages. This is strongly indicative of point source ingress followed by lateral diffusion into the active layer. This mechanism is also consistent with the dramatic increase in device lifetime when thicker contacts are used. If pinhole ingress can be arrested by filling or creating a tortuous path for diffusion, one should be able to see additional gains in device lifetime. We show that Ag/Al composite electrodes, although only 200 nm in combined thickness, extend the lifetime of these devices to ~5000 hrs.









Lloyd, et al., Sol. Energy Mater. Sol. Cells (2011), doi:10.1016/j.solmat.2010.12.036

Conclusions

- Degradation in conventional devices stems from the reactivity of low work function metals, not the active organic layers
- In larger area devices, electrode thickness dependence studies indicate gas permeability in thin metal electrodes. Photocurrent mapping measurements show nucleation and growth of dark spots in the photocurrent, indicating pinhole ingress of oxygen and water vapor.
- Multilayer electrodes yield surprisingly high stability demonstrating unecapsulated lifetimes of 5000 hours.

This work was funded through the U.S. Department of Energy under Contract No. DOE-AC36-08GO28308 with the National Renewable Energy Laboratory DOE SETP program through the National Center for Photovoltaics. This poster does not contain any proprietary or confidential information. NREL is a national laboratory of the U.S. Department of Energy, Office of Energy Efficiency and Renewable Energy, operated by the Alliance for Sustainable Energy, LLC. • NREL/PO-5200-50739